

Final Report

January 1, 2011 – September 30, 2015

Cooperative Agreement No. R10AC80283

between

New Mexico State University and the US Bureau of Reclamation

submitted by

New Mexico Water Resources Research Institute

Table of Contents

Summary	3
2011 Annual Report	9
2012 Annual Report	18
2013 Annual Report	29
2014 Annual Report	84
2015 Tier I Project Completion Reports	215
Consequences and Possible Solutions for Small Scale Saline Water Residue Disposal in New Mexico – Proof of Concept	216
Construction of MED Component of Pyrolyzer-Desalination Unit for Resiliency Testing	245
Desalination Concentrate Management for Sustainable Agriculture: A preliminary study on transport behavior and plant viability at BGNDRF	310
Design of Pyrolyzer-Desalination Unit Interface for Distributed Biochar and Clean Water Production	357
Developing a Biotechnology with a Reactor to Grow Microalgae for Biodiesel Production from Reusing Waste Concentrate and Anaerobic Digested Sludge	444
Investigating and Understanding the Selectivity of the Conventional Ion-exchange Membranes Used in Electrodialysis Process	539
Optimization of Electrode Design for Electrodialysis Reversal	628
Optimization of Algae Production Using Concentrate	734
Mesophase Templated Porous Polymers as Ultrafiltration Membrane	829
Primary Evaluation of Algae Biofuel Production from Concentrate Stream	896
Producing Polymeric Membrane for Ultrafiltration by High Internal Phase Emulsion Templating	986

Summary

The U.S. Bureau of Reclamation (Reclamation) entered into a Cooperative Agreement (No. R10AC80283) with New Mexico State University (NMSU) to meet several objectives: 1) utilize the collective capabilities and facilities of Reclamation and NMSU to develop research plans and projects, share technical knowledge, and provide professional enhancement for Reclamation and NMSU faculty, staff, and students; 2) facilitate cooperation among universities and research centers, and 3) promote education and transfer of knowledge and technology to the public and private sectors, communities and municipalities, and government and regulatory agencies, as well as the general public. Also, NMSU was to undertake a research program for the development and commercialization of water treatment technology in collaboration with federal agencies, national laboratories, state agencies, local agencies, industry, educational institutions or other water research entities.

The program also was to support desalination research, of which part was to be carried out at or in association with the Brackish Groundwater National Desalination Research Facility (BGNDRF), located in Alamogordo, NM.

New Mexico has large supplies of groundwater available in many aquifers that underlie the state. However, almost 75 percent of this water is considered brackish, containing high levels of total dissolved solids (TDS), ranging from fresh water to a TDS level of more than 300,000 ppm. For small communities and rural homes to utilize New Mexico's groundwater, less expensive technologies must be developed and the cost per unit of treatment must fall.

This Cooperative Agreement is a comprehensive approach to determining how to implement currently available and nascent technologies for desalination of New Mexico's brackish waters. Results of funded projects over the five-year agreement, 2011 to 2015, are contained in this report. Significant progress was made during this period toward developing and deploying cost-effective water treatment technologies and communicating the results to various water-research entities and interested persons.

Project Summary Information

Over the five-year Cooperative Agreement reporting period (2011-2015), 11 projects were funded, 29 students participated on projects (10 received degrees, 16 are continuing in degree programs), and 14 publications have been published or are in the process of publication. After providing summary information below for the projects, individual project summaries indicate publication activity, student participation, and special recognition or notable achievements as a result of the research if any, and new university course offerings as a result of project support if applicable.

Student Participation Summary (all chemical engineering students)

BS	MS	PhD	Degrees Rec'd	Current Students
13	13	3	10	16

Project Publication Summary

Publications published - 2

Publications in preparation - 6

Publications submitted - 4

Publications in review – 2

Individual Project Summaries

Optimization of Electrode Design for Electrodialysis Reversal – Jalal Rastegary (original Pls: Drs. Ali Sharbat and Neil Moe)

Publications

None

Student Participation

Fattaneh Naderi Behdani, PhD, chemical engineering, currently PhD student at NMSU
Masoume Jaber, MS, chemical engineering, graduated

Investigating and Understanding the Selectivity of the Conventional Ion-exchange Membranes Used in Electrodialysis Process – Dr. Ali Sharbat

Publications

None

Student Participation

Leila Karimi, PhD chemical engineering, graduated and currently post-doc at NMSU
Virginia Veruette-Maya, BS chemical engineering, not known if graduated

Preliminary Evaluation of Algae Production from Concentrate Stream – Jalal Rastegary

Publications

Shirazi, SA, M Aghajani, J Rastegary, and A Ghassemi. Simultaneous Treatment of Concentrate Water from Desalination Units and Cultivation of Microalgae as Feed Stock for Biofuel Production. *Desalination and Water Treatment*. In review, 2015.

Student Participation

Saeid Aghahosseini Shirazi, MS chemical engineering, graduated
Tracey Fernandez, BS chemical engineering, graduated
Jaquelyn Guerrero, BS, chemical engineering, graduated

Consequences and Possible Solutions for Small Scale Saline Water Residue Disposal in New Mexico – Dr. Blair Stringam, NMSU

Publications

Sigala, J., Unc, A., and B. Stringam. In Vitro Examination of the Application of Saline Concentrate to Septic Tank Wastewater. *Water Environment Research*, Submitted 2015.

Sigala, J., Unc, A., and B. Stringam. Examination of Particle Dispersion from the Application of Saline Concentrate to Septic Tank Wastewater. *GSTF – Journal of Agricultural Engineering*, Submitted 2015.

Student Participation

Jesus Sigala, MS civil engineering, completed degree
David Gamon, MS civil engineering, did not complete degree

Developing a Biotechnology with a Reactor to Grow Microalgae for Biodiesel Production from Reusing Waste Concentrate and Anaerobic Digested Sludge – Dr. Maung Thein Myint

Publications

Hussein, W, MT Myint, and A Ghassemi. 2015. Energy usage and carbon dioxide emission saving in desalination by using desalination concentrate and waste in microalgae production. *Desalination and Water Treatment*. 54:1:69-83.

Student Participation

Waddah Hussein, MS chemical engineering, graduated

Optimization of Algae Growth Using Concentrate – Jalal Rastegary, NMSU

Publications

Abdulqafar, A, L Karimi, J Rastegary, and A Ghassemi. Modifying Desalination Concentrate to Optimize Its Suitability as a Growth Medium for Microalgae, *Journal of Process Safety and Environmental Protection*, Submitted Dec 2015.

Student Participation

Abdulqafar Ali, MS chemical engineering, working on degree
Tracey Fernandez, BS chemical engineering, graduated
Jaquelyn Guerreo, BS, chemical engineering, graduated
Daniel White, BS, chemical engineering, current student

Construction of MED Component of Pyrolyzer-Desalination Unit for Resiliency Testing – Catherine Brewer, NMSU

Publications

Amiri, A, Pena, J, Smith, M, and Brewer, CE, Design and fabrication of small-scale multiple effect distillation unit for investigation of brackish water scaling behavior, In preparation.

Amiri, A., Brewer, C.E., Small-scale thermal water desalination using biomass energy, In preparation.

Student Participation

Ali Amiri, PhD, chemical engineering, expected graduation Fall 2016
Yunhe Zhang, MS, chemical engineering, expected graduation Summer 2016
Brent Carrillo, BS chemical engineering, expected graduation Spring 2018
William Do Prado, BS chemical engineering, exchange student from Brazil, unpaid

Special Recognition Awards or Notable Achievements

Project entitled "Small-Scale, Low-Temp Multiple Effect Distillation for Brackish Groundwater," submitted by Catherine Brewer and Ali Amiri, was selected as one of the finalists for the NMSU Arrowhead Center's 2016 Launch (business development) Program. The Launch competition for \$25,000 of business start-up funds will occur in Spring 2016.

New Courses

Thermal and membrane water desalination case studies/examples based on the fabricated MED and general reverse osmosis systems were incorporated into CHME 306 Transport Phenomena II: Heat & Mass Transfer during Fall 2015 to 43 students.

Design of Pyrolyzer-Desalination Unit Interface for Distributed Biochar and Clean Water Production – Catherine Brewer, NMSU

Publications

Amiri, A, and Brewer, CE, Small-scale thermal water desalination using biomass energy, In preparation.

Zhang, Y, Idowu, OJ, and Brewer, CE, Using agricultural residue biochar to improve soil quality of desert soils, *Agriculture*, In review.

Dominguez, M, Carrillo, BD, Yamashita, FM, Zhang, Y, Idowu, OJ, and Brewer, CE, Biochar impacts on soil water retention of desert agricultural soils, In preparation.

Student Participation

Ali Amiri, PhD, chemical engineering, expected graduation Fall 2016

Yunhe Zhang, MS, chemical engineering, expected graduation Summer 2016

Brent Carrillo, BS, chemical engineering, expected graduation Spring 2018

Flavia Mitsue Yamashita, BS, chemical engineering, exchange student from Brazil

New Course Offerings

CHME 485/585 Materials from Biorenewable Resources. Course was taught for the first time Fall 2015 to 28 students. Course materials included readings and in-class discussion activities on sources of water for agriculture, selection of crops based on water availability, and water management strategies in sustainable agriculture systems.

Mesophase Templated Porous Polymers as Ultrafiltration Membrane – Dr. Reza Foudazi

Publications

Qavi, S, C Kuang, R Foudazi. Mesophase Templated Porous Polymers as Ultrafiltration Membranes, *Journal Membrane Science*, In preparation.

Student Participation

Sahar Qavi, PhD, chemical engineering, currently working on degree

Maryam Omidvarkordshouli, PhD, chemical engineering, student at SUNY
 Justin Milavec, BS, chemical engineering, graduated, working on MS degree at NMSU
 Aaron Lindsay, BS, chemical engineering, working on degree
 Jessica Miller, BS, chemical engineering, working on degree, currently on internship
 Ryan Zowada, BS, chemical engineering, working on degree

Producing Polymeric Membrane for Ultrafiltration by High Internal Phase Emulsion Templating – Dr. Reza Foudazi,

Publications

Malakian, A, R Zowada, R Foudazi. In-situ functionalization of poly (high internal phase emulsions) for Ultrafiltration Membranes. *Journal Membrane Science*, In preparation.

Student Participation

Anna Malakian, MS, chemical engineering, currently working on degree
 Sahar Qavi, PhD, chemical engineering, currently working on degree
 Maryam Omidvarkordshouli, PhD, chemical engineering, student at SUNY
 Chen Kuang, MS, chemical engineering, currently working on degree
 Ryan Zowada, BS, chemical engineering, working on degree

Desalination Concentrate Management for Sustainable Agriculture: A Preliminary Study on Transport Behavior and Plant Viability at BGNDRF - Manoj Shukla, NMSU

Publications

Flores A, B Schutte, MK Shukla, G Pichionni and A Ulery. 2015. Time-Integrated Measurements of Seed Germination for Salt-Tolerant Plant Species. *Seed Science and Technology*. 43: <http://dx.doi.org/10.15258/sst.2015.43.3.09>.

Flores A, MK Shukla, D Daniel, A Ulery, B Schutte, G Pichionni and S Fernald. 2015. Evapotranspiration Changes with Irrigation Using Saline Groundwater and RO Concentrate. *J. Arid Environments*, Submitted.

Student Participation

Alison Flores, MS in soil science, completed
 Jorge Fernandez, BS completed, currently a graduate student in & environmental sciences

Special Recognition Awards or Notable Achievements

NMSU professor experiments with desalination concentrate disposal:
<https://www.youtube.com/watch?v=BNmUAowyTxY>

Newspaper Articles:

- Professor experiments with desalination concentrate disposal: *Las Cruces Sun News*
- Ag uses for highly saline water researched, *Albuquerque Journal*
- Is saline water an answer to drought, *Las Cruces Bulletin*
- Viable farming and water, *Deming Headlight*

Annual Report 2011

Bureau of Reclamation/New Mexico State University

FY 2008/FY 2009 Appropriations

The Institute for Energy and the Environment

and

The Water Resources Research Institute

at

New Mexico State University

Cooperative Agreement Number R10AC80283

Annual Report

January 1, 2011-December 31, 2011

New Mexico State University

Box 30001 MCS WERC

Las Cruces, NM 88003

Telephone: 575.646.2038

Fax Number: 575.646.5474

Telephone: 800.523.5996

Contents

Background and Introduction to Cooperative agreement	3
NMSU Water and Impaired Water Program	3
NMSU IEE/WRRI Water and Impaired Water Program Goals	4
Research	4
Education.....	4
Outreach.....	5
Components.....	5
Activities for Calendar Year 2011.....	6
Introduction	6
Period: January to March 2011.....	6
Period: April through June 2011.....	7
Period: July through September 2011	8
Period: October through December 2011.....	9

Annual Report for Program Management Plan Agreement Number R10AC80283

BACKGROUND AND INTRODUCTION TO COOPERATIVE AGREEMENT

Most of the population in western North America faces significant water-related challenges. Many rural communities are faced with increasing federally mandated water-quality standards that make availability and affordability of this precious commodity even more vital for an improved/sustained standard of living throughout the country. Management of the existing water resources requires technology improvement and availability, research, education, and outreach at all levels. More importantly, the criticality of water quality and quantity must be augmented to increase water availability including harvesting the abundant brackish water.

New Mexico has large supplies of groundwater available in the many aquifers that underlie the state. However, almost 75 percent of this water is considered brackish, containing high levels of total dissolved solids (TDS), ranging from fresh water to a TDS level of more than 300,000 ppm. In California, there are more than 40 existing and proposed water desalination plants, many utilizing inland groundwater. These plants generate approximately 170,000 acre-feet of desalinated water per year and use 1,300-3,250 kWh of energy per acre foot. The range of total costs for treatment, energy, disposal, and facilities ranges from \$130-\$1,250 per acre foot to treat the water. In order for small communities and rural homes to utilize New Mexico's groundwater, less expensive technologies must be developed and the cost per unit of treatment must fall from the current large-scale, expensive treatment solutions as illustrated by California's system of desalination plants.

This Cooperative Agreement is a comprehensive approach to determining how to implement currently available and nascent technologies, develop education, outreach, research, technology development and deployment for desalination of New Mexico's brackish waters. It is critical to create a research/implementation program that first analyzes the full economic costs of each technology and identifies those technologies that can provide for treatment at various scales, as required by the rural, tribal, and small municipal users in New Mexico and the west.

NMSU WATER AND IMPAIRED WATER PROGRAM

The Institute for Energy and the Environment (IEE) and the Water Resource Research Institute (WRRI) Water and Impaired Water Program is a multifaceted program spanning research, education, and outreach. These efforts led by IEE/WRRI and in collaboration with state and federal government bureaus and regulatory agencies, industrial partners active in water treatment technologies, commercialization, and renewable energies, and academic institutions and research staff active in water research, economics, policy and public relations focus on forging a win-win relationship. The entities partner to develop and deploy cost effective water treatment technologies that benefit the public by reducing the cost of treating water and impaired waters in

the areas of pretreatment, treatment and concentrate management. The vision is continuing to be fulfilled and expanded as more partners and resources are added to the program.

NMSU IEE/WRRI WATER AND IMPAIRED WATER PROGRAM GOALS

The primary focus for New Mexico State University (NMSU) IEE/WRRI's Water and Impaired Water Program is to forge a win-win relationship between the entities for developing and deploying cost effective water treatment technologies that benefit the public by reducing the cost of treating water and impaired waters in the areas of pretreatment, treatment and concentrate management. The goals are to:

RESEARCH

- Create knowledge and acquire data that improves scientific understanding of water and impaired water in the areas of pretreatment, treatment and concentrate management
- Develop approaches to address important issues associated with impaired water including water quality, quantity, pretreatment, treatment, concentrate management, policy, economics, and sustainability
- Develop for deployment affordable and maintainable water treatment technologies for small communities and rural homes
- Provide a comprehensive graduate and undergraduate research opportunity for NMSU and other students interested in impaired water and pursuing research in various aspects of water issues
- Evaluate deployment feasibility of impaired water treatment related technologies
- Develop technologies for commercialization through industrial partners

EDUCATION

- Provide professional development opportunities for undergraduate and graduate students that are pursuing water related degrees, minors and certificates
- Provide a comprehensive graduate and undergraduate research opportunity for NMSU and other students interested in water and impaired water and are pursuing research in various aspects of water issues
- Provide an infrastructure that guides development of students as future scientists, engineers, and policy makers
- Develop classes related to advanced water and impaired water pretreatment, treatment and concentrate management
- Develop courses and materials for professional development, continuing education, and distance learning that target specific stakeholders predicated on level of need, technical detail, and interest
- Develop human and technological resources external to the normal education and research channels through the International Environmental Design Contest (IEDC) utilizing real world problems
- Identify current and future needs of the workforce in water and impaired water treatment operations and maintenance

- Develop materials and classes for operators, technicians, maintenance personnel, and others
- Develop certification programs

OUTREACH

- Develop quality, science-based water and impaired water education and training for formal and non-formal educators
- Develop quality, science based water and impaired water information for the general public
- Develop scientific data and environmental impact evaluation for regulators
- Provide scientific data and information on the processes associated with treatment of impaired water to the health community
- Develop transparent and inclusive life cycle costs to water managers, elected officials and other decision makers

COMPONENTS

The program is structured on three major pillars; all other activities are related to these three distinct yet complimentary programs. The Research, Education, and Outreach pillars build on NMSU, IEE/WRRI capabilities to provide state-of-the-art quality research, education, and outreach in disciplines relevant to water quality, quantity, treatment, concentrate management, policy, economics, sustainability and impaired water. Through the integrated capabilities of the partners, our team will establish a world-class center for expanding the nation's capabilities to address current and future water and impaired water issues that require a multi-disciplinary approach. The team's intent is to continue to develop and evolve the program as more partners and resources are added. Using the team's core competencies, IEE/WRRI will leverage this expertise in three distinct yet complimentary programs. Each section targets to build on the core expertise of NMSU, IEE, WRRI, and Reclamation. They are:

- **Research**—The first pillar encompasses the gamut from laboratory to field demonstration scale. The natural extension of research is technology development and demonstration, followed by commercialization and deployment.
- **Education**— The second pillar is not only academics but also includes the all important hands-on component which transcends the normal classroom learning experience with the addition of participation in cutting edge research and international competition on real world problems through the EDC. Both approaches are an integral support for research. Several natural extensions of education are professional development and training which include such activities as certificate programs, continuing education credits, certification, etc. The delivery methods are as diverse as the target audiences include virtual conferences, distance education, classroom, laboratory, field, etc.

- **Outreach**—The third pillar is perhaps the most expansive of the three pillars due to the diversity of stakeholders that must be included to minimize public hesitancy and skepticism. Through outreach the public may learn to embrace the use of new technologies for treating water and impaired waters. In addition, the regulators that are responsible for protection of public health, the environment, and conservation of natural resources need to understand the technologies being implemented.

ACTIVITIES FOR CALENDAR YEAR 2011

As a part of the reporting requirements associated with the Cooperative Agreement the following activities were accomplished from January 1, 2011 to December 31, 2011.

INTRODUCTION

In addition to the daily and weekly activities and interactions with the Reclamation staff, the following are the summary of key activities undertaken each quarter. Our continued interactions with Reclamation include bi-weekly conference calls, meetings at various locations including Denver, Brackish Groundwater National Desalination Research Facility (BGNDRF) in Alamogordo, Las Cruces, and El Paso, programmatic discussions, water direction and energy related issues.

PERIOD: JANUARY TO MARCH 2011

- Continued conference call meetings with Cooperative Agreement (CA) team
- Updated Gantt Chart
- Continued to communicate with the Reclamation through emails and phone calls
- Provided photos of current NMSU/General Electric (GE) research being conducted at BGNDRF as requested
- Provided speaking points on the CA and BGNDRF activities as requested
- Prepared and submitted the quarterly report for October-December 2010
- Prepared and submitted 2010 Annual Report
- Prepared and submitted 2010 Highlights as required by Cooperative Agreement
- Hosted quarterly meeting with Reclamation in Las Cruces, NM
- Submitted minutes from quarterly meeting to Grants Officer Technical Representative (GOTR) for approval
- Continued to develop databases on stakeholders and presentation opportunities
- Continued to develop needs list
- Submitted to the GOTR the format of the forms for the needs and stakeholders identification for Reclamation input
- Submitted to the GOTR a list of documents NMSU is using for needs identification
- Continued to develop weight factors for the needs list
- Started work on congressional drivers
- Continued to update and refine website

- Continued to populated NMSU/Reclamation “share site” with current documents
- Coordinated delivery of testing materials provided by Reclamation for bench scale testing for the IEDC
- Continued recruitment of judges for the IEDC
- Responded to questions on tasks from the IEDC participants
- Continued planning and coordination of IEDC
- Continued to refine equipment needs list for laboratory at BGNDRF
- Provided written feedback to proposers not recommended for funding on issues of compliance and technical review
- Evaluated resubmitted Tier 1 proposals
- Presented results of resubmitted Tier 1 proposal evaluations, research portfolio, and research budget status to Principal Investigators (PI) as specified in the CA
- Received PIs’ approval on two resubmitted Tier 1 proposals for award
- Obtained GOTR’s concurrence with PIs’ approval of Tier 1 proposal awards
- Announced award of two second round Tier 1 (resubmitted) proposals in concentrate management
- Assigned internal accounting codes to the Tier 1 proposals awarded to Dr. Maung Myint for the project “Development of a Biotechnology with a Reactor” and to Dr. Blair Stringam for the project “Water Residual disposal in New Mexico”
- Facilitated Reclamation’s BGNDRF staff attending NMSU’s eight hour safety course
- Submitted amendment language for the CA for consideration by Reclamation as requested by the GOTR
- Began collaborative work on developing a workshop on renewable energy for BGNDRF through WRRI
- Attended the Multistate Salinity Conf in San Antonio, TX
- Presented at the 2011 Membrane Technology Conference & Exposition in Long Beach, CA research conducted at BGNDRF

PERIOD: APRIL THROUGH JUNE 2011

- Conducted the 21st annual IEDC April 3-6, 2011. Ninety-five students representing 19 teams from 14 universities from across the United States, as well as Canada competed to solve environmental challenges posed by government and industry professionals.
- Continued conference call meetings with CA team
- Updated Gantt Chart
- Continued to communicate with the Reclamation through emails and phone calls
- Prepared and submitted the quarterly report for January-March 2011
- Attended the quarterly meeting with Reclamation in Denver, CO
- Submitted minutes from quarterly meeting to GOTR for approval
- Continued to develop databases on stakeholders and presentation opportunities
- Continued to develop needs list
- Discussed the submitted forms for the needs and stakeholders identification for Reclamation input

- Continued to develop weight factors for the needs list
- Continued work on congressional drivers
- Continued to work on agency drivers
- Continued to update and refine website
- Continued to populated NMSU/Reclamation “share site” with current documents
- Continued to refine equipment needs list for laboratory at BGNDRF
- Evaluated submitted Tier 1 proposal
- Presented results of submitted Tier 1 proposal evaluations, research portfolio, and research budget status to PI as specified in the CA Received PIs’ approval on one submitted Tier 1 proposal for award
- Obtained GOTR’s concurrence with PIs’ approval of Tier 1 proposal award
- Awarded Tier I research grants in treatment.
- Submitted amendment language for the CA for consideration by Reclamation as requested by the GOTR
- Began collaborative work on developing a workshop on renewable energy for BGNDRF through WRRI
- Graduated a chemical engineering student with a masters degree; research related to desalination activities at BGNDRF

PERIOD: JULY THROUGH SEPTEMBER 2011

- Continued conference call meetings with CA team
- Updated Gantt Chart
- Continued to communicate with the Reclamation through emails and phone calls
- Prepared and submitted the quarterly report for April-June 2011
- Attended the quarterly meeting with Reclamation in Denver, CO
- Submitted minutes from quarterly meeting to GOTR for approval
- Continued to monitor progress on awarded Tier I research.
- Continued to develop databases on stakeholders and presentation opportunities
- Continued to develop needs list
- Discussed the submitted forms for the needs and stakeholders identification for Reclamation input
- Continued to develop weight factors for the needs list
- Continued work on congressional drivers
- Continued work on agency drivers
- Continued to update and refine website
- Continued to populated NMSU/Reclamation “share site” with current documents
- Continued to refine equipment needs list for laboratory at BGNDRF
- Evaluated four submitted Tier 1 proposals
- Received two resubmitted Tier I proposals
- Submitted amendment language for the CA for consideration by Reclamation as requested by the GOTR

- Began collaborative work as sponsor on developing a workshop, “New Water New Energy; A conference Linking Desalination and Renewable Energy,” for BGNDRF
- Attended International Desalination Association World Congress in Perth, Australia
- Started discussions on collaboration with the Chief Technology Officer (CTO) of the National Centre of Excellence in Desalination (NCED)
- Posted tasks for the 2012 IEDC

PERIOD: OCTOBER THROUGH DECEMBER 2011

The activities for the reporting period from October 2011 through December 2011 included:

- Continued conference calls and meetings with CA team
- Continued to communicate with the Reclamation through emails and phone calls
- Prepared and submitted the quarterly report for July – September 2011
- Continued to monitor progress on awarded Tier I research.
- Continued to develop databases on stakeholders and presentation opportunities
- Continued to develop needs list
- Discussed the submitted forms for the needs and stakeholders identification for Reclamation input
- Continued work on congressional drivers
- Continued work on agency drivers
- Continued to update and refine website
- Continued to populated NMSU/Reclamation “share site” with current documents
- Evaluated two resubmitted Tier I proposals
- Presented results of resubmitted Tier 1 proposal evaluations, research portfolio, and research budget status to PI as specified in the CA
- Received PIs’ approval on two resubmitted Tier 1 proposals for award
- Obtained GOTR’s concurrence with PIs’ approval of Tier 1 proposal awards
- Awarded two Tier I research grants, one in treatment and one in concentrate management
- Assigned internal accounting codes to the Tier 1 proposals awarded to Dr. Moe “Optimization of Electrode Design for Electrodialysis Reversal”; Dr Sharbat “Investigating and Understanding the Selectivity of the Conventional Ion-exchange Membranes used in Electrodialysis Process” and to Dr. Rastegary “Preliminary Evaluation of Algae Production from Concentrate Stream”
- Assisted in conducting and participated in the workshop breakout groups at “New Water New Energy; A Conference Linking Desalination and Renewable Energy”
- Met with, and continued discussions on, collaboration with the CTO of Australia’s NCED
- Presented at the AIChE Conference on Tier 1 research and other research conducted at BGNDRF
- Presented at the “New Water New Energy; A Conference Linking Desalination and Renewable Energy conducted in December at Alamogordo NM
- Submitted A-133 Audit to GOTR

Annual Report 2012

Bureau of Reclamation/New Mexico State University
FY 2008/FY 2009 Appropriations

The Institute for Energy and the Environment
and

The Water Resources Research Institute
at

New Mexico State University
Cooperative Agreement R10AC80283
Annual Report

January 1, 2012 - December 31, 2012

New Mexico State University
Box 30001 MCS WERC
Las Cruces, NM 88003

Telephone: 575.646.2038
Fax Number: 575.646.5474
Telephone: 800.523.5996

Contents

BACKGROUND AND INTRODUCTION TO COOPERATIVE AGREEMENT	3
NMSU WATER AND IMPAIRED WATER PROGRAM	3
NMSU IEE/WRRI WATER AND IMPAIRED WATER PROGRAM GOALS	4
RESEARCH	4
EDUCATION	4
OUTREACH	5
COMPONENTS	5
Activities for Calendar Year 2012	5
Introduction	6
Period: January to March 2012	6
Period: April To June 2012	7
Period: July to September 2012	7
Period: October to December 2012	9

Annual Report for Program Management Plan Agreement Number R10AC80283

BACKGROUND AND INTRODUCTION TO COOPERATIVE AGREEMENT

Most of the population in western North America faces significant water-related challenges. Many rural communities are faced with increasing federally mandated water-quality standards that make availability and affordability of this precious commodity even more vital for an improved/sustained standard of living throughout the country. Management of the existing water resources requires technology improvement and availability, research, education, and outreach at all levels. More importantly, the criticality of water quality and quantity must be augmented to increase water availability including harvesting the abundant brackish water.

New Mexico has large supplies of groundwater available in the many aquifers that underlie the state. However, almost 75 percent of this water is considered brackish, containing high levels of total dissolved solids (TDS), ranging from fresh water to a TDS level of more than 300,000 ppm. In California, there are more than 40 existing and proposed water desalination plants, many utilizing inland groundwater. These plants generate approximately 170,000 acre-feet of desalinated water per year and use 1,300-3,250 kWh of energy per acre foot. The range of total costs for treatment, energy, disposal, and facilities ranges from \$130-\$1,250 per acre foot to treat the water. In order for small communities and rural homes to utilize New Mexico's groundwater, less expensive technologies must be developed and the cost per unit of treatment must fall from the current large-scale, expensive treatment solutions as illustrated by California's system of desalination plants.

This Cooperative Agreement is a comprehensive approach to determining how to implement currently available and nascent technologies, develop education, outreach, research, technology development and deployment for desalination of New Mexico's brackish waters. It is critical to create a research/implementation program that first analyzes the full economic costs of each technology and identifies those technologies that can provide for treatment at various scales, as required by the rural, tribal, and small municipal users in New Mexico and the west.

NMSU WATER AND IMPAIRED WATER PROGRAM

The Institute for Energy and the Environment (IEE) and the Water Resource Research Institute (WRI) Water and Impaired Water Program is a multifaceted program spanning research, education, and outreach. These efforts led by IEE/WRI and in collaboration with state and federal government bureaus and regulatory agencies, industrial partners active in water treatment technologies, commercialization, and renewable energies, and academic institutions and research staff active in water research, economics, policy and public relations focus on forging a win-win relationship. The entities partner to develop and deploy cost effective water treatment technologies that benefit the public by reducing the cost of treating water and

impaired waters in the areas of pretreatment, treatment and concentrate management. The vision is continuing to be fulfilled and expanded as more partners and resources are added to the program.

NMSU IEE/WRRI WATER AND IMPAIRED WATER PROGRAM GOALS

The primary focus for NMSU IEE/WRRI Water and Impaired Water Program is to forge a win-win relationship between the entities for developing and deploying cost effective water treatment technologies that benefit the public by reducing the cost of treating water and impaired waters in the areas of pretreatment, treatment and concentrate management. The goals are:

RESEARCH

- Create knowledge and acquire data that improves scientific understanding of water and impaired water in the areas of pretreatment, treatment and concentrate management.
- Develop approaches to address important issues associated with impaired water including water quality, quantity, pretreatment, treatment, concentrate management, policy, economics, and sustainability
- Develop for deployment affordable and maintainable water treatment technologies for small communities and rural homes
- Provide a comprehensive graduate and undergraduate research opportunity for NMSU and other students interested in impaired water and pursuing research in various aspects of water issues
- Evaluate deployment feasibility of impaired water treatment related technologies
- Develop technologies for commercialization through industrial partners

EDUCATION

- Provide professional development opportunities for undergraduate and graduate students that are pursuing water related degrees, minors and certificates
- Provide a comprehensive graduate and undergraduate research opportunity for NMSU and other students interested in water and impaired water and are pursuing research in various aspects of water issues
- Provide an infrastructure that guides development of students as future scientists, engineers, and policy makers
- Develop classes related to advanced water and impaired water pretreatment, treatment and concentrate management
- Develop courses and materials for professional development, continuing education, and distance learning that target specific stakeholders predicated on level of need, technical detail, and interest
- Develop human and technological resources external to the normal education and research channels through the International Environmental Design Contest (EDC) utilizing real world problems
- Identify current and future needs of the workforce in water and impaired water treatment operations and maintenance
- Develop materials and classes for operators, technicians, maintenance personnel, and others

- Develop certification programs

OUTREACH

- Develop quality, science-based water and impaired water education and training for formal and non-formal educators
- Develop quality, science based water and impaired water information for the general public
- Develop scientific data and environmental impact evaluation for regulators
- Provide scientific data and information on the processes associated with treatment of impaired water to the health community
- Develop transparent and inclusive life cycle costs to water managers, elected officials and other decision makers

COMPONENTS

The program is structured on three major pillars; all other activities are related to these three distinct yet complimentary programs. Research, Education, and Outreach build on NMSU, IEE/WRRI capabilities to provide state-of-the-art quality research, education, and outreach in disciplines relevant to water quality, quantity, treatment, concentrate management, policy, economics, sustainability and impaired water. Through the integrated capabilities of the partners, our team will establish a world-class center for expanding the nation's capabilities to address current and future water and impaired water issues that require a multi-disciplinary approach. The team's intent is to continue to develop and evolve the program as more partners and resources are added. Using the team's core competencies, IEE/WRRI will leverage this expertise in three distinct yet complimentary programs. Each section targets to build on the core expertise of NMSU, IEE, WRRI, and Reclamation. They are:

- **Research**—The first pillar encompasses the gamut from laboratory to field demonstration scale. The natural extension of research is technology development and demonstration, followed by commercialization and deployment.
- **Education**—The second pillar is not only academics but also includes the all important hands-on component which transcends the normal classroom learning experience with the addition of participation in cutting edge research and international competition on real world problems through the EDC. Both approaches are an integral support for research. Several natural extensions of education are professional development and training which include such activities as certificate programs, continuing education credits, certification, etc. The delivery methods are as diverse as the target audiences include virtual conferences, distance education, classroom, laboratory, field, etc.
- **Outreach**—The third pillar is perhaps the most expansive of the three pillars due to the diversity of stakeholders that must be included to minimize public hesitancy and skepticism. Through outreach the public may learn to embrace the use of new technologies for treating water and impaired waters. In addition, the regulators that are responsible for protection of public health, the environment, and conservation of natural resources need to understand the technologies being implemented.

ACTIVITIES FOR CALENDAR YEAR 2012

As a part of the reporting requirements associated with the Cooperative Agreement the following activities were accomplished from January 1, 2012 to December 31, 2012.

INTRODUCTION

In addition to the daily and weekly activities and interactions with the Bureau of Reclamation (Reclamation) staff, the following are the summary of key activities undertaken each quarter. Our continued interactions with Reclamation include bi-weekly conference calls, meetings at various locations including Denver, Brackish Groundwater National Desalination Research Facility (BGNDRF) in Alamogordo, Las Cruces, programmatic discussions, water and energy related issues.

PERIOD: JANUARY TO MARCH 2012

- Continued conference call/meetings with the Cooperative Agreement (CA) team
- Continued to communicate with the Bureau of Reclamation (Reclamation) through emails and phone calls
- Planning quarterly meeting with Reclamation
- Prepared and submitted the annual report for 2011
- Hosted the quarterly meeting with Reclamation on February 6 & 7 in Las Cruces, NM
- Submitted minutes from quarterly meeting to all participants and Grants Officer Technical Representative (GOTR)
- Continued to refine needed changes to the CA based on modification 002
- Continued the development of the Collaborative Research Education Program
- Continued the development of the new fellowship programs
- Continued to monitor progress on awarded Tier I research
- Prepared and submitted quarterly report for October to December 2011
- Continued to update and refine website
- Continued to populated NMSU/Reclamation “share site” with current documents
- Continued to refine equipment needs list for laboratory at BGNDRF
- Announced Tier 1 call for proposals for review in April
- Received one Tier I proposal
- Attended Reclamation sponsored meeting in Tucson, AZ on 2-24-12 with BOR, ASU, and UA for as part of collaborative research education program and possible collaboration on algae and halophyte production for concentrate management as a potential directed Tier II agricultural research project for BGNDRF
- Initiated agriculture working group meetings to determine the needs for initial soil testing and what infrastructure will be needed to support research at BGNDRF
- Attended AWWA/AMTA Membrane Technology Conference and presented on research conducted at BGNDRF , Glendale, AZ, March 2012
- Coordinated delivery of BGNDRF water mixtures to be used in bench scale testing for the Reclamation and ONR task in the International Environmental Design Contest (IEDC)
- Continued to recruit judges for the IEDC
- Continued planning and coordination for the IEDC
- Responded to questions on tasks from IEDC participants
- Met with UA ERL as a follow-up to the meeting Reclamation sponsored in Tucson, AZ with ASU, and UA as part of collaborative research education program and possible

collaboration on algae and halophyte production for concentrate management as a potential directed Tier II agricultural research project for BGNDRF and began the process of developing potential partnerships

PERIOD: APRIL TO JUNE 2012

- Conducted the 22nd Annual International Environmental Design Contest April 1-4 2012. One hundred and five students, representing twenty-two university teams from fifteen schools across the United States participated and competed to solve environmental challenges posed by government and industry professionals in six tasks Continued conference call/meetings with the CA team
- Continued to communicate with the Reclamation through emails and phone calls
- Planning quarterly meeting with Reclamation
- Prepared and submitted the annual report for 2011
- Attended the quarterly meeting with Reclamation on May 14&15 in Denver, CO
- Submitted minutes from quarterly meeting to participants and GOTR
- Continued to refine needed changes to the CA based on modification 002
- Continued the development of the Collaborative Research Education Program with input from the GOTR
- Continued the development of the new fellowship programs with input from the GOTR
- Continued promotion of Tier I open solicitation
- Received three Tier I proposals
- Continued to monitor progress on awarded Tier I research
- Prepared and submitted quarterly report for January to March 2012
- Continued to update and refine website
- Continued to populated NMSU/Reclamation “share site” with current documents
- Continued to refine equipment needs list for laboratory at BGNDRF
- Graduate student, Saeid Shirazi, attended and presented a poster for Tier 1 at the 2nd International Conference on Algal Biomass, Biofuels and Bioproducts, June 16-19 San Diego, CA
- Graduate student, Saeid Shirazi, who participates on a Tier 1 research project Attended (the CleanTech conference, June 18-21 Santa Clara, CA
- Ali Sharbat a post-doctoral staff member and Leila Karimi a graduate student Attended and presented at the North American Membrane Society (NAMS) Annual Meeting, New Orleans, LA., and June 9-13, 2012
- Dr. Ali Sharbat moderated an Electro-separation session at the North American Membrane Society (NAMS) Annual Meeting, New Orleans, LA., June 9-13, 2012

PERIOD: JULY TO SEPTEMBER 2012

- Continued conference call/meetings with the CA team
- Continued to communicate with the Reclamation through emails and phone calls
- Planning quarterly meeting with Reclamation

- Attended the quarterly meeting with Reclamation on September, 20 & 21 in Denver, CO
- Submitted minutes from quarterly meeting to all participants and GOTR
- Continued to refine needed changes to the CA based on modification 002
- Began drafting Mod 3 to address changes on quarterly reporting and tracking
- Continued the development of the Collaborative Research Education Program
- Continued the development of the new fellowship programs
- Continued to monitor progress on awarded Tier I research
- Prepared and submitted quarterly report for April to June 2012
- Continued to update and refine website
- Continued to populated NMSU/Reclamation “share site” with current documents
- Continued to refine equipment needs list for laboratory at BGNDRF
- Announced Tier 1 call for proposals for review 4th quarter
- Conducted compliance and technical review of 3 Tier I proposals
- Presented the 9 following posters at the WRRRI conferences on July 31, 2012, Las Cruces, New Mexico
 - Desalination in a Pilot-Scale Electrodialysis Process: Selective Removal of Divalent Ions in Comparison With Monovalent Ions, Leila Karimil, Ali Sharbat, Neil Moe, Jim Loya, Abbas Ghassemi
 - Concentrate Stream as a New Potential Media for Growing Algae, Saeid Shirazi, Jalal Rastegary, Abbas Ghassemi, Tracey Fernandez
 - Existing Models for Membrane Desalination, Azadeh Ghorbani, Abbas Ghassemi, Ali Sharbat
 - Concentrate Management Strategies for Inland Desalination, Connor Hanrahan, Jim Loya, Ali Sharbat, Neil Moe, Abbas Ghassemi
 - RO / NF Applications in Brackish Water Desalination: Membrane Characterization and Hybridization with EDR, Ghazaleh Vaseghi, Ali Sharbat and Abbas Ghassemi
 - Using Electrodialysis Reversal Concentrate as Medium for Algal Biomass Production, Stephanie Franco, Jalal Rastegary, Tracey Fernandez, Abbas Ghassemi
 - Overview of Desalination Technologies, Azadeh Ghorbani, Abbas Ghassemi, Ali Sharbat
 - Using Electrodialysis Reversal Concentrate as Medium for Algal Biomass Production, Stephanie Franco, Jalal Rastegary, Abbas Ghassemi, Tracey Fernandez
 - Reusing Anaerobic Digested Sludge and Desalination Concentrate as Water Media and Nutrient for Growing *D. salina* and *S. platensis*, Waddah Hussein, Myint Maung, Abbas Ghassemi

- Presented the following 6 posters at the Bi-national Border Water Resources Summit. September 27-28, 2012 Juarez, Chihuahua, MX and El Paso, TX
 - Applications of RO/NF in Brackish Water Desalination: Membrane Characterization and Hybridization with EDR, Ghazaleh Vaseghi, Ali Sharbat and Abbas Ghassemi
 - Pilot-Scale Electrodialysis Performance in Cation Removal from Brackish Water as a Desalination Process , Leila Karimi, Jim Loya, Abbas Ghassemi
 - Concentrate from Desalination Is Good for Microalgae Growth, Waddah Hussein, Myint Maung, Abbas Ghassemi
 - Cultivation of *Dunaliella tertiolecta* (UTEX LB999) on Concentrate Stream of Reverse Osmosis, Saeid Shirazi, Jalal Rastegary, Abbas Ghassemi, Tracey Fernandez
 - Membrane Desalination Models Review, Azadeh Ghorbani, Abbas Ghassemi
 - Concentrate Management Strategies for Inland Desalination, Connor Hanrahan, Jim Loya, Ali Sharbat, Neil Moe, Abbas Ghassemi
- Presented the following poster to the Algae Biomass Summit September 24-27, 2012 Denver, CO
 - Using Concentrate Stream of Electrodialysis Reversal Pilot Plant for Growing *Nannochloropsis oculata*, Saeid Aghahosseini Shirazi, Jalal Rastegary, Abbas Ghassemi, Tracey Fernandez

PERIOD: OCTOBER TO DECEMBER 2012

- Continued conference call/meetings with CA team
- Continued to communicate with the Reclamation through emails and phone calls
- Exchanged e-mail/phone calls in preparation for the meeting with Katie Guerra in Las Cruces discussing cooperation on PV/RO research project as part of the Collaborative Research Education Program's Collaborative Research Partnerships
- Exchanged e-mail/phone calls in preparation for the meeting with Katie Guerra on development and planning of coordinated CA joint outreach program and materials for a joint exhibit booth at conferences
- NMSU and Reclamation staff worked on the PV/RO skid to determine present condition and worked on new instrumentation plan
- Continued to refine needed changes to the CA based on Mod 002
- Requested and received one year extension to the CA Mod 3
- Received CA Mod 4 change of GOTR
- Continued drafting CA Mod 5 to address changes on quarterly reporting and tracking (Milestone chart), directed research, language clean-up from Mod 2 etc.
- Continued the development of the Collaborative Research Education Program

- Continued the development of the new undergraduate Fellowship Program “Water Fellowship”
- Continued discussions and review/development of a path forward with BGNDRF staff for infrastructure development and utilization of the agricultural research area
- Reviewed safety documents and procedures for NMSU research conducted at BGNDRF with site staff, CA PI and Program Manager, and NMSU’s Chemical Engineering Department Head
- Continued to monitor progress on awarded Tier I research
- Prepared and submitted quarterly report for July to September 2012
- Continued to update and refine website
- Continued to populated NMSU/Reclamation “share site” with current documents
- Continued to refine equipment needs list for laboratory at BGNDRF
- Announced Tier 1 call for proposals for review during first quarter
- Received one Tier 1 proposal
- Questions/inquiries related to, Reclamation sponsored Task 3, from prospective and committed teams were addressed. Task 3, Nitrate Removal in Rural Water Treatment Systems, requires that the teams develop a water treatment system for a rural groundwater well with targeted nitrate removal that addresses the challenges associated with rural water treatment
- The seven teams registered for the Design Contest task sponsored by Reclamation are
 - California Polytechnic State Univ., Pomona
 - Duke University
 - Louisiana State University
 - Ohio University
 - University of California Riverside
 - University of Idaho
 - University of Waterloo
- Identified potential judges to evaluate the effectiveness of nitrate removal and the considerations given to designing the system for rural water infrastructure
- Began recruitment of judges for the contest to be held April 7-10, 2013 in Las Cruces
- Advertised the Water Fellowship to NMSU students in all disciplines
- Received, reviewed and interviewed four applicants for Water Fellowship
- Awarded four Water Fellowships to the following undergraduate students
 - Janelle Roybal
 - Rachel Wood
 - Baraka Lwoya
 - Corinne Fox
- Provided mentoring on and monitored progress of undergraduate fellowship students projects

- Leila Karimi, graduate student, presented a paper entitled “Selectivity Studies on Pilot-scale Electrodialysis Reversal” at the 2012 AIChE annual meeting in October, 28 November 2, 2012 in Pittsburgh, Pennsylvania
- Saeid Shirazi, graduate student, working on a Tier 1 project presented a poster entitled “An Innovative Approach for Using Concentrate Stream of Desalination” at the URC Conference, Las Cruces, NM, October 20, 2012
- Saeid Shirazi, graduate student, working on a Tier 1 project submitted an abstract entitled “An Innovative Method to Exploit Concentrate Stream of Desalination Units” to the 17th Annual Water Reuse & Desalination Research Conference, Phoenix, AZ
- Janelle Roybal and Rachel Wood, fellowship students, submitted an abstract entitled “Sustainable Brine Effluent Disposal for Inland Desalination” to the 17th Annual Water Reuse & Desalination Research Conference, Phoenix, AZ

Annual Report 2013

Bureau of Reclamation/New Mexico State University

FY 2008/FY 2009 Appropriations

The Institute for Energy and the Environment

and

The Water Resources Research Institute

at

New Mexico State University

Cooperative Agreement R10AC80283

Annual Report

January 1, 2013-December 31, 2013

New Mexico State University

Box 30001 MCS WERC

Las Cruces, NM 88003

Telephone: 575.646.2038

Fax Number: 575.646.5474

Telephone: 800.523.5996

Contents

BACKGROUND AND INTRODUCTION TO COOPERATIVE AGREEMENT	2
NMSU WATER AND IMPAIRED WATER PROGRAM	2
NMSU IEE/WRRI WATER AND IMPAIRED WATER PROGRAM GOALS	3
RESEARCH	3
EDUCATION	3
OUTREACH	3
COMPONENTS	4
Activities for Calendar Year 2013	4
Introduction	4
Period: January to March 2013	5 - 8
Period: April to June2013	9 - 12
Period: July to September 2013	13 - 45
Period: October to December 2013	46 - 55

Annual Report for Program Management Plan Agreement Number R10AC80283

BACKGROUND AND INTRODUCTION TO COOPERATIVE AGREEMENT

Most of the population in western North America faces significant water-related challenges. Many rural communities are faced with increasing federally mandated water-quality standards that make availability and affordability of this precious commodity even more vital for an improved/sustained standard of living throughout the country. Management of the existing water resources requires technology improvement and availability, research, education, and outreach at all levels. More importantly, the criticality of water quality and quantity must be augmented to increase water availability including harvesting the abundant brackish water.

New Mexico has large supplies of groundwater available in the many aquifers that underlie the state. However, almost 75 percent of this water is considered brackish, containing high levels of total dissolved solids (TDS), ranging from 1000 ppm to a TDS level of more than 300,000 ppm. In California, there are more than 40 existing and proposed water desalination plants, many utilizing inland groundwater. These plants generate approximately 170,000 acre-feet of desalinated water per year and use 1,300-3,250 kWh of energy per acre foot. The range of total costs for treatment, energy, disposal, and facilities ranges from \$130-\$1,250 per acre foot to treat the water. In order for small communities and rural homes to utilize New Mexico's groundwater, less expensive technologies must be developed and the cost per unit of treatment must fall from the current large-scale, expensive treatment solutions as illustrated by California's system of desalination plants.

This Cooperative Agreement is a comprehensive approach to determining how to implement currently available and nascent technologies, develop education, outreach, research, technology development and deployment for desalination of New Mexico's brackish waters. It is critical to create a research/implementation program that first analyzes the full economic costs of each technology and identifies those technologies that can provide for treatment at various scales, as required by the rural, tribal, and small municipal users in New Mexico and the west.

NMSU WATER AND IMPAIRED WATER PROGRAM

The Institute for Energy and the Environment (IEE) and the Water Resource Research Institute (WRRI) Water and Impaired Water Program is a multifaceted program spanning research, education, and outreach. These efforts led by IEE/WRRI and in collaboration with state and federal government bureaus and regulatory agencies, industrial partners active in water treatment technologies, commercialization, and renewable energies, and academic institutions and research staff active in water research, economics, policy and public relations focus on forging a win-win relationship. The entities partner to develop and deploy cost effective water treatment technologies that benefit the public by reducing the cost of treating water and impaired waters in the areas of pretreatment, treatment and concentrate management. The vision is continuing to be fulfilled and expanded as more partners and resources are added to the program.

NMSU IEE/WRRI WATER AND IMPAIRED WATER PROGRAM GOALS

The primary focus for NMSU IEE/WRRI Water and Impaired Water Program is to forge a win-win relationship between the entities for developing and deploying cost effective water treatment technologies that benefit the public by reducing the cost of treating water and impaired waters in the areas of pretreatment, treatment and concentrate management. The goals are:

RESEARCH

- Create knowledge and acquire data that improves scientific understanding of water and impaired water in the areas of pretreatment, treatment and concentrate management.
- Develop approaches to address important issues associated with impaired water including water quality, quantity, pretreatment, treatment, concentrate management, policy, economics, and sustainability
- Develop for deployment affordable and maintainable water treatment technologies for small communities and rural homes
- Provide a comprehensive graduate and undergraduate research opportunity for NMSU and other students interested in impaired water and pursuing research in various aspects of water issues
- Evaluate deployment feasibility of impaired water treatment related technologies
- Develop technologies for commercialization through industrial partners

EDUCATION

- Provide professional development opportunities for undergraduate and graduate students that are pursuing water related degrees, minors and certificates
- Provide a comprehensive graduate and undergraduate research opportunity for NMSU and other students interested in water and impaired water and are pursuing research in various aspects of water issues
- Provide an infrastructure that guides development of students as future scientists, engineers, and policy makers
- Develop classes related to advanced water and impaired water pretreatment, treatment and concentrate management
- Develop courses and materials for professional development, continuing education, and distance learning that target specific stakeholders predicated on level of need, technical detail, and interest
- Develop human and technological resources external to the normal education and research channels through the International Environmental Design Contest (IEDC) utilizing real world problems
- Identify current and future needs of the workforce in water and impaired water treatment operations and maintenance
- Develop materials and classes for operators, technicians, maintenance personnel, and others
- Develop certification programs

OUTREACH

- Develop quality, science-based water and impaired water education and training for formal and non-formal educators
- Develop quality, science based water and impaired water information for the general public
- Develop scientific data and environmental impact evaluation for regulators

- Provide scientific data and information on the processes associated with treatment of impaired water to the health community
- Develop transparent and inclusive life cycle costs to water managers, elected officials and other decision makers

COMPONENTS

The program is structured on three major pillars; all other activities are related to these three distinct yet complimentary programs. Research, Education, and Outreach build on NMSU, IEE/WRII capabilities to provide state-of-the-art quality research, education, and outreach in disciplines relevant to water quality, quantity, treatment, concentrate management, policy, economics, sustainability and impaired water.

Through the integrated capabilities of the partners, our team will work to establish a world-class center for expanding the nation's capabilities to address current and future water and impaired water issues that require a multi-disciplinary approach, as funding and Reclamation allows. The team's intent is to continue to develop and evolve the program as more partners and resources are added. Using the team's core competencies, IEE/WRII will leverage this expertise in three distinct yet complimentary programs. Each section targets to build on the core expertise of NMSU, IEE, WRII, and Reclamation. They are:

- **Research**—The first pillar encompasses the gamut from laboratory to field demonstration scale. The natural extension of research is technology development and demonstration, followed by commercialization and deployment.
- **Education**— The second pillar is not only academics but also includes the all important hands-on component which transcends the normal classroom learning experience with the addition of participation in cutting edge research and international competition on real world problems through the IEDC. Both approaches are an integral support for research. Several natural extensions of education are professional development and training which include such activities as certificate programs, continuing education credits, certification, etc. The delivery methods are as diverse as the target audiences include virtual conferences, distance education, classroom, laboratory, field, etc.
- **Outreach**—The third pillar is perhaps the most expansive of the three pillars due to the diversity of stakeholders that must be included to minimize public hesitancy and skepticism. Through outreach the public may learn to embrace the use of new technologies for treating water and impaired waters. In addition, the regulators that are responsible for protection of public health, the environment, and conservation of natural resources need to understand the technologies being implemented.

ACTIVITIES FOR CALENDAR YEAR 2013

As a part of the reporting requirements associated with the Cooperative Agreement the following activities were accomplished from January 1, 2013 to December 31, 2013.

INTRODUCTION

In addition to the daily and weekly activities and interactions with the Bureau of Reclamation (Reclamation) staff, the following are the summary of key activities undertaken each quarter. Our continued interactions with Reclamation include bi-weekly conference calls, meetings at various locations

including Denver, Brackish Groundwater National Desalination Research Facility (BGNDRF) in Alamogordo, Las Cruces, programmatic discussions, water direction and energy related issues.

PERIOD: JANUARY TO MARCH 2013

- Attended AWWA and AMTA Membrane Technology Conference & Exposition (Jim, and Jalal), exhibited a booth jointly with Reclamation (Randy) and presented the Cooperative Agreement achievements and research conducted at BGNDRF as required by the cooperative agreement, Feb. 25 – 28, 2013, in San Antonio, Texas.
- Graduate students, Leila Karimi, Leili Abkar, and Fattaneh Naderi Behdani attended AWWA and AMTA Membrane Technology Conference & Exposition Feb. 25 – 28, 2013, in San Antonio, Texas. The purpose of their attendance was to benefit from the latest research in the field of RO and EDR and networking opportunities with the researchers in the field of membrane technology. Racheal Jones a graduate student working in drought planning also attend the conference. Rachael’s goal was to participate and listen to a presentation by Michelle Chapman on the research preformed in Texas on drought planning, determine how she can use the data for her research on New Mexico’s drought planning, and also to coordinate with Michelle on her research activities.
- Presented the following papers:
 - M. Myint, W. Hussein, A. Ghassemi, “Managing Brackish Groundwater Desalination Concentrate in Microalgae Production to Improve Sustainability of Inland Desalination, Wastewater Treatment Plant, Farm, and Ranch in Semi-Arid Region of the United States”. Second Water Research Conference. 20-23 January 2013, Singapore EXPO, Singapore.
 - W. Hussein, M. Myint, A. Ghassemi, “Microalgae Process for Treatment of Concentrate from Inland Desalination to Improve Sustainability of Water Supplies for Irrigation, Farm, and Ranch in Cities of Arid Regions”. Second Water Research Conference. 20-23 January 2013, Singapore EXPO, Singapore.
 - L. Karimi, A. Ghassemi, J. Loya, “Selectively Removal of Charged Species from Brackish Water in Desalination Process”. Multi-State Salinity Coalition, Feb. 2013, Las Vegas, NV.
 - A. Ghorbani, A. Ghassemi, “Comparison of Model for Membrane Base System”. Multi-State Salinity Coalition, Feb. 2013, Las Vegas, NV.
 - L. Karimi, A. Ghassemi, J. Loya, “Selectivity Studies in the Desalination Process Using Electrodialysis”. Graduate Research and Arts Symposium, March 11-13, NMSU, Las Cruces, New Mexico

- Arranged the visit for graduate students, Leila Karimi, Leili Abkar, Fattaneh Naderi Behdani and Azadeh Ghorbani and fellowship students Rachel Wood, Troy Sculto, Duy Khanh Nguyen and Baraka Lwoya and undergraduate student Tracey Fernandez to tour the Bureau of Reclamation's facility in Yuma, AZ, GE and Hydronautics in San Diego, CA. The graduate and fellowship students toured the Yuma Desalting Plant on March 25. The next destination on the trip was to the City of San Diego's Public Utilities Water & Wastewater treatment plant on the morning of March 26 and General Electric's Water and Process Technologies membrane production facility on the afternoon of March 26. The next day March 27, the students toured Hydronautics, a Nitto Denko company where students observed the start to the end of membrane rolling and the final testing.
- As part of the education and outreach component of our Cooperative Agreement eight training sessions for STEM students from El Paso Community College on desalinization and concentrate management were organized. Graduate students, Leila Karimi, Saeid Shirazi, and Azadeh Ghorbani participated from February 13 until March 29.
- Continued conference call/meetings with Cooperative Agreement (CA) team
- Continued to communicate with the Bureau of Reclamation (Reclamation) through emails and phone calls
- Planned quarterly meeting with Reclamation
- Prepared and submitted the annual report for 2012
- Attended the quarterly meeting with Reclamation on March 20 and 21 in Denver
- Submitted minutes from quarterly meeting to all participants and Grants Officer Technical Representative (GOTR)
- Continued to refine needed changes to the CA based on modifications 002, 003, 004
- Continued drafting CA Mod 5 to address changes on quarterly reporting and tracking
- Continued the development of the Collaborative Research Education Program
- Continued monitoring progress on awarded Tier I research
- Prepared and submitted quarterly report for October to December 2012
- Announced Tier 1 call for proposals
- Received one Tier I re-submitted proposal
- Approved One Tier I proposal and obtained GOTR concurrence

- Continued to recruit judges for the International Environmental Design Contest (IEDC)
- Continued planning and coordination for the IEDC

- Continued to address questions/inquiries related to, Reclamation sponsored Task 2 and 3, from committed teams.
- Continued the development of the Collaborative Research Education Program
- Continued discussions and review/development of a path forward with BGNDRF staff for infrastructure development and utilization of the agricultural research area
- Advertised the Water Fellowship to NMSU students in all disciplines
- Received, reviewed and interviewed seven applicants for Water Fellowship
- Awarded five Water Fellowships to the following undergraduate students
 - Rachel Wood
 - Baraka Lwoya
 - Corinne Fox
 - Duy Khanh Nguyen
 - Troy Sculto

PERIOD: APRIL TO JUNE 2013

- Provided the Bureau of Reclamation (Reclamation) Grants Officer Technical Representative (GOTR) with five comprehensive notebooks covering the four areas of the cooperative agreement:
 - Research conducted at or in association with BGNDRF - publications, presentations (oral, poster), thesis (presentation & defense), Tier 1, open solicitation, non-disclosure form, compliance evaluation, technical evaluation, and awards
 - Education - 2011, 2012 and 2013 papers, teams and judges for International Environmental Design Contest. Collaborative Research Education Program which included plan for program, collaborative research partnership, S & T one pager summary for potential collaboration and collaboration on PV/ RO and drought planning. Plan for fellowship program, student fellowship awards and reports.
 - Outreach - El Paso Community college, purpose of class and their funding, syllabus, material for the class, class list and presentations. Conference exhibitions and hand out material for the exhibits.
 - Administration - timeline for proposal development, awards, and modifications. Meetings with Reclamation management of project from the Denver Technical Center. Reclamation RFP on NMSU earmarks FY 2008. Scooping tasks, award and modifications, quarterly and annual reports, and quarterly meeting minutes. Media coverage including signing ceremony articles, news release and photos. Budget expenditure and plan for remaining fund thru September 30, 2015.

- Attended AWWA's ACE13 Annual Conference & Exposition (Abbas, Jim, Roseann, Barbara and Jalal), exhibited a booth jointly with Reclamation and presented the Cooperative Agreement achievements and research conducted at BGNDRF as required by the cooperative agreement, June 9-13, 2013, in Denver, Colorado.

- Graduate students, Leila Karimi and Leili Abkar presented a paper at the ACE13 Conference; and Fattaneh Naderi Behdani, Azadeh Ghorbani, Kwonit Mallick and Rafal Alshukri attended AWWA Conference & Exposition June 9-13, 2013, in Denver, Colorado. The purpose of their attendance was to benefit from the latest research in the field of water and to benefit from networking opportunities with the researchers.

- All six graduate students attending the ACE13 conference also attended the quarterly meeting with Reclamation and presented their research to the group.

- Ten abstracts have been submitted to The World Congress on Petrochemistry and Chemical Engineering to take place in San Antonio, November 18-20, 2013; NMSU/ IEE

is actively involved in this conference chairing a session, and is planning an exhibition booth.

- Eight abstracts have been submitted to AIChE conference to take place in San Francisco, November 3-8, 2013. Our group is going to have a session on water treatment/pretreatment. The title is Desalination and Water Management for Rural Communities. NMSU/IEE is also actively involved in this conference by displaying a booth and chairing a session.
- Presented the following papers:
 - Saeid Aghahosseini Shirazi, Jalal Rastegary, Tracey Fernandez, Abbas Ghassemi. An Innovative Method to Exploit Concentrate Stream of Desalination Units, 17th Annual Water Reuse & Desalination Research Conference, May 6-7, 2013 Phoenix, AZ.
 - Saeid Aghahosseini Shirazi, Jalal Rastegary, Abbas Ghassemi, Tracey Fernandez. Evaluation of Different Sources of Nutrient in Combination with Concentrate Stream of Desalination Unit for Growing Algae, EWRI Congress, May 2013, Cincinnati, Ohio.
 - Myint, M. An Innovative Integrating Design System to Improve the Sustainability of Water Supply in Cities of Arid Regions, 2013 World Environmental & Water Resources Congress, May 19-23, 2013, Cincinnati, OH.
 - Leila Karimi, Abbas Ghassemi, Jim Loya. Performance of Membrane Based Systems such as EDR in Selective Removal of Species at Various Operating Conditions. 17th Annual Water Reuse & Desalination Research Conference, May 6-7, 2013, Phoenix, AZ.
 - Leila Karimi, Leili Abkar, Katherine Guerra, Katharine Dahm, Abbas Ghassemi, Jim Loya. Demonstration of a Hybrid Photovoltaic-reverse Osmosis System for Off-grid Desalination. ACE13 Conference and Exposition, June 11-13 Denver, CO.
 - Jalal Rastegary, Abbas Ghassemi, Saeid Aghahosseini Shirazi, Tracey Fernandez. Using Concentrate from Desalination to Grow Microalgae for Biofuel. 2013 UCOWR/ NIWR Annual Conference, June 11-13, Lake Tahoe, California.
- Conducted the 23rd Annual International Environmental Design Contest April 1-4 2013. Ninety-eight students, representing twenty university teams from twelve schools across the United States participated and competed to solve environmental challenges posed by government and industry professionals in four tasks. IEDC's Reclamation judges recommended that four bench scales solar designs be further evaluated and improved.

- Developed application package and advertised for IEDC Fellowships as follow-up to the contest to take the four selected bench scale solar designs to the next level.
- Selected two internship/fellowship students from Cal Poly San Luis Obispo (Chris Pittner and Yakov Suvorov) to work on four bench scale modules from International Design Contest. The students were chosen by submitting an application that included their ideas on continuing their research. One NMSU Fellowship student was also selected to work alongside the Design Contest Fellowship students (Rachel Wood).
- Continued conference call/meetings with Cooperative Agreement (CA) team.
- Continued to communicate with the Reclamation through emails and phone calls.
- Planned quarterly meeting with Reclamation.
- Attended the quarterly meeting with Reclamation on June 12-13 in Denver.
- Provided details of revised budget and expenditure plan to GOTR.
- Submitted minutes from quarterly meeting to all participants and GOTR.
- Continued to refine needed changes to the CA based on modifications 002, 003, 004.
- Submitted CA Mod 5 to address changes on quarterly reporting and tracking and directed research.
- Continued the development of the Collaborative Research Education Program.
- Continued to work on the PV/RO.
- Continued to work on drought planning.
- Reviewed one Tier I proposal.
- Connor Hanrahan a master student defended his thesis titled “High-Recovery Electrolysis Reversal for Desalination of Inland Brackish water”. Connor’s work was conducted at BGNDRF.
- Continued monitoring progress on awarded Tier I research.
- Prepared and submitted quarterly report for January to March 2013.
- Continued the development of the Collaborative Research Education Program.

- Continued discussions and reviewed/developed a path forward with BGNDRF staff for infrastructure development and utilization of the agricultural research area.
- Advertised the Water Fellowship to NMSU students in all disciplines.
- Received, reviewed and interviewed applicants for Water Fellowship.
- Awarded one Water Fellowship to the following undergraduate student
 - Rachel Wood

PERIOD: JULY TO SEPTEMBER 2013

Administration:

- Continued conference calls/meetings with the Cooperative Agreement (CA) team.
- Continued to communicate with the Bureau of Reclamation (Reclamation) through emails and phone calls.
- Planned quarterly meeting with Reclamation.
- Continued the development of the Collaborative Research Education Program.
- Submitted meeting minutes from Quarterly meeting in Denver.
- Prepared and submitted quarterly report for April to June 2013.
- Continued to monitor progress on awarded Tier I research.
- Continued the development of the new research education fellowship programs for graduate students.
- Continued to update and refine website.
- Continued to refine equipment needs list for laboratory and AG area at BGNDRF.
- Participated in conference calls related to the development of BGNDRF AG area as requested.
- Announced Tier1 call for proposals for 4th quarter review.
- Received two Tier1 proposals to be reviewed 4th quarter.
- Awarded funding for one Tier 1 project to Manoj Shukla, a faculty member of the College of Agricultural, Consumer and Environmental Sciences.
- Attended the quarterly meeting with Reclamation on September 19 and 20 in Denver, Colorado.

Education:

- Worked with Reclamation to develop and refine two tasks for Design Contest (DC) 2014.
- Posted DC tasks to the web.
- Began answering questions from potential DC teams.
- Conducted weekly meetings with design contest fellowship students Chris Pittner and Jacob Suvorov. The faculty and staff at the meetings included Abbas Ghassemi, Jim Loya, Jalal Rastegary, and Roseann Thompson. Students presented their research and got feedback from the group on how to proceed and make improvements to their work.
- Conducted weekly meetings with seventeen Ph.D. and master's students. Each week three students gave PowerPoint presentations on their progress; the other students discussed their own progress and acquired feedback and answers to any questions they had.
- Received and reviewed applications for Graduate Research Education Fellowships.
- Awarded Graduate Research Education Fellowships to the following three students:
 - Nasser Khazeni,
 - Leila Karimi, and
 - Racheal Jones.
- The following Ph.D. and Master's students are supported by BOR:
 - Abkar Leili, first year Ph.D.
 - Saeid Aghahosseini Shirazi, second year Master's
 - Rafal Alshukri, first year Master's
 - Navid Attarzadeh, first year Ph.D.
 - Waddah Hussein, second year Master's
 - Jaber Masoume, first year Master's
 - Racheal Jones, second year Master's
 - Leila Karimi, second year Ph.D.
 - Kwonit Mallick, second year Masters

Research

Tier 1 Quarterly Report

1. **“Consequences and Possible Solutions for Small Scale Saline Water Residue Disposal in New Mexico” (Full Report Attached in Appendix C)**
 - Original PI: Dr. Blair Stringam
 - Current PI: Dr. Blair Stringam
 - Graduate Student: Jesus Sigala
 - Start date and anticipated completion date
 - Start Date: February 1, 2011
 - Anticipated Completion Date: December 30, 2013

- Work conducted during the reporting period:
 - o Collected and analyzed data.
- Significant accomplishments during the reporting period:
 - o Data were collected and analyzed.
- Unanticipated delays during the reporting period:
 - o The saline injection system has suffered breakdowns which have been troublesome but repairable.
 - o Original bacterial analysis of the effluent water provided only a general understanding of the effect of saline water on bacterial. A DNA analysis method that is more sensitive to these bacteria strains will be used instead.
- Progress of spending in the task:
 - o 79.2% of the original \$49,982.00 budget was spent as of September 30, 2013. \$10,404.90 of the budget remains.
- Comparison of actual spending to planned spending:
 - o Actual spending closely matches planned spending.
- Schedule discussion:
 - o Although the aforementioned unexpected delays have pushed the project over schedule, the project is on track to meet its goals within the no cost extension.

2. “Developing a Biotechnology with a Reactor to Grow Microalgae for Biodiesel Production from Reusing Waste Concentrate and Anaerobic Digested Sludge” (Full Report Attached in Appendix D)

- Original PI: Dr. Maung Thein Myint
- Current PI: Dr. Jalal Rastegary
- Graduate Student: Waddah Hussein
- Start date and anticipated completion date
 - o Start Date: February 1, 2011
 - o Anticipated Completion Date: December 31, 2013
- Work conducted during the reporting period:
 - o Three species of microalgae – *Dunaliella salina*, *Spirulina platensis*, and an unknown species of microalgae from the desalination concentrate pond at the Brackish Groundwater National Desalination Research Facility – were grown in different ratios of anaerobic digested sludge (ADS) and concentrate from electro dialysis reversal (EDR).
 - o After algae growth, levels of total dissolved salts in the ADS and EDR concentrate were evaluated and compared to initial levels.
- Significant accomplishments during the reporting period:

- All three microalgae species were grown successfully using anaerobic digested sludge, improving the net energy gain in algae biodiesel as compared to the growth of algae using brackish water and Bold's Basal Medium.
 - Algae growth in ADS and EDR concentrate significantly reduced the levels of TDS in these media, improving water quality.
 - Unanticipated delays during the reporting period:
 - There were no unanticipated delays during the reporting period.
 - What is the progress of spending in the task?
 - 96.5% of the original \$49,980.00 budget was spent as of September 30, 2013. \$1,737.20 of the budget remains.
 - Comparison of actual spending to planned spending:
 - Actual spending closely matches planned spending
 - Schedule discussion:
 - The research has been finished, and the student is writing his thesis. The project is on track to meet its goals within the no cost extension.
3. **“Primary Evaluation of Algae Biofuel Production from Concentrate Stream” (Full Report Attached in Appendix E)**
- Original PI: Dr. Jalal Rastegary
 - Current PI: Dr. Jalal Rastegary
 - Graduate Student: Saeid Aghahosseini Shirazi
 - Undergraduate Student: Tracey Fernandez
 - Start date and anticipated completion date:
 - Start Date: January 1, 2012
 - Anticipated Completion Date: July 1, 2014
 - Work conducted during the reporting period:
 - All experiments were conducted.
 - Significant accomplishments during the reporting period:
 - Data were collected and analyzed, and 2 abstracts were presented at conferences.
 - Unanticipated delays during the reporting period:
 - There were no unanticipated delays during the reporting period.
 - What is the progress of spending in the task?
 - 100% of the original budget of \$49,999.11 had been spent as of September 30, 2013.
 - Comparison of actual spending to planned spending :
 - The budget has been spent, and the planned work has been completed.
 - Schedule discussion:
 - The project is on track to meet its goals within the no cost extension.

4. “Investigating and Understanding the Selectivity of Conventional Ion-Exchange Membranes Used in Electrodialysis Process” (Full Report Attached in Appendix F)

- Original PI: Dr. Ali Sharbat
- Current PI: Dr. Jalal Rastegary
- Graduate Student: Leila Karimi
- Undergraduate Student: Virginia Veruette-Maya
- Start date and anticipated completion date
 - o Start Date: January 1, 2012
 - o Anticipated Completion Date: July 1, 2014
- Work conducted during the reporting period:
 - o Designed data acquisition system.
 - o Selected variables.
 - o Selected and purchased sensors.
 - o Began set-up.
 - o Designed pilot-scale experiments.
 - o Conducted pilot-scale experiments.
 - o Collected and analyzed water samples.
- Significant accomplishments during the reporting period:
 - o The most significant accomplishments during this period were designing the data acquisition system and selecting sensitive sensors with high accuracy that makes the operating variable monitoring and recording during the experiments possible.
- Unanticipated delays during the reporting period:
 - o There were some delays in purchasing the data acquisition parts and laboratory scale electro dialyzer. Designing and purchasing the data acquisition parts as well as laboratory-scale electro dialyzer took much more time than anticipated.
- Progress of spending in the task:
 - o 98.1% of the original budget of \$49,996.63 had been spent as of September 30, 2013. \$927.36 remained.
- Comparison of actual spending to planned spending:
 - o Because of unexpectedly high time demands for designing the data acquisition system and acquiring the necessary sensors, salary is over budget and equipment is under budget.
- Schedule discussion:
 - o The activities are on schedule to be completed by the end of June, so the project is on track to meet its goals within the no cost extension.

5. “Optimization of Electrode Design for Electrodialysis Reversal”

- Original PIs: Dr. Ali Sharbat and Dr. Neil Moe
- Current PI: Dr. Jalal Rastegary

- Start date and anticipated completion date:
 - o Start Date: August 22, 2011
 - o Anticipated Completion Date: August 1, 2014
- Work conducted during the reporting period:
 - o The work has been delayed until the availability of a qualified student to travel to BGNDRF on regular basis. We are in the process of hiring a student who can reside in Alamogordo and do the work.
- Progress of spending in the task:
 - o 10.3% of the original \$49,999.00 had been spent as of September 30, 2013. \$44,827.39 of the budget remains.
- Comparison of actual spending to planned spending:
 - o Actual spending is lower than planned spending because of the delay in finding a qualified student to work at BGNDRF.
- Schedule:
 - o We are in the process of hiring a student, and anticipate that the project will meet its goals within the no cost extension.

6. “Desalination Concentrate Management for Sustainable Agriculture: A Preliminary Study on Transport Behavior and Plant Viability at BGNDRF” (Full Report Attached in Appendix G)

- Original PIs: Dr. Manoi Shukla
- Current PI: Dr. Manoi Shukla
- Start date and anticipated completion date:
 - o Start Date: August 1, 2013
 - o Anticipated Completion Date: July 31, 2014
- Work conducted during the reporting period:
 - o Gathered baseline soil analysis data for BGNDRF
- Significant accomplishments during the reporting period:
 - o Determined soil bulk density, hydraulic conductivity, soil water characteristic, particle size distribution, and EC and SAR at the BGNDRF site.
- Unanticipated delays during the reporting period:
 - o There were no unanticipated delays during this reporting period.
- Progress of spending in the task:
 - o 3.3% of the original budget of \$49,874.71 had been spent as of September 30, 2013. \$48,247 of the budget remains.
- Comparison of actual spending to planned spending:
 - o Actual spending matches planned spending. As per the proposed requirement, loose and core samples were collected from BGNDRF site and soil bulk density, hydraulic conductivity, soil water

characteristic, particle size distribution, and EC and SAR were determined prior to the start of the project.

- Schedule discussion:
 - o The activities are on schedule to meet the expected completion date.

Algae Biomass Summit

- Presented the following poster to the Algae Biomass Summit, held September 30-October 3, 2013 in Orlando, Florida:
 - o “*Algae Biofuel Production and Concentrate Management in Inland Brackish Water Desalination.*” Jalal Rastegary, Saeid Aghahosseini Shirazi, Abbas Ghassemi, Tracey Fernandez. (Attachment 1)

Graduate Research

- Three graduate students (Nasser Khazeni, Pedram Mohrdar and Mohammad Tanhaemami) presented their research to the Denver Reclamation group, as did two undergraduate International Environmental Design Contest fellowship students (Yakov Suvorov and Chris Pittner). (Abstracts in attachments 2-5, Presentations in Appendices I, J, K, and L)
- The following abstracts were prepared submitted and accepted for various conferences: (Abstract attachments 6-36)

- o **1-2013 AIChE Annual Meeting**

Oral Acceptance:

Leili Abkar, Kwonit Mallick, Rafal Alshukri, Abbas Ghassemi and James Loya, Solar-Powered Reverse Osmosis Technology for Brackish Water: The State of The Art.

Ghazaleh Vaseghi, Abbas Ghassemi and James Loya, RO/NF Applications in Brackish Groundwater Desalination: Membrane Characterization.

Leili Abkar, Abbas Ghassemi and James Loya, Investigating the Effective Parameters in Optimizing Reverse Osmosis Technology for Water Treatment

Fattaneh Naderi Behdani, Abbas Ghassemi and James Loya, Impact of Silica in Water Treatment Technology.

Leila Karimi, Azadeh Ghorbani, Abbas Ghassemi and Jim Loya, Selectivity Comparison for Two Cation Exchange Membranes in the Electrodialysis Process.

Azadeh Ghorbani, Leila Karimi, Abbas Ghassemi and James Loya, Developing a Mechanistic Transport Model for Electrodialysis/Electrodialysis Reversal Process

Saeid Aghahosseini Shirazi, Alireza Saraeian, Jalal Rastegary and Abbas Ghassemi, a Novel Method to Manage the Concentrate Disposal of Desalination Units.

Poster Acceptance:

Nasser Khazeni, Meitham Naeem, Abbas Ghassemi, Carbonation of Metal Oxide Nanoparticles Caged in MOF Structure

○ **2-World Congress on Petrochemistry and Chemical Engineering**

Oral Acceptance:

Leili Abkar, Different approaches on energy optimization in reverse osmosis desalination plant.

Pedram Mohrdar Ghaemmaghami, Review on aqueous lithium Li-ion battery.

Nasser Khazeni, Utilization of metal organic frameworks in order to encapsulate greenhouse gas to address water availability and drought

Kwonit Mallick, Optimization of pilot scale photovoltaic reverse osmosis desalination system for ground water.

Azadeh Ghorbani, Developing a mechanistic transport model for electro dialysis reversal process.

Waddah Hussein, Using concentrate from desalination and reusing anaerobic digested sludge to grow algae.

Saeid Aghahosseini Shirazi, Innovative method of using brine water to produce energy.

Leila Karimi, The effect of feed water composition in selective removal of ions in electro dialysis process.

Fattaneh Naderi Behdani, Overview of produced water treatment technologies.

○ **3-58th Annual New Mexico Water Conference**

Poster Acceptance:

Racheal Jones, Kenneth C. Carroll, Michelle Chapman, Mick O'Neill, and Alexander G. Fernald, "Estimating available saline water resources in aquifers of New Mexico using GIS", November 21-22, 2013 Albuquerque, NM

Leili Abkar, Abbas Ghassemi, James Loya. "Optimization Techniques in The Membrane Based Desalination Technologies" 58th Annual New Mexico Water Conference, November 21-22, 2013 Albuquerque, NM

○ **4- AWWA/AMTA 2014 Membrane Technology**

Leili Abkar, Rafal Alshukri, Professor Abbas Ghassemi, James Loya, K. Guerra, Membrane operation and design for renewable energy powered desalination systems

Leili Abkar, Professor Abbas Ghassemi, James Loya, Optimize design and configuration of BWRO under different feed water quality

Fattaneh Naderi Behdani, EDR vs. RO: Silica (AMTA)

Kwonit Mallick, Rafal Alshukri, Jim Loya, Abbas Ghassemi, Performance evaluation of reverse osmosis desalination unit for removing chlorine salts from brackish water

Waddah Hussein, Production of Dunaliella Salina and Spirulina Platensis by Reusing Desalination Concentrate to Improve Sustainability of Inland Desalination

Saeid Aghahosseini Shirazi, Concentrate Management Using Microalgae

○ **5- EWRI World Environmental & Water Resources Congress 2014**

Jalal Rastegary, Abbas Ghassemi, Saeid A. Shirazi, Tracey Fernandez, New Approach to Concentrate Management of Inland Desalination

- Leila Karimi, Leili Abkar, Abbas Ghassemi, James Loya, Study of Technical Feasibility of PVEDR and PVRO Desalination in Remote Rural Areas in New Mexico"

○ **6- ACE 2014**

Leili Abkar, Leila Karimi, Abbas Ghassemi, James Loya, Investigation of Economic Feasibility of PVEDR and PVRO Desalination to produce drinking water

○ **7- ACS 2014**

Navid Attarzadeh, Power Efficiency Enhancement of Vacuum-Deposited Organic Solar Cell based on Fluorine molecules via Thermal Post-Annealing

○ **8- Pacific Rim Summit on Industrial Biotechnology and Bioenergy**

Jalal Rastegary, Tracey Fernandez, Abbas Ghassemi, Assessment of Water Use for Microalgae in Open Pond in Southwest USA

○ **9- 2013 Industrial Water Reuse Specialty Conference**

Jalal Rastegary, Abbas Ghassemi, Saeid A. Shirazi, Tracey Fernandez, Concentrate Stream to Green Energy

○ **Outreach:**

Graduate students Nasser Khazeni and Navid Attarzadeh attended the 246th ACS National Meeting & Exposition from September 8-12, 2013 at the Indiana Convention Center in Indianapolis, Indiana. The purpose of their attendance was to expand their ongoing research in energy and water, based on emerging developments. Since Navid is conducting research in photovoltaic solar cells and Nasser is working on the application of PSM to improve CO₂ capture, the various sessions, presentations, and innovations have the potential to further their work.

Ph.D. students Leila Karimi and Leili Abkar presented their research on desalination to the public via the Las Cruces Sun-News. For the full article, see “NMSU brackish water research could save money, prevent pollution,” attached as Appendix A.

Graduate and undergraduate students presented their research findings on desalination using conventional and renewable energy sources to Senator Martin Heinrich during his visit to the BGNDRF on July 12, 2013. For an article on Senator Heinrich’s visit, see “Senator’s visit,” attached as Appendix B.

Appendix A: "NMSU brackish water research could save money, prevent pollution"

NMSU brackish water treatment research could save money, prevent pollution - Las Cruces Sun-News

10/24/2013



LAS CRUCES SUN-NEWS LAS CRUCES NEWS

Weather: LAS CRUCES, NM | Now: 74°F | High: 78°F | Low: 50°F | 5-Day Forecast

Subscribe | Customer Care

Search Site

News Sports Business Entertainment Lifestyle Opinion Obituaries Special Sections Marketplace Tools

HOT TOPICS: Public Salary Domenici Public Policy Conference ObamaCare National Politics Same-sex marriage

Print Email

NMSU brackish water treatment research could save money, prevent pollution

By Emily C. Kelley

ekelley@nmsu.edu

POSTED: 09/29/2013 04:36:29 PM MDT



Courtesy photo by Emily C. Kelley Lela Korink, Ph.D. candidate in NMSU's Institute for Energy and the Environment, adjusts the outlet differential pressure on a machine used for brackish water research at Brackish Groundwater National Desalination Research Facility in Alamogordo.

DISCOUNTS ON ENERGY SAVING BULBS FOR NEW MEXICO RESIDENTS!

[CLICK FOR DETAILS!](#)

THE FLEXIBLE WAY TO SAVE.

www.theeducationplan.com

The 529 College Savings Plan sponsored by New Mexico.

[>](#)



LAS CRUCES -- Standing outside on a hot New Mexico day, you're likely to be unable to escape the sun, and unlikely to find water. Two New Mexico State University researchers are working on a sustainable, cost effective and environmentally friendly method of meeting the most basic of human needs in the Desert Southwest, fresh water, using our most abundant energy resource, the sun.

Their work at the Brackish Groundwater National Desalination Research Facility in Alamogordo,

NMSU brackish water treatment research could save money, prevent pollution - Las Cruces Sun-News 10/24/2013

is exploring which technology -- photovoltaic reverse osmosis or photovoltaic electro dialysis -- both methods of making brackish water safe for human consumption, is most effective with the specific type of brackish water found in this area, and is the most energy efficient.

The goal of the research is to help solve the water scarcity problem experienced by many in the Desert Southwest, using renewable energy resources, rather than fossil fuels, but the findings of their research could potentially help others in remote parts of the world, too.

Leila Karimi, a chemical engineering Ph.D. candidate working at the Institute for Energy and the Environment, part of NMSU's Department of Chemical Engineering, is focusing on studying the electro dialysis reversal process, while Leili Abkar, a chemical engineering Ph.D. student also working at IEE, is studying reverse osmosis.

"The water emergency situation is certainly alarming," Karimi said. "Almost one-fourth of people around the world are suffering from fresh water scarcity. Desalination can be considered a good solution for this problem, but any desalination process requires huge resources of energy. Conventional desalination technologies rely more on fossil fuels, while the required energy can be provided with renewable energy resources such as solar, wind or geothermal. We are focusing on using solar energy to power electro dialysis and reverse osmosis in off-grid, remote areas that have brackish water resources."

Many people are unaware that the southwestern region of the United States has vast resources of brackish water underground. The water is saline, or salty, which must be converted to fresh water to be consumed by humans, though it is much lower in salinity than seawater. Desalination processes require a large amount of energy; in an area where one of our most abundant natural resources is the sun, harnessing the sun's energy to render brackish water usable makes sense.

The two main groups of desalination technologies are thermal and membrane-based desalination. In thermal desalination, the heat produced by fossil fuels powers the desalination processes, and is the driving force for separating salt from water. In membrane-based separation processes, there are two main types of desalination, pressure-driven or electrically driven. Reverse osmosis is pressure-driven and electro dialysis is electrically driven.

Both processes produce fresh, desalted, drinkable water.

In conventional desalination methods, energy sources come from fossil fuels. Karimi and Abkar are studying the use of renewable energy sources instead, as they don't have the adverse environmental impacts fossil fuels have, such as releasing greenhouse gases like carbon dioxide. And, solar energy is free, once the technology to harvest and store it is in place.

"We have a huge source of solar energy here and high solar insulation," Karimi said. "We can utilize this free energy to power the desalination processes we need."

"In the Middle East, they use thermal desalination technologies because they have abundant resources of fossil fuel and because it is cheap for them," Abkar said. "We're comparing brackish water reverse osmosis with electro dialysis reversal to see which one of them, in this condition, with this salinity that we have here, is more effective."

The two researchers hope to design a better system for remote, rural areas because the final goal is finding a feasible and economical process for remote areas where people are suffering from fresh water shortages, and also don't have access to electricity.

"By finding more feasible desalination processes for different saline water qualities and renewable energy resources, we can provide water for people in remote, off-grid areas at a lower cost and in a sustainable way," Karimi said.

"Many people around the world face water scarcity and fossil fuel is an increasingly very important resource nowadays," Abkar said. "When we are using fossil fuel, we have emissions, and one of the consequences is global warming and climate change."

Photovoltaic power in sun-drenched New Mexico could be the solution.

"The desalination group at New Mexico State University would like to be able to provide new water resources for people, especially people suffering from water scarcity," Karimi added. "Water is a basic human right, so it's everyone's right to have access to it."

Karimi and Abkar expect their experimentation at the Brackish Groundwater National Desalination Research Facility to wrap up in October, and plan to publish findings of their research later this academic year.

"Eye on Research" is a weekly feature provided by New Mexico State University. This week's feature was written by Emily C. Kelley of University Communications.

Print Email Return to Top

RELATED

Southwest Fright Night haunts Las Cruces starting Friday

NM Supreme Court hears arguments on same-sex marriage

Halloween masks, face paint not allowed in stores

http://www.lcsun-news.com/las_cruces-news/ci_24202251/nmsu-brackish-water-treatment-research-could-save-money?

2 / 4

<p>Dr. Oz Weight Loss Trick Magic diet pill has people melting fat away fast. www.healthtrendsguide.com</p>	<p>Marriotti We're Not Idea at a Travel-Bill</p>
---	--

Add a comment...

Vernon Albert · University of Oregon
 What happens to the waste water. Do they eva
 Reply · Like · October 12 at 7:17am

Facebook social plugin

27
 Like

Las Cruces Local Guide

Featured Businesses

Big Lots

Find Las Cruces Attractions

Search for a business


Search by keyword or Zip

Add your business here +

Appendix B: “Senator’s visit”

Institute for Energy & the Environment — Senator's visit — New Mexico State University

10/24/2013


New Mexico State University

Home

College of Engineering

Login

Institute for Energy & the Environment

Energy, Environment, Renewable Resources

NMSU → [Institute for Energy & the Environment](#) → [Senator's visit](#)


Senator's visit

Senator Martin Heinrich visited the Brackish Groundwater National Desalination Research Facility to present the Better Buildings Federal Award to the facility past July 12, 2013.


During this visit, IEE faculty, staff and students had the opportunity to speak with the senator and present various programs.

- Graduate students do part of their water treatment, alternative energy and desalination research on this facility.
- Design contest interns showed their work and improvements on four of the projects that were presented in the design contest. These projects include a basin solar distillation created by the University of Maryland, a double parabolic trough distillation by Ohio University, a nitrate removal unit built by the University of Idaho and a combined parabolic and basin distillation project created by the California Polytechnic University-San Luis Obispo.

“It was a really good opportunity for my research team and I to be able to present our projects to the senator,” said Rachel Wood, an intern, “This was a great time to show that the ability to do research on such applications of our field can make breakthroughs to sustainable alternatives in the water-energy nexus.”



The interns showing their work to Senator Heinrich.



Graduate students at the Brackish Groundwater National Desalination Research Facility.

Published: July 25, 2013 • Updated: July 25, 2013 • Categories: [Uncategorized](#) • [Permalink](#)



Appendix C:

1. Consequences and Possible Solutions for Small Scale Saline Water Residue Disposal in New Mexico – Proof of Concept

PI – Dr. Blair Stringam – Associate Professor in Plant and Environmental Sciences, New Mexico State University

2. Award # 605771 / 118543 WATER RESIDUE DISPOSAL IN NM

3. Report period: August, 2013 to October, 2013.

4. Students involved in Project.

David Gamon, hourly employee, Male, Hispanic, dgamon@nmsu.edu

Jesus Sigala, hourly employee, former graduate Environmental Science student, Male, Hispanic

5. A comparison of the actual accomplishments with the goals and objectives established for the period and reasons why the established goals were not met. (see part 6)

Table 1. Project Schedule

MONTH

Tasks/Subtasks	1	2	6	7	8	9	10	11	12	13	14	15	16	17	18	19	20	21	22	23	24	25	26	27	28	29	30	31	32	33
1.) Detailed Literature review																														
2.) Select individual septic system																														
3.) Install septic apparatus									X																					
4.) Collect baseline data									X																					
5.) Collect and analyze data								X	X	X	X	X	X	X	X	X	X	X	X	X	X	X	X	X	X	X	X	X	X	
6.) Restore Septic system																														X
7.) Summary of results																														X
8.) Summary of treatment and disposal options																														X
3																														
4 Final Report																														X

6. We have been continuing to inject saline water into the leach field at critical times of the day. We have had some difficulty with the injection system, but we have been able to repair the breakdowns that have occurred. While the breakdowns have been troublesome, they have been repairable and we have had to

be very careful about managing the injection system. We will be continuing to inject water into the leach field.

We have tried to conduct bacterial analysis of the effluent water and discovered that the results provided only a general understanding of the effect of saline water on bacteria. There are numerous bacteria strains that live in a septic system and it is reasonable to assume that saline water will have different effects on these various strains. We have recently learned about a DNA analysis method that is more sensitive to the various bacteria strains. The no cost extension that was just granted to us will help us determine the effects of saline water on the various bacteria that live in a septic system.

7. Cost Status. Show approved budget by budget period and actual costs incurred.

Cost sharing - break out by recipient share, and total costs.

Category	Budgeted from start to end of this reporting period	Spent to Date	Anticipated Spending Next Quarter	Total Budgeted
Salaries	\$30,825	\$25,438.00	\$5,387	
Fringe Benefits	\$925	\$763	\$162	
Travel	\$2,400	\$311	\$250	
Supplies/Materials	\$2,400	\$350	\$2,050	
Services	\$3,040	\$2,073.18	\$1,000	
Subcontract	\$750	\$175		
Equipment				
IDC	\$9,642	\$6,643.72	\$1,649.00	
Total	\$49,982	\$34,433.90	\$10,498.00	
COST SHARE				
Salaries		\$800	\$2,400	
Fringe Benefits				
Travel		\$276		
Supplies/Materials		\$1141		
Services		\$325	\$2,000	
Equipment				
IDC				
Total		\$1,642	\$4,400	

8. There are no changes in the approach or aims of this project so far.

9. We have been injecting saline effluent into the leach field.

10. A summer student has been assisting with the project this quarter in addition Jesus Sigala has been working on the project. Jesus has been helping prepare samples for DNA analysis.

11. A description of any product produced or technology transfer activities accomplished during this reporting period, such as:

- a. There are no Publications at this time.
- b. There is no web site or other internet site that reflects results of this project.

- c. No collaborative work has occurred this quarter.
- d. No Technologies/Techniques at this time.
- e. No Inventions/Patent applications at this time.
- f. No additional products at this time.

Appendix D:

1. Project Title
Concentrate Management: Developing *A Biotechnology With A Reactor To Grow Microalgae For Biodiesel From Reusing Waste Concentrate And Anaerobic Digested Sludge*

Name of project principal investigator: Dr. Abbas Ghassemi/ Maung Thein Myint
Contact information: Institute for Energy and the Environment, MSC WERC,
P.O Box 30001, New Mexico State University,
Las Cruces, NM 88001,
Telephone (575) 646 2073; Fax (575) 646 5474

2. Award #: 605770/118542
3. Date of report and period covered by report: Nov 05, 2012; sixth quarter report: July 2012 to Sep 2012
4. Students involved in Project.

Name: Waddah Hussein
Classification: MS graduate student
Gender: Male
Ethnicity: Iraq
Race: Arabic
Disability: No
e-mail: waddahzh@nmsu.edu

- A comparison of the actual accomplishments with the goals and objectives established for the period and reasons why the established goals were not met.

(1a) The *first species*: MONOR2 were not available from the University of Texas at Austin (UT) and New Mexico State University (NMSU) Laboratories. The seed from Brackish Groundwater National Desalination Research Facility (BGNDRF) were replaced as the first species. The seeded microalgae from the evaporation pond at BGNDRF were grown in four cylinder (C1, C2, C3, and C4) and four rectangular reactors (R1, R2, R3, and R4) from Oct 03 to Nov 04, 2011. Reactors C1, C2, R1, and R1 were supplied with anaerobic digested sludge (ADS) as nutrients and Reactors C3, C4, R3, and R4 with Bold's Basal Medium (BBM) as nutrients. The conductivity of cultures in Reactors C1, C2, C3, C4, R1, R2, R3, and R4 are 36,400; 25,900; 30200; 25,900; 30900; 26,500; 30,900; 26,300 $\mu\text{S}/\text{cm}$ respectively. The maximum dry weight of microalgae achieved in Reactors C1, C2, C3, C4, R1, R2, R3, and R4 are 1.36; 1.31; 1.03; 0.95; 1.64; 1.70; 1.34; 1.39 g/L respectively. The dry weight data shows that BGNDRF species grows well in both of the nutrients (ADS and BBM). It can be concluded that there is potential for ADS to replace the BBM, which is energy-dependant nutrient, while ADS is a free resource from waste water treatment plant (WWTP). The highest microalgae biomass concentration achieved is 1.70 g/L in our first study.

The BGNDRF species were tested in the higher conductivity concentrate with the conductivity of 24,000; 30,250; 40,500; 49,200; 59,800 $\mu\text{S}/\text{cm}$ in R1, R2, R3, R4, and R5 during Feb 14, 2012 to Apr 24 2012 by using supernatant from centrifuged ADS. The maximum dry weight of microalgae achieved in Reactors R1, R2, R3, R4, R5, and R6 are 2.17; 1.51; 1.43; 1.15; 1.08 g/L respectively. The highest microalgae biomass concentration achieved is 2.17 g/L in our second study. From our secondary study, it can be concluded that microalgae biomass grow well in the higher conductivity from 24,000 to 59800 $\mu\text{S}/\text{cm}$ with the nutrients from supernatant of ADS.

From our studies, the BGNDRF species was found to have ability to degrade total dissolved solid (TDS) from desalination concentrate and supernatant from ADS. From our second studies, it was found that the maximal TDS removal percentages are 61.3 (stdev 3.5), 62 (stdev 3.7), 57.4 (stdev 2.6), 53.3 (stdev 7.0), and 54.4 (stdev 6.7) % from the initial desalination concentrates of 24000, 30250, 40500, 49200, and 59800 $\mu\text{S}/\text{cm}$. These maximal TDS removal percentages were continued to test with leachate from compost from Aug 2012.

(1b) A poster presentation titled “Culturing Microalgae from Desalination Concentrate Reusing Anaerobic Digested Sludge as Nutrient to Improve the Net Energy Ratio” was presented at the Water Resource Research Institute (WRI) and Bureau of Reclamation’s New Water New Energy Conference by Waddah Hussein on December 13-14, 2011 in Alamogordo, NM. Waddah Hussein plans to present this poster presentation.

(1c) A poster presentation titled “Seed Microalgae from Concentrate of Evaporation Pond in Different Conductivities” was presented by Waddah Hussein in AWWA/AMTA 2012 Membrane Technology Conference on Feb 27-Mar01, 2012 Glendale, AZ.

(2) The second species: *Dunaliella salina* were donated by Tracy Fernandez of the Institute for Energy and the Environment (IEE), NMSU and seeded in two reactors – reactor 1 was supplied with supernatant from ADS and reactor 2 with BBM. The seeded microalgae are being grown in four cylinder (C1, C2, C3, and C4) and four rectangular reactors (R1, R2, R3, and R4). Reactors C1, C2, R1, and R2 were supplied with supernatant from ADS as nutrients and Reactors C3, C4, R3, and R4 with BBM as nutrients. The experiment was conducted during the third week of December 2011.

The second species *Dunaliella salina* were tested in our second studies with leachate from compost (dry anaerobic digested sludge) as nutrients. This test was started from June 2012. [The total dissolved solid removal rates were tested with *D. salina* from Aug 2012.](#)

(3) The third species: The seed for *spirulina plaensis* were ordered from UT at Austin on October6, 2011 and arrived to IEE/NMSU during the third-week of December 2011. The pretreatment was done for this species from the third-week of December 2011. The species were grown with nutrient from ADS between Jan 2012 to Feb 2012.

(4) Based on the literature review of this work, the first and second articles “Complete Sustainability in Electrodialysis Reversal Desalination: Reuse Tertiary Treated Municipal Wastewater as Feed in the Concentrate Stream and Electrodes Rinsing Water”; “Electrodialysis Reversal Desalination: Monographs for the Design Parameters” [were accepted for publication in Desalination and Water Treatment.](#)

(5) Another article “A Generic Stoichiometric Equation for Microalgae-bacteria Nexus by Reusing Clarified Domestic Wastewater as [Growth Medium](#)” has written with [100% done for the first draft.](#)

(6) Based on the experimental data from the first species, the [fourth article](#) “Develop a BGDRF Microalgae Species from Desalination Evaporation Pond” was partially (45%) written.

(7) A proposal “Development of a Microalgae Species from Cattle Manure Leachate Evaporation Pond to Convert Cattle Manure Solid Waste into Microalgae for Biodiesel and Green Feedstock for Cattle Reusing Concentrate from Desalination” was submitted to Environmental Research and Education Foundation by Engineering Research Center at Jan 05, 2012.

(8) July 31 2012: An abstract “Microalgae Production By reusing Desalination concentrate as Water Media and Supernatant from Anaerobic Digested Sludge” was submitted to Water Research for publication.

(9) A poster titled “Concentrate from desalination is good for microalgae growth” [presented at Bi-national Border Water Resources Summit, UTEP, El Paso, TX at Sep 28, 2012.](#)

(10) Oct 29, 2012: "An Innovative Integrating Design Systems to Improve the Sustainability of Water Supply in Cities of Arid Region" have been accepted in oral presentation in 2013 World Environmental & Water Resources Congress at Cincinnati, OH, USA, May 19-23, 2013.

Table 1. Project Schedule

Tasks / Number of month	2011			2012												2013													
	Ju	A	S	O	N	D	Ja	F	M	A	M	Ju	Ju	A	S	O	N	D	Ja	F	M	A	M	Ju	Ju	A			
1. Seeding microalgae from concentrate of desalination evaporation pond with chemical nutrients	■	■	■																										
2. Growing microalgae (BGNDRF species) from concentrate of desalination evaporation pond with chemical nutrients in 4 reactors and anaerobic digested sludge in 4 reactors			■	■																									
3. Seeding Dunaliella salina from concentrate of desalination evaporation pond with ADS as nutrients in first reactor and BBM digested sludge in the second reactors					■																								
4. Growing Dunaliella salina from concentrate of desalination evaporation pond with chemical nutrients in 4 reactors and anaerobic digested sludge in 4 reactors							■	■																					
5. Seeding Spirulina plaensis from concentrate of desalination evaporation pond with ADS as nutrients in first reactor and BBM digested sludge in the second reactors									■	■																			
6. Growing Spirulina plaensis from concentrate of desalination evaporation pond with chemical nutrients in 4 reactors and anaerobic digested sludge in 4 reactors										■	■																		
7. Reviewing the growth for (a) BGNDRF species (b) D. Salina species (c) Spirulina plaensis										■	■	■	■	■	■	■	■	■	■	■	■	■	■	■	■	■	■	■	■
7. Analysis										■	■	■	■	■	■	■	■	■	■	■	■	■	■	■	■	■	■	■	■
8. Report	■		■			■	■			■	■			■	■	■	■	■	■	■	■	■	■	■	■	■	■	■	■
9. Publication/ thesis																													
10. Conference																													
11. Proposal based on this seed grant																													

■ Done
 □ Schedule to be performed

5. A discussion of what was accomplished under these goals during this reporting period, including major activities, significant results, major findings or conclusions, key outcomes or other achievements. *This section should not contain any proprietary data or other information not subject to public release.* If such information is important to reporting progress, do not include the information, but include a note in the report advising the reader to contact the Principal Investigator for further information.

The first research found that concentrate from desalination (20,000-24,000 µS/cm) can grow microalgae (BGNDRF species and *D. Salina*) very well (1.25-1.5 g/L dry weight) with the nutrients from supernatant of anaerobic digested sludge from wastewater treatment plant without any energy-dependant nutrients. The secondary research data show that concentrate from desalination (24,000; 30,250; 40,500; 49,200; 59,800 µS/cm) can grow microalgae (BGNDRF species) very well with the maximum dry weight of 2.17; 1.51; 1.43; 1.15; 1.08 g/L respectively with the nutrients from supernatant of anaerobic digested sludge from wastewater treatment plant without any energy-dependant nutrients.

6. Cost Status. Show approved budget by budget period and actual costs incurred.
Cost sharing - break out by recipient share, and total costs.

Category	Budgeted from start to end of this reporting period	Spent to Date	Anticipated Spending Next Quarter	Total Budgeted
Salaries	3160	24,959	5925	27,883
Fringe Benefits	95	803	95	809
Travel	0	150	0	387
Supplies/Materials	1079	3824	1079	11,261
Services	NA	125	NA	NA
Subcontract	NA	NA	NA	NA
Equipment	NA	NA	NA	NA
IDC	1036	6141	1036	9,641
Total	5370	36,002	8135	49,980
COST SHARE				
Salaries	NA	NA	NA	NA
Fringe Benefits	NA	NA	NA	NA
Travel	NA	NA	NA	NA
Supplies/Materials	NA	NA	NA	NA
Services	NA	NA	NA	NA
Equipment	NA	NA	NA	NA
IDC	NA	NA	NA	NA
Total	NA	NA	NA	NA

7. Any changes in approach or aims and reasons for change. Remember significant changes to the objectives and scope require prior approval by the cooperative agreement PI's and concurrent of the GOTR.

The species: chlorophyte *Monoraphidium minutum* (MONOR2) identified in the proposal was not available from any source. Instead, the researchers seeded and grew a species sampled from the evaporation pond at BGNDRF

8. Actual or anticipated problems or delays and actions taken or planned to resolve them.
No.
9. Any absence or changes of key personnel or changes in consortium/teaming arrangement.
No.
10. A description of any product produced or technology *transfer activities* accomplished during this reporting period,
such as:
No.

Pre final report on Tier 1 proposal titled **“Developing a Biotechnology with a Reactor to Grow Microalgae for Biodiesel from Reusing Waste Concentrate and Anaerobic Digested Sludge”**

The Goal

- 1-Utilize two water sources from waste water treatment anaerobic digested sludge (ADS) and desalination concentrate from electrolysis reversal (EDR) to produce a useful algae for biofuel.
- 2- Using alternative source of nutrients from wastewater (such as anaerobic digested sludge) to grow algae and their capability to grow in low quality water.

The objective

The objective of this research was to develop a bio-reactor to grow three species of microalgae *Dunaliella salina* and *Spirulina platensis* and one unknown species of microalgae from the Concentrate of Desalination Evaporation Pond from the Brackish Groundwater National Desalination Research Facility (BGNDRF). These species were grown in different ratio of microalgae to anaerobic digested sludge, ADS to concentrate from electrolysis reversal (EDR).

Outcome

All three microalgae species were grown successfully using anaerobic digested sludge (ADS). The resulted from the lab testes shows that the high desalination concentrates were significantly reduces to improve sustainability of water. The net energy ratio for algal biodiesel is slightly positive as 0.93 MJ consumed/MJ produced by using brackish groundwater and BBM nutrient. To improve the net energy gain in algal biodiesel, microalgae were cultured by reusing concentrate from desalination and anaerobic digested sludge.

Papers, posters and Oral Presentation

- 1-Maung Thein Myint and Waddah Hussein "Seeding Microalgae from Concentrate of Brackish Groundwater National Desalination Result Facility". US Bureau of Reclamation Technical Resource Center, Denver, CO. May 2011
- 1- Waddah Hussein, Myint Maung, Abbas Ghassemi. “Culturing Microalgae from Desalination Concentrate Reusing Anaerobic Digested Sludge as Nutrient to Improve the Net Energy Ratio”. WRRRI Reclamation New Water New Energy Conference. Dec 13-14, 2011. Alamogordo, NM.
- 2- Waddah Hussein, Myint Maung, Abbas Ghassemi. “Seed Microalgae from Concentrate of Evaporation Pond in Different Conductivities ” AWWA/AMTA 2012 Membrane Technology Conference. Feb. 27 – Mar 01, 2012. Glendale, AZ.

3- Waddah Hussein, Myint Maung, Abbas Ghassemi. "Using desalination concentrate and anaerobic digested sludge as waster media and nutrients for growing D. Salina and S. Platensis" 57th Annual New Mexico Water Conference. Aug 28, 2012. Las Cruces, NM.

4- Waddah Hussein, Myint Maung, Abbas Ghassemi. "Concentrate from Desalination Is Good for Microalgae Growth". Bi-national Border Water Resources Summit. Sep 28, 2012. UTEP, El Paso, TX

5- M.T. Myint, W. Hussein, A. Ghassemi "Microalgae process for treatment of concentrate from inland desalination to improve sustainability of water supplies for irrigation, farm, and ranch in cities of arid-regions". 2nd Water Research conference in Singapore 20-23 January 2013

6- W. Hussein, M.T. Myint, A. Ghassemi "Managing brackish groundwater desalination concentrate in microalgae production to improve sustainability of inland desalination, wastewater treatment plant, farm, and ranch in semi-arid region of the United States". 2nd Water Research conference in Singapore 20-23 January 2013

Appendix E:

Project Title: Preliminary Evaluation of Algae Production from Concentrate Stream

Project principal investigator: Jalal Rastegary

Contact information: rastegar@nmsu.edu

Award number: GR0002841

Date of report: 12/18/2013

Period covered by report: January-September

Students involved in Project:

- Saeid Aghahosseini Shirazi, Master of Science candidate, Research Assistant, Persian, saeid@nmsu.edu
- Tracey Fernandez, Bachelor of Science candidate, Research Assistant, Hispanic, tfernann@nmsu.edu

January	February	March
Doing literature review to find novel and cost-effective method to extract oil from biomass and working on methods to mitigate the probable mistakes during the experiments	Preparing requirements needed for the next step of experiments regarding to concentrate management aiming to investigate the impact of using antiscalant in feedstock water on growing of different strains of microalgae	Mentoring EPCC students from UTEP community colleague. Making the familiar with the concept of desalination and the concerns related to the concentrate stream of desalination units and conducting an experiment for them to investigate the effect of concentrate on algae growth

Publications:

The extended abstract was sent in order to be presented in following conferences:

- 17th Annual Water Reuse & Desalination Research Conference, Phoenix, AZ, May 2013
- EWRI Congress, Cincinnati, Ohio, May 2013
- The other activities included
 - 1- Doing literature review to find novel and cost-effective method to extract oil from biomass.

2-Start to prepare a report of what have been done so far on concentrate management project

April May June

Presentations for two coming conferences in May were prepared.

1- Oral presentation in 17th Annual Water Reuse & Desalination Research Conference, Phoenix, AZ.

2- Oral presentation in EWRI Congress, Cincinnati, Ohio.

3- Research proposal was written in which the scope of works for next few months is defined

1- Related papers for literature review has been ordered and received; thus, the literature review will be initiated from 1st of July.

2- Four strains of algae (*Dunaliella tertiolecta* (UTEX-LB 999), *Chlorella sorokiniana* (UTEX-1230), *Nannochloropsis oculata* (UTEX- LB 2164), *Chlorella vulgaris* (UTEX-2714)) were purchased from UTEX culture collection algae collection on 7th of June and it would be estimated to be received by 7th of July.

3- Two media, bold modified basal freshwater nutrient and F/2 marine water enrichment, were purchased from Sigma-Aldrich.

4- For cell counting purpose, Dr. Houston's lab was visited and flow cytometry has been found as an appropriate method to do the cell counting.

5- 500 ml glass Photobioreactors is ready to order.

July August September

Two sets of experiments were conducted: *Dunaliella tertiolecta* (UTEX-LB 999), *Chlorella sorokiniana* (UTEX-1230)

-Last two sets of experiments were conducted: *Nannochloropsis oculata* (UTEX- LB 2164), *Chlorella vulgaris* (UTEX-2714)

-Poster for ABO conference was prepared

-Data analysis on results

Preparation for AIChE conference for oral presentation

Preparation for Petrochemistry and Chemical Engineering conference for oral presentation.

Appendix F:

Investigating and Understanding the Selectivity of the Conventional Ion-exchange Membranes used in Electrodialysis Process

Tier 1

Area: Treatment/Pre-treatment

PI: Dr. Jalal Rastegary

Date of report: 10/10/2013

Period covered by report: 07/01/2013- 09/30/2013

Students involved in Project:

Leila Karimi, Ph.D. Candidate, Female with no disability

Email: lkarimi@nmsu.edu

**Table 1. Project Schedule
MONTH**

Tasks/Subtasks	1	2	3	4	5	6	7	8	9	10	11	12	13	14	15	16	17	18	
1																			*
2	*	*																	
2A																			
3																			
4 Final Report																			

Activities in the period of July- September 2013:

As soon as designing the data acquisition system and selecting the variables, a wide search was started in order to find the analog output sensors, 4-20 mA, with appropriate range. Moreover, searching for the transmitters for sensors with different type of output was completed. Then the most appropriate sensors at the reasonable price were chosen and the purchase orders were placed. Additionally, the appropriate configuration for a Programmable Logic Control, PLC, was chosen and the required parts were purchased. The purpose of using a PLC is controlling the flow rate of

different feed solutions in the electro dialysis set up via remotely controllable pumps as well as recording data using software, Canary Lab's Historian. Working on the hardware as cutting the parts, preparing the frame of set up was started. Meanwhile, pilot-scale experiments were designed. The experiments in the pilot scale were conducted as the preliminary experiments in order to check the effect of operating variables on the selective removal of ions. The water samples were collected and analyzed using the ion chromatography, ICs 5000, and total inorganic carbon analyzer to measure concentrations of anions and cations, and bicarbonate, respectively. Then the results were analyzed. The paper which will be published on the pilot scale data can be considered as the preliminary step of data collection using the laboratory-scale set-up. Recently some of the ordered compartments were received, but as soon as receiving all of them, assembling of the laboratory scale electro dialysis set up will be started.

There were some delays in purchasing the data acquisition parts and laboratory scale electro dialyzer. The designing and purchasing the data acquisition parts as well as laboratory-scale electro dialyzer took much more time than anticipated due to some reasons. First, the first try for purchasing the chosen sensors and transmitters failed due to unavailability of some of those parts. Therefore, the sensor and transmitter selections were done one more time. Second, finding sensors was very challenging, because the diameter of manifolds was very small, and a few suppliers provide very tiny sensors with acceptable accuracy at reasonable price. The third challenge was dealing with some of the vendors that are out of the U.S. because of too many difficulties regarding completing the paper work at university, that caused a big delay in ordering, purchasing and receiving the tiny electro dialyzer. Although it was expected to receive all the equipment in two weeks, there was a big delay in receiving some of the sensors, transmitters, and PLC parts. Some of the sensors and PLC have not been received yet.

The most significant accomplishments during this period was designing the data acquisition system and selecting all the sensitive sensors with high accuracy that makes the operating variable monitoring and recording during the experiments possible. It is predicted that as soon as completing the set-up and programming the PLC, experiments will be started and the data collection will not take too much. Therefore, the significant results will be published in Desalination or any other Journal before end of the June.

1. Cost Status:

	Budget	Committed as of	Spent	Balance Available
Salary	29,319.00	0.00	36,456.05	-7,137.05
Fringe Benefits	714.00	0.00	1,200.97	-486.97
Travel (In-State)	1,800.00		1,647.00	152.20
Supplies/Materials	8,520,000		299.10	8,220.90
Services			0.00	0.00
Subcontract			0.00	0.00
Equipment			0.00	0.00
IDC	9,643.63	0.00	9,465.35	178.28

Total	49,996.63	0.00	49,069.27	927.36
--------------	-----------	------	-----------	--------

Appendix G:

QUARTERLY PROGRESS REPORT FOR THE PERIOD ENDING: Oct 31, 2013**Desalination Concentrate Management for Sustainable Agriculture:****A Preliminary Study on Transport behavior and Plant Viability at BGNDRF**

Tier 1 Proof of Concept Proposal

Principal Investigator:

PI Name: Manoj K Shukla

University: NMSU

Department: PES

Address: N320, Skeen Hall

Telephone: 6-2324

Fax: 6-6041

E-mail: shuklamk@nmsu.edu

Students Participating in the Project:

Name: Alison Flores

College: CAES

Major: PES

Phone #:

Email: amflores@nmsu.edu

Milestones:

Task	Months												
	0	1	2	3	4	5	6	7	8	9	10	11	12
Baseline data for BGNDRF													
Collect soil for Greenhouse work													
Identify and select plants; obtain seeds													
Plant screening experiments													
Transport experiments in greenhouse													
Analyze and interpret results													
Write final report & present results													

Prior to the start of the project, as per the proposed requirement, loose and core samples were collected from BGNDRF site and soil bulk density, hydraulic conductivity, soil water characteristic, particle size distribution, and EC and SAR were determined. A grad student was recruited, equipment and seed orders were made and germination experiments completed with five of the six species using tap water.

Presentations/Publications

No

Research Related Travel

Two trips to Alamogordo to collect soil samples

IEE Budget Status

IEE	Allocation	Expended	Balance
1. Salaries	29000	1168	27832
2. Fringe Benefits	754	46	708
3. Supplies & Expenses	9300	100	9200
4. Travel	1200	0	1200
5. Publication	0	0	0
6. Indirect Costs (23.9%)	9621	314	9307
Total	49875	1628	48247

Cost-Share Status (if applicable) NA**Cost Share Entity:**

Cost Share	Allocation	Expended	Balance
Cost Share provided by:			
1. Salaries			
2. Fringe Benefits			
3. Supplies & Expenses			
4. Publication			
5. Indirect Costs			
Total			

Purpose of Cost-Share funds (list by general category):**Percentage of IEE and cost-share budget expended:****Description of Commercialization Efforts**

None

Progress Report

Summary

We hired a graduate student who was supported by external grants and we completed the project requirement of conducting base-line analysis of soil at the BGNDRF before the start of this project. Subsequently equipment and seeds were ordered, and germination experiments were conducted for all six plant species (Barley, Triticale, Lepidium, Switchgrass, Atriplex and NiPa grass). The soil sieved through 2 mm sieve is packed in the cones and experiments will soon start to test the survival and growth potential of selected plant species as soon as concentrate is made available by BGNDRF.

Work Plan for Next Quarter

To collect the concentrate from BGNDRF to conduct tests on survival and growth potential of selected plant species.

Quarterly Report Attachments Index

1. *"Algae Biofuel Production and Concentrate Management in Inland Brackish Water Desalination"*
2. *"Utilization of Metal Organic Frameworks in order to Encapsulate Greenhouse Gas to Address Water Availability and Drought"*
3. *"Water Desalination via Microbial Desalination Cell"*
4. *"Optimization of Selected Parameters Impacting Microbial Fuel Cells"*
5. *"WERC Design Contest Further Research"*
6. *"Solar-Powered Reverse Osmosis Technology for Brackish Water: The State of The Art"*
7. *"RO/NF Applications in Brackish Groundwater Desalination: Membrane Characterization"*
8. *"Investigating the Effective Parameters in Optimizing Reverse Osmosis Technology for Water Treatment"*
9. *"Impact of Silica in Water Treatment Technology"*
10. *"Selectivity Comparison for Two Cation Exchange Membranes in the Electrodialysis Process"*
11. *"Developing a Mechanistic Transport Model for Electrodialysis/Electrodialysis Reversal Process"*
12. *"A Novel Method to Manage the Concentrate Disposal of Desalination Units"*
13. *"Carbonation of Metal Oxide Nanoparticles Caged in MOF Structure"*
14. *"Different approaches on energy optimization in reverse osmosis desalination plant"*
15. *"Review on aqueous lithium Li-ion battery"*
16. *"Utilization of metal organic frameworks in order to encapsulate greenhouse gas to address water availability and drought"*
17. *"Optimization of pilot scale photovoltaic reverse osmosis desalination system for ground water"*
18. *"Developing a mechanistic transport model for electrodialysis reversal process"*
19. *"Using concentrate from desalination and reusing anaerobic digested sludge to grow algae"*
20. *"Innovative method of using brine water to produce energy"*
21. *"The effect of feed water composition in selective removal of ions in electrodialysis process"*
22. *"Overview of produced water treatment technologies"*
23. *"Estimating available saline water resources in aquifers of New Mexico using GIS"*
24. *"Optimization Techniques in the Membrane Based Desalination Technologies"*
25. *"New Approach to Concentrate Management of Inland Desalination"*
26. *"Investigation of Economic Feasibility of PVEDR and PVRO Desalination to Produce Drinking Water"*
27. *"Power Efficiency Enhancement of Vacuum-Deposited Organic Solar Cell Based on Flourine Molecules via Thermal Post-Annealing"*
28. *"Assessment of Water Use for Microalgae in Open Pond in Southwest USA"*
29. *"Concentrate Stream to Green Energy"*

PERIOD: OCTOBER TO DECEMBER 2013**Administration:**

- Continued conference calls/meetings with the Cooperative Agreement (CA) team.
- Continued to communicate with the Bureau of Reclamation (Reclamation) through emails and phone calls.
- Continued the development of the Collaborative Research Education Program.
- Prepared and submitted quarterly report for June to September 2013.
- Prepared and resubmitted quarterly reports for June to September 2013 with additional requested information.
- Continued to monitor progress on awarded Tier I research.
- Continued the development of the new research education fellowship programs for graduate students.
- Continued to update and refine website.
- Prepared Brochures, Posters, Window shades for AIChE and Petrochemistry and Chemical Engineering Conferences.
- Registered to exhibit at 2014 AWWA/ AMTA Membrane Technology Conference and Exposition March 10-13 in Las Vegas, Nevada.
- Reviewed two Tier 1 proposals from the faculty of Chemical Engineering of NMSU Reza Foudazi and Catherine Brewer.
- Received and reviewed two Tier 1 resubmitted proposals from the faculty of Chemical Engineering of NMSU Reza Foudazi and Catherine Brewer.
- Awarded and set-up account for the two Tier I for Reza Foudazi and Catherine Brewer
- Tracked quarterly spending needed to provide Reclamation with estimates of percent spent in various categories
- Developed, advertised and distributed flyers for Water Fellowships starting Spring 2014

Education:

Addressed questions and inquiries from prospective and committed teams about the Reclamation-sponsored Tasks 2, Drinking Water Stabilization, and 3, Power Point Tracking for Solar Energy. The four teams currently registered for the Design Contest tasks sponsored by Reclamation are Louisiana State University for Task 2, the University of New Hampshire for Task 3, and Northern Arizona University, which has one team registered for Task 2 and one team registered for Task 3.

- The objective of Task 2 is to find the best fortification for desalted water, which is most commonly obtained from Reverse Osmosis processes. Specifically, the teams will: 1) identify minerals that would improve taste and prevent the water from leaching minerals from the skeletal system; 2) review nutritional requirements for people and livestock; and 3) address the additional benefit of fortifying water, the protection of water distribution systems from corrosion. The teams must also address the existing types of bottled water and bottled beverages in North America, including their source of origin, added minerals content, specifics on the types of minerals, and beneficial uses for the minerals. The research must also address how close the actual products are to the optimum mineral composition as determined by the teams, and what impact the optimum composition may have on taste and odor.
- Task 3 teams will develop a novel system for maximum power point tracking, and demonstrate its cost effectiveness by measuring the additional power generation versus the cost of the components and power required for operation. The teams must quantify the difference in power generation with and without the solar tracking device and conduct a lifecycle cost analysis of the solar system with and without the tracking device.
- Potential judges for the Design Contest have been identified, and recruitment of judges for the contest (April 6-9th, 2013 in Las Cruces) has begun. Facilities for the contest have been procured, updates to the web site have been made, supplies have been ordered, and the 2015 Design Contest post card is currently being edited.
- Conducted weekly meetings with seventeen Ph.D. and Master's degree students. Each week three students gave PowerPoint presentations on their progress; the other students discussed their own progress and acquired feedback and answers to any questions they Mentored, reviewed, commented, and edited graduate students poster and oral presentations for conferences and beginning drafts of thesis.
- Prepared two PhD students for successful completion of comprehensive exam
- Received, review, commented and returned for corrections/additions draft report from International Environmental Design Contest interns summer research on solar stills.
- Received and reviewed application for Graduate Research Education Fellowships:
 - Azadeh Ghorbani
- The following Ph.D. and master's students are supported by BOR for the quarter of Oct-Dec. 2013:

- Abkar Leili, first year MS.
- Saeid Shirazi, second year Master's
- Rafal Alshukri, first year Master's
- Navid Attarzadeh, first year Ph.D.
- Waddah Hussein, second year Master's
- Racheal Jones, second year Master's
- Leila Karimi, third year Ph.D.
- Kwonit Mallick, second year MS
- Pedram Ghaemmaghami second year MS
- Nasser Khazeni third year Ph.D.

Research

Graduate Students

- Received, reviewed, commented on, and provided guidance for graduate students weekly progress reports
- PI and various staff members mentored and interacted with individual graduate and undergraduate students conducting research on a daily bases.
- Continued working with various students research projects insuring appropriate safety procedures and documentation required by the department and university are in place to begin/continue research.
- Continued working with various research projects to analysis needs related to safety, accuracy, effectiveness and efficiency; evaluate; select; order; receive; install and trouble shoot components and systems required conducting specified research for thesis and dissertations.

Graduate Research Presentations

- The following oral and poster presentations were made at various conferences: (Presentation attachments 1-20)
 - **1-2013 AIChE Annual Meeting November 3-8, 2013 San Francisco, California**

Oral Presentations:

Leili Abkar, Kwonit Mallick, Rafal Alshukri, Abbas Ghassemi and James Loya, Solar-Powered Reverse Osmosis Technology for Brackish Water: The State of The Art.

Leili Abkar, Abbas Ghassemi and James Loya, Investigating the Effective Parameters in Optimizing Reverse Osmosis Technology for Water Treatment

Fattaneh Naderi Behdani, Abbas Ghassemi and James Loya, Impact of Silica in Water Treatment Technology.

Leila Karimi, Azadeh Ghorbani, Abbas Ghassemi and Jim Loya, Selectivity Comparison for Two Cation Exchange Membranes in the Electrodialysis Process.

Azadeh Ghorbani, Leila Karimi, Abbas Ghassemi and James Loya, Developing a Mechanistic Transport Model for Electrodialysis/Electrodialysis Reversal Process

Saeid Aghahosseini Shirazi, Alireza Saraeian, Jalal Rastegary and Abbas Ghassemi, a Novel Method to Manage the Concentrate Disposal of Desalination Units.

Poster Presentation:

Nasser Khazeni, Meitham Naeem, Abbas Ghassemi, Carbonation of Metal Oxide Nanoparticles Caged in MOF Structure

- **2-World Congress on Petrochemistry and Chemical Engineering, November 18-20, 2013 San Antonio, Texas**

Oral Presentations:

Leili Abkar, Different approaches on energy optimization in reverse osmosis desalination plant.

Pedram Mohrdar Ghaemmaghami, Review on aqueous lithium Li-ion battery.

Nasser Khazeni, Utilization of metal organic frameworks in order to encapsulate greenhouse gas to address water availability and drought

Kwonit Mallick, Optimization of pilot scale photovoltaic reverse osmosis desalination system for ground water.

Azadeh Ghorbani, Developing a mechanistic transport model for electrodialysis reversal process.

Waddah Hussein, Using concentrate from desalination and reusing anaerobic digested sludge to grow algae.

Saeid Aghahosseini Shirazi, Innovative method of using brine water to produce energy.

Leila Karimi, The effect of feed water composition in selective removal of ions in electro dialysis process.

Fattaneh Naderi Behdani, Overview of produced water treatment technologies.

- **3-58th Annual New Mexico Water Conference, 21-22, 2013 Albuquerque, New Mexico**

Poster Presentations:

Racheal Jones, Kenneth C. Carroll, Michelle Chapman, Mick O’Neill, and Alexander G. Fernald, “Estimating available saline water resources in aquifers of New Mexico using GIS”, November 21-22, 2013 Albuquerque, NM

Leili Abkar, Abbas Ghassemi, James Loya. “Optimization Techniques in the Membrane Based Desalination Technologies” 58th Annual New Mexico Water Conference, November 21-22, 2013 Albuquerque, NM

- **4- Pacific Rim Summit on Industrial Biotechnology and Bioenergy**
Jalal Rastegary, Tracey Fernandez, Abbas Ghassemi, Assessment of Water Use for Microalgae in Open Pond in Southwest USA, Dec. 8-11- 2013 San Diego, CA
- **5- 2013 Industrial Water Reuse Specialty Conference**
Jalal Rastegary, Abbas Ghassemi, Saeid A. Shirazi, Tracey Fernandez, Concentrate Stream to Green Energy, Dec. 9-2013 Long Beach, CA

Tier 1 Quarterly Report_[JL1]

7. **“Consequences and Possible Solutions for Small Scale Saline Water Residue Disposal in New Mexico”**
 - Original PI: Dr. Blair Stringam
 - Current PI: Dr. Blair Stringam
 - Student Researchers: Jesus Sigala, David Gamon
 - Start date and anticipated completion date
 - Start Date: February 1, 2011
 - Anticipated Completion Date: December 30, 2013
 - Work conducted during the reporting period:
 - Completed tests for project
 - Analyzed data
 - Completed DNA analysis
 - Significant accomplishments during the reporting period:
 - Tests for this project have been completed, and the analysis of results indicates that saline water injection into the leach field has reduced the

infiltration rate. We are trying to make sure that there are no other factors that may have influenced the results.

- Unanticipated delays during the reporting period:
 - o There were no unanticipated delays during the reporting period.
- Progress of spending in the task:
 - o 93.9% of the original \$49,982.00 budget was spent as of December 31, 2013. \$ \$3029.70 of the budget remains.
- Comparison of actual spending to planned spending:
 - o Actual spending closely matches planned spending.
- Schedule discussion:
 - o The project is on track to meet its goals within the no cost extension.

8. “Investigating and Understanding the Selectivity of Conventional Ion-Exchange Membranes Used in Electrodialysis Process”

- Original PI: Dr. Ali Sharbat
- Current PI: Dr. Jalal Rastegary
- Graduate Student: Leila Karimi
- Undergraduate Student: Virginia Veruette-Maya
- Start date and anticipated completion date
 - o Start Date: January 1, 2012
 - o Anticipated Completion Date: July 1, 2014
- Work conducted during the reporting period:
 - o All the purchase orders were placed.
 - o The sensors and PLC parts were received.
 - o The manifolds were made based on the proposed design of the set up.
 - o The final configuration of sensors for the streams was solved.
 - o Seven manifolds were prepared for attaching the sensors for three inlet and outlet streams to the electrodializer, while one stream was considered for recycling some part of concentrate stream to combine with inlet concentrate stream.
 - o The rack for set-up was procured, painted, and then the control cabinet was installed on it. Additionally, the cabinet and rack were prepared according to the set-up configuration. Then, the parts of PLC such as power supply, analog inputs, and outputs were installed in the cabinet. The next step is programming the PLC as well as installing the manifolds and sensors.
- Significant accomplishments during the reporting period:
 - o Designed the final sensor configuration for the streams
 - o Procured and prepared the set-up rack.
- Unanticipated delays during the reporting period:
 - o As a consequence of the graduate student’s comprehensive exam, there were some delays in making the set-up.
- Progress of spending in the task:

- 98.1% of the original budget of \$49,996.63 had been spent as of December 31, 2013. \$927.36 remained.
- Comparison of actual spending to planned spending:
 - Because of unexpectedly high time demands for designing the data acquisition system and acquiring the necessary sensors, salary is over budget and equipment is under budget.
- Schedule discussion:
 - The activities are on schedule to be completed by the end of June, so the project is on track to meet its goals within the no cost extension.

9. “Optimization of Electrode Design for Electrodialysis Reversal”

- Original PIs: Dr. Ali Sharbat and Dr. Neil Moe
- Current PI: Dr. Jalal Rastegary
- Start date and anticipated completion date:
 - Start Date: August 22, 2011
 - Anticipated Completion Date: August 1, 2014
- Work conducted during the reporting period:
 - Work had been delayed until a qualified student could be found to travel to BGNDRF on regular basis. We interviewed three undergraduate students from the NMSU Alamogordo Campus; Reece Broughton has been selected and will be hired to do the work.
- Progress of spending in the task:
 - 10.3% of the original \$49,999.00 had been spent as of December 31, 2013. \$44,827.39 of the budget remains.
- Comparison of actual spending to planned spending:
 - Actual spending is lower than planned spending because of the delay in finding a qualified student to work at BGNDRF.
- Schedule:
 - With the hiring of a qualified student to travel to BGNDRF on a regular basis, the project is positioned to begin in earnest. One Master’s student will also be working on this Tier1 in the spring semester, and we anticipate that the project will meet its goals within the no cost extension.

10. “Desalination Concentrate Management for Sustainable Agriculture: A Preliminary Study on Transport Behavior and Plant Viability at BGNDRF”

- Original PIs: Dr. Manoj Shukla
- Current PI: Dr. Manoj Shukla
- Start date and anticipated completion date:
 - Start Date: August 1, 2013

- Anticipated Completion Date: July 31, 2014
- Work conducted during the reporting period:
 - The soil texture analysis was conducted and the site was found to have just one type of soil texture. Therefore, silica sand was bought as a second soil and that will be used to conduct plant screening and transport tests.
 - Four water treatments were selected for the germination experiments. These were deionized water (EC of 0 dS/m), irrigation water from Fabien Garcia greenhouse (0.6 dS/m), well water from BGNDRF (4 dS/m), and concentrate from BGNDRF (10 dS/m).
 - Treatment water samples were analyzed for pH, EC, and SAR.
 - The effects of salt treatments on the germination rates of the six species were monitored in the laboratory.
 - A germination chamber was set to maintain a 25°C temperature from 9:00 a.m. to 9:00 p.m. and a 15°C temperature from 9:00 p.m. to 9:00 a.m. Lights in the chamber remained on during the 12 hour day period and off during the 12 hour night period.
 - Experimental set up consisted of 72 Petri dishes (6 species x 4 treatments x 3 replicates). Each Petri dish was lined with two Whatman #2 filter papers (90 mm) and 3 mL of the treatment water was added. Twenty seeds were placed in each dish such that they did not touch. The Petri dishes were sealed with Parafilm "M" laboratory film to reduce evaporation loss. The dishes were arranged in the germination chamber in a randomized design with one replicate per shelf.
 - Seeds were examined every two days and were removed once the length of the radicle surpassed the length of the seed. Treatment water was added as needed.
 - The second set of germination experiments (repeat) is currently underway.
 - Plant screening experiments are underway with silica sand.
 - Hired a graduate student supported by external grants.
 - Soil sieved through 2 mm sieve is packed in the cones, and experiments to test the survival and growth potential of selected plant species will start as soon as concentrate is made available by BGNDRF.
- Significant accomplishments during the reporting period:
 - Completed experimental set up, and completed the first set of germination experiments, and began second set of germination experiments. Experimental set-up to test plant survival and growth is prepared.
- Unanticipated delays during the reporting period:
 - In the plant screening experiment with clay soil from BGNDRF Alamogordo facility, none of the seeds germinated. This is not anticipated to affect the completion date of the study.

- Progress of spending in the task:
 - o 15.1% of the original budget of \$49,874.71 had been spent as of December 31, 2013. \$42,334 of the budget remains.
- Comparison of actual spending to planned spending:
 - o Actual spending matches planned spending.
- Schedule discussion:
 - o The activities are on schedule to meet the expected completion date.

11. “Primary Evaluation of Algae Biofuel Production from Concentrate Stream”

- Original PI: Dr. Jalal Rastegary
- Current PI: Dr. Jalal Rastegary
- Graduate Student: Saeid Aghahosseini Shirazi
- Undergraduate Student: Tracey Fernandez
- Start date and anticipated completion date:
 - o Start Date: January 1, 2012
 - o Anticipated Completion Date: July 1, 2014
- Work conducted during the reporting period:
 - o Published “Water Resources for Algae-Based Biofuels” in the journal *Contemporary Water Research and Education - Universities Council on Water Resources publication*, 151, 117-122(2013).
 - o Published “ASI: Hydrothermal Extraction and Characterization of Bio-crude Oils from Wet *Chlorella Sorokiniana* and *Dunaliella Tertiolecta*” in the journal *Environmental Progress & Sustainable Energy*, 32(4), 910-915(2013).
 - o Submitted “Treatment of Concentrate disposal of desalination units using microalgae” for publication.
 - o Presented findings at 2013 AIChE Conference, San Francisco, California, USA, November 2013; Petrochemistry 2013 conference, San Antonio, Texas, USA, November 2013; 2013 Industrial Water Reuse Specialty Conference; 2013 Algae Biomass Summit ,Orlando, Florida, USA, October 2013; and the 2013 Pacific Rim Summit on Industrial Biotechnology & Bioenergy, December 8-11, Westin San Diego, San Diego, California.
- Significant accomplishments during the reporting period:
 - o Based on the research findings, we can conclude that the cultivation of algae in concentrate streams enables both an increase in the efficiency of removing pollutants and the cultivation of algal biomass for biofuel and feedstock production.
- Unanticipated delays during the reporting period:
 - o There were no unanticipated delays during the reporting period.
- What is the progress of spending in the task?

- 100% of the original budget of \$49,999.11 had been spent as of September 30, 2013.
- Comparison of actual spending to planned spending :
 - The budget has been spent, and the planned work has been completed. The final report will be submitted within the required time frame by cooperative agreement.

Outreach:

- Attended and exhibited at 2013 AIChE Annual Meeting, November 3-8, 2013 in San Francisco, California.
- Attended and exhibited at 2013 World Congress on Petrochemistry and Chemical Engineering November 18-20, 2013 in San Antonio, Texas.

2014 Annual Report

Contents

	<i>Page</i>
Summary of Publications for 2014	1
2014 CONFERENCE ABSTRACTS	3
Mesoscale Science Frontiers Conference, Santa Fe, NM. May 13-16, 2014.....	3
2014 Symposium on Thermal and Catalytic Sciences for Biofuels and Biobased Products, Denver, CO. September 2-5, 2014	4
2014 American Institute of Chemical Engineers Annual Meeting, Atlanta, GA. November 16- 21, 2014	6
2014 ASABE Section meeting Las Cruces, NM, April 11	8
2014 ASA, CSSA & SSSA International Annual Meeting, Long Beach, CA. November 2-5, 2014.....	9
WRRRI 59th Annual New Mexico Water Conference, Santa Fe, NM. November 18-19, 2014	10
POSTERS AND PRESENTATIONS.....	11
Mesoscale Science Frontiers Conference.....	11
2014 TCS.....	12
2014 AICHE.....	14
2014 ASABE.....	21
2014 ASA, CSSA & SSSA	22
WRRRI 59th Annual New Mexico Water Conference.....	23
PAPERS	24
Biomass as Renewable Energy Source for Water Desalination: A Review	24
Simultaneous Treatment of Concentrate Water from Desalination Units and Cultivation of Microalgae as Feed Stock for Biofuel Production	72
Energy usage and carbon dioxide emission saving in desalination by using desalination concentrate and waste in microalgae production	101
Effects of Operating Conditions on Ion Removal from Brackish Water Using a Pilot-Scale Electrodialysis Reversal System	117

Summary of Publications for 2014

1. Mesoscale Science Frontiers Conference, Santa Fe, NM. May 13-16, 2014
A. Lindsay, I. Jaramillo, R. Foudazi, Extraction of Cellulose Nanowhiskers from Algal Biofuel Waste for Applications in Electro-optic devices.
2. 2014 Symposium on Thermal and Catalytic Sciences for Biofuels and Biobased Products, Denver, CO. September 2-5
Ali Amiri, Catherine E. Brewer, Design of a Biomass Slow Pyrolyzer-Multiple Effect Distillation (MED) Prototype.

Catherine E. Brewer, Opportunities for Biomass Thermochemical Processing to Solve Waste Management and Clean Water Problems.

3. 2014 American Institute of Chemical Engineers Annual Meeting, Atlanta, GA. November 16-21
Ali Amiri, Catherine Brewer, and Kyriacos Zygourakis, A Partial-Combustion Pyrolysis Model for an Energy + Biochar Reactor Design

Masoume Jaber, Fattaneh Naderi Behdani, Abbas Ghassemi, Jim Loya, Optimization of Electrode Design for Electrodialysis Reversal

4. 2014 ASABE Section meeting Las Cruces, NM, April 11
Alison Flores, Brian Schutte, Manoj K Shukla, Geno Picchioni, April Ulery, Effects of Saline RO Wastewater on Germination of Salt Tolerant Species
5. 2014 ASA, CSSA & SSSA International Annual Meeting, Long Beach, CA. November 2-5
Alison Flores, Manoj K Shukla, Brian Schutte, Geno Picchioni, April Ulery, David Daniel, Use of Concentrate from Reverse Osmosis for Agricultural Use
6. WRRRI 59th Annual New Mexico Water Conference, Santa Fe, NM. November 18-19, 2014
Alison Flores, Manoj K Shukla, Pore Clogging Due to Irrigation with RO Concentrate

Submitted Papers:

Ali Amiri, Catherine E. Brewer. Biomass as Renewable Energy Source for Water Desalination: A Review. *Renewable Energy*

Saeid Aghahosseini Shirazi, Masoud Aghajani, Jalal Rastergary, Abbas Ghassemi. Simultaneous Treatment of Concentrate Water from Desalination Units and Cultivation of Microalgae as Feed Stock for Biofuel Production. *Desalination and Water Treatment*

Flores A., B. Schutte, M.K. Shukla, G. Pichionni and A. Ulery. 2015. Time-Integrated Measurements of Seed Germination for Salt-Tolerant Plant Species. *Seed Science and Technology*

Publications:

Waddah Hussein, Maung Thein Myint, Abbas Ghassemi. Energy usage and carbon dioxide emission saving in desalination by using desalination concentrate and waste in microalgae production. *Taylor & Francis journal*, 05 Feb 2014

Leila Karimi, Abbas Ghassemi. Effects of Operating Conditions on Ion Removal from Brackish Water Using a Pilot-Scale Electrodialysis Reversal System. *Desalination and Water Treatment*, 18 March 2015

2014 CONFERENCE ABSTRACTS

Mesoscale Science Frontiers Conference, Santa Fe, NM. May 13-16, 2014

Extraction of Cellulose Nanowhiskers from Algal Biofuel Waste for Applications in Electro-optic devices

A. Lindsay, I. Jaramillo, R. Foudazi

Department of Chemical Engineering, New Mexico State University, Las Cruces, NM 88003

Abstract:

One of the current sources of biomass that is of particular interest for both academia and industry is algae. Algae is excellent for CO₂ sequestration, can be used in wastewater treatment, and is currently receiving a great deal of attention as a source of biofuels. Due to the cost of production in comparison to oil, algal biofuels are not yet a viable source of energy. A potential means by which the cost could be reduced is through the derivation of other products from the algal waste. After extracting biofuel, the waste is often discarded. However, this waste material usually contains cellulose, which can be converted to cellulose nanowhiskers through a bleaching pretreatment with NaClO₂ and an acid hydrolysis with H₂SO₄. Cellulose nanowhiskers are nanosized crystals of cellulose with a high length over diameter ratio and a strength to weight ratio eight times that of steel. Due to their surface chemistry, cellulose nanowhiskers can be functionalized with negatively charged sulfate ester groups, which introduces a surface charge density to the nanowhiskers. While previous experiments involving the control of functionalized cellulose nanocrystals derived from cotton under an electric field were not successful, the shape of cellulose nanowhiskers derived from algae may provide a greater difference in surface charge density and, consequently, allow the nanowhiskers to self-assemble under an electric field more efficiently. Because cellulose nanowhiskers exhibit liquid crystalline behavior in solution, an electric field can be used to control their self-assembly with a potential application in electro-optic devices such as liquid crystal displays.

2014 Symposium on Thermal and Catalytic Sciences for Biofuels and Biobased Products, Denver, CO. September 2-5, 2014**Design of a Biomass Slow Pyrolyzer-Multiple Effect Distillation (MED) Prototype**

Ali Amiri, Catherine E. Brewer

Department of Chemical Engineering, New Mexico State University, Las Cruces, NM 88003

Abstract:

Water desalination is one promising solution for freshwater shortages worldwide that can provide large quantities of high quality, potable water. There are two main types of water desalination systems: thermal distillation systems and membrane systems. Membrane systems are usually powered by electricity while thermal systems, including multi-stage flash (MSF), vapor compression (VC), and multiple effect distillation (MED), require low-temperature heat as the main energy input, as well as small amounts of electricity.

In this study, we present a design for a lab-scale biomass slow pyrolyzer-MED system. The thermal and electrical energy needed to operate the MED unit will come from locally-available biomass residues (pecan wood, pecan shells, cotton gin trash, yard waste), while still producing appreciable amounts of biochar for soil applications. The pyrolyzer-MED interface includes a burner to convert low-energy bio-oil and syngas into superheated steam and non-condensable gases, as well as a gas turbine generator to produce electricity. Gases exiting the turbine generator is used as the thermal energy source for production of steam for the first distillation effect. The electricity from the turbine will be used to power the water, brine, and vacuum pumps of the MED unit. The solid biochar product can be applied to improve soil quality and soil water holding capacity.

Specifically, the MED unit consists of three effects in a forward feed arrangement with pre-heaters, able to produce approximately 12 kg/hr (12 L/hr) of distilled water using 3kg/hr of 1.4 bar inlet steam.

Opportunities for Biomass Thermochemical Processing to Solve Waste Management and Clean Water Problems

Catherine E. Brewer

Department of Chemical Engineering, New Mexico State University, Las Cruces, NM 88003

Abstract:

Two of the greatest challenges we will face in this century are sustainable energy and sustainable fresh water. Frequently, these challenges are linked: energy is needed to transport and clean water, and water is a working fluid in energy conversion systems. The connection between water and energy is especially apparent in biomass-based systems: biomass is used to produce energy and water is needed to grow biomass.

In some regions of the world, especially the southwestern U.S., high-quality fresh water for residential, industrial and agricultural purposes is limited. Additional sources of water are available but are brackish or contaminated. These same regions have also unutilized or underutilized supplies of agricultural residues (pecan wood, nut shells, cotton gin trash, alfalfa stems), forestry residues (bark beetle-killed pine, logging wastes, sawdust), and urban residues (yard waste, tumbleweeds). Thermochemical processing provides opportunities to use these biomass resources for value-added energy to treat water and for materials to improve water use efficiency for growing biomass.

In this presentation, we will look at the energy needs for treating brackish and saline waters, ways in which biomass thermochemical processing can meet these needs, and biochars' effects on soil water use efficiencies.

**2014 American Institute of Chemical Engineers Annual Meeting, Atlanta, GA.
November 16-21, 2014**

A Partial-Combustion Pyrolysis Model for an Energy + Biochar Reactor Design

Ali Amiri¹, Catherine Brewer¹, and Kyriacos Zygourakis²,

¹Chemical and Materials Engineering, New Mexico State University, Las Cruces, NM

²Chemical and Biomolecular Engineering, Rice University, Houston, TX

Abstract:

Among the applications of biomass pyrolysis is to simultaneously produce biochar and thermal energy through slow pyrolysis. Partial combustion allows the reactor to be energy self-sufficient. The addition of oxygen (air) to the pyrolyzer, however, alters the pyrolysis reactions and reaction kinetics, and thus the biochar properties. The goals of this study are to develop a partial combustion reaction model to allow the design of a continuous, energy self-sufficient slow pyrolysis system that produces appreciable amounts of biochar for soil application, and thermal and electrical energy to operate a water desalination unit. This water desalination unit will use a thermal desalination method, multiple effect distillation (MED), to treat brackish groundwater. The overall system will be used in rural to convert agricultural residues to water suitable for irrigation or human consumption, and biochar to improve agricultural soil fertility and water holding capacity.

Optimization of Electrode Design for Electrodialysis Reversal

Jaberi, M., NMSU

Naderi Behdani, F., New Mexico State University, Institute for Energy and the Environment/WERC

Ghassemi, A., New Mexico State University, Institute for Energy and the Environment/WERC

Loya, J., New Mexico State University, Institute for Energy and the Environment/WERC

Abstract:

The main advantages of electrodialysis reversal (EDR) technology are high water recovery and great resistance to scaling and fouling. These attractive characteristics make EDR particularly promising in a world of increasing water shortage where communities turn to treating impaired groundwater sources to supplement their supply. However, the relatively high cost of EDR today hinders widespread deployment of this technology, motivating efforts to improve its efficiency. This work targets the electrode, one of the principal components of an EDR device which provides the driving force for desalination.

The shape and functionality of electrodes impacts performance and stack life as well as the operation cost associated with the current utilization and efficiency. The geometric relationship between electrode and membrane also determines the distribution of current density throughout the surface of the electrode and membranes, which in turn dictates the effective limiting current for the membranes. The goal of this work is to develop methods of evaluating current distribution in the stack and compare the optimum electrode design.

2014 ASABE Section meeting Las Cruces, NM, April 11

Effects of Saline RO Wastewater on Germination of Salt Tolerant Species

Alison Flores*, Brian Schutte, Manoj K Shukla, Geno Picchioni, April Ulery

*Department of Plant and Environmental Sciences, New Mexico State University, MSC 3Q,

P.O. Box 30003, Las Cruces, NM

E-mail: amflores@nmsu.edu

Abstract:

Sustainable management of the highly saline concentrate resulting from reverse osmosis and other processes is a major environmental problem that limits widespread implementation of inland groundwater desalination in New Mexico and the southwestern U.S. Water supplies in arid regions are valuable, even when high in salt. Water is a scarce resource in the southwestern United States due to the arid climate. Low rainfall, high evaporation, low quality groundwater, and the dwindling amounts of surface water are exacerbating the irrigation water availability problem. There is a growing need to the use of alternate water sources for irrigation. The Brackish Groundwater National Desalination Research Facility (BGNDRF) is located in the Tularosa Basin Alamogordo, New Mexico. The desalinization process takes place through reverse osmosis, resulting in a highly saline concentrate that must be managed properly to eliminate environmental problems. A possible solution would be to utilize the concentrate as an agricultural treatment for halophytes.

The objective of this research was to determine how saline treatments affect the germination rates of some salt tolerant species. Specifically, the effects on the germination of six species under four different water treatments were determined using a germination chamber. Seeds were examined every two days for 22 days and were removed when the length of the radicle was longer than the seed.

**2014 ASA, CSSA & SSSA International Annual Meeting, Long Beach, CA.
November 2-5, 2014**

Use of Concentrate from Reverse Osmosis for Agricultural Use

Alison M. Flores¹, Manoj K. Shukla¹, Geno A. Picchioni¹, Brian J. Schutte², April L. Ulery³ and David Daniel³, (1)Plant and Environmental Sciences, New Mexico State University, Las Cruces, NM (2)Entomology, Plant Pathology, and Weed Science, New Mexico State University, Las Cruces, NM (3)New Mexico State University, Las Cruces, NM

Abstract:

The Brackish Groundwater National Desalination Research Facility (BGNDRF) in Alamogordo, New Mexico uses reverse osmosis to treat water prior to domestic use. The process of desalination results in a highly concentrated solution that must be disposed of in an environmentally sound way. Land application of desalination concentrate is one approach to its disposal. Objectives in this study are: 1) to evaluate the transport behavior of concentrates for two soil types with contrasting texture, and 2) to measure the effects of BGNDRF concentrate on growth of six plant species *Hordeum vulgare*, *Triticum aestivum x Secale cereale*, *Atriplex canescens*, *Distichlis stricta*, *Lepidium alyssoides*, and *Panicum virgatum*. Plant growth was monitored for 90 days in a greenhouse experiment that used two soils (a clay soil from BGNDRF and commercially available silica sand) and three water treatments: tap water from greenhouses (EC = 1.0 dS/m), well water from BGNDRF (EC =4 dS/cm), and concentrate from BGNDRF (EC =10 dS/cm). Plants were grown in cells (1 plant per cell) that were uniformly watered as needed. Both non-destructive measurements (height, number of leaves, length of leaves, photosynthetic rates) and destructive measurements (stem water potential, osmotic potential, ion uptake) are guiding the selection of candidate plant species for BGNDRF land application sites. Results from experiments related to transport behavior of concentrates have indicated precipitate deposition on the particle surface and in the pores, have shown reductions in hydraulic conductivity caused by pore clogging. Sustainable safe and local management of the highly saline concentrate resulting from reverse osmosis could provide widespread implementation of inland groundwater desalination in New Mexico and the southwestern U.S.

WRRI 59th Annual New Mexico Water Conference, Santa Fe, NM. November 18-19, 2014**Pore Clogging Due to Irrigation with RO Concentrate**

Alison Flores, Plant and Environmental Sciences, New Mexico State University P.O. Box 30003,
Las Cruces, NM 88003 amflores@nmsu.edu 575-496-6265

Manoj Shukla, Plant and Environmental Sciences, New Mexico State University P.O. Box
30003, Las Cruces, NM 88003

Abstract:

In the southwestern United States, water is a scarce resource because of arid climate with low rainfall and high evaporation. Problem is exacerbated by low quality groundwater and dwindling surface water. There is a growing need for use of alternate water sources for agricultural use. About 75% of available groundwater in New Mexico is saline ($EC > 3$ dS/m). Brackish Groundwater National Desalination Research Facility in Alamogordo, NM uses reverse osmosis for desalinization of groundwater. This process results in a highly concentrated saline solution which must be managed in an environmentally sound way. One proposed way to dispose of this concentrate is land application for irrigation of salt tolerant plants. However, its impact on soil porosity is unknown. The objective of this study was to evaluate the effect of irrigation with RO wastewater concentrate on soil hydraulic conductivity. Two soils, clay and silica sand, were repacked and saturated with concentrate and one pore volume of concentrate ($EC \sim 9.5$ dS/m) was applied to the soil once a week. The samples were allowed to dry for one week at temperatures simulating southern NM weather between concentrate applications and the cycle was continued for 22 weeks. The hydraulic conductivity and bulk density of the samples were measured at 4 week intervals. Results from experiments showed reductions in hydraulic conductivity with concentrate application likely due to the precipitation of chemicals from wastewater resulting in pore clogging. Concentrate disposal on soil could aid in the implementation of inland groundwater desalination in the southwestern U.S.

POSTERS AND PRESENTATIONS

Mesoscale Science Frontiers Conference



Extraction of Cellulose Nanowhiskers from Algal Biofuel Waste for Applications in Electro-Optic Devices

Aaron Lindsay¹, Israel Jaramillo¹, and Reza Foudazi¹

¹Department of Chemical and Material Engineering, New Mexico State University, Las Cruces, New Mexico 88003

Introduction

The greatest factor that keeps algal biofuels from being competitive in the fuel market is their cost. A potential means of reducing their cost is by finding a valuable resource in their waste products. Because typical methods for algae biofuel extraction do not generally damage the cellulose, the waste product can potentially be harvested to derive cellulose nanowhiskers, a valuable material resource with a wide range of applications.

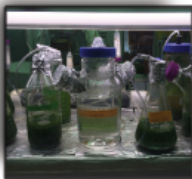


Figure 1: Growing Algae

Cellulose nanowhisker are nanosized crystals of cellulose with a high length over diameter ratio and a strength to weight ratio eight times that of steel¹. Due to their surface chemistry, cellulose nanowhiskers can be functionalized with negatively charged sulfate ester groups, which can introduce a surface charge density to the nanowhiskers. The liquid crystalline behavior in solution, along with the surface charge density, can be manipulated with an electric field to manipulate the birefringence, and thus the polarity of cellulose nanowhiskers. In effect, this has great potential for electro-optical applications, such as LCDs.

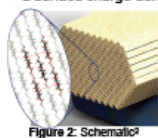


Figure 2: Schematic²

Questions

Can cellulose nanowhiskers be extracted from algal biofuel waste and, if so, can the orientation of the nanowhiskers be controlled with an electric field and used in liquid crystalline displays?

Methods

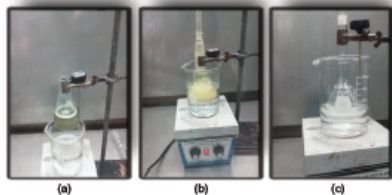


Figure 3: (a) Before bleaching pretreatment; (b) After 15 minutes of bleaching pretreatment; (c) Acid Hydrolysis

Bleaching Pretreatment

- Dried algae biofuel waste was ground into a powder.
- The powder was bleached with NaClO_2 in an acetic buffer system at a pH of 4 for 3 hours at 80°C .
- The microcrystalline cellulose was filtered and washed with dH_2O and 4 wt% NaOH .

Sulfuric Acid Hydrolysis

- The microcrystalline cellulose was hydrolyzed in a 60 wt% H_2SO_4 solution at 40°C for 30 minutes.
- The hydrolyzed microcrystalline cellulose was centrifuged and the supernatant was removed by pipet.
- The hydrolyzed microcrystalline cellulose was dialyzed against water for 3 days.

Data and Results

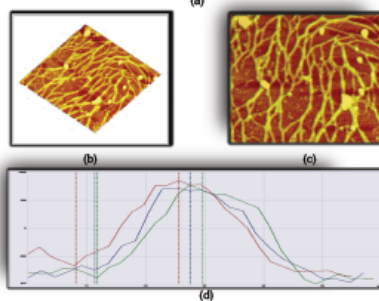
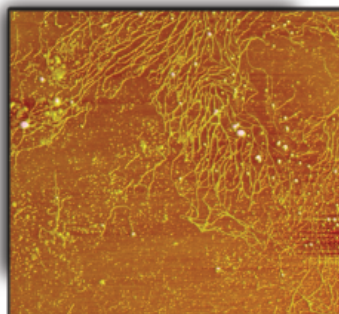


Figure 4: (a) $5\ \mu\text{m} \times 5\ \mu\text{m}$ scale AFM image; (b) $1\ \mu\text{m} \times 1\ \mu\text{m}$ scale AFM (angle) image; (c) $1\ \mu\text{m} \times 1\ \mu\text{m}$ scale AFM (above) image; (d) Plot of height vs. width

Conclusions

The images obtained from the Atomic Force Microscope show branching chains of microcrystalline cellulose, not cellulose nanowhiskers. To obtain the nanowhiskers, further hydrolysis of the microcrystalline cellulose will be needed. Nevertheless, these results suggest that cellulose nanowhiskers can in fact be obtained from algal biofuel wastes.

Future Plans

In the future we intend to study the birefringence by manipulating the cellulose nanocrystals under an electric field and measuring the light intensity through a polarizing filter to assess the potential for use in liquid crystalline displays.

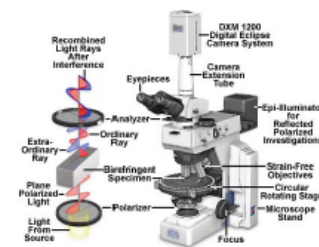


Figure 5: Method for measuring birefringence³

Acknowledgements

- This project was supported by New Mexico State University Institute for Energy and the Environment.
- Special thanks to Dr. Jalal Rastegary and Prof. Abbas Ghassemi.



References

1. R. J. Moon, A. Martini, J. Naim, J. Simonsen and J. Youngblood, *Chem. Soc. Rev.*, 2011, **40**, 3941-3994.
2. D. Hill, *Civil Engineering* (08857024), 2014, **84.3**, 36-37.
3. Nikon Microscopy U - The Source for Microscopy Education. (n.d.). *Nikon MicroscopyU*. Retrieved May 13, 2014, from <http://www.microscopyu.com/articles/polarized/polarizedintro.html>

2014 TCS



Design of a Biomass Slow Pyrolyzer-Multiple Effect Distillation (MED) Prototype

Ali Amiri , Catherine E. Brewer 

Department of Chemical & Materials Engineering, New Mexico State University

Water Desalination

- > Desalination is a promising solution for freshwater shortages that can provide large quantities of high quality, potable water.
- > 50% of desalination plant capacity is located in the Middle East, 20% in the US, 18% in Europe, and 12% in Asia.
- > In 2000, the installed desalination capacity worldwide was about 22 million m³/day, requiring 8.5×10^{18} J per year of energy, equivalent to 203 million tons of crude oil.

> Water quality is categorized in terms of total dissolved solids (TDS) with units of ppm (mg dissolved salts/L of water):

200-700 ppm	• Fresh water
2,000-10,000 ppm	• Brackish water
30,000-60,000 ppm	• Seawater

> Membrane / no-phase-change systems:

- > Are usually powered by only electricity.
- > Include reverse osmosis (RO) and electro dialysis (ED).

> Thermal systems:

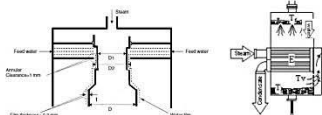
- > Require low-temperature heat as the main energy input and a small amounts of electricity.
- > Include multi-stage flash (MSF), vapor compression (VC), and multiple effect distillation (MED).

> Advantages of MED systems over other technologies:

- > Require less energy compared to MSF
- > Require fewer effects compared to MSF
- > Reduce TDS to less than 10 ppm compared to 10-500 ppm for membrane systems

Multiple Effect Distillation

> Common evaporator combinations:

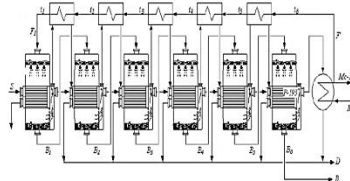


Vertical and horizontal tube evaporator (Sen et al., Desalination, 279 (2011) 15-26)

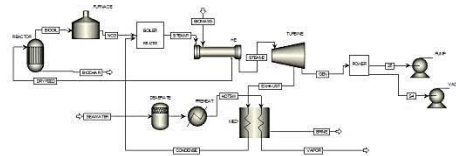
> The feed water and steam may switch their position depending on the design

> Feed arrangements:

- > Forward feed: feed water enters at first effect
 - > May need very large heat transfer area in first effect; this can be mitigated by using regenerative pre-heaters to gradually increase the feed's temperature prior to the first effect
- > Parallel feed: new feed water enters each effect
- > Backward feed: feed water enters at last effect
 - > Requires pumps between stages
 - > High salinity brine in first effect is prone to scaling



Forward feed flow arrangement with regenerative heat exchangers in a six effect, horizontal tube water spray MED Unit (M.A. Darwish, H.K. Abdulrahim, Desalination, 228 (2008) 30-54).



Aspen diagram of biomass pyrolyzer-MED system with interface components.

Our lab-scale biomass pyrolyzer-MED system

- MED system with 3 effects, forward feed arrangement and pre-heaters
- Horizontal, steam tube-side, with falling water film heat exchangers to increase energy efficiency and reduce scaling
- A de-aerator: to reduce dissolved oxygen in the brackish feed water
- Biomass: pecan orchard prunings and shells, cotton gin trash, dairy manure, yard waste
- Pyrolyzer-MED interface components: burner to convert low-energy bio-oil and syngas into superheated steam and non-condensable gases, boiler to produce steam, heat exchanger to dry raw biomass, and gas turbine generator to produce electricity to power system pumps

Acknowledgments

Funding from a cooperative agreement between the NMSU Institute for Energy & the Environment and the U.S. Bureau of Reclamation.

Collaborator Dr. John Idowu, NMSU Plant & Environmental Sciences

Contact Information

cbrewer@nmsu.edu



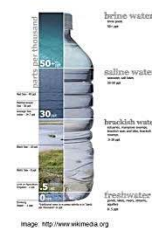
Opportunities for Biomass Thermochemical Processing to Solve Waste Management and Clean Water Problems

Catherine E. Brewer, Department of Chemical & Materials Engineering, New Mexico State University

Biomass Thermochemical Engineering



The Water Problem



- Much of the groundwater in the southwest is brackish: total dissolved solids are in the parts per thousand values.
- Desalination is needed to lower the TDS into parts per million values for drinking and agricultural use.
- Desalination requires significant energy and plans for disposal/use of the concentrated brine.



- An ongoing drought has made irrigation water difficult to obtain and expensive for NM farmers; many spend \$70/acre/year to participate in the Elephant Butte Irrigation District and another \$150-200/acre/year to pump water from their own wells.
- New Mexico soils are frequently saline, which can require use of salt and high pH-tolerant plants, and/or irrigation with clean water to flush salts out of the plant root zone. Brief desert rains often increase soil salinity by dissolving soil minerals then quickly drying.
- Many New Mexico also soils have low organic matter content, resulting in low plant-available water retention capabilities and in susceptibility to wind erosion.

The Waste Management Problem

Southern New Mexico has several biomass waste streams that are not well utilized:



Pecan orchard prunings and shells

- New Mexico ranks 3rd for pecan production in the U.S. with >17,000 orchards over >39,000 acres.
- The Mesilla Valley/Doña Ana County produces ~43 million lbs. of pecans every year, resulting in 30-60 million lbs. of pecan shells and 10-40 million dry tons of orchard prunings.
- Shells have found some use as horticultural mulch and potting media, while orchard prunings are traditionally collected and burned in the fields.

(Llanillo et al. Pecan Marketing Channels in New Mexico, 2010. NMSU, 2010. Rossi et al. Noncommercial Uses of the Pecan Industry. NMSU, 2003. Kaleski et al. Mesilla Valley Pecan Orchard Pruning Residue Disposal Estimates and Value-Added Opportunities. NMSU, 2008.)



Cotton gin trash

- Each 480 lb. bale of cotton contains about 150 lbs. of non-lint, non-seed materials that remaining after ginning.
- The Mesilla Valley grows approximately 30,000 acres of cotton every year, resulting in about 3.3 million tons of cotton gin trash.
- Cotton processors have yet to find a good use for the gin trash and usually have to compost, burn or land-fill it.

(John Howe, NMSU Extension)



Yard waste and tumbleweeds

- The City of Las Cruces (population: ~100,000) receives approximately 2,000-3,000 wet tons of green waste every year at its composting facility.
- Tumbleweeds, commonly Russian thistle, are a regular nuisance across the Southwest. The bone dry plants (with seeds) spread easily and resist treatment by composting.

(Lisa LaRocca, City of Las Cruces Sustainability Office, Rachel Ryan, NMSU Ecology)

Thermal vs. Membrane Water Desalination

While biomass energy could be used to produce electricity to power membrane desalination systems such as reverse osmosis (RO), thermal (phase-change) desalination technologies are better suited since they require mostly low-temperature heat and only some electricity.

Multiple effect distillation (MED) is a promising example:

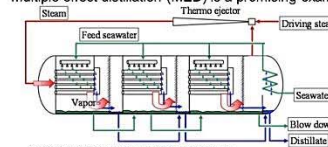


Image: <http://www.nitachosen.com/english/technology/m2/tech/m2.html>

- Operates near 70° C
- Requires 1.5-2.5 kWh of electrical energy and 290 kJ of heat per m³ of feed water
- Has been successfully implemented at the small (farm) scale using solar and geothermal energy sources.

(Water Desalination Using Renewable Energy. International Renewable Energy Agency (IREA) and International Energy Agency Energy Technology Systems Analysis Programme (E3-ETSP). 2012. Feroz, D., Lari, R., Chahga, P., Sassi, L., Maroufi, M., Cotti, M., Miskolczi, N., Hossain, K. Desalination 2009, 242-253. Karanayannis, I. G., Sotiriou, P. G. Desalination 2008, 222-248. Sen, P. K., Sen, P. Y., Moudgal, A., Singh, S. K., Vyas, S. K., Davies, P. Desalination 2001, 279-15)

Pyrolysis vs. Gasification/Combustion

While biomass combustion or gasification could supply the heat and power needs for desalination, pyrolysis can better address the needs of the local system by producing appreciable quantities biochar as well as energy. Applying this biochar to New Mexico soils has the potential to increase soil organic matter content and improve soil water availability.

Acknowledgment

Collaborators Dr. John Idowu (NMSU Plant & Environmental Sciences), Ali Amiri, Yunhe Zhang, Andrea Salazar, and Brent Carrillo
Contact Information
 cbrewer@nmsu.edu

2014 AICHE



A Partial-Combustion Pyrolysis Model for an Energy + Biochar Reactor Design

Ali Amiri,¹ Catherine Brewer,¹ and Kyriacos Zygourakis²

¹Chemical and Materials Engineering, New Mexico State University

²Chemical and Biomolecular Engineering, Rice University

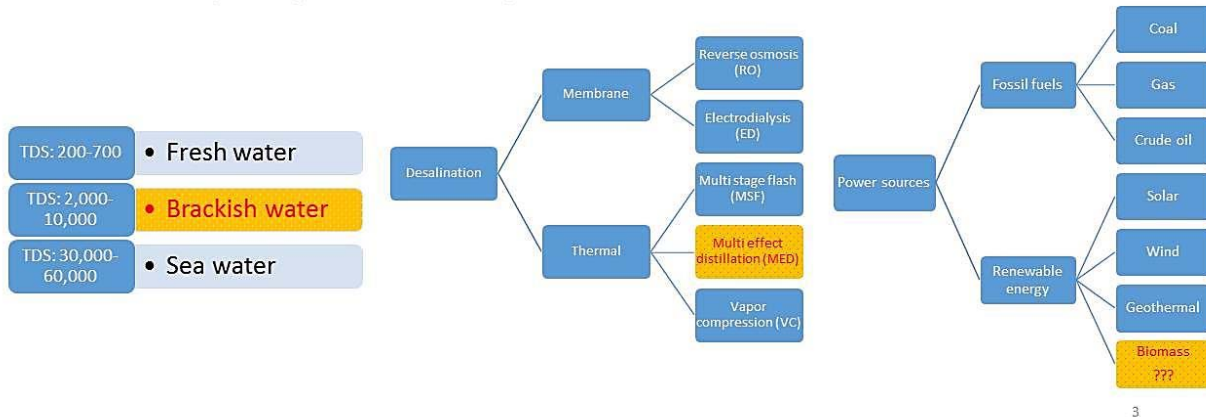
AICHE Annual Meeting 2014

➤ Outline

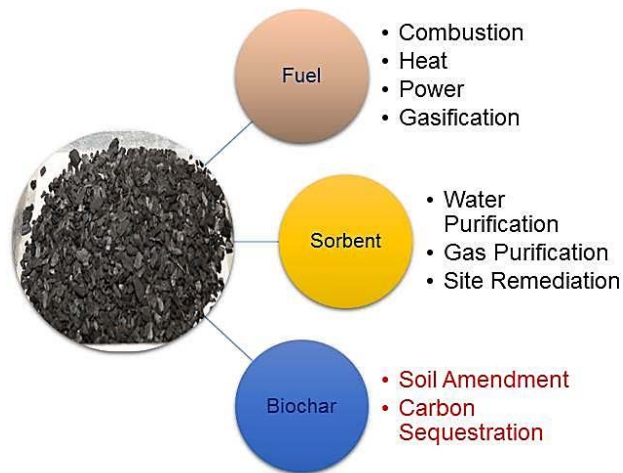
- Why produce thermal energy and biochar?
- Specific design requirements of pyrolyzer
- Reactor model and design

Thermal Energy for Water Desalination

- Water quality is categorized as a function of total dissolved solids (TDS) in parts per million (mg/L)



Biochar for Soil Water Retention

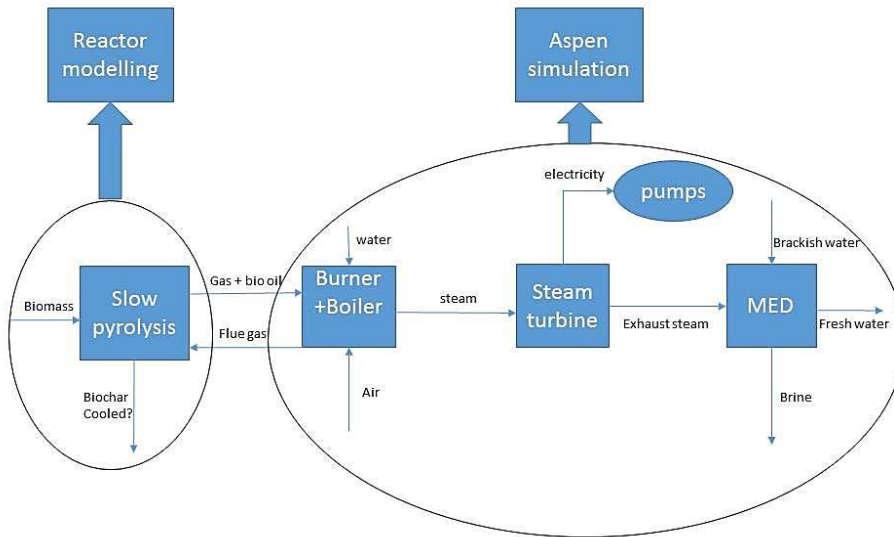


Biomass Available in Southern New Mexico



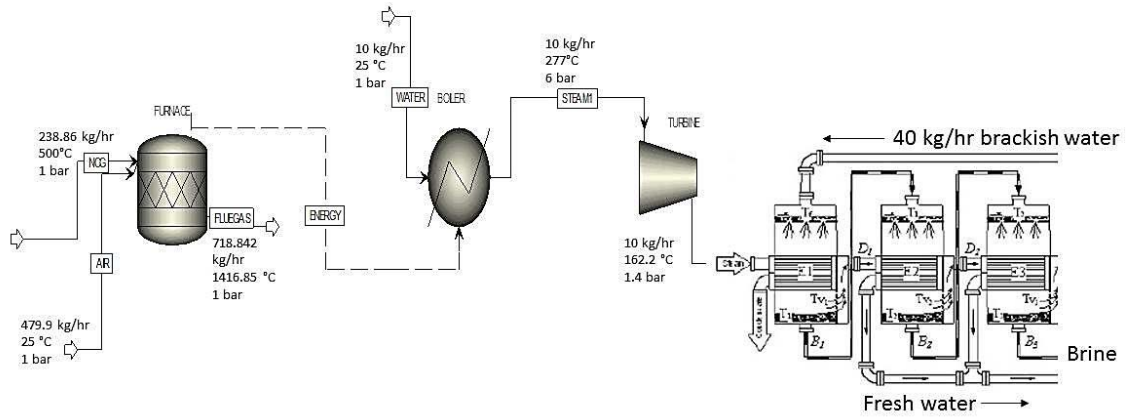
5

Entire Block Diagram



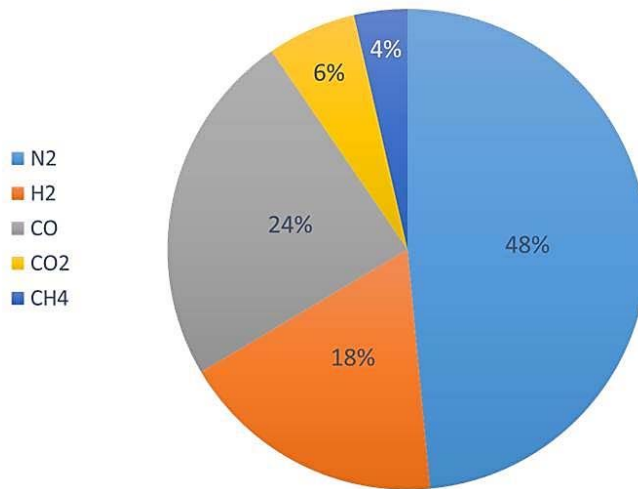
6

Pyrolyzer-MED System Interface



7

Pyrolysis Non-Condensable Gas Composition¹



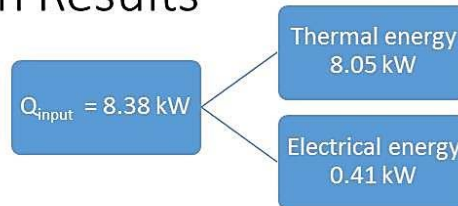
8

Pyrolyzer Requirements Methodology

1. Calculations done based on the following specifications for MED primary steam to make 40 kg/hr distilled water:
 - ✓ Pressure: 1.4 bar
 - ✓ Temperature: 162 °C
 - ✓ Mass flow rate: 10 kg/hr
2. Aspen simulation was run for each block separately in order of distance from MED: Turbine, Boiler, Furnace
3. Once desired material and energy streams were obtained individually, the simulation was run for the whole system.

9

Aspen Simulation Results



- Assuming a pyrolysis producer gas produced from groundnut shell² with HHV of 10 MJ/kg and 80% efficiency³ for the furnace, the lowest rate of biomass required could be:

$$8380 \frac{J}{s} \times \frac{1 \text{ kg}}{10 \times 10^6 J} \times \frac{3600 s}{1 \text{ hr}} \times \frac{1}{0.8} = 3.771 \frac{\text{kg}}{\text{hr}} \text{ of biomass}$$

10

How to model partial combustion for self-heating pyrolyzer to supply desired energy and biochar

- The unknowns to be provided by the reactor modelling?

11

Acknowledgements

- NMSU Institute for Energy and the Environment Tier 1 Proof-of-Concept Grant (through a cooperative agreement with the U.S. Bureau of Reclamation)
- Dr. O. John Idowu
- Brent Carrillo
- Yunhe Zhang

12

References

- 1: Chemical Composition of Biomass Syngas, Coal Syngas, and Natural Gas, from plant power energy and environment: <http://www.treepower.org/fuels/biomasssyngas.html>
- 2: Raveendran, K. et al. 1996. Heating value of biomass and biomass pyrolysis products. Fuel. 75(15): p. 1715-1720.
- 3: Furnaces and Boilers, from energy.gov: <http://energy.gov/energysaver/articles/furnaces-and-boilers>

13

➤ Assumptions

- Peng-Robinson equation of state for material properties
- Isentropic turbine (only turbine model available in Aspen)
- Turbine efficiency: $\eta_{\text{isentropic}} = 70\%$, $\eta_{\text{mechanical}} = 70\%$,
- ~5 bar pressure difference across the turbine
- Non-condensable gases exit pyrolyzer at 500 °C and 1 bar
- NCG composition: 48.6% N₂, 18% H₂, 24% CO, 6% CO₂, 3.4% CH₄
- Combustion reactions in the furnace have 100% conversion:
 1. $2\text{CO} + \text{O}_2 \rightarrow 2\text{CO}_2$
 2. $2\text{H}_2 + \text{O}_2 \rightarrow 2\text{H}_2\text{O}$
 3. $\text{CH}_4 + \text{O}_2 \rightarrow \text{CO}_2 + 2\text{H}_2\text{O}$
 4. $\text{N}_2 + \text{O}_2 \rightarrow 2\text{NO}_2$

<http://www.treepower.org/fuels/biomasssyngas.html>

14

2014 ASABE

ASABE
Las Cruces,
2014

Effects of Saline RO Wastewater on Germination of Salt Tolerant Species



Alison Flores*, Brian Schutte, Manoj K Shukla, Geno Picchioni, April Ulery

*Department of Plant and Environmental Sciences, New Mexico State University, MSC 3Q, P.O. Box 30003, Las Cruces, NM

E-mail: amflores@nmsu.edu

Introduction

Sustainable management of the highly saline concentrate resulting from reverse osmosis and other processes is a major environmental problem that limits widespread implementation of inland groundwater desalination in New Mexico and the southwestern U.S. Water supplies in arid regions are valuable, even when high in salt. Water is a scarce resource in the southwestern United States due to the arid climate. Low rainfall, high evaporation, low quality groundwater, and the dwindling amounts of surface water are exacerbating the irrigation water availability problem. There is a growing need to the use of alternate water sources for irrigation. The Brackish Groundwater National Desalination Research Facility (BGDRF) is located in the Tularosa Basin Alamogordo, New Mexico. The desalination process takes place through reverse osmosis, resulting in a highly saline concentrate that must be managed properly to eliminate environmental problems. A possible solution would be to utilize the concentrate as an agricultural treatment for halophytes.

Objective

- To determine how saline treatments affect the germination rates of some salt tolerant species

Methods & Materials



- The effects of salt treatments on the germination of six species were determined using a germination chamber set to 25/15°C day/night; 12 hour photoperiod.
- Photosynthetic photon flux density within the chamber was approximately 30 μmol m⁻² s⁻¹. 72 Petri dishes (6 species x 4 treatments x 3 replicates) were lined with two Whatman #2 filter papers (90 mm).
- 3 mL of treatment was added to each dish.
- Evaporation loss was reduced by sealing dishes with Parafilm "M" laboratory film.
- A randomized design was used.
- Seeds were examined every two days for 22 days and were removed when the length of the radicle was longer than the seed.

- Six species selected: Atriplex (*Atriplex canescens*), Barley (*Hordeum vulgare*), Lepidium (*Lepidium alyssooides*), Nipa (*Distichlis stricta*), Switchgrass (*Panicum virgatum*), and Triticale (a hybrid of *Triticum aestivum* and *Secale cereale*).
- Four water treatments: Deionized water (EC of 0 dS/m), Irrigation water from Fabian Garcia greenhouse (0.6 dS/m), Well water from BGDRF (4 dS/m), and Concentrate from BGDRF (9.5 dS/m).

Results

Table 1. Final germination percentages of various species under different treatments (* Experiment 1 / ** Experiment 2)

Species	DI Water %	FG Control %	Well Water %	Concentrate %
Atriplex	25.0* / 48.0**	23.3* / 33.3**	26.7* / 26.7**	25.0* / 38.7**
Barley	100.0* / 98.7**	98.3* / 100.0**	96.7* / 100.0**	100.0* / 97.3**
Lepidium	93.3* / 90.7**	93.3* / 90.7**	98.3* / 98.7**	98.3* / 96.0**
NiPa	88.3* / 81.3**	90.0* / 73.3**	90.0* / 80.0**	90.0* / 78.7**
Switchgrass	73.3* / 78.7**	88.3* / 80.0**	66.7* / 86.7**	71.7* / 85.3**
Triticale	100.0* / 98.7**	100.0* / 98.7**	95.0* / 100.0**	95.0* / 98.7**

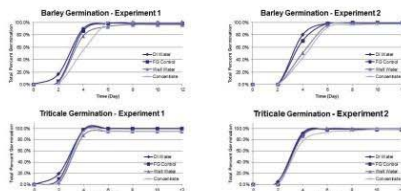


Fig. 1 - Barley and Triticale (Food Plants)

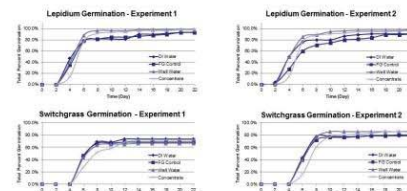


Fig. 2 - Lepidium and Switchgrass (Biomass Plants)

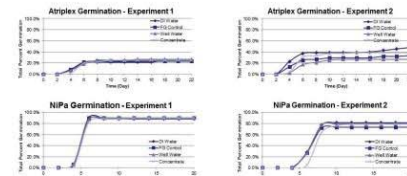


Fig. 3 - Atriplex and NiPa Grass (Fodder Plants)



Fig. 4 - Radicle Length with Increasing Salinity.

Summary

- In both germination studies, the percentages of germination varied with differing plant species.
- It was determined through logistic regression that the final germination percentages remained constant through both trials within the species for various treatments.
- Due to the constant final germination percentages, the data will be analyzed to compare the time taken to reach 50% cumulative germination across water treatments within a species.
- There was a visible difference in radicle length with increasing salinity. A study to further explore this observation is in design.

Acknowledgment: Funding support from Institute for Energy and the Environment (IEE) through NMSU/Bureau of Reclamation Cooperative Agreement, PES and NMSU Agriculture Research Station.

2014 ASA, CSSA & SSSA

Use of Concentrate from Reverse Osmosis for Agricultural Use

Alison Flores^{1*}, Manoj K Shukla¹, Brian Schutte², Geno Picchioni¹, April Ulery¹, David Daniel³

¹Department of Plant and Environmental Sciences, New Mexico State University MSC 3Q, P.O. Box 30003, Las Cruces, NM, ²Department of Entomology, Plant Pathology and Weed Science, NMSU, ³Department of Applied Statistics, NMSU.

*E-mail: amflores@nmsu.edu



2014 ASA, CSSA, SSSA Annual Meeting

Introduction

Sustainable management of the highly saline concentrate resulting from reverse osmosis and other processes is a major environmental problem that limits widespread implementation of inland groundwater desalination in New Mexico and the southwestern U.S. Water is a limited resource in the southwestern United States due to low rainfall, high evaporation, low quality groundwater, and dwindling amounts of surface water. Groundwater is increasingly used to meet the water demand; however, about 75% of this water is saline (EC > 3 dS/m) and requires treatment before it is deemed potable. The Brackish Groundwater National Desalination Research Facility (BGDRF) in Alamogordo, New Mexico uses reverse osmosis (RO) to treat saline groundwater. Using this concentrate for agriculture has the potential to eliminate the need for disposal.

Objectives

- Test the survival and growth of six plant species using the concentrate from RO
- Evaluate the transport behavior of concentrates for two soil types with contrasting texture



Figure 1 – Greenhouse setup. 144 pots (6 species, 3 treatments, 2 soils, 4 replicates), completely randomized design.

Experimental Methods

Plant Selection:

Six salt tolerant species selected are:

Common Name	Barley	Triticale	Mesa Pepperwort	Switchgrass	Fourwing Saltbush	Inland Saltgrass
Scientific Name	<i>Hordeum vulgare</i>	<i>Triticum aestivum</i> x <i>Secale cereale</i>	<i>Lepidium alcyonoides</i>	<i>Panicum virgatum</i>	<i>Atriplex canescens</i>	<i>Distichlis stricta</i>
Type	Food	Food	Biomass	Biomass	Fodder	Fodder

Water Treatments:

Three water treatments were prepared and mixed with a half strength Hoagland's solution. Salinity levels of the treatments varied slightly with time due to fluctuating source water salinity.

- Irrigation water from Fabian Garcia greenhouse (~0.9 dS/m)
- Well water from BGDRF (~4.1 dS/m)
- Concentrate from BGDRF (~8.2 dS/m)

Greenhouse Experiment:

- 144 pots (6 species, 3 treatments, 2 soils, 4 replicates) packed with cheesecloth, small gravel, soil to a consistent bulk density. Repeated once but data for year 1 is presented here.
- Seeds planted and irrigated with control water during seedling establishment to ensure consistent growth pattern. Fertilizer added after at least one leaf had established to prevent salt burn.
- Cells arranged in completely randomized design. Treatments gradually introduced to prevent shock. Species irrigated with same volume and frequency, per soil requirement.
- Physical measurements taken at day 30, 60, 90. Photosynthetic measurements taken after day 60 and 90.
- Leaching fractions determined by collecting and measuring volume of leachate after each irrigation.

Table 1 – Influence of salinity levels on plant physiology. Barley, Inland Saltgrass, and Mesa Pepperwort showed little to no significant difference at 0.05, NS is not significant.

	Clay			
	Height (cm)	Number of Leaves	Leaf Length (cm)	Photosynthetic Rate (µmol CO ₂ m ⁻² s ⁻¹)
Fourwing Saltbush				
Control	31.90± 2.16 a	109.00± 8.30 a	3.55± 0.22 a	7.39± 0.44 a
Well	30.18± 3.29 a	99.50± 4.76 b	4.90± 0.30 b	10.37± 0.39 b
Concentrate	32.13± 1.83 a	168.75± 13.54 b	4.60± 0.36 ab	11.31± 1.16 b
P-value	NS	0.0033	0.0695	0.0047
Switchgrass				
Control	11.50± 1.78 a	7.50± 0.56 a	25.98± 3.12 a	15.40± 1.52 a
Well	4.00± 0.36 b	2.25± 0.22 b	14.08± 1.40 b	12.38± 0.48 ab
Concentrate	4.20± 0.81 b	2.25± 0.22 b	12.53± 1.31 b	8.83± 1.41 b
P-value	0.0047	<0.0001	0.0062	0.0195
Triticale				
Control	10± 0.66 a	14.00± 1.27 a	27.43± 1.35 a	7.35± 0.60 a
Well	12± 0.68 a	21.25± 1.34 b	23.45± 0.75 b	13.74± 1.94 b
Concentrate	11± 0.34 a	17.00± 0.79 a	27.63± 0.32 a	13.59± 0.32 b
P-value	NS	0.0087	0.0344	0.0109
	Sand			
Fourwing Saltbush				
Control	40.2± 2.16 a	180.75± 10.08 a	3.55± 0.27 a	7.91± 0.44 a
Well	45.1± 6.80 a	335.00± 36.07 b	2.48± 0.09 b	7.91± 0.57 a
Concentrate	42.6± 8.33 a	306.25± 24.89 b	2.75± 0.11 ab	10.60± 1.25 b
P-value	NS	0.0322	NS	NS
Switchgrass				
Control	35.55± 5.11 a	18.75± 1.08 a	33.50± 1.33 a	8.02± 0.39 a
Well	29.08± 3.31 a	19.00± 1.70 a	27.38± 3.73 a	15.59± 0.82 b
Concentrate	11.50± 1.82 b	10.50± 2.28 b	17.23± 1.57 b	13.48± 0.99 b
P-value	0.0081	0.0022	0.0008	<0.0001
Triticale				
Control	36.23± 3.75 a	22.25± 2.36 a	20.33± 1.02 a	13.48± 0.70 a
Well	33.13± 4.34 a	33.00± 4.34 a	18.15± 0.56 a	11.89± 0.79 a
Concentrate	18.80± 3.48 b	31.25± 2.41 a	20.28± 2.69 a	11.39± 0.63 a
P-value	0.0484	NS	NS	NS



Figure 2 – Salt effect was visually noticeable in Switchgrass. Species grown in clay (a) is physically stunted more than species grown in sand (b). Plants organized by increasing salinity. Other species did not show visual evidence of differences.

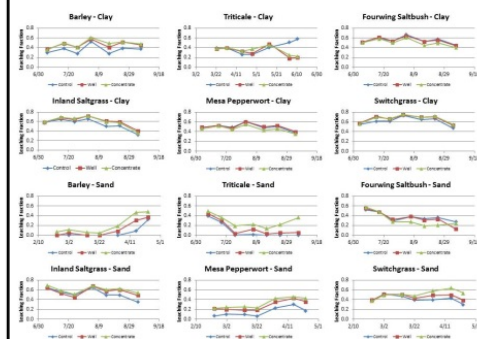


Figure 3 – Leaching fractions (volume of leachate/volume of irrigation) of all species for both soils over time.

Pore Clogging and Solute Movement:

- Two small cores (2 cm x 2 cm) were packed with each soil. Concentrate was applied until cores were saturated and then allowed to dry.
- Cores were subjected to alternate wet and dry cycles.
- Cores were analyzed with a scanning electron microscope, Hitachi S-3400N II.
- Salt deposition was observed both inside the pore and on particle surfaces
- Dual energy CT scans are proposed to distinguish between silicates and other minerals such as calcite (Pacific Northwest National Laboratory, WA)

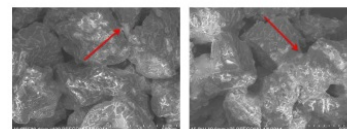


Fig 1 – Salt deposition on sand particles and in the pores.

Summary

- Barley, Triticale, Inland Saltgrass, and Mesa Pepperwort showed little to no variability due to increasing salinity treatments.
- Fourwing Saltbush showed an increase in growth with increasing salinity whereas Switchgrass showed a decrease with increasing salinity.
- Salt accumulation was evident in the pores of the sandy soil columns that could cause reductions in hydraulic conductivity of soil.

Acknowledgment: Funding support from Institute for Energy and the Environment (IEE) through NMSU/Bureau of Reclamation Cooperative Agreement, NMSU Agricultural Experiment Station, Nakayama Endowed Chair

WRRI 59th Annual New Mexico Water Conference

2014 WRRI
59th Annual
New Mexico
Water
Conference

Pore Clogging Due to Irrigation with RO Concentrate

Alison Flores*, Manoj K Shukla

Department of Plant and Environmental Sciences, New Mexico State University, MSC 3Q, P.O. Box 30003, Las Cruces, NM, *E-mail: amflores@nmsu.edu



Introduction

In the southwestern United States, water is a scarce resource due to the arid climate. Low rainfall, high evaporation, low quality groundwater, and dwindling amounts of surface water are contributing to the irrigation water availability problem. There is a growing need for the use of alternate water sources for irrigation. About 75% of the available groundwater is saline (EC>3 dS/m) and requires treatment before it can be used. Often, saline water is treated using reverse osmosis. Brackish Groundwater National Desalination Research Facility (BGNDRF) located in Alamogordo, New Mexico, has a small RO unit for desalination of groundwater. However, the disposal of saline waste (concentrate) generated after desalination is a big challenge. Using the concentrate for agriculture has the potential of cost-effective disposal while sustaining vegetation.

Objective

- Evaluate the effect of irrigation with RO concentrate on soil hydraulic conductivity for two contrasting soil textures.

Methods & Materials

- 16 columns (3.8 cm in diameter and 10 cm in height) were packed (8 with clay soil, 8 with sand) such that the length of displacement was about 8.3 cm.
- One pore volume of RO concentrate from BGNDRF (~9.5 dS/m) applied per week for 20 weeks, then every other week for 4 weeks. Soil allowed to dry between water applications.
- Bulk density was determined just before wetting
- Saturated hydraulic conductivity was determined using the constant head method.

Acknowledgment

Funding support from Institute for Energy and the Environment (IEE) through NMSU/Bureau of Reclamation Cooperative Agreement, PES and NMSU Agricultural Experiment Station and Nakayama Endowment.

Table 1 – Soil texture data for clay and sand

Soil	% Sand	% Silt	% Clay	Texture
1	99.60	0.07	0.33	Fine Sand
2	19.57	28.96	51.47	Clay

Table 2 – Average hydraulic conductivity and bulk density of sand and clay samples

Week	Sand		Clay	
	Hydraulic Conductivity (cm/h)	Bulk Density (g/cm ³)	Hydraulic Conductivity (cm/h)	Bulk Density (g/cm ³)
0	223.30 ± 13.04	0.94 ± 0.01	0	1.57 ± 0.12
4	171.41 ± 3.80	1.29 ± 0.01	4	0.67 ± 0.26
8	180.32 ± 6.00	1.32 ± 0.02	8	0.16 ± 0.02
12	178.82 ± 7.98	1.28 ± 0.02	12	0.15 ± 0.02
16	189.01 ± 11.75	1.27 ± 0.01	16	0.17 ± 0.01
20	204.19 ± 10.12	1.27 ± 0.01	20	0.17 ± 0.01
24	171.90 ± 6.84	1.36 ± 0.01	24	0.22 ± 0.03

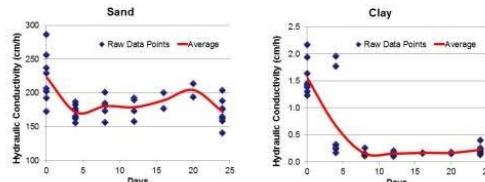


Figure 1 Hydraulic conductivity variations over time during wetting and drying cycles in sand and clay

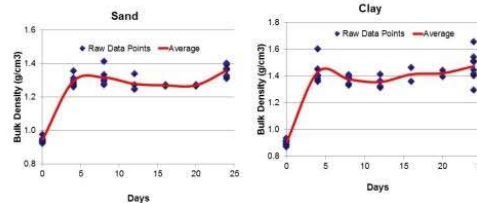


Figure 2 Bulk density variations over time during wetting and drying cycles in sand and clay

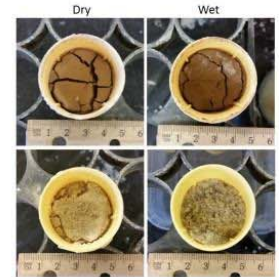


Figure 3 Cracks before and after saturation of clay and sand cells



Figure 4 Salt accumulation at the outlet

Summary

- The decrease in the saturated hydraulic conductivity was observed in both soils (Fig 1).
- An increase in bulk density was observed in both clay and sand columns which could be attributed to settlement during soil wetting.
- Drying produced cracks specially in clay which became smaller after irrigation and attendant swelling (Fig 3)
- Decrease in saturated hydraulic conductivity could be due to accumulation of salt in the soil. Accumulation is also visual at the outlet of the columns (Fig 4).
- Surface crusting occurred in the sand soil that could also have reduced the hydraulic conductivity of sand.
- Pore clogging could be a problem due to continuous RO concentrate application. Clogging could be reduced by maintaining a sufficient leaching fraction.

PAPERS

Biomass as Renewable Energy Source for Water Desalination: A Review

Ali Amiri,^a Catherine E. Brewer^{a,*}

^aDepartment of Chemical & Materials Engineering, New Mexico State University, P.O. Box
30001 MSC 3805, Las Cruces, NM 88003 USA

*Corresponding author: cbrewer@nmsu.edu, phone: 1-575-646-8637, fax: 1-575-646-7706

Abstract

Water desalination is an energy-intensive process needed in many parts of the world to provide fresh water for drinking, agriculture, and industry. The energy for desalination can come from conventional fossil fuels such as petroleum, natural gas and coal, as well as renewable energy sources such as solar, wind, hydro, and geothermal. One renewable energy source that is widely available but currently unused for water desalination is biomass. In this review, we summarize available water desalination technologies, energy requirements and costs, and explore how scale and resource availability create trade-offs in technology selection and design. From there, we present a case for the circumstances in which biomass energy may be suitable for water desalination: small scale capacity needs, infrastructure-poor or rural areas, lower-salinity (brackish) source water, thermal desalination technologies, and an abundant, underutilized biomass supply.

Keywords: water desalination; multiple effect distillation; renewable energy; biomass

1. Introduction

The need for high quality water is dramatically increasing due to rapid population growth, higher per capita water consumption, greater industrial and power generation water use, and expanding agricultural production. Freshwater resources are not capable of meeting these needs as just 3% of earth's water is fresh water. As such, there is need for techniques to purify available but low-quality water. Water desalination is a common technique for providing large quantities of high quality, potable water worldwide. Approximately 50% of the desalination plants are located in the Middle East, 20% in the US, 18% in Europe, and 12% in Asia [1]. The installed desalination capacity throughout the world in 2000 was about 22 million m³ of water per day, requiring approximately 8.5 EJ of energy per year, which is equivalent to 203 million tons of crude oil. Concerns about petroleum-based energy availability and environmental impacts have motivated the exploration of alternative and renewable energy sources for water desalination [2].

In this review, we summarize desalination technologies and energy sources, focusing on multiple effect distillation (MED) and renewable energy. From this summary, we present an argument for the potential of biomass as an energy source for water desalination through a pyrolysis-MED process.

2. Desalination

2.1 Water Quality and Technologies

Water quality is categorized as a function of total dissolved solids (TDS) in parts per million (mg/L): freshwater contains 200 to 700 ppm, treated wastewater contains 700 to 1,500 ppm,

brackish water contains 2,000 to 10,000 ppm, and seawater contains 30,000 to 60,000 ppm. Approximately 58% and 23% of the installed water desalination capacity worldwide are used for treating seawater and brackish water, respectively [3]. In addition to dissolved salts, waters can contain other impurities such as microorganisms, organic matter, suspended solids, silica, etc. that can cause scaling, fouling, and corrosion in the unit. For this reason, efficient pre-treatment and post-treatment techniques to eliminate harmful impurities are often needed.

Depending on the TDS of the water, treatment costs, and infrastructure availability, a variety of desalination techniques can be used; these techniques are grouped into membrane/single-phase processes and thermal/phase-change processes. There are also some new approaches for desalination. Some examples are forward osmosis, ion concentration polarization, super-cavitation evaporation, and capacitive deionization [1, 2, 4, 5].

2.2 Membrane Processes

The two main membrane desalination processes are electro dialysis (ED) and reverse osmosis (RO). Both require electrical energy to drive the separation process. In ED, anion-permeable and cation-permeable membranes, in combination with a cathode and an anode, are used to draw salt ions outward from a dilute feed stream into concentrated brine streams. The electrical power is used to maintain a voltage across the anode and cathode. ED systems, which were developed almost 10 years before RO, are usually used to treat brackish water, and they are more efficient for higher concentrations of highly mobile, small ions.

In RO, which is responsible for more than 88% of the membrane process capacity worldwide, hydraulic pressure is used to overcome osmotic pressure to force water molecules through a semi-permeable membrane (pore sizes less than 10 Å) from a stream with low ion

concentration to a stream with high ion concentration. The osmotic pressure, π , is dependent on the TDS of the dilute and concentrated streams:

$$\pi = \frac{\varphi\gamma cRT}{M}$$

where γ is the number of ions, φ is the osmotic coefficient, c is the difference in salt concentration between the two streams on a mass basis, M is the salt's molecular weight, R is the gas constant, and T is the temperature in Kelvin [4]. For RO to work effectively, the hydraulic pressure provided by a pump on the dilute stream side of the membrane must be significantly higher than the osmotic pressure. RO is usually more cost-effective for water with TDS values less than 5,000 ppm, while ED is more economical for water with TDS values greater than 5,000 ppm [3, 6].

For both ED and RO, membrane scaling and fouling can substantially affect system performance. Water pre-treatments such as filtration, sterilization, and/or chemical additives can be used to prevent scaling and bio-fouling [6, 7]. Compared to thermal desalination systems, membrane processes usually have less risk of scaling and corrosion due to membrane processes' ambient or near-ambient operating temperatures [3]. Post-treatment processes for membrane desalination systems can include hydrogen sulfide removal and/or pH adjustment, depending on the final intended water use. More detailed information on membrane desalination process design and membrane scaling can be obtained in [7, 8].

2.3. Thermal Processes

There are three main types of thermal desalination processes: multi-stage flash distillation (MSF), vapor compression distillation (VC), and multiple effect distillation (MED). All three require low-temperature heat as the main energy input and a small amount of electricity to drive

pumps. Some advantages of thermal desalination processes over membrane desalination processes are higher quality product water, no membrane replacement costs, lower sensitivity to changes in feed water quality, and less rigid monitoring requirements [3, 9, 10].

2.3.1 Multi-Stage Flash Distillation (MSF)

MSF was first developed by Silver at Weir Co. in Glasgow, Scotland in 1960 and is based on seawater evaporation using steam from an external heat source. For many years, MSF has been the “easiest” technology for water desalination and accounts for over 40% of desalination technologies worldwide [5, 6]. The typical capacity for an MSF process is large: 10,000 to 35,000 m³/day. In MSF, seawater is preheated using heat exchangers up to 90-110°C before entering the first stage. Vacuum pumps create a negative pressure difference near seawater’s saturation point in the first stage, causing the seawater to partially flash. The flashed water vapor is condensed by contact with the incoming seawater in the heat exchangers and collected. The remaining concentrated seawater/brine enters the second stage, which is operated at a lower pressure than the first stage. Again, the negative pressure difference causes some of the seawater to flash off and be collected. This process continues until the last stage, which has the lowest temperature and pressure. Sometimes, demisters are used to remove entrained brine droplets from the flashed vapor as these droplets can create salinity in the product water and contribute to scale formation on condenser tubes. The vacuum system removes produced non-condensable gases in order to keep the heat transfer coefficient as high as possible within the stages. To prevent scaling, pre-treatments such as adding acid or advanced scale inhibitors like polyphosphate can be used.

2.3.2 Vapor Compression (VC)

VC is very similar to MSF but only has one evaporation stage and can be run under atmospheric or sub-atmospheric pressure. Hot, pressurized feed water enters the evaporation stage and flashes off, then is condensed and collected. The remaining brine can then be recycled through the process by re-pressurizing it. The VC pressurization can be done using mechanical vapor compression (MVC), which requires additional electricity energy for the pump, or thermal vapor compression (TVC), in which high-pressure steam is injected into the feed stream [4, 6].

2.3.3 Multiple-Effect Distillation (MED)

MED, also known as multiple-effect boiling [2], is the oldest thermal desalination process and has a typical plant capacity of 600 to 300,000 m³/day. MED has been in competition with MSF technically and economically for many years. At the end of 2011, MSF and MED units accounted for approximately 26% and 8.2% of worldwide water production capacity, respectively [11]. Two main advantages of MED over MSF are MED's lower energy consumption due to better heat transfer from the constant temperature difference in MED effects, and the fewer number of effects needed in MED to achieve a given performance ratio (mass of distillate produced per unit mass of input steam) [2, 6].

In the most common configuration of MED, steam from an external heat source is fed into a tube in the first effect. Seawater or brackish water is sprayed onto the steam-filled tube and part of the water flashes into steam. The newly produced steam is then fed into the next effect as the heat source, after which it condenses and is collected. As in MSF, temperature and pressure decrease from the first effect to the last effect [4, 12, 13].

An important design parameter for MED is the gain output ratio (GOR): the ratio of distilled water to input steam flow rates. GOR represents the number of times that the heat of evaporation is reused [5, 6, 14-16]; GOR relates directly to energy efficiency. Yang et al. showed that GOR and water production rate decrease with increasing feed water flow rate and increase with increasing steam flow rate [17]. Zhao et al. observed that, although increasing the feed steam temperature slightly decreased GOR, such a temperature increase decreased the total heat transfer area needed—a result of a greater temperature difference between adjacent evaporators [18].

Another important factor in MED design is the optimization of the number of effects. This number is a function of the temperature difference between the feed steam and the top brine temperature (TBT), as well as the minimum temperature differential within an each evaporator [19]. Having more effects results in more distilled water produced and a higher GOR, however, the capital cost and per kg distilled water cost also increase. Other design factors include TBT and heat transfer area within the effects. At higher TBTs, the number of the effects increases and thus the GOR increases. Generally, an MED can be operated at either a high TBT ($> 90^{\circ}\text{C}$) or a low TBT ($55\text{-}90^{\circ}\text{C}$). Although the heat transfer area and the water production costs for high TBTs are much less than those for low TBTs, high TBTs dramatically increase the amount of corrosion and scaling, as well as the energy consumption. For this reason, low TBT MED is more widely used worldwide than high TBT MED [18, 20, 21].

2.3.3.1 MED Feed Arrangements

There are three main flow arrangements in MED unit design: forward feed, backward feed, and parallel feed; each arrangement has its own advantages and disadvantages [27]. In the

forward feed (FF) arrangement, which is the most common configuration, feed water and steam move in a same direction. As shown in Figure 1.a, the feed water and steam both enter the system in the first effect at their highest temperature and pressure. One of the challenges for the FF arrangement is that a large portion of the energy is required in first evaporator to heat the feed water to its boiling point, meaning that the heat transfer surface area in the first effect is much greater than in the other effects. Regenerative heat exchanges between effects can solve this problem: steam exiting one effect transfers a small amount of its energy to pre-heat the feed stream before moving on to the next effect. Figure 1.b shows how such heat exchangers can be used to heat feed water from an initial feed water temperature to a temperature much closer to the boiling point before entering the first effect.

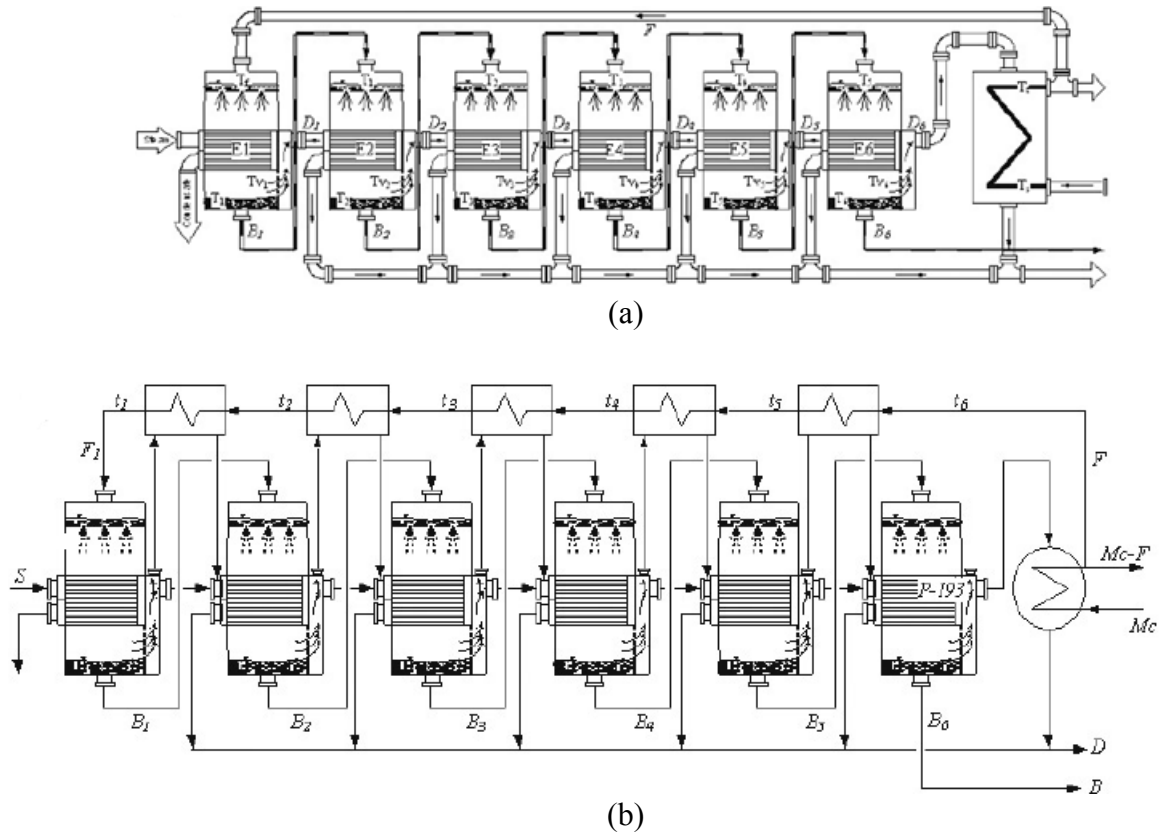


Figure 1. (a) Forward feed flow arrangement and (b) forward feed flow arrangement with regenerative heat exchangers in a six effect, horizontal tube water spray MED unit [22].

In the backward feed (BF) arrangement, the feed water enters the last effect where the temperature and pressure are lowest. The steam enters the system in the first effect, where it comes in contact with the highest salinity brine. The advantage of this system is that high-salinity brine evaporation, which requires the most energy, is done at the highest temperature. The disadvantages of this arrangement are that the high temperatures, pressures, and salinities in the first effect can cause more scaling and fouling, and the movement of feed water from low pressure to high pressure requires additional pumping between effects. Part of the increase in scaling and fouling is because the solubility of calcium salts decreases at higher temperatures.

In the parallel feed (PF) arrangement, new feed water is injected at the top and brine is collected from the bottom of each effect independently, while the heat transfer fluid (feed steam and produced water vapor) still move from one effect to another. In such an arrangement, the salinity within each effect reaches its maximum value, meaning that the greatest amount of fresh water vapor had been removed. Darwish et al. showed that the PF arrangement has larger GORs than FF or BF for 2-6 effects, with the difference in GOR increasing with the number of effects [22].

In addition to the direction of the flow, the side of the heat exchanger (tube side or shell side) in which each steam flows also impacts MED design. Flowing the steam on the tube side and feed water on the shell side has some advantages: less mist carry-over in the produced steam, easier scale removal/cleaning, and easier turbulence generation inside the tubes, which improves heat transfer [12].

2.3.3.2 Scaling and Fouling in MED

Scaling decreases the overall heat transfer coefficient in heat exchangers because of the low thermal conductivity of the scale material. In MED heat exchangers, scale build-up on the outer surface of evaporating tubes increases the wall temperature of the tubes, which, over a prolonged period of time, can lead to crack formation in the tubes, in addition to lower overall MED energy efficiency [23, 24].

Scale formation within MED units is dependent on the concentrations of Ca^{2+} , Mg^{2+} , bicarbonate, and TDS in the water; operating temperature; water residence time; fluid velocity; water pH; rate of CO_2 release; and the roughness of the evaporator construction materials [23, 24]. There are different types of scale deposits including soft, hard, silica, and organic. In research with a MED-VC unit, Al-Jaroudi, et al. observed a 14 mm-thick scale build-up comprised of soft CaCO_3 and hard CaSO_4 , as well as a significant proportion of organic matter [23]. There are three ways to control build-up of CaSO_4 scale: decrease the MED operating temperature, decrease the overall concentration factor (brine TDS/feed water TDS) to keep the brine TDS concentration below the scaling threshold, and soften the feed water by substituting a monovalent cation such as Na^+ for the Ca^{2+} . Magnesium hydroxide is an alkaline scale component that is sometimes observed in MSF or MED systems from high Mg^{2+} ion concentrations in the water. Polyphosphate may be used as a scale inhibitor if the unit's operation temperature is less than 90°C ; hydrolysis of polyphosphate occurs at higher temperatures, which leads to the formation of calcium phosphate. For this reason, polyphosphate is rarely used for MED units. The presence of organic matter in scale build-up may be due to marine life (bio-fouling) or from industrial discharges of oil, grease, wax or paint materials. A hot alkaline treatment can usually remove organic scale build-up. Similar to scale prevention in

MSF, water pre-treatments, a vacuum system, and a demister can also be used to avoid scaling in MED. Even with several management techniques, there is still a chance of scaling in MED units [23].

2.3.3.3 Scaling and Non-Condensable Gases

Non-condensable gases such as CO₂, O₂, and N₂ are released during brine evaporation within the effects or through ambient air leakage into the parts of the unit operating under vacuum. The presence of these gases may cause alkaline scale formation. For example, the combination of dissolved CO₂ in the condensate, which decreases the water pH to acidic conditions, with O₂, may cause corrosion in condenser tubes. De-aeration of the feed water in a titanium tube condenser is a method to decrease the oxygen content within the feed water. CO₂, which dissociates in water to form HCO₃⁻ and CO₃²⁻, is harder to manage. The release rate of CO₂ is highest in the first effect, and at higher water temperatures and salinities [20, 24]. CaCO₃ scale deposition is also highest in the first effect and pH decreases from the first effect to the last effect [25]. Even a low concentration of non-condensable gases within the water can significantly decrease the overall heat transfer coefficient over time, leading to a decrease in evaporator performance [24]. For these reasons, an efficient venting system is critical to control the release of non-condensable gases and prevent scaling, fouling, poor heat transfer, and ultimately, increased energy consumption [26].

2.3.3.4 Scaling and Tube Construction in MED

There are many different ways of arranging the water flow patterns and the steam tubes within MED heat exchangers: water tube-side vs. steam tube-side, falling water film vs. water

spray vs. water immersion, horizontal tubes vs. vertical tubes, smooth tubes vs. corrugated tubes, etc. Four common evaporator combinations are: vertical steam tube-side, vertical water tube-side, horizontal steam tube-side (see Figure 1), and horizontal water tube-side. Among them, horizontal steam tube-side with a falling film water flow has been found to be the most efficient arrangement in terms of energy consumption, thermal characteristics, and simplicity in construction. A tube falling film arrangement is preferred in industry because it lowers the frequency of scaling and carry-over in the tubes due to shorter contact time between the brine and the heat transfer surface, and lowers the vapor velocity which increases the overall heat transfer coefficient, leading to a higher MED system efficiency [5, 19]. Galal et al. showed that the amount of water that can be condensed on the outer surface of corrugated tubes is 1.5 times greater than the amount that can be condensed on smooth tubes. Also, the fouling thermal resistance of corrugated tubes is nearly half that of smooth tubes, leading to higher long-term thermal performance [27].

For low TBT MED, aluminum is preferred over copper because more aluminum tubes can be installed for the same investment costs, leading to more heat transfer area and higher thermal efficiency per amount of produced water; for high TBT MED, however, copper is preferred [19]. Zarkadas et al. studied polymeric hollow fiber (PHF) heat exchangers made of polypropylene (PP) and polyetheretherketone (PEEK), and found that they have the same or even better thermal performance than metal heat exchangers [28]. Other advantages of PHF heat exchangers over metallic ones include smaller volumes, significantly lower pressure drops, less weight, and better resistance to corrosion. The disadvantage of most PHF heat exchangers is that they have a low thermal conductivity (0.1-0.5 W/m·K); this disadvantage can be minimized by using a very small wall thickness [29]. Christmann et al. [34] tested a pilot-scale MED with falling film plate

evaporators composed of PEEK with wall thicknesses of 25 μm and found that the thermal conduction resistance was 10^{-4} K/W, which is the same as that of stainless steel with a wall thickness of 1.5 mm [30]. The low mechanical strength of polymers, however, means that some stabilization measures must be taken if the walls are to withstand pressure differences across the heat transfer surface [30-32].

2.4. Hybrid Desalination Systems

In hybrid desalination systems, a power generation unit is combined with both thermal and membrane processes; such systems are more efficient and economical than “dual-purpose” evaporation systems, where the power generation unit provides both electrical and thermal energy required for desalination but only one kind of process is used [19, 33]. For instance, in RO-MSF, the water exiting the RO unit is fed into an MSF unit. This increases the overall amount of very pure distilled water (since MSF can achieve a lower exit TDS concentration than RO) and decreases the cost of a pre-treatment unit (since the RO system removes most of the salts that would cause scaling problems in the MSF system). An MED-RO or MSF-RO system is also viable, where pre-heated seawater exiting the last effect of an MED or MSF distiller is fed into an RO unit. In this case, a 1°C increase in seawater feed temperature boosts the water production rate in RO by 3% [34]. More information on hybrid systems is available in [34-39].

3. Biomass as an Energy Source

Biomass is unique among renewable energy options in that it can be both a source of energy and a source of materials. In this way, biomass is similar to petroleum and coal. According to the US Department of Energy’s 2011 report, the total annual energy consumption in the US is

approximately 98 billion GJ, 4% of which comes from biomass. The annual biomass production rate in the US is approximately 214 million Mg: 129 million Mg as forest resources and 85 million Mg as agricultural resources [40, 41]. Compared to energy from petroleum or coal, energy from biomass has several disadvantages: 1) lower bulk densities, 2) lower energy contents, 3) higher moisture content (which can create both transportation and storage problems due to weight and decomposition, respectively), and 4) greater heterogeneity [42]. More information about the challenges and prospects of first and second generation biofuel production from biomass is available in Yousuf et al. [43] and Naik et al. [44].

3.1 Biomass Types and Sources

Biomass used for energy usually comes from one of two categories: wastes or dedicated energy crops. Wastes include yard waste, municipal solid waste (MSW), agricultural residues (e.g. rice husks, grain straw, orchard prunings), food waste, logging residues, and animal manure. The main advantage of waste biomass is its relatively low cost; its main disadvantage is the large variation in availability, composition, and characteristics from one season to another, and one location to another [45].

Dedicated energy crops are plants specifically grown for energy production. They include herbaceous crops such as switchgrass and miscanthus, short rotation woody crops such as hybrid poplar, and oleaginous (lipid-rich) crops such as oilseeds and yeasts. Energy crops are optimized for high rates of biomass production and/or high yields of specific plant components, such as fatty acids in oleaginous crops. While food crops (i.e. plant components that contain significant amounts of digestible carbohydrates, proteins, and/or fats) can be used for energy, a goal of dedicated energy crops is to not compete with food production or use prime land resources.

Among woody crops, hardwoods such as willow, poplar, mesquite, and alder, are preferred for most conversion techniques over softwoods due to their lower lignin content. Softwoods, such as pine, are beneficial for construction and thus make up a significant portion of logging and construction residues; these residues are typically used as boiler fuels [41]. In spite of their overall lower productivities compared to herbaceous or woody energy crops, oleaginous crops are popular because they contain long-chain hydrocarbons and relatively low amounts of oxygen, and thus resemble petroleum. For example, soybean and sunflower only produce about 450-1,600 L of biodiesel per hectare compared to corn which can produce 5,800-8,700 L of ethanol per hectare. The hydrocarbons in oleaginous crops include sterols, fatty acids, di-glycerides, tri-glycerides, and waxes; these are frequently used to produce liquid fuels to power engines and generators.

Garcia-Perez et al. provide a useful review of biomass resources, collection methods, transportation considerations, and pretreatments such as drying and grinding in [45].

3.2 Biomass Properties

The suitability of a particular type of biomass for energy production is dependent on several of its properties including composition, heating value, density, and production yield.

One method of characterizing biomass composition is proximate analysis, which measures moisture, volatile matter, fixed carbon, and ash content by thermogravimetric analysis (TGA). Moisture, defined as mass lost upon heating to just above water's boiling point, typically 105°C, represents weight that does not contribute to energy value. Because weight basis can have such large implications for transport, storage, and biomass conversion, it is important to specify whether moisture content is reported on a wet or a dry basis [40]. Dry weight percent is most

commonly used to avoid confusion from large variations in moisture content from one sample to another and over time. Volatile matter is typically defined as the portion of biomass that decomposes into the gas phase under heating in an inert environment. This value is important for designing biomass burners and other thermochemical processing unit operations, especially in relation to the fraction that does not volatilize in an inert environment, i.e. the fixed carbon. Samples with low volatile matter content do not ignite easily (this is why lighter fluid is often needed to start a charcoal barbeque). Ash is composed of the inorganic minerals contained in the plants and any soil contaminating the biomass. Like moisture content, ash represents weight that does not contribute to energy value. In proximate analysis, ash is defined as any material remaining after the sample is combusted in air, usually at temperatures around 750°C.

Another method for characterizing biomass composition is elemental analysis (CHN, CHNO or CHNSO) or ultimate (CHNSO plus Cl) analysis. C and H generally contribute to energy content, while N, O, S, and Cl generally detract from energy content and can lead to emissions problems [40, 41].

Biomass energy content is usually reported as higher heating value (HHV). HHV is the enthalpy released when a fuel reacts with oxygen under isothermal conditions; this measurement assumes the water vapor formed during the reaction is not condensed at the end of the process. Lower heating value (LHV) may also be reported. LHV is defined in the same way as HHV except LHV does not include the latent heat of produced water condensation. HHV is measured directly by oxygen bomb calorimetry. It can also be estimated from correlations using proximate, ultimate, or biochemical composition analyses [40, 46-53].

There are two important kinds of density for evaluating biomass as an energy source: bulk density (kg/m^3), and energy density or volumetric energy content (GJ/m^3). These two

densities are related by HHV and are critical for biomass handling and transportation logistics; the lower the energy density, the more vehicle space is required to transport a given amount of energy. The bulk density of herbaceous biomass typically ranges from 50-200 kg/m³ while that of woody biomass typically ranges from 200-500 kg/m³—well below the densities of fossil fuels (~600-900 kg/m³). Table 1 shows bulk and energy densities for several kinds of fuel. Cellulose is the only plant component with a consistent HHV (~18 MJ/kg) due to its well-defined chemical structure. HHV for lignin varies over a range of 23.3-25.6 MJ/kg [49]. In general, biomass that contains more lignin has a higher energy density than biomass that is mostly carbohydrates.

Table 1. Energy content and densities of different fuels [41, 54]

Fuel	HHV (MJ/kg)	Bulk Density (kg/m ³)	Volumetric Energy Content (GJ/m ³)
Diesel	46	850	39.1
Gasoline	48.24	740	35.7
Coal	18.33-36.67	600-900	11-33
Hardwood	18.92-18.95	280-480	5.3-9.1
Softwood	20	200-340	4-6.8
Agricultural residues	16-18	50-200	0.8-3.6
Nut shells	20.31	64	1.3
Animal manure	17.36	400	6.944
Municipal solid waste (MSW)	19.87	--	--
Orchard prunings	19.05	--	--
Sunflower shells	17.86	64	1.143
Methanol	22.27	790	17.6
Ethanol	29.74	790	23.5
Biomass pyrolysis oil	8.28	1280.2	10.6

3.3 Biomass Densification

One pretreatment method used to overcome the challenges of biomass energy is densification. Densification can increase the bulk and energy densities of biomass by as much as 10 fold. It can also improve particle size and shape homogeneity, and particle durability, making biomass much easier to transport, store, and handle. Densification can be performed with a variety of equipment

including pellet mills, screw extruders, briquette presses, cubers, roller presses, tablet presses, etc.; the first three are the most common methods. Energy consumption and end-product quality differ depending on the densification method. For example, screw extrusion has the highest energy consumption since it shears and mixes the material in addition to compressing it. A hardwood or softwood feedstock with an 8% of moisture content, 2-6 mm particle size, and bulk density of 200 kg/m³ fed through a screw extruder can reach a bulk density of 1400 kg/m³ while its moisture content decreases to 4% [55-57]. Densification end-product quality grades are often determined based on particle size uniformity, durability index, heating value, and moisture, ash, and chloride contents [58]. For some applications, quality certification programs are available. In the case of wood pellets for residential and commercial heating, the common standards are the ENplus quality scheme, the CANplus quality scheme, and the Pellet Fuels Institute (PFI) Standards Program, in the E.U., Canada, and the U.S., respectively [59]. Recent research has focused on expanding the biomass densification market past wood pellets made using pellet mills and standard operating parameters. Adapa et al. [60, 61], Ndiema et al. [62], Li and Liu [63], and Mani et al. [64] have studied the pelletization of agricultural straw, the effects of die pressure (20-140 MPa) on biomass relaxation characteristics, high pressure (34-138 MPa) densification of wood residue, and compaction characteristics of lignocellulosic biomass using an Instron Universal Testing Machine, respectively. Pretreatment processes such as steam explosion, grinding, and torrefaction can be used to decrease densification energy consumption and improve biomass binding. Sarkar et al. showed that the bulk density of switchgrass could be increased from 138 kg/m³ to 499 kg/m³ through densification alone, and up to 598 kg/m³ when densification followed torrefaction at 270°C [65].

3.4 Extracting Energy from Biomass

Due to the exothermic characteristics of carbon-carbon and carbon-hydrogen bond oxidation, lignocellulosic biomass may be burned directly as a solid fuel for process heat, or converted to flammable gases and liquids for later use. There are two broad conversion technology platforms: biological/biochemical and thermochemical/catalytic. The biological/biochemical conversion platform includes hydrolysis, fermentation, anaerobic digestion, and composting; this platform will not be considered here. The thermochemical conversion platform includes gasification, pyrolysis, and torrefaction, (as well as hydrothermal liquefaction (HTL) and solvolysis, which are not considered here).

3.4.1 Combustion

Biomass direct combustion is the complete oxidation of biomass at moderate to high temperatures to produce hot flue gas and ash. The hot flue gas, mostly carbon dioxide and steam, can be used for many applications such as drying and space heating (low pressure), and power generation (high pressure). Combustion furnaces can be direct-fired or indirect fired. In direct-fired furnaces, the fuel is burned in the process steam or the process stream is in direct contact with the flue gases. This contact makes it probable that the process steam will become contaminated by combustion products (tars, ash, etc.) In indirect-fired furnaces, the combustion products are somehow separated from the process stream, such as with thermally conductive walls or with air-to-air heat exchangers.

Furnaces are often integrated with boilers for steam production. The two most common boiler configurations are fire-tube boilers and water-tube boilers. Fire-tube boilers, in which combustion gases are passed through tubes inside a water vessel, are more suitable for gaseous or volatile liquid fuels. Water-tube boilers, as the name implies, pass water through tubes held inside the fire; water-tube boilers

are more complex and are more suitable for solid fuels, such as biomass [41]. Solid fuel furnaces/water-tube boilers can be grouped into grate-fired, suspension, and fluidized bed systems. Grate-fired system combustion efficiency is barely more than 90% due to mass transfer limitations, while the efficiency of the other two systems can exceed 99%. Suspension burners are equipped with pulverizers to reduce the particle size of the fuels and enable entrainment for efficient conversion; their wide-spread implementation, however, has been hindered by their large NO_x emissions caused by high operating temperatures. Fluidized bed burners, due to their excellent mixing and large heat transfer surface areas, can operate at lower temperatures (~850°C) and thus limit their NO_x emissions. Whole tree burners also exist and can decrease wood harvesting and handling costs by eliminating the need for wood chipping [41].

The biomass combustion reaction consists of four stages: 1) warming and drying, 2) pyrolysis, 3) flaming pyrolysis, and 4) char combustion. Oxygen is only needed for the third and fourth stages. The warming and drying stage is endothermic and results in the evolution of associated water. As the temperature increases past 200°C in the second stage, hemicellulose and lignin begin to decompose and volatilize (i.e. pyrolyze). As the volatile gases from pyrolysis exit the biomass particle, they come in contact with oxygen which can result in gas phase reactions to form a flame, H₂O and CO₂. Once the gas phase reactions (third stage) are complete and oxygen can reach the surface of the biomass char remnants, solid-gas oxidation (fourth stage) reactions take place. Depending on the availability of oxygen and char temperature, the produced CO may be oxidized to form CO₂ [41].

Further information about biomass combustion can be found in [42, 66, 67].

3.4.2 Gasification

Gasification is simply combustion at slightly lower temperatures (750-1500°C) with less than the stoichiometric amount of oxygen, forming carbon monoxide and hydrogen (synthesis gas or “syngas”) rather than carbon dioxide and water. Gasification has been in use since 1812 in England, when conversion of coal to gas was needed for illumination purposes (lamps fueled by “town gas”). Syngas is flammable and includes small amounts of CO₂, CH₄, H₂S, and NH₃. If syngas contains a significant amount of N₂ from using air as the oxidant, it is called producer gas. Syngas/producer gas can be used for thermal energy generation in much the same way as natural gas, and as a material feedstock for making liquid fuels and other chemicals. Biomass’ high volatile matter content (70-90%) compared to many coals (30-40%), and the high reactivity of biomass char, make biomass a suitable feedstock for gasification [68]. Two challenges when designing biomass gasification reactors are how to treat incompletely-reacted tars, and how to avoid sintering and other reactor damage from the ash fraction [40]. More information on biomass gasification, syngas cleaning and conditioning, and follow-on reactions can be found in [69-73].

3.4.3 Pyrolysis and Torrefaction

Pyrolysis is the heating and decomposition of biomass in the absence or severe limitation of oxygen to create a distribution of different products. Pyrolysis can be thought of as just the first two stages of combustion. Torrefaction is low temperature pyrolysis (200-300°C) used as a pretreatment to remove water and easily-degradable compounds while increasing biomass friability and energy density [42, 74]. Pyrolysis can be categorized into slow pyrolysis and fast pyrolysis where slow and fast refer to the heating rate (~10°C/min in slow pyrolysis and >500 °C/s in fast pyrolysis) and relative reaction time. Slow pyrolysis is the long-used technology for

producing charcoal; its operating conditions maximize solid yield [42]. Fast pyrolysis uses kinetic controls to optimize the liquid product yield. Both types of pyrolysis are usually conducted at 400-600°C, although slow pyrolysis may be done at lower or higher temperatures to adjust char properties. Biomass pyrolysis products include all three phases: gases (mostly CO, H₂, CO₂, CH₄, C₂H₂, etc.), liquids (bio-oil/tar and water), and solids (biochar and/or ash). The distribution of products changes depending on the biomass used and the operating conditions; a decrease in bio-oil yield results in an increase in biochar and gas yields, and vice versa.

Non-condensable pyrolysis gases can be the product of primary biomass decomposition, as well as the product of secondary tar cracking and char gasification. Gas production is typically favored by higher temperatures, longer reaction times, and smaller particle sizes [42]. Although pyrolysis gas has a low heating value, it is still suitable for thermal energy production and power generation [72, 74]. In a characterization study of pyrolysis gas, Brown et al. [75] showed that carbon monoxide, carbon dioxide, nitrogen, and methane contributed the highest concentrations, respectively. Besides these gases, oxygen and traces of ethylene, ethane, propylene, and C₄ gases were also observed. The heating value increased from 8 to 15 MJ/kg as the pyrolysis temperature increased from 525 to 650 °C, with carbon monoxide and methane providing nearly 80% of the gas heating value [75]. For rice straw pyrolysis, Park et al. [74] also found an increase in gas heating value with temperature: from 4.1-11.4 MJ/kg over 300-700°C, respectively.

Biochar is the carbon-rich solid product of pyrolysis that can be used as a solid fuel, a feedstock for activated carbon adsorbent production, and as a soil amendment to improve soil fertility and sequester carbon [76]. Yields of biochar are usually 15-20% for fast pyrolysis and 20-50% for slow pyrolysis on a dry biomass weight basis. Lignin content in biomass typically favors char formation reactions resulting in higher char yields [76-78]. For a temperature range

of 450-500°C, slow pyrolysis produces about 0.26 kg of char per kg of biomass, with approximately 45% of the biomass carbon being retained in the char [79]. Biochars usually have HHVs similar to those of coals (13-23 MJ/kg), where slow pyrolysis and woody feedstocks favor higher HHVs compared to fast pyrolysis or gasification and herbaceous feedstocks [80].

4. Energy and Water Desalination

4.1 Energy Requirements for Desalination

Water desalination plants use about 4-20 kWh/m³ (14-72 MJ/m³) of electrical energy equivalent to produce fresh water; if thermal energy has to be converted to produce electrical energy (at ~30% efficiency), this value would be approximately 46-240 MJ/m³ [6]. Desalination unit energy consumption contributes about 60% of water production costs [6]. For an energy optimized desalination system, Semiathas showed that the energy costs can be decreased to 30-44% of total water production costs [16].

The amount of energy needed for water desalination is dependent on many factors such as the form of energy (electrical, thermal, etc.), plant capacity, plant design configuration, and feed water TDS. The energy needed for MED and MSF processes is generally much higher than that required for RO because of the water evaporation step in MED and MSF, and significant improvements in RO technology that have lowered its power consumption [2, 81]. Thermal desalination technologies, however, are capable of decreasing the TDS to less than 10 ppm while RO technologies can reduce the TDS to 10 ppm to 500 ppm, depending on the membranes used. The TDS limits for drinking water are typically 400 to 500ppm—much higher than that of water produced in MED and well within the range for RO [6]. For drinking water, therefore, some

untreated feed water can be added to the desalinated water to moderate the TDS concentration and make MED water more cost-effective [82].

Water desalination plant capacities, energy requirements, and produced water costs for small-scale plants are shown in Table 2. As expected, energy and cost requirements for small-scale plants are much higher than those for large-scale plants. All of the energy requirement values assume that chemical energy from biomass is converted to thermal energy and that thermal energy is converted to needed electrical energy at an efficiency of 30% to account for thermodynamics. For example, if 1 kWh/m³ (3.6 MJ/m³) of electrical energy was described in the original reference, the table will list 12 MJ/m³ of thermal energy.

4.1.1 Energy Consumption in RO

A typical RO unit, with an energy recovery system and a plant capacity of up to 128,000 m³/day for seawater and 98,000 m³/day for brackish water, consumes 14.4-21.6 MJ/m³ (4-6 kWh/m³) and 5.4-9 MJ/m³ of electrical energy, respectively. This difference in energy requirements is the main cost difference between treating seawater and brackish water by RO [4]. High TDS concentrations result in more energy consumption at a rate of approximately 3.6 MJ/m³ (1 kWh/m³) per 10,000 ppm [45].

4.1.2 Energy Consumption in MSF

The factors that affect energy consumption in MSF systems are temperature of the heat sink, number and geometry of the stages, feed water TDS concentration, unit construction materials, and heat exchanger configuration. Increasing the GOR, the number of stages, and the heat transfer surface area are all ways to lower energy consumption [6, 8, 16, 21]. From design

information provided by commercial manufacturers, a typical MSF, with a production rate of 50,000-70,000 m³/day and a GOR of 8-12, consumes between 190 MJ/m³ and 282 MJ/m³ of thermal energy, and 13.5 MJ/m³ (3.75 kWh/m³) of electrical energy [6, 16].

4.1.3 Energy Consumption in MED

Similar to MSF, MED needs thermal energy for water evaporation and electrical energy to power pumps. A typical MED unit, with a production rate of 5,000-15,000 m³/day, a top brine temperature (TBT) of 64-70°C, and a GOR of 10-16, requires 145-230 MJ/m³ of thermal energy and 8.1 MJ/m³ (2.25 kWh/m³) of electrical energy. The energy consumption for both MSF and MED could be decreased significantly if they used cogeneration power plants, where waste steam from the power turbine exhaust provides the initial thermal energy [6, 16].

4.1.4 Energy Consumption in VC

Mechanical vapor compression (MVC) only requires electrical energy. A MVC unit, with a production rate of 100-3,000 m³/day and a TBT of 74°C, requires 25.2-43.2 MJ/m³ (7-12 kWh/m³). A thermal vapor compression (TVC) unit, with a production rate of 10,000-30,000 m³/day, a GOR of 12, and a TBT of 63-70°C, requires 227.3 MJ/m³ of thermal energy and 5.7-6.48 MJ/m³ (1.6-1.8 kWh/m³) of electrical energy [6, 16].

4.2 Fossil Fuel Energy and Water Desalination

Conventional water desalination technologies, especially those with the highest capacities in the Middle East, are powered by fossil fuels such as coal, crude oil, and natural gas. Concerns about future availability, greenhouse gas emissions, and environmental impacts of fossil fuels

has helped focus future water desalination technologies (and power generation in general) towards energy efficiency and renewable energy [83].

Nisan et al. showed that, at present coal prices, the integration of RO or MED water desalination systems with circulating fluidized bed, coal-fired power plants would result in the lowest power and desalination costs, while oil-fired power production would result in the highest desalination costs. From an environmental impact analysis perspective, RO with a combined cycle gas turbine power plant had the lowest emissions of NO_x, SO_x, CO₂, and particulates, while MSF with a coal-fired power plant had the highest emissions [83]. Methnani has shown that RO water desalination, coupled with any type of fossil fuel, would have lower costs than MED due to the lower energy requirements for RO. This difference in costs, however, is generally negligible except when treating very high salinity water [84]. The use of pulverized coal rather than lump coal in power plants results in higher efficiency for the boiler (and the whole desalination system) since more of the furnace volume is used and the coal is more completely combusted [85].

4.3. Renewable Energy and Water Desalination

The integration of renewable energy with desalination is especially suitable for remote areas and areas lacking connection to electrical energy grid infrastructure; in some cases, solar is the only feasible option due to distance from other resources [86, 87]. The most popular renewable energy sources for water desalination units have been solar photovoltaic (PV), solar thermal, wind, and geothermal, and hybrids of these options. Factors to consider when pairing renewable energy and desalination technologies include type, amount, and cost of energy available, site topography and geographical conditions, plant size, feed water salinity, capital costs, treatment

requirements, and local infrastructure. 13% of renewable energy powered desalination systems worldwide are solar-MED, while 6% are solar-MSF. Eltawil et al. provide a very useful table of combinations of renewable energy sources and water desalination methods in [3].

4.3.1 Solar Energy and Water Desalination

Solar energy may be used for water desalination unit indirectly, such as by connecting a solar collector to a desalination system, or directly, such as within a solar still where collection and desalination occur in a single unit.

Both MED and MSF can be used with solar collectors providing steam. The first method is direct steam generation (DSG), which uses parabolic trough collectors and fresh water, brine, or seawater as the heat transfer fluid [88]. In a solar DSG-MED system, the solar collector plays the role of the first effect: feed water, pre-heated in the MED, enters the solar collector and is partially evaporated by solar energy. The steam generated in the collector is then used as the heat source in the second effect. In such a system, the initial steam is generated from the feed water/brine rather than fresh water [89]; however, fresh water may also be used for steam production [90]. The second method for steam production in solar-MED systems also uses parabolic trough collectors but uses oil to transfer heat to the first effect. The third method for steam production is flashing pressurized water in a flash drum after it has been heated in the solar collector. Depending on climate conditions, any of these three methods may be used to enhance fresh water production [2, 88, 91, 92].

For direct solar water desalination, a conventional solar still uses a blackened bottom surface to absorb solar energy and the green-house effect to evaporate salty water within a V-shaped glass envelope. Solar still efficiency, the ratio of energy utilized in water evaporation to the solar

energy incident on the glass cover, has a maximum value of approximately 35%. For more information on solar stills, see [2, 93-95].

Raluy et al. observed that for MSF units integrated with solar thermal energy, 63% of airborne emissions, including CO₂, NO_x, SO_x, and non-methane volatile organic compounds, decreased compared to MSF units using conventional fossil fuel boilers. The use of solar energy, however, requires special raw materials for cell and panel production compared to other renewable energies and, therefore, has more environmental impacts. Also, solar energy is available just part of the day (about 25% of the time) and thus, the cost of water produced through solar desalination is higher than that of water produced through conventional energy-powered desalination [1].

4.3.2 Hydroelectric Energy and Water Desalination

Hydropower is generated from the gravitational potential energy stored in water by damming rivers. Low-temperature waste heat from a hydropower turbine can be used as the thermal energy source for MSF and MED. Hydro-MSF has been shown to be the most effective combination in terms of reducing airborne emissions (79% decrease) compared to fossil fuel-MSF; the results were similar (71% emissions decrease) for hydro-MED [1, 96, 97].

4.3.3 Wind Energy and Water Desalination

Wind, the result of atmospheric pressure differences caused by solar energy, is a suitable energy source for powering desalination units, especially for remote areas with high wind speeds such as islands [2, 98]. Because of weather-related wind speed fluctuations, efficient back-up power systems such as diesel generators, batteries, or flywheels are needed to stabilize the

energy production rates [99, 100]. One significant advantage of wind energy is its low cost compared to other renewable technologies. Wind is locally available and does not require much water transportation from treatment location to end user. Wind turbines can be coupled with several desalination technologies, though they have mostly been used with RO systems. The amount of treated water that can be produced effectively by a wind-RO system is 50-2,000 m³/day [3, 6]. A useful overview of wind energy has been provided by Ackermann [101]. More information on wind-powered desalination is available in [87, 98, 102-107].

4.3.4 Geothermal Energy and Water Desalination

Geothermal energy is heat stored beneath the earth's surface. Geothermal reservoirs can be low temperature (<150°C) or high temperature (>150°C); temperature directly affects which applications can make use of the stored energy. Medium to high temperature geothermal reservoirs can provide energy for either membrane or thermal desalination processes. One advantage of geothermal energy is that there is no need for additional energy storage reservoir heat supply is continuous and predictable. Ophir showed that a geothermal-desalination plant would cost as much as a large multi-effect dual-purpose desalination plant [108]. As described in a report by Awerbuch [109], the first geothermal-desalination pilot plant was built in Holtville, California in 1972, funded by U.S. Bureau of Reclamation [3, 6]. Pilot-scale geothermal-MED plants have been designed and tested in France [110] and southern Tunisia [111]; the evaporators and condensers for these units were made of polypropylene and the unit operating temperature was 60-90°C [112]. Sometimes, brine from geothermal desalination systems can be used directly as the feed water/heat source for thermal desalination, or even RO, if the membranes can withstand higher temperatures (60-90°C). If a geothermal reservoir can provide high enough

pressure water, it can provide shaft energy for mechanically driven desalination processes [113, 114].

4.3.5 Biomass Energy and Water Desalination

The literature is nearly silent on biomass energy for water desalination. Eltawil et al. described the use of biomass for water desalination energy as not being “a promising alternative since organic residues are not normally available in arid regions and the growing of biomass requires more fresh water than it could generate in a desalination plant” [3]. For most situations, this conclusion is reasonable, especially when large water treatment capacities are needed, the feed is high salinity seawater, or the biomass is grown only for energy production. In situations where very small plant capacities are needed, where significant amounts of local agricultural, forestry, or urban biomass residues are available and underutilized, and/or where the feed water is of relatively low salinity, biomass use may be feasible alternative.

For example, in New Mexico in the southwestern U.S., the climate is warm to hot and semi-arid to arid, enabling agricultural production through irrigation with ground water. This ground water has varying levels of salinity, from fresh to brackish. Residues from agriculture including pecan orchard prunings and shells [115], cotton gin trash [116], and dairy manure, in addition to urban yard waste, are locally available. In this scenario, biomass might conceivably serve as the energy source for a farm-scale irrigation or neighborhood-scale drinking water thermal water desalination plant. Combustion, gasification, or pyrolysis could be used to directly convert biomass into thermal energy. A slow pyrolysis process would have the added advantage of producing a value-added biochar product that would be used as an adsorbent for additional water treatment or as a soil amendment for improved soil water use efficiency and fertility [117-121].

Table 2. Water desalination plant capacities, thermal energy requirements (assuming a 30% efficiency for conversion of thermal energy to electrical energy if electricity is required), and water production costs for small-scale (<100 m³/day) conventional and renewable energy source-desalination technologies.

Method	Size (m ³ /day)	Water	Energy (MJ/m ³)		Cost (US\$/m ³)	Ref.
			Electrical	Thermal		
Conventional MED (single-purpose)	<100	Seawater	-	-	2.0-8.0	[6]
Diesel MED	4	Brackish	-	1,110	26.50	[122]
Conventional RO	20-1,200	Brackish	-	-	0.78-1.33	[123]
Solar Still	<100	-	0	Passive solar	1.3-6.5	[6]
Solar Multiple Effect Humidification	1-100	-	18	355	2.6-6.5	[6]
Solar MED	1	Brackish	-	-	25.3	[87]
Solar MED	72	Seawater	-	-	3.6-4.35	[87]
Solar Membrane Distillation	0.15-10	-	0	540-708	10.5-19.5	[6]
Solar PV RO	<100	Seawater	48-72	0	11.7-15.36	[6]
Solar PV RO	<100	Brackish	18-48	0	6.5-9.1	[6]
Solar PV ED	<100	-	18-48	0	10.4-11.7	[6]
Wind RO	19	Seawater	-	-	4.4-7.3	[87]
Wind RO	12	Seawater	-	-	2.6	[87]
Wind MVC	<100	-	84-144	0	5.2-7.8	[6]
Geothermal MED	80	-	24-36	149-289	2.0-2.80	[6]

5. Economics

5.1 Economics of Water Desalination Plants

The costs for a water desalination plants may be grouped into capital costs and operational costs. Capital costs are one-time costs and include direct construction costs, such as land, equipment, buildings, and wells/surface water intake and concentrate disposal infrastructure, and indirect construction costs. Operational costs are recurring costs and include fixed costs such as insurance and amortization (usually 0.5% and 5-10% of the total capital costs, respectively) and variable costs such as maintenance, labor, energy, chemicals, supplies, etc. For a typical seawater

RO plant, capital costs and energy costs represent 37% and 44%, respectively, of the total costs. For a similar thermal desalination plant, the capital cost fraction is lower (32%) and the energy costs higher (50%) because of the higher energy requirement per cubic meter of produced water for thermal systems [3, 81].

Energy consumption and hence, the final produced water cost, is significantly reduced in thermal desalination units if the power source is dual-purpose, i.e. the turbine is directly integrated with the desalination unit so that low-temperature exhaust heat energy provides the primary steam for desalination [19]. For example, the produced water cost of a 6 million gallon per day (22,700 m³/day) single-purpose MED unit would be 0.739 cents/gallon (1.95 US\$/m³), while the produced water cost from a similar capacity dual-purpose unit would decrease to 0.330 cents/gallon (0.87 US\$/m³). Use of corrosion-resistant materials for heat transfer surfaces also decreases the capital and long-term energy costs for thermal desalination processes due to reduced scaling [3].

Fresh water produced in conventional (fossil fuel-powered) MED plants with capacities of >90,000 m³/day costs approximately 0.52-1.01 US\$/m³. As the capacity of the MED plant decreases to 12,000-50,000 m³/day, the produced water cost increases to 0.95-1.95 US\$/m³. The estimated produced water cost for an MSF plant with a capacity of 23,000-528,000 m³/day is 1.75-0.52 US\$/m³, respectively [6].

5.2 Economics of Coupling Renewable Energy and Water Desalination

Although many forms of renewable energy are available for free or very low cost, there are often significant capital costs for renewable energy systems, which result in dramatically higher produced water costs, especially at the smaller scale (see Table 2). These costs can be decreased

with continuous improvements in renewable energy systems and power-saving strategies.

Currently, renewable energy-powered water desalination systems are economically feasible only in rural communities with no access to an electrical grid, and/or where solar and wind resources are abundant.

The water production cost for a concentrated solar power-MED system with a production capacity of about 5,000 m³/day, a thermal energy requirement of 147-289 MJ/m³, and an electrical energy requirement of 2.5 kWh/m³ (9 MJ/m³) would be 2.40-2.80 US\$/m³ [6, 81]. A typical geothermal-MED system, with a capacity of 80 m³/day, a 80-100°C energy source, and the same energy requirements as the concentrated solar power system, would have a water production cost of 2.00-2.80 US\$/m³ [6]. Solar PV-RO and PV-ED are promising technologies in terms of economics; the main disadvantages of these systems are the low availability (and therefore high cost) of large PV arrays [3].

6. Small-Scale Water Desalination Technologies

Much of the world's water desalination capacity is large-scale, fossil fuel-powered, seawater desalination. In general, produced water cost increases as plant capacity decreases and renewable energy sources are used. Small-scale desalination systems and their economics, however, are very important for small, rural communities where the available water is brackish or contaminated.

Sen et al. have focused on designing small-scale desalination systems for rural communities in India to address such concerns [82]. They developed a micro-scale MED system, initially powered by diesel, with 3 effects, a FF arrangement, a GOR of 3.6, and a fresh water production rate of 11-12 L/hr (0.27 m³/day). The unit can decrease the TDS of the water from 750 ppm to

<10 ppm, well below the required TDS for potable water [12]. In another series of studies on small-scale MED unit design and operating parameters, Sen et al. experimented with 3, 6 and 9-effect systems, vertical tube evaporators using falling film water flow, and parallel feed alternatives. They found that a steam flow rate of 30 kg/hr at 4 bar, and a feed water flow rate of 100 kg/hr, were satisfactory to meet design goals. The produced steam from the boiler was 130-140°C and the feed water was heated to 110-112°C [12, 122, 124]. The 9-effect MED, at semi-optimized parameters, produced 4 m³/day of distilled water and required approximately 1110 MJ/m³ of thermal energy at a cost of approximately 26.5 US\$/m³ (assuming a diesel energy content of 43 MJ/L, a cost of 0.86 US\$/L, and a density of 0.832 kg/L) [122]. These very high energy and cost values are expected to decrease with improvements in boiler efficiency, insulation to prevent heat losses, and continuing adjustments to the heat exchangers. Long-term goals for this research include increasing ease of fabrication, decreasing costs, and incorporating biomass-derived energy to replace the diesel fuel.

Biomass, with its relatively high moisture, oxygen, and ash content, and low bulk and energy densities, is best suited for small scale applications as transportation costs increase quickly with increasing distances [125]. As such, biomass makes a less-than-ideal energy source compared to fossil fuels and electricity. Non-food biomass, however, is abundant in many places in the form of agricultural residues, forestry residues, yard waste, construction wood waste, and municipal solid wastes (cloth, paper, cardboard, etc.) [126]. Many of these residues go underutilized in landfills, especially in rural areas where there is less pressure for waste valorization. For those rural areas that require small-scale water desalination, communities should consider biomass-powered water treatment systems; such systems may not represent optimized energy efficiency

or costs, but they may allow communities to meet their needs with the resources they already have. Biomass should also be considered as a supplement to solar power during off-peak times.

Conclusions

Different kinds of renewable energy-powered water desalination methods and technologies are available. For most scenarios, using renewable energy sources is much more expensive than conventional energy sources due to high capital costs. Improvements in energy efficiency and renewable energy collection/conversion technologies has somewhat driven down these costs, and the environmental benefits of using renewable energy sources has helped shrink the overall advantages of conventional energy systems. Much more research is needed for optimized site-specific renewable energy-powered water desalination system design.

If biomass is to be a feasible energy source for water desalination, a small-scale thermal desalination system in a rural area with lower salinity (brackish) feed water and abundant waste biomass is the most promising scenario. The economics of such a system would be significantly improved if the energy conversion method can produce other valuable products such as biochar.

Acknowledgements

The authors would like to acknowledge financial support for this research from a cooperative agreement between the Institute for Energy & the Environment at New Mexico State University and the U.S. Bureau of Reclamation.

References

- [1] RG Raluy, L Serra, J Uche. Life cycle assessment of desalination technologies integrated with renewable energies. *Desalination* 2005; 183: 81-93.
- [2] SA Kalogirou. Seawater desalination using renewable energy sources. *Prog. Energ. Combust.* 2005; 31: 242-81.
- [3] MA Eltawil, Z Zhengming, L Yuan. A review of renewable energy technologies integrated with desalination systems. *Renew. Sust. Energ. Rev.* 2009; 13: 2245-62.
- [4] R Semiat, D Hasson. Water desalination. *Rev. Chem. Eng.* 2012; 28: 43-60.
- [5] DS Likhachev, F-C Li. Large-scale water desalination methods: a review and new perspectives. *Desalination and Water Treatment* 2013; 51: 2836-49.
- [6] A Al-Karaghoul, LL Kazmerski. Energy consumption and water production cost of conventional and renewable-energy-powered desalination processes *Renew. Sust. Energ. Rev.* 2013; 24: 343-56.
- [7] G Braun, W Hater, Cz Kolk, C Dupoirion, T Harrer, T Götz. Investigations of silica scaling on reverse osmosis membranes. *Desalination* 2010; 250: 982-4.
- [8] M Elimelech, WA Phillip. The future of seawater desalination: energy, technology, and the environment. *Science* 2011; 333: 712-7.
- [9] A Hanson, W Zachritz, K Stevens, L Mimbela, R Polka, L Cisneros. Distillate water quality of a single-basin solar still: laboratory and field studies. *Sol. Energy* 2004; 76: 635-45.
- [10] S Kalogirou. Survey of solar desalination systems and system selection. *Energy* 1997; 22: 69-81.
- [11] 2011-2012 IDA Desalination Yearbook. Global Water Intelligence, London, 2012.

- [12] PK Sen, PV Sen, A Mudgal, SN Singh, SK Vyas, P Davies. A small scale multiple-effect distillation (MED) unit for rural micro enterprises: Part I--design and fabrication. *Desalination* 2011; 279: 15-26.
- [13] M Al-Shammiri, M Safar. Multi-effect distillation plants: state of the art. *Desalination* 1999; 126: 45-59.
- [14] F Manenti, M Masi, G Santucci, G Manenti. Parametric simulation and economic assessment of a heat integrated geothermal desalination plant. *Desalination* 2013; 317: 193-205.
- [15] H-J Joo, H-Y Kwak. Performance evaluation of multi-effect distiller for optimized solar thermal desalination. *Appl. Therm. Eng.* 2013; 61: 491-9.
- [16] R Semiat. Energy issues in desalination processes. *Environ. Sci. Technol.* 2008; 42: 8193-201.
- [17] L Yang, S Shen, H Hu. Thermodynamic performance of a low temperature multi-effect distillation experimental unit with horizontal-tube falling film evaporation. *Desalination and Water Treatment* 2011; 33: 202-8.
- [18] D Zhao, J Xue, S Li, H Sun, Q-d Zhang. Theoretical analyses of thermal and economical aspects of multi-effect distillation desalination dealing with high-salinity wastewater. *Desalination* 2011; 273: 292-8.
- [19] A Ophir, F Lokiec. Advanced MED process for most economical sea water desalination. *Desalination* 2005; 182: 187-98.
- [20] A Ophir, A Gendel. High performance MED plants. In: R. Semiat, D. Hasson (Eds.) 8th Annual Israel Desalination Society Conference: Innovations and Applications of Sea-Water and Marginal Water Desalination, Haifa, Israel, 2006.

- [21] JE Miller. Review of Water Resources and Desalination Technologies, SAND 2003-0800. Sandia National Laboratories, Albuquerque, NM, 2003, p. 54.
- [22] MA Darwish, HK Abdulrahim. Feed water arrangements in a multi-effect desalting system. *Desalination* 2008; 228: 30-54.
- [23] SS Al-Jaroudi, A Ul-Hamid, JA Al-Matar. Prevention of failure in a distillation unit exhibiting extensive scale formation. *Desalination* 2010; 260: 119-28.
- [24] K Al-Anezi, N Hilal. Scale formation in desalination plants: effect of carbon dioxide solubility. *Desalination* 2007; 204: 385-402.
- [25] AE Al-Rawajfeh. $\text{CaCO}_3\text{-CO}_2\text{-H}_2\text{O}$ system in falling film on a bank of horizontal tubes: model verification. *J. Ind. Eng. Chem.* 2010; 16: 1050-8.
- [26] AE Al-Rawajfeh, H Glade, HM Qiblawey, J Ulrich. Simulation of CO_2 release in multiple-effect distillers. *Desalination* 2004; 166: 41-52.
- [27] T Galal, A Kalendar, A Al-Saftawi, M Zedan. Heat transfer performance of condenser tubes in an MSF desalination system. *J Mech Sci Technol* 2010; 24: 2347-55.
- [28] DM Zarkadas, B Li, KK Sirkar. Polymeric hollow fiber heat exchangers (PHFHES): a new type of compact heat exchanger for lower temperature applications. In: *ASME Summer Heat Transfer Conference*, ASME, San Francisco, 2005.
- [29] X Yan, B Li, B Liu, J Zhao, Y Wang, H Li. Analysis of improved novel hollow fiber heat exchanger. *Appl. Therm. Eng.* 2014; 67: 114-21.
- [30] JBP Christmann, LJ Krätz, H-J Bart. Novel polymer film heat exchangers for seawater desalination. *Desalination and Water Treatment* 2010; 21: 162-74.
- [31] L Zaheed, RJJ Jachuck. Review of polymer compact heat exchangers, with special emphasis on a polymer film unit. *Appl. Therm. Eng.* 2004; 24: 2323-58.

- [32] G Hetsroni, A Mosyak. Heat transfer and pressure drop in a plastic heat exchanger with triangular channels. *Chem. Eng. Process.* 1994; 33: 91-100.
- [33] J Uche, L Serra, A Valero. Thermo-economic optimization of a dual-purpose power and desalination plant. *Desalination* 2001; 136: 147-58.
- [34] OA Hamed. Overview of hybrid desalination systems — current status and future prospects. *Desalination* 2005; 186: 207-14.
- [35] E Cardona, S Culotta, A Piacentino. Energy saving with MSF-RO series desalination plants. *Desalination* 2003; 153: 167-71.
- [36] AM Helal, AM El-Nashar, E Al-Katheeri, S Al-Malek. Optimal design of hybrid RO/MSF desalination plants Part I: Modeling and algorithms. *Desalination* 2003; 154: 43-66.
- [37] AM Helal, AM El-Nashar, ES Al-Katheeri, SA Al-Malek. Optimal design of hybrid RO/MSF desalination plants Part II: Results and discussion. *Desalination* 2004; 160: 13-27.
- [38] D Manolakos, G Papadakis, D Papantonis, S Kyritsis. A simulation-optimisation programme for designing hybrid energy systems for supplying electricity and fresh water through desalination to remote areas: Case study: the Meressini village, Donoussa island, Aegean Sea, Greece. *Energy* 2001; 26: 679-704.
- [39] K Thu, Y-D Kim, G Amy, WG Chun, KC Ng. A hybrid multi-effect distillation and adsorption cycle. *Appl. Energ.* 2013; 104: 810-21.
- [40] P Quaak, H Knoef, H Stassen. *Energy from Biomass: A Review of Combustion and Gasification Technologies.* The World Bank, Washington, D.C., 1999, p. 78.
- [41] RC Brown, TR Brown. *Biorenewable Resources: Engineering New Products from Agriculture.* 2nd ed., Wiley-Blackwell, Danvers, MA, 2014.
- [42] R Zanzi. *Pyrolysis of Biomass In, Kungl Tekniska Hogskolan Stokholm,* 2001.

- [43] A Yousuf. Biodiesel from lignocellulosic biomass - Prospects and challenges. *Waste Management* 2012; 32: 2061-7.
- [44] SN Naik, VV Goud, PK Rout, AK Dalai. Production of first and second generation biofuels: A comprehensive review. *Renewable & Sustainable Energy Reviews* 2010; 14: 578-97.
- [45] M Garcia-Perez, C Kruger, M Fuchs, S Sokhansanj. Methods for Producing Biochar and Advanced Bio-fuels in Washington State (Part II: From field to pyrolysis reactor). Washington State University
2012.
- [46] SA Channiwala, PP Parikh. A unified correlation for estimating HHV of solid, liquid and gaseous fuels. *Fuel* 2002; 81: 1051-63.
- [47] T Cordero, F Marquez, J Rodriguez-Mirasol, JJ Rodriguez. Predicting heating values of lignocellulosics and carbonaceous materials from proximate analysis. *Fuel* 2001; 80: 1567-71.
- [48] KH Kim, X Bai, MR Rover, RC Brown. The effect of low-concentration oxygen in sweep gas during pyrolysis of red oak using a fluidized bed reactor. *Fuel* 2014; 124: 49-56.
- [49] CD Sheng, JLT Azevedo. Estimating the higher heating value of biomass fuels from basic analysis data. *Biomass & Bioenergy* 2005; 28: 499-507.
- [50] D Tillman. *Wood as an energy resource* Academic Press, New York 1978.
- [51] L Jiménez, F González. Study of the physical and chemical properties of lignocellulosic residues with a view to the production of fuels. *Fuel* 1991; 70: 947-50.
- [52] K Annamalai, JM Sweeten, SC Ramalingam. Estimation of gross heating values of biomass fuels. *Transactions of the ASAE* 1987; 30: 1205-8.
- [53] F Shajizadeh, W Degroot. *Thermal uses and properties of carbohydrates and lignins* Academic Press, New York, 1976.

- [54] M Erol, H Haykiri-Acma, S Kucukbayrak. Calorific value estimation of biomass from their proximate analyses data. *Renewable Energy* 2010; 35: 170-3.
- [55] C Thoreson, K Webster, M Darr, E Kapler. Investigation of process variables in the densification of corn stover briquettes. *Energies* 2014; 7: 4019-32.
- [56] YN Shastri, Z Miao, LF Rodríguez, TE Grift, AC Hansen, KC Ting. Determining optimal size reduction and densification for biomass feedstock using the BioFeed optimization model. *Biofuels, Bioproducts and Biorefining* 2014; 8: 423-37.
- [57] JS Tumuluru, CT Wright, JR Hess, KL Kenney. A review of biomass densification systems to develop uniform feedstock commodities for bioenergy application. *Biofuels, Bioproducts and Biorefining* 2011; 5: 683-707.
- [58] Pellet Fuels Institute Standard Specification for Residential/Commercial Densified Fuel. In: Pellet Fuels Institute, Arlington, VA, 2011, p. 10.
- [59] C Wiberg. Wood Pellet Quality Schemes. In: *Biomass Magazine*, BBI International, 2014.
- [60] Adapa PK, Bucko J, Tabil LG, Schoenau G, Sokhansanj S. Pelleting Characteristics of Fractionated Suncure and Dehydrated Alfalfa Grinds. In: ASAE/CSAE North-Central Intersectional Meeting, Saskatoon, Canada, 2002.
- [61] Adapa PK, Schoenau GJ, Tabil LG, Sokhansanj S, Crerar B. Pelleting of Fractionated Alfalfa Products. In: ASAE Annual International Meeting, Las Vegas, Nevada, USA, 2003.
- [62] CKW Ndiema, PN Manga, CR Rutttoh. Influence of die pressure on relaxation characteristics of briquetted biomass. *Energy Conversion and Management* 2002; 43: 2157-61.
- [63] YD Li, H Liu. High-pressure densification of wood residues to form an upgraded fuel. *Biomass & Bioenergy* 2000; 19: 177-86.

- [64] S Mani, LG Tabil, S Sokhansanj. Specific energy requirement for compacting corn stover. *Bioresource Technology* 2006; 97: 1420-6.
- [65] M Sarkar, A Kumar, JS Tumuluru, KN Patil, DD Bellmer. Gasification performance of switchgrass pretreated with torrefaction and densification. *Applied Energy* 2014; 127: 194-201.
- [66] BM Jenkins, LL Baxter, TR Miles. Combustion properties of biomass. *Fuel Processing Technology* 1998; 54: 17-46.
- [67] C Branca, C DiBlasi. Global kinetics of wood char devolatilization and combustion. *Energy Fuels* 2003; 17: 1609-15.
- [68] R Zanzi, K Sjöström, E Björnbom. Rapid pyrolysis of agricultural residues at high temperature. *Biomass and Bioenergy* 2002; 23: 357-66.
- [69] K Matsuoka, K Kuramoto, T Murakami, Y Suzuki. Steam Gasification of Woody Biomass in a Circulating Dual Bubbling Fluidized Bed System. *Energy Fuels* 2008; 22: 1980-5.
- [70] V Skoulou, G Koufodimos, Z Samaras, A Zabaniotou. Low temperature gasification of olive kernels in a 5-kW fluidized bed reactor for H₂-rich producer gas. *International Journal of Hydrogen Energy* 2008; 33: 6515-24.
- [71] KJ Timmer. Carbon conversion during bubbling fluidized bed gasification of biomass. In: *Mechanical Engineering*, Iowa State University, Ames, IA, 2008, p. 171.
- [72] G Chen, J Andries, Z Luo, H Spliethoff. Biomass pyrolysis/gasification for product gas production: the overall investigation of parametric effects. *Energy Conversion and Management* 2003; 44: 1875-84.
- [73] RZ Vigouroux. Pyrolysis of Biomass. In: *Chemical Engineering and Technology*, Royal Institute of Technology, Stockholm, 2001.

- [74] J Park, Y Lee, C Ryu, YK Park. Slow pyrolysis of rice straw: Analysis of products properties, carbon and energy yields. *Bioresource Technology* 2014; 155: 63-70.
- [75] AL Brown, PD Brady, CD Mowry, TT Borek. An Economic Analysis of Mobile Pyrolysis for Northern New Mexico Forests. Sandia National Laboratories Albuquerque 2011.
- [76] TR Brown, MM Wright, RC Brown. Estimating profitability of two biochar production scenarios: slow pyrolysis vs fast pyrolysis. *Biofuel. Bioprod. Bior.* 2011; 5: 54-68.
- [77] JW Lee, M Kidder, BR Evans, S Paik, AC Buchanan, CT Garten, RC Brown. Characterization of biochars produced from cornstovers for soil amendment. *Environ. Sci. Technol.* 2010; 44: 7970-4.
- [78] Y Lee, P-R-B Eum, C Ryu, Y-K Park, J-H Jung, S Hyun. Characteristics of biochar produced from slow pyrolysis of Geodae-Uksae 1. *Bioresource Technology* 2013; 130: 345-50.
- [79] S Shabangu, D Woolf, EM Fisher, LT Angenent, J Lehmann. Techno-economic analysis of biomass slow pyrolysis into different biochar and methanol concepts. *Fuel* 2014; 117: 742-8.
- [80] CE Brewer, K Schmidt-Rohr, JA Satrio, RC Brown. Characterization of biochar from fast pyrolysis and gasification systems. *Environ. Prog. Sustain. Energy* 2009; 28: 386-96.
- [81] G Fiorenza, VK Sharma, G Braccio. Techno-economic evaluation of a solar powered water desalination plant. *Energ. Convers. Manage.* 2003; 44: 2217-40.
- [82] PV Sen, K Bhuwanesh, K Ashutosh, Z Engineer, S Hegde, PK Sen, R Lal. Micro-scale multiple-effect distillation system for low steam inputs. *Procedia Engineering* 2013; 56: 63-7.
- [83] S Nisan, N Benzarti. A comprehensive economic evaluation of integrated desalination systems using fossil fuelled and nuclear energies and including their environmental costs. *Desalination* 2008; 229: 125-46.

- [84] M Methnani. Influence of fuel costs on seawater desalination options. *Desalination* 2007; 205: 332-9.
- [85] L Tian, J Guo, Y Tang, L Cao. A historical opportunity: economic competitiveness of seawater desalination project between nuclear and fossil fuel while the world oil price over \$50 per boe—part A: MSF. *Desalination* 2005; 183: 317-25.
- [86] E Tzen. Successful plants worldwide. In: *Desalination Units Powered by RES: Opportunities & Challenges*, ADU-RES, Hammamet, Tunisia, 2005, p. 15-6.
- [87] A Al-Karaghoul, D Renne, LL Kazmerski. Solar and wind opportunities for water desalination in the Arab regions. *Renew. Sust. Energ. Rev.* 2009; 13: 2397-407.
- [88] L García-Rodríguez, C Gómez-Camacho. Perspectives of solar-assisted seawater distillation. *Desalination* 2001; 136: 213-8.
- [89] L García-Rodríguez, C Gómez-Camacho. Preliminary design and cost analysis of a solar distillation system. *Desalination* 1999; 126: 109-14.
- [90] L García-Rodríguez, AI Palmero-Marrero, C Gómez-Camacho. Application of direct steam generation into a solar parabolic trough collector to multieffect distillation. *Desalination* 1999; 125: 139-45.
- [91] L García-Rodríguez, AI Palmero-Marrero, C Gómez-Camacho. Comparison of solar thermal technologies for applications in seawater desalination. *Desalination* 2002; 142: 135-42.
- [92] HM Qiblawey, F Banat. Solar thermal desalination technologies. *Desalination* 2008; 220: 633-44.
- [93] F Daniels. *Direct Use of the Sun's Energy*. 6th ed., Ballantine Books, New York, 1974.
- [94] JA Eibling, SG Talbert, GOG Löf. Solar stills for community use—digest of technology. *Sol. Energy* 1971; 13: 263-76.

- [95] S Kalogirou. Solar Energy Engineering Processes and Systems. 2nd ed., Academic Press, Oxford, 2014.
- [96] BA Akash, MS Mohsen. Potentials for development of hydro-powered water desalination in Jordan. *Renew. Energ.* 1998; 13: 537-42.
- [97] M Murakami. Hydro-powered reverse osmosis (RO) desalination for co-generation: A Middle East case study. *Desalination* 1994; 97: 301-11.
- [98] CT Kiranoudis, NG Voros, ZB Maroulis. Wind energy exploitation for reverse osmosis desalination plants. *Desalination* 1997; 109: 195-209.
- [99] E Tzen, R Morris. Renewable energy sources for desalination. *Sol. Energy* 2003; 75: 375-9.
- [100] E Tzen, K Perrakis, P Baltas. Design of a stand alone PV - desalination system for rural areas. *Desalination* 1998; 119: 327-33.
- [101] T Ackermann, L Söder. An overview of wind energy-status 2002. *Renew. Sust. Energ. Rev.* 2002; 6: 67-127.
- [102] L García-Rodríguez, V Romero-Ternero, C Gómez-Camacho. Economic analysis of wind-powered desalination. *Desalination* 2001; 137: 259-65.
- [103] MS Miranda, D Infield. A wind-powered seawater reverse-osmosis system without batteries. *Desalination* 2003; 153: 9-16.
- [104] Q Ma, H Lu. Wind energy technologies integrated with desalination systems: Review and state-of-the-art. *Desalination* 2011; 277: 274-80.
- [105] M Lenzen, J Munksgaard. Energy and CO₂ life-cycle analyses of wind turbines—review and applications. *Renew. Energ.* 2002; 26: 339-62.
- [106] SM Habali, IA Saleh. Design of stand-alone brackish water desalination wind energy system for Jordan. *Sol. Energy* 1994; 52: 525-32.

- [107] R Robinson, G Ho, K Mathew. Development of a reliable low-cost reverse osmosis desalination unit for remote communities. *Desalination* 1992; 86: 9-26.
- [108] A Ophir. Desalination plant using low grade geothermal heat. *Desalination* 1982; 40: 125-32.
- [109] L Awerbuch, TE Lindemuth, SC May, AN Rogers. Geothermal energy recovery process. *Desalination* 1976; 19: 325-36.
- [110] K Bourouni, R Martin, L Tadrict. Analysis of heat transfer and evaporation in geothermal desalination units. *Desalination* 1999; 122: 301-13.
- [111] K Bourouni, MT Chaibi, L Tadrict. Water desalination by humidification and dehumidification of air: State of the art. *Desalination* 2001; 137: 167-76.
- [112] K Bourouni, JC Deronzier, L Tadrict. Experimentation and modelling of an innovative geothermal desalination unit. *Desalination* 1999; 125: 147-53.
- [113] I Houcine, F Benjemaa, M-H Chahbani, M Maalej. Renewable energy sources for water desalting in Tunisia. *Desalination* 1999; 125: 123-32.
- [114] E Barbier. Geothermal energy technology and current status: an overview. *Renew. Sust. Energ. Rev.* 2002; 6: 3-65.
- [115] JM Lillywhite, R Heerema, JE Simonsen, E Herrera. Pecan Marketing Channels in New Mexico, 2010, Guide Z-307. New Mexico State University Cooperative Extension Service, Las Cruces, NM, 2010, p. 8.
- [116] A Isci, GN Demirer. Biogas production potential from cotton wastes. *Renewable Energy* 2007; 32: 750-7.

- [117] J Lehmann, J Pereira da Silva, C Steiner, T Nehls, W Zech, B Glaser. Nutrient availability and leaching in an archaeological Anthrosol and a Ferralsol of the Central Amazon basin: fertilizer, manure and charcoal amendments. *Plant Soil* 2003; 249: 343-57.
- [118] J Lehmann, S Joseph. *Biochar for Environmental Management: Science and Technology*. Earthscan, London, 2009.
- [119] DA Laird. The charcoal vision: A win-win-win scenario for simultaneously producing bioenergy, permanently sequestering carbon, while improving soil and water quality. *Agron. J.* 2008; 100: 178-81.
- [120] CJ Barrow. Biochar: potential for countering land degradation and for improving agriculture. *Appl. Geogr.* 2012; 34: 21-8.
- [121] R Lal. Black and buried carbons' impact on soil quality and ecosystem services. *Soil Till. Res.* 2008; 99: 1-3.
- [122] PK Sen, PV Sen, A Mudgal, SN Singh. A small scale multiple-effect distillation (MED) unit for rural micro enterprises: Part II--Parametric studies and performance analysis. *Desalination* 2011; 279: 27-37.
- [123] IC Karagiannis, PG Soldatos. Water desalination cost literature review and assesment. *Desalination* 2008; 223: 448-56.
- [124] PK Sen, PV Sen, A Mudgal, SN Singh. A small scale multi-effect distillation (MED) unit for rural micro enterprises: Part-III Heat transfer aspects. *Desalination* 2011; 279: 38-46.
- [125] M Wright, RC Brown. Establishing the optimal sizes of different kinds of biorefineries. *Biofuels, Bioproducts and Biorefining* 2007; 1: 191-200.

[126] M Downing, LM Eaton, RL Graham, MH Langholtz, RD Perlack, AF Turhollow Jr, B Stokes, CC Brandt. U.S. Billion-Ton Update: Biomass Supply for a Bioenergy and Bioproducts Industry. Oak Ridge National Laboratory, 2011, p. 194.

Simultaneous Treatment of Concentrate Water from Desalination Units and Cultivation of Microalgae as Feed Stock for Biofuel Production

Saeid Aghahosseini Shirazi, New Mexico State University, College of Engineering, Institute for Energy and the Environment, Address: 1060 Frenger Mall, ECIII, Las Cruces, NM, USA 88003, Tel: 575-646-2038, Email: saeid@nmsu.edu

Jalal Rastegary, New Mexico State University, College of Engineering, Institute for Energy and the Environment, Address: 1060 Frenger Mall, ECIII, Las Cruces, NM, USA 88003, Tel: 575-646-1510, Email: rastegar@nmsu.edu

Masoud Aghajani, New Mexico State University, College of Engineering, Institute for Energy and the Environment, Address: 1060 Frenger Mall, ECIII, Las Cruces, NM, USA 88003, Tel: 575-646-2038, Email: masoud@nmsu.edu

Abbas Ghassemi, New Mexico State University, College of Engineering, Institute for Energy and the Environment, Address: 1060 Frenger Mall, ECIII, Las Cruces, NM, USA 88003, Tel: 575-646-2357, Email: aghassem@ad.nmsu.edu

Abstract

Environmental effects associated with concentrate disposal have restricted the practical deployment of desalination technologies for inland brackish water, reducing the ability of desalination to alleviate global water shortages. In order to increase the feasibility of deploying desalination processes for inland brackish water sources, a beneficial use for concentrate from inland desalination systems should be found. The use of concentrate as a growth medium for salt-tolerant microalgae species, which could use the salts and nutrients in concentrate to grow and produce useful products, could help solve the problem of concentrate disposal for inland brackish water desalination plants. Therefore, to investigate the feasibility of using microalgae in pollutant removal and biomass production, a full factorial experiment was conducted on the growth of two strains of marine algae in concentrate under cycles of 16 hours of illumination and 8 hours of

darkness, at a temperature of 25°C. In addition, ion removal from the concentrate was tracked in order to characterize the role of microalgae in removing pollutants.

Keywords: *Concentrate, Desalination, Microalgae, Water, Biofuel*

1. Introduction

The amount of fresh water on planet is finite and fairly constant (only 0.8% of total water) [1]. Besides seas, oceans and glaciers the rest could be categorized as brackish water, which has high levels of total dissolved solids (TDS). Brackish water sources can be subdivided into surface water or groundwater. Since fresh groundwater and rivers are not sustainably used, these resources are either being depleted or becoming saline. In addition, population growth and global development require new water resources to meet the increasing demands. Water reuse and the desalination of salty water have proven to be promising solutions [2]. Since the early 1960s, desalination plants are constructed and produced considerable amount of drinking water. In the majority of new designs, membrane processes have been used instead of thermal processes [3], and reverse osmosis (RO) is the most commonly-used membrane process. By means of various membrane types, this process is capable of treating both seawater (SW) and brackish groundwater.

Brackish water (BW) desalination has satisfied water demands for different purposes in many countries around the world; in the United States, where there are more than 260 desalination plants, more than 95% of them use inland, brackish water sources [4]. Brackish groundwater is available as a significant resource in many inland and dry places, so even more brackish water reverse osmosis (BWRO) desalination projects are expected in the future [5].

Despite the significant potential of BWRO to alleviate global water shortages, an important environmental and financial problem associated with the process is the disposal of the waste stream from the process, which is called concentrate or brine. This concentrate is so saline that it must be disposed of properly, but the costs of doing so can adversely affect the feasibility of needed desalination plants [6]. Seawater plants can return the concentrate to the sea, but inland desalination plants have no such ready options. For BWRO desalination facilities, the most common methods for disposing of concentrate are deep well injection [7], surface water discharge, and evaporation ponds [8, 9]. Surface water discharge and deep well injection are not environmentally sustainable, and all of the options are costly, so novel alternatives for concentrate management are vital [10]. Disposal cost is a very important factor for all desalination plants, since it factors into the total cost of water production. Even when concentrate is diluted back into the sea, disposal costs can comprise between 5 and 33 percent of total desalination costs [11]; depending on the salinity of the concentrate, costs can be even higher for inland BWRO plants [12], sometimes reaching beyond 40% of plants' capital costs [13]. These cost factors emphasize the need for new concentrate management methods.

Energy availability is also critically important to water availability, since energy and water are interconnected: water is essential to the production of energy, and energy is needed to produce safe water. At present, over 80% of total energy usage is supplied from fossil fuels, such as petroleum, coal, and natural gas [14], which are constrained by availability and cost and which also release enormous amounts of CO₂ into the atmosphere. This release results in climate change, affecting food and water resources, ecosystems, and other parts of the environment [15]. Hence, concerted effort is needed to find sustainable, renewable, and CO₂-balanced alternative energy sources that can supplant fossil fuels [16]. In recent years, biofuel has shown the greatest potential

as an alternative to fossil fuels because it is derived from non-toxic, biodegradable, and potentially renewable resources and has less adverse environmental impact [17]. Furthermore, biofuel can be obtained from various different sources, such as sugar crops, starch crops, oilseed crops, and algae. However, a major concern over biomass-based energy, particularly in large-scale fuel production, is that it will consume vast amounts of farmland and water, compete with food production, and drive up food prices [18]. While this concern is relevant to biofuel production from sugar crops, starch crops, and oilseed crops, microalgae can produce biofuels by utilizing undeveloped lands and wastewater, without using resources necessary for food production. Overall, because of their advantages over other crops – which include higher photosynthetic efficiency, higher biomass production, higher growth rate, higher oil yield, and lower land requirements [19, 20] - microalgae appear to be the only source of biofuel that is capable of meeting global demand for energy. Based on calculations done by Chisti, microalgae with an average oil content of 30% dry biomass weight would require only 3% of the U.S. cropping area to meet the needed energy for transportation [21]. Microalgae can produce various renewable biofuels such as methane [22], biodiesel [23] and biohydrogen [24], and, as an additional benefit, microalgae have a voracious appetite for carbon dioxide. Based on estimations, the production of 100 tons of biomass will fix nearly 183 tons of CO₂ [25].

The cultivation of microalgae in concentrate, where the algae could remove ions and salts, could help resolve problems associated with desalination while simultaneously meeting energy needs by providing feedstock for biofuel production. To examine whether concentrate from inland desalination could be an appropriate medium for growing microalgae while investigating whether microalgae can contribute to concentrate treatment, a full factorial experiment with Completely Random Design (CRD) arrangement was conducted. Two strains of algae were cultivated in four

different media (concentrate, f/2, a 50:50 combination of f/2 and concentrate, and deionized water), and then the microalgae growth in the different types of growing media was compared. Additionally, ion removal from concentrate by microalgae was studied.

2. Materials and methods

2.1 Strains of algae

In this research, two strains of microalgae, *Nannochloropsis oculata* (UTEX-LB 2164) and *Dunaliella tertiolecta* (UTEX-LB 999), were obtained from the University of Texas Algae Collection in Austin, Texas. Both *Nannochloropsis oculata* and *Dunaliella tertiolecta* absorb CO₂ efficiently, making those good candidates to test the hypothesis of this paper [26]. The pre-cultures of both strains were cultivated in f/2 medium [27] for about three weeks in a 10 gallon aquarium aerated with ambient air. The air pumps were connected to air stones for better air distribution. When an optical density of approximately 1.00 was obtained at a wave length of 750 nm for each strain, four liters from each strain was taken for the experiment.

Nannochloropsis is a green algae that includes approximately six species. *Nannochloropsis* has been considered as a suitable candidate for biofuel production due to its fast reproduction and high oil content, which ranges from 31 to 68% of dry weight [21,28]. *Nannochloropsis oculata* is known as a marine algae; however, this strain also has been observed growing in fresh and brackish water [29]. This strain was selected for this experiment due to the high salinity of the concentrate. *Dunaliella tertiolecta* is a unicellular algae strain with oil content of approximately 40% of dry weight. *Dunaliella tertiolecta* is a very fast growing strain with a high CO₂ fixation rate [30]. Additionally, *Dunaliella* is green algae capable of growing in water bodies containing more than

10% salt, such as oceans and brine lakes [31]. This strain was selected due to its tolerance of the saline environments.

2.2 Culture and medium

In this research, four different media were used: concentrate, f/2, a 50:50 combination of f/2 and concentrate, and deionized water.

2.2.1 Concentrate medium

Concentrate refers to an 80/20 mixture of concentrate and f/2 in this experiment. The concentrate was obtained from the Reverse Osmosis (RO) water desalination process at the Brackish Groundwater National Desalination Research Facility (BGNDRF) in Alamogordo, New Mexico, and its specifications were as follows: Total Dissolved Solids (TDS) was 6240 ppm, Electroconductivity (EC) was 10260 $\mu\text{S}/\text{cm}$, and pH was 7.83. The ion content of the concentrate is shown in Table 1. Only ions which are vital for algae to grow were targeted, and since NH_4^+ was not available in the concentrate, that ion is not mentioned.

Table 1: Ion content of concentrate medium

Cations (mg/l)	K^+	32.93
	Na^+	1936.8
	Mg^{2+}	608.6
	Ca^{2+}	495.25
Anions (mg/l)	F^-	16.32
	Cl^-	2789.2
	NO_3^-	854.6
	SO_4^{2-}	4729.78
	PO_4^{3-}	21.9
Total Nitrogen(mg/l)		22.88

2.2.2 f/2 medium

The f/2 medium is a common and widely used general enriched seawater medium designed for growing coastal marine algae.

2.2.3 50:50 combination of f/2 and concentrate medium

This combination was incorporated into the experimental design because it is more economical than pure f/2.

2.2.4 Deionized medium

This medium served as the control medium in this experiment.

2.3 Photobioreactors set up

In this study, 32 cylindrical, glass UTEX 500-milliliter photobioreactors were used. Each photobioreactor was 14 cm in height and 7 cm in diameter, with a working volume of 500 ml and an autoclavable body. Each photobioreactor was equipped with five air delivery modules, a water trap, an air pump, an air stone, and one additional access port for sampling and measurements.

2.4 Design of experiment

32 runs were conducted in order to provide the required data for testing the various combinations of the 2 types of microalgae and 4 media. Since the experimental design used was a full-factorial design (2X4), eight combinations of microalgae and media were obtained.

2.5 Experimental Apparatus

An experimental apparatus was constructed using the UTEX glass photobioreactors. In order to pass an air tube into the photobioreactor through a check valve on the top of the lid, each photobioreactor had a quarter inch hole made in the center of the lid. Then, the air tube was

connected to the air stone for better air distribution, as well as to create more homogenous bubbles. Each photobioreactor was aerated by a Fusion Air Pump 200 (1.5 W). The lighting device used consisted of four GE, F40PL/AQ-ECO, wide-spectrum, 40W florescent tubes with a 3100K color temperature, producing 1900 lumens for each rack. The average distance from the bulbs to the experimental medium was 25 cm. For better light distribution, the floor of each rack was covered with aluminum foil. This addition enabled light from the bottom of each rack to reflect to the underbelly of the photobioreactor. All weights were measured using an Acculab AL-204 scale with an accuracy of +/- 0.0001g. An Eppendorf 5804 centrifuge was used to isolate biomass from the medium. The wet biomass was dried in a Fisher vacuum oven. An Eppendorf 1-50 ml pipette was used for the inoculation and transfer of algae. Volumes of the medium were measured using volumetric flasks. The pH was measured using an Accumet AB15/15+ pH meter. Before taking each pH sample, the pH meter was calibrated with standard pH 7 solution. A SANYO MLS-3751L was used to autoclave glassware.

2.6 Test procedure

To avoid any contaminations, all glassware was washed and rinsed with distilled water, and then autoclaved. 8 algae/medium sets with four replications for each treatment were placed separately inside the 32 batch photobioreactors. All the photobioreactors were placed under 16 hours of illumination and 8 hours of darkness at $30^{\circ}\text{C} \pm 2.0^{\circ}\text{C}$. Then, the inoculums of microalgae were cultivated in four media at the ratio of 1 to 4 in photobioreactors.

The next step was filling the photobioreactors with 320 ml of their respective media. Subsequently, the pH of the media was measured and found to be at 7.8, 6.9, 7.5 and 7.1 for concentrate, $f/2$, the 50:50 combination of $f/2$ and concentrate, and deionized water, respectively. Next, 80 ml of stirred homogenous algae was added to each photobioreactor containing 320 ml of

medium. The initial biomass of the inoculating algae was defined by taking four 50 ml samples. The samples were centrifuged at 10,000 rpm for three minutes. The supernatant was discarded from each sample, and the remaining algae in each sample was again rinsed with deionized water and then centrifuged a second time. These samples were then dried for 24 hours at 80° C. The initial biomass added to the photobioreactor was 0.052g and 0.043g for *Dunaliella tertiolecta* (UTEX-LB 999) and *Nannochloropsis oculata* (UTEX- LB 2164), respectively. The photobioreactors were placed randomly in racks. Air with a volumetric flow rate of 5 ml/s entered each photobioreactor through the air hose inserted through the lid. The experiments ran for 10 days. During this period, pH, optical density at 750 nm, TDS, EC and Total Nitrogen (TN) were measured every day. Furthermore, dry biomass and ion content of each concentrate medium were measured on the first and last days of the experiment. The resulting data were analyzed using a GLM (General Linear Model) procedure. Assumptions were checked using SAS 9.1.3. Means were compared using Tukey's Test ($P < 0.05$).

2.7 Analytical method

2.7.1 Algae growth

One of the objectives of this experiment is to compare the growth of microalgae in different conventional media. Currently, there are three basic methods to quantify biomass concentration: measuring the dry weight of biomass, counting cell numbers, and using the optical density. In this experiment, optical density and dry biomass weight were used in tandem to assess biomass production.

2.7.1.1 Dry biomass weight analysis

Although calculating the dry weight of a sample is challenging, it is the most accurate method for determining biomass production [32]. To measure dry biomass, a 50 ml sample of culture suspension was taken. Then, the sample was transferred to a pre-weighed 50 ml plastic tube. The plastic tube, with its content of algal culture, was centrifuged for 3 minutes at 10,000 RPM, after which the supernatant was extracted. Since the dry weight, especially for marine algae, is heavily affected by the salts and nutrients absorbed on the cell surface, the centrifuged content was rinsed with deionized water, based on a suggestion by Lee and Shen [33], in order to reduce the error in determining the amount of dry biomass. Subsequently, the tubes were centrifuged at 10,000 RPM for 3 minutes after rinsing with deionized water. The clear supernatant was discarded, while the tubes containing the biomass were dried in the oven at 80°C for 24 hours. In order to prevent loss of volatile components in algae cells, the temperature was maintained below 90°C. The dry biomass was determined by the difference between the initial weight and the final weight of the tube.

2.7.1.2 Optical density

A HACH DR 5000 Spectrophotometer was used to track the daily algae growth in terms of optical density. Optical density was measured daily at a wavelength of 750 nm, which is the range where chlorophyll is a dominant pigment.

2.7.2 Ion removal

In addition to comparing the growth rates of algae in different media, the other central objective of this experiment is to evaluate whether microalgae can contribute significantly to the removal of environmentally hazardous ions from desalination concentrate. For this purpose, Total

Dissolved Solids (TDS), electroconductivity (EC), and Total Nitrogen (TN) were measured daily. The ion content of concentrate was determined from the first and final days.

2.7.2.1 Salinity (TDS and EC)

TDS and EC were measured using sensION5 Conductivity Meter.

2.7.2.2 Total Nitrogen analysis

Combining the SHIMADZO TNM-1 with a SHIMADZO TOC-VCS/CP analyzer creates a Total Organic Carbon (TOC) / Total Nitrogen (TN) simultaneous analysis system which was used for TN analysis in this experiment. The analysis was conducted at the Freeport-McMoRan Water Quality Lab at New Mexico State University.

2.7.2.3 Ion content analysis

Ion content of the concentrate medium was analyzed using a DIONEX ICS-3000 Ion Chromatography System.

3. Results and discussion

Two one-way experiments were run simultaneously to form a full factorial experiment each for ten days.

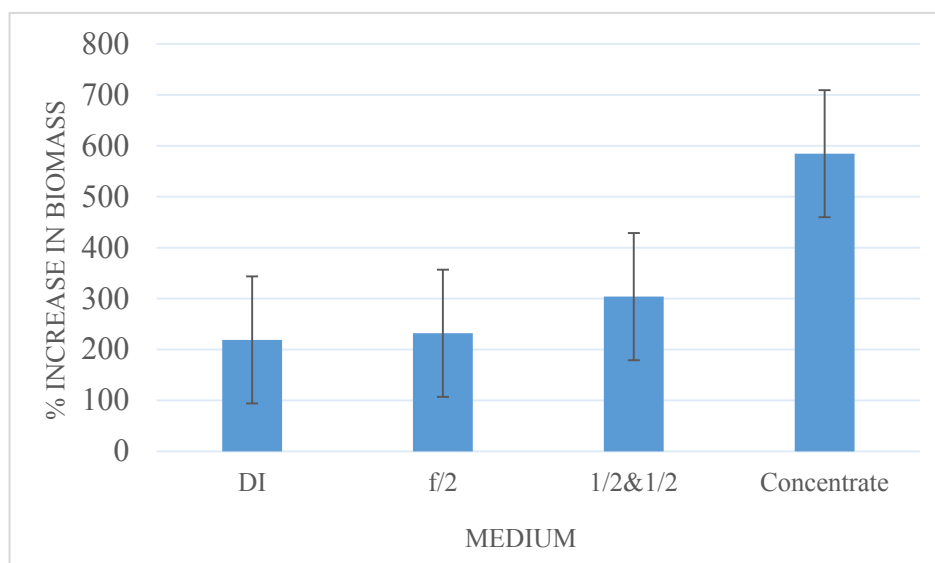
3.1 Experiment 1

In this part of the experiment, *Dunaliella tertiolecta* (UTEX-LB 999) was used in order to investigate microalgae growth in a concentrate medium with TDS of 6240 ppm. For each combination of microalgae and medium, four replications were considered. Thus, sixteen runs for a period of 10 days were conducted for the required data. All factors that might affect the biomass

growth were kept as constant as possible in order to clarify the effects of algae type and medium on biomass growth.

Figure 1 depicts the effect of medium on percent increase in biomass. P-value of 0.004 shows significant difference in biomass production by different media.

Figure 1 Effect of medium on biomass production for *Dunaliella tertiolecta*

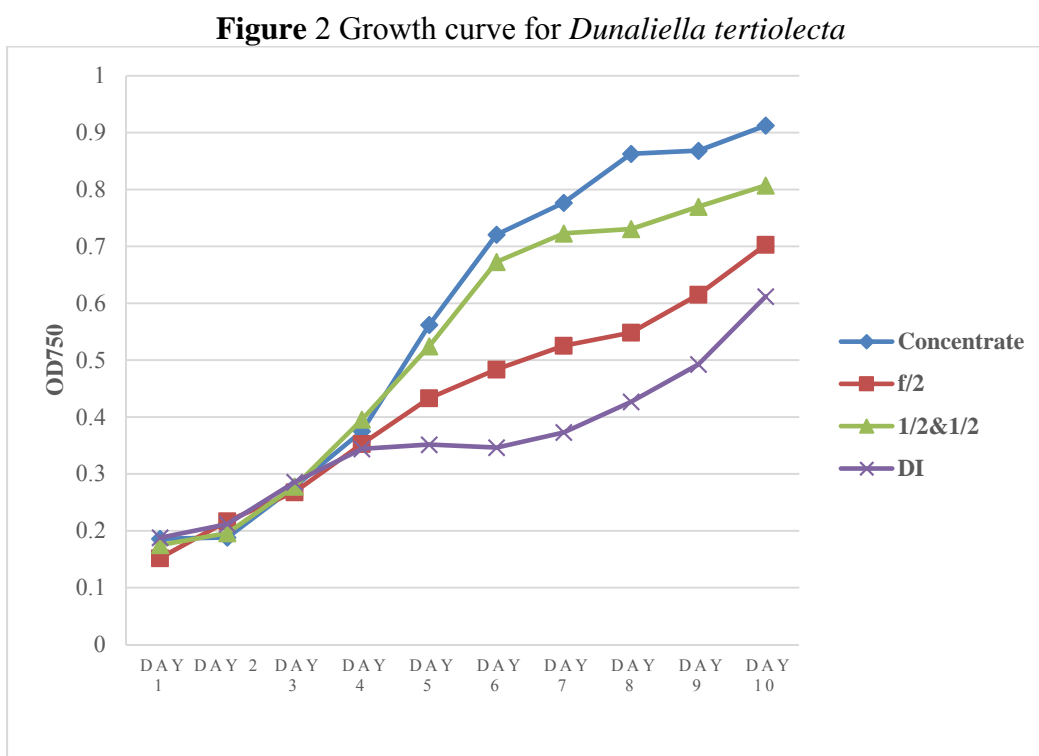


Concentrate was the medium that maximized the biomass production, and there were no significant differences in percent increase of biomass among other media that did not contain concentrate. This analysis reveals that the high salinity and nutrients available in concentrate provided a better environment for this strain of marine algae to grow than did other media. High concentrations of nitrate, phosphate, and NaCl could be possible reasons behind this increased growth.

Compared to f/2 medium, the 50:50 medium demonstrated better performance because it contained the nutrients of both f/2 and the concentrate. This result shows that nutrients available in concentrate can still contribute to algae growth when the nutrients in f/2 are diminishing. Furthermore, there was no significant difference between the growths of the biomass in the f/2

medium when compared with the deionized water medium. This result is because the inoculum algae added to the culture medium at a ratio of 1:4 was pre-cultivated in f/2; therefore, 20% of the deionized water medium was essentially f/2.

Figure 2 displays the growth curve for four different media during the ten days of experimentation.

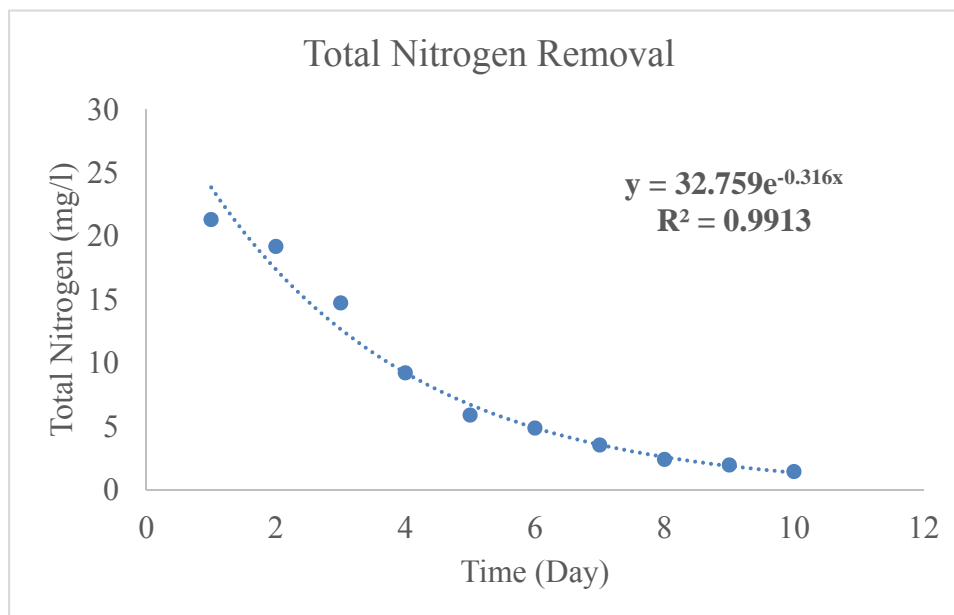


The results obtained from optical density at 750 nm confirm the results obtained from dry weight biomass. Similar to the results gained from the dry weight test, algae grown in concentrate consistently had the highest optical density from day five to day ten. Aside from concentrate, 50:50 and f/2 media had the next highest optical densities, respectively.

During the first three days, the growth trends in all media were slow and almost the same because the algae cultures were in their lag phases. On the fourth day, the cultures began their exponential phases, when the differences in media manifested themselves. The rates of the increase

in concentrate and 50:50 media were significantly higher than f/2 medium during the exponential phase, due to the high concentrations of nitrate and phosphate available in concentrate. On the eighth day, the algae growth in the concentrate medium slowed, mostly because of a depletion of nutrients. The role of light was also important in this stage because the cultures in the concentrate and 50:50 media became very dense and turbid, inhibiting light penetration, especially in the middle of the reactor. However, since the algae cultivated in f/2 and deionized water did not become overly dense, light penetration was better than for the other media. Hence, the cultures in f/2 and deionized water did not exhibit the same inhibitory factor for photosynthesis that the strain in the concentrate medium experienced. It is anticipated that the continuation of the experiment for few more days would have resulted in a similar outcome for the cultures cultivated in f/2 and deionized water, which would eventually collapse due to their photosynthetic inhibitions.

Nitrogen is the main nutrient required for algae to grow, and nitrogen removal is a biotic. Since nitrogen is needed for biomass growth, a high nitrogen concentration is important to support the reproduction of microalgae cells. However, the nitrogen concentration in growth media is eventually depleted without new inputs, and remains at a level that only supports the synthesis of enzymes and critical cell formation. Under these conditions, available carbons are converted into lipids rather than proteins, which slows algal growth because proteins are necessary for continued algal growth [34]. This accentuates the importance of nitrogen removal. Figure 3 shows total nitrogen (TN) removal trending over the period of the experiment, revealing that *Dunaliella tertiolecta* significantly reduced the nitrogen levels in concentrate.

Figure 3 Total nitrogen removal from concentrate by *Dunaliella tertiolecta*

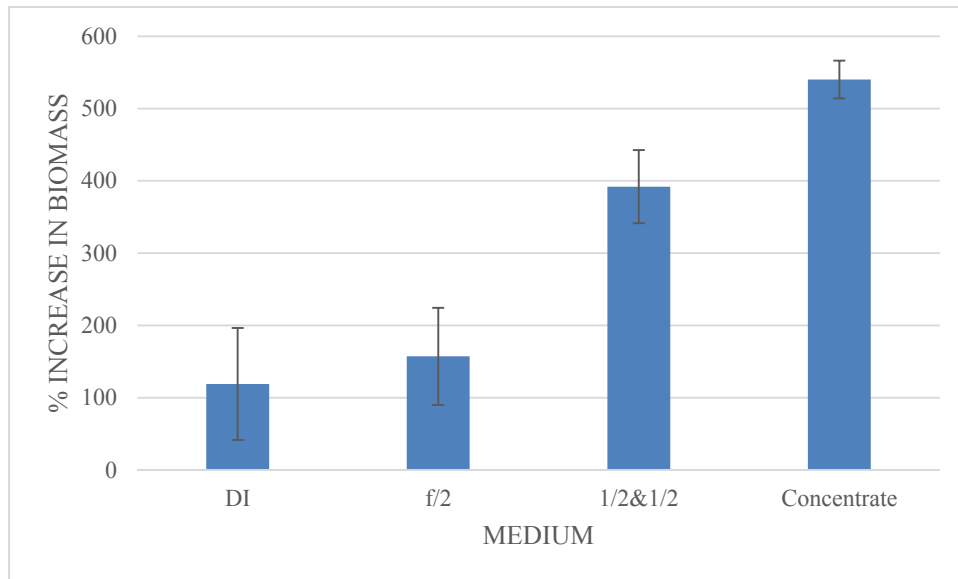
The nitrogen removal yield (Y_N) was 0.93, which is considerable, and the volumetric rate of N removal (Q_N) was $1.99 \text{ mg} \cdot \text{dm}^{-3} \cdot \text{day}^{-1}$.

In addition to TN, the amount of certain ions in the concentrate medium was measured on the first and final days. Table 2 and Table 3 display the concentration of these ions.

3.2 Experiment 2

In second experiment, *Nannochloropsis oculata* (UTEX- LB 2164) was used for concentrate treatment and biofuel production. All the conditions were similar to the first experiment. Sixteen runs were performed in order to obtain the required data for assessing the various combinations of media.

The initial biomass was 0.043 g. Figure 4 shows the effect of each media on percent increase in biomass. The P-value of less than 0.0001 shows significant differences in biomass production for the different media.

Figure 4 Effect of medium on biomass production for *Nannochloropsis oculata*

Concentrate is the medium that produced the greatest amount of biomass, and the 50:50 medium produced a larger biomass than the f/2 medium. However, the deionized water and f/2 media showed little statistical difference. Again, high concentrations of some ions—such as nitrate, phosphate and NaCl—were an important parameter that caused this difference.

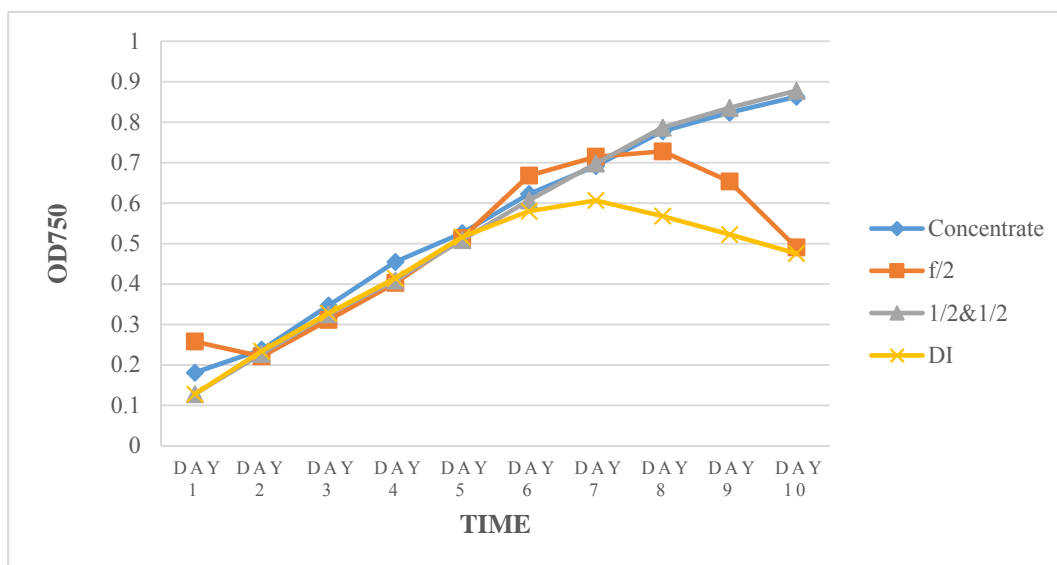
Figure 5 Growth curve for *Nannochloropsis oculata*

Figure 5 depicts the growth curve for the different media in this experiment. The results obtained from the optical density measurements at 750 nm were similar to the results from dry biomass measurement. The vertex point for maximum biomass occurred in the seventh day of the experiment for f/2 and deionized water, indicating that the nutrients in f/2 were diminishing; consequently, growth of algae was decreasing. The lack of nutrients in f/2 and deionized water media caused the stationary phase in these media to be approximately one day, a duration that, compared to the other media, was considerably short. From this information, it can be deduced that the high salinity of concentrated was an advantage that helped promote continuous algae growth. The high salinity of concentrate further explains why the 50:50 medium was still growing after the seventh day.

Table 2: Anions (experiment 1)

		Unit=mg/l				
		F ⁻	Cl ⁻	NO ₃ ⁻	SO ₄ ²⁻	PO ₄ ³⁻
Anions	Initial	15.2	2605.8	834.9	3788.4	18.3
	Final	≈0	2383.3	81.3	3608.1	≈0
	Removal	15.2	222.5	753.6	180.3	18.3
	Ion removal yield	≈1	0.1	0.9	0	≈1
	Volumetric rate of ion removal	1.52	22.2	75.4	18	1.83

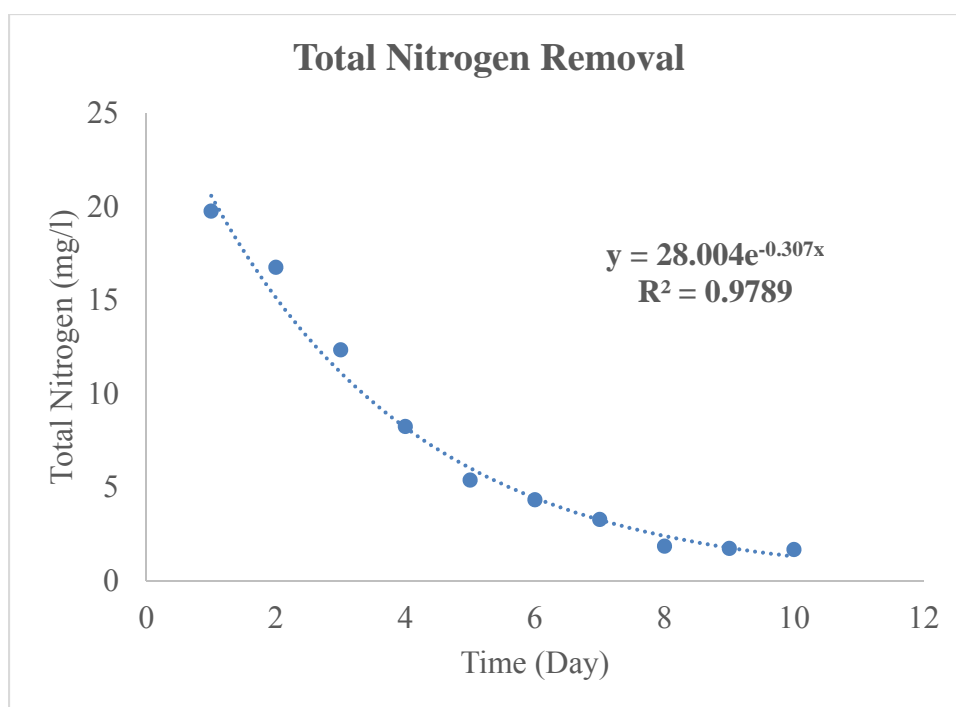
Table 3: Cations (experiment 1)

		Unit=mg/l			
		K ⁺	Na ⁺	Mg ²⁺	Ca ²⁺
Cations	Initial	28.7	1889.2	579	464.2
	Final	24.8	1655	537.4	347.3
	Removal	3.9	234.2	41.6	116.9
	Ion removal yield	0.1	0.1	0.1	0.2
	Volumetric rate of ion removal	0.4	23.4	4.1	11.7

The contribution of *Dunaliella tertiolecta* to fluoride, nitrate, and phosphate removal was significant. In addition, TDS of concentrate decreased from 6290 to 5802.5 mg/l and electroconductivity reduced from 10180 to 9455 $\mu\text{S}/\text{cm}$.

Figure 6 shows the trend of TN removal trend over time for *Nannochloropsis oculata*, which demonstrates that this species meaningfully lessened the amount of nitrogen in concentrate, just as *Dunaliella tertiolecta* did in the first experiment.

Figure 6 Total nitrogen removal from concentrate by *Nannochloropsis oculata*



The nitrogen removal yield (Y_N) was 0.91 and volumetric rate of nitrogen removal (Q_N) was $1.81 \text{ mg}\cdot\text{dm}^{-3}\cdot\text{day}^{-1}$.

Table 4 and Table 5 show anion and cation concentrations in the samples. Similar to *Dunaliella tertiolecta*, *Nannochloropsis oculata* removed fluoride, nitrate, and phosphate significantly. Since the experiment was designed to avoid cross contamination and because the

experiment used pure algae, ion removal was performed by the algae and not any other organisms. TDS of the concentrate decreased from 6270 to 4930 mg/l while EC reduced from 10200 to 8170 $\mu\text{S}/\text{cm}$.

Table 4: Anions (Experiment 2)

		Unit=mg/l				
		F ⁻	Cl ⁻	NO ₃ ⁻	SO ₄ ²⁻	PO ₄ ³⁻
Anion	Initial	15.2	2754.2	834.4	3598.3	20.8
	Final	0	2489.6	72.9	3139.3	0
	Removal	15.2	264.6	761.5	459	20.8
	Ion removal yield	1	0.09	0.9	0.1	1
	Volumetric rate of ion removal	1.52	26.5	76.1	45.9	2.08

Table 5: Cations (Experiment 2)

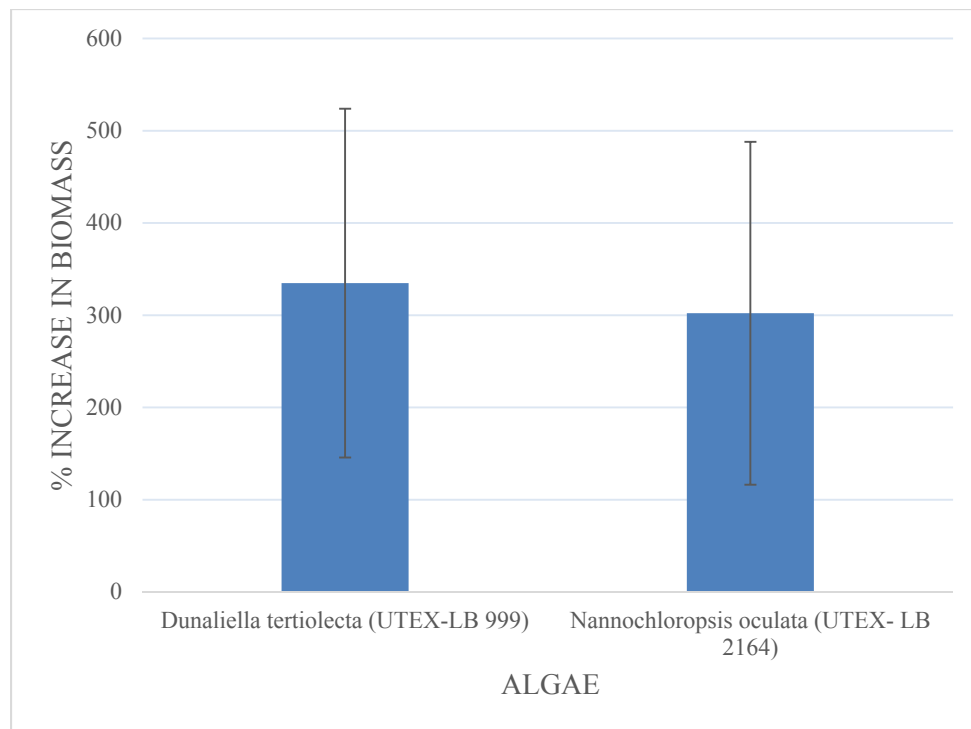
		Unit=mg/l			
		K ⁺	Na ⁺	Mg ²⁺	Ca ²⁺
Cation	Initial	29.6	1987.6	595.4	445.4
	Final	26.8	1797.9	548.2	351.5
	Removal	2.8	189.7	47.3	93.9
	Ion removal yield	0.1	0.09	0.1	0.2
	Volumetric rate of ion removal	0.3	18.9	4.7	9.4

3.3 Growth comparison

The full factorial experiment with two levels for algae and four levels for medium considered the interaction of these two factors. Analyzing algae type, medium, and the interaction between the algae and the medium indicated some effects on final biomass production.

Figure 7 shows that there was not a significant difference in biomass production between *Nannochloropsis oculata* (UTEX-LB 2164) and *Dunaliella tertiolecta* (UTEX-LB 999) (P-value = 0.35).

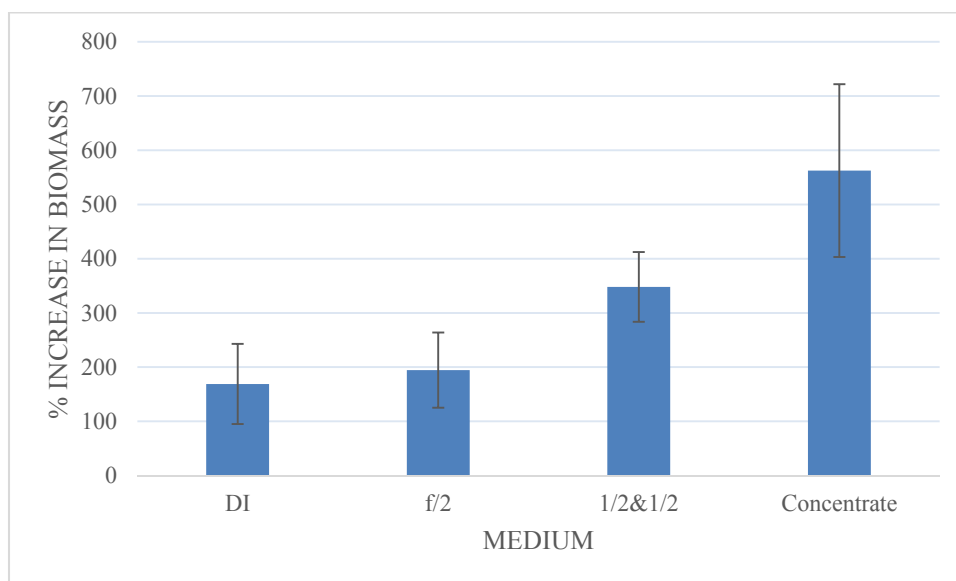
Figure 7 Algae effect on dry biomass production



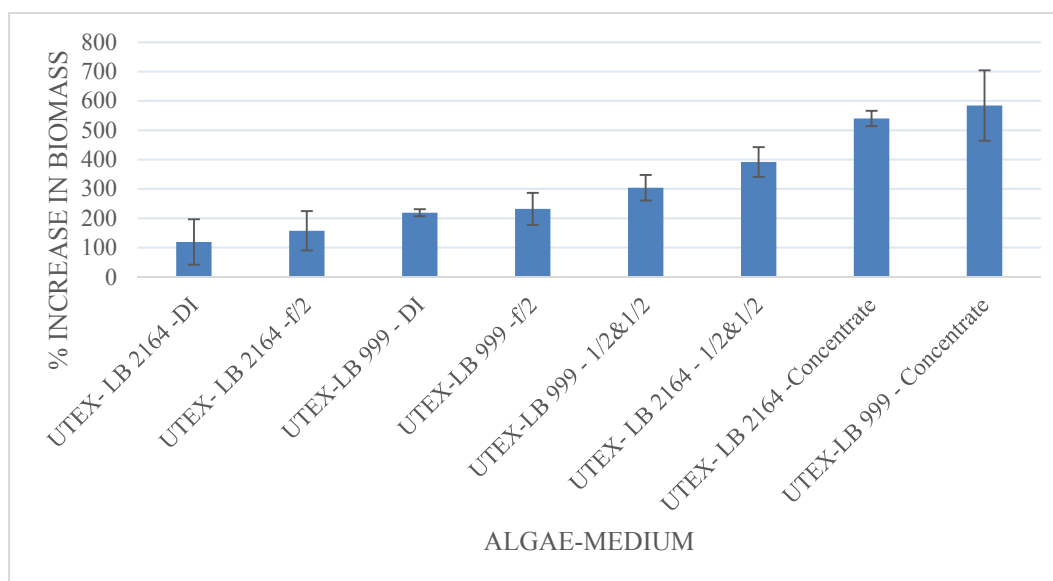
Results showed significant variations in dry biomass produced by the four media (P-value < 0.0001), but no significant variations in biomass production between the two algae species (P-value = .35). Figure 8 illustrates two observations: (1) a significant difference in dry biomass production was observed when concentrate is used, and (2) there was a significant biomass increase in 50:50 medium as compared to f/2. Deionized water and f/2 were essentially the same

in terms of percentage increase in biomass, because the algae inoculum was pre-cultured in f/2, causing the inoculum itself to contain practically all the main nutrients of f/2.

Figure 8 Medium effect on dry biomass production



There were no significant differences among interactions (P-value=0.2470). Figure 9 demonstrates that the interaction of the concentrate medium with *Dunaliella tertiolecta* (UTEX-LB 999) produced the highest dry biomass. Interaction of the concentrate medium with *Nannochloropsis oculata* (UTEX-LB 2164) was substantial as well. Interactions of 50:50 medium with both strains of algae yielded considerable amounts of dry biomass, but these amounts were significantly less than the biomass produced in the concentrate medium. Since concentrate is less expensive than f/2, these results suggest that concentrate is a better choice than both the 50:50 and f/2 media.

Figure 9 Algae-Medium interaction effect on dry biomass

Based on results obtained from dry weight biomass, two kinetic parameters, Volumetric Growth Rate and Specific Growth Rate, are calculated (Table 6).

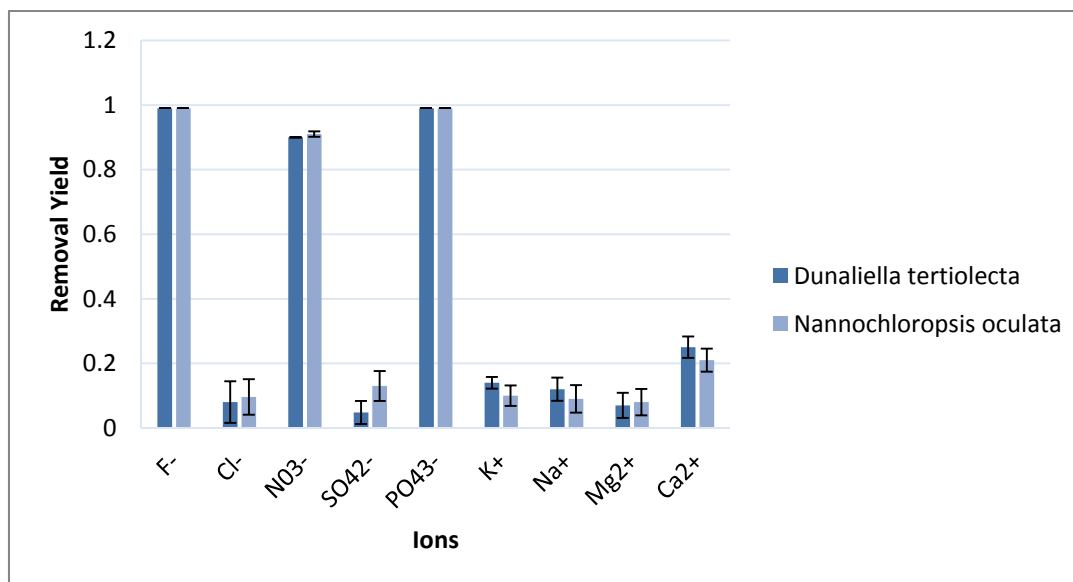
Table 6 Kinetic parameters

		Q_x =Volumetric Growth Rate($\text{gr.dm}^{-3}.\text{day}^{-1}$)	μ =Specific Growth Rate(day^{-1})
<i>Dunaliella tertiolecta</i> (UTEX-LB 999)	Concentrate	0.08	0.19
	f/2	0.03	0.12
	1/2&1/2	0.04	0.14
	DI	0.03	0.11
<i>Nannochloropsis oculata</i> (UTEX-LB 2164)	Concentrate	0.06	0.18
	f/2	0.02	0.09
	1/2&1/2	0.04	0.16
	DI	0.01	0.07

3.4 Ion removal comparison

Ion removal from concentrate by two strains of algae is displayed in figure 10.

Figure 10 Ion removal from concentrate by two cultures of algae

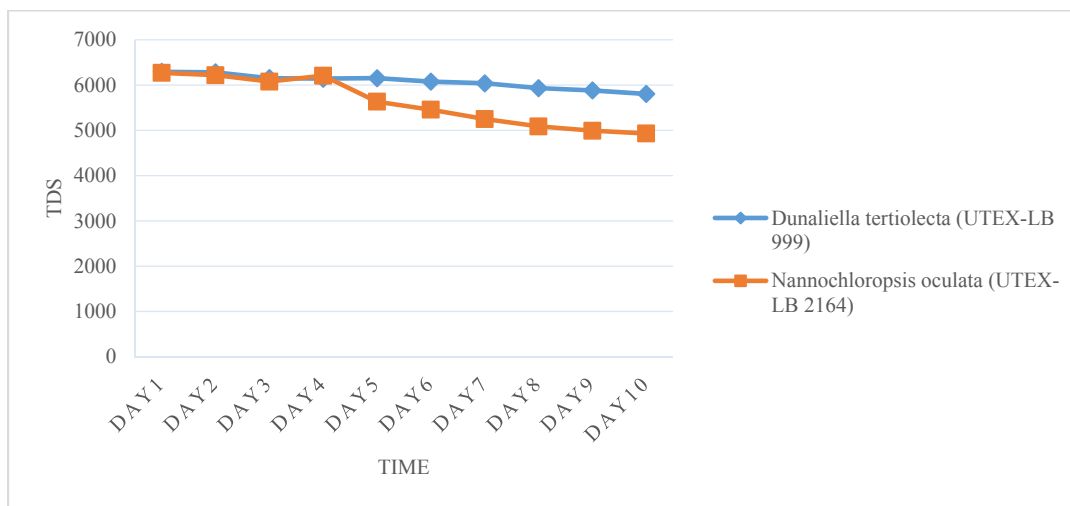


The elementary composition and C: P: N ratio of microalgae cells usually varies with the strain type; therefore, the ability to absorb nitrogen and phosphorous may be different for different species of microalgae. In marine algae, the molecular ratios of carbon, phosphorus, and nitrogen allow the algae to grow quickly by uptaking the nutrients available in waste water and salty water. This uptake can occur especially quickly in water bodies with high concentrations of N and P [35]. The results of this experiment showed that the marine algae were also able to do this when concentrate was used as a growth medium.

Figure 11 shows that the TDS decreased in the concentrate medium during the experimental period as a result of the algae species *Nannochloropsis oculata* and *Dunaliella tertiolecta*. However, because ions such as potassium, chloride, sodium, calcium, and sulphate

cause high TDS [36] and these ions were not removed significantly, TDS did not decrease considerably.

Figure 11 TDS reduction in concentrate medium by two strains of algae



4. Conclusion

Based on research findings, an optimal match between algae and medium was identified. These findings indicated that, among all the investigated media, a concentrate medium maximized the percentage increase of dry weight biomass better than an *f/2* medium, which is a conventional and accepted medium for growing marine algae. The results of optical density at 750nm conveyed the same result as well. There was no significant difference in biomass production and ion removal from concentrate between *Nannochloropsis oculata* (UTEX- LB 2164) and *Dunaliella tertiolecta* (UTEX-LB 999). Both strains are acceptable for the purpose of biomass production and ion removal. The contribution of algal cultures to the removal of ions from concentrate was not significant other than for specific ions, such as nitrate, phosphate and fluoride; however, TN decreased considerably during the experiment. TDS did not change considerably because many of the ions responsible for high TDS were not removed in significant quantities.

Based on the findings, it could be concluded that the cultivation of marine algae strains in the waste concentrate of water desalination units is a unique approach that allows particular pollutants to be removed from concentrate while algal biomass is cultivated for biofuel feedstock production. The results of this research identify a potential approach to reduce the cost of desalination by creating revenue from biofuel production, which could also bring about environmental benefits such as CO₂ mitigation and concentrate disposal treatment.

5. Acknowledgment

The project reported herein was funded by the “Bureau of Reclamation”.

References

- [1] P. H. Gleick, Water resources. In: Encyclopedia of Climate and Weather, ed. by S. H. Schneider, Oxford University Press, New York, 1996, vol. 2, pp. 817-823.
- [2] L.F. Greenlee, D.F. Lawler, B.D. Freeman, B. Marrot and P. Moulin, Reverse osmosis desalination: Water sources, technology and today's challenges, *Water Research*, 43, (2009), 2317-2348.
- [3] Gleick, P.H., 2006. *The World's Water 2006–2007, The Biennial Report on Freshwater Resources*. Island Press, Chicago.
- [4] M. Mickley, "Treatment of Concentrate, Desalination and Water Purification Research and Development Program Report No. 155." US Department of the Interior, Bureau of Reclamation, Denver (2009).
- [5] T. Qiu and P.A. Davies, Comparison of Configurations for High-Recovery Inland Desalination Systems, *Water*, 4 (2012), 690-706.
- [6] D. Squire, J. Murrer, P. Holden and C. Fitzpatrick, Disposal of reverse osmosis membrane concentrate, *Desalination*, 108 (1996) 143–147.
- [7] A. Muniz and S. Skehan, Disposal of concentrate from brackish water desalting plants by use of deep injection wells, *Desalination*, 78 (1) 1990 41-47.
- [8] J.M. Arnal, M. Sancho, I. Iborra, J.M. Gozalvez, A. Santafe, J. Lora, Concentration of brines from RO desalination plants by natural evaporation, *Desalination*, 182 (2005) 435-439.
- [9] C.J. Gabelich, P. Xu and Y. Cohen, Chapter 10 concentrate treatment for inland desalting, *Sustainability Science and Engineering*, 2 (2010) 295-326.

[10] A. Perez-Gonzalez, A.M. Urtiaga, R. Ibanez and I. Ortiz, State of the art and review on the treatment technologies of water reverse osmosis concentrates, *Water Research*, 46 (2012) 267- 283

[11] M. Ahmed, W.H. Shayya, D. Hoey and J. Al-Handaly, Brine disposal from reverse osmosis desalination plants in Oman and the United Arab Emirates, *Desalination*, 133 (2) (2001) 135-147.

[12] B.D. Stanford, J.F. Leising, R.G. Bond and S.A. Snyder, Inland Desalination: Current Practices, Environmental Implications, and Case Studies in Las Vegas, NV. *Sustainability Science and Engineering*, 2 (2010) 327-350.

[13] C. De Vito, S. V. F. Mignardi & R. F. M. Mignardi, Reject brines from desalination as possible sources for environmental technologies, In: *Expanding Issues in Desalination*, Robert Y. Ning (Ed.), ISBN 2011, pp. 978-953.

[14] A. Demirbas & M. F. Demirbas, Importance of algae oil as a source of biodiesel, *Energy Conversion and Management*, 52(1) (2011) 163–170.

[15] R. Foster, M. Ghassemi and A. Cota, *Solar energy: renewable energy and the environment*, CRC Press, 2009.

[16] R. Righelato, and D. V. Spracklen, Carbon mitigation by biofuels or by saving and restoring forests?, *SCIENCE-NEW YORK THEN WASHINGTON*, 317, No. 5840 (2007) 902.

[17]L. Gouveia, and A. C. Oliveira, Microalgae as a raw material for biofuels production, *Journal of Industrial Microbiology & Biotechnology*, 36 (2009) 269–274.

- [18] V. Patil, K. Q. Tran and H. R. Giselrod, Towards sustainable production of biofuels from microalgae, *International Journal of Molecular Sciences*, 9(7) (2008) 1188–1195.
- [19] J. W. Richardson, J. L. Outlaw and M. Allison, Economics of micro algae oil, In: 13th ICABR conference on the emerging bio-economy, Ravello, Italy, (2009).
- [20] T. Minowa, S. Yokoyama, M. Kishimoto, T. Okakura, Oil production from algal cells of *Dunaliella tertiolecta* by direct thermochemical liquefaction, *Fuel*, 74 (1995) 1735–1738.
- [21] Y. Chisti, Biodiesel from microalgae, *Biotechnology Advances*, 25(3) (2007) 294–306.
- [22] P. Spolaore, C. Joannis-Cassan, E. Duran & A. Isambert, Commercial applications of microalgae, *Journal of Bioscience and Bioengineering*, 101 (2006) 87–96.
- [23] T. G. Dunahay, E. E. Jarvis, S. S. Dais & P. G. Roessler, Manipulation of microalgal lipid production using genetic engineering, *Applied Biochemistry and Biotechnology*, 57/58, (1996) 223–231.
- [24] I. Akkerman, M. Janssen, J. Rocha and R. H. Wijffels, Photobiological hydrogen production: Photochemical efficiency and bioreactor design, *International Journal of Hydrogen Energy*, 27 (2002) 1195–1208.
- [25] D. Antoni, V. V. Zverlov and W. H. Schwarz, Biofuels from microbes, *Applied Microbiology and Biotechnology*, 77 (2007) 23–35.
- [26] E. Ono, and J. L. Cuello, Design parameters of solar concentrating systems for CO₂-mitigating algal photobioreactors, *Energy*, 29 (2004) 1651–1657.

- [27] R. R. L. Guillard, Culture of Phytoplankton for Feeding Marine Invertebrates, Culture of Marine Invertebrate Animals, (1975) 29–60.
- [28] K. E. Apt and P. W. Behrens, Commercial development in microalgal biotechnology, Journal of Phycology, 35 (1999) 215-226.
- [29] K. P. Fawley and M. W. Fawley, Observations on the Diversity and Ecology of Freshwater *Nannochloropsis* (Eustigmatophyceae), with Descriptions of New Taxa, Protist, 158 (3) (2007) 325-336.
- [30] A. H. Demirbas, Inexpensive oil and fats feedstocks for production of biodiesel. Energy Education Science and Technology Part A-Energy Science and Research, 23, (1-2) (2009) 1-13.
- [31] Oilgae Report, Academic Edition, Tamil Nadu, India, 2010.
- [32] A. Richmond and Q. Hu, Handbook of Microalgal Culture: Applied Phycology and Biotechnology, Wiley & Sons Publication, 2013.
- [33] Y. K. Lee and H. Shen, In: A. Richmond, Handbook of Microalgal Culture. Biotechnological and Applied phycology, Black-well Publishing, Oxford 2004, pp. 40-56.
- [34] E. Suali and R. Sarbatly, Conversion of microalgae to biofuel, Renewable and Sustainable Energy Reviews, 16(6) (2012) 4316–4342.
- [35] T.J. Lundquist, Production of algae in conjunction with wastewater treatment. In: NREL-AFOSR workshop on algal oil for jet fuel production, 2008.
- [36] M. Bishnoi and S. Arora, Potable groundwater quality in some villages of Haryana, India: Focus on fluoride, Journal of Environmental Biology, 28(2) (2007) 291–294.

Energy usage and carbon dioxide emission saving in desalination by using desalination concentrate and waste in microalgae production

This article was downloaded by: [New Mexico State University], [waddah hussein]

On: 10 February 2014, At: 12:47

Publisher: Taylor & Francis

Informa Ltd Registered in England and Wales Registered Number: 1072954 Registered office: Mortimer House, 37-41 Mortimer Street, London W1T 3JH, UK



Desalination and Water Treatment

Publication details, including instructions for authors and subscription information:

<http://www.tandfonline.com/loi/tdwt20>

Energy usage and carbon dioxide emission saving in desalination by using desalination concentrate and wastes in microalgae production

Waddah Hussein^{ab}, Maung Thein Myint^c & Abbas Ghassemi^{ab}

^a Institute for Energy and the Environment, New Mexico State University, MSC WERC, P.O. Box 30001, Las Cruces, NM 88003, USA

^b Chemical Engineering Department, New Mexico State University, MSC ChE, P.O. Box 30001, Las Cruces, NM 88003, USA

^c Civil Engineering Department, New Mexico State University, MSC 3CE, P.O. Box 30001, Las Cruces, NM 88003, USA Tel. +1 575 312 9300; Fax: +1 575 646 6049

Published online: 05 Feb 2014.

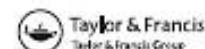
To cite this article: Waddah Hussein, Maung Thein Myint & Abbas Ghassemi, Desalination and Water Treatment (2014): Energy usage and carbon dioxide emission saving in desalination by using desalination concentrate and wastes in microalgae production, Desalination and Water Treatment, DOI: [10.1080/19443994.2014.884476](https://doi.org/10.1080/19443994.2014.884476)

To link to this article: <http://dx.doi.org/10.1080/19443994.2014.884476>

PLEASE SCROLL DOWN FOR ARTICLE

Taylor & Francis makes every effort to ensure the accuracy of all the information (the "Content") contained in the publications on our platform. However, Taylor & Francis, our agents, and our licensors make no representations or warranties whatsoever as to the accuracy, completeness, or suitability for any purpose of the Content. Any opinions and views expressed in this publication are the opinions and views of the authors, and are not the views of or endorsed by Taylor & Francis. The accuracy of the Content should not be relied upon and should be independently verified with primary sources of information. Taylor and Francis shall not be liable for any losses, actions, claims, proceedings, demands, costs, expenses, damages, and other liabilities whatsoever or howsoever caused arising directly or indirectly in connection with, in relation to or arising out of the use of the Content.

This article may be used for research, teaching, and private study purposes. Any substantial or systematic reproduction, redistribution, reselling, loan, sub-licensing, systematic supply, or distribution in any form to anyone is expressly forbidden. Terms & Conditions of access and use can be found at <http://www.tandfonline.com/page/terms-and-conditions>



Energy usage and carbon dioxide emission saving in desalination by using desalination concentrate and wastes in microalgae production

Waddah Hussein^{a,b}, Maung Thein Myint^{c,*}, Abbas Ghassemi^{a,b}

^aInstitute for Energy and the Environment, New Mexico State University, MSC WERC, P.O. Box 30001, Las Cruces, NM 88003, USA

^bChemical Engineering Department, New Mexico State University, MSC ChE, P.O. Box 30001, Las Cruces, NM 88003, USA

^cCivil Engineering Department, New Mexico State University, MSC 3CE, P.O. Box 30001, Las Cruces, NM 88003, USA
Tel. +1 575 312 9300; Fax: +1 575 646 6049; email: mmyint@nmsu.edu

Received 29 August 2013; Accepted 22 December 2013

ABSTRACT

Energy usage and CO₂ emission between traditional electro dialysis reversal (EDR) and innovative EDR desalinations were compared. The difference between traditional and innovative EDR desalination depended on which concentrate treatment was employed. Traditional EDR desalination consists of electro dialysis as concentrate treatment, while innovative EDR desalination consists of *Dunaliella salina* production as concentrate treatment. Microalgae species *D. salina* and *Arthrospira (Spirulina) platensis* were cultured in used bottles (3.7 L) as reactors and using desalination concentrate and supernatant from anaerobic digested sludge (SADS) as growth medium and nutrients. *D. salina* was grown in reactors D₁, D₂, D₃, and D₄. *Spirulina platensis* was in S₁, S₂, S₃, and S₄. SADS was supplied to reactors D₁, D₂, S₁, and S₂ as nutrient. Bold's Basal Medium was supplied to reactors D₃ and D₄ while F2 was supplied to reactors S₃ and S₄ as nutrient. Conductivity of desalination concentrates used in reactors D₁ and D₃ was 31.8 and in D₂ and D₄ 25.4 mS/cm, respectively. Conductivity of concentrate in reactors S₁ and S₃ was 35.9 and in S₂ and S₄ 21.5 mS/cm, respectively. Dry weight concentrations of *D. salina* grown in reactors D₁ and D₂ with SADS (1.36–1.49 g/L) were achieved which were more than that with Bold's Basal Medium (0.84–1.04 g/L) in reactors D₃ and D₄. Dry weight concentrations of *S. platensis* with SADS (1.41–1.98 g/L) in reactors S₁ and S₂ were achieved which were more than that supplied with F2 (0.68–1.20 g/L) in reactors S₃ and S₄. In those cases where SADS was the nutrient, low conductivity mediums provided the higher microalgae dry weight concentrations. Dry weights of both species achieved by reusing concentrate and SADS in our studies were 1.49 g/L (*D. salina*) and 1.98 g/L (*S. platensis*) that are comparable to that of literature data where sea water and pretreated sea water were used. Both species gain a negative net energy ratio. Energy content of 3.02–4.24 kJ/L is required for a positive net energy ratio in microalgae growth culture. Conductivities of growth mediums from all reactors in which *D. salina* were grown are less than the conductivity of drinking water quality required for sheep. Net energy ratio of *D. salina* is less than that of *S. platensis*. For conservative and reusable drinking water for sheep, *D. salina* was used as microalgae to treat concentrate in

*Corresponding author.

our analyses. Energy usage and CO₂ emission saved from innovative integrated desalination were 4–14%.

Keywords: CO₂ emission saving; Desalination concentrate; *Dunaliella salina*; Energy saving; Net energy ratio; *Spirulina platensis*

1. Introduction

1.1. Further treatment required for desalination concentrate

In the past several years, the western USA has suffered and continues to suffer from severe drought. The water level in rivers has decreased along with the water level of the reservoirs downstream. These losses are typically replaced by pumping and desalting brackish groundwater that carries total dissolved solids (TDS) > 1,000 mg/L. Desalination technologies such as reverse osmosis, nanofiltration, and electrodialysis (reversal) (ED(R)) to desalt brackish groundwater into drinking water show promise, but these technologies have a big drawback when applied in large-scale systems because only dissolved ions are physically transferred from one stream to another stream. The transferred ions carried by the stream have very high conductivity and have not received treatment. The direct and indirect discharges of the concentrate pose an environmental risk, both now and, more so, in the future as such CO₂-untreated discharges build up in the atmosphere little by little which, subsequently, contributes to climate change. The literature repeatedly suggests treating desalination concentrate further. Additional treatment, however, raises the desalination cost, energy usage, and carbon dioxide concentration emission.

1.2. Reuse desalination concentrate in culturing microalgae

Spirulina requires dissolved inorganic carbon as a nutrient for growth. *Spirulina* can consume dissolved carbon dioxide in water medium as a primary substrate for its growth [1]. *Spirulina* is a photosynthesizing cyanophyte (blue-green algae) and has the ability to grow energetically in sturdy sunlight under hot temperatures and highly alkaline conditions [2]. *Spirulina* prospers in alkaline lakes where it is difficult or impossible for other organisms to live [1,3]. *Dunaliella* prospers in high-salinity water. In open lakes, microalgae growth cycles are normally limited by the availability of nutrients in the water medium. The growth and carotenogenesis medium cost one-third of the total cost of thorough production of *Dunaliella salina* [4]. If *D. salina* can be cultured from cost-free growth medium and nutrient, not only about

one-third of the total cost but also CO₂ emission from fossil-based manufacturing growth medium and nutrients can be avoided.

1.3. Reuse anaerobic digested sludge in microalgae culture for sustainability

Reusing waste materials improves the net energy gain of the first- and second-generation biofuels and will improve the third-generation biofuel. The first-generation biofuels were fed from energy plants (sugar cane, corn, and soybean), but were accompanied by excessive water and land uses and deforestation. The second-generation biofuels were generated from lignocellulose agriculture and forest residues. However, their conversion rates are slow and they need large areas of reactor footprint land and are economically not feasible. To be environmentally friendly and cost-effective, the literature recommended that the whole energy crops traditionally unused and residues from lignocellulose agriculture and forest be co-fed with animal waste and/or anaerobic digested sludge to stoichiometrically balance the carbon, nutrients, and micro-organisms and accelerate the biochemical conversion rate in the first- and second-biofuel processes, respectively. Microalgae were suggested as third-generation biofuels, thus eliminating the disadvantages of the first- and second-generation biofuel processes. Oil from microalgae process was not yet economically viable in 2007 technologies [5] as revealed by both the key projects funded by the governments of the USA and Japan. Algae biodiesel production cost is almost 10-fold higher than crude oil [6]. Literature everywhere, therefore, has concentrated on finding cost-free sources of carbon, nutrients, growth mediums, and reactor materials as much as possible to further reduce the production costs of microalgae [2,7–9] and to increase the sustainability of the environment.

The reuse of desalination concentrate, supernatant from anaerobic digested sludge (SADS), and used bottles in microalgae production follows the fundamental eco-environmental and ecologically sound practices. Conservation environmentalists recommended that the investigation of the fundamentals of eco-environmental and ecologically sound environmental practices be carried out to initialize the regions specific standards or

best practices for achieving the highest harvests with least environmental impact. That means that processes for sustainable energy production must be environmentally benign, reduce greenhouse gas production, and utilize renewable resources. Desalination concentrate, SADS, and used bottles are renewable resources.

1.4. Hypothesis

HCO_3^- acts as a buffer and protects microalgae growth culture from pH fluctuations that can be harmful to microalgae growths. Additionally, HCO_3^- , as an inorganic carbon source, improves growth cultures in carbon storage compared to CO_2 [10]. Concentrate from brackish groundwater desalination dissolves more HCO_3^- than that from sea water desalination. *Spirulina* prospers in high CO_3^{2-} and HCO_3^- water [11]. CO_3^{2-} , HCO_3^- , and alkaline-rich desalination concentrate with pH (8.5–11.0) is ideally suitable for *Spirulina platensis* growth [1]. *Dunaliella* species are native to salty lake water [12]. *Dunaliella* also has a wide range of pH forbearing ability ranging from pH 1 (*D. acidophila* [13]) to pH 11 (*D. salina*). *D. salina* is one of the most environmentally forbearing eukaryotic organisms recognized and can survive from sea water (= 3% NaCl) to NaCl saturation (= 31% NaCl), and temperature ranging from $<0^\circ\text{C}$ to $>38^\circ\text{C}$ [14,15]. Energy consumed per energy produced for nutrients in microalgae production is 0.455 MJ/MJ [16]. The objectives of this article are: (one) to evaluate the net energy ratio of microalgae (*D. salina* and *Arthrospira* (*Spirulina*) *platensis*) production and (two) to analyze the energy usage and CO_2 saved in these microalgae production in used bottles as reactors.

2. Method

2.1. Analytical method and sampling

Microalgae species *D. salina* were sampled in the New Mexico State University Lab. *Arthrospira* (*Spirulina*) *platensis* were sampled at the University of Texas at Austin. These species were grown in used bottles (3.785 L volume) by reusing desalination concentrate as the growth medium and SADS from wastewater treatment plant as nutrients (Table 1). To narrow the gap between lab- and field-scale studies, natural desalination concentrate samples were used in the research for all the tests [17]. Desalination concentrate samples were collected from desalination concentrate ponds of the Brackish Groundwater National Desalination Research Facility located in Alamogordo, NM, USA. Anaerobic digested sludge was collected from Las

Cruces Wastewater Treatment Plant, NM. Desalination concentrate and anaerobic digested sludge were separately centrifuged for 3 min at 10,000 rpm to collect the supernatants. The supernatants were used in the studies. Dry weight concentration and optical density of growth culture were used to identify the microalgae growth. About 10 mL of cell suspension sample was withdrawn from the reactor, centrifuged for 3 min at 10,000 rpm, the supernatant was decanted, and the remaining microalgae slurries were dried at 103–105°C in an oven to measure the dry weight concentration of microalgae, and the dry weights concentrations of the microalgae were measured according to SM 2540D [18,19]. The same volume of supernatant of each sample was also dried in the same oven to obtain the correct TDS concentration from microalgae slurries to get TDS-free dry weight concentration of microalgae. The optical density of growth culture was measured with the spectrophotometer (Hach DR/2010) at 560 nm wavelength, the same wavelength 560 nm recommended by Concas et al. [20] for the measurement of optical density. The pH was measured with Cole Parmer pH meter AB15 accumet basic. The conductivity was measured with the Hach sension5 conductivity meter. Dry weight concentrations were measured at 13 and 11 points after 41 and 34 d of treatment for *D. salina* and *S. platensis*, respectively. Optical density of growth culture was measured at 15 and 12 points after 41 and 34 d of treatment for *D. salina* and *S. platensis*, respectively. Conductivity of growth culture was measured at 18 and 12 points after 41 and 34 d of treatment for *D. salina* and *S. platensis*, respectively. Optical density of growth culture was measured at 15 and 12 points after 41 and 34 d of treatment for *D. salina* and *S. platensis*, respectively. The pH of growth culture was measured at 17 and 12 points after 41 and 34 d of treatment for *D. salina* and *S. platensis*, respectively.

2.2. Contents in open reactors

All reactors were filled with desalination concentrate and seed microalgae as shown in Table 1. Reactors D_1 , D_2 , S_1 , and S_2 were fed with SADS as nutrients. Reactors D_3 and D_4 were fed with Bold's Basal Medium [21] and S_3 and S_4 with F2 [22] as nutrients. The reactors were bubbled with air from the environment (which contained CO_2 at 0.0387% by volume), 8 hours a day. All reactors were directly exposed to sunlight from 9:00 am to 5:00 pm on non-holidays by taking the reactors outside during daylight hours and moving them back into the lab room at night. The experiments D_1 , D_2 , D_3 , and D_4 were performed during November–December 2011

Table 1
Contents in reactors

Reactor	Desalination concentrate		Seed microalgae		Seed microalgae	Nutrient
	Conductivity $\mu\text{S}/\text{cm}$	Volume L	Weight g/L dry	Volume L		
D_1	31,800	2.00	0.79	0.11	<i>D. salina</i>	SADS
D_2	25,442	2.00	0.79	0.11	<i>D. salina</i>	SADS
D_3	31,800	2.00	0.45	0.08	<i>D. salina</i>	BBM
D_4	25,442	2.00	0.45	0.08	<i>D. salina</i>	BBM
S_1	35,900	1.97	1.01	0.10	<i>S. platensis</i>	SADS
S_2	21,500	1.97	1.01	0.10	<i>S. platensis</i>	SADS
S_3	35,900	1.97	2.68	0.10	<i>S. platensis</i>	F2
S_4	21,500	1.97	2.68	0.10	<i>S. platensis</i>	F2

Notes: SADS = Supernatant from anaerobic digested sludge after centrifugation at 10,000 rpm for 3 min twice. BBM = Bold's Basal Medium.

and S_1 , S_2 , S_3 , and S_4 were performed during January–February 2012 in New Mexico State University, Las Cruces, NM. Sunlight radiation data were not collected since sunlight radiation varies with time (from 9:00 am to 5:00 pm) during the day and location of surface in reactors. The reactors were illuminated with light bulbs on holidays when the reactors were in the lab. The radiations from light bulbs to reactors were also not collected since the exposure time of light bulb is negligible compared to the exposure time of sunlight. SADS was fed periodically as fed-batch culture. The seed microalgae concentrations for *D. salina* and *S. platensis* were 0.029 (stdev 0.014) and 0.089 (stdev 0.047) g/L in reactors D and S , respectively. These different concentrations of seed microalgae between *D. salina* and *S. platensis* affected the growth of these microalgae, differently.

3. Results and discussion

Dry weight concentrations of *D. salina*, and *S. platensis*, optical density, conductivities of growth media, nutrient added as fed-batch, pH, temperature of cultures when the reactors were in lab, and air flow rate vs. culturing time are plotted in Figs. 1 and 2. The temperature of the cultures was 32.8–47.2 °C when the reactors were outside the lab directly under the sun. The volume of the nutrient added to reactors increases with the time of experimentation as shown in Figs. 1(d) and 2(d) because the microalgae's dry weight concentrations and optical density of growth medium increase with time as shown in Figs. 1(a) and (b), and 2(a) and (b). The comparison of dry weight concentrations and specific growth rates of *D. salina* and *S. platensis* between our studies and literature data is presented in Tables 3 and 4.

3.1. Comparison of biomass microalgae between SADS and BBM or F2

Dry weight concentrations of *D. salina* supplied with SADS (1.36–1.49 g/L) were higher than that supplied with BBM (0.84–1.04 g/L) as shown in Fig. 1(a). Dry weight concentrations of *S. platensis* supplied with SADS (1.41–1.98 g/L) were higher than that supplied with F2 (0.68–1.20 g/L) as shown in Fig. 2(a). The reason for this may be that the micro-organism grew in SADS [23] along with microalgae, and the micro-organism promoted microalgae growth. This finding agrees with the finding of Wang et al. [24]. Wang et al. [24] stated that the specific growth rate of microalgae from concentrate (wastewater from sludge centrifuge) is higher than that from wastewater before and after primary settling and aeration tank. Wastewater from sludge centrifuge has more micro-organisms than the wastewater before and after primary settling and aeration tank. In cases of SADS as nutrients, low conductivity mediums provide higher microalgae dry weight concentrations. In cases of Bold's Basal Medium and F2 as nutrients, higher conductivity mediums provided higher microalgae dry weight concentrations.

3.2. Comparison of biomass microalgae between our study and literature

Dry weight concentrations of both species by reusing concentrate and SADS achieved from our studies are 1.49 g/L (*D. Salina*; Fig. 1(a)) and 1.98 g/L (*S. Platensis*; Fig. 2(a)). These results are comparable to that of literature data (*D. salina* 1.06 g/L and *S. platensis* 0.8–2.99 g/L in Tables 3 and 4), where sea water and pretreated sea water were used. Dry weight

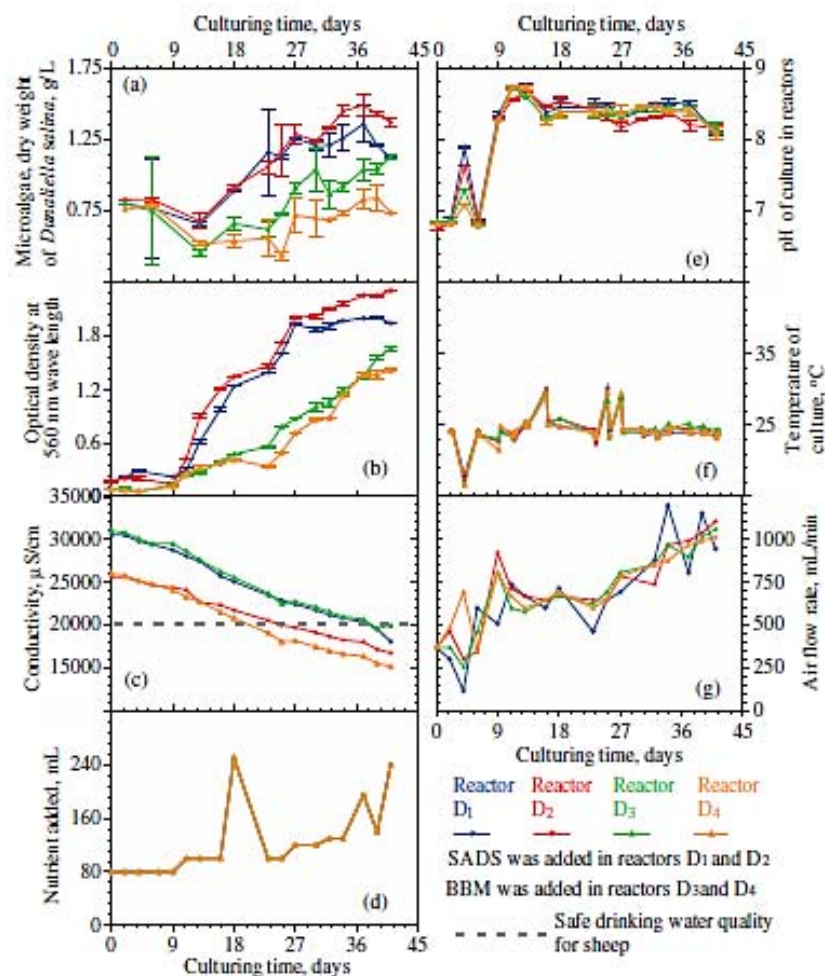


Fig. 1. *D. salina*'s growing characteristics with culturing time (a) dry weight; (b) optical density; (c) conductivities of media in reactors; (d) nutrient added into reactors; (e) pH; (f) temperature when reactors were in the lab; (g) air flow rate.

concentration 2.587 g/L of *S. platensis* was observed in the work of Volkmann et al. [25] in desalinated wastewater. Dry weight concentration of 2.37 g/L of dry biomass was observed by Pandey et al. [26] at pH 8.25, temperature at 30°C, and light intensity of 3 Klux [27]. Dry weight concentration of *S. platensis* 2.34 g/L was found on the 27th day of culturing in 30% petha waste medium supplemented with standard medium (for example, CFIRI medium) in triplicate at 3 Klux light intensity, pH 9.5 ± 0.1, and 30°C ± 2 temperature under 12/12 h light/dark cycles [27]. Dry weight concentration 2.91 g/L of *S. platensis* was observed at input CO₂ concentration of 10% on the 25th day of

culturing by Ramanan et al. [28]. Longer culturing time 37–39 d for *D. salina* was required to reach maximal growth due to higher conductivities in concentrate (Table 2) and color from SADS. The color of SADS decreases the transparency of the used plastic bottles as reactors. The growth rate of microalgae also depends on the amount of seed microalgae in the growth media [29,30].

The growth of *D. salina* may be inhibited in desalination concentrate by brackish groundwater since this concentrate contains high concentration of SO₄²⁻ and high concentration of HCO₃⁻. *D. salina* prefers high pH of 11 while the pH of the growth culture was between

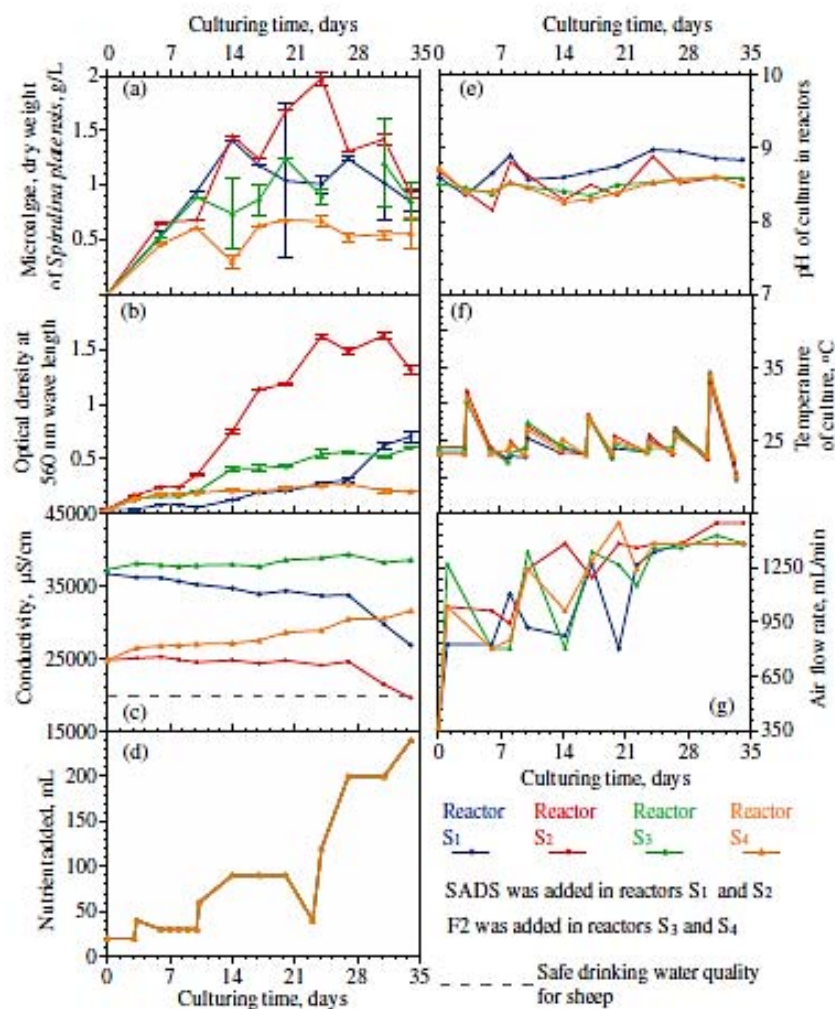


Fig. 2. *S. platensis*'s growing characteristics with culturing time (a) dry weight; (b) optical density; (c) conductivities of media in reactors; (d) nutrient added into reactors; (e) pH; (f) temperature when reactors were in the lab; (g) air flow rate.

6.8 and 8.8 in Fig. 1(e). Therefore, longer culturing time is required for *D. salina* to reach the maximum dry weight concentration compared to *S. platensis*, since *Spirulina* prospers in high CO_3^{2-} and HCO_3^- water [11] in the pH range of 8.5–11.0 [1].

3.3. Specific growth rate

$$\mu = \{\ln(W_y/W_x)\}/\{t_y - t_x\} \quad (1)$$

where W_y and W_x are the microalgae dry weight (W) at the start (t_x) and the end (t_y) of the logarithmic growth phase [31,32].

The specific growth rate was found from the Eq. (1). The available specific growth rates of *D. salina* from literature, culturing with NaCl as growth medium [33], and manufactured chemical nutrient [34] were used to compare with that from our studies. The natural desalination concentrate and SADS were used in our studies (Tables 3 and 4), and the specific growth rates from our studies (0.095–0.114 for *D. salina* in Table 3 and 0.019–0.034 for *S. platensis* in Table 4) were lower than those reported in literature (0.12–0.47 for *D. salina* [34] in Table 3 and 0.255 for *S. platensis* from [51] in Table 4), where sea water and pretreated sea water were used as water medium in

Table 2
Maximal dry weight concentrations in reactors

Reactor	Seed microalgae	Nutrient	At which the highest dry weight occurs				
			Weight g/L dry	Optical density	pH	Temp °C	<i>d</i>
<i>D</i> ₁	<i>D. salina</i>	SADS	1.36	2.002	8.5	24–24	37
<i>D</i> ₂	<i>D. salina</i>	SADS	1.49	2.259	8.2	24–24	37
<i>D</i> ₃	<i>D. salina</i>	BBM	1.04	1.355	8.4	24–25	37
<i>D</i> ₄	<i>D. salina</i>	BBM	0.84	1.369	8.2	23–24	39
<i>S</i> ₁	<i>S. platensis</i>	SADS	1.41	0.125	8.6	23–24	14
<i>S</i> ₂	<i>S. platensis</i>	SADS	1.98	1.625	8.9	23–26	24
<i>S</i> ₃	<i>S. platensis</i>	F2	1.24	0.434	8.5	23–24	20
<i>S</i> ₄	<i>S. platensis</i>	F2	0.68	0.236	8.4	23–25	20

Note: SADS = Supernatant from anaerobic digested sludge after centrifugation at 10,000 rpm for 3 min twice.

closed reactor. Misleading conclusions can be made in comparison in the microalgae growth rate in between different water mediums, different nutrient supplied, and different types and characteristics of reactors used [30]. Pittman et al. [30] states that nutrient removal rates are comparable. However, microalgae growth rates are higher in artificial wastewater than that in natural wastewater [29,35]. This may be due to the increased toxicity of natural wastewaters, or the competitive effects of indigenous bacteria and protozoa, or by the diverse chemical composition of the natural wastewaters [30]. Natural concentrate from desalination of the evaporation pond has to be used for simulating real-world conditions [17] and to reduce the disconnection gap between lab and field. Sheehan et al. [36] stated that there is disengagement between the lab and the field. The lab condition requires simulating the field situation as such using natural concentrate in the experiments.

The lower specific growth rates of microalgae may also be due to the temperature fluctuation between daytime (open outdoor 32.8–47.2°C in our study) and nighttime (in lab 17–30°C in our study), or the illumination problems from the color of SADS (optical density 0.58 at 560 nm wavelength). The higher concentrations of TDS, N, Mg²⁺, and Ca²⁺ can be toxic to the microalgae growth [37]. Tredici and Zittelli [38] found that the outdoor cultures of *S. platensis* (1.09 and 1.26 g/L/d) were lower than that of indoor (1.64–1.93 g/L/d). However, the enthalpies are similar (20.9–21.6 kJ/g). Torzillo et al. [39] concluded that temperature and light irradiance influence the biomass composition and found that dry weight concentrations of biomass were reduced during the night due to the decrease of these two factors.

3.4. Waste materials improve the net energy gain in microalgae production

The energy produced per energy consumed in microalgae processes is in the range of 0.2–2 MJ/MJ [16,40] without reusing waste materials. The analyses of net energy ratio are shown in Table 5. The maximal dry weights of *D. salina* and *S. platensis* grown in desalination concentrate and supplied with SADS are 1.36–1.49 and 1.41–1.98 g/L, respectively, in our study. The lipid contents of *D. salina* and *S. platensis* are in the ranges of 3.29–4.03 and 6.2–10.6% [41–43]. Analyses show that both species gain negative net energy ratio reusing of waste materials (reactor, growth medium, and nutrients) were reused. Energy consumed per energy produced for nutrients in microalgae production is 0.455 MJ/MJ [16], and energy saved from nutrients is about 45.5% of the energy produced.

3.5. Net energy ratio

Net energy ratio was reported in Table 5. Net energy ratio was calculated as energy produced divided by energy used in microalgae process. Energy produced and energy used were calculated by Eqs. (2) and (3) as:

$$\text{Energy produced} = \frac{(\text{DW}_{\text{microalgae}}) (\text{Lipid}_{\text{content}})}{(\text{Energy}_{\text{content}}) (\eta)} \quad (2)$$

where energy produced = energy production from microalgae (dry) grown in 1 L culture, kJ/L_{culture}; DW_{microalgae} = microalgae (dry) concentration grown in 1 L growth culture, g/L_{culture}; Lipid_{content} = lipid content in respective microalgae (dry), %; Energy_{content} = energy content in lipid, kJ/g; and η = efficiency of microalgal oil to biodiesel, %.

Table 3
Comparison of dry weight and specific growth rate between our data and literature values for *D. salina*

<i>D. salina</i> data from our lab				<i>D. salina</i> data from literature				Ref.			
Water media	Nutrient	Dry weight, g/L	Culturing time day	Specific growth rate, d ⁻¹	Water media	Nutrient	Dry weight, g/L	Culturing time day	Specific growth rate, d ⁻¹	Type of reactor	
Conc. ^a	SADS	1.36	37	0.095	Sea water	NaNO ₃	1.06	17			[50]
Conc. ^b	SADS	1.49	37	0.097	Sea water	F2	0.33	Semi-cont.	0.12–0.33	Open	[34]
Conc. ^a	BBM	1.04	37	0.114	Sea water	F3	0.53	25, bench	0.33	Open	[34]
Conc. ^b	BBM	0.84	39	0.106	Sea water	F4	1.65	Semi-cont.	0.22–0.46	Closed	[34]
					Sea water	F5	2.00	25, bench	0.47	Closed	[34]
					10% NaCl	J/1			0.28		[33]

Notes: Conc.^a = desalination concentrate which has conductivity 31,800 µS/cm; Conc.^b = desalination concentrate which has conductivity 25,442 µS/cm. SADS = Supernatant from anaerobic digested sludge after centrifugation at 10,000 rpm for 3 min twice. BBM = Bold's basal medium.

Table 4
Comparison of dry weight and specific growth rate between our data and literature values for *Spirulina platensis*

S. platensis data in our lab		S. platensis literature data								
Water media	Nutrient	Dry weight g/L	Process day	Specific growth rate, d ⁻¹	Water media or reactor	Nutrient medium	Dry weight, g/L	Process day	Specific growth rate, d ⁻¹	Ref.
Conc. ^a	SADS	1.41	14	0.030	PS		2.26-2.99	25	0.255	[51]
Conc. ^a	SADS	1.98	24	0.032	OP	Zarrouk's	1.1	8		[52]
Conc. ^a	F2	1.20	31	0.034	DW	50%ADE	1.23	14		[53]
Conc. ^a	F2	0.68	24	0.019	10% OM	Zarrouk's	0.8-1.0	21-25		[54]
					CP	NO ₃ ⁻ , HCO ₃ ⁻	1.70	NA		[43]
					Desalinated WW		2.59	NA		[25]
					30% petha	CFTRI	2.37	NA		[26,27]
							2.34	27		[27]
							2.91	25		[28]

Notes: Conc.^a = desalination concentrate which has conductivity 35,900 µS/cm. Conc.^b = desalination concentrate which has conductivity 21,500 µS/cm. ADE = anaerobically digested distillery effluent. OM = olive oil mill wastewater; NaOCl was used to decrease the phenol concentration and turbidity. PS = pretreated sea water. OP = open pond 2.5 m². DW = distilled water. CP = closed photobioreactor. CFTRI = prescribed medium [27]. SADS = supernatant from anaerobic digested sludge after centrifugation at 10,000 rpm for 5 min twice.

Table 5
Net energy analysis of microalgae production

Description/reactors	<i>D. salina</i>		<i>S. platensis</i>		Unit	Ref.
	<i>D</i> ₁	<i>D</i> ₂	<i>S</i> ₁	<i>S</i> ₂		
<i>Energy produced from microalgae production</i>						
Dry weight of microalgae from our study	1.36	1.49	1.41	1.98	g/L _{culture}	
Lipid content in respective dry microalgae	3.29	3.29	10.6	10.6	%	[41,42]
Lipid content in respective dry microalgae	4.03	4.03	6.2	6.2	%	[41,43]
Energy content in lipid	38.3	38.3	38.3	38.3	kJ/g	[57]
Energy convertible from microalgae	1.91	2.09	4.54	6.37	kJ/L _{culture}	
Efficiency, algal oil to biodiesel	63.9	63.9	63.9	63.9	%	[55]
Energy produced	1.22	1.33	2.90	4.07	kJ/L _{culture}	
<i>Energy used in microalgae production</i>						
Energy used in supplying CO ₂ from air	0.35	0.35	0.35	0.35	kWh/kg _{biomass}	
Energy used in pumping for harvesting	0.10	0.10	0.10	0.10	kWh/kg _{biomass}	[56]
Energy for centrifugation for harvesting	0.10	0.10	0.10	0.10	kWh/kg _{biomass}	[56]
Energy for oil extraction and conversion to biodiesel	0.05	0.05	0.05	0.05	kWh/kg _{biomass}	[56]
Total energy used	0.60	0.60	0.60	0.60	kWh/kg _{biomass}	[56]
Total energy used	0.60	0.60	0.60	0.60	Wh/g _{biomass}	
Total energy used	0.82	0.89	0.85	1.19	Wh/L _{culture}	
Total energy used	2.91	3.19	3.02	4.24	kJ/L _{culture}	
<i>Net energy ratio</i>						
Energy produced/energy used	0.42	0.42	0.96	0.96	Unit less	
Energy loss in microalgae production	-1.70	-1.86	-0.12	-0.17	kJ/L _{culture}	

$$E_{\text{used}} = E_{\text{CO}_2} + E_{\text{pumping}} + E_{\text{centrifuging}} + E_{\text{extraction}} \quad (3)$$

E_{used} = energy used in microalgae production, E_{CO_2} = energy used in supplying CO₂ from air, kJ/L_{culture}; E_{pumping} = energy used in pumping in microalgae harvesting process, kJ/L_{culture}; $E_{\text{centrifuging}}$ = energy used for centrifugation in microalgae harvesting process, kJ/L_{culture}; $E_{\text{extraction}}$ = energy used for oil extraction, and conversion to biodiesel, kJ/L_{culture}.

The net energy ratios calculated from *D. salina* and *S. platensis* were 0.42 and 0.96, respectively, as shown in Table 5, and these values are less than neutral. The net energy ratios of *D. salina* are less than those of *S. platensis* because *D. salina* had both less dry weight concentration and less lipid content compared to the *S. platensis*. Net energy ratio from *S. platensis* (0.96) is close to neutral. From Table 4, 3.02–4.24 kJ/L of the energy content in microalgae growth culture is required for a positive net energy ratio.

3.6. Using waste concentrate in microalgae (*D. salina*) production for desalination energy reduction

Conductivities of growth mediums at the end of test from all reactors in which *D. salina* were grown

are less than 20,000 μS/cm, which is the maximal allowable conductivity of drinking water quality required for sheep as shown in Fig. 1(c). Net energy ratio of *D. salina* is less than that of *S. platensis*. For conservative and reusable drinking water for sheep, *D. salina* was used as microalgae to treat concentrate in our analyses.

Tables 6 and 7 compare energy consumption in desalinations between traditional EDR desalination with ED as concentrate treatment and innovative integrated desalination with microalgae production as concentrate treatment. Traditional EDR desalination contains two processes as shown in Fig. 3(a). The first process is the EDR desalination, and the data from [45,46] were used in the analyses as shown in Tables 6 and 7. The second process is concentrate treatment, in which the concentrate (TDS 0.2–2%) from the first stage was concentrated to TDS 12–20% using ED with energy consumption of 1–7 kWh/m³ [47–49]. The innovative integrated desalination also contains two processes as shown in Fig. 3(b). The first process is the same as that of the traditional EDR desalination. However, concentrate from the first process was used in microalgae production as concentrate treatment in innovative desalination.

Downloaded by [New Mexico State University], [waddah hussein], [waddah hussein] at 12:47 10 February 2014

Table 6
Traditional vs. innovative EDR desalination: feed TDS 1817 mg/L

1	2	3	4	5	6	7	8	9	10	11
First stage-EDR desalination		Second stage-conc. management	Second stage-conc. management	Second stage-conc. management	Microalgae production using conc.					
Feed dissolved ions 1817 mg/L		Traditional EDR desalination	Traditional EDR desalination	Traditional EDR desalination	Microalgae production using conc.					
Water recovery rate % [45]	Power used in desalination kJ/L p [45]	Power used in pumping kJ/L p	Power used in concentrate management kJ/L c [46-48]	Life cycle desalination power used kJ/L p	Power loss in algae L c*	Power loss in algae kJ/L p	Power loss in algae kJ/L p	Life cycle desalination power used kJ/L p	Power usage saving %	Saving in CO ₂ emission %
70.9	1.90	0.38	2.94	1.21	1.78	0.73	1.78	3.01	13.7	13.7
79.3	2.18	0.44	3.06	0.80	1.78	0.46	1.78	3.08	9.8	9.8
82.8	2.37	0.47	3.53	0.73	1.78	0.37	1.78	3.21	10.2	10.2
85.7	2.64	0.53	3.79	0.63	1.78	0.30	1.78	3.47	8.8	8.8
88.1	2.91	0.58	4.24	0.57	1.78	0.24	1.78	3.73	8.1	8.1
87.4	2.92	0.58	3.96	0.57	1.78	0.26	1.78	3.76	7.7	7.7
79.2	3.16	0.63	4.33	1.14	1.78	0.47	1.78	4.26	13.6	13.6
86.0	3.10	0.62	4.96	0.81	1.78	0.29	1.78	4.01	11.4	11.4
86.0	3.81	0.76	5.72	0.93	1.78	0.29	1.78	4.86	11.7	11.7

Notes: c = conc. = concentrate waste, p = product EDR - electrolysis reversal. Traditional EDR desalination - EDR as first stage for desalination and EDR as second stage for concentrate treatment. Innovative EDR desalination - EDR as first stage for desalination; microalgae as second stage for concentrate treatment. *Referred from the average value of data from columns 2 and 3 of Table 5.

Table 7
Traditional vs. innovative EDR desalination: feed TDS 4,042 mg/L

1	2	3	4	5	6	7	8	9	10	11
First stage-EDR desalination			Second stage-conc. management			Second stage-conc. management				
Feed dissolved ions 1,817 mg/L			Traditional EDR desalination			Microalgae production using conc.				
Water recovery rate % [44]	Power used in desalination kJ/L.p [44]	Power used in pumping kJ/L.p	Power used in concentrate management		Life cycle desalination power used kJ/L.p	Power loss in algae kJ/L.c*	Power loss in algae kJ/L.p	Life cycle desalination power used kJ/L.p	Power usage saving %	Saving in CO ₂ emission %
			kJ/L.c [46-48]	L.p						
73.2	6.5	1.30	4.19	1.53	9.35	1.78	0.65	8.47	9.4	9.4
79.4	6.8	1.37	4.71	1.22	9.43	1.78	0.46	8.67	8.1	8.1
84.0	7.1	1.42	5.50	1.05	9.56	1.78	0.34	8.85	7.4	7.4
86.8	7.7	1.54	6.17	0.94	10.18	1.78	0.27	9.52	6.5	6.5
91.4	8.9	1.77	8.31	0.78	11.41	1.78	0.17	10.79	5.4	5.4
93.1	11.6	2.33	9.83	0.73	14.68	1.78	0.13	14.09	4.1	4.1

Notes: c = conc. = concentrate waste, p = product EDR – electrolysis reversal. Traditional EDR desalination – EDR as first stage for desalination and EDR as second stage for concentrate treatment. Innovative EDR desalination – EDR as first stage for desalination; microalgae as second stage for concentrate treatment. *Referred from the average value of data from columns 2 and 3 of Table 5.

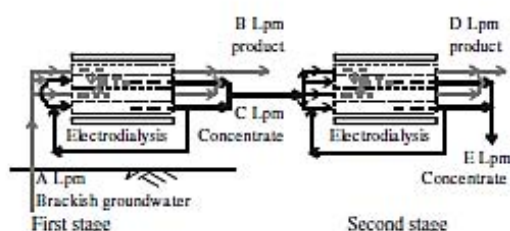


Fig. 3(a). Traditional ED desalination and concentrate management, first stage: traditional ED desalination; second stage: concentrate management in which concentrate from the first stage was fed in the microalgae production; Lpm = litre per minute.

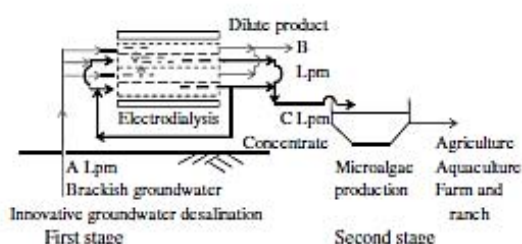


Fig. 3(b). Innovative ED desalination and concentrate management, first stage: traditional ED desalination; second stage: concentrate management in which concentrate from the first stage was fed in the microalgae production; Lpm = litre per minute.

Energy consumption of EDR desalination is 0.528–3.23 kWh/m³ (1901–11,628 J/L as shown in Tables 6 and 7) of desalted product water, depending on water recovery rate and chemical characteristics of feed water [45,46]. The pumping energy was assumed as 20% of energy consumption of EDR desalination as shown in our analysis in Tables 6 and 7.

Data in columns 1, 2, and 3 of Tables 6 and 7 were for first-stage EDR desalination which desalted brackish groundwater into drinking water. Data in columns 1 and 2 of Table 6 were referred from [46]. Data in columns 1 and 2 of Table 7 were referred from [45]. Data in column 3 of Tables 6 and 7 were calculated from 20% of column 2. Data in columns 4, 5, and 6 of Tables 6 and 7 were for second-stage traditional EDR desalination which desalted concentrate from the first stage into drinking water and highly concentrated concentrate. Data in column 4 of Tables 6 and 7 were referred, interpolated, and extrapolated from literature data that stated that

TDS 0.2–2% from the first stage was concentrated to TDS 12–20% by using ED with the energy consumption of 1–7 kWh/m³ [47–49]. Data in column 5 of Tables 6 and 7 were converted to kWh per m³ of product from kWh per m³ of concentrate. Data from column 6 of Tables 6 and 7 were summed from data from columns 2, 3, and 5. Data in columns 7, 8, and 9 of Tables 6 and 7 were for second-stage concentrate management using concentrate from first stage in microalgae production. Data in column 7 of Tables 6 and 7 were calculated from the difference in the energy content of *D. salina* and the energy used as shown in Table 5. Data in column 8 were kWh per m³ of concentrate as shown in column 7 of Tables 6 and 7 into kWh per m³ of product. Data in column 9 of Tables 6 and 7 were the sum of Data columns 2, 3, and 8. Data in column 10 of Tables 6 and 7 were calculated by employing data from columns 6 and 9. CO₂ emissions in column 11 of Tables 6 and 7 were calculated from life cycle CO₂ emission rate 1.001 kg/KW-hr.

Our calculations show that minimal energy usage and CO₂ emission reduction employing innovative integrated EDR desalination are 4–14% as shown in Tables 6 and 7.

The desirable TDS and maximum TDS for drinking water quality guidelines for sheep are 5,000–10,000 mg/L TDS or 10,000–20,000 μS/cm. The range for beef cattle is 4,000–5,000 mg/L TDS or 8,000–10,000 μS/cm according to NSW Public Works [44]. The conductivities from reactors *D*₁, *D*₂, *D*₃, and *D*₄ after 39, 27, 39, and 23 d of *D. salina* treatment were lower than the conductivity requirement in the drinking water quality guidelines for sheep, respectively, as shown in Fig. 1(c). The conductivities from reactors *S*₂ after 34 d of *S. platensis* treatment were lower than the conductivity requirement in the drinking water quality guidelines for sheep as shown in Fig. 2(c). The treated desalination concentrate contains green food, protein, nutrients, minerals, and desalted water; the treated desalination concentrate from reactors *D*₁ to *D*₄ and *S*₂ can be given to sheep in semi-arid regions where green food and water resources are gradually diminishing.

4. Conclusion

The maximal dry weights of *D. salina* and *S. platensis* grown in desalination concentrate and supplied with SADS (1.36–1.49 g/L) were more than that supplied with BBM and F2 due to micro-organism growth along with microalgae. Micro-organism promotes

microalgae growth. The maximal dry weight concentrations of *D. salina* and *S. platensis* grown in desalination concentrate and supplied with SADS were comparable to that in the literature. Energy usage and CO₂ emission reduction employing innovative integrated EDR desalination with microalgae production as concentrate treatment are 4–14% lower than concentrate treatment using ED.

Acknowledgments

This project was supported, in part, by the USA Office of Naval Research (ONR) (Contract # N00014-08-1-0304), Tier I: Reclamation Cooperative Agreement Program through Bureau of Reclamation GR0002841-GHASSEMI BOR COOP, National Science Foundation Engineering Research Center Program (ReNUWIt), and by the Ed & Harold Foreman Endowed Chair.

References

- [1] M.A.B. Habib, M. Parvin, T.C. Huntington, M.R. Hasan, A Review on Culture, Production and Use of *Spirulina* as Food for Humans and Feeds for Domestic Animals and Fish, FAO Fisheries and Aquaculture Circular. No. 1034, FAO, Rome, 2008, p. 33.
- [2] J.A.V. Costa, L.M. Colla, P.F.D. Filho, Improving *Spirulina platensis* biomass yield using a fed-batch process, *Bioresour. Technol.* 92 (2004) 237–241.
- [3] E. Kebede, G. Ahlgren, Optimum growth conditions and light utilization efficiency of *Spirulina platensis* (= *Arthrospira fusiformis*) (Cyanophyta) from Lake Chitu, *Ethiop. Hydrol.* 332 (1996) 99–109.
- [4] C.A. Santos, A.M. Vieira, H.L. Fernandes, J.A. Empis, J.M. Novais, Optimisation of the biological treatment of hypersaline wastewater from *Dunaliella salina* carotenogenesis, *J. Chem. Technol. Biotechnol.* 76 (2001) 1147–1153.
- [5] M.E. Huntley, D.G. Redalje, CO₂ mitigation and renewable oil from photosynthetic microbes: A new appraisal, *Mitig. Adapt. Strat. Global Change* 12 (2007) 573–608.
- [6] Y. Chisti, Biodiesel from microalgae beats bioethanol, *Trends Biotechnol.* 26 (2008) 126–131.
- [7] E.J. Olgun, E. Alarcon, S. Galicia, Recycling of pig waste recovery of *Spirulina* sp. at pilot plant level, under tropical conditions, in: *Proceedings of the Eighth International Conference on Applied Algology*, September 29–October 1, 1999, Montecatini Terme, Italy.
- [8] G. Samorì, C. Samorì, F. Guerrini, R. Pistocchi, Growth and nitrogen removal capacity of *Desmodesmus communis* and of a natural microalgae consortium in a batch culture system in view of urban wastewater treatment: Part I, *Water Res.* 47 (2013) 791–801.
- [9] F.G. Acién, J.M. Fernández, J.J. Magán, Production cost of a real microalgae production plant and strategies to reduce it, *Biotechnol. Adv.* 30 (2012) 1344–1353.
- [10] R.D. Gardner, E. Lohman, R. Gerlach, Comparison of CO₂ and bicarbonate as inorganic carbon sources for triacylglycerol and starch accumulation in *Chlamydomonas reinhardtii*, *Biotechnol. Bioeng.* 110 (2013) 87–96.
- [11] A. Richmond, *Handbook of Microalgal Mass Culture*. CRC Press, Boston, MA, 1990.
- [12] M.A. Borowitzka, The mass culture of *Dunaliella salina*. FAO Corporate Document repository, Murdoch: Murdoch University, 1990. <http://www.fao.org/docrep/field/003/AB728E/AB728E00.htm> (accessed January 18, 2013).
- [13] H. Gimmmler, U. Weis, C. Weis, H. Kugel, B.D. Treffny, *Dunaliella acidophila* (Kalina) Masyuk? An alga with a positive membrane potential, *New Phytol.* 113 (1989) 175–184.
- [14] M. Ginzburg, *Dunaliella*: A green alga adapted to salt, *Adv. Bot. Res.* 14 (1987) 93–183.
- [15] L.J. Borowitzka, M.A. Borowitzka, β -carotene (Provitamin A) production with algae, in: E.J. Vandamme (Ed.), *Biotechnology of Vitamins, Pigments and Growth Factors*, Elsevier Applied Science, London, 1989, pp. 15–26.
- [16] D.L. Sills, V. Paramita, M.J. Franke, M.C. Johnson, T.M. Akabas, C.H. Greene, J.W. Tester, Quantitative uncertainty analysis of life cycle assessment for algal biofuel production, *Environ. Sci. Technol.* 47 (2013) 687–694.
- [17] C. Visvanathan, B.D. Marsono, B. Basu, Removal of THMP by nanofiltration: Effects of interference parameters, *Water Res.* 32 (1998) 3527–3538.
- [18] APHA, *Standard Methods for the Examination of Water & Wastewater*, American Public Health Association, Washington, DC, 2005.
- [19] J.M. Valigore, P.A. Gostomski, D.G. Wareham, A.D. O'Sullivan, Effects of hydraulic and solids retention times on productivity and settleability of microbial (microalgal-bacterial) biomass grown on primary treated wastewater as a biofuel feedstock, *Water Res.* 46 (2012) 2957–2964.
- [20] A. Concas, L. Pisu, G. Cao, Mathematical modelling of *Chlorella vulgaris* growth in semi-batch photobioreactors fed with pure CO₂, *Chem. Eng. Trans.* 32 (2013) 1021–1026.
- [21] H.W. Nichols, H.C. Bold, *Trichosarcina polymorpha* gen. et sp. nov., *J. Phycol.* 1 (1965) 34–38.
- [22] R.R.L. Guillard, J.H. Ryther, Studies of marine planktonic diatoms: I. *Cydotella nana* Hustedt, and *Detonula confervacea* (Cleve) gran, *Can. J. Microbiol.* 8 (1962) 229–239.
- [23] M. Myint, A. Ghassemi, N. Nirmalakhandan, Review of nondestructed anaerobic digested sludge to reinstate concentrate from electrodialysis reversal desalination in bioenergy production, *Environ. Eng. Sci.* 27 (2010) 811–823.
- [24] L. Wang, M. Min, Y. Li, P. Chen, Y. Chen, Y. Liu, Y. Wang, R. Ruan, Cultivation of green algae *Chlorella* sp. in different wastewaters from municipal wastewater treatment plant, *Appl. Biochem. Biotechnol.* 162 (2010) 1174–1186.
- [25] H. Volkmann, U. Imianovsky, J.L.B. Oliveira, E.S.S. Anna, Cultivation of *Arthrospira (Spirulina) platensis* in desalinator wastewater and salinated synthetic medium: Protein content and amino-acid profile, *Braz. J. Microbiol.* 39 (2008) 98–101.

- [26] J.P. Pandey, A. Tiwari, Optimization of biomass production of *Spirulina maxima*, *J. Algal Biomass Utiln.* 1 (2010) 20–32.
- [27] S. Jain, S. Masih, S.G. Singh, Potentiality of petha (*benincasa hispida*) waste for the growth of *spirulina platensis*, *Res. J. Agric. Sci.* 2 (2011) 133–135.
- [28] R. Ramanan, K. Kannan, A. Deshkar, R. Yadav, Enhanced algal CO₂ sequestration through calcite deposition by *Chlorella* sp. and *Spirulina platensis* in a mini-raceway pond, *Bioresour. Technol.* 101 (2010) 2616–2622.
- [29] P.S. Lau, N.F.Y. Tam, Y.S. Wong, Effect of algal density on nutrient removal from primary settled wastewater, *Environ. Pollut.* 89 (1995) 59–66.
- [30] J.K. Pittman, A.P. Dean, O. Osundeko, The potential of sustainable algal biofuel production using wastewater resources, *Bioresour. Technol.* 102 (2011) 17–25.
- [31] A.M. Wood, R.C. Everroad, L.M. Wingard, Chapter 18: Measuring growth rates in microalgal cultures, in: R.A. Andersen (Ed.), *Algal Culturing Techniques*, Elsevier Academic Press, Burlington, MA, 2005, pp. 269–285.
- [32] R. Huerlimann, R. de Nys, K. Heimann, Growth, lipid content, productivity, and fatty acid composition of tropical microalgae for scale-up production, *Biotechnol. Bioeng.* 107 (2010) 245–257.
- [33] F. García, Y. Freile-Pelegrín, D. Robledo, Physiological characterization of *Dunaliella* sp. (Chlorophyta, Volvocales) from Yucatan, Mexico, *Bioresour. Technol.* 98 (2007) 1359–1365.
- [34] A. Prieto, J.P. Cañavate, M. García-González, Assessment of carotenoid production by *Dunaliella salina* in different culture systems and operation regimes, *J. Biotechnol.* 151 (2011) 180–185.
- [35] A. Ruiz-Marin, L.G. Mendoza-Espinosa, T. Stephenson, Growth and nutrient removal in free and immobilized green algae in batch and semi-continuous cultures treating real wastewater, *Bioresour. Technol.* 101 (2010) 58–64.
- [36] J. Sheehan, T. Dunahay, J. Benemann, P. Roessler, A Look Back at the U.S. Department of Energy's Aquatic Species Program—Biodiesel from Algae, U.S. Department of Energy's Office of Fuels Development, National Renewable Energy Laboratory, Midwest Research Institute, Golden, CO, 1998, Contract No. DE-AC36-83CH10093.
- [37] H.W. Kim, R. Vannela, B.E. Rittmann, Responses of *Synechocystis* sp. PCC 6803 to total dissolved solids in long-term continuous operation of a photobioreactor, *Bioresour. Technol.* 128 (2013) 378–384.
- [38] M.R. Tredici, G.C. Zittelli, Efficiency of sunlight utilization: Tubular versus flat photobioreactors, *Biotechnol. Bioeng.* 57 (1998) 187–197.
- [39] G. Torzillo, A. Sacchi, R. Materassi, Temperature as an important factor affecting productivity and night biomass loss in *Spirulina platensis* grown outdoors in tubular photobioreactors, *Bioresour. Technol.* 38 (1991) 95–100.
- [40] L. Batan, J. Quinn, B. Willson, T. Bradley, Net energy and greenhouse gas emission evaluation of biodiesel derived from microalgae, *Environ. Sci. Technol.* 44 (2010) 7975–7980.
- [41] C.D. Tanzi, M.A. Vian, F. Chemat, New procedure for extraction of algal lipids from wet biomass: A green clean and scalable process, *Bioresour. Technol.* 134 (2013) 271–275.
- [42] Z.-Y. Li, S.-Y. Guo, L. Li, Bioeffects of selenite on the growth of *Spirulina platensis* and its biotransformation, *Bioresour. Technol.* 89 (2003) 171–176.
- [43] G. Markou, I. Chatzipavlidis, D. Georgakakis, Cultivation of *Arthrospira (Spirulina) platensis* in olive-oilmill-wastewater treated with sodium hypochlorite, *Water Res.* 112 (2012) 234–241.
- [44] NSW Public Works, Brackish Groundwater: A Viable Community Water Supply Option? The National Water Commission, Australian Government, Canberra, 2011.
- [45] D. Elyanow, R.G. Parent, J.R. Mahoney, Parametric tests of an electrodialysis reversal (EDR) system with aliphatic anion membranes, *Desalination* 38 (1981) 549–565.
- [46] D. Elyanow, E. Sieveka, J. Mahoney, The determination of super-saturation limits in an EDR unit with aliphatic anion membranes, in: *Nineth Annual Conference and International Trade Fair of the National Water Supply Improvement Association*, Washington, DC, Vol. II, May 31–June 4, 1981.
- [47] E. Korngold, L. Aronov, N. Belayev, K. Kock, Electrodialysis with brine solutions oversaturated with calcium sulfate, *Desalination* 172 (2005) 63–75.
- [48] E. Korngold, L. Aronov, N. Daltrophe, Electrodialysis of brine solutions discharged from an RO plant, *Desalination* 242 (2009) 215–227.
- [49] A. Pérez-González, A.M. Urriaga, R. Ibáñez, I. Ortiz, State of the art and review on the treatment technologies of water reverse osmosis concentrates, *Water Res.* 46 (2012) 267–283.
- [50] W.-W. Huang, B.-Z. Dong, Z.-P. Cai, S.-S. Duan, Growth effects on mixed culture of *Dunaliella salina* and *Phaeodactylum tricornutum* under different inoculation densities and nitrogen concentrations, *Afr. J. Biotechnol.* 10 (2011) 13164–13174.
- [51] J.T. Leema, R. Kirubakaran, N.V. Vinithkumar, P.S. Dheenan, S. Karthikayulu, High value pigment production from *Arthrospira (Spirulina) platensis* cultured in seawater, *Bioresour. Technol.* 101 (2010) 9221–9227.
- [52] A.A. Gitelson, S. Laorawat, G.P. Keydan, A. Vonshak, Optical properties of dense algal cultures outdoors and their application to remote estimation of biomass and pigment concentration in *Spirulina platensis* (Cyanobacteria), *J. Phycol.* 31 (1995) 828–834.
- [53] R. Kaushik, R. Prasanna, H.C. Joshi, Utilization of anaerobically digested distillery effluent for the production of *Spirulina platensis* (ARM 730), *J. Sci. Ind. Res.* 65 (2006) 521–525.
- [54] C.C. Reichert, C.O. Reinehr, A.V. Costa, Semicontinuous cultivation of the Cyanobacterium *Spirulina platensis* in a closed photobioreactor, *Braz. J. Chem. Eng.* 23 (2006) 23–28.
- [55] S. Chinnasamy, A. Bhatnagar, R.W. Hunt, Microalgae cultivation in a wastewater dominated by carpet mill effluents for biofuel applications, *Bioresour. Technol.* 101 (2010) 3097–3105.
- [56] D.E. Brune, T.J. Lundquist, J.R. Benemann, Microalgal biomass for greenhouse gas reductions: Potential for replacement of fossil fuels and animal feeds, *J. Environ. Eng.* 135 (2009) 1136–1144.
- [57] L. Lardon, A. Hélias, B. Sialve, Life-cycle assessment of biodiesel production from microalgae, *Environ. Sci. Technol.* 43 (2009) 6475–6481.

Effects of Operating Conditions on Ion Removal from Brackish Water Using a Pilot-Scale Electrodialysis Reversal System

This article was downloaded by: [Leila Karimi]

On: 20 March 2015, At: 11:10

Publisher: Taylor & Francis

Informa Ltd Registered in England and Wales Registered Number: 1072954 Registered office: Mortimer House, 37-41 Mortimer Street, London W1T 3JH, UK



Desalination and Water Treatment

Publication details, including instructions for authors and subscription information:
<http://www.tandfonline.com/loi/tdwt20>

Effects of operating conditions on ion removal from brackish water using a pilot-scale electrodialysis reversal system

Leila Karimi^a & Abbas Ghassemi^a

^a Institute for Energy & the Environment (IEE/WERC), New Mexico State University, P.O. Box 30001, Las Cruces, NM, USA, Tel. +1 575 646 3075, Tel./Fax: +1 575 646 5474
Published online: 18 Mar 2015.



CrossMark

[Click for updates](#)

To cite this article: Leila Karimi & Abbas Ghassemi (2015): Effects of operating conditions on ion removal from brackish water using a pilot-scale electrodialysis reversal system, *Desalination and Water Treatment*, DOI: [10.1080/19443994.2015.1024748](https://doi.org/10.1080/19443994.2015.1024748)

To link to this article: <http://dx.doi.org/10.1080/19443994.2015.1024748>

PLEASE SCROLL DOWN FOR ARTICLE

Taylor & Francis makes every effort to ensure the accuracy of all the information (the "Content") contained in the publications on our platform. However, Taylor & Francis, our agents, and our licensors make no representations or warranties whatsoever as to the accuracy, completeness, or suitability for any purpose of the Content. Any opinions and views expressed in this publication are the opinions and views of the authors, and are not the views of or endorsed by Taylor & Francis. The accuracy of the Content should not be relied upon and should be independently verified with primary sources of information. Taylor and Francis shall not be liable for any losses, actions, claims, proceedings, demands, costs, expenses, damages, and other liabilities whatsoever or howsoever caused arising directly or indirectly in connection with, in relation to or arising out of the use of the Content.

This article may be used for research, teaching, and private study purposes. Any substantial or systematic reproduction, redistribution, reselling, loan, sub-licensing, systematic supply, or distribution in any form to anyone is expressly forbidden. Terms & Conditions of access and use can be found at <http://www.tandfonline.com/page/terms-and-conditions>



Effects of operating conditions on ion removal from brackish water using a pilot-scale electro dialysis reversal system

Leila Karimi*, Abbas Ghassemi

Institute for Energy & the Environment (IEE/WERC), New Mexico State University, P.O. Box 30001, Las Cruces, NM, USA, Tel. +1 575 646 3075; email: lkarimi@nmsu.edu (L. Karimi), Tel./Fax: +1 575 646 5474; email: Aghassem@nmsu.edu (A. Ghassemi)

Received 25 September 2014; Accepted 19 February 2015

ABSTRACT

Understanding the effects of operating factors on ion removal in the electro dialysis/ electro dialysis reversal (ED/EDR) process can significantly benefit industrial applications, enabling process optimization through different combinations of operational factors. Several studies have shown the effects of specific operating factors on ion removal, and it has been established that superficial velocity influences ion removal. However, previous studies have yielded mixed results on whether increases in superficial velocity increase or decrease ion removal; also, since previous studies are based on laboratory-scale ED systems, the results may not be fully applicable to full-scale desalination due to differences in system characteristics such as membrane area, flow path, and degree of superficial velocity's effect on ion removal. Therefore, this experimental study employs a pilot-scale EDR system that is very similar to a full-scale system in order to explore the effects of applied voltage, superficial velocity, and feed water temperature on ion removal. Additionally, a conceptual explanation is developed to explain the inconclusive results from previous research. The findings of this experiment confirmed that increases in superficial velocity decreased ion removal, and this result can help predict and optimize full-scale operations. In the investigated ranges, increasing voltage and temperature resulted in increased ion removal, while increasing superficial velocity resulted in decreased ion removal. The experiments were conducted at the Brackish Groundwater National Desalination Research Facility in Alamogordo, NM, USA on a General Electric Company pilot-scale EDR system with a maximum product flow rate of 45 L/min, using brackish water with a conductivity of 1,700 $\mu\text{S}/\text{cm}$.

Keywords: Desalination; Pilot-scale electro dialysis; Brackish water; Operating conditions

1. Introduction

The electro dialysis reversal (EDR) process, one of the membrane-based desalination technologies, has been used commercially for over 50 years [1], and is most feasible when the level of total dissolved solids

(TDS) in feed water is in the range of 400–6,000 ppm [2]. Although electro dialysis (ED)/EDR has some limitations for the desalination of brackish waters with higher TDS, some researchers have reported success in the use of EDR processes to desalinate saline water with TDS of 30,000 ppm [3]. Compared to reverse osmosis and nanofiltration processes, ED/EDR is more robust against non-ionic species such as silica, which

*Corresponding author.

causes scaling problems, because the EDR process does not affect any uncharged species in the stream, avoiding their accumulation or agglomeration [4,5].

Beside desalination, ED has wide applications, including the removal of heavy metals such as Cu and Pb [6–8]; applications of this process for sodium chloride production have also been demonstrated in Japan [9]. For the treatment of wastewater laden with heavy metals, ED/EDR offers several advantages, including the ability to recover valuable metals such as Cr and Cu, and the ability to produce a highly concentrated waste stream which makes disposal easier. Additionally, the ED processes are used to recover acids and bases from industrial wastewater [1].

In the EDR process, ion transport flux is described by the extended Nernst-Planck equation [10,11]. As shown in Eq. (1), the total flux of ion i in the EDR process is composed of three components, as follows:

$$J_i = -D_i \left(\frac{dC_i}{dx} + z_i C_i \frac{F}{RT} \frac{d\phi}{dx} \right) + C_i V \quad (1)$$

where D_i , C_i , F , R , T , ϕ , z_i , and V are ion diffusion coefficient, ion concentration, Faraday constant, molar gas constant, temperature, electrical potential, valence of the ion, and superficial velocity [10,11], respectively. In ion movement toward the ion exchange membrane in the desalting solution, migration and diffusion are the dominant ion transport mechanisms, while, in the direction of flow, convection has more effect and migration and diffusion can be neglected because of the large Peclet number [12]. The Peclet number, which is defined in Eq. (2), is the ratio of convection mass transport to diffusion mass transport. According to the ion transport direction and Eq. (2), the greater Peclet number in the direction of flow is expected since the superficial velocity value is higher than the mass diffusion coefficient:

$$Pe = \frac{VL}{D} = Re_L \times Sc \quad (2)$$

where V , L , D , Re_L , and Sc are superficial velocity, length of flow path, mass diffusion coefficient, Reynolds number, and Schmidt number, respectively. Based on Eq. (1), the ion transport rate toward the membrane involves ion concentration and applied electrical potential, the ion diffusivity, velocity, Peclet number, and temperature's impact on transport functionality. Additionally, the dependency of ion flux on temperature is embedded in the ion diffusion term. Eq. (3), derived from the Stokes-Einstein equation, reveals that the diffusion coefficient of ions changes linearly with temperature and inversely with viscosity [13]:

$$D_i(T) = \frac{D_i(T_0) \times T \times \mu(T_0)}{T_0 \times \mu(T)} \quad (3)$$

where $D_i(T)$ and $D_i(T_0)$ are diffusion coefficient at temperature T and reference temperature T_0 , and $\mu(T)$ and $\mu(T_0)$ are solution dynamic viscosity at temperature T and reference temperature T_0 , respectively. Although the diffusion coefficient of each ion is not independent of the others and the effective ion diffusion coefficient should be considered as the effective one for combinations of ions, Eq. (3) can give a good approximation of each individual ion diffusion coefficient at different levels of operating temperature. These basic equations clearly depict the kind of operating factors that can affect the removal of individual ions in the ED/EDR process, and will be discussed in the results and discussion section later in this paper.

Generally, the EDR process is affected by controllable factors such as superficial velocity, which is the calculated velocity of fluid through the channels regardless of the presence of spacers in the channel, as well as temperature and applied voltage. Based on membrane type, the process can also be influenced by other factors, commonly referred to as noise effects, such as pH, concentration polarization, ambient temperature, fouling, and electrolysis effects, which are prohibitively difficult or costly to control. By knowing how operating factors affect the removal of different monovalent and divalent ions, it will be possible to produce desalinated water with acceptable quality at lower energy consumption, in a more efficient process. Although there are studies conducted to investigate these effects, they have been in the laboratory scale setting, and different results have been reported for batch and continuous experimental procedures.

Among the saline water sources (feed waters) which are desalinated to produce freshwater, the types and quantities of ions vary. Since desalted water for different applications, such as drinking water, can have different acceptable levels for different types of ions, sometimes desalination plants only need to remove particular types of ions; other ions can be left in the desalted water. Consequently, investigating the removal of ions under different operating conditions is crucially important.

The two most important factors that affect the rate of separation are applied voltage and the superficial velocity. Applying greater voltage increases current density, and causes a greater concentration gradient for each ion in the diffusion boundary layer [4]. Kabay et al. [14] reported that voltage variation affected monovalent ion removal more than divalent ion removal under their experimental conditions, which

consisted of batch mode ED operation using ternary mixtures composed of NaCl-CaCl₂ and KCl-MgCl₂ salts. They also showed that the specific energy consumption is significantly affected by voltage variation. Demircioglu et al. [15] demonstrated the significant role of applied voltage on K⁺ removal in their experiments. Banasiak et al. [16] stated that the removal of F⁻ was affected by voltage changes, while the NO₃⁻ removal was not influenced significantly by voltage variation. However, they explained that the observed effect was due to different initial concentrations of the ions and the ion characteristics.

Superficial velocity, also known as flow rate of feed stream, plays an important role for ion removal in the EDR process. Research, however, has yielded inconclusive results on its effects. Although some researchers reported positive or neutral effects from increasing the feed velocity, which was explained by how increasing the feed velocity decreases the thickness of the concentration boundary layer [4,14,15], several other researchers have reported that increased velocity has adverse effects on ion removal and separation performance. This effect is explained by a lower residence time for ions at increased flow rates, which can have negative effects on ion removal. It is assumed that at higher feed flow rates, the ions do not have enough time to pass through the membrane, and are rinsed from the membrane surface before passing [17–20]. Additionally, both positive and negative effects of superficial velocity on current efficiency and ion removal were reported by Sadrzadeh and Mohammadi in sea water treatment using a small ED system at different flow rates and different feed concentrations [21]. In the present research, a major objective is determining whether increased superficial velocity has an overall positive or overall negative effect on ion removal.

Also, although several valuable studies have been conducted to investigate the effect of operating parameters on the removal of ions in the ED process, nearly all of these studies have been done on very small, laboratory-scale ED systems. In these small systems, the influence of some of the investigated parameters, such as voltage, can be consistent between laboratory-scale and full-scale ED/EDR performance; however, the influence of some other parameters, like fluid velocity, can be different not only at different variable levels, but also at different ED/EDR stack sizes. Additionally, the laboratory-scale ED processes are mostly constrained to low levels of certain factors, such as stream velocity in dilute and concentrate chambers, number of cell pairs, and shape of flow path. Therefore, investigating the influence of operating factors at levels similar to the real values and using a pilot-scale

EDR system—which is very similar to the full-scale EDR systems in terms of size of membrane effective area, flow path of streams, and size of electrodes—increases the findings' applicability to full-scale EDR systems. Consequently, in this study, the effects of the main operating factors such as applied voltage, superficial velocity, and temperature of feed water on ion removal were investigated at the pilot scale, with the major goal of resolving previously reported inconsistencies in the effect of superficial velocity on ion removal. Additionally, to explain the different results previously reported, a conceptual explanation is developed.

2. Materials and methods

The pilot-scale experiments were conducted in the Brackish Groundwater National Desalination Research Facility (BGNDRF) using a General Electric EDR setup with an influent flow rate capacity of 45 L/min. BGNDRF is a federal facility which functions under the United States Department of Interior, Bureau of Reclamation (Reclamation). This facility was established by an Act of Congress, and has the mission to support sustainable advanced water treatment research and technology development for inland brackish groundwater sources. This facility is located in Alamogordo, New Mexico, an optimal environment for desalination research, and is positioned in the Tularosa Basin, which possesses a vast supply of groundwater resources and a wide range of water qualities. A wide range of salinity is accessible inside this basin, within a 5-mile radius. The mission of BGNDRF is to conduct research for the development of cost-effective desalination and alternative energy technologies that produce sustainable sources of water and power for urban, industrial, agricultural, and environmental purposes. The facility includes a central research building located on a 40-acre site. Water for work at the facility is obtained from four wells. The available water sources have been categorized as well 1, which has the comparatively low salinity of 1,000–1,200 mg/L at 40°C and for which a cooling tower is available, and three mid-concentration TDS wells, 3, 4, and 2, with salinities of 3,450–6,400 mg/L at 21°C [22]. The schematic of the whole EDR setup, which is located in the fourth test bay in the facility, is shown in Fig. 1. In this set up, a feed pump pressurizes feed water for delivery to the test bay, after which the water is sent to the multi-media filter (MMF). The MMF removes suspended solids from the feed water due to its sieving functions of different media layers. The MMF employs ordered sizes of anthracite (0.85–0.95 mm),

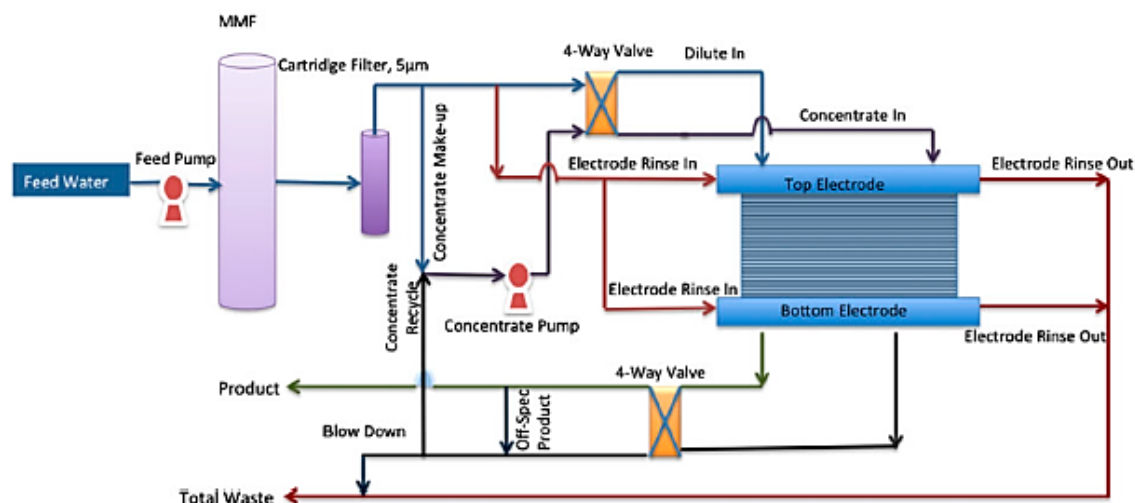


Fig. 1. Schematic of the pilot-scale EDR setup.

sand (0.85 mm), and garnet (0.42–0.6 mm) to remove suspended particles. The largest particles that can pass through the MMF are 10–15 μ in size [23]. Although the electro dialysis process does not generally require special pretreatment, applying an MMF can help to prevent damage and fouling of the membranes from sands and suspended solids in the feed water. Next, the feed water was passed through a cartridge filter, which was the final step before feed water entered the EDR stack. This filter had a pore size of 5 μ m, and removed remaining suspended solids from the feed water.

The GE electro dialyzer was composed of one hydraulic and one electrical stage. The anion exchange membranes, cation exchange membranes, and spacers used in the experiment were GE AR908, GE CR67-HMR, and GE MK-IV, with a membrane effective area of 0.3 m² per ion exchange membrane, respectively. The EDR stack components were the same size as the components of a full-scale stack, and the only difference between this stack and a full-scale process was the number of cell pairs: the stack used in the experiments had 40 cell pairs, while in full-scale applications the number of cell pairs exceeds 600. The feed water used was from well 1, which provided brackish water with nominal conductivity of 1,700 μ s/cm. The research facility could provide water from well 1 at two different temperatures: 24 °C after passing the cooling tower, or 38 °C directly from the storage tank. This provided the opportunity for researchers to conduct the experiments at two different temperatures. However, the temperature levels vary throughout the year. The feed water chemical condition and

composition, which were obtained from analyzing the collected feed water samples in the process, are given in Tables 1 and 2. The feed water had total organic carbon (TOC) levels of 36.62 ppm, turbidity of 0.99 nephelometric turbidity units, and clear coloration.

As shown in Tables 1 and 2, the composition of water changed slightly at each operating temperature. This small difference was observed because some of the water evaporates in the cooling tower, and concentrates the feed water to some extent. Therefore, the conductivity of feed water was subject to change. The electrode rinse solution had the same feed composition, and was dosed with 15% hydrochloric acid. The injected acid was consumed to neutralize the hydroxide ions formed in the cathode, preventing scaling problems in the electrodes.

The experiments were carried out at two levels of temperature and superficial velocity, and six levels of voltage, as shown in Table 3.

The levels of superficial velocity were chosen based on the minimum and maximum flow rates recommended by the manufacturer. The maximum permissible voltage was chosen based on the examined

Table 1
Feed water conductivity and pH

Brackish ground water BGNDRF well 1		
Temperature (°C)	Conductivity (μ s/cm)	pH
24	1,765	8–8.1
38	1,650	8–8.3

Table 2
Feed water composition in the pilot-scale experiments

Temperature (°C)	Brackish ground water BGNDRF well 1								
	Average concentration of cations (standard deviation), ppm					Average concentration of anions (standard deviation), ppm			
	Ca ²⁺	Mg ²⁺	Na ⁺	Sr ²⁺	K ⁺	Cl ⁻	SO ₄ ²⁻	HCO ₃ ⁻	F ⁻
24	50.5 (1.8)	8.6 (0.3)	376.9 (3.2)	<2 (NA)	2.1 (0)	35.9 (1.3)	664.0 (17.6)	185.1 (2.5)	2.0 (0.1)
38	47.0 (3.0)	7.5 (0.5)	363.6 (5.1)	<2 (NA)	2.0 (0)	31.6 (0.7)	628.2 (11.6)	187.2 (1.8)	2.0 (0.2)

*May have a negligible source of CO₃²⁻ due to a feed water pH above 8.

Table 3
Operating condition levels in the pilot-scale experiments

Factor	Factor level	Factor experimental value
Feed linear velocity	1	8.8 cm/s
	2	13.1 cm/s
Temperature	1	24 °C
	2	38 °C
Voltage	1	2.6 V
	2	9.8 V
	3	21.7 V
	4	33.4 V
	5	45.3 V
	6	57.7 V

conditions using results from previously conducted limiting current tests. The voltage range was selected to represent a wide range of applied voltage.

The experiments were conducted in continuous system. Therefore, new feed water was used for every experiment. The feed water condition of temperature was controlled. For experiments at higher temperature, the well water was sent to the test bay directly from the storage tank, while experiments at lower temperature, water was delivered to the test bay after passing the cooling tower. The stream flow rates, superficial velocity of the streams, and the applied voltage were controlled through the experimental setup. Before applying electricity to the system, the flow rates were adjusted to provide the proposed superficial velocity. The system was allowed to run for 5 min to reach the steady state condition after applying the electricity to the stack. All of the experiments were conducted at the same polarity—i.e. the EDR system was running at positive polarity for half an hour when the experiments and water sample collections were done. However, to prevent scaling problems, it was also necessary to run the system at negative polarity, in the reversal condition. After polarity reversal, the system was allowed to run for 10 min to reach the steady state

condition before sample collection started. Additionally, during the experiments, the flow rates were controlled carefully to reduce the noise effects. For each experiment, 250 ml water samples of feed, product, and concentrate streams were collected, and then the experiment and water sample collection were repeated for the next voltage level. The collected water samples were kept in the refrigerator to prevent any evaporation before they were analyzed. The water samples were analyzed using a Dionex ICS-5000 Dual Channel IC System, an ion chromatography system capable of measuring cations via an analytical compartment and anions via a capillary compartment. Additionally, samples were analyzed for their pH levels to detect the presence of carbonate and bicarbonate. Then, the titrations were done for water samples to determine the amount of any possible carbonate. However, the titration procedure cannot be considered an accurate method for very small amounts of species. Therefore, the samples were analyzed using a TOC analyzer, Shimadzu TOC-VCSH, to determine the total inorganic carbon (TIC). Due to the pH level of the samples, all of the reported TIC was assumed to be from an HCO₃⁻ source, but later experimental results suggested a negligible CO₃²⁻ presence.

3. Results and discussions

3.1. Effect of applied voltage and ion size on ion removal

Generally, under normal operating conditions below limiting current, increasing the amount of applied voltage increases the removal of ions and current density. The effect of applied voltage on ion removal depends on certain ion characteristics, such as charge and hydrated radius. Ions with greater electrical charges are affected more strongly by an electrical field than ions with a smaller electrical charge. This effect is distinctly shown for cations and anions in Figs. 2 and 3. In order to show this effect in conducted experiments, the percent removal of each ion was calculated using Eq. (4). Then, the percent

removal of ions was plotted vs. the applied voltage to the stack.

$$\% \text{Removal} = \frac{(C_{F,i} - C_{P,i})}{C_{F,i}} \times 100 \quad (4)$$

where $C_{F,i}$ and $C_{P,i}$ are the concentrations of ion i in the feed and product streams, respectively.

In this experiment, the removal rates of different ions were not compared to a reference species due to the different concentrations of different ions. When the initial concentration of a specific ion is greater than the other ions, more ions of that type are available to be affected by applied voltage which results in better removal of that type ion. By analyzing ion

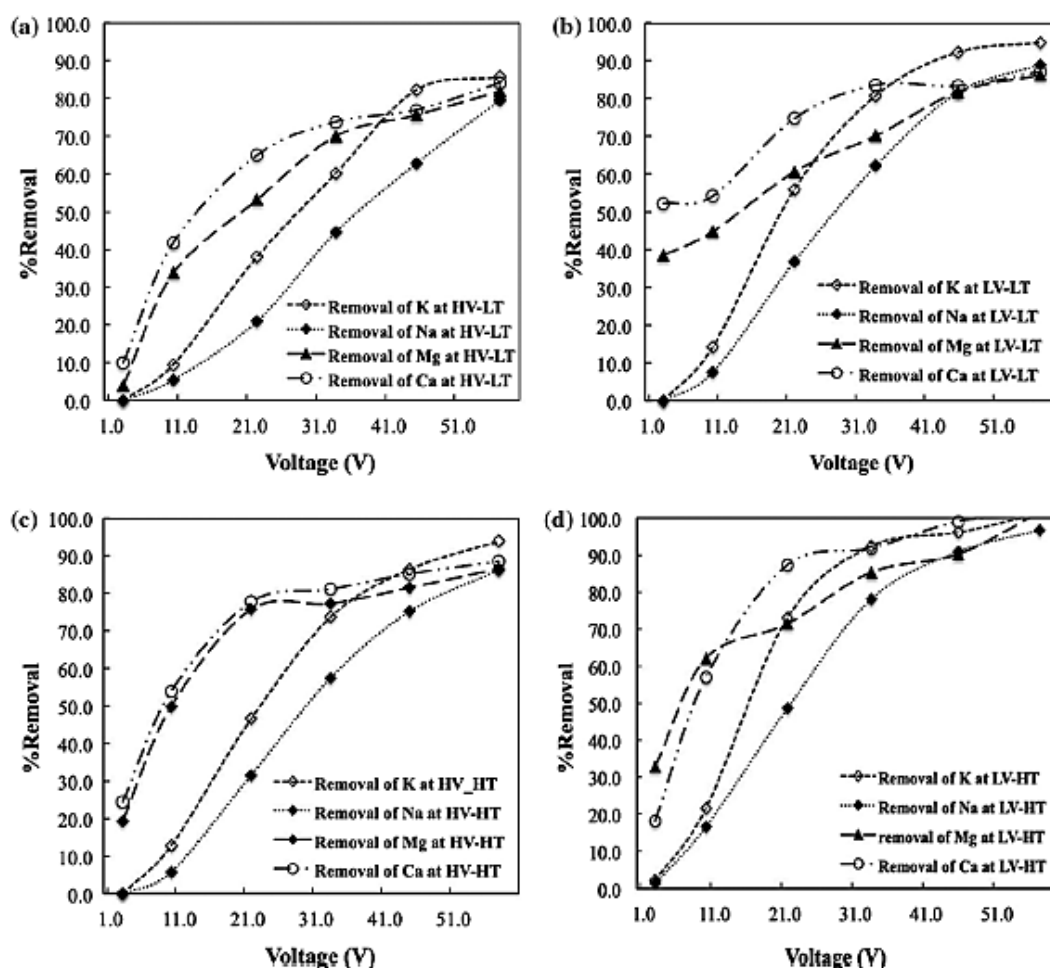


Fig. 2. Effect of voltage on removal of cations at (a) high velocity–low temperature, (b) low velocity–low temperature, (c) high velocity–high temperature, and (d) low velocity–high temperature.

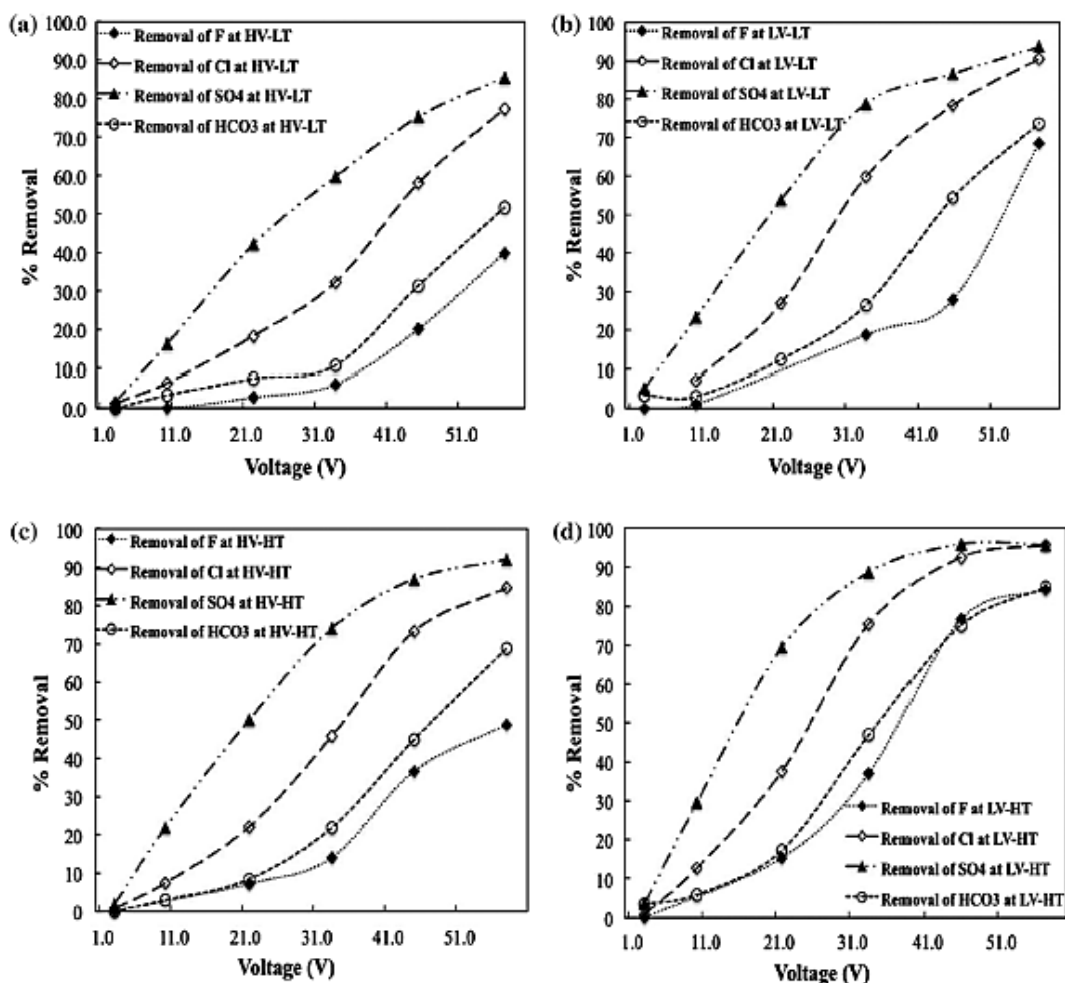


Fig. 3. Effect of voltage on removal of anions at (a) high velocity–low temperature, (b) low velocity–low temperature, (c) high velocity–high temperature, and (d) low velocity–high temperature.

removal based on percent change rather than absolute removal in comparison to a reference ion, it is possible to normalize the effect of different initial ion concentrations.

The data from Fig. 2 depicts how the divalent cations, Ca²⁺ and Mg²⁺, were removed better than monovalent cations such as K⁺ and Na⁺. However, while this trend was shown in almost all of the plots of this figure at lower voltage, at higher applied voltages the percent removal of the ions converged to a unique value, especially at lower velocity and higher temperature, under which conditions the greatest amount of removal was observed. According to the graphs within Fig. 2, the effect of applied voltage on the removal of ions was not consistent in all ranges of applied voltage. Additionally, it was shown that

when applied voltage was constant, the percent removal of Ca²⁺ was greater than the percent removal of Mg²⁺. Since Ca²⁺ has a smaller hydrated radius than Mg²⁺ [24, 25], the better removal of Ca²⁺ could be explained by its smaller size. The effect from the size of ions' hydrated radii was also observed in the higher removal percentage of K⁺ as compared to the removal percentage of Na⁺. K⁺ has a smaller hydrated radius than Na⁺ [24, 25], so as with Ca²⁺ and Mg²⁺, K⁺ ions were removed more effectively than Na⁺ ions.

The same effects from voltage, electrical charge, and hydrated ion size that were observed with cations were also observed in the removal of anions, as shown in Fig. 3. Divalent anions, such as SO₄²⁻, were removed better than monovalent anions, such as Cl⁻, F⁻, and

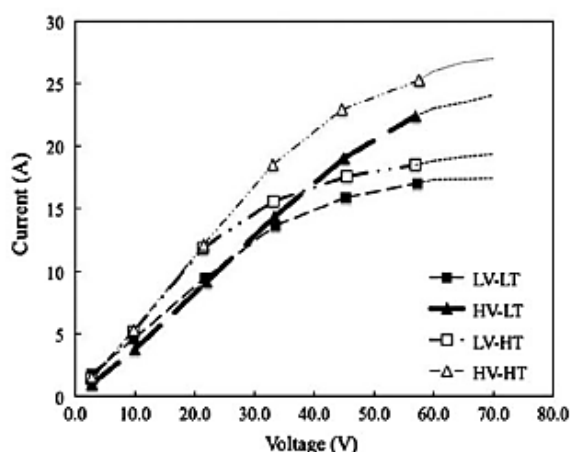


Fig. 4. Variation of current vs. voltage.

HCO_3^- . Since HCO_3^- has a larger hydrated radius than F^- [26], it was expected that less removal of HCO_3^- would be observed in comparison to F^- . The observed difference in the removal of these two monovalent anions implies that the total inorganic carbon, which was initially identified as HCO_3^- on the basis of the pH measurements and titration results that confirmed the absence of CO_3^{2-} in samples with a pH level lower than 8.3 [27], must have had a negligible amount of CO_3^{2-} which was not high enough to be detected by titration method.

During the experiments, the current was measured and recorded. Current was not considered as an independent variable for ion removal studies because the current efficiency varies with ion concentration; therefore, according to the previous studies, the voltage can be considered as a more universal and independent parameter to analyze different rates of ion removal under different conditions [7,8,15,21]. Fig. 4 shows the variation of current vs. applied voltage at different operating conditions.

Fig. 4 shows that the measured current during the experiments at different conditions was affected by ion removal and superficial velocity (flow rate) differently at lower and higher levels of voltage at both low and high temperatures. It illustrates that the current at high voltages increased at both levels of temperature when superficial velocity increased, while its value was not affected by superficial velocity variations at lower levels of voltages. In order to verify this observation and confirm the inconsistent current behavior shown in Fig. 4, the percent change in product flow rate (L/s) was multiplied by total ion removal (molar), and plotted vs. voltage in Fig. 5(a) and (b) alongside the percent change in current, which was calculated for different conditions.

The theoretical value for current through the stack can be calculated from Faraday's law as follows:

$$I = \frac{zFQ\Delta C_i}{\eta N_{cp}} \quad (5)$$

where I , z , F , Q , ΔC_i , η , and N_{cp} are electrical current (A), ion valence, Faraday constant (As/eq), flow rate (cm^3/s), desired ion concentration difference between feed and dilute streams (mol/cm^3), current efficiency, and number of cell pairs, respectively. The plotted values in Fig. 5(a) and (b) explain the different behavior of measured current at the different levels of voltage shown in Fig. 4. Although, based on Eq. (5), a positive effect on current was expected from an increase in superficial velocity, such positive effect was compromised by the negative effect on the current from reduction in ion removal. Additionally, the greater slope of current at higher velocity, as shown in Fig. 4, demonstrates that the limiting current should be achieved at higher levels of voltage (virtual dot lines). This observation confirms the positive effect of velocity on decreasing the concentration polarization and reducing the thickness of the boundary layer. However, at lower superficial velocity levels, limiting current can be obtained at lower voltage levels, as shown in Fig. 4 using the dotted lines.

Table 4
Mobility of individual ions at different operating conditions

V (cm/s)	T (°C)	Mobility ($\text{m}^2/\text{V}/\text{s}$) $\times 10^8$							
		Cations				Anions			
		Ca^{2+}	Mg^{2+}	Na^+	K^+	F^-	Cl^-	CO_3^{2-}	SO_4^{2-}
8.8	24	6.04	5.39	5.09	7.47	5.63	7.75	452	8.13
	38	7.95	7.09	6.70	9.83	7.41	10.20	595	10.69
13.1	24	5.94	5.29	5.00	7.34	5.53	7.62	444	7.99
	38	7.97	7.10	6.71	9.84	7.42	10.22	596	10.71

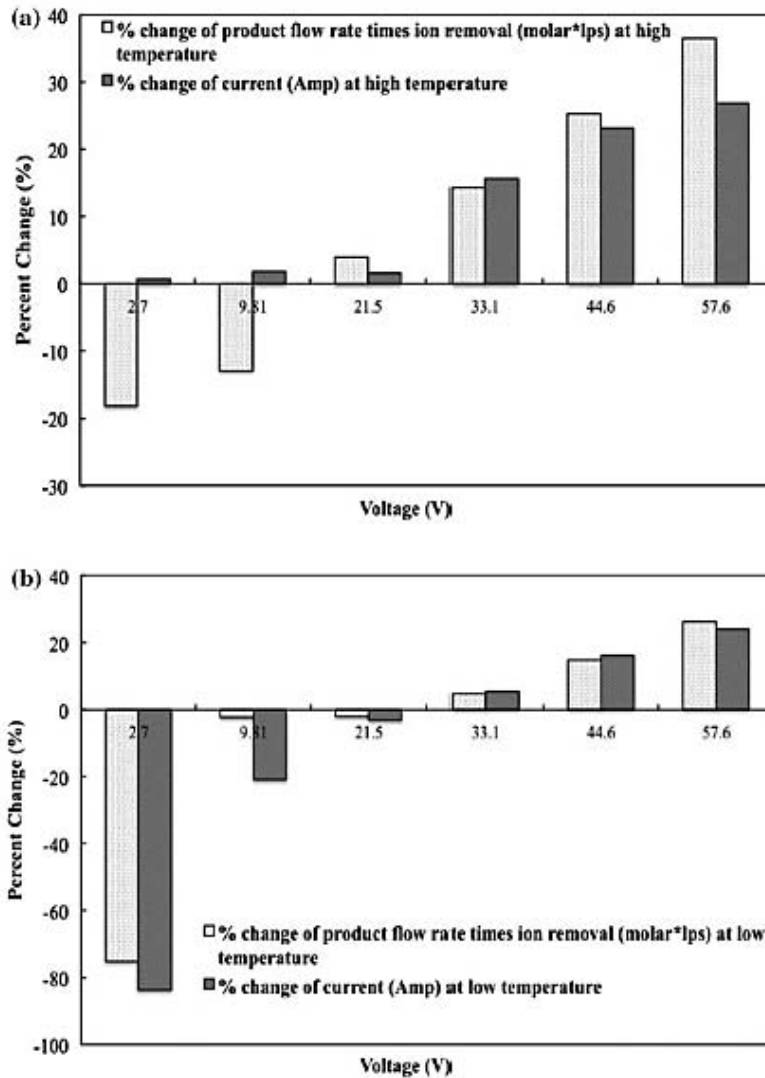


Fig. 5. Values for percent change of product flow rate times total ion removal and percent change of current at different levels of voltage at (a) high temperature and (b) low temperature.

3.2. Effect of superficial velocity and temperature on ion removal

As discussed before, two of the other parameters that affect ion removal in the EDR process are superficial velocity, also called flow rate, and the temperature of the dilute stream. Based on the results obtained from this experiment, the impact of these parameters on the removal of cations and anions is shown in Figs. 6 and 7.

Notably, several previous experiments have reported that increases in the superficial velocity can have either positive or negative effects on ion removal.

Positive effects are attributed to increased turbulence of flow, decreased thickness of the boundary layer, and reductions in the concentration polarization. Negative effects are attributed to decreased residence time. As can be seen in Figs. 6 and 7, the plotted curves from this experiment confirmed the overall negative influence of increased superficial velocity.

This observed reduction trend in the removal of all ions can be explained by decreased residence time, a characteristic which can be defined as follows:

$$t_{\text{resid}} = \frac{L}{V} \quad (6)$$

where t_{resid} , L , and V are residence time, flow path length, and superficial velocity, respectively.

According to this equation, the residence time decreases 33% over the constant flow path in the EDR stack when the linear velocity is increased from 8.8 to 13.1 cm/s. The observed reduction in ion removal is due to the decrease in the residence time, meaning the ions had less time to pass through the membranes and transfer from dilute stream to the concentrate stream.

According to the obtained results, the reduction in residence time did not affect the removal of all ions linearly and consistently. The nonlinearity of this relationship can be explained by the hidden positive effect of superficial velocity on the thickness of the boundary layer, which affects ion removal rate. Additionally, the non-homogeneous influence of residence time

reduction on the removal of different ions can be justified by accounting for the different behavior of ions and their removal rate in the EDR process due to their different characteristics.

To develop a conceptual explanation for why several previous experiments report overall positive or neutral effects on ion removal from increases in superficial velocity, it can first be noted that these results are reported only from experiments using batch processes and a constant experimental duration for different superficial velocities. In batch experiments, the system operates as a closed loop, where the outputs of the system cycle back as inputs. In such a system, therefore, if the experiment's time duration is held constant for different levels of velocity, an increase in superficial velocity increases not only the velocity, but also the number of times that

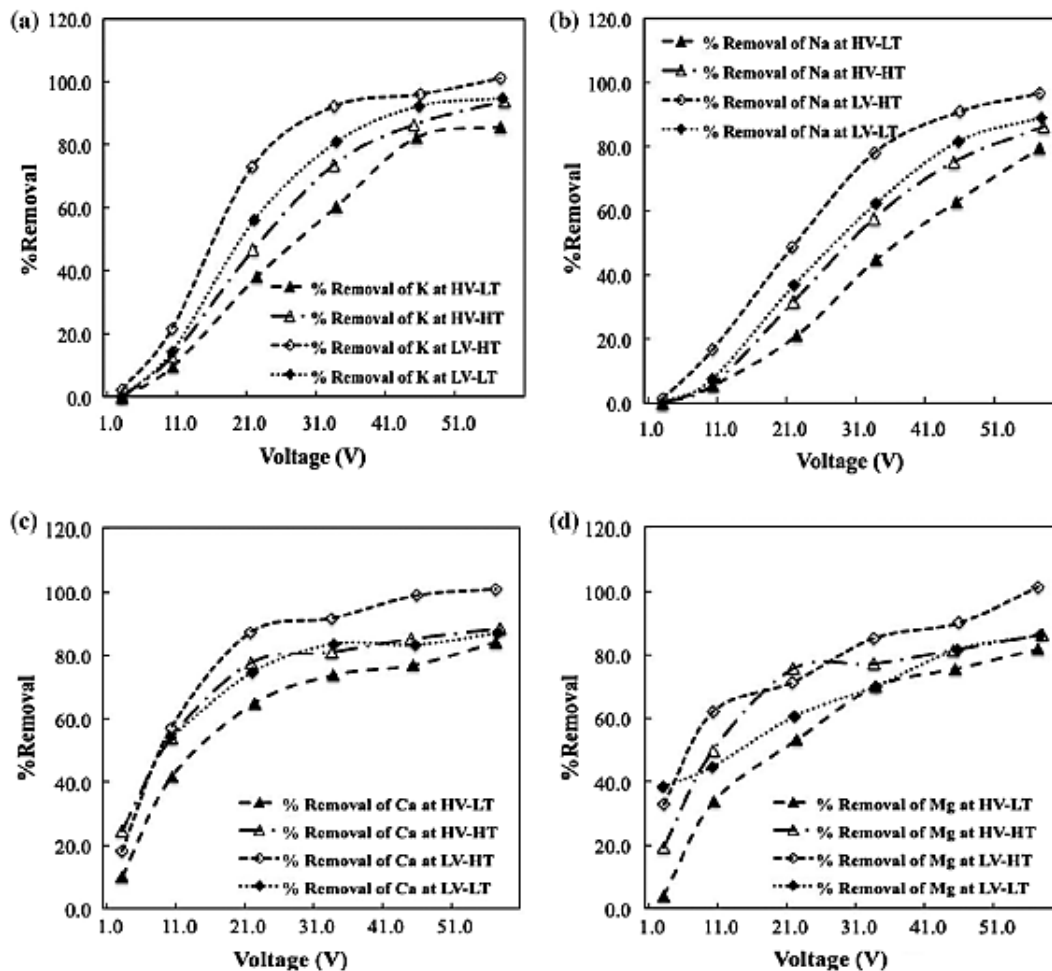


Fig. 6. Effect of velocity and temperature on removal of cations, (a) K^+ , (b) Na^+ , (c) Ca^{2+} , and (d) Mg^{2+} .

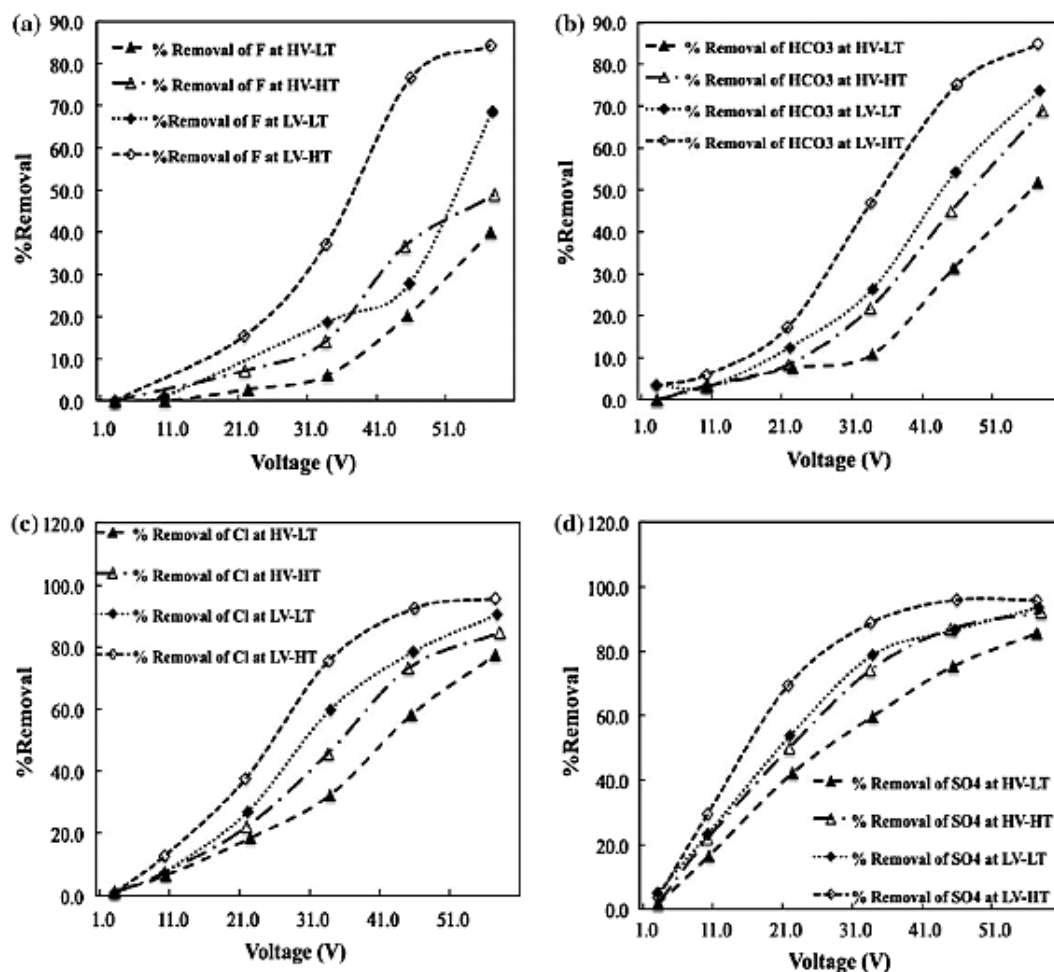


Fig. 7. Effect of velocity and temperature on removal of anions, (a) F^- , (b) HCO_3^- , (c) Cl^- , and (d) SO_4^{2-} .

the solution passes through the membrane. Therefore, experiments using a batch system with a constant time duration for different velocities may be recording the positive effect of additional passages through the ED stack, which could offset the negative effect of increased velocity to yield overall positive or neutral results.

One of the other operating factors which impacts ion removal is operational temperature. According to the curves shown in Figs. 6 and 7, increasing the temperature of feed water from 24 to 38°C improved ion removal for both cations and anions. It appears that increasing the temperature improves ion mobility and consequently increases the ion removal. The ion mobility at different temperatures can be calculated using the Nernst–Einstein equation as follows:

$$u_i = \frac{|z_i|FD_i}{RT} \quad (7)$$

where u_i , z_i , F , D_i , R , and T are ion mobility, ion charge, Faraday constant, ion diffusion coefficient, molar gas constant, and absolute temperature, respectively. By incorporating the effect of temperature on the diffusion coefficient of ions using Eq. (3) into the Nernst–Einstein equation, the ratio of ion mobility was calculated and reported in Table 4 for individual ions. The results showed that when temperature was increased from 24 to 38°C, individual ion mobility increased 1.3 times for both cations and anions when the diffusion coefficients of ions were assumed to be independent of each other. However, because of the

nature of the Nernst–Planck equation, Eq. (1), in which the temperature term is the denominator term of ion flux, this ratio is not the same as the observed ratio at which ion removal increased under the effect of temperature.

4. Conclusion

Since operating factors play an important role in the technical, economic, and product quality aspects of the desalination process, the influence of operating factors on pilot-scale EDR was investigated in this paper. Of special interest, due to inconsistent findings in previous research, was the question of whether increases in superficial velocity have positive or negative effects on ion removal. Generally, the experiments conducted in this research at the pilot-scale confirmed that feed superficial velocity and feed temperature both affect the removal of anions and cations in the pilot scale electro dialysis desalination process. Increases in the superficial velocity of the feed stream in the given range had a negative effect on ion removal due to decreases in the ion residence time. Although the superficial velocity increases had a positive effect by decreasing the concentration polarization and the thickness of the boundary layer, the negative effect from the decrease in residence time had a greater influence in the range of velocities studied. Additionally, the observed effect on the removal of different ions from superficial velocity was not consistent across the whole range of applied voltage, as shown in Figs. 5–7. Moreover, increases in temperature in the examined range improved ion removal at both levels of superficial velocity. In addition, the applied voltage in the stack had a different effect on different ions due to their electrical charges and different hydrated radii. However, at higher levels of voltage, the removal of ions converged to a unique value; so, the comparative effect of voltage on different ions can be better investigated at lower levels of voltage. Studying the effects of the above-mentioned operating factors on pilot-scale EDR confirmed that the EDR process can be controlled at specific levels of operating conditions in order to obtain the desired removal of specific ions in full-scale applications.

Acknowledgments

The authors would like to thank the US Bureau of Reclamation Brackish Groundwater National Desalination Research Facility. This work was supported by the US Bureau of Reclamation [R10AC80283].

Symbols

C_i	—	ion concentration (mol/cm ³)
D_i	—	ion diffusion coefficient (cm ² /s)
F	—	Faraday constant (A s/eq)
I	—	electrical current (A)
L	—	flow path length (cm)
N_{cp}	—	number of cell pairs
Q	—	flow rate (cm ³ /s)
R	—	molar gas constant (J/mol K)
Re	—	Reynolds number
Sc	—	Schmidt number
T	—	temperature (K)
T_0	—	reference temperature (K)
t_{resid}	—	residence time (s)
u_i	—	ion mobility (cm ² /V s)
V	—	superficial velocity (cm/s)
z_i	—	charge of the ion

Greek

ϕ	—	Electrical potential (V)
μ	—	Dynamic viscosity (Pa s)
η	—	Current efficiency

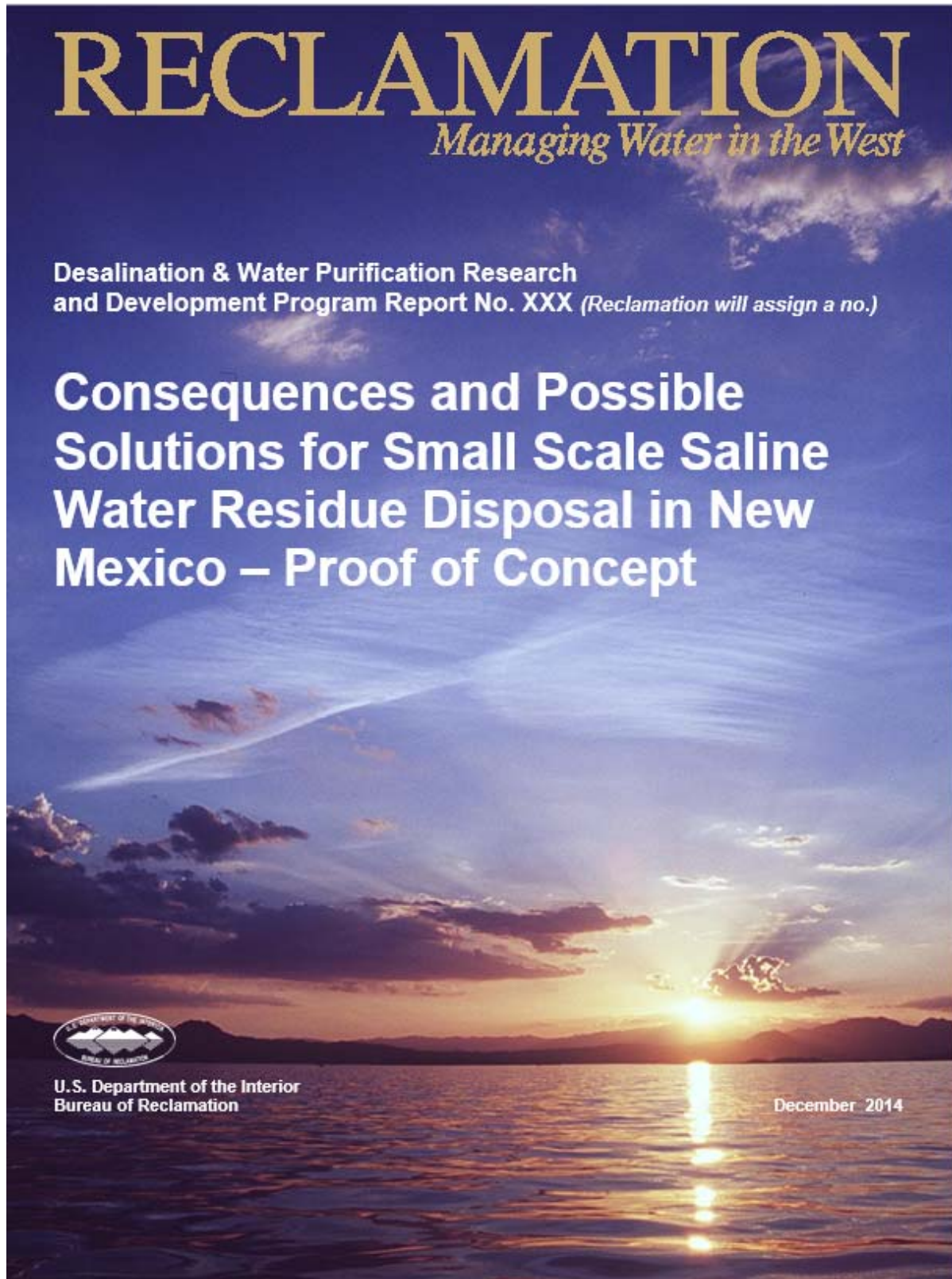
References

- [1] H. Strathmann, Electrodialysis, mature technology with a multitude of new applications, *Desalination* 264 (2010) 268–288. doi: 10.1016/j.desal.2010.04.069.
- [2] S. Kalogirou, Seawater desalination using renewable energy sources, *Prog. Energy Combust. Sci.* 31 (2005) 242–281. doi: 10.1016/j.pecs.2005.03.001.
- [3] Y. Tanaka, R. Ehara, S. Itoi, T. Goto, Ion-exchange membrane electrodialytic salt production using brine discharged from a reverse osmosis seawater desalination plant, *J. Membr. Sci.* 222 (2003) 71–86. doi: 10.1016/S0376-7388(03)00217-5.
- [4] W.S. Walker, Improving Recovery in Reverse Osmosis Desalination of Inland Brackish Groundwaters via Electrodialysis, University of Texas, Austin, TX, 2010.
- [5] P.V. Brady, R.J. Kottenstette, T.M. Mayer, M.M. Hightower, Inland desalination: Challenges and research needs, *J. Contemp. Water Res. Edu.* 132 (2005) 46–51. doi: 10.1111/j.1936-704X.2005.mp132001007.x.
- [6] T. Mohammadi, A. Moheb, M. Sadrzadeh, A. Razmi, Modeling of metal ion removal from wastewater by electrodialysis, *Sep. Purif. Technol.* 41 (2005) 73–82. doi: 10.1016/j.seppur.2004.04.007.
- [7] M. Sadrzadeh, T. Mohammadi, J. Ivakpour, N. Kasiri, Separation of lead ions from wastewater using electrodialysis: Comparing mathematical and neural network modeling, *Chem. Eng. J.* 144 (2008) 431–441. doi: 10.1016/j.ccej.2008.02.023.
- [8] A. Abou-Shady, C. Peng, J. Almeria O, H. Xu, Effect of pH on separation of Pb (II) and NO₃⁻ from aqueous solutions using electrodialysis, *Desalination* 285 (2012) 46–53. doi: 10.1016/j.desal.2011.09.032.
- [9] R. Yamane, M. Ichikawa, Y. Mizutani, Y. Onoue, Concentrated brine production from sea water by electrodialysis using exchange membranes, *Ind. Eng. Chem. Process Des. Dev.* 8 (1969) 159–165.

- [10] H. Strathmann, Ion-exchange Membrane Separation Processes, first ed., Elsevier, Amsterdam, 2004. doi: 10.1016/S0927-5193(04)80031-7.
- [11] A.J. Bard, L.R. Faulkner, Electrochemical Methods: Fundamentals and Applications, second ed., Wiley, New York, NY, 2000.
- [12] P. Moon, G. Sandí, D. Stevens, R. Kizilel, Computational modeling of ionic transport in continuous and batch electrodialysis, *Sep. Sci. Technol.* 39 (2004) 2531–2555. doi: 10.1081/SS-200026714.
- [13] F.M.T. Gimmi, Diffusion in methods of soil analysis, Part 4, Physical Methods, Science Society of America, Madison, WI, 2002.
- [14] N. Kabay, H. Kahveci, Ö. İpek, M. Yüksel, Separation of monovalent and divalent ions from ternary mixtures by electrodialysis, *Desalination* 198 (2006) 74–83. doi: 10.1016/j.desal.2006.09.012.
- [15] M. Demircioglu, N. Kabay, I. Kurucaovali, E. Ersoz, Demineralization by electrodialysis (ED)—Separation performance and cost comparison for monovalent salts, *Desalination* 153 (2002) 329–333.
- [16] L.J. Banasiak, T.W. Kruttschnitt, A.I. Schäfer, Desalination using electrodialysis as a function of voltage and salt concentration, *Desalination* 205 (2007) 38–46. doi: 10.1016/j.desal.2006.04.038.
- [17] V.M.M. Aponte, G. Colón, Sodium chloride removal from urine via a six-compartment ED cell for use in advanced life support systems (Part 1: Salt removal as a function of applied voltage and fluid velocity), *Desalination* 140 (2001) 121–132. doi: 10.1016/S0011-9164(01)00362-9.
- [18] M. Sadrzadeh, A. Razmi, T. Mohammadi, Separation of monovalent, divalent and trivalent ions from wastewater at various operating conditions using electrodialysis, *Desalination* 205 (2007) 53–61. doi: 10.1016/j.desal.2006.04.039.
- [19] M. Sadrzadeh, A. Kaviani, T. Mohammadi, Mathematical modeling of desalination by electrodialysis, in: Tenth International Water Technology Conference IWTC10, Alexandria, Egypt, 2006, pp. 221–233.
- [20] T. Mohammadi, a. Razmi, M. Sadrzadeh, Effect of operating parameters on Pb²⁺ separation from wastewater using electrodialysis, *Desalination* 167 (2004) 379–385. doi: 10.1016/j.desal.2004.06.150.
- [21] M. Sadrzadeh, T. Mohammadi, Treatment of sea water using electrodialysis: Current efficiency evaluation, *Desalination* 249 (2009) 279–285. doi: 10.1016/j.desal.2008.10.029.
- [22] Analysis of water from four wells at the brackish groundwater national research facility, Bureau of Reclamation, Tetra Tech, Inc., Albuquerque, 2011.
- [23] J.P. Fues, High-efficiency filtration as pretreatment to membrane-based demineralization systems, in: American Filtration Separation Society AFS Annual Conference 21st, Valley Forge, 2008.
- [24] E.R. Nightingale, E.R. Nightingale Jr., Phenomenological theory of ion solvation. Effective radii of hydrated ions, *J. Phys. Chem.* 63 (1959) 1381–1387. doi: 10.1021/j150579a011.
- [25] B.L. Railsback, Some Fundamentals of Mineralogy and Geochemistry, Dep. Geol. Univ. Georg. Athens, GA. 30602-2501. U.S.A. (2006). www.gly.uga.edu/railsback/FundamentalsIndex.html.
- [26] J. Kielland, Individual activity coefficients of ions in aqueous solutions, *J. Am. Chem. Soc.* 59 (1937) 1675–1678.
- [27] C.N. Sawyer, P.L. Mccarty, Chemistry for Environmental Engineering, third ed., New York, NY, 1978.

2015 Tier 1 Project Completion Reports

Consequences and Possible Solutions for Small Scale Saline Water Residue Disposal in New Mexico — Proof of Concept



REPORT DOCUMENTATION PAGE			<i>Form Approved</i> <i>OMB No. 0704-0188</i>		
<p>The public reporting burden for this collection of information is estimated to average 1 hour per response, including the time for reviewing instructions, searching existing data sources, gathering and maintaining the data needed, and completing and reviewing the collection of information. Send comments regarding this burden estimate or any other aspect of this collection of information, including suggestions for reducing the burden, to Department of Defense, Washington Headquarters Services, Directorate for Information Operations and Reports (0704-0188), 1215 Jefferson Davis Highway, Suite 1204, Arlington, VA 22202-4302. Respondents should be aware that notwithstanding any other provision of law, no person shall be subject to any penalty for failing to comply with a collection of information if it does not display a currently valid OMB control number.</p> <p>PLEASE DO NOT RETURN YOUR FORM TO THE ABOVE ADDRESS.</p>					
1. REPORT DATE (DD-MM-YYYY) (24-11-2014)		2. REPORT TYPE Proof of Concept Final Report		3. DATES COVERED (From - To) (From 13-01-2011 To 31-13-2013)	
4. TITLE AND SUBTITLE Consequences and Possible Solutions for Small Scale Saline Water Residue Disposal in New Mexico – Proof of Concept			5a. CONTRACT NUMBER R10AC80283		
			5b. GRANT NUMBER		
			5c. PROGRAM ELEMENT NUMBER		
6. AUTHOR(S) Dr. Blair L Stringam			5d. PROJECT NUMBER		
			5e. TASK NUMBER		
			5f. WORK UNIT NUMBER		
7. PERFORMING ORGANIZATION NAME(S) AND ADDRESS(ES) Plant and Environmental Sciences, New Mexico State University, Box 30003 MSC 3Q, Skeen Hall Room N127 Las Cruces, N.M. 88003-8003			8. PERFORMING ORGANIZATION REPORT NUMBER		
9. SPONSORING/MONITORING AGENCY NAME(S) AND ADDRESS(ES) IEE/WERC New Mexico State University PO Box 30001 Las Cruces, NM 88003			10. SPONSOR/MONITOR'S ACRONYM(S)		
			11. SPONSOR/MONITOR'S REPORT NUMBER(S)		
12. DISTRIBUTION/AVAILABILITY STATEMENT					
13. SUPPLEMENTARY NOTES					
14. ABSTRACT <p>This study examines the consequences of depositing the saline concentrate into a septic system. The study was separated into two experiments. First, effluent was collected from a septic tank. Various samples of this waste water were mixed with varying concentrations of saline water. Particle dispersion and survivability of various bacterial strains were measured. Comparison of the distribution of microbial diversity of wastewater control and salinity treatments showed recovered populations had undergone a slight degree of selection with salinity treatment.</p> <p>The second experiment was conducted where saline water was injected directly into the upstream side of the leach field. Infiltration tests were taken at the beginning and the end of the experiment. These tests indicated that there was a decrease in infiltration over the time that saline water was injected into the leach field. The main contributor to this decrease is believed to be the dissipation of precipitates from a chemical reaction between the various salts in the saline concentrate and carbon dioxide that is emitted from the bacterial activity in the leach field soil.</p>					
15. SUBJECT TERMS					
16. SECURITY CLASSIFICATION OF:			17. LIMITATION OF ABSTRACT	18. NUMBER OF PAGES	19a. NAME OF RESPONSIBLE PERSON
a. REPORT	b. ABSTRACT	a. THIS PAGE			19b. TELEPHONE NUMBER (Include area code)

**Desalination & Water Purification Research
and Development Program Report No. XXX**

Consequences and Possible Solutions for Small Scale Saline Water Residue Disposal in New Mexico – Proof of Concept

Prepared for Reclamation Under Agreement No. R10AC80283

by

Blair L. Stringam, PhD



**U.S. Department of the Interior
Bureau of Reclamation
Technical Service Center
Water and Environmental Services Division
Water Treatment Engineering Research Team
Denver, Colorado**

December 2014

MISSION STATEMENTS

The mission of the Department of the Interior is to protect and provide access to our Nation's natural and cultural heritage and honor our trust responsibilities to Indian tribes and our commitments to island communities.

The mission of the Bureau of Reclamation is to manage, develop, and protect water and related resources in an environmentally and economically sound manner in the interest of the American public.

Disclaimer

The views, analysis, recommendations, and conclusions in this report are those of the authors and do not represent official or unofficial policies or opinions of the United States Government, and the United States takes no position with regard to any findings, conclusions, or recommendations made. As such, mention of trade names or commercial products does not constitute their endorsement by the United States Government.

Acknowledgements

I would like to thank the Bureau of Reclamation for providing the support to conduct this research. Dr. Adrian Unc, Jesus Sigala, and David Gamon also contributed significantly to this research.

Contents

	<i>Page</i>
Glossary	vi
Executive Summary	1
Background	2
Conclusions and Recommendations	4
Saline Concentrate Lab Test Conclusions	4
Leach Field Test Conclusions	5
Final Conclusions.....	5
Recommendations.....	6
Methods for Mixing Saline Concentrate with Septic Tank Effluent	6
Sampling	6
Physico-chemical analyses.....	7
Experimental setup.....	7
UV/Vis Spectrophotometry	7
Bacteria viability	7
DNA extraction and sequencing	8
Methods for Addition of Saline Concentrate in the Leach Field Test	8
Results and Discussion	10
Chemical and Physical Parameter.....	10
Bacterial Diversity	15
References.....	18

Glossary

454-pyrosequencing – An advanced lower cost method of pyrosequencing (see pyrosequencing).

Ascomycota – A division name from the kingdom Fungi.

Biomat – A moist layer of bacteria that forms under a septic tank leach field. As leach field water passes through this layer into the soil below, bacteria is removed from the water.

Desalinization – refers to many different processes where varying amounts of salt and or other minerals are removed from saline water.

Dothideomycetes – A large diverse class of fungi.

Gammaproteobacteria – A class of several groups of bacteria. A number of pathogens belong to this class.

Heterotrophic Bacteria – Bacteria that use organic compounds that contain carbon as a source of energy and carbon.

Humidification – The process of adding water.

mothur – An open-source software platform that is used to analyze community sequence data.

Pyrosequencing – is a method of DNA sequencing. It is used to determine the order of nucleotides in DNA.

Reverse osmosis – A water purification process where water is forced through a semipermeable membrane. This process removes many types of molecules and ions. This process leaves a concentrate that must be disposed of.

Spectrophotometry – A method that measures the amount of light that a solution absorbs.

Executive Summary

Large amounts of saline water in New Mexico are not suitable for household, agricultural, or industrial uses. In some areas, extraction and desalination is the only viable way to deliver useable water to locations. As the water is desalinated, disposal of the resulting residue becomes a problem. It is believed that land owners will deposit the majority of this concentrate back into waste water treatment systems such as septic tanks. Very little is known about the consequences of this practice.

This study examines the consequences of depositing the saline concentrate into a septic system. The study was separated into two experiments. First effluent was collected from a septic tank. Various samples of this waste water were mixed with varying concentrations of saline water. Particle dispersion and survivability of various bacterial strains were measured.

Salinity concentrations up to 10 ppt were included. Initial microbial populations were lowest for control and treatments with a range from log 4.5 to 4.8 cfu mL⁻¹. A regrowth period followed at the end of the experiment with log 6 cfu mL⁻¹ being most common. UV absorbance was used to quantify dispersion of solids and treatments produced statistically significant differences of absorbance. Diversity of bacteria and fungi were determined using 454-pyrosequencing. Treatments shared a similar distribution and richness of bacterial and fungal diversity. Operational taxonomic units (OTUs) from Gammaproteobacteria were common throughout treatments and WW control, but increased with treatment. Fungi diversity showed all OTUs belonged to Ascomycota with most being represented by Dothideomycetes members. Comparison of the distribution of microbial diversity of wastewater control and salinity treatments showed recovered populations had undergone a slight degree of selection with salinity treatment.

The second experiment was conducted on the leach field. In this experiment, saline water was injected directly into the upstream side of the leach field. Infiltration tests were taken at the beginning and the end of the experiment. These tests indicated that there was a decrease in infiltration over the time that saline water was injected into the leach field.

While the 5% clay content in the leach field soil would likely result in dispersion of clay particles that would influence the reduction in infiltration, it is believed that the soil clay content is not the governing factor. Instead the main contributor is believed to be the dissipation of precipitates from a chemical reaction between the various salts in the saline concentrate and carbon dioxide that is emitted from the bacterial activity in the leach field soil. Biomat formation may also reduce infiltration, but there was not enough time for a significant formation of the biomat.

As reverse osmosis technology is refined and efficiency improves, the concentration of contaminants will increase to levels that have been shown to negatively impact the performance of small flow wastewater systems. As septic systems are permitted and installed using existing standards, a septic system that has been compromised by the disposal of salt-rich reject water presents a risk to the surrounding environment and the public health.

This study tried to address the following questions. What are the impacts of concentrate disposal into small sewage systems? Are existing standards for small flow systems sufficient to allow for disposal of reject flows without presenting a risk to public health?

Background

Many water sources in New Mexico contain varying concentrations of dissolved inorganic salts and are not suitable for human consumption or use. Whittier and Goldstein (1986) estimate that New Mexico has about 200 billion acre feet of saline groundwater. Much of this water has a saline content of 1000 ppm or higher of total dissolved solids (TDS). This water is not suitable for human consumption unless it undergoes a desalinization process.

There are a number of farms, ranches, and small communities throughout New Mexico where the only source of water is saline water. In order to make these water sources useable for human consumption, some form of desalinization must be performed. There are a number of desalinization processes ranging from various distillation processes, reverse osmosis, and humidification (Whitworth and Lee, 2003). Regardless of the process, there is always a residue/byproduct that is left after desalinization (Whitworth and Lee, 2003). While small scale desalinization technologies become cost effective, there is very little information available about economically viable disposal of the residue/byproduct. There is a risk that the desalination technologies may be applied without regard for managing the residual concentrate and in the absence of a proven solution, inappropriate disposal may occur.

As reverse osmosis technology has advanced, the reported efficiency of the systems has increased several fold. The first commercially available residential systems wasted upwards of 80 percent of the source stream. Newer systems are efficient enough to produce a more concentrated reject stream of less than 10%. The technology has outpaced the understanding of its potential impact on a small waste water system treatment system. Where previous systems could be installed based on historical performance, risk that a newer system is installed and plumbed into a septic system without a better understanding of the impact is significant.

Additionally, the risk is not limited to the septic system performance itself. It is believed that the concentrations of pollutants may reach a level where the biomat

of the leach field distribution piping is compromised. If this is the case, commonly accepted design and implementation practices would no longer apply and the potential for under-treated sewage reaching the groundwater is increased. The potential of pathogens passing through a damaged or compromised leach field biomat present a risk to the public health.

Most of the research directed at the impact of salt-rich discharge into small systems has focused on the use of chemical water softeners. In these cases, the risk is sufficient that most reputable wastewater treatment manufacturers have clauses in their warranties voiding the warranties if water softener brine is discharged to the treating system (Gross and Bounds, 2007). As the efficiency of reverse osmosis systems improve, the resulting concentrations will reach levels that have been shown to impact the ability of a typical bio-system (Gross and Bounds, 2007).

A number of regional water budgeting and planning efforts in New Mexico have used a rule-of-thumb assumption that approximately 50 percent of the water pumped from onsite domestic wells is returned to the aquifer through the septic system (McQuillan and Basset, 2009). However in New Mexico, widespread ground-water contamination has occurred in many rural areas utilizing on-site wells and septic systems (N.M. WQCC, 2002a). Effluent discharged to the subsurface by drainfields often percolates into the same aquifer tapped by wells for domestic supply. In New Mexico, on-site septic systems have contaminated more acre-feet of ground water, and more public and private water supply wells, than all other sources combined (McQuillan, 2004)

It was suspected that additions of concentrate to a septic system can have both immediate and accumulated impacts. In this study two separate sets of experiments were designed to estimate both immediate and accumulated impacts. The sensitivity of a bio-system to increasing levels of concentrate can be accomplished in a laboratory setting using field samples. In other words, field samples will be collected from a septic system and taken to a lab where saline concentrates will be mixed into the sample. The samples will then be analyzed for the effect that the concentrate has on the biological organisms within the sample.

There is a gap in knowledge on the impact to the microbial community of the septic system. Previous work has shown that septic systems and associated leach field biomats are unique at the microbial level (Tomaras, Sahl, et al., 2009). Sudden changes such as increasing the concentration of NaCl can have an impact on the activity of bacteria involved in reduction of organic pollutants (Cortés-Lorenzo, Rodríguez-Díaz, et al., 2012). Here we investigate the impact of saline concentrate application into wastewater by studying microbial diversity and viability.

The original plan for this project was to inject saline water into the septic tank and

try to determine the effect on the septic tank water as well as the leach field. Prior to the selection of a research site, the researchers became concerned with the possible results of injecting the saline water into the septic tank. Moore (2001) claimed that organic particles in the septic tank would disperse with the introduction of saline water. If this occurred the septic field would likely see an increase in particle deposits from this dispersion. While this is an important conclusion to draw from this research, it was determined that the same possible outcome could be determined by taking samples from the septic system and conducting experiments in the lab where the saline water is mixed with the septic tank effluent. Conducting these tests in the laboratory would make particle dispersion measurement easier.

In addition, the study wanted to determine the effect that saline water had in the leach field. It would be very difficult to separate the effect that saline water had on the leach field with the addition of particles from the effluent stream. It was concluded that if the saline water was injected into the leach field the effect that this would have on the leach field could be separated from the deposit of effluent particles.

For these reasons, this study was separated into two experiments. One focused on the effect that saline water had on the septic tank effluent and the other examined the effect that saline water had on the leach field. The findings from these two experiments are reported below.

While this study will help to understand the consequences of introducing saline concentrates into the waste streams of small septic systems, there is more that will need to be understood. Additional studies should address what the consequences of adding these concentrates into larger municipal systems and industrial treatment systems. While the data from this study can be used to make assumptions, complete understanding can only be accomplished by studying these larger systems as well.

Conclusions and Recommendations

Saline Concentrate Lab Test Conclusions

Increased salinity selected for bacterial populations that included a subset of the WW sample. Results suggest that increased salinity produced shifts in the microbial diversity. Implementation of this method is likely to reduce some bacterial activity but bacterial viability is not much of a concern. The data suggest an increase in dispersion will be observed with increased salinity. Particle dispersion will likely send particles into the leach field before they are completely digested. As these particles are deposited, there would be a reduction in infiltration.

Leach Field Test Conclusions

The change in permeability rate for the leach field may be attributed to three things. The first may be due to the incorporation of salts into the clay soil below the leach field. This would likely disperse the clay particles and reduce the rate of water movement through the soil. However, considering that the clay content in the soil was about 5%, it is believed that the clay dispersion would have a limited effect. Corey *et al.*, (1977) claims that clay is not a problem unless the soil has a clay content over 15%.

The second thing that could contribute to the lower water movement is possibly the formation of a biomat below the leach field. A properly functioning leach field will have a biomat develop below it, but it takes 3 to 8 years for a biomat to completely form (Farrell-Poe, 2014). Farrell-Poe (2014) indicates that at the most a biomat could only have formed under half of the leach field in one year. If this is the case, the biomat will have little to no effect on the infiltration of water into the leach field.

It is believed that the main contributing factor to the infiltration reduction is the deposition of precipitates in the leach field. The bacterial action in the leach field will produce carbon dioxide. This will likely combine with calcium, magnesium, potassium, and sodium in the saline concentrate. The result would be the formation of carbonate precipitates. These precipitates will also fill soil voids and reduce infiltration.

Final Conclusions

Depositing saline concentrate into a septic system appears to have multiple consequences. While there is limited impact on survivability of the organic particles in the septic system, the particles are dispersed and will likely become part of the stream that flows into the leach field. This will eventually limit the infiltration of the leach field.

It also appears that depositing saline concentrate in the septic system will dissipate clay particles and likely cause chemical reactions that will result in the deposit of precipitates in the soil. Both of these results will reduce leach field infiltration rates.

Presently it appears that there is no elegant solution for how saline concentrate can or should be treated when it is removed from the water supply. This waste stream should not be deposited into the septic system. Instead, this concentrate should be deposited in a properly designed evaporation pond or some other safe place. This would also apply to a small community that may have to remove salts from their water supply. However, a small community may be able to develop an

underground injection site that the concentrate can be safely deposited into.

It may be suggested to add chemicals such as acid from time to time to try to free salts from the leach field soil. This would likely damage the biomat and risk polluting the ground water.

Recommendations

This work has only considered the consequences of depositing saline water into the septic tank for a 1 year period. Further study is needed to understand the long term consequences. While this work showed that there is limited negative effects on the bacteria in the septic tank we were not able to determine what would happen to the biomat under a leach field. It takes several years to form a biomat and we do not understand if saline water would limit biomat formation. The biomat helps to purify septic water before it flows into the ground water. Understanding the effects that saline concentrate has on biomat formation needs to be understood.

In addition, the deposition of participates in the leach field over a longer period of time needs to be understood. It is believed that the reaction between carbon dioxide and the salts in the saline water would eventually reduce leach field permeability to zero. However, this needs to be verified.

Methods for Mixing Saline Concentrate with Septic Tank Effluent

Sampling

Saline solution was sampled from a desalination plant located in Alamogordo, NM. A volume of 8 L was collected in plastic containers which were DI washed and sterilized prior to sampling. The solutions were kept at room temperature in the lab until use.

Wastewater was collected from a residential septic tank located near Las Cruces, NM. The septic tank is a one family unit featuring a typical two-chamber system. A wastewater sample was retrieved from the septic tank outlet to leach-field (i.e. tank effluent). The wastewater sample was immediately transported to the lab, stored at 4 °C, and used the same day.

Physico-chemical analyses

EC was tested using a bench top Fisher Scientific conductivity meter. pH was tested using a Beckman Phi 72 pH meter. Dissolved oxygen (DO) was determined at the time of sampling using a multi-parameter Hach field test kit (FF-1A). TSS was determined using gravimetric methods.

A survey of the chemical profile of both wastewater and saline solution was carried out on an ICP/OES Optima 4300 DV system according to the standard EPA method 200.7 (EPA, 1994).

Experimental setup

For most tests, a 100 mL 1:1 saline concentrate to wastewater reaction mixtures were prepared. Four levels of saline concentrate treatments were used including a 10 ppt stock and three dilutions of the stock using DI water yielding saline solutions at 6 ppt, 4 ppt, and 2.6 ppt. A reaction with only wastewater (WW) served as one control and a second reaction with only saline concentrate (SS) served as a second control. A third control included wastewater mixed with deionized water (WW-DI).

In a second experiment, a higher ratio of 3:1 saline concentrate to wastewater volume was prepared while maintaining the same overall volume of 100 mL. The same final salinity concentrations were as above.

All reactions were performed in triplicate in 500 mL Erlenmeyer flasks. All glassware were acid bath washed and autoclaved. Flasks were aluminum sealed and placed on orbital shaking at 30 rpm. Reactions were held at room temperature and in dark conditions.

UV/Vis Spectrophotometry

Absorbance as an indicator of dispersion was detected by UV/Vis spectrophotometry using a Genesys 20 spectrophotometer at 600 nm wavelength and 1 cm path length. Plastic disposable cuvettes were used using 2 mL assay volume. All readings were performed in triplicate.

Bacteria viability

Heterotrophic bacterial counts were determined by incubation on Mueller-Hinton Agar (MHA). High motility/swarming was observed on pre-test, therefore the filter plate method was performed instead of the agar sweep method. Dilutions

ranging from 10^{-3} to 10^{-5} mL were prepared. Incubation was carried out for 36 hours at 37 °C.

DNA extraction and sequencing

Several centrifugation steps were performed to pellet and wash the bacteria from the 80 mL samples. DNA was extracted using a MoBio PowerSoil DNA isolation kit according to the manufacturer's protocol. The final dilution volume was 100 μ L. All extractions were performed in duplicate and were composited for downstream application.

DNA was quantified on a NanoDrop 1000. For most samples DNA yields were 20 ng μ L⁻¹ range. Only 2 ng of DNA were measured per μ L of the saline concentrate (SS). Samples were analyzed by 454 pyrosequencing at Molecular Research MRDNA in Shallowater, TX. Bacterial tag-encoded FLX-Titanium amplicon pyrosequencing (bTEFAP) was performed using primers 28F (GAGTTTGATCNTGGCTCAG) and 519R (GTNTTACNGCGGCKGCTG) covering the V1 to V3 region of the 16S rRNA (Erb-Downward et al., 2011). Fungal primers EndoITSF (AAGGTCTCCGTAGGTGAAC) and EndoITSR (GTATCCCTACCTGATCCGAG) were used which sequence the internal transcribed spacer region (Lucero, Unc, et al., 2011). As described previously (Dowd et al., 2008) a 30-cycle single amplification with 1 U HotStarTaq Plus Master Mix kit (Qiagen) was used to amplify sequences prior to sequencing on Roche 454 Titanium instrument using recommended guidelines and reagents.

For bacteria, mothur 1.32.0 (Schloss et al., 2011) was used for analysis of sequencing results using a standard analysis approach. Sequences 200 bp or greater of high quality (qwindowaverage criteria in mothur) and with homopolymer not greater than 6 were kept. Clustering was calculated at 0.03 and OTUs were classified using the RDP taxonomy in mothur. A taxonomic approach was used for fungi pyrosequencing results. A similar workflow to bacteria was implemented for fungi to eliminate bad quality sequences. BLASTn was performed using a custom curated GreenGenes database at MRDNA (Dowd, Callaway, et al., 2008).

Methods for Addition of Saline Concentrate in the Leach Field Test

The goal of this portion of the project was to determine the impact that concentrated saline water would have on the leach field of a septic system. Richards et al. (1954) and Brady and Weil (2010) report that if saline water is allowed to flow over and through a soil that contains clay, there will be a dispersal of clay particles. As clay particles disperse, they will fill soil voids and reduce

infiltration. In order to see if this occurred in a septic tank leach field, the researchers tried to find a septic system that had a leach field located in a clay soil.

A functioning septic system that was in good condition was needed for this project. Saline concentrate was originally going to be injected into the waste stream that went into the septic tank, but that was determined to be risky considering that Moore (2001) indicates that saline water would disperse the particles in the septic tank. If this occurred, the particles would likely flow with the septic water into the leach field. This would likely reduce infiltration in the leach field. If this occurred, the experiment may not be able to determine if changes in septic field infiltration were from saline concentrate interacting with soil particles or from organic particles in the waste stream.

In case the study had a long lasting negative effect on the septic leach field, it was determined that a second leach field would be installed on a septic system. Using an actual septic system that served a household would give the most realistic results. Several sites were examined to determine their suitability for the study. One site showed promise, but as the addition of a second leach field was considered, New Mexico State representatives informed us that all other septic tanks on the property would have to be brought to state standard requirements. The particular property had 5 septic systems. All of these sites would have to be upgraded and this requirement exceeded the funding that was available for the project.

A second site was inspected for use as a possible research site. However, the water table was high and the site would have required the addition of a soil mound and pumping system to operate the leach field. Again the cost would have exhausted the funds that were available. The high water table may also have given none typical results.

Multiple other sites were inspected for use as a research site but the area that would be required for the leach field was made up of sand and it was suspected that a leach field that was placed over a sandy soil would not give any measureable results. It was determined that the most significant results would occur if the soil below the septic tank leach field contained some clay. However, the sites that were available for this study had only sand in the leach field area.

A site was finally located where a septic system had been installed 2 years prior to this research project. An additional leach field could be connected to the original septic system with no negative effects to the system. The soil was sampled for the leach field area and sand was the primary component of the soil located in this area. As mentioned earlier, it was desired to have clay soil in the soil mix. It was suggested that a clay soil be incorporated/mixed into the sandy soil below where the leach field would be located. A trench was excavated for the leach field and clay soil was spread out over the leach field area. The clay soil was then mixed

into the sandy soil. This created a clay-sand soil layer below the leach field that was about 8 to 10 inches thick. After mixing, the soil was analysed for proportions of sand, silt, and clay. It was determined that the soil was 87.8% sand, 7.23 % silt, and 4.96 % clay.

Once the soil was in place, the leach field was installed and connected to the septic system. The septic system was operated with the new leach field for approximately one month. After a month, tests were conducted to determine the leach field permeability rate. This was accomplished by pouring water down into the leach field through an observation tube. The amount of water that was poured into the leach field and the time that was required for the water to infiltrate were measured

After the permeability tests were completed, a salinity metering injection system was connected into the observation tube so that saline water could be injected into the system. A saline solution with an approximate EC of 2700 $\mu\text{S}/\text{cm}$ was injected into leach field. The chemical analysis for this saline solution is shown in table 1. The metering pump was incorporated into the saline injection system with a timer so that saline water would be injected into the leach field in the morning and evening. This was done to simulate the removal of salts using an IO system at key times of the day when there would be high water use. During these high use periods, the waste concentrate would be dropped back into the house waste stream. However as mentioned earlier, the concentrate was injected into the leach field.

Injection of the saline water into the leach field continued for a period of about one year. At the end of a year the leach field was again tested to determine the permeability rate.

Results and Discussion

Chemical and Physical Parameter

Stock saline solution had a salinity of about 10,000 mg L^{-1} or 1% (w/v) solution (10 ppt). Physical and chemical parameters of both saline and wastewater solution are shown in table 1.

In the first experiment, solutions of 1:1 saline concentrate to wastewater were prepared with varying concentrations of salinity. UV absorbance results were measured daily during the experiment. Absorbance of experimental controls WW and SS at initial t_0 were statistically different (figure 1). Throughout the experiment, both controls had statistically significant differences in absorbance between each other and compared to the treatments. Among treatments, assays from t_0 and t_3 yielded non-significant differences in absorbance. At day t_4 , two

treatments, 10 ppt and 4 ppt had the highest mean absorbance; this difference was statistically significant between 10 ppt and both 2.6 and 6 ppt.

Table 1. Physico-chemical parameters of to wastewater and saline concentrate samples.

	Wastewater	Saline Solution
pH	6.85	6.89
DO (mg/L)	< 0.2	1.6
EC (mS/cm)	1.04	8.98
SAR	2.47	6.98
TSS (mg/L)	34	10,600
Mg	14.46	459.27
Ca	71.74	593.18
Na	87.86	931.5
K	18	6.737
Al	0.2167	Nd
As	0.1042	0.5425
B	0.3733	0.8825
Ba	0.057	0.0369
Be	Nd	Nd
Cd	0.0018	Nd
Co	0.0023	Nd
Cr	Nd	Nd
Fe	0.274	Nd
Mn	0.0474	Nd
Mo	Nd	Nd
Ni	0.0052	0.0188
Pb	Nd	Nd
Se	0.0515	Nd
Tl	Nd	Nd
V	Nd	Nd
Zn	0.055	0.1033
Bi	Nd	Nd
Li	0.067	0.0973
P	6.006	Nd
Sr	0.6683	14.14
Si (as SiO ₂)	31.33	47.64
S	11.74	1271
Cu	Nd	0.6135

Note: Elemental concentration in mg/L

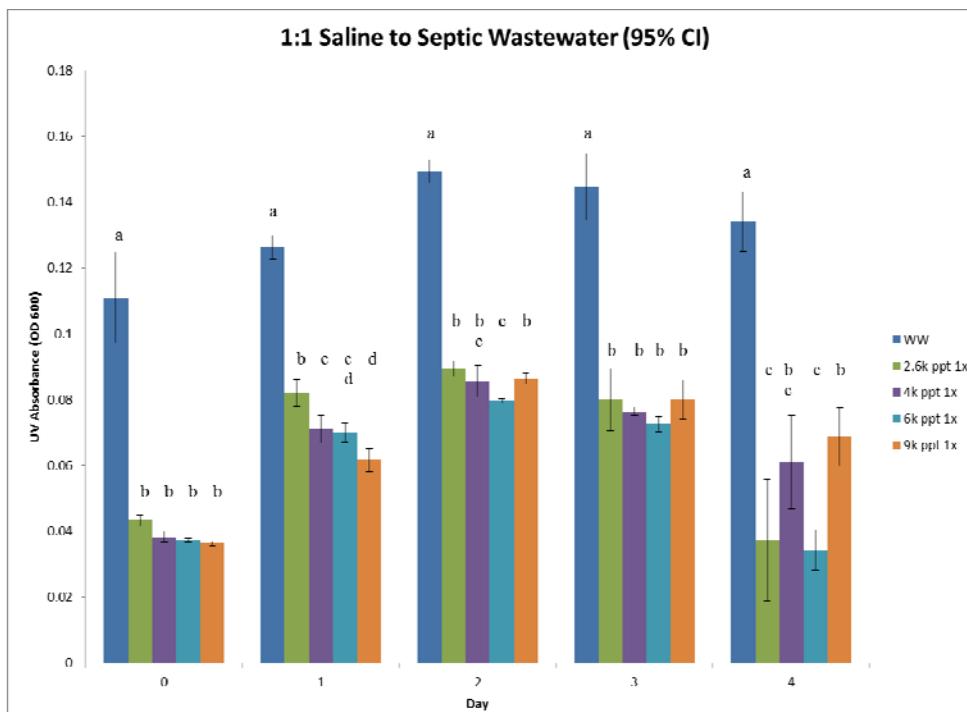


FIGURE 1. UV/Vis absorbance of WW control and treatments with statistical inference shown (95% CI). GLM ANOVA method performed in MiniTab with Tukey pairwise comparison, all test of significance at $\alpha < 0.05$.

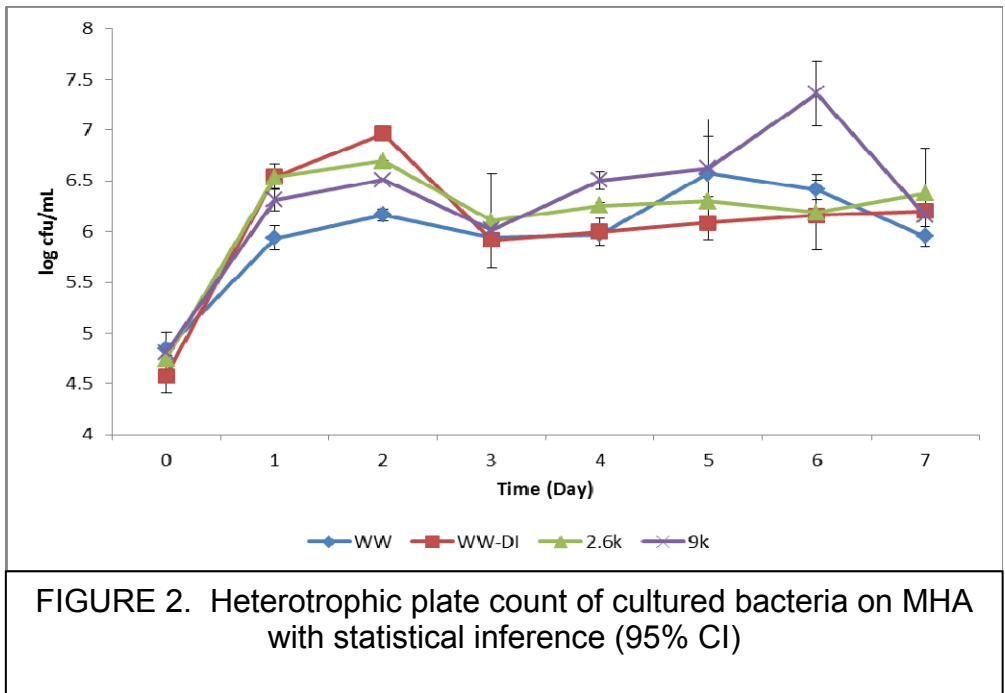
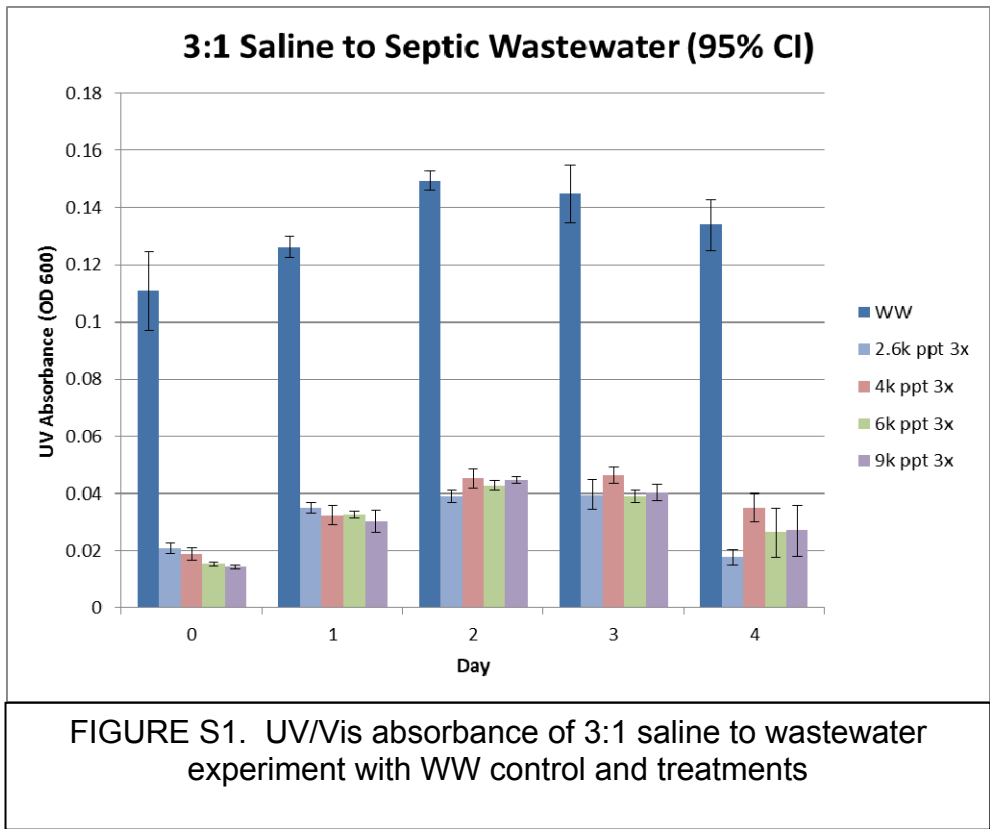
These results show that WW control and treatments increase in absorbance temporarily with a peak at t_2 followed by a decrease. The same trend was observed in the experiments with 3:1 ratio of saline to wastewater.

In the 3:1 ratio experiments, differences in the absorbance among treatments were mostly non-significant (Fig S1). At t_4 , only the 4 ppt treatment had statistically higher absorbance compared to 2.6 ppt, while it was higher but not statistically significant than the absorbance measured for the 6 and 10 ppt treatments.

Bacterial viability, i.e. heterotrophic counts, were determined by MHA agar plate incubation (figure 2). The MHA agar plate incubation confirmed the lower count of recoverable bacteria at the start of the experiment with log 4.5 to 4.8 cfu mL⁻¹. The bacterial population steadily increased with a peak at t_2 associated with short-term regrowth. One treatment at 10 ppt, had a second peak in late phase monitoring (time = 6). A steady bacterial population in SS control could be detected with an average population of log 5.0 cfu mL⁻¹.

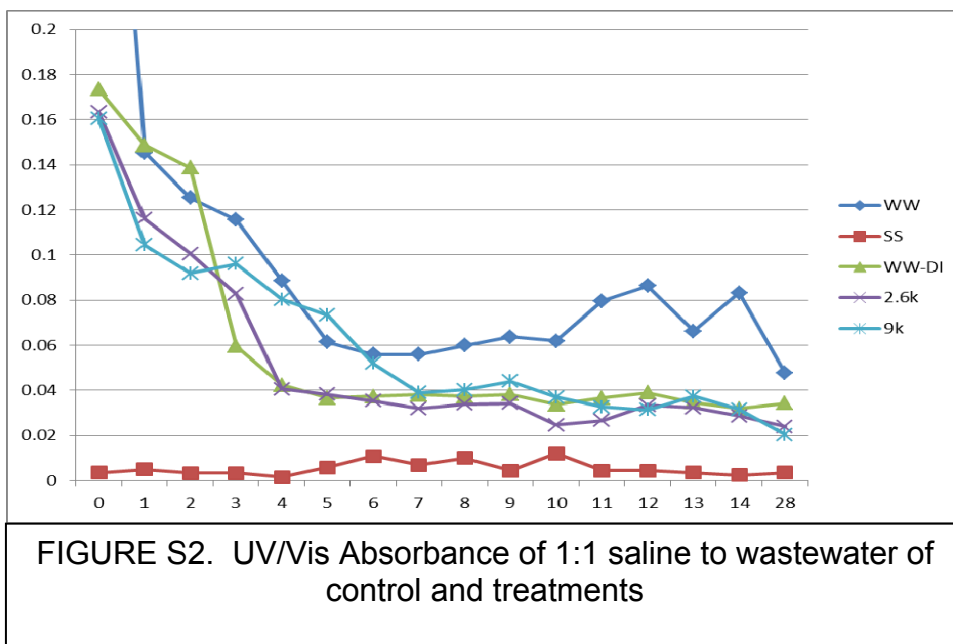
Long term bacterial abundance was monitored using spectrophotometry as described (Fig S2). These were performed in parallel to the heterotrophic counts. Results show that for most treatments and controls a baseline was reached at day

6. The one exception was the WW control for which more variability in the absorbance profiles were observed after day 10.



The data showed that there was a significant difference among treatments when examining the UV/Vis absorbance. This would be in agreement with several studies showing selection of bacteria with salt increase (Ríos et al., 2010). Salt stress affects the microbial cell reducing the amount of solutes in the cell membrane. These effects are counteracted by different mechanisms that have been explored in salt tolerant bacteria (Tsuzuki, Moskvina, et al., 2011; Steil, Hoffmann, et al., 2003). In addition to selection of bacteria, salts are known to disperse dissolved organic carbon in soils, effects that were however related to increases in soil pH (Green et al., 2008).

Varying concentrations of salts are known to influence microbial parameters in several ways (Wong et al., 2008). Some of these are dispersion of soils and organic matter related to increase of bacterial biomass with increasing salinity. The results point to dispersion increasing at a statistically significant difference for greater concentrations of salt. Ng et al. (2005) found that wastewater in SBR encountered problems of high turbidity with increasing concentrations of NaCl up to 60 g L⁻¹. Yet, the sludge volume index was low at higher NaCl, indicating better compaction properties of sludge. In septic tanks, longer retention time have to be taken into account, which is likely to see both greater sludge compaction in both chambers and increased dispersion of small particles which will be introduced to the leach field.



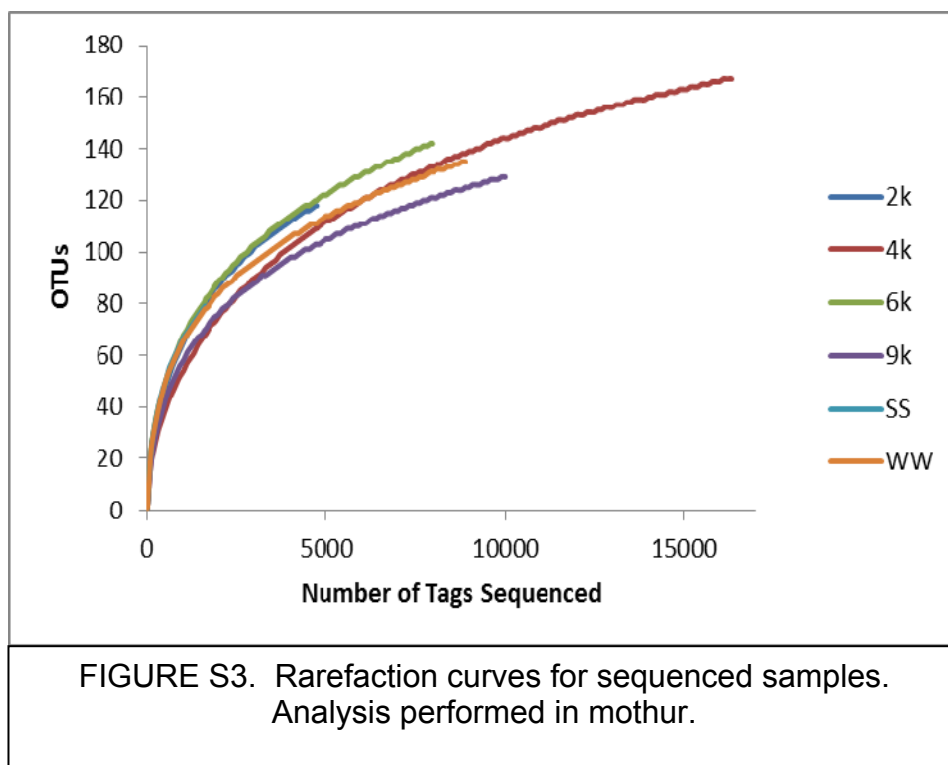
Bacterial Diversity

454-pyrosequencing was performed to analyze the bacterial diversity related to treatments and controls of analyzed samples. Coverage and estimators of richness and abundance are shown in table 2. Results indicate high sequence (>98%) coverage for all samples. Control SS showed the lowest bacterial richness with 105 OTUs (Ace and Chao estimators). WW and 4 ppt samples had the greatest richness at 200 OTUs.

TABLE 2. Summary of sequences results as performed in mothur

Sample	Number of Sequences	Coverage	Ace	Chao1	Inverse Simpson
2k	4730	0.992389	155.18	148	5.02553
4k	16337	0.997062	206.9441	220.7143	3.920377
6k	7960	0.994347	192.1834	197	6.863835
9k	10008	0.996303	166.5482	170.625	3.863572
SS	1616	0.983292	106.0041	104.0714	7.374596
WW	8904	0.99562	204.6678	176.1667	7.321451

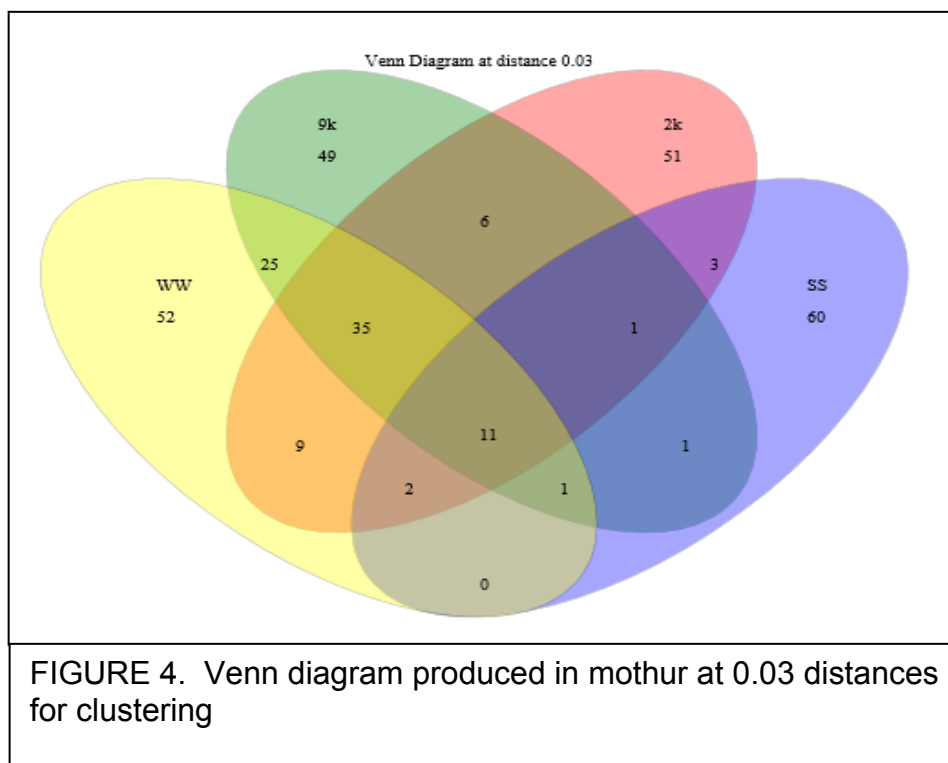
Rarefaction curves for the sequencing efforts on these samples were produced (figure S3). Results showed samples did not asymptote, but most featured very similar shapes and lengths. Treatment 4 ppt showed the most richness but this was likely a result of a higher number of tags sequenced from this sample.

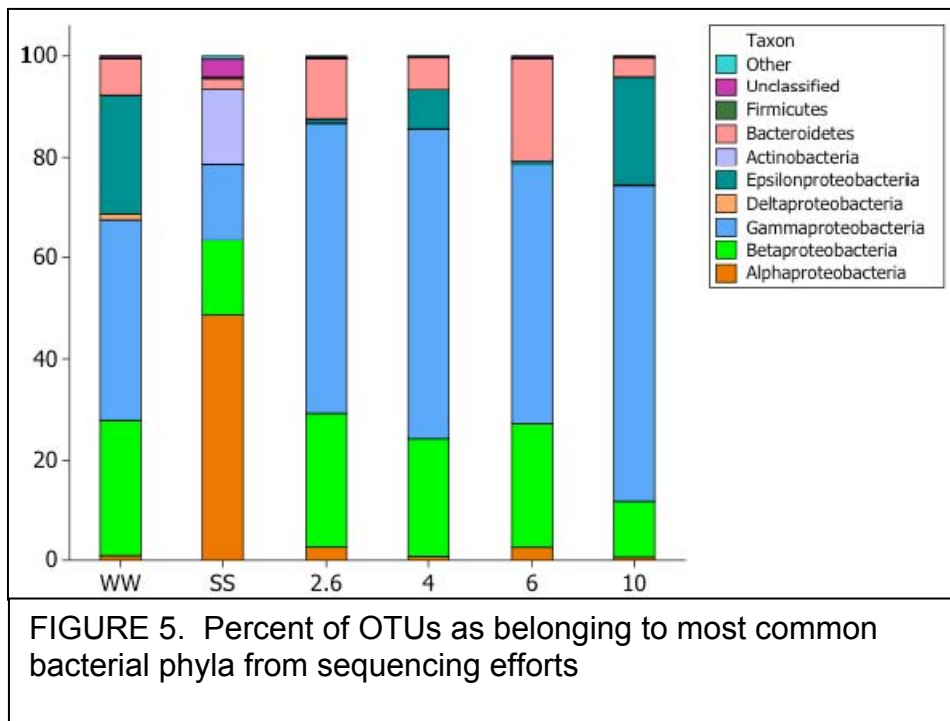


Sample similarity is graphically presented in figure 4. Results indicate that treatments are similar with each other and dissimilar from the SS control. An examination of phyla (figure 5) showed two bacterial classes in SS were Alphaproteobacteria and Actinobacteria. These were among the most common for that sample. Alternatively, Actinobacteria were not detected for WW and treatments.

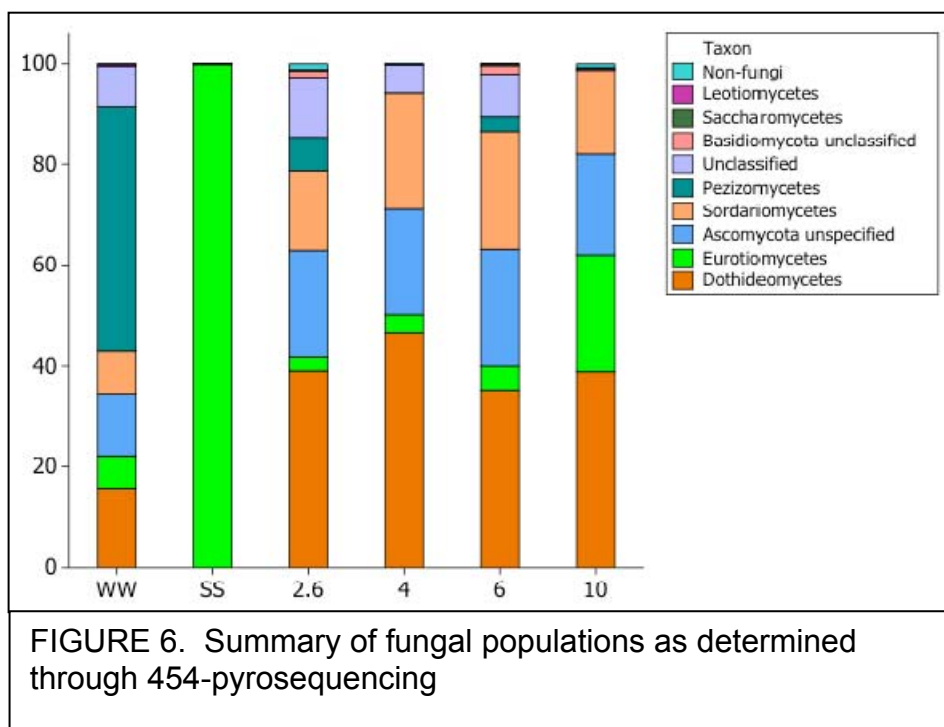
For fungi, pyrosequencing efforts showed very clearly control SS to be dominated by Ascomycota members belonging to Eurotiomycetes (figure 6). Of which, all sequences were assigned putatively to the genus *Penicillium*. Sequences from this genus have been observed previously in a high salt environment (Smolyanyuk and Bilanenko, 2011).

Selection of bacteria did take place among treatments compared to the native WW microbial population. One possibility is that introduced saline offers different mechanisms and substrates which in turn offer different strategies of survival. Another possibility is that osmotic stress effects drove changes in survival by selection. For wastewater, this is a concern because of the attribution of some species to important wastewater processes. One study found that salinity concentrations of 0.5% and higher decreased the removal of nutrients from sequencing batch reactors (Intrasungka, Keller, et al., 1999). Ammonia oxidizing bacteria, an important group of bacteria for wastewater treatment, are also known to be affected negatively by increasing salt concentration (Cantera, Jordan, et al., 2006).





The survival of indicator bacteria as well as pathogenic species are a valid concern. Increasing salt reduces wastewater bacterial activity in most aspects that are measured such as DOC and ammonia removal (Johir, Vigneswaran, et al., 2013) for very high salinity (60 g L⁻¹). At a moderate salinity concentration (10 g L⁻¹) acclimation has been reported (Linarić, Markić, et al., 2013). With longer retention time of waste in a septic tank system, acclimation of bacterial population is likely to take place with Gammaproteobacteria being abundant.



References

Brady, N.C. and Weil, R.R. (2010). *Elements of the nature and properties of soils third edition*. Prentice Hall, New York, New York.

Cantera, J. J. L., Jordan, F. L., and Stein, L. Y. (2006) Effects of irrigation sources on ammonia-oxidizing bacterial communities in a managed turf-covered aridisol. *Biology and Fertility of Soils*, 43(2), 247–255. [online] <http://link.springer.com/10.1007/s00374-006-0101-x> (Accessed January 16, 2014).

Corey, R.B., Tyler, E.J., Olotu, M.U. (1977). “Effects of water softener use on the permeability of septic tank seepage fields” In *Proceedings of the Second National Home Sewage Treatment Symposium*. ASAE Publication 5-77. ASAE, St. Joseph, MI, pp. 226-235.

Cortés-Lorenzo, C., Rodríguez-Díaz, M., López-Lopez, C., Sánchez-Peinado, M., Rodelas, B., and Gonzalez-Lopez, J. (2012) Effect of salinity on enzymatic activities in a submerged fixed bed biofilm reactor for municipal sewage treatment. *Bioresource technology*, 121, 312–319.

Dowd, S. E., Callaway, T. R., Wolcott, R. D., Sun, Y., McKeehan, T., Hagevoort, R. G., and Edrington, T. S. (2008) Evaluation of the bacterial diversity in the feces of cattle using 16S rDNA bacterial tag-encoded FLX amplicon pyrosequencing (bTEFAP). *BMC microbiology*, 8, 125. [online] <http://www.pubmedcentral.nih.gov/articlerender.fcgi?artid=2515157&tool=pmcentrez&rendertype=abstract> (Accessed June 28, 2011).

EPA (1994) Determination of metals and trace elements in water and wastes by inductively coupled plasma-atomic emission spectrometry,

Erb-Downward, J. R., Thompson, D. L., Han, M. K., Freeman, C. M., McCloskey, L., Schmidt, L. a, Young, V. B., Toews, G. B., Curtis, J. L., Sundaram, B., Martinez, F. J., and Huffnagle, G. B. (2011) Analysis of the lung microbiome in the “healthy” smoker and in COPD. *PloS one*, 6(2), e16384. [online] <http://www.pubmedcentral.nih.gov/articlerender.fcgi?artid=3043049&tool=pmcentrez&rendertype=abstract> (Accessed November 19, 2013).

Farrell-Poe, K.L. (2014). "Can you rejuvenate failing soil treatment areas?" University of Arizona draft Bulletin

Green, S. M., Machin, R., and Cresser, M. S. (2008) Long-term road salting effects on dispersion of organic matter from roadside soils into drainage water. *Chemistry and Ecology*, 24(3), 221–231.

Gross, M. and Bounds, T. (2007) “Water Softener Backwash Brine Stresses Household Septic Tanks and Treatment Systems”. *Small Flows Magazine*, Vol. 8, No 2, 8 – 10.

Intrasungkha, N., Keller, J., and Blackall, L. L. (1999) Biological nutrient removal efficiency in treatment of saline wastewater. *Water science and technology*, 39(6), 183–190.

Johir, M. a. H., Vigneswaran, S., Kandasamy, J., BenAim, R., and Grasmick, a. (2013) Effect of salt concentration on membrane bioreactor (MBR) performances: Detailed organic characterization. *Desalination*, 322, 13–20. [online] <http://linkinghub.elsevier.com/retrieve/pii/S0011916413002014> (Accessed January 16, 2014).

Linarić, M., Markić, M., and Sipos, L. (2013) High salinity wastewater treatment. *Water science and technology: a journal of the International Association on Water Pollution Research*, 68(6), 1400–5. [online] <http://www.ncbi.nlm.nih.gov/pubmed/24056440> (Accessed January 16, 2014).

Lucero, M. E., Unc, A., Cooke, P., Dowd, S., and Sun, S. (2011) Endophyte microbiome diversity in micropropagated *Atriplex canescens* and *Atriplex torreyi* var *griffithsii*. *PloS one*, 6(3), e17693. [online] <http://www.pubmedcentral.nih.gov/articlerender.fcgi?artid=3060086&tool=pmcentrez&rendertype=abstract> (Accessed November 2, 2011).

McQuillan, D. and Bassett, E. (2009) “Return Flow to Ground Water from Onsite Wastewater Systems”. 18th Annual NOWRA Technical Conference and Expo, April 6-9, 2009, Milwaukee, WI

McQuillan, D. (2004) “Ground-Water Quality Impacts from On-Site Septic Systems”. Proceedings, National Onsite Wastewater Recycling Association, 13th Annual Conference, Albuquerque, NM, November 7 – 10, 2004

Moore, M., (2001) “Water Softener Use Raises Questions for System Owners”. Pipeline 12:1. National Small Flows Clearinghouse.

Ng, H. Y., Ong, S. L., and Ng, W. J. (2005) Effects of Sodium Chloride on the Performance of a Sequencing Batch Reactor. *Journal of environmental engineering*, 131(11), 1557–1565.

Richards, L.A., Allison, L.E., Bernstein, L., Bower, C.A., Brown, J.W., Fireman, M., Hatcher, J.T., Hayward, H.E., Pearson, G.A., Reeve, R.C., Richards, L.A., and L.V. Wilcox. (1954). *Diagnosis and improvement of saline and alkali soils*. Agriculture Handbook No. 60, US Dept of Agriculture, US Government Printing Office

Ríos, A. D. L., Valea, S., Ascaso, C., Davila, A., Kastovsky, J., Mckay, C. P., Gómez-silva, B., and Wierchos, J. (2010) Comparative analysis of the microbial communities inhabiting halite evaporites of the Atacama Desert. *International Microbiology*, 13, 79–89.

Schloss, P. D., Gevers, D., and Westcott, S. L. (2011) Reducing the effects of PCR amplification and sequencing artifacts on 16S rRNA-based studies. *PLoS one*, 6(12), e27310. [online] <http://www.pubmedcentral.nih.gov/articlerender.fcgi?artid=3237409&tool=pmcentrez&rendertype=abstract> (Accessed November 7, 2013).

Smolyanyuk, E. V. and Bilanenko, E. N. (2011) Communities of halotolerant micromycetes from the areas of natural salinity. *Microbiology*, 80(6), 877–883. [online] <http://link.springer.com/10.1134/S002626171106021X> (Accessed January 16, 2014).

Steil, L., Hoffmann, T., Budde, I., Völker, U., and Bremer, E. (2003) Genome-wide transcriptional profiling analysis of adaptation of *Bacillus subtilis* to high salinity. *Journal of bacteriology*, 185(21), 6358–6370.

Tomaras, J., Sahl, J. W., Siegrist, R. L., and Spear, J. R. (2009) Microbial diversity of septic tank effluent and a soil biomat. *Applied and environmental microbiology*, 75(10), 3348–51. [online] <http://www.pubmedcentral.nih.gov/articlerender.fcgi?artid=2681617&tool=pmcentrez&rendertype=abstract> (Accessed January 16, 2014).

Tsuzuki, M., Moskvina, O. V., Kuribayashi, M., Sato, K., Retamal, S., Abo, M., Zeilstra-Ryalls, J., and Gomelsky, M. (2011) Salt stress-induced changes in the transcriptome, compatible solutes, and membrane lipids in the facultatively phototrophic bacterium *Rhodobacter sphaeroides*. *Applied and environmental microbiology*, 77(21), 7551–9. [online] <http://www.pubmedcentral.nih.gov/articlerender.fcgi?artid=3209165&tool=pmcentrez&rendertype=abstract> (Accessed January 16, 2014).

Whittier, J. and Goldstein, B. (1986). “Use of Saline Water for Buffalo Gourd Production in New Mexico”. New Mexico Water Resources Research Institute, New Mexico State University, Project No. 1423614

Whitworth, T.M and Lee, R. (2003). “Desalting of Saline Waters-Applications to New Mexico”. *New Mexico Geology*, 25(1), 16-20.

Wong, V. N. L., Dalal, R. C., and Greene, R. S. B. (2008) Salinity and sodicity effects on respiration and microbial biomass of soil. *Biol Fertil Soils*, 44, 943–953.

Construction of MED Component of Pyrolyzer-Desalination Unit
for Resiliency Testing



REPORT DOCUMENTATION PAGE		Form Approved OMB No. 0704-0188
<p>The public reporting burden for this collection of information is estimated to average 1 hour per response, including the time for reviewing instructions, searching existing data sources, gathering and maintaining the data needed, and completing and reviewing the collection of information. Send comments regarding this burden estimate or any other aspect of this collection of information, including suggestions for reducing the burden, to Department of Defense, Washington Headquarters Services, Directorate for Information Operations and Reports (0704-0188), 1215 Jefferson Davis Highway, Suite 1204, Arlington, VA 22202-4302. Respondents should be aware that notwithstanding any other provision of law, no person shall be subject to any penalty for failing to comply with a collection of information if it does not display a currently valid OMB control number.</p> <p>PLEASE DO NOT RETURN YOUR FORM TO THE ABOVE ADDRESS.</p>		
1. REPORT DATE (DD-MM-YYYY)	2. REPORT TYPE	3. DATES COVERED (From - To)
30-09-2015		From 01-07-2014 to 31-07-2015
4. TITLE AND SUBTITLE Construction of MED Component of Pyrolyzer-Desalination Unit for Resiliency Testing		5a. CONTRACT NUMBER
		5b. GRANT NUMBER
		5c. PROGRAM ELEMENT NUMBER
		5d. PROJECT NUMBER
6. AUTHOR(S) Catherine E. Brewer		5e. TASK NUMBER
		5f. WORK UNIT NUMBER
7. PERFORMING ORGANIZATION NAME(S) AND ADDRESS(ES)		8. PERFORMING ORGANIZATION REPORT NUMBER

<p>9. SPONSORING/MONITORING AGENCY NAME(S) AND ADDRESS(ES)</p>	<p>10. SPONSOR/MONITOR'S ACRONYM(S)</p>
	<p>11. SPONSOR/MONITOR'S REPORT NUMBER(S)</p>
<p>12. DISTRIBUTION/AVAILABILITY STATEMENT</p>	
<p>13. SUPPLEMENTARY NOTES</p>	
<p>14. ABSTRACT</p> <p>This study was the second part of a study to assess the potential of using biomass energy through pyrolysis to treat brackish groundwater on the small-scale in a multiple effect distillation (MED) unit. We designed, fabricated and conducted shakedown tests on a two-effect, lab-scale unit intended to produce 1 m³/day of distilled water under partial vacuum conditions (~200 kPa) and moderate temperatures (55-70°C). Hot water was used to supply heat and a vacuum pump provided pressure. Smooth, horizontal copper pipes and a falling film feedwater configuration were selected to maximize water evaporation while limiting scaling from precipitation of calcium carbonate and calcium sulfate—salts found in relatively high concentrations in brackish groundwater in New Mexico. While shakedown tests showed that the fabricated MED prototype is capable of producing high quality distilled water, insufficient preheating of the feedwater limited the length of time that the effects could stay warm enough to maintain feedwater evaporation. Identified targets for prototype improvement include unit fabrication materials and size, heat exchange, corrosion prevention, pump selection, vacuum maintenance, and incorporation of economic modeling data. Future research will focus on MED unit performance relative to water chemistry and scaling.</p> <p>Outcomes of this project include two manuscripts to be published as peer-reviewed journal articles, portions of two graduate student theses, three conference presentations, research capacity and expertise building in the Water-Energy Nexus for a junior faculty member, five follow-on grant proposals, real-world case studies in water treatment for a chemical engineering heat transfer class, and a lab-scale unit that can be used for thermal water desalination and heat transfer research.</p>	
<p>15. SUBJECT TERMS</p>	

brackish water, thermal desalination, multiple effect distillation, scaling, solubility, partial vacuum conditions, proof-of-concept prototype, water chemistry

16. SECURITY CLASSIFICATION OF:			17. LIMITATION OF ABSTRACT	18. NUMBER OF PAGES	19a. NAME OF RESPONSIBLE PERSON
a. REPORT	b. ABSTRACT	a. THIS PAGE			19b. TELEPHONE NUMBER <i>(Include area code)</i>

Standard Form 298 (Rev. 8/98)

Prescribed by ANSI Std. Z39.18

Construction of MED Component of Pyrolyzer-Desalination Unit for Resiliency Testing

by

Catherine E. Brewer

MISSION STATEMENTS

The mission of the Department of the Interior is to protect and provide access to our Nation's natural and cultural heritage and honor our trust responsibilities to Indian tribes and our commitments to island communities.

The mission of the Bureau of Reclamation is to manage, develop, and protect water and related

Disclaimer

The views, analysis, recommendations, and conclusions in this report are those of the authors and do not represent official or unofficial policies or opinions of the United States Government, and the United States takes no position with

regard to any findings, conclusions, or recommendations made. As such, mention of trade names or commercial products does not constitute their endorsement by the United States Government.

Acknowledgements

Funding for this research was provided by a supplemental extension to a Tier 1 Proof of Concept Grant through the New Mexico State University Institute for Energy and the Environment as part of a cooperative agreement with the Desalination and Water Purification Research and Development Program, U.S. Bureau of Reclamation.

The authors would like to acknowledge the NMSU Manufacturing Engineering & Technology Center for their assistance with designing, fabricating and testing the lab-scale MED unit, Mr. Brent Carrillo and Mr. Willian Do Prado for their assistance with the MED testing, and the staff of the NMSU Department of Chemical & Materials Engineering for their support.

Contents

Page

Acknowledgements	iii
Contents.....	v
Glossary	vii
Executive Summary.....	1
1. Introduction.....	3
1.1 Motivation.....	3
1.2 Design Project.....	4
1.2.1 Project Objectives	4
1.2.2 Project Tasks	4
1.2.3 Project Deliverables	5
1.3 Organization of Report	5
1.4 Conclusions and Recommendations	6
2. Resiliency in Thermal Water Desalination	7
2.1 Thermal Desalination Technologies	7
2.2 Scaling and Fouling.....	9
2.3 Brackish Water Chemistry in New Mexico	10
2.4 Design Considerations to Prevent Scaling.....	12
3. Biomass Pyrolysis for Small-Scale Water Desalination	14
3.1 System Components and Parameters.....	14
3.2 Furnace and Boiler	16
3.2.1 VOC Combustion Methods	16
3.2.2 Steam or Hot Water	21
3.3 Supplying Vacuum	22
3.4 Feedwater Preheating	24
4. Design and Fabrication of Multiple Effect Distillation Lab Unit.....	26
4.1 Horizontal Tubes and Falling Film	26
4.2 Fabrication Considerations.....	27
4.3 Material and Parts Selection.....	30
4.4 Monitoring and Data Collection	31
4.5 Shakedown Trials and Safety Review	32
4.5.1 Vertical Unit Orientation and Pump Pressure Head	33
4.5.2 Water Vapor and Vacuum Pump	34
4.5.3 Polycarbonate Sheeting and Vacuum Pressure....	34
4.5.4 Preheating Feedwater.....	35

4.6 Future Unit Improvements	35
5. Water Testing	39
5.1 Negative Control Benchmark.....	39
5.2 Positive Control Benchmark	42
5.3 Future Work	42
6. Project Outcomes	44
6.1 Research Capacity Building	44
6.2 Theses, Publications, and Presentations.....	44
6.3 Follow-On Proposals	45
6.4 Other Products	46
Reference List	48
Appendix	51
Surface Area Calculations for Heat Exchangers.....	51

Glossary

AWWA	American Water Works Association
BGNDRF	Brackish Groundwater National Desalination Research Facility
EC	electrical conductivity
IEE	Institutue for Energy & the Environment
MED	multiple effect distillation
MSF	multiple stage flash
NMSU	New Mexico State University
NPSH	net positive suction head
PFPE	perfluoropoly ether
TDS	total dissolved solids
TOC	total organic carbon
VC	vapor compression
VOC	volatile organic carbon(s)

Executive Summary

Communities located in rural, arid areas face the challenge of finding local and affordable energy supplies to operate water desalination equipment. A renewable distributed energy source that has great potential for water desalination is biomass: agricultural wastes, forestry residues, residential yard waste, byproducts from biofuels production, etc.

Pyrolysis, a process that transforms biomass through heating under limited-oxygen conditions, can be used to produce char, bio-oil, and non-condensable gas products. The liquid and gas products can be combusted to drive the pyrolysis process, and to provide heat and power to a desalination process. The char product can be applied to soils as biochar to improve soil quality and soil water holding capacity.

This project represents the second stage in a proof-of-concept study for a biomass slow pyrolysis system that could be coupled to a multiple effect distillation (MED) unit for the small-scale desalination of brackish water. Information learned from the first stage of the study was used to design, build, and test a laboratory-scale MED unit prototype that could be used for water chemistry research. The unit contains two effects and one condenser, and was designed to produce approximately 1 m³/day of distilled water. Hot water (80°C) was used to provide the heat energy and a vacuum pump to maintain the system pressure at around 200 kPa (~1/5th atmospheric pressure) to enable feedwater to evaporate at temperatures around 60°C. These conditions were selected to help prevent scaling on heat transfer surfaces caused by the low solubility of salts commonly found in brackish groundwater, namely CaCO₃ and CaSO₄. Smooth copper tubes in a horizontal orientation were used for the primary heat transfer surfaces with feedwater applied as a spray to create a falling film; these design parameters were chosen due to their tendency to enhance heat transfer rates and prevent scaling. Sensors were installed at select locations on the unit to enable calculations of heat transfer coefficients and identify effects of scaling.

After the initial design and fabrication process, a series of shakedown trials on desalination of a model feedwater helped assess base design performance and identify prototype improvements. Among the identified improvements are increased preheating of feedwater to maintain system temperatures for sustained operation, modified unit size for easier fabrication and handling, pump selection, and increased resistance to corrosion. Follow-on work will continue the performance benchmarking process and track performance changes as functions of water chemistry, as well as incorporate economic process modeling.

Outcomes of this project include two manuscripts to be published as peer-reviewed journal articles, portions of two graduate student theses, three conference presentations, research capacity and expertise building in the Water-Energy Nexus for a junior faculty member and a PhD student, five follow-on grant proposals, real-world case studies in water treatment for a chemical engineering heat transfer class, and a lab-scale MED unit that can be used for thermal water desalination and heat transfer research.

1. Introduction

1.1 Motivation

Water for agricultural use has become expensive and difficult to obtain in New Mexico and other southwestern states due primarily to an on-going drought. Well water used for irrigation can frequently be brackish and can result in the accumulation of salt in irrigated soils. Soil salinity can result in lower crop yields due to plant salt stress. Treatment of soil salinity often requires flushing the soil with fresh water to transport salts below the root zone. Use of brackish well water to meet temporary water needs can lead to the need for even more fresh water in the long term to maintain crop yield.

Desalination of brackish groundwater is one way to obtain fresh water for irrigation from available water sources. However, desalination requires energy. In rural locations, electricity from a grid, or electricity generation using solid or liquid fuels, is often unavailable or prohibitively expensive at the necessary scale. Some desalination systems are designed to use what farmers have available on or near their farms: sunlight, wind, and geothermal energy. Such systems have been employed with some success, although per unit costs remain high and energy storage can be difficult.

One resource that farmers have available but that has not been much explored for desalination is biomass in the form of agricultural residues and yard waste. In a previous project, we studied water desalination technologies that might be paired with biomass pyrolysis to produce biochar and thermal energy for fresh water. We found that low-temperature multiple effect distillation (MED) was promising for the small scale because of its reuse of the heat of vaporization and the opportunity to use the heat resource available. We designed and simulated an interface that would use the output of biomass pyrolysis (bio-oil and non-condensable gases) to produce electricity and thermal energy in the form of low-temperature steam.

This project was the first step towards a prototype of the pyrolyzer-MED system. The primary goal of this project was to construct a laboratory-scale prototype of the MED and to compare that prototype's operation to the simulation. Laboratory scale (1-2 m³ produced water per day) was chosen to represent the small end of the applications for this system while still being large enough to identify real-world challenges.

A major challenge to consistent operation of thermal desalination systems is scaling and fouling, especially the formation of hard scale at elevated water temperatures. *A secondary goal of this project was to design an MED system that would be resilient to differing water chemistries and minimize scaling to increase system longevity.*

1.2 Design Project

1.2.1 Project Objectives

The objectives of this project were to:

- Build and operate a lab-scale multiple effect distillation unit to enable thermal water desalination research and future incorporation of biomass-based thermal energy.
- Evaluate ability of MED unit design to accommodate a wide variety of water chemistries and resist fouling.
- Develop faculty and graduate student expertise in thermal water desalination and water chemistry.

1.2.2 Project Tasks

The specific tasks undertaken in the project were:

1. Design and source/fabricate boiler/heater to supply steam/hot water for lab-scale MED unit.
2. Fabricate and assemble lab-scale MED unit with associated equipment (pumps, boiler, monitoring) and plumbing.
3. Perform MED unit shakedown trials.
4. Use MED unit to desalinate water with a range of chemistries to evaluate energy requirements and resiliency to fouling.
5. Build water chemistry and desalination expertise through conference attendance, on-campus networking, and literature review.

6. Evaluate MED unit energy efficiency and fouling resistance in relation to potential implemental scenarios.
7. Prepare final report and external proposals to fund construction of pyrolyzer and interface, and follow-on fouling resistance and energy efficiency research.

1.2.3 Project Deliverables

The deliverables of this project are:

- a. Fabrication designs and part lists for lab-scale MED unit.
- b. Working MED unit installed in the laboratory and available for research projects.
- c. Results from shakedown trials and water treatment experiments.
- d. Final project report.
- e. Proposals submitted to external funding agencies.

1.3 Organization of Report

This chapter is intended to provide context for the project and to summarize the take-away messages from the project results.

The second chapter presents a literature review of relevant thermal desalination technologies and the challenges of scaling. Sections of the chapter were selected from a review article manuscript prepared by the PhD student. Also included is background information about local water chemistry that influenced the design of water treatment experiments. This text will serve as part of the literature review and introduction for Mr. Ali Amiri's PhD dissertation.

The third chapter describes the pyrolysis-MED interface design on which this project is based and the considerations leading to decisions made for how to supply heat and vacuum for the lab MED unit. This work was part of Mr. Yunhe Zhang's MS thesis.

The fourth chapter describes the design, fabrication and shakedown process for the MED unit in the laboratory. This will serve as a methods chapter in Mr. Ali Amiri's PhD dissertation.

The fifth chapter presents the methods of water treatment experiments for the laboratory MED unit to benchmark energy use, water production efficiency, and occurrences of scaling. This will serve as another chapter in Mr. Ali Amiri's PhD dissertation.

The final chapter summarizes the outcomes from the project.

1.4 Conclusions and Recommendations

Although it requires more overall energy than membrane water treatment methods, thermal water desalination methods, especially multiple effect distillation, provide the opportunity to produce high purity distilled water using available low-temperature heat sources. These sources can include heat from biomass thermochemical processing, solar heat, geothermal heat, and industrial waste heat. The water chemistry of brackish groundwater creates challenges for thermal water desalination due to the low solubility of certain calcium and magnesium salts, namely carbonates and sulfates, at increasing temperatures. Carefully controlling the temperature of every heat transfer surface and conducting the feedwater evaporation process under partial vacuum can prevent scaling; these two strategies require special considerations for MED unit construction. The lab-scale, first prototype of such a unit showed that distilled water of the desired quality can be produced, as long as the heat transfer into and within the unit are properly controlled. Further prototype development is needed to increase feedwater preheating capabilities, reduce corrosion, enhance evaporation heat transfer, simplify unit construction, and ensure reliable vacuum operation. Water chemistry testing in relation to MED operation performance, combined with economic modeling, can guide the unit development process to achieve robust and economically feasible thermal desalination of brackish groundwater at the small scale.

2. Resiliency in Thermal Water Desalination

2.1 Thermal Desalination Technologies

There are three main types of thermal desalination processes: multi-stage flash distillation (MSF), vapor compression distillation (VC), and multiple effect distillation (MED). All three require low-temperature heat as the main energy input and a small amount of electricity to drive pumps. Some advantages of thermal desalination processes over membrane desalination processes are higher quality product water, no membrane replacement costs, lower sensitivity to changes in feed water quality, and less rigid monitoring requirements (Eltawil, et al., 2009, Hanson, et al., 2004, Kalogirou, 1997).

MSF was first developed by Silver at Weir Co. in Glasgow, Scotland in 1960 and is based on seawater evaporation using steam from an external heat source. For many years, MSF has been the “easiest” technology for water desalination and accounts for over 40% of desalination technologies worldwide (Al-Karaghoul and Kazmerski, 2013, Likhachev and Li, 2013). The typical capacity for an MSF process is large: 10,000 to 35,000 m³/day. In MSF, water is preheated using heat exchangers up to 90-110°C before entering the first stage. Vacuum pumps create a negative pressure difference near water’s saturation point in the first stage, causing the water to partially flash. The flashed water vapor is condensed by contact with incoming feedwater in the heat exchangers and collected. The remaining brine enters the second stage, which is operated at a lower pressure than the first stage. Again, the negative pressure difference causes some of the water to flash off and be collected. This process continues until the last stage, which has the lowest temperature and pressure.

VC is very similar to MSF but only has one evaporation stage and can be run under atmospheric or sub-atmospheric pressure. Hot, pressurized feed water enters the evaporation stage and flashes off, then is condensed and collected. The remaining brine can then be recycled through the process by

re-pressurizing it. Pressurization can be done using mechanical vapor compression, which requires additional electricity energy for the pump, or thermal vapor compression, in which high-pressure steam is injected into the feed stream (Al-Karaghoul and Kazmerski, 2013, Semiat and Hasson, 2012).

Multiple effect distillation (MED) or multiple effect boiling is similar to MSF in that multiple units are operated at gradually decreasing temperatures and pressures. The difference is that steam from the first effect is used as the heat source in the second effect in MED; this means that the heat of vaporization is reused. In MED, steam enters through a pipe into the first stage or effect. Feed water is sprayed onto this hot pipe. Since the effect environment is kept under partial vacuum, some of the feed water flashes into vapor, leaving behind a concentrated brine solution. The flashed water vapor is carried into a pipe and into the next effect, which is at a lower temperature and pressure than the first effect. The freshly formed vapor provides the heat for the vaporization of more feed water within the second effect. This cycle continues and results in desalinated water and brine. MED is the oldest thermal desalination process and often has a plant capacity of 600 to 300,000 m³/day (Kalogirou, 2005). A typical MED unit operates at 55-90°C, and requires 135-230 MJ and 5-9 MJ (1.5-2.5 kWh) of thermal and electrical energy, respectively, per cubic meter of feed water (Al-Karaghoul and Kazmerski, 2013). MED has been in competition with MSF technically and economically for many years. At the end of 2011, MSF and MED units accounted for approximately 26% and 8.2% of worldwide water production capacity, respectively (2012). Two main advantages of MED over MSF are MED's lower energy consumption due to better heat transfer from the constant temperature difference in MED effects, and the fewer number of effects needed in MED to achieve a given performance ratio (mass of distillate produced per unit mass of input steam) (Al-Karaghoul and Kazmerski, 2013, Kalogirou, 2005).

2.2 Scaling and Fouling

There are different types of scale deposits including soft, hard, silica, organic and bio-fouling. Soft scale is the precipitation of inorganic compounds due to their concentrations exceeding their solubility. They are called soft because they can be removed relatively easily through increases in temperature and/or decreasing the pH by adding acid. An example of soft scale is calcium bicarbonate. Hard scale forms by precipitation like soft scale but is much more difficult to remove and often requires mechanical cleaning. Hard scale is usually composed of divalent alkaline cations and sulfates or chlorides. An example of hard scale is calcium sulfate. Organic matter build-up may be due to marine life (i.e. bio-fouling) or from industrial discharges such as crude oil, greases, waxes and paint materials. A hot alkaline treatment can usually remove organic scale.

Scale formation can be especially damaging for heat transfer surfaces because scale build-up has a low thermal conductivity, which slows conduction and decreases thermal efficiency. Slower conduction increases heat transfer plate or tube wall temperatures and these prolonged higher temperatures can lead to corrosion and/or crack formation (Al-Jaroudi, et al., 2010). For this reason, prevention and treatment of scaling is critical to heat exchanger maintenance.

Scale formation within the effects of MED units is dependent on the feedwater concentrations of Ca^{2+} , Mg^{2+} , and bicarbonate ions, the feedwater total dissolved solids (TDS) concentration, MED operating temperature, water residence time, fluid velocity, water pH, rate of CO_2 release, and roughness of evaporator materials (Al-Anezi and Hilal, 2007, Al-Jaroudi, et al., 2010). In research conducted with a MED-vapor compression (VC) unit, Al-Jaroudi, et al. observed a 14 mm-thick scale build-up comprised of soft CaCO_3 and hard CaSO_4 , which are major scaling contributors, as well as a significant proportion of organic matter (Al-Jaroudi, et al., 2010). These build-ups greatly inhibited evaporator function. $\text{Mg}(\text{OH})_2$ is another alkaline scale that is sometimes observed

in MSF or MED systems due to Mg^{2+} ions in the water. Non-condensable gases such as CO_2 , O_2 , and N_2 released during brine evaporation within the effects or ambient air leakage into the evaporator, may cause alkaline scale formation. For example, dissolved CO_2 in the condensate decreases the water pH to acidic conditions such that, with O_2 , the condenser tubes are subject to corrosion. The release rate of CO_2 is highest in the first effect, and increases with higher water temperatures and salinities (Al-Anezi and Hilal, 2007). This causes $CaCO_3$ deposition to be highest in the first effect while the pH decreases from the first effect to the last effect (Al-Rawajfeh, 2010). Even a low concentration of non-condensable gases within the water can significantly decrease the overall heat transfer coefficient over time, leading to a decrease in evaporator performance (Al-Anezi and Hilal, 2007).

2.3 Brackish Water Chemistry in New Mexico

Groundwater available in New Mexico ranges from fresh to very brackish depending on the location, the aquifer depth, and the time of year. Water chemistry for this research was based on baseline data from water tests of the well water at the Brackish Groundwater National Desalination Research Facility (BGNDRF) in Alamogordo, NM. Water tests were conducted by Tetra Tech in 2011 and 2012, and the results presented in a 2013 report (Inc., 2013). A summary of relevant data is presented in Table 2.1.

Table 2.1 Water test results from 2011-2012 analyses of the four groundwater wells at the Brackish Groundwater National Desalination Research Facility (Inc., 2013). TDS: total dissolved solids; TOC: total organic carbon; HCO_3^- : bicarbonate; CO_3^{2-} : carbonate; SO_4^{2-} : sulfate; SiO_2 : silicon dioxide.

Component/Parameter	Well 1	Well 2	Well 3	Well 4
Temperature (°C)	32.0- 41.2	21.0- 22.5	19.9- 22.1	19.5- 21.3
pH	7.71- 8.16	7.25- 7.65	7.28- 7.67	7.22- 7.70

TDS (mg/L)	1,040- 1,710	5,320- 5,900	3,590- 4,380	3,970- 4,380
TOC (mg/L)	0-1.0	0.97- 1.30	0.56- 1.30	0.70- 0.83
Na (mg/L)	310- 340	640- 720	410- 530	420- 540
Ca (mg/L)	48-89	550	440- 450	490- 530
Mg (mg/L)	11-22	320- 340	220- 250	220- 240
K (mg/L)	4.6- 5.4	2.6- 4.0	2.9- 3.4	2.6- 3.4
SiO ₂ (mg/L)	24-26	23-24	21-22	19
SO ₄ (mg/L)	580- 990	3,000- 3,800	1,800- 2,500	1,900- 2,600
Cl (mg/L)	33-35	580- 650	620- 690	620- 680
HCO ₃ ⁻ (mg/L CaCO ₃)	130- 160	240- 250	190- 210	210
CO ₃ ²⁻ (mg/L CaCO ₃)	0	0	0	0

Brackish groundwater at BGNDRF can be characterized as mildly alkaline (pH of 7-8), low (Well 1) to high salinity (Wells 2-4) for brackish water, with relatively little organic carbon or silica compounds. Most of the ions are sodium, calcium, magnesium, sulfate, chloride and bicarbonate, which implies a substantial risk of producing hard scale (mostly calcium sulfate) during thermal desalination. Relative to drinking water standards, Wells 2-4 contain too much chloride and sulfate, and all wells would require desalination to a TDS concentration below 500 mg/L (Inc., 2013). As can be seen from the data, which represents four different sampling times over the course of a year, the water chemistry is quite variable. This means that desalination systems would need to be robust enough to accommodate the changes with time while still producing water with the desired quality.

2.4 Design Considerations to Prevent Scaling

There are several management options for preventing and treating scale formation. Demisters (specially designed screens) are used to remove entrained brine droplets from the flashed vapor to prevent those droplets from adding salinity into the product water and contributing to scale formation on condenser tubes. Dissolved gases such as O_2 and N_2 can be removed through a suitable venting system such as the vacuum pump used to maintain effect pressure. CO_2 , which dissociates in water to form bicarbonate (HCO_3^-) and carbonate (CO_3^{2-}), is harder to manage through venting alone although efficient ventilation does help (Al-Rawajfeh, et al., 2004). Feedwater pretreatments, such as adding acid or scale inhibitors like polyphosphate, can be used. The hydrolysis of polyphosphate at high temperatures ($90^\circ C$), however, leads to the formation of calcium phosphate and means that polyphosphate is rarely used in ambient pressure MED units.

While soft scale is troublesome for MED units, hard scale, namely $CaSO_4$, is a major concern since hard scale requires unit disassembly and mechanical cleaning. Prevention is the preferred management for hard scale and can be done in three ways: decreasing the MED operating temperature (solubility is higher at lower temperatures), decreasing the concentration factor within the effect to keep the produced brine below the concentration scaling threshold, and softening the feedwater by substitution with a monovalent cation. Lowering the temperature means simultaneously decreasing the effect pressure, which requires the use of a (more powerful) vacuum pump. Decreasing the concentration factor means increasing the feedwater flow rate and thus increasing the amount of brine that must be collected or recycled. Softening the feedwater requires an additional unit operation and creates another waste water stream. Selection of one option or a combination of options is a critical design choice and must be weighed against system cost, complexity, down-time, and available labor. Even with several management techniques, there is still a chance of scaling in MED units (Al-Jaroudi, et al., 2010).

Tube orientation with the MED unit's effects can also impact the likelihood of scaling. Steam tubes within the effects can be oriented vertically or horizontally. Vertical tubes tend to have greater scaling and carryover since flashing water vapor has to pass through liquid feedwater/brine on the way to the next effect. The horizontal orientation is usually preferred in MED units since it lowers the frequency of this scaling and carryover, and increases the overall heat transfer coefficient, leading to higher MED system efficiency.

3. Biomass Pyrolysis for Small-Scale Water Desalination

3.1 System Components and Parameters

In a previous U.S. Bureau of Reclamation Desalination and Water Purification Research Program project, a biomass pyrolysis-MED unit interface was designed to model how local biomass residues might provide the energy needed to power an MED unit for desalination of brackish water at the farm or co-op scale. Briefly, that system consists of 12 unit operations in the following order:

1. Biomass is added to a *feed hopper*;
2. From the feed hopper, biomass enters the *auger slow pyrolysis unit* and is converted into chars, bio-oil (as vapors and aerosols) and non-condensable gases (NCG) through partial combustion of the biomass;
3. Chars are fed into a *char collection* container where some of the cooled flue gases are warmed before being recycled into the pyrolysis unit;
4. Bio-oil vapors, aerosols and NCG flow into a *furnace* where they are combusted with additional air to form carbon dioxide and water;
5. Heat from the combustion furnace heats water in a *boiler* to produce steam;
6. Steam from the boiler is fed through a *steam turbine* to produce electricity;
7. Low pressure, low temperature steam is fed into the *first effect of the MED unit* to provide process heat; condensed steam is recycled to the boiler or collected with the distillate;
8. Electricity from the turbine generator is used to power the *vacuum pump* and the *water pumps* (feed water, brine, and distillate) of the MED;
9. Brackish feedwater is preheated using the *condenser unit of the MED* then a *heat exchanger* connected to the warm flue gas stream exiting the combustion furnace;

10. Preheated feedwater is sprayed into the *effects* in a parallel feed arrangement, creating a falling film over horizontal heat transfer tubes and producing low-pressure steam that flows into the next effect;
11. Brine collected at the bottom of each effect is removed to *brine storage* or recycled into the *feedwater tank*;
12. Distilled water collected in the condenser is pumped through a valve into *fresh water storage*; the *valve* allows the diversion of the produced water into the feedwater if the electrical conductivity is too high.

More information about the system and interface design, and the process computer simulation, can be found in that final project report (Brewer and Idowu, 2015). Process flows, temperatures, pressures, and heat rates from the Aspen Plus® simulation are taken from that report and shown here as Figure 3.1.

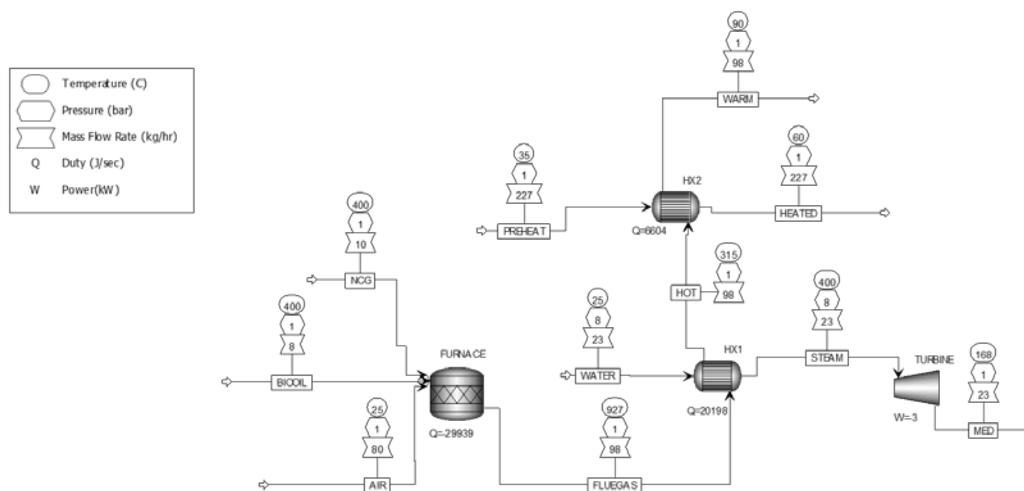


Figure 3.1 Aspen Plus® process flow diagram for pyrolyzer-MED interface showing stream temperatures, pressures, mass flow rates, heat duties and electrical power. HX1: heat exchanger 1, boiler; HX2: heat exchanger 2, preheater for the MED brackish feedwater; NCG: non-condensable gases; MED, multiple effect distillation unit (Brewer and Idowu, 2015).

Process needs identified with the Aspen Plus® simulations were used to specify parameters for the furnace/boiler and the vacuum for the design of the lab-scale MED unit such that the MED portion of the system prototype could be fabricated and tested. The remaining sections of this chapter detail the background information and design process going from the process simulation to equipment selection for the physical unit.

3.2 Furnace and Boiler

3.2.1 VOC Combustion Methods

Biomass thermochemical processes produce large amounts of volatile organic compounds (VOCs). Many such organic compounds are toxic and some have been classified as carcinogens, such as formaldehyde, vinyl chloride, benzene, and polycyclic aromatic hydrocarbons. If these compounds are emitted directly without treatment, the resultant pollution poses a risk to the environment and public health (Urashima and Chang, 2000). Thus, a system that produces VOCs must include VOC treatment in the material and energy management considerations. Traditional VOC treatment methods include combustion, freezing, absorption, and adsorption. Some treatment methods are described in Table 3.1. For this project, different combustion methods were considered for biomass pyrolysis VOC treatment and energy recovery.

Table 3.1 Example treatment methods for VOCs (Urashima and Chang, 2000).

Method	Mechanism	Optimal Usage	Advantages	Disadvantages
Thermal Combustion	VOCs are mixed with hot gases at high temperatures, resulting in complete combustion.	High concentration, low volume, combustible VOCs	Efficient Removes VOCs fully	Tar accumulation Consumes CH ₄ Polluting and costly if combustion is incomplete
Absorption in Water	VOCs are dissolved in water,	Point-source, water-soluble VOCs	Easy to operate and manage Low costs of operation	Water pollution Inefficient Aromatics require extra processing
Chemical Absorption	VOCs dissolve in and react with solvents, producing harmless compounds.	High concentration, high volume VOCs	Customizable Mature technology	Inefficient Consumes solvent Incomplete reactions result in secondary pollution

Adsorption	VOCs are bound, adsorbed into a solid material.	Low concentration VOCs; when very high purity is required.	Very high efficiency Can treat many types of VOCs	Adsorbents are expensive and not easily reusable Cannot treat high concentration or high temperature VOCs
------------	---	--	--	--

Also known as direct spark combustion, direct combustion uses combustible VOCs as the fuel in a combustion reaction. Direct combustion is best suited for VOCs that contain combustible compounds and/or compounds that are strongly exothermic upon oxidation as this will best sustain the combustion reaction (Kim, et al., 2005). Direct combustion can be performed in a regular stove, kiln, or torch. At temperatures in excess of 1100°C, direct combustion fully breaks down VOCs into carbon dioxide and water vapor. Direct combustion is generally simple to operate and inexpensive. Torches are a type of open direct combustion device that can burn in air and do not require an initial input of natural gas. Torches often rise dozens of meters into the air and are many factories' main method for processing combustible VOCs. Torches can be designed to separate emissions by type and can incorporate ordinary (fuel-based) or electrical combustion devices to ensure safer, more stable, and reliable combustion processes (Hewitt, 1971). The advantages of direct combustion are:

- 1) No pre-heating of the combustion chamber or gases is needed.
- 2) Combustion occurs at high temperatures with minimal flame, which makes the heat recyclable.
- 3) Systems can handle high concentration and/or high temperature VOC streams.

Thermal combustion is used when there are not enough combustibles to sustain a direct combustion reaction. Thermal combustion relies on the heat produced by secondary fuels to raise the flame/chamber temperature to expedite the oxidation of hydrocarbons into carbon dioxide and water. Thermal combustion can be broken down into three steps (Cao, 2012):

- 1) Combustion of supplementary fuel to increase the temperature.
- 2) Mixing of VOCs with heated secondary fuel combustion gases to reach the reaction temperature.
- 3) Oxidation of VOC combustibles where the reactants are burned at the designated temperature for a specified amount of time.

A thermal combustion oven is composed of the supplementary combustion chamber to produce the desired temperature by burning supplementary fuel and the main combustion chamber used to mix the heated gases with VOCs for oxidation. Assuming sufficient oxygen, the primary combustion reaction is governed by temperature (usually $\sim 760^{\circ}\text{C}$), time (usually ~ 0.5 s), and turbulence. Within a certain range, these three governing parameters are synergistic: increasing one parameter usually decreases the minimum requirements for the other two. Increasing temperature increases fuel consumption and increasing reaction time requires a larger combustion oven, so the most economical approach is usually to increase flow turbulence. The relationship between reaction time and combustion oven size is:

$$\tau = \frac{V_R}{Q_s \left(\frac{T}{293}\right)} \times 3600$$

where, τ is the residence time in the chamber in seconds, V_R is the volume of the chamber in m^3 , Q_s is the total volumetric flow rate in m^3/hr . at standard conditions, 3600 is the conversion factor from hours to seconds, and T is the temperature of the chamber in degrees K. Table 3.2 lists the theoretical reaction times and temperatures of various types of

VOCs. In practice, if steam or black smoke is emitted, additional reaction time is needed.

Table 3.2. Required temperatures and reaction times for treatment of various types of VOCs (Tong, 2001).

Off-Gas Description	Combustion efficiency (%)	Residence time (s)	Reaction temperature (°C)
Hydrocarbons	>90	0.3-0.5	590-680
Hydrocarbons + CO	>90	0.3-0.5	680-820
VOCs	50-90	0.3-0.5	540-650
	90-99	0.3-0.5	590-700
	>99	0.3-0.5	650-820
White smoke	>90	0.3-0.5	680-820
Black smoke (particulate)	100	0.7-1	760-1100

Catalytic combustion uses catalyst to oxidize gaseous pollutants at relatively low temperatures (250-450°C) (Cai, et al., 2008). Catalytic combustion requires a solid catalyst reaction bed and a heat exchanger. Influx gases cross the pre-heated catalyst bed and both oxygen and hydrocarbon molecules adsorb to the catalyst surface. Once both molecules are present on the catalyst surface, oxygen can directly react with the hydrocarbons. The advantages of catalytic combustion are:

- 1) Reaction temperature is low compared to direct combustion (600-800°C).
- 2) Reaction has low resource consumption; it is possible for the reaction to sustain itself once the reaction temperature is reached, allowing recycling of the excess energy produced (Kim, et al., 2005).
- 3) Catalytic conversions can treat nearly any hydrocarbon or VOC feedstock from many industries (electronics, organics, oil and gas, etc.)
- 4) Reactions produce virtually no secondary pollution.

For biomass pyrolysis operated under continuous flow conditions, direct combustion of the vapors and non-condensable gases (NCG) is possible and desirable as long as the concentration and heating value of the combustible compounds remain high enough. Reactor start-up will likely require addition of supplementary fuel to bring the furnace up to temperature until the pyrolysis process off-gases can maintain the flame. Direct combustion is unlikely to be suitable for batch pyrolysis reaction systems since the flow, concentration, and composition of VOCs in the vapors and NCGs are variable. While catalytic conversion is suitable for VOC treatment, the goal of this project was to produce flue gas at high temperatures ($>900^{\circ}\text{C}$) for steam at high temperature and pressures (400°C and 8 bar), so catalytic combustion was not considered.

3.2.2 Steam or Hot Water

The two primary inputs into an MED unit are the feedwater and a heat carrier at the desired feedwater vaporization temperature. That heat carrier is usually steam or liquid water for simplicity, safety and water's high heat capacity and high latent heat of vaporization. The feedwater vaporization temperature, i.e. the operating temperature in each effect, is determined by the vapor-liquid equilibrium of the feedwater. The higher the temperature, the higher the vapor pressure. Once the vapor pressure exceeds the ambient pressure, the water freely boils as long as sufficient heat for the phase change is continuously supplied. Water chemistry and TDS impacts the feedwater's vapor pressure; in general, the higher the TDS, the lower the vapor pressure and the more elevated the boiling point.

To prevent formation of hard scale in MED, the effects must be kept at as low a temperature as possible. Lowering the temperature, however, creates a trade off in that lower pressure would also now be required. For example, Table 3.3 shows a comparison of the vapor pressures heats of vaporization for pure water at various temperatures. The heat of vaporization also increases as temperature decreases. For low-temperature MED of brackish water containing CaSO_4

and CaCO_3 , this means that all heat transfer surfaces must be kept at temperatures below approximately 80°C , the whole system must be at pressures between one half and one tenth of atmospheric pressure, and more heat must be transferred to maintain vaporization. These three factors are the principle challenge for low-temperature MED design.

Table 3.3 Properties of water at temperatures between room temperature and its atmospheric-pressure boiling point (CRC, 2003).

Temperature ($^\circ\text{C}$)	Vapor pressure (kPa)	Heat of vaporization (kJ/mol)
25	3.2	44.0
50	12.3	
60	19.9	42.5
70	31.2	
80	47.4	41.6
100	101.3	40.7

While steam can be used as the primary heat transfer fluid in low-temperature MED, i.e. the heat transfer fluid used to boil water in the first effect, controlling the temperature of the steam is difficult because the pressures must be below atmospheric pressure. In this case, hot water may be as a better primary heat transfer fluid as it can be used at atmospheric pressure. Using water, however, means that all heat transfer happens as sensible heat instead of getting both sensible heat and latent heat of vaporization from the heat transfer fluid. As a result, higher flow rates and/or greater heat transfer surface areas would be needed. (Low pressure steam as the heat transfer medium for the later effects is not a problem because this steam is produced at the needed pressure and temperature in the first effect.)

3.3 Supplying Vacuum

There are two general methods for providing vacuum: through a vacuum pump or through a gas ejector. In a pump, gas is moved mechanically through sealed chambers using

differences in pressures. There are many configurations and types of pumps; choice of pumps is dependent on the level of vacuum needed, the system volume, the gas removal rate, properties of the gas, cost, etc. Fluid ejectors, most typically steam ejectors, use Bernoulli's principle to provide vacuum. Motive fluid enters a nozzle-shaped compression tube, which increases the motive fluid's velocity. When the high-speed (low pressure) motive fluid exits the compression tube into the larger mixing tube, suction is generated. A schematic of a fluid ejector is shown in Figure 3.1. Fluid ejectors have no moving parts and thus require no power and little maintenance.

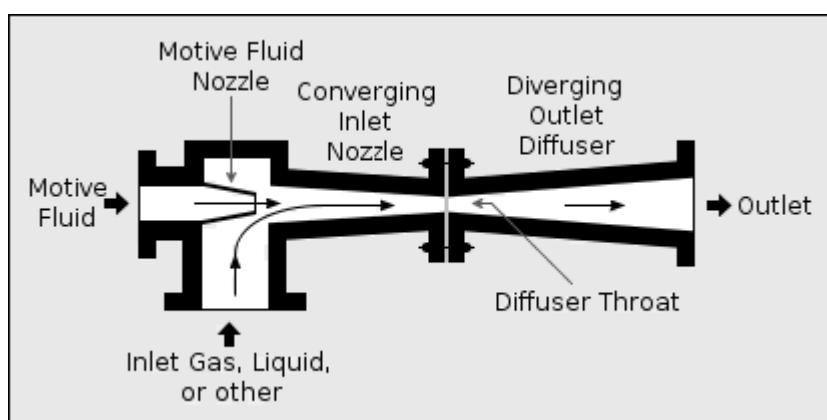


Figure 3.1 Schematic diagram of a fluid ejector (image: Milton Beychock, 2012, public domain).

For MED units, steam ejectors would use motive steam from a boiler to provide vacuum for the effects and to remove non-condensable gases. A heat exchanger at the steam ejector outlet could be used to condense the motive steam and return it to the boiler for reuse, as long as there was a way to vent the non-condensable gases. If the steam can be brought to a low-enough temperature using a de-superheater after the steam ejector, this steam might even be used as the primary heat transfer fluid in the first effect.

As with any unit operation, market availability plays a key role in design feasibility. For this project, the target effect temperature to prevent scale was 60-70°C, which would require a vacuum system to maintain pressures around 20 kPa or 1/5th of atmospheric pressure. The smallest steam

ejector available on the market for this pressure and effect volume required 265 kg/hr. of motive steam and would require significant de-superheating. As such, the flow rate and cost (approximately \$18,000) of a steam ejector system were too great to be practical at the laboratory scale. At a slightly larger scale, such as farm or co-op scale, a fluid ejector system may be more practical and should be considered over a vacuum pump to lower system maintenance and electrical requirements.

3.4 Feedwater Preheating

Multiple effect distillation requires several heat exchange steps. Feedwater must be warmed to vaporization temperature, boiled, and then cooled after vaporization. In low-temperature MED, the use of sub-atmospheric pressure for the vaporization step means that at least some volume of the unit must be kept under vacuum. Energy conservation and manufacturing principles dictate that the volume under vacuum should be minimized. This can be done by preheating the feedwater as much as possible prior to its entrance into the sub-atmospheric section of the unit. In practical terms, this means using the low pressure region only for the vaporization step of the distillation and doing the sensible heat increase elsewhere.

Preheating feedwater can occur in several places in the MED and is a major consideration when choosing an MED flow configuration such as forward flow, backward flow, parallel flow, etc. (Darwish and Abdulrahim, 2008). Near all MED units have a condenser unit where the coldest feedwater is used to condense the steam produced in the last effect. After the condenser, regenerative preheaters can be used to remove some heat from generated vapor to warm feedwater between effects. If other waste heat is available nearby, heat exchangers can be used to further warm the feedwater. In all case, heat losses should be minimized through insulation, material selection, and other strategies as heat losses directly impact an MED units gain output ratio (GOR), i.e. how many times the heat of vaporization can be recycled to treat more

water. GOR is a measure of MED efficiency and is generally the factor used for unit optimization.

4. Design and Fabrication of Multiple Effect Distillation Lab Unit

A two stage laboratory-scale multi effect distillation (MED) unit was designed and fabricated to be used for desalination of brackish water. The intention of the lab unit is to assist with design of future units at the application scale (farm or co-op) and to enable research on the impacts of brackish water chemistry on scaling at different thermal desalination operating conditions. The design was based on using 80 kg/hr. of brackish feedwater to produce about 20 kg/hr. of fresh water in two effects. From preliminary design work, hot water was selected as the primary heat transfer fluid and a vacuum pump was selected to provide system pressure. The main components of the system include: a heater and pump to provide the heat transfer water, two evaporator effects, a condenser, a vacuum pump, brine and distillate pumps, a feedwater pump, and assorted liquid storage and plumbing parts. The effects and condenser were set to operate 63.5, 60, and 59°C, respectively, at steam saturation conditions, which represents an absolute pressure of approximately 26 kPa.

4.1 Horizontal Tubes and Falling Film

The MED system design started from the second effect heat exchange surfaces as this would be the portion of the unit replicated to create more effects and would dictate unit size and flow requirements. Among the various heat tube and fluid flow configurations available, horizontal steam tubes with falling water film were selected due to their greater rates of heat transfer per surface area and their lower incidence of scaling (Darwish and Abdulrahim, 2008). Falling water film would be achieved by spraying feedwater over the pipes arranged to be directly over the top of each other with a space in between to optimize fluid flow and heat exchange. The number and size of the tubes was selected based on calculations of the needed heat transfer surface area from the estimation of overall heat transfer coefficients and the expected change in temperature within the effect (Incropera, et al., 2007). To ensure even heat transfer and less tube

bending/joining, a manifold system was selected to distribute steam evenly between all the steam tubes rather than to have the steam travel in a winding path.

Once the flow rate and temperature for the steam in the second effect were determined, the heat transfer area and flow rates for the first effect were calculated also assuming a horizontal tube arrangement and a falling liquid film. For the hot water, however, a single, serpentine tube was used to carry the water in a continuous loop rather than splitting the water flow with a manifold.

The condenser was designed next, this time with the feedwater being the fluid inside the horizontal tubes rather than the steam. Steam from the second effect would enter at the top of the unit and condense as it contacted the cool tubes.

After many iterations and optimization, the calculated surface areas for the first effect, second effect and condenser were 0.45 m², 0.44 m² and 0.126 m², respectively. Sample calculations are shown in the Appendix. Tubing diameter (2.54 cm) was selected to balance number of tubes, lengths of tubes, and heat transfer fluid dynamics of the steam and water flows.

4.2 Fabrication Considerations

After the heat transfer surface area calculations, the rest of the unit design proceeded under the following considerations:

- Space and fabrication equipment limitations within the NMSU Manufacturing Engineering & Technology Center (MTEC) machine shop,
- Number and complexity of fabrication steps,
- Number of unit components available commercially compared to number of unit components that have to be special ordered or fabricated,
- Ability to visually observe and instrumentally monitor heat transfer process for teaching and research purposes,

- Ease of unit assembly and disassembly for modification and cleaning,
- Ease of unit operation in terms of number of operators and level of operator involvement, and,
- Ability to stay within fabrication budget for parts and labor, and within fabrication schedule in the case of backordered and custom parts.

Fabrication drawings were developed using CAD software and as many hardware components as possible were found from commercial vendors; the drawing process was repeated as parts were identified and additional component capability information became available.

While rounded and single part components are generally best for pressure systems, rectangles using welded or fastened flat sheets are far easier to fabricate. For this reason, the MED units were designed as tall, rectangular boxes with attached feet so that they could be placed on a floor or other surface. Dimensions were determined based on the needed space for water to be sprayed and to flow over the pipes, saving room at the bottom for water to collect and be drained. Figures 4.1 and 4.2 show a 2-D dimensional fabrication cross section of the effects and condenser, and a 3-D rendering, respectively.

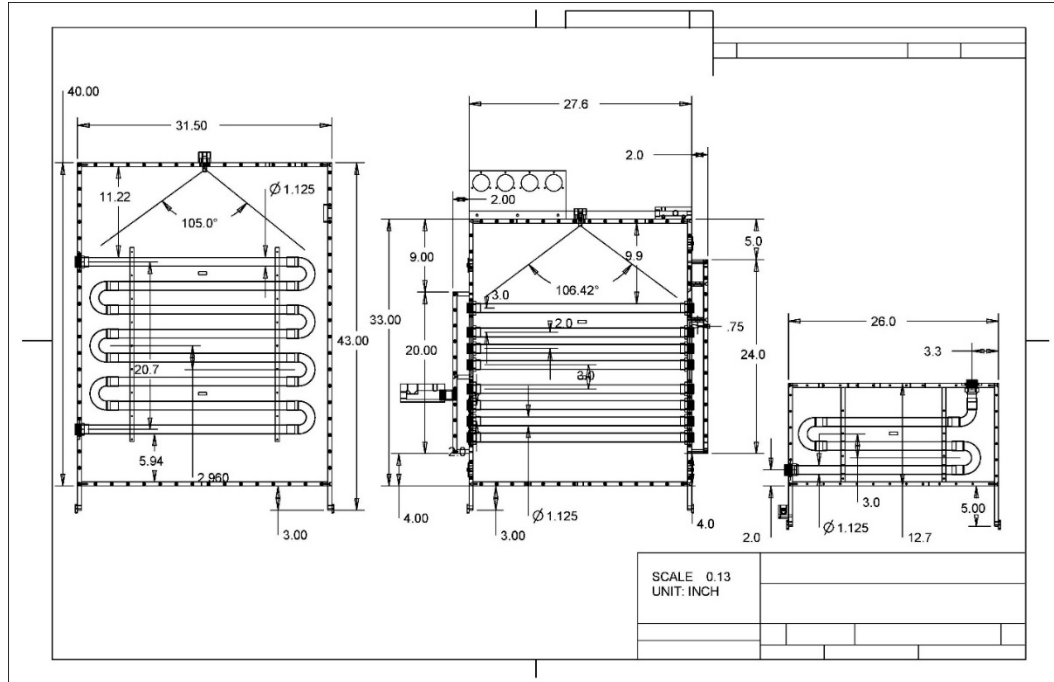


Figure 4.1 Two dimensional fabrication drawing of the first and second effects, and the condenser of the designed lab-scale MED unit. Measurements are shown in inches.

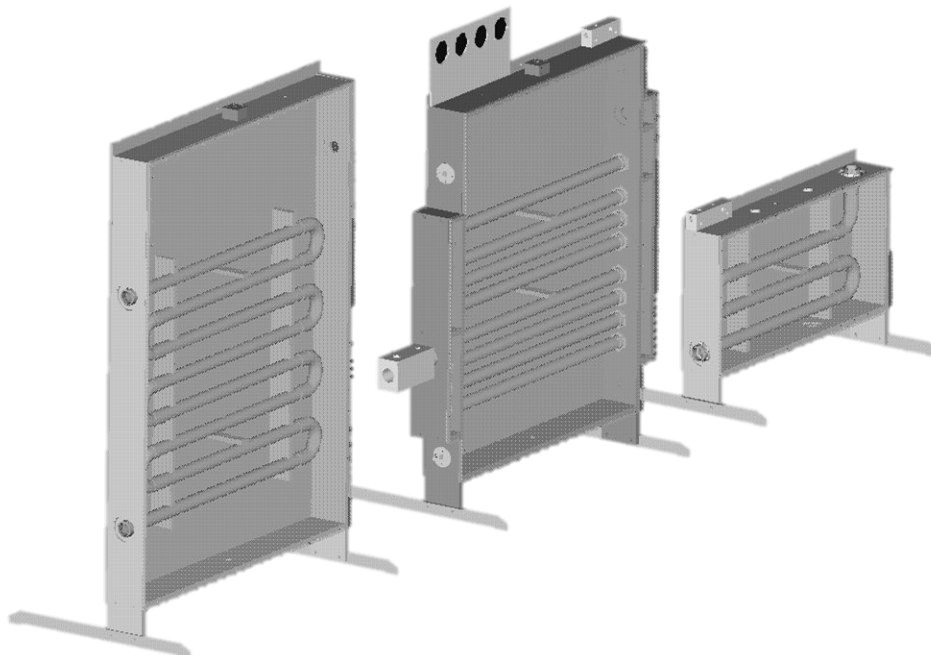


Figure 4.2 Three dimensional rendering of lab-scale MED unit using SOLIDWORKS CAD design software showing copper

heat exchange tubing, box configuration, locations for instrumental monitoring, and stands.

4.3 Material and Parts Selection

Copper was selected as the tubing material for the effects due to its very high thermal conductivity and reasonable resistance to corrosion and biological fouling. The raw materials were available commercially at the required sizes as straight tubes and 180° bends of copper coil. The coil and straight tubes were soldered together.

The effect and condenser boxes were constructed out of aluminum sheet and bar stock, which enabled easier machining in-house. The sides and back of the boxes were welded together while a sheet of polycarbonate was used for the front cover. The polycarbonate enabled direct visual observation of the insides of the effects and provided relative thermal insulation. A multi-purpose, high-strength Aramid/Buna-N gasket between the aluminum frame and the polycarbonate provided sealing at the front; screws provided the closure. Due to the size limits of MTEC equipment, the larger aluminum sheets and polycarbonate had to be cut with a water jet to size elsewhere. Again, the raw materials were purchased directly, mostly from McMaster-Carr (Elmhurst, Illinois).

For ease of assembly, most plumbing was constructed using NPT piping and fittings. Hydraulic hose that could withstand the pressure differences were used between the effects. Special vacuum hose and clamps were used to connect the unit to the vacuum pump. The spray nozzles for inside the effects were targeted to deliver a flat spray with dimensions of 22.8 in. x 1.5 in. x 8 in. (57.9 cm x 3.8 cm x 20.3 cm) at 20 psi (138 kPa) for flows less than 1 gal/min (3.78 L/min); an H-VV series low-flow flat spray with a 110° spray angle was selected (Spraying Systems Company, Wheaton, IL).

Feedwater and heat transfer water were stored in 65 gallon (240L) polyethylene tanks designed for drinking and irrigation

water (Chem-Tainer, West Babylon, NY). Brine and distillate were collected in heavy duty 5 gallon (18 L) HDPE square carboys (Dynalab Corp, Rochester, NY). Feedwater was fed into the system using a 1/125 hp compact submersible pump (McMaster-Carr). Heat transfer water was heated to 70-80°C and pumped using a 1.5 kW portable water heater/recirculator (McMaster-Carr).

System pressure was achieved using a D40BCS vacuum pump (Oerlikon Leybold, Export, PA) operated at 0.1 bar absolute pressure. To prevent issues with the water vapor from the MED unit, a liquid nitrogen cold trap was installed between the pump and the condenser, and perfluoropolyether (PFPE) oil was used in the pump.

Produced brine and distillate were removed from the effects using moderate-flow positive displacement bypass diaphragm pumps (Cole Palmer, Vernon Hills, IL). The pumps created a 45 psi (310 kPa) pressure differential, which was able to work with the vacuum conditions.

4.4 Monitoring and Data Collection

To enable research on MED operation, pressure gauges, thermometers, and a flow meter were incorporated into the MED unit design, as shown in Figure 4.3.

Four vacuum steam pressure gauges (Ashcroft, Stratford, CT) were installed to read the pressures within the two effects and the condenser, and in the transfer line between the first and second effects.

Temperatures within the effects and the condenser were measured using adjustable-angle dry dial thermometers (McMaster-Carr) capable of measuring between 0-150°C. Temperatures of the feedwater after the pump and before the effects, of the steam between the first and second effects, and of the heat transfer water before and after the first effect were measured with bottom-connection dry dial thermometers (McMaster-Carr) capable of measuring between 0-150°C.

Temperatures of the heat transfer surfaces within the second effect were measured using remote-reading dial thermometers (McMaster-Carr) with a tin-plated copper stems capable of measuring between 0-115°C, located at the inlets and outlets of the top-most and bottom-most heat transfer tubes.

A water flow meter with control valve capable of measuring 0.8-8 L/min (McMaster-Carr) was installed between the feed water tank and the first effect.

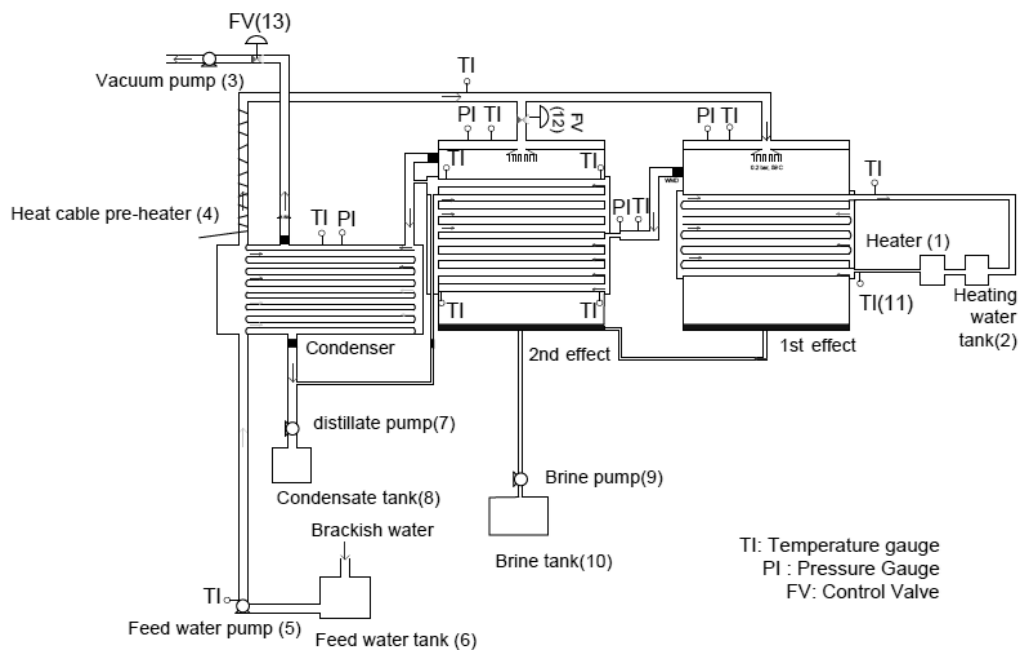


Figure 4.3 Schematic of entire lab-scale MED unit showing the unit operations and relative locations of temperature and pressure gauges, control valves, and flow meter.

4.5 Shakedown Trials and Safety Review

After fabrication and assembly of the MED components, a series of shakedown trials was conducted with tap water to assess the operation of the unit compared to design specifications. A thorough safety review was also conducted and an experimental safety plan prepared and approved as per NMSU College of Engineering procedures. A panoramic view of the completed unit in the lab near the end of the shakedown trials and modifications is shown in Figure 4.4.



Figure 4.4 Panoramic photograph of fabricated MED unit in the laboratory showing the vacuum pump with cold trap on the left, to the feedwater holding tank, to the MED condenser, second effect, first effect and heat transfer water holding tank on the far right. Photo was taken near the completion of the shakedown trials.

4.5.1 Vertical Unit Orientation and Pump Pressure Head

The original design had the effects and condenser units placed on the floor. However, this created insufficient head for the brine and distillate pumps chosen, partially because the units are operated under vacuum. Centrifugal pumps require a high net positive suction head (NPSH). Even after raising the units to on top of a table (~1 m elevation) and then on top of supports on top of a table (~1.7 m), there was still not enough NPSH. A search for alternative pumps yielded three options: piston pumps, metering diaphragm pumps, and bypass diaphragm pumps. Piston pumps are generally the best option to pump water out of sub-atmospheric pressure chambers but they are about 10 times more expensive than other types of pumps. Both metering and bypass diaphragm pumps are able to run dry and are self-priming, important considerations for easy operation if the water levels in the effects will vary over time. A metering diaphragm pump with 20 psi (145 kPa) maximum differential pressure was tested first but did not provide enough suction. Finally, a moderate-flow, positive displacement bypass diaphragm with a 45 psi (310 kPa) pressure differential was found to work. This solution is not perfect because the increased elevation of the entire unit creates the need for climbing to read meters and make adjustments. Future designs need to either incorporate the

vertical orientation from the beginning, such as building the unit onto frames that include steps, or selecting brine and distillate pumps that can provide greater pressure differential.

4.5.2 Water Vapor and Vacuum Pump

During one of the first test runs of the MED unit, it was noticed that a portion of vapor entering the condenser was being transferred into the vacuum pump along with non-condensable gases. This resulted in substantial cloudiness in the pump oil, jeopardizing the long-term durability of the pump, and steam losses from the system. To address the problem, a liquid nitrogen cold trap was added between the condenser and vacuum pump to condense vapors coming from the condenser. A butterfly valve was also installed at the pump intake port to enable isolation of the pump from the MED for liquid nitrogen refilling. Because the vapors and gases coming from the condenser are warm, the frequency of liquid nitrogen refills is higher than would be desired (approximately 4-6 L per hour of operation). Using crushed dry ice instead of liquid nitrogen did increase the cold trap's capacity but required additional handling for crushing and trap filling. Future designs need to adjust the location of the vacuum outlet in the condenser to be farther away from the steam inlet to prevent vapors from flowing past the condenser tubes and directly out the vacuum outlet. Adding baffles to direct the steam flow over the pipes are another option. If a vacuum pump is to be used to provide unit pressure, an additional heat exchanger to further cool outlet gases prior to the cold trap would lower the liquid nitrogen/dry ice consumption.

4.5.3 Polycarbonate Sheeting and Vacuum Pressure

The front panels of the two effects and the condenser are made from polycarbonate to allow direct observation into the units. Upon running the vacuum pump, the polycarbonate covers on the first and second effects of the MED buckled inward, putting pressure on the seals at the unit corners and threatening to crack the cover in the middle. To address this, three aluminum bars, shaped to prevent impeding water flow in the effects, were added horizontally to stabilize the polycarbonate sheet. Bars were not needed for the condenser

unit as the surface area of the condenser is much smaller than that of the effects. Future problems with buckling can be prevented by using metal for all sides of the units or selecting a polymer shape and thickness that better withstand vacuum; both options would eliminate direct visual observation, so some form of sight glass might also be considered.

4.5.4 Preheating Feedwater

One of the main obstacles to distilled water recovery rates is the low temperature of the feedwater entering the effects. In the current unit, the feedwater temperature after the condenser and before the first effect does not exceed 35°C, which is much lower than the first effect's designed operating temperature of 61°C. A decrease in the first effect's temperature decreases the amount of steam that is produced to heat the second effect, which then reduces the amount of steam flowing into the condenser to produce distillate and to warm the feedwater. After a few minutes of successful operation, the unit cools too much and the distilled water production rate is reduced to the tiny amount of feedwater that flashes under the vacuum conditions. Addition of insulation around exterior surfaces of the units, exposed plumbing, and holding tanks, and a heat tape on the piping between the condenser and the first effect, was not sufficient. (Preheating the feedwater in the feedwater holding tank would help as long as the temperature increase is not too much or the feedwater will not be cool enough to condense the water vapor in the condenser.) Future designs will need to consider an additional heat exchanger between the condenser and the first effect. In a lab research unit such as this one, heat for the heat exchanger could again come from a hot water supply as with the heat exchanger water used to warm the first effect. In a field unit, heat to preheat the feedwater could come from the final cooling step of flue gases coming from the biomass pyrolysis off-gas combustion chamber.

4.6 Future Unit Improvements

As with any design project and proof-of-concept prototype, the fabrication and shakedown trial process highlighted many opportunities for unit improvement.

The first improvements have to do with the fabrication materials. While aluminum is relatively inexpensive, lightweight and easy to machine, aluminum is also susceptible to corrosion over time, especially in a continuously wet environments. Corrosion can be partially mitigated using an anodization process. A better option may be to construct the effects and condenser out of a rigid, molded polymer or polymer composite that can be machined, can stand up to the vacuum pressures, and can tolerate the moderate temperatures (50-80°C). A polymer molding process would also enable the corners of the effects to be rounded instead of square, a shape that is more suitable for pressurized chambers, and the addition of exterior flanges. Polymer materials generally have lower densities and lower thermal conductivities than aluminum, which would lower the weight of the unit for easier set-up handling and reduce heat losses to the environment.

The heat transfer surfaces in the current MED are horizontal smooth copper tubes, chosen to simplify fabrication while lowering incidents of scaling/fouling. To improve heat transfer and the amount of produced water, enhanced geometry (i.e. corrugated) tubes, such as GEWA B and GEWA C available from Weiland Materials, can be used. These tubes have various surface microstructures; examples are shown in Figure 4.5. Some past research has shown that heat transfer improvement can be as much as 150% (Galal, et al., 2010, Kalendar and Griffiths, 2001, Nae-Hyun and Webb, 1991). If such improvement could be done with this unit, small-scale MED units for rural communities and farmers could produce more water at lower costs without needing to increase the size of the entire MED unit.

The next two improvements are related to heat exchange outside of the effects. An additional heat exchangers to preheat the feedwater would help maintain temperature in the first and second effects, thus increasing distilled water production and overall unit efficiency. Future work should focus on how to take advantage of heat from other sources,

as well as to manage how heat is retained within the unit. The cold trap for the vacuum pump is effective for removing small amounts of water vapor from room temperature non-condensable gases. The off-gases being vented from the current MED condenser are too warm and contain too much water vapor. Relocating the inlets and outlets on the condenser, increasing the tortuosity of the steam flow in the condenser, and/or adding a heat exchanger to lower the vent gas temperature would lower the consumption rate of liquid nitrogen in the lab.

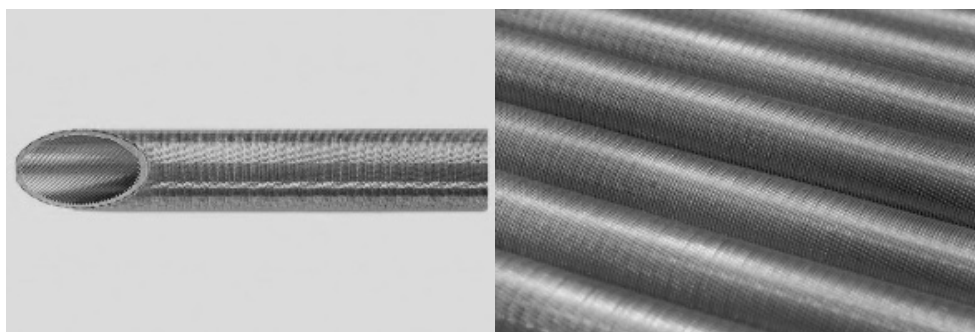


Figure 4.5. Examples of enhanced geometry (corrugated) copper tubes (http://www.wieland.com.sg/internet/en/products/tubes/product_catalogue_2/finned_tubes___gewa/gewa_b___gewa_c/gewa_bgewac_1.jsp).

Framing and wall-mounting for the unit components would improve unit stability and enable clean-up of overlapping water and steam piping. Framing could include climbing mechanisms to simplify the process of reading meters. Selection of brine and distillate pumps with greater maximum displacement pressures would also enable the units to be mounted closer to the floor.

A longer-term and larger-scale improvement would be the use of a gas ejector instead of a vacuum pump for providing system vacuum. This switch would lower the maintenance and electrical power requirements of the system and would remove the need for cryogenics to operate a cold trap. Combined with optimization of heat exchangers and selection

of water pumps, the electrical power requirements for the unit might be substantially reduced, thus reducing the load on the pyrolyzer-MED interface turbine generator.

All potential improvements will be evaluated using capital and operating cost estimates through Aspen Plus® simulations of the MED and overall biomass pyrolysis-MED processes building on simulation work begun in our previous project.

5. Water Testing

Water desalination research on the fabricated MED unit is centered on the interaction of water chemistry and thermal desalination conditions to reduce mineral scale on heat transfer surfaces. Initial tests focused on water chemistries like that of Well 1 at the Brackish Groundwater National Desalination Research Facility (BGNDRF,) which contain sodium, calcium, chloride, bicarbonate, and sulfate as the primary ions at total dissolved solids (TDS) concentrations between 1000-2000 ppm (mg/L) and pH values of 7.0-8.5 (see Table 2.1). A negative control water chemistry was designed to benchmark operation of the MED. This data would be contrasted to operation performance data from treating a positive control water chemistry that was purposefully designed to promote scaling. Follow-on experiments will use the two negative control and positive control benchmarks to identify operating conditions for various brackish water chemistries that optimize distilled water production and prevent scaling.

5.1 Negative Control Benchmark

For the negative control water chemistry, a TDS of 1,200 ppm and a pH of 7.1 with 600 ppm of NaCl and 600 ppm of CaCl₂ was chosen to represent the mildest scenario for brackish groundwater in terms of the likelihood of forming CaCO₃ and CaSO₄ scale. The relatively low pH was to ensure that any carbon dioxide from the air that dissolved into the solution would remain as bicarbonate (HCO₃⁻) ions rather than less-soluble carbonate (CO₃²⁻) ions.

Enough negative control water to fill the MED feedwater holding tank (245 L) was prepared by dissolving 147 g each of NaCl and CaCl₂ salts in distilled water, adjusting the pH to 7.1 using dilute hydrochloric acid and sodium hydroxide solutions, and diluting to final volume. The MED operation for the negative control runs was conducted as follows: the heat transfer water temperature was preheated to 78°C, the vacuum pump run to evacuate the system for 30 minutes prior to starting the test, and the feedwater set to recirculate

through the holding tank to ensure good mixing. Once the MED was at the desired operating conditions (system pressure ≈ 0.2 bara and first effect temperature = 61°C), the valve between the feedwater tank and the first effect was opened to spray feed water into the first effect at a rate of approximately 1 gal/min (3.7 L/min). After about five minutes, the valve was opened to allow feedwater to spray into the second effect. As brine and distillate water collected in the effects and the condenser, the brine and distillate water pumps were switched on. The unit was allowed to run for about 80 minutes; temperatures, pressures, and flow rates were monitored and the values recorded every 2-5 minutes using the sensors at several locations on the MED (see Figure 4.3). The temperature of the cold trap was also monitored; as soon as the trap's outer surface felt warm to the touch, the vacuum pump was temporarily isolated from the system and the liquid nitrogen reservoir refilled. Once the test was complete, the volumes of feedwater, brine, distillate water collected in the condenser, and distillate water collected in the cold trap were recorded. A pH and electrical conductivity (EC) meter (Fisher Scientific, Waltham, MA) was used to measure the pH and TDS concentrations of the feedwater and the collected water samples.

The test runs were hampered by a relatively rapid temperature decrease in the system that led to almost no distilled water production after the first five or ten minutes of operation. An example of the temperatures observed in the system over the course of the test are shown in Figure 5.1. The temperature in the first effects started at 61°C , then decreased to $50\text{-}55^{\circ}\text{C}$ after five minutes, then continued to decrease gradually to about 40°C by the end of the test. At the current system pressure, temperatures much below 60°C do not allow evaporation of water from the feedwater stream to produce steam. From about 5 to 15 minutes into the test, the temperature in the second effect and the condenser was briefly warmed by steam from the first effect from room temperature to about 37°C and 35°C , respectively. After steam was produced in the effects and traveled to the condenser, the temperature of the feedwater did increase

from room temperature to about 35°C—warm but not warm enough to maintain the temperature in the first effect and to ensure effective MED operation.

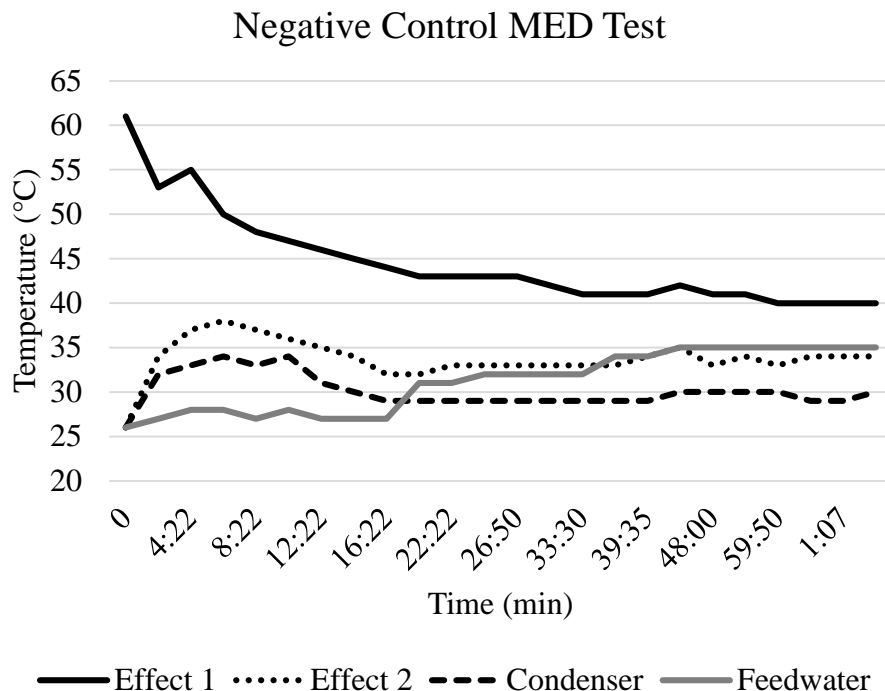


Figure 5.1 Temperatures of the feedwater and the interiors of the effects and the condenser of the MED unit during a desalination test run of the negative control feedwater formulation.

Given the temperatures within the unit, the produced water volumes were as expected: approximately 2 L of distilled water was collected in the condenser in the first five minutes of operation and almost no water thereafter. In the 1 hour+ operation time, approximately 200 ml of distilled water was collected in the vacuum cold trap, indicating that substantial produced steam was being vented prematurely from the system. The pH, EC, and TDS data for the water samples from the negative control test shown in Figure 5.1 are shown in Table 5.1. As expected, the TDS of the distillate water was very low (5 ppm) and the TDS of the feedwater (1150 ppm) was less than that of the collected brine (1231 ppm). The measured pH values, however, were lower than expected (5.9-6.7) given that the pH of the prepared feedwater was

adjusted to 7.1; the decrease in pH was likely caused by the dilution with distilled water from prepared volume (~20 L) to final volume (245 L) within the feedwater holding tank. In the future, the pH of the feedwater will be checked and adjusted as needed immediately before each test.

Table 5.1 Total dissolved solids (TDS), electrical conductivity (EC) and pH of water samples measured before and after a negative control water desalination test using the MED unit.

Water Sample	pH	EC ($\mu\text{S}/\text{cm}$)	TDS (ppm)
Feedwater before test	6.48	2843	1150
Collected brine	6.68	2924	1231
Collected clean distillate	5.91	13	5

5.2 Positive Control Benchmark

For the positive control water chemistry, a TDS of 1,520 ppm and a pH of 7.1 with 400 ppm of NaCl, 1000 ppm of CaCl_2 , and 120 ppm of Na_2CO_3 was chosen. This chemistry was selected so that CaCO_3 would be at its saturated condition at 55°C (120 ppm) and would precipitate on the MED heat transfer surfaces at the MED temperature (60°C). Compared to the brackish groundwater chemistry at BGNDRF (Table 2.1), the positive control conditions are still relatively mild with the goal of forming easier-to-clean soft scale at the upper MED operating temperatures. Desalination tests will be conducted with this feedwater after the feedwater preheating adjustments are made in order to test MED function under sustainable operation conditions.

5.3 Future Work

Once the MED performance is benchmarked using the negative and positive control water chemistries, desalination experiments will be expanded to include higher feedwater TDS concentrations and pH values, and magnesium and sulfate ions. Heat transfer performance evaluations will focus on the four evaporator tube temperatures in the second effect

(to enable calculations of experimental heat transfer coefficients) and the distilled water production rates. Scaling will be observed visually and through heat transfer calculations. Periodically, the unit will be disassembled to test scale removal (cleaning) methods.

6. Project Outcomes

6.1 Research Capacity Building

This developed the expertise and laboratory research capabilities of a new assistant professor in Chemical & Materials Engineering (Brewer). Funds from this project, combined with faculty start-up funds, contributed to the purchase and set up of several pieces of equipment associated with the MED unit. Collaborations were fostered between the PI and researchers/staff at New Mexico State University in the Institute for Energy & the Environment (IEE), the Manufacturing Technology & Engineering Center, the Department of Mechanical Engineering, Extension Food Technology, and the NMSU Agricultural Experiment Stations. Two graduate students and two undergraduate students received training in research methods, sample analysis, and laboratory safety, as well as experience in conducting original research.

In addition to conference presentations, travel funding provided through this project enabled Dr. Brewer to attend the American Water Works Association (AWWA) Sustainable Water Management Conference and Mr. Amiri to attend the Water Reuse Research Foundation (WateReuse) 19th Annual Water Reuse and Desalination Research Conference as part of the expertise building process.

6.2 Theses, Publications, and Presentations

Work on this project has resulted in two manuscripts in preparation (titles are tentative), part of one in-progress Ph.D. dissertation, part of one completed M.S. thesis, and three conference presentations (two upcoming with abstract accepted):

Amiri, A., Zhang, Y., Idowu, O.J., Brewer, C.E., Design of biomass pyrolyzer-multiple effect distillation system interface, *in preparation*.

Amiri, A., Brewer, C.E., Small-scale brackish water thermal desalination using low-temperature multiple effect distillation to prevent scaling, *in preparation*.

Amiri, A., Biomass as a renewable energy source for brackish water thermal desalination, Ph.D. Dissertation, Engineering: Chemical Engineering, New Mexico State University, expected Fall 2016.

Zhang, Y., Design of biomass pyrolyzer-multiple effect distillation system components for laboratory testing, M.S. Thesis, Chemical Engineering, New Mexico State University, June 2015.

Amiri, A., Zhang, Y., Brewer, C.E., Design and Fabrication of a Lab-Scale Multiple Effect Distillation (MED) Unit to Investigate Different Water Chemistry and Scaling Behavior, *2015 American Institute of Chemical Engineers Annual Meeting*, Salt Lake City, UT, November 10, 2015.

Amiri, A., Brewer, C.E., Small-scale Thermal Desalination of Brackish Water Using Biomass Energy, *Water Resources Research Institute 60th Annual New Mexico Water Conference*, Taos, NM, October 9, 2015.

Zhang, Y., Amiri, A., Brewer, C.E., Idowu, O.J., Design and testing of biomass pyrolyzer-multiple effect distillation system components for laboratory testing, *2015 American Institute of Chemical Engineers Spring Meeting*, Austin, TX, April 28, 2015.

6.3 Follow-On Proposals

Research conducted during this project has resulted in the submission of two directly related follow-on proposals, the first of which progressed to Phase II consideration and is currently be revised for resubmission, and the second of which was prepared by Mr. Amiri and was not funded:

"Halophytes and Biochar for Desalination Concentrate Management"

US Department of Interior/Bureau of Reclamation Desalination and Water
Purification Research & Development
12/1/15-12/31/16, \$149,977, PIs: Brewer, Rastegary, Idowu

“Corrugated Tubes for Brackish Water Desalination Improvement”
New Mexico Water Resources Research Institute
FY 16 Student Water Research Grant Program
10/1/15-6/30/16, \$6,000, PI: Amiri (Brewer as faculty sponsor)

Collaborations fostered through this research project have resulted in the submission of three additional related proposals, the first of which is currently pending; the other two are under revision for resubmission:

“Holistic Approach for Sustainable Agriculture”
USDA AFRI Water for Agriculture
1/1/16-12/31/19; \$10,000,000, PIs: Ghassemi, et al.
Large, multi-institutional, long-term integrated research, extension and education project focusing on water desalination techniques, use of algal and halophyte biomass, algal food products, and on-farm nutrient, water and energy use.

"Integrated Training Network for Water and Energy Process Improvement Impacting WAMS"
USDA NIFA Women and Minorities in STEM Fields
5/16/16-5/15/18, \$141,230, PIs: Brewer, Sullivan, Flores, Valles-Rosales
Train-the-trainer program to incorporate water audits, energy audits and cost benefit analysis into freshmen engineering classes and extension outreach.

"Design of a Mobile Torrefaction System for Invasive Species Biomass Utilization"
USDA AFRI Engineering
8/16/15-8/15/18, \$479,279, PIs: Brewer, Conley
Construction and testing of biomass torrefaction/pyrolysis field unit that could be used to pretreat tumbleweed and salt cedar biomass on-farm.

6.4 Other Products

Other products that are the result of this project include:

- a lab-scale, two-effect thermal multiple effect distillation unit available for thermal water desalination and general heat exchanger research;

- an updated Aspen Plus® simulation file allowing model experimentation with different scales and conditions for the biomass pyrolyzer-MED interface;
- a long-term case study and example problems for teaching conduction and convection heat transfer used in Dr. Brewer's Fall 2015 CHME 306 Transport Phenomena II: Heat and Mass Transfer class (43 students, mostly juniors majoring in chemical engineering);
- a webpage describing the project and results:
<http://wordpress.nmsu.edu/cbrewer/projects/>

Reference List

2012. *2011-2012 IDA Desalination Yearbook*, Global Water Intelligence, London.

Al-Anezi, K. and N. Hilal, 2007. Scale formation in desalination plants: effect of carbon dioxide solubility, *Desalination*, 204, 385-402.

Al-Jaroudi, S.S., A. Ul-Hamid and J.A. Al-Matar, 2010. Prevention of failure in a distillation unit exhibiting extensive scale formation, *Desalination*, 260, 119-128.

Al-Karaghoul, A. and L.L. Kazmerski, 2013. Energy consumption and water production cost of conventional and renewable-energy-powered desalination processes *Renew. Sust. Energ. Rev.*, 24, 343-356.

Al-Rawajfeh, A.E., 2010. CaCO₃-CO₂-H₂O system in falling film on a bank of horizontal tubes: model verification, *J. Ind. Eng. Chem.*, 16, 1050-1058.

Al-Rawajfeh, A.E., H. Glade, H.M. Qiblawey and J. Ulrich, 2004. Simulation of CO₂ release in multiple-effect distillers, *Desalination*, 166, 41-52.

Brewer, C.E. and O.J. Idowu, 2015. Design of Pyrolyzer-Desalination Unit Interface for Distributed Biochar and Clean Water Production, Report No. ###, USBOR, Denver, CO.

Cai, H., X. Li and S. Xu, 2008. Purification technology for removing volatile organic carbons, *Journal of Chemical Industry and Engineering*, 3, 6 (in Chinese).

Cao, Q.W., 2012. Investigate the combustion of organic waste treatment, *Technology Vision*, 27, 356-357 (in Chinese).

CRC, 2003. *CRC Handbook of Chemistry and Physics*, Chemical Rubber Publishing Company, Boca Raton, FL.

Darwish, M.A. and H.K. Abdulrahim, 2008. Feed water arrangements in a multi-effect desalting system, *Desalination*, 228, 30-54.

Eltawil, M.A., Z. Zhengming and L. Yuan, 2009. A review of renewable energy technologies integrated with desalination systems, *Renew. Sust. Energ. Rev.*, 13, 2245-2262.

Galal, T., A. Kalendar, A. Al-Saftawi and M. Zedan, 2010. Heat transfer performance of condenser tubes in an MSF desalination system, *Journal of Mechanical Science and Technology*, 24, 2347-2355.

Hanson, A., W. Zachritz, K. Stevens, L. Mimbela, R. Polka and L. Cisneros, 2004. Distillate water quality of a single-basin solar still: laboratory and field studies, *Sol. Energy*, 76, 635-645.

Hewitt, W.L., 1971, Direct spark igniter combustion safeguard apparatus, U.S. Patent 3,574,496.

Inc., T.T., 2013. 2012 Analysis of Water from Four Wells and Three Ponds at the Brackish Groundwater National Desalination Research Facility, Report No. Albuquerque, NM.

Incropera, F.P., D.P. Dewitt, T.L. Berman and A.S. Lavine, 2007. *Fundamentals of Heat and Mass Transfer*, John Wiley and Sons, Hoboken, NJ.

Kalendar, A. and A. Griffiths, 2001. Performance study of enhanced and smooth surface tubes in a system condenser of a multistage flash desalination unit, *Desalination*, 134, 269-283.

Kalogirou, S., 1997. Survey of solar desalination systems and system selection, *Energy*, 22, 69-81.

Kalogirou, S.A., 2005. Seawater desalination using renewable energy sources, *Prog. Energ. Combust.*, 31, 242-281.

Kim, H.-H., S.-M. Oh, A. Ogata and S. Futamura, 2005. Decomposition of gas-phase benzene using plasma-driven catalyst (PDC) reactor packed with Ag/TiO₂ catalyst, *Applied Catalysis B: Environmental*, 56, 213-220.

Likhachev, D.S. and F.-C. Li, 2013. Large-scale water desalination methods: a review and new perspectives, *Desalination and Water Treatment*, 51, 2836-2849.

Nae-Hyun, K. and R.L. Webb, 1991. Particulate fouling of water in tubes having a two-dimensional roughness geometry, *International Journal of Heat and Mass Transfer*, 34, 2727-2738.

Semiat, R. and D. Hasson, 2012. Water desalination, *Rev. Chem. Eng.*, 28, 43-60.

Tong, Z.-Q., 2001. *The Purification and Utilization of Industrial Exhaust Gas*, Chemical Industry Press, Beijing (in Chinese).

Urashima, K. and J.-S. Chang, 2000. Removal of volatile organic compounds from air streams and industrial flue gases by non-thermal plasma technology, *IEEE Transactions on Dielectrics and Electrical Insulation*, 7, 602-614.

Appendix

Surface Area Calculations for Heat Exchangers

First Effect

$$Q_{steam} = m_{steam} \times h_{63.5C} = \frac{10kg}{hr} \times \frac{2350kJ}{kg} = \frac{23500kJ}{hr}$$

$$= 6527.78W$$

$$6527.78 = m_{water} \times C_p \times \Delta T \Rightarrow \text{assuming } \Delta T = 10^{\circ}C:$$

$$m_{water} = \frac{6527.78}{4.12 \times 10} = 158.45 \frac{g}{s} = \frac{570.42kg}{hr}$$

$$\Delta T_{LMTD} = \frac{6527.78 = U \times A \times \Delta T_{LMTD},}{\ln \frac{\Delta T_1}{\Delta T_2}} = \frac{[(70 - 63.5) - (63.5 - 60)]}{\ln \left(\frac{6.5}{3.5} \right)} = 4.84^{\circ}C$$

Assuming $U = 3000 \text{ W/m}^2\text{C}$:

$$6527.78 = 3000 \times A \times 4.84$$

$$A = 0.45m^2 = \pi DL$$

For $D = 1'' = 0.0254 \text{ m}$

$$L_{coil} = \frac{0.45}{\pi \times 0.0254} = 5.64m = 18.5ft$$

The amount of feed water evaporated within the first effect will be:

$$6527.78 = M_{f1} \times C_{pf} \times (T_{b1} - T_{Fh}) + M_{s1} \times h_{s1}$$

Where T_{b1} is the top brine temperature which is $63.5^{\circ}C$ and T_F is the temperature of feed water being sprayed into the first effect which is set to be $55^{\circ}C$. M_{f1} is the mass flow rate of feed water in the first effect which is $40 \text{ kg/hr} = 11.11 \text{ g/s}$. Also, if

we neglect the BPE the h_{s1} will be the same as $h_{63.5} = 2350$ kJ/kg:

$$M_{s1} = \frac{6527.78 - 11.11 \times 4.12 \times (63.5 - 55)}{2350} = 2.61 \frac{g}{s} = 9.4 \frac{kg}{hr}$$

2nd Effect

Assuming OD = 1", U = 3409 W/m²°C, ΔT = 4°C, L = 700 mm,

$$M_{s1} \times h_{s1} = U \times A \times \Delta T \Rightarrow A = 0.44 \text{ m}^2 = n\pi DL \Rightarrow n = 8$$

$$M_{s1} \times h_{s1} = M_{f2} \times C_{pf} \times (T_{b2} - T_F) + M_{s2} \times h_{s2@60C}$$

$$\frac{2.61g}{s} \times 2350 = 11.11 \times 4.12 \times (60 - 55) + M_{s2} \times 2358.6 \rightarrow$$

$$M_{s2} = 2.31 \text{ g/s} = 8.31 \text{ kg/hr}$$

Condenser

$$LMTD = \frac{(T_c - T_{Fc}) - (T_c - T_{Fh})}{\ln \frac{(T_c - T_{Fc})}{(T_c - T_{Fh})}} = \frac{(59 - 25) - (59 - 55)}{\ln \left(\frac{34}{4}\right)}$$

$$= 14^\circ\text{C}$$

Where T_c is the temperature at condenser shell, T_{Fc} , the temperature of incoming feed water, T_{Fh} the temperature of pre-heated feed water. Assuming $U = 3000 \text{ W/m}^2\text{°C}$:

$$M_f \times C_p \times \Delta T_F = U \times A \times \Delta T_{LMTD} \rightarrow 43 \frac{g}{s} \times 4.12 \times 30 = 3000 \times$$

$$A \times 14 \rightarrow$$

$$A = 0.126 \text{ m}^2 = 126542 \text{ mm}^2$$

$$A = \pi \times D \times L \text{ assuming OD} = 1" \rightarrow L = 1585 \text{ mm} = 1.585 \text{ m} = 5.2 \text{ ft}$$

**Desalination Concentrate Management for Sustainable Agriculture:
A Preliminary Study on Transport behavior and Plant Viability at
BGNDRF**



REPORT DOCUMENTATION PAGE			Form Approved OMB No. 0704-0188		
<p>The public reporting burden for this collection of information is estimated to average 1 hour per response, including the time for reviewing instructions, searching existing data sources, gathering and maintaining the data needed, and completing and reviewing the collection of information. Send comments regarding this burden estimate or any other aspect of this collection of information, including suggestions for reducing the burden, to Department of Defense, Washington Headquarters Services, Directorate for Information Operations and Reports (0704-0188), 1215 Jefferson Davis Highway, Suite 1204, Arlington, VA 22202-4302. Respondents should be aware that notwithstanding any other provision of law, no person shall be subject to any penalty for failing to comply with a collection of information if it does not display a currently valid OMB control number.</p> <p>PLEASE DO NOT RETURN YOUR FORM TO THE ABOVE ADDRESS.</p>					
1. REPORT DATE (DD-MM-YYYY) 08/16/2015		2. REPORT TYPE		3. DATES COVERED (From - To)	
4. TITLE AND SUBTITLE Desalination Concentrate Management for Sustainable Agriculture: A Preliminary Study on Transport behavior and Plant Viability at BGNDRF			5a. CONTRACT NUMBER R10AC80283		
			5b. GRANT NUMBER		
			5c. PROGRAM ELEMENT NUMBER		
6. AUTHOR(S) Manoj K Shukla Alison Flores			5d. PROJECT NUMBER		
			5e. TASK NUMBER		
			5f. WORK UNIT NUMBER		
7. PERFORMING ORGANIZATION NAME(S) AND ADDRESS(ES) Plant and Environmental Sciences New Mexico State University 945 College Ave., Las Cruces, NM-88003			8. PERFORMING ORGANIZATION REPORT NUMBER		
9. SPONSORING/MONITORING AGENCY NAME(S) AND ADDRESS(ES)			10. SPONSOR/MONITOR'S ACRONYM(S)		
			11. SPONSOR/MONITOR'S REPORT NUMBER(S)		
12. DISTRIBUTION/AVAILABILITY STATEMENT					
13. SUPPLEMENTARY NOTES					
14. ABSTRACT The objective of the study was to improve knowledge of six candidate halophyte species (<i>Atriplex canescens</i> , <i>Hordeum vulgure</i> , <i>Lepidium alyssoides</i> , <i>Distichlis stricta</i> , <i>Panicum virgatum</i> , and \times <i>Triticosecale</i>) for cultivation on wastewater land application sites. Study was divided into three parts, a germination, pore clogging, and a plant survival and utilized water and RO concentrate from the Brackish Groundwater National Desalination Research Facility (BGNDRF) in Alamogordo, NM. Candidate species showed the potential to grow and survive under RO concentrate irrigation.					
15. SUBJECT TERMS					
16. SECURITY CLASSIFICATION OF:			17. LIMITATION OF ABSTRACT	18. NUMBER OF PAGES	19a. NAME OF RESPONSIBLE PERSON
a. REPORT X	b. ABSTRACT	a. THIS PAGE			19b. TELEPHONE NUMBER (Include area code)

**Desalination & Water Purification Research
and Development Program Report No. XXX**

**Desalination Concentrate Management for Sustainable
Agriculture: A Preliminary Study on Transport behavior and
Plant Viability at BGNDRF**

Prepared for Reclamation Under Agreement No. R10AC80283

by

Author(s)

Manoj K Shukla, Professor, New Mexico State University

Alison Flores, graduate student, New Mexico State University



U.S. Department of the Interior
Bureau of Reclamation
Technical Service Center
Water and Environmental Services Division
Water Treatment Engineering Research Team
Denver, Colorado

Month Year

MISSION STATEMENTS

The mission of the Department of the Interior is to protect and provide access to our Nation's natural and cultural heritage and honor our trust responsibilities to Indian tribes and our commitments to island communities.

The mission of the Bureau of Reclamation is to manage, develop, and protect water and related resources in an environmentally and economically sound manner in the interest of the American public.

Disclaimer

The views, analysis, recommendations, and conclusions in this report are those of the authors and do not represent official or unofficial policies or opinions of the United States Government, and the United States takes no position with regard to any findings, conclusions, or recommendations made. As such, mention of trade names or commercial products does not constitute their endorsement by the United States Government.

Acknowledgements

Authors thank NMSU Agricultural Experiment Station, NIFA, Nakayama Chair and Institute for Energy and the Environment through the NMSU/Bureau of Reclamation Cooperative Agreement for support.

Contents

	<i>Page</i>
Glossary	iii
Executive Summary	1
Introduction	2
Materials and Methods	6
Plant Selection	6
Water Treatments	6
Germination Experiment	7
Soil Sampling	8
Pore Clogging Experiment	9
Greenhouse Plant Survival Cylinder Preparation	10
Water Balance Experiment	10
Plant Growth Measurements	10
Statistical Analysis	12
Results and Discussions	12
Water Treatments	12
Germination Study	13
Soil Sampling	15
Pore Clogging	17
Water Balance	19
Evapotranspiration and Deep Percolation	19
Leaching Fractions	21
Plant Growth Measurements	24
Dry Biomass	24
Height and Number of Leaves	26
Photosynthetic Rates	28
Ion Uptake	30
Conclusion	33
References	34

Glossary

Brackish Groundwater National Desalination Research Facility – Facility in Alamogordo, NM that was created to develop technologies for the desalination of brackish and impaired groundwater in the inland states. Abbreviated as BGNDRF.

Cl⁻ – Abbreviation of chloride ion.

Deep percolation – Amount of water leached through soil past the root zone. Abbreviated as DP.

Desalination – Many different processes where salt and other minerals are removed from saline water.

Electrical conductivity – A measure of the ability of water to conduct electrical currents via dissolved ions. Abbreviated as EC.

Evapotranspiration – The sum of the water evaporation from the soil and the plant transpiration to the atmosphere. Abbreviated as ET.

Germinability – The capacity of a seed sample to germinate.

Germination Index – A measure of the time for a seed sample to germinate that uses the number of seeds germinated by the end of the experiment to cancel the effect of the seed sample size. Abbreviated as GI.

Halophyte – Plant species that grows and thrives in high salinity.

Irrigation – Amount of water applied to plants as water source. Abbreviated as IR.

K⁺ – Abbreviation of potassium ion.

Leaching fraction – The volumetric ratio of water applied (irrigated) to water leached (via deep percolation). Abbreviated as LF.

Mean germination time – The weighted mean of the time a seed sample takes to germinate. Abbreviated as MGT.

Na⁺ – Abbreviation of sodium ion.

Reverse osmosis – Water purification process where water is forced through a semipermeable membrane to remove various molecules and ions, leaving both potable water and a saline concentrate. Abbreviated as RO.

Sodium Adsorption Ratio – A measure of the suitability of water for use in agricultural irrigation determined by concentrations of dissolved solids. Measures sodicity of water and soils. Abbreviated as SAR.

Timson's Index – A measure of the time it takes a seed sample to germinate that combines germination rate with the final germination percentage. Abbreviated as T.

Timson's Modified Index – A measure of time for a seed sample to germinate that minimized the effect of final germination percentage in Timson's index. Abbreviated as T_{mod} .

Ks- saturated hydraulic conductivity of soil

Executive Summary

Water scarcity in arid regions has led to a decline of surface water available for agriculture and put constraints on saline groundwater resources. It has also necessitated the use of nontraditional water sources for augmenting irrigation water portfolio. One way to expand the irrigation water supply is to pump saline groundwater, run it through an inland reverse osmosis (RO) system, and utilize fresh water to grow food crops and saline RO concentrate to grow salt-tolerant plants including forage crops.

The objective of the study was to improve knowledge of six candidate halophyte species (*Atriplex canescens*, *Hordeum vulgure*, *Lepidium alyssoides*, *Distichlis stricta*, *Panicum virgatum*, and \times *Triticosecale*) for cultivation on wastewater land application sites. Study was divided into three parts, a germination study, pore clogging study, and a plant survival study and utilized water from the Brackish Groundwater National Desalination Research Facility (BGNDRF) in Alamogordo, NM.

The purpose of the germination study was to improve knowledge of halophyte germination by comparing time-integrated measurements of germination among seed populations exposed to saline groundwater and RO concentrate. The germination of six halophyte species was studied in 22-day germination tests conducted in growth chambers set to 25/15°C day/night temperatures with 12-hour photoperiods. Seeds of each species were placed in Petri dishes lined with filter papers moistened with one of the four saline treatments (electrical conductivity [EC] = 0, 0.6, 4.0, and 10.0 dS/m). Germinability, mean germination time, germination index, Timson's index, and Timson's index modified were calculated. Results showed that although final germination percentages remained similar within a species across treatments for all species except *L. alyssoides*, germination time varied to some degree, showing a germination time dependency.

The pore clogging study was conducted to determine how concentrated saline water affects the saturated hydraulic conductivity (Ks) of two soils (sand and clay) over time and to observe the effects of concentrated saline solution on soil. The effect of saline water application to two soils was studied in a 24-day test. Columns measuring 3.8 cm in diameter and 10 cm in height were packed with either a clay or sand and received one pore volume of concentrate each week for 20-weeks, then every two weeks for 4-weeks. Columns were allowed to dry between applications. The Ks was measured every 4-weeks for the duration of the study. Comparisons of the Ks over time showed initial decreases in Ks that were variable in the sand but fairly consistent in the clay. The salt deposition was observed on the soil surface as well as in the pores indicating that problems with Ks could arise with regular application of saline RO concentrate to soil.

The plant survival study was conducted in the greenhouse because NMDA does not allow land application of water above 4 dS/m. Columns were packed with two contrasting soils, clay and sand, to a constant bulk density. Seeds of the six halophyte species were planted and allowed to grow for 30-days prior to the start of the experiment using control water to ensure a consistent growth pattern. Plants were arranged in a completely randomized design and treatments were applied for 90-days.

The objectives greenhouse study were to components of water balance including amounts of irrigation, drainage (or deep percolation), evapotranspiration (ET), and volumetric leaching fractions (LF) under a salinity gradient. ET for the six species was obtained from water balance equation. Results showed that the ET was higher and DP was lower for the control plants than the saline water-grown plants and values were more evident in the sand than in the clay. Additionally, with increasing irrigation water salinity, ET decreased but LF increased.

Other objectives of the greenhouse study was to quantify plant growth and ion uptake due to irrigation with saline groundwater and RO concentrate. Five physical measurements (height, number of stem nodes, average internodal length, number of leaves, and leaf length), four non-destructive measurements (photosynthetic rates, stomatal conductance rates, leaf temperatures, and transpiration rates), and five destructive measurements (stem water potential, osmotic potential, dry biomass, ion uptake, and chloride content) were made at the different times and frequency. Plant height was measured along the main live stem from the base of the stem to the highest node. The number of leaves were counted for the entire plant. A LiCor LI-6400XT was used to determine the photosynthetic rates, stomatal conductance, leaf temperatures, and transpiration rates. Dry biomass was determined after cutting the plant at the soil surface and drying at 65°C for 3-days. The Na⁺ and K⁺ ion concentrations were determined through microwave digestion and Cl⁻ ion concentration was determined by mixing samples with 2% acetic acid. Results showed that *A. canescens* and *L. alyssoides* saw an increase in biomass while the others saw a decrease. *P. virgatum* was the only species to see a consistent decrease in plant height with increasing salinity and all species (except *A. canescens* which showed an increase) noted a decrease in the number of leaves per plant. There were no clear trends with respect to photosynthetic rates for the species. The concentrations of Na⁺ and Cl⁻ both increased with increasing salinity, whereas K⁺ decreased. Based on these results, all of the tested species have the potential for establishment on land application sites.

Introduction

In arid and semi-arid regions around the world, water is a limited resource. These areas are characterized by low rainfall and high evaporation. A significant amount of water is required for agricultural production, and thus, any water, even saline, must be used. (Smedema and Shiati, 2002). In southern New Mexico,

groundwater is often the saline water source utilized for agricultural irrigation. The groundwater salinity is highly variable and about 75% of available groundwater is saline having an electrical conductivity (EC) > 3 dS/m (Lansford *et al.*, 1990; WRRRI, 1997). Low quality groundwater, along with persistent drought and diminishing fresh water supplies, has prompted urgent searches for novel water resources in arid and semi-arid regions (Schwabe *et al.*, 2013). Such searches have led to increased efforts to produce water suitable for both human consumption and cropland irrigation through the use of reverse osmosis (RO) desalination. The RO desalination of brackish groundwater produces potable, low saline water, and high saline-sodic RO concentrate (UNEP, 1998). Land application of RO concentrate, either by itself or mixed with wastewater effluent, is one approach to its disposal (Nemmers *et al.*, 2012) but the likelihood of deleterious environmental impacts has made the disposal of wastewater from inland desalination systems challenging and limits the widespread implementation of inland groundwater desalination (Soliz *et al.*, 2011).

The Brackish Groundwater National Desalination Research Facility (BGNDRF) located in Alamogordo, New Mexico utilizes a reverse osmosis (RO) treatment to desalinate groundwater from its four saline wells and produce potable water. The resulting concentrated saline wastewater, also known as concentrate, typically has an EC of 10 dS/m. In arid and semi-arid environments, the waste is often disposed of using evaporation ponds but this method of disposal is expensive and causes the loss of valuable water (Gonzalez *et al.*, 2009; Soliz *et al.*, 2011). Another possibility is to reuse it for irrigating salt-tolerant plants (Noaman and El-Haddad, 2000; Babcock *et al.*, 2009).

Unlike plant species intolerant of salinity (i.e., glycophytes), halophytes can germinate, grow and survive under osmotic tensions potentially limiting to plant water uptake and ionic conditions possibly toxic to plant columns (Ries and Hofmann, 1983; Hussain *et al.*, 1997; Kim *et al.*, 2012). Halophytes have been introduced for revegetation on salt-contaminated soils because they are capable of growing on soil with more than 0.2% salt concentration; however, such revegetation efforts are often characterized by low rates of seedling survival and variability among halophyte species in plant establishment (Barbour *et al.*, 1987; Keiffer and Ungar, 2002). Plants tend to grow more slowly when subjected to salinity and often end up stunted but there is less growth inhibition in salt tolerant plants because they can store the salts within the plant tissue or excrete the salt through salt glands (Miyamoto *et al.*, 1994). Furthermore, application of highly saline-sodic water can produce contiguous patches of soil with high sodium content and low soil hydraulic conductivity (Adhikari *et al.*, 2012).

Germination of an individual seed is the sequence of physiological processes from imbibition to radicle protrusion (Bewley and Black, 1994). Typically, radicle protrusion is treated as a binary variable and is combined across individual seeds to provide insights on the germination percentages across seed populations. Final germination percentages have often been used to determine salinity effects on

seed germination; however, more information on the alleged impacts of salinity on population-level germination dynamics can be discerned by utilizing binary measures of radicle protrusion integrated over time. Studies have shown that despite comparable final germination percentages of seeds treated with water of increasing salinity, there is often a delay in germination (Shalaby, 1993; Almansouri, 2001; Flores *et al.*, 2015). Delayed germination under field conditions may increase the potential for seed mortality caused by pathogen infection (Dalling *et al.*, 2011). Thus, revegetation efforts on salt-contaminated soils should utilize halophyte species capable of rapid germination at the population level.

Another major concern with adding saline solution to a soil system is the affect the aqueous salts could have on soils. A study of factors affecting saturated hydraulic conductivity (Ks) showed that an increase in the sodium absorption ratio (SAR) decreased Ks (McNeal *et al.*, 1968). Soils with higher clay contents, like most agricultural soils, tend to show a larger decrease in Ks (Pupisky and Shainberg, 1979). The high salt content of RO wastewater concentrate could potentially accumulate within the soil and cause pore clogging. This could subsequently lead to further reduction in Ks and effectively change the soil profile. For this reason, concentrate-applied soil would also need to be monitored for pore clogging.

It has been shown that total shoot biomass and cumulative ET are directly related (Allen *et al.*, 1998). A recent study showed that increasing salinity decreased the yield of broccoli plants and the ET also decreased as a consequence of the salt increase (Smith *et al.*, 2013). Diaz *et al.* (2013) found that plants producing higher biomass under lower salinity levels generally had higher ET. However, they also noted that some halophytic species could tolerate high salt levels to produce acceptable biomass yields while maintain ET. A leaching fraction of 0.30 is reported to maintain a salt distribution conducive to plant growth, but some species, like many in the genus *Distichlis*, prefer wetter soils and others, like many *Atriplex* species, prefer drier soils (Miyamoto *et al.*, 1994). Studies have shown that the average leaching fraction is not only related to biomass but also ET: as leaching fraction increases, dry biomass increases and ET increase (Khan, 1996; Noaman and El-Haddad, 2000). However, ET still decreased with increasing salinity when leaching fractions were comparable among treatments.

Plants exposed to salinity tend to grow slower and are often stunted in growth. A study on bell peppers showed that as the EC of the irrigation water increased from 0.5 to 7 dS/m, the shoot and fruit weight both decreased (Ben-Gal *et al.*, 2008). Similarly, a study on *Panicum virgatum* and *Spartina pectinata* saw a decrease in plant growth with increasing salinity and increased ion uptake (Kim *et al.*, 2012) and another study on broccoli found that there was a decrease in the plant yield as a consequence of a salt increase (Smith *et al.*, 2013). Sometimes, the plants do not show any signs of growth interference at higher salinity and differences such as

thicker leaves or decreased grain yields are not apparent until they are compared to unaffected plants (Bernstein, 1975; Noaman and El-Haddad, 2000).

It has been noted that for moderate levels of salinity, photosynthetic rates were unaffected by salinity, although an eventual decrease with increasing salinity is sometimes observed (Alvarez *et al.*, 2012; Koyro *et al.*, 2013; Ge *et al.*, 2014). It was often seen that the photosynthetic rates had little effect on plant growth, an indication of salt tolerance (Koyro *et al.*, 2013; Ge *et al.*, 2014). Conversely, it has been seen that growth and osmotic potential are related: the higher the osmotic potential, the taller the plants (Saber *et al.*, 2011). Osmotic potential is reported to be a better index for ion affect on plants because different concentrations of salts cause similar reactions (Souza *et al.*, 2012). In general, salinity causes a reduction in leaf water potential as well as osmotic potential (Scholberg and Locascio 1999; Souza *et al.*, 2012) and the uptake of ions has been hypothesized to cause this reduction (Hussain *et al.*, 2014).

Some researchers have been studying the effects of land application of saline-sodic waters for agriculture but often use wastewaters with ECs between 4 and 6 dS/m which is similar to that of groundwater (Soliz *et al.*, 2011; Picchioni *et al.*, 2012; Ghermandi *et al.*, 2013). There is little guidance, however, concerning species selection and management. Because of the potential problems that could arise due to the land application, a better knowledge of candidate species and their responses to increasing salinity as well as management techniques can be crucial to making wastewater disposal safer and ultimately making inland desalination possible.

Because one of the main problems limiting the implementation of inland groundwater desalination systems is sustainable management of the highly saline RO wastewater concentrate, we believe that finding an acceptable method of disposal is the first step to employing these processes. Most studies on wastewater land application utilize various salt mixtures to determine the effects of salinity. This study improves our knowledge of candidate species for land application sites by making use of both saline groundwater and wastewater from the RO process.

Our general hypothesis is that with proper plant selection and the adoption of appropriate management techniques, saline groundwater and RO concentrate can be used to irrigate halophytes year-round. The objectives of the study were to: 1) improve knowledge of candidate species for cultivation on land application sites by comparing time-integrated measurements of germination among seed populations exposed to saline groundwater and concentrate from RO facilities, 2) determine how concentrated saline water affects the saturated hydraulic conductivity of two soils over time and to observe the effects of concentrated saline solution on soil, 3) evaluate the ET and leaching fractions under a salinity gradient, and 4) determine suitable species for land application sites by comparing growth parameters and ion uptake among greenhouse grown plants exposed to saline groundwater and concentrate from RO facilities.

Methods and Materials

Plant selection

Six plant species were selected for the study due to their high levels of salt tolerance: *Atriplex canescens* (Pursh) Nutt. (also known as fourwing saltbush or atriplex), *Hordeum vulgare* L. (barley), *Lepidium alyssoides* A. Gray (mesa pepperwort or lepidium), *Distichlis stricta* (Torr.) Rydb. (inland saltgrass or nipa grass), *Panicum virgatum* L. (switchgrass), and \times *Triticosecale* Wittm. (triticale). All seeds were purchased from Curtis & Curtis Inc. in Clovis, NM with the exception of the *L. alyssoides* seeds which were collected locally in Las Cruces, NM (32°16'N, 106°54'W).

To improve the germination rates for the *D. stricta* and the *A. canescens*, seeds of both species were pretreated prior to planting (Flores *et al.* 2015). The *D. stricta* seeds were placed into mesh packets which were then placed in a hydrated soil mixture at 4°C for 30 days. The soil mixture consisted of a 1:1, sand to soil volumetric ratio of QUIKRETE all-purpose sand (No. 1152) and soil from Leyendecker Plant Science Center in Las Cruces, NM that had been passed through a 4 mm sieve. The *A. canescens* seeds were treated using a method described by Twitchell (1955) that consisted of taking 30g of seed and soaking in 3L of water for two hours, followed by rinsing with 3L of distilled water, and air drying the seeds for seven days. Seeds of *D. stricta* feature a physiological dormancy that is presumably reduced during cool seasons under natural conditions. For this study, seeds were stratified in a hydrated soil mixture at 4°C for 30 days prior to the start of germination assays (Baskin and Baskin, 1998). For the *A. canescens* seeds, Twitchell's (1955) method of taking 30 g of seeds and soaking in 3 L of water for two hours, rinsing with 3 L of distilled water and air-drying for seven days to reduce seed dormancy was used to prepare the seeds.

Water treatments

This study utilized groundwater taken from the Brackish Groundwater National Desalination Research Facility (BGNDRF) located in the Tularosa Basin in Alamogordo, New Mexico (32°52'N, 105°58'W) which uses RO to desalinate well water. Four water treatments were selected to create a salinity gradient for the germination study: deionized water (electrical conductivity [EC] = 0 dS/m, sodium adsorption ratio [SAR] = non-detectable, pH = 5.6), university greenhouse irrigation tap water (EC = 0.6 dS/m, SAR = 2.1, pH = 8.1), BGNDRF well water (EC = 4 dS/m, SAR = 4.3, pH = 7.9), and BGNDRF RO concentrate (EC = 10 dS/m, SAR = 6.1, pH = 8.2). The germination study utilized the deionized water as the control whereas the greenhouse study considered the tap water as the control. The well from BGNDRF chosen for the study provided both the well

water and, after the RO process, the concentrate. The dominant cation in all treatments was calcium followed by sodium.

Treatment water samples were analysed for pH and EC according to EPA method 150.2 and EPA 120.1, respectively. The concentrations of Mg^{+2} , Na^{+1} , and Ca^{+2} ions were determined by analysing samples in a PerkinElmer Optima 4300 DV ICP-OES according to EPA 200.7 and the sodium adsorption ratios (SAR) were subsequently calculated (Robbins, 1983):

$$SAR = \frac{[Na^{+}]}{\sqrt{\frac{([Ca^{2+}] + [Mg^{2+}])}{2}}} \quad (1)$$

where $[Na^{+}]$ is the concentration of sodium ion (meq/L), $[Ca^{2+}]$ is the concentration of calcium ion (meq/L), and $[Mg^{2+}]$ is the concentration of magnesium ion in the sample (meq/L).

For the greenhouse study, each treatment was mixed with a half strength Hoagland's solution, giving a fertilizer to source water ratio of approximately 1:5. This resulted in ECs of approximately 0.9 dS/m, 4.1 dS/m, and 8.0 dS/m for the control, well water, and concentrate treatments, respectively. The fertilizer was applied to the plants with every irrigation.

Germination Experiment

The effects of the salt treatments on the germination of the species were determined using an experimental set-up consisting of 72 Petri dishes, each lined with two Whatman #2 filter papers (90 mm-diameter) and 3 mL treatment water. The experiment included two runs separated in time. For the first run, three samples of 20 seeds were separated out in each dish while 25 seeds were used for the second experiment. The Petri dishes were sealed with parafilm to reduce evaporation loss, but water was added as needed. The dishes were randomly arranged in a germination chamber set with 25/15°C (day/night) alternating temperatures, with a 12 hour photoperiod. Photosynthetic photon flux density within the chamber was approximately $30 \mu\text{mol m}^{-2} \text{s}^{-1}$. Seeds were considered germinated and removed once the length of the radicle surpassed the length of the seed. Ungerminated seeds remained in the dish until the conclusion of the study and their viability was determined using the imbibed crush test. The study ran for 22 days.

Parameters used to evaluate the effect of water treatment were germinability, mean germination time, germination index, Timson's index, and Timson's index modified and calculated using the following formulas (Ranal and Santana, 2006):

$$\text{Germinability} = \left(\sum_{i=1}^k n_i / S \right) \times 100\% \quad (2)$$

$$MGT = \sum_{i=1}^k n_i t_i / \sum_{i=1}^k n_i \quad (3)$$

$$GI = \sum_{i=1}^k |(23 - t_i)n_i|/S \quad (4)$$

$$T = \sum_{i=1}^K (g_i(K - j)) \quad (5)$$

$$T_{mod} = T/\sum_{i=1}^K g_i \quad (6)$$

Where k is the last day of germination, n_i is the number of newly germinated seeds on day i, S is the number of seeds in the experiment (germinated and viable, non-germinated), t_i is the number of days from the start of the experiment to day i, 23 is the number of days spent in the germination test plus 1, g_i is the number of newly germinated seeds in the time interval i, K is the total number of time intervals (days) and $j = 1-i$.

These parameters were chosen to: show the total percentage of viable seeds in a sample that complete the germination process (germinability), measure the time it takes seeds to germinate (GI and T), and give a time measurement that accounts for the total number of seeds that germinated within the Petri dish (MGT and T_{mod}). GI is limited because it includes non-germinated seeds in the calculation, making the calculation dependent on seed sample size. T is limited because it is only suitable when germination percentages of seed samples are comparable. MGT and T_{mod} both take into account the final germinability, which can vary from trial to trial, which minimizes the effect of germination percentage.

Soil Sampling

Soil samples were collected from BGNDRF on July 31, 2013 (32:53.081N and 105:58.624W). Soil samples were collected from the top 30 cm of soil, and were air-dried and sieved through a 2-mm sieve. A commercially available silica sand was selected to provide a contrasting soil for the experiment. Texture analysis was performed for both soils using the hydrometer method (Gee and Bauder, 1986), and Ks using the constant head method (Klute and Dirksen, 1986). For the soil moisture characteristics, a pressure plate extractor was used and soil moisture contents were determined for the potentials of 0, -0.03, -0.1, -0.2, -0.3, -0.5, -1.0, and -1.5 MPa (Klute, 1986) and a van Genuchten curve was fitted to the data using the equation (Shukla, 2014):

$$\theta_i = \theta_r + \frac{\theta_s - \theta_r}{[1 + (\alpha\phi_i)^n]^m} \quad (7)$$

Where θ_i is the moisture content at pressure i, θ_r is the residual water content at the permanent wilting point (PWP), θ_s is the water content at saturation, α is a fitting parameter, ϕ_i is the ith pressure, n is a fitting parameter, and $m = 1 - 1/n$.

Saturated paste extracts from soil samples were prepared to determine the pH, EC, and the concentrations of Mg^{+2} , Na^{+1} , and Ca^{+2} ions, also analyzed in a

PerkinElmer Optima 4300 DV ICP-OES. The sodium adsorption ratio (SAR) was then calculated according to equation (1).

Pore Clogging Experiment

Sixteen columns (3.8 cm-diameter, 10 cm-height) were packed for the study: eight with clay, eight with sand. A piece of cheesecloth and small gravel were packed first to prevent the soil loss through the drainage holes at the bottom of the columns. Soil was loosely packed in the columns, giving a height of soil of approximately 8.3 cm.

The bulk density of each column was determined and assuming a particle density of 2.65 g/cm³, the porosity was calculated for each column. Prior to any treatments, the clay was washed with 3 pore volumes of deionized water to remove salts in the soil. The 16 columns were then wetted from the bottom over the course of 24 hours to ensure that there was no entrapped air in the sample. The initial K_s of the samples was determined using the constant head method (Klute and Dirksen, 1986).

The soil columns were irrigated with one pore volume of the concentrate and given a week to dry. The day of treatment and the following 2 days columns were left to air drying in the laboratory. The following 3 days drying was done in a chamber to simulate the southern New Mexico climate. The chamber was set to maintain a 35°C/25°C (day/night) temperatures, with a 12 hour photoperiod. The columns were removed from the chamber on the day prior to the subsequent irrigation and were allowed to equilibrate with room temperature. This cycle was continued for 20 weeks. For weeks 21-24, the time between irrigation was reduced to one application every two weeks. The same procedure was followed throughout irrigation –drying events.

The change in K_s was assessed by conducting tests every 4 weeks. The second and all subsequent K_s tests were performed using concentrate rather than tap water to avoid clearing any salt-clogged pores.

Greenhouse Plant Survival Cylinder Preparation

Larger size cylindrical columns (6.4 cm-diameter, 25.4 cm-height) were used for the greenhouse study and cheesecloth and small gravel were placed at the bottom of the columns to prevent soil loss. Columns were then packed with two contrasting soils, one collected from the BGNDRF site and a commercially available fine silica sand, to a constant bulk density. Prior to the planting of seeds, it was determined that the columns containing clay contained a large amount of salts and therefore, the columns were leached until the average EC of the leachate was < 5 dS/m. The columns with sand were slowly saturated from the bottom through sub-irrigation.

The experiment was conducted at NMSU Fabian Garcia greenhouse located in Las Cruces, NM (32°16'43"N, 106°46'23"W). The first sand experiment ran from January 2014 to April 2014 and the second experiment ran from June 2014 to September 2014. The first clay experiment was conducted from March 2014 to June 2014 and the second experiment from June 2014 to September 2014.

Seeds were planted in the top 1 cm of soil. Control water was used during the plant establishment to ensure a consistent growth pattern. Fertilizer was not applied to the seedlings until at least one leaf had established to prevent burning. To prevent shock, treatments were gradually introduced to the plants after a seedling establishment period of four weeks. The plants were arranged in a completely randomized design by generating random number using Data Analysis in MS Excel (2013).

Water Balance Experiment

Plant species were irrigated with the same volume of treatment water and with the same frequency within an experiment. This was done to maintain a consistent irrigation schedule rather than a consistent leaching fraction to represent a field containing all species intermixed. The volumetric leaching fractions for the plants were determined using the following equation (Ayers and Wescott, 1985):

$$LF = V_{\text{drainage}}/V_{\text{irrigation}} \quad (8)$$

Where V_{drainage} is the volume of water applied (cm^3) and $V_{\text{irrigation}}$ is the volume of leachate (cm^3).

The evapotranspiration (ET) rates of the plants were calculated for each species and water treatment. The following water balance equation was used for this calculation (Shukla, 2014):

$$ET = IR + R - \Delta S - RO - DP \quad (9)$$

Where IR is the irrigation depth (cm; = 0), R is rainfall (cm), ΔS is the change in soil water content (cm), RO is runoff (cm; = 0), and DP is the deep percolation (cm; leachate collected from the bottom of the column).

Plant Growth Measurements

Five physical measurements were taken to measure the plant growth over the course of 90 days: height, number of stem nodes, average internodal length, number of leaves, and leaf length. These measurements were taken at day 30, 60, and 90 from the start of each experiment. The height of the main, live stem was measured from the base of the stem to the highest node. The stem nodes were designated as any area where one or more branches away from the stem were noted and were counted and recorded. For the average intermodal length, the

distance between the nodes was measured along the main stem and the mean was calculated and recorded. The number of leaves for each plant were counted and recorded. The leaf length was determined by measuring from the node, up the midrib, to the apex of the third leaf from the top of the main stem. The exception for this measurement was the *P. virgatum* plants grown in the clay soil due to the fact that several of these plants did not grow more than two leaves. In this case, the second leaf from the top of the main stem was measured.

Using a LiCor LI-6400XT Portable Photosynthesis System unit, photosynthetic rates, conductance rates, leaf temperatures, and transpiration rates were measured. These measurements were taken on days 60 and 90.

Other measurements include, stem water potential, osmotic potential, dry biomass, ion uptake, and chloride content. The stem water potential of the plants were measured using a pressure bomb and were measured after 90 days of growth had been achieved. Osmotic potential was determined by taking leaf samples, placing them in a freezer for at least 24 hours, crushing the leaves, and then centrifuging the samples for 5 minutes at 13000 rpm to extract the cell sap. A Wescor Vapro osmometer was used to measure the concentration of the solution and the following equation was used to calculate the osmotic potential (Ψ_s) (Shukla, 2014):

$$\Psi_s = -CiRT \quad (10)$$

Where C is the concentration of the solution (as determined by the osmometer), i is the ionization constant (taken as 1.8 for saline solutions), R is the gas constant ($0.00831 \text{ kg MPa mol}^{-1} \text{ K}^{-1}$), T is temperature in Kelvin.

At the conclusion of the greenhouse study, the plants were harvested by cutting the plant at the soil surface. The plants were dried at 65°C for 3 days and weighed to determine the dry biomass. The dry biomass was used to determine the ion uptake via microwave digestion by taking 0.5 g of plant matter ground to pass through a 40 mesh and mixing with 5 mL of concentrated nitric acid (HNO_3) and 2 mL of 30% hydrogen peroxide (H_2O_2). The mixture was heated in a Microwave Accelerated Reaction System (MARS5 HP-500 Plus) and following a cooling period, the samples were filtered, diluted, and analyzed using the PerkinElmer Optima 4300 DV ICP-OES according to EPA methods 3051A and 200.7. This process determined the concentrations of S, B, Zn, P, Fe, Mn, Mg, Ca, Cu, Al, Na, and K. The dry biomass was also used to determine the chloride content of the plant samples and was determined by taking 0.2 g of plant matter (< 40 mesh) and mixing with 50 mL of 2% acetic acid. The solution was shaken for 30 minutes before being filtered and analyzed on a Technicon Autoanalyzer II.

Saturated soil paste extracts were prepared at the conclusion of the experiment. One sample was analyzed for each soil-species-water treatment combination for the first experiment with clay, however, both soils were analyzed during second

experiment. The extract was prepared according to the method described by Gavlak *et al.* (1994) and samples were analyzed for pH and EC. Using the PerkinElmer Optima 4300 DV ICP-OES, saturated paste extracts were analyzed for Mg^{+2} , Na^{+1} , and Ca^{+2} ions according to EPA 200.7. The sodium adsorption ratio (SAR) was calculated according to equation (1).

Statistical Analysis

Statistical analyses for the germination study were performed using the open source statistical software program R (R Core Team, 2015). For each species, solution effects on germination metrics were determined using analyses of variance. To meet the assumptions of constant variance as indicated by visual inspections of plots of residuals versus predicted values, specific datasets were square-root transformed prior to analysis.

Statistical analyses for the water balance and greenhouse study were performed using SAS software, v 9.2 and v 9.4, respectively. For each species, differences due to water treatments were determined using analyses of variance (ANOVA). Means were separated by least significant difference (LSD) and were considered significant for an alpha (α) value of 0.05. Results were modeled using a general linear model.

Results and Discussion

Water treatments

The ECs for the deionized, greenhouse, well, and concentrate waters, prior to the addition of fertilizer, were 0.6, 4.0, and 10.0 dS/m, respectively (Table 1). The SAR was 2.1, 4.3, and 6.1 for the greenhouse water, well water, and RO concentrate, respectively. However, SAR was <13 for all waters, making the greenhouse tap neither saline nor sodic, and the well and concentrate water treatments saline but not sodic.

Table 1 – Treatment analysis of waters used in study: deionized water; water from the Fabian Garcia (FG) greenhouses in Las Cruces, NM; well water from Brackish Groundwater National Desalination Research Facility (BGNDRF) in Alamogordo, NM; RO waste concentrate from BGNDRF. *ND indicates non-detection.

Type of Water	Mg (meq/L)	Ca (meq/L)	Na (meq/L)	K (meq/L)	EC (dS/m)	SAR	pH
Deionized	ND*	ND	ND	ND	0	ND	5.6
FG Greenhouse	0.7	2.5	2.6	4.5	0.6	2.1	8.1
BGNDRF Well	13.1	17.4	16.9	6.9	4.0	4.3	7.9
BGNDRF Concentrate	42.7	52.1	42.2	12.8	10.0	6.1	8.2

In the well water, the dominant cation was calcium with 17.4 meq/L, followed by sodium (16.9 meq/L) and magnesium (13.1 meq/L). The dominant cation in the RO concentrate was calcium (52.1 meq/L), while sodium and magnesium were 42.2 and 42.7 meq/L, respectively. These results were consistent with the large amount of calcium in the soil in the form of CaCO₃ (Gypsum).

Germination Study

The five response variables MGT, GI, T and T_{mod} were analyzed at $\alpha = 0.05$ for each halophyte species across saline water treatments. There were statistically significant differences noted in all species but for different indices and to different extents (Table 2).

Table 2 – Effect of salinity on germination parameters of seeds of *A. canescens*, *H. vulgare*, *L. alyssoides*, *D. stricta*, *P. virgatum* and *×Triticosecale*. Abbreviations: MGT, mean germination time; GI, germination index; T, Timson's index; T_{mod}, Timson's modified index. The values followed by different letters were significantly different within a species at $P < 0.05$. Results are means of six replicates and standard errors (SE) were calculated using the formula $SE = S / \sqrt{n}$, where S is the standard deviation of the replicate mean and n is the number of replicates.

Species	EC	Germination Indices				
		Germinability (%) ± SE	MGT (day) ± SE	GI (seeds day ⁻¹) ± SE	T (% day) ± SE	T _{mod} (day) ± SE
<i>A. canescens</i>	0	36.5 ± 5.6	7.11 ± 0.94	5.7 ± 0.8	70.00 ± 12.44	8.45 ± 0.47
	0.9	28.3 ± 3.4	6.36 ± 0.46	4.7 ± 0.5	56.67 ± 8.09	8.82 ± 0.23
	4.1	26.7 ± 3.4	6.80 ± 0.48	4.3 ± 0.6	51.67 ± 7.00	8.60 ± 0.24
	8	31.8 ± 6.7	6.43 ± 0.20	5.2 ± 1.1	63.83 ± 13.55	8.78 ± 0.10
<i>H. vulgare</i>	0	99.3 ± 0.7	4.14 ± 0.14 a	18.7 ± 0.2 a	221.50 ± 9.28 a	9.93 ± 0.07 a
	0.9	99.2 ± 0.8	4.37 ± 0.15 a	18.5 ± 0.2 ab	218.83 ± 10.63 ab	9.81 ± 0.07 a
	4.1	98.3 ± 1.7	4.74 ± 0.17 b	18.0 ± 0.3 bc	213.00 ± 10.95 bc	9.63 ± 0.08 b
	8	98.7 ± 1.3	5.06 ± 0.14 c	17.7 ± 0.3 c	209.67 ± 8.48 c	9.47 ± 0.07 c
<i>L. alyssoides</i>	0	92.0 ± 2.1 a	5.98 ± 0.23 bc	15.6 ± 0.3 bc	186.33 ± 9.95 bc	9.01 ± 0.12 ab
	0.9	92.0 ± 2.6 a	6.96 ± 0.26 a	14.8 ± 0.5 c	175.50 ± 7.14 c	8.52 ± 0.13 c
	4.1	98.5 ± 1.0 b	5.60 ± 0.22 c	17.1 ± 0.3 a	203.83 ± 10.16 a	9.20 ± 0.11 a
	8	97.2 ± 1.4 b	6.51 ± 0.16 bc	16.0 ± 0.2 b	190.83 ± 8.65 b	8.74 ± 0.08 bc
<i>D. stricta</i>	0	84.8 ± 5.0	6.67 ± 0.34 a	13.9 ± 1.0	164.17 ± 9.31	8.66 ± 0.17 a
	0.9	81.7 ± 4.8	6.59 ± 0.34 a	13.5 ± 1.0	158.17 ± 6.95	8.70 ± 0.17 a
	4.1	85.0 ± 4.8	6.70 ± 0.36 a	13.9 ± 0.9	163.83 ± 8.01	8.65 ± 0.18 a
	8	84.3 ± 3.7	7.26 ± 0.48 b	13.3 ± 0.9	157.17 ± 5.02	8.37 ± 0.24 b
<i>P. virgatum</i>	0	76.0 ± 4.1	7.08 ± 0.15 a	12.1 ± 0.7	145.50 ± 12.50	8.46 ± 0.08
	0.9	74.2 ± 5.9	7.09 ± 0.23 a	11.8 ± 0.9	141.50 ± 13.74	8.46 ± 0.12
	4.1	76.7 ± 5.1	7.20 ± 0.21 a	12.1 ± 0.7	146.17 ± 14.98	8.40 ± 0.11
	8	78.5 ± 4.6	8.43 ± 0.17 b	11.4 ± 0.5	138.17 ± 12.19	7.78 ± 0.09
<i>×Triticosecale</i>	0	99.3 ± 0.7	3.85 ± 0.11 a	19.0 ± 0.2	224.83 ± 9.71	10.08 ± 0.05 a
	0.9	99.3 ± 0.7	4.01 ± 0.09 ab	18.9 ± 0.2	223.00 ± 9.65	9.99 ± 0.04 ab
	4.1	97.5 ± 1.7	4.17 ± 0.08 b	18.4 ± 0.3	218.00 ± 13.19	9.91 ± 0.04 b
	8	96.8 ± 1.6	4.22 ± 0.18 b	18.2 ± 0.2	215.33 ± 11.05	9.89 ± 0.09 b

Because the weighted MGT and T_{mod} take into account the final cumulative germinability of the seed samples which minimizes the effect of the germination percentage, these differences were more pronounced. Analyses of the final

germination percentages determined that the difference among water treatments within a species was not significant for five of the six halophytes studied. The *L. alyssoides* seeds were the only ones to show a difference in final germination with higher germinations observed for the higher salinity treatments.

Although the final germination percentages across the treatments were comparable within the species, there was evidence of variability among treatments between the onset of germination and the final seed germination, indicating a delay for some species (Figure 1). This is supported by the results from the MGT, GI, T, and T_{mod} comparisons for each species (Table 2). Significant differences were noted in the MGT of all species except *A. canescens*. The largest differences were noted for *H. vulgare*, *D. stricta*, and *P. virgatum*. The GI and T, which take into account total final germinability, only showed differences for two species, *H. vulgare* and *L. alyssoides*. Like the weighted MGT, T_{mod} takes into account the cumulative germination of the seed sample and showed a significant difference for four species: *H. vulgare*, *L. alyssoides*, *D. stricta*, and \times *Triticosecale*.

Seeds from *L. alyssoides* were most sensitive to changes in water salinity, as indicated by the significant differences observed in all five calculated indices. *A. canescens* was the least susceptible with no significant differences noted in indices. *H. vulgare* had the second highest number of significant differences with four of the five indices showing significance. *D. stricta* and \times *Triticosecale* each contained significant differences for MGT and T_{mod} while *P. virgatum* noted a significant difference solely in MGT. All the indices, aside from the germinability, are related to the germination time of a species. These results show that increasing salinity delayed germination of all species, except *A. canescens*, and germination was time dependent, indicating a delay. The final germination percentage (germinability) showed no significant differences for the species (except *L. alyssoides*) indicating that the germinability was not affected by the water treatment.

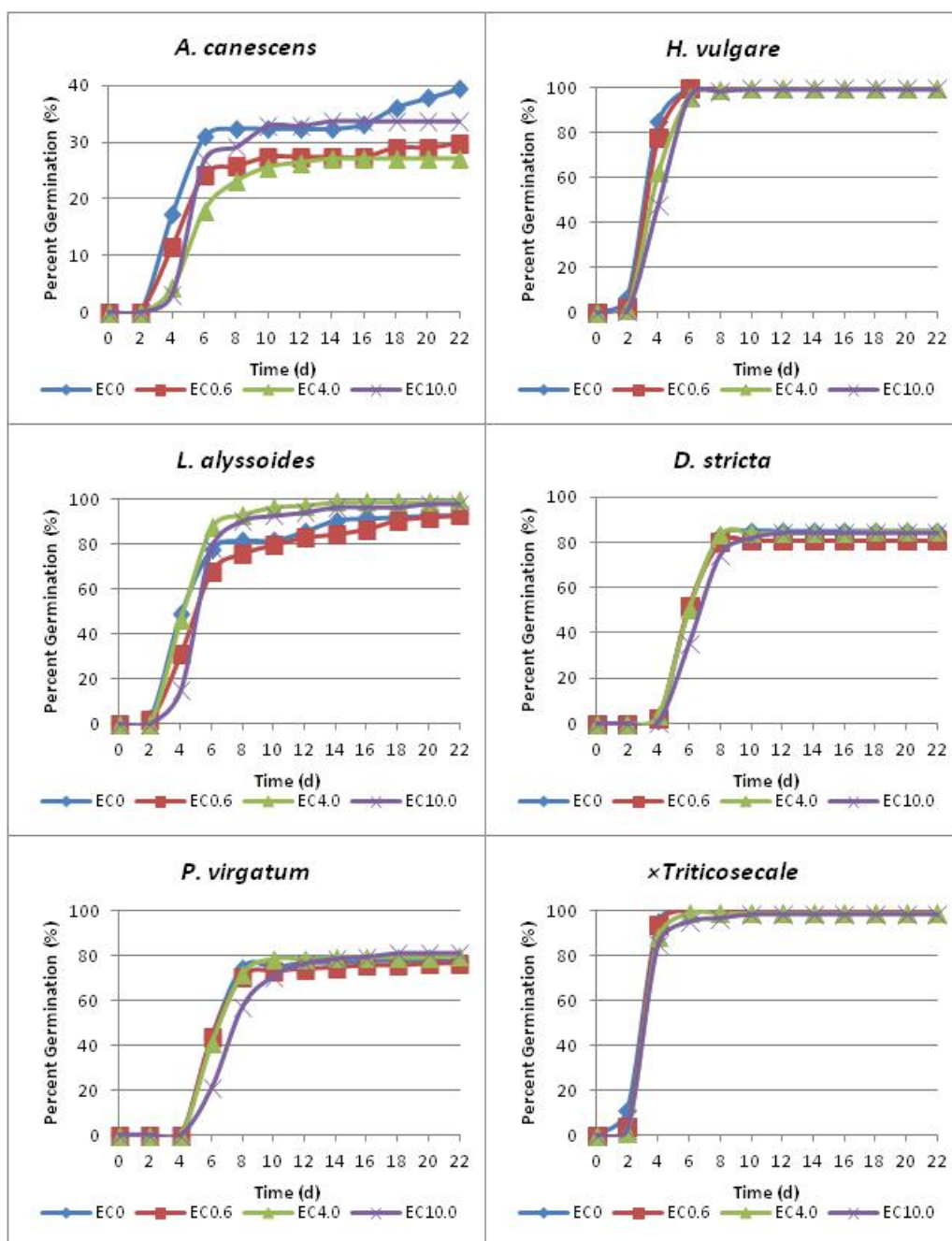


Figure 1 – Cumulative germination of halophyte seeds of *A. canescens*, *H. vulgare*, *L. alyssoides*, *D. stricta*, *P. virgatum* and *Tritico-secale* over 22 days, under different salt concentration treatments: EC 0, 0.6, 4.0, and 10.0 dS/m. Results are means of six replicates across two runs.

Soil Sampling

According to USDA textural classification, the soil collected from BGNDRF was classified as clay and commercial soil was sand (Table 3). The K_s was 5.9 ± 2.5 cm/h from clay and 150.4 ± 13.5 cm/h from sand. The clay soil from BGNDRF contained large amounts of salts. The concentrations of magnesium, calcium, and

sodium were found to be 70.1, 155, and 127 meq/L, respectively (Table 4). With an EC of 28.9 dS/m, the soil was classified as highly saline and with an SAR of 11.95 and it was classified as borderline sodic. The dominant cation found in the clay soil was calcium, which was consistent with the groundwater at the site. The commercial sand had a significantly lower amount of salt than the clay with magnesium, calcium, and sodium concentrations of 0.8, 4.7, and 5.2 meq/L, respectively. Although dominant cation was sodium, sand had an EC of 1.2 dS/m and an SAR of 3.15 making it neither saline nor sodic.

Table 3 – Hydrometer method, texture analysis results for two soils in the study. Bulk density results are the packing readings for the study's plant column preparations.

Property	% Sand	% Silt	% Clay	Soil Texture	Bulk Density (g/cm ³)
Soil 1	19.57	28.96	51.47	Clay	1.07
Soil 2	99.60	0.07	0.32	Fine Sand	1.00

Table 4 – Mg²⁺, Ca²⁺, Na⁺, and K⁺ ion concentrations for the clay soil collected at BGNDRF, along with the EC, SAR, and pH readings for the soil.

Property	Mg (meq/L)	Ca (meq/L)	Na (meq/L)	EC (dS/m)	SAR	pH
Clay Soil	70.1	155.0	127.0	28.9	11.95	7.5
Sand Soil	0.9	4.7	5.2	1.2	3.15	7.5

The van Genuchten parameters from soil moisture retention curves (Figure 2) were found to be very different for the clay and the sand. The α value for the clay was $0.002582 \pm 0.000073 \text{ cm}^{-1}$ whereas the α for sand was $0.009198 \pm 0.002340 \text{ cm}^{-1}$. The n values were 1.7425 ± 0.0471 and 3.1466 ± 0.1481 for clay and sand, respectively.

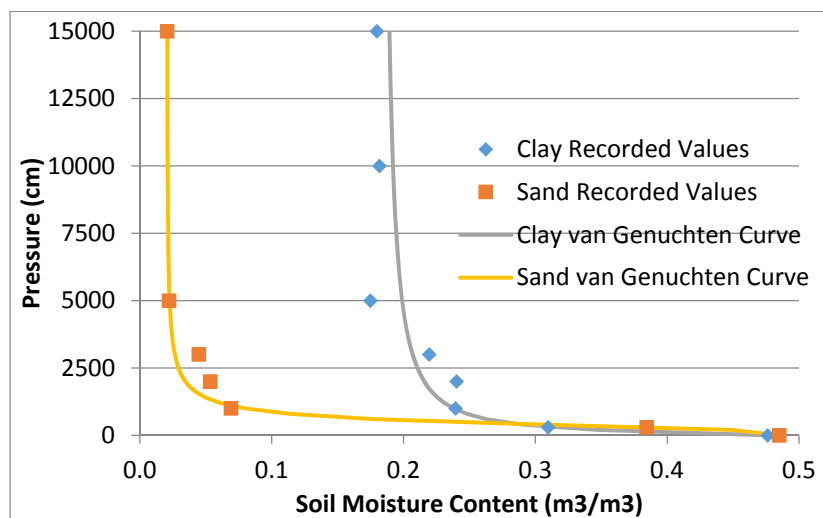


Figure 2 – van Genuchten drying curves for the clay and sand. 1 cm water = 0.001 MPa.

Pore Clogging

Overall, the soils maintained Ks with the application of the saline RO concentrate, although both showed a decrease in Ks. Both the sand and clay samples experienced a decrease in Ks from week 0 to week 4 (Figure 3). Some of this decrease can be attributed to the accumulation of salts within the pore which was also visually evident around the drainage holes (Figure 4). Additionally, the settling of soil particles within the samples, particularly in the clay could be the cause of the decrease in Ks as the movement of finer particles into pores can cause blockage (Pupisky and Shainberg, 1979). A high amount of sodium in water is another cause of hydraulic conductivity reduction shown in previous studies (McNeal *et al.*, 1968; Pupisky and Shainberg, 1979; Adhikari *et al.*, 2014). The pore clogging mechanism study by deVries (1972) suggested that allowing soils to drain daily may have helped maintain Ks. It has also been observed that when calcium and magnesium are present in similar amounts as sodium in the saline solution (like the BGNDRF RO concentrate), the deterioration of soil structure is reduced, helping permeability (Singh *et al.*, 2011).

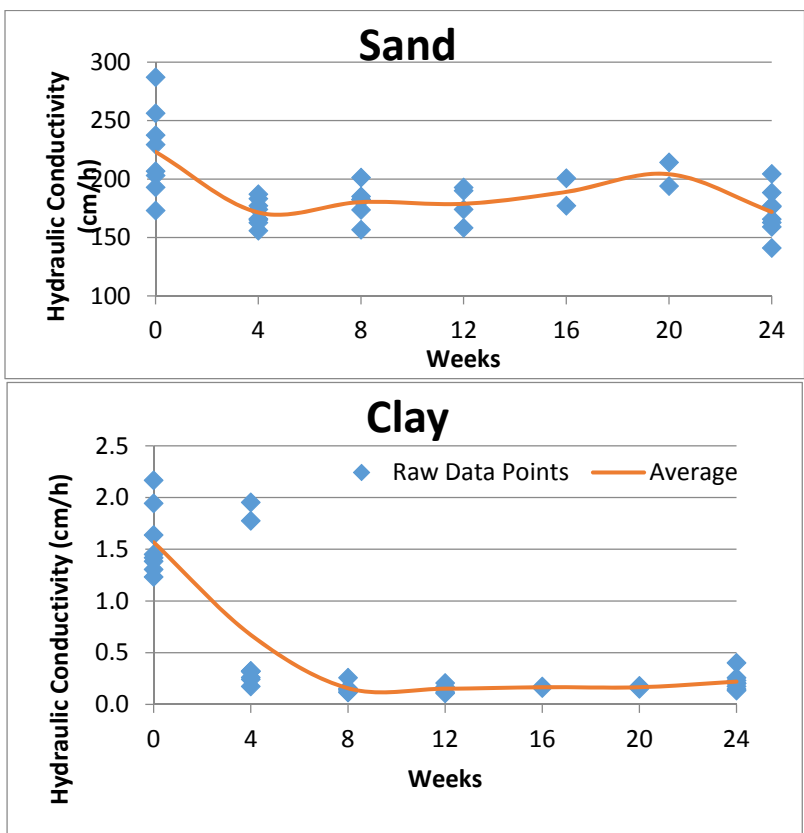


Figure 3 – Graphs showing the change in hydraulic conductivity over time for sand and clay samples.

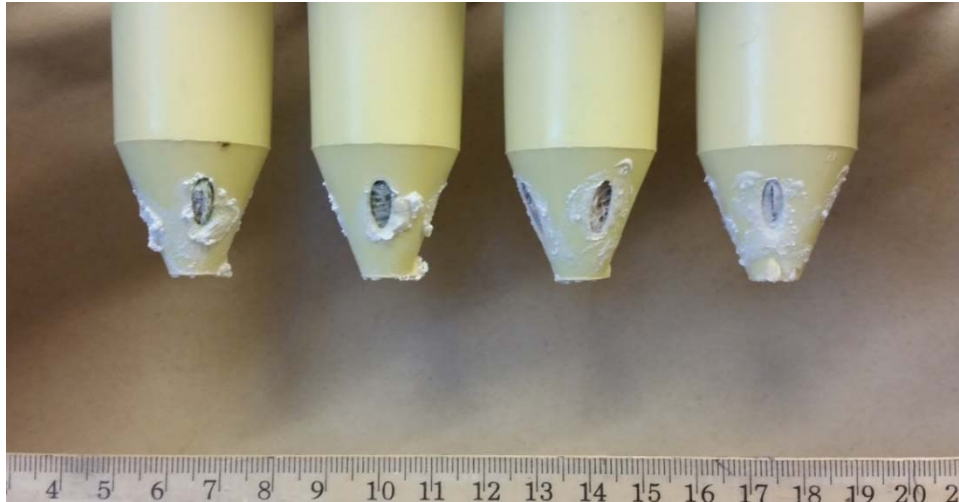


Figure 4 – Salt accumulation at drainage holes of columns. Salt buildup was evident in all clay and sand samples.

The clay soil showed little variability in K_s after the initial drop as opposed to the sand soil. The clay soil also had a much lower K_s than the sand which can be expected as other studies have noted that an increase in clay content can cause a decrease in K_s (McNeal *et al.*, 1968). Although the clay showed some cracks with drying, this likely did not increase K_s as the clay swelled with the addition of concentrate, closing the cracks (Figure 5). However, it has been observed that clay swelling can lead to a sealing of pores which could, in addition to salt accumulation, lower permeability (Pupisky and Shainberg, 1979).

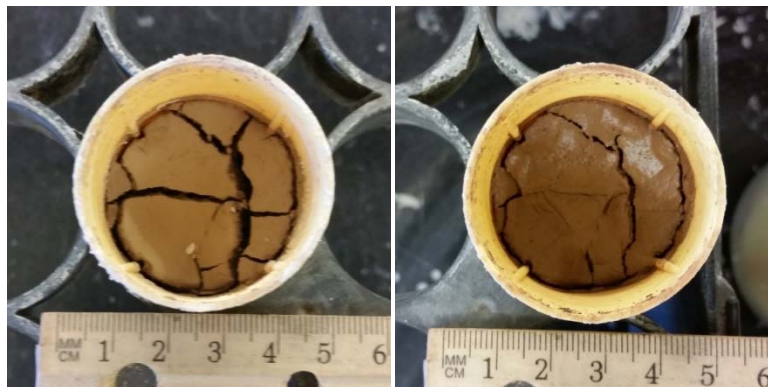


Figure 5 – Cracks formed in clay samples following a drying cycle. All clay samples showed evidence of cracking with drying. On the left, dry clay just prior to concentrate application. On the right, wet clay just after application.

The sand soil was much more variable than the clay and showed increasing as well as decreasing K_s over time. This could be due to the surface crusting that was observed in the sand columns (Figure 6). The buildup of salt and the clogging of pores at the soil surface can lead to decreased K_s . The surface clogging is typically responsible for most of the decrease in K_s (Rice, 1974). Because the

majority of the Ks issues are at the surface of the soil, any disruption in the layer could temporarily increase water flow (deVries, 1972; Lal and Shukla, 2004). However, despite the varying Ks over time, the sand soil maintained a high level of permeability, something that has been previously observed (deVries, 1972).

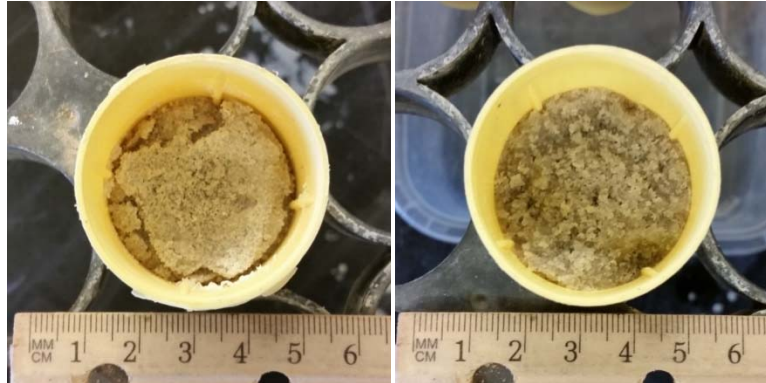


Figure 6 – Surface crusting in the sand samples. Crusting was evident in all sand samples. On the left, dry sand just prior to concentrate application. On the right, wet sand just after application.

This section of the study has shown that a problem with water retention and water movement can arise with land application of RO concentrate and thus a management plan, such as leaching, is needed.

Water Balance

Evapotranspiration and Deep Percolation

The sand-grown plants showed varying results for different species and showed more significant differences for the mean total ET and DP (Table 5). *H. vulgare* and *×Triticosecale* plants responded similarly and showed statistically significant differences with increasingly salinity in both experiments. Both saw decreases in ET with increasing salinity and consequently significant increases in DP as well. In the first experiment, 3% of the control irrigation water was lost to DP for both species, but this number increased during the second experiment to 25% and 14% for the *H. vulgare* and *×Triticosecale*, respectively. In contrast, the concentrate plants saw DP of 17% and 33% for *H. vulgare* and 20% and 32% for *×Triticosecale* for the first and second experiments, respectively. These two species saw the greatest ET losses and lowest DP amounts of all species studied. Only the *D. stricta* plants grown in the sand showed any difference in ET or DP. For both experiments, the highest values for ET and the lowest values of DP were found in the control plants. The *L. alyssoides* plants saw a difference in ET and DP for the first experiment only, whereas the *P. virgatum* plants only showed a difference in the second experiment. However, like the other species, the highest ET and lowest DP values were seen in the control. There were no significant differences in ET or DP for either sand experiment for the *A. canescens* plants: the plants treated with well water and RO concentrate showed ET and DP values

close to the control. This species was the only one of the six to show no differences for ET or DP with increasing salinity.

Table 5 – Total water balance readings (cm) for the six halophyte species at the conclusion of each of the two study periods for the sand soil. Different letters across a row correspond to a statistically significant difference in total irrigation (IR), deep percolation (DP), and evapotranspiration (ET) means within a species at $\alpha = 0.05$. Measurements were not compared across species.

		Water Balance Calculations (cm)											
		Sand 1					Sand 2						
Species	Water	EC 0.9 ± SE	EC 4.1 ± SE	EC 8.0 ± SE	EC 0.9 ± SE	EC 4.1 ± SE	EC 8.0 ± SE	EC 0.9 ± SE	EC 4.1 ± SE	EC 8.0 ± SE	EC 0.9 ± SE		
<i>A. canescens</i>	IR (cm)	80.58 ± 0.00	a	80.58 ± 0.00	a	80.58 ± 0.00	a	97.89 ± 0.00	a	97.89 ± 0.00	a	97.89 ± 0.00	a
	DP (cm)	22.67 ± 4.49	a	23.31 ± 3.24	a	22.66 ± 1.25	a	40.40 ± 3.30	a	40.57 ± 3.93	a	34.38 ± 2.35	a
	ET (cm)	57.91 ± 4.49	a	57.27 ± 3.24	a	57.92 ± 1.25	a	57.49 ± 3.30	a	57.32 ± 3.93	a	63.51 ± 2.35	a
<i>H. vulgare</i>	IR (cm)	80.58 ± 0.00	a	80.58 ± 0.00	a	80.58 ± 0.00	a	97.89 ± 0.00	a	97.89 ± 0.00	a	97.89 ± 0.00	a
	DP (cm)	2.51 ± 0.78	c	6.37 ± 0.27	b	13.85 ± 1.59	a	24.48 ± 1.39	b	28.02 ± 1.30	ab	32.52 ± 1.65	a
	ET (cm)	78.07 ± 0.78	a	74.21 ± 0.27	b	66.73 ± 1.59	c	73.41 ± 1.39	a	69.87 ± 1.30	ab	65.37 ± 1.65	b
<i>L. alyssoides</i>	IR (cm)	80.58 ± 0.00	a	80.58 ± 0.00	a	80.58 ± 0.00	a	97.89 ± 0.00	a	97.89 ± 0.00	a	97.89 ± 0.00	a
	DP (cm)	12.00 ± 1.53	b	22.52 ± 1.26	a	25.59 ± 2.01	a	45.40 ± 2.43	a	49.48 ± 2.59	a	50.20 ± 2.22	a
	ET (cm)	68.58 ± 1.53	a	58.06 ± 1.26	b	54.99 ± 2.01	b	52.49 ± 2.43	a	48.41 ± 2.59	a	47.69 ± 2.22	a
<i>D. stricta</i>	IR (cm)	80.58 ± 0.00	a	80.58 ± 0.00	a	80.58 ± 0.00	a	97.89 ± 0.00	a	97.89 ± 0.00	a	97.89 ± 0.00	a
	DP (cm)	30.02 ± 0.83	b	30.31 ± 3.14	ab	36.61 ± 1.37	a	52.35 ± 1.39	b	56.62 ± 2.75	ab	60.18 ± 1.71	a
	ET (cm)	50.56 ± 0.83	a	50.27 ± 3.14	ab	43.97 ± 1.37	b	45.54 ± 1.39	a	41.27 ± 2.75	ab	37.71 ± 1.71	b
<i>P. virgatum</i>	IR (cm)	80.58 ± 0.00	a	80.58 ± 0.00	a	80.58 ± 0.00	a	97.89 ± 0.00	a	97.89 ± 0.00	a	97.89 ± 0.00	a
	DP (cm)	34.05 ± 1.87	a	36.76 ± 1.81	a	39.56 ± 1.64	a	50.39 ± 1.17	c	53.70 ± 1.12	b	58.42 ± 0.58	a
	ET (cm)	46.53 ± 1.87	a	43.82 ± 1.81	a	41.02 ± 1.64	a	47.50 ± 1.17	a	44.19 ± 1.12	b	39.47 ± 0.58	c
× <i>Triticosecale</i>	IR (cm)	80.58 ± 0.00	a	80.58 ± 0.00	a	80.58 ± 0.00	a	97.89 ± 0.00	a	97.89 ± 0.00	a	97.89 ± 0.00	a
	DP (cm)	2.80 ± 0.56	c	8.11 ± 1.74	b	16.16 ± 1.91	a	14.06 ± 0.83	c	20.04 ± 1.75	b	30.92 ± 0.50	a
	ET (cm)	77.78 ± 0.56	a	72.47 ± 1.74	b	64.42 ± 1.91	c	83.83 ± 0.83	a	77.85 ± 1.75	b	66.97 ± 0.50	c

The species did not necessarily perform better in the sand than in the clay (Table 6). The ET tended to be lower and the DP tended to be higher for all species grown in clay than in the sand. Both experiments showed a difference in ET and DP with increasing salinity for ×*Triticosecale* and it was the only one of the six species to show a difference for the first clay experiment. Unlike the sand, however, the ×*Triticosecale* saw higher values for the ET and lower values for the DP in the concentrate grown plants than in the control grown plants. For the first experiment, the control plants saw 39% of the irrigation water lost to DP whereas the RO concentrate irrigated plants only lost 33% of the irrigation water to DP. Despite this deviation from the norm for the ET and DP, the values for the species were still the highest ones noted for any of the plants grown in the clay. For the ×*Triticosecale*, it was observed that as salinity increased, ET decreased and DP increased. Like the sand plants, the control plants saw higher ET and lower DP values than the RO concentrate grown plants with 22% and 35% of the irrigation water lost to DP, respectively. The *H. vulgare* and *P. virgatum* plants only saw a difference in ET and DP for the second experiment and like the second experiment for ×*Triticosecale*, an increase in salinity saw a decrease in ET and an increase in DP. The *A. canescens*, *L. alyssoides*, and *D. stricta* plants did not show any difference in ET or DP with increasing salinity in the clay soil. Within these species, the values for the plants treated with saline irrigation water were consistent with the control values.

Table 6 – Total water balance readings (cm) for the six halophyte species at the conclusion of each of the two study periods for the clay soil. Different letters across a row correspond to a statistically significant difference in total irrigation (IR), deep percolation (DP), and evapotranspiration (ET) means within a species at $\alpha = 0.05$. Measurements were not compared across species.

Species	Water	Water Balance Calculations (cm)											
		Clay 1					Clay 2						
		EC 0.9 ± SE	EC 4.1 ± SE	EC 8.0 ± SE	EC 0.9 ± SE	EC 4.1 ± SE	EC 8.0 ± SE	EC 0.9 ± SE	EC 4.1 ± SE	EC 8.0 ± SE			
<i>A. canescens</i>	IR (cm)	80.90 ± 0.00	a	80.90 ± 0.00	a	80.90 ± 0.00	a	84.94 ± 0.00	a	84.94 ± 0.00	a	84.94 ± 0.00	a
	DP (cm)	36.04 ± 1.85	a	39.31 ± 1.03	a	36.67 ± 1.35	a	46.32 ± 1.21	a	46.23 ± 0.62	a	43.12 ± 1.59	a
	ET (cm)	44.86 ± 1.85	a	41.59 ± 1.03	a	44.23 ± 1.35	a	38.62 ± 1.21	a	38.71 ± 0.62	a	41.82 ± 1.59	a
<i>H. vulgare</i>	IR (cm)	80.90 ± 0.00	a	80.90 ± 0.00	a	80.90 ± 0.00	a	84.94 ± 0.00	a	84.94 ± 0.00	a	84.94 ± 0.00	a
	DP (cm)	29.15 ± 0.46	a	26.06 ± 1.71	a	29.78 ± 1.47	a	29.09 ± 3.71	b	37.25 ± 2.71	ab	38.19 ± 0.83	a
	ET (cm)	51.75 ± 0.46	a	54.84 ± 1.71	a	51.12 ± 1.47	a	55.85 ± 3.71	a	47.69 ± 2.71	ab	46.75 ± 0.83	b
<i>L. alyssoides</i>	IR (cm)	80.90 ± 0.00	a	80.90 ± 0.00	a	80.90 ± 0.00	a	84.94 ± 0.00	a	84.94 ± 0.00	a	84.94 ± 0.00	a
	DP (cm)	35.41 ± 2.13	a	35.96 ± 1.98	a	37.04 ± 0.68	a	41.09 ± 0.88	a	41.53 ± 1.14	a	38.22 ± 2.79	a
	ET (cm)	45.49 ± 2.13	a	44.94 ± 1.98	a	43.86 ± 0.68	a	43.85 ± 0.88	a	43.41 ± 1.14	a	46.72 ± 2.79	a
<i>D. stricta</i>	IR (cm)	80.90 ± 0.00	a	80.90 ± 0.00	a	80.90 ± 0.00	a	84.94 ± 0.00	a	84.94 ± 0.00	a	84.94 ± 0.00	a
	DP (cm)	38.64 ± 1.24	a	38.71 ± 2.77	a	38.49 ± 0.99	a	46.73 ± 2.56	a	51.45 ± 1.63	a	51.17 ± 1.84	a
	ET (cm)	42.26 ± 1.24	a	42.19 ± 2.77	a	42.41 ± 0.99	a	38.21 ± 2.56	a	33.49 ± 1.63	a	33.77 ± 1.84	a
<i>P. virgatum</i>	IR (cm)	80.90 ± 0.00	a	80.90 ± 0.00	a	80.90 ± 0.00	a	84.94 ± 0.00	a	84.94 ± 0.00	a	84.94 ± 0.00	a
	DP (cm)	42.11 ± 1.46	a	41.27 ± 2.05	a	43.77 ± 0.77	a	50.93 ± 0.52	b	54.48 ± 0.37	a	54.84 ± 1.32	a
	ET (cm)	38.79 ± 1.46	a	39.63 ± 2.05	a	37.13 ± 0.77	a	34.01 ± 0.52	a	30.46 ± 0.37	b	30.10 ± 1.32	b
× <i>Triticosecale</i>	IR (cm)	80.90 ± 0.00	a	80.90 ± 0.00	a	80.90 ± 0.00	a	84.94 ± 0.00	a	84.94 ± 0.00	a	84.94 ± 0.00	a
	DP (cm)	31.81 ± 0.66	a	25.45 ± 1.16	b	26.70 ± 1.13	b	19.34 ± 2.04	b	21.93 ± 1.84	b	29.97 ± 0.70	a
	ET (cm)	49.09 ± 0.66	b	55.45 ± 1.16	a	54.20 ± 1.13	a	65.60 ± 2.04	a	63.01 ± 1.84	a	54.97 ± 0.70	b

The total amount of irrigation water varied depending on the soil type and the experiment, but was consistent within each experiment and soil for all treatments. As was noted, the DP was inversely related to the ET for a given treatment-plant combination. Despite the values of ET and DP varying for different halophytes, the trends remained similar: i) in both soils (with the exception of the first clay experiment), when a significant difference was detected, the ET was higher and the DP was lower for the control plants than that for either the well water or the concentrate irrigated plants, ii) the ET values were higher and the DP values were lower in the sand than in the clay, and iii) the spread of values was much smaller in the clay across treatments within a species than sand.

Leaching Fractions

During the growth period, leaching fractions remained fairly steady for most species in both soils. *D. stricta* and ×*Triticosecale* showed results typical of these observations (Figure 7). *H. vulgare* was an exception to this because the plants began to flower around day 60 and subsequently started dying. This decreased the water uptake for the plants and increased the leaching.

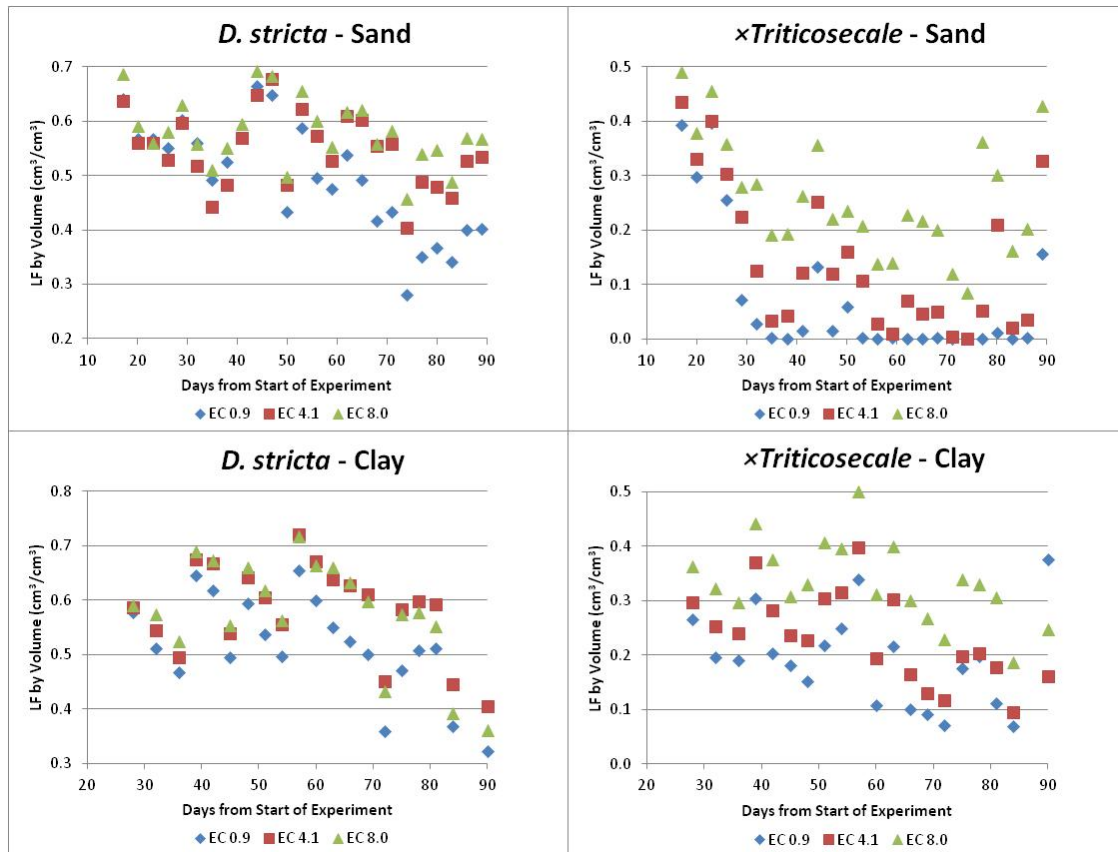


Figure 7 – Graphs of the leaching fractions by volume (volume deep percolation / volume irrigation) for *D. stricta* and *×Triticosecale* for the second experiment in both sand and clay soil.

The sand showed a lot of variability in average leaching fractions within a species for both experiments (Table 7). In the first sand experiment, only one trend appeared: as the salinity of the irrigation water increased, the leaching fraction also increased. This was evident in the *H. vulgare*, *L. alyssooides*, *P. virgatum*, and *×Triticosecale* plants. Two species, *A. canescens* and *D. stricta*, did not see any statistical differences in the leaching fractions with changing salinity. In the second experiment, three species showed increasing leaching fractions with increasing salinity, *D. stricta*, *P. virgatum*, and *×Triticosecale*, but none showed any difference in ET. Although it did not show any difference in the first experiment, *A. canescens* saw a decrease in leaching fraction with increasing salinity, which was coupled with an increase in dry biomass. There were no differences noted in either *H. vulgare* or *L. alyssooides* for the second sand experiment. Despite a modification that increased the amount of total irrigation water in the second experiment, *D. stricta*, *P. virgatum*, and *×Triticosecale* all showed similar average leaching fractions across the two experiments. The largest decrease was seen in the *H. vulgare* plants which decreased from 0.17 to 0.15 and to 0.09 for the control, well water, and concentrate treatments, respectively. Regardless of how the change affected the average leaching fraction, the trends seen in the first experiment were the same as those in the second experiment, even when no significant difference was detected.

Table 7 – Average leaching fractions by volume (volume deep percolation / volume irrigation) for the six halophyte species over the course of the two study periods for both the sand and clay soils. Different letters down a column correspond to a statistically significant difference in leaching fraction means within a species at $\alpha = 0.05$. Measurements were not compared across species.

Species	EC	Leaching Fraction by Volume (cm^3/cm^3)							
		Sand 1		Sand 2		Clay 1		Clay 2	
		Mean \pm SE	a	Mean \pm SE	a	Mean \pm SE	a	Mean \pm SE	a
<i>A. canescens</i>	0.9	0.28 \pm 0.02	a	0.38 \pm 0.01	a	0.45 \pm 0.01	b	0.53 \pm 0.01	a
	4.1	0.28 \pm 0.02	a	0.37 \pm 0.01	a	0.49 \pm 0.01	a	0.52 \pm 0.01	a
	8	0.27 \pm 0.01	a	0.29 \pm 0.01	b	0.45 \pm 0.01	ab	0.48 \pm 0.01	b
<i>H. vulgare</i>	0.9	0.05 \pm 0.02	b	0.22 \pm 0.02	a	0.35 \pm 0.02	a	0.33 \pm 0.01	b
	4.1	0.10 \pm 0.02	b	0.25 \pm 0.02	a	0.31 \pm 0.02	a	0.43 \pm 0.01	a
	8	0.21 \pm 0.02	a	0.30 \pm 0.01	a	0.36 \pm 0.01	a	0.46 \pm 0.01	a
<i>L. alyssoides</i>	0.9	0.17 \pm 0.02	b	0.41 \pm 0.01	a	0.46 \pm 0.02	a	0.46 \pm 0.01	a
	4.1	0.30 \pm 0.01	a	0.46 \pm 0.01	a	0.45 \pm 0.01	a	0.46 \pm 0.01	a
	8	0.35 \pm 0.01	a	0.46 \pm 0.01	a	0.47 \pm 0.01	a	0.42 \pm 0.01	a
<i>D. stricta</i>	0.9	0.41 \pm 0.01	a	0.49 \pm 0.01	b	0.49 \pm 0.01	a	0.52 \pm 0.01	b
	4.1	0.40 \pm 0.02	a	0.55 \pm 0.01	a	0.49 \pm 0.01	a	0.58 \pm 0.01	a
	8	0.47 \pm 0.01	a	0.58 \pm 0.01	a	0.49 \pm 0.01	a	0.58 \pm 0.01	a
<i>P. virgatum</i>	0.9	0.44 \pm 0.01	b	0.48 \pm 0.01	b	0.53 \pm 0.01	a	0.58 \pm 0.01	a
	4.1	0.48 \pm 0.01	ab	0.51 \pm 0.01	b	0.51 \pm 0.01	a	0.63 \pm 0.01	a
	8	0.53 \pm 0.01	a	0.56 \pm 0.01	a	0.54 \pm 0.01	a	0.63 \pm 0.01	a
× <i>Triticosecale</i>	0.9	0.05 \pm 0.02	c	0.09 \pm 0.01	b	0.39 \pm 0.02	a	0.19 \pm 0.01	b
	4.1	0.11 \pm 0.01	b	0.15 \pm 0.01	b	0.31 \pm 0.02	a	0.23 \pm 0.01	b
	8	0.21 \pm 0.01	a	0.27 \pm 0.01	a	0.34 \pm 0.01	a	0.33 \pm 0.01	a

The clay soil showed much less variability in the leaching fractions within a species than the sand soil (Table 7). In the first experiment, only the *A. canescens* showed a statistical difference; however, there was no corresponding difference in either ET or dry biomass for the species even with this difference in leaching fraction across the treatments. There was more variability seen in the second experiment. The *H. vulgare*, *D. stricta*, and ×*Triticosecale* all showed an increase in average leaching fraction with increasing salinity. For *D. stricta* and ×*Triticosecale*, there were no differences noted in ET or dry biomass, but the *H. vulgare* plants did see a trend with respect to biomass: as the leaching fraction increased, the dry biomass decreased. *A. canescens* showed a decrease in leaching fraction with an increase in salinity, but this was accompanied by an increase in biomass. Neither *L. alyssoides* nor *P. virgatum* showed any difference with respect to leaching fraction for the second experiment. The change in total amount of irrigation water changed much less for the clay than for the sand from the first to the second experiment; however, average leaching fractions did not change drastically from the first experiment to the second experiment, with the exception of ×*Triticosecale*. This exception can be explained by the cracking that occurred when the clay soil dried: if the cracks became too large because the plants were taking up a lot of water and the clay was contracting (which happened most often in the control), then less water penetrated the soil and quickly leached through the cracks, increasing the leaching fraction.

For all species, the leaching fractions were higher in the clay than in the soil. This can be seen in both experiments. Even when similar fractions were seen in both soils as in *D. stricta* for experiment 2 and *P. virgatum* in experiment 1, it was still slightly higher in the clay than in the sand for those cases. Unless otherwise noted, an increase in average leaching fraction was accompanied by a decrease in total final ET and vice versa. Although differences with respect to soils were noted, trends that were seen in the sand could also be seen in the clay for the species.

Plant Growth Measurements

Dry Biomass

The plant species that responded similarly for the biomass results responded similarly for ET and DP. The *A. canescens* plants showed an increase in dry biomass with increasing salinity for both sand experiments, indicating that the plants grew slightly better with the higher salinity treatments (Table 8). Similarly, the *L. alyssoides* plants showed a greater dry biomass for the concentrate treatments for the second sand experiment and although there was not a significant difference for the first experiment, the means for the concentrate treatment were still found to be higher than the control. The *D. stricta* plants showed the least amount of variability in dry biomass yields with no significant differences found for any combination of soils and experiments except for the second sand experiment, which showed lower yields for the saline treatments than the control. The *P. virgatum* plants had the most variability in growth with notably different dry biomass yields for the sand plants. The first sand experiment showed control plants with a mean biomass of over one and a half times the mean biomass for the well treatment plants and three times the mean for the concentrate treatment plants. The *P. virgatum* plants irrigated with the saline treatments grew considerably better in the second sand experiment but no significant difference was detected; however, the biomass yields were still lower in the higher saline treatments than they were for the control. Neither *H. vulgare* nor *×Triticosecale* showed any significant difference in dry biomass yields for the sand.

The *A. canescens* plants also showed an increase in dry biomass with increasing salinity in the clay (Table 8). There was a statistically significant difference in the second clay experiment for the species and despite not having a significant difference in the means for the first experiment, it was still evident that the average dry biomass yield for the concentrate treatment was higher than that for the control treatment. The *L. alyssoides* plants also showed a greater dry biomass for the concentrate treatments in the second experiment and like the *A. canescens*, although there was not a significant difference detected in the first experiment, the means for the concentrate treatment were higher than the control. In the first clay experiment, both *H. vulgare* and *×Triticosecale* showed the highest biomass yield for the well water treatment, followed by the concentrate treatment and then the control. For the second clay experiment, both showed the highest biomass yield in the control but only *H. vulgare* showed a statistically significant difference. The

P. virgatum plants had the most difficult time growing in the clay soil of all six halophyte species and the plants barely survived with final mean biomass readings measuring no more than 0.22 g for either experiment in any treatment. However, despite the low dry biomass yields for the species, the control treatment plants still showed a statistically higher mean than the saline treatments. There was no significant difference detected for the *D. stricta* plants in the clay soil.

Table 8 – Dry biomass readings (g) for the six halophyte species at the conclusion of each of the two study periods for both the sand and clay soils. Different letters down a column correspond to a statistically significant difference in dry biomass means within a species at $\alpha = 0.05$. Measurements were not compared across species.

Species	EC	Dry Biomass (g)							
		Sand 1		Sand 2		Clay 1		Clay 2	
		Mean \pm SE		Mean \pm SE		Mean \pm SE		Mean \pm SE	
<i>A. canescens</i>	0.9	2.12 \pm 0.24	b	2.53 \pm 0.18	b	1.73 \pm 0.22	a	1.27 \pm 0.09	b
	4.1	2.37 \pm 0.19	ab	3.02 \pm 0.18	b	1.51 \pm 0.28	a	1.29 \pm 0.13	b
	8	3.00 \pm 0.24	a	4.18 \pm 0.10	a	1.98 \pm 0.17	a	1.82 \pm 0.14	a
<i>H. vulgare</i>	0.9	4.97 \pm 0.27	a	2.93 \pm 0.24	a	2.48 \pm 0.23	b	2.59 \pm 0.14	a
	4.1	5.29 \pm 0.09	a	2.85 \pm 0.56	a	3.36 \pm 0.16	a	1.83 \pm 0.27	b
	8	5.11 \pm 0.29	a	3.61 \pm 0.20	a	2.88 \pm 0.20	ab	1.98 \pm 0.09	b
<i>L. alyssoides</i>	0.9	0.86 \pm 0.07	a	0.86 \pm 0.03	c	0.54 \pm 0.09	a	0.56 \pm 0.01	b
	4.1	0.91 \pm 0.08	a	1.01 \pm 0.06	b	0.72 \pm 0.14	a	0.63 \pm 0.06	ab
	8	1.05 \pm 0.11	a	1.17 \pm 0.05	a	0.60 \pm 0.10	a	0.86 \pm 0.13	a
<i>D. stricta</i>	0.9	1.26 \pm 0.09	a	1.54 \pm 0.10	a	0.87 \pm 0.12	a	0.83 \pm 0.24	a
	4.1	1.58 \pm 0.12	a	0.99 \pm 0.18	b	0.78 \pm 0.11	a	0.73 \pm 0.13	a
	8	1.55 \pm 0.11	a	1.17 \pm 0.08	ab	0.94 \pm 0.04	a	0.91 \pm 0.18	a
<i>P. virgatum</i>	0.9	2.99 \pm 0.10	a	2.56 \pm 0.21	a	0.09 \pm 0.02	a	0.22 \pm 0.05	a
	4.1	1.72 \pm 0.07	b	2.54 \pm 0.21	a	0.02 \pm 0.01	b	0.04 \pm 0.01	b
	8	0.89 \pm 0.10	c	1.93 \pm 0.40	a	0.02 \pm 0.00	b	0.04 \pm 0.01	b
× <i>Triticosecale</i>	0.9	4.58 \pm 0.34	a	3.09 \pm 0.13	a	1.61 \pm 0.14	b	1.93 \pm 0.09	a
	4.1	4.36 \pm 0.14	a	3.38 \pm 0.14	a	2.14 \pm 0.15	a	1.89 \pm 0.09	a
	8	4.20 \pm 0.22	a	3.55 \pm 0.16	a	1.94 \pm 0.09	ab	1.68 \pm 0.07	a

Although there was some variability seen in the different soils, the trends tended to be similar across soils. Two plant species, *A. canescens* and *L. alyssoides*, had runs that resulted in higher amounts of dry biomass from the plants irrigated with the higher salinity water. *H. vulgare*, ×*Triticosecale*, and *D. stricta* showed little difference in overall final biomass amounts and *P. virgatum* had the most variation, with the control plants containing the highest amounts of biomass. There was not a clear overall trend as some combinations showed the highest yields in the control treatment and some saw the highest in the RO concentrate. Similar to the results for *A. canescens* and *L. alyssoides*, one study showed no statistically significant difference among the dry weights of plants exposed to varying levels of salt but did note a slight increase in means with increasing salinity (Muhammad and Hussain, 2010). However, this is in contrast to the majority of salinity studies which typically show a decrease in dry biomass with increasing salinity (Hussain *et al.*, 1997; Glenn and Brown, 1998; Kim *et al.*,

2012). Other studies have shown that although dry biomass tends to decrease with increasing salinity, many differences are not noticeable until the treatment is higher (waters with ECs higher than 10 dS/m) than what was tested in this study, which could explain the lack of noted differences here (Shalaby *et al.* 1993; Marcum, 1999).

Height and Number of Leaves

At the conclusion of the study, four species (*A. canescens*, *H. vulgare*, *L. alyssoides*, and *D. stricta*) showed no significant difference in height with respect to increasing salinity in either soil or in either experiment (Table 9). The *×Triticosecale* plants showed a much larger difference in height for the first sand experiment than for the second sand experiment or either clay experiment. This was due to the fact that in the first sand experiment, the plants reached maturity near the end of the plant cycle, whereas they did not in any of the subsequent experiments. The second sand experiment was the only one that showed a difference in heights for the *×Triticosecale* plants with the control and well water plants being nearly twice as tall as the concentrate plants. The *P. virgatum* plants were the only ones to show a statistical difference in heights for both soils and both experiments. Even when severely stunted as in the clay soil, the plants were still tallest in the low saline treatments and shortest in the saline treatments.

The number of leaves at the conclusion of the study was much more varied than the plant height for the species in the study (Table 10). The *P. virgatum* plants showed a difference in the total number of leaves for the first sand experiment and both clay experiments. The concentrate grown plants had a significantly lower number of leaves than the control or well water grown plants in the first sand experiment, but both saline treatments showed less leaves than the control for the clay experiments. *A. canescens* showed differences in the second experiment for both soils with the concentrate grown plants having the most leaves of the treatments. Although not statistically different, the trend was the same for the first experiments. Three species, *L. alyssoides*, *D. stricta*, and *×Triticosecale* all showed only one statistical difference in number of leaves but the results varied. *L. alyssoides* showed that the salinity treatments tended to have the higher number of leaves. *D. stricta* showed the most leaves in the well water, control, and concentrate treatments for the first sand, second sand, and both clay experiments, respectively. The *×Triticosecale* plants had no clear trend either with the first sand experiment showing the most leaves in the control, the second sand with the most in the saline treatments, the first clay with the most in the well, and the second clay with the number of leaves equal for all treatments. The *H. vulgare* plants had no significant differences noted for either soil or either experiment but like the other species, showed varied results with the lowest number of leaves in the control for the second sand and the first clay experiments but the highest number in the control for the second clay experiment.

Table 9 – Average plant height (cm) for the six halophyte species at the conclusion of each of the two study periods for both the sand and clay soils. Different letters down a column correspond to a statistically significant difference in dry biomass means within a species at $\alpha = 0.05$. Measurements were not compared across species.

		90 Day Plant Height (cm)											
		Sand 1			Sand 2			Clay 1			Clay 2		
Species	EC	Mean	±	SE	Mean	±	SE	Mean	±	SE	Mean	±	SE
<i>A. canescens</i>	0.9	29.05	±	1.97	a	40.23	±	2.49	a	35.68	±	2.25	a
	4.1	34.53	±	5.84	a	45.13	±	7.85	a	33.43	±	4.06	a
	8.0	39.90	±	4.53	a	42.58	±	9.61	a	37.10	±	1.72	a
	LSD		NS			NS			NS			NS	
<i>H. vulgare</i>	0.9	44.85	±	1.33	a	42.38	±	1.09	a	42.28	±	1.84	a
	4.1	46.95	±	0.90	a	39.63	±	3.78	a	47.03	±	1.19	a
	8.0	45.88	±	1.10	a	44.25	±	1.67	a	43.93	±	1.79	a
	LSD		NS			NS			NS			NS	
<i>L. alyssoides</i>	0.9	4.73	±	0.98	a	9.78	±	0.52	a	5.23	±	0.79	a
	4.1	3.98	±	0.52	a	11.40	±	1.52	a	6.80	±	0.71	a
	8.0	4.95	±	1.54	a	9.60	±	1.48	a	5.13	±	1.24	a
	LSD		NS			NS			NS			NS	
<i>D. stricta</i>	0.9	34.25	±	2.45	a	36.75	±	1.00	a	34.10	±	0.91	a
	4.1	34.10	±	4.44	a	34.93	±	2.03	a	29.93	±	3.53	a
	8.0	30.78	±	2.25	a	34.65	±	2.80	a	31.93	±	3.15	a
	LSD		NS			NS			NS			NS	
<i>P. virgatum</i>	0.9	35.55	±	5.90	a	43.23	±	2.60	a	5.78	±	1.08	a
	4.1	29.08	±	3.83	a	44.35	±	1.87	a	2.43	±	0.49	b
	8.0	11.50	±	2.10	b	32.70	±	4.04	b	2.30	±	0.37	b
	LSD		13.55			9.53			2.50			4.26	
× <i>Triticosecale</i>	0.9	97.23	±	0.80	a	36.23	±	4.34	a	9.50	±	0.76	a
	4.1	90.75	±	3.79	a	33.13	±	5.01	a	11.63	±	0.78	a
	8.0	93.40	±	7.24	a	18.80	±	4.02	b	11.48	±	0.39	a
	LSD		NS			14.31			NS			NS	

Typically there is a decrease in growth when plants are exposed to salinity. Many salinity studies have supported this observation. Scholberg and Locascio (1999) saw a decrease in dry plant matter with increasing salinity and Kim *et al.* (2012) found that plants were stunted as the salinity increased. But despite usually showing an obvious difference in growth due to salinity, occasionally plants do not appear stunted until they are compared to control plants (Bernstein, 1975; Noaman and El-Haddad, 2000). For example, it was noted in one study that at salinity levels up to approximately 13.5 dS/m, there was no difference in dry weight between saline affected and unaffected plants (Koyro *et al.*, 2013). Similarly, many studies have shown that salt affected plants generally have fewer leaves than their unaffected counterparts (Saber *et al.*, 2011; Alvarez *et al.*, 2012); however, some species did show a slight increase in the number of leaves with irrigation salinity up to approximately 21 dS/m (Redondo-Gomez *et al.*, 2007).

Table 10 – Average number of leaves per plant for the six halophyte species at the conclusion of each of the two study periods for both the sand and clay soils. Different letters down a column correspond to a statistically significant difference in dry biomass means within a species at $\alpha = 0.05$. Measurements were not compared across species.

		90 Day Number of Leaves											
Species	EC	Sand 1			Sand 2			Clay 1			Clay 2		
		Mean	±	SE	Mean	±	SE	Mean	±	SE	Mean	±	SE
<i>A. canescens</i>	0.9	151.00	±	14.28 a	180.75	±	11.64 b	118.75	±	11.09 a	109.00	±	9.58 b
	4.1	125.50	±	14.48 a	335.00	±	41.65 a	106.25	±	12.85 a	99.50	±	5.50 b
	8.0	164.00	±	20.38 a	306.25	±	28.74 a	137.75	±	12.96 a	168.75	±	15.63 a
LSD				NS			95.90			NS			35.36
<i>H. vulgare</i>	0.9	3.25	±	1.18 a	3.75	±	2.84 a	6.75	±	1.11 a	7.25	±	0.75 a
	4.1	3.50	±	0.65 a	6.50	±	1.50 a	9.00	±	0.41 a	5.00	±	1.41 a
	8.0	3.00	±	1.29 a	11.25	±	3.42 a	7.00	±	1.29 a	5.25	±	1.89 a
LSD				NS			NS			NS			NS
<i>L. alyssoides</i>	0.9	25.75	±	1.25 a	29.00	±	0.71 b	19.25	±	1.31 a	21.50	±	0.87 a
	4.1	24.00	±	1.96 a	61.00	±	12.83 a	17.67	±	1.20 a	21.25	±	1.44 a
	8.0	28.50	±	1.26 a	47.25	±	7.95 ab	21.67	±	1.76 a	26.50	±	2.90 a
LSD				NS			27.90			NS			NS
<i>D. stricta</i>	0.9	92.25	±	5.36 a	150.50	±	11.03 a	73.75	±	8.05 a	70.50	±	16.98 a
	4.1	105.25	±	11.99 a	87.75	±	17.71 b	66.00	±	10.98 a	62.75	±	23.22 a
	8.0	95.75	±	8.08 a	90.00	±	3.94 b	82.00	±	5.21 a	82.00	±	17.15 a
LSD				NS			39.22			NS			NS
<i>P. virgatum</i>	0.9	18.75	±	1.25 a	18.75	±	1.25 a	4.00	±	0.41 a	7.50	±	0.65 a
	4.1	19.00	±	1.96 a	17.00	±	1.68 a	2.00	±	0.00 b	2.25	±	0.25 b
	8.0	10.50	±	2.63 b	16.50	±	2.66 a	2.50	±	0.29 b	2.25	±	0.25 b
LSD				6.48			NS			1.05			1.36
× <i>Triticosecale</i>	0.9	7.25	±	2.81 a	22.25	±	2.72 a	14.00	±	1.47 b	13.25	±	1.93 a
	4.1	3.00	±	1.08 a	33.00	±	4.78 a	21.25	±	1.31 a	13.75	±	1.84 a
	8.0	2.50	±	0.87 a	31.25	±	2.78 a	17.00	±	0.91 b	12.75	±	1.55 a
LSD				NS			NS			4.02			NS

Photosynthetic Rates

In the first sand experiment, only *H. vulgare* showed a significant difference in photosynthetic rates (Table 11). It saw the highest rates in the well water treatment, followed by the control then the concentrate. *A. canescens*, *D. stricta*, and *P. virgatum* all showed the highest values in the control, whereas *L. alyssoides* had higher rates in the saline treatments than in the control. The ×*Triticosecale* plants had treatment values much closer to each other than the other species and saw the highest rates in the control, then the concentrate and well water. In the second sand experiment, four species showed significant difference. *A. canescens*, *L. alyssoides*, and *P. virgatum* all showed the highest photosynthetic rates in the concentrate treatment plants whereas *H. vulgare* had the highest values in the control. The *D. stricta* plants saw higher values in the saline treatments than the control and ×*Triticosecale* showed the highest photosynthetic values in the control, despite neither species showing a significant difference.

Table 11 – Average photosynthetic rates ($\mu\text{mol CO}_2 \text{ m}^{-2}\text{s}^{-1}$) for the six halophyte species at the conclusion of each of the two study periods for both the sand and clay soils. Different letters down a column correspond to a statistically significant difference in dry biomass means within a species at $\alpha = 0.05$. Measurements were not compared across species.

Species	EC	Photosynthetic Rates ($\mu\text{mol CO}_2 \text{ m}^{-2}\text{s}^{-1}$)											
		Sand 1			Sand 2			Clay 1			Clay 2		
		Mean	\pm SE		Mean	\pm SE		Mean	\pm SE		Mean	\pm SE	
<i>A. canescens</i>	0.9	19.94	\pm 3.19	a	7.94	\pm 0.47	b	7.39	\pm 0.47	b	5.69	\pm 1.22	a
	4.1	13.70	\pm 1.69	a	7.91	\pm 0.61	b	10.37	\pm 0.42	a	7.18	\pm 1.29	a
	8.0	13.66	\pm 1.09	a	10.60	\pm 1.33	a	11.51	\pm 1.24	a	7.17	\pm 1.02	a
	LSD		NS		2.62			2.37			NS		
<i>H. vulgare</i>	0.9	16.56	\pm 0.99	ab	8.47	\pm 0.92	a	11.43	\pm 0.15	a	7.83	\pm 2.26	a
	4.1	18.36	\pm 0.76	a	6.37	\pm 0.24	b	10.51	\pm 0.76	a	3.50	\pm 1.64	a
	8.0	15.43	\pm 0.56	b	7.35	\pm 0.61	ab	7.68	\pm 0.59	b	9.49	\pm 1.78	a
	LSD		2.37		1.64			2.12			NS		
<i>L. alyssoides</i>	0.9	16.79	\pm 0.69	a	9.33	\pm 0.88	b	15.92	\pm 2.00	a	5.44	\pm 1.21	a
	4.1	18.17	\pm 1.87	a	13.48	\pm 1.41	a	12.69	\pm 1.43	a	7.60	\pm 2.26	a
	8.0	18.04	\pm 3.50	a	14.01	\pm 1.22	a	13.19	\pm 3.00	a	8.07	\pm 1.53	a
	LSD		NS		3.49			NS			NS		
<i>D. stricta</i>	0.9	13.30	\pm 0.98	a	5.66	\pm 1.10	a	10.33	\pm 1.83	b	6.42	\pm 1.82	a
	4.1	12.20	\pm 1.29	a	9.21	\pm 1.69	a	13.10	\pm 1.03	ab	7.57	\pm 2.43	a
	8.0	11.49	\pm 0.76	a	6.26	\pm 1.07	a	14.12	\pm 0.69	a	9.10	\pm 1.01	a
	LSD		NS		NS			3.75			NS		
<i>P. virgatum</i>	0.9	20.66	\pm 1.02	a	8.02	\pm 0.42	b	15.97	\pm 1.43	a	5.32	\pm 1.63	a
	4.1	17.82	\pm 1.39	a	15.59	\pm 0.88	a	13.30	\pm 0.25	a	-1.59	\pm 1.82	b
	8.0	17.36	\pm 1.17	a	13.48	\pm 1.06	a	8.43	\pm 1.78	b	-1.25	\pm 0.99	b
	LSD		NS		2.44			4.80			4.47		
\times <i>Triticosecale</i>	0.9	13.88	\pm 0.57	a	13.48	\pm 0.75	a	7.35	\pm 0.64	b	10.55	\pm 0.29	a
	4.1	12.03	\pm 0.92	a	11.89	\pm 0.85	a	13.17	\pm 2.07	a	9.76	\pm 0.60	a
	8.0	13.19	\pm 0.36	a	11.29	\pm 0.67	a	11.59	\pm 0.34	a	10.20	\pm 0.80	a
	LSD		NS		NS			3.73			NS		

In the first clay experiment, the photosynthetic rate varied a lot with respect to species and treatment (Table 11). *A. canescens*, *D. stricta*, and \times *Triticosecale* showed their highest readings for photosynthetic rate in the concentrate while the highest rates for *H. vulgare* and *P. virgatum* were found in the control. *L. alyssoides* saw no significant difference, but the photosynthetic rates in the control were shown to be higher than the saline treatments. Far fewer differences were evident for the second clay experiment and only *P. virgatum* saw a statistically significant difference. Four plant species (*A. canescens*, *H. vulgare*, *L. alyssoides*, and *D. stricta*) saw the highest values of photosynthetic rate in the saline treatments. *P. virgatum* and \times *Triticosecale* had their highest values in the control.

For all combinations of soil and experiment, any significant differences for conductance or transpiration followed the trends that the photosynthetic rate measurements saw. The average leaf temperature did not vary by more than 4°C for any combination of species, soil, and experiment.

There are many contrasting reports concerning salinity and photosynthetic rates in previous studies. Some studies showed that at moderate levels of salinity, especially in halophytic species, photosynthetic rates remained unaffected as compared to the control treatment (Koyro *et al.*, 2013; Ge *et al.*, 2014). Other studies showed little variability in photosynthetic rates for the first several weeks of saline treatments but eventually showed a decrease in rates with increasing salinity (Alvarez *et al.*, 2012). Many halophytes showed an eventual decrease in photosynthetic rates with increasing salinity (Redondo-Gomez *et al.*, 2006; Redondo-Gomez *et al.*, 2007; Ge *et al.*, 2014) but this was not always the case. Some halophytes saw an increase in photosynthetic rate until the EC of the irrigation water reached approximately 14 dS/m (Koyro *et al.*, 2013) and one extreme halophyte showed an increase in rates with increasing salinity up to an EC of approximately 52 dS/m (Redondo-Gomez *et al.*, 2010). For each of these studies, the stomatal conductance and transpiration rates responded in the same way that photosynthetic rates did.

Ion Uptake

Generally, an increase in irrigation water salinity caused an increase in sodium (Na^+) concentration for all species, soils, and experiments, even when no significant difference was detected, but there were two deviations from this trend (Table 12). The first sand experiment showed a decrease in sodium ion concentration with increasing salinity for *H. vulgare* and the first clay experiment for *A. canescens* had a much lower concentration for the well water treatment than either the control or the concentrate treatments. *D. stricta* and *×Triticosecale* both saw significant differences in both soils and both experiments. *H. vulgare* had a statistical difference for all combinations of soil and experiment except for the one mentioned above. *L. alyssoides* and *P. virgatum* both only had differences for the second sand experiment and *A. canescens* showed no differences for either soil or experiment.

Chloride (Cl^-) concentration was much more varied than the Na^+ concentration (Table 13). In general, Cl^- concentration increased with increasing salinity, however, a few instances of decreasing concentration were noted for *A. canescens* in the first clay experiment and *A. canescens* and *P. virgatum* in the second sand experiment, but not all were significantly different. In the second clay experiment, *D. stricta* saw a significant difference with the highest concentration in the well water treatment, and although not statistically different, the same was noted for *H. vulgare* in the second experiment for both soils.

Far fewer differences were noted for potassium (K^+) concentration than for Na^+ or Cl^- (Table 14). The general trend for K^+ was that as irrigation salinity increased, the concentration of the ion decreased. Although a couple species showed slightly different values for the well water treatment than either the control or the concentrate, they still followed the trend in that the treatments exposed to less salinity had higher K^+ concentrations than those exposed to higher salinity. The

one exception to this was the *P. virgatum* plants in the second sand experiment which showed a significantly different increase in ion concentration with increasing salinity.

Table 12 – Sodium (Na⁺) ion concentrations (%) for the six halophyte species at the conclusion of each of the two study periods for both the sand and clay soils. Different letters down a column within a species correspond to a statistically significant difference in concentration at $\alpha = 0.05$. Measurements were not compared across species. Final *P. virgatum* dry biomass samples were combined due to low individual plant biomass for analysis and therefore, only one data point (and thus no standard error data) could be obtained for the species.

Species	EC	Sodium Concentration (%)															
		Sand 1			Sand 2			Clay 1			Clay 2						
		Mean	±	SE	Mean	±	SE	Mean	±	SE	Mean	±	SE				
<i>A. canescens</i>	0.9	1.31	±	0.74	a	1.93	±	0.60	a	1.10	±	0.41	a	0.46	±	0.40	a
	4.1	0.83	±	0.54	a	1.54	±	0.78	a	0.50	±	0.34	a	1.12	±	0.67	a
	8.0	0.85	±	0.44	a	2.31	±	0.72	a	1.46	±	0.70	a	1.15	±	0.85	a
	LSD		NS			NS			NS			NS					
<i>H. vulgare</i>	0.9	0.32	±	0.12	a	0.19	±	0.01	c	0.19	±	0.01	b	0.18	±	0.03	b
	4.1	0.30	±	0.03	a	0.40	±	0.04	b	0.29	±	0.04	b	0.39	±	0.03	ab
	8.0	0.24	±	0.09	a	0.60	±	0.04	a	0.55	±	0.12	a	0.56	±	0.14	a
	LSD		NS			0.10			0.23			0.27					
<i>L. alyssooides</i>	0.9	0.07	±	0.03	b	0.05	±	0.01	b	0.03	±	0.02	a	0.12	±	0.07	a
	4.1	0.09	±	0.02	b	0.13	±	0.03	b	0.31	±	0.21	a	0.11	±	0.04	a
	8.0	0.21	±	0.05	a	0.34	±	0.06	a	0.13	±	0.04	a	0.19	±	0.02	a
	LSD		0.12			0.12			NS			NS					
<i>D. stricta</i>	0.9	0.32	±	0.06	b	0.60	±	0.01	b	0.50	±	0.07	b	0.64	±	0.10	c
	4.1	0.57	±	0.07	ab	1.39	±	0.23	a	0.79	±	0.07	ab	0.98	±	0.06	b
	8.0	0.78	±	0.17	a	1.56	±	0.09	a	1.01	±	0.12	a	1.30	±	0.07	a
	LSD		0.36			0.46			0.30			0.28					
<i>P. virgatum</i>	0.9	0.03	±	0.01	b	0.06	±	0.03	b	0.06	±	.	.	0.06	±	.	.
	4.1	0.13	±	0.06	b	0.05	±	0.00	b	0.22	±	.	.	0.40	±	.	.
	8.0	0.32	±	0.07	a	0.14	±	0.03	a	1.22	±	.	.	1.68	±	.	.
	LSD		0.17			0.08			N/A			N/A					
× <i>Triticosecale</i>	0.9	0.13	±	0.03	c	0.07	±	0.01	c	0.07	±	0.01	b	0.11	±	0.01	c
	4.1	0.29	±	0.04	b	0.42	±	0.06	b	0.48	±	0.12	a	0.31	±	0.07	b
	8.0	0.70	±	0.06	a	0.73	±	0.05	a	0.52	±	0.03	a	0.66	±	0.03	a
	LSD		0.15			0.15			0.23			0.14					

With respect to Na⁺, Cl⁻, and K⁺ ion concentrations, ×*Triticosecale* and *D. stricta* were the species that were most susceptible to ion uptake due to differing amounts of salt in its irrigation water. These species each noted 9 statistically significant differences for various combinations of soil and experiment for these ions. The least susceptible was *A. canescens* with only 1 difference and the remaining three species, *H. vulgare*, *L. alyssooides*, and *P. virgatum*, were similar in the amount of noted differences with 5, 5, and 4, respectively.

Table 13 – Chloride (Cl⁻) ion concentrations (%) for the six halophyte species at the conclusion of each of the two study periods for both the sand and clay soils. Different letters down a column within a species correspond to a statistically significant difference in concentration at $\alpha = 0.05$. Measurements were not compared across species. No data could be recorded for some species

(noted with a ‘.’) because of low total final dry biomass. Following microwave digestion, there was not enough remaining plant matter for chloride analysis.

Species	EC	Chloride Concentration (%)															
		Sand 1			Sand 2			Clay 1			Clay 2						
		Mean	±	SE	Mean	±	SE	Mean	±	SE	Mean	±	SE				
<i>A. canescens</i>	0.9	2.02	±	0.37	a	4.12	±	0.32	a	2.03	±	0.77	a	2.41	±	0.29	a
	4.1	1.76	±	0.44	a	2.66	±	0.54	a	1.62	±	0.25	a	2.48	±	0.88	a
	8.0	2.43	±	0.29	a	3.63	±	0.53	a	1.94	±	0.44	a	2.91	±	0.17	a
	LSD			NS				NS				NS				NS	
<i>H. vulgare</i>	0.9	1.08	±	0.09	b	1.64	±	0.13	a	1.88	±	0.08	ab	2.14	±	0.56	a
	4.1	1.13	±	0.06	b	1.93	±	0.09	a	1.62	±	0.16	b	2.29	±	0.18	a
	8.0	1.76	±	0.25	a	1.66	±	0.18	a	2.12	±	0.18	a	2.03	±	0.20	a
	LSD			0.51				NS				0.46				NS	
<i>L. alyssoides</i>	0.9	0.77	±	0.05	b	0.97	±	0.12	b	.	±	.	.	.	±	.	.
	4.1	0.84	±	0.07	ab	1.40	±	0.08	a	0.88	±	.	.	.	±	.	.
	8.0	1.37	±	0.24	a	1.47	±	0.11	a	0.71	±	.	.	1.63	±	0.12	.
	LSD			0.54				0.32				N/A				N/A	
<i>D. stricta</i>	0.9	0.91	±	0.12	a	1.38	±	0.15	b	1.21	±	0.29	a	1.44	±	0.08	b
	4.1	1.34	±	0.49	a	1.95	±	0.14	ab	1.39	±	0.23	a	2.21	±	0.10	a
	8.0	1.43	±	0.19	a	2.24	±	0.27	a	1.85	±	0.27	a	1.87	±	0.22	ab
	LSD			NS				0.62				NS				0.60	
<i>P. virgatum</i>	0.9	0.58	±	0.16	b	1.37	±	0.95	a	.	±	.	.	.	±	.	.
	4.1	0.72	±	0.13	b	0.53	±	0.04	a	.	±	.	.	.	±	.	.
	8.0	1.38	±	0.11	a	0.80	±	0.04	a	.	±	.	.	.	±	.	.
	LSD			0.53				NS				N/A				N/A	
× <i>Triticosecale</i>	0.9	0.79	±	0.09	b	0.88	±	0.07	b	1.83	±	0.30	a	1.63	±	0.24	b
	4.1	0.92	±	0.07	b	1.82	±	0.05	a	2.00	±	0.16	a	1.93	±	0.22	b
	8.0	1.64	±	0.16	a	2.03	±	0.07	a	2.39	±	0.12	a	2.69	±	0.14	a
	LSD			0.36				0.21				NS				0.65	

In order to facilitate water uptake when the soil solution is saline, many plants take up some of the ions in order to adjust the internal osmotic potential and it is important to look at all the ions and interactions because similar reactions occur within plants even when the individual ion concentrations vary (Alvarez *et al.*, 2012; Souza *et al.*, 2012). Many studies showed that as the salinity of the irrigation water increased, the concentration of Na⁺ also increased (Scholberg and Locascio, 1999; Redondo-Gomez *et al.*, 2007; Redondo-Gomez *et al.*, 2010; Alvarez *et al.*, 2012). Chloride was suggested to be more toxic than Na⁺ and tended to appear in larger concentrations when salinity was higher (Alvarez *et al.*, 2012). Potassium ions are generally excluded from plant uptake in the presence of Na⁺ and various salinity studies have shown that an increase in salinity stress causes a decrease in K⁺ (Scholberg and Locascio, 1999; Redondo-Gomez *et al.*, 2010; Hussain *et al.*, 2014). However, this was more variable as one study showed little difference after 3 dS/m in K⁺ concentration (Redondo-Gomez *et al.*, 2007) and another even showed a slight increase with increasing salinity (Scholberg and Locascio, 1999).

Table 14 – Potassium (K⁺) ion concentrations (%) for the six halophyte species at the conclusion of each of the two study periods for both the sand and clay soils. Different letters down a column within a species correspond to a statistically significant difference in concentration at $\alpha = 0.05$. Measurements were not compared across species. Final *P. virgatum* dry biomass samples were combined due to low individual plant biomass for analysis and therefore, only one data point (and thus no standard error data) could be obtained for the species.

Species	Potassium Concentration (%)																
	EC	Sand 1			Sand 2			Clay 1			Clay 2						
		Mean	±	SE	Mean	±	SE	Mean	±	SE	Mean	±	SE				
<i>A. canescens</i>	0.9	3.37	±	0.54	a	2.83	±	0.18	a	4.63	±	0.35	a	4.74	±	0.51	a
	4.1	2.75	±	0.27	a	2.32	±	0.10	b	4.11	±	0.53	a	5.00	±	1.03	a
	8.0	2.23	±	0.20	a	1.65	±	0.11	c	4.33	±	0.29	a	4.40	±	0.39	a
	LSD			NS			0.43					NS				NS	
<i>H. vulgare</i>	0.9	1.25	±	0.03	a	1.99	±	0.20	a	2.10	±	0.12	a	2.28	±	0.13	a
	4.1	1.14	±	0.04	a	1.75	±	0.15	a	1.84	±	0.09	a	2.60	±	0.22	a
	8.0	1.35	±	0.13	a	1.67	±	0.09	a	1.95	±	0.07	a	2.36	±	0.22	a
	LSD			NS			NS					NS				NS	
<i>L. alyssoides</i>	0.9	2.14	±	0.15	a	3.36	±	0.21	a	2.25	±	0.12	a	2.72	±	0.28	a
	4.1	2.27	±	0.29	a	3.59	±	0.26	a	1.93	±	0.40	a	2.13	±	0.09	b
	8.0	1.89	±	0.21	a	3.04	±	0.39	a	2.37	±	0.12	a	2.49	±	0.07	ab
	LSD			NS			NS					NS				0.55	
<i>D. stricta</i>	0.9	1.17	±	0.01	a	1.38	±	0.04	ab	1.32	±	0.07	a	1.48	±	0.07	a
	4.1	1.03	±	0.06	a	1.50	±	0.07	a	1.21	±	0.07	a	1.43	±	0.06	ab
	8.0	1.05	±	0.09	a	1.18	±	0.11	b	0.88	±	0.04	b	1.12	±	0.13	b
	LSD			NS			NS					0.20				0.33	
<i>P. virgatum</i>	0.9	0.90	±	0.07	b	1.15	±	0.09	a	1.47	±	.	.	1.60	±	.	.
	4.1	1.13	±	0.12	b	1.01	±	0.09	a	0.23	±	.	.	0.76	±	.	.
	8.0	1.68	±	0.04	a	1.12	±	0.13	a	0.36	±	.	.	0.47	±	.	.
	LSD			0.27				NS				N/A				N/A	
× <i>Triticosecale</i>	0.9	1.34	±	0.06	a	1.97	±	0.12	a	2.78	±	0.11	a	2.63	±	0.08	a
	4.1	1.13	±	0.06	b	1.75	±	0.03	a	2.11	±	0.14	b	2.46	±	0.07	a
	8.0	1.02	±	0.04	b	1.72	±	0.10	a	2.15	±	0.08	b	2.51	±	0.18	a
	LSD			0.18				NS				0.36				NS	

Conclusions

1. The germination study showed that for these seed lots, levels of germination obtained with deionized water can also be achieved with saline water treatments up to an EC of 10.0 dS/m. Five of the six species showed some delay in germination with increasing salinity, which is consistent with the findings of previous studies (Ries and Hofmann, 1983; Almansouri *et al.*, 2001). These six species, *A. canescens*, *H. vulgare*, *L. alyssoides*, *D. stricta*, *P. virgatum* and ×*Triticosecale*, can potentially survive the germination and re-vegetation process with saline water and are adequate candidate species for land application sites.
2. Pore clogging study showed that continuous application of RO concentrate will cause salt deposition in the pores leading to pore clogging with attendant decreases in hydraulic conductivity of soil.

3. The greenhouse plant survival experiments showed that for these six species, salinity can affect their growth but at the levels of salinity tested, all species were able to tolerate the salt and survive. Two species, *A. canescens* and *L. alyssoides* saw increases in dry biomass with increasing salinity whereas the others saw a decrease. This increase is in contrast to most studies which see a reduction in biomass with increasing salinity (Glenn and Brown, 1998; Kim *et al.*, 2012), but indicates that they are indeed halophytic species and grow slightly better with salts, rather than just tolerating them. K^+ is often replaced by Na^+ in plants when sodium ions are present which is evident in this study as well. Based on the results from this study, these six species (*A. canescens*, *H. vulgare*, *L. alyssoides*, *D. stricta*, *P. virgatum*, and \times *Triticosecale*) could be adequate candidate species for land application sites.

References

- Adhikari, P., Shukla, M.K., and Mexal, J.G. (2012). Spatial variability of soil properties in an arid ecosystem irrigated with treated municipal and industrial wastewater. *Soil Science*, **177**, 458-469.
- Adhikari, P., Shukla, M.K., Mexal, J.G., and Daniel, D. (2014). Irrigation with treated wastewater: quantification of changes in soil physical and chemical properties. *Irrigation & Drainage Systems Engineering*, **3**, 1-10.
- Allen, R.G., Pereira, L.S., Raes, D., and Smith, M. (1998). Crop evapotranspiration – Guidelines for computing crop water requirements. *FAO Irrigation and Drainage Paper 56*.
- Almansouri, M., Kinet, J.-M., and Lutts, S. (2001). Effect of salt and osmotic stresses on germination in durum wheat (*Triticum durum* Desf.). *Plant and Soil*, **231**, 243-254.
- Alvarez, S., Gomez-Bellot, M.J., Castillo, M., Bañon, S., and Sanchez-Blanco, M.J. (2012). Osmotic and saline effect on growth, water relations, and ion uptake and translocation in *Phlomis purpurea* plants. *Environmental and Experimental Botany*, **78**, 138-145.
- Ayers, R.S. and D.W. Wescot. (1985). *Water quality for agriculture*. Retrieved from <http://www.fao.org/docrep/003/T0234E/T0234E02.htm>.
- Babcock, M., Shukla, M.K., Picchioni, G., Mexal, J., and Daniel, D. (2009). Chemical and physical properties of Chihuahuan desert soils irrigated with industrial effluent. *Arid Land Research and Management*, **23**, 47-66.
- Barbour, M.G., Burk, J.H., and Pitts, W.D. (1987). *Terrestrial Plant Ecology*. 2nd ed. pp. 112, Benjamin-Cummings Publishing Company, San Francisco.

- Baskin, C.C. and Baskin, J.M. (1998). *Seeds: Ecology, Biogeography, and Evolution of Dormancy and Germination*. 1st ed. pp. 402, Academic Press, San Diego.
- Ben-Gal, A., Ityel, E., Dudley, L., Cohen, S., Yermiyahu, U., Presnov, E., Zigmund, L., and Shani, U. (2008). Effect of irrigation water salinity on transpiration and on leaching requirements: A case study for bell peppers. *Agricultural Water Management*, **95**, 587-597.
- Bernstein, L. (1975). Effects of salinity and sodicity on plant growth. *Annual Review of Phytopathology*, **13**, 295-312.
- Bewley, J.D. and Black, M. (1994). *Seeds: Physiology of Development and Germination*. 2nd ed. pp. 445, Plenum Press, New York.
- Dalling, J.W., Davis, A.S., Schutte, B.J., and Arnold, A.E. (2011). Seed survival in soil: interacting effects of predation, dormancy and the soil microbial community. *Journal of Ecology*, **99**, 85-95.
- deVries, J. (1972). Soil filtration of wastewater effluent and the mechanism of pore clogging. *Water Pollution Control Federation*. 44(4):565-573.
- Diaz, F.J., Benes, S.E., and Grattan, S.R. (2013). Field performance of halophytic species under irrigation with saline drainage water in the San Joaquin Valley of California. *Agricultural Water Management*, **118**, 59-69.
- Flores, A.M., Schutte, B.J., Shukla, M.K., Picchioni, G.A., and Ulery, A.L. (2015). Time-integrated measurements of seed germination for salt-tolerant plant species. *Seed Science and Technology*, **43**.
- Gavlak, R.G., Horneck, D.A., and Miller, R.O. (1994). Plant, soil, and water reference methods for the western region. W. Reg. Ext. Publ. 125. Version 4.1.
- Ge, Z.-M., Zhang, L.-Q, Yuan, L. and Zhang, C. (2014). Effects of salinity on temperature-dependent photosynthetic parameters of a native C₃ and a non-native C₄ marsh grass in the Yangtze Estuary, China. *Photosynthetica*, **52**, 484-492.
- Gee, G.W. and J.W. Bauder. (1986). Particle size analysis. p. 404–407. *In* A. Klute (ed.) *Methods of soil analysis*. Part 1. 2nd ed. Agron. Monogr. 9. ASA and SSSA, Madison, WI.
- Ghermandi, A., Messalem, R., Offenbach, R., and Cohen, S. (2013). Solar desalination for sustainable brackish water management in arid land agriculture. *Renewable Agriculture and Food Systems*, **29**, 255-264.

- Glenn, E.P., and Brown, J.J. (1998). Effects of soil salt levels on the growth and water use efficiency of *Atriplex canescens* (Chenopodiaceae) varieties in drying soil. *American Journal of Botany*, **85**, 10-16.
- Gonzalez-Delgado, A.M., Shukla, M.K., Ulery, A.L., Bawazir, A.S., and Brady, P.V. (2011). Saturated hydraulic conductivity of self-sealing lining materials for desalination evaporation ponds. *Desalination and Water Treatment*, **29**, 187-195.
- Hussain, G., Al-Jaloud, A.A., Al-Shammary, S.A., Karimulla, S., and Al-Aswad, S.O. (1997). Effect of saline irrigation on germination and growth parameters of barley (*Hordeum vulgare* L.) in a pot experiment. *Agricultural Water Management*, **34**, 125-135.
- Hussain, R.A., Ahmad, R., Waraich, E.A., and Nawaz, F. (2014). Nutrient uptake, water relations, and yield performance of different wheat cultivars (*Triticum aestivum* L.) under salinity stress, *Journal of Plant Nutrition*.
- Katerji, N., Mastrorilli, M., van Hoorn, J.W., Lahmer, F.Z., Hamdy, A., and Oweis, T. (2009). Durum wheat and barley productivity in saline-drought environments. *European Journal of Agronomy*, **31**, 1-9.
- Keiffer, C.H. and Ungar, I.A. (2002). Germination and establishment of halophytes on brine-affected soils. *Journal of Applied Ecology*, **39**, 402-415.
- Khan, M.J. (1996). Yield and evapotranspiration of two barley varieties as affected by sodium chloride salinity and leaching fraction in lysimeter tanks. *Communications in Soil Science and Plant Analysis*, **27**, 157-177.
- Kim, S., Rayburn, A.L., Voigt, T., Parrish, A., and Lee, D.K. (2012). Salinity effects on germination and plant growth of prairie cordgrass and switchgrass. *BioEnergy Research*, **5**, 225-235.
- Klute, A. (1986). Water retention: Laboratory methods. p. 635–662. In A. Klute (ed.) *Methods of soil analysis. Part 1*. 2nd ed. Agron. Monogr. 9. ASA and SSSA, Madison, WI.
- Klute, A. and Dirksen, C. (1986). Hydraulic conductivity and diffusivity: Laboratory methods. p. 687–734. In A. Klute (ed.) *Methods of soil analysis. Part 1*. 2nd ed. Agron. Monogr. 9. ASA and SSSA, Madison, WI.
- Koyro, H.-W., Hussain, T., Huchzermeyer, B., and Khan, M.A. (2013). Photosynthetic and growth responses of a perennial halophytic grass *Panicum turgidum* to increasing NaCl concentrations. *Environmental and Experimental Botany*, **91**, 22-29.

- Lal, R. and Shukla, M.K. (2004). Principles of Soil Physics. Marcel Dekker, New York: pp. 165-178.
- Lansford, R., Hernandez, J., Enis, P., Truby, D., and Mapel, C. (1990). Evaluation of available saline water resources in New Mexico for the production of microalgae. Solar Energy Research Institute, Golden, CO.
- Marcum, K.B. (1999). Salinity tolerance mechanisms of grasses in the subfamily Chloridoideae. *Crop Science*, **39**, 1153-1160.
- McNeal, B. L., Layfield, D.A., Norvell, W.A., and Rhoades, J.D. (1968). Factors influencing hydraulic conductivity of soils in the presence of mixed salt solutions. *Soil Science Society of America Proceedings*, **32**, 187-190.
- Miyamoto, S., Glenn, E.P., and Singh, N.T. (1994). Utilization of halophytic plants for fodder production with brackish water in subtropic deserts. In *Halophytes as a Resource for Livestock and for Rehabilitation of Degraded Lands*, (eds. V.R. Squires and A.T. Ayoub), pp. 43-75, Springer, Netherlands.
- Muhammad, Z. and Hussain, F. (2010). Effect of NaCl salinity on the germination and seedling growth of some medicinal plants. *Pakistan Journal of Botany*, **42**, 889-897.
- Nemmers, Sylvia J., April L. Ulery, and Manoj K. Shukla. (2012). Wastewater effluent effects on arsenic sorption in arid New Mexico soils. *New Mexico Journal of Science*, **46**, 137-148.
- Noaman, M.N. and El-Haddad, E-S. (2000). Effects of irrigation water salinity and leaching fraction on the growth of six halophyte species. *Journal of Agricultural Science*, **135**, 279-285.
- Picchioni, G.A., Shukla, M.K., Mexal, J.G., Babcock, M., Ruiz, A., Sammis, T.W., Rodriguez, D.S. (2012). Application of treated industrial wastewater on a Chihuahuan desert shrubland: Implications for water quality and mineral deposition. *Arid Land Research and Management*, **26**, 211-226.
- Pupisky, H. and Shainberg, I. (1979). Salt effects on the hydraulic conductivity of a sandy soil. *Soil Science Society of America Journal*, **43**, 429-433.
- R Core Team. (2015). *R: A Language and Environment for Statistical Computing*, R Foundation for Statistical Computing, Vienna, Austria. v.2.12.1, <http://www.R-project.org>.
- Ranal, M.A. and Santana, D.G. (2006). How and why to measure the germination process? *Revista Brasileira de Botanica*, **29**, 1-11.

Redondo-Gomez, S., Wharmby, C., Castillo, J.M., Mateos-Naranjo, E., Luque, C.J., de Cires, A., Luque, T., Davy, A.J., and Figueroa, M.E. (2006). Growth and photosynthetic responses to salinity in an extreme halophyte, *Sarcocornia fruticosa*. *Physiologia Plantarum*, **128**, 116-124.

Redondo-Gomez, S., Mateos-Naranjo, E., Davy, A.J., Fernandez-Munoz, F., Castellanos, E.M., Luque, T., and Figueroa, M.E. (2007). Growth and photosynthetic responses to salinity of the salt-marsh shrub *Atriplex portulacoides*. *Annals of Botany*, **100**, 555-563.

Redondo-Gomez, S., Mateos-Naranjo, E., Figueroa, M.E., and Davy, A.J. (2010). Salt stimulation of growth and photosynthesis in an extreme halophyte, *Arthrocnemum macrostachyum*. *Plant Biology*, **12**, 79-87.

Rice, R.C. (1974). Soil clogging during infiltration of secondary effluent. *Water Pollution Control Federation*, **46**, 708-716.

Ries, R.E. and Hofmann, L. (1983). Effect of sodium and magnesium sulfate on forage seed germination. *Journal of Range Management*, **36**, 658-662.

Robbins, C.W. (1983). Sodium adsorption ration-exchangeable sodium percentage relationships in a high potassium saline-sodic soil. *Irrigation Science*, **5**, 173-179.

Saberi, A.R., Siti Alshah, H., Halim, R.A., and Zaharah, A.R. (2011). Morphological responses of forage sorghums to salinity and irrigation frequency. *African Journal of Biotechnology*, **10**, 9647-9656.

Scholberg, J.M.S. and Locascio, S.J. (1999). Growth response of snap bean and tomato as affected by salinity and irrigation method. *HortScience*, **34**, 259-264.

Schwabe, K., Albiac, J., Connor, J.D., Hassan, R., and Meza-Gonzalez, L. (2013). Introduction. In *Drought in Arid and Semi-Arid Regions*, (eds. K. Schwabe, J. Albiac, J. D. Connor, R. Hassan, and L. Meza-Gonzalez), pp. 1-21, Springer, New York.

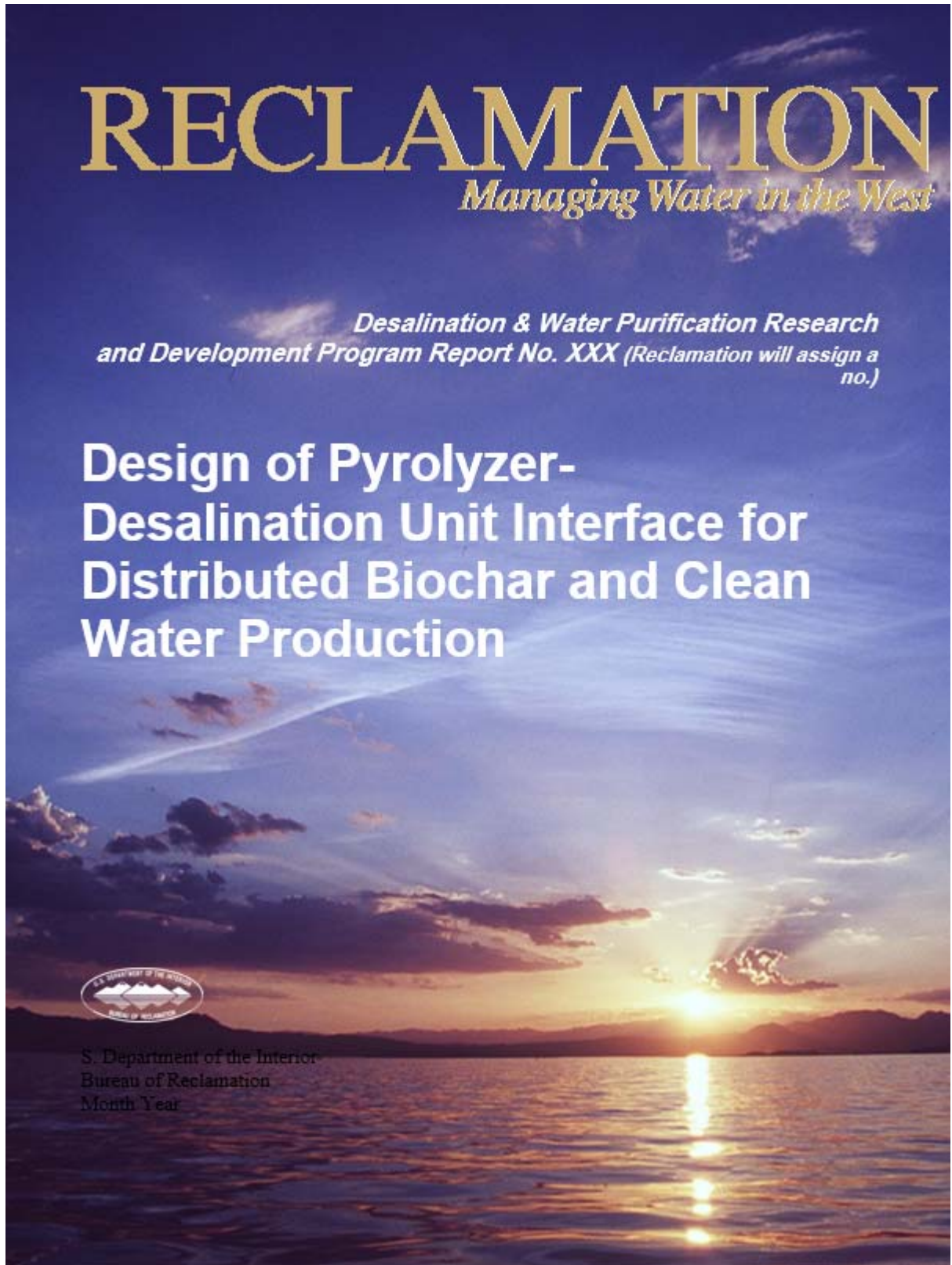
Shalaby, E.E., Epstein, E., and Qualset, C.O. (1993). Variation in salt tolerance among some wheat and triticale genotypes. *Journal of Agronomy and Crop Science*, **171**, 298-304.

Shukla, M.K. (2014). Soil physics, an introduction. CRC Press, Boca Raton.

Singh, A.P., Singh, A., Tiwari, H.I., and Dwivedi, P.K. 2011. The effect of salts of the hydraulic conductivity of the saline alkali soil. *Indian Journal of Scientific Research*, **2**, 117-119.

- Smedema, L. K. and K. Shiati. (2002). Irrigation and salinity: a perspective review of the salinity hazards of irrigation development in the arid zone. *Irrigation and Drainage Systems*, 16: 161-174.
- Smith, T.E., Grattan, S.R., Grieve, C.M., Poss, J.A., Läuchli, A.E., and Suarez, D.L. (2013). pH dependent salinity-boron interactions impact yield, biomass, evapotranspiration and boron uptake in broccoli (*Brassica oleracea* L.). *Plant Soil*, **370**, 541-554.
- Soliz, D., Glenn, E.P., Seaman, R., Yoklic, M., Nelson, S.G., and Brown, P. (2011). Water consumption, irrigation efficiency and nutritional value of *Atriplex lentiformis* grown on reverse osmosis brine in a desert irrigation district. *Agriculture, Ecosystems and Environment*, **140**, 473-483.
- Souza, E.R., Freire, M.B.G., dos, S., Cunha, K.P.V., Nascimento, C.W.A., Ruiz, H.A., Lins, C.M.T. (2012). Biomass, anatomical changes and osmotic potential in *Atriplex nummularia* Lindl. cultivated in sodic saline soil under water stress. *Environmental and Experimental Botany*, **82**, 20-27.
- Twitchell, L.F.T. (1955). Germination of fourwing saltbush seed as affected by soaking and chloride removal. *Journal of Range Management*, **8**, 218-220.
- UNEP International Environmental Technology Center. (1998). Desalination by reverse osmosis. *Sourcebook of Alternative Technologies for Freshwater Augmentation in Latin America and the Caribbean*. Retrieved from <https://www.oas.org/dsd/publications/Unit/oea59e/begin.htm#Contents>.
- WRRI (Water Resources Research Institute). (1997). Transboundary aquifers of the El Paso/Ciudad Juarez/Las Cruces region. *Texas Water Development Board and New Mexico Water Resources Research Institute*. U.S. Environmental Protection Agency, Region VI.

Design of Pyrolyzer-Desalination Unit Interface for Distributed Biochar and Clean Water Production



REPORT DOCUMENTATION PAGE		Form Approved OMB No. 0704-0188
<p>The public reporting burden for this collection of information is estimated to average 1 hour per response, including the time for reviewing instructions, searching existing data sources, gathering and maintaining the data needed, and completing and reviewing the collection of information. Send comments regarding this burden estimate or any other aspect of this collection of information, including suggestions for reducing the burden, to Department of Defense, Washington Headquarters Services, Directorate for Information Operations and Reports (0704-0188), 1215 Jefferson Davis Highway, Suite 1204, Arlington, VA 22202-4302. Respondents should be aware that notwithstanding any other provision of law, no person shall be subject to any penalty for failing to comply with a collection of information if it does not display a currently valid OMB control number. PLEASE DO NOT RETURN YOUR FORM TO THE ABOVE ADDRESS.</p>		
1. REPORT DATE (DD-MM-YYYY) 30-08-2015	2. REPORT TYPE	3. DATES COVERED (From - To) From 01-01-2014 To 30-06-2015
4. TITLE AND SUBTITLE Design of Biomass Pyrolyzer-Desalination Unit Interface for Distributed Biochar and Clean Water Production	5a. CONTRACT NUMBER R10AC80283	
	5b. GRANT NUMBER	
	5c. PROGRAM ELEMENT NUMBER	
6. AUTHOR(S) Catherine E. Brewer O. John Idowu	5d. PROJECT NUMBER	
	5e. TASK NUMBER	
	5f. WORK UNIT NUMBER	
7. PERFORMING ORGANIZATION NAME(S) AND ADDRESS(ES) New Mexico State University		8. PERFORMING ORGANIZATION REPORT NUMBER
9. SPONSORING/MONITORING AGENCY NAME(S) AND ADDRESS(ES)		10. SPONSOR/MONITOR'S ACRONYM(S)
		11. SPONSOR/MONITOR'S REPORT NUMBER(S)
12. DISTRIBUTION/AVAILABILITY STATEMENT		
13. SUPPLEMENTARY NOTES		
14. ABSTRACT <p>In this study, we explored the concept of connecting biomass pyrolysis to water desalination. The first component was the design of a biomass pyrolyzer that could be coupled with a multiple effect distillation (MED) unit for the small-scale desalination of brackish water. The design included unit selection and sizing, and development of an interface to connect the two units. The second component was the lab-scale production of biochar from locally-available biomass residues and the measurement of those biochars effects on New Mexico soils, especially soil water holding capacity and soil quality.</p> <p>We found that an MED producing 1-2 m³/day of distilled water, approximately 475-550 kg of dry biomass is needed per m³ of produced distilled water, yielding 160-190 kg of biochar. The pyrolysis-MED concept has potential now as a value-added waste management system; water costs are currently too high (~20-50 US\$/m³) for the system to be feasible based on water production</p>		

<p>alone. Amendment with biochar showed the potential to increase soil organic matter and soil nutrients; biochar salinity is a concern, especially for the cotton gin trash biochar. Biochar appeared to increase the available water capacity of the sandy loam soil although more data is needed to demonstrate statistical significance and evaluate the effect on irrigation management. Outcomes of this project include four manuscripts to be published as peer-reviewed journal articles, two graduate student theses, four conference presentations, research capacity building in the Water-Energy Nexus for two junior faculty, five follow-on grant proposals, and a process simulation that can be used in future process design.</p>					
<p>15. SUBJECT TERMS water desalination, biomass, pyrolysis, multiple effect distillation, brackish water, biochar, process simulation, pecan shell, pecan orchard prunings, cotton gin trash, yard waste, soil quality, soil salinity, soil available water capacity</p>					
16. SECURITY CLASSIFICATION OF:			17. LIMITATION OF ABSTRACT	18. NUMBER OF PAGES	19a. NAME OF RESPONSIBLE PERSON
a. REPORT	b. ABSTRACT	a. THIS PAGE			19b. TELEPHONE NUMBER (<i>Include area code</i>)

Standard Form 298 (Rev. 8/98)
Prescribed by ANSI Std. Z39.18

DESIGN OF PYROLYZER-DESALINATION UNIT INTERFACE FOR DISTRIBUTED BIOCHAR AND CLEAN WATER PRODUCTION

by

Catherine E. Brewer and O. John Idowu



**U.S. Department of the Interior
Bureau of Reclamation
Technical Service Center
Water and Environmental Services Division
Water Treatment Engineering Research Team
Denver, Colorado**

Month Year

MISSION STATEMENTS

The mission of the Department of the Interior is to protect and provide access to our Nation's natural and cultural heritage and honor our trust responsibilities to Indian tribes and our commitments to island communities.

The mission of the Bureau of Reclamation is to manage, develop, and protect water and related resources in an environmentally and economically sound manner in the interest of the American public.

Disclaimer

The views, analysis, recommendations, and conclusions in this report are those of the authors and do not represent official or unofficial policies or opinions of the United States Government, and the United States takes no position with regard to any findings, conclusions, or recommendations made. As such, mention of trade names or commercial products does not constitute their endorsement by the United States Government.

Acknowledgements

Funding for this research was provided by a Tier 1 Proof of Concept Grant through the New Mexico State University Institute for Energy and the Environment as part of a cooperative agreement with U.S. Bureau of Reclamation.

The authors would like to acknowledge the NMSU Manufacturing Engineering & Technology Center for their assistance with fabricating the lab-scale pyrolyzer, Dr. Kyriacos Zygourakis for his input on the interface design, Mr. Brent Carrillo for his assistance with the pyrolysis runs, Ms. Barbara Hunter for her assistance with soil chemical analyses, Dr. Wayne Van Voohries and Ms. Andrea Salazar for their assistance with HHV analyses, Mr. Graham Hoffman and Mr. Kodanda Phani Raj Dandamudi for their assistance with biochar characterizations, the Idowu research group for their help with the soil incubations, and the staff of the NMSU Department of Chemical & Materials Engineering for their support.

Contents

	<i>Page</i>
Acknowledgements.....	iii
Contents	v
Glossary	vii
Executive Summary	1
1. Introduction.....	2
1.1 Motivation	2
1.2 Proof-of-Concept Study	2
1.2.1 Project Objectives	2
1.2.2 Project Tasks.....	3
1.2.3 Project Deliverables.....	3
1.3 Organization of Report	3
1.4 Conclusions and Recommendations	4
2. Energy Sources for Water Desalination Literature Review.....	6
Abstract	6
2.1 Introduction	6
2.2 Desalination	6
2.2.1 Water Quality and Technologies	6
2.2.2 Membrane Processes	7
2.2.3 Thermal Processes	8
2.2.4 MED Design Considerations	10
2.2.5 Hybrid Desalination Systems	13
2.3 Biomass as an Energy Source	14
2.3.1 Biomass Types and Sources	14
2.3.2 Biomass Properties	15
2.3.3 Biomass Densification	16
2.3.4 Extracting Energy from Biomass.....	17
2.4. Energy and Water Desalination	20
2.4.1 Energy Requirements for Desalination.....	20
2.4.2 Fossil Fuel Energy and Water Desalination	22
2.4.3. Renewable Energy and Water Desalination	23
2.5 Economics	26
2.5.1 Economics of Water Desalination Plants	26
2.5.2 Economics of Coupling Renewable Energy and Water Desalination	27
2.6 Small-Scale Water Desalination Technologies	27
Conclusions	28
3. Design Parameters for Biomass Pyrolyzer-MED System	29
3.1 System Scale and Desired Qualities	29
3.2 Unit Operations	29
3.2.1 Process Flow	29
3.2.2 Steam for the MED	30
3.2.3 Electricity for the MED	31

3.2.4 Aspen Plus® Simulation.....	31
3.3.4 Calculating Biomass Needs	34
3.3 System Design Results	34
3.4 Conclusions and Future Research	34
4. Producing Biochar from Locally-Available Biomass Resources	36
4.1 Lab-Scale Pyrolyzer Design and Fabrication	36
4.1.1 Pyrolysis Literature Review	36
4.1.2 Pyrolyzer Design Considerations	38
4.1.3 Design of Lab-Scale Slow Pyrolyzer.....	40
4.2 Biomass Feedstocks	41
4.3 Biochar Production	42
4.4 Biochar Characterization	42
4.5 Results	42
4.6 Conclusion	43
5. Biochar Effects on New Mexico Soil Properties	44
5.1 Study Goals and Objectives	44
5.2 Soil Incubation Materials and Methods	46
5.3 Soil Property Measurement Methods	46
5.4 Results and Implications	48
5.4.1 Coarse Textured Soil (Sandy Loam)	48
5.4.2 Fine Textured Soil (Clay Loam Soil)	49
5.4.3 Soil Quality Implications of This Study	50
5.4.4 Soil Moisture Desorption Results	51
5.5 Conclusions and Future Work	54
6. Outcomes of This Research	55
6.1 Research Capacity Building	55
6.2 Theses, Publications, and Presentations	55
6.3 Follow-On Proposals	56
6.4 Other Products	57
Reference List	58
Appendix: Data Record.....	72

Glossary

AWC	available water capacity
BF	backward feed
BGNDRF	Brackish Groundwater National Desalination Research Facility
CGT	cotton gin trash
DSG	direct steam generation
EC	electrical conductivity
ED	electrodialysis
FC	field capacity
FF	forward feed
GOR	gain output ratio
HHV	higher heating value
HX	heat exchanger
IEE	Institute for Energy and the Environment
LHV	lower heating value
MED	multiple effect distillation
MSF	multiple stage flash
MSW	municipal solid waste
MVC	mechanical vapor compression
NCG	non-condensable gases
NMSU	New Mexico State University
NO _x	nitrogen oxides
PEEK	polyetheretherketone
PF	parallel feed
PHF	polymeric hollow fiber
PP	polypropylene
PP	pecan (orchard) prunings
ppm	parts per million
PS	pecan sheels
psia	pounds per square inch absolute
PWP	permanent wilting point
PV	photovoltaic
RO	reverse osmosis
SAR	sodium adsorption ratio
SOM	soil organic matter
SO _x	sulfur oxides
TBT	top brine temperature
TDS	total dissolved solids
TGA	thermogravimetric analysis
TVC	thermal vapor compression
VC	vapor compression
VOCs	volatile organic carbons
YW	yard waste

Executive Summary

Communities located in rural, arid areas face the challenge of finding local and affordable energy supplies to operate water desalination equipment. A renewable distributed energy source that has great potential for water desalination and has yet to be explored is biomass: agricultural wastes, forestry residues, residential yard waste, byproducts from biofuels production, etc. Pyrolysis, a process that transforms biomass through heating under limited-oxygen conditions, can be used to produce char, bio-oil or tar, and non-condensable gas products. The liquid and gas products can be combusted to drive the pyrolysis process, and to provide heat and power to a desalination process. The char product can be applied to soils as biochar to improve soil quality and soil water holding capacity.

The first component of this proof-of-concept project was the theoretical design of a biomass slow pyrolysis system that could be coupled through an interface to a multiple effect distillation (MED) unit for the small-scale desalination of brackish water. The process began with a review of the literature in the overlapping areas of water desalination technologies and renewable energy sources. From the literature review, a low-temperature, parallel feed MED was selected. An ASPEN Plus® chemical engineering process modeling simulation was developed for the interface (furnace, boiler, turbine and heat exchangers) to enable rapid determination of unit operation size and flow stream properties for multiple system size scales and operating conditions. This simulation was used to estimate how much biomass would be needed to produce a given amount of distilled water. The second component of the project was the production of biochar from locally-available biomass residues and the measurement of those biochars effects on New Mexico soils. Production of the biochars required the design and fabrication of a lab-scale slow pyrolysis reactor system. Pecan shell, pecan orchard prunings, cotton gin trash, and yard waste were used to produce biochars that were amended to and incubated with two agricultural soils. After incubation, multiple soil quality indicators and soil water desorption curves were measured to compare the agricultural potential of amended and unamended soils.

Results indicated that, for an MED producing 1-2 m³/day of distilled water, approximately 475-550 kg of dry biomass is needed per m³ of produced distilled water, yielding 160-190 kg of biochar. The pyrolysis-MED concept has potential now as a value-added waste management system; water costs are currently too high (~20-50 US\$/m³) for the system to be feasible based on water production alone. Amendment with biochar showed the potential to increase soil organic matter and soil nutrients; biochar salinity is a concern, especially for the cotton gin trash biochar. Biochar appeared to increase the available water capacity of the sandy loam soil although more data is needed to demonstrate statistical significance and evaluate the effect on irrigation management.

Outcomes of this project include four manuscripts to be published as peer-reviewed journal articles, two graduate student theses, four conference presentations, research capacity building in the Water-Energy Nexus for two junior faculty, five follow-on grant proposals, and a process simulation that can be used in future process design.

1. Introduction

1.1 Motivation

Water for agricultural use has become expensive and difficult to obtain in New Mexico and other southwestern states due primarily to an on-going drought. For example, even though they pay approximately \$70/acre/year to participate in the Elephant Butte Irrigation District, many NM farmers spend an additional \$150-200/acre/year to pump water from their own wells to obtain enough water for cotton or alfalfa crops. This well water can frequently be brackish and its use for irrigation can result in the accumulation of salt in irrigated soils. Soil salinity can result in lower crop yields due to plant salt stress. Treatment of soil salinity often requires flushing the soil with fresh water to transport salts below the root zone. Use of brackish well water to meet temporary water needs can lead to the need for even more fresh water in the long term to maintain crop yield.

Desalination of brackish groundwater is one way to obtain fresh water for irrigation from available water sources. However, desalination requires energy. In rural locations, where many farms are located, electricity from a grid or electricity generation using solid or liquid fuels is often unavailable or prohibitively expensive at the necessary scale. Some desalination systems are designed to use what farmers have available on or near their farms: sunlight, wind, and geothermal energy. Such systems have been employed with some success, although per unit costs remain high. One resource that farmers also have available but that has not been much explored for desalination is biomass in the form of agricultural residues and yard waste. *The primary goal of this project is to explore the feasibility of using biomass to provide the energy needed to desalinate water at the farm scale in rural areas.*

Many agricultural soils in New Mexico are characterized by very low organic matter content and are often poorly positioned to withstand drought and erosion. Thermochemical processing of biomass to produce heat energy for thermal desalination would result in a co-product, biochar, which may help address this soil quality problem. The potential of biochar to increase available soil water is related to its highly porous nature which acts as a sponge and modifies the soil texture. Improvements in soil water use efficiency, and thus, extensions of the time between irrigation events, represent significant potential irrigation water savings. Therefore, *the secondary goal of this project is to measure biochar's ability to improve soil quality and soil water retention properties.*

1.2 Proof-of-Concept Study

1.2.1 Project Objectives

The objectives of this project were to:

- Quantify the resources and conditions needed to enable biomass pyrolysis-powered brackish water desalination.

- Evaluate the potential for biomass pyrolysis-powered brackish water desalination in the context of other desalination technologies.
- Develop the capacity to produce biochars and to conduct biochar-amended soil quality and water use research.
- Evaluate the potential of biochars produced from local biomass resources to improve local agricultural soils.

1.2.2 Project Tasks

The specific tasks undertaken in this project were:

1. Identify scale and configuration of pyrolyzer and desalination unit, including mass and energy balances.
2. Design and prepare fabrication drawings for pyrolyzer-MED unit system components.
3. Construct and perform shakedown trials on lab-scale pyrolyzer.
4. Produce biochars for soil water retention measurements.
5. Prepare and incubate biochar-amended soil samples for soil water retention measurements.
6. Measure soil water potential curves for biochar-amended soils.
7. Prepare final report and proposals for additional external funding.

1.2.3 Project Deliverables

The deliverables of this project are:

- a. Selection and sizing of pyrolyzer-desalination unit including mass and energy balances.
- b. Design for pyrolyzer-desalination unit system fabrication.
- c. Characteristics of slow pyrolysis biochars produced on lab-scale pyrolyzer.
- d. Results from biochar-amended soil incubation study.
- e. Results and recommendations from biochar-amended soil water potential tests.
- f. Final project report.
- g. Proposals submitted to external funding agencies.

1.3 Organization of Report

This chapter is intended to provide context for the project and to summarize the take-away messages from the project results.

The second chapter is the text of a review article manuscript prepared by the PhD student on the project during his review of the relevant literature. The manuscript expands on the justification for selection multiple effect distillation (MED) as the desalination technology to be coupled with pyrolysis. The manuscript also provides baseline data of water desalination production rates, water quality and

costs. This text will serve as the literature review chapter of Mr. Ali Amiri's PhD dissertation.

The third chapter presents the results from the pyrolysis-MED interface design process including an Apsen Plus® process simulation and calculations. Assumptions needed for the design led to a reaction and process modeling collaboration with Dr. Kyriacos Zygourakis at Rice University. The results have been presented at two conferences and will be used to prepare an article manuscript and a chapter of Mr. Amiri's PhD dissertation.

The fourth chapter describes the construction and operation of a lab-scale pyrolyzer used to produce biochars from locally available biomass resources. The reactor design, testing, and biochar characterization served as half of the MS thesis work of Mr. Yunhe Zhang, and have contributed to one conference presentation and one article manuscript currently under review.

The fifth chapter presents the methods and results of a soil incubation study using the produced biochars. The soil work is split into two components: general soil fertility and quality, and soil water retention and physical properties. The soil quality results were used in the biochar article currently under review. The soil water retention results are being used to prepare another article manuscript for submission in the near future. The soil water retention work was conducted primarily by two undergraduate researchers, Mr. Brent Carrillo and Ms. Flavia Mitsue Yamashita; continuation and expansion of the work will serve as the MS thesis topic of a new graduate student.

The final chapter summarizes the outcomes from the project.

1.4 Conclusions and Recommendations

Low temperature multiple effect distillation (MED) is the most appropriate water desalination technology to be coupled with biomass pyrolysis due to MED's use of low grade thermal energy, system simplicity, history of coupling with other renewable energy sources at the small scale, and potential for low maintenance operation from the prevention of scaling. Biomass residues contain sufficient energy to provide the heat and power for small-scale water desalination although predicted water costs are still too high for a biomass pyrolysis-MED system to be feasible based on water production alone. Pyrolysis of local agricultural residues produced acceptable yields of biochar with acceptable properties, although the high ash content of the cotton gin trash biochar raises concerns about soil salinity if biochar derived from that feedstock is to be used as a soil amendment.

Further development of biomass pyrolysis-MED systems should be pursued in situations where biomass waste management is the primary objective and where the on-site production of small amounts of high-purity water is needed; soil quality and soil water effects of applied biochars may provide additional value to the system and should be investigated. Design of biomass pyrolysis-MED

prototypes should be based on scale and suitability of unit operations (especially steam turbine generators), followed by the availability (amount, seasonality, cost) of biomass in the near vicinity. More research is needed on the relationship between biochar ash content and its effect on soil salinity and crop yields. In some cases, the effects of increased salinity might be offset by changes in other soil quality indicators; if biochar salinity is limiting, methods for quantifying that limitation are needed. More research is needed to understand the impacts of biochar amendments on soil's available water capacity, especially for irrigated cropping systems. Research efforts should strive to align instrumental/theoretical measurements with crop-relevant impacts in the field.

2. Energy Sources for Water Desalination Literature Review

Abstract

Water desalination is an energy-intensive process needed in many parts of the world to provide fresh water for drinking, agriculture, and industry. The energy for desalination can come from conventional fossil fuels such as petroleum, natural gas and coal, as well as renewable energy sources such as solar, wind, hydro, and geothermal. One renewable energy source that is widely available but currently unused for water desalination is biomass. In this review, we summarize available water desalination technologies, energy requirements and costs, and explore how scale and resource availability create trade-offs in technology selection and design. From there, we present a case for the circumstances in which biomass energy may be suitable for water desalination: small scale capacity needs, infrastructure-poor or rural areas, lower-salinity (brackish) source water, thermal desalination technologies, and an abundant, underutilized biomass supply.

2.1 Introduction

The need for high quality water is dramatically increasing due to rapid population growth, higher per capita water consumption, greater industrial and power generation water use, and expanding agricultural production. Freshwater resources are not capable of meeting these needs as just 3% of earth's water is fresh water. As such, there is need for techniques to purify available but low-quality water. Water desalination is a common technique for providing large quantities of high quality, potable water worldwide. Approximately 50% of the desalination plants are located in the Middle East, 20% in the US, 18% in Europe, and 12% in Asia (Raluy, et al., 2005). The installed desalination capacity throughout the world in 2000 was about 22 million m³ of water per day, requiring approximately 8.5 EJ of energy per year, which is equivalent to 203 million tons of crude oil. Concerns about petroleum-based energy availability and environmental impacts have motivated the exploration of alternative and renewable energy sources for water desalination (Kalogirou, 2005).

In this review, we summarize desalination technologies and energy sources, focusing on multiple effect distillation (MED) and renewable energy. From this summary, we present an argument for the potential of biomass as an energy source for water desalination through a pyrolysis-MED process.

2.2 Desalination

2.2.1 Water Quality and Technologies

Water quality is categorized as a function of total dissolved solids (TDS) in parts per million (mg/L): freshwater contains 200 to 700 ppm, treated wastewater contains 700 to 1,500 ppm, brackish water contains 2,000 to 10,000 ppm, and

seawater contains 30,000 to 60,000 ppm. Approximately 58% and 23% of the installed water desalination capacity worldwide are used for treating seawater and brackish water, respectively (Eltawil, et al., 2009). In addition to dissolved salts, waters can contain other impurities such as microorganisms, organic matter, suspended solids, silica, etc. that can cause scaling, fouling, and corrosion in the unit. For this reason, efficient pre-treatment and post-treatment techniques to eliminate harmful impurities are often needed.

Depending on the TDS of the water, treatment costs, and infrastructure availability, a variety of desalination techniques can be used; these techniques are grouped into membrane/single-phase processes and thermal/phase-change processes. There are also some new approaches for desalination. Some examples are forward osmosis, ion concentration polarization, super-cavitation evaporation, and capacitive deionization (Kalogirou, 2005, Likhachev and Li, 2013, Raluy, et al., 2005, Semiat and Hasson, 2012).

2.2.2 Membrane Processes

The two main membrane desalination processes are electro dialysis (ED) and reverse osmosis (RO). Both require electrical energy to drive the separation process. In ED, anion-permeable and cation-permeable membranes, in combination with a cathode and an anode, are used to draw salt ions outward from a dilute feed stream into concentrated brine streams. The electrical power is used to maintain a voltage across the anode and cathode. ED systems, which were developed almost 10 years before RO, are usually used to treat brackish water, and they are more efficient for higher concentrations of highly mobile, small ions.

In RO, which is responsible for more than 88% of the membrane process capacity worldwide, hydraulic pressure is used to overcome osmotic pressure to force water molecules through a semi-permeable membrane (pore sizes less than 10 Å) from a stream with low ion concentration to a stream with high ion concentration. The osmotic pressure, π , is dependent on the TDS of the dilute and concentrated streams:

$$\pi = \frac{\phi \gamma c R T}{M}$$

where γ is the number of ions, ϕ is the osmotic coefficient, c is the difference in salt concentration between the two streams on a mass basis, M is the salt's molecular weight, R is the gas constant, and T is the temperature in Kelvin (Semiat and Hasson, 2012). For RO to work effectively, the hydraulic pressure provided by a pump on the dilute stream side of the membrane must be significantly higher than the osmotic pressure. RO is usually more cost-effective for water with TDS values less than 5,000 ppm, while ED is more economical for water with TDS values greater than 5,000 ppm (Al-Karaghoul and Kazmerski, 2013, Eltawil, et al., 2009).

For both ED and RO, membrane scaling and fouling can substantially affect system performance. Water pre-treatments such as filtration, sterilization, and/or

chemical additives can be used to prevent scaling and bio-fouling (Al-Karaghoul and Kazmerski, 2013, Braun, et al., 2010). Compared to thermal desalination systems, membrane processes usually have less risk of scaling and corrosion due to membrane processes' ambient or near-ambient operating temperatures (Eltawil, et al., 2009). Post-treatment processes for membrane desalination systems can include hydrogen sulfide removal and/or pH adjustment, depending on the final intended water use. More detailed information on membrane desalination process design and membrane scaling can be obtained in (Braun, et al., 2010, Elimelech and Phillip, 2011).

2.2.3 Thermal Processes

There are three main types of thermal desalination processes: multi-stage flash distillation (MSF), vapor compression distillation (VC), and multiple effect distillation (MED). All three require low-temperature heat as the main energy input and a small amount of electricity to drive pumps. Some advantages of thermal desalination processes over membrane desalination processes are higher quality product water, no membrane replacement costs, lower sensitivity to changes in feed water quality, and less rigid monitoring requirements (Eltawil, et al., 2009, Hanson, et al., 2004, Kalogirou, 1997).

2.2.3.1 Multi-Stage Flash Distillation (MSF)

MSF was first developed by Silver at Weir Co. in Glasgow, Scotland in 1960 and is based on seawater evaporation using steam from an external heat source. For many years, MSF has been the “easiest” technology for water desalination and accounts for over 40% of desalination technologies worldwide (Al-Karaghoul and Kazmerski, 2013, Likhachev and Li, 2013). The typical capacity for an MSF process is large: 10,000 to 35,000 m³/day. In MSF, seawater is preheated using heat exchangers up to 90-110°C before entering the first stage. Vacuum pumps create a negative pressure difference near seawater's saturation point in the first stage, causing the seawater to partially flash. The flashed water vapor is condensed by contact with the incoming seawater in the heat exchangers and collected. The remaining concentrated seawater/brine enters the second stage, which is operated at a lower pressure than the first stage. Again, the negative pressure difference causes some of the seawater to flash off and be collected. This process continues until the last stage, which has the lowest temperature and pressure. Sometimes, demisters are used to remove entrained brine droplets from the flashed vapor as these droplets can create salinity in the product water and contribute to scale formation on condenser tubes. The vacuum system removes produced non-condensable gases in order to keep the heat transfer coefficient as high as possible within the stages. To prevent scaling, pre-treatments such as adding acid or advanced scale inhibitors like polyphosphate can be used.

2.2.3.2 Vapor Compression (VC)

VC is very similar to MSF but only has one evaporation stage and can be run under atmospheric or sub-atmospheric pressure. Hot, pressurized feed water

enters the evaporation stage and flashes off, then is condensed and collected. The remaining brine can then be recycled through the process by re-pressurizing it. The VC pressurization can be done using mechanical vapor compression (MVC), which requires additional electricity energy for the pump, or thermal vapor compression (TVC), in which high-pressure steam is injected into the feed stream (Al-Karaghoul and Kazmerski, 2013, Semiat and Hasson, 2012).

2.2.3.3 Multiple-Effect Distillation (MED)

MED, also known as multiple-effect boiling (Kalogirou, 2005), is the oldest thermal desalination process and has a typical plant capacity of 600 to 300,000 m³/day. MED has been in competition with MSF technically and economically for many years. At the end of 2011, MSF and MED units accounted for approximately 26% and 8.2% of worldwide water production capacity, respectively (2012). Two main advantages of MED over MSF are MED's lower energy consumption due to better heat transfer from the constant temperature difference in MED effects, and the fewer number of effects needed in MED to achieve a given performance ratio (mass of distillate produced per unit mass of input steam) (Al-Karaghoul and Kazmerski, 2013, Kalogirou, 2005).

In the most common configuration of MED, steam from an external heat source is fed into a tube in the first effect. Seawater or brackish water is sprayed onto the steam-filled tube and part of the water flashes into steam. The newly produced steam is then fed into the next effect as the heat source, after which it condenses and is collected. As in MSF, temperature and pressure decrease from the first effect to the last effect (Al-Shammiri and Safar, 1999, Semiat and Hasson, 2012, Sen, et al., 2011).

An important design parameter for MED is the gain output ratio (GOR): the ratio of distilled water to input steam flow rates. GOR represents the number of times that the heat of evaporation is reused (Al-Karaghoul and Kazmerski, 2013, Joo and Kwak, 2013, Likhachev and Li, 2013, Manenti, et al., 2013, Semiat, 2008); GOR relates directly to energy efficiency. Yang et al. showed that GOR and water production rate decrease with increasing feed water flow rate and increase with increasing steam flow rate (Yang, et al., 2011). Zhao et al. observed that, although increasing the feed steam temperature slightly decreased GOR, such a temperature increase decreased the total heat transfer area needed—a result of a greater temperature difference between adjacent evaporators (Zhao, et al., 2011).

Another important factor in MED design is the optimization of the number of effects. This number is a function of the temperature difference between the feed steam and the top brine temperature (TBT), as well as the minimum temperature differential within an each evaporator (Ophir and Lokiec, 2005). Having more effects results in more distilled water produced and a higher GOR, however, the capital cost and per kg distilled water cost also increase. Other design factors include TBT and heat transfer area within the effects. At higher TBTs, the number of the effects increases and thus the GOR increases. Generally, an MED can be

operated at either a high TBT ($> 90^{\circ}\text{C}$) or a low TBT ($55\text{-}90^{\circ}\text{C}$). Although the heat transfer area and the water production costs for high TBTs are much less than those for low TBTs, high TBTs dramatically increase the amount of corrosion and scaling, as well as the energy consumption. For this reason, low TBT MED is more widely used worldwide than high TBT MED (Miller, 2003, Ophir and Gendel, 2006, Zhao, et al., 2011).

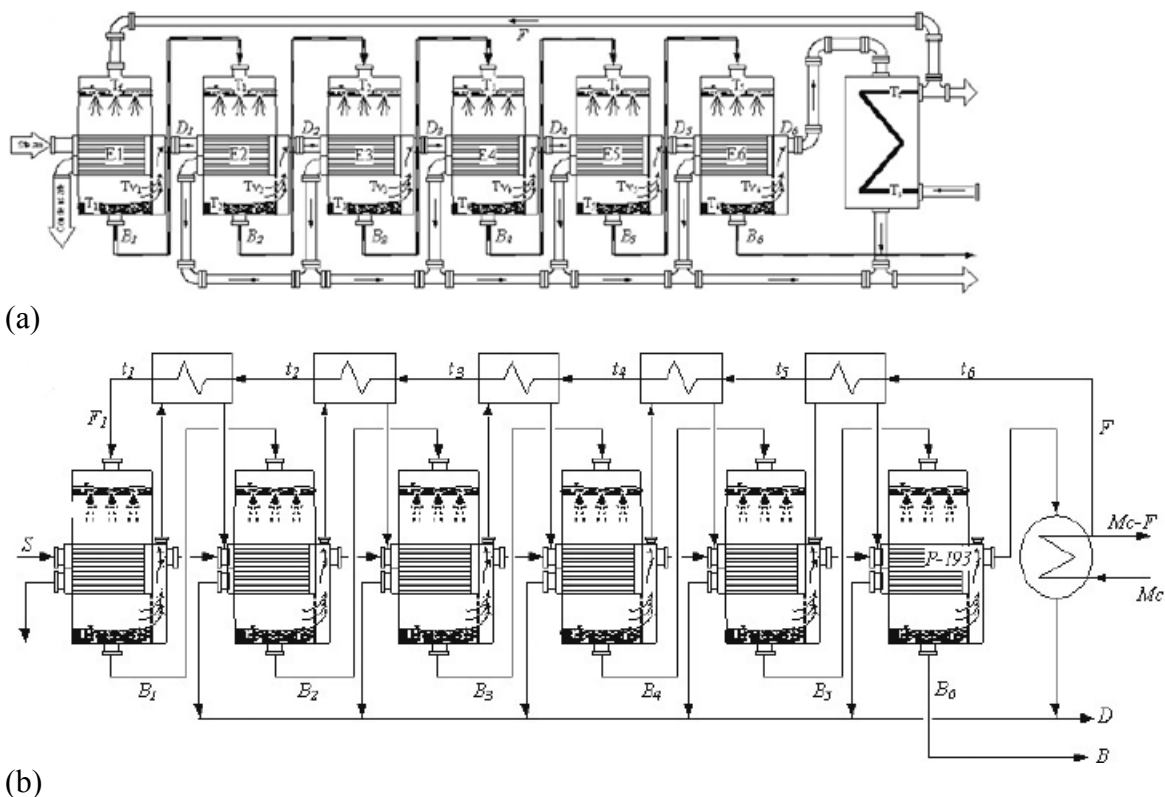
2.2.4 MED Design Considerations

2.2.4.1 Feed Arrangements

There are three main flow arrangements in MED unit design: forward feed, backward feed, and parallel feed; each arrangement has its own advantages and disadvantages. In the forward feed (FF) arrangement, which is the most common configuration, feed water and steam move in a same direction. As shown in Figure 2.1.a, the feed water and steam both enter the system in the first effect at their highest temperature and pressure. One of the challenges for the FF arrangement is that a large portion of the energy is required in first evaporator to heat the feed water to its boiling point, meaning that the heat transfer surface area in the first effect is much greater than in the other effects. Regenerative heat exchanges between effects can solve this problem: steam exiting one effect transfers a small amount of its energy to pre-heat the feed stream before moving on to the next effect. Figure 2.1.b shows how such heat exchangers can be used to heat feed water from an initial feed water temperature to a temperature much closer to the boiling point before entering the first effect.

In the backward feed (BF) arrangement, the feed water enters the last effect where the temperature and pressure are lowest. The steam enters the system in the first effect, where it comes in contact with the highest salinity brine. The advantage of this system is that high-salinity brine evaporation, which requires the most energy, is done at the highest temperature. The disadvantages of this arrangement are that the high temperatures, pressures, and salinities in the first effect can cause more scaling and fouling, and the movement of feed water from low pressure to high pressure requires additional pumping between effects. Part of the increase in scaling and fouling is because the solubility of calcium salts decreases at higher temperatures.

In the parallel feed (PF) arrangement, new feed water is injected at the top and brine is collected from the bottom of each effect independently, while the heat transfer fluid (feed steam and produced water vapor) still move from one effect to another. In such an arrangement, the salinity within each effect reaches its maximum value, meaning that the greatest amount of fresh water vapor had been removed. Darwish et al. showed that the PF arrangement has larger GORs than FF or BF for 2-6 effects, with the difference in GOR increasing with the number of effects (Darwish and Abdulrahim, 2008).



(b)
Figure 2.1. (a) Forward feed flow arrangement and (b) forward feed flow arrangement with regenerative heat exchangers in a six effect, horizontal tube water spray MED unit (Darwish and Abdulrahim, 2008).

In addition to the direction of the flow, the side of the heat exchanger (tube side or shell side) in which each steam flows also impacts MED design. Flowing the steam on the tube side and feed water on the shell side has some advantages: less mist carry-over in the produced steam, easier scale removal/cleaning, and easier turbulence generation inside the tubes, which improves heat transfer (Sen, et al., 2011).

2.2.4.2 Scaling and Fouling in MED

Scaling decreases the overall heat transfer coefficient in heat exchangers because of the low thermal conductivity of the scale material. In MED heat exchangers, scale build-up on the outer surface of evaporating tubes increases the wall temperature of the tubes, which, over a prolonged period of time, can lead to crack formation in the tubes, in addition to lower overall MED energy efficiency (Al-Anezi and Hilal, 2007, Al-Jaroudi, et al., 2010).

Scale formation within MED units is dependent on the concentrations of Ca^{2+} , Mg^{2+} , bicarbonate, and TDS in the water; operating temperature; water residence time; fluid velocity; water pH; rate of CO_2 release; and the roughness of the evaporator construction materials (Al-Anezi and Hilal, 2007, Al-Jaroudi, et al., 2010). There are different types of scale deposits including soft, hard, silica, and organic. In research with a MED-VC unit, Al-Jaroudi, et al. observed a 14 mm-

thick scale build-up comprised of soft CaCO_3 and hard CaSO_4 , as well as a significant proportion of organic matter (Al-Jaroudi, et al., 2010). There are three ways to control build-up of CaSO_4 scale: decrease the MED operating temperature, decrease the overall concentration factor (brine TDS/feed water TDS) to keep the brine TDS concentration below the scaling threshold, and soften the feed water by substituting a monovalent cation such as Na^+ for the Ca^{2+} . Magnesium hydroxide is an alkaline scale component that is sometimes observed in MSF or MED systems from high Mg^{2+} ion concentrations in the water. Polyphosphate may be used as a scale inhibitor if the unit's operation temperature is less than 90°C ; hydrolysis of polyphosphate occurs at higher temperatures, which leads to the formation of calcium phosphate. For this reason, polyphosphate is rarely used for MED units. The presence of organic matter in scale build-up may be due to marine life (bio-fouling) or from industrial discharges of oil, grease, wax or paint materials. A hot alkaline treatment can usually remove organic scale build-up. Similar to scale prevention in MSF, water pre-treatments, a vacuum system, and a demister can also be used to avoid scaling in MED. Even with several management techniques, there is still a chance of scaling in MED units (Al-Jaroudi, et al., 2010).

2.2.4.3 Scaling and Non-Condensable Gases

Non-condensable gases such as CO_2 , O_2 , and N_2 are released during brine evaporation within the effects or through ambient air leakage into the parts of the unit operating under vacuum. The presence of these gases may cause alkaline scale formation. For example, the combination of dissolved CO_2 in the condensate, which decreases the water pH to acidic conditions, with O_2 , may cause corrosion in condenser tubes. De-aeration of the feed water in a titanium tube condenser is a method to decrease the oxygen content within the feed water. CO_2 , which dissociates in water to form HCO_3^- and CO_3^{2-} , is harder to manage. The release rate of CO_2 is highest in the first effect, and at higher water temperatures and salinities (Al-Anezi and Hilal, 2007, Ophir and Gendel, 2006). CaCO_3 scale deposition is also highest in the first effect and pH decreases from the first effect to the last effect (Al-Rawajfeh, 2010). Even a low concentration of non-condensable gases within the water can significantly decrease the overall heat transfer coefficient over time, leading to a decrease in evaporator performance (Al-Anezi and Hilal, 2007). For these reasons, an efficient venting system is critical to control the release of non-condensable gases and prevent scaling, fouling, poor heat transfer, and ultimately, increased energy consumption (Al-Rawajfeh, et al., 2004).

2.2.4.4 Scaling and Tube Construction in MED

There are many different ways of arranging the water flow patterns and the steam tubes within MED heat exchangers: water tube-side vs. steam tube-side, falling water film vs. water spray vs. water immersion, horizontal tubes vs. vertical tubes, smooth tubes vs. corrugated tubes, etc. Four common evaporator combinations are: vertical steam tube-side, vertical water tube-side, horizontal steam tube-side (see Figure 2.1), and horizontal water tube-side. Among them, horizontal steam

tube-side with a falling film water flow has been found to be the most efficient arrangement in terms of energy consumption, thermal characteristics, and simplicity in construction. A tube falling film arrangement is preferred in industry because it lowers the frequency of scaling and carry-over in the tubes due to shorter contact time between the brine and the heat transfer surface, and lowers the vapor velocity which increases the overall heat transfer coefficient, leading to a higher MED system efficiency (Likhachev and Li, 2013, Ophir and Lokiec, 2005). Galal et al. showed that the amount of water that can be condensed on the outer surface of corrugated tubes is 1.5 times greater than the amount that can be condensed on smooth tubes. Also, the fouling thermal resistance of corrugated tubes is nearly half that of smooth tubes, leading to higher long-term thermal performance (Galal, et al., 2010).

For low TBT MED, aluminum is preferred over copper because more aluminum tubes can be installed for the same investment costs, leading to more heat transfer area and higher thermal efficiency per amount of produced water; for high TBT MED, however, copper is preferred (Ophir and Lokiec, 2005). Zarkadas et al. studied polymeric hollow fiber (PHF) heat exchangers made of polypropylene (PP) and polyetheretherketone (PEEK), and found that they have the same or even better thermal performance than metal heat exchangers (Zarkadas, et al., 2005). Other advantages of PHF heat exchangers over metallic ones include smaller volumes, significantly lower pressure drops, less weight, and better resistance to corrosion. The disadvantage of most PHF heat exchangers is that they have a low thermal conductivity (0.1-0.5 W/m·K); this disadvantage can be minimized by using a very small wall thickness (Yan, et al., 2014). Christmann et al. [34] tested a pilot-scale MED with falling film plate evaporators composed of PEEK with wall thicknesses of 25 μm and found that the thermal conduction resistance was 10^{-4} K/W, which is the same as that of stainless steel with a wall thickness of 1.5 mm (Christmann, et al., 2010). The low mechanical strength of polymers, however, means that some stabilization measures must be taken if the walls are to withstand pressure differences across the heat transfer surface (Christmann, et al., 2010, Hetsroni and Mosyak, 1994, Zaheed and Jachuck, 2004).

2.2.5 Hybrid Desalination Systems

In hybrid desalination systems, a power generation unit is combined with both thermal and membrane processes; such systems are more efficient and economical than “dual-purpose” evaporation systems, where the power generation unit provides both electrical and thermal energy required for desalination but only one kind of process is used (Ophir and Lokiec, 2005, Uche, et al., 2001). For instance, in RO-MSF, the water exiting the RO unit is fed into an MSF unit. This increases the overall amount of very pure distilled water (since MSF can achieve a lower exit TDS concentration than RO) and decreases the cost of a pre-treatment unit (since the RO system removes most of the salts that would cause scaling problems in the MSF system). An MED-RO or MSF-RO system is also viable, where pre-heated seawater exiting the last effect of an MED or MSF distiller is fed into an RO unit. In this case, a 1°C increase in seawater feed temperature boosts the water

production rate in RO by 3% (Hamed, 2005). More information on hybrid systems is available in (Cardona, et al., 2003, Hamed, 2005, Helal, et al., 2003, Helal, et al., 2004, Manolakos, et al., 2001, Thu, et al., 2013).

2.3 Biomass as an Energy Source

Biomass is unique among renewable energy options in that it can be both a source of energy and a source of materials. In this way, biomass is similar to petroleum and coal. According to the US Department of Energy's 2011 report, the total annual energy consumption in the US is approximately 98 billion GJ, 4% of which comes from biomass. The annual biomass production rate in the US is approximately 214 million Mg: 129 million Mg as forest resources and 85 million Mg as agricultural resources (Brown and Brown, 2014, Quaak, et al., 1999). Compared to energy from petroleum or coal, energy from biomass has several disadvantages: 1) lower bulk densities, 2) lower energy contents, 3) higher moisture content (which can create both transportation and storage problems due to weight and decomposition, respectively), and 4) greater heterogeneity (Zanzi, 2001). More information about the challenges and prospects of first and second generation biofuel production from biomass is available in (Yousuf, 2012) and (Naik, et al., 2010).

2.3.1 Biomass Types and Sources

Biomass used for energy usually comes from one of two categories: wastes or dedicated energy crops. Wastes include yard waste, municipal solid waste (MSW), agricultural residues (e.g. rice husks, grain straw, orchard prunings), food waste, logging residues, and animal manure. The main advantage of waste biomass is its relatively low cost; its main disadvantage is the large variation in availability, composition, and characteristics from one season to another, and one location to another (Garcia-Perez, et al., 2012).

Dedicated energy crops are plants specifically grown for energy production. They include herbaceous crops such as switchgrass and miscanthus, short rotation woody crops such as hybrid poplar, and oleaginous (lipid-rich) crops such as oilseeds and yeasts. Energy crops are optimized for high rates of biomass production and/or high yields of specific plant components, such as fatty acids in oleaginous crops. While food crops (i.e. plant components that contain significant amounts of digestible carbohydrates, proteins, and/or fats) can be used for energy, a goal of dedicated energy crops is to not compete with food production or use prime land resources. Among woody crops, hardwoods such as willow, poplar, mesquite, and alder, are preferred for most conversion techniques over softwoods due to their lower lignin content. Softwoods, such as pine, are beneficial for construction and thus make up a significant portion of logging and construction residues; these residues are typically used as boiler fuels (Brown and Brown, 2014). In spite of their overall lower productivities compared to herbaceous or woody energy crops, oleaginous crops are popular because they contain long-chain hydrocarbons and relatively low amounts of oxygen, and thus resemble

petroleum. For example, soybean and sunflower only produce about 450-1,600 L of biodiesel per hectare compared to corn which can produce 5,800-8,700 L of ethanol per hectare. The hydrocarbons in oleaginous crops include sterols, fatty acids, di-glycerides, tri-glycerides, and waxes; these are frequently used to produce liquid fuels to power engines and generators.

Garcia-Perez et al. provide a useful review of biomass resources, collection methods, transportation considerations, and pretreatments such as drying and grinding in (Garcia-Perez, et al., 2012).

2.3.2 Biomass Properties

The suitability of a particular type of biomass for energy production is dependent on several of its properties including composition, heating value, density, and production yield.

One method of characterizing biomass composition is proximate analysis, which measures moisture, volatile matter, fixed carbon, and ash content by thermogravimetric analysis (TGA). Moisture, defined as mass lost upon heating to just above water's boiling point, typically 105°C, represents weight that does not contribute to energy value. Because weight basis can have such large implications for transport, storage, and biomass conversion, it is important to specify whether moisture content is reported on a wet or a dry basis (Quaak, et al., 1999). Dry weight percent is most commonly used to avoid confusion from large variations in moisture content from one sample to another and over time. Volatile matter is typically defined as the portion of biomass that decomposes into the gas phase under heating in an inert environment. This value is important for designing biomass burners and other thermochemical processing unit operations, especially in relation to the fraction that does not volatilize in an inert environment, i.e. the fixed carbon. Samples with low volatile matter content do not ignite easily (this is why lighter fluid is often needed to start a charcoal barbeque). Ash is composed of the inorganic minerals contained in the plants and any soil contaminating the biomass. Like moisture content, ash represents weight that does not contribute to energy value. In proximate analysis, ash is defined as any material remaining after the sample is combusted in air, usually at temperatures around 750°C.

Another method for characterizing biomass composition is elemental analysis (CHN, CHNO or CHNSO) or ultimate (CHNSO plus Cl) analysis. C and H generally contribute to energy content, while N, O, S, and Cl generally detract from energy content and can lead to emissions problems (Brown and Brown, 2014, Quaak, et al., 1999).

Biomass energy content is usually reported as higher heating value (HHV). HHV is the enthalpy released when a fuel reacts with oxygen under isothermal conditions; this measurement assumes the water vapor formed during the reaction is not condensed at the end of the process. Lower heating value (LHV) may also be reported. LHV is defined in the same way as HHV except LHV does not include the latent heat of produced water condensation. HHV is measured directly

by oxygen bomb calorimetry. It can also be estimated from correlations using proximate, ultimate, or biochemical composition analyses (Annamalai, et al., 1987, Channiwala and Parikh, 2002, Cordero, et al., 2001, Jiménez and González, 1991, Kim, et al., 2014, Quaak, et al., 1999, Shajizadeh and Degroot, 1976, Sheng and Azevedo, 2005, Tillman, 1978).

There are two important kinds of density for evaluating biomass as an energy source: bulk density (kg/m^3), and energy density or volumetric energy content (GJ/m^3). These two densities are related by HHV and are critical for biomass handling and transportation logistics; the lower the energy density, the more vehicle space is required to transport a given amount of energy. The bulk density of herbaceous biomass typically ranges from 50-200 kg/m^3 while that of woody biomass typically ranges from 200-500 kg/m^3 —well below the densities of fossil fuels ($\sim 600\text{-}900 \text{ kg/m}^3$). Table 2.1 shows bulk and energy densities for several kinds of fuel. Cellulose is the only plant component with a consistent HHV ($\sim 18 \text{ MJ/kg}$) due to its well-defined chemical structure. HHV for lignin varies over a range of 23.3-25.6 MJ/kg (Sheng and Azevedo, 2005). In general, biomass that contains more lignin has a higher energy density than biomass that is mostly carbohydrates.

Table 2.1. Energy content and densities of different fuels (Brown and Brown, 2014, Erol, et al., 2010)

Fuel	HHV (MJ/kg)	Bulk Density (kg/m^3)	Energy Content (GJ/m^3)
Diesel	46	850	39.1
Gasoline	48.24	740	35.7
Coal	18.33-36.67	600-900	11-33
Hardwood	18.92-18.95	280-480	5.3-9.1
Softwood	20	200-340	4-6.8
Agricultural residues	16-18	50-200	0.8-3.6
Nut shells	20.31	64	1.3
Animal manure	17.36	400	6.944
Municipal solid waste (MSW)	19.87	--	--
Orchard prunings	19.05	--	--
Sunflower shells	17.86	64	1.143
Methanol	22.27	790	17.6
Ethanol	29.74	790	23.5
Biomass pyrolysis oil	8.28	1280.2	10.6

2.3.3 Biomass Densification

One pretreatment method used to overcome the challenges of biomass energy is densification. Densification can increase the bulk and energy densities of biomass

by as much as 10 fold. It can also improve particle size and shape homogeneity, and particle durability, making biomass much easier to transport, store, and handle. Densification can be performed with a variety of equipment including pellet mills, screw extruders, briquette presses, cubers, roller presses, tablet presses, etc.; the first three are the most common methods. Energy consumption and end-product quality differ depending on the densification method. For example, screw extrusion has the highest energy consumption since it shears and mixes the material in addition to compressing it. A hardwood or softwood feedstock with an 8% of moisture content, 2-6 mm particle size, and bulk density of 200 kg/m³ fed through a screw extruder can reach a bulk density of 1400 kg/m³ while its moisture content decreases to 4% (Shastri, et al., 2014, Thoreson, et al., 2014, Tumuluru, et al., 2011). Densification end-product quality grades are often determined based on particle size uniformity, durability index, heating value, and moisture, ash, and chloride contents (2011). For some applications, quality certification programs are available. In the case of wood pellets for residential and commercial heating, the common standards are the ENplus quality scheme, the CANplus quality scheme, and the Pellet Fuels Institute (PFI) Standards Program, in the E.U., Canada, and the U.S., respectively (Wiberg, 2014). Recent research has focused on expanding the biomass densification market past wood pellets made using pellet mills and standard operating parameters. Adapa et al. (Adapa PK, et al., 2002, Adapa PK, et al., 2003), Ndiema et al. (Ndiema, et al., 2002), Li and Liu (Li and Liu, 2000), and Mani et al. (Mani, et al., 2006) have studied the pelletization of agricultural straw, the effects of die pressure (20-140 MPa) on biomass relaxation characteristics, high pressure (34-138 MPa) densification of wood residue, and compaction characteristics of lignocellulosic biomass using an Instron Universal Testing Machine, respectively. Pretreatment processes such as steam explosion, grinding, and torrefaction can be used to decrease densification energy consumption and improve biomass binding. Sarkar et al. showed that the bulk density of switchgrass could be increased from 138 kg/m³ to 499 kg/m³ through densification alone, and up to 598 kg/m³ when densification followed torrefaction at 270°C (Sarkar, et al., 2014).

2.3.4 Extracting Energy from Biomass

Due to the exothermic characteristics of carbon-carbon and carbon-hydrogen bond oxidation, lignocellulosic biomass may be burned directly as a solid fuel for process heat, or converted to flammable gases and liquids for later use. There are two broad conversion technology platforms: biological/biochemical and thermochemical/catalytic. The biological/biochemical conversion platform includes hydrolysis, fermentation, anaerobic digestion, and composting; this platform will not be considered here. The thermochemical conversion platform includes gasification, pyrolysis, and torrefaction, (as well as hydrothermal liquefaction (HTL) and solvolysis, which are not considered here).

2.3.4.1 Combustion

Biomass direct combustion is the complete oxidation of biomass at moderate to

high temperatures to produce hot flue gas and ash. The hot flue gas, mostly carbon dioxide and steam, can be used for many applications such as drying and space heating (low pressure), and power generation (high pressure). Combustion furnaces can be direct-fired or indirect fired. In direct-fired furnaces, the fuel is burned in the process steam or the process stream is in direct contact with the flue gases. This contact makes it probable that the process steam will become contaminated by combustion products (tars, ash, etc.) In indirect-fired furnaces, the combustion products are somehow separated from the process stream, such as with thermally conductive walls or with air-to-air heat exchangers.

Furnaces are often integrated with boilers for steam production. The two most common boiler configurations are fire-tube boilers and water-tube boilers. Fire-tube boilers, in which combustion gases are passed through tubes inside a water vessel, are more suitable for gaseous or volatile liquid fuels. Water-tube boilers, as the names implies, pass water through tubes held inside the fire; water-tube boilers are more complex and are more suitable for solid fuels, such as biomass (Brown and Brown, 2014). Solid fuel furnaces/water-tube boilers can be grouped into grate-fired, suspension, and fluidized bed systems. Grate-fired system combustion efficiency is barely more than 90% due to mass transfer limitations, while the efficiency of the other two systems can exceed 99%. Suspension burners are equipped with pulverizers to reduce the particle size of the fuels and enable entrainment for efficient conversion; their wide-spread implementation, however, has been hindered by their large NO_x emissions caused by high operating temperatures. Fluidized bed burners, due to their excellent mixing and large heat transfer surface areas, can operate at lower temperatures (~850°C) and thus limit their NO_x emissions. Whole tree burners also exist and can decrease wood harvesting and handling costs by eliminating the need for wood chipping (Brown and Brown, 2014).

The biomass combustion reaction consists of four stages: 1) warming and drying, 2) pyrolysis, 3) flaming pyrolysis, and 4) char combustion. Oxygen is only needed for the third and fourth stages. The warming and drying stage is endothermic and results in the evolution of associated water. As the temperature increases past 200°C in the second stage, hemicellulose and lignin begin to decompose and volatilize (i.e. pyrolyze). As the volatile gases from pyrolysis exit the biomass particle, they come in contact with oxygen which can result in gas phase reactions to form a flame, H₂O and CO₂. Once the gas phase reactions (third stage) are complete and oxygen can reach the surface of the biomass char remnants, solid-gas oxidation (fourth stage) reactions take place. Depending on the availability of oxygen and char temperature, the produced CO may be oxidized to form CO₂ (Brown and Brown, 2014).

Further information about biomass combustion can be found in (Branca and DiBlasi, 2003, Jenkins, et al., 1998, Zanzi, 2001).

2.3.4.2 Gasification

Gasification is simply combustion at slightly lower temperatures (750-1500°C) with less than the stoichiometric amount of oxygen, forming carbon monoxide and hydrogen (synthesis gas or “syngas”) rather than carbon dioxide and water. Gasification has been in use since 1812 in England, when conversion of coal to gas was needed for illumination purposes (lamps fueled by “town gas”). Syngas is flammable and includes small amounts of CO₂, CH₄, H₂S, and NH₃. If syngas contains a significant amount of N₂ from using air as the oxidant, it is called producer gas. Syngas/producer gas can be used for thermal energy generation in much the same way as natural gas, and as a material feedstock for making liquid fuels and other chemicals. Biomass’ high volatile matter content (70-90%) compared to many coals (30-40%), and the high reactivity of biomass char, make biomass a suitable feedstock for gasification (Zanzi, et al., 2002). Two challenges when designing biomass gasification reactors are how to treat incompletely-reacted tars, and how to avoid sintering and other reactor damage from the ash fraction (Quaak, et al., 1999). More information on biomass gasification, syngas cleaning and conditioning, and follow-on reactions can be found in (Chen, et al., 2003, Matsuoka, et al., 2008, Skoulou, et al., 2008, Timmer, 2008, Vigouroux, 2001).

2.3.4.3 Pyrolysis and Torrefaction

Pyrolysis is the heating and decomposition of biomass in the absence or severe limitation of oxygen to create a distribution of different products. Pyrolysis can be thought of as just the first two stages of combustion. Torrefaction is low temperature pyrolysis (200-300°C) used as a pretreatment to remove water and easily-degradable compounds while increasing biomass friability and energy density (Park, et al., 2014, Zanzi, 2001). Pyrolysis can be categorized into slow pyrolysis and fast pyrolysis where slow and fast refer to the heating rate (~10°C/min in slow pyrolysis and >500 °C/s in fast pyrolysis) and relative reaction time. Slow pyrolysis is the long-used technology for producing charcoal; its operating conditions maximize solid yield (Zanzi, 2001). Fast pyrolysis uses kinetic controls to optimize the liquid product yield. Both types of pyrolysis are usually conducted at 400-600°C, although slow pyrolysis may be done at lower or higher temperatures to adjust char properties. Biomass pyrolysis products include all three phases: gases (mostly CO, H₂, CO₂, CH₄, C₂H₂, etc.), liquids (bio-oil/tar and water), and solids (biochar and/or ash). The distribution of products changes depending on the biomass used and the operating conditions; a decrease in bio-oil yield results in an increase in biochar and gas yields, and vice versa.

Non-condensable pyrolysis gases can be the product of primary biomass decomposition, as well as the product of secondary tar cracking and char gasification. Gas production is typically favored by higher temperatures, longer reaction times, and smaller particle sizes (Zanzi, 2001). Although pyrolysis gas has a low heating value, it is still suitable for thermal energy production and power generation (Chen, et al., 2003, Park, et al., 2014). In a characterization study of pyrolysis gas, Brown et al. showed that carbon monoxide, carbon

dioxide, nitrogen, and methane contributed the highest concentrations, respectively (Brown, et al., 2011). Besides these gases, oxygen and traces of ethylene, ethane, propylene, and C4 gases were also observed. The heating value increased from 8 to 15 MJ/kg as the pyrolysis temperature increased from 525 to 650 °C, with carbon monoxide and methane providing nearly 80% of the gas heating value (Brown, et al., 2011). For rice straw pyrolysis, Park et al. also found an increase in gas heating value with temperature: from 4.1-11.4 MJ/kg over 300-700°C, respectively (Park, et al., 2014).

Biochar is the carbon-rich solid product of pyrolysis that can be used as a solid fuel, a feedstock for activated carbon adsorbent production, and as a soil amendment to improve soil fertility and sequester carbon (Brown, et al., 2011). Yields of biochar are usually 15-20% for fast pyrolysis and 20-50% for slow pyrolysis on a dry biomass weight basis. Lignin content in biomass typically favors char formation reactions resulting in higher char yields (Brown, et al., 2011, Lee, et al., 2010, Lee, et al., 2013). For a temperature range of 450-500°C, slow pyrolysis produces about 0.26 kg of char per kg of biomass, with approximately 45% of the biomass carbon being retained in the char (Shabangu, et al., 2014). Biochars usually have HHVs similar to those of coals (13-23 MJ/kg), where slow pyrolysis and woody feedstocks favor higher HHVs compared to fast pyrolysis or gasification and herbaceous feedstocks (Brewer, et al., 2009).

2.4. Energy and Water Desalination

2.4.1 Energy Requirements for Desalination

Water desalination plants use about 4-20 kWh/m³ (14-72 MJ/m³) of electrical energy equivalent to produce fresh water; if thermal energy has to be converted to produce electrical energy (at ~30% efficiency), this value would be approximately 46-240 MJ/m³ (Al-Karaghoul and Kazmerski, 2013). Desalination unit energy consumption contributes about 60% of water production costs (Al-Karaghoul and Kazmerski, 2013). For an energy optimized desalination system, Semiathas showed that the energy costs can be decreased to 30-44% of total water production costs (Semiath, 2008).

The amount of energy needed for water desalination is dependent on many factors such as the form of energy (electrical, thermal, etc.), plant capacity, plant design configuration, and feed water TDS. The energy needed for MED and MSF processes is generally much higher than that required for RO because of the water evaporation step in MED and MSF, and significant improvements in RO technology that have lowered its power consumption (Fiorenza, et al., 2003, Kalogirou, 2005). Thermal desalination technologies, however, are capable of decreasing the TDS to less than 10 ppm while RO technologies can reduce the TDS to 10 ppm to 500 ppm, depending on the membranes used. The TDS limits for drinking water are typically 400 to 500ppm—much higher than that of water produced in MED and well within the range for RO (Al-Karaghoul and Kazmerski, 2013). For drinking water, therefore, some untreated feed water can

be added to the desalinated water to moderate the TDS concentration and make MED water more cost-effective (Sen, et al., 2013).

Water desalination plant capacities, energy requirements, and produced water costs for small-scale plants are shown in Table 2.2. As expected, energy and cost requirements for small-scale plants are much higher than those for large-scale plants. All of the energy requirement values assume that chemical energy from biomass is converted to thermal energy and that thermal energy is converted to needed electrical energy at an efficiency of 30% to account for thermodynamics. For example, if 1 kWh/m³ (3.6 MJ/m³) of electrical energy was described in the original reference, the table will list 12 MJ/m³ of thermal energy.

2.4.1.1 Energy Consumption in RO

A typical RO unit, with an energy recovery system and a plant capacity of up to 128,000 m³/day for seawater and 98,000 m³/day for brackish water, consumes 14.4-21.6 MJ/m³ (4-6 kWh/m³) and 5.4-9 MJ/m³ of electrical energy, respectively. This difference in energy requirements is the main cost difference between treating seawater and brackish water by RO (Semiati and Hasson, 2012). High TDS concentrations result in more energy consumption at a rate of approximately 3.6 MJ/m³ (1 kWh/m³) per 10,000 ppm (Garcia-Perez, et al., 2012).

2.4.1.2 Energy Consumption in MSF

The factors that affect energy consumption in MSF systems are temperature of the heat sink, number and geometry of the stages, feed water TDS concentration, unit construction materials, and heat exchanger configuration. Increasing the GOR, the number of stages, and the heat transfer surface area are all ways to lower energy consumption (Al-Karaghoul and Kazmerski, 2013, Elimelech and Phillip, 2011, Miller, 2003, Semiati, 2008). From design information provided by commercial manufacturers, a typical MSF, with a production rate of 50,000-70,000 m³/day and a GOR of 8-12, consumes between 190 MJ/m³ and 282 MJ/m³ of thermal energy, and 13.5 MJ/m³ (3.75 kWh/m³) of electrical energy (Al-Karaghoul and Kazmerski, 2013, Semiati, 2008).

2.4.1.3 Energy Consumption in MED

Similar to MSF, MED needs thermal energy for water evaporation and electrical energy to power pumps. A typical MED unit, with a production rate of 5,000-15,000 m³/day, a top brine temperature (TBT) of 64-70°C, and a GOR of 10-16, requires 145-230 MJ/m³ of thermal energy and 8.1 MJ/m³ (2.25 kWh/m³) of electrical energy. The energy consumption for both MSF and MED could be decreased significantly if they used cogeneration power plants, where waste steam from the power turbine exhaust provides the initial thermal energy (Al-Karaghoul and Kazmerski, 2013, Semiati, 2008).

2.4.1.4 Energy Consumption in VC

Mechanical vapor compression (MVC) only requires electrical energy. A MVC unit, with a production rate of 100-3,000 m³/day and a TBT of 74°C, requires 25.2-43.2 MJ/m³ (7-12 kWh/m³). A thermal vapor compression (TVC) unit, with a production rate of 10,000-30,000 m³/day, a GOR of 12, and a TBT of 63-70°C, requires 227.3 MJ/m³ of thermal energy and 5.7-6.48 MJ/m³ (1.6-1.8 kWh/m³) of

electrical energy (Al-Karaghoulouli and Kazmerski, 2013, Semiat, 2008).

Table 2.2. Water desalination plant capacities, thermal energy requirements (assuming a 30% efficiency for conversion of thermal energy to electrical energy if electricity is required), and water production costs for small-scale (<100 m³/day) conventional and renewable energy source-desalination technologies.

Method	Size (m ³ /day)	Water	Energy (MJ/m ³)		Cost (US\$/m ³)	Ref.
			Electrical	Thermal		
Conventional MED (single-purpose)	<100	Seawater	-	-	2.0-8.0	(Al-Karaghoulouli and Kazmerski, 2013)
Diesel MED	4	Brackish	-	1,110	26.50	(Sen, et al., 2011)
Conventional RO	20-1,200	Brackish	-	-	0.78-1.33	(Karagiannis and Soldatos, 2008)
Solar Still	<100	-	0	Passive solar	1.3-6.5	(Al-Karaghoulouli and Kazmerski, 2013)
Solar Multiple Effect Humidification	1-100	-	18	355	2.6-6.5	(Al-Karaghoulouli and Kazmerski, 2013)
Solar MED	1	Brackish	-	-	25.3	(Al-Karaghoulouli, et al., 2009)
Solar MED	72	Seawater	-	-	3.6-4.35	(Al-Karaghoulouli, et al., 2009)
Solar Membrane Distillation	0.15-10	-	0	540-708	10.5-19.5	(Al-Karaghoulouli and Kazmerski, 2013)
Solar PV RO	<100	Seawater	48-72	0	11.7-15.36	(Al-Karaghoulouli and Kazmerski, 2013)
Solar PV RO	<100	Brackish	18-48	0	6.5-9.1	(Al-Karaghoulouli and Kazmerski, 2013)
Solar PV ED	<100	-	18-48	0	10.4-11.7	(Al-Karaghoulouli and Kazmerski, 2013)
Wind RO	19	Seawater	-	-	4.4-7.3	(Al-Karaghoulouli, et al., 2009)
Wind RO	12	Seawater	-	-	2.6	(Al-Karaghoulouli, et al., 2009)
Wind MVC	<100	-	84-144	0	5.2-7.8	(Al-Karaghoulouli and Kazmerski, 2013)
Geothermal MED	80	-	24-36	149-289	2.0-2.80	(Al-Karaghoulouli and Kazmerski, 2013)

2.4.2 Fossil Fuel Energy and Water Desalination

Conventional water desalination technologies, especially those with the highest capacities in the Middle East, are powered by fossil fuels such as coal, crude oil,

and natural gas. Concerns about future availability, greenhouse gas emissions, and environmental impacts of fossil fuels has helped focus future water desalination technologies (and power generation in general) towards energy efficiency and renewable energy (Nisan and Benzarti, 2008).

Nisan et al. showed that, at present coal prices, the integration of RO or MED water desalination systems with circulating fluidized bed, coal-fired power plants would result in the lowest power and desalination costs, while oil-fired power production would result in the highest desalination costs. From an environmental impact analysis perspective, RO with a combined cycle gas turbine power plant had the lowest emissions of NO_x, SO_x, CO₂, and particulates, while MSF with a coal-fired power plant had the highest emissions (Nisan and Benzarti, 2008). Methnani has shown that RO water desalination, coupled with any type of fossil fuel, would have lower costs than MED due to the lower energy requirements for RO. This difference in costs, however, is generally negligible except when treating very high salinity water (Methnani, 2007). The use of pulverized coal rather than lump coal in power plants results in higher efficiency for the boiler (and the whole desalination system) since more of the furnace volume is used and the coal is more completely combusted (Tian, et al., 2005).

2.4.3. Renewable Energy and Water Desalination

The integration of renewable energy with desalination is especially suitable for remote areas and areas lacking connection to electrical energy grid infrastructure; in some cases, solar is the only feasible option due to distance from other resources (Al-Karaghoul, et al., 2009, Tzen, 2005). The most popular renewable energy sources for water desalination units have been solar photovoltaic (PV), solar thermal, wind, and geothermal, and hybrids of these options. Factors to consider when pairing renewable energy and desalination technologies include type, amount, and cost of energy available, site topography and geographical conditions, plant size, feed water salinity, capital costs, treatment requirements, and local infrastructure. 13% of renewable energy powered desalination systems worldwide are solar-MED, while 6% are solar-MSF. Eltawil et al. provide a very useful table of combinations of renewable energy sources and water desalination methods in (Eltawil, et al., 2009).

2.4.3.1 Solar Energy and Water Desalination

Solar energy may be used for water desalination unit indirectly, such as by connecting a solar collector to a desalination system, or directly, such as within a solar still where collection and desalination occur in a single unit.

Both MED and MSF can be used with solar collectors providing steam. The first method is direct steam generation (DSG), which uses parabolic trough collectors and fresh water, brine, or seawater as the heat transfer fluid (García-Rodríguez and Gómez-Camacho, 2001). In a solar DSG-MED system, the solar collector plays the role of the first effect: feed water, pre-heated in the MED, enters the solar collector and is partially evaporated by solar energy. The steam generated in the collector is then used as the heat source in the second effect. In such a system,

the initial steam is generated from the feed water/brine rather than fresh water (García-Rodríguez and Gómez-Camacho, 1999); however, fresh water may also be used for steam production (García-Rodríguez, et al., 1999). The second method for steam production in solar-MED systems also uses parabolic trough collectors but uses oil to transfer heat to the first effect. The third method for steam production is flashing pressurized water in a flash drum after it has been heated in the solar collector. Depending on climate conditions, any of these three methods may be used to enhance fresh water production (García-Rodríguez and Gómez-Camacho, 2001, García-Rodríguez, et al., 2002, Kalogirou, 2005, Qiblawey and Banat, 2008).

For direct solar water desalination, a conventional solar still uses a blackened bottom surface to absorb solar energy and the green-house effect to evaporate salty water within a V-shaped glass envelope. Solar still efficiency, the ratio of energy utilized in water evaporation to the solar energy incident on the glass cover, has a maximum value of approximately 35%. For more information on solar stills, see (Daniels, 1974, Eibling, et al., 1971, Kalogirou, 2014, Kalogirou, 2005).

Raluy et al. observed that for MSF units integrated with solar thermal energy, 63% of airborne emissions, including CO₂, NO_x, SO_x, and non-methane volatile organic compounds, decreased compared to MSF units using conventional fossil fuel boilers. The use of solar energy, however, requires special raw materials for cell and panel production compared to other renewable energies and, therefore, has more environmental impacts. Also, solar energy is available just part of the day (about 25% of the time) and thus, the cost of water produced through solar desalination is higher than that of water produced through conventional energy-powered desalination (Raluy, et al., 2005).

2.4.3.2 Hydroelectric Energy and Water Desalination

Hydropower is generated from the gravitational potential energy stored in water by damming rivers. Low-temperature waste heat from a hydropower turbine can be used as the thermal energy source for MSF and MED. Hydro-MSF has been shown to be the most effective combination in terms of reducing airborne emissions (79% decrease) compared to fossil fuel-MSF; the results were similar (71% emissions decrease) for hydro-MED (Akash and Mohsen, 1998, Murakami, 1994, Raluy, et al., 2005).

2.4.3.3 Wind Energy and Water Desalination

Wind, the result of atmospheric pressure differences caused by solar energy, is a suitable energy source for powering desalination units, especially for remote areas with high wind speeds such as islands (Kalogirou, 2005, Kiranoudis, et al., 1997). Because of weather-related wind speed fluctuations, efficient back-up power systems such as diesel generators, batteries, or flywheels are needed to stabilize the energy production rates (Tzen and Morris, 2003, Tzen, et al., 1998). One significant advantage of wind energy is its low cost compared to other renewable technologies. Wind is locally available and does not require much water transportation from treatment location to end user. Wind turbines can be coupled

with several desalination technologies, though they have mostly been used with RO systems. The amount of treated water that can be produced effectively by a wind-RO system is 50-2,000 m³/day (Al-Karaghoulis and Kazmerski, 2013, Eltawil, et al., 2009). A useful overview of wind energy has been provided by Ackermann (Ackermann and Söder, 2002). More information on wind-powered desalination is available in (Al-Karaghoulis, et al., 2009, García-Rodríguez, et al., 2001, Habali and Saleh, 1994, Kiranoudis, et al., 1997, Lenzen and Munksgaard, 2002, Ma and Lu, 2011, Miranda and Infield, 2003, Robinson, et al., 1992).

2.4.3.4 Geothermal Energy and Water Desalination

Geothermal energy is heat stored beneath the earth's surface. Geothermal reservoirs can be low temperature (<150°C) or high temperature (>150°C); temperature directly affects which applications can make use of the stored energy. Medium to high temperature geothermal reservoirs can provide energy for either membrane or thermal desalination processes. One advantage of geothermal energy is that there is no need for additional energy storage reservoir heat supply is continuous and predictable. Ophir showed that a geothermal-desalination plant would cost as much as a large multi-effect dual-purpose desalination plant (Ophir, 1982). As described in a report by Awerbuch (Awerbuch, et al., 1976), the first geothermal-desalination pilot plant was built in Holtville, California in 1972, funded by U.S. Bureau of Reclamation (Al-Karaghoulis and Kazmerski, 2013, Eltawil, et al., 2009). Pilot-scale geothermal-MED plants have been designed and tested in France (Bourouni, et al., 1999) and southern Tunisia (Bourouni, et al., 2001); the evaporators and condensers for these units were made of polypropylene and the unit operating temperature was 60-90°C (Bourouni, et al., 1999). Sometimes, brine from geothermal desalination systems can be used directly as the feed water/heat source for thermal desalination, or even RO, if the membranes can withstand higher temperatures (60-90°C). If a geothermal reservoir can provide high enough pressure water, it can provide shaft energy for mechanically driven desalination processes (Barbier, 2002, Houcine, et al., 1999).

2.4.3.5 Biomass Energy and Water Desalination

The literature is nearly silent on biomass energy for water desalination. Eltawil et al. described the use of biomass for water desalination energy as not being “a promising alternative since organic residues are not normally available in arid regions and the growing of biomass requires more fresh water than it could generate in a desalination plant” (Eltawil, et al., 2009). For most situations, this conclusion is reasonable, especially when large water treatment capacities are needed, the feed is high salinity seawater, or the biomass is grown only for energy production. In situations where very small plant capacities are needed, where significant amounts of local agricultural, forestry, or urban biomass residues are available and underutilized, and/or where the feed water is of relatively low salinity, biomass use may be a feasible alternative.

For example, in New Mexico in the southwestern U.S., the climate is warm to hot and semi-arid to arid, enabling agricultural production through irrigation with ground water. This ground water has varying levels of salinity, from fresh to brackish. Residues from agriculture including pecan orchard prunings and shells

(Lillywhite, et al., 2010), cotton gin trash (Isci and Demirer, 2007), and dairy manure, in addition to urban yard waste, are locally available. In this scenario, biomass might conceivably serve as the energy source for a farm-scale irrigation or neighborhood-scale drinking water thermal water desalination plant. Combustion, gasification, or pyrolysis could be used to directly convert biomass into thermal energy. A slow pyrolysis process would have the added advantage of producing a value-added biochar product that would be used as an adsorbent for additional water treatment or as a soil amendment for improved soil water use efficiency and fertility (Barrow, 2012, Laird, 2008, Lal, 2008, Lehmann and Joseph, 2009, Lehmann, et al., 2003).

2.5 Economics

2.5.1 Economics of Water Desalination Plants

The costs for a water desalination plants may be grouped into capital costs and operational costs. Capital costs are one-time costs and include direct construction costs, such as land, equipment, buildings, and wells/surface water intake and concentrate disposal infrastructure, and indirect construction costs. Operational costs are recurring costs and include fixed costs such as insurance and amortization (usually 0.5% and 5-10% of the total capital costs, respectively) and variable costs such as maintenance, labor, energy, chemicals, supplies, etc. For a typical seawater RO plant, capital costs and energy costs represent 37% and 44%, respectively, of the total costs. For a similar thermal desalination plant, the capital cost fraction is lower (32%) and the energy costs higher (50%) because of the higher energy requirement per cubic meter of produced water for thermal systems (Eltawil, et al., 2009, Fiorenza, et al., 2003).

Energy consumption and hence, the final produced water cost, is significantly reduced in thermal desalination units if the power source is dual-purpose, i.e. the turbine is directly integrated with the desalination unit so that low-temperature exhaust heat energy provides the primary steam for desalination (Ophir and Lokiec, 2005). For example, the produced water cost of a 6 million gallon per day (22,700 m³/day) single-purpose MED unit would be 0.739 cents/gallon (1.95 US\$/m³), while the produced water cost from a similar capacity dual-purpose unit would decrease to 0.330 cents/gallon (0.87 US\$/m³). Use of corrosion-resistant materials for heat transfer surfaces also decreases the capital and long-term energy costs for thermal desalination processes due to reduced scaling (Eltawil, et al., 2009).

Fresh water produced in conventional (fossil fuel-powered) MED plants with capacities of >90,000 m³/day costs approximately 0.52-1.01 US\$/m³. As the capacity of the MED plant decreases to 12,000-50,000 m³/day, the produced water cost increases to 0.95-1.95 US\$/m³. The estimated produced water cost for an MSF plant with a capacity of 23,000-528,000 m³/day is 1.75-0.52 US\$/m³, respectively (Al-Karaghoul and Kazmerski, 2013).

2.5.2 Economics of Coupling Renewable Energy and Water Desalination

Although many forms of renewable energy are available for free or very low cost, there are often significant capital costs for renewable energy systems, which result in dramatically higher produced water costs, especially at the smaller scale (see Table 2.2). These costs can be decreased with continuous improvements in renewable energy systems and power-saving strategies. Currently, renewable energy-powered water desalination systems are economically feasible only in rural communities with no access to an electrical grid, and/or where solar and wind resources are abundant.

The water production cost for a concentrated solar power-MED system with a production capacity of about 5,000 m³/day, a thermal energy requirement of 147-289 MJ/m³, and an electrical energy requirement of 2.5 kWh/m³ (9 MJ/m³) would be 2.40-2.80 US\$/m³ (Al-Karaghoul and Kazmerski, 2013, Fiorenza, et al., 2003). A typical geothermal-MED system, with a capacity of 80 m³/day, a 80-100°C energy source, and the same energy requirements as the concentrated solar power system, would have a water production cost of 2.00-2.80 US\$/m³ (Al-Karaghoul and Kazmerski, 2013). Solar PV-RO and PV-ED are promising technologies in terms of economics; the main disadvantages of these systems are the low availability (and therefore high cost) of large PV arrays (Eltawil, et al., 2009).

2.6 Small-Scale Water Desalination Technologies

Much of the world's water desalination capacity is large-scale, fossil fuel-powered, seawater desalination. In general, produced water cost increases as plant capacity decreases and renewable energy sources are used. Small-scale desalination systems and their economics, however, are very important for small, rural communities where the available water is brackish or contaminated. Sen et al. have focused on designing small-scale desalination systems for rural communities in India to address such concerns (Sen, et al., 2013). They developed a micro-scale MED system, initially powered by diesel, with 3 effects, a FF arrangement, a GOR of 3.6, and a fresh water production rate of 11-12 L/hr. (0.27 m³/day). The unit can decrease the TDS of the water from 750 ppm to <10 ppm, well below the required TDS for potable water (Sen, et al., 2011). In another series of studies on small-scale MED unit design and operating parameters, Sen et al. experimented with 3, 6 and 9-effect systems, vertical tube evaporators using falling film water flow, and parallel feed alternatives. They found that a steam flow rate of 30 kg/hr. at 4 bar, and a feed water flow rate of 100 kg/hr., were satisfactory to meet design goals. The produced steam from the boiler was 130-140°C and the feed water was heated to 110-112°C (Sen, et al., 2011, Sen, et al., 2011, Sen, et al., 2011). The 9-effect MED, at semi-optimized parameters, produced 4 m³/day of distilled water and required approximately 1110 MJ/m³ of thermal energy at a cost of approximately 26.5 US\$/m³ (assuming a diesel energy content of 43 MJ/L, a cost of 0.86 US\$/L, and a density of 0.832 kg/L) (Sen, et

al., 2011). These very high energy and cost values are expected to decrease with improvements in boiler efficiency, insulation to prevent heat losses, and continuing adjustments to the heat exchangers. Long-term goals for this research include increasing ease of fabrication, decreasing costs, and incorporating biomass-derived energy to replace the diesel fuel.

Biomass, with its relatively high moisture, oxygen, and ash content, and low bulk and energy densities, is best suited for small scale applications as transportation costs increase quickly with increasing distances (Wright and Brown, 2007). As such, biomass makes a less-than-ideal energy source compared to fossil fuels and electricity. Non-food biomass, however, is abundant in many places in the form of agricultural residues, forestry residues, yard waste, construction wood waste, and municipal solid wastes (cloth, paper, cardboard, etc.) (Downing, et al., 2011). Many of these residues go underutilized in landfills, especially in rural areas where there is less pressure for waste valorization. For those rural areas that require small-scale water desalination, communities should consider biomass-powered water treatment systems; such systems may not represent optimized energy efficiency or costs, but they may allow communities to meet their needs with the resources they already have. Biomass should also be considered as a supplement to solar power during off-peak times.

Conclusions

Different kinds of renewable energy-powered water desalination methods and technologies are available. For most scenarios, using renewable energy sources is much more expensive than conventional energy sources due to high capital costs. Improvements in energy efficiency and renewable energy collection/conversion technologies has somewhat driven down these costs, and the environmental benefits of using renewable energy sources has helped shrink the overall advantages of conventional energy systems. Much more research is needed for optimized site-specific renewable energy-powered water desalination system design.

If biomass is to be a feasible energy source for water desalination, a small-scale thermal desalination system in a rural area with lower salinity (brackish) feed water and abundant waste biomass is the most promising scenario. The economics of such a system would be significantly improved if the energy conversion method can produce other valuable products such as biochar.

3. Design Parameters for Biomass Pyrolyzer-MED System

3.1 System Scale and Desired Qualities

The low energy density nature of biomass dictates that biomass for energy be used close to its source. Close, by many estimates, is within several tens of miles (km) (Wright and Brown, 2007). Therefore, a water desalination system using biomass residues for energy will need to be on the scale of a single farm or a co-op of farms or residences. Within those constraints, the designed system must also account for the amount of biomass available on a seasonal basis and/or from storage. If the water is needed year-round, then the biomass must also be available year-round. On the other hand, if the produced water is to be used for a short-term purpose, such as flushing salts out of the root zone prior to planting or irrigating salt-sensitive seedlings, the seasonality of biomass residue supplies must be matched to the needed times.

The design of this system was based on the available water and biomass residues in the Mesilla Valley region of southern New Mexico. Brackish water chemistry was modeled off of wells 2, 3, and 4 at the Brackish Groundwater National Desalination Research Facility (BGNDRF) at Alamogordo, NM. These waters ranged in total dissolved solids (TDS) from 3,450 to 6,400 mg/L and pH values from 7.0 to 7.8 (Munoz-Guerra, et al., 2011). Target biomass residues were pecan shells, pecan orchard prunings, cotton gin trash, and yard waste. Other abundant residues that might be considered for this region are invasive species, namely tumbleweed and salt cedar, and dairy manure.

The design process started with the thermal and electrical energy needs of the multiple effect distillation (MED) water desalination unit and worked backwards to determine the needed biomass feed rate. The target fresh water production rate was 1-2 m³/day or approximately 50 kg/hr.; this rate is considered micro-scale for water desalination technologies. The process would be continuous flow, use unit operations that could be installed on a mobile platform such as a trailer pulled by a pickup truck or a semi and be operated by two people. All of the energy needed for the water desalination would come from the biomass with the exception of start-up energy that might come from propane, diesel, or electricity. The pyrolysis process would be energy self-sufficient. Other sources of energy might be used for biomass size reduction (splitting, chipping) and drying. The process would be clean such that the only products were fresh water, brine, biochar and carbon dioxide.

3.2 Unit Operations

3.2.1 Process Flow

The process flow consists of 12 unit operations:

1. Biomass is added to a *feed hopper*;
2. From the feed hopper, biomass enters the *auger slow pyrolysis unit* and is converted into chars, bio-oil (as vapors and aerosols) and non-condensable gases (NCG) through partial combustion of the biomass;
3. Chars are fed into a *char collection* container where some of the cooled flue gases are warmed before being recycled into the pyrolysis unit;
4. Bio-oil vapors, aerosols and NCG flow into a *furnace* where they are combusted with additional air to form carbon dioxide and water;
5. Heat from the combustion furnace heats water in a *boiler* to produce steam;
6. Steam from the boiler is fed through a *steam turbine* to produce electricity;
7. Low pressure, low temperature steam is fed into the *first effect of the MED unit* to provide process heat; condensed steam is recycled to the boiler or collected with the distillate;
8. Electricity from the turbine generator is used to power the *vacuum pump* and the *water pumps* (feed water, brine, and distillate) of the MED;
9. Brackish feedwater is preheated using the *condenser unit of the MED* then a *heat exchanger* connected to the warm flue gas stream exiting the combustion furnace;
10. Preheated feedwater is sprayed into the *effects* in a parallel feed arrangement, creating a falling film over horizontal heat transfer tubes and producing low-pressure steam that flows into the next effect;
11. Brine collected at the bottom of each effect is removed to *brine storage* or recycled into the *feedwater tank*;
12. Distilled water collected in the condenser is pumped through a valve into *fresh water storage*; the *valve* allows the diversion of the produced water into the feedwater if the electrical conductivity is too high.

3.2.2 Steam for the MED

The energy required for primary steam for the MED was calculated as follows assuming the use of two evaporation effects.

For steam flow rate = 23 kg/hr., pressure = 0.5 bar absolute (7.3 psia), and temperature = 81.3°C (178°F), the amount of energy released by the steam within the MED first effect as latent heat is:

$$Q_{total} = Q_{latent} = M_{steam} \times H_{vap} \quad (1)$$

where M_{steam} is the steam flow rate and H_{vap} is the latent heat of vaporization. From steam tables for saturated steam at 0.5 bar and 81°C, the enthalpy of condensation is 2306.3 kJ/kg, which results in an energy transfer rate:

$$Q_{latent} = 23 \frac{kg}{hr} \times 2306.3 \text{ kJ/kg} = 53,045 \frac{kJ}{hr} = 14.73 \text{ kW} \quad (2)$$

This amount of thermal energy is appropriate to produce approximately 55 kg/hr. of fresh water if 227 kg/hr. of brackish water (TDS = 1,000-3,000 mg/L) is fed into the effect.

In the case that the exhaust steam from turbine is superheated (to a temperature higher than 81°C for the same steam pressure) the amount of energy released by steam within the MED effect would be:

$$Q_{total} = Q_{sensible} + Q_{latent} = M_{steam} \times C_p \times \Delta T + M_{steam} \times H_{vap} \quad (3)$$

where C_p is the heat capacity and ΔT is the temperature difference between the superheated steam and saturated steam. The heat capacity of the steam was estimated for the steam using a standard temperature-dependent heat capacity model from Table C.1 of (Smith, et al., 2005).

3.2.3 Electricity for the MED

The electrical power requirements for the MED unit assumed that four unit operations would be needed with individual power requirements of:

- 2.2 kW for a vacuum pump to provide vacuum at approximately 0.1-0.2 bar within the MED unit;
- 58 W for the distillate pump;
- 58 W for the brine pump;
- 108W for the feedwater pump;

which results in a total electrical power requirement of 2.45 kW.

3.2.4 Aspen Plus® Simulation

Process simulation software, Aspen Plus®, was used to model the mass and energy balances associated with the pyrolyzer-MED interface unit operations based on the thermal and electrical power needs of the MED unit. The model included four continuous, steady-state unit operations: a furnace to combust the non-condensable gases (NCG) and bio-oil to produce hot flue gas, a shell-and-tube heat exchanger (boiler) to use heat from the flue gases to produce steam, a turbine to convert the steam to electricity, and a second shell-and-tube heat exchanger to use residual heat in the flue gas to preheat the MED feedwater. The complete process flow is shown in Figure 3.1. Simulations were first run on as individual blocks using results from other block simulations. Once input and output streams were near converging on individual block bases, the unit operation blocks were combined into one single process block and the simulations repeated until convergence was achieved.

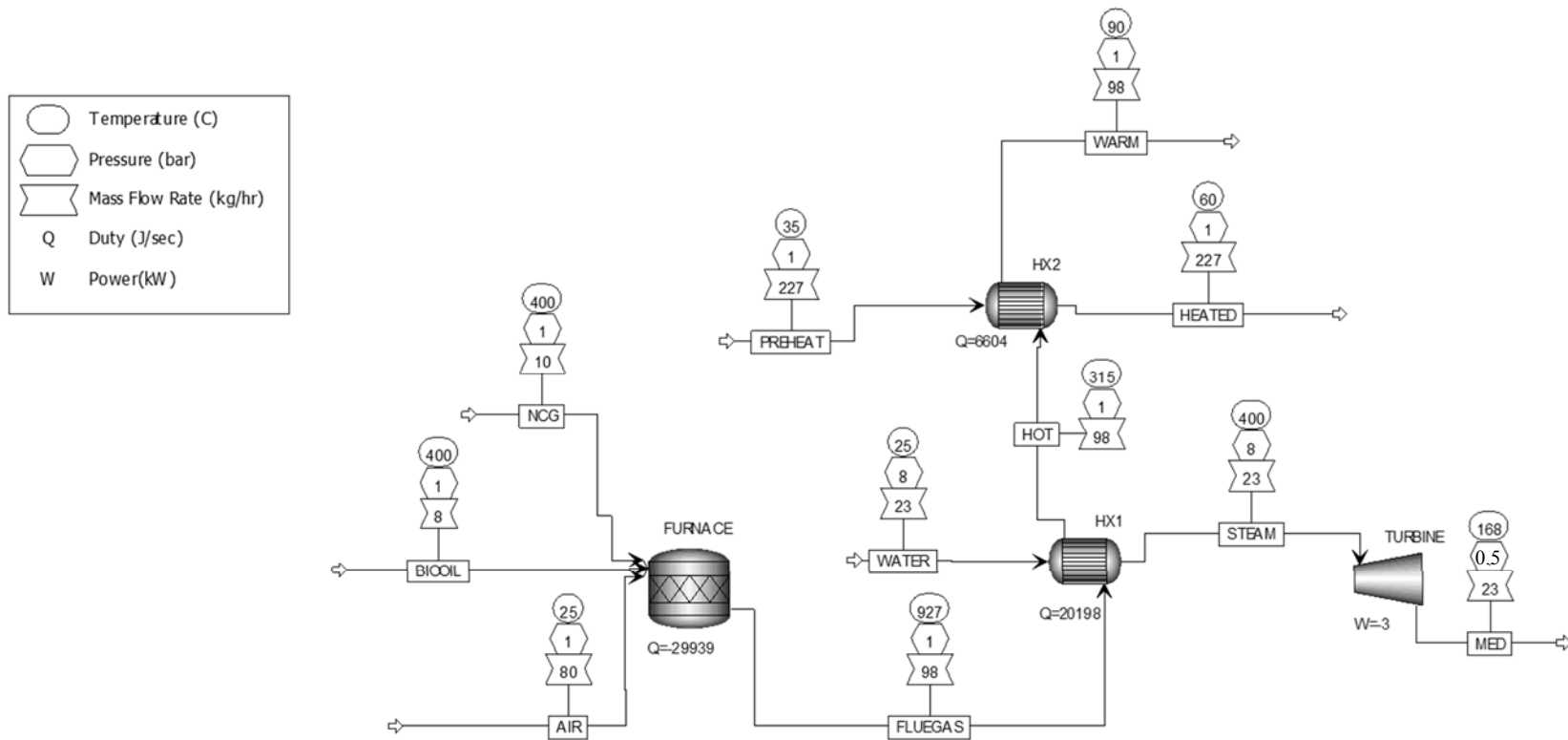


Figure 3.1 Aspen Plus® process flow diagram for pyrolyzer-MED interface showing stream temperatures, pressures, mass flow rates, heat duties and electrical power. HX1: heat exchanger 1, boiler; HX2: heat exchanger 2, preheater for the MED brackish feedwater; NCG: non-condensable gases; MED, multiple effect distillation unit.

3.2.4.1 Turbine Simulation

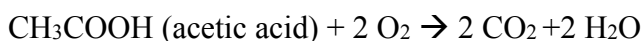
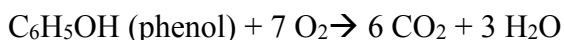
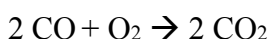
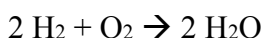
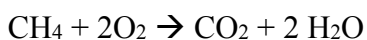
The only available option for a turbine in Aspen Plus® is the isentropic turbine. However, Aspen provides two temperatures for the outlet stream, one for the actual requirements and one for the idealized isentropic conditions, which are usually the same value initially. Turbine efficiency was set to the default value of 72%. The property method used was IAPWS-95, and the free-water phase properties were determined using STEAM-TA and water solubility method 3. The discharge pressure and indicated horsepower were 0.5 bar and 3 kW, respectively.

3.2.4.2 Boiler Simulation

From the turbine simulation preliminary results, the output requirements for the boiler heat exchanger were set to provide 23 kg of steam at 8 bar and 400°C. As with the turbine, the free-water phase properties were determined using STEAM-TA and water solubility method 3. The hot (steam) side of the boiler was modeled using Peng-Robinson vapor only; the cold (water) side was modeled using STEAM-NBS vapor and liquid. Heat exchanger configuration was set to countercurrent shell-and-tube with a minimum approach temperature of 1°C

3.2.4.3 Furnace Simulation

The furnace model was more complicated because NCG and bio-oil compositions and combustion reactions had to be specified. Using literature about slow pyrolysis NCG and bio-oil composition as guidance, five complete combustion reactions available in Aspen Plus® were selected in the following order:



The mole fractions for the NCG input stream were assumed to be 68% CO₂, 28% CO, 2% H₂ and 2% CH₄, at a temperature of 400°C and atmospheric pressure (Phan, et al., 2008, Wijayantia and Tanoue, 2013). The bio-oil input stream was set at 400 °C and atmospheric pressure with mole fractions of 53% phenol, 28.1% acetic acid, 9.2% furfural, 5.4% methyl acetate and 4.3% hydroxyacetone (Kim, et al., 2014, Phan, et al., 2008). Air was assumed to have a molar composition of 79% N₂ and 21% O₂ at an input temperature and pressure of 25°C and 1 bar, respectively. The property model used for the furnace calculations was Peng Robinson with free-water phase properties treated as ideal (due to the high temperatures and low pressures). The furnace efficiency was assumed to be 80% based on a standard gas-fueled boiler (2015). Furnace operation was optimized by varying the air flow rate and the combustion temperature. Input flow rates had to be adjusted when different heat duties were needed to avoid heat transfer

temperature cross over in the boiler.

3.2.4.4 Brackish Feedwater Preheater Simulation

The heat exchanger used to further cool the flue gas and to preheat the MED unit brackish feedwater was modeled as a countercurrent shell-in-tube exchanger. The cold side was modeled as liquid only using STEAM-NBS with an outlet temperature of 60°C; the hot side was modeled using gas-phase only Peng-Robinson. The minimum approach temperature was limited to 1°C.

3.3.4 Calculating Biomass Needs

The necessary flow rates of bio-oil and NCG from the pyrolyzer were calculated from the Aspen Plus® simulation of the furnace; from that calculation, the amount of biomass needed per m³ of produced water from the MED unit can be estimated. In the slow pyrolysis of lignocellulosic biomass, approximately 60-70% of the dry feedstock mass is converted into bio-oil vapors and NCG, while the remaining 30-40% of the mass is converted into char (Lee, et al., 2013, Phan, et al., 2008). To get the amount of biomass needed, the combined mass flow rates from the bio-oil and NCG streams of the converged simulation were simply divided by the pyrolysis yields on a dry basis. Based on the bio-oil and NCG gas compositions assumed for the simulation, the combined bio-oil and NCG would have a higher heating value (HHV) of approximately 7.5 MJ/kg; with the 80% assumed furnace efficiency, 6.0 MJ/kg of this energy would be converted into usable energy for the boiler.

3.3 System Design Results

The results of the converged Aspen Plus® simulation are shown in Figure 3.1. The overall inlet streams into the furnace were 10 kg/hr. and 8 kg/hr. of NCG and bio-oil, respectively, at 400°C and 1 bar, and 80 kg/hr. of air. An optimum combustion temperature was calculated at 927°C and released 29.9 kW of thermal energy. The surface area needed for the boiler was 0.057 m² to produce 23 kg/hr. of steam at 400°C and 8 bars using 98 kg/hr. of hot flue gas at 1 bar and 927°C. Exiting the turbine was superheated steam at 168°C and 0.5 bar; the turbine produced 3 kW of work for an electrical generator. The surface area needed for the brackish water preheater was 0.06 m² and warmed 227 kg/hr. of brackish feedwater from 35°C to 60°C.

Assuming a 65% yield of bio-oil and NCG from slow pyrolysis, approximately 27.6 kg/hr. or 0.66 Mg/day of dry biomass is needed to produce 55 kg/hr. or 1.3 m³ of distilled water. Put another way, approximately 475-550 kg of dry biomass is needed per m³ of produced distilled water. Assuming a biomass purchase cost of US\$50-75 per dry ton, treated water at this scale would cost 23-41 US\$/m³.

3.4 Conclusions and Future Research

Biomass contains enough energy to feasibly provide the energy for brackish water desalination using multiple effect distillation. The water production rates, unit operations and costs modeled here using Aspen Plus® represent the very low end

of small scale throughput, that is, what could be achieved in a laboratory-scale system. As expected at this scale, the produced water costs are approximately one order of magnitude higher than what could be achieved with economies of scale and an optimized number of effects. The mass and energy balances from the simulation demonstrate the proof-of-concept for a biomass pyrolyzer-MED system and provide a tool for designing real-world systems at different scales.

One challenge of pursuing a proof-of-concept prototype at such a small scale is the limited availability of optimized unit operations. For this system interface to be built for field testing, the scale will likely be selected based on the equipment available on the commercial market. Here, the steam turbine is likely to be the limiting equipment component, followed by the heat exchangers; the steam turbine should be selected first, then the simulation used to size the other components based on the available biomass feedstocks.

The cost estimate presented here is based on literature values for biomass purchase prices, such as in (Brown, et al., 2011), and does not consider capital and operating costs. The more likely scenario in the field is that the capital and operating (labor, maintenance, start-up fuel) costs will dictate the produced water cost while the biomass will be obtained onsite rather than being purchased. Future work with the developed simulation should be to add techno-economic analysis.

Three ways that the interface might be improved are the addition of water recovery from the biomass drying and combustion processes, the addition of heat exchanger to warm the boiler feed water using the superheated steam exiting the turbine, and the addition of an electrical air blower for the furnace to ensure adequate oxygen. Biomass from the field is usually wet and must be dried to less than approximately 10% moisture by weight prior to pyrolysis. A major product of combustion is water that currently is not recovered from the flue gas stream. Both sources of water represent opportunities to increase distilled water recovery rates. While the latent heat of the superheated steam might be used in the MED, the high temperature (168°C) would cause substantial scaling as the brackish water boiled in the effect; scaling is most likely at temperatures greater than 80°C. Since the boiler feed water does not contain salts, there is the potential for heat recovery without the risk of scaling. Finally, an air blower would give the furnace operator greater control over the combustion reaction to target an optimum temperature and increase combustion efficiency.

The interface modeled here assumes set rates and compositions of bio-oil vapors and non-condensable gases from biomass pyrolysis. Even though this model uses values that have been demonstrated in the literature, a complete design of a pyrolyzer-MED system will need to include pyrolysis reactor models that account for the variability with time inherent in pyrolysis reactions (start-up vs. steady state) and biomass composition. Such modeling is especially important for pyrolyzers that use direct heating through partial combustion of the biomass to provide the energy for the pyrolysis reactions, as anticipated to be the case here.

4. Producing Biochar from Locally-Available Biomass Resources

4.1 Lab-Scale Pyrolyzer Design and Fabrication

4.1.1 Pyrolysis Literature Review

Biomass pyrolysis is a thermochemical process that heats organic material to temperatures over 300°C in an oxygen-free environment to convert low energy density biomass into a high energy density oil (~22 GJ m⁻³ or ~17 MJ kg⁻¹), biochar (~18 MJ kg⁻¹) and syngas (~6 MJ kg⁻¹) (Bridgwater, et al., 1999, Ioannidou, et al., 2009). Biomass is composed of water, carbohydrates (cellulose, hemicellulose, starches, etc.), aromatic molecules (lignin), minerals (ash), and other compounds (extractives). The products of pyrolysis are 20–57% char, 32–58% oil, and 9–48% gas (Babu, 2008). Recently, more attention has been paid to biomass pyrolysis because pyrolysis can convert many types of organic material, such as municipal solid waste (MSW), agricultural waste, and forestry waste; and pyrolysis gas can be used for heating, power, and the creation of syngas, methane, hydrogen, etc.

As seen in the thermogravimetric analysis (TGA) results in Figure 4.1, there are significant behavioral differences between the three components of plant material. Cellulose starts decomposing at about 315°C and is mostly pyrolyzed by 400°C. On the other hand, hemicellulose is the first component in organic material to decompose, starting at 215–315°C but 20% hemicellulose is left unreacted in the solid residual, despite temperatures as high as 900°C. Lignin is the most difficult component to decompose with also the worst mass loss rate, leaving 47% by weight in the residual at 900°C (Fantozzi, et al., 2007, Yang, et al., 2007).

For biomass pyrolysis, there are three main stages (Fantozzi, et al., 2007):

1. Dehydration (25°C–100°C) removes moisture from the biomass.
2. Thermal cracking (100–350°C) decomposes biomass under oxygen free conditions. With the rise in temperature, a variety of volatile organic compounds (VOCs) will form, resulting in a loss of the majority of the original mass. Although the temperature reaches the ignition point of the material, the oxygen free conditions prevent the formation of a flame, as flame is gas phase oxidation reaction.
3. Carbonization (> 400°C) is generally considered to be caused by the further cracking of C-C and C-H bonds. Decomposition occurs very slowly in this stage and the resulting mass loss is much smaller than in the second stage. Biochar is formed when the C-C and C-H bonds in the VOCs are broken, dispersing them as gases.

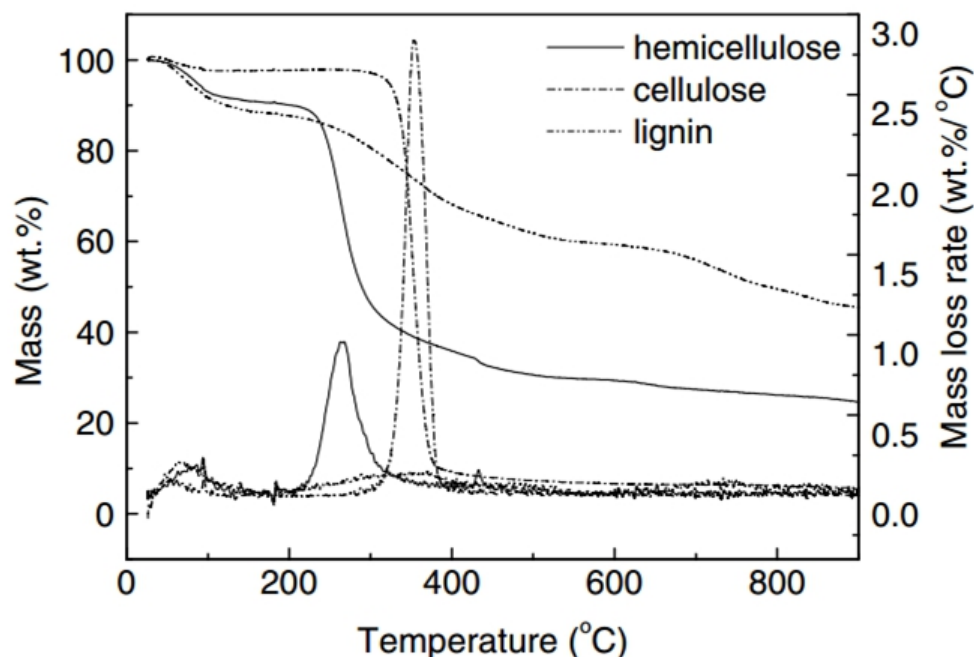


Figure 4.1. Pyrolysis curves of hemicellulose, cellulose and lignin in a thermogravimetric analyzer (Yang, et al., 2007).

Table 4.1. Parameters for different pyrolysis processes (Brewer and Brown, 2012).

Process	Residence time	Heating rate	Temperature range (°C)	Primary product
Carbonization	hours-days	Very slow	400-600	Biochar
Slow pyrolysis	5-30 min	Slow	350-600	Syngas, bio-oil, biochar
Fast pyrolysis	0.5-5 sec	High	650	Bio-oil

There are two primary methods of pyrolysis, slow pyrolysis and fast pyrolysis. These two methods vary in physical parameters like temperature, heating rate, residence time and primary products. Slow pyrolysis is mainly used to produce biochar from low-value biomass feedstock like yard waste, but can also be used to generate energy (Downie, et al., 2012). The heating rate is usually below 100 K/min, the reaction temperature range is from 300°C to 800°C, and the residence time varies from minutes to days. The yields of slow pyrolysis are roughly 35% biochar, 30% bio-oil, and 35% syngas by mass. Slow pyrolysis units are typically connected to an afterburner to burn the off-gases, often for heat or electricity generation (Brown, et al., 2011). Fast pyrolysis was developed from the slow pyrolysis process to maximize bio-oil production. It is operated at moderate temperatures with very high heating rates and short residence times. Several fast pyrolysis experiments have managed to convert 70-80% of the starting dry biomass weight into bio-oil (Winsley, 2007). The size and type of the pyrolyzer is

determined by the size of the feedstock. If the feedstock is too large, the heating rate will be too low to achieve fast pyrolysis. Typical particle sizes for fast pyrolysis are < 2 mm.

Table 4.2. Typical product yields (dry basis) obtained by different modes of wood pyrolysis (Winsley, 2007).

Mode	Conditions	Bio-oil	Biochar	Gas
Fast	Moderate temperature (500°C) for 1s	75%	12%	13%
Intermediate	Moderate temperature (500°C) for 10-20s	50%	20%	30%
Slow	Low temperature (400°C) with very long solids residence time	30%	35%	35%
Gasification	High temperature (800°C) with long vapor residence time	5%	10%	85%

4.1.2 Pyrolyzer Design Considerations

There are three main methods for heating pyrolyzers: direct heating, auto-thermal heating, and indirect heating. In direct heating, biomass, petroleum, or natural gas is burned outside of the pyrolyzer to generate hot combustion gases which enter the pyrolysis chamber and drive the pyrolysis reactions. In auto-thermal heating, some of the feedstock is burned/oxidized to generate the heat needed to pyrolyze the rest of the feedstock (Emrich, 1985). In indirect heating, hot gas flows through an external heating tube adjacent to the tube and heats the biomass by thermal conduction; this method ensures that pyrolysis will occur in an oxygen-free environment, but this also means that one must either recycle or remove the VOCs produced during pyrolysis. Figure 4.2 shows these various types of heating. In commercial applications, direct heating is usually chosen because it is cheap and easy to operate. In lab-scale applications, indirect heating methods give better control of the reaction temperature, heating rate, and residence time.

The batch reaction cycle includes a heating phase to create the biochar and a cooling phase to lower the biochar's temperature to prevent combustion upon exposure to air. Feedstock particles are kept stationary during the reaction while produced VOCs are released into the sweep gas. Semi-batch systems are more efficient at utilizing heat because the hot steam generated in one reaction cycle is reused in the next reaction cycle. Although some systems can also recycle liquid byproducts, most systems only recycle hot steam in producing biochar (Garcia-Perez, et al., 2010). In general, a continuous reaction chamber is operational 90-95% of the time because the reaction is only discontinued during the occasional maintenance of the chamber. Most reaction chambers are adjusted for continuous operation when the biomass feedstock flow rate is sufficiently high.

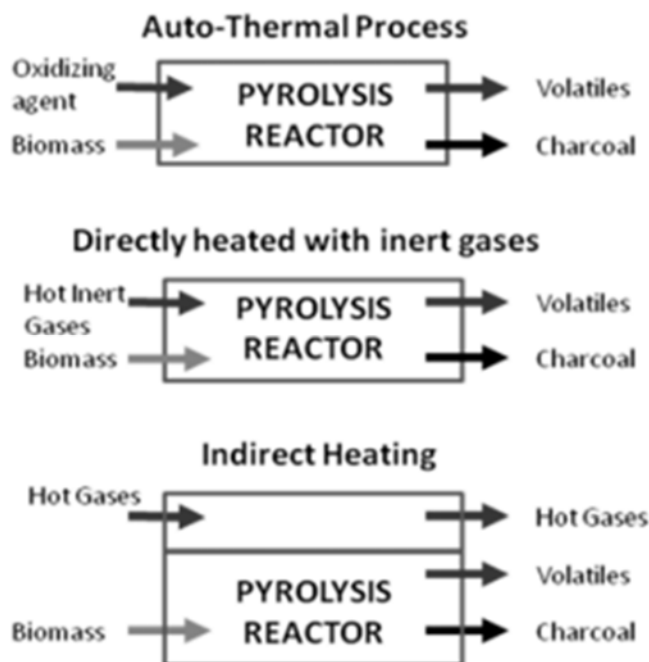


Figure 4.2. Types of pyrolysis heating methods (Garcia-Perez, et al., 2010).

Several lab-scale slow pyrolyzers have been developed for biochar research. The “buried sand” reactor was designed at Rice University to produce biochar for small-scale testing. Instead of using nitrogen as an inert purge gas, the entire reaction chamber was buried in 9 kg of sand, which allowed volatiles to escape through the sand and greatly limiting the diffusion of oxygen into the reactor. The reactor itself was a steel vessel covered by a loose-fitting porcelain lid containing the biomass (30-60g), glass wool and a thermocouple. Heat was provided by a box furnace with snorkel ventilation. This setup (thermocouple + furnace) gave the users good temperature control. Long wait times were common because the large mass of sand for heating and cooling. The sand insulation cannot be scaled to higher-yield applications because the mass, cooling time, and pressure generated by the sand. Nor was it possible to measure emissions due to the lack of an outflow collection mechanism (Kinney, et al., 2012).

The “meat smoker” reactor was a custom-built, pilot-scale batch reactor designed at Baylor University to produce large amounts of biochar using cheap, relatively common equipment including a truck-mounted, propane-powered pyrolyzer, and to collect bio-oils for further analysis. Biomass was sealed in a 20L soup pot coated with sealing grease. A custom lid and clamp kept the pot shut as the reactor was placed in a backyard smoker box equipped with an extra propane burner. The propane tank that was weighed before and after each reaction cycle (4 hours) to estimate energy usage. Each cycle produced roughly 2 kg of biochar. To remove VOCs, the lid contained a large vent connected to a series of large, air-cooled condenser tubes with openings at the bottom for bio-oil collection. Non-condensable gases were returned to and combusted in the second burner (Li, et al.,

2011). Despite its many advantages, this reactor did have a few problems. Reaction conditions were variable because temperature control was based on the imprecise dials of the smoker while the temperature of the biomass in the large pot was monitored by only one thermocouple. This often resulted in reaction temperatures above desired targets. The sealant also proved difficult to use and would sometimes fail.

The “paint can” reactor was designed at Iowa State University to produce slow-pyrolysis biochar for a biochar comparison study. A 0.95L (1 quart) paint can containing the biomass was placed inside a box furnace. An inflow line of nitrogen (1 L/min flow rate) and an outflow line for VOCs into an ice water impinger was included, as was a thermocouple for temperature measurement. A flow meter measured the gas outflow after non-condensable gases were cooled by the impinger (Brewer, et al., 2009). With relatively few parts, this system was cheap and easy to build. However, such a system required much maintenance: the outflow line often would clog because the tubing got too cold; this clogging created back pressure and sometimes fires in the lab furnace. The sealing material covering both ports would deteriorate after repeated heating cycles.

4.1.3 Design of Lab-Scale Slow Pyrolyzer

The goals of our pyrolyzer design were to produce relatively large amounts of reproducible biochar while managing VOCs and allowing for easy assembly, disassembly and cleaning. Integrated temperature control and VOC collection features are included. (Since we currently have no plans to analyze or recycle the produced VOCs, combustion would be the best approach. However, space constraints of the fume hood prevent the construction of a burner, so a condenser was built instead.)

The system consists of a GHA 12/450 single zone horizontal tube furnace (Carbolite, Hope Valley, UK) sized to fit a 5.5 in. (14 cm) O.D. 304 stainless steel reaction tube with a 1/4 in (6 mm) wall thickness. The programmable furnace provided an 18 in. (46 cm) heated zone for indirect heating. Inside the reaction tube, two circular 303 stainless steel plates with large holes were held in place with screws; 304 stainless steel 40-mesh wire cloth was placed between the plates on the biomass side to contain the biomass particles while allowing for gas flow. End caps for the reaction tube, with high temperature glass-mica ceramic O-rings, were held in place by clamps. One end cap contained openings for a thermocouple (Super OMEGACLAD XL, Omega) and a nitrogen gas inlet. A handheld data logger (OM-EL-ENVIROPAD-TC, Omega) was connected to the thermocouple to record the temperature of the biomass every 5 minutes. Pyrolysis vapors exited through the other end cap into a 0.95 cm O.D. tube maintained at 200°C by heat tape (XtremeFLEX BWH, BriskHeat Corp, Columbus, OH) with a temperature controller (SDC Digital Benchtop, BriskHeat Corp.) to prevent early vapor condensation and clogging. Vapors were bubbled through approximately 700 mL of distilled water in a large, glass Erlenmeyer flask set in an ice bath. The entire pyrolysis system was operated inside of a fume hood, as shown in Figure 4.3. The

fabrication process included cold-flow and hot-flow shakedown trials.

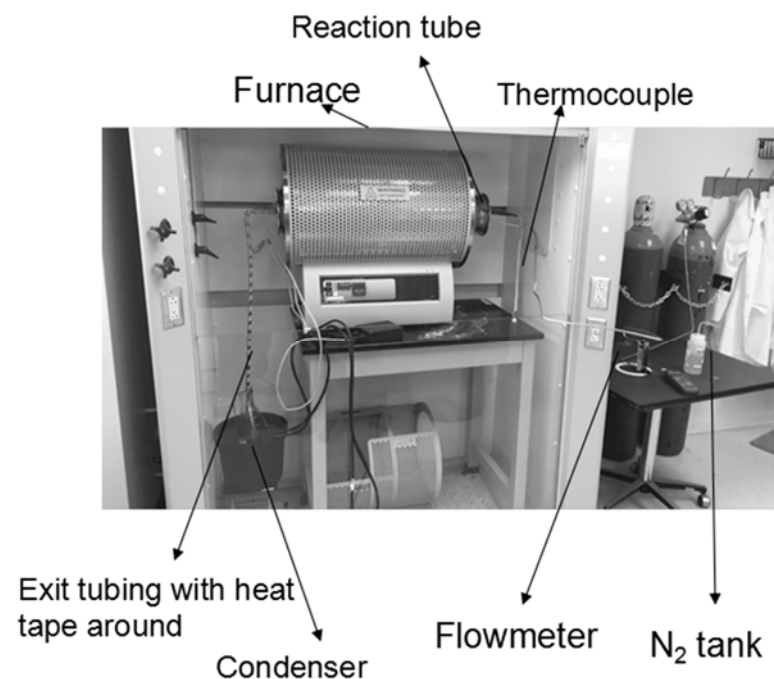


Figure 4.3. Custom-built lab-scale slow pyrolysis system used to produce biochar.

4.2 Biomass Feedstocks

Four feedstocks were selected for this study to represent underutilized biomass available locally. All feedstocks were air dried and stored in sealed buckets prior to pyrolysis.

Pecan (*Carya illinoensis* (Wangenh.) K. Koch) orchard prunings were collected from the NMSU Leyendecker Plant Science Center in Las Cruces, NM. Prunings consisted primarily of small branches and twigs, with some leaf material.

Prunings were allowed to dry in the field, then were collected and chipped in a standard yard waste chipper. Pecan shells were collected from a local pecan processing facility and were used as received.

Cotton (*Gossypium hirsutum* L.) gin trash was collected from Mesa Farmers Coop - Cotton Gin in Vado, NM. The gin trash contained mostly cotton leaf and stem pieces, with noticeable amounts of lint and seed residues, and some other materials such as soil.

Yard waste was collected from the NMSU green waste yard on 17 April 2014. The waste consisted primarily of freshly cut and chipped wood waste from tree pruning around campus, with a small amount of mixed leaves, shrubs, and grasses collected from maintenance of xeriscaped areas.

4.3 Biochar Production

Biochars were produced from the four biomass feedstocks using the custom-built, lab-scale slow pyrolysis system. Biomass (200-250 g) was loaded into the reaction tube between the perforated plates. The furnace was heated at a rate of $5^{\circ}\text{C min}^{-1}$ to 450°C and maintained at 450°C for 60 minutes, after which the furnace and heat tape were turned off and the system allowed to cool overnight. An inert atmosphere was maintained by flowing nitrogen gas through the reactor at a rate of 1.0 L min^{-1} . Once the biochar had cooled to room temperature, the reactor was disassembled and the biochar removed, weighed, and stored in sealed containers. Bio-oil yields were estimated from the change in mass in the water condenser; this yield did not include the non-trivial amounts of tar that had condensed inside the pyrolyzer and exit tubing. Non-condensable gas plus tar yield was estimated by difference. The reactor was cleaned by placing the reaction tube in the tube furnace without the end caps and heating the tube to 600°C for an hour to burn off tar residues.

4.4 Biochar Characterization

Moisture content of the biomass feedstocks and biochars was measured by heating ground samples in an oven at 105°C for 2 hours. Ash content was measured by heating 0.5 g of sample in a muffle furnace to 600°C and 750°C for 6 hours for biomass and biochar, respectively. Ash measurements were done in duplicate.

Higher heating values (HHV) of the biomass feedstocks and biochars were determined in duplicate using a Model 6725 semi-micro bomb calorimeter (Parr Instrument Co., Moline, IL). Mineral oil of known energy content was used as a spike for samples which did not easily ignite in order to ensure complete combustion.

4.5 Results

Pyrolysis product yields, and biomass and biochar characteristics are shown in Table 1. There was a lag of approximately $25\text{-}50^{\circ}\text{C}$ during pyrolysis between the biomass temperature and the furnace set temperature due to heat transfer limitations; the actual highest heating temperatures were 433 , 423 , 425 and 419°C for pecan shell, pecan prunings, cotton gin trash, and yard waste, respectively. Biochars retained the particle size distribution and shape of the biomass feedstocks. Biochars were uniformly black in color, had little or no perceivable odor, and left no oily residue when smeared; these observations are consistent with complete biomass conversion. One exception was the cotton gin trash biochar, which had some interspersed dark brown particles, especially in the shape of the cotton lint residues, suggesting a slightly less severe pyrolysis intensity (Brewer, et al., 2012). The cotton gin trash feedstock also had a significantly higher ash content (12% on a feedstock weight basis, compared to 1-5%), which resulted in a higher biochar yield (42%, compared to 28-35%), higher

biochar ash content (31%, compared to 4-19%) and lower biochar HHV (24 MJ kg⁻¹, compared to 31-32 MJ kg⁻¹); these results indicate that the feedstock's mineral matter was concentrated in the biochar ash fraction. The biomass feedstock pyrolysis properties, yields, and higher heating values were consistent with other biomass slow pyrolysis processes. The collected bio-oil yields (11-18%) were lower, and the non-condensable gas (NCG) yields higher, than would generally be expected for this slow pyrolysis temperature since the tars coating the reactor and exit plumbing were not measured and thus were included in the NCG estimation.

Table 4.1. Yields of biochar, collected bio-oil, non-condensable gases (NCG) and uncollected tars from biochar production, reported on a wet feedstock basis. Moisture content, ash content, and higher heating values (HHV) of biomass feedstocks and biochars reported on a wet, unground basis; \pm is standard deviation where $n = 2$.

Sample	Biochar Yield (wt. %)	Bio-oil Yield (wt. %)	NCG + Tar Yield (wt. %)	Moisture (wt. %)	Ash (wt. %)	HHV (MJ kg ⁻¹)
Pecan shell	--	--	--	5.8	1.4 \pm 0.3	18 \pm 0.5
Pecan prunings	--	--	--	5.7	2.7 \pm 0.2	23 \pm 3
Cotton gin trash	--	--	--	6.1	12 \pm 1	17 \pm 1
Yard waste	--	--	--	4.2	4.7 \pm 0.3	22 \pm 2
Pecan shell biochar	28	18	54	3.9	4.2 \pm 0.1	31 \pm 1
Pecan prunings biochar	35	13	52	4.3	10.8 \pm 0.1	31 \pm 2
Cotton gin trash biochar	42	11	57	3.3	31 \pm 4	24 \pm 3
Yard waste biochar	32	17	51	2.4	19 \pm 2	32 \pm 4

4.6 Conclusion

Biochar yields for 450°C slow pyrolysis of pecan shells, pecan orchard prunings, yard waste and cotton gin trash ranged from 28-42 wt.%, within the expected range for these conditions. From the characterizations available, these feedstocks and conditions produce biochars of acceptable quality for soil application; the CGT exhibited the high ash content and low HHV of feedstocks higher in mineral content which may impact its suitability for ash-sensitive applications.

5. Biochar Effects on New Mexico Soil Properties

5.1 Study Goals and Objectives

Soil quality is “the capacity of a specific kind of soil to function, within natural or managed ecosystem boundaries, to sustain plant and animal productivity, maintain or enhance water and air quality, and support human health and habitation” (Karlen, et al., 1997). Generally, arid soils have poor quality due to very low levels of soil organic matter (Idowu and Flynn, 2013). Organic matter is very central to the quality of any soil (Reeves, 1997). The organic matter levels of arid soils, particularly in New Mexico where this study was conducted, are often less than 1% (Ulery and Tugel, 1999); to improve the soil organic matter, considerable efforts are needed to add organic materials to the soil. Traditional ways for improving soil organic matter, such as cover cropping, leaving crop residues after harvest, and applying manure, are often difficult to achieve in arid soils due to water availability and salinity (Magdoff, 2001). For example, cover cropping has been very challenging for farmers in the arid desert southwest of the United States due to the reduced amounts of available water for agriculture (Idowu, et al., 2012). This region has suffered severe drought over several years and using scarce water for raising cover crops is perceived by many growers as uneconomical.

In order to improve soil organic matter of arid soils, innovative methods that will not compete with water for crop production need to be developed. One such innovative method is to convert locally available waste biomass materials into biochar for soil application. Biochar is a predominantly recalcitrant organic carbon (C) material, created when biomass is heated to temperatures between 300 and 1000°C under low oxygen concentrations (i.e. pyrolysis) (Jeffery, et al., 2011). Since the organic carbon produced in biochar is very stable, addition of biochar to the soil has the potential to both improve soil quality and sequester carbon, which is important for mitigation of excessive carbon dioxide in the atmosphere (McHenry, 2009).

Biochar application to the soil has been shown by different studies to have significant impacts on several soil quality parameters (Barrow, 2012, Laird, 2008, Lal, 2008, Lehmann, et al., 2003). Positive impacts of biochar amendment on soils include:

- i) increasing soil capacity to sorb plant nutrients, consequently reducing leaching losses of nutrients (Cheng, et al., 2008, Liang, et al., 2006);
- ii) decreasing soil bulk density, leading to less-compacted soil conditions favorable for root growth and water permeability (Laird, et al., 2010);
- iii) increasing the soil cation exchange capacity (Steiner, et al., 2008);
- iv) increasing soil microbial activity and diversity (Lehmann, et al., 2011, Steinbeiss, et al., 2009);
- v) increasing plant available water retention (Karhu, et al., 2011, Laird, et al.,

- 2010); and
vi) increasing crop yields (Kimetu, et al., 2008, Steiner, et al., 2007).

From a biomass systems engineering perspective, using available biomass resources to meet the community's needs is critical to ecological sustainability. In arid agricultural communities, crop residues are often the primary available biomass feedstock and fresh water is often the primary need. Biomass can be used to help meet water needs in several ways, including providing the energy needed for water treatment. A way in which biomass for water treatment and biomass for soil amendments can be combined is to use slow pyrolysis to produce thermal energy for brackish groundwater desalination and biochars for application to agricultural soils.

New Mexico state usually ranks 3rd for pecan production in the United States with >17,000 pecan orchards covering more than 15,800 ha. Doña Ana County is New Mexico's highest pecan producing county at approximately 19,500 Mg yr⁻¹ (Lillywhite, et al., 2010). Pecan production creates two residual biomass streams: pecan shells and pecan orchard prunings (leaves, branches, etc.). Estimates of the amount of pecan shells available from the New Mexico/western Texas pecan industries range from 14,000-26,000 Mg yr⁻¹; some of these shells have been used in the horticulture as a mulch and alternative potting media (Mexal, et al., 2003). Estimates of orchard pruning residues available from the Mesilla Valley region of New Mexico range from 11,000-37,000 Mg yr⁻¹ on a dry basis. Air quality restrictions have caused pecan farmers to look for alternatives to conventional open-air pruning residue burning (Kallestad, et al., 2008).

After harvest and prior to textile production, cotton bolls must be ginned to remove the seeds (used to make cottonseed oil and cottonseed meal) and other non-lint materials. The non-seed, non-lint materials, such as stems, leaves and dirt, are collectively referred to as cotton gin trash. An average of 68 kg of gin trash is generated for each 218 kg bale of cotton. In 2013, approximately 12,000 ha of cotton were grown in New Mexico at an average yield of 0.89 bales/ha, resulting in over 725,000 Mg of cotton gin trash (unpublished cooperative extension service data).

Many municipalities collect tree branches, grass clippings, garden residues, and other yard wastes from residential and commercial properties for composting, mulching, and other uses. The City of Las Cruces, New Mexico (population approximately 100,000) receives 1,800-2,700 Mg yr⁻¹ of wet green waste for processing into compost (Lisa LaRocque, City of Las Cruces Sustainability Officer, 23 September 2013). This represents a significant source of biomass that could be used for pyrolysis, especially for municipalities that are looking for alternative, higher-value uses for yard waste.

Pyrolysis of locally available waste biomass can help produce energy that can potentially be used for desalinization of increasingly salty well waters used for

irrigation and, at the same time, improve soil quality through the application of biochars. Therefore, the objectives of this study were:

- Assess the impacts of biochar amendments (derived from pecan shells, pecan orchard prunings, urban yard waste, and cotton gin trash) on multiple soil quality indicators in two different soil textures, sandy loam and clay loam.
- Assess the impacts of biochar amendments on soil water retention (moisture desorption) in two different soil textures, sandy loam and clay loam.

5.2 Soil Incubation Materials and Methods

Two local arid soils used for agriculture, a sandy loam and a clay loam, were amended with the biochars at a rate of 45 Mg ha⁻¹. The sandy loam soil (a Thermic Typic Torrifuvents (Staff, 1999)) was collected from the NMSU Fabian Garcia Agriculture Experiment Station in Las Cruces, NM. The clay loam soil (a Thermic Vertic Torrifuvents (Staff, 1999)) was collected from the NMSU Leyendecker Plant Science Center in Las Cruces, NM. Biochars were ground to pass a 2 mm sieve prior to addition to the soil. Soil samples were thoroughly mixed then packed into pots. Soils were first slowly saturated with water then allowed to drain for 24 h, after which they were placed into a growth chamber for 3 weeks. About 100 cm³ of water was added twice a week to prevent the soil from drying out. The temperature of the growth chamber was set at a day temperature of 28°C and a night temperature of 20°C.

5.3 Soil Property Measurement Methods

Soil chemical analyses were conducted on the biochar-amended soils after incubation using standard procedures. The pH, electrical conductivity, calcium, magnesium, sodium, and sodium adsorption ratio of the soils were measured using the filtered solution from a saturated paste preparation (Laboratory, 1954). Soil organic matter (SOM) was measured using the Walkley-Black method (Nelson and Sommers, 1996). Sodium bicarbonate-extractable phosphorus (Olsen, et al., 1954) and potassium were measured by inductively coupled plasma (ICP) spectroscopy (Cihacek, 1983). Nitrate-N concentration was measured by water extract using a cadmium reduction column (Ludwick and Reuess, 1974). Copper, iron, manganese and zinc micronutrients were measured by DPTA extract and analyzed by ICP (Ludwick and Reuess, 1974).

The experimental design for the biochar soil amendment trial was a randomized complete block design, with treatment combinations replicated four times. Experimental treatments consisted of biochars from four different feedstocks [pecan shells (PS), pecan prunings (PP), yard waste (YW) and cotton gin trash (CGT)] and a control treatment with no biochar addition, tested in two soil types (sandy loam and clay loam), for a total of ten treatment combinations. Analysis of

variance was performed on soil measurements and the means of the treatment values were separated using the Student Newman Keuls test after a significant F-ratio.

Moisture desorption curves were used to assess the effect of biochar amendments on soil water retention in the plant available range, namely from field capacity (FC) at -33 kPa tension (336 cm or 132 in. of water, $pF = 2.53$ where $pF = -\log [h$ (in cm)]) to permanent wilting point (PWP) at -1,500 kPa tension (15,296 cm or 6,022 in. of water, $pF = 4.19$). Soil moisture desorption curves were measured using a HYPROP tensiometer system (UMS GmbH, Munich, Germany) and a WP4C Dewpoint potentiometer (Decagon Devices, Pullman, WA). The dewpoint potentiometer measures water potential in the based on measurements of humidity above a sample in a closed chamber.

Soil samples were prepared for tensiometer analysis by partially saturating them for several hours in their incubation pots, then inverting the pots onto a tray. The potentiometer sample ring was pushed over the sample and any soil sticking above the rim was gently pushed down to completely fill the sample ring. Excess soil was removed and saved for chemical analysis. The saturation base and a coffee filter were placed over the soil and the sample was completely saturated overnight. The HYPROP was run as per manufacturer instructions in multiple device mode with weight measurements taken 2-3 times per day until analysis runs were complete. Refilling was done overnight using a vacuum system that provided 850 kPa when connected to the HYPROP base. The HYPROP provides data in the wet range, from approximately -1 kPa ($pF = 1$) to -1,000 kPa ($pF = 3$).

To gain more information about the water capacity in the PWP range, samples from the HYPROP were removed as soon as the analysis was finished and analyzed using the dewpoint potentiometer according to manufacturer instructions. After each measurement, samples were allowed to air dry for a few hours then remeasured until the water potential was below the PWP. Soil dry weights were measured by drying in an oven at 105°C for 2 hours; these dry weights were then used to back calculate volumetric water contents of the soil samples for the dewpoint potential measurements.

The data was fitted to the unimodal van Genuchten/Mualem model (van Genuchten, 1980) and to the bimodal modification to the Genuchten model (Durner, 1994) using TensioVIEW software version 1.9 build 104 and HYPROP software version 2.0 build 89. The unimodal van Genuchten equation uses the Mualem model for conductivity (van Genuchten, 1980) and is presented in Equation 1:

$$\frac{\theta - \theta_r}{\theta_s - \theta_r} = \frac{1}{[1 + (\alpha|h|)^n]^{(1-1/n)}} \quad (1)$$

where θ is the volumetric water content, h is the soil water tension or “height”, and θ_s , θ_r , α and n are model parameters. Information regarding the tensiometer

measurement theory and data fitting method are available in (Abel, et al., 2013, Peters, et al., 2011, Schindler, et al., 2010) and from the manufacturer. Plant available water capacity was calculated as the difference in volumetric water content between FC at $pF = 2.53$ and PWP at $pF = 4.19$ using the fitted models.

5.4 Results and Implications

Mean values of soil quality indicator measurements are presented in Tables 5.1 and 5.2. The results were analyzed separately according to soil textures to evaluate the impacts of biochar from different feedstocks on soil quality indicators.

5.4.1 Coarse Textured Soil (Sandy Loam)

While pH did not show a significant difference with biochar treatment (Table 5.1), the trends of the biochar treatment impact on soil EC, SOM, Na, Ca, and Mg were similar across the coarse textured soil samples. CGT led to significantly higher EC, SOM, Na, Ca, and Mg compared to the control treatment and the other biochar treatments (Table 5.2). The EC increase in the soil amended with CGT (7.12 dS m^{-1}) is of a great concern and implies that biochar produced from CGT may lead to high salinity. Since salinity management is very critical to the success of the cropping systems in the desert southwest region, it is important to avoid the addition of materials that will exacerbate salinity problems. Although the SOM was significantly increased by the CGT in sandy soil, the corresponding increase in salinity may limit the use of CGT biochar. SAR gave significant differences in the sandy soil, but these values were well below the SAR level at which sodicity becomes a problem ($\text{SAR} > 13$).

While $\text{NO}_3\text{-N}$ was not significantly affected by different biochars, both P and K were significantly increased by the biochar from CGT (Table 5.2). Amending sandy soil with CGT biochar led to a P increase of about 4.2 times and a K increase of about 13.9 times compared with the control treatment. These increases are considerable in terms of nutrient additions to the soil. For micronutrients, Cu was not significantly affected by the biochar treatments, but Mn was significantly increased by the biochar treatments relative to the control (Table 5.2). There were statistical significant differences in Fe for the coarse textured soil, however, these differences do not have crop management significance since all the Fe values measured were in the medium range based on soil nutrient sufficiency levels for arid soils (Flynn, 2012). Addition of CGT and PP biochars led to significantly higher Zn levels in soil compared to the control, PS, and YW treatments. Based on crop sufficiency level, the Zn level moved to the high range with the addition of CGT and PP biochars, while it stayed in the medium range for the control, PS and YW biochar treatments (Flynn, 2012).

Table 5.1. Soil quality measurements of biochar-amended soils including pH, electrical conductivity (EC), soil organic matter (SOM), cations (Na, Ca, Mg), and calculated sodium adsorption ratio (SAR). PS: pecan shell; PP: pecan prunings; YW: yard waste; CGT: cotton gin trash.

Soil	Biochar Treatment	pH	EC (dS m ⁻¹)	SOM (g kg ⁻¹)	Na (mg kg ⁻¹)	Ca (mg kg ⁻¹)	Mg (mg kg ⁻¹)	SAR
Sandy loam	Control	7.45	1.45 a	0.55 a	8.3 a	5.0 a	1.4 a	4.5 b
	PS	7.48	1.28 a	0.49 a	6.6 a	4.9 a	1.2 a	3.7 ab
	PP	7.40	2.00 a	0.51 a	9.5 a	8.8 a	2.6 a	3.9 ab
	CGT	7.41	7.12 b	1.16 b	17.0 b	49.6 b	16.3 b	2.9 a
	YW	7.43	1.25 a	0.65 a	6.7 a	4.8 a	1.4 a	3.8 ab
		ns						
Clay loam	Control	6.90 a	6.86 a	1.19 a	23.5 a	47.2 a	13.8 a	4.3 a
	PS	7.03 ab	7.47 a	1.20 a	28.4 a	52.0 a	15.4 a	4.9 ab
	PP	6.88 a	15.5 c	1.24 a	62.9 c	133 c	35.3 b	6.9 c
	CGT	7.08 b	9.12 ab	1.89 b	35.2 ab	64.5 ab	23.0 a	5.3 b
	YW	6.90 a	12.0 b	1.33 a	44.5 b	94.9 b	24.7 a	5.7 b

Data are separated by soil type; entries in the same column labeled with different letters had statistically significant differences ($P < 0.05$, $n = 4$); ns: not significant at $P < 0.05$.

Table 5.2. Extractable macronutrients (NO₃-N, P, K) and micronutrients (Cu, Mn, Fe, Zn) of biochar-amended soils. PS: pecan shell; PP: pecan prunings; YW: yard waste; CGT: cotton gin trash.

Soil	Biochar Treatment	NO ₃ -N	P	K	Cu	Mn	Fe	Zn
		(mg kg ⁻¹)						
Sandy loam	Control	3.7	6.0 a	26 a	1.2	3.4 a	2.7 b	0.86 a
	PS	2.5	6.1 a	34 a	1.1	6.1 b	2.8 b	0.88 a
	PP	2.7	7.1 a	43 a	1.0	8.4 c	2.6 ab	1.12 b
	CGT	0.8	25 b	361 b	0.9	11.6 d	2.4 a	1.08 b
	YW	1.9	6.4 a	35 a	1.2	8.7 c	2.5 ab	0.90 a
		ns			ns			
Clay loam	Control	136 a	12 a	60 a	2.3	4.5 a	3.4 b	0.88
	PS	138 a	13 a	70 a	1.6	7.0 b	3.6 b	0.95
	PP	759 c	12 a	113 c	2.1	7.5 bc	2.5 a	1.19
	CGT	1 a	28 b	252 d	1.7	8.2 cd	2.8 a	1.07
	YW	466 b	13 a	92 b	1.5	8.8 d	2.7 a	1.94
					ns			ns

Data are separated by soil type; entries in the same column labeled with different letters had statistically significant differences ($P < 0.05$, $n = 4$); ns: not significant at $P < 0.05$.

5.4.2 Fine Textured Soil (Clay Loam Soil)

In the fine textured soil, the CGT led to slightly higher pH (7.08) compared to the

control treatment (pH = 6.90, see Table 5.1). This slight rise in pH was statistically significant yet would not have much management significance since nutrient availability, which is governed by soil pH, would be similar within the range of pH differences measured in this experiment. EC in the fine textured soil was highest with PP biochar amendment (15.5 dS m⁻¹) followed by YW biochar (12.0 dS m⁻¹) and CGT biochar (9.12 dS m⁻¹); these high EC levels show the need for caution in using these biochars in clay soils. As previously discussed, high EC can limit crop productivity and act as a yield constraint. Similar to the sandy soil results, CGT led to a significant increase in SOM. Na, Ca, and Mg concentrations were also affected by biochar treatments, with PP biochar-amended soils having the highest concentrations of these elements.

The NO₃-N levels were generally very high in the fine textured soil relative to the coarse textured soil, except for the CGT treatment, which was very low (Table 5.2). NO₃-N was significantly highest under the PP biochar treatment followed by YW. The reason for the very low level of NO₃-N for CGT treatment in fine textured soil is not clear, however, similar observation was made in the coarse textured soil in which the NO₃-N was quantitatively the lowest, though not significantly different. One possible explanation is that the CGT contained sufficient quantity of labile carbon such that soil microbial consumption of the labile carbon led to immobilization of plant-available nitrogen (Deenik, et al., 2010); this possibility is supported by the observation of some dark brown rather than black components of the CGT biochar.

Similar to the coarse textured soil, the CGT treatment had the highest P and K levels (Table 5.2) suggesting the possibility of nutrient additions to the soil through biochar produced from CGT. For micronutrients in the fine textured soil, Cu and Zn did not give any significant treatment effects, while Mn was highest in YW biochar treatment and Fe was highest in PS treatment. Such increases in Fe and Mn may not have significant crop management effects, however, since the measurements for all treatments belong to the same crop management ranges (medium for Fe and high for Mn (Flynn, 2012)).

5.4.3 Soil Quality Implications of This Study

This study has demonstrated the potential of biochar from different feedstocks for soil amendment. While different biochars have shown the potential to add nutrients such as nitrate, phosphate and potassium to the soil, care has to be taken with respect to the potential of each biochar to cause soil salinity. Also, the reaction of the soil to biochar produced from different feedstocks varies with soil texture. The CGT biochar, with its higher mineral content, exhibits a great potential to add organic matter to the soil and high quantities of nutrients such as P and K in both fine and coarse textured soil (Brewer, et al., 2011); however, for arid soils, the high level of salinity encountered in the CGT biochar-amended soil may serve as critical limitation to the use of this biomass feedstock. In the coarse textured soil, other biochars apart from CGT did not appear to deliver much nutrient benefits to the soil, however, they did not raise the salinity of the soil significantly when compared to the control treatment, indicating that they might

be used for long term building of the soil organic matter and soil quality. In the fine textured soil, though the control soil had initially high salinity, all the biochars tend to lead to increased salinity, except the PS biochar. Therefore, pecan shell biochar may be the best choice among the locally available feedstocks for the clay soil when salinity is considered. In order to better understand the effects of these biochar on soil quality, especially the effects on soil salinity, biochar amendments need to be tested under real field conditions and under different cropping systems.

5.4.4 Soil Moisture Desorption Results

An example of the data and the fitted model curves is show in Figure 5.1, as well as the locations of definitions of field capacity (FC) and permanent wilting point (PWP). Unimodal and bimodal van Genuchten model parameters are tabulated for the biochar-amended soils in Tables 5.3 and 5.4, respectively, as well as the estimated soil bulk densities and calculated available water capacities (AWC).

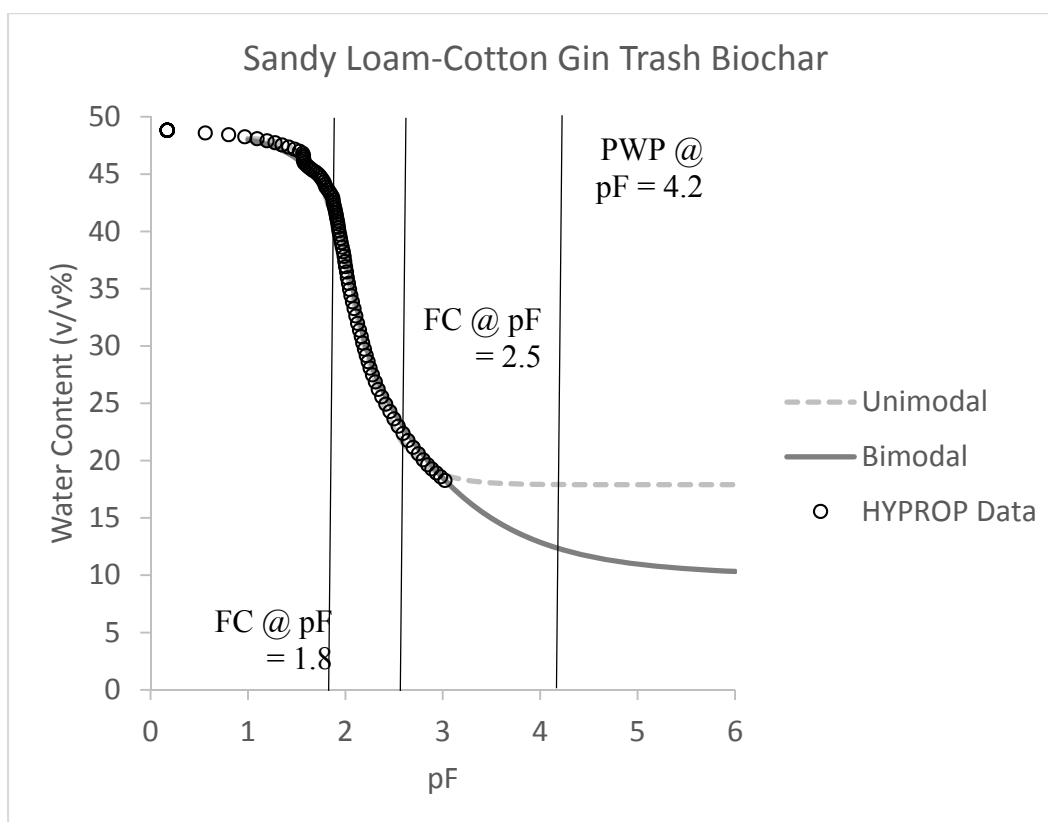


Figure 5.1 Water desorption curve data for cotton gin trash biochar-amended sandy loam soil. $pF = -\log(h)$ where h is water tension in cm of water; unimodal: water desorption curve using van Genuchten unimodal model data fit (van Genuchten, 1980); bimodal: water desorption curve using van Genuchten bimodal model data fit (Durner, 1994). Vertical lines indicate commonly-used definitions of field capacity (FC) and permanent wilting point (PWP).

Table 5.3. Soil bulk density, van Genuchten unimodal model parameters (van Genuchten, 1980), and available water content (AWC) of biochar-amended soils from water desorption measurements. AWC assumes field capacity at -33 kPa and permanent wilting point at -1.5 MPa. PS: pecan shell; PP: pecan prunings; YW: yard waste; CGT: cotton gin trash; number indicates replicate identifier from soil incubation. *Model was fit after data from dewpoint potentiometer was included.

Soil	Biochar Treatment	Bulk Density (g cm ⁻³)	θ_r (cm ³ cm ⁻³)	θ_s (cm ³ cm ⁻³)	α (cm ⁻¹)	n	AWC (cm ³ cm ⁻³)
Sandy Loam	Control 3	1.48	0.054	0.346	0.0116	2.474	3.8
	Control 4	1.45	0.113	0.375	0.0100	2.465	4.2
	PP 3	1.26	0.232	0.512	0.0113	2.322	4.6
	PP 3*	1.26	0.133	0.519	0.0146	1.534	13.8
	CGT 2	1.33	0.109	0.412	0.0107	2.480	4.4
	CGT 3	1.45	0.046	0.343	0.0098	2.663	3.9
	YW 3	1.40	0.081	0.392	0.0120	2.152	5.9
	YW 4	1.41	0.083	0.380	0.0104	2.399	4.9
Clay Loam	Control 3	1.22	0.051	0.447	0.0150	1.355	15.9
	PS 3	1.16	0	0.496	0.0215	1.184	16.8
	PP 2	1.17	0.176	0.548	0.0116	1.334	16.1
	PP 3	1.07	0	0.588	0.0148	1.182	21.0
	CGT 2	1.14	0	0.549	0.0137	1.216	21.1
	YW 4	1.01	0.212	0.608	0.0129	1.458	15.9

In general, the unimodal van Genuchten model was able to fit the data well near saturation but began to deviate from the tensiometer measured data as the water tensions approached PWP. This deviation would result in an underestimation of the AWC (Figure 5.1 and Table 5.3). The addition of available data from the dewpoint potentiometer for the sandy loam amended with pecan pruning biochar caused a substantial change in the fitted model parameters and increased the estimated AWC from 4.6 to 13.8 cm³ cm⁻³. This additional data supports the likelihood of the unimodal model underestimating the AWC.

For the sandy loam soils using the unimodal model fit, amendment with biochar did not appear to impact the AWC, except for the yard waste biochar, which showed a slight increase in AWC. More data is needed to determine if this increase is statistically significant. For the clay loam soils using the unimodal model fit, amendment with all of the biochars except for the yard waste biochar appeared to increase the AWC, although only slightly. Again, more data would be needed to determine statistical significance.

Table 5.4. Van Genuchten bimodal model parameters (Durner, 1994) and available water content (AWC) of biochar-amended soils from water desorption measurements. AWC assumes field capacity at -33 kPa and permanent wilting point at -1.5 MPa. PS: pecan shell; PP: pecan prunings; YW: yard waste; CGT: cotton gin trash; number indicates replicate identifier from soil incubation. *Model was fit after data from dewpoint potentiometer was included.

Soil	Biochar Treatment	θ_r (cm^3 cm^{-3})	θ_s (cm^3 cm^{-3})	α_1 (cm^{-1})	n_1	α_2 (cm^{-1})	n_2	ω_2	AWC (cm^3 cm^{-3})
Sandy Loam	Control 3	0	0.350	0.0099	4.557	0.0176	1.487	0.646	7.9
	Control 4	0	0.380	0.0084	4.500	0.0198	1.260	0.669	9.8
	PP 3	0	0.517	0.0099	4.474	0.0185	1.179	0.764	13.8
	PP 3*	0.074	0.516	0.0099	4.599	0.0170	1.254	0.739	12.7
	CGT 2	0	0.384	0.0089	5.844	0.0127	1.474	0.744	11.5
	CGT 3	0	0.344	0.0094	7.018	0.0107	1.771	0.733	8.5
	YW 3	0	0.393	0.0118	3.655	0.0124	1.430	0.693	11.6
	YW 4	0	0.384	0.0090	5.841	0.0129	1.474	0.744	11.4
Clay Loam	Control 3	0	0.445	0.0211	1.936	0.0041	1.330	0.703	18.8
	PS 3	0.213	0.494	0.0269	1.493	0.0020	2.561	0.262	11.9
	PP 2	0.257	0.548	0.0129	1.468	0.0021	5.469	0.052	12.4
	PP 3	0.268	0.586	0.0209	1.498	0.0022	2.107	0.327	14.8
	CGT 2	0.211	0.547	0.0234	1.697	0.0030	1.729	0.557	16.0
	YW 4	0	0.608	0.0135	1.536	0.0003	1.895	0.425	32.1

From the bimodal model parameters, it appeared that amending sandy loam soil with pecan pruning and yard waste biochars increased the AWC by approximately 20-50%, which would be a substantial improvement if this difference were shown to be significant. Cotton gin trash biochar amendment did not appear to affect the AWC of the sandy loam soil. For the clay loam soil, amendment with biochar appeared to actually decrease AWC with the exception of yard waste biochar. As with the previous results, more data is needed to determine if these differences are consistent across replications and statistically significant. For the bimodal model, addition of the data from the dewpoint potentiometer decreased the estimated AWC slightly.

Results from previous attempts to study the impact of biochar amendment on AWC can be difficult to interpret depending on how FC and PWP are defined. For example, the FC was defined as 10 kPa ($pF = 2$) for a study of grass biochar added at four rates on a coarse sand soil (Jeffery, et al., 2015), while FC was defined as 6 kPa ($pF = 1.8$) for a study of maize silage biochar and hydrochar added to two sandy soils and four loamy sand soils (Abel, et al., 2013). As can be seen in Figure 5.1, defining FC at $pF = 1.8$ for the sandy loam soils here would greatly increase the absolute values of the AWC measurements and should be considered in future work. Another possibility is attempt to match the model definitions with practical measurements as was done in a study of wood mill waste gasification char study on a range of soils from loamy sand to silty clay

loam; in this case, FC was defined by the moisture content of soil that no longer wet a paper towel through drainage holes in the bottom of the pot and PWP was defined as the moisture content when wheat seedlings wilted and did not recover (Peake, et al., 2014).

5.5 Conclusions and Future Work

Amending clay loam and sandy loam agricultural soils with biochars from pecan shells, pecan orchard prunings, and yard waste had few significant impacts, positive or negative, on the soil quality indicators measured in this study after a short soil incubation. Biochar effects were different for the two different soil textures. Cotton gin trash biochar showed the greatest potential to increase soil organic matter and plant nutrients, however, the increases in salinity for both soils is a serious concern.

Biochar application rate in this trial was very high (45 Mg ha^{-1}), and the biochar materials were ground to pass through 2-mm sieve before application to the soil in order to accelerate the biochar's interactions within the soil system. It is possible that the effects seen in this trial, such as biochar's impact on soil salinity, may not be as severe if biochars are applied as larger fragments and at lower rates.

More research is needed on the effects of different biochar amendments on soil quality and plant available water retention in arid agricultural soils. Trials involving impacts of different sizes and rates of biochar are needed in arid regions, to help balance the utility of this potential soil organic matter source without delivering any negative side effect such as increased soil salinity. Work to understand the effects of biochar amendment on AWC needs to include an expanded set of instrumental data (tensiometer, dewpoint potentiometer, pressure plate) and complementary data from plant measurements. For irrigated crop systems, biochar amendments needs to be considered from both the soil water desorption and adsorption directions.

6. Outcomes of This Research

6.1 Research Capacity Building

This project served as the launching point for research laboratory and collaboration development, and several student research opportunities for one new assistant professor in Chemical & Materials Engineering (Brewer) and one assistant professor in Extension Plant Science/Plant & Environmental Science who has now been promoted to associate professor with tenure (Idowu). Funds from this project, combined with faculty start-up funds, contributed to the purchase and set up of several pieces of equipment, namely a lab-scale pyrolysis system and additional test units for soil water retention equipment. Collaborations were created or fostered between the PIs and researchers/staff at New Mexico State University in the Institute for Energy & the Environment (IEE), the Manufacturing Technology & Engineering Center, the Office of Sustainability, the Department of Building & Grounds, and the Department of Plant & Environmental Sciences, and with a research group in Chemical & Biomolecular Engineering at Rice University. Two graduate students and two undergraduate students received training in research methods, sample analysis, and laboratory safety, as well as experience in conducting original research.

6.2 Theses, Publications, and Presentations

Work on this project has resulted in one manuscript under peer review, one manuscript in revision, and two manuscripts in preparation (titles are tentative), part of one in-progress Ph.D. dissertation, part of one completed M.S. thesis, and four conference presentations:

Amiri, A., Brewer, C.E., Biomass as a renewable energy source for water desalination: a review, *in revision*.

Zhang, Y., Idowu, O.J., Brewer, C.E., Using agricultural residue biochar to improve soil quality of desert soils, *under review*.

Amiri, A., Zhang, Y., Idowu, O.J., Brewer, C.E., Design of biomass pyrolyzer-multiple effect distillation system interface, *in preparation*.

Carrillo, B.D., Yamashita, F.M., Zhang, Y., Idowu, O.J., Brewer, C.E., Biochar impacts on soil water retention of desert agricultural soils, *in preparation*.

Amiri, A., Biomass as a renewable energy source for brackish water thermal desalination, Ph.D. Dissertation, Engineering: Chemical Engineering, New Mexico State University, expected Fall 2016.

Zhang, Y., Design of biomass pyrolyzer-multiple effect distillation system components for laboratory testing, M.S. Thesis, Chemical Engineering, New Mexico State University, June 2015.

Amiri, A., Brewer, C.E., Idowu, O.J., Aspen simulation of biomass slow pyrolyzer-multiple effect distillation (MED) prototype, *1st Annual Rocky Mountain Section American Water Works Association/RMWEA Conference*, Albuquerque, NM, April 30, 2015.

Zhang, Y., Amiri, A., Brewer, C.E., Idowu, O.J., Design and testing of biomass pyrolyzer-multiple effect distillation system components for laboratory testing, *2015 American Institute of Chemical Engineers Spring Meeting*, Austin, TX, April 28, 2015.

Amiri, A., Brewer, C., Zygourakis, K., A partial-combustion model for an energy + biochar reactor design, *2014 American Institute of Chemical Engineers Annual Meeting*, Atlanta, GA, November 16, 2014.

Amiri, A., Brewer, C.E., Design of a biomass slow pyrolyzer-multiple effect distillation (MED) prototype, *Symposium on Thermal and Catalytic Sciences for Biofuels and Biobased Products*, Denver, CO, September 3, 2014.

6.3 Follow-On Proposals

Research conducted during this project has resulted in the submission of two directly related follow-on proposals, the first of which was funded and recently competed, and the second of which was not funded but did progress to Phase II consideration and is currently be revised for resubmission:

“Construction of MED Component of Pyrolysis-Desalination Unit for Resiliency Testing”

NMSU Institute of Energy & the Environment Tier 1 Supplemental Extension
8/1/14-7/31/15, \$104,237, PI: Brewer

Construction and testing of a lab-scale prototype of the multiple effect distillation (MED) component of a biomass pyrolysis-water desalination unit.

"Halophytes and Biochar for Desalination Concentrate Management"

US Department of Interior/Bureau of Reclamation Desalination and Water Purification Research & Development

12/1/15-12/31/16, \$149,977, PIs: Brewer, Rastegary, Idowu

Collaborations fostered through this research project have resulted in the submission of three additional related proposals, the first of which was funded and is underway; the other two of which are currently pending:

“Sustainable Use of Biomass Resources in a Semi-Arid Landscape: Connecting Chemical Engineering, Soil Science, and Extension”

USDA NIFA National Needs Fellowship

7/15/15-7/14/20, \$241,000, PIs: Brewer, Ulery, Idowu, Archarya, Rockstraw

A multidisciplinary graduate fellowship program with training in chemical

engineering and soil science. This program will prepare four fellows (2 MS, 2 PhD) to address the challenges of producing food, fiber, and fuel from biomass while improving soil quality in water-limited regions.

“Invasive Plant Biomass Conversion to Biochar: A Conservation Practice to Restore Ecosystem Health”

USDA Natural Resources Conservation Service Conservation Innovation Grant
10/1/15-9/30/18, \$577,666, PIs: Ganguli, Bockness, Sterling, Brewer, Ulery,
Conley, Brown

Collaboration with range sciences from several universities to study the use of slow pyrolysis in the field to mitigate the spread and damage from woody invasive species.

“Holistic Approach for Sustainable Agriculture”

USDA AFRI Water for Agriculture

1/1/16-12/31/19; \$10,000,000, PIs: Ghassemi, et al.

Large, multi-institutional, long-term integrated research, extension and education project focusing on water desalination techniques, use of algal and halophyte biomass, algal food products, and on-farm nutrient, water and energy use.

6.4 Other Products

Other products that are the result of this project include:

- soil samples amended with biochars made from local biomass that are available for further analysis and study;
- an Aspen Plus® simulation file allowing model experimentation with different scales and conditions for the biomass pyrolyzer-MED interface;
- a press release and extension materials about the biochar-amended soil analysis results (in preparation); and
- a webpage describing the project and results:
<http://wordpress.nmsu.edu/cbrewer/projects/>

Reference List

- [International Desalination Association] 2012. *2011-2012 IDA Desalination Yearbook*, Global Water Intelligence, London.
- [U.S. Department of Energy] 2015. *Furnaces and Boilers*, Energy Savers, U.S. Department of Energy, Washington D.C., Available at: <http://energy.gov/energysaver/articles/furnaces-and-boilers> [Accessed 28 August 2015].
- Abel, S., A. Peters, S. Trinks, H. Schonsky, M. Facklam and G. Wessolek, 2013. Impact of biochar and hydrochar addition on water retention and water repellency of sandy soil, *Geoderma*, 202–203, 183-191.
- Ackermann, T. and L. Söder, 2002. An overview of wind energy-status 2002, *Renew. Sust. Energ. Rev.*, 6, 67-127.
- Akash, B.A. and M.S. Mohsen, 1998. Potentials for development of hydro-powered water desalination in Jordan, *Renew. Energ.*, 13, 537-542.
- Al-Anezi, K. and N. Hilal, 2007. Scale formation in desalination plants: effect of carbon dioxide solubility, *Desalination*, 204, 385-402.
- Al-Jaroudi, S.S., A. Ul-Hamid and J.A. Al-Matar, 2010. Prevention of failure in a distillation unit exhibiting extensive scale formation, *Desalination*, 260, 119-128.
- Al-Karaghoul, A. and L.L. Kazmerski, 2013. Energy consumption and water production cost of conventional and renewable-energy-powered desalination processes *Renew. Sust. Energ. Rev.*, 24, 343-356.
- Al-Karaghoul, A., D. Renne and L.L. Kazmerski, 2009. Solar and wind opportunities for water desalination in the Arab regions, *Renew. Sust. Energ. Rev.*, 13, 2397-2407.
- Al-Rawajfeh, A.E., 2010. CaCO₃-CO₂-H₂O system in falling film on a bank of horizontal tubes: model verification, *J. Ind. Eng. Chem.*, 16, 1050-1058.
- Al-Rawajfeh, A.E., H. Glade, H.M. Qiblawey and J. Ulrich, 2004. Simulation of CO₂ release in multiple-effect distillers, *Desalination*, 166, 41-52.
- Al-Shammiri, M. and M. Safar, 1999. Multi-effect distillation plants: state of the art, *Desalination*, 126, 45-59.
- Annamalai, K., J.M. Sweeten and S.C. Ramalingam, 1987. Estimation of gross heating values of biomass fuels, *Transactions of the ASAE*, 30, 1205-1208.

- Awerbuch, L., T.E. Lindemuth, S.C. May and A.N. Rogers, 1976. Geothermal energy recovery process, *Desalination*, 19, 325-336.
- Babu, B.V., 2008. Biomass pyrolysis: a state-of-the-art review, *Biofuels, Bioproducts and Biorefining*, 2, 393-414.
- Barbier, E., 2002. Geothermal energy technology and current status: an overview, *Renew. Sust. Energ. Rev.*, 6, 3-65.
- Barrow, C.J., 2012. Biochar: potential for countering land degradation and for improving agriculture, *Appl. Geogr.*, 34, 21-28.
- Bourouni, K., M.T. Chaibi and L. Tadrist, 2001. Water desalination by humidification and dehumidification of air: State of the art, *Desalination*, 137, 167-176.
- Bourouni, K., J.C. Deronzier and L. Tadrist, 1999. Experimentation and modelling of an innovative geothermal desalination unit, *Desalination*, 125, 147-153.
- Bourouni, K., R. Martin and L. Tadrist, 1999. Analysis of heat transfer and evaporation in geothermal desalination units, *Desalination*, 122, 301-313.
- Branca, C. and C. DiBlasi, 2003. Global kinetics of wood char devolatilization and combustion, *Energy Fuels*, 17, 1609-1615.
- Braun, G., W. Hater, C.z. Kolk, C. Dupoirion, T. Harrer and T. Götz, 2010. Investigations of silica scaling on reverse osmosis membranes, *Desalination*, 250, 982-984.
- Brewer, C., R. Unger, K. Schmidt-Rohr and R. Brown, 2011. Criteria to select biochars for field studies based on biochar chemical properties, *Bioenergy Res.*, 4, 312-323.
- Brewer, C.E. and R.C. Brown, 2012. Biochar, Sayigh, A., *Comprehensive Renewable Energy*, Elsevier, Oxford.
- Brewer, C.E., Y.-Y. Hu, K. Schmidt-Rohr, T.E. Loynachan, D.A. Laird and R.C. Brown, 2012. Extent of pyrolysis impacts on fast pyrolysis biochar properties, *J. Environ. Qual.*, 41, 1115-1122.
- Brewer, C.E., K. Schmidt-Rohr, J.A. Satrio and R.C. Brown, 2009. Characterization of biochar from fast pyrolysis and gasification systems, *Environ. Prog. Sustain. Energy*, 28, 386-396.
- Bridgwater, A.V., D. Meier and D. Radlein, 1999. An overview of fast pyrolysis

of biomass, *Organic Geochemistry*, 30, 1479-1493.

Brown, A.L., P.D. Brady, C.D. Mowry and T.T. Borek, 2011. *An Economic Analysis of Mobile Pyrolysis for Northern New Mexico Forests*, Report No. Albuquerque

Brown, R.C. and T.R. Brown, 2014. *Biorenewable Resources: Engineering New Products from Agriculture*, Wiley-Blackwell, Danvers, MA.

Brown, T.R., M.M. Wright and R.C. Brown, 2011. Estimating profitability of two biochar production scenarios: slow pyrolysis vs fast pyrolysis, *Biofuel. Bioprod. Bior.*, 5, 54-68.

Cardona, E., S. Culotta and A. Piacentino, 2003. Energy saving with MSF-RO series desalination plants, *Desalination*, 153, 167-171.

Channiwala, S.A. and P.P. Parikh, 2002. A unified correlation for estimating HHV of solid, liquid and gaseous fuels, *Fuel*, 81, 1051-1063.

Chen, G., J. Andries, Z. Luo and H. Spliethoff, 2003. Biomass pyrolysis/gasification for product gas production: the overall investigation of parametric effects, *Energy Conversion and Management*, 44, 1875-1884.

Cheng, C.-H., J. Lehmann and M.H. Engelhard, 2008. Natural oxidation of black carbon in soils: Changes in molecular form and surface charge along a climosequence, *Geochim. Cosmochim. Acta*, 72, 1598-1610.

Christmann, J.B.P., L.J. Krätz and H.-J. Bart, 2010. Novel polymer film heat exchangers for seawater desalination, *Desalination and Water Treatment*, 21, 162-174.

Cihacek, L.J., 1983. *Interpreting Soil Analysis*, Report No. University, N.M.S., Las Cruces, NM.

Cordero, T., F. Marquez, J. Rodriguez-Mirasol and J.J. Rodriguez, 2001. Predicting heating values of lignocellulosics and carbonaceous materials from proximate analysis, *Fuel*, 80, 1567-1571.

Daniels, F., 1974. *Direct Use of the Sun's Energy*, Ballantine Books, New York.

Darwish, M.A. and H.K. Abdulrahim, 2008. Feed water arrangements in a multi-effect desalting system, *Desalination*, 228, 30-54.

Deenik, J.L., T. McClellan, U. Goro, M.J. Antal and S. Campbell, 2010. Charcoal volatile matter content influences plant growth and soil nitrogen transformations, *Soil Sci. Soc. Am. J.*, 74, 1259-1270.

- Downie, A., P. Munroe, A. Cowie, L. Van Zwieten and D.M.S. Lau, 2012. Biochar as a Geoengineering Climate Solution: Hazard Identification and Risk Management, *Critical Reviews in Environmental Science and Technology*, 42, 225-250.
- Downing, M., L.M. Eaton, R.L. Graham, M.H. Langholtz, R.D. Perlack, A.F. Turhollow Jr, B. Stokes and C.C. Brandt, 2011. *U.S. Billion-Ton Update: Biomass Supply for a Bioenergy and Bioproducts Industry*, Report No. ORNL/TM-2011/224,
- Durner, W., 1994. Hydraulic conductivity estimation for soils with heterogeneous pore structure, *Water Resources Research*, 30, 221-223.
- Eibling, J.A., S.G. Talbert and G.O.G. Löf, 1971. Solar stills for community use—digest of technology, *Sol. Energy*, 13, 263-276.
- Elimelech, M. and W.A. Phillip, 2011. The future of seawater desalination: energy, technology, and the environment, *Science*, 333, 712-717.
- Eltawil, M.A., Z. Zhengming and L. Yuan, 2009. A review of renewable energy technologies integrated with desalination systems, *Renew. Sust. Energ. Rev.*, 13, 2245-2262.
- Emrich, W., 1985. *Handbook of Charcoal Making: The Traditional and Industrial Methods*, Solar Energy R&D in the European Community, Series E: Energy from Biomass, Springer, Luxembourg.
- Erol, M., H. Haykiri-Acma and S. Kucukbayrak, 2010. Calorific value estimation of biomass from their proximate analyses data, *Renewable Energy*, 35, 170-173.
- Fantozzi, F., S. Colantoni, P. Bartocci and U. Desideri, 2007. Rotary kiln slow pyrolysis for syngas and char production from biomass and waste--Part 1. Working envelope of the reactor, *Journal of Engineering for Gas Turbines and Power*, 129, 901-907.
- Fiorenza, G., V.K. Sharma and G. Braccio, 2003. Techno-economic evaluation of a solar powered water desalination plant, *Energ. Convers. Manage.*, 44, 2217-2240.
- Flynn, R., 2012. Appropriate Analyses for New Mexico Soils, Guide A-146, Report No. Las Cruces, NM.
- Galal, T., A. Kalendar, A. Al-Saftawi and M. Zedan, 2010. Heat transfer performance of condenser tubes in an MSF desalination system, *Journal of Mechanical Science and Technology*, 24, 2347-2355.

- Garcia-Perez, M., C. Kruger, M. Fuchs and S. Sokhansanj, 2012. Methods for Producing Biochar and Advanced Bio-fuels in Washington State (Part II: From field to pyrolysis reactor), Report No. 12-07-033,
- Garcia-Perez, M., T. Lewis and C.E. Kruger, 2010. Methods for Producing Biochar and Advanced Biofuels in Washington State, Part 1: Literature Review of Pyrolysis Reactors, Report No. 11-07-017, Ecology, S.o.W.D.o., Pullman, WA.
- García-Rodríguez, L. and C. Gómez-Camacho, 1999. Preliminary design and cost analysis of a solar distillation system, *Desalination*, 126, 109-114.
- García-Rodríguez, L. and C. Gómez-Camacho, 2001. Perspectives of solar-assisted seawater distillation, *Desalination*, 136, 213-218.
- García-Rodríguez, L., A.I. Palmero-Marrero and C. Gómez-Camacho, 1999. Application of direct steam generation into a solar parabolic trough collector to multieffect distillation, *Desalination*, 125, 139-145.
- García-Rodríguez, L., A.I. Palmero-Marrero and C. Gómez-Camacho, 2002. Comparison of solar thermal technologies for applications in seawater desalination, *Desalination*, 142, 135-142.
- García-Rodríguez, L., V. Romero-Ternero and C. Gómez-Camacho, 2001. Economic analysis of wind-powered desalination, *Desalination*, 137, 259-265.
- Habali, S.M. and I.A. Saleh, 1994. Design of stand-alone brackish water desalination wind energy system for Jordan, *Sol. Energy*, 52, 525-532.
- Hamed, O.A., 2005. Overview of hybrid desalination systems — current status and future prospects, *Desalination*, 186, 207-214.
- Hanson, A., W. Zachritz, K. Stevens, L. Mimbela, R. Polka and L. Cisneros, 2004. Distillate water quality of a single-basin solar still: laboratory and field studies, *Sol. Energy*, 76, 635-645.
- Helal, A.M., A.M. El-Nashar, E. Al-Katheeri and S. Al-Malek, 2003. Optimal design of hybrid RO/MSF desalination plants Part I: Modeling and algorithms, *Desalination*, 154, 43-66.
- Helal, A.M., A.M. El-Nashar, E.S. Al-Katheeri and S.A. Al-Malek, 2004. Optimal design of hybrid RO/MSF desalination plants Part II: Results and discussion, *Desalination*, 160, 13-27.
- Hetsroni, G. and A. Mosyak, 1994. Heat transfer and pressure drop in a plastic heat exchanger with triangular channels, *Chem. Eng. Process.*, 33, 91-100.

- Houcine, I., F. Benjemaa, M.-H. Chahbani and M. Maalej, 1999. Renewable energy sources for water desalting in Tunisia, *Desalination*, 125, 123-132.
- Idowu, O.J. and R. Flynn, 2013. Understanding Soil Health for Production Agriculture in New Mexico, Guide A-148, Report No. Service, C.E., Las Cruces, NM.
- Idowu, O.J., M. Marsalis and R. Flynn, 2012. *Agronomic Principles to Help with Farming During Drought Periods, Guide A-147*, Report No. Service, C.E., Las Cruces, NM.
- Ioannidou, O., A. Zabaniotou, E.V. Antonakou, K.M. Papazisi, A.A. Lappas and C. Athanassiou, 2009. Investigating the potential for energy, fuel, materials and chemicals production from corn residues (cobs and stalks) by non-catalytic and catalytic pyrolysis in two reactor configurations, *Renewable and Sustainable Energy Reviews*, 13, 750-762.
- Isci, A. and G.N. Demirer, 2007. Biogas production potential from cotton wastes, *Renewable Energy*, 32, 750-757.
- Jeffery, S., M.B.J. Meinders, C.R. Stoof, T.M. Bezemer, T.F.J. van de Voorde, L. Mommer and J.W. van Groenigen, 2015. Biochar application does not improve the soil hydrological function of a sandy soil, *Geoderma*, 251–252, 47-54.
- Jeffery, S., F.G.A. Verheijen, M. van der Velde and A.C. Bastos, 2011. A quantitative review of the effects of biochar application to soils on crop productivity using meta-analysis, *Agriculture, Ecosystems & Environment*, 144, 175-187.
- Jenkins, B.M., L.L. Baxter and T.R. Miles, 1998. Combustion properties of biomass, *Fuel Processing Technology*, 54, 17-46.
- Jiménez, L. and F. González, 1991. Study of the physical and chemical properties of lignocellulosic residues with a view to the production of fuels, *Fuel*, 70, 947-950.
- Joo, H.-J. and H.-Y. Kwak, 2013. Performance evaluation of multi-effect distiller for optimized solar thermal desalination, *Appl. Therm. Eng.*, 61, 491-499.
- Kallestad, J.C., J.G. Mexal and T.W. Sammis, 2008. Mesilla Valley Pecan Orchard Pruning Residues: Biomass Estimates and Value-Added Opportunities, Research Report 764, Report No. Las Cruces, NM.
- Kalogirou, S., 1997. Survey of solar desalination systems and system selection, *Energy*, 22, 69-81.

Kalogirou, S., 2014. *Solar Energy Engineering Processes and Systems*, Academic Press, Oxford.

Kalogirou, S.A., 2005. Seawater desalination using renewable energy sources, *Prog. Energ. Combust.*, 31, 242-281.

Karagiannis, I.C. and P.G. Soldatos, 2008. Water desalination cost literature review and assesment, *Desalination*, 223, 448-456.

Karhu, K., T. Mattila, I. Bergström and K. Regina, 2011. Biochar addition to agricultural soil increased CH₄ uptake and water holding capacity – Results from a short-term pilot field study, *Agr. Ecosyst. Environ.*, 140, 309-313.

Karlen, D.L., M.J. Mausbach, J.W. Doran, R.G. Cline, R.F. Harris and G.E. Schuman, 1997. Soil quality: a concept, definition, and framework for evaluation (a guest editorial), *Soil Sci Soc Am J*, 61, 4-10.

Kim, K.H., X. Bai, M.R. Rover and R.C. Brown, 2014. The effect of low-concentration oxygen in sweep gas during pryolysis of red oak using a fluidized bed reactor, *Fuel*, 124, 49-56.

Kimetu, J., J. Lehmann, S. Ngoze, D. Mugendi, J. Kinyangi, S. Riha, L. Verchot, J. Recha and A. Pell, 2008. Reversibility of soil productivity decline with organic matter of differing quality along a degradation gradient, *Ecosystems*, 11, 726-739.

Kinney, T.J., C.A. Masiello, B. Dugan, W.C. Hockaday, M.R. Dean, K. Zygourakis and R.T. Barnes, 2012. Hydrologic properties of biochars produced at different temperatures, *Biomass Bioenerg.*, 41, 34-43.

Kiranoudis, C.T., N.G. Voros and Z.B. Maroulis, 1997. Wind energy exploitation for reverse osmosis desalination plants, *Desalination*, 109, 195-209.

Laird, D.A., 2008. The charcoal vision: A win-win-win scenario for simultaneously producing bioenergy, permanently sequestering carbon, while improving soil and water quality, *Agron. J.*, 100, 178-181.

Laird, D.A., P. Fleming, D.D. Davis, R. Horton, B. Wang and D.L. Karlen, 2010. Impact of biochar amendments on the quality of a typical Midwestern agricultural soil, *Geoderma*, 158, 443-449.

Lal, R., 2008. Black and buried carbons' impact on soil quality and ecosystem services, *Soil Till. Res.*, 99, 1-3.

Lee, J.W., M. Kidder, B.R. Evans, S. Paik, A.C. Buchanan, C.T. Garten and R.C. Brown, 2010. Characterization of biochars produced from cornstovers for soil

amendment, *Environ. Sci. Technol.*, 44, 7970-7974.

Lee, Y., P.-R.-B. Eum, C. Ryu, Y.-K. Park, J.-H. Jung and S. Hyun, 2013. Characteristics of biochar produced from slow pyrolysis of Geodae-Uksae 1, *Bioresource Technology*, 130, 345-350.

Lehmann, J. and S. Joseph, 2009. *Biochar for Environmental Management: Science and Technology*, Earthscan, London.

Lehmann, J., J. Pereira da Silva, C. Steiner, T. Nehls, W. Zech and B. Glaser, 2003. Nutrient availability and leaching in an archaeological Anthrosol and a Ferralsol of the Central Amazon basin: fertilizer, manure and charcoal amendments, *Plant Soil*, 249, 343-357.

Lehmann, J., M.C. Rillig, J. Thies, C.A. Masiello, W.C. Hockaday and D. Crowley, 2011. Biochar effects on soil biota - A review, *Soil Biol. Biochem.*, 43, 1812-1836.

Lenzen, M. and J. Munksgaard, 2002. Energy and CO₂ life-cycle analyses of wind turbines—review and applications, *Renew. Energ.*, 26, 339-362.

Li, D., W.C. Hockaday, C.A. Masiello and P.J.J. Alvarez, 2011. Earthworm avoidance of biochar can be mitigated by wetting, *Soil Biol. Biochem.*, 43, 1732-1737.

Li, Y.D. and H. Liu, 2000. High-pressure densification of wood residues to form an upgraded fuel, *Biomass & Bioenergy*, 19, 177-186.

Liang, B., J. Lehmann, D. Solomon, J. Kinyangi, J. Grossman, B. O'Neill, J.O. Skjemstad, J. Thies, F.J. Luizao, J. Petersen and E.G. Neves, 2006. Black carbon increases cation exchange capacity in soils, *Soil Sci. Soc. Am. J.*, 70, 1719-1730.

Likhachev, D.S. and F.-C. Li, 2013. Large-scale water desalination methods: a review and new perspectives, *Desalination and Water Treatment*, 51, 2836-2849.

Lillywhite, J.M., R. Heerema, J.E. Simonsen and E. Herrera, 2010. *Pecan Marketing Channels in New Mexico, 2010, Guide Z-307*, Report No. Las Cruces, NM.

Ludwick, A.E. and J.O. Reuess, 1974. *Guide to fertilizer recommendations in Colorado*, Report No. University, C.S., Fort Collins, CO.

Ma, Q. and H. Lu, 2011. Wind energy technologies integrated with desalination systems: Review and state-of-the-art, *Desalination*, 277, 274-280.

Magdoff, F., 2001. Concepts, components, and strategies of soil health in

agroecosystems, *Journal of Nematology*, 33, 169.

Manenti, F., M. Masi, G. Santucci and G. Manenti, 2013. Parametric simulation and economic assessment of a heat integrated geothermal desalination plant, *Desalination*, 317, 193-205.

Mani, S., L.G. Tabil and S. Sokhansanj, 2006. Specific energy requirement for compacting corn stover, *Bioresource Technology*, 97, 1420-1426.

Manolakos, D., G. Papadakis, D. Papantonis and S. Kyritsis, 2001. A simulation-optimisation programme for designing hybrid energy systems for supplying electricity and fresh water through desalination to remote areas: Case study: the Mersini village, Donoussa island, Aegean Sea, Greece, *Energy*, 26, 679-704.

Matsuoka, K., K. Kuramoto, T. Murakami and Y. Suzuki, 2008. Steam Gasification of Woody Biomass in a Circulating Dual Bubbling Fluidized Bed System, *Energy Fuels*, 22, 1980-1985.

McHenry, M.P., 2009. Agricultural bio-char production, renewable energy generation and farm carbon sequestration in Western Australia: Certainty, uncertainty and risk, *Agriculture, Ecosystems & Environment*, 129, 1-7.

Methnani, M., 2007. Influence of fuel costs on seawater desalination options, *Desalination*, 205, 332-339.

Mexal, J.G., E. Herrera, T.W. Sammis and W.H. Zachritz, 2003. *Noncommensurable Values of the Pecan Industry, Guide H-654*, Report No. Las Cruces, NM.

Miller, J.E., 2003. Review of Water Resources and Desalination Technologies, SAND 2003-0800, Report No. Laboratories, S.N., Albuquerque, NM.

Miranda, M.S. and D. Infield, 2003. A wind-powered seawater reverse-osmosis system without batteries, *Desalination*, 153, 9-16.

Munoz-Guerra, J.A., P. Prado and S.V. Garcia-Tenorio, 2011. Use of hydrogen as a carrier gas for the analysis of steroids with anabolic activity by gas chromatography/mass spectrometry, *Journal of Chromatography A*, 1218, 7365-7370.

Murakami, M., 1994. Hydro-powered reverse osmosis (RO) desalination for co-generation: A Middle East case study, *Desalination*, 97, 301-311.

Naik, S.N., V.V. Goud, P.K. Rout and A.K. Dalai, 2010. Production of first and second generation biofuels: A comprehensive review, *Renewable & Sustainable Energy Reviews*, 14, 578-597.

Ndiema, C.K.W., P.N. Manga and C.R. Ruttoh, 2002. Influence of die pressure on relaxation characteristics of briquetted biomass, *Energy Conversion and Management*, 43, 2157-2161.

Nelson, D.W. and L.E. Sommers, 1996. Total carbon, organic carbon and organic matter, Sparks, D.L., *Methods of Soil Analysis Part 3. Chemical Methods*, SSSA and ASA, Madison, WI.

Nisan, S. and N. Benzarti, 2008. A comprehensive economic evaluation of integrated desalination systems using fossil fuelled and nuclear energies and including their environmental costs, *Desalination*, 229, 125-146.

Olsen, S.R., C.V. Cole, F.S. Watanabe and L.A. Dean, 1954. Estimation of available phosphorus in soils by extraction with sodium bicarbonate, *U.S. Dept. of Agric. Circ.*, 939,

Ophir, A., 1982. Desalination plant using low grade geothermal heat, *Desalination*, 40, 125-132.

Ophir, A. and F. Lokiec, 2005. Advanced MED process for most economical sea water desalination, *Desalination*, 182, 187-198.

Park, J., Y. Lee, C. Ryu and Y.K. Park, 2014. Slow pyrolysis of rice straw: Analysis of products properties, carbon and energy yields, *Bioresource Technology*, 155, 63-70.

Peake, L.R., B.J. Reid and X. Tang, 2014. Quantifying the influence of biochar on the physical and hydrological properties of dissimilar soils, *Geoderma*, 235–236, 182-190.

Peters, A., W. Durner and G. Wessolek, 2011. Consistent parameter constraints for soil hydraulic functions, *Advances in Water Resources*, 34, 1352-1365.

Phan, A.N., C. Ryu, V.N. Sharifi and J. Swithenbank, 2008. Characterisation of slow pyrolysis products from segregated wastes for energy production, *Journal of Analytical and Applied Pyrolysis*, 81, 65-71.

Qiblawey, H.M. and F. Banat, 2008. Solar thermal desalination technologies, *Desalination*, 220, 633-644.

Quaak, P., H. Knoef and H. Stassen, 1999. *Energy from Biomass: A Review of Combustion and Gasification Technologies*, Report No. Bank, T.W., Washington, D.C.

Raluy, R.G., L. Serra and J. Uche, 2005. Life cycle assessment of desalination

technologies integrated with renewable energies, *Desalination*, 183, 81-93.

Reeves, D.W., 1997. The role of soil organic matter in maintaining soil quality in continuous cropping systems, *Soil and Tillage Research*, 43, 131-167.

Robinson, R., G. Ho and K. Mathew, 1992. Development of a reliable low-cost reverse osmosis desalination unit for remote communities, *Desalination*, 86, 9-26.

Sarkar, M., A. Kumar, J.S. Tumuluru, K.N. Patil and D.D. Bellmer, 2014. Gasification performance of switchgrass pretreated with torrefaction and densification, *Applied Energy*, 127, 194-201.

Schindler, U., W. Durner, G. von Unold, L. Mueller and R. Wieland, 2010. The evaporation method: Extending the measurement range of soil hydraulic properties using the air-entry pressure of the ceramic cup, *Journal of Plant Nutrition and Soil Science*, 173, 563-572.

Semiati, R., 2008. Energy issues in desalination processes, *Environ. Sci. Technol.*, 42, 8193-8201.

Semiati, R. and D. Hasson, 2012. Water desalination, *Rev. Chem. Eng.*, 28, 43-60.

Sen, P.K., P.V. Sen, A. Mudgal and S.N. Singh, 2011. A small scale multi-effect distillation (MED) unit for rural micro enterprises: Part-III Heat transfer aspects, *Desalination*, 279, 38-46.

Sen, P.K., P.V. Sen, A. Mudgal and S.N. Singh, 2011. A small scale multiple-effect distillation (MED) unit for rural micro enterprises: Part II--Parametric studies and performance analysis, *Desalination*, 279, 27-37.

Sen, P.K., P.V. Sen, A. Mudgal, S.N. Singh, S.K. Vyas and P. Davies, 2011. A small scale multiple-effect distillation (MED) unit for rural micro enterprises: Part I--design and fabrication, *Desalination*, 279, 15-26.

Sen, P.V., K. Bhuwanesh, K. Ashutosh, Z. Engineer, S. Hegde, P.K. Sen and R. Lal, 2013. Micro-scale multiple-effect distillation system for low steam inputs, *Procedia Engineering*, 56, 63-67.

Shabangu, S., D. Woolf, E.M. Fisher, L.T. Angenent and J. Lehmann, 2014. Techno-economic analysis of biomass slow pyrolysis into different biochar and methanol concepts, *Fuel*, 117, 742-748.

Shajizadeh, F. and W. Degroot, 1976. *Thermal uses and properties of carbohydrates and lignins* Academic Press, New York.

Shastri, Y.N., Z. Miao, L.F. Rodríguez, T.E. Grift, A.C. Hansen and K.C. Ting,

2014. Determining optimal size reduction and densification for biomass feedstock using the BioFeed optimization model, *Biofuels, Bioproducts and Biorefining*, 8, 423-437.

Sheng, C.D. and J.L.T. Azevedo, 2005. Estimating the higher heating value of biomass fuels from basic analysis data, *Biomass & Bioenergy*, 28, 499-507.

Skoulou, V., G. Koufodimos, Z. Samaras and A. Zabaniotou, 2008. Low temperature gasification of olive kernels in a 5-kW fluidized bed reactor for H₂-rich producer gas, *International Journal of Hydrogen Energy*, 33, 6515-6524.

Smith, J.M., H.C. Van Ness and M.M. Abbott, 2005. *Introduction to Chemical Engineering Thermodynamics*, McGraw Hill Higher Education, Columbus, OH.

Staff, S.S., 1999. *Soil Taxonomy: A Basic System of Soil Classification for Making and Interpreting Soil Surveys*, U.S. Department of Agriculture Handbook 436, Natural Resources Conservation Service,

Steinbeiss, S., G. Gleixner and M. Antonietti, 2009. Effect of biochar amendment on soil carbon balance and soil microbial activity, *Soil Biol. Biochem.*, 41, 1301-1310.

Steiner, C., B. Glaser, W.G. Teixeira, J. Lehmann, W. Blum and W. Zech, 2008. Nitrogen retention and plant uptake on a highly weathered central Amazonian Ferralsol amended with compost and charcoal, *J. Plant Nutr. Soil Sci.*, 171, 893-899.

Steiner, C., W. Teixeira, J. Lehmann, T. Nehls, J. de Macêdo, W. Blum and W. Zech, 2007. Long term effects of manure, charcoal and mineral fertilization on crop production and fertility on a highly weathered Central Amazonian upland soil, *Plant Soil*, 291, 275-290.

Thoreson, C., K. Webster, M. Darr and E. Kapler, 2014. Investigation of process variables in the densification of corn stover briquettes, *Energies*, 7, 4019-4032.

Thu, K., Y.-D. Kim, G. Amy, W.G. Chun and K.C. Ng, 2013. A hybrid multi-effect distillation and adsorption cycle, *Appl. Energ.*, 104, 810-821.

Tian, L., J. Guo, Y. Tang and L. Cao, 2005. A historical opportunity: economic competitiveness of seawater desalination project between nuclear and fossil fuel while the world oil price over \$50 per boe—part A: MSF, *Desalination*, 183, 317-325.

Tillman, D., 1978. *Wood as an energy resource* Academic Press, New York

Tumuluru, J.S., C.T. Wright, J.R. Hess and K.L. Kenney, 2011. A review of

- biomass densification systems to develop uniform feedstock commodities for bioenergy application, *Biofuels, Bioproducts and Biorefining*, 5, 683-707.
- Tzen, E. and R. Morris, 2003. Renewable energy sources for desalination, *Sol. Energy*, 75, 375-379.
- Tzen, E., K. Perrakis and P. Baltas, 1998. Design of a stand alone PV - desalination system for rural areas, *Desalination*, 119, 327-333.
- Uche, J., L. Serra and A. Valero, 2001. Thermoeconomic optimization of a dual-purpose power and desalination plant, *Desalination*, 136, 147-158.
- Ulery, A.L. and A.J. Tugel, 1999. Farming in New Mexico: Soil quality and productivity maintenance, *New Mexico Journal of Science*, 39, 86-108.
- van Genuchten, M.T., 1980. A closed form of the equation for predicting the hydraulic conductivity of unsaturated soils, *Soil Sci Soc Am J*, 44, 892-898.
- Wijyantia, W. and K.-i. Tanoue, 2013. Char formation and gas products of woody biomass pyrolysis, *Energy Procedia* 32, 145-152.
- Winsley, P., 2007. Bioenergy and biochar production for climate change mitigation, *N. Z. Sci. Rev.*, 64, 5-10.
- Wright, M. and R.C. Brown, 2007. Establishing the optimal sizes of different kinds of biorefineries, *Biofuels, Bioproducts and Biorefining*, 1, 191-200.
- Yan, X., B. Li, B. Liu, J. Zhao, Y. Wang and H. Li, 2014. Analysis of improved novel hollow fiber heat exchanger, *Appl. Therm. Eng.*, 67, 114-121.
- Yang, H., R. Yan, H. Chen, D.H. Lee and C. Zheng, 2007. Characteristics of hemicellulose, cellulose and lignin pyrolysis, *Fuel*, 86, 1781-1788.
- Yang, L., S. Shen and H. Hu, 2011. Thermodynamic performance of a low temperature multi-effect distillation experimental unit with horizontal-tube falling film evaporation, *Desalination and Water Treatment*, 33, 202-208.
- Yousuf, A., 2012. Biodiesel from lignocellulosic biomass - Prospects and challenges, *Waste Management*, 32, 2061-2067.
- Zaheed, L. and R.J.J. Jachuck, 2004. Review of polymer compact heat exchangers, with special emphasis on a polymer film unit, *Appl. Therm. Eng.*, 24, 2323-2358.
- Zanzi, R., K. Sjöström and E. Björnbom, 2002. Rapid pyrolysis of agricultural residues at high temperature, *Biomass and Bioenergy*, 23, 357-366.

Zhao, D., J. Xue, S. Li, H. Sun and Q.-d. Zhang, 2011. Theoretical analyses of thermal and economical aspects of multi-effect distillation desalination dealing with high-salinity wastewater, *Desalination*, 273, 292-298.

Appendix: Data Record

Table A.1 Yields of biochar and bio-oil from lab scale slow pyrolysis

Material	Feedstock (g)	Biochar (g)	Yield of biochar (%)	Collected bio-oil (g)	Yield of bio-oil (%)
Pecan Shell	242.1	66.8	27.6	44	18
Pecan Prunings	250.7	87.7	35.0	33	13
Yard Waste	195.0	61.5	31.5	33	17
Cotton Gin Trash	252.3	106.1	42.1	28	11

Table A.2 Moisture content of biochars and feedstocks

Product	Sample + holder (g)	Wet sample (g)	Dry sample (g)	Moisture (%)
Pecan Shell	6.04	5.17	5.83	3.9
Pecan Prunings	2.87	1.95	2.79	4.3
Yard Waste	2.23	1.27	2.20	2.4
Cotton Gin Trash	3.49	2.83	3.39	3.3
Feedstock				
Pecan Shell	24.26	22.04	22.99	5.8
Pecan Prunings	23.47	21.02	22.27	5.7
Yard Waste	25.91	23.92	24.91	4.2
Cotton Gin Trash	14.60	12.92	13.81	6.1

Table A.3 Ash contents of biochars and feedstocks.

Products	Rep.	Crucible (g)	Sample + crucible (g)	Ash + crucible (g)	Ash content (%)
Pecan Shell	1	12.41	13.41	12.45	4.19
	2	12.43	13.37	12.47	4.27
Pecan Prunings	1	11.85	12.55	11.93	10.90
	2	13.32	14.34	13.43	10.62
Yard Waste	1	12.02	12.47	12.09	16.96
	2	17.79	18.41	17.92	21.90
Cotton Gin Trash	1	12.93	13.70	13.14	27.58
	2	18.06	19.31	18.49	34.54
Feedstock					
Pecan Shell	1	16.02	16.59	16.03	1.74
	2	17.19	17.74	17.19	1.08
Pecan Prunings	1	28.29	28.85	28.31	2.52
	2	15.55	16.03	15.56	2.87
Cotton Gin Trash	1	28.29	28.84	28.36	11.40
	2	15.55	16.05	15.61	13.41
Yard Waste	1	16.02	16.56	16.04	4.39
	2	17.19	17.69	17.21	5.02

Table A.4 Higher heating values (HHV) of biochars and feedstocks, measured by bomb calorimetry.

Sample	HHV (MJ/kg)	
Feedstocks		
Pecan shell	18.6	17.9
Cotton gin trash	17.6	16.0
Yard Waste	23.5	20.2
Pecan prunings	20.5	24.6
Biochars		
Pecan shell	31.7	29.7
Cotton gin trash	21.7	26.0
Pecan prunings	32.6	29.4
Yard waste	28.5	34.4

Table A.5 Analysis results for biochar-amended sandy loam soils after incubation. EC: electrical conductivity; SAR: sodium adsorption ratio; OM: organic matter.

BiocharTrt	Block	pH	EC	Mg	Ca	Na	SAR	OM	Nitrate-N	K	P	Zn	Mn	Fe	Cu	% Saturation
			dS/m	mg/kg				g/kg	mg/kg							
Control	1	7.40	0.582	0.46	1.87	3.16	2.93	0.53	1.05	23.4	6.21	0.85	3.28	2.89	1.38	27.04
Control	2	7.50	1.52	1.4	4.83	8.03	4.55	0.47	1.47	25.0	5.88	0.85	3.28	2.64	1.33	19.95
Control	3	7.40	2.26	2.61	8.58	14.25	6.02	0.53	10.8	28.3	5.69	0.87	4.17	2.56	1.08	21.97
Control	4	7.50	1.42	1.15	4.58	7.72	4.56	0.66	1.44	26.0	6.08	0.85	3.03	2.78	1.20	22.15
YardWaste	1	7.40	0.614	0.56	2.08	3.6	3.13	0.58	0.65	33.0	6.34	0.82	7.56	2.39	1.14	29.17
YardWaste	2	7.30	1.14	1.8	5.5	5.0	2.62	0.71	0.24	29.4	6.21	1.0	8.69	2.58	1.85	25.34
YardWaste	3	7.50	1.58	1.49	5.48	7.98	4.27	0.59	2.91	37.4	6.21	0.87	9.14	2.52	1.0	26.58
YardWaste	4	7.50	1.68	1.72	6.05	10.2	5.17	0.72	3.72	40.8	6.73	0.91	9.3	2.61	0.99	28.37
PecanSh	1	7.53	0.786	0.85	3.45	3.31	2.26	0.47	1.91	29.1	6.47	0.86	5.46	2.81	1.09	24.89
PecanSh	2	7.50	1.22	1.15	4.54	6.19	3.67	0.52	5.87	34.6	6.08	0.9	5.59	2.85	1.2	31.50
PecanSh	3	7.50	1.43	1.25	5.09	7.58	4.26	0.51	0.70	36.4	5.95	0.86	6.47	2.73	1.07	25.93
PecanSh	4	7.40	1.67	1.68	6.35	9.14	4.56	0.44	1.57	36.8	5.95	0.91	6.73	2.7	1.07	26.46

Table A.5, continued.

BiocharTrt	Block	pH	EC	Mg	Ca	Na	SAR	OM	Nitrate-N	K	P	Zn	Mn	Fe	Cu	% Saturation
			dS/m	mg/kg				g/kg	mg/kg							
CotTrash	1	7.32	4.41	8.28	24.8	9.48	2.33	1.42	0.70	204.0	23.3	1.02	10.0	2.68	1.03	27.81
CotTrash	2	7.42	8.08	18.6	53.2	18.6	3.10	0.93	1.05	476.0	25.97	1.05	12.71	2.14	0.85	32.15
CotTrash	3	7.40	8.11	18.6	55.9	19.4	3.18	1.18	0.73	379.0	24.53	1.08	11.65	2.27	0.74	26.90
CotTrash	4	7.50	7.86	19.7	64.4	20.5	3.16	1.11	0.71	386.0	25.61	1.15	11.96	2.35	1.08	28.43
PecanTree	1	7.50	0.837	0.89	3.73	3.51	2.31	0.47	1.18	32.5	8.33	1.05	7.57	2.52	0.78	28.07
PecanTree	2	7.40	2.44	3.18	10.4	11.5	4.41	0.62	1.66	48.4	7.13	1.12	8.95	2.58	1.05	29.48
PecanTree	3	7.40	2.24	2.8	9.46	11.3	4.56	0.45	1.21	42.0	6.34	1.11	8.37	2.73	1.14	26.83
PecanTree	4	7.30	2.47	3.38	11.8	11.5	4.17	0.49	6.94	48.4	6.6	1.2	8.61	2.61	1.02	26.85

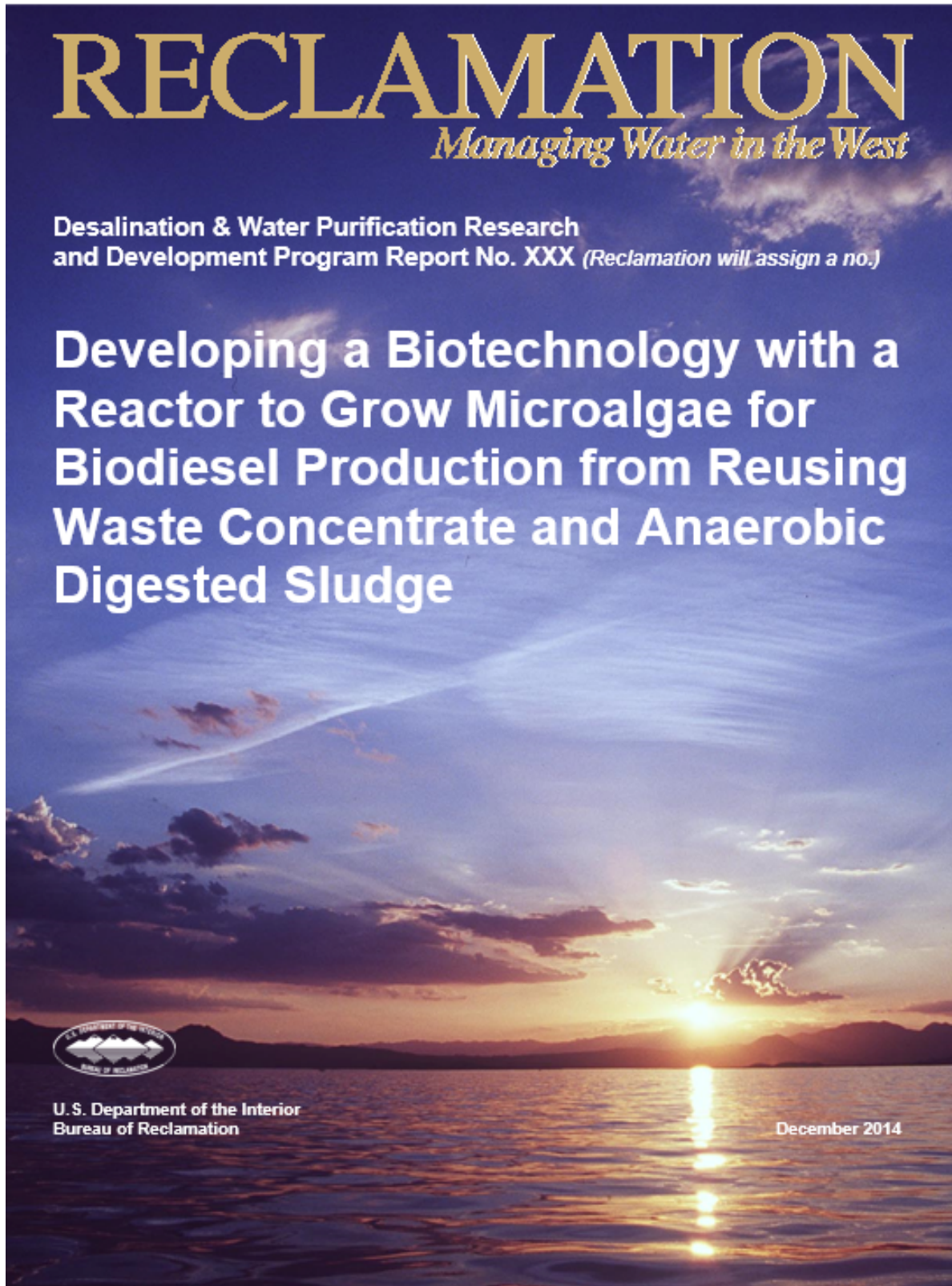
Table A.6 Analysis results for biochar-amended clay loam soils after incubation. EC: electrical conductivity; SAR: sodium adsorption ratio; OM: organic matter.

BiocharTrt	Block	pH	EC	Mg	Ca	Na	SAR	OM	Nitrate-N	K	P	Zn	Mn	Fe	Cu	% Saturation
			dS/m	mg/kg				g/kg	mg/kg							
Control	1	6.90	6.02	12.6	41.8	20.9	4.01	1.31	128.9	63.4	11.09	0.86	5.42	3.35	1.99	41.93
Control	2	6.90	6.86	13.8	45.2	25.1	4.62	1.17	92.2	55.6	11.8	0.87	4.26	3.50	1.49	44.90
Control	3	6.90	6.18	12.1	42.3	21.6	4.14	1.15	109.3	58.2	12.52	0.74	3.82	3.42	1.44	51.79
Control	4	6.90	8.36	16.8	59.3	26.2	4.25	1.11	215.4	63.9	13.4	1.05	4.55	3.26	4.35	45.82
YardWaste	1	7.00	8.61	17.0	59.7	29.8	4.81	1.26	283.9	82.8	12.09	5.36	8.03	3.06	1.43	54.05
YardWaste	2	6.80	10.8	24.6	85.9	43.9	5.91	1.32	345.6	89.1	12.67	0.78	7.67	2.77	1.32	43.11
YardWaste	3	6.88	14.4	30.7	114.0	59.1	6.95	1.47	585.3	98.2	12.52	0.85	8.68	2.55	1.69	46.90
YardWaste	4	6.90	14.2	26.3	120.0	45.3	5.30	1.28	650.3	95.9	12.82	0.75	8.49	2.47	1.48	53.49
PecanSh	1	7.10	5.3	9.56	32.6	19.8	4.31	1.14	41.8	54.6	12.24	0.82	6.53	3.67	1.41	44.07
PecanSh	2	7.10	7.35	15.0	50.7	25.2	4.40	1.19	110.2	73.3	13.7	0.90	7.19	3.35	1.44	39.47
PecanSh	3	7.00	8.21	16.4	54.3	31.0	5.21	1.25	149.6	71.0	12.67	0.93	6.52	3.51	1.77	41.83
PecanSh	4	6.90	9.03	20.8	70.4	37.6	5.57	1.22	250.0	80.2	12.09	1.14	7.61	3.87	1.73	42.29

Table A.6, continued.

BiocharTrt	Block	pH	EC	Mg	Ca	Na	SAR	OM	Nitrate-N	K	P	Zn	Mn	Fe	Cu	% Saturation
			dS/m	mg/kg				g/kg	mg/kg							
CotTrash	1	7.10	9.82	25.5	70.1	36.6	5.29	1.95	1.69	257.0	27.82	1.07	8.65	2.80	1.22	47.04
CotTrash	2	7.10	9.55	24.5	67.6	34.4	5.07	1.59	0.52	249.0	28.57	1.06	8.45	2.63	1.79	45.08
CotTrash	3	7.00	8.95	21.4	61.3	35.5	5.52	1.77	1.34	266.0	28.57	1.02	8.55	2.97	1.72	44.08
CotTrash	4	7.10	8.15	20.4	59.0	34.4	5.46	2.24	0.42	234.0	28.38	1.13	9.40	2.97	2.15	44.24
PecanTree	1	6.90	14.9	31.0	125.0	56.8	6.43	1.20	661.4	107.0	12.09	1.04	6.49	2.61	1.67	39.06
PecanTree	2	6.80	18.1	48.4	174.0	77.5	7.35	1.32	930.4	126.0	11.66	1.30	8.35	2.10	2.28	40.03
PecanTree	3	6.80	17.20	36.2	146.0	67.2	7.04	1.17	995.8	122.0	12.09	1.14	7.19	2.22	1.86	40.62
PecanTree	4	7.02	11.8	25.4	87.9	50.1	6.66	1.26	450.1	98.1	12.52	1.29	8.06	2.91	2.41	43.56

Developing a Biotechnology with a Reactor to Grow Microalgae for Biodiesel Production from Reusing Waste Concentrate and Anaerobic Digested Sludge



REPORT DOCUMENTATION PAGEForm Approved
OMB No. 0704-0188

The public reporting burden for this collection of information is estimated to average 1 hour per response, including the time for reviewing instructions, searching existing data sources, gathering and maintaining the data needed, and completing and reviewing the collection of information. Send comments regarding this burden estimate or any other aspect of this collection of information, including suggestions for reducing the burden, to Department of Defense, Washington Headquarters Services, Directorate for Information Operations and Reports (0704-0188), 1215 Jefferson Davis Highway, Suite 1204, Arlington, VA 22202-4302. Respondents should be aware that notwithstanding any other provision of law, no person shall be subject to any penalty for failing to comply with a collection of information if it does not display a currently valid OMB control number.

PLEASE DO NOT RETURN YOUR FORM TO THE ABOVE ADDRESS.

1. REPORT DATE (DD-MM-YYYY) (15-12-2014)	2. REPORT TYPE Proof of Concept Final Report	3. DATES COVERED (From - To) (01-02-2011)-(31-12-2013)
4. TITLE AND SUBTITLE Developing a Biotechnology with a Reactor to Grow Microalgae for Biodiesel Production from Reusing Waste Concentrate and Anaerobic Digested Sludge		5a. CONTRACT NUMBER R10AC80283
		5b. GRANT NUMBER
		5c. PROGRAM ELEMENT NUMBER
6. AUTHOR(S) Waddah Hussein, Jalal Rastegary, Abbas Ghassemi		5d. PROJECT NUMBER
		5e. TASK NUMBER
		5f. WORK UNIT NUMBER
7. PERFORMING ORGANIZATION NAME(S) AND ADDRESS(ES)		8. PERFORMING ORGANIZATION REPORT NUMBER
9. SPONSORING/MONITORING AGENCY NAME(S) AND ADDRESS(ES) IEE/WERC New Mexico State University P.O. Box 30001 Las Cruces, NM 88003		10. SPONSOR/MONITOR'S ACRONYM(S)
		11. SPONSOR/MONITOR'S REPORT NUMBER(S)
12. DISTRIBUTION/AVAILABILITY STATEMENT		
13. SUPPLEMENTARY NOTES		
14. ABSTRACT Desalination technologies have significant potential to alleviate global water shortages, but they also produce a highly saline byproduct, desalination concentrate, that must be disposed of properly to avoid adverse environmental impacts. One possible solution is additional treatment of the concentrate, but this increases desalination's costs and energy use; other current options for the disposal of the concentrate, including evaporation ponds and deep well injection, are not sustainable. To help resolve the problem of concentrate disposal and make inland desalination systems more sustainable and economically feasible, the objective of this research is to provide an alternative method for disposing of concentrate from inland desalination systems by using the concentrate as a nutrient for the production of microalgae, turning a substance that is typically a waste product into a potentially useful resource. Since this same approach could possibly be used to safely and productively dispose of certain other wastes, the use of supernatant anaerobic digested sludge (SADS) from wastewater treatment plants (WWTPs) as a nutrient for microalgae production was also investigated. The research hypothesis is that microalgae can effectively treat both the reject brine and the SADS, decreasing the financial cost and environmental effects of disposing of these substances. In this experiment, bioreactors were constructed to grow microalgae using concentrate from the desalination of inland brackish water at the Brackish Groundwater National Desalination Research Facility (BGNDRF) in Alamogordo, New Mexico. Additional experiments were conducted to evaluate SADS as a nutrient supplement. The SADS was provided by a wastewater treatment plant in Las Cruces, NM. The experiment included three microalgae species: <i>Dunaliella salina</i> , <i>Spirulina platensis</i> , and a third, unknown species of microalgae from the BGNDRF evaporation pond. These species, selected because of their ability to grow in highly saline environments, were grown in bioreactors that were filled with concentrate with different levels of salinity and directly exposed to sunlight, CO ₂ , and nutrient resources. To evaluate the growth of the microalgae species, both optical density measurements and dry weight measurements were used.		

15. SUBJECT TERMS					
16. SECURITY CLASSIFICATION OF:			17. LIMITATION OF ABSTRACT	18. NUMBER OF PAGES	19a. NAME OF RESPONSIBLE PERSON
a. REPORT	b. ABSTRACT	a. THIS PAGE			19b. TELEPHONE NUMBER <i>(Include area code)</i>

Standard Form 298 (Rev. 8/98)
 Prescribed by ANSI Std. Z39.18

**Desalination & Water Purification Research
and Development Program Report No. XXX**

Developing a Biotechnology with a Reactor to Grow Microalgae for Biodiesel Production from Reusing Waste Concentrate and Anaerobic Digested Sludge

Prepared for Reclamation Under Agreement No.

R10AC80283

By

Waddah Hussein, Jalal Rastegary, Abbas Ghassemi



**U.S. Department of the Interior
Bureau of Reclamation
Technical Service Center
Water and Environmental Services Division
Water Treatment Engineering Research Team
Denver, Colorado
December 2014**

MISSION STATEMENTS

The mission of the Department of the Interior is to protect and provide access to our Nation's natural and cultural heritage and honor our trust responsibilities to Indian tribes and our commitments to island communities.

The mission of the Bureau of Reclamation is to manage, develop, and protect water and related resources in an environmentally and economically sound manner in the interest of the American public.

Disclaimer

The views, analysis, recommendations, and conclusions in this report are those of the authors and do not represent official or unofficial policies or opinions of the United States Government, and the United States takes no position with regard to any findings, conclusions, or recommendations made. As such, mention of trade names or commercial products does not constitute their endorsement by the United States Government.

Acknowledgements

This thesis is an achievement that I accomplished with help from a group of people whom I respect and am proud to know in person. I first would like to thank my advisor, Dr. Abbas Ghassemi, for his guidance and support. I am grateful to him for making me a part of his research group and giving me the opportunity to pursue my passion for optics. I am honored to have been his student.

I would also like to thank the members of my thesis committee, Dr. Paul Andersen, Dr. Reza Foudazi, and Dr. Delia Valles-Rosales, for taking time out of their busy schedules to evaluate my thesis and provide valuable advice.

In addition, I want to take this opportunity to thank Dr. Jalal Rastegary, the program manager Jim Loya, Dr. Myint Maung, Roseann Thompson, Eahsan Shahriary, Patrick DeSimio, and Marzie Ghasempour for helping me during my thesis.

I would like to thank Nasser Khazeni for being my mentor and providing his support, especially in statistical analysis.

Certainly, I would like especially to thank the Bureau of Reclamation for their support under the contract R10AC80283.

Contents

	<i>Page</i>
Glossary	iv
Acronyms and Abbreviations	iv
Chemical Symbols	v
Executive Summary	1
Chapter 1: INTRODUCTION.....	2
1.1 Water Scarcity	2
1.2 Desalination Technologies	5
1.3 Comparison	7
1.4 EDR and RO Comparison	7
1.5 Wastewater Treatment Plant	7
1.6 Research Issue and Solution.....	8
1.7 Hypothesis.....	9
1.8 Research Objective.....	9
1.9 Approach	10
Conclusions.....	10
Recommendations.....	11
Chapter 2: LITERATURE REVIEW.....	12
2.1 Concentrate Disposal Methods.....	12
2.2 Algae Species Selection	13
2.3 Algae-based Concentrate Treatment	14
2.4 Carbon Dioxide Emissions (Global Warming).....	15
Chapter 3: MATERIALS AND METHODS.....	18
3.1 Analytical Method and Sampling (Experiment Design)	18
3.2 Contents in Reactors.....	19
3.3 Statistical Analysis	20
Chapter 4: RESULT AND DISCUSSION	21
4.1 Introduction	21
4.2 Batch Reactors (<i>Dunaliella salina</i> and <i>Spirulina platensis</i>)	21
4.3 Specific Growth Rate	26
4.4 The Comparison of Microalgae Biomass between SADS – BBM, and SADS – F/2	27
4.5 Comparison of Microalgae Biomass between Study and Literature.....	27
4.6 The Microalgae Strains from the Desalination Evaporation Pond at the Brackish Groundwater National Desalination Research Facility (BGNDRF)..	28
4.7 Results	28
4.8 Mass of Conductivity Reduction.....	29
Chapter 5 – CONCLUSIONS.....	31
Chapter 6 - FUTURE RECOMMENDATIONS	32
References.....	33
Tables.....	43
Chapter 1	43
Chapter 2	46
Chapter 3	47

Chapter 4	48
Figures.....	54
Chapter 1	54
Chapter 4	55
Chapter 7 – APPENDIX.....	65
Appendix A	65
<i>Units of Measure</i>	65
Appendix B	66
<i>Elements/Ions in Anaerobic Digested Sludge (EPA, 2006)</i>	66
Appendix C	67
<i>BBM Recipe</i>	67
Appendix D	68
<i>F/2 Recipe</i>	68
Appendix E.....	68
<i>Data Record</i>	68

Glossary

Acronyms and Abbreviations

BBM	Bold's Basal Medium
BGNDRF	Brackish Groundwater National Desalination Research Facility
CFTRI	Prescribed medium
CWA	Clean Water Act
DC	Direct current
dH ₂ O	Desalinated Water
ED	Electrodialysis
EDR	Electrodialysis Reversal
EPA	U.S. Environmental Protection Agency
GHG	Greenhouse gas
GMO	Genetically modified organisms
IGD	Imperial gallon(s) per day
IPPC	The International Panel on Climate Change
J/1	Modified Johnson medium
MED	Multi-effect distillation
MF	Microfiltration
Mgal	Millions of gallons
MSF	Multistage flash evaporation
MVC	Mechanical vapor compressor
MWCO	Molecular weight cutoff
NF	Nanofiltration
NM	New Mexico State
NMSU	New Mexico State University
NPDES	National Pollutant Discharge Elimination System
RO	Reverse Osmosis
SADS	Supernatant from Anaerobic Digested Sludge
TDS	Total dissolved solids
TVC	Thermo vapor compressor
UF	Ultra filtration
U.S	United States
US \$	United States Dollar(s)
VC	Vapor compression
WHO	World Health Organization
WWTP	Wastewater treatment plant

Chemical Symbols

CO ₂	Carbon Dioxide
CO	Carbon Monoxide
HCO ₃ ⁻	Bicarbonate
CO ₃ ²⁻	Carbonate
BaCl	Barium Chloride
NaH ₂ PO ₄	Monosodium Phosphate
NaCl	Sodium Chloride
NaNO ₃	Sodium Nitrate
Na ₂ SiO ₃	Sodium Silicate
NO ₃	Nitrate
N ₂ O	Nitrous Oxide
H ₂ O	Water
H ₂	Hydrogen
HPO ₄ ²⁻	Phosphoric Acid
O ₂	Oxygen
NO ₂	Nitrogen Dioxide
CH ₄	Methane
NO _x	Nitrogen Oxides
SO _x	Sulfur Dioxide
Mg ²⁺	Magnesium
Ca ²⁺	Calcium
N	Nitrogen
SO ₄ ²⁻	Sulfate Ion
NaNO ₃	Sodium Nitrate

Executive Summary

Desalination technologies have significant potential to alleviate global water shortages, but they also produce a highly saline byproduct, desalination concentrate, which must be disposed of properly to avoid adverse environmental impacts. One possible solution is additional treatment of the concentrate, but this increases desalination's costs and energy use; other current options for the disposal of the concentrate, including evaporation ponds and deep well injection, are not sustainable.

To help resolve the problem of concentrate disposal and make inland desalination systems more sustainable and economically feasible, the objective of this research is to provide an alternative method for disposing of concentrate from inland desalination systems by using the concentrate as a nutrient for the production of microalgae, turning a substance that is typically a waste product into a potentially useful resource. Since this same approach could possibly be used to safely and productively dispose of certain other wastes, the use of supernatant anaerobic digested sludge (SADS) from wastewater treatment plants (WWTPs) as a nutrient for microalgae production was also investigated. The research hypothesis is that microalgae can effectively treat both the reject brine and the SADS, decreasing the financial cost and environmental effects of disposing of these substances.

In this experiment, bioreactors were constructed to grow microalgae using concentrate from the desalination of inland brackish water at the Brackish Groundwater National Desalination Research Facility (BGNDRF) in Alamogordo, New Mexico. Additional experiments were conducted to evaluate SADS as a nutrient supplement. The SADS was provided by a wastewater treatment plant in Las Cruces, NM.

The experiment included three microalgae species: *Dunaliella salina*, *Spirulina platensis*, and a third, unknown species of microalgae from the BGNDRF evaporation pond. These species, selected because of their ability to grow in highly saline environments, were grown in bioreactors that were filled with concentrate with different levels of salinity and directly exposed to sunlight, CO₂, and nutrient resources.

To evaluate the growth of the microalgae species, both optical density measurements and dry weight measurements were used.

Chapter 1: INTRODUCTION

1.1 Water Scarcity

According to the U.S. Census Bureau (U.S. Census, 2011), the world population reached seven billion on March 12, 2012, and is expected to reach 8 billion in 2026. By 2042, the global population is expected to reach 9 billion (EPA, 2012). With such an extraordinary rise in population, the demand for fresh water will continue to increase over the subsequent decades: in the last century, water withdrawals increased six fold, while the global population only increased by three fold (United Nations Population Fund, 2003) (EPA, 2012). The water scarcity resulting from population growth is exacerbated by the facts that water resources are unevenly distributed on the earth's surface and only a small percentage of fresh water is readily accessible for human use as fresh surface water. Although the total volume of water on earth is approximately 1.4 billion m³, only about 2.5 percent of it is fresh water (about 35 million m³) (UNESCO, 1999), and most of this freshwater is either underground or locked in glaciers. Surface fresh water, easily usable by humans, constitutes only 0.01 percent of the total water on earth (Gunawansa and Bhullar, 2013). In terms of water distribution, Canada has fully a tenth of the global surface fresh water (Kalogirou, 2005), while Brazil, China, Russia, the U.S., Canada, India, Indonesia, Colombia, and the Democratic Republic of Congo collectively possess 60 percent of the available fresh water in the globe (World Business Council for Sustainable Development, 2005). In sum, fresh water is already scarce throughout much of the world, and it is expected that the global water consumption will double in the next 20 years. Therefore, finding a new source of fresh water is essential.

President John F. Kennedy, during a speech dedicated to the first seawater desalination plant in the U.S., said:

“No water resources program is of greater long-range importance than our efforts to convert water from the world’s greatest and cheapest natural resources – our oceans – into water fit for our homes and industry. Such a break-through would end bitter struggles between neighbors, states and nations.”

Today, more than 50 years later, this statement is still true.

In 2005, the average daily water consumption in the U.S. was about 410,000 million gallons, of which 328,000 million gallons per day (80%) were withdrawn from surface water and the remaining 20 percent were from ground water (Barber, 2009). As demonstrated by Figure 1.1, the main uses of water include agriculture, industrial use, and domestic use. According to the United States Geological Survey (USGS, 2009), the total withdrawal of fresh water for

agricultural applications in the year 2005 was estimated to be 128,000 million gallons per day, while the industrial sector had a share of 228,600 million gallons per day (with thermoelectric power withdrawals of 210,000 million gallons per day) and the water withdrawal for domestic applications was estimated to be 25,600 million gallons per day (USGS, 2009). As can be seen in Figure 1.1, as the income of countries increases, the use of water for industrial purposes increases, rising from 10 percent in low- and middle-income countries to 59 percent in high-income countries (World Business Council for Sustainable Development, 2005).

Water security is a major feature of national security due to its direct impact on national independence. With the world population's current growth rate and the expansion of the global economy, it is expected that, by 2025, 60 percent of people who live in arid countries will have limited access to fresh water (Alameddine and El-Fadel, 2007). It is also anticipated that by 2025, approximately 90 percent of the fresh water now available worldwide will have been consumed and rendered unusable (Pasta et al., 2012), leading to a major portion of the world's population (about 75 percent) facing water shortages in 2050 (UNESCO, 2003). Currently, almost 1.8 million people – most of them children – die annually due to water-borne diseases (World Health Organization, 2004). Such conditions are compelling motivations to find new water resources, and desalination – a process which removes salts from salty water to produce fresh water – could provide such a resource.

Fresh water is differentiated from various forms of salty water by its levels of total dissolved solids (TDS), identified by the World Health Organization (WHO) as the measure of all organic and inorganic substances that are dissolved in water; usually, the main constituents are calcium, chloride, sodium, magnesium, and sulfates (WHO, 2008). According to the Water Quality Association (WQA), water is classified into the following categories, based on the level of TDS (WQA, 1999).

In the past several years, the western United States has suffered, and continues to suffer, from moderate to severe drought. This, coupled with fast economic growth in the Southwest which has led to increased demand for water (Brady et al., 2009), has stressed the existing water resources in the region. Throughout most of the western U.S., the water level in rivers has decreased and the water levels in reservoirs have been reduced. To help meet demand, these scarce water resources could be augmented by pumping and desalting brackish groundwater that has total dissolved solids exceeding 1000 mg per liter. However, the potential for desalination is limited in inland areas due to economic factors and the challenges associated with disposing of concentrate, a highly saline waste byproduct of desalination.

Nevertheless, desalination is a promising approach for meeting water needs, and it has a long and proven history in the United States. The first seawater desalination plant in the U.S. was built in 1961 in Freeport, Texas (Arroyo et al., 2012). Currently, there are more than 260 desalination plants in the United States, and more than 95 percent of them are considered inland, brackish groundwater facilities (Mickley, 2009) as opposed to seawater desalination facilities, which

are located in coastal areas. For seawater desalination facilities, the concentrate (also called reject brine) can affordably be returned to the ocean, where it is diluted. However, the disposal of concentrate is a major problem for inland water desalination plants.

When water is desalinated, only a certain percentage of the original water volume is turned into fresh water. This fact is reflected in the water recovery rate, which is the ratio of the volume of desalinated water to the initial water volume used in the desalination unit as feedwater. The recovery rate is an important subject in the desalination industry, which has two primary subsectors: inland brackish water desalination, and seawater desalination. There are two main differences between brackish and seawater desalination systems: recovery rates and the handling of reject brine.

Inland brackish water desalination plants face finite feedwater sources and have high recovery rates of 50 percent to 75 percent; in some cases the recovery rate can reach 94 percent. As a result of this high recovery rate, the reject brine is highly concentrated, which makes concentrate disposal problematic (the high concentration is also the main reason for fouling and scaling of the membrane). To dispose of concentrate, inland desalination plants can employ several different methods, including evaporation ponds, deep well injection, and surface water discharge – among others – but all of these methods are costly and environmentally problematic.

In contrast, seawater desalination plants generally have a lower recovery rate of 40 percent to 60 percent, which is acceptable because the ocean provides a practically unlimited supply of feed water. The lower recovery rate is also prudent because the ocean has high levels of TDS, which would cause fouling at higher recovery rates. Generally, concentrate from seawater desalination plants is returned directly back to the sea, which is a cost-effective but environmentally problematic approach.

For desalination systems themselves, there are three main classes of technology (Younos and Tulou, 2005):

- Pressure-driven (membrane) processes;
- Heat- or temperature-driven processes; and
- Chemical processes.

Pressure-driven and heat-driven processes are used mainly in industrial water purification. Pressure-driven technology is less energy-intensive than temperature driven technology, but this method also delivers a lower permeate quality. The cost of desalination is subject to a plant's location and the technologies used, but, as a result of millions of dollars of research (Yuhua and Daniles, 2006), the average cost of desalination has decreased from US\$20 per thousand gallons in 1980 to under US\$4 per thousand gallons in 2005. The research on this subject is ongoing, and it is predicted that in the future the cost of desalination will decrease even more.

The water which is desalinated to produce fresh water is known as feedwater. As indicated in Figure 1.2, seawater is the source for about 60 percent of the total

feedwater worldwide, and brackish water, the second largest source in the world, has a share of 21.24 percent.

1.2 Desalination Technologies

As mentioned earlier, the two most commonly-used desalination methods are:

1. Pressure-driven processes (membrane desalination); and
2. Heat- or temperature-driven processes.

Pressure-driven processes (membrane processes) include the technologies of reverse osmosis (RO), microfiltration (MF), ultrafiltration (UF), and nanofiltration (NF). Electrodialysis (ED) and electrodialysis reversal (EDR) can also be classified as pressure-driven processes. Each of these technologies is described below.

Reverse Osmosis (RO): RO is an example of a pressure-driven membrane process, where high pressure is used to overcome the osmotic pressure of the membrane. The high pressure forces the solid particles present in the feedwater into the membrane, where the solid particles are retained; the feedwater, however, passes through the membranes, leaving most of its solid particles behind and becoming fresh water. Over time, the membrane will be contaminated by biological fouling, causing scaling to occur. Chemical treatments can be used to remove scaling, but if chemical clearing is not effective, then the RO membrane will require replacement (Carter, 2009). RO membranes have a total recovery rate of 70-85 percent (Greenlee et al., 2009). RO is the leading technology for treating both seawater and brackish water; there are more than 16,000 desalination plants worldwide, and about half of them are RO plants (Kurz et al., 2011). In the United States, around 70 percent of desalination plants use this technology. About 7 percent of the plants using the RO method use seawater as the feedwater source (Carter, 2013; Greenlee et al., 2009; Wetterau, 2011).

Microfiltration (MF), ultrafiltration (UF), and nanofiltration (NF) are systems distinguished by the pore size of their filters. NF membranes remove bacteria from the water using the same method as RO. The pore size of NF membranes is 0.001 μm . In UF membranes, the pore size is 10 times larger than NF (typically between 0.01-0.05 μm), and the UF membranes are capable of filtering a higher molecular weight than the NF membranes. The MF filter is used to remove larger particles, and has a comparatively large pore size of 0.1-0.2 μm . MF filters are generally used in drinking water applications (Wang et al., 2008). For MF, molecular weight cutoff (MWCO) has become the central measurement instead of the normal measurement of pore size (EPA, 2010), on account of some larger organic macromolecules that can be retained in the membranes. In addition to their use in industrial desalination, the aforementioned filters are used in a wide range of industries such as pharmaceuticals, food, and metal processes, among others.

Electrodialysis (ED) and electrodialysis reversal (EDR): ED/EDR technologies are electrochemical methods that function on the principle of the movement of an electrolyte that is subjected to an electrical field. The ED/EDR

base unit consists of a number of cells, and each cell pair contains ion- and cation-permeable membranes and a spacer. The spacer helps direct the flow of the water as the feed water passes simultaneously through all the cells. Under the influence of direct current (DC) electricity, the electrodes will split the feed into positive and negative ions. The positive ions will leave the feedwater by travelling toward the cathode through a cation exchange membrane, while the negative ions move in the opposite direction, leaving the feed stream by travelling toward the anode through an anion exchange membrane. After leaving the feed water stream (which, at this point, is desalinated), the positive and negative ions from the feedwater are trapped by oppositely charged membranes, producing the concentrate stream that contains the salts and other dissolved minerals (U.S. Department of the Interior Bureau of Reclamation, 2010; Greenlee et al., 2009). To achieve a high recovery rate and provide a self-cleaning process with less fouling and scaling of the membrane, the polarities of the electrodes are periodically reversed in EDR. With the EDR method, the recovery rate can go up to 94 percent.

Temperature-driven processes include multistage flash evaporation (MSF), multiple-effect distillation (MED), and vapor compression (VC). Each of these processes is described below.

Multiple-effect distillation: MED is the oldest desalination process used, and it consists of multiple stages or “effects.” Each of these stages makes use of a series of tubes heated by internal steam. As the first step of the MED process, the salty feed water is dispersed over the tubes, and as the water reaches its boiling point, the vapor generated from the heat in the first tube transfers heat to the second tube. At this point, the process repeats itself. Distillate – the desalinated water – and brine are collected in each stage. MED is energy-efficient since it uses latent heat to boil the feedwater without any additional supply of heat after the first tube. However, MED has its problems – notably, scaling – and therefore, after MSF technology was released, the use of MED decreased significantly.

Multistage Flash Evaporation: In 1957, the first large MSF units were installed and built in the Middle East by Westinghouse Company. This system consisted of four flash stages with two units, which produced a total of 1 million imperial gallons per day (IGD) of fresh water from seawater (Al-Modaf and Al-Wazzan, 2001). MSF units, in general, are composed of three sections: heat rejection, heat recovery, and heat input (brine heater). The first two sections comprise a plant. These stages are connected to each other, and each stage consists of a heat exchanger and a condensate collector. The input feed will start boiling and evaporating by keeping the pressure in the first flash chamber lower than the corresponding saturation pressure. This will cause the water vapors to cool down and condense to form the distillate, and the latent heat generated from the condensation is used to heat the new seawater in the tubes. Finally, the distillate produced in each stage is collected and then pumped into a storage tank (Khawaji et al., 2008).

Vapor Compression: In this type of desalination technology, mechanical energy replaces thermal energy. VC operates by reducing the vapor pressure in

order to reduce the boiling point temperature (EPA, 2005). Two methods are used to compress vapor pressure: an ejector system, thermal vapor compression (TVC), which is driven by an external source of pressure, and mechanical vapor compression (MVC). TVC units are larger than the MVC units, yet both of these units have small capacities compared to MEDs or MSDs.

A problem with all desalination processes is the difficulty disposing of reject brine. This is one of the key factors that must be considered before a desalination plant is installed. This issue is particularly important for inland desalination plants. When a method for disposing concentrate has been selected, the two main concerns are the economic costs and the environmental effects (Mickley, 2009) that result from the highly saline nature of the concentrate; some studies indicate that the salinity of reject brine (concentrate) can reach 85,000 mg/L (Abdul-Wahab and Al-Weshahi, 2009), which is double the salinity of seawater.

1.3 Comparison

As shown in Table 1.2, the cost of electro dialysis desalination techniques is lower than the cost of the other technologies. Multiple effect distillation (MED) and multi-stage flash desalination (MSF) have a higher cost than RO processes and produce the same efficiency.

1.4 EDR and RO Comparison

As shown in Table 1.3, in which RO and EDR are compared, EDR has a higher efficiency and lower cost, while RO has the upper hand when the feed has a higher conductivity.

1.5 Wastewater Treatment Plant

The purpose of treating wastewater is to avoid pollution problems in receiving waters. In particular, the main water quality concern in the wastewater treatment plants is nitrogen (Richard et al., 2009). To minimize pollution problems, the first objective of wastewater treatment is to reduce the volume of the waste by removing its liquid portion, producing a sludge. The second objective is to decompose the highly putrescible organic matter into relatively stable or inert organic and inorganic compounds. When these two objectives are achieved, an anaerobic digested sludge is produced. The characteristics of such sludge are shown in Appendix B.

Within wastewater treatment plants, there are three fundamental levels of treatment:

1. Primary treatment, in which water is piped into large tanks and allowed to settle to remove particulate solids. This level is sometimes referred to as mechanical treatment;
2. Secondary (biological) treatment, in which microorganisms are used to remove more contaminating solids. In the absence of oxygen, the microorganisms consume the organic matter as food and convert it to carbon dioxide, methane, water, and energy for their own growth and reproduction. This step removes the dissolved organic matter that escapes primary treatment. The resulting product is called anaerobic digested sludge. The process itself is sometimes called biological treatment; and
3. Tertiary treatment, which is simply additional treatment beyond secondary treatment. This step can remove more than 99 percent of all the impurities from sewage, producing an effluent of almost drinking-water quality through disinfection, typically with chlorine.

1.6 Research Issue and Solution

The main difference between seawater and brackish water is the amount of TDS each contains, as can be seen in Table 1.1. Desalination technologies have significantly increased worldwide access to large quantities of drinkable water by converting non-potable saltwater into fresh water. Most of the seawater desalination units dispose of the reject brine back into the ocean, as this approach is less expensive; however, this procedure is very harmful to the environment because the high salt concentration, high temperature, and other chemical elements such as anti-scaling additives affect the aquatic environment.

The disposal methods for concentrate from inland water desalination plants are not very efficient due to their high cost and the harm they cause to the environment. After the dissolved salt is removed from saltwater to make freshwater, the salt is left in a concentrate stream (also called a reject brine) which has a very high level of total dissolved salt. Despite the problem mentioned above, approximately half of the concentrate streams produced from desalination plants in the United States are disposed of by the following standard disposal methods: discharge to surface water or sewers, containment in deep wells, or disposal in evaporation ponds and land applications (Mickley, 2009).

From an economic standpoint, disposing of the concentrate can be very expensive, and can vary from 5 percent to 30 percent of the total cost of desalination (Hordagui, 1997; Mohamed et al., 2005). The desalination industry and its customers are affected by the significant cost associated with disposing of the concentrate; therefore, reducing the costs is one of the main concerns in the industrial desalination sector.

An affordable and sustainable method for disposing of the concentrate could preserve the environment and reduce the cost of potable water by reducing the financial burden on the industrial desalination plants. This present study showed that microalgae can be used to treat the concentrate from desalination

plants by using the dissolved carbon and nutrients in the waste stream as media for growth, eliminating the salts by metabolizing them. The microalgae species can also produce biofuels and other useful products while they treat the waste concentrate.

1.7 Hypothesis

The hypothesis of this research is that concentrate can be used as a growth medium for algae because it contains nutrients and minerals that can be used by algae; Table 1.4 shows some of the results from an analysis of the four groundwater wells from the Brackish Groundwater National Desalination Research Facility, highlighting the elements that algae can use as nutrients.

In addition to these elements, the groundwater wells at BGNDRF also contained other elements such as dissolved oxygen chloride, bicarbonate silica, bromide, barium, iron, silica, organic carbon, selenium, copper, chloride, and fluoride.

The elements listed in Table 1.5 and Appendix B can be consumed by algae, providing a possible path for using the concentrate as a growth medium for algae and reducing the environmental impacts of the reject brine, potentially making this an affordable and sustainable method. This approach could also be combined with another waste stream: supernatant anaerobic digested sludge (SADS) from wastewater treatment plants (WWTP). This stream contains phosphorus and nitrogen, critical elements for algae growth (Pankaj and Awasthi, 2013). By utilizing these two waste streams (SADS and concentrate) it should be possible to produce a useful microalgae.

The bicarbonate identified in the groundwater wells at BGNDRF is an inorganic carbon source, and can improve the growth of algae cultures in carbon storage compared to CO₂ (Gardner et al., 2013). Concentrate from brackish groundwater desalination dissolves more HCO₃⁻ than that from seawater desalination. *Spirulina* grows in high CO₃²⁻ and HCO₃⁻ water (Richmond, 1986). CO₃²⁻, HCO₃⁻ and alkaline-rich microalgae consume dissolved inorganic carbon as a primary carbon source and sulfate as a macronutrient. Desalination concentrate from brackish groundwater can be treated by microalgae which consume bicarbonate and sulfate. *Dunaliella* species are native to salt water (Borowitzka, 2009) and can tolerate a wide pH range (Gimmler et al., 1989), making them one of the most environmentally tolerant eukaryotic organisms recognized, capable of surviving in salinities ranging from seawater (3% NaCl) to NaCl saturation (31% NaCl) (Ginzburg, 1989).

1.8 Research Objective

As part of ongoing water research on treatment of desalination concentrate at New Mexico State University, this study was conducted to:

1. Determine the feasibility of integrated algae cultivation (*Dunaliella salina*, *Spirulina platensis*, and the strain from the BGNDRF evaporation pond) by using desalination concentrate as a growth medium and SADS as nutrients; and
2. Determine the feasibility of reducing the salinity level of concentrate by using it as a medium for microalgae production.

1.9 Approach

The experimental evaluation of the research objective was performed by varying the level of conductivity in the bioreactors, using the native non-GMO microalgae *Dunaliella salina*, *Spirulina platensis*, an unknown species of microalgae strain acquired from the BGNDRF evaporation pond, SADS from the wastewater treatment plant, and natural concentrate from the Brackish Groundwater National Desalination Research Facility in Alamogordo, NM. During each experiment, measurements were taken for dry weight, optical density, temperature, conductivity, and pH, and algae samples were collected and analyzed.

Conclusions

Based on the experiments conducted in this study, the following conclusions can be made:

- Due to microorganisms growing with microalgae, the maximum dry weights of *D. salina* and *S. platensis* grown in desalination concentrate and supplied with SADS (1.36–1.49 g/L) are more than the dry weights of these same species when supplied with BBM and F/2, due to the manner in which the microorganism promotes microalgae growth. The maximum dry weight concentrations of *D. salina* and *S. platensis* grown in desalination concentrate and supplied with SADS are comparable to those in the literature.
- This study demonstrates the feasibility of using concentrate as a growth medium using SADS as a nutrient to grow algae culture.
- A combination of lower conductivity in the medium (25,442 and 25,100 $\mu\text{S}/\text{cm}$) and the use of SADS enhanced the growth of *D. salina* and *S. platensis*.
- The amount of the conductivity reduction was significant in BGNDRF species strains in 110 days.

These results suggest that using microalgae for reducing the conductivity of desalination concentrate and SADS by using the concentrate as a growth medium and SADS as an additional source of nutrients is better than using traditional methods for disposing of the concentrate from the desalination units, which have high costs and adverse environmental effects. High TDS levels, however, limited the ability of specific algae species to grow in the concentrate and reduce its conductivity.

The results also suggested that the BGNDRF strain can be used for concentrate management at salinity levels below 35,000 $\mu\text{S}/\text{cm}$. The BGNDRF species grew well at these levels, and since SADS is known to contain elements and ions that algae consume in their growth process – namely, ammonia nitrogen, sodium, calcium, magnesium, and potassium – it can be deduced that the BGNDRF species consumed some of these elements and ions in order to grow, reducing the overall salinity of the concentrate. The extent of this reduction could be explored in future research.

Recommendations

Recommendations for future research are listed below:

- Experiments can be conducted at different TDS levels to establish the optimal growth rate and can be performed on a large scale.
- Different species of microalgae can be cultured with the reject concentrate to study their growths and the conductivity reductions.
- The ion and element content of the growth media could be determined before and after algae growth to identify the specific ions and elements that the algae species remove.

Chapter 2: LITERATURE REVIEW

This chapter offers a description of the seven typical disposal methods for concentrate and provides details on these methods. This topic is followed by a discussion of algae species selection, and then algae-based concentrate treatment, energy security, and the potential for biofuel production from microalgae. The chapter concludes with a broad outline on carbon dioxide emissions.

2.1 Concentrate Disposal Methods

The list below shows the different methods used by desalination plants for the disposal of reject brine, starting with the most common. The information is based on a survey conducted by Michael C. Mickley that explored the concentrate disposal methods used by desalination plants that have more than 300 membranes (Mickley, 2009) and which treat at least 25,000 gallons of water per day (GPD). As reported in Mickley's research, the leading methods for concentrate disposal are:

- Surface water discharge,
- Discharge to sewer,
- Land application,
- Deep well injection,
- Evaporation ponds,
- Spray irrigation, and
- Zero liquid discharge.

Each of these methods is discussed below.

Surface Water Discharge: In this method, concentrate is discharged into surface water such as oceans or lakes. Since 1977, as a result of the Clean Water Act (CWA) passed in 1972, desalination plants have had to obtain a permit from the National Pollutant Discharge Elimination System (NPDES) to dispose of the concentrate in any surface water. The administrator of the EPA may also issue a permit to discharge. The concentrate is permitted to contain a medium or high level of TDS, depending on the technology used by the plants (Doremus and Tarlock, 2013).

Discharge to Sewer: In this method, concentrate is discharged into sewer systems. To make sure the disposed concentrate meets wastewater regulations designed to prevent adverse effects to the sewer system, this method also requires a permit issued under the NPDES (Mickley, 2006).

Land Application: This method is the most efficient option in locations where the climate is dry and sunny and where large plots of land are available at low cost. This method is usually used for small desalination plants (Mickley, 2009).

Deep Well Injection: This method consists of injecting wastewater 1000 to 8000 feet into the earth through a deep well. Generally, only large plants use this disposal method. This method may be considered storage instead of disposal, since the wastewater stays in the wells and does not disperse. Due to increase

concerns over the contamination of 300,000 injection wells (Mickley, 2006), the United States Congress added regulations for underground injection control to the CWA in 1979.

Evaporation Ponds: This method follows the same basic approach used to produce salt from seawater, and it works by pumping concentrate into shallow, artificial ponds, where the water evaporates and leaves the solids behind. These residual solids can then be dumped into landfills or sold if they are considered a valuable substance. This disposal method is usually used by small-sized plants (< 1 million gallons) in the southwestern United States, where evaporation ponds are the most suitable method for disposing of concentrate as evaporation rates are high in the dry, sunny climate, and large plots of land are available at low cost. The NPDSE currently does not require a permit for disposal of concentrate using evaporation ponds (Mickley, 2006).

Spray Irrigation: This method is similar to the sprinklers commonly used to water lawns, gardens, and golf courses. As with evaporation ponds, this process requires a relatively dry, sunny climate and available land, and is usually used for small desalination plants with low concentrate flow rates. For spray irrigation, the concentrate must be pre-treated or diluted to reduce the salinity of the wastewater; this method requires a permit from NPDSE (Mickley, 2006).

Zero Liquid Discharge: This method works by recycling the concentrate for different purposes within the desalination plant and reducing the amount of waste water. At the end of this process, the concentrate is reduced to a sludge-like material or dry salt (zero liquid), which can be disposed of as a solid. This is the most expensive method for disposing of the concentrate – because of its high energy demands, it can encompass more than 60 percent of a plant’s capital cost. Consequently, this method is usually followed only when no other disposal options are feasible (Mickley, 2006).

Table 2.1 indicates the percentages at which the five conventional concentrate disposal methods are used for municipal membrane desalination plants in the U.S. Such plants account for 98 percent of disposal cases in the U.S.

2.2 Algae Species Selection

The microalgae strain from the desalination evaporation pond at BNGDRF and two other species of halophytic microalgae, *Spirulina platensis* and *Dunaliella salina*, were selected for this study.

Spirulina platensis is a photosynthesizing cyanophyte (blue-green algae) that has the shape of a spiral coil and the ability to grow energetically in sturdy sunlight under hot temperatures and highly alkaline conditions (Richmond, 1986). *Spirulina* prospers in alkaline lakes where it is difficult or impossible for other organisms to live (Habib and Parvin, 2008; Kebede and Ahlgren, 1996), and it also can grow in brackish water and in high bicarbonate concentrations (Mallick, 2002). *Spirulina* can consume dissolved carbon dioxide in a water medium as a primary substrate for its growth (Habib and Parvin, 2008). For many decades, *Spirulina* has been used as a food source worldwide because it contains several

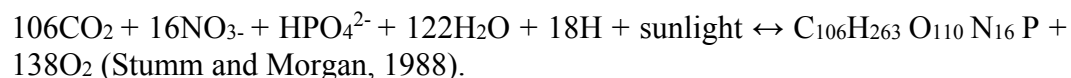
nutrients such as proteins, carbohydrates, minerals, different vitamins, and γ -linoleic acid (Ramadan et al., 1996; Teimouri, 2013). The oil content in *Spirulina platensis* ranges from 6-13 percent of algae dry weight (Chaiklahan et al., 2008).

Dunaliella salina is a unicellular green microalgae that is capable of prospering in high-salinity water (Fisher et al., 1997) and in strong shifts in salinity due to its intracellular osmotic metabolites (Ben-Amotz and Avron, 1973; Mishra et al., 2008; Chen and Jiang, 2009). The size of *Dunaliella salina* ranges between 5-25 μm in length and 3-13 μm in width. This species contains β -carotene in a range of 10-14 percent of algae dry weight, and is therefore often used in natural foods. The total lipid content in *Dunaliella salina* is in the range from 3.8 to 4.4 percent in terms of dry weight (Abd El-Baky et al., 2004; Weldy et al., 2007). In open lakes, microalgae growth cycles are normally limited by the availability of nutrients in the water medium. In commercial cultivation, the growth and carotenogenesis media comprise one-third of the total production cost of *Dunaliella salina* (Santos et al., 2001). If *D. salina* can be cultured from a cost-free growth medium and a cost-free nutrient, this would avoid not only about one-third of the total cost but also the CO₂ emissions from the fossil fuel-based manufacturing of conventional growth media and nutrients.

Spirulina and *Dunaliella* have been successfully cultured in a scale larger than 0.1 ha (Sheehan et al., 1998). Most of the commercial production of microalgae is from open ponds.

2.3 Algae-based Concentrate Treatment

Microalgae require water, light, CO₂, appropriate pH, suitable salinity, macronutrients (nitrates and phosphates), vitamins, and trace elements for their growth (Chisti, 2007; Brennan and Owende, 2010). By using photosynthesis, microalgae convert light into new algae biomass as the following equation indicates:



By rearranging the above equation, the microalgae component can be expressed as:



The ratio of carbon-to-nitrogen-to-phosphorus is the main requirement for the growth of algae. Microalgae will grow well if all these components are available in an appropriate ratio; if fresh water is used, it takes 3726 kg water, 0.33 kg nitrogen, and 0.71 kg of phosphate to produce 1 kg of biodiesel from algae. Recycling harvested water reduces the water and nutrient usage by 84 percent and 55 percent, respectively. Using seawater or wastewater decreases the water requirement by 90% and reduces the need to supply all of the nutrients except phosphate (Yang et al., 2011). To grow 1 kg of dry microalgae, 20.3 L of water, 134 g of salt, 147 g of nitrogen, and 20 g of phosphorus are required (Batan et al., 2010). Chisti's 2008 analysis shows that algae biomass with a lipid content of 42

percent and production costs of US\$217.22 per ton becomes competitive with petroleum at the price of US\$60.00 per barrel. Using a value of US\$0.22 per kWh for energy consumption, the production cost of 1 ton of algae biomass from desalination concentrate that had already been used to produce a crop of microalgae was estimated to be US\$808.79. One ton of algal biomass can be produced during the treatment of 1443 m³ of wastewater. If the credit for wastewater treatment at US\$0.4 per m³ is considered, the cost of 1 ton of biomass would be reduced to US\$231.59. This calculation concludes that if the price of petroleum is US\$63.97 per barrel, algae biomass can be a viable energy alternative.

The financial costs of both desalinization and microalgae production can be reduced by reusing the concentrate from desalination to grow the microalgae. This same practice could also reduce the environmental costs of desalinization. As mentioned before, the financial costs associated with disposing of concentrate are currently very high: in the case of inland sites, concentrate disposal adds a minimum of 15 percent to the cost of desalination (Glueckstern and Priel, 1997; Oren et al., 2010). For disposal by evaporation pond, the cost is US\$1.18-10.04 per m³ (Samimi and Zarinabadi, 2012). At present, the top available disposal methods – surface water disposal or discharge to wastewater treatment plants – are also highly debatable due to environmental concerns. In sum, the literature supports the contention that desalination could be made more sustainable and be done with a dramatically lower cost by using the waste concentrate produced by desalinization to grow microalgae.

Microalgae can also reduce the presence of many heavy materials in wastewater through the phycoremediation process (Pankaj and Awasthi, 2013).

2.4 Carbon Dioxide Emissions (Global Warming)

As sunlight reaches the earth's atmosphere and strikes the planet, the surface of the earth is heated and a portion of the sunlight is reflected back to space as infrared radiation. The main greenhouse gases - carbon dioxide (CO₂), nitrogen dioxide (NO₂), methane (CH₄) and steam (H₂O) (EPA, 2012) – absorb the infrared radiation and trap the heat, causing the earth's temperature to rise about 32 °C (59 °F) to an average of 14-15 °C. This natural phenomenon makes the environment warmer and more suitable for the development of human civilization; without it, the surface of the planet would be covered with a thick layer of ice (Chen et al., 2001; Samimi and Zarinabadi, 2012; Loriuset et al., 1990).

However, since the Industrial Revolution (mid-1700s) (Hettiarachchi, 2012), the use of fossil fuels and other energy sources that produce greenhouse gases (GHG) such as carbon dioxide and methane has increased dramatically, and the concentrations of these gases in the earth's atmosphere have increased by 36 percent and 148 percent, respectively; other studies indicate that the concentrations of the aforementioned gases in the atmosphere have increased by 40 percent and 160 percent, respectively (EPA, 2013).

The Intergovernmental Panel on Climate Change (IPCC) has identified carbon dioxide as the most significant anthropogenic greenhouse gas, with an 80 percent annual emission growth between 1970 and 2004 (Greenwell et al., 2010). The largest share of the total greenhouse gas emissions is also carbon dioxide (about 70 percent) (Stewart and Hessami, 2005). Increasing the presence of CO₂ and other greenhouse gases in the atmosphere has kept a large portion of infrared radiation from exiting the earth's atmosphere, causing the weather to become warmer (Wang et al., 2008).

Carbon dioxide alone is responsible for about 25 percent of the effect from all greenhouse gases, due to its absorption of half of the infrared radiation wavelength reflected back to space from the earth. According to the National Energy Technology Laboratory, the total CO₂ emissions from industrial sources is about 100 trillion cubic feet (5,090 million metric tons) per year (Nakamura, 2006), and according to the U.S. Department of Energy's Carbon Dioxide Information Analysis Center, in 2013 the global carbon dioxide emission was approximately 36 billion tons from the combustion of fossil fuels only; that same year, the cumulative emission of CO₂ due to all human activity since the mid-1800s reached 2015 billion tons of CO₂ (Carbon Dioxide Information Analysis Center, 2013). Currently, the level of carbon dioxide concentration in the atmosphere is between 300 and 400 ppm (Rosenberg et al., 2011). According to Hettiarachchi (2012), "the IPCC Special Report on Emissions Scenarios gives a wide range of future CO₂ scenarios, ranging from 541 to 970 ppm by the year 2100" (IPCC, 2012).

Microalgae have the capability of capturing CO₂ from various sources such as the atmosphere, industrial exhaust gases, and fixed CO₂ sources. Generally, microalgae are cultivated in two methods: open ponds (raceways), and closed systems, which are exposed to air or aerated in order for air-tolerating microalgae to capture CO₂ from the atmosphere for cell growth. Microalgae are considered to be the most productive carbon user, and can fix a larger amount of CO₂ per land area than can higher plants such as trees and sugar cane. In addition, microalgae are not subject to the loss of plant leaves due to weather and environmental conditions, a problem in higher plants which adversely affects the process of photosynthesis and therefore reduces CO₂ uptake (Brown and Sprague, 1992). Some studies show that CO₂ is captured by microalgae with an efficiency up to 50 times greater than that of higher plants (Nakamura, 2006; Demirbas, 2006). Such efficient CO₂ capture could help alleviate climate change effects from elevated CO₂ levels.

In the southwestern desert of the United States, there are favorable conditions for algae growth, such as expansive lands, warm temperatures, brackish water, and large sources of carbon dioxide (in the form of fossil fuel power plants). The feasibility of using such CO₂ sources to grow microalgae has already been demonstrated: in Kona, Hawaii, a commercial production plant for biofuel already supplies CO₂ for *Spirulina* growth using flue gases from a power plant. About 75 percent of the flue gas, which provides 67 tons of CO₂ per month, is efficiently absorbed into the system, supporting 36 tons/month of *Spirulina* (Pedroni et al., 2001). Globally, approximately 7 percent of CO₂ emissions is due

to power plant flue gases (Fisher et al., 1997). In 2010, EIA estimated that the total emission of CO₂ from coal power plants in New Mexico and Arizona has been 68.5 million metric tons (EIA, 2013), which can be absorbed by algae farms covering only 0.3425 percent of the area of those states (Demirbas, 2006).

Emissions from the use of fossil fuels will add more carbon dioxide to the atmosphere, and will therefore increase the climatic effects of greenhouse gases. Using biofuel from microalgae as an alternative to fossil fuels reduces the emission of greenhouse gases such as carbon dioxide, methane, and nitrous oxide. During the process of microalgae cultivation, the algae consume the carbon dioxide necessary for their growth and then release the same amount of this greenhouse gas (carbon dioxide) when they are used as biofuels. The advantage of this method is that the balance of the gas in the atmosphere will not be affected during the combustion of the biodiesel.

The application of microalgae to reduce greenhouse gas emissions can come through the development of a wastewater treatment and aquatic farming process that combines algae's waste treatment features with their ability to reduce GHG emissions and produce biofuel (Havlík et al., 2011).

As compared with petroleum diesel, the percentage decrease in greenhouse gas components and the reduction in net emissions for the production of biodiesel from microalgae and soybean feedstocks are evident in Table 2.2.

Chapter 3: MATERIALS AND METHODS

3.1 Analytical Method and Sampling (Experiment Design)

Two experiments of the three experiments (for *D. salina* and *S. platensis*) are designed based on a two-level factorial design (2^2) with two replications for each level of conductivity in the medium. The nutrient types were considered as treatments, and dry weight and optical density were measured as responses. The third experiment (for the BGNDRF species) is designed with five different levels of conductivity as treatments, and dry weight and optical density as responses.

In all three experiments, temperature, pH, conductivity, and flow rate were monitored and measured.

The lengths of the experiments were determined by the growth behavior of the microalgae, which, in fed batch reactors, is characterized by five phases: 1) the lag phase, in which the microalgae are acclimating to the new environment and only a small increase in cell density happens; 2) the exponential phase, in which cell density increases as a function of time; 3) the phase of declining growth rate, in which the increases in cell density slow; 4) the stationary phase, in which cell density stabilizes; and 5) the death or crash phase, when cell densities drop precipitously as a result of algae die-off. This may happen due to an obstruction of light caused by the high cell density, an increase in the toxicity of the growth medium due to the buildup of algae's natural wastes, the competitive effects of indigenous bacteria and protozoa, and/or a depletion of nutrients. The experiments were run until the algae reached their death or crash phase, so the lengths of the experiments varied with the lengths of the algae's different growth phases. The BGNDRF strain, since its characteristics were previously unknown, was allowed to grow for a longer period to ensure that it had reached the crash phase.

The *D. salina* microalgae species was cultivated at the New Mexico State University Laboratory. *Arthrospira (Spirulina) platensis* was cultivated at the University of Texas at Austin. A previously unknown species from a desalination concentrate pond in Alamogordo, NM was also grown in a single reactor. The three species were grown in cleaned used bottles (3.785 L volume) with desalination concentrate as the growth medium and SADS from a wastewater treatment plant as a nutrient (Table 3.1). Desalination concentrate samples were collected from the desalination concentrate ponds of the Brackish Groundwater National Desalination Research Facility located in Alamogordo, New Mexico. Anaerobic digested sludge was collected from the wastewater treatment plant in

Las Cruces, NM. Desalination concentrate and anaerobic digested sludge were separately centrifuged for 3 minutes at 10,000 rpm to separate the heavy particles and collect the supernatants. These supernatants were used in the studies as a nutrient. Dry weight concentration and the optical density of growth culture were used to identify the microalgae growth. About 10 mL of cell suspension samples were withdrawn from the reactor and centrifuged for 3 minutes at 10,000 rpm; then, the supernatant was decanted, and the remaining wet microalgae (slurries) were dried at 103-105 °C in an oven to measure the dry weight concentrations of the microalgae. These measurements were taken in accordance with the SM 2540D procedures (American Public Health Association, 2005; Valigore et al., 2012). The same volume of supernatant of each sample was also dried in the same oven to obtain the correct TDS concentration from the wet microalgae (slurries) to get the TDS-free dry weight concentration of the microalgae. The optical density of the growth culture was measured with a spectrophotometer (Hach DR/2010) at a 560 nm wavelength, the same wavelength recommended by Concaset et al., 2013. The 560 nm wavelength was chosen to correspond to the peak absorption rate for chlorophyll. Scans were performed in cuvette tubes. The pH was measured with a Cole Parmer pH meter AB15 Accumet Basic. The conductivity was measured with the Hach sensION5 conductivity meter. Information on the growth of each of the three algae species is presented below.

- *D. salina*: This experiment was performed during November-December 2011, for a total of 41 days. The parameter measurements were taken on an average of every two days. Dry weight concentrations were measured at 18 points, the optical density of the growth culture was measured at 17 points, the conductivity of growth culture was measured at 18 points, and the pH was measured at 17 points of treatment.
- *S. platensis*: This experiment was performed during January-February 2012, for a total of 34 days. The parameter measurements were taken on an average of every three days. Dry weight concentrations were measured at 10 points, optical density of growth culture was measured at 12 points, the conductivity of growth culture was measured at 13 points, and the pH was measured at 13 point of treatment.
- BGNDRF species: This experiment was performed during February-September 2012, for a total of 110 days. The parameter measurements were taken on an average of every five days. Dry weight concentrations were measured at 20 points, the optical density of the growth culture was measured at 22 points, the conductivity of growth culture was measured at 22 points, and the pH was measured at 24 points of treatment.

3.2 Contents in Reactors

All reactors were filled with desalination concentrate and seed microalgae as shown in Table 3.1. Reactors D1, D2, S1, and S2 were fed with SADS as

nutrients. Reactors D3 and D4 were fed with Bold's Basal Medium (BBM) (Nichols and Bold, 1965), and reactors S3 and S4 were fed with F/2 (Guillard and Ryther, 1962). Reactors R1, R2, R3, R4, and R5 were fed with SADS. The characteristics of SADS, Bold's Basal Medium, and F/2 are shown in Appendices B, C, and D, respectively. The reactors were bubbled 8 hours a day with air from the environment, which contained CO₂ at 0.0387 percent by volume. All reactors were directly exposed to sunlight from 9:00 a.m. to 5:00 p.m. in New Mexico State University, Las Cruces, NM. Sunlight radiation data were not collected since sunlight radiation varies with time (from 9:00 a.m. to 5:00 p.m.) during the day and also with the location of the reactor surface. The reactors were illuminated with light bulbs on holidays when the reactors were in the lab. The radiation from the light bulbs to the reactors was not collected since the exposure time to the light bulbs was negligible compared to the exposure time to sunlight. SADS, F/2, and BBM were fed periodically as fed-batch culture.

The conductivities of the concentrate varied somewhat due to the process used to increase the salinity to needed levels. The concentrate taken from the desalination systems at BGNDRF had relatively low levels of conductivity, which varied slightly around 6280 $\mu\text{S}/\text{cm}$. Since the goal of this research was to investigate the growths of different algae species at elevated and significantly different salinities (differences of about 7000 $\mu\text{S}/\text{cm}$), the concentrate salinity had to be increased. This was done by boiling the concentrate to reach the desired salinity levels, and since this process is not completely controllable, the final salinity levels for different experiments were slightly different.

3.3 Statistical Analysis

After data collection (biomass measurement), based on the hypothesis and research questions, two way analysis of variance and regression techniques were used to find the differences and relationships between predictors (nutrients and conductivities) and response (biomass).

Chapter 4: RESULT AND DISCUSSION

4.1 Introduction

A 2² factorial experiment was conducted for two experiments (*D. salina* and *S. platensis*) and the third experiment (BGNDRF species) was designed using five different levels of conductivity. These experiments were carried out for two reasons: (1) to evaluate microalgae's ability to reduce conductivity in desalination concentrate; and (2) to investigate the feasibility of integrated algae cultivation using desalination concentrate and supernatant from anaerobic digested sludge (SADS). This chapter presents the results obtained from these experiments.

4.2 Batch Reactors (*Dunaliella salina* and *Spirulina platensis*)

Table 4.1 shows the highest dry weight achieved from the study, along with optical density, pH, culturing day, and temperature at which the highest dry weight was attained.

The growths of *D. salina* and *S. platensis* in two different nutrients with time are shown in Figures 4.1(a) and 4.2(a). Reactors D1, D2, S1, and S2 were supplied with SADS, while D3, D4, S3, and S4 were supplied with BBM and F/2, respectively. *D. salina* required 37-39 days to reach maximal growth. With SADS as a nutrient, *D. salina* needed 37 days to reach maximal growth, which was 1.40 g/L of dry weight when grown in 31,800 $\mu\text{S/cm}$ conductivity and 1.56 g/L dry weight when grown in a conductivity of 25,442 $\mu\text{S/cm}$. With BBM as a nutrient, *D. salina* required 37-39 days to reach maximal growth, which was 1.04 g/L of dry weight when grown in 31,800 $\mu\text{S/cm}$ conductivity and 0.84 g/L dry weight when grown in 25,442 $\mu\text{S/cm}$ conductivity. *S. platensis* needed less time than *D. salina* to reach maximal growth, taking 14-20 days to reach the maximal growth as determined by the highest point in the dry weight graph. With SADS as a nutrient, *S. platensis* needed 14-24 days to reach maximal growth, which was 1.46 g/L of dry weight when grown in 35,800 $\mu\text{S/cm}$ conductivity and 1.96 g/L dry weight when grown in 25,100 $\mu\text{S/cm}$ conductivity. In F/2 nutrient, *S. platensis* required 20 days to reach the maximal growth of 1.28 g/L of dry weight when grown in 35,800 $\mu\text{S/cm}$ conductivity and 0.66 g/L dry weight when grown in

25,100 $\mu\text{S}/\text{cm}$ conductivity. SADS provided higher yields than BBM (*D. salina*) and F/2 (*S. platensis*). The lower conductivity improved the yield while SADS was fed into reactors.

Figures 4.1(b) and 4.2(b) show the optical density of the cultures with time. The highest optical densities (*D. salina* 2.25; *S. platensis* 1.62) occurred in the lower conductivities (*D. salina* 25,442 $\mu\text{S}/\text{cm}$; *S. platensis* 25,100 $\mu\text{S}/\text{cm}$) with the SADS as nutrient for both *D. salina* and *S. platensis*.

Figures 4.1(c) and 4.2(c) depict the conductivity changes in the growth media with culturing time. The conductivities in cultures of *D. salina* in reactors D1 and D2 decreased with time, as shown in Figure 4.1(c). This decrease is due to microalgae consuming the necessary ions (phosphorus, nitrate+nitrite, calcium, sulfate, magnesium, sodium, and potassium) for their growth in the concentrate stream. The conductivities of the cultures in reactors S3 and S4 increased with time, as shown in Figure 4.2(c). Although *S. platensis* consumed the ions in the medium necessary for its growth, the F/2 nutrient had a higher conductivity than the culturing desalination concentrate, so the conductivity level increase may have been due to the contribution from F/2 nutrient. The nutrients added into reactors S1, S2, S3, and S4 are shown in Figure 4.2(d). As algae grow, they require more nutrients; therefore, the amount of nutrient added was increased with time.

Figures 4.1(e) and 4.2(e) show the pH of the media with time. These data show that *D. salina* and *S. platensis* grew in pH 8-9, as shown in Figures 4.1(e) and 4.2(e). The temperature of medium for *D. salina* was 60-90 °F, as shown in Figure 4.1(f); the temperature of medium for *S. platensis* was 65-95 °F, as shown in Figure 4.2(f). CO₂ was supplied from air, which was bubbled into reactors.

As previously mentioned, this experiment was a full-factorial design (2²). The Analysis of Variance for the experiment (*D. salina*) is shown in Table 4.2

After finding a statistically significant difference, it was necessary to use multiple comparisons to find the significant nutrient and the best combination of conductivity and nutrient to control Type I error and increase the power of our statistical analysis; we therefore used Tukey's test.

As can be seen in the ANOVA in Table 4.2, conductivity levels had no effect on the level of biomass production for *D. salina* (P-value >0.05). Tukey's test also showed no difference, a result that could be due to *D. salina*'s ability to grow in high levels of salinity and in strong changes in salinity. Therefore, the level of conductivity, in the range between 25,443 and 31,800 $\mu\text{S}/\text{cm}$, did not significantly affect the growth rate of *D. salina*, as shown in Figure 4.3.

Tukey's test did, however, show a significant difference between the different types of nutrient; in this system, using SADS as a nutrient provided more biomass than BBM did, as indicated in Figure 4.4.

Tukey's test showed no significant difference among means of nutrient-conductivity interaction when using the same type of nutrient at different conductivity levels, as indicated in Figure 4.5.

The four treatment combinations in the design are shown graphically in Figure 4.6, where "A" refers to the effect of Factor A (level of conductivity), "B" refers to the effect of Factor B (type of nutrient), and "AB" refers to the AB

interaction. In the 2^2 design, the low and high levels of A and B are denoted by “-” and “+,” respectively, on the A and B axes.

The four treatment combinations in the design are also represented by lowercase letters as shown in Figure 4.6.

The main effective parameter on this system is type of nutrient (factor B) and the interaction between the level of conductivity and type of nutrient (factor AB), as shown in Table 4.3.

The regression model in a (2^2) factorial design is:

$$Y = \beta_0 + \beta_1 X_1 + \beta_2 X_2 + \beta_{12} X_1 X_2 + \varepsilon$$

Where X_1 is a coded variable that represents the level of conductivity, X_2 is a coded variable that represents the type of nutrient, and the β s are regression coefficients.

$$X_1 = \frac{\text{Cond} - \left(\frac{\text{Cond at low} + \text{Cond at high}}{2} \right)}{(\text{Cond at high} - \text{Cond at low})/2}$$

$$X_1 = \frac{\text{Cond} - 28,621}{3,179}$$

If the level of conductivity is at a high level (Conductivity = 31,800 $\mu\text{S}/\text{cm}$), then $X_1 = +1$; if the level of conductivity is at low level (25,442 $\mu\text{S}/\text{cm}$), then $X_1 = -1$.

$$X_2 = \frac{\text{TN} - ((\text{TN at low} + \text{TN at high}))/2}{(\text{TN at high} - \text{TN at low})/2}$$

$$X_2 = \frac{\text{TN} - (\text{BBM} - \text{SADS})/2}{(\text{SADS} - \text{BBM})/2}$$

If the type of nutrient is at a high level (SADS), then $X_2 = +1$, and if the level of conductivity is at a low level (BBM), then $X_1 = -1$.

The fitted regression model is:

$$Y = 1.19 + \left(\frac{0.045}{2} \right) X_2 + \left(\frac{0.145}{2} \right) X_1 X_2$$

This model can be used to obtain the predicted value of Y; the residuals are the difference between the observed and the fitted values of Y.

$$Y = \beta_0 + \beta_2 (-1) + \beta_{12} (-1) (-1) = 1.24$$

$$e_1 = 1.56 - 1.24 = 0.32$$

$$e_2 = 1.42 - 1.24 = 0.18$$

$$Y = \beta_0 + \beta_2 (-1) + \beta_{12} (+1) (-1) = 1.095$$

$$e_3 = 1.38 - 1.095 = 0.285$$

$$e4 = 1.4 - 1.095 = 0.305$$

$$Y = \beta_0 + \beta_2 (+1) + \beta_{12} (-1) (+1) = 1.14$$

$$e5 = 0.84 - 1.14 = -0.3$$

$$e6 = 0.8 - 1.14 = -0.34$$

$$Y = \beta_0 + \beta_1 (+1) + \beta_{12} (+1) (+1) = 1.285$$

$$e7 = 1.04 - 1.285 = -0.245$$

$$e8 = 0.98 - 1.285 = -0.305$$

After substituting the relationships between the natural and coded variables, the following regression model is obtained:

$$Y = 1.19 + \left(\frac{0.045}{2}\right) \left(\frac{TN - (BBM + SADS)/2}{(SADS - BBM)/2}\right) + \left(\frac{0.145}{2}\right) \left(\frac{Cond - 28,261}{3,179}\right) \left(\frac{TN - (BBM + SADS)/2}{(SADS - BBM)/2}\right)$$

Where Y is maximum biomass (g/L), TN is type of nutrient, BBM is Bold's Basal Medium, SADS is supernatant from anaerobic digested sludge, and Cond is conductivity ($\mu\text{S}/\text{cm}$).

Figure 4.7 shows that there are no points further than + 0.4 or - 0.4, and that there is no issue of outliers; therefore, we can trust our regression analysis.

As for *S. platensis*, the analysis of variance for this full-factorial design (2^2) experiment is shown in Table 4.4.

Again, after finding a significant difference, we needed to use multiple comparisons to find the significant nutrient and best combination of conductivity and nutrient to control Type I error and increase the power of our statistical analysis; we therefore used Tukey's test.

As can be seen in the ANOVA in Table 4.4, conductivity had no impact on biomass production (P-value > 0.05). Tukey's test also showed no difference. Therefore, it can be concluded that the level of conductivity, in the range between 25,100 and 35,800 $\mu\text{S}/\text{cm}$, did not affect the growth rate of *S. platensis* significantly, as shown in Figure 4.8.

Tukey's test did show a significant difference between the types of nutrients (P-value < 0.05); in this system, the use of SADS as a nutrient provided more biomass in comparison to F/2, as indicated in Figure 4.9.

Tukey's test showed significant difference among means of nutrient-conductivity interaction, and the highest levels of biomass were seen in the combination of a conductivity of 25,100 $\mu\text{S}/\text{cm}$ and SADS as a nutrient; also, the lowest biomass production was seen in the interaction between a conductivity of 25,100 $\mu\text{S}/\text{cm}$ and F/2 (P-value < 0.05), as indicated in Figure 4.10.

Again, the four treatment combinations in the design are shown graphically in Figure 4.11, where "A" refers to the effect of Factor A (level of conductivity), "B" refers to the effect of Factor B (type of nutrient), and "AB" refers to the AB interaction. In the 2^2 design, the low and high levels of A and B are denoted by "-" and "+," respectively, on the A and B axes. The four treatment

combinations in the design are also represented by lowercase letters, as shown in Figure 4.11.

The main effective parameter on this system is type of nutrient (Factor B) and the interaction between the level of conductivity and the type of nutrient (Factor AB).

The regression model in a 2^2 factorial design is:

$$Y = \beta_0 + \beta_1 X_1 + \beta_2 X_2 + \beta_{12} X_1 X_2 + \varepsilon$$

Where X_1 is a coded variable that represents the level of conductivity, X_2 is a coded variable that represents the type of nutrient, and the β s are regression coefficients.

$$X_1 = \frac{\text{Cond} - \left(\frac{\text{Cond at low} + \text{Cond at high}}{2}\right)}{(\text{Cond at high} - \text{Cond at low})/2}$$

$$X_1 = \frac{\text{Cond} - 28,700}{5350}$$

If the level of conductivity is at a high level (Conductivity = 35,800 $\mu\text{S}/\text{cm}$), then $X_1 = +1$; if the level of conductivity is at low level (25,100 $\mu\text{S}/\text{cm}$), then $X_1 = -1$.

$$X_2 = \frac{\text{TN} - (\text{TN at low} + \text{NT at high})/2}{(\text{TN at high} - \text{NT at low})/2}$$

$$X_2 = \frac{\text{TN} - (\text{F2} + \text{SADS})/2}{(\text{SADS} - \text{F2})/2}$$

If the type of nutrient is at a high level (SADS), then $X_2 = +1$, and if the level of conductivity is at low level (F/2), then $X_2 = -1$.

The fitted regression model for *S. platensis* is:

$$Y = 1.32 + \left(\frac{0.09}{2}\right) X_2 + \left(\frac{0.52}{2}\right) X_1 X_2$$

Similar to the previous calculations, this model can be used to obtain the predicted value of Y and the residuals.

$$Y = \beta_0 + \beta_2 (-1) + \beta_{12} (-1) (-1) = 1.53$$

$$e_1 = 1.88 - 1.535 = 0.345$$

$$e_2 = 1.96 - 1.535 = 0.425$$

$$Y = \beta_0 + \beta_2 (-1) + \beta_{12} (+1) (-1) = 1.32$$

$$e_3 = 1.52 - 1.32 = 0.2$$

$$e_4 = 1.46 - 1.32 = 0.14$$

$$Y = \beta_0 + \beta_2 (+1) + \beta_{12} (-1) (+1) = 1.58$$

$$e5 = 0.6 - 1.58 = -0.98$$

$$e6 = 0.66 - 1.58 = -0.92$$

$$Y = \beta_0 + \beta_1 (+1) + \beta_2 (+1) (+1) = 1.32$$

$$e7 = 1.2 - 1.32 = -0.12$$

$$e8 = 1.28 - 1.32 = -0.04$$

The final regression model is:

$$Y = 1.32 + \left(\frac{0.09}{2}\right) \left(\frac{TN-(F2+SADS)/2}{(SADS-F2)/2}\right) + \left(\frac{0.52}{2}\right) \left(\frac{Cond-28,700}{5350}\right) \left(\frac{TN-(F2+SADS)/2}{(SADS-F2)/2}\right)$$

where Y is maximum biomass (g/L), TN is type of nutrient, F2 is F/2 Medium, SADS is supernatant from anaerobic digested sludge, and COND is conductivity ($\mu\text{S/cm}$).

Figure 4.12 shows that there are no points further than +1 or -1, and that there is no issue of outliers; therefore, we can trust our regression analysis.

4.3 Specific Growth Rate

The specific growth rate was found from Equation 1:

$$\mu = \frac{\ln(W_y/W_x)}{t_y - t_x} \quad \text{Eq.1}$$

where W_y and W_x are the microalgae dry weight (W) at the beginning (t_x) and at the end (t_y) of the logarithmic growth phase (Wood et al., 2005; Huerlimann et al., 2010). The available literature found for specific growth rates of *D. salina* while culturing with NaCl solutions as a growth medium (García et al., 2007) and a manufactured chemical nutrient (Prieto et al., 2011) were used for comparison with the results from this study. The natural desalination concentrate and SADS that were used in the study and the specific growth rates (0.095-0.114) for *D. salina* in Table 4.6 and 0.019-0.034 for *S. platensis* in Table 4.7 were lower than those reported in the literature (0.12-0.47 for *D. salina* (Prieto et al., 2011) in Table 4.6 and 0.255 for *S. platensis* (Leema et al., 2010) in Table 4.7, where seawater and pretreated seawater were used as the water medium in a closed reactor. Misleading conclusions could be made when comparing the microalgae growth rate between different water mediums, different nutrients supplied, and different types and characteristics of reactors used by Pittman et al., 2011, leading to a statement that nutrient removal rates are comparable. However, microalgae growth rates are higher in artificial wastewater than in natural wastewater (Lau et al., 1995; Ruiz-Marin et al., 2010). This may be due to the increased toxicity of natural wastewaters, the competitive effects of indigenous bacteria and protozoa, or the diverse chemical composition of the natural wastewaters (Pittman et al., 2011). Natural desalination concentrate from the evaporation pond has to be used

for simulating real-world conditions (Samori et al., 2013) and to reduce the disconnection between lab and field, noted by Sheehan et al. in 1998. The lab conditions should simulate the field situation, through approaches such as using natural concentrate in the experiments.

The lower specific growth rates of microalgae may also be due to the temperature fluctuation between daytime (open outdoor, 91.0-116.9 °F) and nighttime (in the lab, 62.5-86 °F), or the illumination problems from the color of SADS (optical density 0.58 at 560 nm wavelength). Additionally, the higher concentrations of TDS, N, Mg²⁺, and Ca²⁺ can be toxic to the microalgae, inhibiting their growth (Kim et al., 2013). Tredici and Zittelli, 1998 found that the biomass growth rates of outdoor cultures of *S. platensis* (1.09 and 1.26 g/L/d) were lower than those of indoor cultures (1.64-1.93 g/L/d). However, the enthalpies are similar (20.9-21.6 kJ/g). Torzillo et al., 1991 concluded that temperature and light irradiance influence the biomass composition and found that dry weight concentrations of biomass were reduced during the night due to the decrease of these two factors.

4.4 The Comparison of Microalgae Biomass between SADS – BBM, and SADS – F/2

Dry weight concentrations of *D. salina* supplied with SADS (1.40-1.56 g/L) were higher than the dry weight concentrations of *D. salina* supplied with BBM (0.84-1.04 g/L), as shown in Figure 4.1(a). Dry weight concentrations of *D. salina* supplied with SADS (1.46-1.96 g/L) were higher than those supplied with F/2 (0.68-1.28 g/L), as shown in Figure 4.2(a). The reason for this may be that micro-organisms grew in SADS along with microalgae, and the microorganism promoted microalgae growth. This finding agrees with the finding of Wang et al., 2010, which states that the specific growth rate of microalgae from concentrate (wastewater from sludge centrifuge) is higher than that from wastewater before and after primary settling and aeration tank. Wastewater from sludge centrifuge has more micro-organisms than the wastewater before and after primary settling and aeration tank. In cases of SADS as nutrient, low conductivity media provide higher microalgae dry weight concentrations. In the case of Bold's Basal Medium and F/2 as nutrients, higher conductivity media provided higher microalgae dry weight concentrations.

4.5 Comparison of Microalgae Biomass between Study and Literature

By reusing concentrate as a growth medium and SADS as a nutrient, this study achieved dry weight concentrations of 1.56 g/L for *D. Salina* (Figure 4.1(a)) and 1.96 g/L for *S. Platensis* (Figure 4.2(a)). These dry weight concentrations are comparable to the results in the literature data where seawater was used, which

are 1.06 g/L for *D. salina* and 0.8–2.9 g/L for *S. platensis*, as shown in Tables 4.4 and 4.5.

A dry weight concentration of 2.587 g/L for *S. platensis* was observed in the work of Volkmann et al., 2008, in desalinated wastewater. A dry weight concentration of 2.37 g/L of dry biomass was observed by Pandey and Tiwari, 2010, at a pH of 8.25, a temperature of 30 °C, and a light intensity of 3 Klux (Jain et al., 2011). A dry weight concentration of 2.34 g/L for *S. platensis* was found on the 27th day of culturing in a 30 percent petha waste medium supplemented with a standard medium (for example, CFTRI medium) in triplicate at 3 Klux light intensity, pH 9.5 ± 0.1 , and $30 \text{ °C} \pm 2$ under 12/12 h light/dark cycles (Jain et al., 2011). A dry weight concentration of 2.91 g/L for *S. platensis* was observed at an input CO₂ concentration of 10 percent on the 25th day of culturing by Ramanant et al., 2010. In the current research, a longer culturing time of 37–39 days for *D. salina* was required to reach maximal growth due to higher conductivities in the concentrate (Table 4.1) and the color from SADS, which decreased the transparency of the plastic bottles used as reactors. The growth rate of microalgae also depends on the amount of seed microalgae in the growth medium (Pittman et al., 2011; Lau et al., 1995). The growth of *D. salina* may be inhibited in desalination concentrate by brackish groundwater since this concentrate contains a high concentration of SO₄²⁻ and a high concentration of HCO₃⁻. *D. salina* prefers high pH of 11, while the pH of the growth culture was between 6.8 and 8.8, as shown in Figure 1(e). Therefore, a longer culturing time was required for *D. salina* to reach the maximum dry weight concentration compared to *S. platensis*, since *Spirulina* prospers in high CO₃²⁻ and HCO₃⁻ water (Richmond, 1986) in the pH range of 8.5–11.0 (Habib and Parvin, 2008).

The highest dry weight yields from reused concentrate as a water medium and SADS as a nutrient are comparable to the data from the literature (Tables 4.6 and 4.7). Most of the culturing time in the study is higher than the culturing time from literature, which may be due to the desalination concentrate that was used in the experiment.

4.6 The Microalgae Strains from the Desalination Evaporation Pond at the Brackish Groundwater National Desalination Research Facility (BGNDRF)

4.7 Results

The study had a duration of about 110 days in order to analyze the growths of these strains, measuring factors such as dry weight, optical density, salinity, pH, and temperature.

Table 4.8 shows the highest dry weight achieved from the study along with the optical density, pH, culturing day, and temperature at which the highest dry weight was gained.

The growth of the Brackish Ground Water National Desalination Facility (BGNDRF) species with time is shown in Figure 4.13(a) in five different conductivities; all reactors were supplied with the same amount of nutrient (SADS).

The BGNDRF species required 80-100 days to reach the maximal growth. The lower conductivity (21000 $\mu\text{S}/\text{cm}$) improved the yield of biomass (2.08 g/L); the highest conductivity (52500 $\mu\text{S}/\text{cm}$) resulted in a lower yield (1.59 g/L).

Figure 4.13(b) shows the optical density of the culture with time. The highest optical density (2.08) occurred in the lowest conductivity (21000 $\mu\text{S}/\text{cm}$); the lowest optical density (1.68) occurred in the highest conductivity (52500 $\mu\text{S}/\text{cm}$).

Figure 4.13(c) depicts the conductivity changes with culturing time. Figure 4.13(d) shows the amount of nutrient that was added during the experiment period. Unlike the experiments with *D. salina* and *S. platensis*, the nutrient addition rate was held constant for the BGNDRF strain. This was done because the BGNDRF strain was previously undiscovered and its growth characteristics and nutrient requirements were unknown.

Figure 4.13(e) displays the pH of the media with time. Data show that the BGNDRF species grew in pH 8-9.2. The temperature of medium for BGNDRF species was 75-100 °F, as shown in Figure 4.13(f). CO₂ was supplied from air which was bubbled into reactors, as shown in Figure 4.13(g).

4.8 Mass of Conductivity Reduction

Mass of conductivity is the result of multiplying the conductivity ($\mu\text{S}/\text{cm}$) of the microalgae in the bioreactor by the actual volume of the microalgae (L) in the bioreactor; the mass of conductivity deduction from concentrate and nutrient percentage is shown in Figure 4.14. Microalgae growth rates are depicted in Figure 4.13(a) and Figure 4.15.

Overall, the mass of conductivity deductions from concentrate and nutrients (57, 54, 46, 40, and 37 percent) are inversely proportional to the original mass of conductivities (51,191; 64,502; 80,517; 104,950; 120,720 ($\mu\text{S}/\text{cm}$) (L)) in 110 days of treatment (Figure 4.14). The maximum dry weights of microalgae (2.08, 1.92, 1.85, 1.75 and 1.59 g/L) in the five different conductivities of concentrate are shown in Figure 4.15. Conductivities of culture in 110 days are significantly less than that of original concentrate from desalination. Mass of conductivity deduction is significant in 0-110 days of treatment, as shown in Figure 4.14. Desalted culture included water, green food, protein, and nutrients, which can be fed to sheep by mixing dry feed stocks to sustain cities in arid-regions (State of New South Wales, 2007; Government of Western Australia, 2007).

The ANOVA regression model in Table 4.9 shows that conductivity (predictor) explains the variation in biomass (response) (P-value <0.05).

A regression model was developed based on the maximum biomass in each reactor and the five levels of conductivity in each one.

The regression equation is:

$Y = 2.353 - 0.000015 \text{ Conductivity}$

Y: Maximum Dry Weight (g/L)

Conductivity ($\mu\text{S/cm}$)

The regression fit for the maximum biomass and conductivity obtained has an R-squared value of 97.4% (P-value < 0.05).

Figure 4.15 shows that low conductivity of the concentrate results in a high dry weight.

The results in Figure 4.16 indicate that we can trust the regression analysis because all residuals are around the best fit line (there is no problem of normality), there are no points further than -0.04 or $+0.04$, there is no issue of outliers, and all the data have the same frequency.

Chapter 5 – CONCLUSIONS

Based on the experiments conducted in this study, the following conclusions can be made:

- Due to microorganisms growing with microalgae, the maximum dry weights of *D. salina* and *S. platensis* grown in desalination concentrate and supplied with SADS (1.36–1.49 g/L) are more than the dry weights of these same species when supplied with BBM and F/2, due to the manner in which the microorganism promotes microalgae growth. The maximum dry weight concentrations of *D. salina* and *S. platensis* grown in desalination concentrate and supplied with SADS are comparable to those in the literature.
- This study demonstrates the feasibility of using concentrate as a growth medium using SADS as a nutrient to grow algae culture.
- A combination of lower conductivity in the medium (25,442 and 25,100 $\mu\text{S}/\text{cm}$) and the use of SADS enhanced the growth of *D. salina* and *S. platensis*.
- The amount of the conductivity reduction was significant in BGNDRF species strains in 110 days.

These results suggest that using microalgae for reducing the conductivity of desalination concentrate and SADS by using the concentrate as a growth medium and SADS as an additional source of nutrients is better than using traditional methods for disposing of the concentrate from the desalination units, which have high costs and adverse environmental effects. High TDS levels, however, limited the ability of specific algae species to grow in the concentrate and reduce its conductivity.

The results also suggested that the BGNDRF strain can be used for concentrate management at salinity levels below 35,000 $\mu\text{S}/\text{cm}$. The BGNDRF species grew well at these levels, and since SADS is known to contain elements and ions that algae consume in their growth process – namely, ammonia nitrogen, sodium, calcium, magnesium, and potassium – it can be deduced that the BGNDRF species consumed some of these elements and ions in order to grow, reducing the overall salinity of the concentrate. The extent of this reduction could be explored in future research.

Chapter 6 - FUTURE RECOMMENDATIONS

Recommendations for future research are listed below:

- Experiments can be conducted at different TDS levels to establish the optimal growth rate and can be performed on a large scale.
- Different species of microalgae can be cultured with the reject concentrate to study their growths and the conductivity reductions.
- The ion and element content of the growth media could be determined before and after algae growth to identify the specific ions and elements that the algae species remove.

References

- Abd El-Baky, H.H., El-Baz, F.K., El-Baroty, G.S. (2004). Production of lipids rich in omega 3 fatty acids from the halotolerant alga *Dunaliella salina*. *Biotechnology*, 3, (1), 102-108.
- Abdul-Wahab, S.A., Al-Weshahi, M.A. (2009). Brine management: substituting chlorine with on-site produced sodium hypochlorite for environmentally improved desalination processes. *Water resources management*, 23, 2437-2545.
- Alameddine, I., and El-Fadel, M. (2006). Brine discharge from desalination plants: a modeling approach to an optimized outfall design. *Desalination*, 214, 241-260.
- Al-Wazzan, Y., and Al-Modaf, F. (2001). Seawater desalination in Kuwait using multistage flash evaporation technology — historical overview. *Desalination*, 134, 257-267.
- Alley, W.M. (2003). Desalination of ground water: earth science perspectives. Retrieved July 6, 2013, from <http://pubs.usgs.gov/fs/fs075-03/pdf/AlleyFS.pdf>.
- American Public Health Association. (2005). Standard methods for the examination of water and wastewater. APHA. Washington, DC.
- Arnal, J.M., Sancho, M., Iborra, I., González, J.M., Santafé, A., and Lora, J. (2005). Concentration of brine from RO desalination plants by natural evaporation. *Desalination*. 182,435-439.
- Arroyo, S., and Shirazi, S. (2012). Cost of the brackish groundwater desalination in Texas. Retrieved July 10, 2013, from https://www.twdb.state.tx.us/innovativewater/desal/doc/Cost_of_Desalination_in_Texas.pdf.
- Barber, N. (2009). Summary of estimated water use in the United States in 2005. Retrieved August 11, 2013, from <http://pubs.usgs.gov/fs/2009/3098/pdf/2009-3098.pdf>.
- Baten, L., Quinn, J., Willson, B., and Bradley, T. (2010). Net Energy and Greenhouse Gas Emission Evaluation of Biodiesel Derived from Microalgae. *Environmental Science and Technology*, 44, 7975–7980.
- Ben-Amotz, A. and Avron, M. (1973). The role of glycerol in the osmotic

regulation of the halophilic alga *Dunaliella parva*. *Plant Physiol.* 51, 875-878.

Biofuel. (n.d.). In *Wikipedia*. Retrieved October 14, 2013, from <http://en.wikipedia.org/wiki/Biofuel>.

Borowitzka, M. (1990). The Mass Culture of *Dunalella Salina*. *Technical Resource Papers Regional Workshop on the Culture and Utilization of Seaweeds Volume II*. Retrieved July 17, 2013, from <http://www.fao.org/docrep/field/003/ab728e/ab728e06.htm>

Brady, P.V., Kottenstette, R.J., Mayer, T.M. and Hightower, M.M. (2009). Inland Desalination: Challenges and Research Needs. *Journal of Contemporary Water Research and Education* 132, 46–51.

Brennan, L., Owende, P. (2010). Biofuels from microalgae – A Review of technologies for production, processing, and extractions of biofuels and co-products. *Renewable and Sustainable Energy Reviews.* 14,(2), 557–577.

Brown, L.M., and Sprague, S. (1992). Aquatic species project report: FY 1989-90. Golden, CO: National Renewable Energy Laboratory

Carbon Dioxide Information Analysis Center. (2013). 2013 Global Carbon Project. Retrieved May 4, 2014 from <http://cdiac.ornl.gov/GCP/carbonbudget/2013/>

Carter, N.T. (2013). *Desalination and Membrane Technologies: Federal Research and Adoption Issues* (CRS Report No. R40477). Washington, DC: Congressional Research Service. Retrieved March 15, 2014, from <http://www.fas.org/sgp/crs/misc/R40477.pdf>.

Chaiklahan, R., Chirasuwan, N., Loha, V., and Bunnag, B. (2008). Lipid and fatty acids extraction from the cyanobacterium *Spirulina*. *Science Asia*, 34, 299–305.

Chen, H. and Jiang, J.G. (2009). Osmotic responses of *Dunaliella* to the changes of salinity. *Journal of Cellular Physiology.* 219, (2), 251-258.

Chisti, Y. (2007). Biodiesel from microalgae. *Biotechnology Advance*, 25, 294–306.

Chisti, Y. (2008). Biodiesel from microalgae beats bioethanol. *Trends in Biotechnol.* 26, (3), 126–131.

Cooley, H., Gleick, P. H., and Wolff, G. (2006). Desalination with a Grain of Salt, A California perspective. Pacific Institute for Studies in Development, Environment, and Security. Retrieved June 26, 2013, from http://www.pacinst.org/wpcontent/uploads/2013/02/desalination_report3.pdf

Demirbaş, A. (2006). Oily Products from Mosses and Algae via Pyrolysis. *Energy Part A: Recovery, Utilization, and Environmental Effects*. 28,10, 933–940.

Eltawi, M., Zhengming, Z., Yuan, L. (2009). A review of renewable energy technologies integrated with desalination systems. *Renewable and Sustainable Energy Reviews* 13, 2245–2262

Fisher, M., Gokhman, I., Pick, U., Zamir, A. (1997). A structurally novel transferrin-like protein accumulates in the plasma membrane of the unicellular green alga *Dunaliella salina* grown in high salinities. *The Journal of Biological Chemistry*, 272,(3), 1565 – 70.

García, F., Freile-Pelegri, Y., Robledo, D. (2007). Physiological characterization of *Dunaliella* sp. (Chlorophyta, Volvocales) from Yucatan, Mexico. *Bioresour. Technol.* 98,(7), 1359–1365.

Gardner, R.D., Lohman, E., Gerlach, R. (2013). Comparison of CO₂ and Bicarbonate as inorganic carbon sources for triacylglycerol and starch accumulation in *Chlamydomonas reinhardtii*, *Biotechnol. and Bioeng.* 110, 1, 87–96.

Gimmler, H., Weis, U., Weis, C., Kugel, H., Treffny, B. D. (1989). *Dunaliella acidophila* (Kalina) Masyuk - An alga with a positive membrane potential. *New Phytol.* 113, 175–184.

Ginzburg, M. (1989). *Dunaliella*: A green alga adapted to salt. *Adv Bot. Res* 114,93-183.

Gitelson, A.A., Laorawat, S., Keydan, G.P., Vonshak, A. (1995). Optical properties of dense algal cultures outdoors and their application to remote estimation of biomass and pigment concentration in *Spirulina platensis* (Cyanobacteria), *J. Phycol.* 31, 828–834.

Glueckstern, P., Priel, M. (1997). Optimized brackish water desalination plants with minimum impact on the environment. *Desalination*. 108, 19-26.

Government of Western Australia, Department of Water. (2007). Rural Water Note: water quality in broadacre farming. Retrieved July 16, 2012, from <http://www.water.wa.gov.au/PublicationStore/first/76924.pdf>.

Greenlee, L.F., Lawler, D.F., Freeman, B.D., Marrot, B., Moulin, P. (2009). Reverse osmosis desalination: water sources, technology, and today's challenges. *Water Research*. 43, 2317-2348.

- Greenwell, H.C., Laurens, L.M., Shields, R.J., Lovitt, R.W., and Flynn, K. J. (2010). Placing microalgae on the biofuels priority list: a review of the technological challenges. *Journal of the Royal Society, Interface / the Royal Society*, 7(46), 703–26.
- Guillard, R.R.L. and Ryther, J.H. (1962). Studies of marine planktonic diatoms: I. *Cyclotella nana* Hustedt, and *Detonula confervacea* (Cleve) gran, *Canadian Journal Microbiology*. 8,(2), 229–239.
- Gunawansa, A. and Bhullar, L. (2013). *Water Governance: An Evaluation of Alternative Architectures*. Northampton, MA: Edward Elgar Publishing Limited.
- Habib, M., and Parvin, M. (2008). *A review on culture, production, and use of Spirulina as food for humans and feeds for domestic animals and fish*. Fisheries and Aquaculture Circular. No.1034, FAO, Rome, Italy: Food and Agriculture Organization of the United Nations.
- Havlik, P., Schneider, U.A., Schmid, E., Böttcher, H., Fritz, S., Skalský, R., Obersteiner, M. (2011). Global land-use implications of first and second generation biofuel targets. *Energy Policy*, 39(10), 5690–5702.
- Hettiarachchi, N. D. G. (2012). Integrated approach of regulate global temperature rises and climate changes for sustainable planet. *Journal of Physics: Conference Series* 433, 012032.
- Hordagui, H. (1997). Environmental Aspects of Brine Reject from Desalination Industry in ESCWA Region. United Nations Economic and Social Commission for Western Asia, Beirut, Lebanon.
- Howe, K.J. (2004). Technical Challenges to Concentrate Disposal from Inland Desalination. In Proceedings of Identifying Technologies to Improve Regional Water Stewardship: North – Middle Rio Grande Corridor. 234–239. Albuquerque, NM.
- Huang, W.W., Dong, B.Z., Cai, Z.P., Duan, S.S. (2011). Growth effects on Mixed culture of *Dunaliella salina* and *Phaeodactylum tricornutum* under Different inoculation densities and nitrogen concentrations, *African Journal of Biotechnology*. 10,(61), 13164–13174.
- Huerlimann, R., De Nys, R., Heimann, K. (2010). Growth, lipid content, productivity and fatty acid composition of tropical microalgae for scale-up production. *Biotechnol. Bioeng.* 107, (2), 245–257.
- Intergovernmental Panel on Climate Change. (2012). Special report. Managing the Risks of Extreme Events and Disasters to Advance Climate Change Adaptation Cambridge University Press, New York, USA.

- International Energy Agency. (2010). Sustainable production of second-generation Biofuels. Retrieved May 18, 2014, from www.iea.org/publications/freepublications/publication/biofuels_exec_summary.pdf.
- Jain, S., Masih, S., Singh, S.G. (2011). Potentiality of petha (*benincasahispida*) waste for the growth of *spirulina platensis*, *Res. J. Agric. Sci.* 2, 133–135.
- Kalogirou, S. (2005). Seawater desalination using renewable energy sources. *Progress in Energy and Combustion Science.* 31, 242–281.
- Kaushik, P., Prasanna, R., Joshi, H.C. (2006). Utilization of anaerobically digested distillery effluent for the production of *Spirulina platensis* (ARM 730), *J. Sci. Ind. Res.* 65,521–525.
- Kebede, E., and Ahlgren, G. (1996). Optimum growth conditions and light utilization efficiency of *Spirulina platensis* (*Arthrospira fusiformis*) (Cyanophyta) from Lake Chitu, Ethiopia. *Hydrobiologia*, 332,(2), 99-109.
- Khawaji, A.D., Kutubkhanah, I.K., Wie, J.M. (2008). Advances in seawater desalination technologies. *Desalination.* 221, 47–69.
- Kim, H., Vannela, R., and Rittmann, B. (2013). Responses of *Synechocystis* sp. PCC 6803 to total dissolved solids in long-term continuous operation of a Photobioreactor. *Bioresour. Technology*, 128, 378-384.
- Kurz, B. A., Stepan, D.J., Harju, J.A., Stevens, B.G. and Cowan, R.M. (2011). Evaluation of Brackish Groundwater Treatment for Use in Hydraulic Fracturing of the Bakken Play, North Dakota. Retrieved April 15, 2014, from <http://www.undeerc.org/Water/pdf/BakkenWaterOppPhase2.pdf>.
- Lachica, R. (2013). How the army needs to lead transformation in the operational energy campaign. *Army Sustainment*, 45(2), 11-13.
- Lau, P.S, Tam, N.F.Y., Womg, Y.S. (1995). Effect of algal density on nutrient removal from primary settled wastewater, *Environ. Pollut.* 89, 59–66.
- Leema, J.T., Kirubakaran, R., Vinithkumar, N.V., Dheenan, P.S., Karthikayulu, S. (2010). High value pigment production from *Arthrospira* (*Spirulina*) *platensis* cultured in seawater, *Bioresour.Technol.* 101, 9221–9227.
- Lorius, C., Jouzel, J., Reynaud, D., Hansen, J. H. L. T. (1990). The ice-core record: climate sensitivity and future greenhouse warming. *Nature* 347, 139–145.
- Mallick, N. (2002). Biotechnological potential of immobilized algae for wastewater N, P and metal removal: A review. *Biometals.* 15, 377-390.
- Markou, G., Chatzipavlidis, I., Georgakakis, D. (2012) Cultivation of *Arthrospira*

- (Spirulina) platensis in olive-oil mill wastewater treated with sodium hypochlorite, *Water Res.* 112, 234–241.
- Mickley, M. (2009). Treatment of Concentrate. U.S. Department of the Interior, Bureau of Reclamation. Report No. 155.
- Mickley, M. (2006). Membrane Concentrate Disposal: Practices and Regulation Purification Research and Development Program. U.S. Department of the Interior Bureau of Reclamation. Report No.123.
- Mishra, A., Mandoli, A. and Jha, B. (2008). Physiological characterization and stress-induced metabolic responses of *Dunaliella salina* isolated from salt pan. *Journal of industrial microbial and biotechnology.* 35,(10), 1093-1101.
- Mohamed, A.M.O., Maraqa, M., and Al Handhaly, J. (2005). Impact of land disposal of reject brine from desalination plants on soil and groundwater. *Desalination* 182, 411–433.
- Nakamura, DN. (2006). Journal speaking: the mass appeal of biomass. *Oil Gas J.* 104:15.
- Nichols, H.W., Bold, H.C. (1965). *Trichosarcina polymorpha* gen. et sp. Nov. *Journal of phycology.* 1, 1, 34–38.
- NSW Public Works, 2011. Brackish Groundwater: A Viable Community Water Supply Option? The National Water Commission, Australian Government, Canberra.
- Oren, Y., Korngold, E., Daltrophe, N., Messalem, R., Volkman, Y., Aronov, L., Weismann, M., Bouriakov, N., Glueckstern, P., Gilron, J. (2010). Pilot studies on high recovery BWRO-EDR for near zero liquid discharge approach. *Desalination.* 261, 321–330.
- Pandey, J.P., Tiwari, A. (2010) Optimization of biomass production of *Spirulina maxima*, *J. Algal Biomass Utiln.* 1, 20–32.
- Pankaj, V. P. and Awasthi, M. (2013). Use of algae through different approaches. *International Journal of Sustainable Development and Green Economics.* 2, 1, 100-108.
- Pankratz, T. (2012). International Desalination Yearbook 2011 – 2012.
- Pasta, M., Wessells, C.D., Cui, Y. and La Mantia, F A. (2012). A desalination battery. *Nano letters.* 12, 839–43.

- Pedroni, P., Davison, J., Beckert, H. (2001). A Proposal to Establish an International Network on Biofixation of CO₂ and Greenhouse Gas Abatement with Microalgae. *Journal of Energy and Environmental Research*. 1, 136-150.
- Pittman, J.K., Dean, A.P., Osundeko, O. (2011). The potential of sustainable algal biofuel production using wastewater resources, *Bioresour. Technol.* 102, 17-25.
- Prieto, A., Cañavate, J.P., García-González, M. (2011). Assessment of Carotenoid production by *Dunaliella salina* in different culture systems and operation regimes, *J. Biotechnol.* 151, 180–185.
- Ramanan, R., Kannan, K., Deshkar, A., Yadav, R. (2010). Enhanced algal CO₂ sequestration through calcite deposition by *Chlorella* sp. and *Spirulina platensis* in a miniraceway pond, *Bioresour. Technol.* 101, 2616–2622.
- Reichert, C.C., Reinehr, C.O., Costa, A.V. (2006). Semicontinuous cultivation of the Cyanobacterium *Spirulina platensis* in a closed photobioreactor, *Braz. J. Chem. Eng.* 23, 23–28.
- Richard O. Carey & Kati W. Migliaccio (2009). Contribution of Wastewater Treatment Plant Effluents to Nutrient Dynamics in Aquatic Systems: A Review, *Environmental Management*. 44,205–217
- Richmond, A. (1986). Handbook of Microalgae Mass Culture. *CRC Press*, Boston, MA.
- Rosenberg, J.N., Mathias, A., Korth, K., Betenbaugh, M.J., and Oyler, G.A. (2011). Microalgal biomass production and carbon dioxide sequestration from an integrated ethanol biorefinery in Iowa: A technical appraisal and economic feasibility evaluation. *Biomass and Bioenergy*, 35(9), 3865–3876.
- Ruiz-Marin, A., Mendoza-Espinosa, L.G., Stephenson, .T. (2010). Growth and nutrient removal in free and immobilized green algae in batch and semi-continuous cultures treating real wastewater, *Bioresour. Technol.* 101, 58-64.
- Samimi, Amir. Zarinabadi, S. (2012). Reduction of Greenhouse gases emission and effect on environment. *Journal of American Science* 8(8), 1011–1015.
- Samorí, G., Samorí, C., Guerrini, F., Pistocchi, R. (2013). Growth and nitrogen removal capacity of *Desmodesmus communis* and of a natural microalgae consortium in a batch culture system in view of urban wastewater treatment: Part I, *Water Research*. 47,(2), 791–801.
- Santos, C.A., Vieira, A.M., Fernandes, H.L., Empis, .J.A., Novais, J.M. (2001). Optimization of the biological treatment of hypersaline wastewater from *Dunaliella salina* carotenogenesis. *J. Chem. Technol. Biotechnol.* 76, 1147-1153.

Sheehan, J., Dunahay, T., Benemann, J., Roessler, P. (1998). A Look Back at the U.S. Department of Energy's Aquatic Species Program—Biodiesel from Algae, U.S. Department of Energy's Office of Fuels Development. National Renewable Energy Laboratory, Midwest Research Institute, Golden, CO, Contract No. DE-AC36-83CH10093.

State of New South Wales, Department of Primary Industries. (2007). Water for live stocks: interpreting water quality tests. Retrieved April 25, 2013 from http://www.dpi.nsw.gov.au/__data/assets/pdf_file/0018/111348/water-for-livestock-interpreting-water-quality-tests.pdf.

Stumm, W. and Morgan, J.J. (1988). An introduction emphasizing chemical-equilibria in natural waters. *Agriculture Biology and Environmental Sciences* (41):18.

Teimouri, M., Amirkolaie, A. K., Yeganeh, S., Agricultural, S., and Boulevard, K. D. (2013). Effect of Spirulina platensis Meal as a Feed Supplement on Growth Performance and Pigmentation of Rainbow Trout (*Oncorhynchus mykiss*), *World Journal of Fish and Marine sciences*. 5,(2), 194–202.

Tetra Tech. (2011). Analysis of water from four wells at the Brackish Groundwater National Desalination Research Facility, Contract No. R10PC40009. U.S. Department of the Interior, Bureau of Reclamation.

Torzillo, G., Sacchi, A., Materassi, R. (1991). Temperature as an important factor affecting productivity and night biomass loss in *Spirulina platensis* grown outdoors in tubular photobioreactors, *Bioresour. Technol.* 38, 95–100.

Tredici, M. R., and Zittelli, G. C. (1998). Efficiency of sunlight utilization: Tubular versus flat photobioreactors. *Biotechnology and Bioengineering*, 57, 187-197.

United Nations Educational, Scientific and Cultural Organization (UNESCO). (2003). World Water Development, Water and Energy Report. Retrieved March 2014, from <http://unesdoc.unesco.org/images/0012/001297/129726e.pdf>.

United Nations Educational, Scientific and Cultural Organization (UNESCO). (1999). Summary of the monograph “World Water Resource at the beginning of the 21st century.” Retrieved July 27, 2013, from <http://webworld.unesco.org/water/ihp/db/shiklomanov/summary/html/summary.html>.

United Nations Population Fund (UNFPA). (2003). Population Global population and water, access and sustainability number 6. Retrieved July 27, 2013, from http://www.unwater.org/downloads/190_filename_globalwater_eng.pdf.

- United States Census Bureau. (2011). The World Population at 7 Billion. Retrieved May 5, 2012 from <http://blogs.census.gov/2011/10/31/the-world-population-at-7-billion/>.
- United States Department of the Interior, Bureau of Reclamation. (2010). Reclamation Managing Water in the West. Water Treatment Primer for Communities in Need. Desalination Series Report No. 68.
- United States Environmental Protection Agency. (2005). Membrane Filtration Guidance Manual, Retrieved May 17, 2013 from http://www.epa.gov/safewater/disinfection/lt2/pdfs/guide_lt2_membranefiltration_final.pdf.
- United States Environmental Protection Agency. (2006). Biosolids Technology Fact Sheet Multi-Stage Anaerobic Digestion. Retrieved from http://water.epa.gov/scitech/wastetech/upload/2006_10_16_mtb_multi-stage.pdf
- United States Environmental Protection Agency. (2012). Climate change indicators in the United States, (EPA 430-R-12-004). Retrieved April 23, 2014, from <http://www.epa.gov/climatechange/pdfs/climateindicators-full-2012.pdf>.
- United States Environmental Protection Agency. (2013). Inventory of U.S. Greenhouse Gas Emissions and Sinks: 1990-2010, (EPA 430-R-12-001). Retrieved from <http://www.epa.gov/climatechange/emissions/usinventoryreport.html>.
- United States Energy Information Administration. (2013). State-Level Energy-Related Carbon Dioxide Emissions 2001-2010. Retrieved June 15, 2014 from <http://www.eia.gov/environment/emissions/state/analysis/pdf/stateanalysis.pdf>.
- United States Geological Survey. (2009). Survey Fact Sheet 2009–3098, Summary of estimated water use in the United States in 2005. Department of the Interior, USGS, Retrieved from <http://pubs.usgs.gov/fs/2009/3098/pdf/2009-3098.pdf>.
- Valigore, J.M., Gostomski, P.A., Wareham, D.G., O’Sullivan, A.D. (2012). Effects of hydraulic and solids retention times on productivity and settleability of microbial (microalgal-bacterial) biomass grown on primary treated wastewater as a biofuel feedstock, *Water Research*. 46,(9), 2957–2964.
- Volkman, H., Imianovsky, U., Oliveira, J.L.B., Anna, E.S.S. (2008). Cultivation of *Arthrospira* (spirulina) platensis in desalinator wastewater and salinated synthetic medium: Protein content and amino-acid profile, *Braz. J. Microbiol.* 39, 98–101.
- Wang, B., Li, Y., Wu, N. and Lan, C. Q. (2008). CO₂ bio-mitigation using

microalgae. *Applied microbiology and biotechnology* 79, 707–18.

Wang, L., Min, M., Li, Y., Chen, P., Chen, Y., Liu, Y., Wang, Y., Ruan, R. (2010). Cultivation of green algae *Chlorella* sp. in different wastewaters from municipal wastewater treatment plant, *Appl. Biochem. Biotechnol.* 162, 1174–1186.

Wang, L.K., Chen, J.P., Hung, Y., and Shamma, N.K. (2008). Membrane and desalination technologies. New York: Humana Press. Water Quality Association. (1999). Retrieved May 23, 2012 from <http://www.wqa.org/glossary.cfm?gl=1874>

Weldy, C. S., Huesemann, M. (2007). Lipid production by *Dunaliella salina* in batch culture: effects of nitrogen limitation and light intensity. U.S. Department of Energy. *Journal of Undergraduate Research.* 7, 115-122.

Wetterau, G. (2011). *Desalination of seawater: AWWA manual M61*. Denver, CO: American Water Works Association.

Wood, A.M., Everroad, R.C., Wingard, L.M. (2005). Chapter 18: Measuring growth rates in microalgal cultures, in: R.A.Andersen (Ed.), *Algal Culturing Techniques*, Elsevier Academic Press, Burlington, MA, pp. 269–285.

World Business Council for Sustainable Development (WBCSD). (2005). Water facts and trends. Retrieved October 7, 2012, from http://www.unwater.org/downloads/Water_facts_and_trends.pdf.

World Health Organization. (2004). Facts and figures: Water, sanitation and hygiene links to health. Retrieved July 13, 2013, from http://www.who.int/water_sanitation_health/publications/factsfigures04/en/

World Health Organization. (2008). Guidelines for Drinking-water Quality. Retrieved August 15, 2012, from http://www.who.int/water_sanitation_health/dwq/fulltext.pdf

Yang, J., Xu, M., Zhang, X., Hu, Q., Sommerfeld, M., Chen, Y. (2011). Life-cycle analysis on biodiesel production from microalgae: Water footprint and nutrients balance. *Bioresource Technology* 10 2 (1) 159-165.

Younos, T., Tulou, K. E. (2005), Overview of Desalination Techniques. *Journal of Contemporary water research and education.* 132, 3-10

Younos, Tamim. (2005), The Economics of Desalination. *Contemporary water research and education.* 132, 39-45

Yuhas, E., Daniles, T. (2006). The US Freshwater Supply Shortage: Experiences with Desalination as Part of the Solution, *Journal of Environmental Planning and Management*, 49,(4), 571 – 585.

Tables

Chapter 1

Table 1.1. Classification of Water Based on TDS Levels (WQA, 1999)

Water type	Range mg/L TDS
Fresh water	< 1,000
Brackish water	1,000 - 5,000
Highly brackish water	5,000 - 15,000
Saline water	15,000 - 30,000
Saline water	15,000 - 30,000
Seawater	30,000-40,000
Brines	>40,000

Table 1.2. Desalination cost for various desalination technologies (\$/m³ freshwater - multiply by 3.8 for \$/1000 gal) (Younos, 2005)

Process	
Multistage flash (Seawater)	1.32-5.36
Multiple-effect distillation (Seawater)	0.46-8.5
Reverse osmosis (Seawater)	0.45-0.92
Reverse osmosis (Brackish Water)	0.37-0.7
Electrodialysis (Brackish water)	0.58

Table 1.3. Comparison between RO and EDR (Eltawi et al., 2009)

Process	Recovery and Total dissolved solids	Pros	Cons
RO	<ul style="list-style-type: none"> • 30–60% recovery • Possible for single pass (higher recoveries are possible for multiple passes) • Product water has less than 200 mg/L TDS when brackish water is the feed water source 	<ul style="list-style-type: none"> • Lower energy requirements • Relatively lower investment cost • No cooling water flow • Has a modular design, so maintenance does not require entire plant to shut down 	<ul style="list-style-type: none"> • Higher costs for chemical and membrane replacement • Membranes susceptible to biofouling • Minimum membrane life expectancy around 5–7 years • Mechanical failures possible due to high pressure operation
ED/EDR	<ul style="list-style-type: none"> • 85–94% recovery possible • Product water has 140–600 mg/L TDS 	<ul style="list-style-type: none"> • Energy usage is proportional to salts removed • Operational at low to moderate pressures • Higher membrane life of 7–10 years 	<ul style="list-style-type: none"> • Only suitable for feed water up to 12,000 mg/L TDS • Periodic cleaning of membranes required • Leaks may occur in membrane stacks

Table 1.4. Analysis of the four groundwater walls from (BGNDRF) (Tetra Tech, 2010).

Elements/ions	Range (mg/L)
Phosphorus Total (as P)	0.015-0.03
Nitrate+Nitrite (as N)	2.8-8.3
Bicarbonate Alkalinity (as CaCO ₃)	150-250
Calcium	49-550
Sulfate	580-3200
Magnesium	13-340
Sodium	310-720
Potassium	2.6-5.0

Chapter 2

Table 2.1. Methods of inland concentrate disposal in the U.S. (Mickley, 2009)

Disposal Method	(%)
Discharged to surface water	45
Discharged to wastewater treatment plants	27
Land application	8
Deep well injection	13
Evaporation ponds	4

Table 2.2. Net greenhouse gas emissions of conventional diesel, soybean biodiesel, and microalgae biodiesel (Batan et al., 2010)

Contribution	Conventional diesel	Soybean biodiesel	Microalgae biodiesel
CO ₂ (g. MJ ⁻¹)	14.69	-72.73	-59.49
CH ₄ (g. MJ ⁻¹)	2.48	2.48	0.74
N ₂ O (g. MJ ⁻¹)	0.07	0.58	-16.54
Net “strain to pump” GHG (gCO ₂ -eq/MJ)	17.24	-71.73	-75.29

Chapter 3

Table 3.1. Composition in reactors

	Reactor Conductivity ($\mu\text{S}/\text{cm}$)	Desalination Volume (L)	Concentrate Seed Microalgae	Seed Microalgae	Nutrient
D11,D12	31,800	2.0	0.1	<i>D. Salina</i>	SADS
D21,D22	25,442	2.0	0.1	<i>D. Salina</i>	SADS
D31,D32	31,800	2.0	0.08	<i>D. Salina</i>	BBM
D41,D42	25,442	2.0	0.08	<i>D. Salina</i>	BBM
S11,S12	35,800	1.9	0.1	<i>S. platensis</i>	SADS
S21,S22	25,100	1.9	0.1	<i>S. platensis</i>	SADS
S31,S32	35,800	1.9	0.1	<i>S. platensis</i>	F/2
S41,S42	25,100	1.9	0.1	<i>S. platensis</i>	F/2
R11,R12	21,000	2.1	0.1	BGNDRF species	SADS
R21,R22	27,100	2.1	0.1	BGNDRF species	SADS
R31,R32	35,500	2.1	0.1	BGNDRF species	SADS
R41,R42	48,500	2.1	0.1	BGNDRF species	SADS
R51,R52	52,600	2.1	0.1	BGNDRF species	SADS

Note: SADS is Supernatant from Anaerobic Digested Sludge after centrifuging at 10,000 rpm for 3 min twice. BBM is Bold's Basal Medium.

Chapter 4

Table 4.1. Maximum dry weight concentration in reactors

Reactors	Seed microalgae	Nutrient	Where highest dry weight occurs (Average)				
			Dry weight (g/L)	Optical density	pH	Temp (°F)	Culturing day
D1	<i>D. salina</i>	SADS ¹	1.36	2.00	8.5	75	37
D2	<i>D. salina</i>	SADS ¹	1.49	2.25	8.2	76	37
D3	<i>D. salina</i>	BBM ²	1.04	1.35	8.4	76	37
D4	<i>D. salina</i>	BBM ²	0.84	1.36	8.2	74	39
S1	<i>S. platensis</i>	SADS ¹	1.41	0.12	8.6	74	14
S2	<i>S. platensis</i>	SADS ¹	1.98	1.62	8.9	78	24
S3	<i>S. platensis</i>	F/2	1.24	0.43	8.5	73	20
S4	<i>S. platensis</i>	F/2	0.68	0.23	8.4	74	20

¹SADS is supernatant from anaerobic digested Sludge after centrifuging at 10,000 rpm for 3 min twice.

²BBM is Bold's Basal Medium.

Table 4.2. Analysis of variance for *D. salina*.

SOV	df	ss	adj ss	Ms	F	P-value
Conductivity	1	0.00405	0.00405	0.00405	1.29	0.32
Nutrient	1	0.55125	0.55125	0.55125	175.00	0.000
Conductivity*Nutrient	1	0.04205	0.04205	0.04205	13.35	0.000
Error	4	0.01260	0.01260	0.00315		
Total	7	0.60995				

Table 4.3. Analysis of variance for *D. salina*

Factors	P-value	Effect
A (level of conductivity)	>0.05	Non-Significant
B (type of nutrient)	<0.05	Significant
AB	<0.05	Significant

Table 4.4. Analysis of variance for *S. platensis*

SOV	df	ss	adj ss	Ms	F	P-value
Conductivity	1	0.01620	0.01620	0.01620	6.48	0.064
Nutrient	1	1.18580	1.18580	1.18580	474.32	0.000
Conductivity*Nutrient	1	0.54080	0.54080	0.54080	474.32	0.000
Error	4	0.01000	0.01000	0.00250		
Total	7	1.75280				

Table 4.5. Analysis of variance for *S. platensis*

Factors	P-value	Effect
A (level of conductivity)	>0.05	Non-Significant
B (type of nutrient)	<0.05	Significant

AB

<0.05

Significant

Table 4.6. Comparison of dry weight and specific growth rate between the study data and literature values for *D. salina*

<i>D. salina</i> data from the study		<i>D. salina</i> data from literature									
Water medium	Nutrient	Dry weight, g/L	Culturing time, day	Specific growth rate, d ⁻¹	Water medium	Nutrient	Dry weight, g/L	Culturing time, day	Specific growth rate, d ⁻¹	Type of reactor	Ref.
Conc. ^a	SADS	1.56	37	0.095	Sea Water	NaNO ₃	1.06	17	N/A	N/A	Huang et al., 2011
Conc. ^b	SADS	1.4	37	0.097	Sea Water	F/2	0.33	Semi- continuous	0.12-0.33	Open	Prieto et al., 2011
Conc. ^a	BBM	1.04	37	0.114	Sea Water	F/2	0.53	25, bench	0.33	Open	Prieto et al., 2011
Conc. ^b	BBM	0.84	39	0.106	Sea Water	F/2	1.65	Semi- continuous	0.22-0.46	Closed	Prieto et al., 2011
					Sea Water	F/2	2	25, bench	0.47	Closed	Prieto et al., 2011
					10% NaCl	J/1	N/A	N/A	0.28	N/A	García et al., 2007

Note: BBM is Bold's Basal Medium; Conc.^a is desalination concentrate which has conductivity 31,800 µS/cm; Conc.^b is desalination concentrate which has conductivity 25,442 µS/cm; and SADS is supernatant from anaerobic digested sludge after centrifugation at 10,000 rpm for 3 minutes twice.

Table 4.7. Comparison of dry weight and specific growth rate between study data and literature values for *S. platensis*

S. <i>platensis</i> data from the study		S. <i>platensis</i> data from literature								
Water medium	Nutrient	Dry weight, g/L	Culturing time, day	Specific growth Rate, d ⁻¹	Water medium	Nutrient	Dry weight, g/L	Culturing time, day	Specific growth rate, d ⁻¹	Ref.
Conc. ^a	SADS	1.52	14	0.03	PS	N/A	2.26-2.99	25	0.225	Leema et al., 2010
Conc. ^b	SADS	1.96	24	0.032	OP	Zarrouk's	1.1	8	N/A	Gitelson et al., 1995
Conc. ^a	F/2	1.28	31	0.034	DW	50%ADE	1.23	14	N/A	Kaushik et al., 2006
Conc. ^b	F/2	0.66	24	0.019	10% OM	Zarrouk's	0.8-1.0	21-25	N/A	Reichert et al., 2006
					CP	NO ₃ ⁻ , HCO ₃ ²⁻	1.7	N/A	N/A	Markou et al., 2012
					Desalination WW	N/A	2.59	N/A	N/A	Pandey et al., 2010; Jain et al., 2011
					30% petha	CFTRI	2.34	27	N/A	Ramanan et al., 2010

Note: Conc.^a is desalination concentrate which has conductivity 35,800 µS/cm; Conc.^b is desalination concentrate which has conductivity 25,100 µS/cm; ADE is anaerobically digested distillery effluent; OM is olive oil mill wastewater; NaOCl was used to decrease the phenol concentration and turbidity; PSS is pretreated sea water; OP is open pond, 2.5 m²; DW is distilled water; CP is closed photo bioreactor; CFTRI is prescribed medium (Jain et al., 2011); and SADS is supernatant from anaerobic digested sludge after centrifugation at 10,000 rpm for 3 minutes twice.

Table 4.8. Maximum dry weight concentration in reactors

Reactors	Seed microalgae	Desalination concentrate conductivity ($\mu\text{S/cm}$)	Nutrient	Where highest dry weight occurs				
				(Average)				
				Dry weight (g/L)	Optical density	pH	Temp ($^{\circ}\text{F}$)	Culturing time (days)
R1	BGNDRF	21,000	SADS	2.08	4.7	8.2	77	90
R2	BGNDRF	27,000	SADS	1.92	3.85	8.4	77	80
R3	BGNDRF	35,000	SADS	1.85	3.96	8.4	77	80
R4	BGNDRF	42,500	SADS	1.75	1.86	8.7	82	100
R5	BGNDRF	52,500	SADS	1.59	1.68	8.6	84	100

Note: BGNDRF is the Brackish Groundwater National Desalination Research Facility Microalgae species; and SADS is supernatant from anaerobic digested sludge after centrifugation at 10,000 rpm for 3 min twice.

Table 4.9. Analysis of variance for BGNDF species

SOV	df	ss	F	P-value
Regression	1	0.140206	150.54	0.001
Error	3	0.002794	0.000931	
Total	4	0.143000		

Figures

Chapter 1

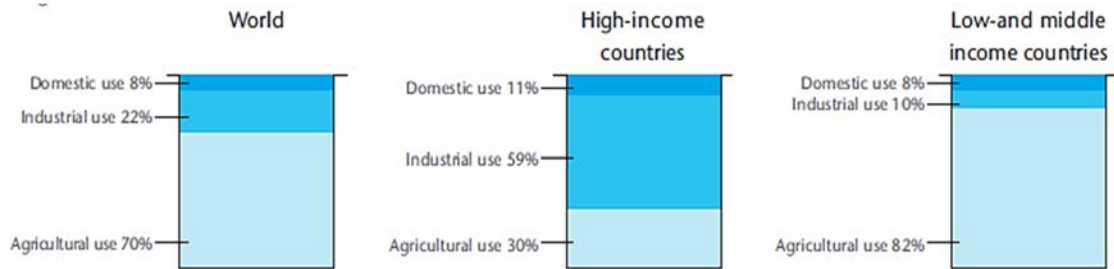


Figure 1.1. Main uses of water (WBCSD, 2005)

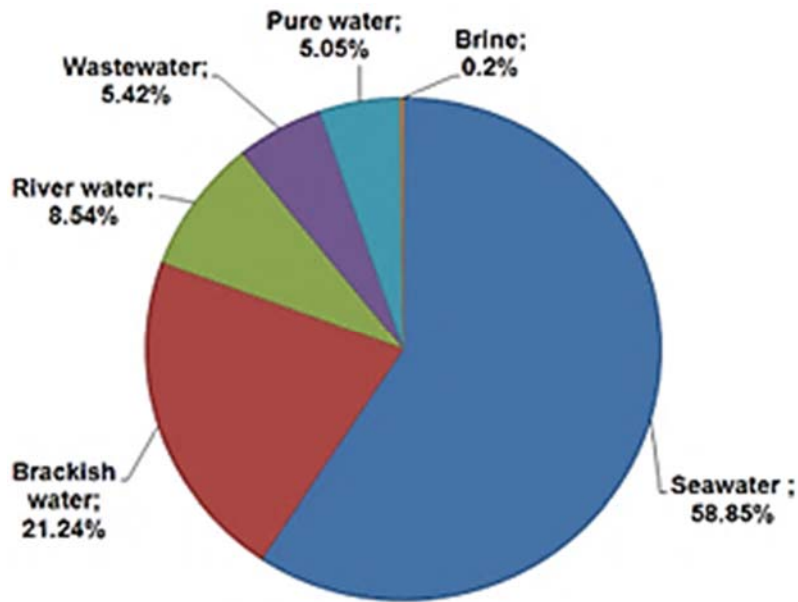
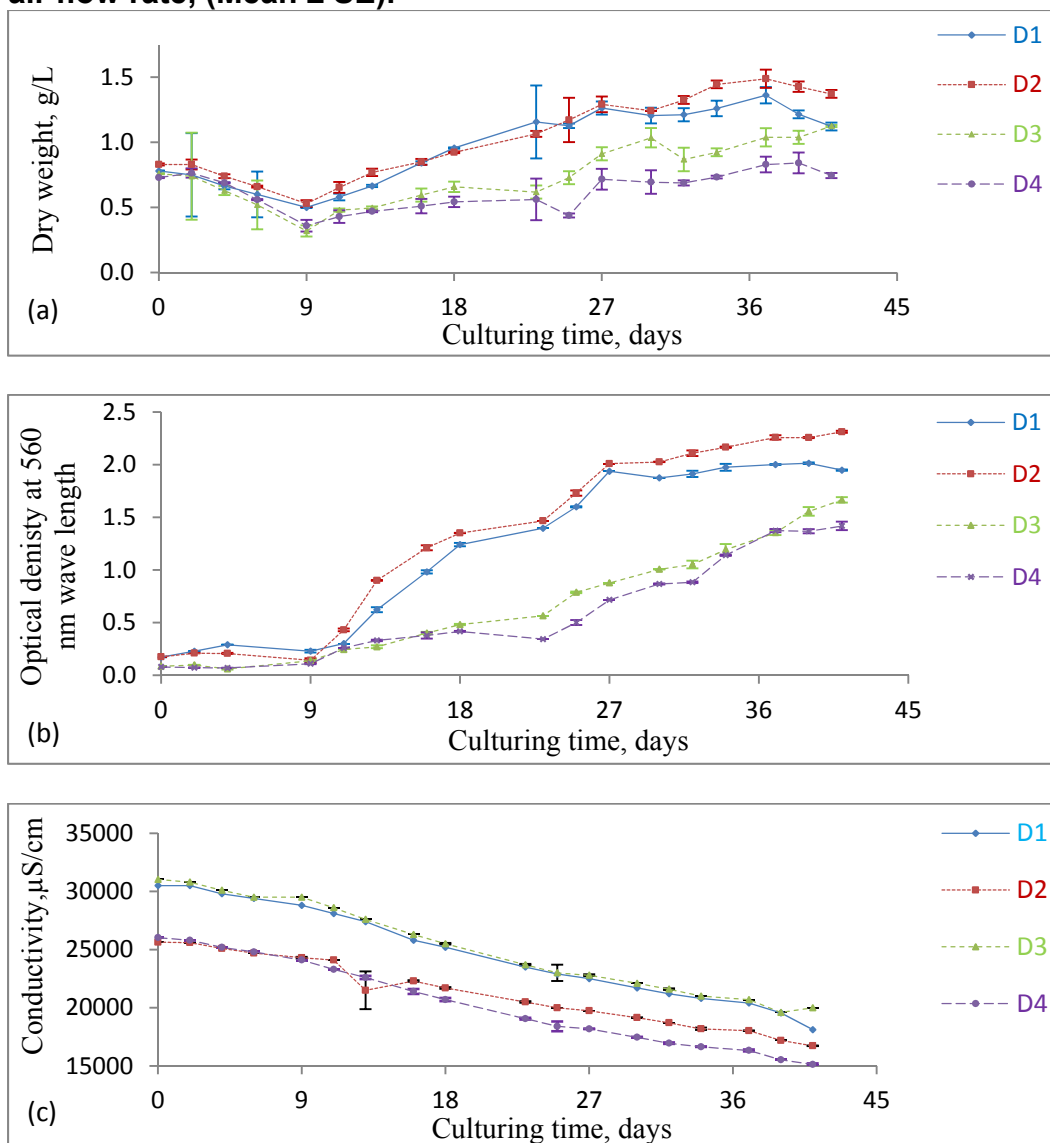
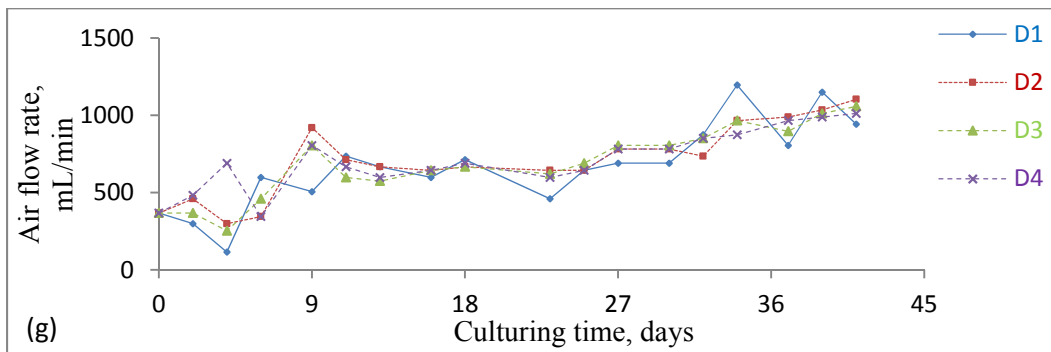
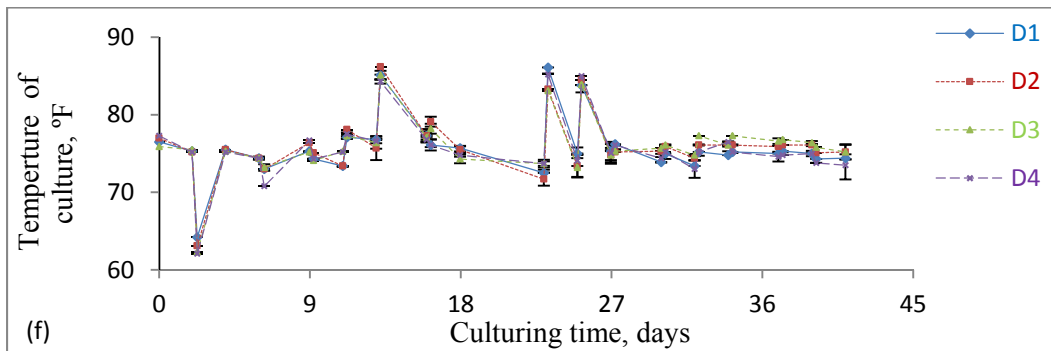
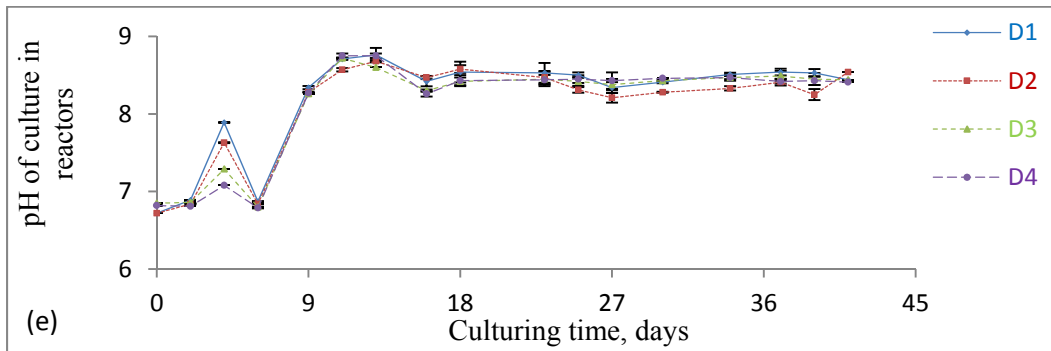
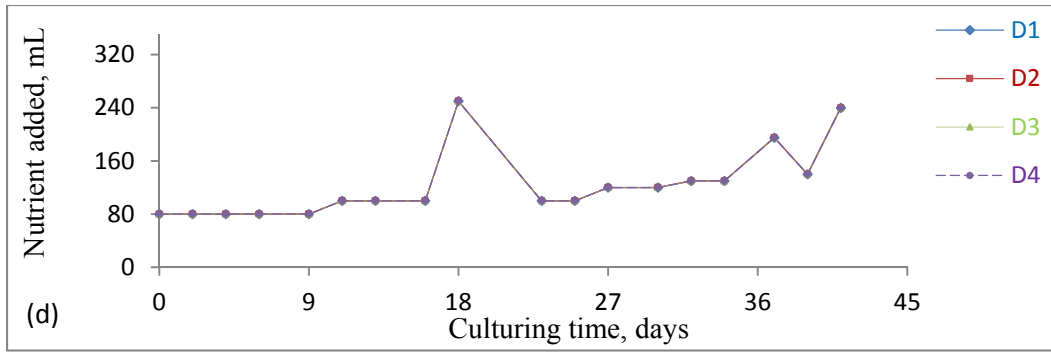


Figure 1.2. Worldwide sources of feedwater (Pankratz, 2012)

Chapter 4

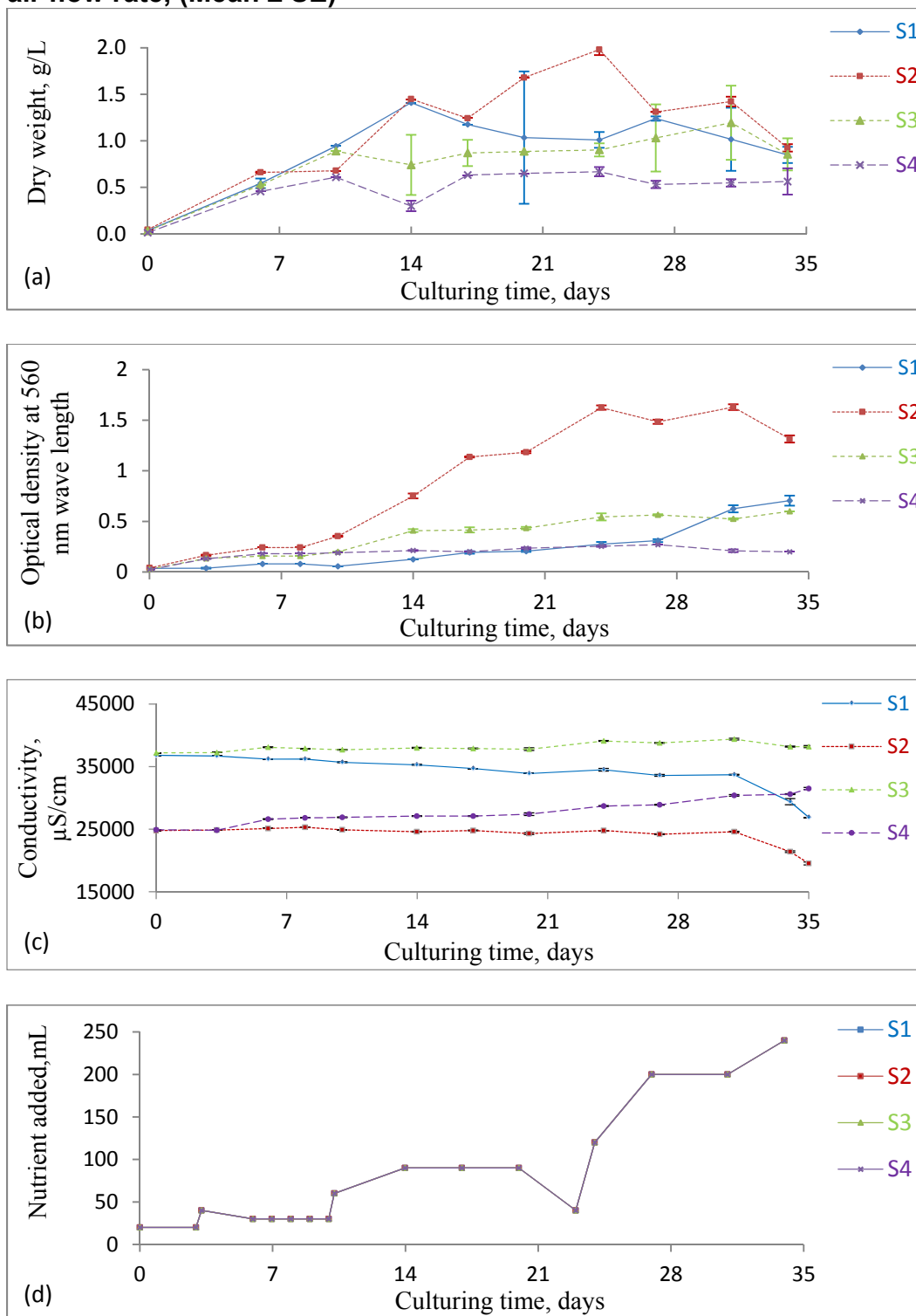
Figure 4.1. *D. salina's* growing characteristics with culturing time: (a) dry weight; (b) optical density; (c) conductivities of medium in reactors; (d) nutrient added into reactors; (e) pH; (f) temperature; (g) air flow rate, (Mean \pm SE).

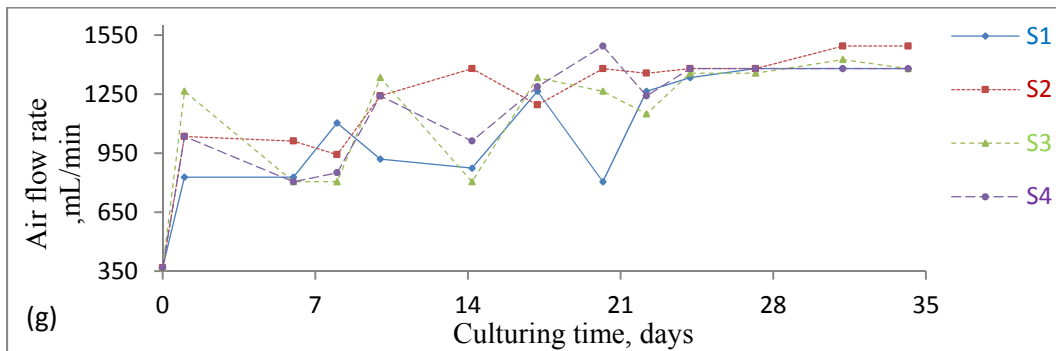
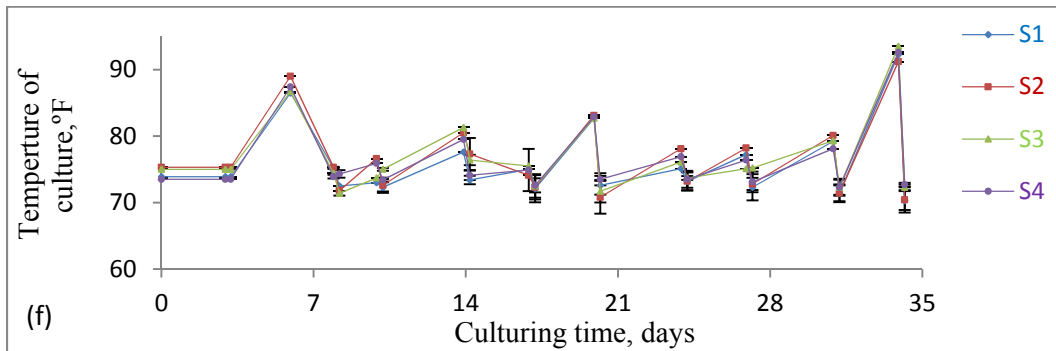
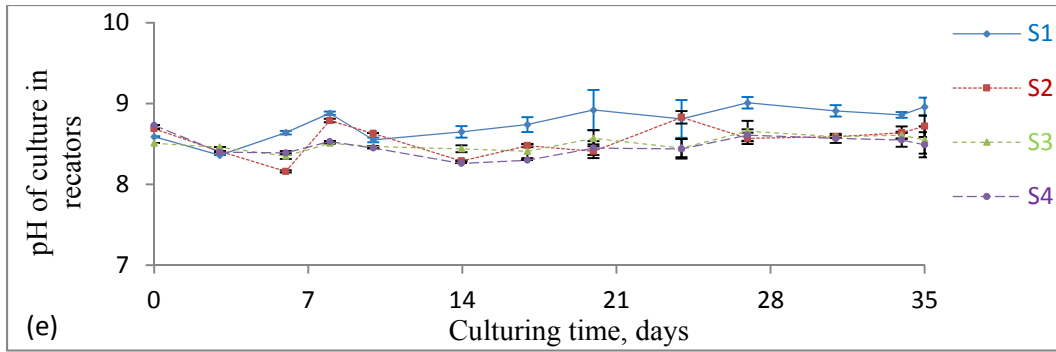




Note. SADS was added in reactors; D1 (31,800 $\mu\text{S/cm}$), D2 (25,442 $\mu\text{S/cm}$). BBM was added in Reactors; D3 (31,800 $\mu\text{S/cm}$), D4 (25,442 $\mu\text{S/cm}$).

Figure 4.2. *S. platensis*'s growing characteristics with culturing time: (a) dry weight; (b) optical density; (c) conductivities of medium in reactors; (d) nutrient added into reactors; (e) pH; (f) temperature; (g) air flow rate, (Mean \pm SE)





Note: SADS was added in reactors S1 (35,900 $\mu\text{S/cm}$), S2 (25500 $\mu\text{S/cm}$). F/2 was added in Reactors S3 (35,900 $\mu\text{S/cm}$), S4 (25500 $\mu\text{S/cm}$)

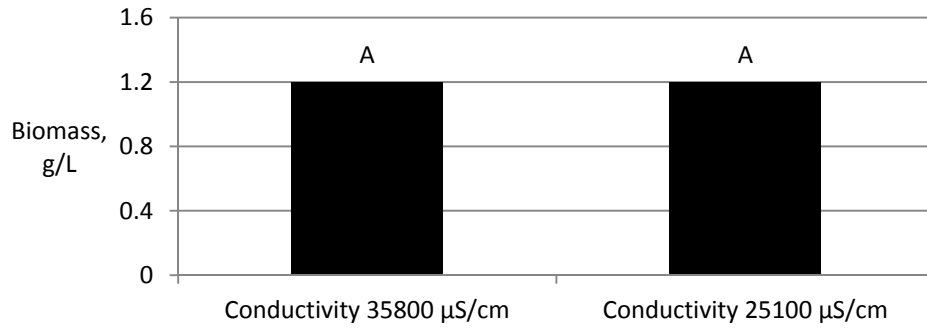


Figure 4.3. Effect of conductivity on biomass

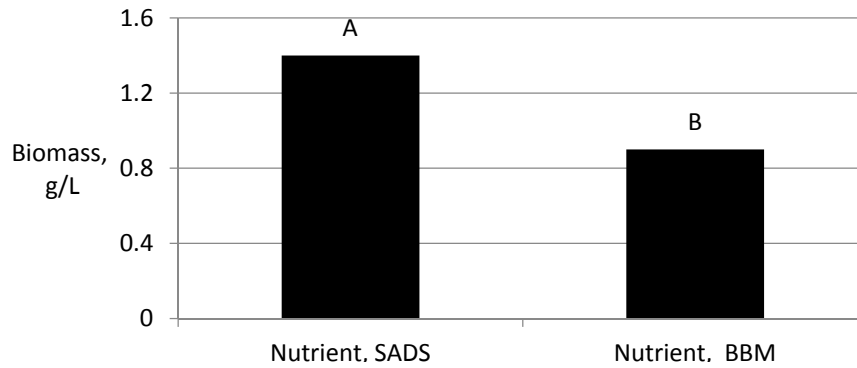


Figure 4.4. Effect of nutrient type on biomass

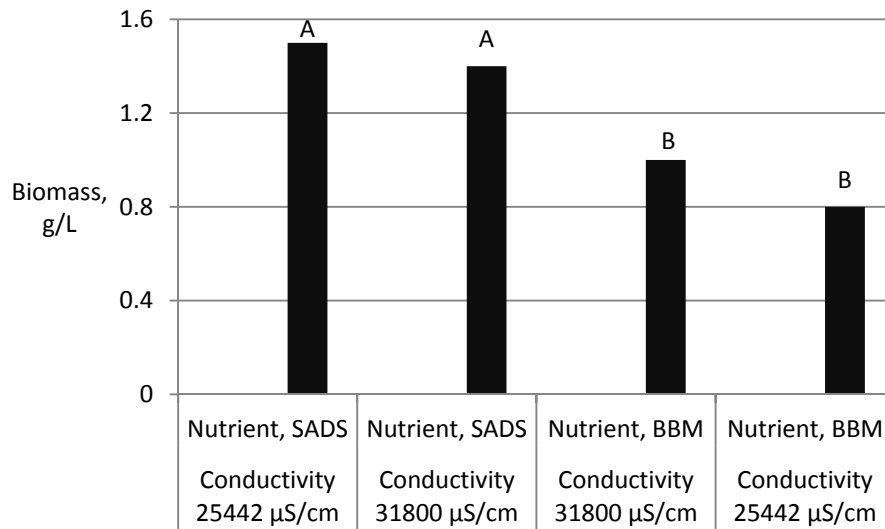


Figure 4.5. Effect of conductivity and nutrient type on biomass

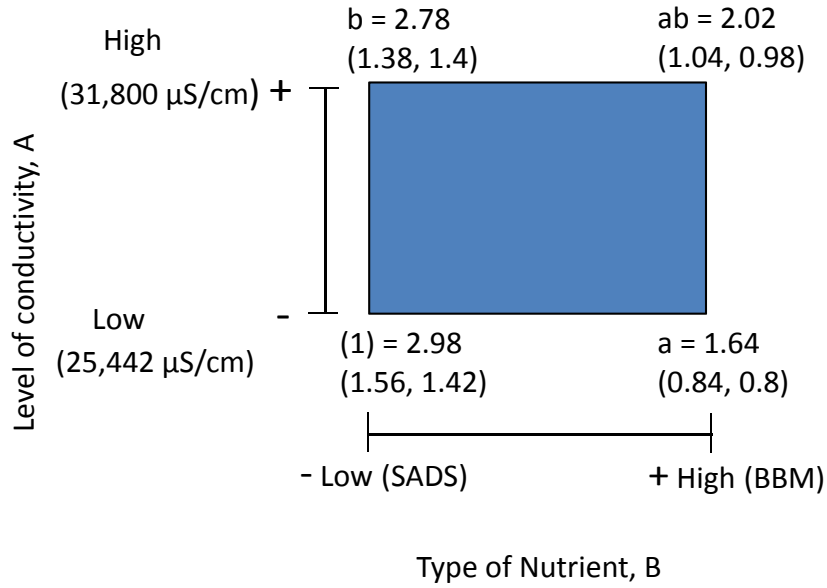


Figure 4.6. Combination in the 2² design

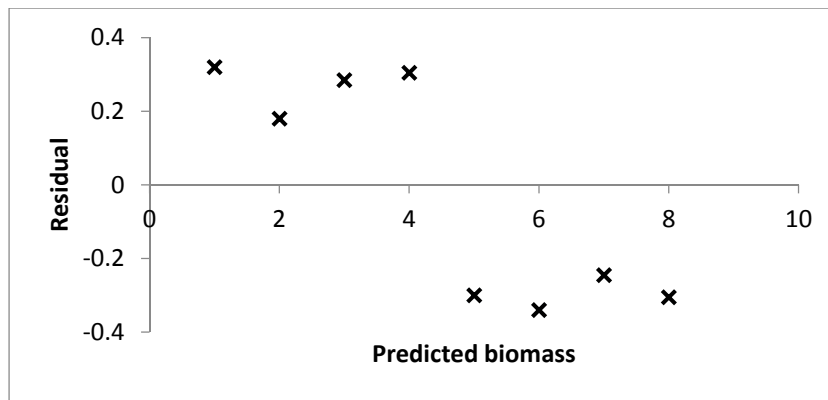


Figure 4.7. Residuals vs. predicted maximum biomass

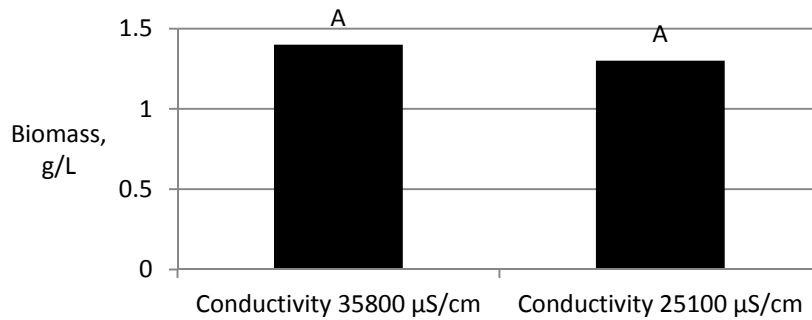


Figure 4.8. Effect of conductivity on biomass

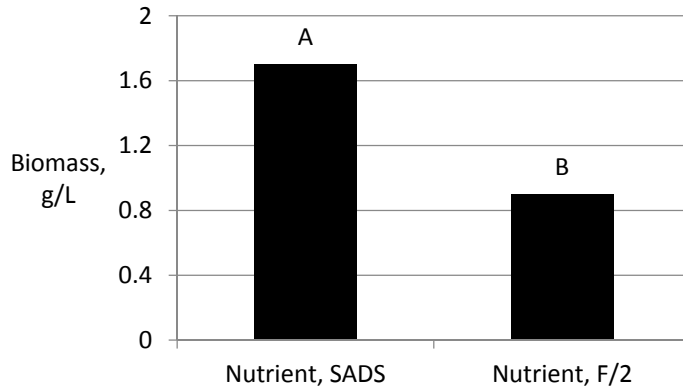


Figure 4.9. Effect of conductivity and nutrient type on biomass

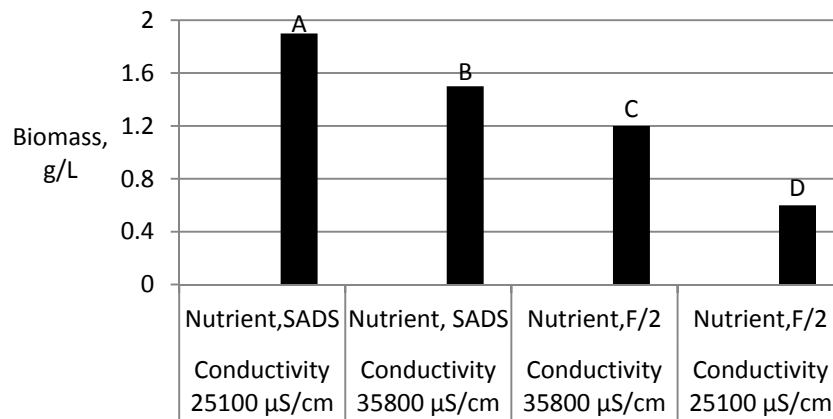


Figure 4.10. Effect of conductivity and nutrient type on biomass

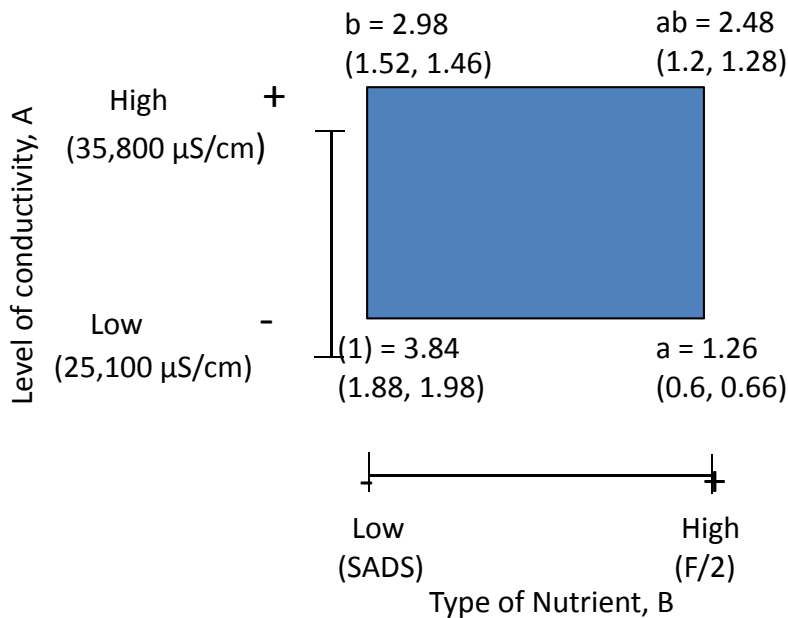


Figure 4.11. Combination in the 2² design

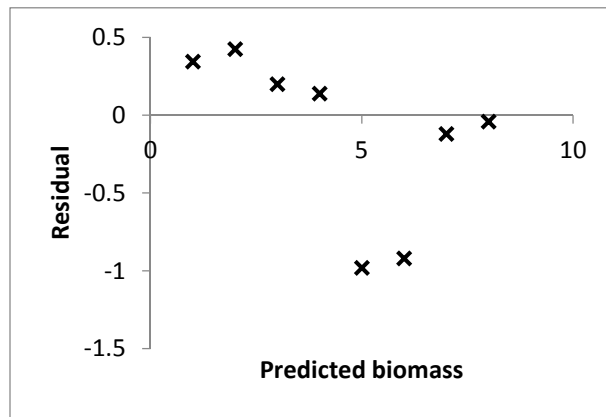
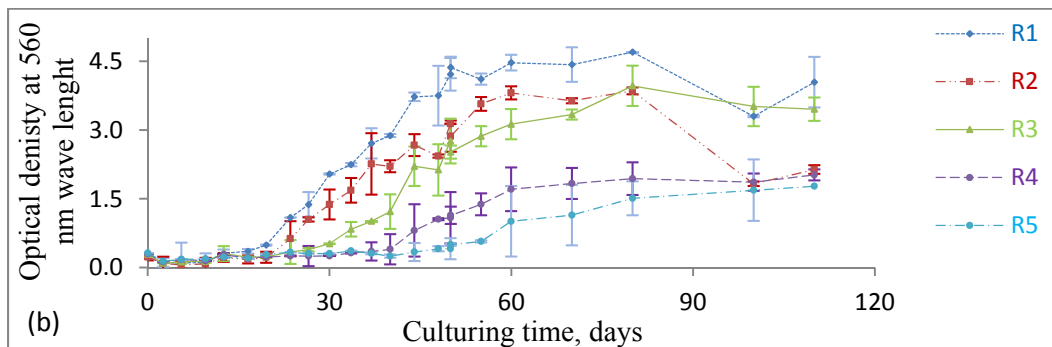
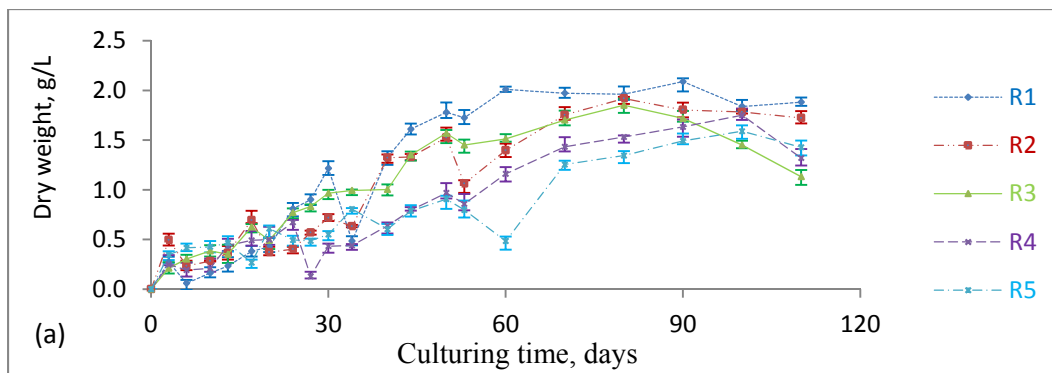
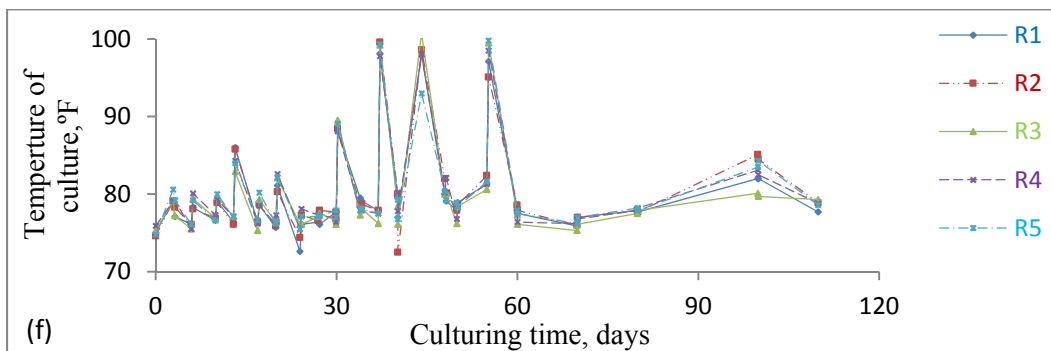
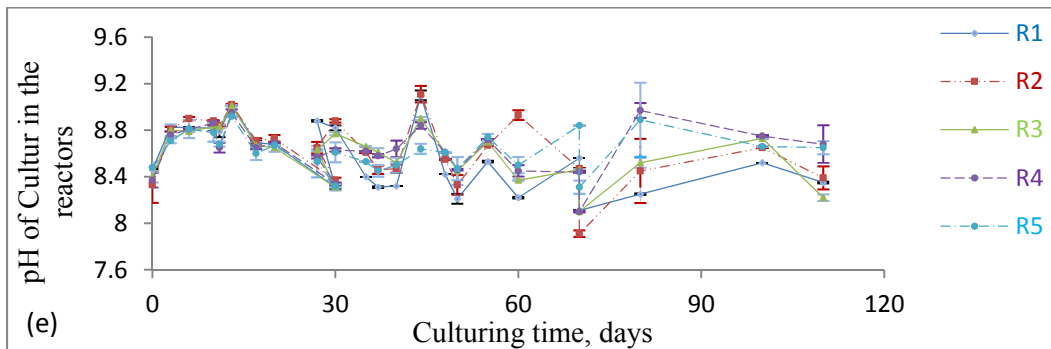
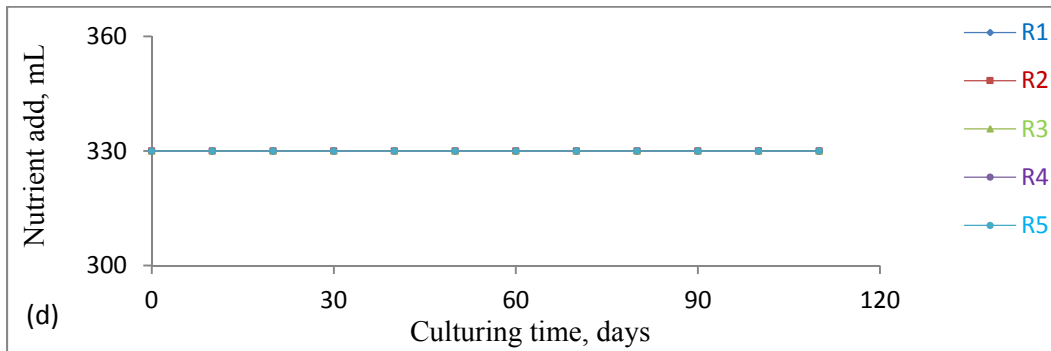
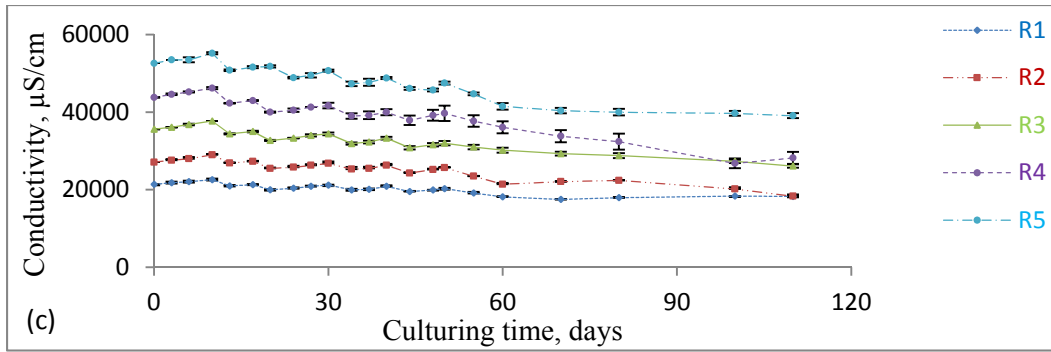


Figure 4.12. Residuals vs. predicted maxima biomass

Figure 4.13. BGNDRF species growing characteristics with time: a) dry weight; (b) optical density; (c) conductivities of medium in reactors; (d) nutrient added into reactors; (e) pH; (f) temperature; (g) air flow rate, (Mean \pm SE).





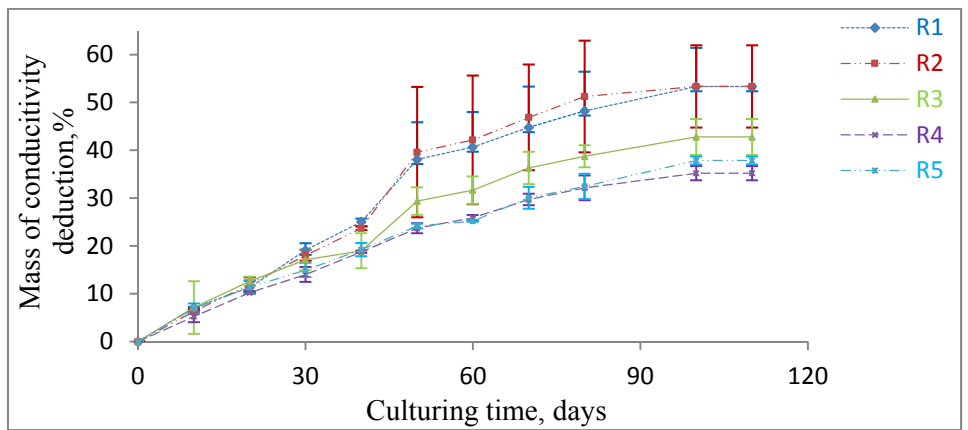
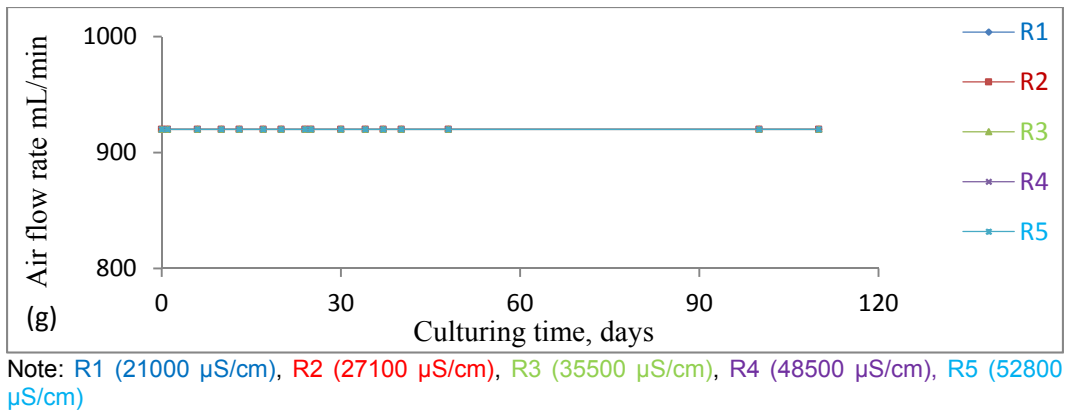


Figure 4.14. Mass of conductivity deduction vs. culturing time (Mean \pm SE).

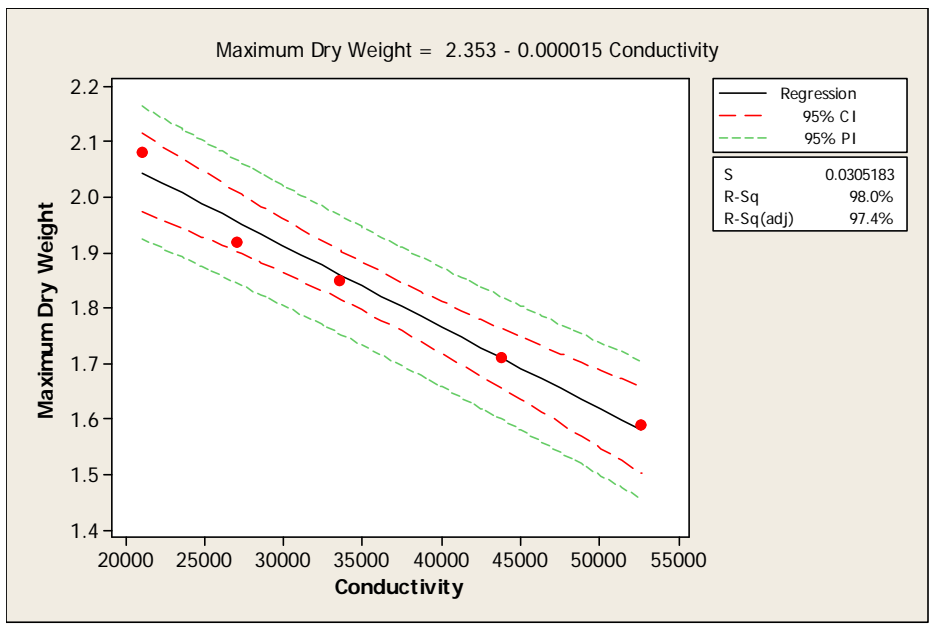


Figure 4.15. Maximum dry weights vs. initial conductivity

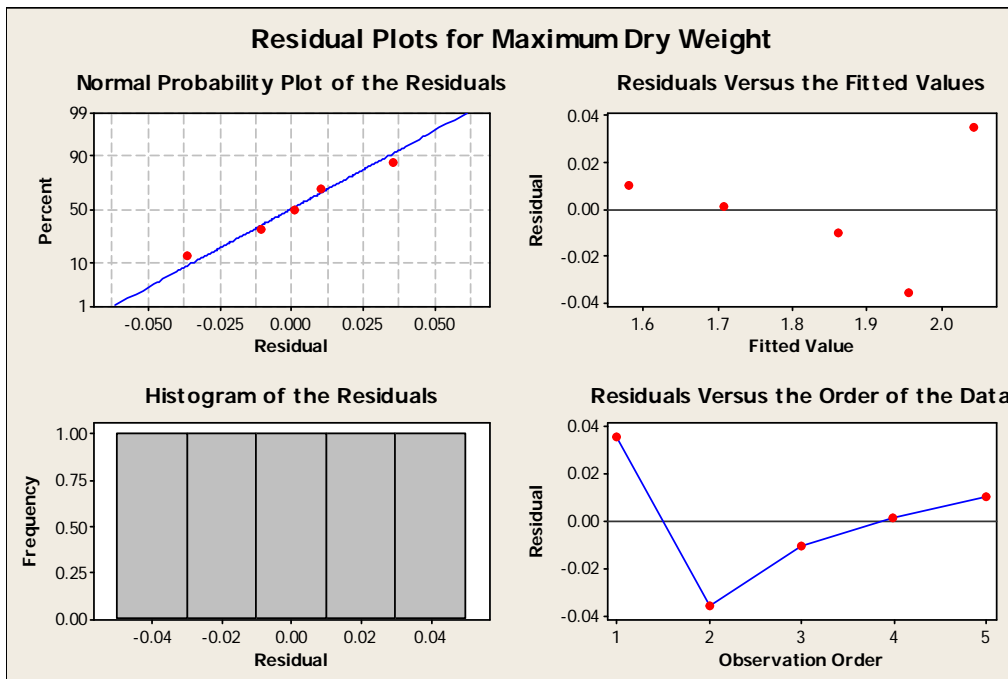


Figure 4.16. Residual Plots for Maximum Dry Weight

Chapter 7 – APPENDIX

Appendix A

Units of Measure

°C	Degree(s) Celsius
°F	Degree(s) Fahrenheit
ft	Feet
g	Gram(s)
g/L	Gram(s) per liter
g/L/d	Gram(s) per liter per day
g. MJ ⁻¹	Gram(s) per mega joule(s)
GPD	Gallon(s) per day
Kg	kilogram
KWh	kilowatt hour

L	Liter(s)
m ³	Cubic meter(s)
mg/L	Milligram(s) per liter
MJ	Mega Joule
MGD	Million gallon(s) per day
ppm	Part per million
Rpm	Revolutions per minute
μm	Micrometer(s)
μS/cm	Micro-Siemens per centimeter
%	Percentage

Appendix B

Elements/Ions in Anaerobic Digested Sludge (EPA, 2006)

Elements/ions	Range (mg/L)
Ammonia Nitrogen	1,500–3,000
Sodium	3,500–5,500
Calcium	1,500–4,500
Magnesium	1,000–1,500
Potassium	2,500–4,500

Anaerobic digested sludge also contains other elements such as copper, chromium VI, chromium, nickel and zinc.

Appendix C

BBM Recipe

To 940 ml of distilled water	Salt	g/400 ml dH ₂ O
Add 10 ml of each of the	NaNO ₃	10.0
Following stock solutions:	CaCl ₂ .2H ₂ O	1.0
	MgSO ₄ .7H ₂ O	3.0
	KH ₂ PO ₄	3.0
	NaCl	1.0

Next, add 1 ml of each of the trace element stock solution:

(1) EGTA: 50 g

KOH: 31 g

1.0 L dH₂O

(2) FeSO₄.7H₂O: 4.98 g

1.0 ml H₂SO₄

999ml dH₂O

(3) H₃BO₃: 11.42 g

1.0 dH₂O

(4) ZnSO₄.7H₂O: 8.82 g

MnCl₂.4H₂O: 1.44 g

MoO₃: 0.71 g

CuSO₄.5H₂O: 1.57 g

Co(NO₃).6H₂O: 0.49 g

1.0 L dH₂O

Appendix D

F/2 Recipe

For one liter of F/2

1. To approximately 950 mL of non-pasteurized seawater, add each of the components in the order specified in the table (except vitamins) while stirring continuously.
2. Bring total volume to 1 L with non-pasteurized seawater.
3. Cover and autoclave medium.
4. When cooled add sterile vitamins.
5. Store at refrigerator temperature.

Component	Amount	Stock Solution
NaNO ₃	1 mL	7.5 g/100 mL dH ₂ O
NaH ₂ PO ₄ •H ₂ O	1 mL	0.5 g/100 mL dH ₂ O
Na ₂ SiO ₃ •9H ₂ O	1 mL	3 g/100 mL dH ₂ O
Trace Metals Solution	1 mL/L	
Vitamin B12	1 mL/L	
Biotin Vitamin Solution	1 mL/L	
Thiamine Vitamin Solution		

Appendix E

Data Record

Nutrient (mL)

Reactors: D1-D4; Seed microalgae: *D. salina*

Day	D1-1 (SADS)	D1-2 (SADS)	D1 (average)	D2-1 (SADS)	D2-2 (SADS)	D2 (average)
0	80	80	80	80	80	80
2	80	80	80	80	80	80
4	80	80	80	80	80	80
6	80	80	80	80	80	80
9	80	80	80	80	80	80
11	100	100	100	100	100	100
13	100	100	100	100	100	100
16	100	100	100	100	100	100
18	250	250	250	250	250	250
23	100	100	100	100	100	100
25	100	100	100	100	100	100
27	120	120	120	120	120	120
30	120	120	120	120	120	120
32	130	130	130	130	130	130
34	130	130	130	130	130	130
37	195	195	195	195	195	195

39	140	140	140	140	140	140
41	240	240	240	240	240	240

Day	D3-1 (BBM)	D3-2 (BBM)	D3 (average)	D4-1 (BBM)	D4-2 (BBM)	D4 (average)
0	80	80	80	80	80	80
2	80	80	80	80	80	80
4	80	80	80	80	80	80
6	80	80	80	80	80	80
9	80	80	80	80	80	80
11	100	100	100	100	100	100
13	100	100	100	100	100	100
16	100	100	100	100	100	100
18	250	250	250	250	250	250
23	100	100	100	100	100	100
25	100	100	100	100	100	100
27	120	120	120	120	120	120
30	120	120	120	120	120	120
32	130	130	130	130	130	130
34	130	130	130	130	130	130
37	195	195	195	195	195	195
39	140	140	140	140	140	140
41	240	240	240	240	240	240

Reactors: S1-S4; Seed microalgae: *S. platensis*

Day	S1-1 (SADS)	S1-2 (SADS)	S1 (average)	S2-1 (SADS)	S2-2 (SADS)	S2 (average)
0	20	20	20	20	20	20
6	20	20	20	20	20	20
7	40	40	40	40	40	40
8	30	30	30	30	30	30
9	30	30	30	30	30	30
10	30	30	30	30	30	30
14	90	90	90	90	90	90
17	90	90	90	90	90	90
20	90	90	90	90	90	90
24	120	120	120	120	120	120
27	200	200	200	200	200	200
31	200	200	200	200	200	200
34	240	240	240	240	240	240

Day	S3-1 (f/2)	S3-2 (f/2)	S3 (average)	S4-1 (f/2)	S4-2 (f/2)	S4 (average)
0	20	20	20	20	20	20
6	20	20	20	20	20	20
7	40	40	40	40	40	40
8	30	30	30	30	30	30
9	30	30	30	30	30	30
10	30	30	30	30	30	30
14	90	90	90	90	90	90
17	90	90	90	90	90	90
20	90	90	90	90	90	90
24	120	120	120	120	120	120
27	200	200	200	200	200	200
31	200	200	200	200	200	200
34	240	240	240	240	240	240

Dry Biomass (g/L)

Reactors: D1-D4; Seed microalgae: *D. salina*

Day	D1-1	D1-2	D1 (average)	D2-1	D2-2	D2 (average)
0	0.76	0.76	0.76	0.83	0.83	0.83
2	0.43	1.08	0.755	0.79	0.87	0.83
4	0.67	0.69	0.68	0.72	0.76	0.74
6	0.42	0.78	0.6	0.64	0.68	0.66

9	0.5	0.5	0.5	0.55	0.51	0.53
11	0.66	0.64	0.65	0.68	0.62	0.65
13	0.69	0.63	0.66	0.79	0.75	0.77
16	0.87	0.83	0.85	0.86	0.84	0.85
18	0.97	0.93	0.95	0.91	0.93	0.92
23	0.88	1.43	1.155	1.08	1.04	1.06
25	1.1	1.14	1.12	0.98	1.36	1.17
27	1.22	1.3	1.26	1.31	1.27	1.29
30	1.15	1.28	1.215	1.25	1.23	1.24
32	1.16	1.26	1.21	1.28	1.36	1.32
34	1.2	1.32	1.26	1.39	1.49	1.44
37	1.31	1.41	1.36	1.41	1.55	1.48
39	1.27	1.15	1.21	1.38	1.46	1.42
41	1.13	1.11	1.12	1.41	1.34	1.375
Day						
	D3-1	D3-2	D3 (average)	D4-1	D4-2	D4 (average)
0	0.76	0.76	0.76	0.73	0.73	0.73
2	0.41	1.08	0.745	0.71	0.81	0.76
4	0.58	0.68	0.63	0.66	0.7	0.68
6	0.35	0.7	0.525	0.54	0.58	0.56
9	0.33	0.32	0.325	0.31	0.41	0.36
11	0.47	0.49	0.48	0.44	0.42	0.43
13	0.28	0.3	0.29	0.46	0.48	0.47
16	0.6	0.58	0.59	0.56	0.46	0.51
18	0.64	0.66	0.65	0.55	0.53	0.54
23	0.6	0.62	0.61	0.73	0.39	0.56
25	0.73	0.71	0.72	0.42	0.44	0.43
27	0.93	0.89	0.91	0.67	0.76	0.715
30	1.08	0.98	1.03	0.61	0.76	0.685
32	0.78	0.94	0.86	0.67	0.69	0.68
34	0.9	0.94	0.92	0.72	0.74	0.73
37	0.88	1.19	1.035	0.78	0.88	0.83
39	0.9	1.17	1.035	0.76	0.92	0.84
41	1.1	1.14	1.12	0.746	0.744	0.745

Reactors: S1-S4; Seed microalgae: *S. platensis*

Day	S1-1	S1-2	S1 (average)	S2-1	S2-2	S2 (average)
0	0.0326	0.0366	0.0346	0.0427	0.0487	0.0457
6	0.548	0.538	0.543	0.66	0.662	0.661
10	0.941	0.945	0.943	0.69	0.67	0.68
14	1.13	1.15	1.14	1.445	1.466	1.4555
17	1.166	1.187	1.1765	1.223	1.263	1.243
20	1.641	0.43	1.0355	1.689	1.67	1.6795
24	1.05	0.97	1.01	1.995	1.98	1.9875
27	1.25	1.23	1.24	1.3	1.32	1.31
31	1.315	0.7182	1.0166	1.43	1.41	1.42
34	0.9528	0.744	0.8484	0.928	0.923	0.9255

Day	S3-1	S3-2	S3 (average)	S4-1	S4-2	S4 (average)
0	0.031	0.031	0.031	0.0137	0.0137	0.0137
6	0.502	0.551	0.5265	0.446	0.466	0.456
10	0.88	0.9	0.89	0.6	0.62	0.61
14	0.39	1.09	0.74	0.28	0.32	0.3
17	0.739	0.999	0.869	0.613	0.653	0.633
20	0.884	0.886	0.885	0.66	0.64	0.65
24	0.8996	0.908	0.9038	0.67	0.666	0.668
27	0.6528	1.4102	1.0315	0.525	0.538	0.5315
31	0.692	1.689	1.1905	0.546	0.55	0.548
34	0.845	0.865	0.855	0.674	0.452	0.563

Optical Density at 560 nmReactors: D1-D4; Seed microalgae: *D. salina*

Day	D1-1	D1-2	D1 (average)	D2-1	D2-2	D2 (average)
0	0.1715	0.1715	0.1715	0.1715	0.1715	0.1715
2	0.02273	0.02277	0.02275	0.2104	0.2106	0.2105
4	0.2898	0.2892	0.2895	0.2071	0.2079	0.2075
6	0.2291	0.2289	0.229	0.1425	0.1435	0.143
9	0.3	0.301	0.3005	0.4318	0.4312	0.4315
11	0.6223	0.6228	0.62255	0.9007	0.9013	0.901
13	0.98	0.984	0.982	1.198	1.222	1.21
16	1.237	1.245	1.241	1.351	1.353	1.352
18	1.397	1.396	1.3965	1.4677	1.4673	1.4675
23	1.59	1.61	1.6	1.737	1.725	1.731
25	1.9371	1.9379	1.9375	2.0108	2.0102	2.0105
27	1.877	1.873	1.875	2.02	2.034	2.027
30	1.898	1.929	1.9135	2.1212	2.098	2.1096
32	1.955	1.996	1.9755	2.1668	2.1662	2.1665
34	2.001	2.003	2.002	2.257	2.261	2.259
37	2.019	2.009	2.014	2.251	2.266	2.2585
39	1.9482	1.9488	1.9485	2.311	2.315	2.313
41	0.1715	0.1715	0.1715	0.1715	0.1715	0.1715

Day	D3-1	D3-2	D3 (average)	D4-1	D4-2	D4 (average)
0	0.0855	0.0855	0.0855	0.08	0.08	0.08
2	0.0978	0.0982	0.098	0.0725	0.0725	0.0725
4	0.062	0.06	0.061	0.0705	0.0695	0.07
6	0.1398	0.1382	0.139	0.107	0.113	0.11
9	0.2442	0.2448	0.2445	0.2606	0.2594	0.26
11	0.2711	0.2699	0.2705	0.33	0.332	0.331
13	0.395	0.407	0.401	0.378	0.378	0.378
16	0.489	0.475	0.482	0.414	0.42	0.417
18	0.5649	0.5661	0.5655	0.3439	0.3431	0.3435
23	0.789	0.787	0.788	0.5	0.502	0.501
25	0.8769	0.8781	0.8775	0.7163	0.7168	0.71655
27	1.002	1.012	1.007	0.8664	0.8686	0.8675
30	1.0519	1.0531	1.0525	0.8827	0.8843	0.8835
32	1.1932	1.1938	1.1935	1.1412	1.1398	1.1405
34	1.359	1.351	1.355	1.371	1.377	1.374
37	1.5561	1.5569	1.5565	1.3671	1.3699	1.3685
39	1.6651	1.6659	1.6655	1.418	1.42	1.419
41	0.0855	0.0855	0.0855	0.08	0.08	0.08

Reactors: S1-S4; Seed microalgae: *S. platensis*

Day	S1-1	S1-2	S1 (average)	S2-1	S2-2	S2 (average)
0	0.036	0.036	0.036	0.0405	0.0405	0.0405
3	0.037	0.038	0.0375	0.165	0.167	0.166
6	0.082	0.078	0.08	0.243	0.241	0.242
8	0.081	0.079	0.08	0.241	0.243	0.242
10	0.057	0.056	0.0565	0.3537	0.3533	0.3535
14	0.124	0.126	0.125	0.7517	0.7513	0.7515
17	0.191	0.195	0.193	1.138	1.136	1.137
20	0.2054	0.2056	0.2055	1.183	1.185	1.184
24	0.271	0.279	0.275	1.657	1.594	1.6255
27	0.316	0.305	0.3105	1.486	1.484	1.485
31	0.641	0.609	0.625	1.6505	1.6095	1.63
34	0.754	0.656	0.705	1.361	1.27	1.3155

Day	S3-1	S3-2	S3 (average)	S4-1	S4-2	S4 (average)
0	0.028	0.028	0.028	0.0255	0.0255	0.0255
3	0.137	0.133	0.135	0.131	0.132	0.1315
6	0.1585	0.1575	0.158	0.182	0.18	0.181

8	0.159	0.157	0.158	0.182	0.18	0.181
10	0.198	0.2	0.199	0.195	0.185	0.19
14	0.407	0.411	0.409	0.211	0.215	0.213
17	0.418	0.414	0.416	0.203	0.201	0.202
20	0.437	0.431	0.434	0.2358	0.2352	0.2355
24	0.542	0.548	0.545	0.252	0.258	0.255
27	0.564	0.566	0.565	0.2701	0.2699	0.27
31	0.524	0.526	0.525	0.2107	0.2094	0.21005
34	0.609	0.592	0.6005	0.205	0.195	0.2

pH**Reactors: D1-D4; Seed microalgae: *D. salina***

Day	D1-1	D1-2	D1 (average)	D2-1	D2-2	D2 (average)
0	6.72	6.72	6.72	6.72	6.72	6.72
2	6.9	6.9	6.9	6.82	6.86	6.84
4	7.88	7.9	7.89	7.61	7.65	7.63
6	6.89	6.85	6.87	6.82	6.86	6.84
9	8.35	8.33	8.34	8.3	8.26	8.28
11	8.7	8.72	8.71	8.59	8.55	8.57
13	8.87	8.65	8.76	8.7	8.66	8.68
16	8.38	8.46	8.42	8.48	8.48	8.48
18	8.45	8.63	8.54	8.59	8.57	8.58
23	8.44	8.62	8.53	8.38	8.56	8.47
25	8.57	8.43	8.5	8.33	8.29	8.31
27	8.25	8.43	8.34	8.18	8.25	8.215
30	8.4	8.42	8.41	8.29	8.27	8.28
32	8.52	8.5	8.51	8.34	8.32	8.33
34	8.55	8.53	8.54	8.34	8.48	8.41
37	8.52	8.54	8.53	8.36	8.14	8.25
39	8.43	8.45	8.44	8.55	8.56	8.555
41	6.72	6.72	6.72	6.72	6.72	6.72

Day	D3-1	D3-2	D3 (average)	D4-1	D4-2	D4 (average)
0	6.85	6.85	6.85	6.82	6.82	6.82
2	6.86	6.86	6.86	6.79	6.83	6.81
4	7.26	7.22	7.24	7.07	7.09	7.08
6	6.8	6.8	6.8	6.76	6.82	6.79
9	8.25	8.27	8.26	8.28	8.26	8.27
11	8.71	8.73	8.72	8.74	8.76	8.75
13	8.65	8.55	8.6	8.72	8.78	8.75
16	8.31	8.29	8.3	8.2	8.2	8.2
18	8.41	8.43	8.43	8.38	8.48	8.43
23	8.52	8.38	8.45	8.43	8.45	8.44
25	8.43	8.41	8.42	8.43	8.42	8.425
27	8.37	8.39	8.38	8.52	8.34	8.43
30	8.44	8.42	8.43	8.46	8.46	8.46
32	8.48	8.46	8.47	8.46	8.49	8.475
34	8.47	8.52	8.495	8.41	8.43	8.42
37	8.48	8.42	8.45	8.38	8.48	8.43
39	8.44	8.44	8.44	8.42	8.4	8.41
41	6.85	6.85	6.85	6.82	6.82	6.82

Reactors: S1-S4; Seed microalgae: *S. platensis*

Day	S1-1	S1-2	S1 (average)	S2-1	S2-2	S2 (average)
0	8.59	8.59	8.59	8.69	8.69	8.69
3	8.35	8.37	8.36	8.4	8.42	8.41
6	8.62	8.66	8.64	8.17	8.15	8.16
8	8.89	8.87	8.88	8.77	8.81	8.79
10	8.56	8.54	8.55	8.61	8.65	8.63
14	8.66	8.64	8.65	8.3	8.28	8.29
17	8.79	8.69	8.74	8.47	8.49	8.48
20	9.22	8.62	8.92	8.43	8.39	8.41

24	8.98	8.64	8.81	8.95	8.71	8.83
27	9.02	9	9.01	8.54	8.6	8.57
31	8.9	8.92	8.91	8.6	8.58	8.59
34	8.87	8.86	8.865	8.69	8.59	8.64

Day	S3-1	S3-2	S3 (average)	S4-1	S4-2	S4 (average)
0	8.51	8.51	8.51	8.73	8.73	8.73
3	8.47	8.45	8.46	8.4	8.4	8.4
6	8.34	8.36	8.35	8.4	8.38	8.39
8	8.53	8.49	8.51	8.53	8.53	8.53
10	8.49	8.45	8.47	8.46	8.44	8.45
14	8.45	8.46	8.455	8.26	8.26	8.26
17	8.51	8.31	8.41	8.28	8.32	8.3
20	8.46	8.68	8.57	8.51	8.39	8.45
24	8.54	8.36	8.45	8.52	8.38	8.45
27	8.75	8.57	8.66	8.58	8.64	8.61
31	8.57	8.61	8.59	8.58	8.56	8.57
34	8.6	8.62	8.61	8.53	8.57	8.55

Temperature (°F)

Reactors: D1-D4; Seed microalgae: *D. salina*

Day	D1-1	D1-2	D1 (average)	D2-1	D2-2	D2 (average)
0	76.5	76.5	76.5	77	77	77
2	63	63.2	63.1	63.1	62.9	63
4	75.6	75.4	75.5	75.5	75.5	75.5
6	74.5	74.3	74.4	74.3	74.5	74.4
9	75.4	75.2	75.3	76.6	76.2	76.4
11	73.5	73.3	73.4	75.6	74.6	75.1
13	76.9	76.8	76.85	73.7	73.1	73.4
16	77.1	78.5	77.8	77.4	73.5	75.45
18	75.6	75.8	75.7	77.7	76.9	77.3
23	72.6	72.4	72.5	75.6	75.4	75.5
25	75.1	74.9	75	72.9	70.5	71.7
27	75.2	75.4	75.3	71.9	74.9	73.4
30	73.7	74.1	73.9	75.2	75.2	75.2
32	73.4	73.4	73.4	74.3	74.5	74.4
34	74.9	74.7	74.8	76	76.2	76.1
37	75.2	74.8	75	75.7	76.1	75.9
39	75.1	74.9	75	76	76.2	76.1
41	74.6	74.2	74.4	74.6	75.8	75.2

Day	D3-1	D3-2	D3 (average)	D4-1	D4-2	D4 (average)
0	75.9	75.9	75.9	77.3	77.3	77.3
2	62.3	62.3	62.3	62.4	61.9	62.15
4	74.2	74.6	74.4	75.1	75.3	75.2
6	73.1	73.3	73.2	74.9	73.9	74.4
9	75.5	74.9	75.2	76.9	76.5	76.7
11	75.3	75.3	75.3	75.1	75.3	75.2
13	75.4	77.4	76.4	76.9	76.3	76.6
16	77	77.2	77.1	76.5	77.1	76.8
18	74.2	74.4	74.3	74.9	74.7	74.8
23	73.8	73.6	73.7	73.8	73.6	73.7
25	73	73.4	73.2	74.1	74.1	74.1
27	74.9	74.7	74.8	76	76.2	76.1
30	75.7	75.9	75.8	76.1	76.1	76.1
32	76	76.2	76.1	76.3	76.7	76.5
34	76.6	76.6	76.6	74.8	74.8	74.8
37	76.7	76.5	76.6	75.3	74.7	75
39	75.7	75.9	75.8	73.6	74	73.8
41	76	74.4	75.2	71.5	74.5	73

Reactors: S1-S4; Seed microalgae: *S. platensis*

Day	S1-1	S1-2	S1 (average)	S2-1	S2-2	S2 (average)
0	73.9	73.9	73.9	75.3	75.3	75.3
3	73.9	73.9	73.9	75.3	75.3	75.3
6	86.6	86.4	86.5	89.1	88.9	89
8	75.1	75.3	75.2	75.4	75.2	75.3
10	73	73	73	76.4	76.8	76.6
14	77.7	77.6	77.65	80	81	80.5
17	75.2	74.8	75	72.3	72.3	72.3
20	82.5	82.9	82.7	83	83.2	83.1
24	75	75.2	75.1	78.3	77.9	78.1
27	77.3	76.7	77	78.5	77.9	78.2
31	79.5	78.9	79.2	80.1	80.1	80.1
34	92.6	92	92.3	91.3	91.1	91.2

Day	S3-1	S3-2	S3 (average)	S4-1	S4-2	S4 (average)
0	75	75	75	73.5	73.5	73.5
3	75	75	75	73.5	73.5	73.5
6	86.6	86.8	86.7	87.3	87.5	87.4
8	74.3	74.5	74.4	73.9	73.9	73.9
10	73.2	74.2	73.7	75.8	76	75.9
14	81.6	81	81.3	79.1	79.9	79.5
17	75.7	75.3	75.5	74.8	75	74.9
20	82.7	82.7	82.7	82.9	82.9	82.9
24	76	76.2	76.1	76.7	77.1	76.9
27	75.4	74.8	75.1	76.4	76.4	76.4
31	79	79.6	79.3	78	78.2	78.1
34	93.4	93.6	93.5	92.7	92.5	92.6

Conductivity ($\mu\text{S/cm}$)**Reactors: D1-D4; Seed microalgae: *D. salina***

Day	D1-1	D1-2	D1 (average)	D2-1	D2-2	D2 (average)
0	30,499	30,499	30,499	25,634	25,634	25,634
2	30,450	30,550	30,500	25,660	25,540	25,600
4	30,120	30,080	30,100	25,000	25,200	25,100
6	29,525	29,475	29,500	24,750	24,650	24,700
9	28,860	28,740	28,800	24,270	24,330	24,300
11	28,040	28,160	28,100	24,200	24,000	24,100
13	27,420	27,380	27,400	23,100	19,900	21,500
16	25,875	25,725	25,800	25,880	25,720	25,800
18	25,150	25,250	25,200	21,770	21,630	21,700
23	23,520	23,480	23,500	20,950	20,050	20,500
25	22,910	22,890	22,900	20,100	19,900	20,000
27	22,470	22,530	22,500	19,770	19,710	19,740
30	21,660	21,740	21,700	19,170	19,130	19,150
32	21,150	21,250	21,200	18,730	18,690	18,710
34	20,830	20,770	20,800	18,200	18,180	18,190
37	20,450	20,350	20,400	18,060	18,000	18,030
39	19,530	19,590	19,560	17,230	17,150	17,190
41	18,100	18,120	18,110	16,790	16,670	16,730

Day	D3-1	D3-2	D3 (average)	D4-1	D4-2	D4 (average)
0	31,030	31,030	31,030	26,030	26,030	26,030
2	30,780	30,820	30,800	25,880	25,720	25,800
4	30,000	30,200	30,100	25,100	25,300	25,200
6	29,450	29,550	29,500	24,890	24,710	24,800
9	29,450	29,550	29,500	24,000	24,200	24,100
11	28,660	28,540	28,600	23,450	23,150	23,300
13	27,500	27,700	27,600	22,660	22,540	22,600
16	26,400	26,200	26,300	21,440	21,360	21,400
18	25,580	25,420	25,500	20,660	20,740	20,700

23	23,770	23,630	23,700	19,100	19,020	19,060
25	23,700	22,300	23,000	18,100	18,700	18,400
27	22,810	22,790	22,800	18,200	18,220	18,210
30	22,000	22,200	22,100	17,400	17,520	17,460
32	21,650	21,550	21,600	16,920	16,980	16,950
34	21,040	20,960	21,000	16,620	16,660	16,640
37	20,650	20,750	20,700	16,300	16,360	16,330
39	19,620	19,580	19,600	15,520	15,540	15,530
41	20,000	20,000	20,000	15,150	15,110	15,130

Reactors: S1-S4; Seed microalgae: *S. platensis*

Day	S1-1	S1-2	S1 (average)	S2-1	S2-2	S2 (average)
0	36,800	36,800	36,800	24,800	24,800	24,800
3	36,000	36,400	36,200	25,000	25,200	25,100
6	35,750	35,650	35,700	25,000	24,800	24,900
8	35,150	35,450	35,300	26,670	26,530	26,600
10	34,680	34,720	34,700	24,810	24,790	24,800
14	33,920	33,880	33,900	24,250	24,350	24,300
17	34,520	34,480	34,500	24,875	24,725	24,800
20	33,630	33,570	33,600	24,100	24,300	24,200
24	33,745	33,655	33,700	24,625	24,575	24,600
27	26,920	26,880	26,900	19,440	19,600	19,520
31	36,800	36,800	36,800	24,800	24,800	24,800
34	36,000	36,400	36,200	25,000	25,200	25,100

Day	S3-1	S3-2	S3 (average)	S4-1	S4-2	S4 (average)
0	37,200	37,200	37,200	24,900	24,900	24,900
3	38,050	38,150	38,100	26,400	26,800	26,600
6	37,750	37,650	37,700	26,950	26,850	26,900
8	38,000	38,000	38,000	26,850	27,350	27,100
10	37,850	37,950	37,900	27,130	27,070	27,100
14	37,825	37,775	37,800	27,410	27,390	27,400
17	39,110	39,090	39,100	28,770	28,630	28,700
20	38,750	38,850	38,800	28,930	28,870	28,900
24	39,550	39,250	39,400	30,480	30,320	30,400
27	38,130	38,270	38,200	30,640	30,560	30,600
31	37,200	37,200	37,200	24,900	24,900	24,900
34	38,050	38,150	38,100	26,400	26,800	26,600

Air flow rate (mL/min)**Reactors: D1-D4; Seed microalgae: *D. salina***

Day	D1-1	D1-2	D1 (average)	D2-1	D2-2	D2 (average)
0	368	368	368	368	368	368
2	299	299	299	460	460	460
4	115	115	115	299	299	299
6	596	596	596	345	345	345
9	506	506	506	920	920	920
11	736	736	736	713	713	713
13	667	667	667	667	667	667
16	598	598	598	664	664	664
18	713	713	713	667	667	667
23	460	460	460	644	644	644
25	644	644	644	644	644	644
27	690	690	690	782	782	782
30	690	690	690	782	782	782
32	874	874	874	736	736	736
34	1196	1196	1196	966	966	966
37	805	805	805	989	989	989
39	1150	1150	1150	1035	1035	1035
41	943	943	943	1104	1104	1104

Day	D3-1	D3-2	D3 (average)	D4-1	D4-2	D4 (average)
0	368	368	368	368	368	368
2	368	368	368	483	483	483
4	253	253	253	690	690	690
6	460	460	460	345	345	345
9	805	805	805	805	805	805
11	598	598	598	667	667	667
13	575	575	575	598	598	598
16	644	644	644	644	644	644
18	667	667	667	690	690	690
23	621	621	621	598	598	598
25	690	690	690	644	644	644
27	805	805	805	782	782	782
30	805	805	805	782	782	782
32	851	851	851	851	851	851
34	966	966	966	874	874	874
37	897	897	897	966	966	966
39	1012	1012	1012	989	989	989
41	1058	1058	1058	1012	1012	1012

Reactors: S1-S4; Seed microalgae: *S. platensis*

Day	S1-1	S1-2	S1 (average)	S2-1	S2-2	S2 (average)
0	368	368	368	368	368	368
3	828	828	828	1012	1012	1012
6	1104	1104	1104	943	943	943
8	920	920	920	1242	1242	1242
10	874	874	874	1380	1380	1380
14	1265	1265	1265	1196	1196	1196
17	805	805	805	1380	1380	1380
20	1334	1334	1334	1357	1357	1357
24	1380	1380	1380	1380	1380	1380
27	1380	1380	1380	1495	1495	1495
31	1380	1380	1380	1495	1495	1495
34	368	368	368	368	368	368

Day	S3-1	S3-2	S3 (average)	S4-1	S4-2	S4 (average)
0	368	368	368	368	368	368
3	805	805	805	805	805	805
6	805	805	805	851	851	851
8	1334	1334	1334	1242	1242	1242
10	805	805	805	1288	1288	1288
14	1334	1334	1334	1495	1495	1495
17	1265	1265	1265	1242	1242	1242
20	1357	1357	1357	1380	1380	1380
24	1357	1357	1357	1380	1380	1380
27	1426	1426	1426	1380	1380	1380
31	1380	1380	1380	1380	1380	1380
34	368	368	368	368	368	368

Nutrient (mL)

Reactors: R1-R5; Seed microalgae: BGNDRF; Nutrient: SADS

Day	R1-1	R1-2	R1 (average)	R2-1	R2-2	R2 (average)
0	330	330	330	330	330	330
3	330	330	330	330	330	330
6	330	330	330	330	330	330
10	330	330	330	330	330	330
13	330	330	330	330	330	330
17	330	330	330	330	330	330
20	330	330	330	330	330	330
24	330	330	330	330	330	330

27	330	330	330	330	330	330
30	330	330	330	330	330	330
34	330	330	330	330	330	330
40	330	330	330	330	330	330
44	330	330	330	330	330	330
50	330	330	330	330	330	330
53	330	330	330	330	330	330
60	330	330	330	330	330	330
70	330	330	330	330	330	330
80	330	330	330	330	330	330
90	330	330	330	330	330	330
100	330	330	330	330	330	330
110	330	330	330	330	330	330

Day	R3-1	R3-2	R3 (average)	R4-1	R4-2	R4 (average)
0	330	330	330	330	330	330
3	330	330	330	330	330	330
6	330	330	330	330	330	330
10	330	330	330	330	330	330
13	330	330	330	330	330	330
17	330	330	330	330	330	330
20	330	330	330	330	330	330
24	330	330	330	330	330	330
27	330	330	330	330	330	330
30	330	330	330	330	330	330
34	330	330	330	330	330	330
40	330	330	330	330	330	330
44	330	330	330	330	330	330
50	330	330	330	330	330	330
53	330	330	330	330	330	330
60	330	330	330	330	330	330
70	330	330	330	330	330	330
80	330	330	330	330	330	330
90	330	330	330	330	330	330
100	330	330	330	330	330	330
110	330	330	330	330	330	330

Day	R5-1	R5-2	R5 (average)
0	330	330	330
3	330	330	330
6	330	330	330
10	330	330	330
13	330	330	330
17	330	330	330
20	330	330	330
24	330	330	330
27	330	330	330
30	330	330	330
34	330	330	330
40	330	330	330
44	330	330	330
50	330	330	330
53	330	330	330
60	330	330	330
70	330	330	330
80	330	330	330
90	330	330	330
100	330	330	330
110	330	330	330

Dry Biomass (g/L)

Reactors: R1-R5; Seed microalgae: BGNDRF; Nutrient: SADS

Day	R1-1	R1-2	R1 (average)	R2-1	R2-2	R2 (average)
0	0	0	0	0	0	0
3	0.3005	0.2429	0.2717	0.5505	0.4395	0.495
6	0.066	0.055	0.0605	0.19	0.28	0.235
10	0.2032	0.1234	0.1633	0.2837	0.2829	0.2833
13	0.3184	0.1482	0.2333	0.2969	0.4347	0.3658
17	0.4207	0.3423	0.3815	0.7706	0.618	0.6943
20	0.5277	0.3273	0.4275	0.4025	0.3409	0.3717
24	0.7402	0.8801	0.81015	0.3857	0.4209	0.4033
27	0.9514	0.8516	0.9015	0.5718	0.5682	0.57
30	1.2963	1.1371	1.2167	0.6964	0.7403	0.71835
34	0.5025	0.4675	0.485	0.6303	0.6363	0.6333
40	1.3764	1.2802	1.3283	1.2985	1.3481	1.3233
44	1.6498	1.5718	1.6108	1.2996	1.3621	1.33085
50	1.8316	1.7284	1.7800	1.6241	1.4310	1.52755
53	1.6714	1.7801	1.7258	0.9990	1.1260	1.0625
60	2.0116	2.0099	2.0108	1.4173	1.3777	1.3975
70	2.007	1.939	1.9730	1.8255	1.6830	1.75425
80	2.0020	1.923	1.9625	1.9401	1.8999	1.92
90	2.1984	1.98	2.0892	1.7110	1.8990	1.805
100	1.9129	1.7654	1.8392	1.7833	1.7835	1.7834
110	1.9263	1.8386	1.8825	1.8036	1.6448	1.7242

Day	R3-1	R3-2	R3 (average)	R4-1	R4-2	R4 (average)
0	0	0	0	0	0	0
3	0.1712	0.2523	0.21175	0.312	0.202	0.257
6	0.2821	0.3245	0.3033	0.2213	0.1653	0.1933
10	0.352	0.418	0.385	0.301	0.12	0.2105
13	0.4513	0.2521	0.3517	0.3771	0.501	0.43905
17	0.664	0.5761	0.62005	0.5429	0.4417	0.4923
20	0.5164	0.467	0.4917	0.4006	0.6003	0.50045
24	0.81	0.73	0.77	0.5992	0.6994	0.6493
27	0.8644	0.799	0.8317	0.144	0.116	0.13
30	0.9665	0.9669	0.9667	0.4312	0.4354	0.4333
34	0.9902	0.9963	0.9933	0.4409	0.4390	0.4400
40	1.0122	0.994	1.0031	0.6347	0.642	0.63835
44	1.311	1.39	1.3505	0.7928	0.7988	0.7958
50	1.6464	1.492	1.5692	1.0184	0.9201	0.96925
53	1.3518	1.5498	1.4508	0.8585	0.8599	0.8592
60	1.4712	1.5538	1.5125	1.1617	1.1599	1.1608
70	1.8045	1.6005	1.7025	1.4834	1.3851	1.43425
80	1.905	1.797	1.851	1.5319	1.5321	1.532
90	1.8188	1.6196	1.7192	1.6849	1.5831	1.634
100	1.4013	1.5003	1.4508	1.8108	1.6912	1.751
110	1.048	1.2185	1.13325	1.2221	1.4195	1.3208

Day	R5-1	R5-2	R5 (average)
0	0	0	0
3	0.3078	0.3862	0.347
6	0.384	0.448	0.416
10	0.3775	0.4759	0.4267
13	0.5159	0.4147	0.4653
17	0.2674	0.2666	0.267
20	0.6602	0.5599	0.61005
24	0.5257	0.4643	0.495
27	0.4853	0.4898	0.48755
30	0.551	0.5524	0.5517
34	0.8034	0.8100	0.8067
40	0.6321	0.578	0.60505
44	0.8162	0.7604	0.7883
50	0.8762	0.9373	0.90675

53	0.7181	0.8785	0.7983
60	0.5223	0.4477	0.485
70	1.2566	1.2534	1.255
80	1.2967	1.3951	1.3459
90	1.5204	1.473	1.4967
100	1.6111	1.569	1.59005
110	1.5197	1.3369	1.4283

Optical Density at 560 nm**Reactors: R1-R5; Seed microalgae: BGNDRF; Nutrient: SADS**

Day	R1-1	R1-2	R1 (average)	R2-1	R2-2	R2 (average)
0	0.22	0.22	0.22	0.23	0.23	0.23
3	0.12	0.1	0.11	0.087	0.093	0.09
6	0.106	0.104	0.105	0.063	0.057	0.06
10	0.115	0.105	0.11	0.078	0.082	0.08
13	0.33	0.27	0.3	0.21	0.23	0.22
17	0.359	0.351	0.355	0.176	0.174	0.175
20	0.4855	0.4955	0.4905	0.227	0.223	0.225
24	1.11	1.07	1.09	0.31	0.95	0.63
27	1.57	1.18	1.375	1.07	1.03	1.05
30	2.01	2.07	2.04	1.072	1.678	1.375
34	2.248	2.242	2.245	1.52	1.84	1.68
37	2.347	3.075	2.711	1.59	2.94	2.265
40	2.89	2.87	2.88	2.22	2.2	2.21
44	3.723	3.727	3.725	2.46	2.88	2.67
47	3.75	3.75	3.75	2.44	2.42	2.43
48	4.306	3.204	3.755	3.132	3.138	3.135
50	4.367	4.363	4.365	2.482	3.248	2.865
55	4.15	4.07	4.11	3.37	3.77	3.57
60	4.45	4.49	4.47	3.832	3.789	3.8105
70	4.0273	4.8258	4.42655	3.64	3.641	3.6405
80	4.702	4.7	4.701	3.8532	3.8538	3.8535
100	3.3	3.3	3.3	1.829	1.825	1.827
110	3.65	4.49	4.07	1.9752	2.2998	2.1375

Day	R3-1	R3-2	R3 (average)	R4-1	R4-2	R4 (average)
0	0.29	0.29	0.29	0.3	0.3	0.3
3	0.093	0.097	0.095	0.125	0.115	0.12
6	0.124	0.126	0.125	0.178	0.172	0.175
10	0.139	0.131	0.135	0.15	0.15	0.15
13	0.196	0.415	0.3055	0.25	0.31	0.28
17	0.227	0.223	0.225	0.18	0.24	0.21
20	0.236	0.234	0.235	0.238	0.222	0.23
24	0.152	0.528	0.34	0.257	0.253	0.255
27	0.37	0.41	0.39	0.04	0.46	0.25
30	0.521	0.523	0.522	0.257	0.253	0.255
34	0.767	0.893	0.83	0.315	0.325	0.32
37	1	1.02	1.01	0.192	0.51	0.351
40	0.82	1.62	1.22	0.176	0.624	0.4
44	1.82	2.6	2.21	0.24	1.38	0.81
47	2.15	2.11	2.13	1.057	1.053	1.055
48	1.58	2.68	2.13	1.089	1.081	1.085
50	2.21	2.83	2.52	0.52	1.62	1.07
55	2.66	3.07	2.865	1.181	1.579	1.38
60	2.82	3.434	3.127	1.2	2.3015	1.75075
70	3.332	3.34	3.336	1.534	2.034	1.784
80	3.688	4.238	3.963	1.458	2.42	1.939
100	3.213	3.816	3.5145	1.698	1.998	1.848
110	3.251	3.655	3.453	1.862	2.18	2.021

Day	R5-1	R5-2	R5 (average)
0	0.315	0.315	0.315

3	0.143	0.137	0.14
6	0.186	0.174	0.18
10	0.191	0.189	0.19
13	0.221	0.229	0.225
17	0.207	0.203	0.205
20	0.286	0.284	0.285
24	0.334	0.336	0.335
27	0.309	0.301	0.305
30	0.306	0.304	0.305
34	0.36	0.371	0.3655
37	0.32	0.3	0.31
40	0.26	0.24	0.25
44	0.15	0.53	0.34
47	0.41	0.41	0.41
48	0.4	0.42	0.41
50	0.192	0.63	0.411
55	0.57	0.57	0.57
60	0.242	1.766	1.004
70	0.497	1.794	1.1455
80	1.111	1.912	1.5115
100	1.177	2.198	1.6875
110	1.77	1.779	1.7745

pH**Reactors: R1-R5; Seed microalgae: BGNDRF**

Day	R1-1	R1-2	R1 (average)	R2-1	R2-2	R2 (average)
0	8.46	8.46	8.46	8.33	8.33	8.33
3	8.82	8.84	8.83	8.82	8.8	8.81
6	8.81	8.83	8.82	8.9	8.9	8.9
10	8.81	8.83	8.82	8.89	8.87	8.88
11	8.8	8.78	8.79	8.85	8.84	8.845
13	9.01	9.03	9.02	9.04	9	9.02
17	8.7	8.68	8.69	8.7	8.72	8.71
20	8.7	8.66	8.68	8.71	8.75	8.73
24	8.34	8.28	8.31	8.39	8.35	8.37
27	8.88	8.88	8.88	8.66	8.64	8.65
30	8.81	8.83	8.82	8.89	8.87	8.88
35	8.4	8.4	8.4	8.6	8.62	8.61
37	8.3	8.32	8.31	8.47	8.45	8.46
40	8.31	8.33	8.32	8.47	8.47	8.47
44	9.11	9.19	9.15	9.09	9.13	9.11
48	8.43	8.41	8.42	8.56	8.54	8.55
50	8.23	8.19	8.21	8.32	8.34	8.33
55	8.51	8.55	8.53	8.68	8.66	8.67
60	8.23	8.21	8.22	8.94	8.92	8.93
70	8.58	8.54	8.56	8.49	8.45	8.47
80	8.12	8.1	8.11	7.9	7.92	7.91
90	8.24	8.26	8.25	8.46	8.44	8.45
100	8.5	8.54	8.52	8.66	8.64	8.65
110	8.37	8.33	8.35	8.4	8.38	8.39

Day	R3-1	R3-2	R3 (average)	R4-1	R4-2	R4 (average)
0	8.4	8.4	8.4	8.37	8.37	8.37
3	8.83	8.93	8.88	8.75	8.77	8.76
6	8.8	8.78	8.79	8.83	8.79	8.81
10	8.85	8.81	8.83	8.85	8.87	8.86
11	8.81	8.85	8.83	8.66	8.64	8.65
13	9.01	9.01	9.01	8.97	8.93	8.95
17	8.66	8.68	8.67	8.66	8.64	8.65
20	8.66	8.64	8.65	8.7	8.68	8.69
24	8.32	8.3	8.31	8.35	8.33	8.34
27	8.62	8.64	8.63	8.56	8.58	8.57
30	8.76	8.78	8.77	8.61	8.65	8.63

35	8.65	8.67	8.66	8.62	8.63	8.625
37	8.6	8.62	8.61	8.59	8.57	8.58
40	8.52	8.52	8.52	8.63	8.65	8.64
44	8.91	8.89	8.9	8.83	8.85	8.84
48	8.61	8.61	8.61	8.63	8.59	8.61
50	8.47	8.43	8.45	8.48	8.44	8.46
55	8.7	8.7	8.7	8.73	8.71	8.72
60	8.38	8.36	8.37	8.46	8.44	8.45
70	8.47	8.45	8.46	8.45	8.45	8.45
80	8.1	8.1	8.1	8.16	8.04	8.1
90	8.54	8.5	8.52	8.9	9.04	8.97
100	8.71	8.75	8.73	8.71	8.79	8.75
110	8.21	8.23	8.22	8.7	8.66	8.68

Day	R5-1	R5-2	R5 (average)
0	8.48	8.48	8.48
3	8.71	8.71	8.71
6	8.84	8.78	8.81
10	8.79	8.77	8.78
11	8.69	8.67	8.68
13	8.91	8.93	8.92
17	8.65	8.55	8.6
20	8.68	8.66	8.67
24	8.3	8.34	8.32
27	8.52	8.54	8.53
30	8.6	8.62	8.61
35	8.52	8.54	8.53
37	8.46	8.44	8.45
40	8.55	8.46	8.505
44	8.63	8.65	8.64
48	8.62	8.6	8.61
50	8.49	8.45	8.47
55	8.75	8.73	8.74
60	8.5	8.5	8.5
70	8.83	8.85	8.84
80	9.35	8.59	8.97
90	8.83	8.96	8.895
100	8.69	8.63	8.66
110	8.67	8.63	8.65

Temperature (°F)

Reactors: R1-R5; Seed microalgae: BGNDRF

Day	R1-1	R1-2	R1 (average)	R2-1	R2-2	R2 (average)
0	75	75	75	74.6	74.6	74.6
3	79.5	78.7	79.1	79.1	79.1	79.1
6	77.1	77.1	77.1	78.4	78.2	78.3
10	76.4	75.9	76.15	76.1	76.1	76.1
13	78.8	77.9	78.35	78.3	77.9	78.1
17	76.6	76.6	76.6	76.8	77	76.9
20	79.3	78.9	79.1	78.2	79.6	78.9
24	76.1	76.7	76.4	76.1	76.1	76.1
27	86	86	86	85.7	85.9	85.8
30	76.9	75.9	76.4	76.8	76	76.4
33	78.3	78.9	78.6	78.7	78.7	78.7
37	75.9	75.5	75.7	75.8	76	75.9
40	76.3	76.1	76.2	76.8	76	76.4
48	81.9	80.08	81.0	80.7	79.9	80.3
50	72.8	72.4	72.6	74.4	74.4	74.4
55	76.4	75.8	76.1	77.2	77.4	77.3
60	76.8	76.0	76.4	76.7	76.5	76.6
70	76.1	76.1	76.1	77.7	78.1	77.9
80	77.9	77.5	77.7	77.2	78.1	77.7
100	76.9	76.7	76.8	76.9	76.7	76.8

110	77.6	77.8	77.7	78.9	78.8	78.9
Day	R3-1	R3-2	R3 (average)	R4-1	R4-2	R4 (average)
0	75.3	75.3	75.3	75.9	75.9	75.9
3	79.3	78.9	79.1	79.5	78.7	79.1
6	77.1	77.3	77.2	79.2	79.2	79.2
10	75.6	75.4	75.5	75.7	75.3	75.5
13	79.5	79.3	79.4	80.3	79.9	80.1
17	76.9	76.9	76.9	77.3	77.3	77.3
20	79.4	80	79.7	79.8	78.8	79.3
24	77.1	77.1	77.1	77.5	76.7	77.1
27	82.4	83.4	82.9	84.3	84.3	84.3
30	75.7	74.9	75.3	76.5	75.9	76.2
33	79.1	79.5	79.3	78.8	78.2	78.5
37	76.9	75.9	76.4	76.1	76.1	76.1
40	76.4	77.2	76.8	77.1	77.5	77.3
48	82.1	83.1	82.6	82.9	82.3	82.6
50	76.1	76.1	76.1	75.7	75.3	75.5
55	76.8	75.4	76.1	78.4	77.8	78.1
60	77.1	77.1	77.1	77.2	77.4	77.3
70	77.8	77.2	77.5	77.2	77.2	77.2
80	76.4	76.8	76.6	77.6	76.4	77
100	76.1	76.1	76.1	76.9	75.9	76.4
110	79.6	79.0	79.3	78.9	78.7	78.8

Day	R5-1	R5-2	R5 (average)
0	74.8	74.8	74.8
3	80.6	80.6	80.6
6	79.5	78.9	79.2
10	76.1	76.1	76.1
13	78.9	79.5	79.2
17	76.8	76.4	76.6
20	80	80	80
24	77.7	76.5	77.1
27	84.7	83.3	84
30	76.8	76.4	76.6
33	80.7	79.7	80.2
37	76.8	75.6	76.2
40	76.9	75.9	76.4
48	82.7	81.8	82.25
50	75.5	75.5	75.5
55	77.6	76.6	77.1
60	77.5	76.7	77.1
70	77.8	76.6	77.2
80	77.4	78.4	77.9
100	77.4	76.6	77
110	78.7	78.5	78.6

Conductivity ($\mu\text{S}/\text{cm}$)

Reactors: R1-R5; Seed microalgae: BGNDRF

Day	R1-1	R1-2	R1 (average)	R2-1	R2-2	R2 (average)
0	21,400	21,400	21,400	27,100	27,100	27,100
3	21,700	21,900	21,800	27,500	27,700	27,600
6	22,000	22,200	22,100	28,400	27,600	28,000
10	22,500	22,700	22,600	30,000	28,000	29,000
13	21,100	20,900	21,000	26,800	27,000	26,900
17	21,200	21,400	21,300	27,300	27,300	27,300
20	21,900	21,700	21,800	28,100	27,900	28,000
23	20,500	20,300	20,400	25,900	25,700	25,800
27	21,000	20,800	20,900	26,200	26,400	26,300
30	21,100	21,300	21,200	26,700	26,900	26,800
33	19,940	19,980	19,960	25,200	25,400	25,300

38	20,000	20,200	20,100	25,400	25,600	25,500
40	20,700	21,100	20,900	26,100	26,500	26,300
44	19,430	19,630	19,530	24,200	24,400	24,300
48	19,830	20,090	19,960	25,100	25,300	25,200
50	20,200	20,400	20,300	25,500	25,900	25,700
55	19,200	19,140	19,170	23,600	23,400	23,500
60	20,000	20,200	20,100	24,200	24,400	24,300
70	18,300	18,060	18,180	21,300	21,500	21,400
80	19,410	19,210	19,310	25,600	25,600	25,600
90	19,860	20,020	19,940	26,100	26,300	26,200
100	20,700	20,700	20,700	23,400	23,200	23,300
110	20,300	20,500	20,400	23,200	23,400	23,300

Day	R3-1	R3-2	R3 (average)	R4-1	R4-2	R4 (average)
0	35,600	35,600	35,600	43,800	43,800	43,800
3	36,200	36,000	36,100	44,600	44,600	44,600
6	36,500	37,100	36,800	45,000	45,400	45,200
10	37,600	37,800	37,700	46,100	46,300	46,200
13	34,500	34,300	34,400	42,200	42,400	42,300
17	35,100	34,900	35,000	43,100	42,900	43,000
20	36,400	36,600	36,500	44,000	44,000	44,000
23	33,100	33,500	33,300	40,600	40,400	40,500
27	34,000	34,000	34,000	41,200	41,400	41,300
30	34,300	34,500	34,400	41,800	41,600	41,700
33	31,800	32,000	31,900	39,200	38,800	39,000
38	32,100	32,500	32,300	39,100	39,300	39,200
40	33,200	33,400	33,300	40,100	39,900	40,000
44	30,900	30,700	30,800	37,800	38,000	37,900
48	31,400	31,800	31,600	39,100	39,300	39,200
50	32,000	32,000	32,000	37,400	42,000	39,700
55	31,100	30,900	31,000	36,600	38,800	37,700
60	32,900	32,700	32,800	34,100	38,100	36,100
70	30,150	30,250	30,200	33,300	34,300	33,800
80	33,200	32,800	33,000	37,200	37,400	37,300
90	32,700	32,700	32,700	31,000	33,800	32,400
100	31,200	30,800	31,000	26,000	27,600	26,800
110	29,000	29,200	29,100	26,200	30,200	28,200

Day	R5-1	R5-2	R5 (average)
0	52,600	52,600	52,600
3	53,300	53,700	53,500
6	53,400	53,600	53,500
10	55,100	55,300	55,200
13	50,600	51,000	50,800
17	51,500	51,700	51,600
20	52,800	53,000	52,900
23	48,800	49,000	48,900
27	49,400	49,600	49,500
30	50,600	50,800	50,700
33	47,400	47,200	47,300
38	47,600	47,800	47,700
40	48,900	48,700	48,800
44	46,100	46,100	46,100
48	45,600	45,800	45,700
50	47,400	47,600	47,500
55	44,800	44,600	44,700
60	46,200	46,400	46,300
70	41,650	41,350	41,500
80	45,000	45,200	45,100
90	44,600	44,600	44,600
100	44,500	44,300	44,400
110	43,400	43,600	43,500

Air flow rate (mL/min)**Reactors: R1-R5; Seed microalgae: BGNDRF**

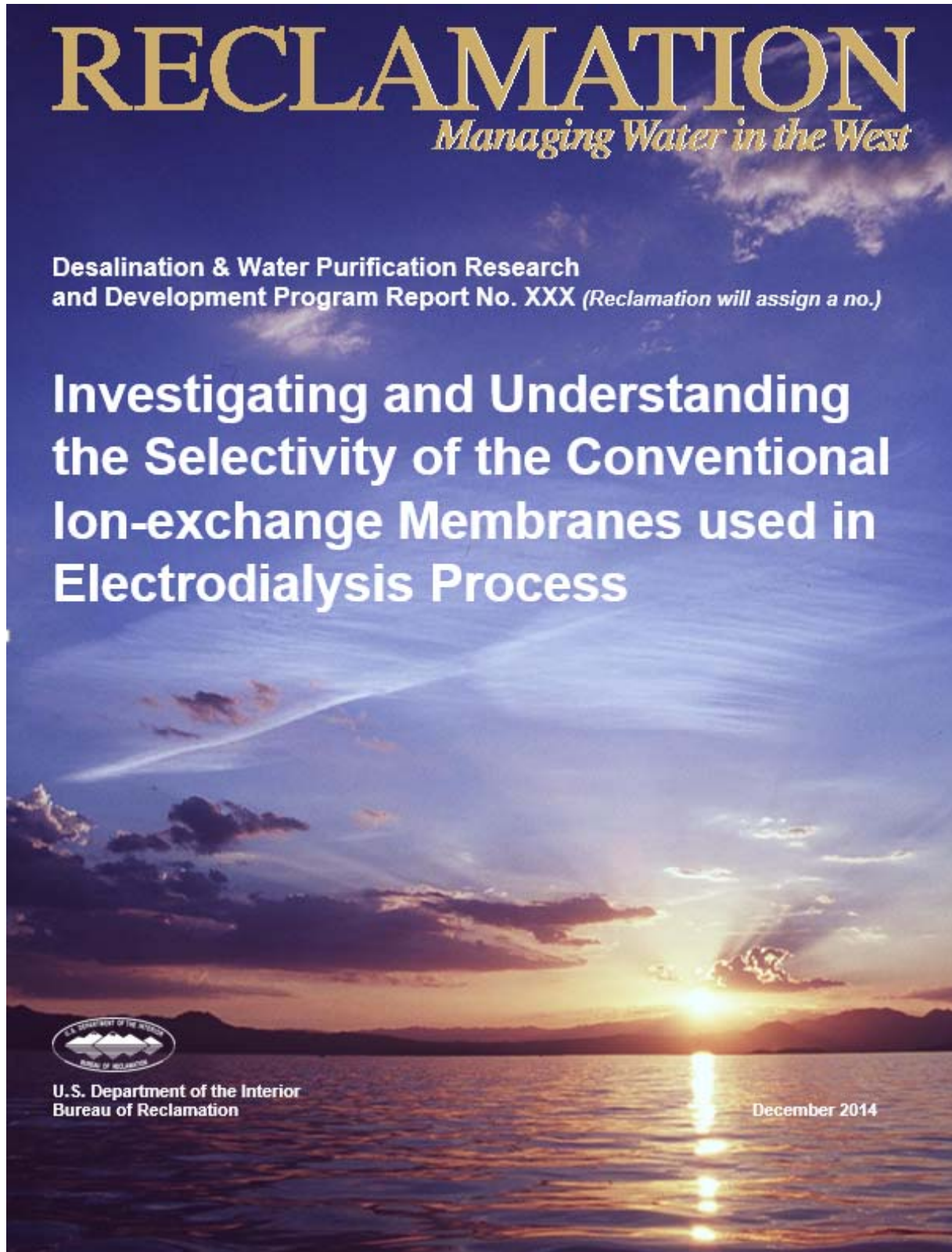
Day	R1-1	R1-2	R1 (average)	R2-1	R2-2	R2 (average)
0	920	920	920	920	920	920
3	920	920	920	920	920	920
6	920	920	920	920	920	920
10	920	920	920	920	920	920
11	920	920	920	920	920	920
13	920	920	920	920	920	920
17	920	920	920	920	920	920
20	920	920	920	920	920	920
23	920	920	920	920	920	920
27	920	920	920	920	920	920
30	920	920	920	920	920	920
35	920	920	920	920	920	920
37	920	920	920	920	920	920
40	920	920	920	920	920	920
44	920	920	920	920	920	920
48	920	920	920	920	920	920
50	920	920	920	920	920	920
55	920	920	920	920	920	920
60	920	920	920	920	920	920
70	920	920	920	920	920	920
70	920	920	920	920	920	920
80	920	920	920	920	920	920
100	920	920	920	920	920	920
110	920	920	920	920	920	920

Day	R3-1	R3-2	R3 (average)	R4-1	R4-2	R4 (average)
0	920	920	920	920	920	920
3	920	920	920	920	920	920
6	920	920	920	920	920	920
10	920	920	920	920	920	920
11	920	920	920	920	920	920
13	920	920	920	920	920	920
17	920	920	920	920	920	920
20	920	920	920	920	920	920
23	920	920	920	920	920	920
27	920	920	920	920	920	920
30	920	920	920	920	920	920
35	920	920	920	920	920	920
37	920	920	920	920	920	920
40	920	920	920	920	920	920
44	920	920	920	920	920	920
48	920	920	920	920	920	920
50	920	920	920	920	920	920
55	920	920	920	920	920	920
60	920	920	920	920	920	920
70	920	920	920	920	920	920
70	920	920	920	920	920	920
80	920	920	920	920	920	920
100	920	920	920	920	920	920
110	920	920	920	920	920	920

Day	R5-1	R5-2	R5 (average)
0	920	920	920
3	920	920	920
6	920	920	920
10	920	920	920
11	920	920	920
13	920	920	920
17	920	920	920
20	920	920	920

23	920	920	920
27	920	920	920
30	920	920	920
35	920	920	920
37	920	920	920
40	920	920	920
44	920	920	920
48	920	920	920
50	920	920	920
55	920	920	920
60	920	920	920
70	920	920	920
70	920	920	920
80	920	920	920
100	920	920	920
110	920	920	920

Investigating and Understanding the Selectivity of the Conventional Ion-exchange Membranes used in Electrodialysis Process



REPORT DOCUMENTATION PAGE			Form Approved OMB No. 0704-0188		
<p>The public reporting burden for this collection of information is estimated to average 1 hour per response, including the time for reviewing instructions, searching existing data sources, gathering and maintaining the data needed, and completing and reviewing the collection of information. Send comments regarding this burden estimate or any other aspect of this collection of information, including suggestions for reducing the burden, to Department of Defense, Washington Headquarters Services, Directorate for Information Operations and Reports (0704-0188), 1215 Jefferson Davis Highway, Suite 1204, Arlington, VA 22202-4302. Respondents should be aware that notwithstanding any other provision of law, no person shall be subject to any penalty for failing to comply with a collection of information if it does not display a currently valid OMB control number.</p> <p>PLEASE DO NOT RETURN YOUR FORM TO THE ABOVE ADDRESS.</p>					
1. REPORT DATE (DD-MM-YYYY) (12-12-2014)		2. REPORT TYPE Proof of Concept Final Report		3. DATES COVERED (From - To) (01-01-2012)-(09-15-2014)	
4. TITLE AND SUBTITLE Investigating and Understanding the Selectivity of the Conventional Ion-exchange Membranes used in Electrodialysis Process			5a. CONTRACT NUMBER R10AC80283		
			5b. GRANT NUMBER		
			5c. PROGRAM ELEMENT NUMBER		
6. AUTHOR(S) Leila Karimi, Abbas Ghassemi			5d. PROJECT NUMBER		
			5e. TASK NUMBER		
			5f. WORK UNIT NUMBER		
7. PERFORMING ORGANIZATION NAME(S) AND ADDRESS(ES) IEE/WERC New Mexico State University PO Box 30001 Las Cruces, NM 88003			8. PERFORMING ORGANIZATION REPORT NUMBER		
9. SPONSORING/MONITORING AGENCY NAME(S) AND ADDRESS(ES)			10. SPONSOR/MONITOR'S ACRONYM(S)		
			11. SPONSOR/MONITOR'S REPORT NUMBER(S)		
12. DISTRIBUTION/AVAILABILITY STATEMENT					
13. SUPPLEMENTARY NOTES					
<p>14. ABSTRACT</p> <p>Drinking water shortage is a worsening issue in the world. After surface water resources, groundwater supplies are very important sources of drinking water in many parts of the world as well as southwest region of the United States. One of the common technologies used for the desalination of brackish water is electrodialysis/electrodialysis reversal (ED/EDR). Among the saline water sources which are desalinated to produce freshwater, the types and quantities of ions vary. Since drinking water standards allow different types of ions to be present at different levels, sometimes desalination plants only need to remove particular types of ions, while other ions can remain. Consequently, the development of preferential ion removal in the ED/EDR process could increase the efficiency of the technology in cases where the ion composition of a feedwater is well-known. Additionally, selective removal of ions would help reduce the cost of desalination or anionic contaminant removal by reducing the number of moles of ions that must be removed to get appropriate results. In this study, the experiments were conducted at the Brackish Groundwater National Desalination Research Facility (BGNDRF), on a General Electric Company pilot-scale EDR system with an influent flow rate capacity of 12 gpm (0.775 L/s). Brackish feedwater with a conductivity of 1700 µS/cm was acquired from the aquifer in Tularosa Basin. The experiment operated with single electrical/hydraulic stage using CR67HMR cation-exchange membranes and three types of AR908, AR204 and aged-AR204 anion-exchange membranes, and Spacer-Mark IV with an effective membrane surface area of 3,540 cm². The objective of this research is to study the effect of operating conditions on the selective removal of ions in the EDR process. Additionally, three different types of anion exchange membranes were used to show their behavior in the selective removal of ions. Then, the sensitivities of selectivity values for cations and anions were explored. Finally, the influences of two different phases, solution phase and membrane phase, were defined using a dimensionless number.</p>					
15. SUBJECT TERMS					
16. SECURITY CLASSIFICATION OF:			17. LIMITATION OF ABSTRACT	18. NUMBER OF PAGES	19a. NAME OF RESPONSIBLE PERSON
a. REPORT	b. ABSTRACT	a. THIS PAGE			19b. TELEPHONE NUMBER (Include area code)

**Desalination & Water Purification Research
And Development Program Report No. XXX**

Investigating and Understanding the Selectivity of the Conventional Ion- exchange Membranes used in Electrodialysis Process

Prepared for Reclamation Under Agreement No. R10AC80283

by

Leila Karimi, Abbas Ghassemi



**U.S. Department of the Interior
Bureau of Reclamation
Technical Service Center
Water and Environmental Services Division
Water Treatment Engineering Research Team
Denver, Colorado**

December 2014

MISSION STATEMENTS

The mission of the Department of the Interior is to protect and provide access to our Nation's natural and cultural heritage and honor our trust responsibilities to Indian tribes and our commitments to island communities.

The mission of the Bureau of Reclamation is to manage, develop, and protect water and related resources in an environmentally and economically sound manner in the interest of the American public.

Disclaimer

The views, analysis, recommendations, and conclusions in this report are those of the authors and do not represent official or unofficial policies or opinions of the United States Government, and the United States takes no position with regard to any findings, conclusions, or recommendations made. As such, mention of trade names or commercial products does not constitute their endorsement by the United States Government.

Acknowledgements

The authors would like to thank the U.S. Bureau of Reclamation and the Brackish Groundwater National Desalination Research Facility.

Some parts of this report were retrieved from Leila Karimi's Ph.D. dissertation, which is in progress as of the writing of this report.

Table of Contents

Glossary	iv
Chapter 1: Introduction	2
1.1 Background	2
1.2 Conclusions and Recommendations	4
Chapter 2: Literature Review	6
2.1 Introduction	6
2.1.1 Fresh Water Scarcity	6
2.1.2 Different water categories and availabilities.....	6
2.2 Desalination as a solution to drinking water scarcity.....	6
2.2.1 Electrodialysis/ Electrodialysis Reversal	6
2.2.1.1 Ion Exchange Membrane	6
2.2.1.2 Donnan Potential.....	7
2.2.1.3 Electrodialysis Applications	8
2.2.1.4 Electrodialysis stack.....	8
2.2.1.5 Mass Transport in Electrodialysis Process	9
2.2.1.6 Ion Transport in the Solution Phase.....	9
2.2.1.7 Transport models and selectivity in membrane phase	11
2.2.1.8 Selectivity in ED/EDR process.....	13
2.2.1.9 Effective Parameters in the Selective Removal of Ions in ED/EDR process.....	13
2.2.1.9.1 Voltage	13
2.2.1.9.2 Velocity	14
2.2.1.9.3 Ion Type	15
2.2.1.9.4 Feed composition	15
2.2.1.9.5 Pressure	15
2.2.1.9.6 pH.....	16
Chapter 3: Material and Methods	17
3.1 Pilot Scale Experiment Site.....	17
3.2 Pilot-Scale Experimental Set-up	17
3.2.1 Pretreatment Process Before EDR	17
3.2.2 EDR Stack.....	18
3.2.3 Analytical Analysis	18
3.3 Pilot-Scale Experiments.....	19
3.4 Design of Experiments	19
3.4.1 Pilot-Scale	19

Chapter 4: Results and Discussion.....	20
4.1 Effect of Applied Voltage and Ion Size on Ion removal.....	20
4.2 Effect of Superficial Velocity on Ion Removal.....	21
4.3 Effect of Temperature on Ion Removal	21
4.4 Comparing the Effect of Linear Velocity and temperature on Ion Removal 22	
4.5 Selectivity of different Ion exchange membranes under different conditions	22
4.5.1 Selective Removal of Cations	22
4.5.2 Selective Removal of Anions.....	23
4.5.3 Selectivity Sensitivity for Cations Vs. Na ⁺	23
4.5.4 Selectivity Sensitivity for Anions Vs. Cl ⁻	23
4.5.5 Ion Exchange Membrane Selectivity Comparison	23
Chapter 5: References	26
Tables	30
Chapter 2	30
Chapter 3	30
Chapter 4	32
Figures.....	33
Chapter 2	33
Chapter 3	34
Chapter 4	35
Appendix.....	70
Data Record.....	70

Glossary

Variable	Description
ΔC	desired ion concentration difference between feed and dilute streams
C	ion concentration
D	ion diffusion coefficient
D	desalting cell width
F	Faraday constant
f	molar activity
I	electrical current
i	total current density
IEC	anion exchange membrane
J	total flux of ion i
L	flow path length
N	number of cell pairs
n	number of anions and cations in the solution
P	swelling pressure of the membrane
Q	flow rate
R	molar gas constant
T	temperature
t	transport number of ion i
t	residence time
u	ion mobility
v	velocity of bulk flow
V	solution linear velocity in the dilute chamber
z	electrical charge
$\frac{d\bar{\phi}^{CM \text{ or } AM}}{dx}$	electrical potential gradient in the cation or anion exchange membrane

PS_i^j permselectivity of ion i against j in the membrane phase

Greek Variable

μ chemical potential
 φ electrical potential
 α ion activity
 v partial molar volume
 η current efficiency
 λ individual ion conductivity
 ξ a dimensionless number
 Λ equivalent conductivity

Superscript

m membrane phase
s solution phase

Subscript

i ion type
j ion type
cp cell pair
diff diffusion
mig migration
AM anion exchange membrane
CM cation exchange membrane
resid residence time
conv convection
Don Donnan

Executive Summary

Drinking water shortage is a worsening issue in the world. After surface water resources, groundwater supplies are very important sources of drinking water in many parts of the world as well as southwest region of the United States. One of the common technologies used for the desalination of brackishwater is electro dialysis/electrodialysis reversal (ED/EDR). The basic design of ED and EDR is the same, except that in ED the direction of the electrical current and ion flow is constant, while in EDR the direction of the electrical current and ion flow is reversed periodically. The reversal of the electrical current and ion flow in EDR gives the system self-cleaning characteristics and decreases scaling, a universal problem for membrane-based systems in which minerals create a hard build-up that clogs the filter membrane. Because EDR is relatively resistant to scaling, especially from silica, EDR is better suited for desalination than other membrane-based technologies such as reverse osmosis (RO). This is particularly important in the case of the desalinization of saline water with significantly high silica content. Among the saline water sources (feedwaters) which are desalinated to produce freshwater, the types and quantities of ions vary. Since drinking water standards allow different types of ions to be present at different levels, sometimes desalination plants only need to remove particular types of ions, while other ions can remain. Consequently, the development of preferential ion removal in the ED/EDR process could increase the efficiency of the technology in cases where the ion composition of a feedwater is well-known. Additionally, the selective removal of ions would help reduce the cost of desalination or anionic contaminant removal by reducing the number of moles of ions that must be removed to get appropriate results.

In this study, the experiments were conducted at the Brackish Groundwater National Desalination Research Facility (BGNDRF) in Alamogordo, NM, on a General Electric Company pilot-scale EDR system with an influent flow rate capacity of 12 gpm (0.775 L/s). Brackish feedwater with a conductivity of 1700 $\mu\text{S}/\text{cm}$ was acquired from the aquifer in Tularosa Basin. The experiment operated with a single electrical/hydraulic stage using CR67HMR cation-exchange membranes and three types anion-exchange membranes - AR908, AR204, and aged-AR204 – as well as a Spacer-Mark IV with an effective membrane surface area of 3,540 cm^2 .

The objective is to study the effect of operating conditions on the removal of ions in EDR, and to investigate the selective removal of different ions in this process. Additionally, three different types of anion exchange membranes were used to show their behavior in the removal of ions. Then, the sensitivities of selectivity values for cations and anions were explored. Finally, the influence of two different phases, solution phase and membrane phase, were defined using a dimensionless number.

Chapter 1: Introduction

1.1 Background

Drinking water in the southwestern region of the United States is heavily dependent upon groundwater (United States Geological Survey, 2011). Groundwater supplies have various water chemistries. Depending on the geological formation, the regional precipitation level, and an aquifer's characteristics, groundwater can contain various amounts of anions such as chloride, sulfate, and alkalinity species (i.e., carbonate/bicarbonate), which contribute to high total dissolved solids (TDS) and/or salinity. In addition to these regular species, the presence of small contamination levels from some other anions such as nitrate, perchlorate, and fluoride poses a risk to public health. If the amount of one or more of these anions in a groundwater resource is higher than the levels established in national primary/secondary drinking water standards (EPA, 2011) or local standards, there is a need to reduce the level of the ions that have exceeded the maximum allowed level.

Reverse osmosis (RO), electrodialysis (ED), ion-exchange (IX), and coagulation/filtration are efficient technologies for removing both: 1) anionic species that cause high TDS/salinity, and 2) contamination from some specific anions (MWH, 2005; Clifford and Ghurye, 2002). Although some development has occurred, the lack of selectivity is a considerable issue in these technologies. In general, there are always competitor ions that interfere with the removal of ion(s) of interest, which makes the process more costly. For instance, if there is some nitrate contamination in a groundwater, but other anions in that groundwater are at acceptable levels, then the other ions would interfere in nitrate removal using IX, RO, or ED technologies, making the actual cost of nitrate removal much higher than the theoretical cost of nitrate removal might have been. Another example is Tularosa Basin's typical groundwater, where most of its salinity is due to sulfate salts and chloride is in acceptable level; therefore, the removal of sulfate using RO or ED technologies encounters interference from other ions including chloride, and this interference imposes extra cost to this desalination technology. Thus, selectively removing ion(s) of interest is an area that needs more research.

Selective IX resins have been produced and are available to remove nitrate and perchlorate. Nitrate-selective resins are developed by increasing the length of the functional group from trimethyl amines to triethyl amines and/or tributyl amines (Guter, 1984). The distance between functional groups affects the divalent/monovalent selectivity (Guter, 1984). For perchlorate-selective resins, the order of the selectivity is known to be perchlorate > nitrate > chloride > bicarbonate (Gu and Coates, 2006). Still, there are interferences of other ions in selective resin applications. For instance, increasing the sulfate/nitrate ratio in water from 1 to 10 decreases the percent capacity of the resin allocated to nitrate adsorption from 98% to 85%, and the unwanted removal of sulfate increases.

RO membranes are more selective for divalent ions than monovalent ions. In natural waters, the order of ion rejection using conventional RO membranes is $\text{SO}_4^{2-} > \text{Ca}^{+2} > \text{Mg}^{+2} > \text{HCO}_3^- > \text{Na}^+ > \text{K}^+ > \text{Cl}^- > \text{Br}^-$ (Sata et al., 1997). Although RO membranes reject more divalent ions, there are always amounts of monovalent ions that are removed from water. This removal causes more osmotic pressure in the RO chamber, which increases pressure drop and makes the desalination process more costly.

Some advancements have been reported in the manufacturing of ion-exchange membranes used in the ED systems, increasing the process selectivity for some ions of interest compared to the rest of the ionic species. Monovalent and divalent species separation has been studied (Van der Bruggen et al., 2004; Sadrzadeh et al., 2007). Charge repulsion, attraction, and ionic size are important factors that affect separation between monovalent and multivalent anions (Sata et al., 1997). In addition, operating conditions such as current density, influent flow rate, and acidity (pH) have influences on the permselectivity of the ED ion-exchange membranes used to separate monovalent and multivalent anions. It has been demonstrated that a decrease in current density increases the selectivity of both conventional (non-selective) and monovalent selective ED anion-exchange membranes (Zhang et al., 2009). Still, these membranes are not 100% selective for divalent or monovalent anions and there is always interference of other ions involved in ED removing anions of interest.

To the best of available knowledge, there has not been an extensive study that investigates the selectivity of anion-exchange membranes for various divalent (e.g., sulfate (SO_4^{2-}) and selenate (SeO_4^{2-})) or various monovalent (e.g., nitrate (NO_3^-) and chloride (Cl^-)) species. There is a need to understand the selectivity of available anion-exchange membranes for various divalent and various monovalent species in the case of desalination. In addition, there is a need to comprehend and characterize the selectivity of available anion-exchange membranes for removing trace amounts of anion contaminants, such as fluoride, in the presence of other anions that are normally present in drinking water. The reason is that the amount of energy used in the ED process for desalination or contaminant removal is proportional to the number of moles of ions that are removed from water. The selective removal of ions would help to reduce the cost of desalination or anionic contaminant removal by reducing the number of moles of ions needed to be removed to get appropriate results.

The ion removal not only depends on the selectivity of the ion exchange membranes, but also on how quickly ions move toward the boundary layers and ion exchange membranes. Therefore, the ion removal rate depends on both the affinity of membrane for a certain ion in aqueous solution and the ion movement in the solution phase.

In membrane phase, the selectivity is the affinity of a membrane for a certain ion in aqueous solution, and depends on physical and chemical characteristics of the ion. The magnitude of the valence and the atomic number of the ion are two important factors in determining selectivity (Crittenden et al., 2005). The pore size distribution and the types of functional groups on the polymer chain are also determinant factors for the selectivity. The most important

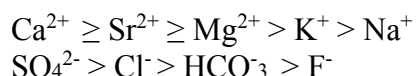
factor affecting the selectivity is the spacing of functional groups (Clifford and Weber, 1986). A divalent ion requires two adjacent active functional groups to connect to and to satisfy the electroneutrality of the exchange chemical reaction. Therefore, increasing the distance between active functional groups decreases the selectivity for divalent ions (e.g. sulfate) (Crittenden et al., 2005). Alternately, monovalent selectivity can be obtained by coating the surface of the anion exchange membrane with a negatively charged layer (Strathmann, 2004).

Both monovalent and divalent selective membranes have been developed. Commercially, monovalent selective membranes are mostly used in the desalination of sea water.

1.2 Conclusions and Recommendations

Conclusion

- Operating parameters, such as applied voltage, solution superficial velocity, temperature, and ion characteristics, have a significant effect on ion removal in the EDR process.
- Increasing the applied voltage in the stack improves ion removal before reaching the limiting current conditions.
- Increasing the solution flow rate (velocity) has an adverse effect on the removal of all ions, due to decreases in the residence time of ions in the EDR stack.
- Increasing the temperature has a positive influence on ion removal due to increases in the ion mobility in both membrane and solution phases.
- Ion characteristics, such as ion size and charge, have a significant effect on the removal of ions; ions with a smaller size and larger charge are removed more than the others.
- The selectivity values of cations, compared to Na⁺ removal, and anions, compared to Cl⁻ removal, are as follows using CR67 and AR204 cation and anion exchange membranes, respectively:



- Sensitivity analysis of selectivity shows that selectivity values for cations and anions were more sensitive at lower values of ξ compared to its higher values, with ξ representing the operating conditions. Therefore, the selectivity studies can be investigated better at mild operating conditions.
- The obtained results confirmed that the aged anion exchange membranes (aged-AR204) which were used in a waste water treatment plant, showed lower selectivity values for divalent ions compared to the new anion exchange membranes, which showed higher selectivity values for divalent

anions. This observation strengthens the idea of a negative surface charge on the aged-AR204 anion exchange membranes, which cause divalent anions' repulsion.

- The removal of ions in the EDR process can be considered in three distinct regions based on the ξ values. In the first region, the membrane phase has a strong role in the selective removal of ions. In the second region, a combination of the membrane phase and the solution phase affects the ion removal. However, in the high values of ξ (region III), all ions are removed simultaneously regardless of the type of ion, or the effects of solution phase and ion exchange membrane phase.

Recommendations

- Characterization of aged-AR204 membranes can confirm, or reject, the hypothesis of a negative surface charge on the membrane surface.
- Testing different water compositions can add more valuable results to this study.
- Studying the removal of ions individually, and mixture of ions, can provide a better picture of ion removal and the role of ions' interaction in selectivity studies.
- Theoretical models can be developed for the selective removal of ions in the EDR process, and these models can be verified with experimental work.
- The selectivity behavior of cation exchange membranes can be investigated using the same approach as for anion exchange membranes.

Chapter 2: Literature Review

2.1 Introduction

2.1.1 Fresh Water Scarcity

Water is an essential chemical material for every living organism on this planet, and it is necessary to maintain proper body function. Naturally, fresh water resources are limited by their quantity. However, there are other factors – such as population increase, industrial development, environmental parameters, and pollution introduction – that affect its availability. Today, fresh water scarcity has drawn the world's attention. It presents the most significant challenge to economic and social development in many countries. By the year 2030, it is estimated that world water needs will increase from 4500 billion cubic meters to 6900 billion cubic meters, 40% greater than current supplies (Addams et al., 2009).

2.1.2 Different water categories and availabilities

With regard to their levels of total dissolved solids (TDS), water resources are categorized into four types, as shown in table 2-2 (Anon., 2014).

2.2 Desalination as a solution to drinking water scarcity

Desalination is the physical-chemical process of removing salt from water. There are different desalination technologies, and the applicability of each depends on factors such as saline water type, energy availability, product application, and required treatment capacity. One of the most applicable desalination technologies across many conditions, especially brackish water treatment, is electrodialysis/ electrodialysis reversal.

2.2.1 Electrodialysis/ Electrodialysis Reversal

Electrodialysis is a membrane-based separation process in which ions are transferred through an ion exchange membrane under the influence of an applied electrical field (Mulder, 1951).

2.2.1.1 Ion Exchange Membrane

Ion exchange membranes are divided into two main groups: cation exchange membranes (CEM) and anion exchange membranes (AEM). Cation exchange membranes are negatively charged polymeric membranes, mostly charged with sulfonic or carboxylic acid groups. In contrast, anion exchange membranes are positively charged with quaternary ammonium salts. Co-ions, the ions with similar charges, are repelled from the membrane surface as a result of

interaction with these fixed charged groups. These ion exchange membranes can be synthesized in two different forms, as either heterogeneous or homogenous structures. Due to a higher mechanical strength and lower electrical resistance, the homogeneous structure tends to be preferred. The synthesis of these membranes is achieved through the introduction of an ionic group into a polymeric film. The charges are distributed uniformly in the polymer matrix, while a degree of cross-linking sufficient enough to prevent excessive swelling should be present in the polymer structure (Mulder, 1951). Although ion exchange membranes were designed for electrodialysis applications, they are also used extensively in several other processes such as fuel cells, bipolar membrane electrodialysis, and electrodeionization (Tanaka, 2007). Ion exchange membranes are characterized by their properties of electrical resistance, ion exchange capacity, water content, ion transport number, solute permeability coefficient, electroosmotic coefficient, water permeation coefficient, swelling ratio, and mechanical strength (Tanaka, 2007).

2.2.1.2 Donnan Potential

As discussed in the previous section, the two groups of ion exchange membranes contain counter ions in their polymeric structures; cation exchange membranes have fixed anions and mobile cations, while anion exchange membranes have fixed cations and mobile anions. When a cation exchange membrane is placed into a strong electrolyte solution, a significant difference in the concentration of ions between the membrane and solution phases occurs. Specifically, the concentration of cations in the membrane phase far exceeds that of the solution phase, while the concentration of anions in the solution phase is much greater than that of the membrane phase. The tendency to eliminate this concentration difference causes the cations to diffuse into the solution phase while the anions diffuse into the membrane phase. However, during the diffusion of the first few ions, a very strong electrical potential occurs that pulls the counter ions (cations) back into the membrane phase, and co-ions (anions) back into the solution phase; this is known as the Donnan potential. Through this, equilibrium is achieved because the tendency of ions to eliminate the concentration difference is neutralized by the effect of the electrical field. As a result, the co-ions are repelled from the membrane, and effect that is called Donnan exclusion (Strathmann, 1995; Helfferich, 1962). The Donnan potential cannot be measured experimentally, but it can be calculated from electrochemical equilibrium between the two phases as follows (Strathmann, 1995):

$$\eta_i^M = \eta_i^S \quad \text{Eq. 2-1}$$

where η is the electrochemical potential. The superscripts m and s are membrane and solution phases and the subscript i , represents the ion type. The electrochemical potential of ion i can be calculated using the following equation:

$$\eta_i = \mu_i + z_i F \varphi \quad \text{Eq. 2-2}$$

where μ_i , z_i , F , and φ are chemical potential, electrical charge, Faraday constant, and electrical potential. By assuming that the temperature of the membrane and

solution phases are equal, the Donnan potential can be calculated by the following equation:

$$\Delta\varphi_{Don} = \varphi^M - \varphi^S = \frac{1}{z_i F} \left(RT \ln \frac{a_i^S}{a_i^M} - v_i P_s \right) \quad \text{Eq. 2-3}$$

where $\Delta\varphi_{Don}$, φ^M , φ^S , α^S_i , α^M_i , v_i , and P_s are Donnan potential, electrical potential in membrane, electrical potential in solution, temperature, activity of ion i in solution, activity of ion i in the membrane, partial molar volume of the ion i , and swelling pressure of the membrane phase, respectively.

2.2.1.3 Electrodialysis Applications

The ED process has been applied commercially for more than 50 years (Strathmann, 2010). This technology is the most applicable desalination process when the total TDS of feed water is within 400-6000 ppm (Kalogirou, 2005). However, some researchers have reported success in desalinating saline water with TDS of 30,000 ppm (Tanaka et al., 2003). Nonetheless, very wide applications for electrodialysis exist aside from desalination, including the removal of Cr, Cu (Barakat, 2011; Mohammadi et al., 2005), Co(II), Ni(II) (Tzanetakis et al., 2003), and Cd (Marder et al., 2004) (Jakobsen et al., 2004), Pb^{2+} (Abou-Shady et al., 2012). There have also been demonstrations in Japan and Korea of several applications that use this process for the production of sodium chloride. ED also has several advantages for the treatment of wastewater loaded with heavy metals, including the ability to recover valuable metals such as Cr and Cu, and the benefit of easier disposal due to the production of a highly concentrated waste stream. Additionally, ED processes are also used to recover acids and bases from industrial waste water (Kedem et al., 2010).

2.2.1.4 Electrodialysis stack

The electrodialysis stack is the major unit of an electrodialysis system. It is composed of alternating series of cation and anion exchange membranes. These ion exchange membranes are the walls of dilute and concentrate chambers. Between each pair of ion exchange membranes, a spacer is used which creates the thickness of the desalting and concentrating chambers as well as introducing the turbulence to the flows. The stack of ion exchange membranes and spacers is placed between two electrodes which are in contact with electrode rinse solutions. An electrical field is then created by applying differential electrical potential on these electrodes; this generates ionic movement, with the anions attempting to move toward the anode, and the cations attempting to move in the opposite direction toward the cathode. The affected anions pass through the anion exchange membranes, but are blocked by cation exchange membranes in the next chamber. Similarly, the cations pass through the cation exchange membranes but are blocked by the anion exchange membranes in the same chamber where the cations are trapped. This results in what is known as the concentrate chamber, where cations are held on one side by the anion exchange membrane, and anions are held on the other side by the cation exchange membrane. The other type of chamber, which now has far fewer cations and anions, is referred to as the dilute

chamber. Therefore, two different solutions, one dilute and the other concentrate, are generated in the electro dialysis process. The schematic figure of the electro dialysis stack is shown in figure 1-1.

The electro dialysis reversal (EDR) process utilizes the same fundamentals that electro dialysis (ED) does. However, it has an additional feature, which is polarity reversal. This feature adds more advantages to the electro dialysis process due to decreases in the scaling risk and increases in the recovery rate of the process (Kalogirou, 2005; Tanaka et al., 2003).

2.2.1.5 Mass Transport in Electro dialysis Process

The quantity of ion transport in electro dialysis processes is correlated with the electrical current density in the process based on Faraday's law as shown below:

$$I = \frac{zFQ\Delta C_i}{\eta N_{cp}} \quad \text{Eq. 2-4}$$

where I , z , F , Q , ΔC_i , η , and N_{cp} are electrical current (A), ion valence, Faraday constant (As.eq⁻¹), flow rate (cm³/s), desired ion concentration difference between feed and dilute streams (eq.cm⁻³), current efficiency, and number of cell pairs, respectively (Mulder, 1951).

Assuming the bulk solution is mixed well due to spacer design, the ion removal is influenced by the ion transport rate in both the solution boundary layer and the membrane phase. Therefore, separately studying ion transport through the boundary layer and through the membrane is crucially important.

2.2.1.6 Ion Transport in the Solution Phase

According to Nernst-Planck equation, the total flux of ion i in the EDR process is composed of three components, as follows:

$$J_i = J_{i,diff} + J_{i,mig} + J_{i,conv} \quad \text{Eq. 2-5}$$

where J_i , $J_{i,diff}$, $J_{i,mig}$, and $J_{i,conv}$ are total, diffusion, migration, and convection flux through an ion exchange membrane, respectively.

The three diffusion, migration, and convection fluxes are represented by equations 2-6 through 2-8, respectively.

$$J_{i,diff} = -D_i \frac{dC_i}{dx} \quad \text{Eq. 2-6}$$

$$J_{i,mig} = -\frac{F}{RT} D_i z_i C_i \frac{d\phi}{dx} = u_i C_i \frac{d\phi}{dx} \quad \text{Eq. 2-7}$$

$$J_{i,conv} = C_i v_i \quad \text{Eq. 2-8}$$

These ion transport mechanisms occur due to concentration gradient, electrical potential gradient, and imbalanced forces on the ion in the solution, respectively (Bard & Faulkner, 2001).

Due to the significant role of two first ion transfer mechanisms, the convection term in the above equation can be neglected (Strathmann, n.d.).

$$J_{i,diff} = -D_i \frac{dC_i}{dx} \quad \text{Eq. 2-6}$$

$$J_{i,mig} = -\frac{F}{RT} D_i z_i C_i \frac{d\phi}{dx} = u_i C_i \frac{d\phi}{dx} \quad \text{Eq. 2-7}$$

$$J_{i,conv} = C_i v_i \quad \text{Eq. 2-8}$$

where D_i , C_i , F , R , T , ϕ , z_i , u_i , and v are ion diffusion coefficient, ion concentration, Faraday constant, molar gas constant, temperature, electrical potential, charge magnitude and sign of the ion, ion mobility, and velocity of bulk flow (Bard & Faulkner, 2001; Strathmann, 2004). The ion mobility applied in the above equation can be calculated using Nernst– Einstein equation as follows (Tanaka, 2003):

$$u_i = \frac{|z_i|FD_i}{RT} \quad \text{Eq. 2-9}$$

The electrical current is carried by ions that are transferred through the ion exchange membrane. The component of current which is carried by ion i shown as below.

$$i_i = z_i F J_i \quad \text{Eq. 2-10}$$

According to the Nernst-Planck equation, $i_i = z_i F J_i$ Eq. 2-10 can be written as equation 2-11

$$i_i = z_i F \left(D_i \frac{dC_i}{dx} + \frac{z_i F}{RT} D_i C_i \frac{d\phi}{dx} \right) \quad \text{Eq. 2-11}$$

The fraction of total electrical current that is carried by each individual species is called transport number. The transport number of each ion can be calculated from following equation:

$$t_i = \frac{i_i}{i} = \frac{|z_i| u_i C_i}{\sum_k |z_k| u_k C_k} = \frac{|z_i| \lambda_i C_i}{\sum_k |z_k| \lambda_k C_k} \quad \text{Eq. 2-12}$$

where t_i , i , u_i , and λ_i are transport number of ion i , total current density, ion mobility, and individual ion conductivity, respectively. Most researchers consider the transport number as the current portion from occurred ion flux due to the migration mechanism only, as shown in $t_i = \frac{i_i}{i} = \frac{|z_i| u_i C_i}{\sum_k |z_k| u_k C_k} = \frac{|z_i| \lambda_i C_i}{\sum_k |z_k| \lambda_k C_k}$

Eq. 2-12, while the total flux includes diffusion and migration mechanisms. Consequently, the ion transport number of each ion in the whole process can be described by the following equation:

$$t_i = \frac{z_i F J_i}{\sum_k z_k F J_k} \quad \text{Eq. 2-13}$$

where J_i is the total flux of ion i from dilute cell to concentrate cell.

Additionally, the total flux can be defined by the extended Nernst-Planck equation as follows:

$$-D_i \left(\frac{dC_i}{dx} + z_i C_i \frac{F}{RT} \frac{d\phi}{dx} + C_i \frac{d \ln f_i}{dx} \right) + C_i v \quad \text{Eq. 2-14}$$

where the D_i , c_i , ϕ , f_i and v are ion diffusion coefficient, ion concentration, electrical potential, molar activity, and velocity of bulk flow, respectively.

The governing ion transport mechanisms in ion movement toward the ion exchange membrane are Electrical migration and diffusion in the desalting solution; however, convection has greater influence in the direction of flow. Therefore, migration and diffusion can be neglected due to great Pecklet number (Moon et al., 2004).

2.2.1.7 Transport models and selectivity in membrane phase

The ion transport through the ion exchange membrane as well as the solution phase is explained by Nernst-Planck equation as follows:

$$\bar{J}_i = -\bar{D}_i \left(\frac{d\bar{C}_i}{dx} + n_i \frac{F \bar{C}_i}{RT} \frac{d\bar{\phi}}{dx} \right) - \frac{RT}{F} \bar{u}_i \frac{d\bar{C}_i}{dx} - z_i \bar{u}_i \bar{C}_i \frac{d\psi}{dx} \quad \text{Eq. 2-15}$$

where J_i , \bar{u}_i , \bar{C}_i , z_i , ϕ , and v are the flux, mobility, concentration, electrical charge, and electrical potential in the membrane phase. In equation 2-15, ion diffusion, migration, and convection through the membrane phase are introduced by the first, second, and the third terms of the equation, respectively. Although all of these three mechanisms occur, the two diffusion and convection terms can be neglected because of the compact and solid structure of ion exchange membranes, so the ion transfer through the membrane can be simplified as the following equation (Tanaka, 2007):

$$J_i = -\bar{D}_i \left(\frac{z_i F \bar{C}_i}{RT} \frac{d\phi}{dx} \right) \quad \text{Eq. 2-16}$$

Assuming ideal passing of counter ions through the membranes, resulting in the replacement of all co-ions, the current density is described by following equation:

$$\sum_i |z_i| \bar{J}_i = \frac{I}{F} \quad \text{Eq. 2-17}$$

where \bar{I}_i is current density in the membrane phase. Multiplying equation 2-16 by z_i and combining by Eq. 2-17 will present the following equation as below:

$$\frac{\bar{I}}{F} = \sum_i \left(-z_i \bar{D}_i \left(\frac{z_i F \bar{C}_i}{RT} \frac{d\phi}{dx} \right) \right) \quad \text{Eq. 2-18}$$

therefore, the electrical potential gradient in the membrane phase is calculated as follows:

$$\frac{d\bar{\phi}^{CM \text{ or } AM}}{dx} = - \frac{RT\bar{I}}{-\sum z_i^2 \bar{C}_i^2 F^2 \bar{D}_i} \quad \text{Eq. 2-19}$$

where $\frac{d\bar{\phi}^{CM \text{ or } AM}}{dx}$ is the electrical potential gradient in the cation or anion exchange membrane.

By assuming that the ion exchange membranes are ideally selective to counter ions, and co-ions are completely repelled with functional groups, only counter ions are absorbed to fixed charge sites. If it is assumed that only a monolayer of counter ions is absorbed to the fixed charged sites, the ion exchange capacity of membranes is equal to concentration of counter ions in the membrane phase as equation 2-20. The absorbed counter ions on the fixed charged sites migrate through the membranes when an electrical potential gradient is applied.

$$\sum_i |z_i| \bar{C}_i = IEC_{AM} \text{ or } IEC_{CM} \quad i = 1, 2, \dots, n \quad \text{Eq. 2-20}$$

where IEC_{AM} , IEC_{CM} , and n are ion exchange capacity for anion exchange membrane and cation exchange membrane, and number of anions and cations in the solution, respectively (Moon et al., 2004).

The term permselectivity refers to the different rates at which different ions move through the ion exchange membrane. In the membrane phase, the permselectivity term can be defined by the following equation (Tanaka, 2007):

$$PS_j^i = \frac{\bar{t}_i / \bar{t}_j}{C_i / C_j} \quad \text{Eq. 2-21}$$

where the \bar{t}_i , C_i , C_j , and PS_j^i are transport number through the ion exchange membrane, concentration of ions i and j in the dilute solution, and the permselectivity of ion i against j in the membrane phase, respectively (Sata et al., 2002). The ion transport number, defined as the portion of current carried by a particular ion passing the membrane, can be written as follows (Tanaka, 2007).

$$\bar{t}_i = \frac{z_i I_i}{\sum z_i I_i} = \frac{z_i^2 \bar{u}_i \bar{C}_i}{\sum z_i^2 \bar{u}_i \bar{C}_i} \quad \text{Eq. 2-22}$$

where the parameters of the aforementioned equation were defined before.

Several factors affect ion transfer in the membrane phase, where the mobility of monovalent and divalent ions is approximately 1/10 and 1/20, respectively, of their mobility in the solution phase. This decrease in mobility can be attributed to the pore size distribution of ion exchange membranes (0.005-0.1

µm), electrical interaction between counter ions and fixed functional groups in the membrane structure and hydrated radius of monovalent and divalent counter ions - not including proton and hydroxide ions (Tanaka, 2007).

The divalent ions are kept in the membrane phase longer than monovalent ions due to their stronger interactions between divalent ions and fixed charged groups, so the divalent ions move more slowly than monovalent ions in the membrane phase (Kabay et al., 2002; Kabay, İpek, et al., 2006). In addition to ion charge, the hydrated ion size affects the ion transport through the membrane phase. The larger ions pass through membranes more slowly than smaller ones (Kabay, İpek, et al., 2006).

Additionally, Donnan equilibrium theory explains the movement of ions through the cation and anion exchange membranes, describing permselectivity both for ions with different charge types and ions with the same charge type. In the concentrated solutions, the effect of Donnan exclusion decreases (Mulder, 1951).

2.2.1.8 Selectivity in ED/EDR process

ED/EDR is one of the most selective membrane-based processes for the removal of ions (Aponte & Colón, 2001). Although ED is a high-cost process for removing F^- and NO_3^- , it is also highly efficient in selectively removing these species (Oldani et al., 1992; Kesore et al., 1997). According to the well-defined definition of selectivity in the membrane phase, the overall selectivity term for the ED process can be defined as follows.

$$S_j^i = \frac{t_i/t_j}{c_i/c_j} \quad \text{Eq. 2-23}$$

where t and C are observed transport number of ion in the ED process, and the concentration of ions in the dilute chamber. The subscripts i and j are related to the two ions whose removals are compared.

The membrane characteristics that affect ion transport through the IEM are the characteristics of the polymer matrix, the type and concentration of fixed ions, and the degree of crosslinking in the membrane structure (Bataillon, 2002).

2.2.1.9 Effective Parameters in the Selective Removal of Ions in ED/EDR process

On the one hand, the controllable factors such as flow rate, temperature, applied voltage, and membrane type can affect the EDR process. On the other hand, some of the noise factors such as pH, concentration polarization, ambient temperature, fouling, and electrolysis effects can also have an influence on the process.

2.2.1.9.1 Voltage

Applied voltage is the most important factor that affects the rate of separation. Walker demonstrated that at higher applied voltages, sodium and

sulfate ions are removed faster in relation to total ion removal. Applying greater voltage, which increases current density, causes a greater concentration gradient for each ion in the diffusion boundary layer (Walker, 2010). Monovalent ion removals were greater affected by voltage variation than are divalent ions under their experimental condition (Kabay, Kahveci, et al., 2006). Kabay et al. showed that voltage variation significantly affects the specific energy consumption (Kabay, Kahveci, et al., 2006). Demircioglu et al. demonstrated the significant role of applied voltage on K^+ removal in their experiments, and also showed that the effect is similar for the removal of Na^+ ions (Demircioglu et al., 2002). Balster et al. showed that calcium transport through the positively charged CEM is low at lower current densities, while it strongly increases at higher current densities (Balster et al., 2005). Banasiak et al. stated that the removal of F^- was affected by voltage changes, while the NO_3^- removal was not influenced significantly by voltage variation. However, they explained that the observed results was due to different initial concentration of the ions and the ion features (Banasiak et al., 2007a).

2.2.1.9.2 Velocity

There are two different reasons for which the rate of ion removal is affected by flow velocity. First, an increased flow velocity can change the thickness of the diffusion boundary layer and cause a positive effect on the rate of ion removal. Particularly, a decrease in the diffusion boundary layer along with an increase in the dilute concentration on the membrane surface occurs from an increasing velocity; in turn, the electrical resistance decreases and a higher current density results in higher rates of ion removal (Walker, 2010). The positive effect of feed velocity variation was distinctly detected on sulfate and sodium removal, along with a negligible and barely detectible effect on calcium and chloride removal (Walker, 2010). Furthermore, the significant effect of velocity was observed at higher concentration polarizations which occurs at applied higher voltage, due to thicker diffusion boundary layer (Walker, 2010). However, Kabay et al. could not observe any specific effect of velocity on ion removal in their experiments (Kabay, Kahveci, et al., 2006), and Demircioglu and et al. did not report any significant effect of flow velocity on K^+ and Na^+ ions in their experiments (Demircioglu et al., 2002). The second means by which flow velocity may affect ion removal is a lower residence time for ions at increased flow rates, which can have negative effects on ion removal. Different researchers have reported the unfavorable effect of increased velocity on ion removal rate and separation performance. It is assumed that ions do not have enough time to pass through the membrane at higher feed flow rates, and are instead rinsed from the membrane surface before passing (Sadrzadeh et al., 2006). Aponte and Colon used the ED process to examine sodium chloride recovery from urine; they reported that at a lower flow velocity, which causes higher residence time, greater sodium chloride removal from urine was achieved (Aponte & Colón, 2001). The negative effect of velocity on the separation of different ions was reported (Sadrzadeh et al., 2006),(Sadrzadeh et al., 2007),(Mohammadi et al., 2004). On the other hand, both positive and negative effects of velocity on current efficiency

in sea water treatment using small ED was reported by Sadrzadeh and Mohammadi at different flow rates and different feed concentrations (Sadrzadeh & Mohammadi, 2009).

2.2.1.9.3 Ion Type

Ions with lower diffusivity reach limiting current faster than the ions with greater diffusivity, due to faster depletion on the membrane surface (Walker, 2010). In the matter of specific energy consumption in electro dialysis, the effect of ion valance on the separation was investigated (Kabay et al., 2003). Due to interaction between ion exchange membrane characteristics, ion charge also affects ion removal. Balster et al. studied the effects of the feed composition's current density and calcium ion concentration on the selectivity of different commercial ion exchange membranes. They demonstrated that calcium ion transport through the membrane is affected by the membrane's charge density and conductivity, as well as its water uptake and ion exchange capacity. It was also mentioned that IEMs with lower charge density have a greater tendency to remove monovalent ions selectively. Additionally, it was reported that membrane charge density also affects multivalent ion removal rate more than monovalent ion removal rate (Balster et al., 2005).

2.2.1.9.4 Feed composition

Kabay et al. examined the feed composition effect in the electro dialysis process using different 0.01 N binary mixtures on monovalent and divalent ion removal at room temperature, and at a constant flow rate of 1.6 l/min. It was shown that at lower voltage, the monovalent cations are removed more efficiently in the presence of only monovalent anions than under conditions where divalent anions are present in the feed solution; this is because the monovalent cations are more strongly attracted by divalent anions, thus affecting their removal rate. At higher voltages, however, this effect disappeared (Kabay, İpek, et al., 2006). While investigating the effect of initial NaCl concentrations in the feedwater, Banasiak et al. demonstrated the efficiency of removing F^- and NO_3^- ions from brackish water through the use of electro dialysis processes. The results confirmed that the rate of removal was greater at higher initial concentrations of NaCl (Banasiak et al., 2007b).

2.2.1.9.5 Pressure

Most electro dialysis manufacturers recommend that static head difference between the dilute and concentrate solutions be kept close to zero to prevent convection mechanisms and water transport from a dilute stream to a concentrate one. Despite this, the differential pressure at the inlet and outlet points of the stack between the dilute and concentrate chambers in the real large-scale operation of EDR systems is kept within the 0.5-1 psi range. Although the recommended difference can be applied well in the lab-scale EDR process, this is done in the large-scale operation in order to prevent any leakage from the concentrate chamber to the dilute chamber (Murray, 1996).

2.2.1.9.6 pH

Removal of anions occurs best in acidic, low-pH environments while removal of cations works best in alkaline high-pH environments; this effect is explained by the tendency of OH^- to compete with anions, and likewise of H^+ with cations. The effect of pH on important parameters such as current efficiency, concentration polarization, and energy consumption in the ED process was investigated by About-Shady et al.; it was shown that pH variations influence the distribution of NO_3^- and Pb^{2+} on the surface membrane, and thus affects their removal (Abou-Shady et al., 2012). Additionally, Kabay et al. investigated the effect of pH on the separation of monovalent ions such as NaCl and KCl, and divalent ions such as MgCl_2 and CaCl_2 , at pH levels of 6.5, 6.0, 4.0, and 2.0 (Kabay et al., 2003). It was shown that a higher energy consumption was required to remove ions at a lower pH (defined as less than 4), regardless of whether the ions were monovalent or divalent. However, pH changes did not affect competitive separation of monovalent and divalent ions (Kabay et al., 2003).

Chapter 3: Material and Methods

3.1 Pilot Scale Experiment Site

The Bureau of Reclamation constructed the Brackish Groundwater National Desalination Research Facility (BGNDRF), a federal research facility located in Alamogordo, New Mexico, to provide national and international researchers an environment where they can conduct work on brackish ground water desalination. The facility's location in the Tularosa Basin provides access to four brackish groundwater wells with a wide range of salinity, ranging from 1000 to 6400 ppm. One of the wells, well 1, is a geothermal well with a normal temperature of 40 °C. The brackish water from this well can be supplied at two different temperatures: 24 °C after passing the cooling tower which is subject to change due to seasonal temperature changes, or 40 °C straight from the storage tank. At this facility test bay number 4, where the pilot-scale EDR set-up was installed, was used for the EDR experiments.

In the process of well water delivery to the test bays, water from the aquifer was pumped to a storage tank, where it was then sent to a hydrostatic tank to be pressurized to 350 kPa. With the use of a valve, the pressure was then reduced to less than 70 kPa before it was delivered to the test bay.

3.2 Pilot-Scale Experimental Set-up

A General Electric EDR set-up with an influent flow rate capacity of 12 gallons per minute (0.775 L/s) was used to conduct these pilot-scale experiments. figures 3-1 and 3-2 present a schematic and a photograph of the entire set-up. The nature and purpose of each component is explained in the following sections.

3.2.1 Pretreatment Process Before EDR

Before being sent to the EDR stack, the feed water is pressurized in the feed pump and then sent to the Multi-Media filter (MMF) and cartridge filter. Generally, the EDR process does not need special pretreatment. However, applying a MMF can help prevent potential damage and fouling of the membranes from sands and suspended solids in the feed water; filters of different pore sizes in the MMF provide the means in which the suspended solids can be removed. The feed water then passes through the cartridge filter, which contains a pore size of 10 µm, to remove any remaining suspended or dissolved particles before finally entering the stack.

3.2.2 EDR Stack

The GE electro dialyzer that was used in this set-up was composed of spacers and anion and cation exchange membranes. These stack components are of industrial-size, but the number of cell pairs differs from that of industrial stacks; the stack used in the experiments had 40 cell pairs, while the number of cell pairs in industrial applications exceeds 600. A cell pair is constituted of three ion exchange membranes that provide two dilute and two concentrate chambers. The spacers serve to separate the ion exchange membranes from each other, and establish the required channel thickness for dilute and concentrate streams to flow in the channels; they also introduce turbulence in the streams. The membranes are fixed between two top and bottom electrodes. Both streams pass once through the chambers and exit the stack as shown in figure 3-1. Therefore, the stack is constituted of one hydraulic and one electrical stage. Heavy spacers and heavy cation exchange membranes precede the electrodes whose coatings give them the capability of charge reversal. The reason behind the use of the heavy spacers and heavy cation exchange membranes is to facilitate the flow of the electrode rinse solution over the top and bottom electrodes. This flow washes out the produced gases from electrode chambers' reactions and sends them to the degasifier to prevent any damage to membranes, especially from the chlorine produced in the cathode. Although the electrode solution conductivity should match that of the feed water in order to decrease the effect of osmotic pressure (Abou-Shady et al., 2012), large scale operations dose the electrode rinse solution with 15% hydrochloric acid. The injected acid is consumed in order to neutralize the hydroxide ions formed in the cathode, which prevents scaling problems in the electrodes. After leaving the stack, the electrode rinse solution is sent to the degasifier and is then either disposed of as waste, or recycled, in order to improve the process's recovery rate. The detailed specification of the EDR components is introduced in table 3-1.

3.2.3 Analytical Analysis

The operating conditions were monitored and recorded during the experiments. By using inline float type flow meters, made by Plast-O-matic valves, Inc., product flow rates and concentrate blow down were measured and then recorded manually. The set-up was equipped with Mettler Toledo inline pH and conductivity sensors, and temperature sensors were used to monitor these parameters during the experiments to ensure a steady system operation. Additionally, an oscilloscope from Fluke Co. was used to measure the applied voltage between the two electrodes on the stack. The DC current probe, also from Fluke Co., was used to measure the direct current in the stack.

During the experiments, water samples were collected and analyzed using the Dionex ICS-5000 Dual Channel IC System, an ion chromatography system with the capability of measuring the cations and the anions via analytical channels and capillary channels, respectively. Additionally, pH levels of the samples were analyzed to detect the amount of carbonate. Titration was then performed for water samples to determine the amount of any possible carbonate. However, for very small mounts of species, the titration procedure cannot be considered as an

accurate method of analysis. Therefore, the samples were analyzed to determine the inorganic carbon source using Total Organic Carbon Analyzer, Shimadzu TOC-Vcsh.

3.3 Pilot-Scale Experiments

The pilot-scale experiments were conducted at BGNDRF using brackish well water. The used feed water was provided from well 1, and as explained previously, could be delivered at two different temperatures. The feed water composition is given in table 3-2; it can be seen from the data that the water composition slightly varies at each operating temperature. These small differences were observed because some of the water in the cooling tower evaporates, further concentrating the feed water to some extent.

3.4 Design of Experiments

The experiments were designed in two different sets. The first set was preliminary experiments at pilot-scale, and the next set will be at laboratory-scale.

3.4.1 Pilot-Scale

In order to show the effect of operating parameters, such as velocity, temperature, and voltage on ion removal in EDR process, the experiments were conducted at two levels of temperature and velocity, and six levels of voltage, as shown in table 3-3. The ratios of dilute and concentrate streams were chosen based on the manufacturer's recommended numbers. The experiments were conducted at four different combinations of temperature and flow. In order to detect the effect of velocity (flow rate), and temperature, the experiments were run at the same voltage levels for all four combinations. The overall design of the conducted experiments is shown in table 3-4.

The most significant operating factors will be determined after conducting the experiments, shown in table 2-8, and analyzing the obtained results. Then another set of detailed experiments will be designed to obtain an empirical model for ion removal in EDR process.

However, for the purpose of anion exchange membrane comparison, the next phase of experiments were conducted in a wider range of operating conditions and used three different anion exchange membranes, but used the same cation exchange membranes in the pilot-scale EDR. The first set of conducted experiments consisted of using AR204 under a wide range of operating conditions. The second and third sets of experiments were done using AR908 and aged-AR204. The aged-AR204 were used anion exchange membranes from a San Diego wastewater treatment site (North City Water Reclamation). In order to assure that the aged-AR204 membranes were in good condition, the membranes were carefully scrubbed, washed, and tested with the leakage test.

Chapter 4: Results and Discussion

4.1 Effect of Applied Voltage and Ion Size on Ion removal

As discussed in the first chapter, ions are removed in the EDR process because of the applied voltage in the stack. Under normal operating conditions before limiting current is reached, increasing the amount of applied voltage increases the removal of ions. The effect of applied voltage on ion removal depends on some of the ion characteristics such as charge and hydrated radius. According to the literature mentioned in the first chapter, ions with greater electrical charges are affected more strongly by an electrical field than ions with a smaller electrical charge. This effect is distinctly shown for cations in figures 4-1 and 4-2.

The data from all these figures depicts that the divalent cations, Ca^{2+} and Mg^{2+} , are removed better than monovalent cations, such as K^+ and Na^+ . However, while this trend is shown in almost all of the figures at lower voltage, at higher applied voltages the percent removal of the ions converges to a unique value, especially at lower velocity and high temperature under which the greatest amount of removal is observed. According to all of these figures, the effect of applied voltage on the removal of ions is not constant in all ranges of applied voltage. Additionally, it is shown that when applied voltage is constant, the percent removal of Ca^{2+} is greater than percent removal of Mg^{2+} due to the smaller hydrated radius of Ca^{2+} in comparison to Mg^{2+} , as shown in table 4-1 (Nightingale & Nightingale Jr., 1959; Railsback, 2006). The effect of the hydrated radius of ions is also observed in the higher removal percentage of K^+ as compared to the removal percentage of Na^+ , an effect which is due to the greater hydrated radius of Na^+ in comparison to K^+ (Nightingale & Nightingale Jr., 1959; Railsback, 2006). The same effects from voltage, electrical charge, and hydrated ion size that are observed with cations are also observed in the removal of anions, as shown in figures 4-3 and 4-4. Although it was predicted to observe less removal of HCO_3^- in comparison to F^- due to its bigger hydrated radius (Kielland, 1937), in some experiments the removal of HCO_3^- is higher than, or close to, the F^- removal. The observed difference in the removal of these two monovalent anions implies that the negligible amount of CO_3^{2-} was counted in the obtained results from total inorganic carbon analysis which was initially assumed as HCO_3^- concentration; however, its concentration could not be detected by pH measurements and titration method due to its very small amount.

4.2 Effect of Superficial Velocity on Ion Removal

As discussed in chapter 1, one of the other parameters that affect ion removal in the EDR process is superficial velocity, or flow rate. The impact of this effect on the removal of cations and anions is shown in figures 4-5 through 4-12 based on the results obtained from this experiment.

The plotted curves show that when linear velocity increases from 8.8 to 13.1 cm/s, the removal rate decreases for both cations and anions. This reduction trend in the removal of ions can be explained by decreased residence time, a characteristic which can be defined as follows:

$$t_{resid} = \frac{L}{V} \quad \text{Eq. 4-1}$$

which t_{resid} , L , and V are residence time, flow path length, and linear velocity, respectively.

According to this equation, the residence time decreases 33% over the constant flow path in the EDR stack when the linear velocity is increased from 8.8 to 13.1 cm/s. The observed reduction in the ion removal due to the decrease in the residence time means the ions have less time to pass through the membranes and transfer from dilute stream to the concentrate stream. The ions which reach the membrane's surface are washed from the surface without being able to pass through the membranes.

4.3 Effect of Temperature on Ion Removal

One of the impactful operating factors in ion removal is temperature. According to the shown curves in figures 4-13 to 4-20, increasing the temperature of feed water from 24 to 38 °C improves ion removal. The experimental results from pilot-scale experiments confirm this effect for the removal of both cations and anions.

The observed effect of temperature can be explained theoretically by considering the positive effect of temperature on ion diffusion coefficient in the solution phase as shown in equation 2-15. By incorporating the effect of temperature on the diffusion coefficient of ions into the Nernst- Einstein equation, the ratio of ion mobility was calculated, confirming that when temperature was increased from 24 to 38 °C, ion mobility increased 1.3 times for both cations and anions, when the diffusion coefficient of ions are assumed independent of each other. However, because of the nature of the Nernst-Planck equation in which the temperature term is the denominator term of ion flux, this ratio is not the same as the observed ratio of ion removal increasing under the effect of temperature.

4.4 Comparing the Effect of Linear Velocity and temperature on Ion Removal

The percent removal of all cations and anions was also plotted in order to compare the effect of linear velocity and temperature in the proposed levels. According to the plotted results in figure 4-21, it seems that increasing temperature from 24 to 38 °C can compensate for the negative effect of velocity increase on the removal of divalent ions Ca^{2+} , SO_4^{2-} , and Mg^{2+} .

The effects of linear velocity and temperature on the removal of monovalent ions are compared in the figures 4-22 and 4-23. Based on the removal results for monovalent anions and cations, shown in these figures, the greatest removal of ions is obtained at a low linear velocity of 8 cm/s; this causes higher residence time and higher temperature, which creates higher ion mobility. For the removal of monovalent ions, low velocity and low temperature was the second most effective set of operating conditions. It appears that, due to the important role of residence time in the removal of monovalent ions, increases in the operating temperature cannot compensate for the way higher flow velocity decreases the residence time of ions in the stack at higher velocity, as what was observed in the removal of divalent ions.

4.5 Selectivity of different Ion exchange membranes under different conditions

In order to show the effect of operating conditions on ion removal in a combined form, a dimensionless number, ξ was applied. This number was introduced by Kitamoto and Takashima (Kitamoto & Takashima, 1970) using the following equation.

$$\xi = \frac{\Lambda \Delta \phi}{2FDV} \quad \text{Eq 4-2}$$

where Λ , $\Delta \phi$, F , D , and V are equivalent conductivity, effective applied voltage, Faraday constant, desalting cell width, and solution linear velocity in the dilute chamber.

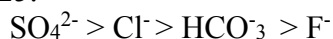
4.5.1 Selective Removal of Cations

In order to show the preferential cation removal in the EDR process, Na^+ was chosen as the reference cation. The selectivity of the EDR process toward different ions was calculated using equation 2-23, as introduced in the previous chapter. The results of the conducted pilot-scale experiments using the CR-67 cation exchange membrane showed the following order in removal of cations, as shown in figure 4-24.



4.5.2 Selective Removal of Anions

In order to show the preferential anion removal in the EDR process, Cl^- was chosen as reference anion. Similar to cations, the selectivity of the EDR process toward different anions was calculated using equation 2-23. The results of the conducted pilot-scale experiments using the AR204 anion exchange membranes showed the following order in removal of anions as shown in figure 4-25.



4.5.3 Selectivity Sensitivity for Cations Vs. Na^+

In order to investigate the sensitivity of selectivity values for different cations at different operating conditions, the selectivity values were calculated when the removal of Na^+ was increased 0.5 ppm at different ξ values. As it is shown in figures 4-26 through 4-29, the selectivity values for cations are more sensitive at lower values of ξ compared to its higher values. This observation confirms that the removal of cations in a selective way is more feasible in lower values of ξ , which means the mild operating conditions, specifically lower voltage values, because, as shown in previous figures, the selectivity values approach to one at higher levels of applied voltages.

4.5.4 Selectivity Sensitivity for Anions Vs. Cl^-

The similar sensitivity analysis was conducted to verify the selectivity sensitivity for different anions at different operating conditions. The selectivity values were calculated when the removal of Cl^- was increased 0.5 ppm at different ξ values. As it is shown in figures 4-30 through 4-32, the selectivity values for cations are more sensitive at lower values of ξ compared to its higher values. The anions' removal results showed that the selectivity of anions using AR204 anion exchange membranes is more sensitive at lower values of ξ which confirms divalent selective behavior of this type of membrane. Like cations' removal, this observation confirms that the removal of anions in a selective way is more achievable at lower values of ξ which means the mild operating conditions, specifically lower voltage values.

4.5.5 Ion Exchange Membrane Selectivity Comparison

The next phase of experiments was conducted to compare the performance of different anion exchange membranes under different operating conditions. The examined anion exchange membranes in the pilot-scale experiments were AR204, AR908, and aged-AR204. However, the same type of cation exchange membranes, CR-67, was used in all of the experiments. The operating conditions, as explained before, are shown in the form of ξ . The obtained results are shown in the following figures. Figures 4-33 through 4-35 show the selectivity of EDR process using different anion exchange membranes.

As depicted in figure 4-33, the new AR204 and AR908 membranes showed more selective behavior toward SO_4^{2-} compared to Cl^- at lower ξ values, which represent mild operating conditions. This behavior can be explained

according to the type of functional groups in the structure of these ion exchange membrane types and the electrical charge of SO_4^{2-} , which causes their fast migration under the influence of an electrical field. However, aged-AR204 anion exchange membranes showed values less than 1 for selectivity of SO_4^{2-} over Cl^- in a wide range of ξ . This observation can be explained hypothetically by the nature of microorganisms built up on the surface of anion exchange membranes, which are negatively charged. The accumulation of negative charge on the surface of the membrane can cause a repulsion force between the anions with greater electrical charge as SO_4^{2-} , but let monovalent ions as Cl^- pass through them much faster and more easily.

Figures 4-33 and 4-35 show that the selectivity of EDR process for monovalent ions, such as F^- and HCO_3^- , are less than Cl^- due to their larger hydrated sizes as compared to Cl^- hydrated size. Additionally, the graphs confirm that the selectivity of the Anion exchange membranes for F^- were not affected by aging and the negative layer of microorganisms on the aged-AR204 anion exchange membranes.

Figures 4-36 through 4-39 showed that the type of used anion exchange membrane did not have any significant effect on selectivity of cations while the type of cation exchange membrane was same. However, the electronuetality is affected when one of the anion or cation exchange membranes are selective toward any specific species.

These figures confirmed that the EDR process is more selective for removal of divalent cations, such as Ca^{2+} , Mg^{2+} , and Sr^{2+} compared to monovalent cations as Na^+ when CR-67 cation exchange membranes are used. However, at higher values of ξ , which mostly represent higher applied voltage in the process, the selectivity values approach to 1 for all species.

In general, three different regions can be assumed for the effect of ξ as shown in figures 4-40 through 4-48. These figures depict that at small ξ values (Region I) the removal of ions is mostly under the influence of ion exchange membrane types rather than other factors. In the mid-range of ξ values (region II) both solution phase and ion exchange membranes play a significant role in ion removal. This means factors the behavior of ions in the solution phase and affinity of ion exchange membrane to the ion and the behavior of ion in the membrane have a significant role on ion removal. In the high values of ξ (region III) all ions are removed simultaneously regardless of the type of ion, or effects of solution phase and ion exchange membrane phase.

As it is shown in the figures 4-40 through 4-43, the range of ξ values for three different regions is constant in removal of divalent cations. The small ξ values which represent the first region are ξ values less than 6.5×10^{-5} . If ξ parameter is in the range of $6.5 \times 10^{-5} < \xi < 5.9 \times 10^{-4}$, it is called region II. ξ values great than 5.9×10^{-4} represent region III.

As shown in figures 4-44 through 4-47, the lower range of ξ values is slightly different for the removal of monovalent ions. However, this difference cannot be strongly claimed due to variation of the data.

Chapter 5: References

Abou-Shady, A. et al., 2012. Effect of pH on separation of Pb (II) and NO₃⁻ from aqueous solutions using electrodialysis. *Desalination*, 285, pp.46–53.

Addams, L. et al., 2009. *Charting Our Water Future Economic frameworks to inform decision-making*,

Anon, 2014. Salinity. Available at:
http://www.seagrassli.org/ecology/physical_environment/salinity.html.

Aponte, V.M.M. & Colón, G., 2001. Sodium chloride removal from urine via a six-compartment ED cell for use in Advanced Life Support Systems (Part 1: salt removal as a function of applied voltage and fluid velocity). *Desalination*, 140(2), pp.121–132.

Balster, J. et al., 2005. Preparation and characterisation of monovalent ion selective cation exchange membranes based on sulphonated poly(ether ether ketone). *Journal of Membrane Science*, 263(1-2), pp.137–145.

Banasiak, L.J., Kruttschnitt, T.W. & Schäfer, A.I., 2007a. Desalination using electrodialysis as a function of voltage and salt concentration. *Desalination*, 205(1-3), pp.38–46.

Banasiak, L.J., Kruttschnitt, T.W. & Schäfer, A.I., 2007b. Desalination using electrodialysis as a function of voltage and salt concentration. *Desalination*, 205(1-3), pp.38–46.

Barakat, M.A., 2011. New trends in removing heavy metals from industrial wastewater. *Arabian Journal of Chemistry*, 4(4), pp.361–377.

Bard, A.J. & Faulkner, L.R., 2001. *Electrochemical Methods: Fundamentals and Applications* second., John Wiley an Sons, INC.

Bataillon, P.E., 2002. Conductivity and selectivity of ion exchange membranes : *Desalination*, 147, pp.359–361.

Demircioglu, M. et al., 2002. Demineralization by electrodialysis (ED) - separation performance and cost comparison for monovalent salts. *Desalination*, 153, pp.329–333.

Helfferich, F.G., 1962. *Ion Exchange*, New York: Courier Dover Publications.

Jakobsen, M.R. et al., 2004. Electrodialytic removal of cadmium from wastewater sludge. *Journal of Hazardous Materials*, 106(2–3), pp.127–132.

- Kabay, N. et al., 2003. Effect of feed characteristics on the separation performances of monovalent and divalent salts by electrodialysis. *Desalination*, 158, pp.95–100.
- Kabay, N., İpek, Ö., et al., 2006. Effect of salt combination on separation of monovalent and divalent salts by electrodialysis. *Desalination*, 198(1-3), pp.84–91.
- Kabay, N. et al., 2002. Removal of calcium and magnesium hardness by electrodialysis. *Desalination*, 149(1), pp.343–349.
- Kabay, N., Kahveci, H., et al., 2006. Separation of monovalent and divalent ions from ternary mixtures by electrodialysis. *Desalination*, 198(1-3), pp.74–83.
- Kalogirou, S., 2005. Seawater desalination using renewable energy sources. *Progress in Energy and Combustion Science*, 31(3), pp.242–281.
- Kedem, O., Wilf, M. & Strathmann, H., 2010. Electrodialysis, a mature technology with a multitude of new applications. *Desalination*, 264(3), pp.268–288.
- Kesore, K., Janowski, F. & Shaposhnik, V.A., 1997. Highly effective electrodialysis for selective elimination of nitrates from drinking water. *Journal of Membrane Science*, 127(1), pp.17–24.
- Kielland, J., 1937. Individual Activity Coefficients of Ions in Aqueous Solutions. *Journal of the American Chemical Society*, 58(9), pp.1675–1678.
- Kitamoto, A. & Takashima, Y., 1970. Preferential ion transport through ion exchange membranes by electrodialysis. *Journal of Chemical Engineering of ...*, 3(1957), pp.54–61.
- Marder, L., Bernardes, A.M. & Ferreira, J.Z., 2004. Cadmium electroplating wastewater treatment using a laboratory-scale electrodialysis system. *Separation and Purification Technology*, 37(3), pp.247–255.
- Mohammadi, T. et al., 2005. Modeling of metal ion removal from wastewater by electrodialysis. *Separation and Purification Technology*, 41(1), pp.73–82.
- Mohammadi, T., Razmi, a. & Sadrzadeh, M., 2004. Effect of operating parameters on Pb²⁺ separation from wastewater using electrodialysis. *Desalination*, 167, pp.379–385.
- Moon, P. et al., 2004. Computational Modeling of Ionic Transport in Continuous and Batch Electrodialysis. *Separation Science and Technology*, 39(11), pp.2531–2555.

- Mulder, M., 1951. *Basic Principles of membrane technology* first., Enschede: Kluwer Academic Publishers.
- Murray, P. ed., 1996. *Electrodialysis and Electrodialysis Reversal* first., Denver: American Water Works Association.
- Nightingale, E.R. & Nightingale Jr., E.R., 1959. Phenomenological Theory of Solvation. Effective Radii of Hydrated Ions. *The Journal of Physical Chemistry*, 63(9), pp.1381–1387.
- Oldani, M. et al., 1992. On the nitrate and monovalent cation selectivity of ion exchange membranes used in drinking water purification. *Journal of Membrane Science*, 75(3), pp.265–275.
- Railsback, B.L., 2006. Some Fundamentals of Mineralogy and Geochemistry. *Department of Geology, University of Georgia Athens, Georgia 30602-2501 U.S.A.* Available at: www.gly.uga.edu/railsback/FundamentalsIndex.html.
- Sadrzadeh, M., Kaviani, A. & Mohammadi, T., 2006. Mathematical Modeling of Desalination by Electrodialysis. In *Tenth International Water Technology Conference, IWTC10*. Alexandria, Egypt, pp. 221–233.
- Sadrzadeh, M. & Mohammadi, T., 2009. Treatment of sea water using electrodialysis: Current efficiency evaluation. *Desalination*, 249(1), pp.279–285.
- Sadrzadeh, M., Razmi, A. & Mohammadi, T., 2007. Separation of monovalent, divalent and trivalent ions from wastewater at various operating conditions using electrodialysis. *Desalination*, 205(1-3), pp.53–61.
- Sata, T., Sata, T. & Yang, W., 2002. Studies on cation-exchange membranes having permselectivity between cations in electrodialysis. *Journal of Membrane Science*, 206(1-2), pp.31–60.
- Strathmann, H., Assessment of Electrodialysis Water Desalination Process Costs.pdf. Available at: <http://gwri-ic.technion.ac.il/pdf/IDS/82.pdf>.
- Strathmann, H., 2010. Electrodialysis, a mature technology with a multitude of new applications. *Desalination*, 264(3), pp.268–288.
- Strathmann, H., 2004. *Ion-exchange Membrane separation processes* first., Elsevier.
- Strathmann, H., 1995. *Membrane Separation Technology- Principles and Applications* second. S. Noble, R.D., Stern, ed., New York: Elsevier.

Tanaka, Y., 2003. Concentration polarization in ion-exchange membrane electrodialysis—the events arising in a flowing solution in a desalting cell. *Journal of Membrane Science*, 216(1-2), pp.149–164.

Tanaka, Y., 2007. *Ion Exchange Membranes: Fundamentals and Applications* First., Amsterdam: Elsevier.

Tanaka, Y. et al., 2003. Ion-exchange membrane electro-dialytic salt production using brine discharged from a reverse osmosis seawater desalination plant. *Journal of Membrane Science*, 222(1), pp.71–86.

Tzanetakis, N. et al., 2003. Comparative performance of ion exchange membranes for electrodialysis of nickel and cobalt. *Separation and Purification Technology*, 30(2), pp.113–127.

Walker, W.S., 2010. *Improving Recovery in Reverse Osmosis Desalination of Inland Brackish Groundwaters via Electrodialysis*. Austin: University of Texas at Austin.

Tables

Chapter 2

TABLE 2-1 Water resource categories regarding the salinity ²

Water Type and Salinity				
Water Type	Fresh Water	Brackish Water	Saline Water	Brine
TDS (ppt*)	<0.5	0.5-30	30-50	>50

* parts per thousands

Chapter 3

TABLE 3-1 Specification of the EDR stack

Component	Detail	
EDR Stack	One Electrical Stage	Two Electrodes
	One Hydraulic Stage	40 Cell pairs
Ion Exchange Membranes	Anion Exchange Membranes	GE AR908 114×60×0.6 (cm)
	Cation Exchange Membranes	GE CR67-HMR 114×60×0.6 (cm)
Spacer	Normal	Mk-IV Effective Membrane Area: 0.3 m ² /IEM
	Heavy	

TABLE 3-2 Feed water composition

Brackish Ground Water BGNDRF well 1									
Temperature (°C)	Cations (ppm)					Anions (ppm)			
	Ca ²⁺	Mg ²⁺	Na ⁺	Sr ²⁺	K ⁺	Cl ⁻	SO ₄ ²⁻	HCO ₃ ^{-*}	F ⁻
24	50.5	8.6	376.9	<2	2.1	35.9	664.0	185.1	2.0
38	47.0	7.5	363.6	<2	2.0	31.6	628.2	187.2	2.0

* It may have a negligible source of CO₃²⁻

TABLE 3-2 Operating conditions levels in the pilot-scale experiments

Factor	Level	Real Value
Feed Linear Velocity (V: cm/s)	1	8.8
	2	13.1
Temperature (°C)	1	24
	2	38
Voltage (V)	1	2.6
	2	9.8
	3	21.7
	4	33.4
	5	45.3
	6	57.7

TABLE 3-3 Overall design of preliminary experiments in the pilot-scale experiments

Feed Linear Velocity	Temperature (°C)	Applied Voltage (V)
1	1	1
		2
		3
		4
		5
		6
1	2	1
		2
		3
		4
		5
		6

Chapter 4

TABLE 4-1
Hydrated radii
of examined
cations and
anions

Ion hydrated radius (°A)						
Ca ²⁺	Cations			Anions		
	Mg ²⁺	Na ⁺	K ⁺	Cl ⁻	SO ₄ ²⁻	F ⁻
4.12	4.28	3.58	3.31	3.32	3.79	3.52

1
2
3
4
5
6
1
2
3
4
5
6

Figures

Chapter 2

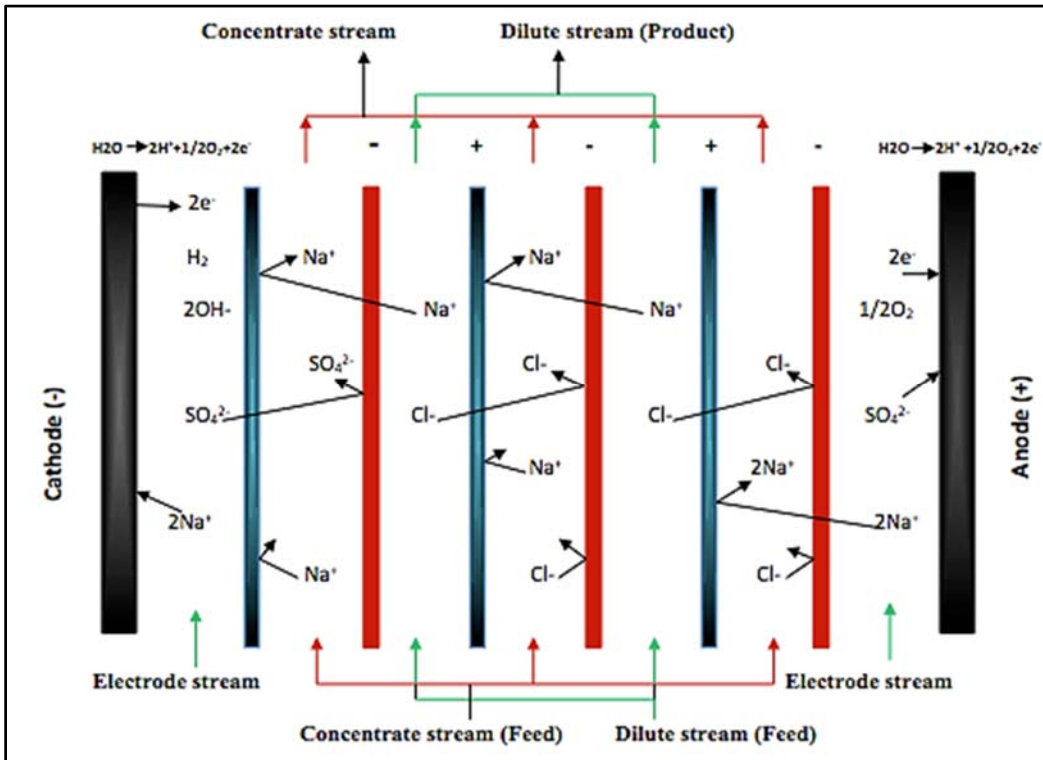


FIGURE 1-1 Schematic of electrodialysis process

Chapter 3

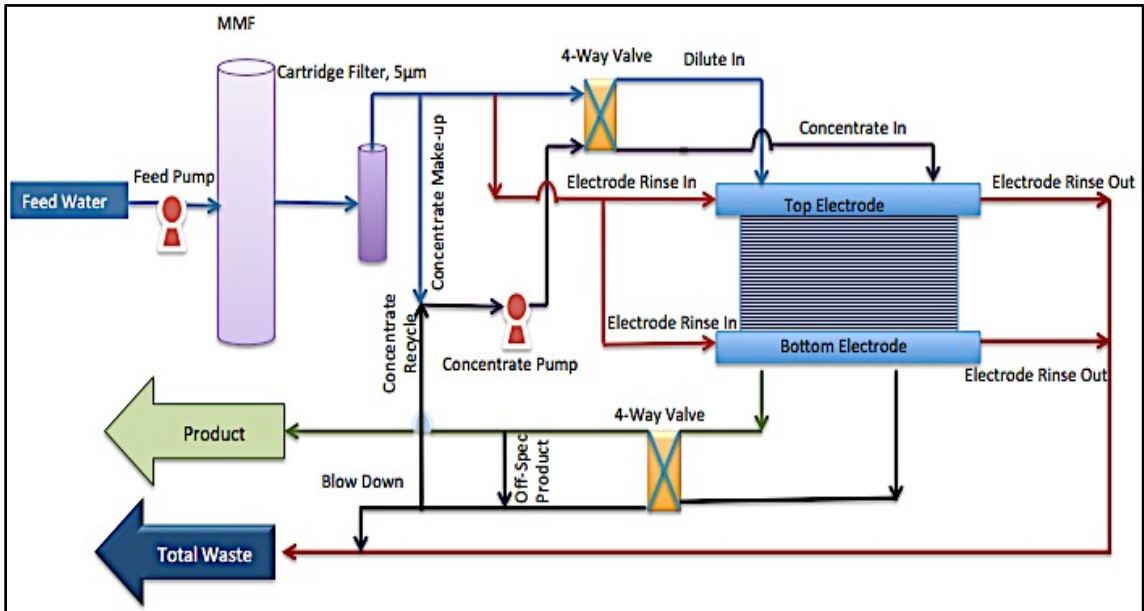


FIGURE 3-1 Schematic of the pilot-scale EDR set-up

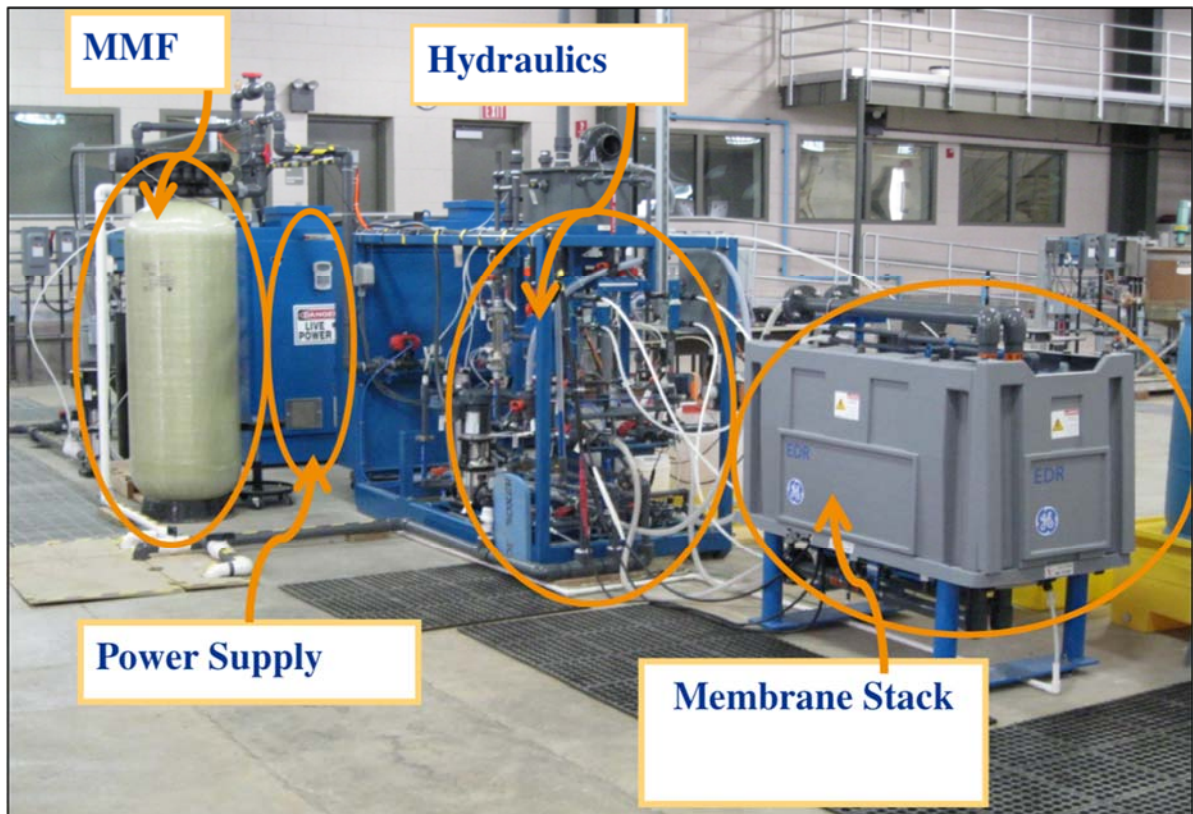
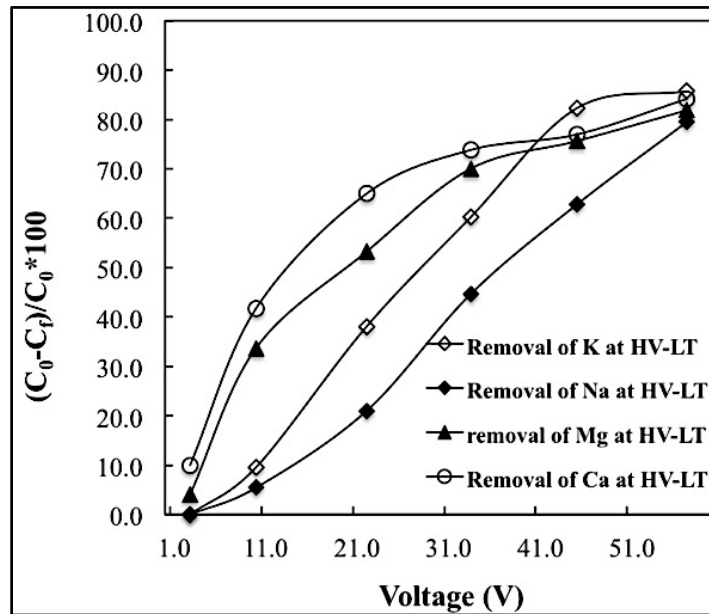
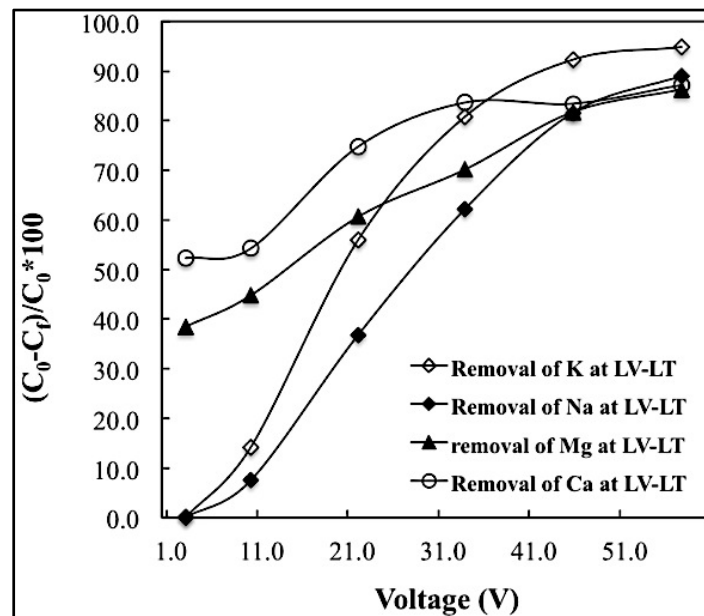


FIGURE 3-2 Pilot-scale EDR set-up

Chapter 4

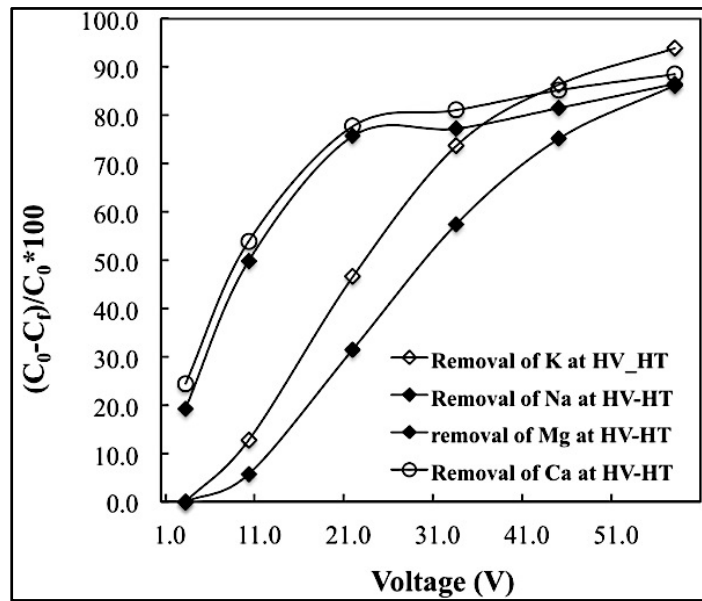


(a)

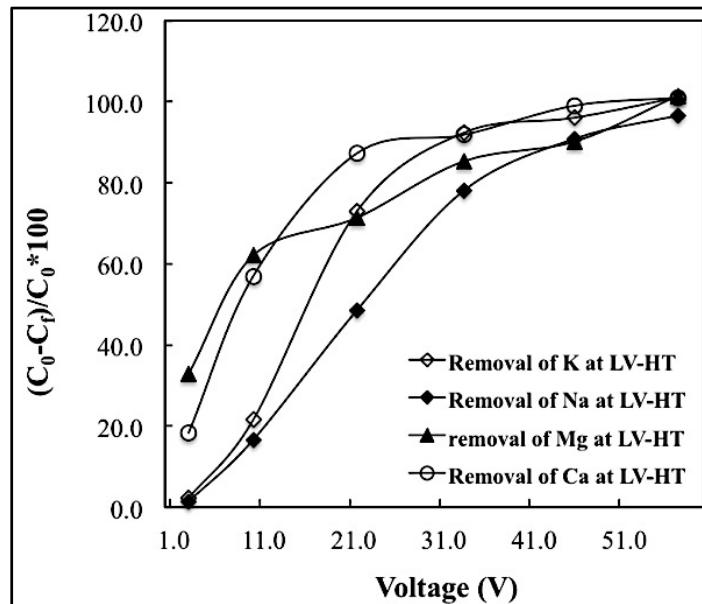


(b)

FIGURE 0-3 Effect of voltage on removal of cations at low temperature, high velocity (a), and low velocity (b)

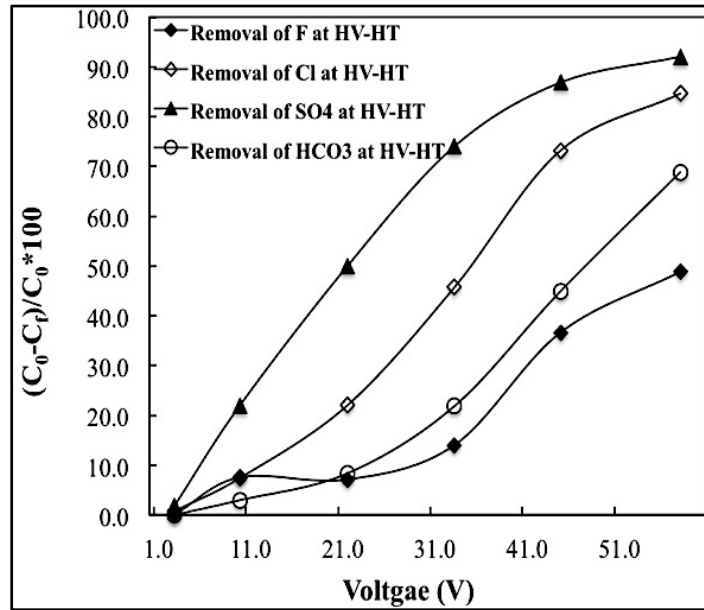


(a)

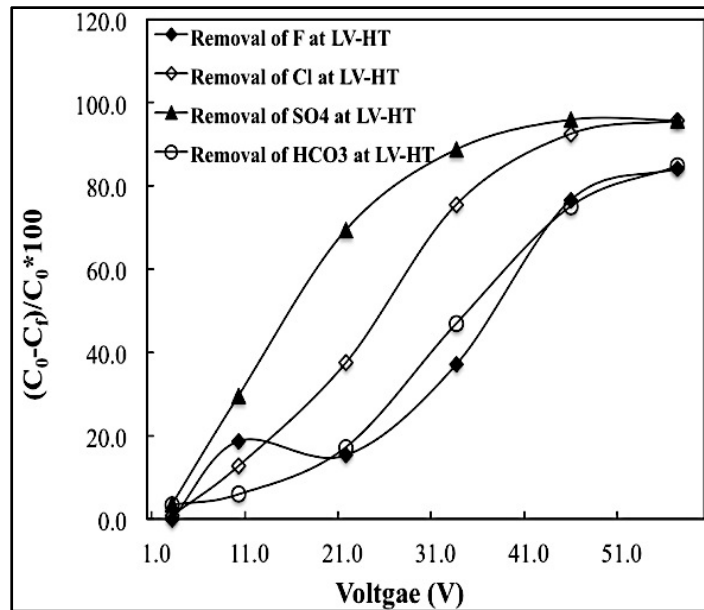


(b)

FIGURE 0-4 Effect of voltage on removal of cations at high temperature, high velocity (a) and low velocity (b)

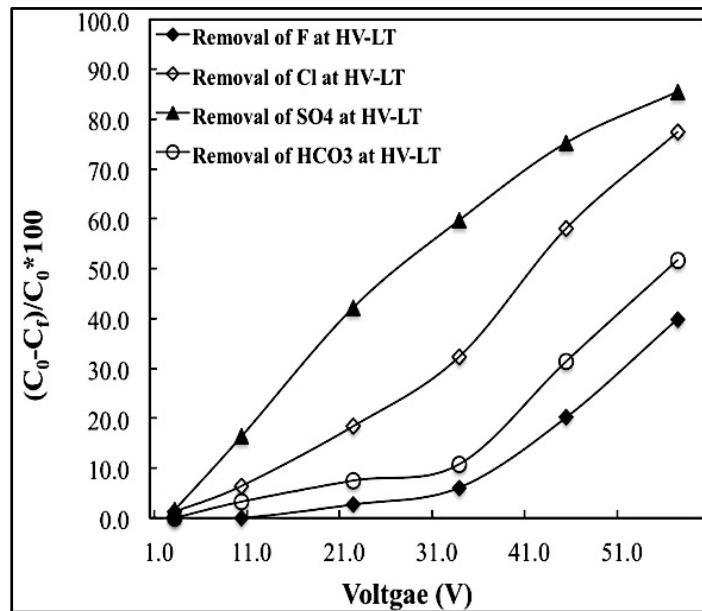


(a)

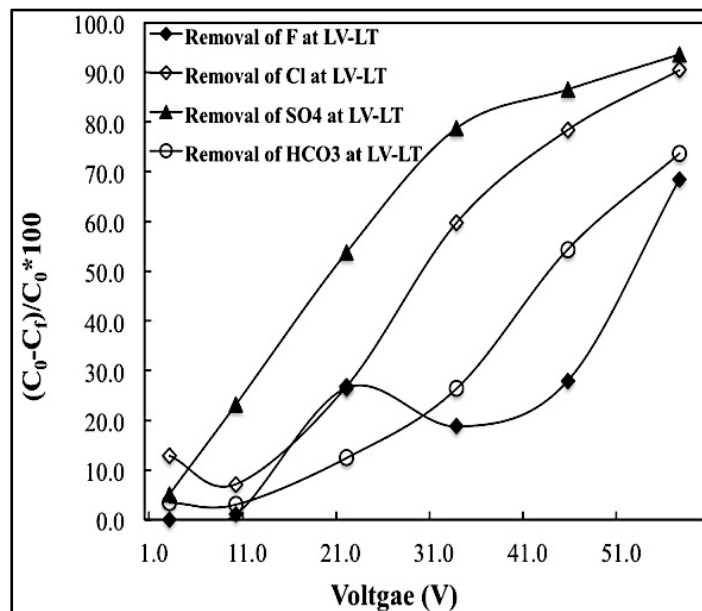


(b)

FIGURE 0-5 Effect of voltage on removal of anions at high temperature, high velocity (a), and low velocity (b)

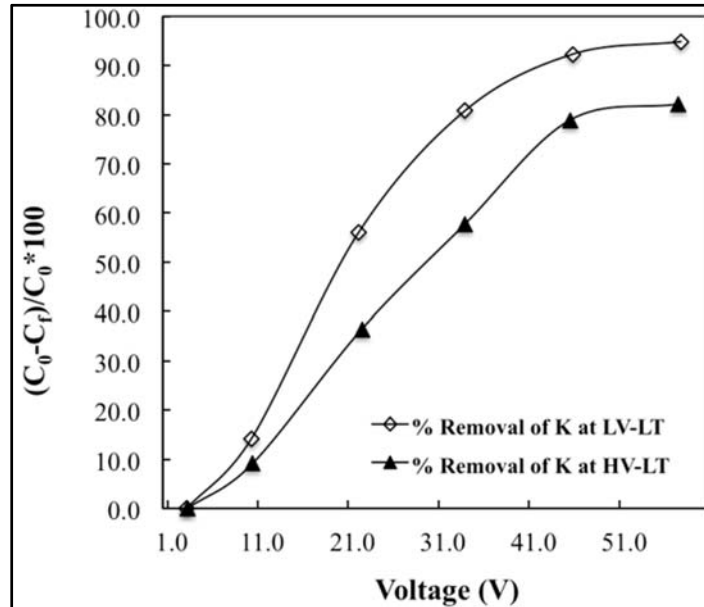


(a)

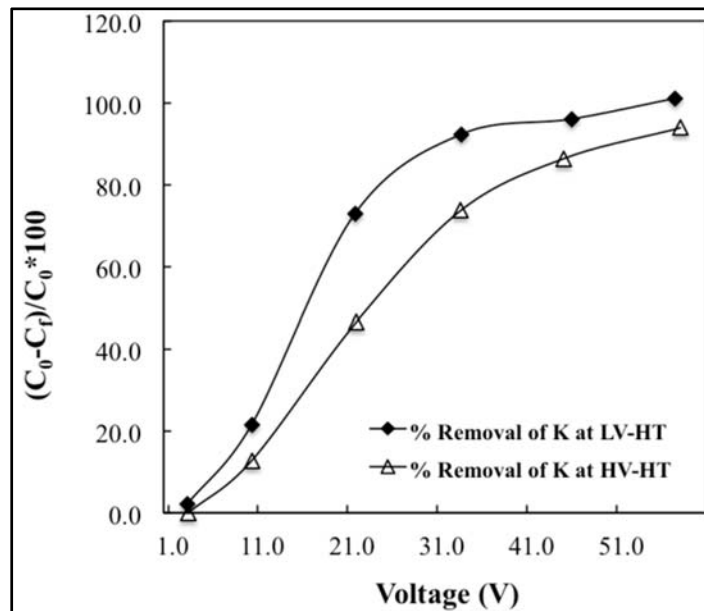


(b)

FIGURE 0-6 Effect of voltage on removal of anions at low temperature, high velocity (a), and low velocity (b)

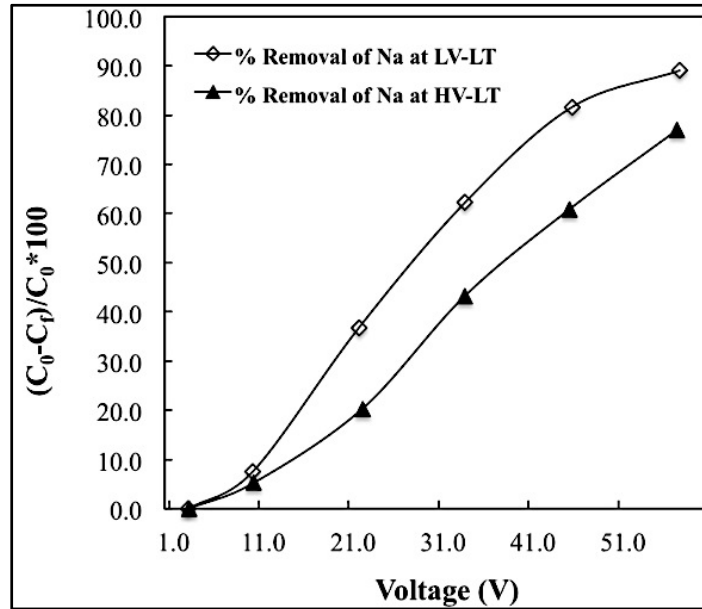


(a)

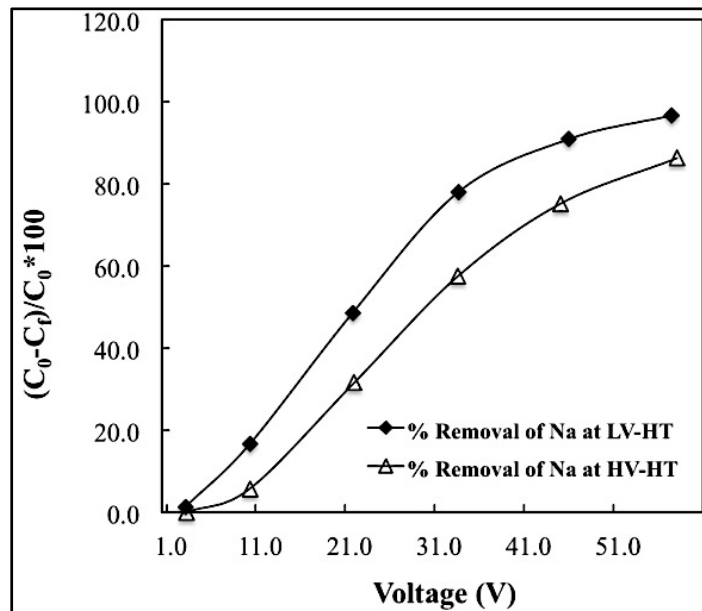


(b)

FIGURE 0-7 Effect of velocity on removal of K⁺ at low temperature (a), and at high temperature (b)

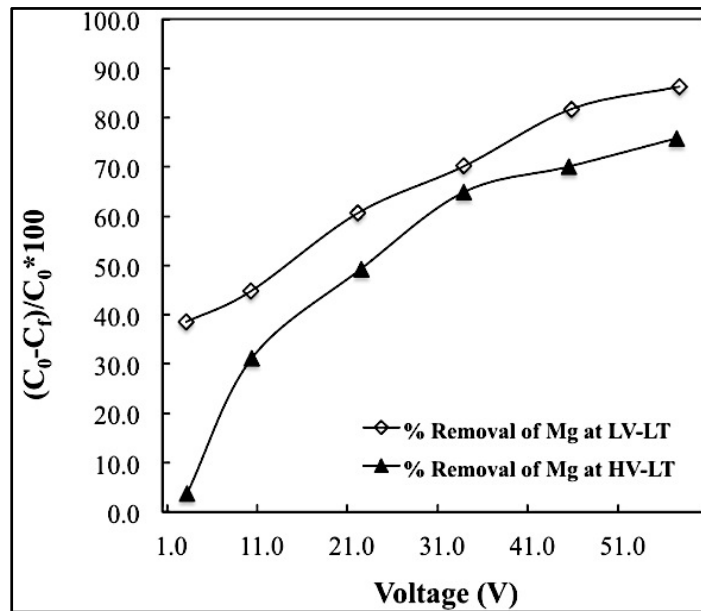


(a)

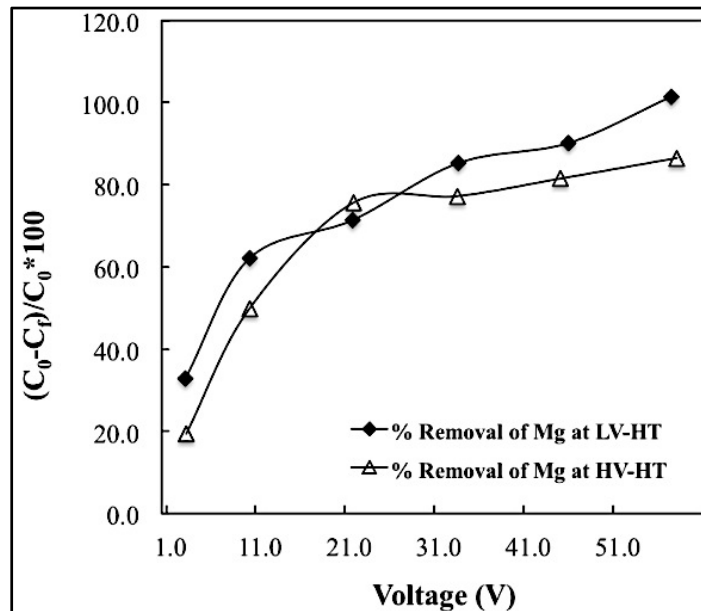


(b)

FIGURE 0-8 Effect of velocity on removal of Na⁺ at low temperature (a), and at high temperature (b)

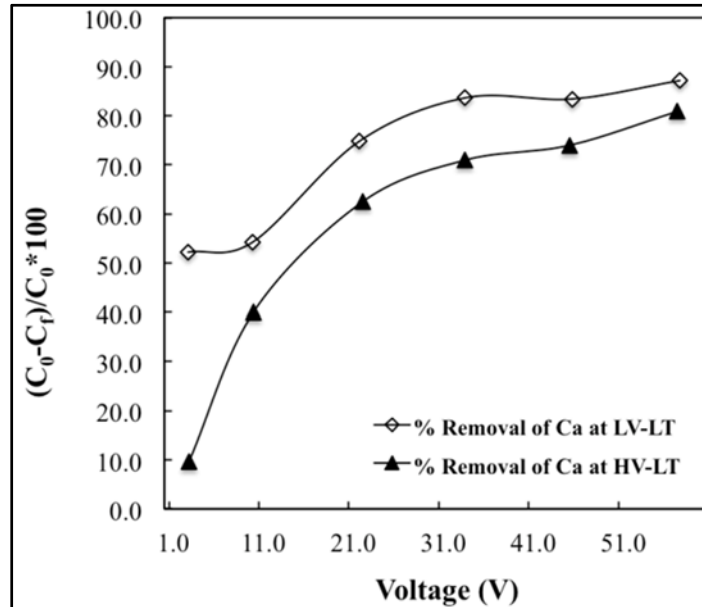


(a)

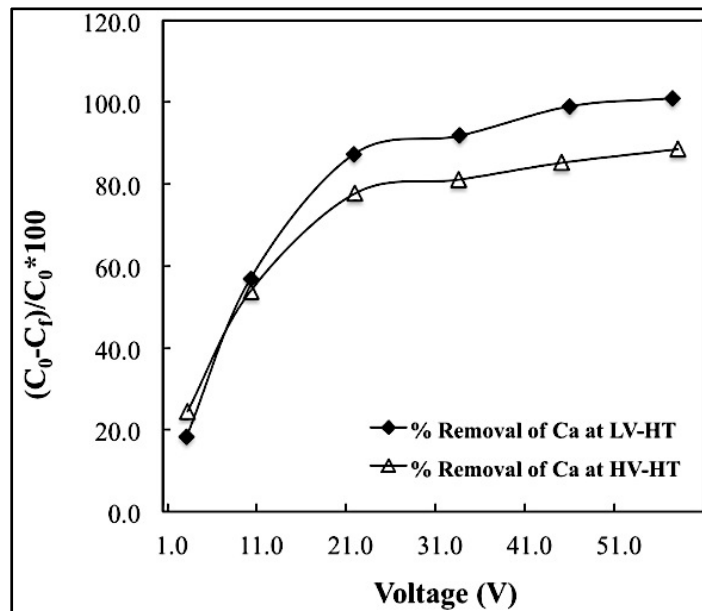


(b)

FIGURE 0-9 Effect of velocity on removal of Mg^{2+} at low temperature (a), and at high temperature (b)

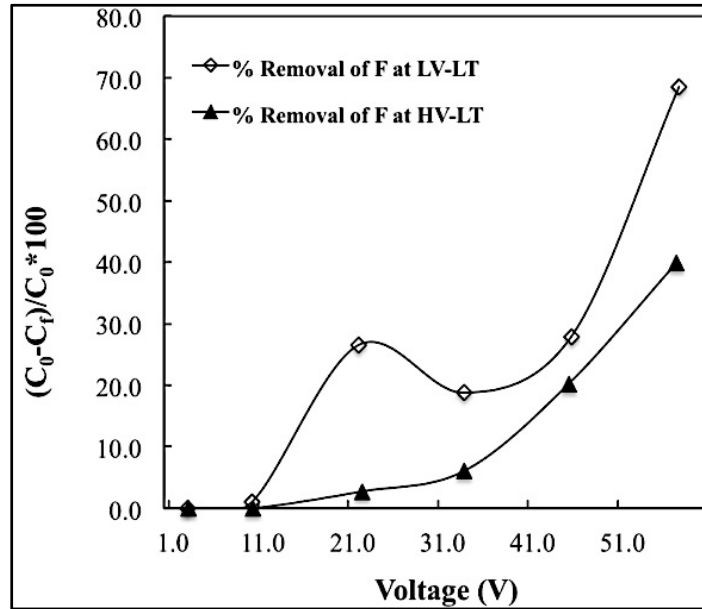


(a)

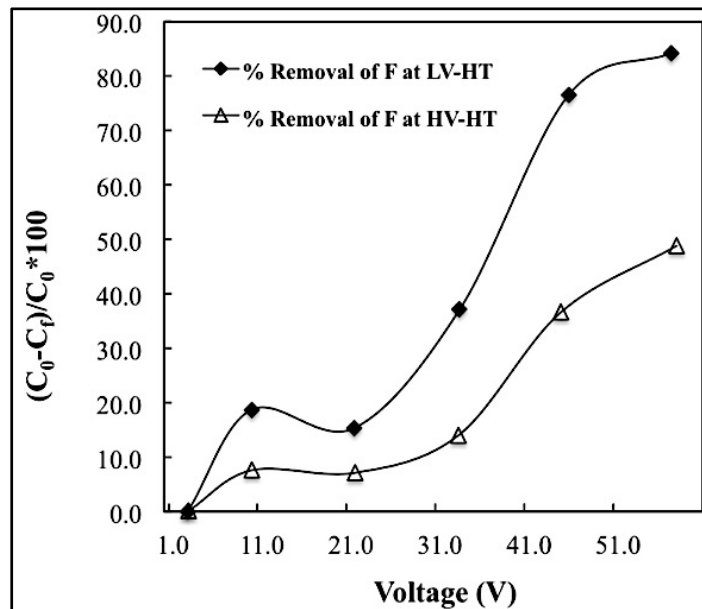


(b)

FIGURE 0-10 Effect of velocity on removal of Ca^{2+} at low temperature (a), and at high temperature (b)

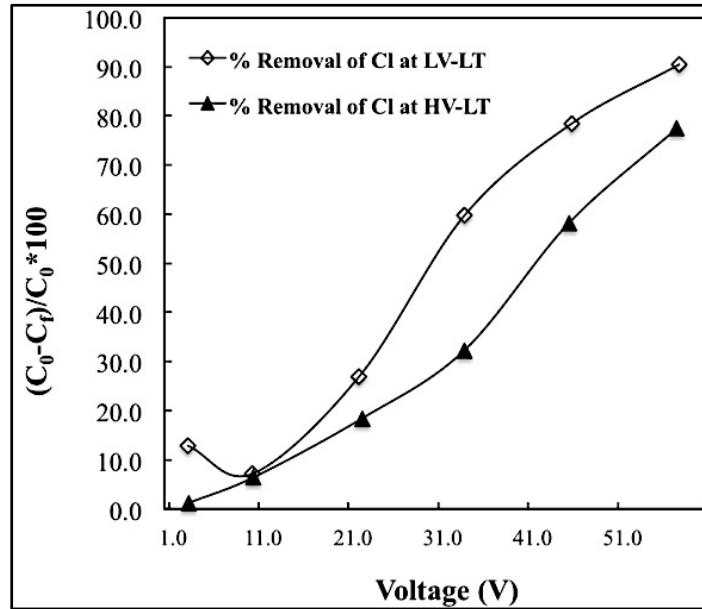


(a)

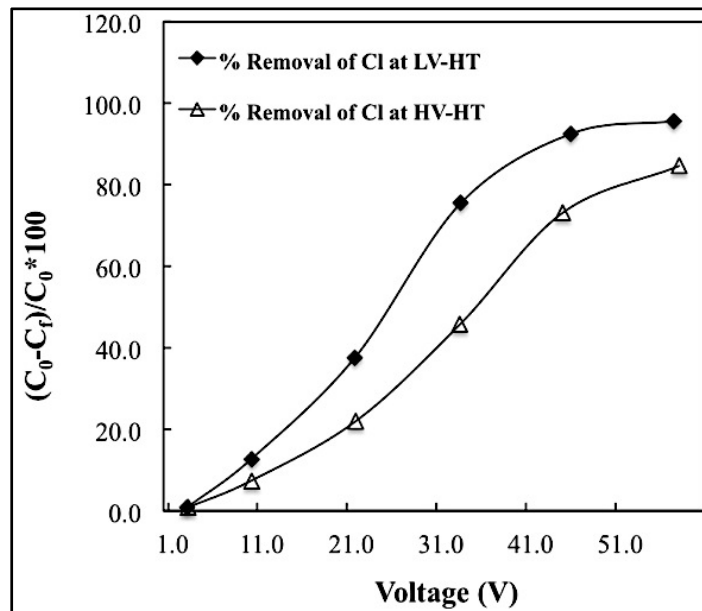


(b)

FIGURE 0-11 Effect of velocity on removal of F⁻ at low temperature (a), and at high temperature (b)

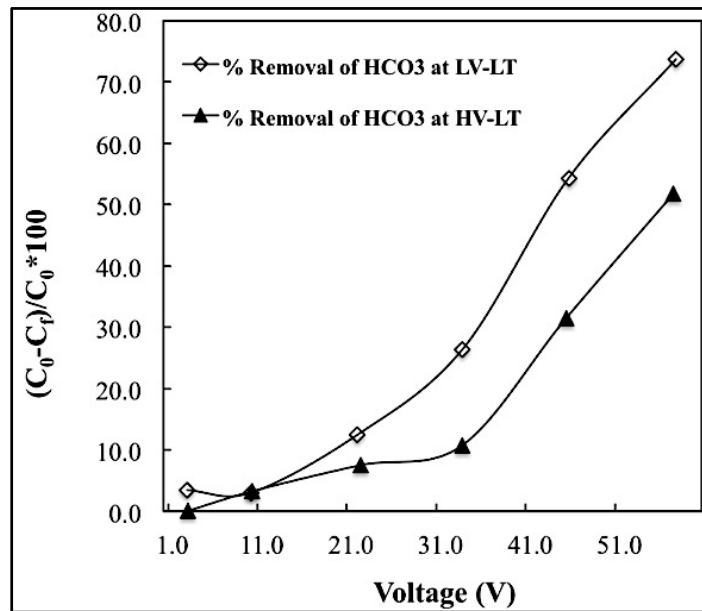


(a)

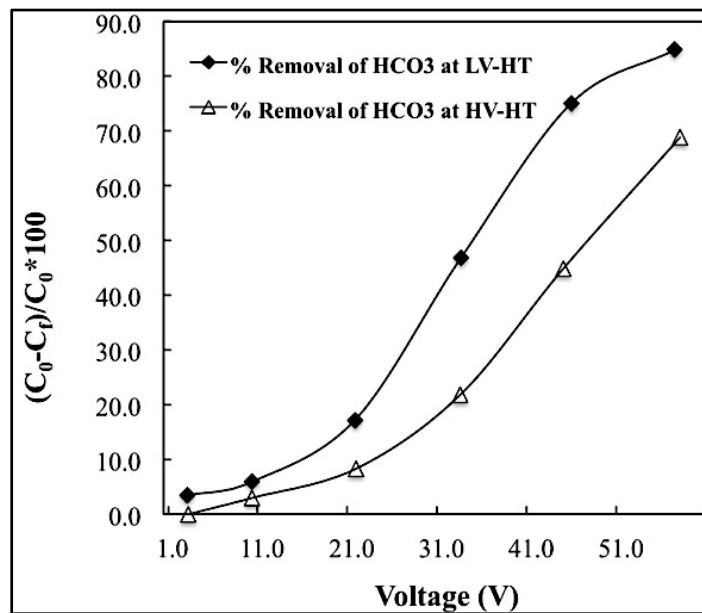


(b)

FIGURE 0-12 Effect of velocity on removal of Cl⁻ at low temperature (a), and at high temperature (b)

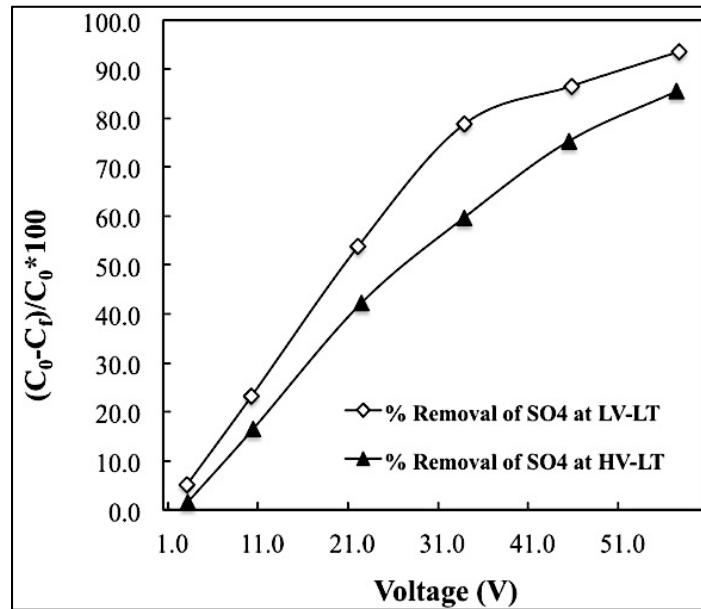


(a)

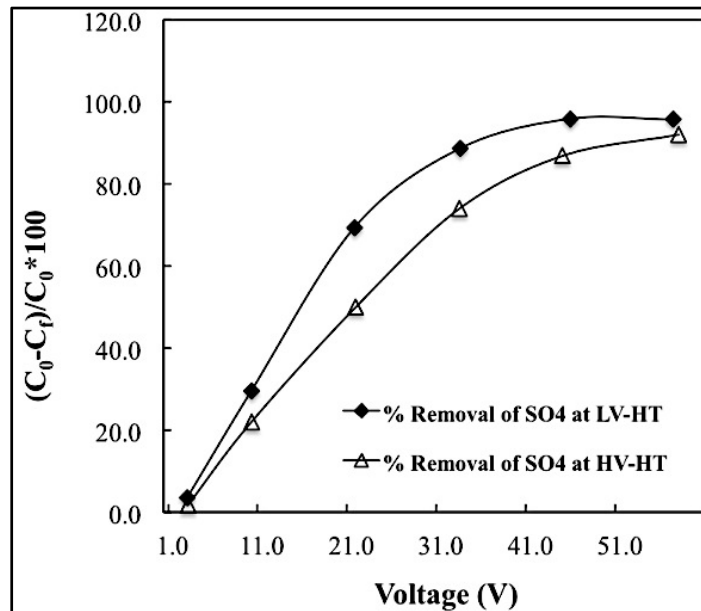


(b)

FIGURE 0-13 Effect of velocity on removal of HCO_3^- at low temperature (a), and at high temperature (b)

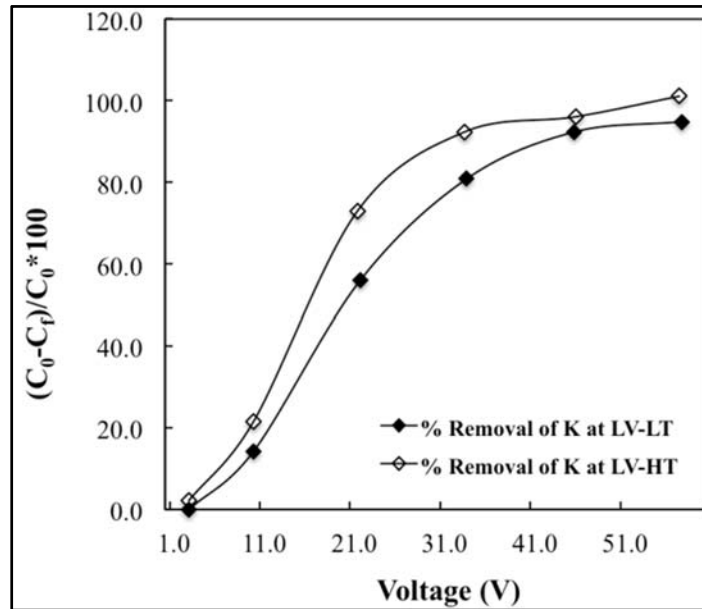


(a)

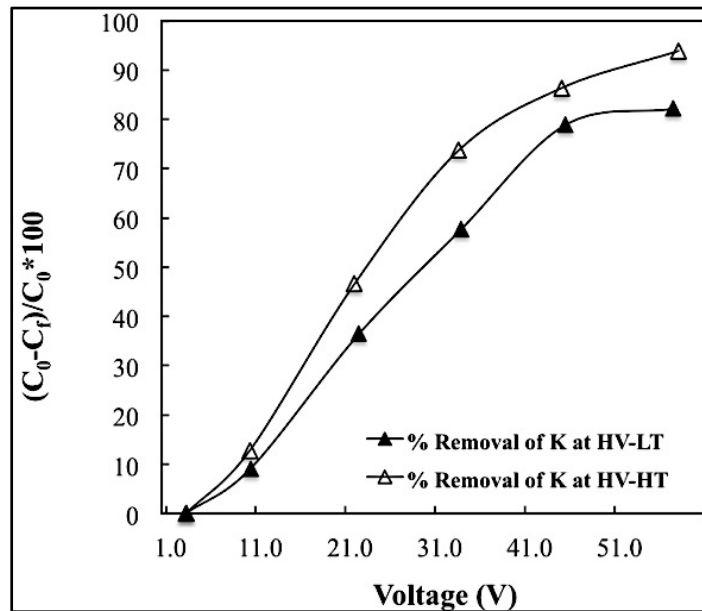


(b)

FIGURE 0-14 Effect of velocity on removal of SO_4^{2-} at low temperature (a), and at high temperature (b)

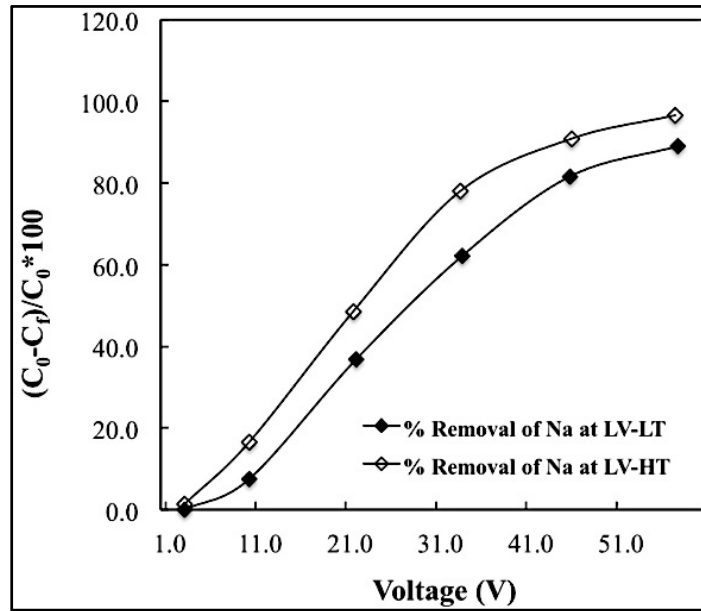


(a)

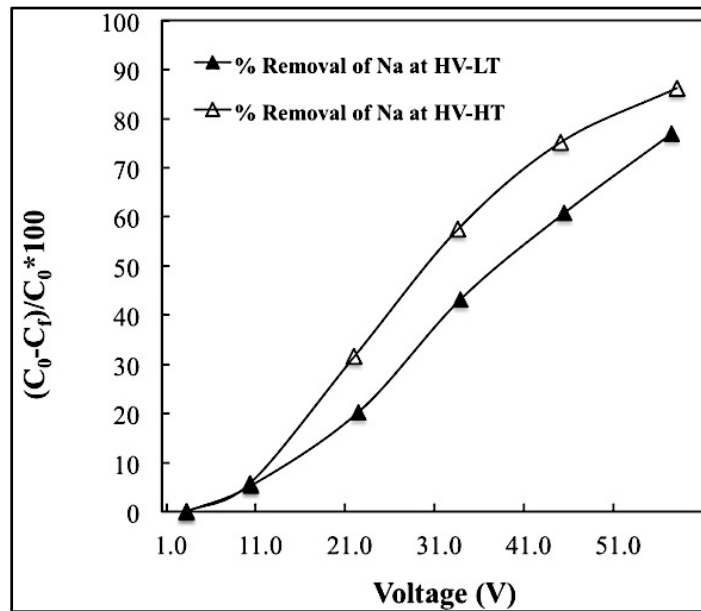


(b)

FIGURE 0-15 Effect of temperature on removal of K⁺ at low velocity (a), and high velocity (b)

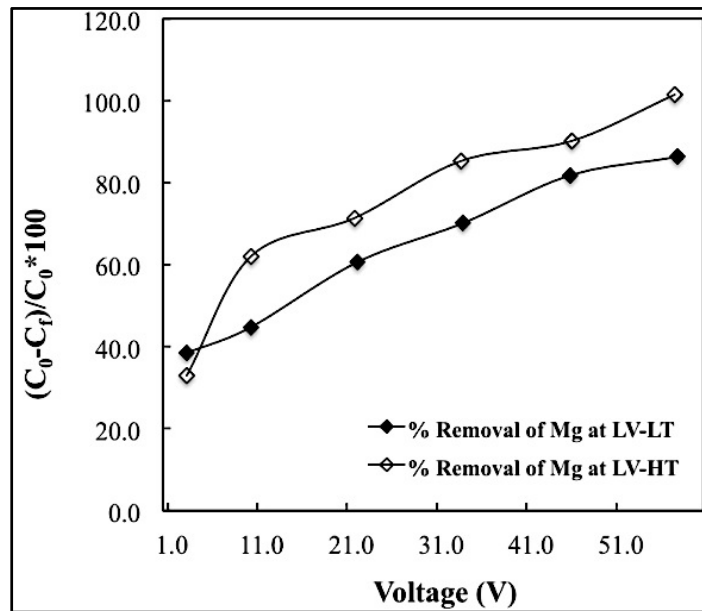


(a)

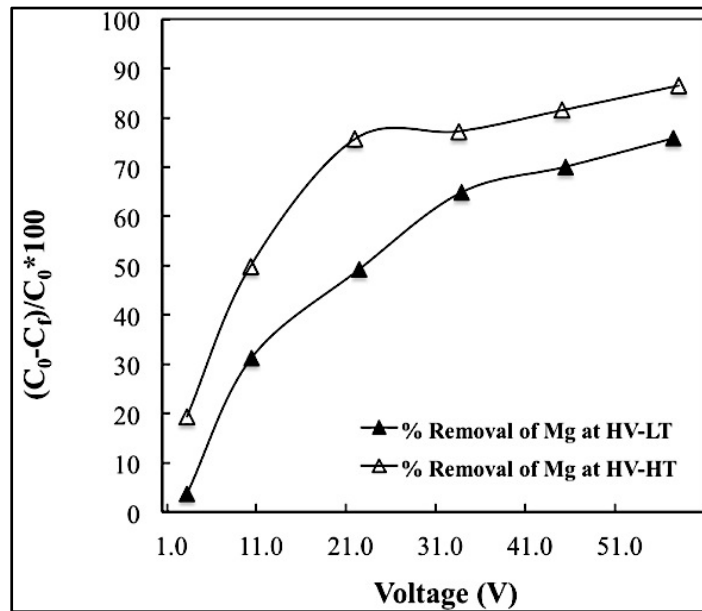


(b)

FIGURE 0-16 Effect of temperature on removal of Na⁺ at low velocity (a), and high velocity (b)

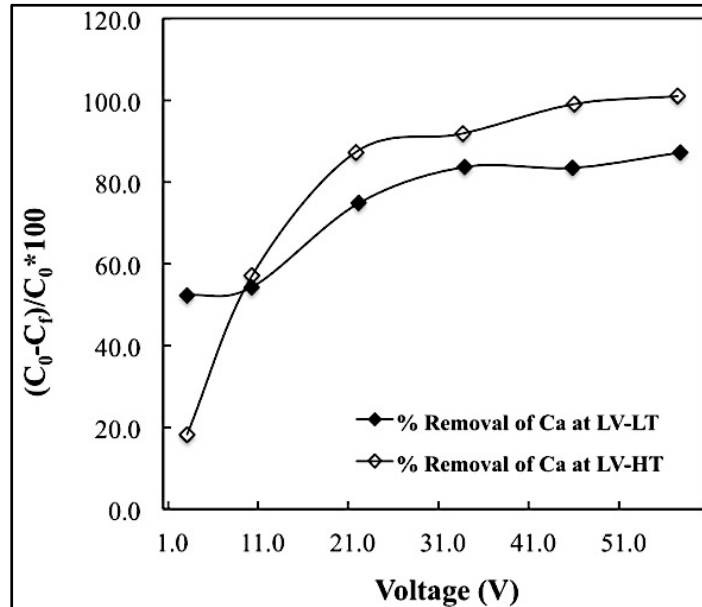


(a)

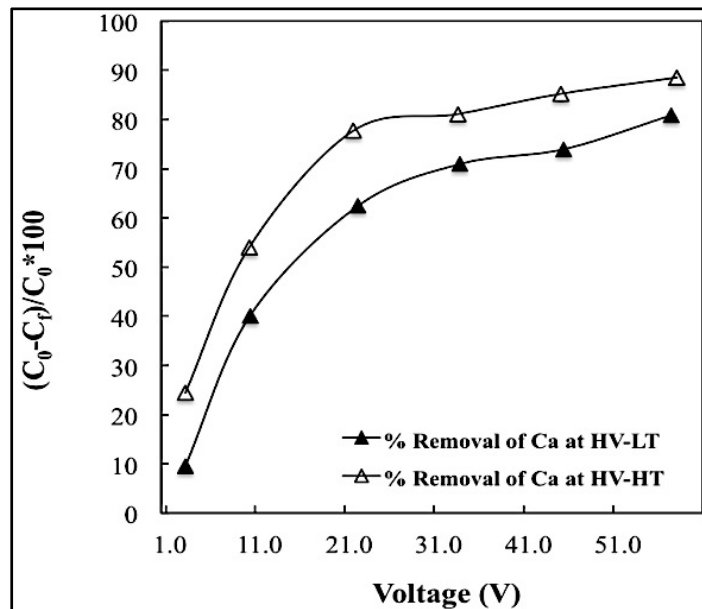


(b)

FIGURE 0-17 Effect of temperature on removal of Mg^{2+} at low velocity (a), and high velocity (b)

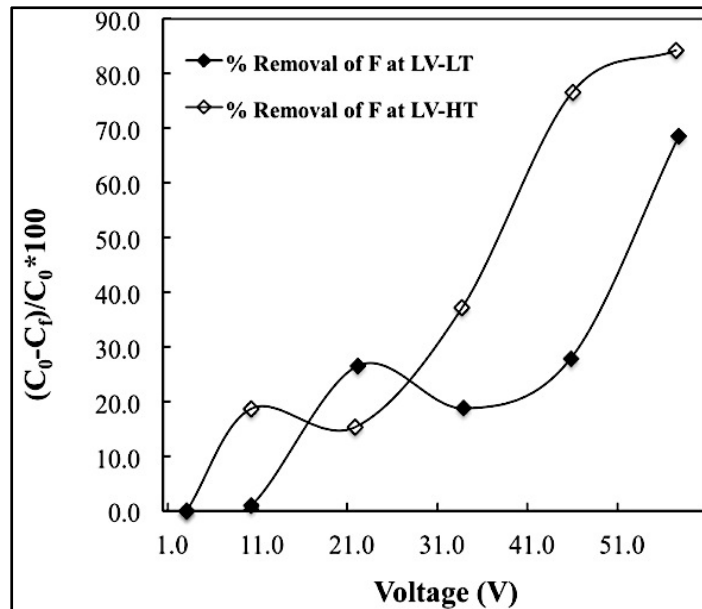


(a)

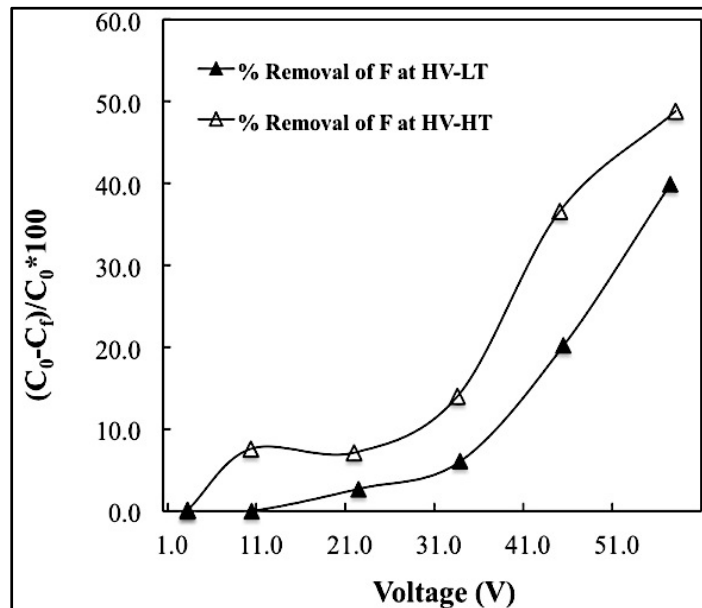


(b)

FIGURE 0-18 Effect of temperature on removal of Ca²⁺ at low velocity (a), and high velocity (b)

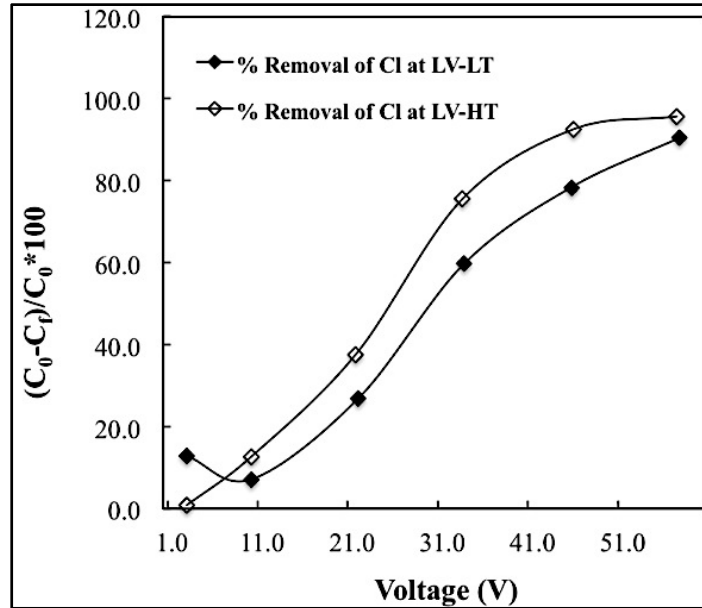


(a)

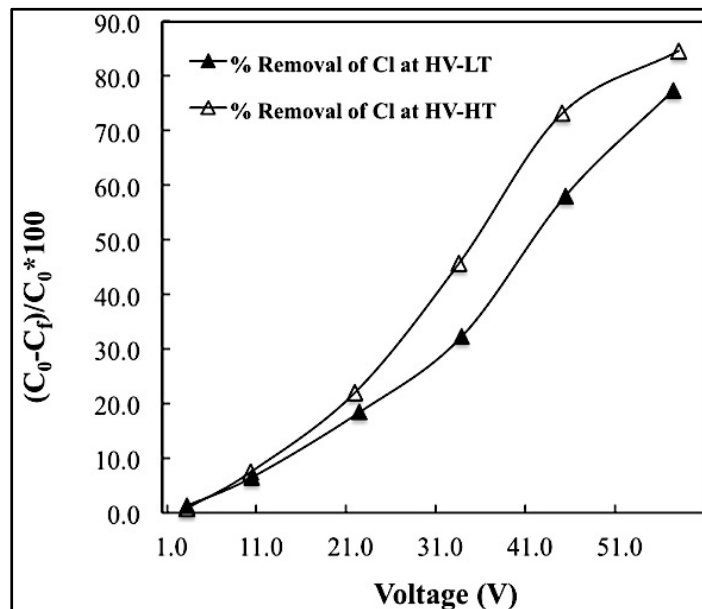


(b)

FIGURE 0-19 Effect of temperature on removal of F^- at low velocity (a), and high velocity (b)

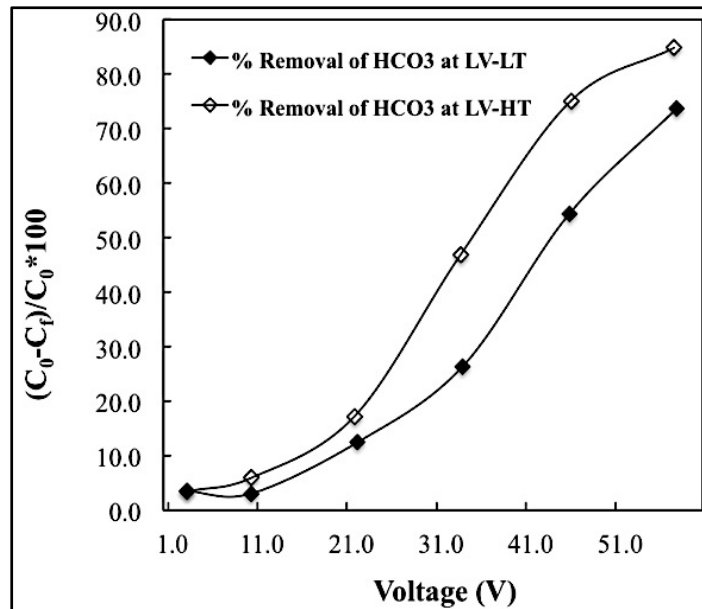


(a)

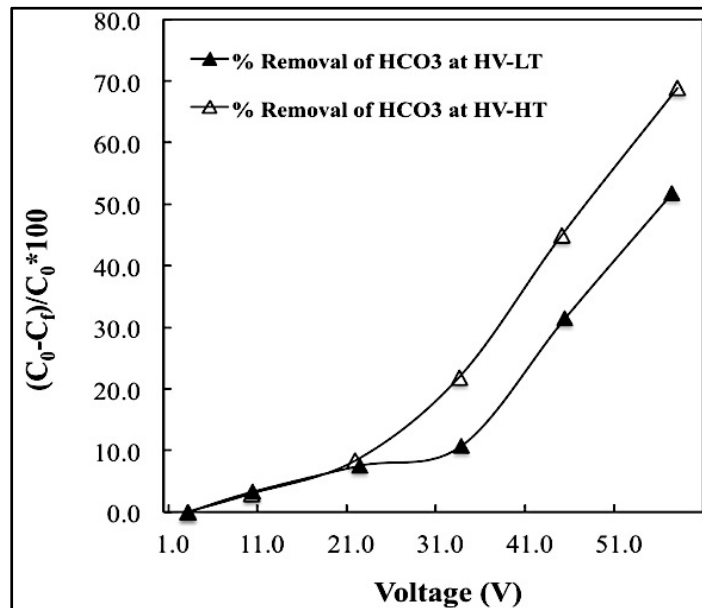


(b)

FIGURE 0-20 Effect of temperature on removal of Cl⁻ at low velocity (a), and high velocity (b)

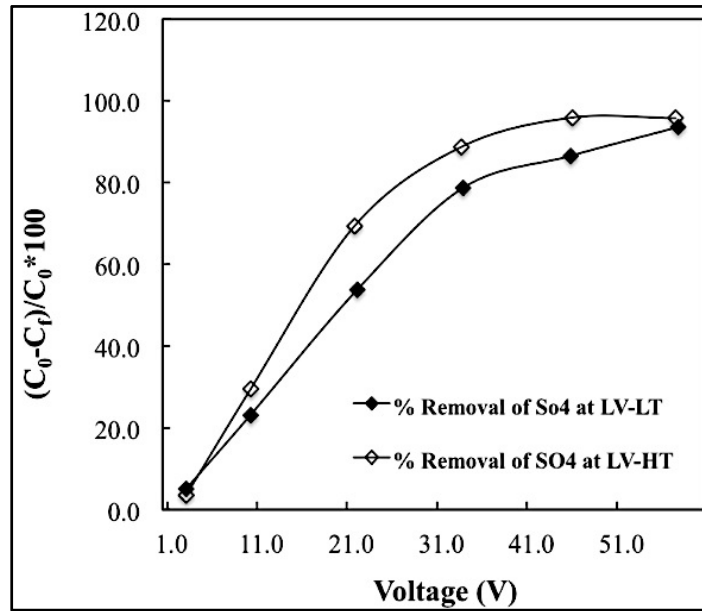


(a)

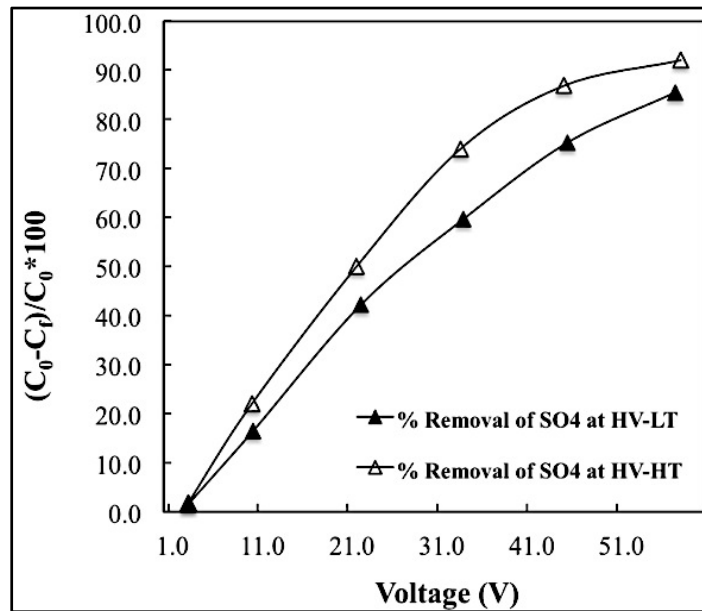


(b)

FIGURE 0-21 Effect of temperature on removal of HCO_3^- at low velocity (a), and high velocity (b)

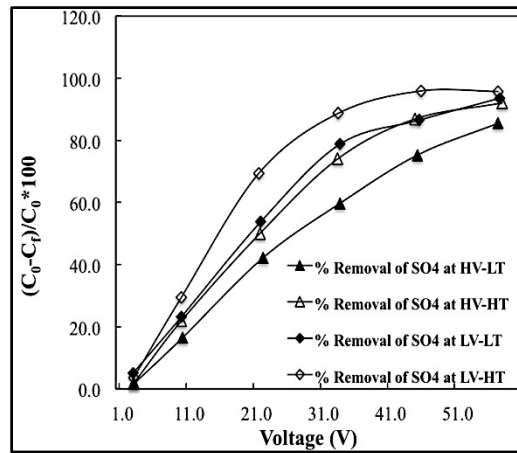


(a)

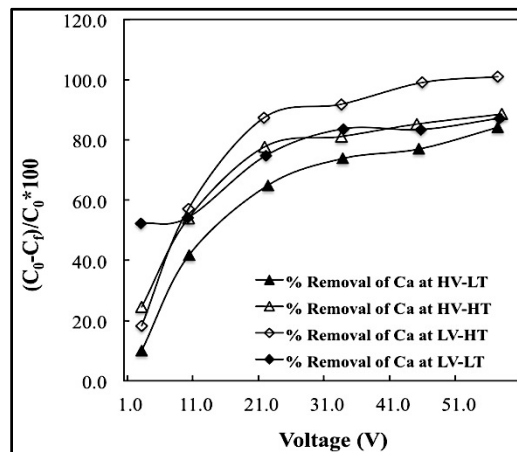


(b)

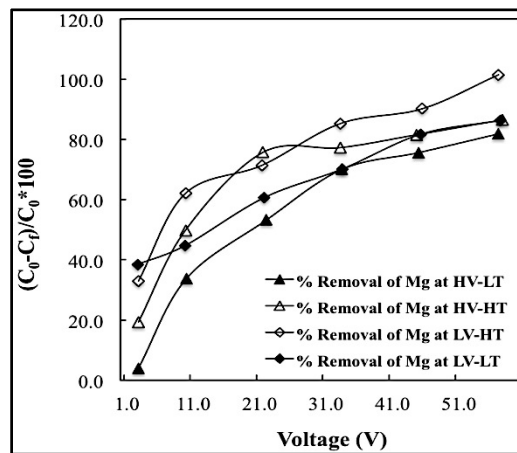
FIGURE 0-22 Effect of temperature on removal of SO_4^{2-} at low velocity (a), and high velocity (b)



(a)

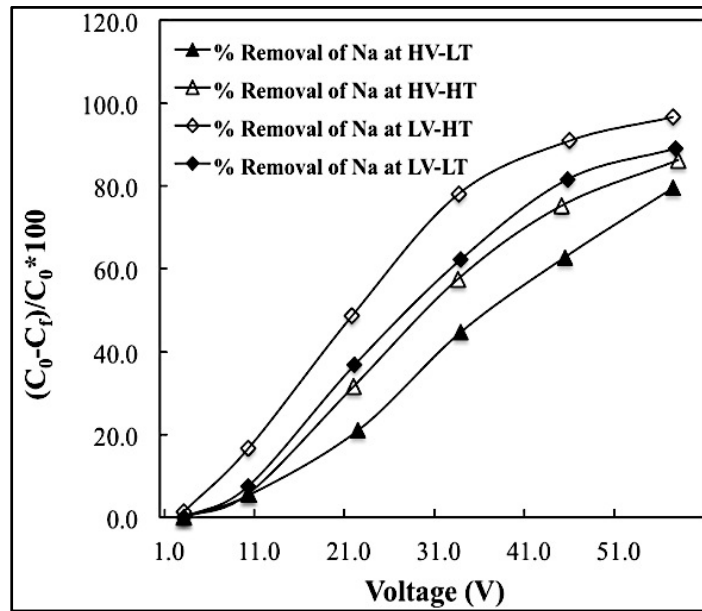


(b)

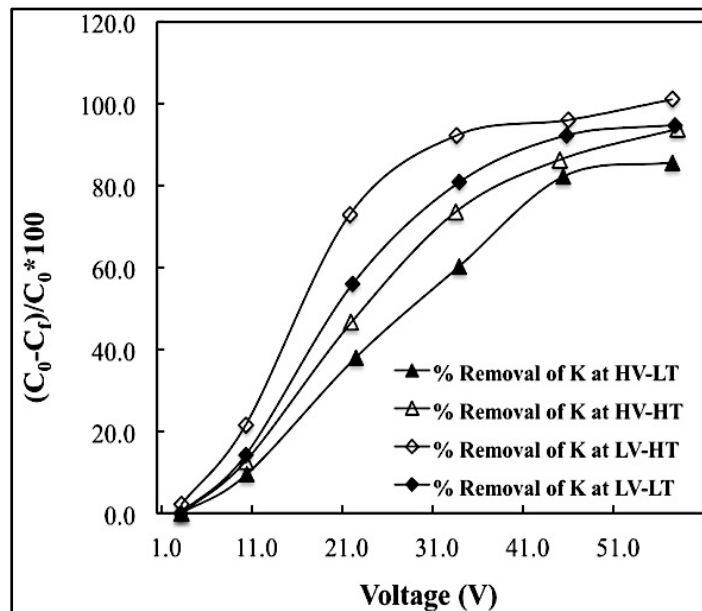


(c)

FIGURE 0-23 Comparison of the effects velocity and temperature on removal of SO_4^{2-} (a), Ca^{2+} (b), and Mg^{2+} (c)

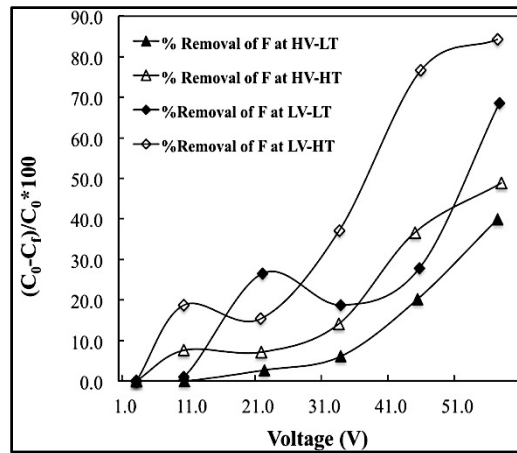


(a)

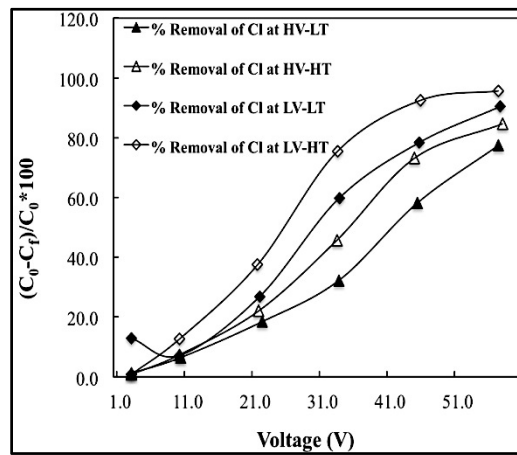


(b)

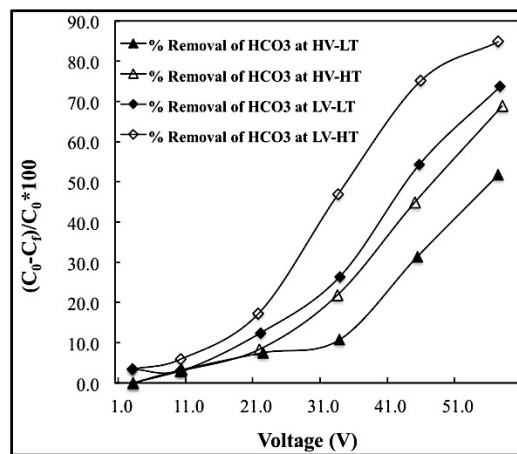
FIGURE 0-24 Comparison of the velocity and temperature effects on removal of Na⁺ (a), and K⁺ (b)



(a)



(b)



(c)

FIGURE 0-25 Comparison of the effects of velocity and temperature on removal of F⁻ (a), Cl⁻ (b), and HCO₃⁻ (c)

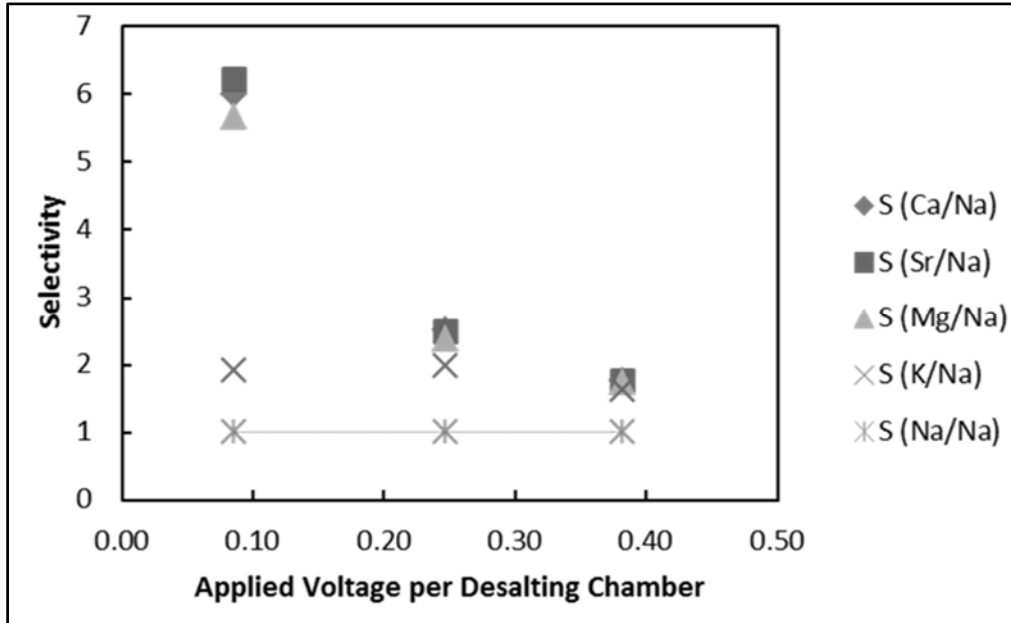


FIGURE 0-26 The general trend of cations' selective removal in the EDR process using CR-67 cation exchange membrane

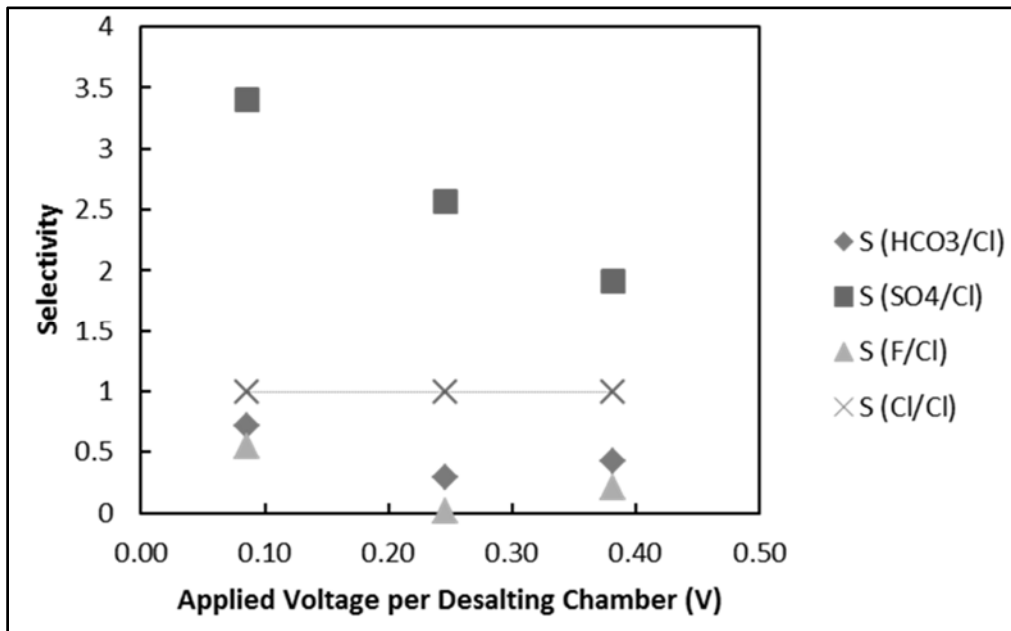


FIGURE 0-27 The general trend of anions' selective removal in the EDR process using AR204 anion exchange membrane

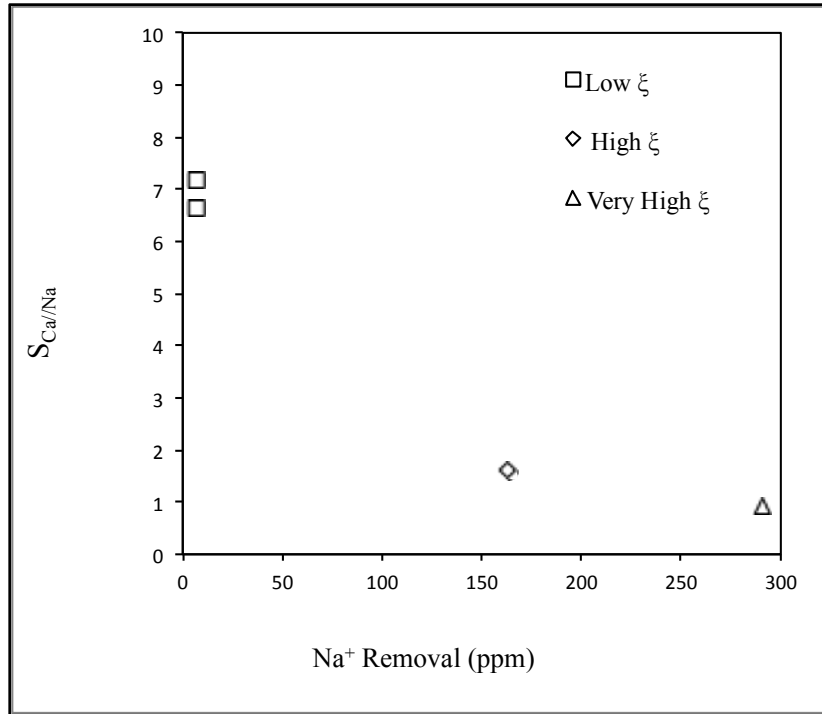


FIGURE 0-28 Selectivity sensitivity for Ca²⁺ vs. Na⁺

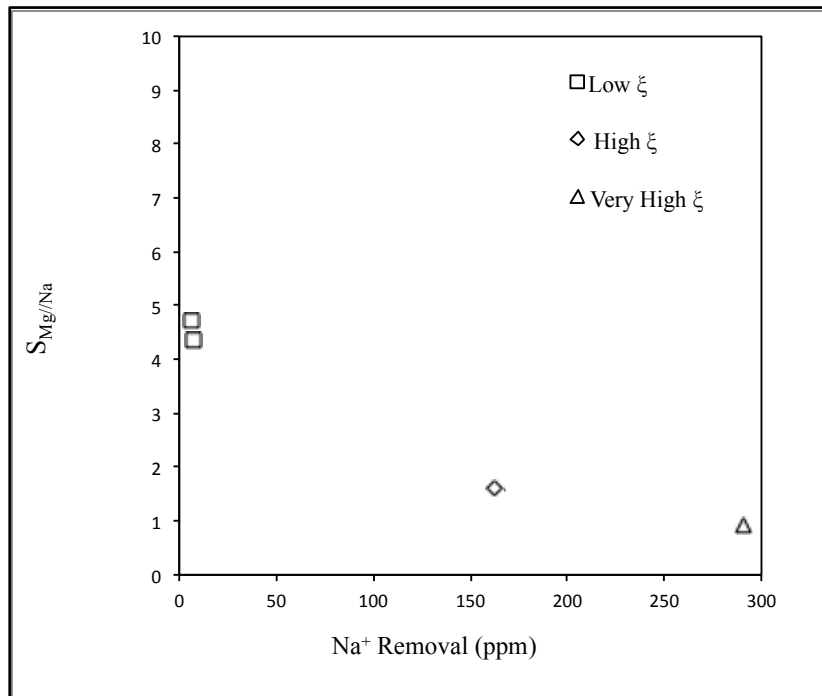


FIGURE 0-29 Selectivity sensitivity for Mg²⁺ vs. Na⁺

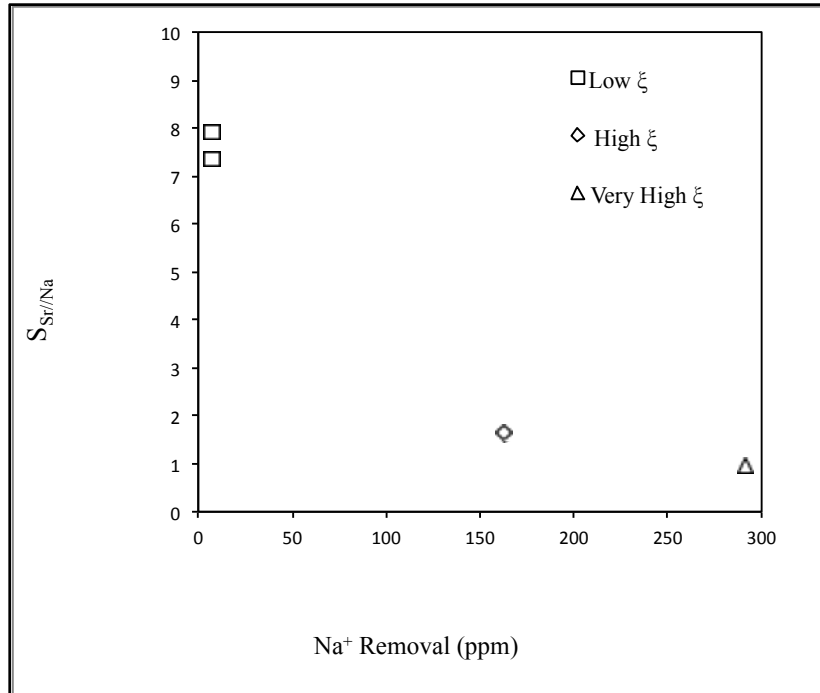


FIGURE 0-30 Selectivity sensitivity for Sr²⁺ vs. Na⁺

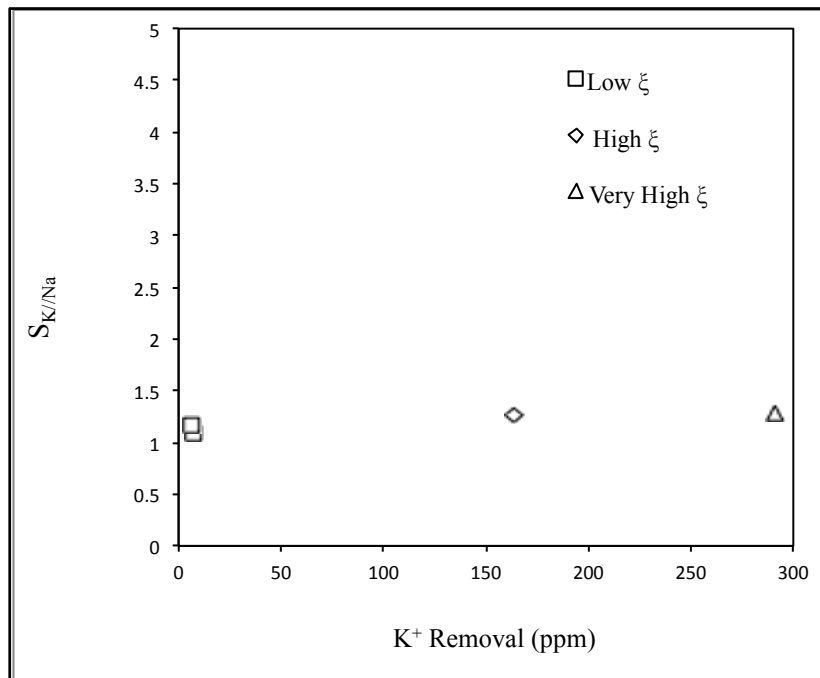


FIGURE 0-31 Selectivity sensitivity for K⁺ vs. Na⁺

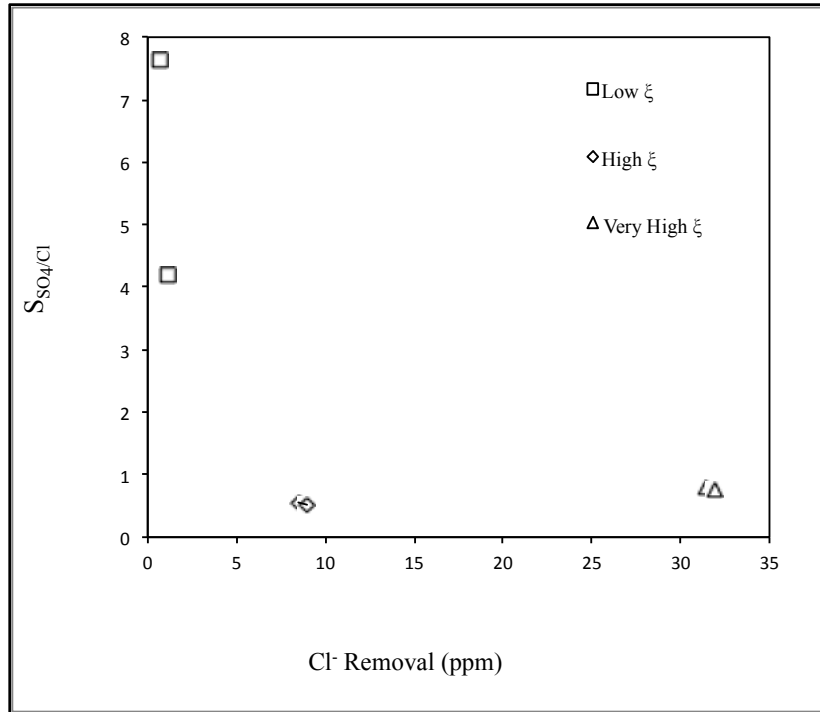


FIGURE 0-32 Selectivity sensitivity for SO_4^{2-} vs. Cl^-

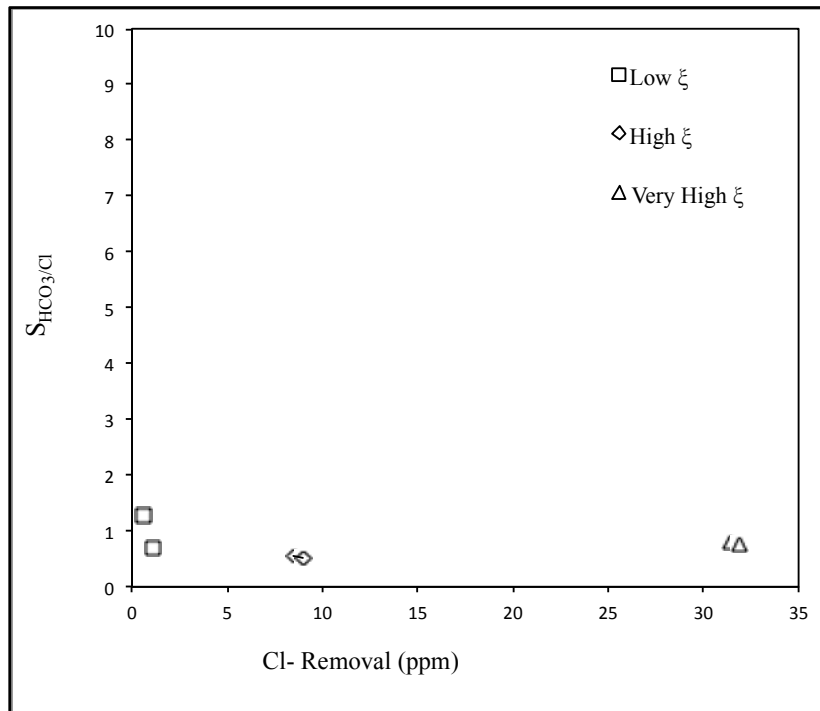


FIGURE 0-33 Selectivity sensitivity for HCO_3^- vs. Cl^-

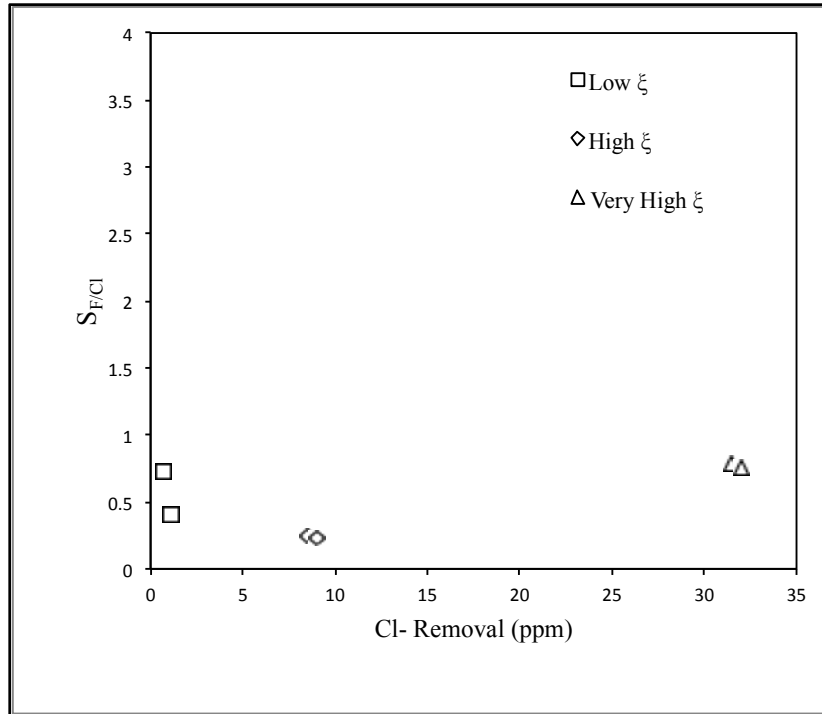


FIGURE 0-34 Selectivity sensitivity for F^- vs. Cl^-

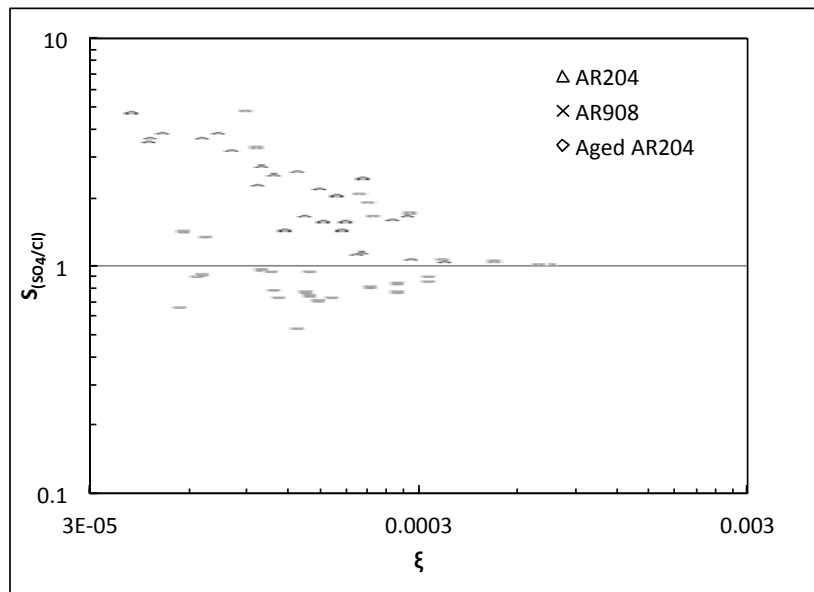


FIGURE 0-35 Selectivity values of SO_4^{2-} vs Cl^- in EDR process, using different anion exchange membranes

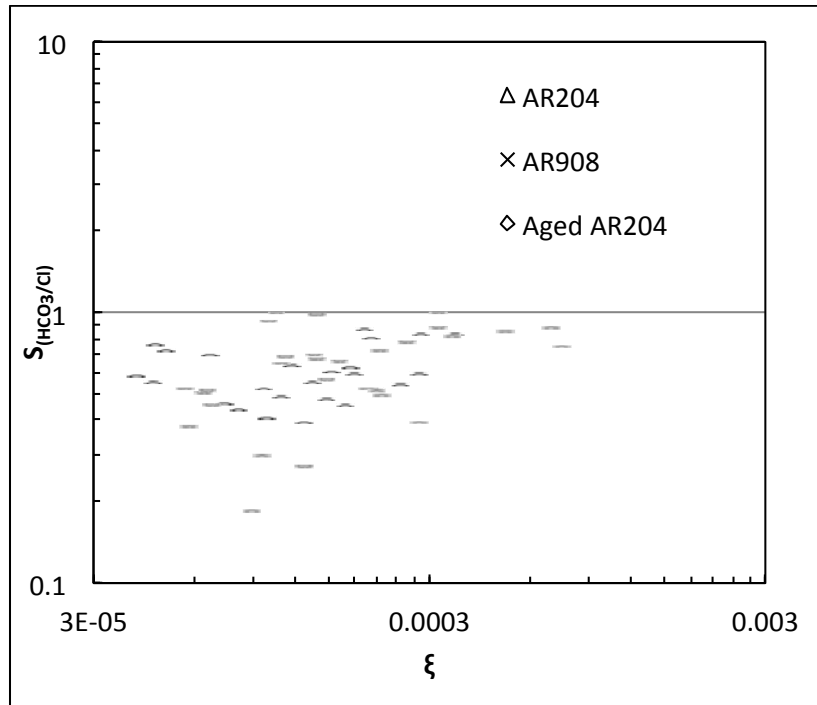


FIGURE 0-36 Selectivity values of HCO_3^- vs Cl^- in EDR process, using different anion exchange membranes

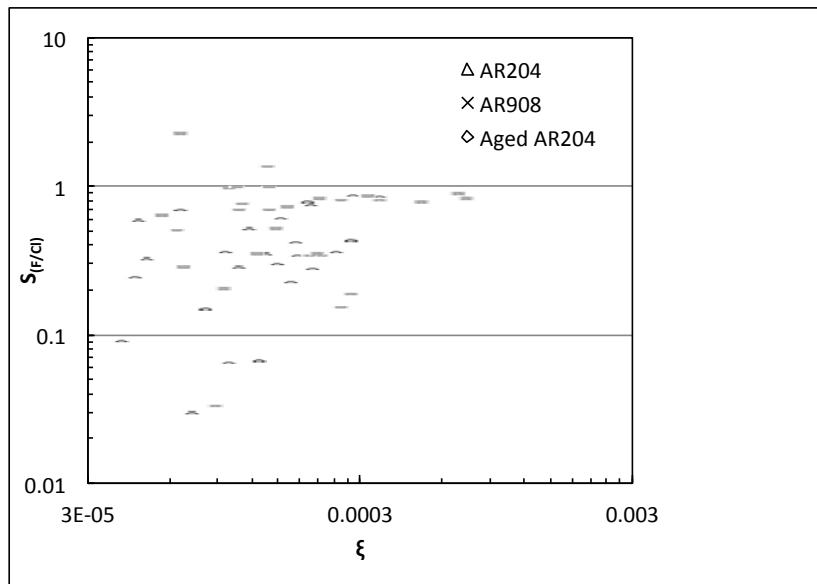


FIGURE 0-37 Selectivity values of F^- vs Cl^- in EDR process, using different anion exchange membranes

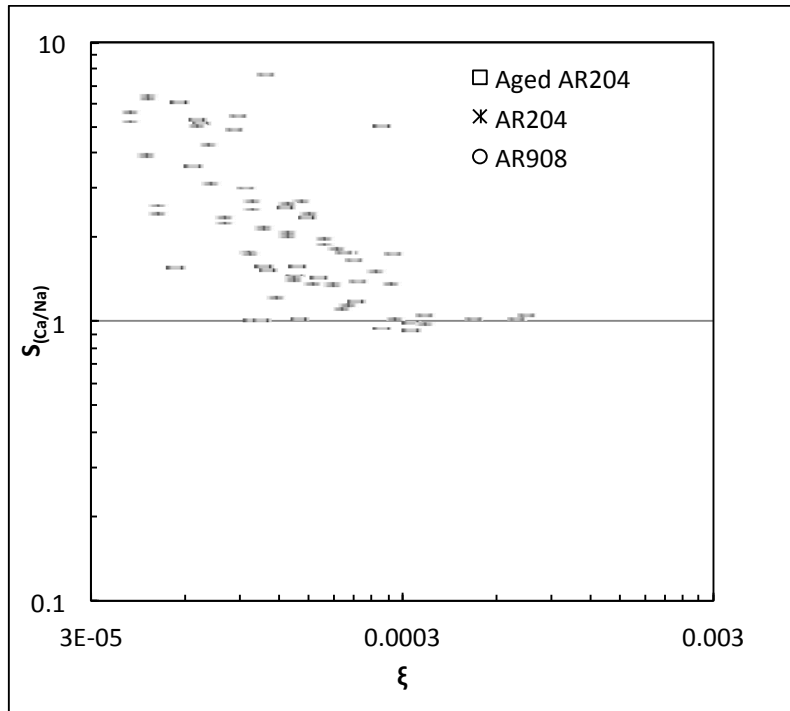


FIGURE 0-38 Selectivity values of Ca^{2+} vs Na^{+} in EDR process, using cation exchange membrane type CR-67 and different anion exchange membranes

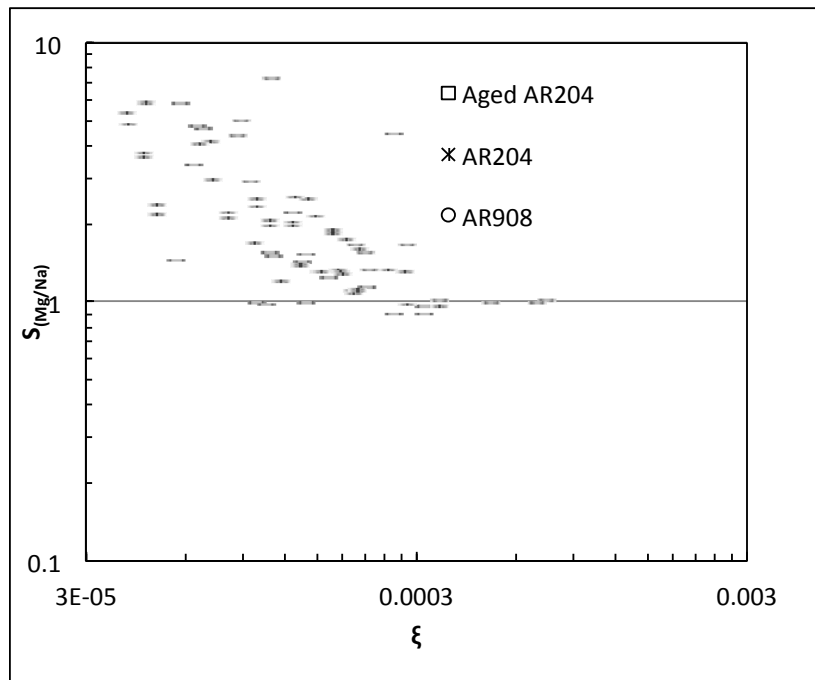


FIGURE 0-39 Selectivity values of Mg^{2+} vs Na^{+} in the EDR process, using cation exchange membrane type CR-67 and different anion exchange membranes

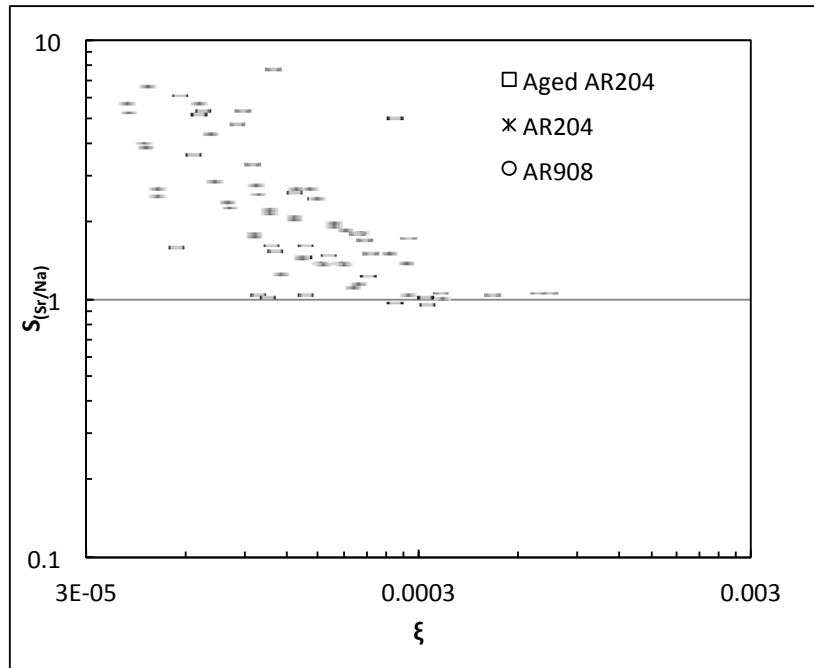


FIGURE 0-40 Selectivity values of Sr²⁺ vs Na⁺ in EDR process, using cation exchange membrane type CR-67 and different anion exchange membranes

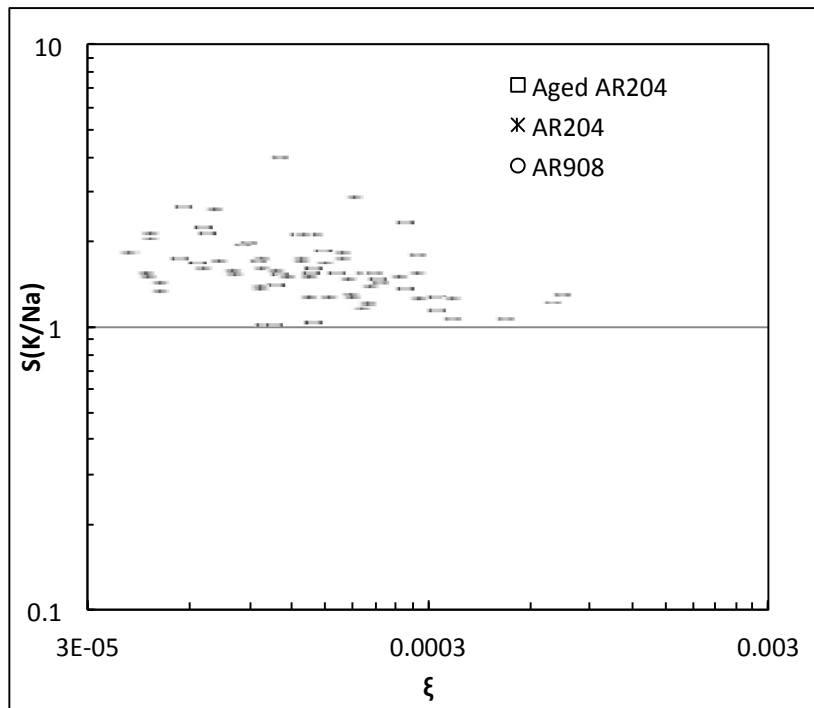


FIGURE 0-41 Selectivity values of K⁺ vs Na⁺ in the EDR process, using cation exchange membrane type CR-67 and different anion exchange membranes

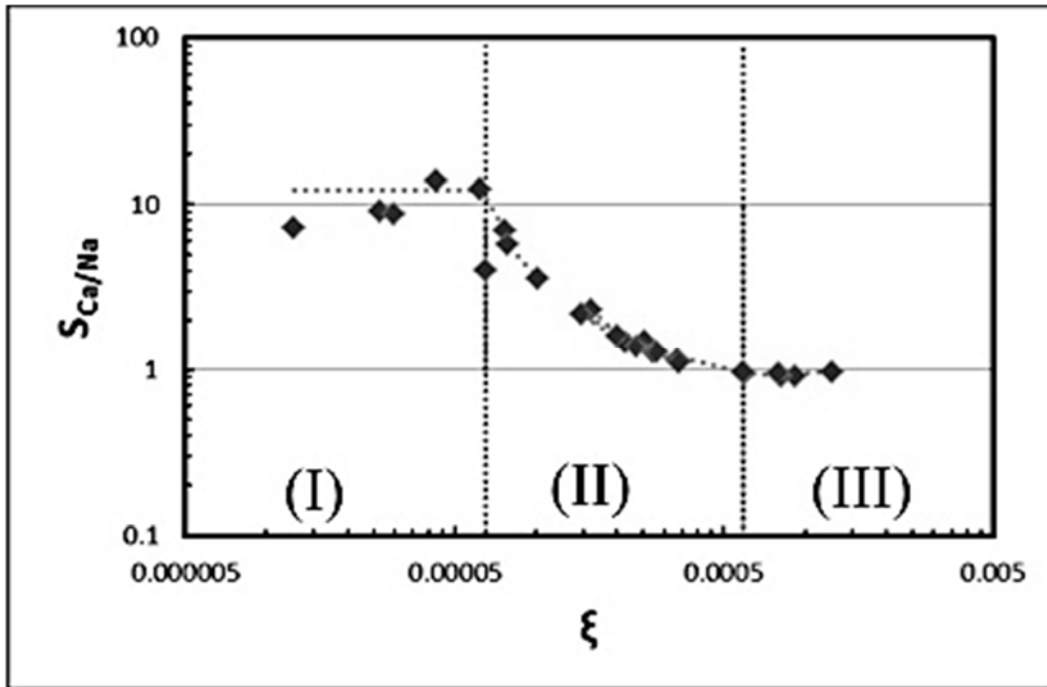


FIGURE 0-42 Different regions for effect of dimensionless number, ξ , in selectivity of Ca^{2+} vs Na^+

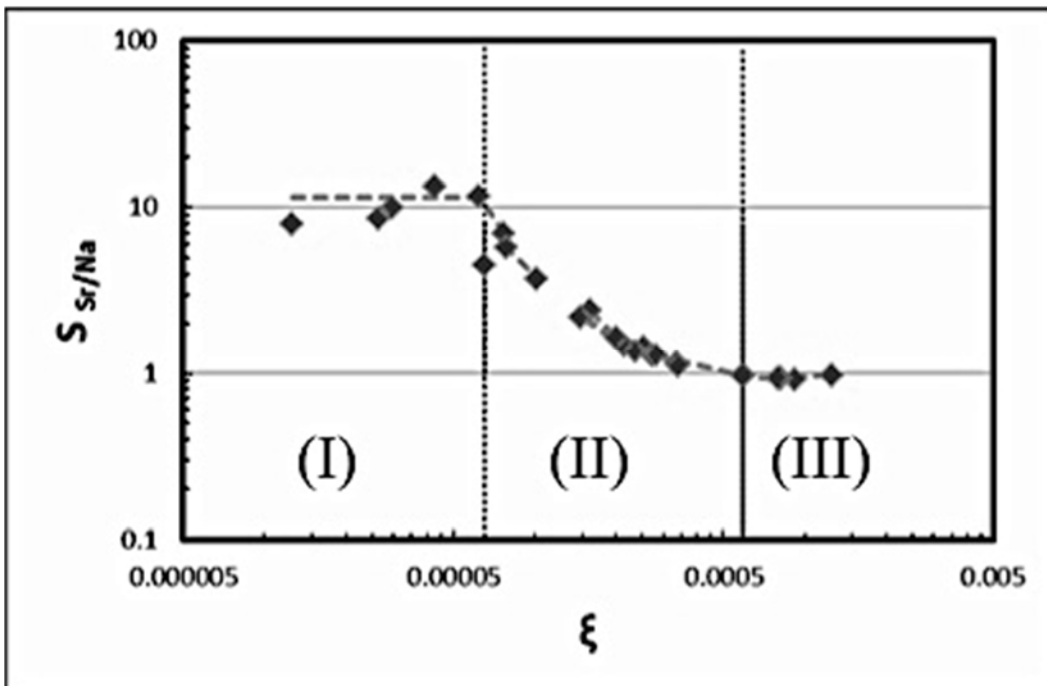


FIGURE 0-43 Different regions for effect of dimensionless number, ξ , in selectivity of Sr^{2+} vs Na^+

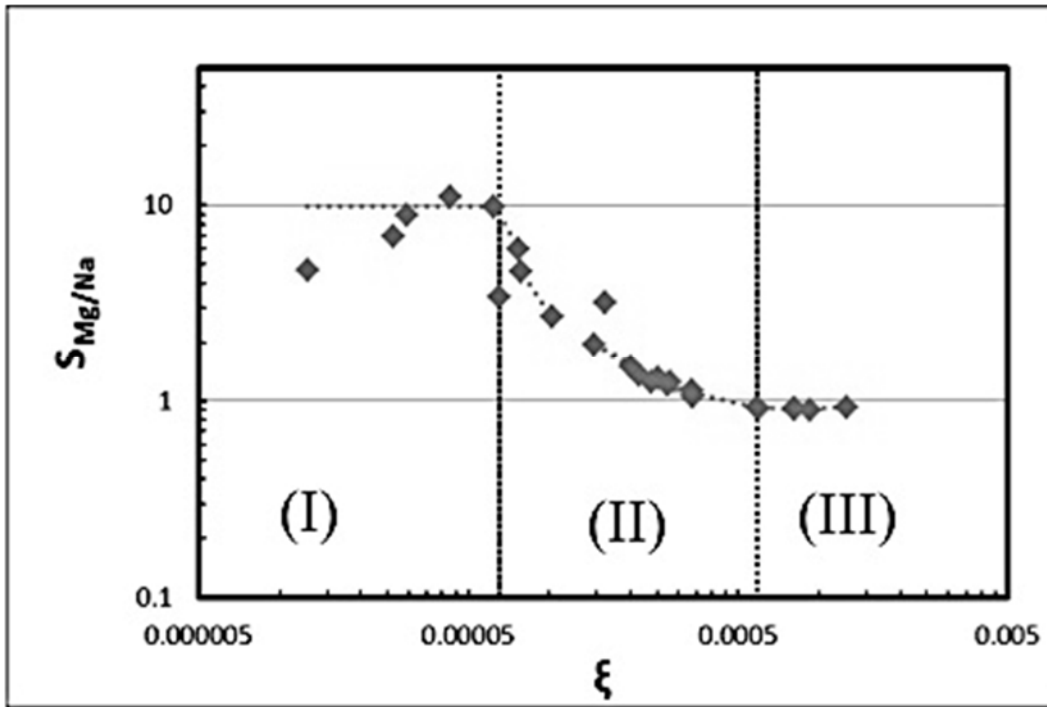


FIGURE 0-44 Different regions for effect of dimensionless number, ξ , in selectivity of Mg^{2+} vs Na^+

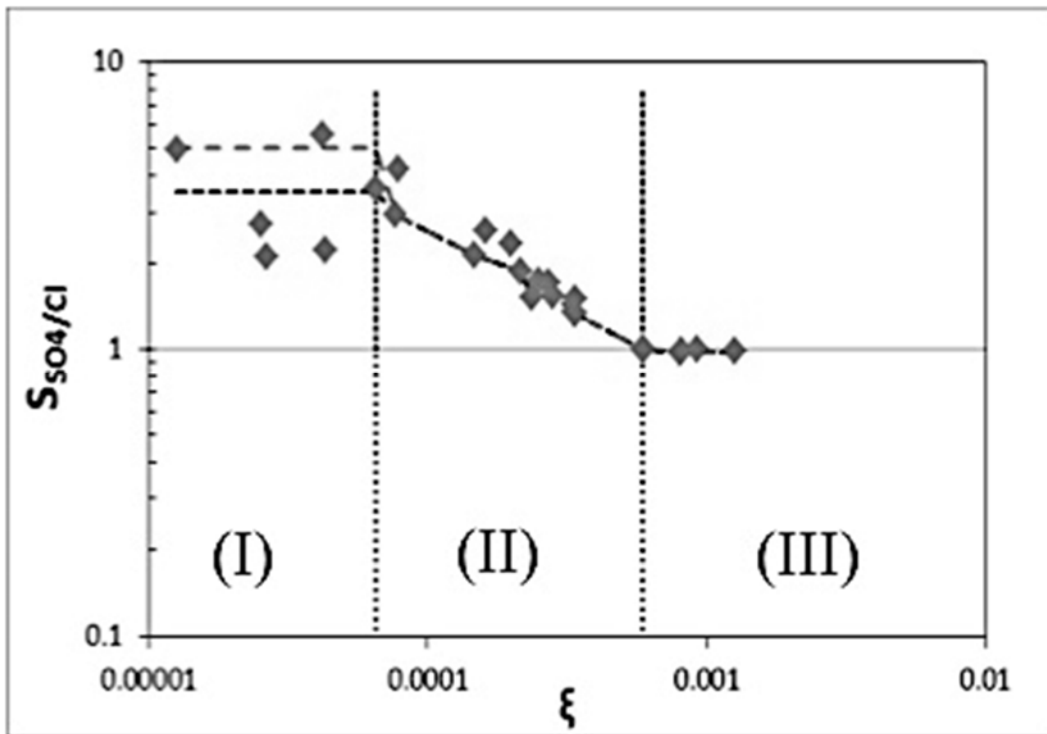


FIGURE 0-45 Different regions for effect of dimensionless number, ξ , for selectivity of SO_4^{2-} vs Cl^-

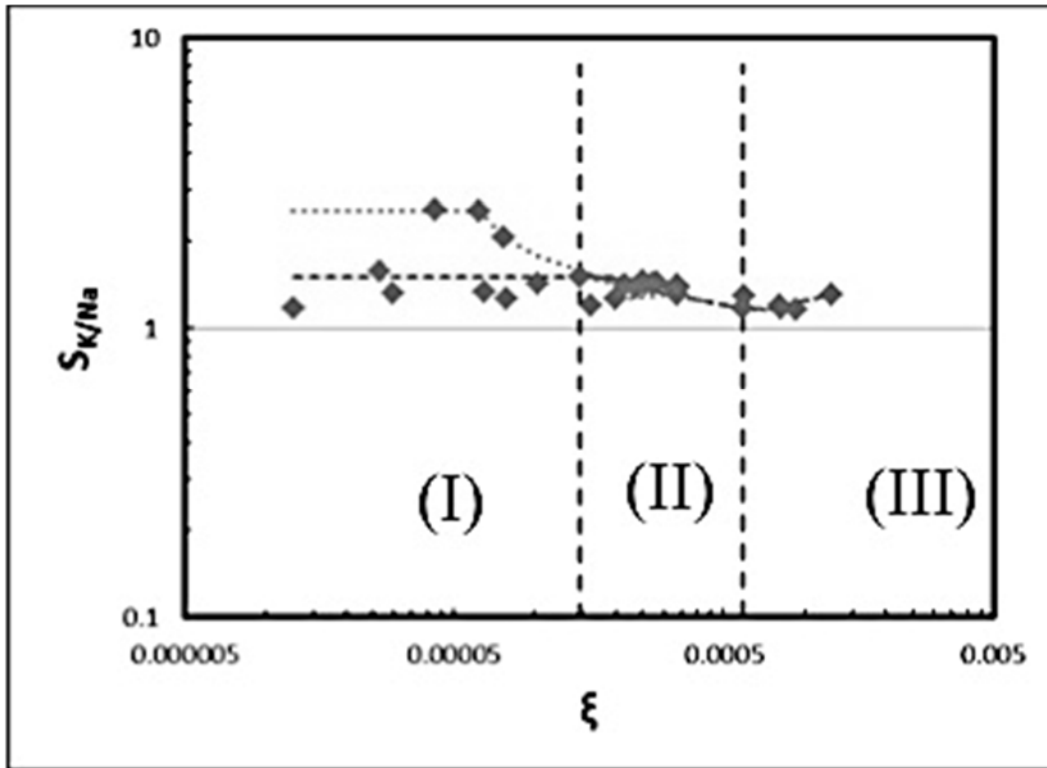


FIGURE 0-46 Different regions for effect of dimensionless number, ξ , in selectivity of K^+ vs Na^+

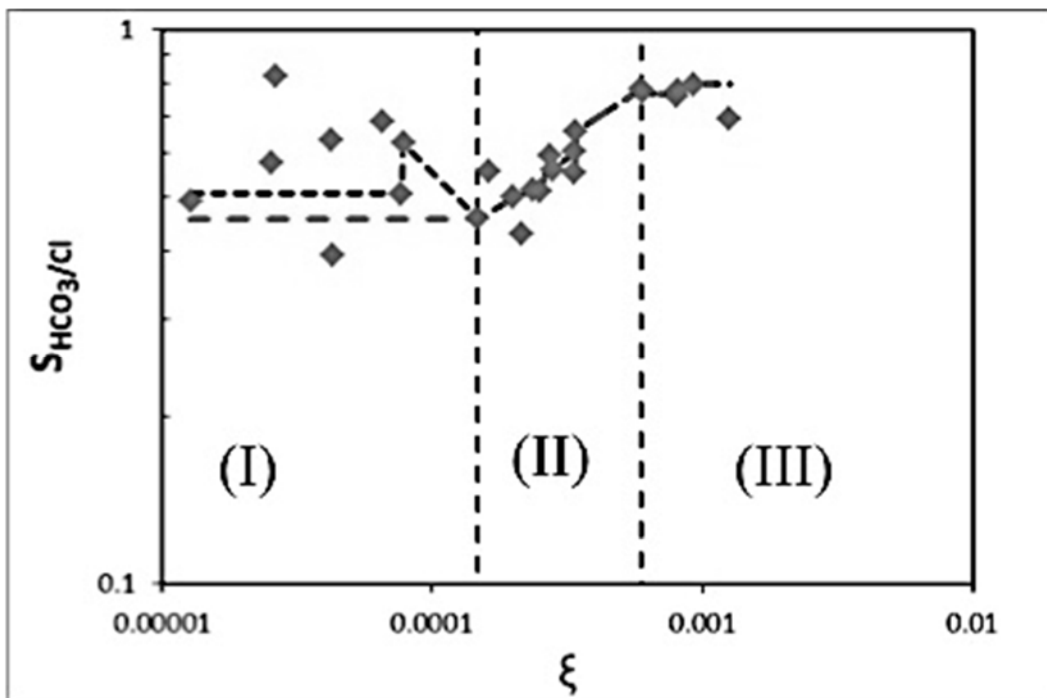


FIGURE 0-47 Different regions for effect of dimensionless number, ξ , for selectivity of HCO_3^- vs Cl^-

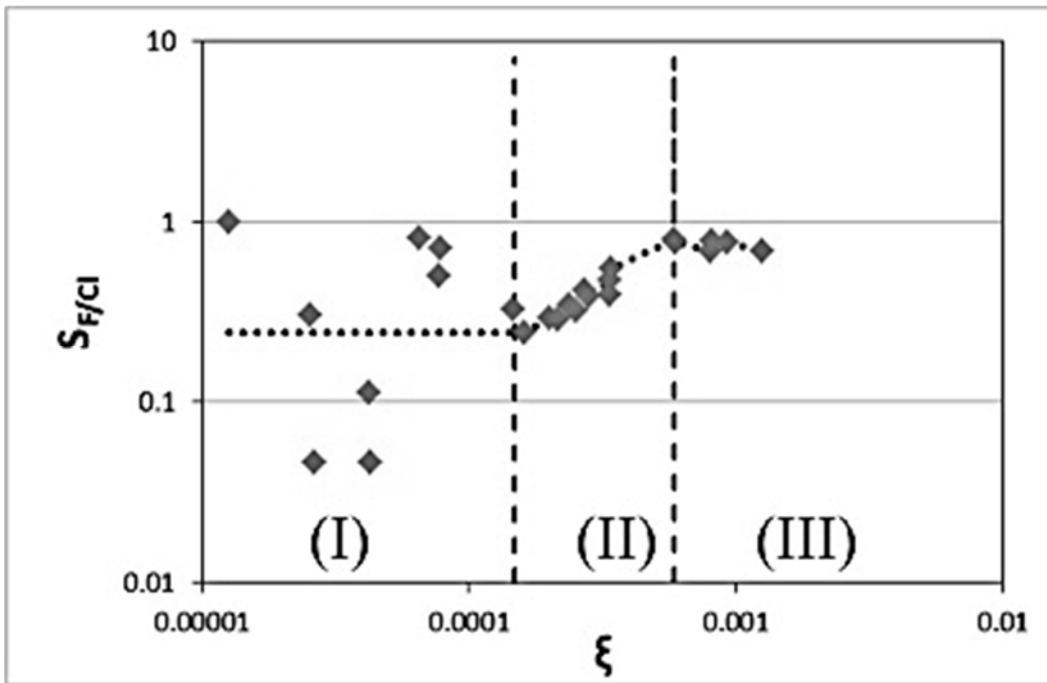


FIGURE 0-48 Different regions for effect of dimensionless number, ξ , for selectivity of F^- vs Cl^-

Appendix

Data Record

Effect of Operating Conditions on Cation Removal

High Temperature-Low Velocity				
Voltage (volts)	K ⁺ (ppm)	Na ⁺ (ppm)	Mg ²⁺ (ppm)	Ca ²⁺ (ppm)
2.67	0.0	5.0	2.4	8.5
9.81	0.4	60.2	4.4	26.6
21.34	1.5	176.4	5.1	40.8
33.2	1.8	283.3	6.1	42.9
45.5	1.9	329.7	6.5	46.2
57	2.0	350.6	7.3	47.1
High Temperature-High Velocity				
Voltage (volts)	K ⁺ (ppm)	Na ⁺ (ppm)	Mg ²⁺ (ppm)	Ca ²⁺ (ppm)
2.7	0.0	0.0	1.5	11.5
9.81	0.3	20.8	3.9	25.5
21.5	0.9	114.9	5.9	36.7
33.1	1.5	209.4	6.1	38.3
44.6	1.7	273.8	6.4	40.2
57.6	1.9	314.1	6.8	41.8

Low Temperature -Low Velocity				
Voltage (volts)	K ⁺ (ppm)	Na ⁺ (ppm)	Mg ²⁺ (ppm)	Ca ²⁺ (ppm)
2.6	0.0	0.0	3.3	27.1
9.8	0.3	28.3	3.9	28.1
21.7	1.2	139.1	5.3	38.8
33.4	1.7	235.0	6.1	43.4
45.3	1.9	308.1	7.1	43.3
57.3	2.0	336.3	7.5	45.2
Low Temperature -High Velocity				
Voltage (volts)	K ⁺ (ppm)	Na ⁺ (ppm)	Mg ²⁺ (ppm)	Ca ²⁺ (ppm)
2.7	0.0	0	0.3	4.7
9.94	0.2	19.8	2.6	19.7
22	0.8	76.4	4.2	30.7
33.4	1.2	162.6	5.5	34.9
45	1.6	228.7	5.9	36.3
57	1.7	289.5	6.4	39.7

High Temperature-Low velocity				
	Removal/Initial*100			
Voltage (volts)	K ⁺ (ppm)	Na ⁺ (ppm)	Mg ²⁺ (ppm)	Ca ²⁺ (ppm)
2.7	2.2	1.4	32.9	18.2
9.8	21.5	16.6	62.1	57.0
21.3	73.0	48.6	71.4	87.3
33.2	92.3	78.1	85.3	91.9
45.5	96.1	90.9	90.2	99.0
57.0	101.1	96.6	101.5	101.0
High Temperature-High Velocity				
	Removal/Initial*100			
Voltage (volts)	K ⁺ (ppm)	Na ⁺ (ppm)	Mg ²⁺ (ppm)	Ca ²⁺ (ppm)
2.7	0.0	0.0	19.3	24.4
9.81	12.7	5.7	49.8	53.9
21.5	46.6	31.6	75.7	77.7
33.1	73.7	57.5	77.2	81.1
44.6	86.4	75.2	81.5	85.2
57.6	93.9	86.2	86.5	88.5

Low Temperature-Low Velocity				
	Removal/Initial*100			
Voltage (volts)	K ⁺ (ppm)	Na ⁺ (ppm)	Mg ²⁺ (ppm)	Ca ²⁺ (ppm)
2.6	0.0	0.0	38.5	52.2
9.8	14.2	7.5	44.8	54.2
21.7	56.0	36.8	60.6	74.8
33.4	80.8	62.2	70.2	83.7
45.3	92.3	81.6	81.7	83.4
57.3	94.9	89.1	86.3	87.2
Low Temperature-High Velocity				
	Removal/Initial*100			
Voltage (volts)	K ⁺ (ppm)	Na ⁺ (ppm)	Mg ²⁺ (ppm)	Ca ²⁺ (ppm)
2.7	0.0	0.0	4.0	10.0
9.9	9.6	5.4	33.7	41.7
22.0	38.0	21.0	53.2	65.0
33.4	60.2	44.6	70.0	73.8
45.0	82.3	62.8	75.6	77.0
57.0	85.7	79.5	81.8	84.1

Effect of Operating Conditions on Anion Removal

High Temperature-Low Velocity				
Voltage (volts)	F ⁻ (ppm)	Cl ⁻ (ppm)	SO ₄ ²⁻ (ppm)	HCO ₃ ⁻ (ppm)
2.67	0.0	0.3	23.0	6.4
9.81	0.4	4.3	189.7	11.1
21.34	0.3	12.8	445.6	32.4
33.2	0.8	25.8	569.7	88.9
45.5	1.7	31.6	615.7	141.2
57	1.8	32.7	614.6	159.4
Low Temperature-Low Velocity				
Voltage (volts)	F ⁻ (ppm)	Cl ⁻ (ppm)	SO ₄ ²⁻ (ppm)	HCO ₃ ⁻ (ppm)
2.6	0.0	4.7	34.6	6.4
9.8	0.0	2.6	157.0	5.6
21.7	0.5	9.8	364.4	23.1
33.4	0.4	21.9	533.3	49.2
45.3	0.6	28.7	585.7	101.1
57.3	1.4	33.2	633.5	137.2

High Temperature-High Velocity				
Voltage (volts)	F ⁻ (ppm)	Cl ⁻ (ppm)	SO ₄ ²⁻ (ppm)	HCO ₃ ⁻ (ppm)
2.7	0.0	0.3	11.0	0.0
9.9	0.2	2.5	137.1	5.5
22.0	0.1	7.5	312.5	15.6
33.4	0.3	15.6	462.5	40.8
45.0	0.7	24.9	542.6	83.8
57.0	1.0	28.8	575.1	128.4
Low Temperature-High Velocity				
Voltage (volts)	F ⁻ (ppm)	Cl ⁻ (ppm)	SO ₄ ²⁻ (ppm)	HCO ₃ ⁻ (ppm)
2.7	0.0	0	10.0	0.0
9.9	0.0	2.3	106.9	6.0
22.0	0.1	6.5	275.1	13.8
33.4	0.1	11.4	388.7	19.8
45.0	0.4	20.4	490.2	57.8
57.0	0.8	27.2	556.9	95.2

High Temperature-Low Velocity				
	Removal/Initial*100			
Voltage (volts)	F ⁻ (ppm)	Cl ⁻ (ppm)	SO ₄ ²⁻ (ppm)	HCO ₃ ⁻ (ppm)
2.67	0.0	0.8	3.6	3.4
9.81	18.7	12.7	29.6	5.9
21.34	15.3	37.5	69.4	17.2
33.2	37.1	75.5	88.8	46.9
45.5	76.6	92.5	95.9	75.1
57	84.3	95.7	95.8	84.8
Low Temperature-Low Velocity				
	Removal/Initial*100			
Voltage (volts)	F ⁻ (ppm)	Cl ⁻ (ppm)	SO ₄ ²⁻ (ppm)	HCO ₃ ⁻ (ppm)
2.6	0.0	12.9	5.1	3.4
9.8	1.0	7.1	23.2	3.0
21.7	26.5	26.9	53.8	12.4
33.4	18.8	59.8	78.8	26.4
45.3	27.9	78.4	86.5	54.3
57.3	68.5	90.5	93.6	73.7

High Temperature-High Velocity				
	Removal/Initial*100			
Voltage (volts)	F ⁻ (ppm)	Cl ⁻ (ppm)	SO ₄ ²⁻ (ppm)	HCO ₃ ⁻ (ppm)
2.7	0.1	0.8	1.8	0.0
9.81	7.6	7.4	22.0	3.0
21.5	7.1	22.0	50.0	8.4
33.1	14.0	45.7	74.0	21.9
44.6	36.6	73.2	86.9	44.9
57.6	48.8	84.7	92.1	68.9
Low Temperature-High Velocity				
	Removal/Initial*100			
Voltage (volts)	F ⁻ (ppm)	Cl ⁻ (ppm)	SO ₄ ²⁻ (ppm)	HCO ₃ ⁻ (ppm)
2.7	0.0	1.2	1.5	0.0
9.94	0.0	6.4	16.4	3.3
22	2.7	18.4	42.2	7.5
33.4	6.1	32.3	59.7	10.7
45	20.2	58.1	75.3	31.4
57	39.9	77.4	85.5	51.7

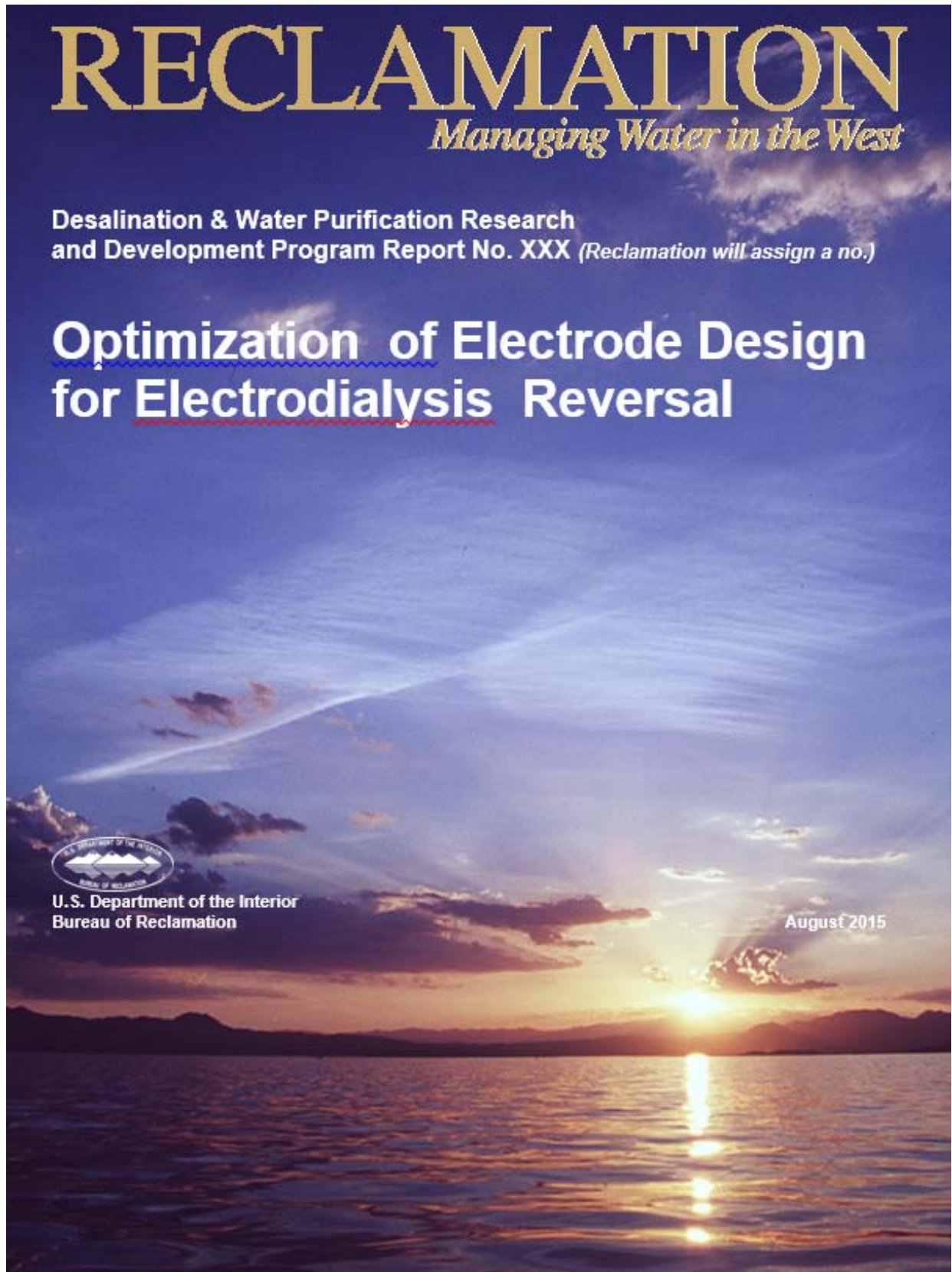
Anion Exchange Membrane Comparison

AR204 Membrane Tests							
Temp	Applied effective Volt	Velocity (cm/s)	ξ	HCO ₃ /Cl	SO ₄ /Cl	Cl/Cl	F/Cl
17	0.08	14.13	4.56625E-05	0.72	3.41	1.00	0.54
17	0.08	14.13	4.57191E-05	0.48	2.53	1.00	0.41
17	0.31	14.25	0.000168124	0.43	1.91	1.00	0.20
17	0.31	14.25	0.000167604	0.37	1.93	1.00	0.18
30	0.13	14.13	7.28511E-05	0.43	3.58	1.00	0.03
31	0.24	14.13	0.000127302	0.37	2.46	1.00	0.06
33	0.33	14.13	0.000174793	0.58	1.35	1.00	0.38
33	0.33	14.13	0.000182984	0.49	1.71	1.00	0.34
22	0.13	14.25	6.59202E-05	0.65	3.39	1.00	0.62
22	0.30	14.25	0.000148946	0.45	2.07	1.00	0.27
24	0.39	13.89	0.000202162	0.49	2.29	1.00	0.25
24	0.49	14.25	0.000246722	0.49	2.29	1.00	0.25
13	0.07	8.50	4.9391E-05	0.67	3.59	1.00	0.29
13	0.07	8.50	4.93667E-05	0.57	3.21	1.00	0.44
13	0.13	8.98	9.82558E-05	0.38	2.58	1.00	0.06
13	0.13	8.98	9.83541E-05	0.45	2.53	1.00	0.12
22	0.24	8.62	0.000177674	0.56	1.47	1.00	0.31
22	0.24	8.62	0.000179681	0.55	1.50	1.00	0.36
31	0.11	8.38	8.09165E-05	0.41	3.01	1.00	0.13
31	0.11	8.38	8.0354E-05	0.40	3.02	1.00	0.08
32	0.19	8.98	0.000134198	0.52	1.56	1.00	0.32
32	0.19	8.98	0.000133633	0.52	1.55	1.00	0.27
33	0.28	8.98	0.000192475	0.81	1.05	1.00	0.71
33	0.28	8.98	0.000192636	0.81	1.05	1.00	0.71
25	0.36	8.97	0.000277602	0.56	1.54	1.00	0.39
25	0.16	9.34	0.000116476	0.60	1.35	1.00	0.48
23	0.37	8.98	0.000283017	0.78	1.01	1.00	0.80
23	0.48	9.34	0.00035501	0.78	0.99	1.00	0.78
32	0.07	10.78	4.4827E-05	0.52	3.31	1.00	0.22
32	0.07	10.78	4.50794E-05	0.71	3.55	1.00	0.16
34	0.17	11.61	9.63874E-05	0.49	2.12	1.00	0.33
34	0.17	11.61	9.64512E-05	0.49	2.11	1.00	0.33
34	0.36	11.73	0.000199366	0.76	1.08	1.00	0.68
34	0.36	11.73	0.000199583	0.76	1.07	1.00	0.68
24	0.07	11.97	4.013E-05	0.55	4.44	1.00	0.08
24	0.07	11.97	3.99063E-05	0.45	3.33	1.00	0.03
24	0.19	11.97	0.000107795	0.46	2.37	1.00	0.26
24	0.19	11.97	0.000107576	0.45	2.55	1.00	0.30
31	0.28	12.09	0.000153463	0.57	1.47	1.00	0.56
31	0.28	12.09	0.000154488	0.56	1.51	1.00	0.35

AR908 Membrane Tests						
Linear velocity	Feed T	Applied effective Volt	ξ	SO ₄ /Cl	HCO ₃ /Cl	F/Cl
8.98	19.20	0.33	2.80E-04	1.59	0.37	0.17
8.98	19.40	0.88	7.45E-04	0.95	0.71	0.76
14.37	24.25	0.20	9.48E-05	3.12	0.28	0.18
14.37	24.47	0.46	2.16E-04	1.56	0.47	0.31
14.37	24.48	1.52	6.93E-04	0.96	0.83	0.81
8.98	33.97	0.12	8.88E-05	4.47	0.17	0.03
8.98	33.91	0.31	1.96E-04	1.94	0.49	0.31
8.98	33.77	0.59	3.53E-04	1.01	0.77	0.73
14.37	33.72	0.37	2.09E-04	1.79	0.48	0.32
14.37	33.81	1.11	5.05E-04	0.99	0.79	0.72

Aged-AR204 Membrane Tests									
	% Removal in Conductivity	Feed Temp	Effective Applied Voltage per desalting cell	ξ	HCO ₃ /Cl	SO ₄ /Cl	Cl/Cl	F/Cl	velocity in desalting chamber (cm/s)
7.5/3.5	30	11.29	0.26	1.4778614E-04	0.52	0.66	1.00	0.48	9.27
7.5/3.5	60	11.32	0.62	2.1243066E-04	0.67	0.76	1.00	0.75	9.39
7.5/3.5	85	11.33	1.95	3.1849595E-04	0.93	0.85	1.00	0.80	9.34
12/5.3	30	9.85	0.46	1.6219957E-04	0.62	0.68	1.00	0.66	14.76
12/5.3	60	9.8	1.13	2.5595399E-04	0.72	0.78	1.00	0.74	14.83
12/5.3	70	9.84	1.86	3.1903570E-04	0.83	0.80	1.00	0.78	15.08
7.5/3.5	30	31.32	0.09	5.7604390E-05	0.36	1.33	1.00		9.25
7.5/3.6	60	31.73	0.26	1.0798076E-04	0.61	0.73	1.00	0.62	9.67
7.5/3.7	90	30.95	0.77	9.8831609E-05	0.87	0.90	1.00	0.88	9.17
12/5.3	30	30.68	0.16	6.3460618E-05	0.48	0.85	1.00	0.46	14.71
12/5.3	60	30.89	0.42	1.1089885E-04	0.64	0.68	1.00	0.70	14.55
12/5.3	90	31.15	1.34	1.0563340E-04	0.94	0.89	1.00	0.90	14.60
7.5/3.5	30	21.96	0.10	6.7394326E-05	0.43	1.26	1.00	0.26	9.12
7.5/3.5	60	21.9	0.30	1.3847771E-04	0.63	0.70	1.00	0.63	9.12
7.5/3.5	90	22.13	1.02	1.3861039E-04	0.92	0.89	1.00	0.90	9.22
12/5.3	30	22.02	0.16	6.5341490E-05	0.49	0.86	1.00	2.10	14.97
12/5.3	60	21.98	0.47	1.3607558E-04	0.65	0.72	1.00	1.25	14.82
12/5.3	90	21.81	1.79	1.5844046E-07	1.01	0.90	1.00	1.01	14.84

Optimization of Electrode Design for Electrodialysis Reversal



REPORT DOCUMENTATION PAGE				<i>Form Approved</i> <i>OMB No. 0704-0188</i>	
<p>The public reporting burden for this collection of information is estimated to average 1 hour per response, including the time for reviewing instructions, searching existing data sources, gathering and maintaining the data needed, and completing and reviewing the collection of information. Send comments regarding this burden estimate or any other aspect of this collection of information, including suggestions for reducing the burden, to Department of Defense, Washington Headquarters Services, Directorate for Information Operations and Reports (0704-0188), 1215 Jefferson Davis Highway, Suite 1204, Arlington, VA 22202-4302. Respondents should be aware that notwithstanding any other provision of law, no person shall be subject to any penalty for failing to comply with a collection of information if it does not display a currently valid OMB control number.</p> <p>PLEASE DO NOT RETURN YOUR FORM TO THE ABOVE ADDRESS.</p>					
1. REPORT DATE (DD-MM-YYYY)		2. REPORT TYPE		3. DATES COVERED (From - To)	
31 August 2015		Final Report			
4. TITLE AND SUBTITLE Optimization of Electrode Design for Electrodialysis Reversal				5a. CONTRACT NUMBER R10AC80283	
				5b. GRANT NUMBER	
				5c. PROGRAM ELEMENT NUMBER	
6. AUTHOR(S) Masoume Jaberi, Fattaneh Naderi Behdani Abbas Ghassemi				5d. PROJECT NUMBER	
				5e. TASK NUMBER	
				5f. WORK UNIT NUMBER	
7. PERFORMING ORGANIZATION NAME(S) AND ADDRESS(ES) IEEE/WERC New Mexico State University PO Box 30001 Las Cruces, NM 88003				8. PERFORMING ORGANIZATION REPORT NUMBER	
9. SPONSORING/MONITORING AGENCY NAME(S) AND ADDRESS(ES)				10. SPONSOR/MONITOR'S ACRONYM(S)	
				11. SPONSOR/MONITOR'S REPORT NUMBER(S)	
12. DISTRIBUTION/AVAILABILITY STATEMENT					
13. SUPPLEMENTARY NOTES					
14. ABSTRACT <p>The worsening global scarcity of freshwater threatens worldwide peace and prosperity, which are intimately tied to the availability of clean, fresh water (J. E. Miller, 2003). One approach for alleviating this threat is desalination, which can turn brackish and saline water sources into freshwater, and electrodialysis reversal (EDR) is a proven and widely used technology that can desalinate brackish waters in inland areas such as the southwestern United States. In a significant advantage over other membrane-based systems like reverse osmosis, EDR's ability to clean itself renders the system resistant to scaling and fouling and allows it to operate at high levels of water recovery. In a further benefit, this system typically requires less energy than thermal distillation to desalinate brackish water, leading to a reduction in overall desalination costs.</p> <p>To identify the operating limits of EDR and find the parameters that maximize its performance, this research investigated the performance sensitivity and limitations of EDR for treating brackish groundwater through careful experimental and statistical analyses of selected electrical, hydraulic, and chemical variables. Experimental evaluation was performed using a pilot-scale EDR system and natural feedwaters at the Brackish Groundwater National Desalination Research Facility in Alamogordo, NM; statistical analyses were carried out using SAS software. Based on the experimental results and statistical analyses, multi-linear regression models were developed for EDR systems for removal ratio, current, and specific energy consumption.</p>					
15. SUBJECT TERMS					
16. SECURITY CLASSIFICATION OF:			17. LIMITATION OF ABSTRACT	18. NUMBER OF PAGES	19a. NAME OF RESPONSIBLE PERSON
a. REPORT	b. ABSTRACT	a. THIS PAGE			19b. TELEPHONE NUMBER (Include area code)

**Desalination & Water Purification Research
and Development Program Report No. XXX**

Optimization of Electrode Design for Electrodialysis Reversal

Prepared for Reclamation Under Agreement No. R10AC80283

By

Masoume Jaberi, Abbas Ghassemi



**U.S. Department of the Interior
Bureau of Reclamation
Technical Service Center
Water and Environmental Services Division
Water Treatment Engineering Research Team
Denver, Colorado**

August 2015

MISSION STATEMENTS

The mission of the Department of the Interior is to protect and provide access to our Nation's natural and cultural heritage and honor our trust responsibilities to Indian tribes and our commitments to island communities.

The mission of the Bureau of Reclamation is to manage, develop, and protect water and related resources in an environmentally and economically sound manner in the interest of the American public.

Disclaimer

The views, analysis, recommendations, and conclusions in this report are those of the authors and do not represent official or unofficial policies or opinions of the United States Government, and the United States takes no position with regard to any findings, conclusions, or recommendations made. As such, mention of trade names or commercial products does not constitute their endorsement by the United States Government.

Acknowledgements

I would like to acknowledge The Desalination and Water Purification Research and Development Program, U.S. Bureau of Reclamation, for their financial support to carry out this research project.

Contents

	<i>Page</i>
Executive Summary	1
Chapter 1 - Introduction.....	2
1.1 Background	2
1.2 Desalination.....	3
1.3 Research Challenge	4
1.4 Research Objective.....	5
1.5 Research Approach	5
Conclusions	5
Recommendations	7
Chapter 2 - Literature Review.....	8
2.1 EDR System Description	8
2.2 Polarity Reversal Phenomenon	9
2.3 EDR Stack Components.....	10
2.3.1 Electrode Chamber	11
2.3.2 EDR Cell Pair	11
2.3.2.1 Ion-Exchange Membranes	11
2.3.2.2 Spacers	13
2.4 Mass Transport in EDR Stack.....	14
2.4.1 Diffusion.....	14
2.4.2 Migration	14
2.4.3 Convection.....	14
2.5 Electrodialysis Reversal Challenges	16
2.5.1 Concentration Polarization	16
2.5.2 Scaling and Fouling: A Concentrate Problem	17
2.5.3 Limiting Current Density: A Dilute Problem.....	17
2.6 EDR Process Performance Metrics	19
2.6.1 Chemical Efficiency: Removal Ratio	19
2.6.2 Hydraulic Efficiency: Recovery Ratio	20
2.6.3 Electrical Efficiency: Specific Energy Consumption (SEC).....	20
2.6.3.1 Direct Energy Requirements.....	21
2.6.3.2 Pumping Energy Requirement.....	22
2.6.4 Electrical Efficiency: Current Efficiency (CE)	23
2.7 Electrodialysis Reversal Optimization	23
2.7.1 Hydraulic: Improving the Rate of Mass Transfer.....	24
2.7.2 Hydraulic: Improving Recovery Ratio	25
2.7.3 Electrical: Decreasing the Electrical Resistance of the Stack	25
2.7.4 Chemical: Preventing Scaling and Fouling	26
2.8 Summary	26

Chapter 3 - Materials and Methods.....	27
3.1 Experimental Design.....	28
3.2 Experimental Set-up.....	29
3.3 Experimental Location	30
3.3.1 Influent Pumping Equipment	30
3.3.2 Multimedia Filter System	30
3.3.3 Cartridge Filtration System	30
3.3.4 EDR stack.....	31
3.3.5 Concentrate Recycle and Waste Blowdown System.....	31
3.3.6 Chemical Dosing System.....	32
3.4 Experimental procedure	32
3.5 Characterization and Control systems.....	33
3.6 Data Analysis	34
Chapter 4 - Results and Discussion	34
4.1 Experimental Results.....	35
4.1.1 Electrical: Determining Limiting Current	35
4.1.2 Electrical: Effects of Stack Voltage.....	36
4.1.2.1 Chemical Efficiency.....	37
4.1.2.2 Electrical Efficiency.....	37
4.1.3 Hydraulic: Effects of Flow Rate.....	37
4.1.3.1 Chemical Efficiency.....	38
4.1.3.2 Electrical Efficiency.....	38
4.1.4 Chemical: Effects of Feed Concentration.....	38
4.1.4.1 Chemical Efficiency.....	39
4.1.4.2 Electrical Efficiency.....	39
4.1.5 Design: Effect of Electrode Geometry	39
4.2 Modeling Results.....	40
4.2.1 Chemical Efficiency: Removal Ratio.....	41
4.2.2 Electrical Efficiency: Current.....	41
4.2.3 Electrical Efficiency: Specific Energy Consumption.....	42
4.3 Conclusion.....	42
4.4 Future Work	44
References.....	45
Tables.....	52
Figures.....	58
Appendices.....	82
Data Record.....	82

Glossary

List of Abbreviations

AEM	Anion Exchange Membrane
ANOVA	Analysis of Variance
BGNDRF	Brackish Groundwater National Desalination Research Facility
CE	Current Efficiency
CEM	Cation Exchange Membrane
DC	Direct Current
ED	Electrodialysis
EDR	Electrodialysis Reversal
GPM	Gallon Per Minute
HMI	Human-Machine Interface
IC	Ion Chromatography
LCD	Limiting Current Density
LSI	Langelier Saturation Index
MED	Multiple Effect Distillation
MEE	Multi-Effect Evaporation
MLR	Multi Linear Regression
MMF	Multi Media Filterage
MSF	Multi-Stage Flash
NMSU	New Mexico State University
RO	Reverse Osmosis
SEC	Specific Energy Consumption
TDS	Total Dissolved Solids
VC	Vapor Compression
VIF	Variance Inflation Factor
ZLD	Zero-Liquid Discharge

Executive Summary

The worsening global scarcity of freshwater threatens worldwide peace and prosperity, which are intimately tied to the availability of clean, fresh water (J. E. Miller, 2003). One approach for alleviating this threat is desalination, which can turn brackish and saline water sources into freshwater, and electro dialysis reversal (EDR) is a proven and widely used technology that can desalinate brackish waters in inland areas such as the southwestern United States. In a significant advantage over other membrane-based systems like reverse osmosis, EDR's ability to clean itself renders the system resistant to scaling and fouling and allows it to operate at high levels of water recovery. In a further benefit, this system typically requires less energy than thermal distillation to desalinate brackish water, leading to a reduction in overall desalination costs.

To identify the operating limits of EDR and find the parameters that maximize its performance, this research investigated the performance sensitivity and limitations of EDR for treating brackish groundwater through careful experimental and statistical analyses of selected electrical, hydraulic, and chemical variables. Experimental evaluation was performed using a pilot-scale EDR system and natural feedwaters at the Brackish Groundwater National Desalination Research Facility in Alamogordo, NM; statistical analyses were carried out using SAS software. Based on the experimental results and statistical analyses, multi-linear regression models were developed for EDR systems for removal ratio, current, and specific energy consumption.

Chapter 1 - Introduction

1.1 Background

Water is the essential substance for life on earth, and the demand for it is increasing rapidly. There is about 1.4 billion km³ of water on earth, but less than 3% of it is freshwater, and most of that is inaccessible since it is locked up in ice caps and glaciers. The remaining 23% of freshwater is held as groundwater, surface water, in plants, and in the atmosphere (P. H. Gleick, 1993).

The lack of fresh water prevents economic development, results in environmental degradation, and causes political instability. This challenge has forced many governments to look for technologies that conserve water and improve the efficiency of water use.

Many areas that are facing the highest water stress have access to groundwater resources, but the quality of the groundwater often renders it unsuitable for human consumption: the main disadvantage of groundwater reservoirs is the high amount of dissolved solids such as calcium, magnesium, iron, sulfate, sodium, chloride, and silica. Before water from these supplies can be used for drinking, agriculture, industrial applications, and myriad other purposes, such groundwater has to be desalinated (Elsaid, Bensalah, & Abdel-wahab, 2012).

Desalination is a process by which excess salts are removed from saline water to make it suitable for human consumption and other uses.

The global online capacity for desalination plants has increased from 5.1 million m³/day in 1980 (Pankratz, 2012), to more than 80 million m³/day in 2013 (International Desalination Association, 2013). Saudi Arabia is currently the world leader in desalination production capacity at approximately 16% of the global capacity, followed by the United States at approximately 13% (Greenlee, Lawler, Freeman, Marrot, & Moulin, 2009).

However, although there are plentiful sources of saline water, the high costs of desalination and other forms of advanced water treatment have limited the use of these technologies (J. E. Miller, 2003). There are currently 16,000 desalination plants on the planet, but their total capacity is only about 1% of the freshwater used every day in just the United States (P. Gleick, 2012; J. E. Miller, 2003; Pankratz, 2012). This capacity is expected to double over the next 20 years with a predicted \$20 billion in spending (Brady, Kottenstette, Mayer, & Hightower, 2009; Martin-lagardette, 2003), but large-scale desalination systems are fairly recent technological developments, dating back only to the mid-1900s, and there are still significant research opportunities for improving the energy consumption, cost, and reliability of desalination technologies.

1.2 Desalination

Desalination is defined as a process for removing various salts from saline water to produce fresh water. There are multiple desalination technologies, but the applicability of each one is heavily dependent on the type of water to be desalinated. Water is typically characterized by the amount of total dissolved solids (TDS), and based on that, there are different water types including:

- Fresh water, with less than 1,000 mg/L TDS,
- Brackish water, with between 1,000 and 5,000 mg/L TDS,
- Highly brackish water, with between 5,000 and 15,000 mg/L TDS,
- Saline water, with between 15,000 and 30,000 mg/L TDS,
- Seawater, with between 30,000 and 40,000 mg/L TDS, and
- Brines, with greater than 40,000 mg/L TDS

In addition to water type, the other main factors in choosing the best desalination technology for a particular application include the availability of energy, the intended use for the produced water, and the required treatment capacity. The basic types of desalination techniques are categorized into two main groups: (a) thermal technologies, and (b) membrane.

The driving force of thermal processes is heat, which is used to induce a phase change in water, causing it to evaporate and leave dissolved solids behind. Because of the energy needed to achieve this, thermal techniques are not usually used for brackish water treatment due to their high cost. However, these technologies produce water with very low levels of TDS, and they are used extensively in the Middle East where there are abundant sources of fossil fuels. Some examples of thermal desalination technologies include multiple stage flash distillation (MSF), multiple effect distillation (MED), multi-effect evaporation (MEE), and vapor compression (VC).

The other main category of desalination approaches, membrane based technologies, is usually divided into two groups based on the driving force, which can be either pressure or electricity. Pressure driven processes include reverse osmosis (RO), nanofiltration, microfiltration, ultrafiltration, and forward osmosis; electrically-driven membrane processes include electrodialysis (ED) and electrodialysis reversal (EDR) (Shaffer & Mintz, 1966).

RO is currently the most popular desalination technology comprising 60% of the total global desalination capacity in 2012 (Pankratz, 2012). However, in comparison to the widely used RO technology, ED has higher water recovery (the fraction of feed water that becomes product water). Low recovery rate prevents widely implementation of RO to desalinate brackish ground waters, because the disposal of large volumes of waste is environmentally and financially unfeasible (Subcommittee, 2004; Nicot & Chowdhury, 2005). The other advantage of ED over RO is greater resistance to scaling and fouling, which makes them particularly promising technologies for brackish water treatment (Murray, 1995).

Electrodialysis (ED) is an electrically driven membrane process in which ions are selectively transferred through ion-exchange membranes under the electric potential of DC voltage. Since the driving force for separation is an electric field, ED only removes charged components from solution. ED cannot

safely remove organic elements that do not carry an electrical charge, but it can be used on waters with high levels of silica that would foul pressure-driven membranes.

Electrodialysis Reversal (EDR) was introduced in the 1970's as an innovative modification of existing ED technology (Elsaid, Bensalah, & Abdelwahab, 2007). EDR works the same way as ED, except that the polarity of the DC power is reversed at specified time intervals, allowing for a 'self-cleaning' of the membrane surfaces. With the reversal modification, EDR process has proven to operate at higher solution concentrations of dissolved solids, suspended solids, scale-prone salts, and non-ionic species (such as silica) with higher recovery rates and low chemical pretreatment than other desalination technologies (Reahl, 2006).

1.3 Research Challenge

Fueled by rapid population growth, much of the Southwest United States is witnessing an increased demand on their limited freshwater supply, and looking towards their extensive brackish water as part of the mix of available resources to address this issue. Texas and Arizona have an estimated 2.7 billion acre-feet and 600 million acre-feet of brackish water, respectively. In New Mexico, there is a significant amounts of brackish groundwater., but three-quarters of this brackish water has salinities high enough to require treatment before it can be used for most purposes (Eden, Glass, & Herman, 2011; National Ground Water Association, 2010).

The challenge of balancing water scarcity and increasing water demands has drawn attention toward utilizing technology to produce drinking water from non-potable resources. However, the implementation of large-scale inland desalination is hindered by the relatively high cost of treating brackish waters (Staff, 1996; Strathmann, 2004; Lee, Hong, Han, Cho, & Moon, 2009; Jefferies & Comstock, 2001).

Electrodialysis Reversal (EDR) has been used for half a century to desalinate brackish and saline waters for potable use and shows promise as a viable brackish water treatment process for two primary reasons: it can achieve greater product recovery than RO, and it is more robust than RO with respect to feed turbidity, feed silica concentration, and biological growth (*i.e.*, ion-exchange membranes can tolerate a mild chlorine dose) (AWWA, 1995; Reahl, 2006).

While the brackish water desalination using EDR process has been successfully implemented in a few situations, there is lack of wide approach that identifies the various operating aspects of EDR and finds the parameters that maximize its performance,

Therefore, our research challenge is to conduct a complete investigation of performance sensitivity and limitations of EDR for treating brackish groundwater through careful experimental and statistical analyses of selected electrical, hydraulic, and chemical variables.

1.4 Research Objective

One goal of this research was to systematically and quantitatively analyze the performance of a pilot-scale EDR plant in the treatment of several brackish groundwaters under various electrical, hydraulic, and chemical conditions; another goal was to determine the operating conditions that contribute to higher removal ratios and lower energy consumption.

More specifically, the objectives of this research were to:

1. Experimentally determine the sensitivity of EDR to hydraulic, electrical, and chemical operational parameters;
2. Determine and compare how the three electrode designs (full, recessed, and tapered) affect EDR performance;
3. Identify the operating parameters that maximizes the performance of EDR;
4. Perform statistical analyses of the investigated parameters (electrical, hydraulic, and chemical) to determine their impacts on EDR performance.

The hypothesis for this research is that EDR desalination systems perform differently under different operating and design conditions, including applied stack voltage, flow rate, source water salinity, and electrode design.

1.5 Research Approach

These goals were accomplished using an existing infrastructure in order to be most economical. We used an existing 1-stage pilot-scale EDR owned by NMSU and located at the Brackish Groundwater National Desalination Research Facility (BGNDRF) in Alamogordo, NM. In order to do the investigations on the operating factors, the experiments were done where the effects of operating variables: feed flow rate, feed salinity, voltage and type of electrode were verified.

The introduction presented here is followed in Chapter 2 by a review of EDR technologies and operations. Then, Chapter 3 details the experimental methodology including the experimental location, experimental set-up, and a detailed summary of the data collection procedure. In Chapter 4, a discussion of experimental results is presented in response to the objectives. Finally, a summary of the conclusions resulting from this research is also presented in Chapter 4.

Conclusions

The following is a brief overview of the conclusions and recommendations made based on the results of the experiment; a more detailed discussion is given in sections 4.3 and 4.4.

- EDR performance depends on operating conditions such as, stack voltage, flow rate and feed salinity. However, the design of the

electrodes has no significant effect on EDR performance.

- Brackish groundwater experiments demonstrated that stack voltage applications in the range of 30-40 Volts and feed flow rates in the range of 7-11 GPM effectively separated up to 70% of the initial feed salinity in the range of approximately 1000-5500 mg/L at single-stage EDR recovery of 80%.
- The rate of separation and current are approximately proportional to the applied voltage.
- The specific energy consumption increases with increasing the applied voltage.
- A decrease in the rate of separation was observed with increases in the feed flow rate, which increase the stack superficial velocity leading to a decrease in residence time.
- An increase in flow rate causes an increase in the energy required for pumping, and consequently an increase in total energy.
- Specific energy consumption decreases with increases in the feed flow rate while product water volume increases when feed flow rate increases.
- As the concentration of solution increases, the removal ratio drops when feed concentration increases.
- Since current is proportional to feed conductivity, the specific energy consumption increases as feed water becomes more saline.
- In order to increase the removal ratio, lower feed concentrations, higher voltages, and lower flow rates should be utilized.
- In order to reduce the specific energy consumption, lower voltages, lower feed concentrations, and higher flow rates are suggested.
- The data gathered in these experiments are from conditions that still left salinity levels above 1,000 $\mu\text{S}/\text{cm}$ in the product water. Therefore, real-world desalination processes would require further treatment to bring the quality of the produced water to acceptable levels.
- Given that specific energy consumption is strongly determined by the removal ratio, further salt removal to produce truly potable water would significantly increase the specific energy consumption of the systems.
- As a consequence of an expanded hydrodynamic boundary layer and concentration boundary layer, the system is likely to experience progressively poorer electrochemical/hydrodynamic behavior.
- As the removal ratio increases, there is a higher likelihood of salt precipitation in the hydrodynamic/concentration boundary layer.
- Additional testing should be conducted before designing industrial-

scale systems due to the preceding reasons.

Recommendations

- Expansion of the EDR experiment could be made to study how additional operating conditions, such as temperature and recovery ratio, affect EDR performance.
- The experiments could be done with more than one hydraulic stage to improve the removal ratio and study how energy consumption changes when more stages are added.
- The models for the pilot-scale plant could be extended to simulate full-scale EDR systems. This would allow them to quantify limitations in the tradeoff between energy consumption and removal ratio associated with voltage application and feed flow rate, making it possible to optimize the design of EDR systems.

Chapter 2 - Literature Review

In this chapter, the principles of electrodialysis reversal are described and the thermodynamic basics for separation and overall mass transfer are explained. Then, the chapter moves on to describe the coupled hydraulic/electrochemical behavior of the system. This is followed by an introduction to basic performance metrics of each EDR system, including energy consumption, desalting ratio, current efficiency and recovery ratio. Lastly, the chapter moves on to present and explain strategies that contribute to improved EDR performance.

EDR is an electrochemical separation process that selectively removes dissolved solids, based on their electrical charge, by transferring the brackish water ions through a semipermeable ion exchange membrane charged with an electrical potential (Younos & Tulou, 2009). The ions are transferred through ion exchange membranes by means of a direct current (DC) voltage. The process uses a driving force to transfer ionic species from the source water toward a cathode (positively charged ions) and anode (negatively charged ions) to a concentrate wastewater stream, creating a more dilute stream (Walker, 2010). The overall schematic for the EDR process is shown in Figure 2.1.

2.1 EDR System Description

As illustrated in Figure 2.2 (Hanrahan, 2013), EDR works as follows. First, the influent source water is split into three streams: feed in, concentrate makeup, and electrode in. The feed in stream, which receives the largest portion of the source water, enters the dilute flow-paths and is demineralized until it exits the stack as product water. A smaller portion of the source water becomes the concentrate makeup stream, which combines with the concentrate recycle at the suction end of the concentrate pump and enters the concentrate flow-paths as the concentrate in stream. This water is progressively concentrated until going to waste as concentrate blowdown, and the remainder enters the concentrate recycle. The source water flows in parallel only through demineralizing compartments, whereas the concentrate stream flows in parallel only through concentrating compartments. The last part of the source water becomes the electrode in stream. This stream is dosed with acid and continuously circulates through the space provided by heavy spacers in order to prevent scaling by neutralizing the hydroxyl ions at the cathode and flushing the electrode chambers of precipitates and gases such as oxygen, hydrogen, and chlorine, which are formed as part of the electrochemical reactions at the surface of the electrodes.

Within the electrode chambers, different oxidation and reduction reactions will occur, depending on the polarity of the electrode. When DC potential is applied across the electrodes, the following processes take place (Murray, 1995):

At the cathode, pairs of water molecules dissociate, producing two hydroxyl (OH⁻) ions plus hydrogen gas (H₂). This reaction, shown in Equation

2.1, is called the reduction of water by the half reaction:



As a result, hydroxide raises the pH of the water, causing calcium carbonate (CaCO_3) precipitation.

At the anode, pairs of water molecules break down to produce four hydrogen ions (H^+), one molecule of oxygen (O_2), and four electrons (e^-), a process which is called the oxidation of water by the half reaction. This is shown in Equation 2.2.



The acid produced by this reaction tends to dissolve any calcium carbonate present to inhibit scaling. In this reaction, in the case of having chloride at the anode, the oxidation of chloride results in chlorine gas (Cl_2) formation, as shown in Equation 2.3.



Flows from the two electrode compartments do not mix with other streams. Concentrate from the electrode stream is sent to a degasifier to remove and safely dispose of any reaction gases. In many applications, after being passed through the degasifier, concentrate from the electrode stream is recycled back to the feed in order to increase the overall recovery of the system (Valero, Barceló, & Arbós, 2010).

2.2 Polarity Reversal Phenomenon

Across all ED/EDR systems and almost all membrane-based desalination processes, membrane fouling is a major problem. In this phenomenon, suspended solids that carry electrical charges adhere to the surface of the membranes and drastically increase membrane resistance, significantly reducing membrane efficiency.

Despite the almost universal prevalence of the membrane fouling problem, this difficulty has been largely overcome in EDR through periodic reversals in the polarity of the electrodes. This reversal tends to expel charged particles that have precipitated onto the membranes. This process, which is called “clean in place” or simply electro dialysis reversal (Pilat, 2001; Reahl, 2006), is illustrated in Figure 2.3. (Allison, 2008).

While the source water flows in the chambers between the cationic and anionic membranes, the DC voltage supplied by the cathode draws anions toward the cathode through the anion exchange membrane (AEM). Over time, the cathodic attraction leads anions to accumulate on the AEM surface, forming a

barrier termed a “fouling layer.” Polarity reversal disrupts the fouling layer by driving the negatively charged components away from the AEM and back into the feed stream, restoring membrane properties to their pre-fouling condition (H.-J. Lee et al., 2009).

In addition to the polarity reversal, the flows of the hydraulic streams at the stack inlet and outlet are also reversed. The hydraulic streams in an EDR stack consist of concentrate streams and dilute streams, and when the EDR stack is operating with reversed polarity, the concentrate cells become the dilute cells, and vice versa. The interval between polarity reversals can range from several minutes to several hours.

For a short period of time while the polarity and streams are being reversed, the salinity of the dilute stream exceeds the salinity levels required of the product water. To avoid producing unacceptable product water, a more complicated flow control process is required. Therefore, the outlet for the product water is monitored by a concentration sensor that regulates a 3-way valve. When conductivity passes a pre-determined threshold, the valve shunts product water with overly high salinity into the brine stream. This is continued until the feed stream has completely replaced the concentrate stream in the newly-dilute flow path, resulting in the production of permeate water with acceptable quality. At this point, the conductivity sensor at the outlet detects salinities below the required threshold and returns the product stream to the product tank.

In the use of EDR systems, some of the product water is always lost into the waste stream during polarity reversal. Usually, this loss varies between 2 and 4% of the volume of product water in industrial EDR plants (AWWA, 1995). Although such loss may not be acceptable when feed solutions contain high value products (e.g., in particular applications within the food and drug industry), product water loss generally is not a problem in the desalination of brackish water.

Overall, periodically reversing the polarity of the electrical field in the EDR process results in several positive impacts to the operation of the system (Katz, 1979):

- The polarization films are broken up several times every hour, which avoids scaling;
- Newly precipitated scales are dissolved before they can damage the membrane;
- As the directional movement of colloidal particles is reversed, slime formation on the membrane surface is reduced; and
- Drawbacks resulting from the need to continuously add chemicals (e.g., antiscalants and acids) are eliminated.

2.3 EDR Stack Components

The basic structure of an EDR stack consists of electrode chamber and cell pairs, as shown in Figure 2.4.

2.3.1 Electrode Chamber

Each electrode compartment consists of an electrode, an electrode water-flow spacer, and a heavy cation membrane. This spacer prevents the electrode waste from entering the main flow paths of the stack and typically is thicker than a normal spacer, which increases water velocity to prevent scaling (Ionics, 1984).

In order to withstand a greater degree of hydraulic pressure difference between the electrode streams and the adjacent flow-paths, heavy cation exchange membranes are required. These membranes have all the properties of regular cationic membranes but are twice as thick (Valerdi-Perez, Berna-Amoros, & Ibanes-Mengual, 2000).

Another component, the electrode, is located at each end of the membrane stack and conducts electric current into the stack. Because of the corrosive nature of the anode compartments, electrodes are usually made of titanium and plated with platinum.

The life span of an electrode is dependent on the amperage applied to the electrode and the ionic composition of the source water. High amperages and large amounts of chlorides in the source water reduce electrode life (AWWA, 1995).

Generally, electrode life in the last decade varied with the application and type of feed water, the capability of the operators, and other factors. Over time, material science has been developing new techniques for plating and deposition, and electrode materials have changed over the years as experience and process understanding have increased. For instance, with the advent of EDR, Ionics, Inc., undertook an extensive research and development program designed to produce an electrode that has a reasonable life, is reasonably inexpensive, and is relatively electrically efficient. (Purification & Program, 2003).

2.3.2 EDR Cell Pair

Each assembled stack is composed of the two electrodes and groups of cell pairs. A cell pair consists of the following (Valero & Arbós, 2010):

- Anion permeable membrane,
- Concentrate spacer,
- Cation permeable membrane, and
- Dilute stream spacer.

This basic cell pair is repeated until it is capped on both ends by the electrode compartments, which consist of: a heavy flow-path spacer, a heavy cation-exchange membrane, and an electrode (Figure 2.5).

2.3.2.1 Ion-Exchange Membranes

Typically, ion-exchange membranes are dense hydrophobic polymers, such as polystyrene, polyethylene, or polysulfone, which are fixed with charged functional groups (Walton, 1962). There are two different types of ion-exchange membranes, which are classified based on the ions that they interact with in solutions: (1) cation-exchange membranes (CEMs), which contain negatively charged groups fixed to the polymer matrix; and (2) anion-exchange membranes (AEMs), which contain positively charged groups fixed to a polymer matrix.

Figure 2.6 (Strathmann, 2010) schematically illustrates the matrix of a CEM with fixed anions and mobile cations. In a cation-exchange membrane, the fixed anions are in electrical equilibrium with mobile cations in the interstices of the polymer. For a CEM, the mobile cations and anions are called counter-ions and co-ions respectively. The co-ions are excluded from the membrane matrix because of their electrical charge, which is identical to that of the fixed ions. In other words, CEMs are preferentially permeable to cations. AEMs, conversely, carry positive charges fixed on the polymer matrix. AEMs exclude cations, and therefore are preferentially permeable to anions (Tanaka, Uchino, & Murakami, 2012). The extent of exclusion from an ion-exchange membrane depends on the properties of both the membrane and the solution (Strathmann, 2010).

In addition to classifying the membranes based on their ionic functionality, it is useful to distinguish them, according to their structure, as homogeneous or heterogeneous (Walton, 1962). Homogeneous membranes are prepared by introducing an ion-exchange moiety directly into the structure of the polymer, leading to a relatively even distribution of charged groups over the entire membrane matrix. Heterogeneous membranes are prepared by mixing a fine ion-exchange resin powder with a binder polymer and pressing and sintering the mixture at an elevated temperature. This results in a structure where the ion-exchange groups are clustered and very unevenly distributed in membrane matrix as shown in Figure 2.6 a) and b) (Strathmann, 2004).

Generally, to produce commercial cation membranes, the polymer film is sulfonated and cross-linked in a sulfuric acid solution, producing $-\text{SO}_3\text{H}$ groups attached to the polymer. The $-\text{SO}_3\text{H}$ groups ionize in water, producing a mobile counter ion (H^+) and a fixed charge ($-\text{SO}_3^-$). Additionally, commercial AEMs usually have fixed positive charges from quaternary ammonium groups ($-\text{NR}_3^+\text{OH}^-$), which repel positive ions (Strathmann, 2011).

The most desired properties of ion-exchange membranes are: high permselectivity, low electrical resistance, good mechanical and form stability, high chemical and thermal stability, and low production costs (Toshikatsu Sata, 2004). In other words, to contribute to the success of EDR plants treating saline water, both AEMs and CEMs must possess common properties including: low electrical resistance; insolubility in aqueous solutions; semi-rigidity for ease of handling during stack assembly; ability to operate in temperatures above $46\text{ }^\circ\text{C}$; resistance to osmotic swelling; long life expectancies; resistance to fouling; ability to be hand-washed; and resistance to change in pH from 1 to 10, allowing the use of strong acid solutions to remove scales and metal hydroxide deposits (Miller, 2009).

In general, EDR technologies have a membrane life of 7 to 10 years, after which membranes must be replaced. Bacterial growth and hot spots or voltage short circuits inside the stack will damage membranes, requiring stack disassembly and the replacement of membranes and spacers, which is tedious and time consuming, particularly if not all membranes in a stack are to be replaced. In order to extend membrane life, improve product quality, and reduce power consumption, cleanings-in-place can be effective (Purification & Program, 2003).

2.3.2.2 Spacers

Spacers typically are made of polypropylene or low density polyethylene and are positioned in the spaces between the membranes that represent the flow paths of the dilute and concentrated streams. These spacers are called dilute and concentrate spacers, respectively. The spacers match the ion-exchange membrane area and are generally about 1 mm thick.

The spacers not only separate the membranes, they both direct the flow of water uniformly across the exposed face of the membrane and create independent flow-paths through the stack (Balster, Stamatialis, & Wessling, 2009). The identical spacers rotate 180° between membranes; as a consequence, all the demineralized streams are combined with each other and all the concentrated streams are combined with each other, allowing the separation of the product and concentrate streams as seen in Figure. 2.7 (Strathmann, 2010). Various spacer designs such as the sheet flow or tortuous path flow are used in practical applications, as illustrated in Figure 2.7 (Scott, 1996).

Generally, the main difference in spacer models is the number of flow paths, which determines water velocity across the membrane stack and the contact time of the source water with the membrane.

The “sheet flow spacer” consists of an open frame with a plastic screen separating the membranes. In these spacers, the compartments are vertically arranged and the process path is relatively short. These compartments give better support for thinner membranes. The second type of spacers, “tortuous flow spacers” are horizontally arranged and folded back upon themselves. These spacers have a long, narrow channel for the flow path, providing much longer flow path. The feed flow velocity in the stack is relatively high, which provides better control over concentration polarization and allows higher limiting current densities. Despite this, the pressure loss in the feed flow channels is still quite high (*Process Technologies for Water Treatment*, 2013; Scott, 1996).

The spacer geometry dictates the proper usage of the available membrane area and the mobility of the feed water along the membrane surfaces. In general, spacers increase the turbulence and promote the mixing of the water, the use of the membrane area, and the transfer of ions. Turbulence resulting from spacers also breaks up particles or slime on the membrane surface, attracts ions to the membrane surface, and increases the availability of ions near the membrane surface, which in turn decreases concentration polarization (Chiapello & Bernard, 1993).

Velocity is an important design parameter for spacer choice because both the amount of desalting that occurs across the membranes and the amount of turbulence are a function of the solution velocity through the spacer, and higher velocity results in higher turbulence (A. A. Von Gottberg & Manager, 2010).

On the first impression, it seems that we should increase the velocity as much as we can. However, the operating velocity in an EDR stack is limited by the pressure drop along the spacer, which also increases with increasing turbulence. Additionally, to prevent external leakage, the maximum inlet pressure of the stack is limited. In conclusion, the optimal spacer provides a balance between promoting turbulence and minimizing the pressure drop (Valero et al.,

2010).

2.4 Mass Transport in EDR Stack

In membrane processes, the transport rate is determined by the driving force or forces acting on the individual components and their mobility and concentration in the membrane. The driving force for the transport of a component A from a phase (') to a phase (") through a membrane can be expressed as a gradient in its concentration, its electrical potential, and its pressure (Figure 2.8) (Strathmann, 2011).

As indicated in Figure 2.8, depending on the driving force and the transport mechanism in the membrane, three different forms of transport are distinguished:

2.4.1 Diffusion

A mass transport process is referred to as diffusion and described by Fick's laws when the individual components move independently of each other under the driving force of a chemical potential gradient. The permeation rate in a diffusion process depends on its diffusion coefficient, which is determined by friction between the diffusing component and other components in a mixture (Philibert, 2005).

2.4.2 Migration

A mass transport is referred to as migration and described by Ohm's law when charged components move through a matrix under the driving force of an electrical potential (ϕ) difference. The migration rate depends on the electrical potential gradient and the mobility of the components in the matrix, which itself is directly related to its diffusion coefficient and is determined by the friction between the migrating component and other components in a mixture (Verbrugge & Hill, 1990).

2.4.3 Convection

A mass transport process is referred to as convection when bulk flow occurs under the driving force of a hydrostatic pressure difference. The flow velocity depends on the hydrostatic pressure difference and hydrodynamic permeability coefficient, determined by the friction between the solution and the matrix.

In membrane processes, all three forms of mass transport can contribute to the overall flux. However, one transport form generally is dominant while the others contribute to a lesser extent to the overall mass flux. In microfiltration and ultrafiltration, the convection of a bulk solution is the dominant form of transport while diffusion is generally insignificant. In reverse osmosis, mass transport through the membrane occurs mainly by the diffusion of individual molecules through a more-or-less homogeneous membrane matrix, but convection can

become significant with high flux membranes. In EDR cell pairs, migration of ions in an electric field is the dominant form of transport (Strathmann, Giorno, & Drioli, 2000).

The transport of a particular ion (i), within an EDR system can be approximated by the Nernst-Planck Equation (Equation 2.4) which is the summation of the diffusion, electromigration, and convection fluxes.

$$J_i = -z_i u_i C_i F \nabla \varphi - D_i \nabla C_i + C_i v \quad \text{Eq. 2.4}$$

where J is the molar flux of species i , z is the sign and magnitude of the charge of the ion, u_i is mobility, C is the molar concentration of species i , F is the Faraday constant (which is a product of Avogadro's number, N_A , and the elementary charge, q_e), $\nabla \varphi$ is the electric potential difference, D is the ionic diffusivity, and v is the fluid velocity (Moon, Sandí, Stevens, & Kizilel, 2004).

Then, the molar flux of species i is described as in Equation 2.5, where i_i is the current density species i .

$$J_i = \frac{i_i}{z_i F} \quad \text{Eq. 2.5}$$

The total electrical current density (i_t) passing through the ED stack is the summation of the fluxes of all charged species in solution (Moon et al., 2004), as shown in Equation 2.6.

$$i_t = \sum_i i_i = F \sum_i z_i J_i \quad \text{Eq. 2.6}$$

The fraction of the current that a particular ion carries is called the transport number (t_i), defined in Equation 2.7:

$$t_i = \frac{i_i}{i_{\text{tot}}} = \frac{z_i J_i}{\sum_i z_i J_i} \quad \text{Eq. 2.7}$$

where:

$$\sum_i t_i = 1 \quad \text{Eq. 2.8}$$

In an ideal system, the rate of separation of ions is proportional to the electrical current density. However, in reality, the number of salt ions separated is less than the electrical equivalent of the current density (Kim, Walker, & Lawler, 2012; Sadrzadeh, Kaviani, & Mohammadi, 2007; Shaposhnik, 1997). Inefficiencies with the ion-exchange membranes, the loss of current through manifolds, and concentration polarization across the ion-exchange membranes can significantly diminish the current efficiency, and each of these sources of inefficiency will be discussed in the following sections (Bard, Faulkner, Swain, & Robey, 1944; Mandersloot & Hicks, 1966; Stuttgart, 2002).

2.5 Electrodialysis Reversal Challenges

The EDR process faces several challenges, especially concentration polarization, scaling and fouling, and limiting current density. These obstacles are discussed in Sections 2.5.1 through 2.5.3.

2.5.1 Concentration Polarization

Let us consider a basic system consisting of an ion-exchange membrane separating two aqueous solutions of 1:1 electrolyte at bulk concentrations of C_0 and C_1 with the same temperature and pressure, as illustrated in Figure 2.9 (Valerdi-Pérez, López-Rodríguez, & Ibáñez-Mengual, 2001).

When an electric potential is applied, there are two types of currents in the system: one, in the membrane, is comprised solely by counter-ions, and the other one is in the solution because of the co-ions and counter-ions in the solution and in contact with the membrane.

Assuming that the transfer number of chloride ions in solution is t_i while it is \bar{t}_i in the membrane and the solution volumes are so large that bulk concentrations are not affected by the passage of current, the subsequent results follow. At current density i (mA/cm²), an electrical flow of chloride ions will take place within the membrane equal to $\bar{t}_i i/F$ (meq/s.cm²), and within the solution, equal to $t_i i/F$ (meq/s.cm²), where F is Faraday's constant (96.5 A.s/meq.). The difference between t_i and \bar{t}_i leads to an unbalanced electrical transfer, and a net shortage of $(\bar{t}_i - t_i) i/F$ (meq/s.cm²) occurs. Therefore, the solution concentration of sodium chloride drops in the region, and nonelectrical diffusion of sodium chloride salt takes place into the immediate vicinity.

At steady state, interfacial concentration is determined by equating the diffusion into the region with net electrical transfer out of the region:

$$\frac{D_s (C_0 - C_1)}{\delta} = \frac{(\bar{t}_i - t_i) i}{F} \quad \text{Eq. 2.9}$$

where D_s is the diffusion coefficient of the salt (cm²/s), C_0 is the bulk solution concentration (meq./cm³), C_1 is the solution concentration at the membrane surface (meq./cm³), δ is the solution film thickness (cm) across which the concentration gradient exists, and F is Faraday's constant.

The passage of current causes a reduction in the electrolyte concentration on one side of the membrane, a phenomenon known as depletion layer (C_1) that arises due to differences in the mobility of the counterions in the two phases of membrane and solution. Alternately, the concentration of the electrolytes increases on the opposite side of the membrane (C_2), a phenomenon that is called the concentration layer. Consequently, a concentration gradient is formed in the

boundary layers on both sides of the membrane, which results in polarization layers. In these layers, the electric potential gradient drives cations and anions in opposite directions, whereas the concentration gradient drives both types of ions in the same direction – an effect known as diffusion (Tanaka, 1991; Ślezak et al., 2005).

The magnitude of the concentration gradient adjacent to a CEM would be different than the concentration gradient adjacent to an AEM due to the differences between the diffusivities of cations and anions (Walker, 2010).

Concentration polarization in EDR cells leads to an accumulation of ions on the membrane surface facing the concentrate cell and a depletion of ions at the membrane surface in the diluate compartment. Both of these occurrences are problematic, as shown subsequently.

2.5.2 Scaling and Fouling: A Concentrate Problem

Brackish groundwater often has relatively high concentrations of calcium, magnesium, carbonate, and sulfate, leading to the supersaturation of one or more salts within the concentrate stream. The precipitation of salts is most likely to occur in the concentrate diffusion boundary layer where concentration polarization causes an accumulation of ions on the membrane surface facing the concentrate cell, which can decrease the mass-transfer efficiency, increase electrical resistance, and damage the membrane.

The supersaturation of a solution with respect to a particular compound can be described by the Langelier Saturation Index (LSI). For a water sample containing Calcium Carbonate, LSI is dependent on pH, alkalinity, calcium concentration, total dissolved solids, and water temperature, and is calculated as the difference between the actual pH (pH_{act}) of the solution and the pH under which precipitation of the given ion concentrations would occur (pH_{eq}).

Thus, a negative LSI means the water is under saturated with calcium carbonate and will tend to dissolve solid calcium carbonate, an LSI close to zero indicates water is not quite saturated with calcium carbonate and would not be strongly scale forming, and a positive LSI shows that the water is over saturated with calcium carbonate and will tend to deposit calcium carbonate, forming scales.

2.5.3 Limiting Current Density: A Dilute Problem

As the concentration gradient phenomenon explained in Section 2.5.1 continues, the interfacial concentration C_1 falls to zero eventually (as indicated in Figure 2.9) and the depletion layer resistance tends to infinity. After this point, the current density value reaches a limiting value called limiting current density (LCD) and therefore,

$$i_{lim} = \frac{D_s F C_o}{\Delta t_i \delta} \quad \text{Eq. 2.10}$$

where $\Delta t_i = \bar{t}_i - t_i$, or the difference between the counter-ion transport number

in the membrane and the solution, $t_i = J_i F / i$ and $\bar{t}_i = \bar{J}_i F / i$ (univalent ions); i is the current density; J_i and \bar{J}_i are flux associated with ions in the bulk solution and membrane, respectively; D_s is the electrolyte diffusion coefficient; and δ is the boundary layer's thickness (Valerdi-Pérez et al., 2001).

In an ion-exchange membrane surface, if the bulk dilute concentration is raised or if the diffusion boundary layer thickness is dropped, then the limitation on electrical current is increased, allowing the maximum rate of desalination (Walker, 2010).

Concentration polarization has been studied widely, and current-voltage curves have been developed to reflect the relationship between the current through the membrane and the corresponding voltage drop over that membrane and its adjacent boundary layers. According to the classical theory of concentration polarization for ion-exchange membranes, the steady-state current-voltage response shows three sections as illustrated in Figure 2.10 (Długołęcki, Anet, Metz, Nijmeijer, & Wessling, 2010).

At low voltage values, the resistance of the stack is constant - i.e., the current intensity and imposed voltage are linearly dependent according to Ohm's law. Therefore, the first region is called the Ohmic region. In the second region, the current varies very slowly with voltage, denoting an almost unconstrained current applied voltage ("plateau") that corresponds to the limiting current (Helfferich, 1962). When the LCD is reached, the cell resistance increases drastically and an increase in the applied voltage does not lead to a significant increase in the current density until, at a certain applied voltage, the current density increases again with the applied voltage (Rubinstein & Shtilman, 1979). In the post-limiting current region, the current intensity once again increases with the applied voltage. In this section, the current density is referred to as overlimiting current density and is caused by the transport of H⁺ and OH⁻ ions which are generated at the membrane/solution interface by water dissociation. The water dissociation affects the current utilization and can lead to a drastic pH-value decrease in the diluate and an equally drastic pH increase in the concentrate solution, which may cause the precipitation of carbonates and sulfates of calcium and magnesium (Ibanez, Stamatialis, & Wessling, 2004).

In an EDR stack, a commonly used technique to decide maximum operating current that can be used without coupled effects with concentration polarization of the membranes, the relationship between the applied potential and the current intensities have to be achieved.

Traditionally, LCD is the point where the current (I) -potential (V) and cell resistance (R) - 1/current curves deflect from linearity, as shown in parts a) and b), respectively, of Figure 2.11 (H. J. Lee, Strathmann, & Moon, 2006). However, this does not always yield unambiguous estimates of the limiting condition when applied to a practical electro dialysis apparatus (Valerdi-perez, 2001).

Considering that the aim of ED is to obtain high desalting efficiency, the optimal operating current may be obtained by combining the curves for V/I-I and η -I (where η is removal ratio) as shown in Figure 2.12 (Meng et al., 2005). The feasibility of the combined method was assessed, and this method proved to be more efficient and simple compared to the traditional V-I curve.

Since the basic function of EDR is to obtain a high desalting efficiency and since there is a maximum desalting ratio with current change, the maximum point of the removal ratio under the optimal operating current can be considered a limiting factor (Meng et al., 2005).

It is evident from studies that limiting current densities depend on the concentration of the solution (J.-H. Choi, Lee, & Moon, 2001; Długołęcki et al., 2010), the flowrate (E. Choi, Choi, & Moon, 2002; Tsiakis & Papageorgiou, 2005; VALERDI-PÉREZ et al., 2000), and temperature (Hwang & Lai, 2007). Therefore, the limiting current can be determined empirically. In the case of the EDR pilot plant located at the Brackish Groundwater National Desalination Research Facility (BGNDRF) in Alamogordo, NM, R. V. Chintakindi (2010) studied the operating parameters and indicated that the limiting current is in a relationship with the aforementioned factors in the manner shown by Equation 2.11:

$$I_{lim} \propto C_f U^{0.8} T^{0.67} \quad \text{Eq. 2.11}$$

The results prove that the resistance of ion exchange membranes strongly depends on the solution concentration. We observe a very strong increase in membrane resistance with decreasing concentration, leading to an increase in the LCD. The LCD is also influenced by the liquid flow rate, because higher solution flow rates generate turbulence in the bulk of the streams and reduce the diffusion boundary layer thickness at the membrane surface. This results directly in an increased LCD. Furthermore, resistance in general strongly depends on the temperature, and the diffusion boundary layer resistance decreases with increasing temperature due to the increase in ion mobility with increasing temperature. In result, temperature increases could increase the LCD.

In this study, the LCD has been experimentally measured and the operating current ranges have been determined considering the limitations in order to avoid challenges associated with concentration polarization.

2.6 EDR Process Performance Metrics

Several metrics may be used to evaluate the performance of the EDR process. These metrics – removal ratio, recovery ratio, specific energy consumption (SEC), and current efficiency – are discussed in Sections 2.6.1 to 2.6.4 of the present work.

2.6.1 Chemical Efficiency: Removal Ratio

The ability of a desalination process to remove salt from a feed stream and produce a product stream of lower salinity measures the technical feasibility of that process. The degree to which that technical goal is accomplished by a desalination process is quantified by the removal ratio (R), which represents the “chemical efficiency” of the system. The removal ratio is defined by Equation 2.12:

$$R = 1 - \frac{C_p}{C_f} \quad \text{Eq. 2.12}$$

where C_p is the salt concentration of the dilute effluent (typically in the units of mass of salt per volume of solution), and C_f is the salt concentration of the feed solution (Tanaka, 2015).

The degree of desalination that can be achieved in passing the feed solution through a stack is a function of the solution concentration, the applied current density, and the residence time of the solution in the stack. If the degree of desalination or concentration that can be achieved in a single pass through the stack is insufficient, several stacks are operated in series (Strathmann, 2010). A typical removal ratio for a single-stage EDR system is between 50% and 99%, depending on the source water quality and product water specifications (American Water Works Association, 1995).

2.6.2 Hydraulic Efficiency: Recovery Ratio

Another aspect of the EDR desalination process is its “recovery ratio” which is considered to be a form of hydraulic efficiency defined by Equation 2.13:

$$r = \frac{Q_p}{Q_f} \quad \text{Eq. 2.13}$$

where Q_p is the volumetric flow rate of the product and Q_f is the volumetric flow rate of the feed (Valero & Arbós, 2010). In a single stage of an EDR stack, where the geometries of the diluate and concentrate cells as well as the linear flow velocities are identical, the recovery rate is 50%. This operation results in a similar pressure in the concentrate and diluate cells. However, in EDR processes, the system often is intentionally operated so that the concentrate cells have a slightly lower pressure than the diluate cells. This prevents trans-membrane pressure and contamination of the diluate stream from leaks.

If the amount of product volume that can be achieved in a single path through the stack is insufficient, part of the diluate or concentrate can be fed back to the feed solution. With such an approach, EDR systems can achieve water recovery rates of up to 95%, which reduces feed water costs and waste water discharge (Strathmann, 2010); however, high-recovery EDR desalination is limited by the scaling tendency of salts in the concentrate stream.

2.6.3 Electrical Efficiency: Specific Energy Consumption (SEC)

Another evaluation metric for the desalination process efficiency is SEC, which quantifies how much energy is consumed by the desalination process to produce a given volume of product water. SEC can be calculated by Equation 2.14:

$$SEC = \frac{E_t}{V_p} \quad \text{Eq. 2.14}$$

where SEC is specific energy consumption (kWh/m³), E_t is the total energy consumption (kWh), and V_p is the product volume (m³) (Stuttgart, 2002).

For full-scale membrane desalination systems with feedwaters ranging from brackish water to sea water, the SEC typically ranges from 1-10 kWh/m³, depending on source water TDS, process technology, recovery ratio, and removal ratio. To be compared, the equivalent SEC of a full-scale thermal process such as MED and MSF typically ranges from 20-40 kWh/m³ (Walker, 2010).

The total energy E_t required in an EDR process is the summation of two terms, as shown in Equation 2.15:

$$E_t = E_{des} + E_p \quad \text{Eq. 2.15}$$

where E_{des} is the electrical energy needed to transfer the ionic components from one solution through the membranes into another solution, and E_p is the energy required to pump the solutions through the EDR unit.

The energy consumption due to electrode reactions and the energy required for operating the process control devices can generally be neglected in large industrial-size plants, since the electrical and pumping typically are the dominant energy consumers in the process (Strathmann, 2010).

Generally, the SEC for EDR is a function of cell geometry, feed water linear flow and electro-chemical characteristics, membrane properties, concentration potential, total area resistance of the membranes, and electrical resistance of the solutions (Myint, Ghassemi, & Nirmalakhandan, 2011).

2.6.3.1 Direct Energy Requirements

The actual desalination process in EDR occurs when the required energy is given by the current passing through the stack multiplied with the total voltage drop encountered between the electrodes (E. Choi et al., 2002).

$$E_{des} = I_{st}U_{st}t \quad \text{Eq. 2.16}$$

Furthermore:

$$U_{st} = I_{st}R_{st} \quad \text{Eq. 2.17}$$

where E_{des} is the energy consumed in a stack for the transfer of ions from a feed to the concentrate solution, I_{st} is the current passing through the stack, U_{st} is the voltage applied between the electrodes, and R_{st} is the stack resistance, defined as:

$$R_{st} = R_{AEM} + R_{CEM} + R_c + R_d \quad \text{Eq. 2.18}$$

Four resistances can be taken into account in a single cell: R_{CEM} , the resistance of cation exchange membranes; R_{AEM} , the resistance of anion exchange

membranes; R_d , the resistance of dilute compartments; and R_c , the resistance of concentrate compartments (Myint et al., 2011). The electrical resistance of a solution can be expressed as a function of concentration as shown in Equation 2.19 (Sadrzadeh & Mohammadi, 2009).

$$R = \frac{h}{\kappa A} \quad \text{Eq. 2.19}$$

Here, κ is the electrical conductivity (S/m), h is the thickness of the dilute or concentrate solution compartment (m), and A is the effective area of the ion exchange membrane (m²). The electrical conductivity is an aggregate of the ionic composition as shown in Equation 2.20:

$$\kappa = \sum_i C_i \lambda_i |z_i| \quad \text{Eq. 2.20}$$

For species i , λ_i is the molar conductivity (Sm²/mol), z_i is the valence, and C_i is the concentration (mol/m³) (Anderko & Lencka, 1997).

It is evident that the required desalination energy is a function of the stack resistance, the amount of the produced water, and the feed and dilute concentration.

2.6.3.2 Pumping Energy Requirement

An EDR unit requires pumps to circulate the diluate, the concentrate, and the electrode rinse solution through the stack. The energy required for pumping these solutions is determined by the volumes of the solutions to be pumped and the pressure drop, as expressed by Equation 2.21:

$$E_p = k_{eff}(Q_d \Delta p_d + Q_c \Delta p_c + Q_e \Delta p_e) \quad \text{Eq. 2.21}$$

Here, E_p is the total energy for pumping the diluate, the concentrate, and the electrode rinse solution through the stack per unit diluate water, k_{eff} is an efficiency term for the pumps, Q_d , Q_c and Q_e are the volume flow rates of the diluate, the concentrate, and the electrode rinse solution through the stack, and Δp_d , Δp_c , and Δp_e are the pressure difference between the inlet and outlet of dilute, concentrate, and electrode rinse solution, respectively (E. Choi et al., 2002; MCGovern, Zubair, & V, 2014; Turek & Dydo, 2001; Zhou & Tol, 2005).

Since the volume of the electrode rinse solution is very small compared to the volumes of the diluate and concentrate, the energy consumption due to the pressure loss in the electrode rinse solution is negligible in most practical applications.

The pressure losses in the various cells are determined by the solution flow velocities and the cell design. The energy requirements for circulating the solution through the system may dominate over the direct energy consumption for solutions with rather low salt concentrations (Strathmann, 2010).

2.6.4 Electrical Efficiency: Current Efficiency (CE)

CE is an important parameter that determines the optimum range of applicability of ED and is a measure of how effectively ions are transported across the ion exchange membranes for a given applied current. CE is calculated using the Equation 2.22:

$$CE(\%) = \frac{Q_p F (C_f - C_p)}{N I_{st}} * 100 \quad \text{Eq. 2.22}$$

Here, Q_p is the volume flow (m^3/s); F is Faraday constant, equal to 96.5 A s /eq ; C_f is feed concentration (mol/m^3 or eq/m^3), C_p is product concentration (mol/m^3 or eq/m^3), I_{st} is the current passing through the stack (A), and N is the number of cell pairs in the stack (Sadrzadeh & Mohammadi, 2009).

In any practical EDR system, it is generally found that the amount of current required to produce a given amount of desalting exceeds the requirement that can be calculated on the basis of current flow through ideal membranes. Several undesirable phenomena occurring in the EDR cell pairs may contribute to low current efficiency in an EDR stack:

- Back diffusion phenomena due to non-perfect permselectivity of membranes (Turek, 2002);
- Shunt or stray current running in the non-active cell areas (Veerman, Post, Saakes, Metz, & Harmsen, 2008);
- Electrical leakage through the manifolds due to short circuit between electrodes (Mandersloot & Hicks, 1966); and
- Osmotic and electro-osmotic water transport through the membranes (Shaposhnik, 1997).

Literature review on the investigation of CE values for different ED and EDR processes indicates that CE values were most frequently observed in the range of 60-80 (Demircio, Kabay, & Gizli, 2001; Demircioglu, Kabay, Kurucaovali, & Ersoz, 2002; A. A. Von Gottberg & Manager, 2010; Ions, Rod, & Is, n.d.; H.-J. Lee et al., 2009; Meng et al., 2005; Rosenberg & Tirrell, 1957; Sadrzadeh et al., 2007; Sadrzadeh & Mohammadi, 2009; T Sata, 1986; Shaposhnik & Grigorchuk, 2010; Shaposhnik, 1997; Turek & Dydo, 2001; Turek, 2002; Veerman et al., 2008). However, values both higher and lower than this have been reported. For instance, Turek & Dydo (2001) reported a current efficiency of 90% for the removal of sodium chloride through the use of a laboratory scale ED system; as an example of low reported current efficiencies, Sadrzadeh & Mohammadi (2009) identified current efficiencies from 0-50% for laboratory scale seawater desalination using an ED cell under different operating parameters.

2.7 Electrodialysis Reversal Optimization

There are several approaches for optimizing the performance of EDR

systems, and these approaches – two hydraulic, one electrical, and one chemical – are discussed in Sections 2.7.1 through 2.7.4.

2.7.1 Hydraulic: Improving the Rate of Mass Transfer

With respect to optimization, a key parameter that must be considered in EDR performance is the velocity of the solution flowing through a concentrate or diluate cell. This parameter is called inter-membrane velocity.

Dimensionless parameters associated with the transport rates are the Reynolds and Schmidt numbers. The Reynolds number (Re) characterizes the ratio of inertial and viscous forces of the fluid dynamics, quantifying the relative importance of these two types of forces for given flow conditions. For flow in a tube or channel, Re is related to the flow velocity in the boundary layer at the membrane surface, as shown in Equation 2.23:

$$Re = \frac{\rho h u}{\mu} \quad \text{Eq. 2.23}$$

where ρ is the solution mass-density (kg/m), h is the channel height (spacer thickness) (m), u is the superficial flow velocity (m/s), and μ is the absolute (dynamic) viscosity of the solution (kg/m.s). Assuming that the solution density and viscosity and the channel height are approximately constant, the Reynolds number is essentially a scalar of velocity for a particular system.

The dimensionless parameter that represents the ratio of viscous and diffusive forces within the solution is the Schmidt number (Sc), defined as in Equation 2.24:

$$Sc = \frac{\mu}{\rho D} \quad \text{Eq. 2.24}$$

where μ is the absolute (dynamic) viscosity of the solution (kg/m.s), ρ is the solution mass-density (kg/m³), and D is the ion diffusivity (m²/s), which depends on solution concentration.

By relating the Schmidt and Reynolds numbers, the non-dimensional mass-transfer coefficient can be created, known as the Sherwood number (Sh). This is defined in Equation 2.25.

$$Sh = \alpha_0 Re^{\alpha_1} Sc^{\alpha_2} \quad \text{Eq. 2.25}$$

where α_0 , α_1 , and α_2 are positive fitting parameters for which numerous attempts have been made to theoretically approximate and empirically validate these parameters; the present study is not concerned with the specific determination of the mass transfer parameters.

Equation 2.25 indicates the relationship of the hydraulic and electrochemical behavior and demonstrates that the limiting rate of mass-transport in an EDR system increases with increases in the velocity. Consequently, as increasing the inter-membrane velocity in a diluate cell promotes mixing and turbulence, which decreases the diffusion boundary layer thickness in the dilute

cell and thereby improves the rate-limiting mass-transport through the diluate diffusion boundary layer, decreases in the electrical resistance of the stack thus improve the electrical efficiency and reduce salt scaling at the membrane surfaces.

Furthermore, an increase in mixing in the concentrate cell can prevent scale formation in the stagnant regions that first show accumulation of precipitates (Berger and Lurie, 1962). However, decreasing the inter-membrane velocity decreases the cost of pumping energy required. In result, there is an optimum value for the flow velocity through the EDR cell pairs, and it needs to be considered while defining the operating solution flowrate values.

2.7.2 Hydraulic: Improving Recovery Ratio

Another important strategy for improving the efficiency of EDR is to increase the recovery ratio. In a single stage EDR system, this improvement can be accomplished by recycling part of the diluate or concentrate to the feed solution. As illustrated in Figure 2.2, the general material balances based on the flows and the species material balance for the total dissolved solids (TDS) are shown in Equation 2.26 and 2.27:

$$Q_f = Q_p + Q_c \quad \text{Eq. 2.26}$$

$$Q_f C_f = Q_p C_p + Q_c C_c \quad \text{Eq. 2.27}$$

Consequently, the waste concentration factor (CF) can be calculated (for the entire system, independently of internal concentrate recycle) by material balance as in Equation 2.28:

$$CF = \frac{C_c}{C_f} = 1 + \frac{rR}{1-r} \quad \text{Eq. 2.28}$$

where C_c is the concentrate waste concentration, C_f is the feed concentration, r is the removal ratio, and R is the recovery ratio.

As the recovery ratio increase, the concentration of salt in the concentrate waste stream increases approaching zero liquid discharge (ZLD), but the challenge in this type of operation is that, as the recovery ratio increases, precipitation in the concentrate stream is more likely to occur because of the elevated ionic concentrations causing problems associated with scaling.

2.7.3 Electrical: Decreasing the Electrical Resistance of the Stack

The resistance of the stack is the summation of the resistances all cell pairs. As illustrated in Figure 2.13, each cell pair of the ED stack can be divided into eight district regions as follows: (1) the CEM, (2) the concentrate diffusion boundary layer adjacent to the CEM, (3) the concentrate bulk, (4) the concentrate diffusion boundary layer adjacent to the AEM, (5) the AEM, (6) the diluate boundary layer adjacent to the AEM, (7) the diluate bulk, and (8) the diluate boundary layer adjacent to the other CEM.

The electrical resistance of an ion-exchange membrane is determined by its capacity and the mobility of ion species in the membrane matrix (Toshikatsu Sata, 2004; Strathmann et al., 2006), and typical values of real resistances in many commercial AEMs and CEMs are in the range of 1-10 $\Omega\text{-cm}^2$.

The solution phase resistances are functions of chemical composition, total conductivity, and the dimensions of each solution, as explained in Equations 2.19 and 2.20.

Developing ion exchange membranes with lower electrical resistance can be accomplished by decreasing width and increasing conductivity. Also, as the resistance of the bulk region decreases with increasing salinity, the electrical resistance of the dilute cell can be reduced by sending part of the concentrate to the feed stream. In addition, the electrical resistance of the dilute diffusion boundary layer can be reduced by reducing its thickness through enhanced mixing.

2.7.4 Chemical: Preventing Scaling and Fouling

In order to implement effective scale-control measures in EDR desalination plants, it is necessary to know the permissible water recovery level at which the plant may be operated under given process conditions without the risk of scale precipitation. Process conditions that influence the permissible water recovery level are numerous and include the supersaturation level of the concentrate stream, the residence time of the concentrated solution, the nature of the antiscalant used, and the dose of the antiscalant used (Hasson, Drak, & Semiat, 2009). Antiscalants are compounds that are added to the concentrate stream of the EDR system in order to alter the precipitation kinetics of low-solubility salts by disrupting one or more aspects of the crystallization stages. Antiscalants inhibit crystal growth through increasing the ion concentration threshold required for clustering, distorting normal crystal growth and produce an irregular crystal structure with poor scale forming ability, or using dispersants which place a surface charge on the crystals. Consequently, the crystals repel one other and are dispersed into the water bulk.

Antiscalants are able to work at relatively low concentrations (< 100 mg/L), where the ion concentrations are stoichiometrically much higher. In many water treatment systems, Phosphonate antiscalants are widely and effectively used to inhibit scale, corrosion and gypsum precipitation (Akyol, Öner, Barouda, & Demadis, 2009; R. P. Allison, 1995).

In another approach to preventing fouling and scaling, the EDR process employs periodic polarity reversal, reducing or eliminating the need for adding acid to the feed water (Fubao, 1985).

2.8 Summary

The fundamentals of the hydraulic, electrical, and chemical phenomena employed in EDR systems are integrally connected to the overall performance, which can be evaluated through different aspects including removal ratio, recovery ratio, current efficiency, specific power consumption and total cost.

As explained in Section 2.6, most of the parameters of the EDR process are inherently overlapping and improving any one aspect could change other aspects in either beneficial or harmful ways.

Within EDR systems, the rate of separation (removal ratio) is proportional to the electrical current density. Since current density is limited by a lack of ions in the diluate diffusion boundary layer and a supersaturation of ions in the concentrate diffusion boundary layer, the diffusion boundary layer thickness must be sufficiently thin and the applied voltage sufficiently low to avoid both cases. The thickness of diffusion boundary layer is controlled by the hydraulic intermembrane velocity. The scaling tendency of the salts existing in the concentrate stream not only reduces the removal ratio, but also limits high-recovery inland desalination.

The electrical behavior of an EDR system is dominated by the resistance of the stack described in Section 2.6.3, and different stack design parameters and operating parameters can change the total resistance in the stack.

The hydraulic efficiency of an EDR system can be improved by increasing the recovery ratio or velocity of intermembrane streams, which are limited by scale formation and pumping energy, respectively.

Therefore, although experimental and full-scale EDR treatments of brackish waters have been proven technically and economically feasible (American Water Works Association, 1995; Reahl, 2005; Strathmann, 2004; Tanaka, 2007; Xu et al., 2008), the EDR process still needs to be optimized for removal ratio, recovery ratio, current efficiency, and power consumption in order to improve its efficiency for widespread deployment. Hence, thorough and systematic experimentation and documentation of EDR performance is required for understanding the optimally beneficial use of EDR to treat saline water.

Chapter 3 - Materials and Methods

The objective of the experimental work was to quantitatively observe the

hydraulic, electrical, and chemical behavior of EDR treatment of brackish groundwater. The effects of process variables on the performance of the EDR were evaluated through precise EDR experimentation. The experimental plan and descriptions of the experimental design, experimental set-up and location, experimental procedure, characterization and control systems, and data analysis are presented here.

3.1 Experimental Design

Regarding the research goal and objectives presented in Chapter 1 and the fundamental concepts outlined in Chapter 2, the experiments performed sketch the EDR performance sensitivities and limitations with respect to the following variables:

1. Chemical – feed water salinity,
2. Electrical – applied voltage, and
3. Hydraulic – feed flow rate.

Among the different operating conditions that impact the EDR process, four parameters were selected; product flow rate, conductivity, applied voltage, and electrode type. These parameters can be briefly described as:

Flow rate: The volumetric flow rate is the volume of fluid which passes through a given surface per unit time. Although the SI unit for flow rate is cubic meters per second (m^3/s), in the EDR pilot scale plant used for our experimentation, flow rate is measured based on gallons per minute (GPM). The flow rate for each of the inlet and outlet streams, dilute, feed, and concentrate streams, are measured and presented. In our experimental set-up, flow rates are measured by flow meters and can be monitored and read on both the flow meters and on a human-machine interface (HMI) screen on the machine.

Conductivity: Conductivity is a measure of the ability of water to pass an electrical current. How well a solution conducts electricity depends on a number of factors including the concentration of ions, mobility of ions, valence of ions, and the temperature of the solution. The conductivity is linked to the level of total dissolved solids (TDS) and is measured in micro-Siemens per centimeter ($\mu\text{S}/\text{cm}$).

Voltage: The electrical voltage and current applied to the electrodialyzer were controlled and monitored by a switching mode, regulated, and programmable power supply. Voltage increments are modified and increased for every reading of the experiment and the accuracy of the applied voltage and current was verified by a handheld digital multi-meter. The voltage applied to an electrodialyzer is indicated by the Equation 3.1:

$$V = N V_{\text{cell}} + V_p \quad \text{Eq. 3.1}$$

where N is the number of cell pairs, V_p the voltage in the electrode cell, and V_{cell} is cell voltage as follows, defined in Equation 3.2:

$$V_{\text{cell}} = I R + E_M \quad \text{Eq. 3.2}$$

where I is current, R is the resistance of the cell pair (Eq. 2.18), and E_M is the membrane potential. (Purification & Program, 2003; Rosenberg & Tirrell, 1957). The manufacturer recommended a maximum voltage application of 1.5 V per cell-pair. Voltage increments are modified and increased for every reading of the experiment.

Electrode type: Electrodes are integral to the EDR process, providing the driving force for desalination. It has been hypothesized that the shape of the electrodes, as well as their location with respect to the solution manifolds, could impact both performance and stack life. Manifold shorting current, which is a parasitic current to the overall desalination process and reduces current efficiency, is a function of electrode design. Based on contemporary design practices and historical knowledge of the GE EDR stack configurations, three electrode designs are proposed and classified based on their geometry: full, recessed and tapered.

The motivation for this particular component of the study arises from GE's hypothesis that changing the electrode from full to recessed could result in reduced stray current, higher allowed stack voltage, and more demineralization. Therefore, there is a strong need to evaluate the three proposed electrode designs.

In each test, input parameters are defined for the experiment. The parameters can be changed between different tests, and subsequently change the outputs. All other operating conditions are recorded. To accomplish the experimental design, three different levels of feed conductivity (salinity) were considered: low, medium, and high. Also, three levels of feed flow rate are considered so that the input flow rate, in its low level, is set to the lowest possible value, and for the high level, it is set to the highest value possible recommended by the manufacturer of the EDR pilot plant used. Since the experimental setup is pilot scale, the single center point is used to check the validity of results from low and high levels. The center points are set to the numbers closely reflecting the average of the low and high levels. The applied voltage has five levels; the highest value is limited by the limiting current values and the lowest is limited by the separation rate.

For flow rate, the values for low, middle and high level were 7, 9 and 11 GPM, respectively. Levels of conductivity were varying among various feed waters depending on the well utilized in the experiment. The lowest value obtained was in Well1 (cold and warm), with low-level conductivity at 1700 $\mu\text{S}/\text{cm}$, and the highest one was with Well2, with high-level conductivity at 6100 $\mu\text{S}/\text{cm}$. Middle points, accordingly, were obtained by a combination of well1 and well2, giving approximately 3700 $\mu\text{S}/\text{cm}$ conductivity.

The experimental plan was designed to study the impact of each variable through performing a full factorial design with three replicates. The order of the all tests was randomized in order to raise the level of quality assurance. The resulting design of experiment is shown in Table 3.1.

3.2 Experimental Set-up

The EDR experimental setup is shown in Figure 3.1.

3.3 Experimental Location

The laboratory site is located at the Brackish Groundwater National Desalination Research Facility (BGNDRF), first opened on August 16, 2007, in Alamogordo, New Mexico. BGNDRF is a federal facility that operates under the U.S. Bureau of Reclamation, whose mission is “to promote sustainable advanced water treatment research and technology development for inland brackish groundwater sources”. The available feed waters consist of four brackish groundwater wells with TDS levels between 1,000 and 6,400 mg/L. The EDR pilot is located at inside bay #4, where all of the wells – well1, well2, and their combination – are used for performing this experiment. Well1 is a geothermal well with medium salinity (~1700 μS) and well2 is a cold well with very high salinity (~6200 μS).

3.3.1 Influent Pumping Equipment

At the BGNDRF, well water is first pumped from the aquifer to a large outside storage tank, and then to a smaller hydrostatic tank, which pressurizes the water to 350 kPa. When water enters the facility, a valve is used to reduce the feed pump inlet pressure to less than 70 kPa and make it ready to reach the EDR pilot system. The source water then flows into the pretreatment system comprised of a multi-media filter (MMF) and a 5 micron cartridge filter.

3.3.2 Multimedia Filter System

The discharge from the feed pump is ejected through an MMF prior to entering the cartridge filtration system. The MMF removes suspended solids from the source water as it sieves through the filter’s various media layers. The feed water is fed in the top of a container through a header which distributes the water evenly. The filter media start with fine sand on the top and then become gradually coarser sand in a number of layers followed by gravel on the bottom, in progressively larger sizes. The top sand physically removes particles from the water. The job of the subsequent layers is to support the finer layer above and provide efficient drainage.

The utilized MMF starts with anthracite (0.85-0.95 mm) on the top, then gradually coarser sand (0.85 mm), followed by garnet (0.42-0.6 mm) in gradually larger sizes to remove suspended particles from the source water, down to a 10-15 micron size (Fues, 2008).

3.3.3 Cartridge Filtration System

Downstream of the MMF, a cartridge filter (5 μm) is employed to protect the membranes from fine suspended particles in the feed water and prevent damage to either the pumps or the membranes. One of the suspended particles is iron (Fe^{2+}), which reacts strongly with hydrogen peroxide (H_2O_2) to produce hydroxyl radicals (OH^\cdot) that could destroy the function of antiscalants (D.F. Lawler, M. Cobb, 2010; Yang & Ma, 2004).

Although no signs of significant pressure loss were observed during the

experiments, the MMF was backwashed and the cartridge filter was replaced approximately every 3 months, between experiments.

After the pretreatment system, the source water enters the EDR hydraulics, which are detailed in Figure 2.1 and explained in Section 2.1.

3.3.4 EDR stack

The EDR Stack is comprised of 40 cell pairs stacked one on top of another. Each cell pair consists of a cation-exchange membrane and an anion-exchange membrane, separated by flow-path spacers, with another spacer on one side of the cell pair.

All the membranes are flexible sheets of cloth-reinforced resin. The properties of the membranes include long life-expectancy, resistance to fouling, impermeability to water under pressure, and operability in temperatures in excess of 46° C.

The spacers separating the membranes, as illustrated in Figure 3.2, provide a U-shaped tortuous path. The solution enters the compartment from the one above it, makes two bends, and finally goes out of the compartment to the one below it.

The spacers are manufactured by using two sheets of low-density polyethylene with die-cut flow channels, which are glued together to form an over-under flow-path that promotes mixing and turbulence (A. von Gottberg, 1998).

These spacers have an effective transfer area of 0.34 m² per membrane and been designed specifically to optimize the turbulence and pressure drop.

This basic cell pair is repeated until it is capped on both ends by the electrode compartments, which consist of a heavy flow-path spacer, a heavy cation-exchange membrane, and an electrode. Heavy cation exchange membranes have all the properties of regular cationic membranes but are twice as thick and can withstand a greater degree of hydraulic pressure.

The electrodes are constructed of platinized titanium and act as either a cathode or an anode, depending on the polarity reversal period. GE Water and Process Technologies has manufactured three kinds of electrode (presented in Figure 3.3):

1. Old Design (Full): Electrode area fully covers active membrane area, but also extends into manifold area;
2. Current Design (Recessed): Geometry mismatch between electrode and spacer; and
3. New Design (Tapered): No geometry mismatch between spacer and electrode.

The polarity reversal cycle for this experiment is 15 min. A steady state was achieved in 10 min, so the 15 min polarity setting was acceptable. Table 3.2 summarizes the specifications of the EDR stack components.

3.3.5 Concentrate Recycle and Waste Blowdown System

The concentrate enters the concentrate pump located in the hydraulic section, then part of it is recycled to the stack. The waste is sent to drain, while

some feed water is also added to the recycle as makeup to prevent the dissolved solids from precipitating on the membranes.

3.3.6 Chemical Dosing System

The chemical dosing system has the following chemicals added:

1. Hydrochloric Acid (15%): The hydrochloric acid is continuously added to the electrode in stream to neutralize the OH^- ions formed at the cathode, in order to prevent the precipitation of pH dependent salts, such as CaCO_3 and $\text{Mg}(\text{OH})_2$.
2. Antiscalant, HYPERSPERSE MDC 706: These chemicals are added to concentrate instream control various scaling and precipitation processes occurring in the equipment during operation.

3.4 Experimental procedure

This experiment studied how different operating and design parameters, including applied voltage, electrode type, product flowrate, and salinity of the feed solution, affect the efficiency of the EDR process. The efficiency of EDR systems can be evaluated by studying the salt removal ratio, produced current density, and amount of specific energy consumed. Table 3.3 shows the design of experiment, where finally the significance of each variable to change the EDR efficiency will be modeled empirically.

In each cycle of polarity reversal, the time is set for a 15 minute reversal. By trial and error, it has been determined that after 10 minutes of reversal, the system attains a steady state. Then, various measurements are taken accordingly. In this study, temperature and recovery ratio have been constant and their effects are not considered to be studied.

Unfortunately, because of the variation in the temperature of the source water coming from the wells, it is difficult to have a constant operating temperature. It was observed that the temperature changes during different seasons in the range of 8-37 °C and it also changes during the day up to 5 °C. Therefore, the experiments were conducted in a range of 20-25°C.

The highest recovery ratio in the EDR pilot-scale located at BGNDRF was determined to be 80%. The product and feed flow rates were monitored closely to ensure constant recovery throughout the long-term experiments; minor variation (< 0.2 GPM) could be observed. The effect of this slight variation was difficult to quantify, and must be considered a noise signal throughout the results.

The feed salinity has been classified as low, medium and high because the feed water quality varies slightly due to its deep-basin origin, leading to variations in conductivity and TDS levels.

Low salinity is the water sourced from well1, high salinity is the water coming from well2, and medium salinity is the combination of the well1 and well2. Table 3.4 shows the composition of each level of salinity considered in this experiments.

The general experimental procedure was as follows:

1. Voltage increments are modified and increased for every reading of the experiment so that they are in ascending order.
2. Measurements for voltage and current for the stage are taken using a voltmeter and an ammeter.
3. The HMI screen gives the measurement of flow rate, temperature, conductivity, and pH of feed, product, and concentrate, and energy consumed.
4. Samples of product, feed, and concentrate water were collected to be subjected to dissolved species analysis. The samples were withdrawn in the final 5 minutes of the polarity reversal period in order to allow enough time for the performance characteristics to stabilize.
5. Water samples were sent to the laboratory of Water and Energy at New Mexico State University and analyzed by ion chromatography.

Prior to the experiments, regarding the study of EDR efficiency factors, it is necessary to achieve the limiting current for each feed flow rate, applied voltage, feed salinity, and electrode type combination. To find the limiting current for each mentioned combination, all of the first three steps have been taken for a large range of voltage values, and then the limiting current was found based on current-voltage and removal ratio-current curves. Operating current values that exceed the limiting current will be problematic, as discussed in Section 2.4.

3.5 Characterization and Control systems

EDR system conditions – including hydraulic flow rates, the stack voltage and current, the pH, temperature, and electrical conductivity of each process stream – were continuously monitored to ensure stable operation. Table 3.5 represents a data collection log of the system conditions that were recorded daily during all the experiments.

The stage voltage (electrode-to-electrode) was measured using an oscilloscope, and the stage current was measured using a DC current probe. The temperature, conductivity, and pH were measured on site, using in-system probes and bench top laboratory devices. The temperature dependence relationship built into the measurement devices converts all the conductivities measured to conductivities at the temperature of 25 °C.

The monitoring the feed stream provides information on the consistency of the inlet water quality, which was expected to vary slightly due to its deep-basin origin. Measurements of the pH, conductivity, and temperature of outlet streams also provide important information on the system performance.

Conductivity and pH have to be monitored constantly because significant changes in pH can imply that concentration polarization is occurring, leading to water-splitting within the stack. Changes in conductivity can be an indication that concentration polarization or scaling is affecting the removal process. The

conductivity measurements of the outlet streams were particularly important during operation to achieve the separation rate of desalination.

3.6 Data Analysis

In the first step of data analysis for this study, the normality of the data was checked using the Shapiro-Wilk test. Additionally, the correlations between independent parameters were examined to eliminate the covariates from the regression relationship. Also, regression analysis between the response variables (removal ratio, specific energy consumption, and the current) and independent variables (feed conductivity, applied voltage, feed flow rate, and electrode type) was completed. Results of SAS programming were confirmed using Excel.

In order to find both the correlation between different parameters and a model to predict the characteristics of response variables based on operating conditions, multiple linear regression (MLR) was utilized. MLR is a statistical method to model the linear relationship between a dependent variable (predicted) and one or more independent variables (predictors).

In order to validate that the data have met the regression assumptions and to identify whether the regression model sufficiently represents the data, "regression diagnostics" methods such as R-squared and variance inflation factor (VIF) were used. During the data analysis of this study, the predictors were always defined in such a way that the regression model gives us the closest R-squared to 1. In addition, the predictors on the regression model could be intercorrelated. Intercorrelation can make it difficult or impossible to determine the relative importance of individual predictors from the estimated coefficients of the regression equation.

Multicollinearity, which is defined as extremely high intercorrelation of predictors, makes the interpretation of the regression coefficients more difficult, and may call for the combination of subsets of predictors into a new set of less-intercorrelated predictors (Curto & Pinto, 2011). Therefore, the VIF method was used to identify multicollinearity in a matrix of predictor variables. Multicollinearity is problematic when the variance inflation factors of one or more predictors becomes large. Therefore, the predictor without which the other VIF numbers would all change to a number close to 1 was eliminated from the list of independent variables.

Once the regression model was estimated, the residuals were defined as the differences between the observed and predicted values in order to measure the closeness of fit of the predicted and actual values (Dowdy, Wearden, & Chilko, 2011).

Chapter 4 - Results and Discussion

Experimentation and empirical modeling were used to systematically and quantitatively analyze the treatment performance of a pilot-scale EDR plant on several brackish groundwater under various electrical, hydraulic, and chemical conditions. The experimental results are described and discussed in Section 4.1, and the modeling results are covered in Section 4.2.

4.1 Experimental Results

Experimental evaluation of EDR's ability to treat brackish groundwater was performed according to the methods detailed in Chapter 3.

The limiting current, which is dependent on flow rate, feed salinity, and temperature, is obtained for each electrode. The effects of electrical, hydraulic, and chemical variables are presented in Sections 4.1.1 through 4.1.4, along with the effect of electrode type in Section 4.1.5.

4.1.1 Electrical: Determining Limiting Current

An applied electrical potential (voltage) is the driving force for ionic separation in EDR, and it is the primary controlling factor for the rate of separation. The current increases along with voltage until the limiting current is reached. Once the system reaches limiting current, the voltage drop across the boundary layer increases drastically, resulting in water dissociation, and consequently changes in the pH of the solution in dilute and concentrate channels. This may cause precipitation of carbonates and sulphates of calcium and magnesium. Thus, to identify operating parameters for EDR that avoid salt precipitation, the limiting current must be determined.

To avoid the many aforementioned problems associated with exceeding limiting current, it is very important to work with operating current values less than limiting current. Measurements of the limiting current for each combination of variables shown are taken through the following procedure:

1. The flow rates of the feed, product, and concentrate streams are set;
2. Voltage increments are modified and increased for every reading of the experiment in ascending order;
3. The polarity reversal time is set for 15 minutes, and after 10 minutes, a time period which is required for the system to reach stability, measurements are taken;
4. The current for each voltage set is taken;
5. The pH and conductivity of feed, product, and concentrate stream are measured.
6. The current vs. voltage, current vs. stack resistance, and removal ratio vs. current curves are plotted to observe the limiting current.

The limiting current curves measured through the aforementioned approach are shown in Figures 4.1 through 4.3.

As the current density through the EDR stack is increased from zero by

increasing the voltage at the electrodes, the concentration gradient in the diffusion boundary layer becomes steeper. If the concentration gradient becomes too steep and consequently the diffusion boundary layer thickness becomes large, then the salt concentration in the dilute diffusion boundary layer approaches zero at the membrane surface; as a result, stack resistance increases drastically, causing a drastic decrease in current produced. As a result of the current decrease, the desalting (removal) ratio decreases. As shown in Figures 4.1 through 4.3, the limiting current is the point where current starts to reach plateau, stack resistance increases drastically, and further increase in removal ratio is prevented.

The resistance, in general, strongly depends on the temperature, since the diffusion boundary layer resistance decreases with increasing temperature due to the increase in ion mobility with increasing temperature. Therefore, since a temperature increase could change the limiting current and this work does not focus on temperature's effect, the temperature has been maintained approximately constant during these experiments ($\sim 20^\circ\text{C}$).

Also, as presented in Eq. 2.11 ($I_{\text{lim}} \propto C_f U^{0.8} T^{0.67}$) and indicated in Figures 4.1 through 4.3, the limiting current is influenced by the flow rate, because higher solution flow rates generate turbulence in the bulk of the streams, reducing the diffusion boundary layer thickness at the membrane surface, and resulting directly in an increased limiting current value.

Furthermore, the results show that the resistance strongly depends on the solution concentration. We observe a very strong decrease in the resistance with increasing concentration, leading to an increase in the limiting current. All the plots presented are for feed water with low-level conductivity ($\sim 1700\ \mu\text{S}/\text{cm}$), as summarized in Table 4.1.

In this study, it was not possible to measure the limiting current for feeds with medium ($\sim 3700\ \mu\text{S}/\text{cm}$) and high salinity ($\sim 6000\ \mu\text{S}/\text{cm}$), because the manufacture has recommended a maximum voltage application of 1.5 V per cell-pair (40 cell pairs used), which limits the total possible applied voltage to 60 V. The experiments conducted indicate that for voltages less than 40 V, the limiting current is not reached, and working with operating current less than 40 V is safe for all levels of flow rate for both medium and high levels of salinity.

Among all the combinations of feed salinity and feed flow rate levels, the lowest limiting current occurs for 7 GPM and low salinity at 45 V. Therefore, the highest voltage applied to the stack was adjusted to be 40 V and the data collected were constantly monitored to make sure that operating currents were in the Ohmic section of the voltage-current curves. In addition, the pH of the dilute and concentrate was monitored constantly, and most significantly, no precipitation occurred in the concentrate solution during the experiments, which demonstrates that the concentration polarization of EDR was sufficiently small.

4.1.2 Electrical: Effects of Stack Voltage

Experiments were performed at five different voltage applications (30, 32.5, 35, 37.5, 40 V) for treating the brackish water from a deep aquifer at BGNDRF in Alamogordo, New Mexico. The measurements were repeated for

three levels of feed flow rate, and the experiment simulated 80% single-stage recovery.

4.1.2.1 Chemical Efficiency

The ionic separation of each experiment is shown in Figure 4.4. As the ions were continuously separated from the dilute and transported to the concentrate, the conductivity of the dilute decreased from its initial value and the removal ratio based on dilute conductivity increased.

As expected, the separation rate increased with increasing voltage because the increased electric field strength increases the rate of electromigration, as shown by the Nernst-Planck equation (Equation 2.4). Also, the rate of removal was approximately proportional to the applied stack voltage.

To determine the removal ratio, the concentration of the effluent dilute and the salt concentration of the feed solution are typically measured in the units of mass of salt per volume of solution. Therefore, the relationship between concentration and conductivity must be obtained. Chintakindi (2011) showed that there is a linear relationship between concentration and conductivity, and Table 4.2 provides the conversion factors of conductivity ($\mu\text{S}/\text{cm}$) to concentration (meq/L).

4.1.2.2 Electrical Efficiency

As expected, current increases with voltage increases based on Ohm's law. Also, there is an approximate linearity between current and voltage (Figure 4.5) which can be attributed to the relatively stable resistance within the stack.

The resistance of dilute solution increases as the dilute conductivity decreases, and conversely, the concentrate resistance decreases as the concentrate conductivity increases. In EDR brackish water treatment systems, the resistance of the ion exchange membranes can be neglected compared to the resistance of dilute and concentrate solutions.

Another metric for evaluating the electrical efficiency of the EDR process is specific energy consumption (SEC), which is the amount of invested energy per unit volume of product water. SEC often is reported in kWh/gallon, and it is approximately proportional to the stack voltage, as shown in Figure 4.6. The SEC includes the electrical energy applied to the stack as well as the hydraulic energy invested to pump the solution through the process.

As shown in Equation 2.16, the actual desalination energy required in an EDR stack is given by the current passing through the stack multiplied by the total voltage drop encountered between the electrodes. Also, the current and voltage have a proportional relationship. Therefore, a voltage increase leads to a higher SEC.

4.1.3 Hydraulic: Effects of Flow Rate

To explore the effect of flow velocity on EDR performance, three different levels of feed flow rate (7, 9, 11 GPM) with a constant recovery ratio (80%) have been considered. In terms of temperature, recovery, stack design parameters, etc.,

the experiments were performed under conditions equivalent to those listed for the investigations of the effects of stack voltage.

4.1.3.1 Chemical Efficiency

While the applied voltage is the main controlling factor for the rate of separation, the solution velocity controls the residence time limitation. At higher flow rates, removal ratio values fall and separation performance decreases. Because a greater flow rate means a lower residence time, ions that are between the membranes do not have enough time to transfer through the membranes (Mohammadi & Kaviani, 2003; Sadrzadeh & Mohammadi, 2008). The rate of separation was decreased approximately 30% by increasing the feed flow rate from 7 to 11 GPM. The effects of flow rate on ion removal are shown in Figure 4.7.

4.1.3.2 Electrical Efficiency

As the velocity increases, the thickness of the diffusion boundary layer decreases due to the increased shear near the membrane surface. A thinner diffusion boundary layer results in lower electrical resistance, which allows a higher current density, as shown in Figure 4.8. However, flow rate here does not seem to have a very significant effect on current generated (the main effect of flow rate on current will be discussed in detail with the modeling results in Section 4.2).

As shown in Figure 4.9, the specific energy required to achieve a removal ratio is decreases with the velocity based on Equation 2.21.

On average, the hydraulic energy accounted for approximately 15% of the total specific energy consumptions of all 7, 9, and 11 GPM experiments. Therefore, the hydraulic energy required is typically a small fraction of the total EDR energy consumption and final operating cost.

As shown in Figures 4.16 – 4.21, as velocity increases within the conditions of this experimentation, the current and SEC improve, while the separation rate results indicate that the marginal improvement in energy consumption alone is not sufficient to justify the increase in capital and operating costs associated with the increase in superficial velocity. The removal ratio decreases with increased velocity. Therefore, the optimal superficial velocity (for a treatment system operating with similar conditions as these) is expected to be optimized to improve the total performance of EDR process.

4.1.4 Chemical: Effects of Feed Concentration

Inlet conductivity, one of inputs changing from low to high levels, has a direct and proportional impact on product conductivity. In order to investigate the effect of feed inlet concentration, three levels of salinity have been considered. For well1, which has the lowest TDS compared with other well waters, the conductivity ranged between 1600 and 1800 $\mu\text{S}/\text{cm}$; for well2, the conductivity was between 5800 and 6200 $\mu\text{S}/\text{cm}$; and for blend water, conductivities varied from 4700 to 4900 $\mu\text{S}/\text{cm}$. Experiments were conducted under conditions equivalent to those listed for previous investigations.

4.1.4.1 Chemical Efficiency

At higher feed concentrations – in spite of the fact that solution conductivity increases, diminishing resistances of dilute and concentrate compartments in the cell pair – the separation percent decreases (Figure 4.10). Hence, it was demonstrated that EDR is more efficient at lower concentrations and can be applied as a treatment process for desalination.

4.1.4.2 Electrical Efficiency

Generally, higher ionic content of the source water results in lower electrical resistance of the EDR concentrate and dilute cells, allowing a higher current density for the same voltage application based on Ohm's law (Figure 4.11). However, higher current densities create a larger potential loss through membrane resistance and concentration polarization. Thus, it is assumed that the electrical resistance of the membranes was small compared to the electrical resistance of the solutions, which provided the predominant stack resistance drop.

Another key parameter for evaluating the electrical efficiency of the EDR system is SEC, and as illustrated in Figure 4.12, the SEC was proportional to the concentration of ionic content removed from the dilute in streams.

Recognizing that the SEC is correlated with the financial cost of an EDR system, it is important to note that, at some point, the energy required to concentrate a solution by EDR would be greater than the energy required by a thermal process, which is practically insensitive to salinities in this range (brackish water salinity range). In order to achieve a lower SEC for high salinity brackish water, one solution is operating at a lower voltage application.

4.1.5 Design: Effect of Electrode Geometry

Based on current design practices and historical knowledge of the GE EDR stack configurations, three electrode designs are investigated: full, recessed, and tapered.

In this project, to compare the three proposed electrode designs, EDR performance was studied as a function of chemical, electrical and hydraulic operating parameters to introduce optimized electrode design, which directly contributes to higher removal ratio, less current loss, and a lower SEC.

To compare the performances of the three investigated electrodes, analysis of variance (ANOVA) was used with current, removal ratio, and SEC as response (dependent) variables, with the null hypothesis as follows:

$$H_0: \mu_{\text{full}} = \mu_{\text{recessed}} = \mu_{\text{tapered}}$$

The null hypothesis for ANOVA is that the mean (average value of the dependent variable) is the same for all different electrode designs. The alternative or research hypothesis is that the average is not the same for all groups.

For the ANOVA test procedure in this experiment, the p-values obtained from statistical data analyses are shown in Table 4.3.

As shown in Table 4.3, we fail to reject the null hypothesis since the p-values are greater than 0.05. Consequently, it can be concluded that the average of the dependent variable is the same for all groups.

In addition to the p-values, looking at the standard error bars lets us compare the difference between the mean and the amount of scatter within the groups. As shown in Figures 4.13-4.15, since the standard error bars for all three electrode designs overlap, the differences between the three means are statistically insignificant.

Therefore, although it has been hypothesized that the shape of the electrodes and their locations with respect to the solution manifolds could impact EDR performance, based on the statistical results, there is no significant difference between these three electrode designs in terms of current, removal ratio, and specific energy consumption.

However, there is a possibility that experimental errors have affected the accuracy of experimental results and conclusions made based on the results. All measurements are subject to some uncertainty, as several types of errors and inaccuracies can happen.

The main sources of possible experimental errors include:

1. Poorly maintained instruments;
2. Fluctuation of the operating conditions during the measurements;
3. Assumption of linear relationship between conductivity and concentration of sample waters; and
4. Assumption of constant temperature and recovery during all the experiments.

4.2 Modeling Results

Several researchers have developed mathematical simulations of the performance of ED and EDR systems (Kabay et al., 2003; Mohammadi, Moheb, Sadrzadeh, & Razmi, 2005; Moon et al., 2004; Myint et al., 2011; Sadrzadeh et al., 2007; Shaposhnik, 1997; Tanaka, 2009). Unfortunately, many of them are limited to binary ionic solutions, and they are limited to low concentrations of brackish water (up to 1000 mg/L TDS or 0.1 mol/L) or small EDR lab scale systems with low input flow rate values.

In this experiment, statistical modeling of the experimental system was employed using SAS programming to predict characteristics of response variables based on operating conditions and the interactions of the hydraulic, electrical, and chemical phenomena within EDR system.

For all the statistical models provided, residual plots have been evaluated. (Residuals are defined as the difference between the original data and the predicted values from the regression equation.) The residuals should be centered on zero throughout the range of fitted values and have a constant spread throughout the range to make sure that variances of residuals are equal.

In addition, in the regression problem, we are looking for a model that explains a substantial proportion of the variation in the response variable. The

analysis of residuals, which is a simple graphic technique (plotting residual vs. predicted value) is required to see if there are any obvious patterns left within the unexplained portion of the variation of the response variable. The emphasis is upon not missing patterns that might suggest a relationship between the predictor and predicted variables.

4.2.1 Chemical Efficiency: Removal Ratio

Based on the results obtained, there is no statistical significance between three different designs of electrode in aspect of EDR performance. Thus, a similar multilinear regression model has been achieved and proposed for all of them. Table 4.4 shows the variation in removal ratio (response) with predictor variables (P-value < 0.05).

The p-value for each term tests the null hypothesis that the coefficient is equal to zero. A low p-value (< 0.05) indicates that the null hypothesis can be rejected. In other words, a predictor that has a low p-value is likely to be a meaningful addition to a model because changes in the predictor's value are related to changes in the response variable.

As shown in the Table 4.4, salinity, flow rate, voltage, and the interactions between them are likely to have a significant effect on removal ratio as a response variable.

However, variance inflation factors (VIF) are another parameter that must be considered while evaluating a regression model. VIF is used to describe how much multicollinearity (correlation between predictors) exists in a regression analysis and measures how much the variances of the estimated regression coefficients are inflated as compared to when the predictor variables are not linearly related.

Multicollinearity is problematic because it can increase the variance of the regression coefficients, making them unstable and difficult to interpret.

In a full factorial design, for estimating removal ratio with stack voltage (V), feed flow rate (GPM) and feed conductivity (mS/cm), the regression model, with the R-square value of 0.95, is:

$$\text{Removal Ratio} = -0.6886 + 0.0122 * \text{Voltage} + 2.8734 / \text{Flow Rate} + 0.8818 / \text{Conductivity}$$

The parameter estimates for this regression model are shown in Table 4.5.

Although the interaction of predictors appears to be significant, the high values of VIF indicate that there is a strong multicollinearity between predictors and their interactions.

As illustrated in Figures 4.4, 4.7, and 4.10, and as explained in Section 1.1, removal ratio increases with increasing the voltage, decreasing the feed flow rate, and decreasing the feed conductivity. Figures 4.16, 4.17, and 4.18, show that the regression model introduced to predict the removal ratio fits the experimental data very well.

4.2.2 Electrical Efficiency: Current

Table 4.6 shows the variation in current (response) with predictor variables (P-value < 0.05) for the multilinear regression model.

The regression model in a full factorial design to estimate current with stack voltage (V), feed flow rate (GPM) and feed conductivity (mS/cm) is (R-square = 0.95):

$$\text{Current} = -15.2230 + 3.5116 * \text{Conductivity} + 0.6017 * \text{Voltage} + 0.0055 * \text{Voltage} * \text{Flow Rate}$$

Table 4.7 shows the parameter estimates for this model of current.

As discussed in Section 1.1, current increases as the conductivity of feed increases due to decreases in the resistance of solutions in the cell pair. Based on Ohm's law, there is a linear relationship between voltage and current, and the model confirms that. Also, as Faraday's law indicates, there is an interaction between the dilute mass transfer and dilute flow rate, as shown in the model. Figures 4.19, 4.20, and 4.21 show that the regression model introduced to predict the current fits the experimental data very well.

4.2.3 Electrical Efficiency: Specific Energy Consumption

Table 4.8 shows the variation in specific energy consumption (response) with predictor variable (P-value <0.05) for the multilinear regression model.

The regression model in a full factorial design for estimating specific energy consumption with stack voltage (V), feed flow rate (GPM) and feed conductivity (mS/cm) is (R-square = 0.95):

$$\text{Specific Energy Consumption} = 0.0013 + 0.0413 / \text{Flow Rate} + 6.475\text{E-}05 * \text{Voltage}^2 * \text{Conductivity} / \text{Flow Rate}$$

The parameter estimates for specific energy consumption based on this model are shown in Table 4.9.

The main effects and interaction effects of independent variables on specific energy consumption are quite reasonable and match with Eq. 2.15, Eq. 2.16, and Eq. 2.21. Additionally, Figures 4.22, 4.23, and 4.24 show that the regression model introduced to predict the specific energy consumption fits the experimental data very well.

4.3 Conclusion

The hypothesis for this research is that EDR desalination systems perform differently under changing operating and design conditions, including applied stack voltage, flow rate, source water salinity, and electrode design. The objectives of this research were to:

1. Experimentally determine the sensitivity of EDR to hydraulic, electrical, and chemical operational parameters;
2. Determine and compare how the three electrode designs (full, recessed, and tapered) affect EDR performance;
3. Identify the operating parameters that maximizes the performance

of EDR;

4. Perform statistical analyses of the investigated parameters (electrical, hydraulic, and chemical) to determine their impacts on EDR performance.

Objective 1 and 2 were accomplished with a pilot-scale continuous EDR system, the performance of which was investigated with respect to applied stack voltage, flow rate, source water salinity, and electrode design. Objectives 3 and 4 were accomplished through the statistical analysis and development of regression models.

Based on the results obtained, EDR performance depends on the operating conditions (stack voltage, flow rate and feed salinity). However, changing the design of electrodes has no significant effect on EDR performance.

Experiments performed with brackish groundwater demonstrated that stack voltage applications in the range of 30-40 Volts and feed flow rates in the range of 7-11 GPM effectively separated up to 70% of the initial feed salinity in the range of approximately 1000-5500 mg/L at single-stage EDR recovery of 80%.

The stack voltage application is a process controlling parameter, and the rate of separation and current are approximately proportional to the applied voltage. The specific energy consumption increases with increasing the applied voltage.

With the feed flow rates tested here, a decrease in the rate of separation was observed with increases in the feed flow rate, which increase the stack superficial velocity leading to a decrease in residence time. Also, increases in flow rate cause an increase in energy required for pumping and consequently an increase in total energy.

However, the specific energy consumption decreases with increases in the feed flow rate because the pumping energy does not change when recovery is kept constant, while product water volume increases when feed flow rate increases.

As the concentration of solution increases, the removal ratio drops when feed concentration increases due to the magnification in the concentration factor (i.e., from 0.011 to 0.014) and limited ion exchange capacity of the membranes. Furthermore, since current is proportional to feed conductivity, the specific energy consumption increases as feed water becomes more saline.

In order to increase the removal ratio, lower feed concentrations, higher voltages, and lower flow rates should be utilized. Also, to reduce the specific energy consumption, lower voltages, lower feed concentrations, and higher flow rates are suggested. Table 4.10 summarizes and demonstrates the best choice of voltage, feed flow rate and feed salinity as operating conditions to maximize each EDR performance metric.

It should be noted, however, that the data gathered in these experiments are from conditions that still left salinity levels above 1,000 $\mu\text{S}/\text{cm}$ in the product water. Therefore, although the developed regression models do predict the effects of the different parameters, real-world desalination processes would require further treatment to bring the quality of the produced water to acceptable levels. Given that specific energy consumption is strongly determined by the removal

ratio, further salt removal to produce truly potable water would significantly increase the specific energy consumption of the systems. Furthermore, as a consequence of an expanded hydrodynamic boundary layer (the results of viscous forces) and concentration boundary layer (the product of mass transfer rates through the desalination membrane), the system is likely to experience progressively poorer electrochemical/hydrodynamic behavior. Additionally, as the removal ratio increases, there is a higher likelihood of salt precipitation in the hydrodynamic/concentration boundary layer, the area in which the most saline part of the solution is moving slowest. For all of these reasons, additional testing should be conducted before designing industrial-scale systems.

4.4 Future Work

Several logical extensions can stem from this work. First, the EDR experimentation could be expanded to study how additional operating conditions, such as temperature and recovery ratio, affect EDR performance. Also, the experiments could be done with more than one hydraulic stage to improve the removal ratio, especially for higher feed salinities, and study how energy consumption changes when more stages are added.

Furthermore, the models for the pilot-scale plant could be extended to simulate full-scale EDR systems. This would allow them to quantify limitations in the tradeoff between energy consumption and removal ratio associated with voltage application and feed flow rate, making it possible to optimize the design of EDR systems.

References

- Akyol, E., Öner, M., Barouda, E., & Demadis, K. D. (2009). Systematic Structural Determinants of the Effects of Tetrakisphosphonates on Gypsum Crystallization. *Crystal Growth & Design*, 9(12), 5145–5154.
- Allison, A. R. P. (2008). Surface and Wastewater Desalination by Electrodialysis Reversal, 86(0).
- Allison, R. P. (1995, November). Electrodialysis reversal in water reuse applications. *Desalination*.
- Anderko, A., & Lencka, M. M. (1997). Computation of Electrical Conductivity of Multicomponent Aqueous Systems in Wide Concentration and Temperature Ranges. *Industrial & Engineering Chemistry Research*, 36(5), 1932–1943.
- Balster, J., Stamatialis, D. F., & Wessling, M. (2009). Towards spacer free electrodialysis. *Journal of Membrane Science*, 341(1-2), 131–138.
- Bard, A. J., Faulkner, L. R., Swain, E., & Robey, C. (n.d.). *Fundamentals and Applications*.
- Brady, P. V., Kottenstette, R. J., Mayer, T. M., & Hightower, M. M. (2009). Inland Desalination: Challenges and Research Needs. *Journal of Contemporary Water Research & Education*, 132(1), 46–51.
- Chiapello, J.-M., & Bernard, M. (1993). Improved spacer design and cost reduction in an electrodialysis system. *Journal of Membrane Science*, 88(1), 251–256.
- Choi, E., Choi, J., & Moon, S. (2002). An electrodialysis model for determination of the optimal current density, 153, 399–404.
- Choi, J.-H., Lee, H.-J., & Moon, S.-H. (2001). Effects of Electrolytes on the Transport Phenomena in a Cation-Exchange Membrane. *Journal of Colloid and Interface Science*, 238(1), 188–195.
- Hanrahan, C. (2013). *High-Recovery Electrodialysis Reversal for the Desalination of Inland Brackish Waters*. New Mexico State University.
- Walker, S. (2010). *Improving recovery in reverse osmosis desalination of inland brackish groundwaters via electrodialysis*. University of Texas at Austin.
- Curto, J. D., & Pinto, J. C. (2011). The corrected VIF (CVIF). *Journal of Applied Statistics*, 38(7), 1499–1507.

- D.F. Lawler, M. Cobb, B. F. (2010). *Improving Recovery: A Concentrate Management Strategy for Inland Desalination*. Austin, TX.
- Demircio, M., Kabay, N., & Gizli, N. (2001). Cost comparison and efficiency modeling in the electro dialysis of brine, *9164(01)*.
- Demircioglu, M., Kabay, N., Kurucaovali, I., & Ersoz, E. (2002). Demineralization by electro dialysis (ED) - separation performance and cost comparison for monovalent salts, *153*, 329–333.
- Długołęcki, P., Anet, B., Metz, S. J., Nijmeijer, K., & Wessling, M. (2010). Transport limitations in ion exchange membranes at low salt concentrations. *Journal of Membrane Science*, *346(1)*, 163–171.
- Dowdy, S., Wearden, S., & Chilko, D. (2011). *Statistics for Research* (p. 640). John Wiley & Sons.
- Eden, S., Glass, T. W., & Herman, V. (2011). Desalination in Arizona. *Arroyo*.
- Electrodialysis and Electrodialysis Reversal: M38*. (1995) (p. 62). American Water Works Association.
- Elsaid, K., Bensalah, N., & Abdel-wahab, A. (2007). Inland Desalination : Potentials and Challenges. *Rivers*.
- Elsaid, K., Bensalah, N., & Abdel-wahab, A. (2012). Inland Desalination : Potentials and Challenges. In Z. Nawaz (Ed.), *Advances in Chemical Engineering* (pp. 449–480). In Tech.
- Fubao, Y. (1985). Study on electro dialysis reversal (EDR) process. *Desalination*, *56*, 315–324.
- Fues, J. (2008). High-Efficiency Filtration as Pretreatment to Membrane-Based Demineralization Systems. In *American Filtration & Separations Society Annual Conference*. Valley Forge, PA.
- Gleick, P. (2012). *The World's Water Volume 7: The Biennial Report on Freshwater Resources*. *The Biennale Report on Freshwater Resources* (Vol. 7). Island Press.
- Gleick, P. H. (1993). *Water in Crisis: A Guide to the World's Fresh Water Resources*. New York: Oxford University Press.

- Gottberg, A. von. (1998). New High Performance Spacers in Electrodialysis Reversal (EDR) Systems. *Proceedings, American Water Works Assoc. Annual*
- Gottberg, A. A. Von, & Manager, P. (2010). New High-Performance Spacers in Electro- Dialysis Reversal (EDR) Systems.
- Greenlee, L. F., Lawler, D. F., Freeman, B. D., Marrot, B., & Moulin, P. (2009). Reverse osmosis desalination: water sources, technology, and today's challenges. *Water Research, 43*(9), 2317–48.
- Hasson, D., Drak, A., & Semiat, R. (2009). Induction times induced in an RO system by antiscalants delaying CaSO₄ precipitation, *157*(May 2003), 193–207.
- Helfferich, F. G. (1962). *Ion Exchange* (p. 624). Courier Corporation.
- Hwang, J.-Y., & Lai, J.-Y. (2007). The effect of temperature on limiting current density and mass transfer in electrodialysis. *Journal of Chemical Technology & Biotechnology, 37*(2), 123–132.
- Ibanez, R., Stamatialis, D. ., & Wessling, M. (2004). Role of membrane surface in concentration polarization at cation exchange membranes. *Journal of Membrane Science, 239*(1), 119–128.
- Ions, C. A. T., Rod, E., & Is, A. (n.d.). PROCESS A P P L I C A T I O N S O F ELECTRODIALYSIS, (6), 29–35.
- Jefferies, M., & Comstock, D. (2001). Predicting calculating scaling tendency in membrane plants. *Desalination, 139*(1-3), 341–344.
- Kabay, N., Ardab, M., Ersoza, E., Kahveci, H., Can, M., Dal, S., ... Yuksel, M. (2003). Effect of feed characteristics on the separation performances of monovalent and divalent salts by electrodialysis, *58*, 95–100.
- Katz, W. E. (1979). The electrodialysis reversal (EDR) process. *Desalination, 28*(1), 31–40.
- Kim, Y., Walker, W. S., & Lawler, D. F. (2012). Competitive separation of di- vs. mono-valent cations in electrodialysis: effects of the boundary layer properties. *Water Research, 46*(7), 2042–56.
- Lee, H. J., Strathmann, H., & Moon, S. H. (2006). Determination of the limiting current density in electrodialysis desalination as an empirical function of linear velocity. *Desalination, 190*(1-3), 43–50.

- Lee, H.-J., Hong, M.-K., Han, S.-D., Cho, S.-H., & Moon, S.-H. (2009). Fouling of an anion exchange membrane in the electro dialysis desalination process in the presence of organic foulants. *Desalination*, 238(1-3), 60–69.
- Mandersloot, W. G. B., & Hicks, R. E. (1966). Leakage currents in electro dialytic desalting and brine production. *Desalination*, 1(2), 178–193.
- Martin-lagardette, B. J. L. (2003). Desalination of Seawater. *Water Engineering and Management*.
- McGovern, R. K., Zubair, S. M., & V, J. H. L. (2014). The cost effectiveness of electro dialysis for diverse salinity applications, 348, 57–65.
- Meng, H., Deng, D., Chen, S., & Zhang, G. (2005). A new method to determine the optimal operating current (I_{lim}) in the electro dialysis process. *Desalination*, 181(1-3), 101–108.
- Miller, A. W. S., Water, G. E., & Technolo-, P. (2009). Understanding Ion-Exchange Resins For Water Treatment Systems.
- Miller, J. E. (2003). Review of Water Resources and Desalination Technologies. *Exchange Organizational Behavior Teaching Journal*, (March), 3–54.
- Mohammadi, T., & Kaviani, A. (2003). Water shortage and seawater desalination by electro dialysis. *Desalination*, 158(1-3), 267–270.
- Mohammadi, T., Moheb, A., Sadrzadeh, M., & Razmi, A. (2005). Modeling of metal ion removal from wastewater by electro dialysis. *Separation and Purification Technology*, 41(1), 73–82.
- Moon, P., Sandí, G., Stevens, D., & Kizilel, R. (2004). Computational Modeling of Ionic Transport in Continuous and Batch Electro dialysis. *Separation Science and Technology*, 39(11), 2531–2555.
- Murray, P. (1995). *Electro dialysis and Electro dialysis Reversal (M38): AWWA Manual of Water Supply Practice*. American Water Works Association.
- Myint, M. T., Ghassemi, A., & Nirmalakhandan, N. (2011). Modeling in desalination—electro-dialysis reversal. *Desalination and Water Treatment*, 27(1-3), 255–267.
- National Ground Water Association. (2010). NGWA Information Brief: Brackish Groundwater, 1–4.
- Nicot, J.-P., & Chowdhury, A. H. (2005). Disposal of brackish water concentrate into depleted oil and gas fields: a texas study. *Desalination*, 181(1-3), 61–74.

- Pankratz, T. (2012). *IDA Desalination Yearbook 2011-2012*. Oxford, UK.
- Philibert, J. (2005). One and a Half Century of Diffusion : Fick , Einstein , before and beyond, 2, 1–10.
- Pilat, B. (2001). Practice of water desalination by electrodialysis, *139*(May), 385–392.
- Process Technologies for Water Treatment*. (2013) (p. 239). Springer Science & Business Media.
- Purification, W., & Program, D. (2003). Handbook, (72).
- Reahl, A. E. R. (2006). Half A Century of Desalination With Electrodialysis.
- Rosenberg, N. W., & Tirrell, C. E. (1957). Limiting Currents in Membrane Cells. *Industrial & Engineering Chemistry*, *49*(4), 780–784.
- Rubinstein, I., & Shtilman, L. (1979). Voltage against current curves of cation exchange membranes. *Journal of the Chemical Society, Faraday Transactions 2*, *75*, 231.
- Sadrzadeh, M., Kaviani, A., & Mohammadi, T. (2007). Mathematical modeling of desalination by electrodialysis. *Desalination*, *206*(1-3), 538–546.
- Sadrzadeh, M., & Mohammadi, T. (2008). Sea water desalination using electrodialysis. *Desalination*, *221*(1-3), 440–447.
- Sadrzadeh, M., & Mohammadi, T. (2009). Treatment of sea water using electrodialysis: Current efficiency evaluation. *Desalination*, *249*(1), 279–285.
- Sata, T. (1986). Recent trends in ion exchange membrane research. *Pure Appl. Chem*, *58*(1), 1613–1626.
- Sata, T. (2004). *Ion Exchange Membranes: Preparation, Characterization, Modification and Application* (p. 314). Royal Society of Chemistry.
- Scott, K. (1996). *Industrial Membrane Separation Technology* (p. 305). Springer Science & Business Media.
- Shaffer, L. H., & Mintz, M. S. (1966). Electrodialysis. In K. S. Spiegler (Ed.), *Principles of Desalination* (pp. 199–289). Academic Press.
- Shaposhnik, V. (1997). Analytical model of laminar flow electrodialysis with ion-exchange membranes. *Journal of Membrane Science*, *133*(1), 27–37.

- Shaposhnik, V. a., & Grigorchuk, O. V. (2010). Mathematical model of electro dialysis with ion-exchange membranes and inert spacers. *Russian Journal of Electrochemistry*, 46(10), 1182–1188.
- Ślezak, A., Ślezak, I. H., & Ślezak, K. M. (2005). Influence of the concentration boundary layers on membrane potential in a single-membrane system. *Desalination*, 184(1-3), 113–123.
- Staff, A. (1996). *Electrodialysis and Electrodialysis Reversal (M38)* (p. 72). American Water Works Association.
- Strathmann, H. (2004a). Assessment of Electrodialysis Water Desalination Process Costs. *Proceedings of the International Conference on Desalination Costing*, 32–54.
- Strathmann, H. (2004b). *Ion-Exchange Membrane Separation Processes* (p. 360). Elsevier.
- Strathmann, H. (2010). Electrodialysis, a mature technology with a multitude of new applications. *Desalination*, 264(3), 268–288.
- Strathmann, H. (2011). *Introduction to Membrane Science and Technology*. Weinheim, Germany: Wiley-VCH.
- Strathmann, H., Giorno, L., & Drioli, E. (n.d.). An Introduction to Membrane.
- Stuttgart, U. (2002). Designing of an electro dialysis desalination plant, 142, 267–286.
- Subcommittee, A. M. R. M. (2004). Committee Report: Current Perspectives on Residuals Management for Desalting Membranes. *Journal - American Water Works Association*, 96(12), 73–87.
- Tanaka, Y. (1991, April). Concentration polarization in ion exchange membrane electro dialysis. *Journal of Membrane Science*.
- Tanaka, Y. (2009). A computer simulation of continuous ion exchange membrane electro dialysis for desalination of saline water. *Desalination*, 249(2), 809–821.
- Tanaka, Y. (2015). *Ion Exchange Membranes: Fundamentals and Applications* (p. 522). Elsevier Science.

- Tanaka, Y., Uchino, H., & Murakami, M. (2012). Continuous ion-exchange membrane electrodialysis of mother liquid discharged from a salt-manufacturing plant and transport of Cl⁻ ions and SO₄²⁻ ions, *3*(1), 63–76.
- Tsiakis, P., & Papageorgiou, L. G. (2005). Optimal design of an electrodialysis brackish water desalination plant. *Desalination*, *173*(2), 173–186.
- Turek, M. (2002). Cost effective electrodialytic seawater desalination, *153*, 371–376.
- Turek, M., & Dydo, P. (2001). OPTIMISATION OF ELECTRODIALYTIC DESALINATION.
- Valerdi-perez, R. (2001). Current-voltage curves for an electrodialysis reversal pilot plant : determination of limiting currents, *141*, 23–37.
- VALERDI-PÉREZ, R., BERNÁ-AMORÓS, L. M., & IBÁÑEZ-MENGUAL, J. A. (2000). Determination of the Working Optimum Parameters for an Electrodialysis Reversal Pilot Plant. *Separation Science and Technology*, *35*(5), 651–666.
- Valerdi-Pérez, R., López-Rodríguez, M., & Ibáñez-Mengual, J. A. (2001). Characterizing an electrodialysis reversal pilot plant. *Desalination*, *137*(1-3), 199–206.
- Valero, F., & Arbós, R. (2010). Desalination of brackish river water using Electrodialysis Reversal (EDR). *Desalination*, *253*(1-3), 170–174.
- Valero, F., Barceló, A., & Arbós, R. (2010). Theory and Applications ., 3–22.
- Veerman, J., Post, J. W., Saakes, M., Metz, S. J., & Harmsen, G. J. (2008). Reducing power losses caused by ionic shortcut currents in reverse electrodialysis stacks by a validated model. *Journal of Membrane Science*, *310*(1-2), 418–430.
- Verbrugge, M. W., & Hill, R. F. (1990). Ion and Solvent Transport in Ion-Exchange Membranes) F (~), *137*(3), 886–893.
- Walker, S. (2010). *Improving recovery in reverse osmosis desalination of inland brackish groundwaters via electrodialysis*. University of Texas at Austin.
- Walton, H. F. (1962). Ion Exchange. F. G. Helfferich. McGraw-Hill, New York, 1962. ix + 624 pp. Illus. \$16. *Science*, *138*(3537), 133–133.

- Yang, Q., & Ma, Z. (2004). DESTRUCTION OF ANTI-SCALANTS IN RO CONCENTRATES BY ELECTROCHEMICAL OXIDATION. *Journal of Chemical Industry and Engineering (China)*, 55(2), 339–340.
- Younos, T., & Tulou, K. E. (2009). Overview of Desalination Techniques. *Journal of Contemporary Water Research & Education*, 132(1), 3–10.
- Zhou, Y., & Tol, R. S. J. (2005). Evaluating the costs of desalination and water transport. *Water Resources Research*, 41(3), n/a–n/a.

Tables

Table 3-1. Experimental variables and discrete value ranges

Variables	Levels
-----------	--------

Stack voltage (V)	30, 32.5, 35, 37.5, 40
Feed flow rate (GPM)	7, 9, 11
Feed water	Low, Medium, High
Electrode type	Full, Recessed, Tapered

Table 3-2. EDR stack specifications

Type	Filter press	GE MkIV 2
EDR Stack	Number	1
	Polarity reversal cycle	15 min
	Electric stage	1
	Hydraulic stage	1/electric stage
	Number of cell pairs	40
Membrane	Heavy cation-exchange	GE CR67-HMR
	Cation-exchange	GE CR67-LLMR
	Anion-exchange	GE AR204-SZRA
	Membrane dimensions	102*46 *0.6 cm
	Effective membrane area	0.47 m ² /membrane
Electrode Information	Spacer model	Mk-IV
	Spacer surface area	0.34m ² /membrane (flow path = 2 m)
	Type and active area	Full : 511.4 in ² Recessed: 493.4 in ² Tapered: 511.4 in ²

Table 3-3. Design of experiments

Factors	Levels	Values
Electrode type	3	Full, Recessed, Tapered
Feed flowrate (GPM)	3	7, 9, 11
Feed salinity classification	3	Low, Medium, High

Applied voltage (V) 5 30, 32.5, 35, 37.5, 40

Table 3-4. Composition and concentration of feed water at BGNDRF

Parameter Name	Units	Low	High	Medium
Bicarbonate	mg/L	150	250	200
Chloride	mg/L	34	580	305
Fluoride	mg/L	2.40	0.35	1.38
Sulfate	mg/L	730	3000	1870
Calcium	mg/L	63	550	306
Magnesium	mg/L	16	320	169
Potassium	mg/L	5.0	2.9	3.9
Silicon Dioxide	mg/L	25	24	24
Sodium	mg/L	320	640	480
Strontium	mg/L	2.0	8.8	5.40
Total Concentration	meq/L	37	160	99
pH	pH units	8.16	7.25	7.40
Conductivity	µs/cm	1700	6100	3900
Total Dissolved Solids	mg/L	1240	5550	3395
Water Temperature	°C	22	21	23

Table 3-5. Data collection log

	Daily Record
Date	-
Time	-
Comment	-
Polarity	-
Feed Conductivity (µS/cm)	-

Feed Temperature (°C)	-
Feed pH	-
Inter-Stage Dilute pH	-
Product Conductivity (µS/cm)	-
Product pH	-
Concentrate Conductivity (µS/cm)	-
Concentrate pH	-
Stage 1 Voltage (V)	-
Stage 1 Current (A)	-
Product Flow Rate (GPM)	-
Concentrate Blow-Down Flow Rate (GPM)	-

Table 3-6. Material specifications

Product	Model	Manufacturer
Pretreatment		
Pressure Reducing Valve	PR150-EP	Plastomatic, Cedar Grove, NJ
Cartridge Filter	Zplex MuniZ 5µm Professional Series	GE WPT, Minnetonka, MN
Multi-Media Filter	Tanks	GE WPT, Minnetonka, MN
Water Measurement		
Flow Meters	Polysulfone Flowmeter	King Instrument Company, Garden Grove, CA
System Conductivity Meters	Elec.inpro 4260/120/PT1000	Thorton Medler Toledo, Bedford, MA
Handheld Conductivity Meter	Sension5	HACH, Loveland, CO
Electrical Measurement		
Oscilloscope	Industrial Scopemeter	Fluke, Everett, WA
Handheld Voltmeter	115 True RMS Multimeter	Fluke, Everett, WA

Table 4-1. Limiting current values for low-level salinity

Electrode Type	Feed Flow Rate	Limiting Current
Full	7 GPM	15.6
	9 GPM	19.0

	11 GPM	26.6
Recessed	7 GPM	14.8
	9 GPM	18.9
	11 GPM	23.8
Tapered	7 GPM	14.9
	9 GPM	18.1
	11 GPM	24.0

Table 4-2. Conversion factors of conductivity to concentration.

Feed Salinity Level	Conversion Factor
Low	0.011
Medium	0.012
High	0.014

Table 4-3. P-values for different dependent variables

Response variable	P-value
Current	0.1596
Removal Ratio	0.2218
Specific Energy Consumption	0.0815

Table 4-4. Analysis of variance for removal ratio

Source	DF	SS	MS	F value	P value
Salinity	1	2.74463	2.74463	1443.11	<.0001
Flow Rate	1	0.50242	0.50242	264.17	<.0001

Voltage	1	0.25328	0.25328	133.17	<.0001
Salinity*Flow Rate	1	0.02277	0.02277	11.97	0.0007
Flow Rate*Voltage	1	0.00564	0.00564	2.96	0.0876
Salinity*Voltage	1	0.02083	0.02083	10.95	0.0012
Salinity*Flow Rate*Voltage	1	0.00188	0.00188	0.99	0.3216
Error	127	0.24154	0.0019		
Total	134	3.79297			

Table 4-5. Parameter estimates for removal ratio

	DF	Parameter Estimate	Standard Error	P-value	VIF
Intercept	1	-0.6886	0.03651	<.0001	0
Voltage	1	0.0122	0.0009	<.0001	1
1/Flow Rate	1	2.8734	0.14874	<.0001	1
1/Conductivity	1	0.8818	0.01929	<.0001	1

Table 4-6. Analysis of variance for current

Source	DF	SS	MS	F-value	P-value
Conductivity	1	4819.44	4819.44	3188.78	<.0001
Flow Rate	1	12.0167	12.0167	7.95	0.0056
Voltage	1	715.457	715.457	473.38	<.0001
Salinity*Flow Rate	1	17.7158	17.7158	11.72	0.0008
Flow Rate*Voltage	1	17.7158	17.7158	11.72	0.0008
Salinity*Voltage	1	3.67753	3.67753	2.43	0.1213
Salinity*Flow Rate*Voltage	1	5.4E-05	5.4E-05	0	0.9952
Error	127	191.945	1.51138		
Total	134	5819.78			

Table 4-7. Parameter estimates - current

	DF	Parameter Estimate	Standard Error	P-value	VIF
Intercept	1	-15.223	1.26678	<.0001	0
Conductivity	1	3.5116	0.073	<.0001	1

Voltage	1	0.6017	0.04013	<.0001	1.3068
Voltage*Flow Rate	1	0.0055	0.00216	0.0128	1.3068

Table 4-8. Analysis of variance for specific energy consumption

Source	DF	SS	MS	F value	P value
Conductivity	1	4819.44	4819.44	3188.78	<.0001
Flow Rate	1	12.0167	12.0167	7.95	0.0056
Voltage	1	715.457	715.457	473.38	<.0001
Salinity*Flow Rate	1	17.7158	17.7158	11.72	0.0008
Flow Rate*Voltage	1	3.67753	3.67753	2.43	0.1213
Salinity*Voltage	1	59.5278	59.5278	39.39	<.0001
Salinity*Flow Rate*Voltage	1	5.4E-05	5.4E-05	0	0.9952
Error	127	191.945	1.51138		
Total	134	5819.78			

Table 4-9. Parameter estimates for specific energy consumption

	DF	Parameter Estimate	Standard Error	P-value	VIF
Intercept	1	0.00127	0.00052	0.0156	0
Voltage ² *Conductivity/Flow Rate	1	1.4E-05	3.44E-07	<.0001	1.1405
1/Flow Rate	1	0.05419	0.00473	<.0001	1.1405

Table 4-10. Best choices of the operating conditions

Response Variable	Minimum Value	Maximum Value
SEC (kWh/Gallon)	0.0075 (30 V, 11 GPM, Low Salinity)	0.0279 (40 V, 7 GPM, High Salinity)
Current (A)	10.2 (30 V, 7 GPM, Low Salinity)	32.5 (40 V, 11 GPM, High Salinity)
Removal Ratio	0.11 (30 V, 11 GPM, High Salinity)	0.73 (40 V, 7 GPM, Low Salinity)

Figures

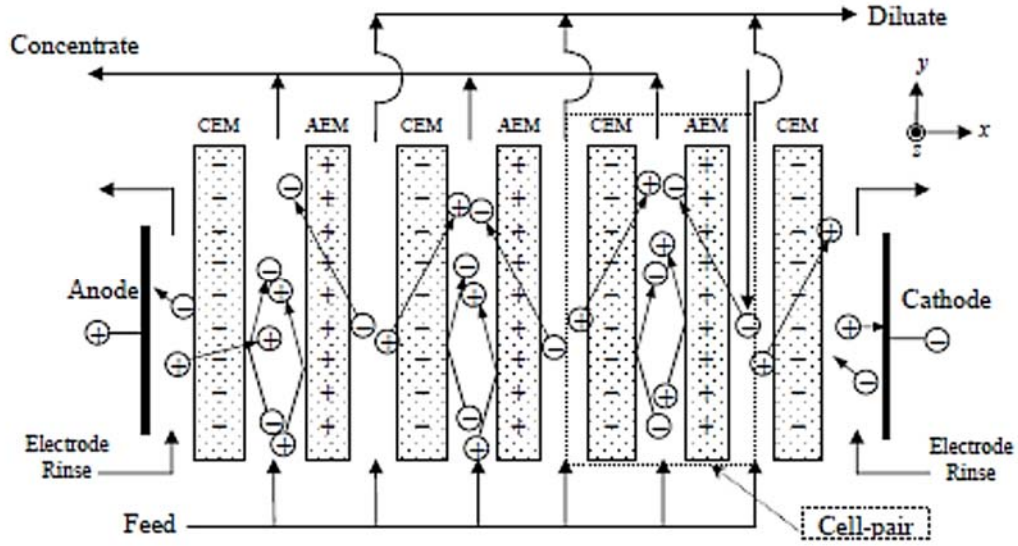


Figure 2.1. Schematic of EDR System. Reprinted from Walker, 2010.

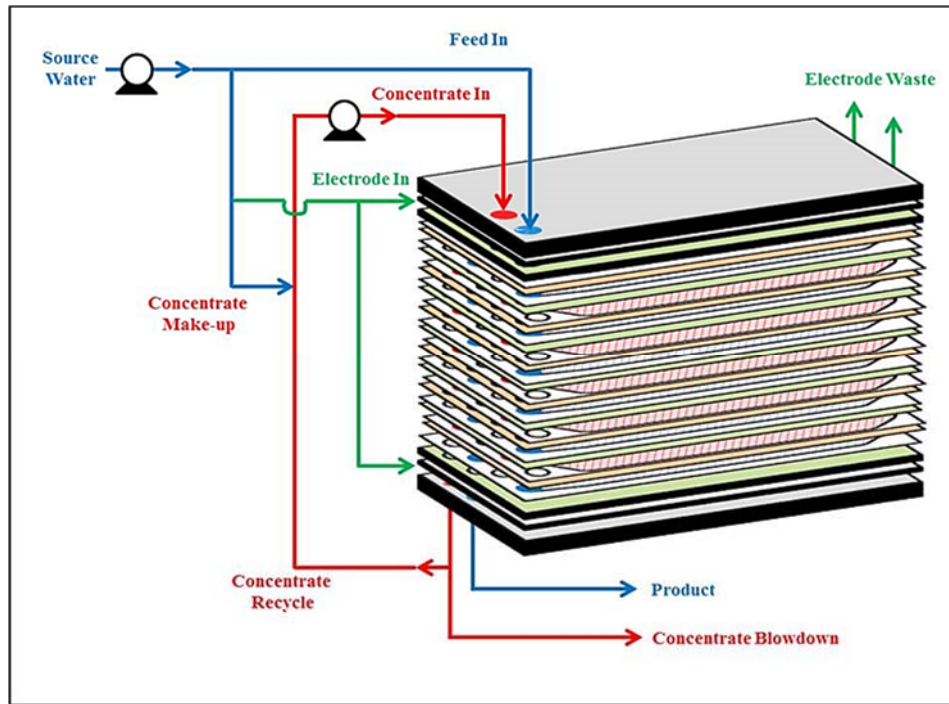


Figure 2.2. Electrodialysis Process Schematic. Reprinted from Hanrahan, 2013.

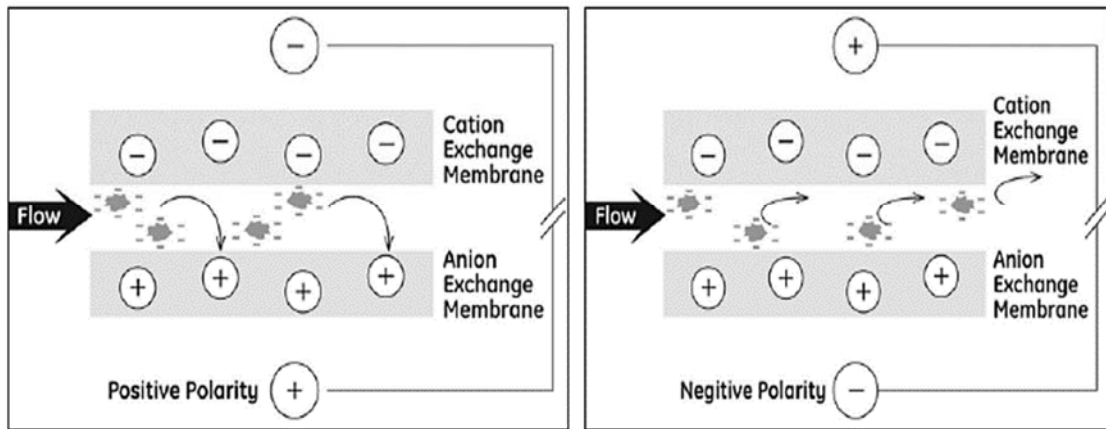


Figure 2.3. Scale Deposition and Scale Removal in EDR. Reprinted from A. R. P. Allison, 2008.

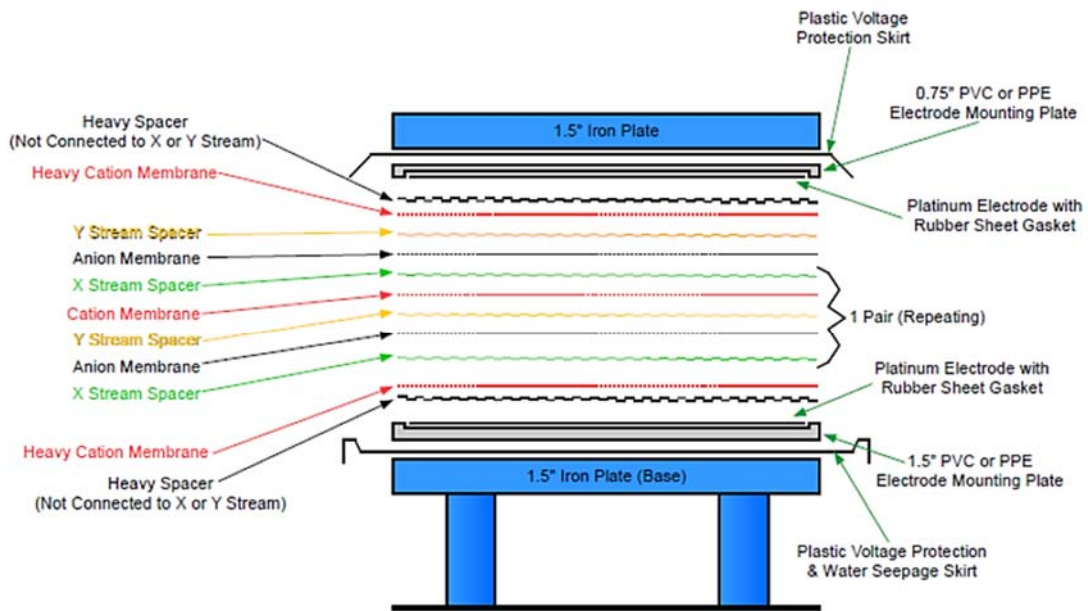


Figure 2.4. EDR Stack Diagram

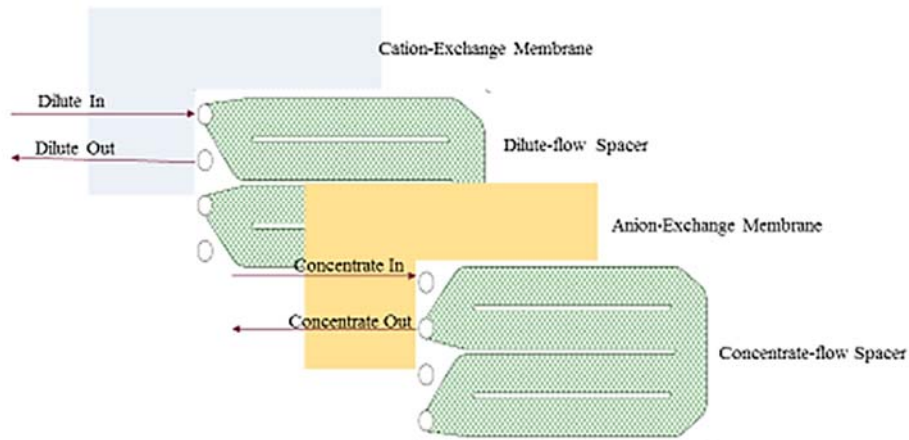


Figure 2.5. Cell Pair Schematic.

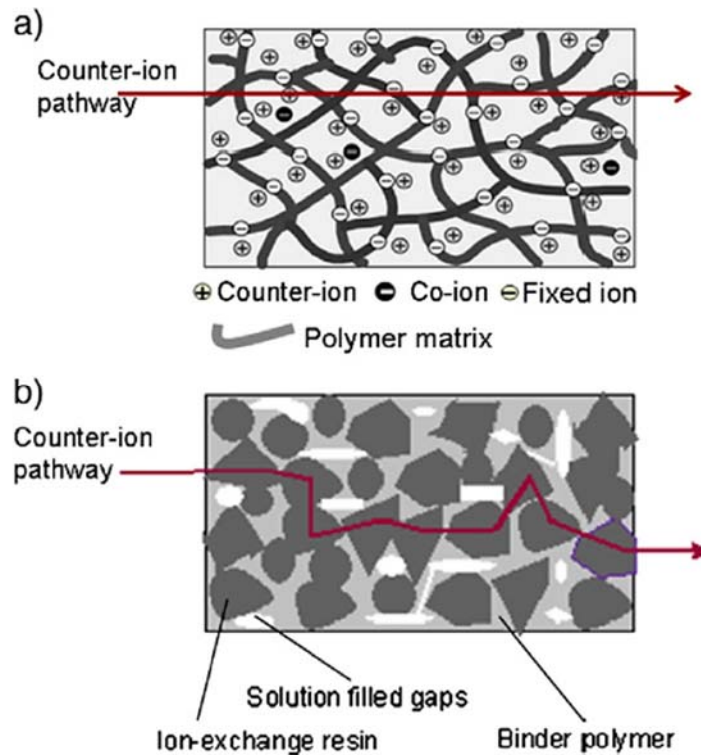


Figure 2.6. Schematic drawing illustrating a) a cation-exchange membrane with a homogeneous structure and b) an ion-exchange membrane with a heterogeneous structure prepared from anion-exchange resin powder and a binder polymer. Reprinted from Strathmann, 2004.

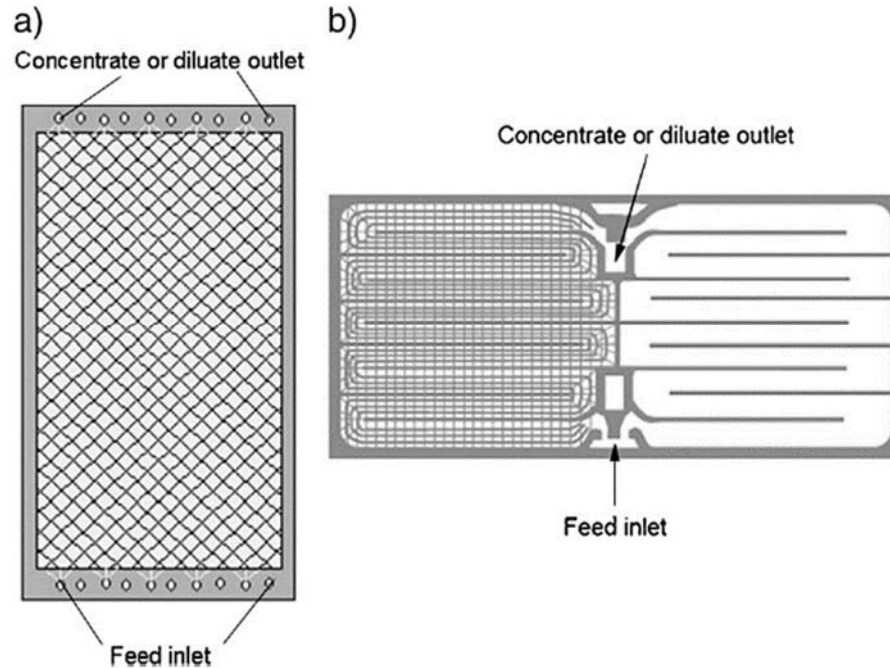


Figure 2.7. Schematic drawing illustrating a) the design of a sheet flow and b) a tortuous path flow spacer. Reprinted from Strathmann, 2010.

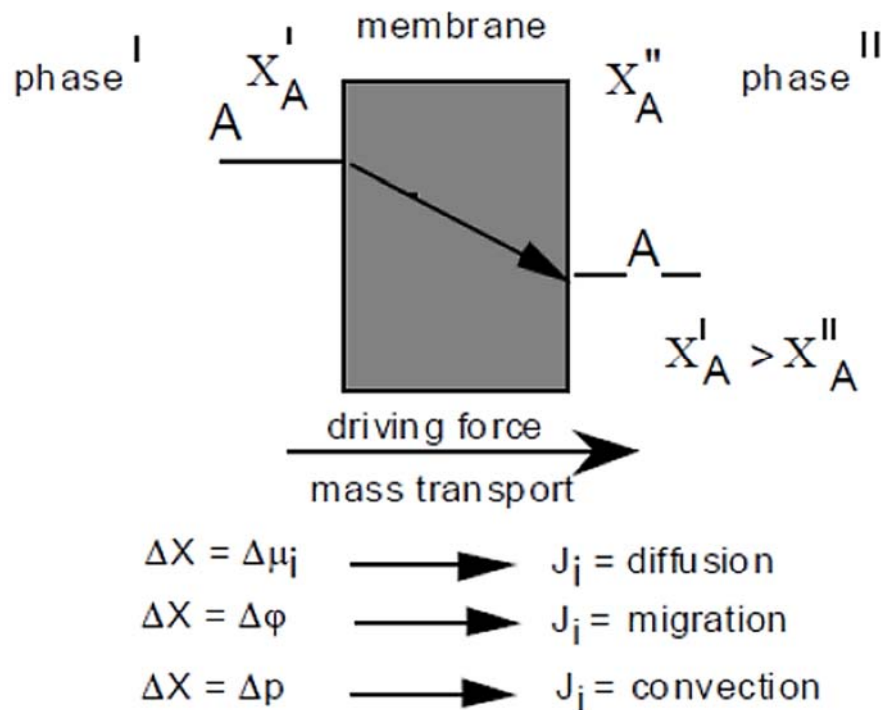


Figure 2.8. General forms of mass transport through the membrane. Reprinted from *Introduction to Membrane Science and Technology*, by H. Strathmann, 2011, Weinheim, Germany: Wiley-VCH.

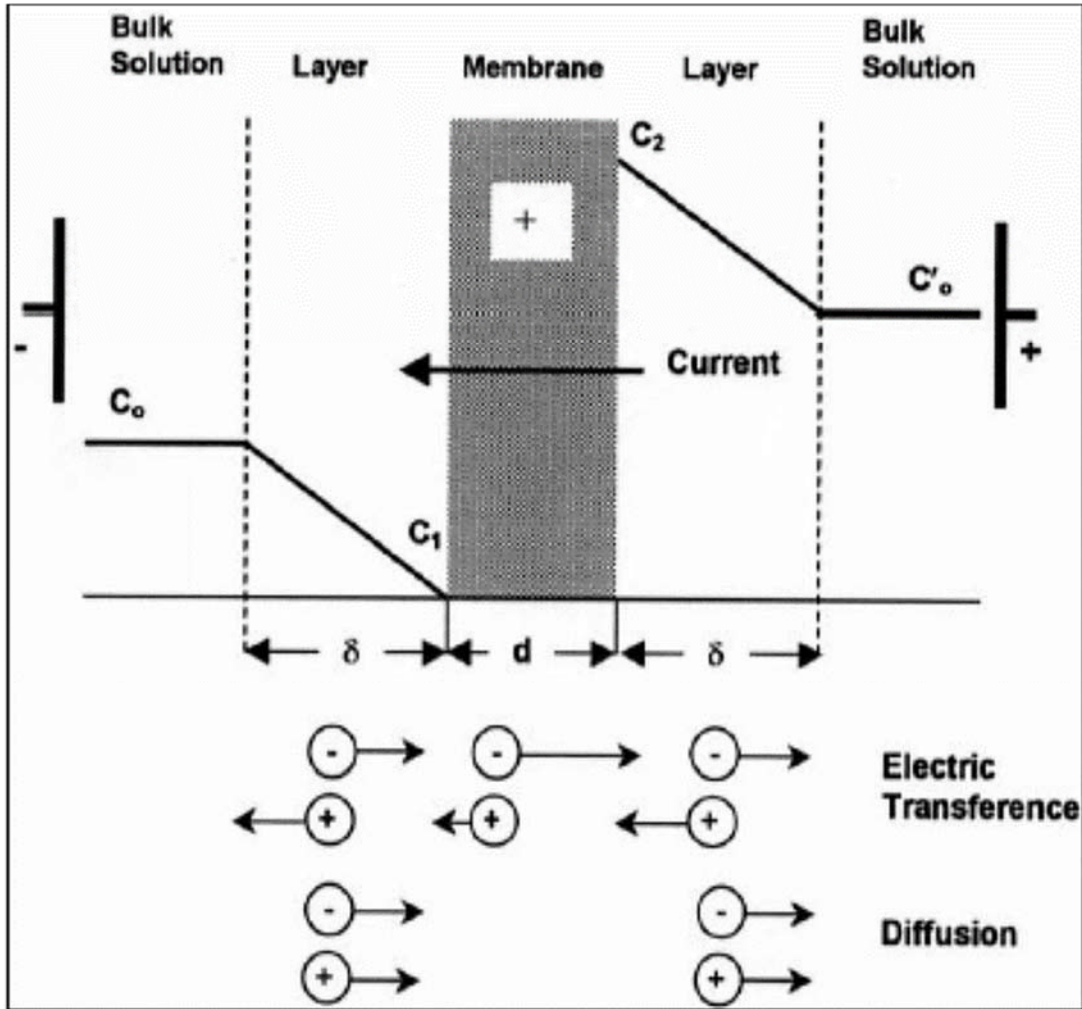


Figure 2.9. Counterion Concentration Profile in the Polarization Layers of an Ion-Exchange Membrane. Reprinted from Valerdi-Pérez et al., 2001.

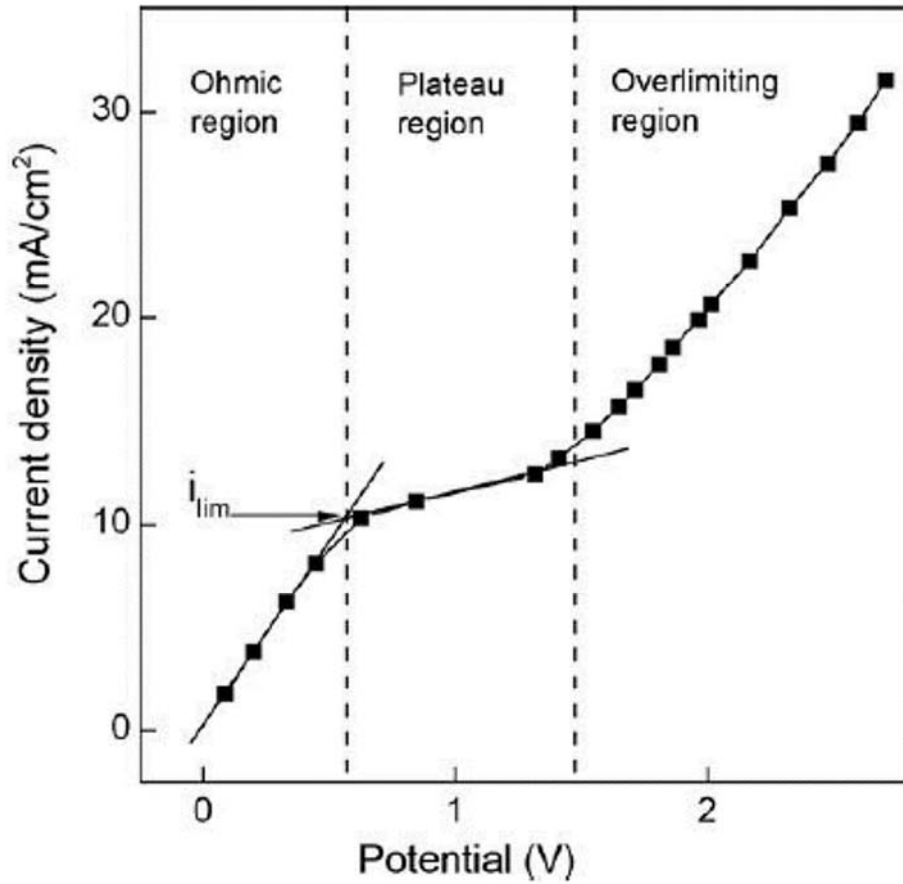


Figure 2.10. Typical Example of a Current-Voltage Curve. Reprinted from Długolecki et al., 2010.

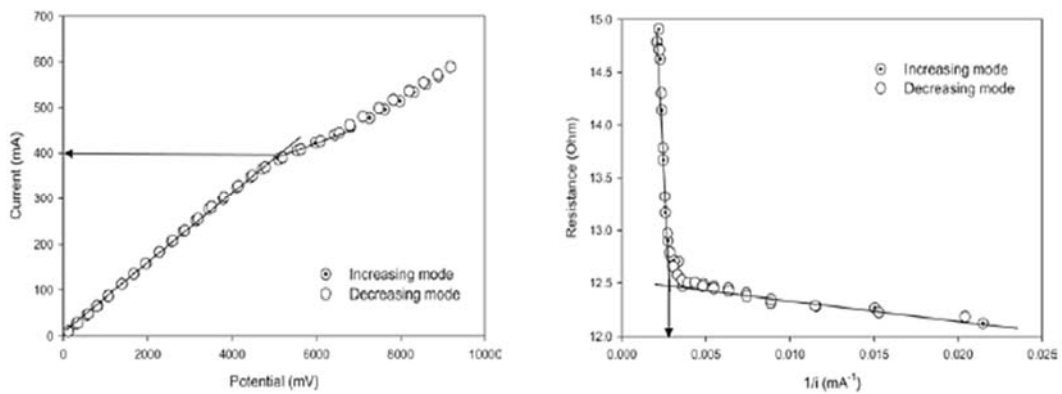


Figure 2.11. a) Current-Potential Relationship, and b) Cell Resistance-1/current Relationship Reprinted from H. J. Lee et al., 2006.

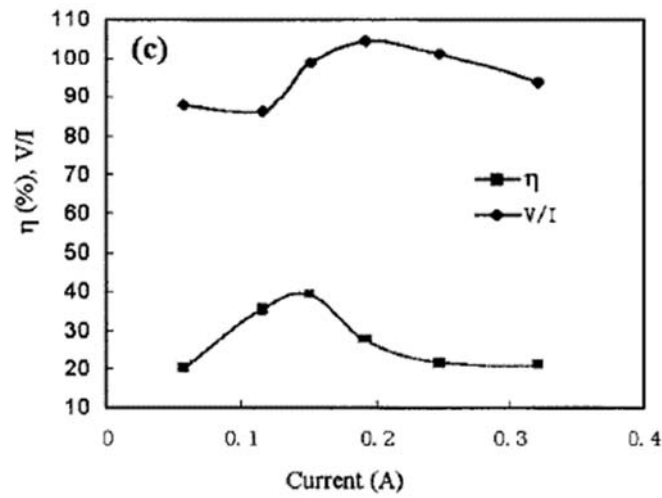


Figure 2.5. Removal Ratio-Current Relationship. Reprinted from Meng et al., 2005.

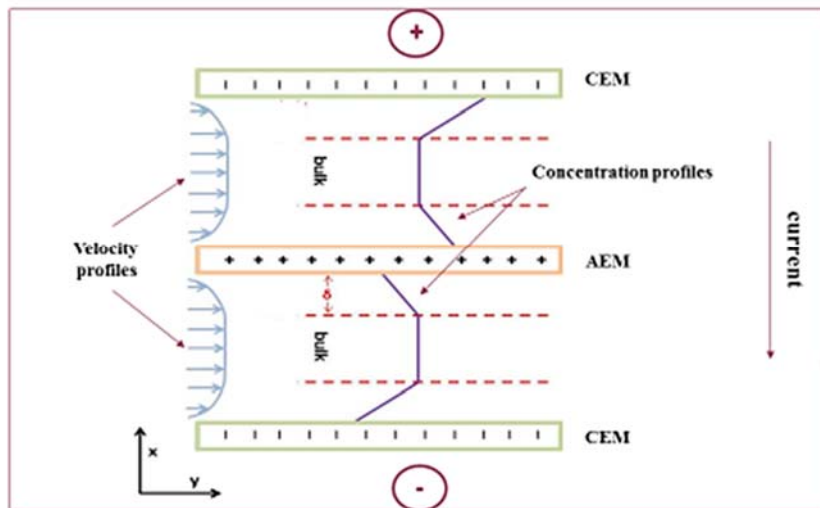


Figure 2.13. Schematic of Regions in a Cell Pair. Adapted from Moon et al., 2004

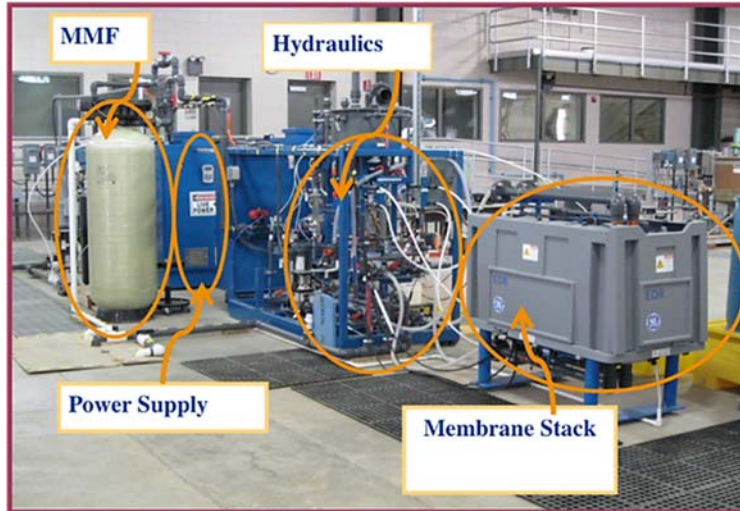


Figure 3.1. EDR pilot-scale set-up

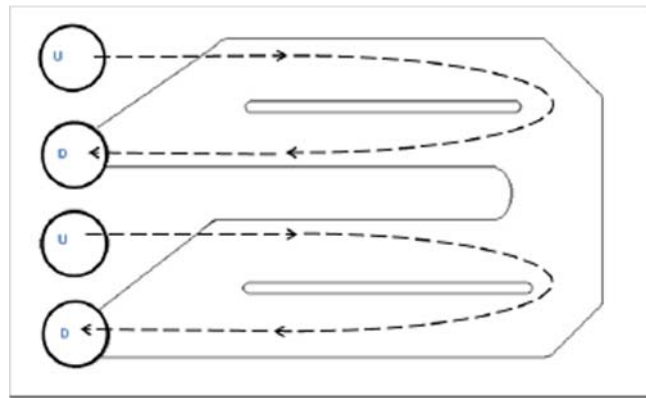


Figure 3.2. GE "MkIV-2" tortuous path spacer

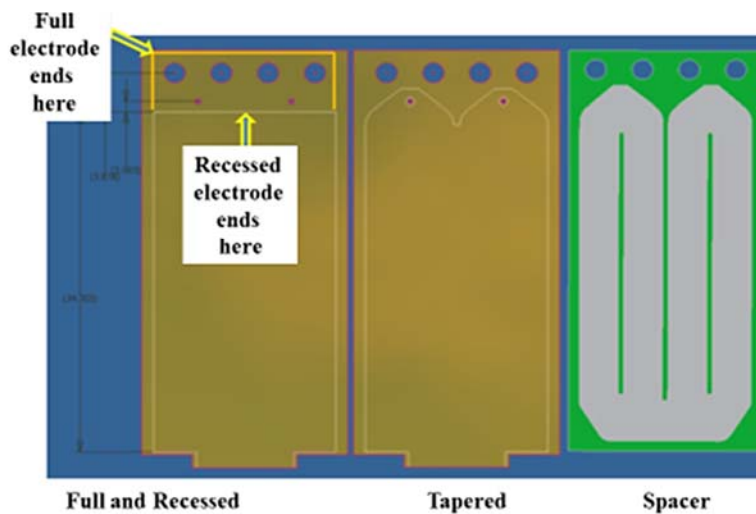
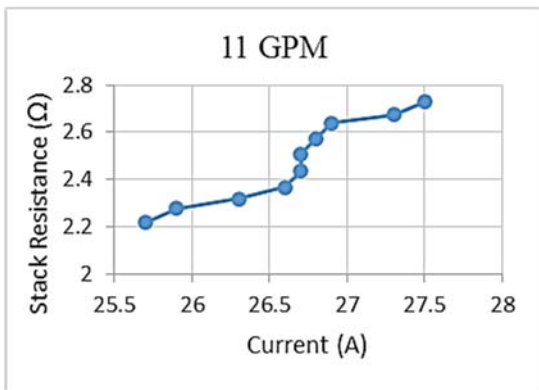
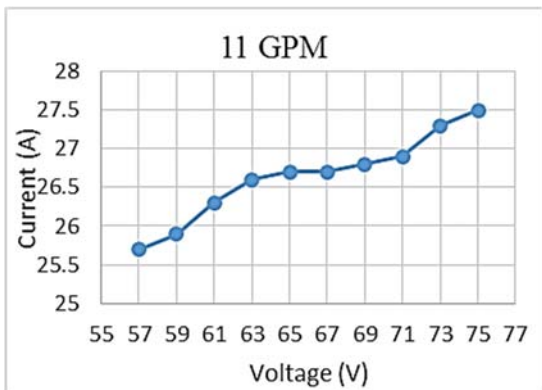
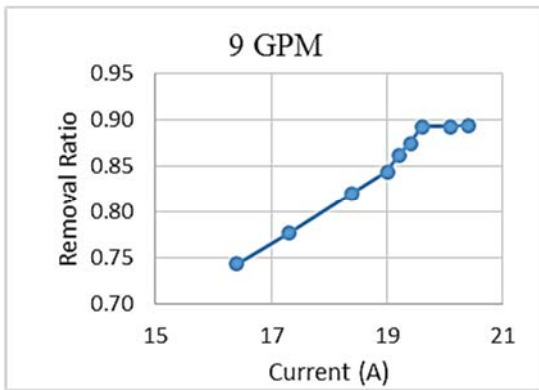
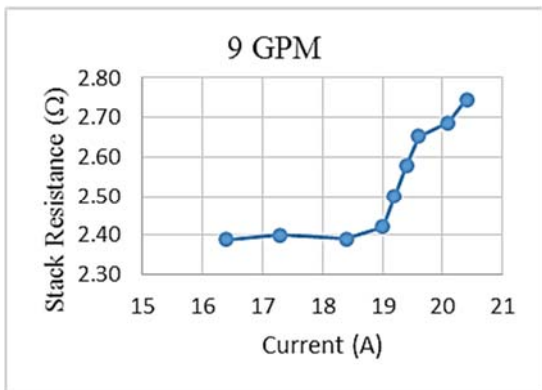
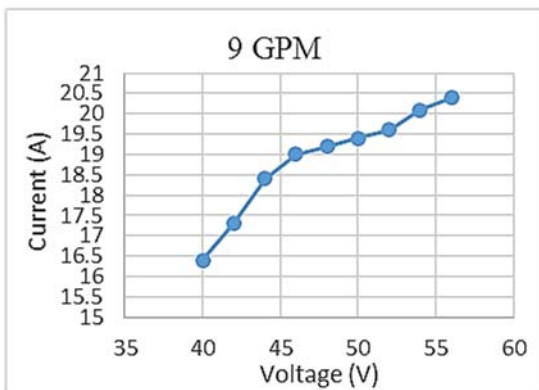
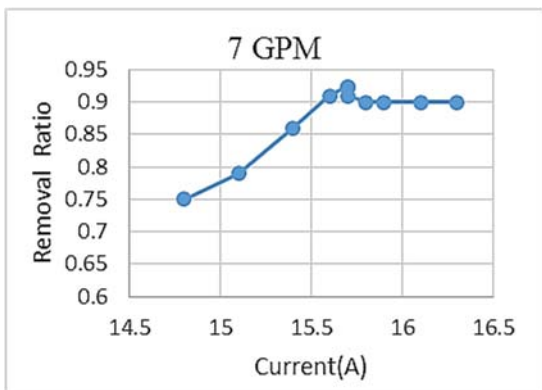
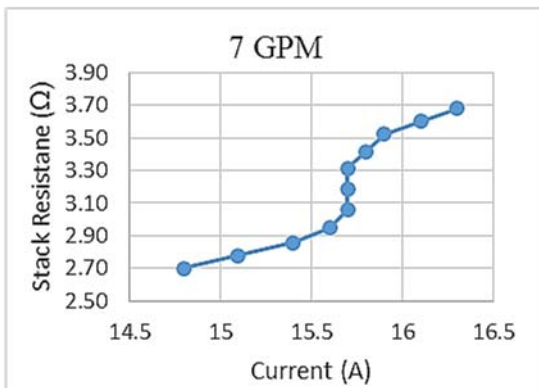
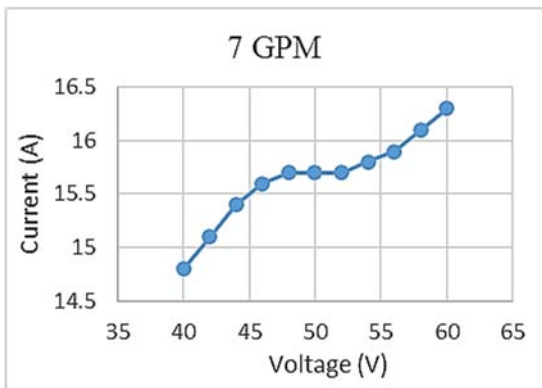


Figure 3.3. Illustration of electrode shapes



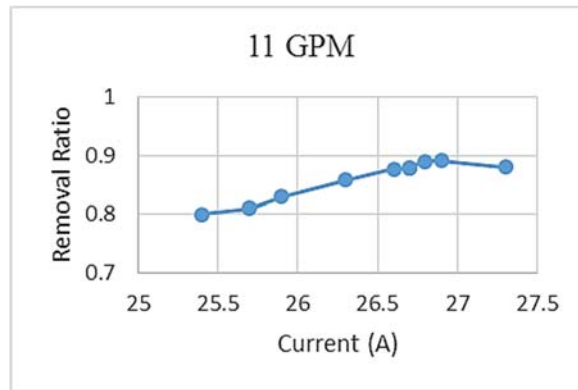
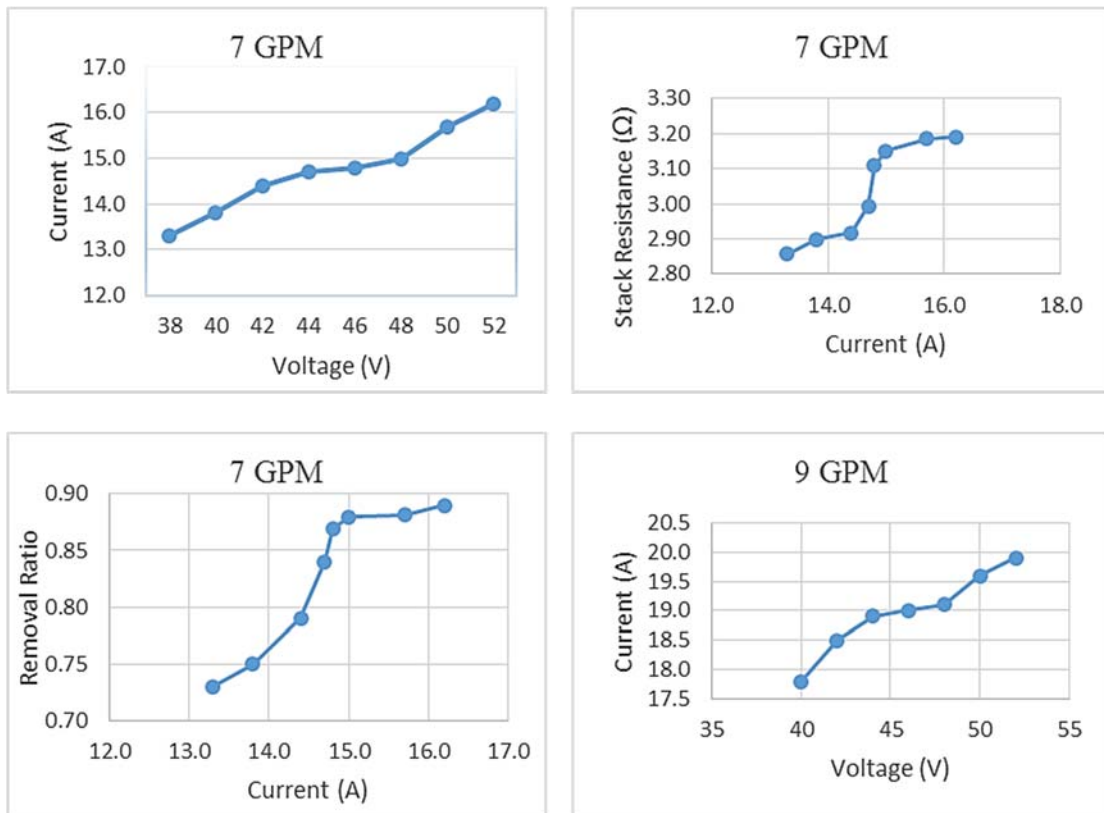


Figure 4.1. Limiting current curves for different feed flow rates – full electrode



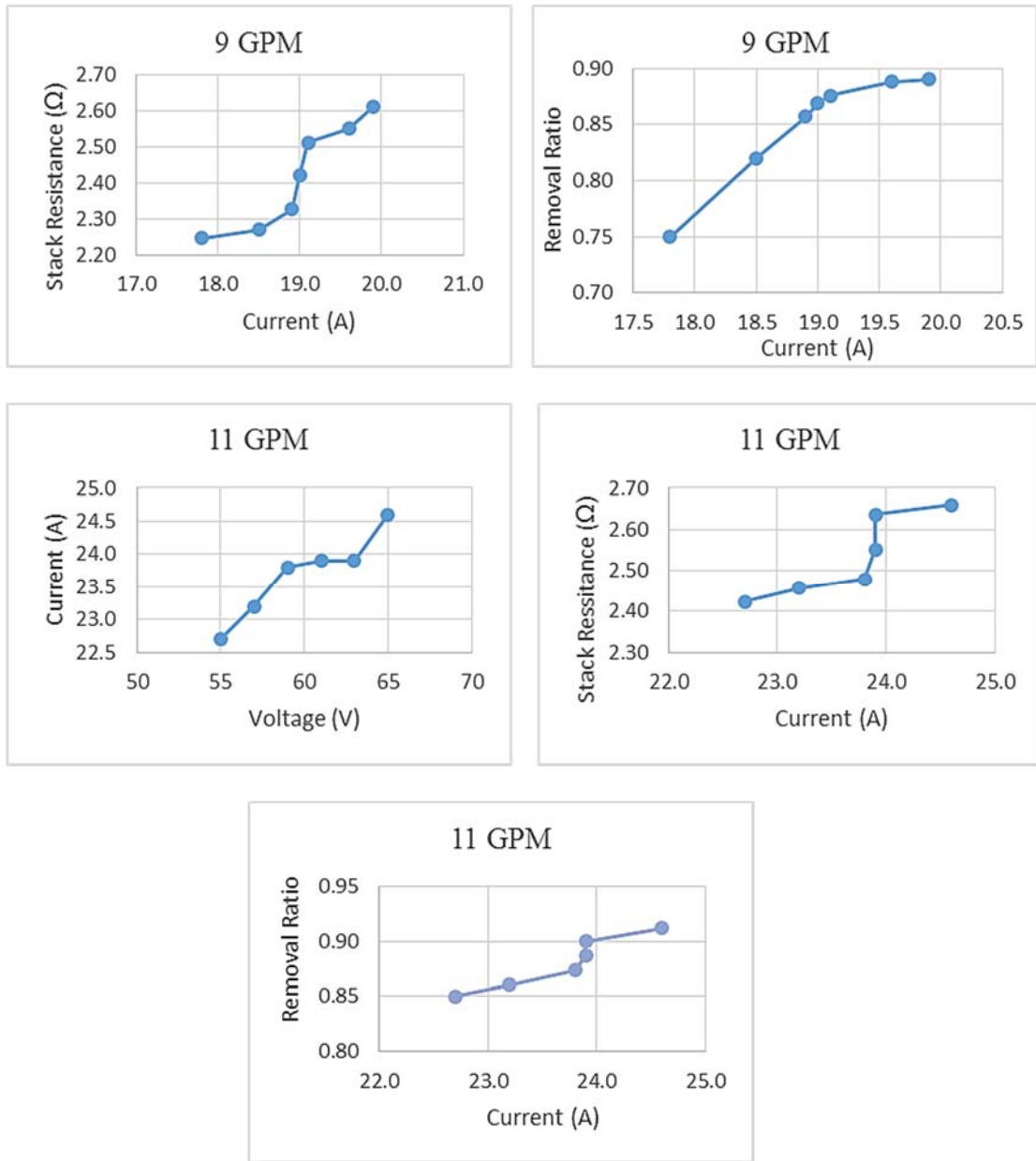
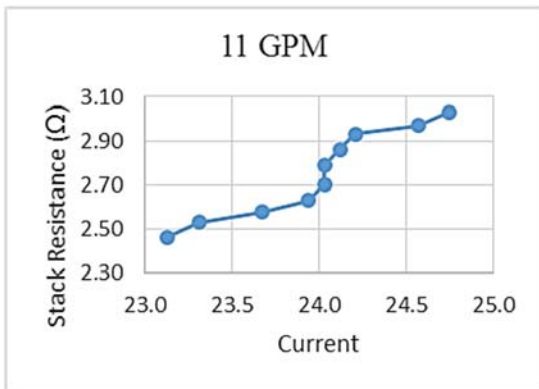
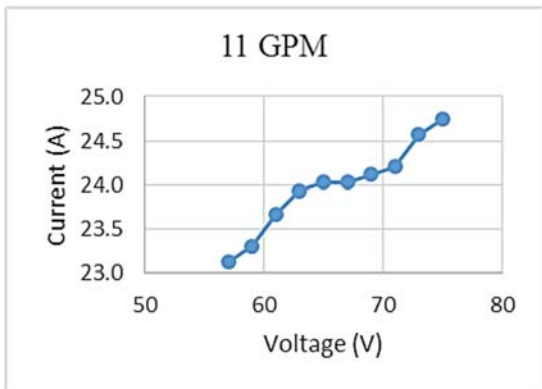
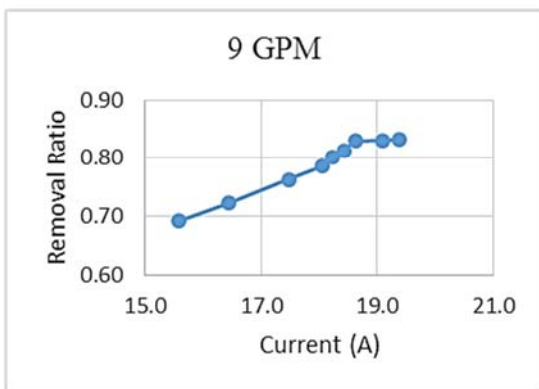
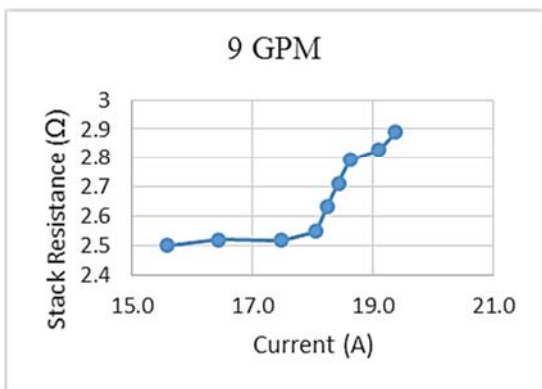
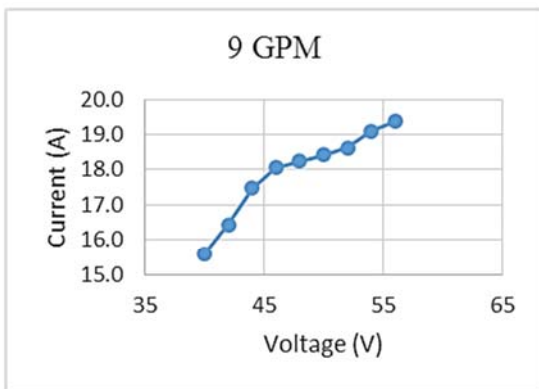
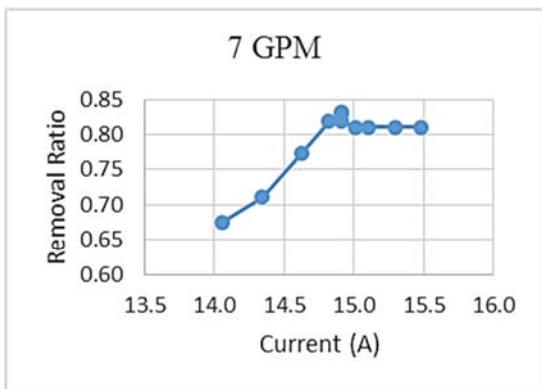
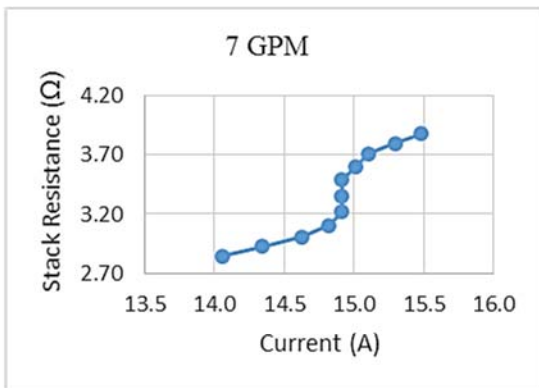
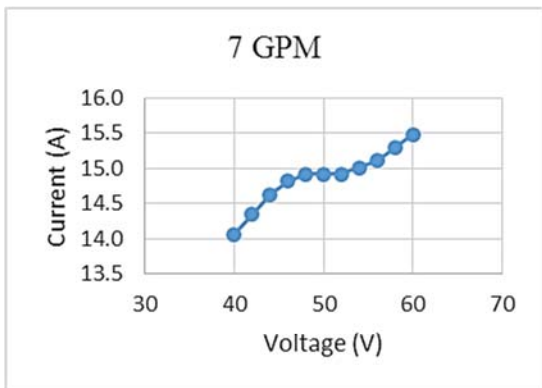


Figure 4.2. Limiting current curves for different feed flow rates – recessed electrode



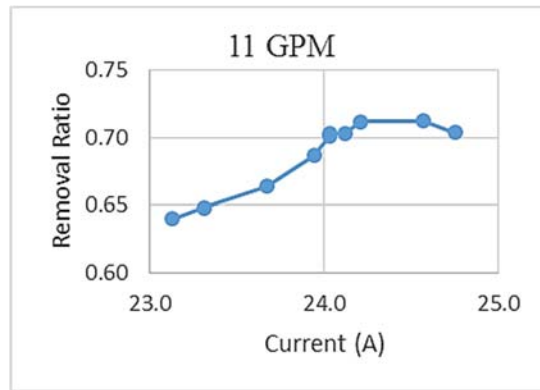


Figure 4.3. Limiting current curves for different feed flow rates – tapered electrode

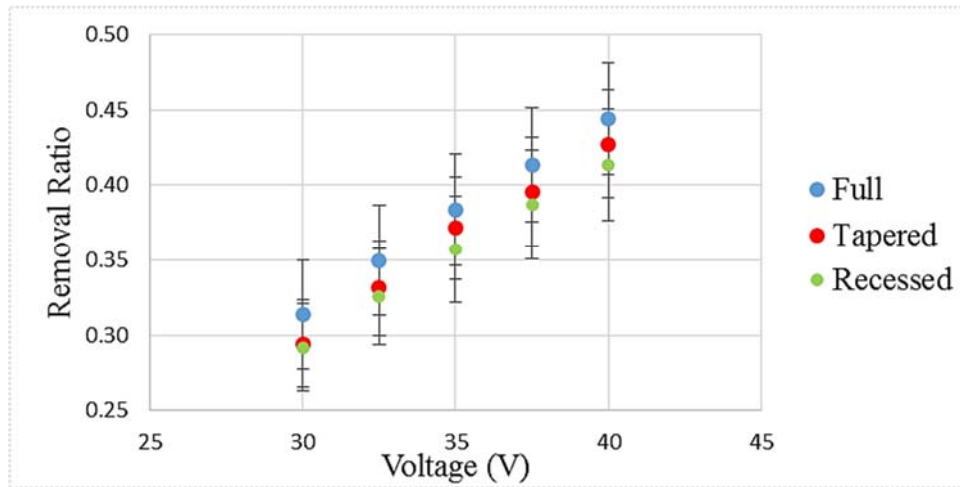


Figure 4.4. Effect of stack voltage on removal ratio

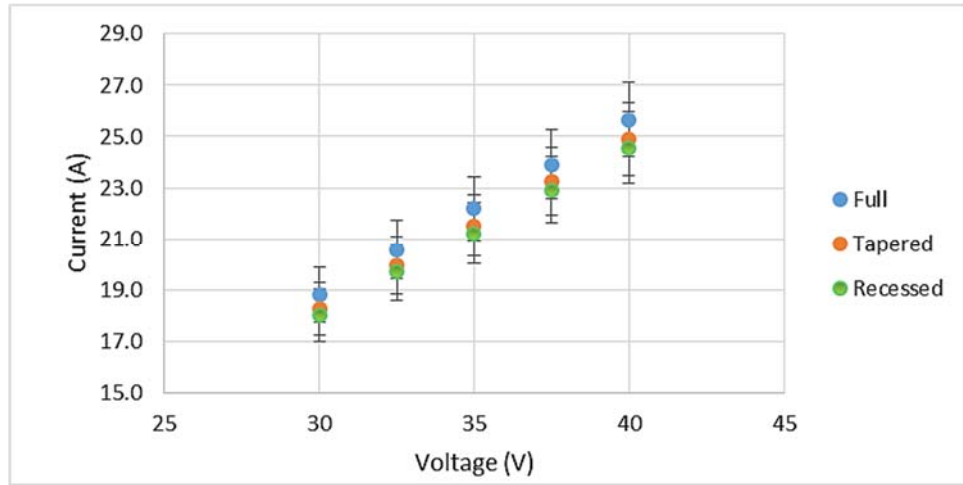


Figure 4.5. Effect of stack voltage on current

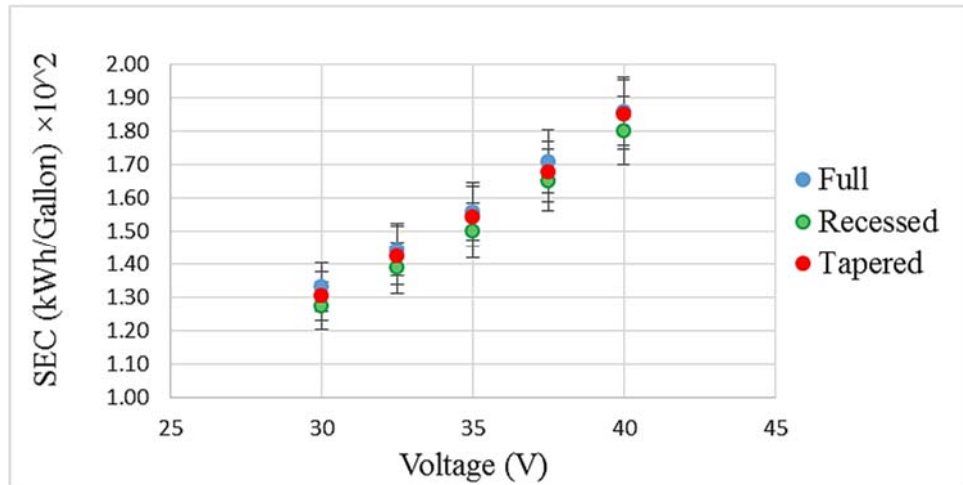


Figure 4.6. Effect of stack voltage on specific energy consumption

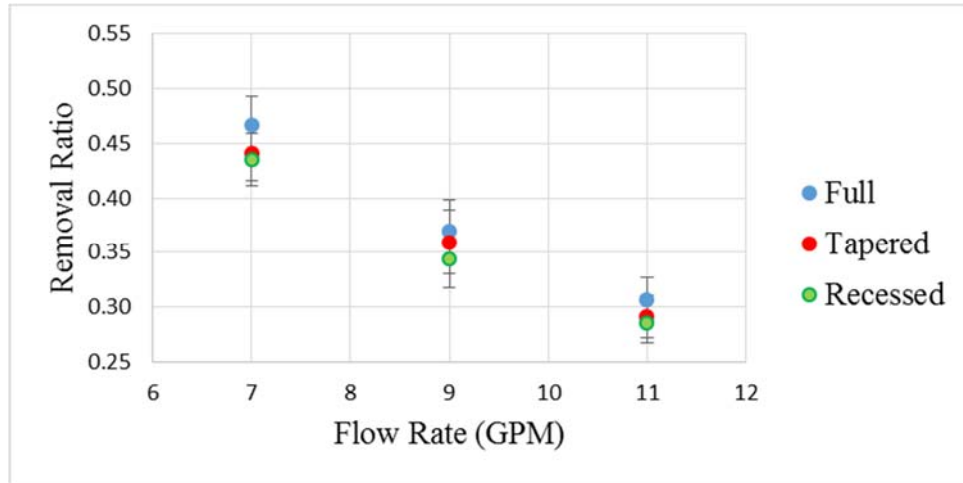


Figure 4.7. Effect of flow rate on removal ratio

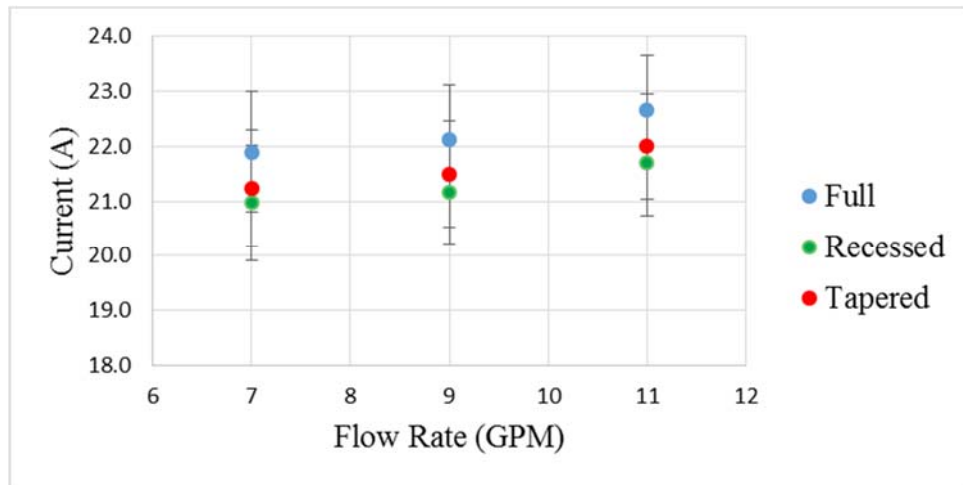


Figure 4.8. Effect of flow rate on current

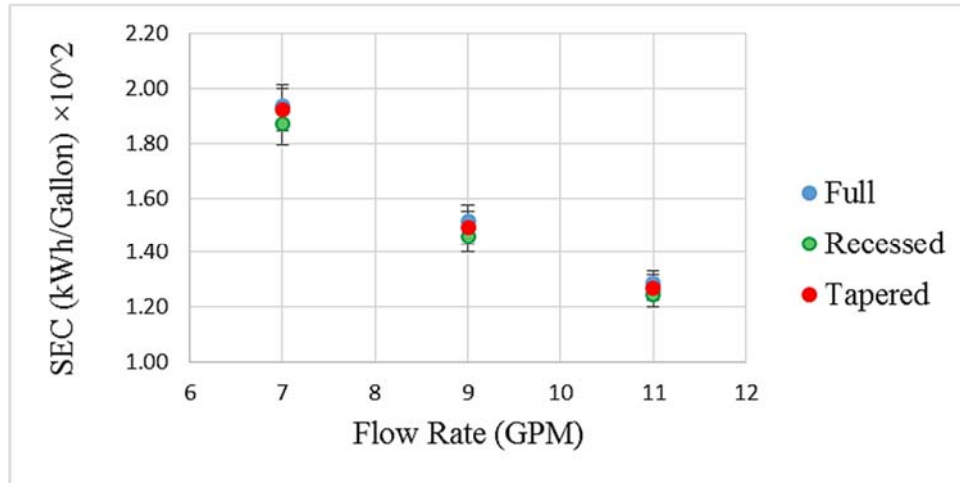


Figure 4.9. Effect of flow rate on specific energy consumption

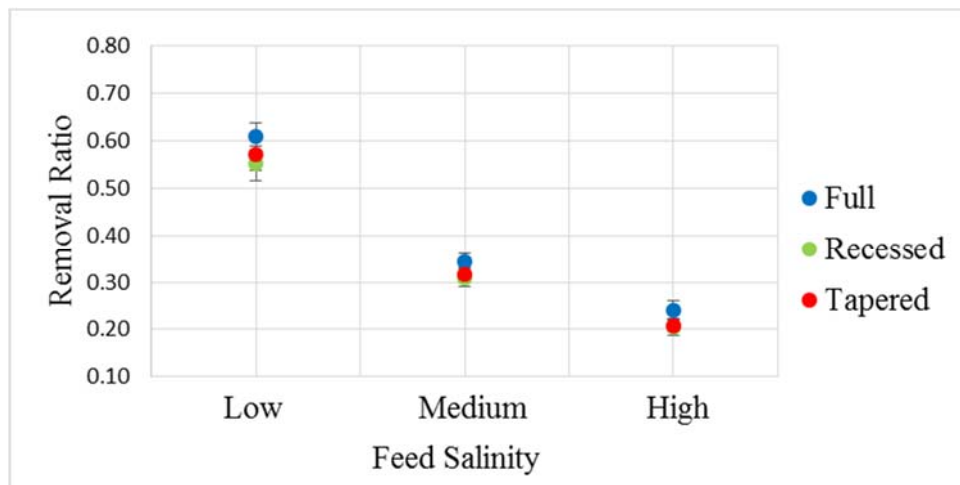


Figure 4.10. Effect of feed salinity on removal ratio

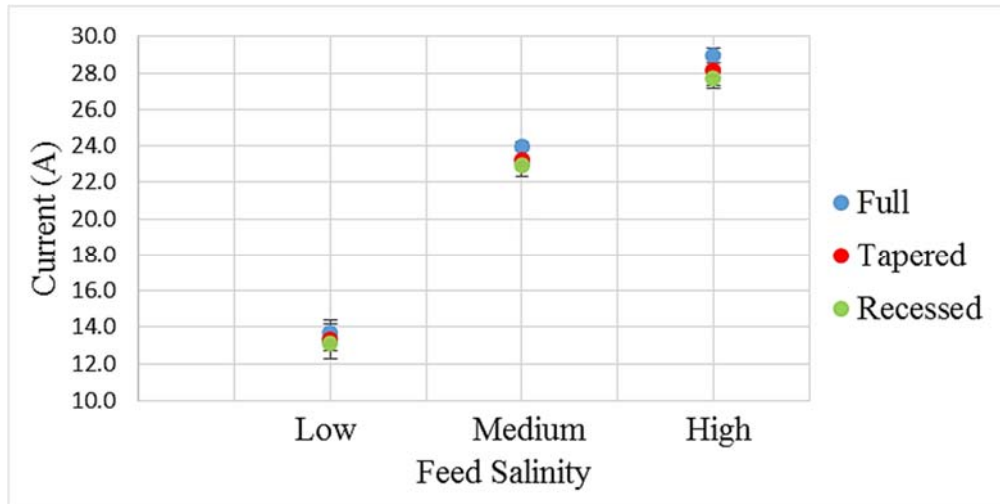


Figure 4.11. Effect of feed salinity on current

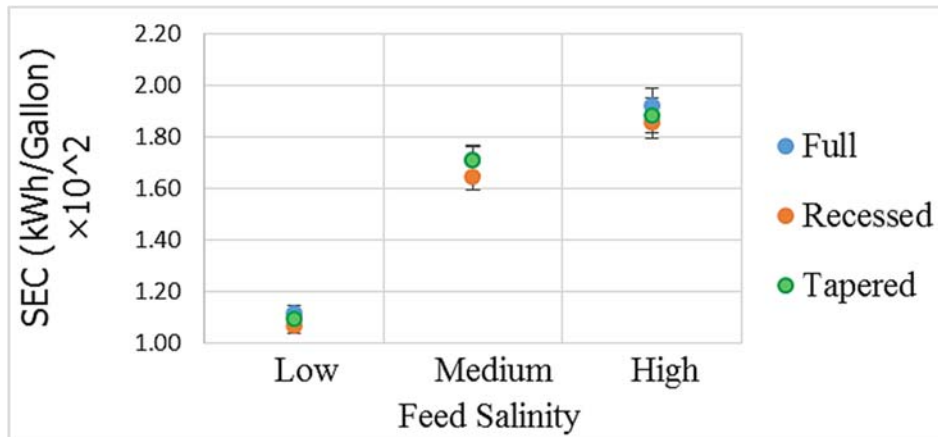


Figure 4.12. Effect of feed salinity on specific energy consumption

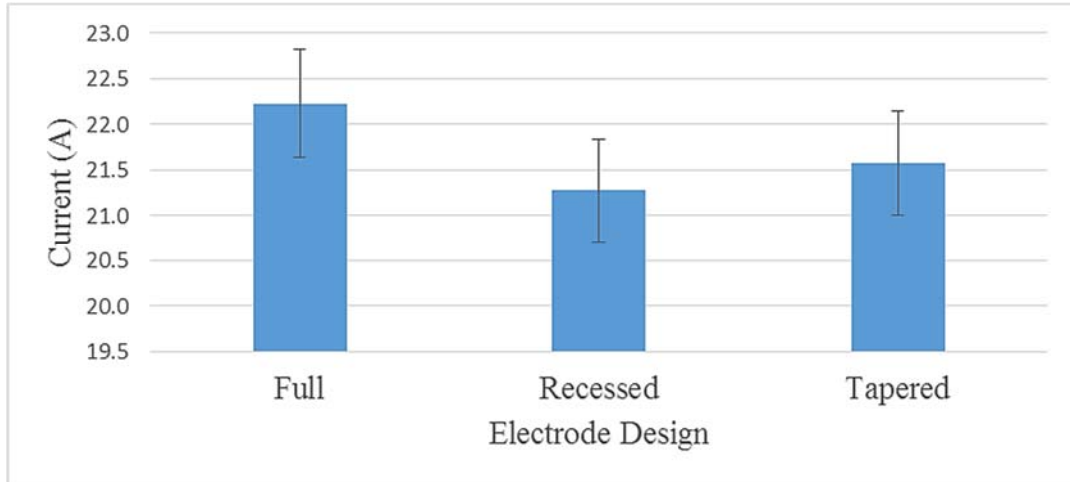


Figure 4.13. Effect of electrode design on current

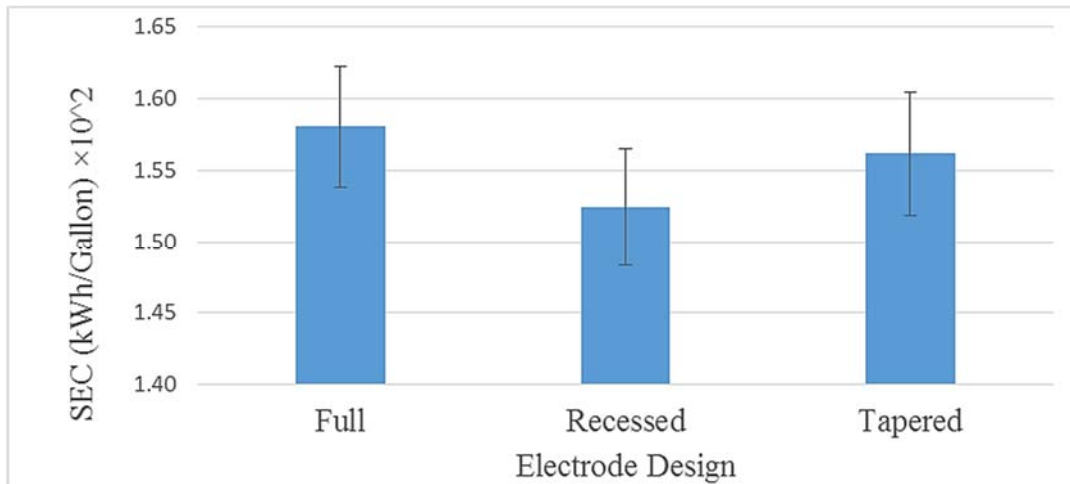


Figure 4.14. Effect of electrode design on specific energy consumption

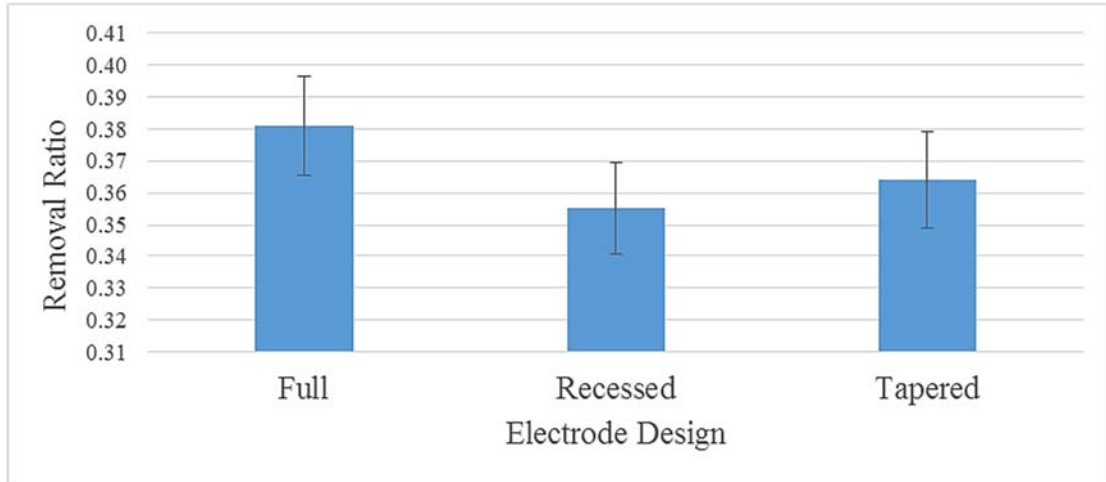


Figure 4.15. Effect of electrode design on removal ratio

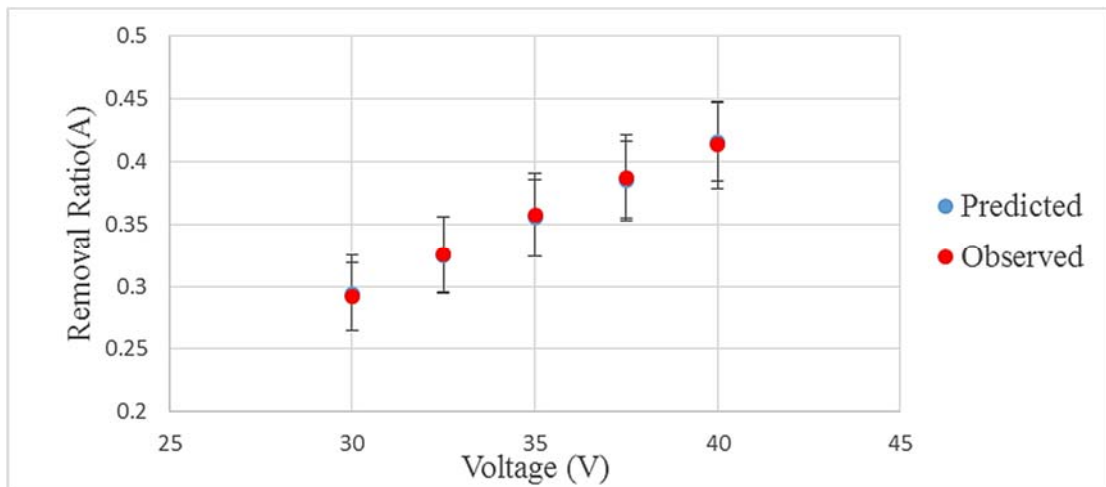


Figure 4.16. Effect of voltage on observed and predicted removal ratio

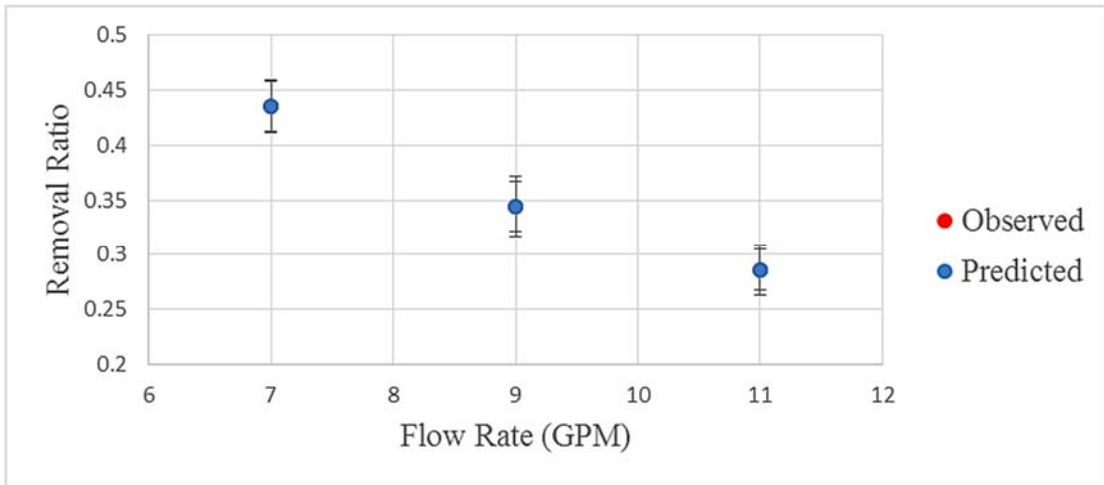


Figure 4.17. Effect of flow rate on observed and predicted removal ratio

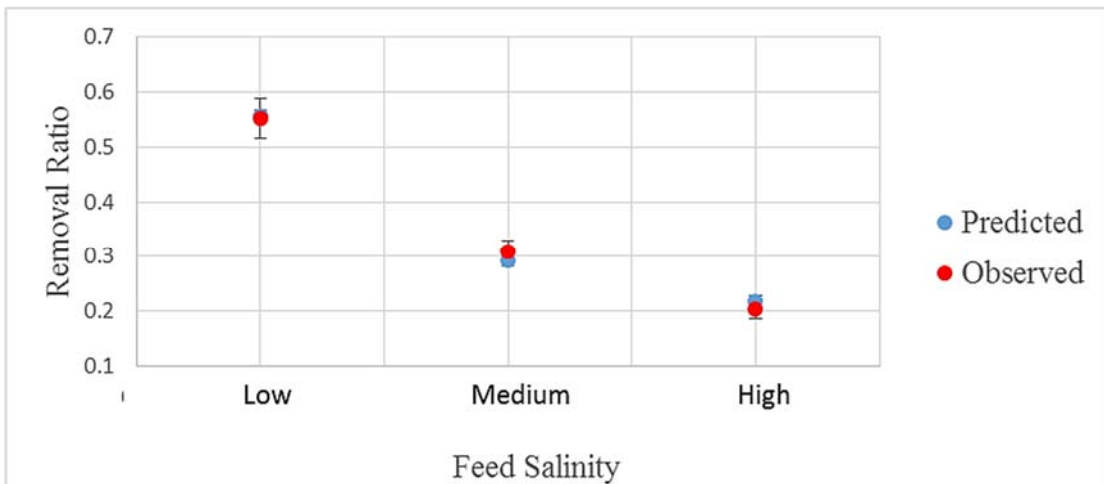


Figure 4.18. Effect of feed salinity on observed and predicted removal ratio

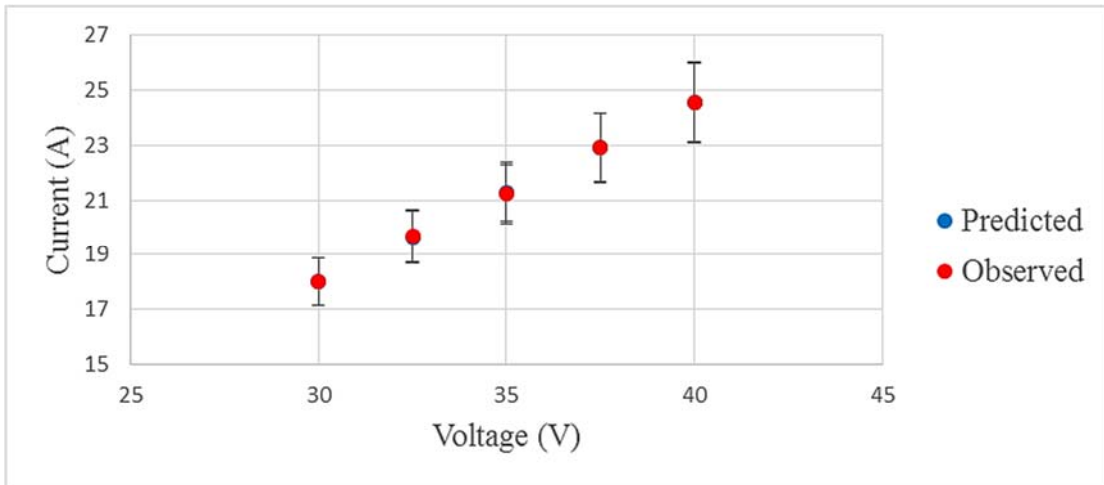


Figure 4.19. Effect of voltage on observed and predicted current

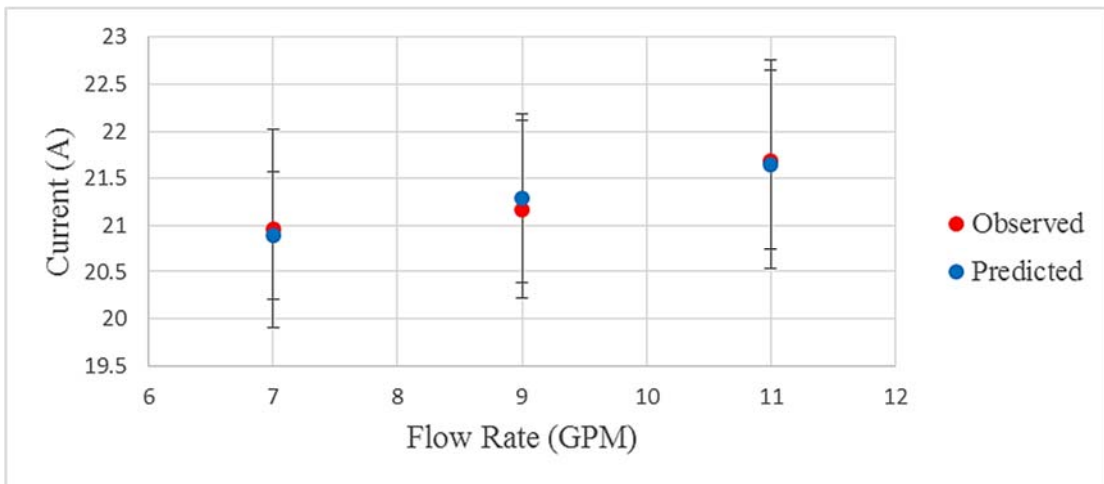


Figure 4.20. Effect of flow rate on observed and predicted current

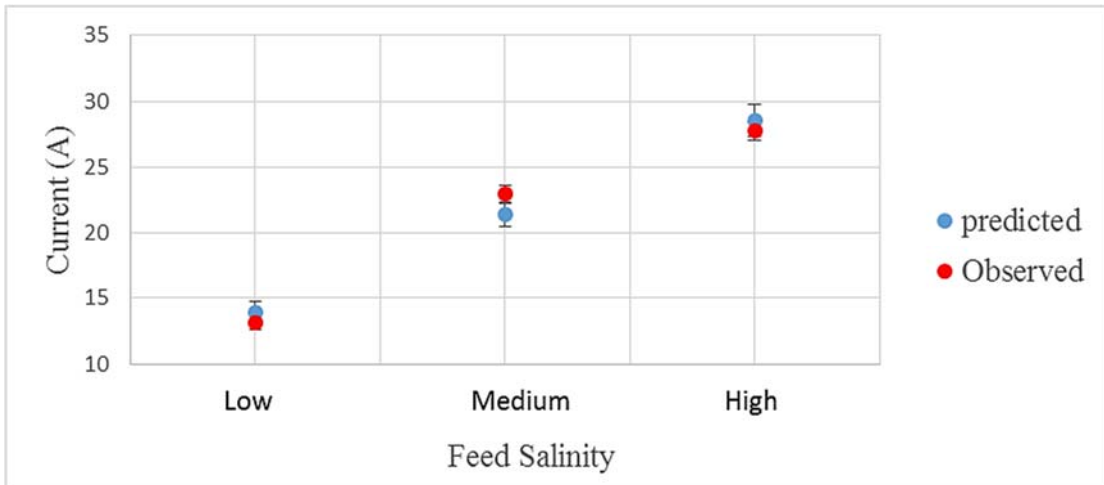


Figure 4.21. Effect of feed salinity on observed and predicted current

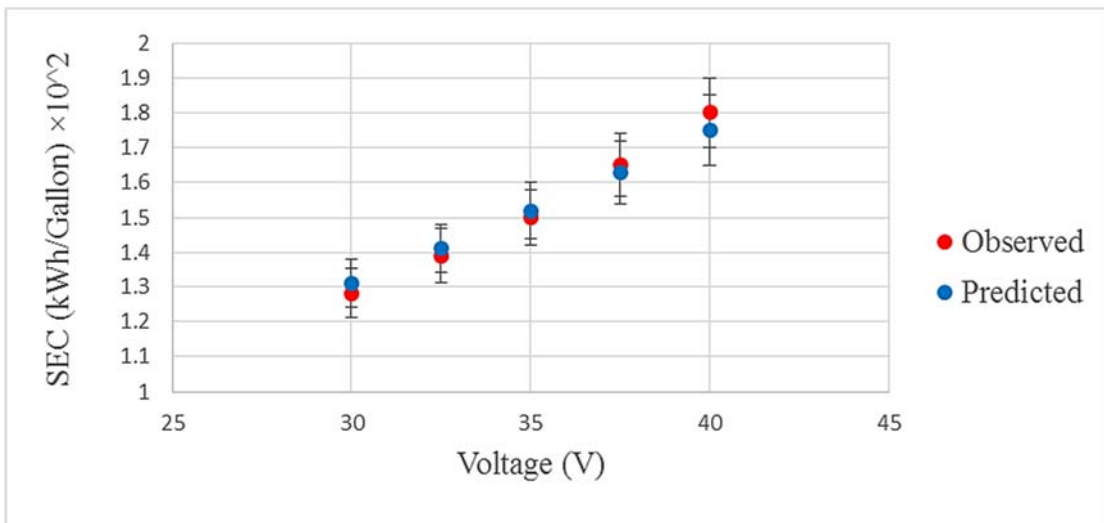


Figure 4.22. Effect of voltage on observed and predicted specific energy consumption

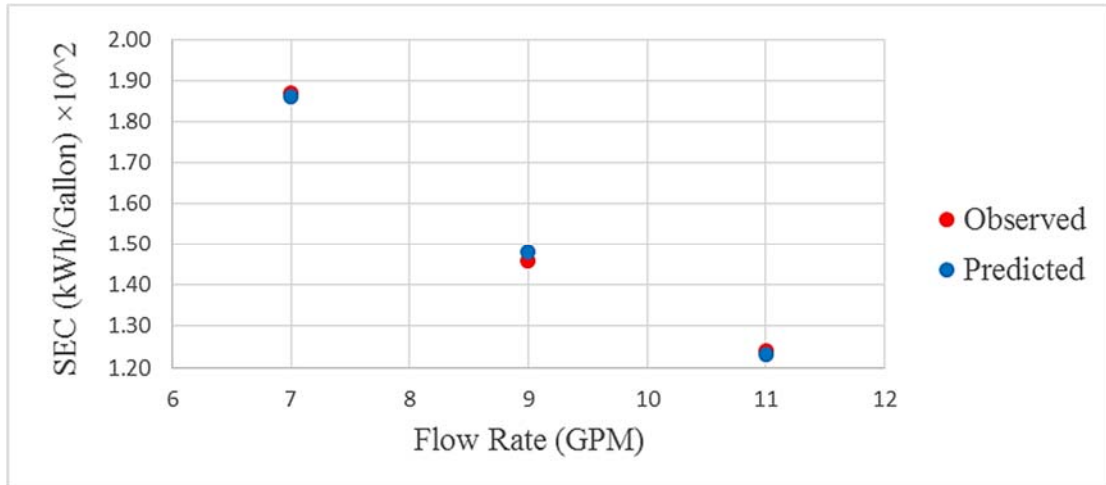


Figure 4.23. Effect of flow rate on observed and predicted specific energy consumption

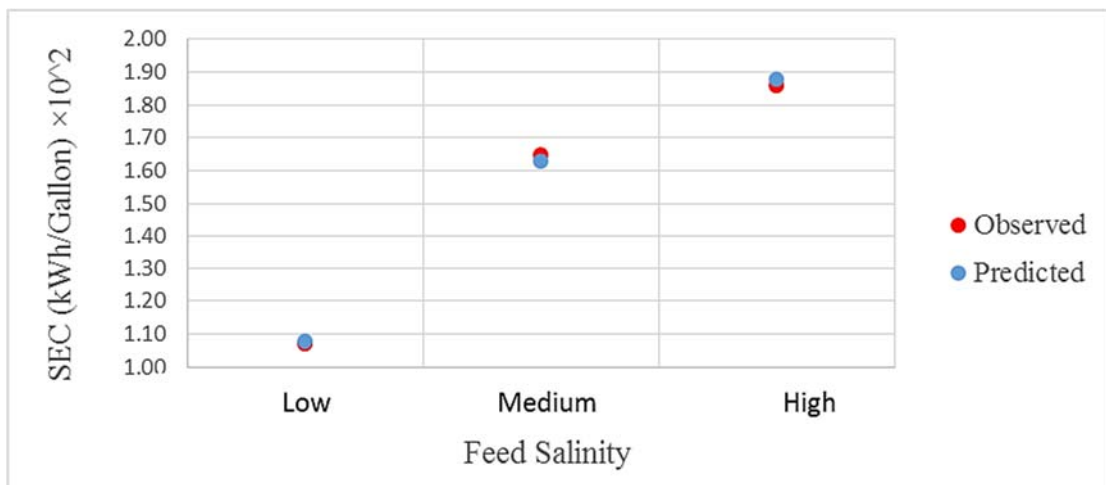


Figure 4.24. Effect of feed salinity on observed and predicted specific energy consumption

Appendices

Data Record

Table-1 data table for response variables

Electrode Type	Well Salinity	Feed Flow Rate (GPM)	Feed Conductivity (ms/cm)	Voltage (V)	Current (A)	Removal Ratio	SEC (kWh/GPM)
Recessed	Low	7	1.811	30.0	10.4	0.52	0.0115
Recessed	Low	7	1.814	32.5	11.2	0.59	0.0121
Recessed	Low	7	1.814	35.0	12.0	0.66	0.0128
Recessed	Low	7	1.813	37.5	12.8	0.69	0.0133
Recessed	Low	7	1.816	40.0	13.6	0.72	0.0137
Recessed	Low	9	1.813	30.0	11.6	0.50	0.0080
Recessed	Low	9	1.813	32.5	12.8	0.54	0.0092
Recessed	Low	9	1.814	35.0	13.4	0.59	0.0103
Recessed	Low	9	1.813	37.5	14.4	0.62	0.0116
Recessed	Low	9	1.814	40.0	15.4	0.64	0.0129
Recessed	Low	11	1.816	30.0	11.6	0.36	0.0082
Recessed	Low	11	1.815	32.5	12.8	0.40	0.0083
Recessed	Low	11	1.815	35.0	13.9	0.43	0.0084
Recessed	Low	11	1.814	37.5	15.1	0.50	0.0095
Recessed	Low	11	1.814	40.0	16.2	0.53	0.0106
Recessed	Low	7	1.809	30.0	10.6	0.54	0.0120
Recessed	Low	7	1.811	32.5	11.3	0.62	0.0125
Recessed	Low	7	1.810	35.0	12.3	0.67	0.0132
Recessed	Low	7	1.807	37.5	13.0	0.71	0.0139

Recessed	Low	7	1.809	40.0	14.0	0.73	0.0141
Recessed	Low	9	1.811	30.0	11.9	0.51	0.0085
Recessed	Low	9	1.810	32.5	12.9	0.57	0.0096
Recessed	Low	9	1.807	35.0	13.6	0.61	0.0108
Recessed	Low	9	1.809	37.5	14.7	0.63	0.0120
Recessed	Low	9	1.806	40.0	15.7	0.67	0.0133
Recessed	Low	11	1.810	30.0	12.0	0.39	0.0086
Recessed	Low	11	1.811	32.5	13.0	0.41	0.0086
Recessed	Low	11	1.807	35.0	14.0	0.44	0.0087
Recessed	Low	11	1.809	37.5	15.4	0.52	0.0100
Recessed	Low	11	1.807	40.0	16.5	0.56	0.0111
Recessed	Low	7	1.811	30.0	10.2	0.50	0.0109
Recessed	Low	7	1.809	32.5	11.1	0.57	0.0117
Recessed	Low	7	1.810	35.0	11.7	0.65	0.0124
Recessed	Low	7	1.808	37.5	12.6	0.66	0.0126
Recessed	Low	7	1.809	40.0	13.2	0.70	0.0133
Recessed	Low	9	1.811	30.0	11.3	0.48	0.0075
Recessed	Low	9	1.808	32.5	12.6	0.52	0.0087
Recessed	Low	9	1.809	35.0	13.2	0.57	0.0098
Recessed	Low	9	1.810	37.5	14.1	0.60	0.0112
Recessed	Low	9	1.809	40.0	15.1	0.61	0.0125
Recessed	Low	11	1.810	30.0	11.2	0.34	0.0078
Recessed	Low	11	1.807	32.5	12.6	0.38	0.0079
Recessed	Low	11	1.807	35.0	13.8	0.41	0.0080
Recessed	Low	11	1.809	37.5	14.8	0.48	0.0091
Recessed	Low	11	1.808	40.0	15.9	0.51	0.0102
Recessed	Medium	7	3.940	30.0	19.3	0.32	0.0168
Recessed	Medium	7	3.930	32.5	21.2	0.36	0.0186

Recessed	Medium	7	3.940	35.0	22.8	0.39	0.0203
Recessed	Medium	7	3.950	37.5	24.6	0.41	0.0221
Recessed	Medium	7	3.940	40.0	26.2	0.45	0.0238
Recessed	Medium	9	3.930	30.0	18.8	0.24	0.0125
Recessed	Medium	9	3.930	32.5	20.8	0.27	0.0141
Recessed	Medium	9	3.930	35.0	22.7	0.30	0.0156
Recessed	Medium	9	3.940	37.5	24.5	0.33	0.0172
Recessed	Medium	9	3.940	40.0	26.4	0.35	0.0188
Recessed	Medium	11	3.940	30.0	19.6	0.20	0.0113
Recessed	Medium	11	3.930	32.5	21.6	0.22	0.0124
Recessed	Medium	11	3.940	35.0	23.5	0.24	0.0134
Recessed	Medium	11	3.950	37.5	25.3	0.27	0.0145
Recessed	Medium	11	3.950	40.0	27.1	0.29	0.0156
Recessed	Medium	7	3.940	30.0	19.7	0.35	0.0174
Recessed	Medium	7	3.930	32.5	21.5	0.38	0.0190
Recessed	Medium	7	3.940	35.0	23.2	0.41	0.0210
Recessed	Medium	7	3.940	37.5	24.9	0.44	0.0227
Recessed	Medium	7	3.940	40.0	26.4	0.47	0.0245
Recessed	Medium	9	3.940	30.0	19.1	0.26	0.0129
Recessed	Medium	9	3.940	32.5	21.0	0.28	0.0146
Recessed	Medium	9	3.940	35.0	23.1	0.31	0.0160
Recessed	Medium	9	3.940	37.5	24.8	0.35	0.0176
Recessed	Medium	9	3.940	40.0	26.7	0.36	0.0192
Recessed	Medium	11	3.940	30.0	19.9	0.21	0.0115
Recessed	Medium	11	3.930	32.5	21.9	0.24	0.0127
Recessed	Medium	11	3.950	35.0	23.9	0.27	0.0137
Recessed	Medium	11	3.950	37.5	25.5	0.29	0.0148
Recessed	Medium	11	3.950	40.0	27.2	0.32	0.0160

Recessed	Medium	7	3.930	30.0	18.9	0.30	0.0163
Recessed	Medium	7	3.930	32.5	20.9	0.33	0.0181
Recessed	Medium	7	3.940	35.0	22.4	0.37	0.0196
Recessed	Medium	7	3.940	37.5	24.3	0.39	0.0215
Recessed	Medium	7	3.940	40.0	26.0	0.43	0.0231
Recessed	Medium	9	3.930	30.0	18.5	0.22	0.0121
Recessed	Medium	9	3.930	32.5	20.6	0.26	0.0136
Recessed	Medium	9	3.930	35.0	22.3	0.28	0.0153
Recessed	Medium	9	3.930	37.5	24.2	0.30	0.0168
Recessed	Medium	9	3.940	40.0	26.1	0.34	0.0183
Recessed	Medium	11	3.940	30.0	19.3	0.19	0.0110
Recessed	Medium	11	3.940	32.5	21.3	0.20	0.0120
Recessed	Medium	11	3.940	35.0	23.1	0.21	0.0132
Recessed	Medium	11	3.940	37.5	25.1	0.24	0.0142
Recessed	Medium	11	3.940	40.0	27.0	0.26	0.0153
Recessed	High	7	5.990	30.0	24.7	0.21	0.0196
Recessed	High	7	5.990	32.5	26.3	0.25	0.0211
Recessed	High	7	5.987	35.0	27.8	0.29	0.0225
Recessed	High	7	5.945	37.5	29.8	0.32	0.0250
Recessed	High	7	5.945	40.0	31.8	0.35	0.0274
Recessed	High	9	5.950	30.0	22.7	0.13	0.0144
Recessed	High	9	5.975	32.5	25.0	0.14	0.0158
Recessed	High	9	6.000	35.0	27.2	0.15	0.0172
Recessed	High	9	6.005	37.5	29.7	0.18	0.0195
Recessed	High	9	6.010	40.0	32.2	0.20	0.0217
Recessed	High	11	5.935	30.0	23.3	0.15	0.0125
Recessed	High	11	5.940	32.5	25.5	0.16	0.0135
Recessed	High	11	5.965	35.0	27.7	0.17	0.0146

Recessed	High	11	5.990	37.5	30.0	0.18	0.0161
Recessed	High	11	5.990	40.0	32.2	0.19	0.0177
Recessed	High	7	5.990	30.0	24.9	0.23	0.0200
Recessed	High	7	5.990	32.5	26.4	0.26	0.0215
Recessed	High	7	5.987	35.0	28.0	0.31	0.0231
Recessed	High	7	5.945	37.5	29.9	0.33	0.0255
Recessed	High	7	5.945	40.0	31.9	0.37	0.0279
Recessed	High	9	5.950	30.0	23.0	0.14	0.0149
Recessed	High	9	5.975	32.5	25.4	0.16	0.0163
Recessed	High	9	6.000	35.0	27.5	0.18	0.0175
Recessed	High	9	6.005	37.5	29.9	0.20	0.0199
Recessed	High	9	6.010	40.0	32.5	0.22	0.0220
Recessed	High	11	5.935	30.0	23.7	0.16	0.0128
Recessed	High	11	5.940	32.5	25.7	0.18	0.0140
Recessed	High	11	5.965	35.0	27.9	0.20	0.0150
Recessed	High	11	5.990	37.5	30.2	0.19	0.0165
Recessed	High	11	5.990	40.0	32.4	0.22	0.0179
Recessed	High	7	5.990	30.0	24.5	0.19	0.0192
Recessed	High	7	5.990	32.5	26.2	0.24	0.0207
Recessed	High	7	5.987	35.0	27.6	0.27	0.0220
Recessed	High	7	5.945	37.5	29.7	0.30	0.0245
Recessed	High	7	5.945	40.0	31.7	0.33	0.0269
Recessed	High	9	5.950	30.0	22.4	0.11	0.0139
Recessed	High	9	5.975	32.5	24.6	0.12	0.0153
Recessed	High	9	6.000	35.0	26.9	0.13	0.0169
Recessed	High	9	6.005	37.5	29.5	0.15	0.0190
Recessed	High	9	6.010	40.0	31.9	0.17	0.0214
Recessed	High	11	5.935	30.0	22.9	0.13	0.0122

Recessed	High	11	5.940	32.5	25.3	0.14	0.0131
Recessed	High	11	5.965	35.0	27.5	0.14	0.0142
Recessed	High	11	5.990	37.5	29.8	0.17	0.0157
Recessed	High	11	5.990	40.0	32.0	0.17	0.0174
Full	Low	7	1.76	30.0	10.9	0.56	0.0116
Full	Low	7	1.76	32.5	11.7	0.64	0.0123
Full	Low	7	1.765	35.0	12.5	0.71	0.0135
Full	Low	7	1.765	37.5	13.4	0.74	0.0139
Full	Low	7	1.765	40.0	14.1	0.77	0.0145
Full	Low	9	1.763	30.0	12.1	0.54	0.0086
Full	Low	9	1.763	32.5	13.4	0.58	0.0095
Full	Low	9	1.763	35.0	14.0	0.64	0.0109
Full	Low	9	1.763	37.5	15.1	0.67	0.0120
Full	Low	9	1.763	40.0	16.0	0.69	0.0133
Full	Low	11	1.77	30.0	12.1	0.39	0.0085
Full	Low	11	1.768	32.5	13.4	0.43	0.0086
Full	Low	11	1.76	35.0	14.5	0.46	0.0089
Full	Low	11	1.758	37.5	15.7	0.54	0.0100
Full	Low	11	1.759	40.0	17.0	0.57	0.0111
Full	Low	7	1.751	30.0	11.1	0.58	0.0126
Full	Low	7	1.752	32.5	11.8	0.67	0.0131
Full	Low	7	1.751	35.0	12.8	0.72	0.0135
Full	Low	7	1.753	37.5	13.6	0.76	0.0148
Full	Low	7	1.751	40.0	14.7	0.79	0.0150
Full	Low	9	1.756	30.0	12.4	0.55	0.0091
Full	Low	9	1.751	32.5	13.5	0.61	0.0103
Full	Low	9	1.754	35.0	14.2	0.65	0.0112

Full	Low	9	1.751	37.5	15.3	0.68	0.0130
Full	Low	9	1.752	40.0	16.5	0.72	0.0139
Full	Low	11	1.756	30.0	12.6	0.42	0.0093
Full	Low	11	1.758	32.5	13.6	0.44	0.0090
Full	Low	11	1.757	35.0	14.6	0.47	0.0088
Full	Low	11	1.752	37.5	16.1	0.56	0.0108
Full	Low	11	1.758	40.0	17.3	0.60	0.0120
Full	Low	7	1.768	30.0	10.6	0.54	0.0117
Full	Low	7	1.762	32.5	11.6	0.61	0.0123
Full	Low	7	1.763	35.0	12.2	0.70	0.0130
Full	Low	7	1.763	37.5	13.2	0.71	0.0136
Full	Low	7	1.762	40.0	13.8	0.75	0.0139
Full	Low	9	1.762	30.0	11.8	0.52	0.0077
Full	Low	9	1.765	32.5	13.2	0.56	0.0092
Full	Low	9	1.763	35.0	13.8	0.61	0.0101
Full	Low	9	1.762	37.5	14.7	0.64	0.0112
Full	Low	9	1.762	40.0	15.7	0.66	0.0129
Full	Low	11	1.765	30.0	11.6	0.37	0.0082
Full	Low	11	1.764	32.5	13.2	0.41	0.0083
Full	Low	11	1.762	35.0	14.4	0.44	0.0083
Full	Low	11	1.762	37.5	15.5	0.52	0.0096
Full	Low	11	1.763	40.0	16.7	0.55	0.0109
Full	Medium	7	3.710	30.0	20.3	0.35	0.0175
Full	Medium	7	3.700	32.5	22.2	0.39	0.0192
Full	Medium	7	3.700	35.0	23.8	0.42	0.0208
Full	Medium	7	3.700	37.5	25.8	0.44	0.0236
Full	Medium	7	3.700	40.0	27.4	0.48	0.0254
Full	Medium	9	3.710	30.0	19.7	0.26	0.0129

Full	Medium	9	3.700	32.5	21.7	0.29	0.0146
Full	Medium	9	3.700	35.0	23.7	0.32	0.0158
Full	Medium	9	3.700	37.5	25.6	0.35	0.0184
Full	Medium	9	3.700	40.0	27.6	0.38	0.0194
Full	Medium	11	3.710	30.0	20.6	0.22	0.0119
Full	Medium	11	3.700	32.5	22.5	0.24	0.0127
Full	Medium	11	3.700	35.0	24.7	0.26	0.0140
Full	Medium	11	3.700	37.5	26.4	0.29	0.0155
Full	Medium	11	3.700	40.0	28.3	0.31	0.0159
Full	Medium	7	3.710	30.0	20.7	0.38	0.0182
Full	Medium	7	3.700	32.5	22.6	0.41	0.0196
Full	Medium	7	3.710	35.0	24.2	0.44	0.0213
Full	Medium	7	3.700	37.5	26.0	0.47	0.0236
Full	Medium	7	3.710	40.0	27.5	0.51	0.0246
Full	Medium	9	3.700	30.0	19.9	0.28	0.0136
Full	Medium	9	3.710	32.5	21.9	0.30	0.0154
Full	Medium	9	3.710	35.0	24.2	0.33	0.0166
Full	Medium	9	3.710	37.5	26.0	0.38	0.0190
Full	Medium	9	3.710	40.0	28.0	0.39	0.0198
Full	Medium	11	3.710	30.0	20.8	0.23	0.0118
Full	Medium	11	3.700	32.5	22.9	0.26	0.0127
Full	Medium	11	3.700	35.0	24.9	0.29	0.0147
Full	Medium	11	3.700	37.5	26.7	0.31	0.0152
Full	Medium	11	3.700	40.0	28.4	0.35	0.0163
Full	Medium	7	3.710	30.0	19.7	0.32	0.0171
Full	Medium	7	3.710	32.5	21.8	0.36	0.0186
Full	Medium	7	3.710	35.0	23.3	0.40	0.0206
Full	Medium	7	3.700	37.5	25.5	0.42	0.0223

Full	Medium	7	3.700	40.0	27.1	0.46	0.0246
Full	Medium	9	3.700	30.0	19.3	0.24	0.0130
Full	Medium	9	3.710	32.5	21.5	0.28	0.0141
Full	Medium	9	3.710	35.0	23.3	0.30	0.0159
Full	Medium	9	3.710	37.5	25.4	0.32	0.0181
Full	Medium	9	3.710	40.0	27.4	0.37	0.0197
Full	Medium	11	3.700	30.0	20.3	0.20	0.0118
Full	Medium	11	3.700	32.5	22.2	0.21	0.0129
Full	Medium	11	3.700	35.0	24.1	0.23	0.0135
Full	Medium	11	3.710	37.5	26.1	0.26	0.0150
Full	Medium	11	3.700	40.0	28.2	0.28	0.0158
Full	High	7	6.060	30.0	25.9	0.23	0.0197
Full	High	7	6.070	32.5	27.5	0.27	0.0221
Full	High	7	6.090	35.0	29.0	0.31	0.0233
Full	High	7	6.020	37.5	31.0	0.34	0.0266
Full	High	7	6.060	40.0	33.2	0.37	0.0276
Full	High	9	6.110	30.0	23.8	0.14	0.0152
Full	High	9	6.100	32.5	26.2	0.15	0.0162
Full	High	9	6.090	35.0	28.4	0.16	0.0185
Full	High	9	6.110	37.5	31.1	0.19	0.0202
Full	High	9	6.110	40.0	33.8	0.21	0.0225
Full	High	11	6.100	30.0	24.3	0.16	0.0129
Full	High	11	6.100	32.5	26.6	0.17	0.0135
Full	High	11	6.100	35.0	29.0	0.18	0.0152
Full	High	11	6.100	37.5	31.4	0.19	0.0168
Full	High	11	6.100	40.0	33.5	0.20	0.0189
Full	High	7	6.060	30.0	26.0	0.25	0.0208
Full	High	7	6.070	32.5	27.7	0.28	0.0221

Full	High	7	6.090	35.0	29.3	0.33	0.0235
Full	High	7	6.020	37.5	31.3	0.36	0.0274
Full	High	7	6.060	40.0	33.2	0.40	0.0295
Full	High	9	6.110	30.0	24.1	0.15	0.0161
Full	High	9	6.100	32.5	26.5	0.17	0.0164
Full	High	9	6.090	35.0	28.7	0.19	0.0189
Full	High	9	6.110	37.5	31.3	0.21	0.0212
Full	High	9	6.060	40.0	34.0	0.24	0.0229
Full	High	11	6.100	30.0	24.8	0.17	0.0129
Full	High	11	6.100	32.5	26.9	0.19	0.0148
Full	High	11	6.060	35.0	29.1	0.21	0.0157
Full	High	11	6.100	37.5	31.7	0.20	0.0170
Full	High	11	6.090	40.0	33.7	0.24	0.0180
Full	High	7	6.060	30.0	25.6	0.20	0.0206
Full	High	7	6.070	32.5	27.4	0.26	0.0221
Full	High	7	6.090	35.0	28.9	0.29	0.0222
Full	High	7	6.020	37.5	31.0	0.32	0.0255
Full	High	7	6.060	40.0	33.1	0.36	0.0280
Full	High	9	6.110	30.0	23.5	0.12	0.0144
Full	High	9	6.100	32.5	25.7	0.13	0.0156
Full	High	9	6.090	35.0	28.2	0.14	0.0177
Full	High	9	6.110	37.5	30.8	0.16	0.0203
Full	High	9	6.090	40.0	33.3	0.18	0.0225
Full	High	11	6.100	30.0	24.0	0.14	0.0126
Full	High	11	6.100	32.5	26.3	0.15	0.0134
Full	High	11	6.090	35.0	28.7	0.15	0.0151
Full	High	11	6.100	37.5	31.2	0.18	0.0167
Full	High	11	6.100	40.0	33.4	0.18	0.0179

Tapered	Low	7	1.685	30.0	10.5	0.47	0.0129
Tapered	Low	7	1.650	32.5	11.4	0.60	0.0137
Tapered	Low	7	1.648	35.0	12.1	0.72	0.0141
Tapered	Low	7	1.647	37.5	13.0	0.78	0.0139
Tapered	Low	7	1.644	40.0	13.8	0.76	0.0152
Tapered	Low	9	1.654	30.0	11.7	0.47	0.0084
Tapered	Low	9	1.648	32.5	13.2	0.59	0.0105
Tapered	Low	9	1.647	35.0	13.7	0.58	0.0104
Tapered	Low	9	1.648	37.5	14.8	0.71	0.0116
Tapered	Low	9	1.648	40.0	15.6	0.58	0.0138
Tapered	Low	11	1.647	30.0	11.7	0.38	0.0089
Tapered	Low	11	1.644	32.5	13.1	0.41	0.0090
Tapered	Low	11	1.654	35.0	14.2	0.47	0.0090
Tapered	Low	11	1.648	37.5	15.4	0.52	0.0091
Tapered	Low	11	1.647	40.0	16.4	0.55	0.0110
Tapered	Low	7	1.645	30.0	10.7	0.50	0.0111
Tapered	Low	7	1.644	32.5	11.5	0.59	0.0123
Tapered	Low	7	1.645	35.0	12.3	0.65	0.0145
Tapered	Low	7	1.645	37.5	13.3	0.74	0.0144
Tapered	Low	7	1.646	40.0	14.1	0.83	0.0127
Tapered	Low	9	1.640	30.0	12.1	0.46	0.0094
Tapered	Low	9	1.611	32.5	13.0	0.52	0.0102
Tapered	Low	9	1.636	35.0	13.8	0.65	0.0104
Tapered	Low	9	1.617	37.5	15.0	0.66	0.0113
Tapered	Low	9	1.624	40.0	16.0	0.75	0.0151
Tapered	Low	11	1.647	30.0	12.3	0.39	0.0099
Tapered	Low	11	1.644	32.5	13.0	0.44	0.0086

Tapered	Low	11	1.654	35.0	14.4	0.46	0.0082
Tapered	Low	11	1.648	37.5	15.8	0.51	0.0104
Tapered	Low	11	1.647	40.0	17.0	0.61	0.0100
Tapered	Low	7	1.650	30.0	10.4	0.45	0.0107
Tapered	Low	7	1.645	32.5	11.3	0.52	0.0130
Tapered	Low	7	1.647	35.0	11.7	0.66	0.0121
Tapered	Low	7	1.646	37.5	12.8	0.65	0.0129
Tapered	Low	7	1.646	40.0	13.4	0.77	0.0123
Tapered	Low	9	1.601	30.0	11.5	0.53	0.0079
Tapered	Low	9	1.609	32.5	12.7	0.52	0.0093
Tapered	Low	9	1.644	35.0	13.6	0.64	0.0111
Tapered	Low	9	1.641	37.5	14.5	0.66	0.0112
Tapered	Low	9	1.620	40.0	15.3	0.57	0.0143
Tapered	Low	11	1.647	30.0	11.5	0.31	0.0073
Tapered	Low	11	1.644	32.5	13.0	0.36	0.0083
Tapered	Low	11	1.654	35.0	14.2	0.40	0.0072
Tapered	Low	11	1.648	37.5	15.0	0.54	0.0099
Tapered	Low	11	1.647	40.0	16.1	0.48	0.0115
Tapered	Medium	7	3.710	30.0	19.6	0.33	0.0170
Tapered	Medium	7	3.680	32.5	21.6	0.40	0.0206
Tapered	Medium	7	3.670	35.0	23.5	0.38	0.0222
Tapered	Medium	7	3.680	37.5	25.1	0.40	0.0199
Tapered	Medium	7	3.680	40.0	27.0	0.48	0.0223
Tapered	Medium	9	3.700	30.0	19.3	0.26	0.0144
Tapered	Medium	9	3.680	32.5	21.2	0.29	0.0150
Tapered	Medium	9	3.680	35.0	23.0	0.31	0.0163
Tapered	Medium	9	3.680	37.5	24.8	0.31	0.0155
Tapered	Medium	9	3.670	40.0	26.8	0.35	0.0215

Tapered	Medium	11	3.680	30.0	19.6	0.23	0.0107
Tapered	Medium	11	3.680	32.5	21.9	0.22	0.0135
Tapered	Medium	11	3.680	35.0	23.6	0.25	0.0129
Tapered	Medium	11	3.680	37.5	25.3	0.29	0.0137
Tapered	Medium	11	3.680	40.0	27.5	0.32	0.0142
Tapered	Medium	7	3.710	30.0	20.0	0.34	0.0181
Tapered	Medium	7	3.680	32.5	21.9	0.37	0.0185
Tapered	Medium	7	3.700	35.0	23.5	0.46	0.0216
Tapered	Medium	7	3.680	37.5	24.9	0.44	0.0216
Tapered	Medium	7	3.680	40.0	26.5	0.44	0.0221
Tapered	Medium	9	3.700	30.0	19.3	0.26	0.0133
Tapered	Medium	9	3.700	32.5	21.5	0.27	0.0143
Tapered	Medium	9	3.710	35.0	23.6	0.30	0.0150
Tapered	Medium	9	3.680	37.5	25.0	0.38	0.0188
Tapered	Medium	9	3.680	40.0	27.4	0.38	0.0175
Tapered	Medium	11	3.680	30.0	20.4	0.24	0.0123
Tapered	Medium	11	3.680	32.5	22.5	0.25	0.0140
Tapered	Medium	11	3.670	35.0	23.9	0.25	0.0145
Tapered	Medium	11	3.680	37.5	26.1	0.27	0.0157
Tapered	Medium	11	3.680	40.0	27.6	0.35	0.0174
Tapered	Medium	7	3.670	30.0	19.4	0.32	0.0168
Tapered	Medium	7	3.680	32.5	21.2	0.31	0.0192
Tapered	Medium	7	3.670	35.0	22.6	0.37	0.0218
Tapered	Medium	7	3.680	37.5	24.3	0.43	0.0209
Tapered	Medium	7	3.680	40.0	26.1	0.47	0.0216
Tapered	Medium	9	3.680	30.0	19.0	0.20	0.0124
Tapered	Medium	9	3.680	32.5	21.0	0.29	0.0126
Tapered	Medium	9	3.670	35.0	22.4	0.25	0.0161

Tapered	Medium	9	3.680	37.5	24.9	0.28	0.0159
Tapered	Medium	9	3.670	40.0	26.2	0.33	0.0210
Tapered	Medium	11	3.680	30.0	19.7	0.20	0.0122
Tapered	Medium	11	3.680	32.5	21.9	0.19	0.0136
Tapered	Medium	11	3.670	35.0	23.7	0.22	0.0120
Tapered	Medium	11	3.680	37.5	25.8	0.27	0.0129
Tapered	Medium	11	3.680	40.0	27.2	0.28	0.0173
Tapered	High	7	6.020	30.0	25.0	0.24	0.0199
Tapered	High	7	6.020	32.5	26.6	0.25	0.0220
Tapered	High	7	6.000	35.0	28.5	0.29	0.0228
Tapered	High	7	6.000	37.5	30.2	0.35	0.0256
Tapered	High	7	6.020	40.0	32.4	0.33	0.0279
Tapered	High	9	6.030	30.0	23.3	0.12	0.0132
Tapered	High	9	6.030	32.5	25.1	0.16	0.0166
Tapered	High	9	6.030	35.0	27.8	0.16	0.0193
Tapered	High	9	6.030	37.5	29.9	0.18	0.0183
Tapered	High	9	6.030	40.0	33.1	0.21	0.0207
Tapered	High	11	6.040	30.0	23.7	0.15	0.0121
Tapered	High	11	6.040	32.5	26.2	0.18	0.0147
Tapered	High	11	6.040	35.0	28.0	0.16	0.0160
Tapered	High	11	6.030	37.5	30.0	0.20	0.0182
Tapered	High	11	6.030	40.0	32.4	0.19	0.0180
Tapered	High	7	6.030	30.0	25.5	0.25	0.0198
Tapered	High	7	6.020	32.5	26.8	0.27	0.0214
Tapered	High	7	6.010	35.0	28.8	0.33	0.0240
Tapered	High	7	6.010	37.5	30.0	0.34	0.0290
Tapered	High	7	6.010	40.0	32.4	0.39	0.0310
Tapered	High	9	6.020	30.0	23.5	0.13	0.0160

Tapered	High	9	6.000	32.5	26.1	0.18	0.0177
Tapered	High	9	6.030	35.0	27.9	0.17	0.0172
Tapered	High	9	6.010	37.5	30.2	0.23	0.0206
Tapered	High	9	6.020	40.0	32.6	0.21	0.0239
Tapered	High	11	6.000	30.0	24.0	0.15	0.0131
Tapered	High	11	6.020	32.5	25.9	0.21	0.0130
Tapered	High	11	6.030	35.0	28.2	0.23	0.0160
Tapered	High	11	6.010	37.5	30.5	0.20	0.0152
Tapered	High	11	6.010	40.0	33.3	0.24	0.0184
Tapered	High	7	6.010	30.0	25.0	0.20	0.0189
Tapered	High	7	6.010	32.5	26.5	0.25	0.0202
Tapered	High	7	6.020	35.0	28.1	0.27	0.0217
Tapered	High	7	6.010	37.5	30.0	0.34	0.0226
Tapered	High	7	6.020	40.0	32.6	0.38	0.0294
Tapered	High	9	6.010	30.0	22.6	0.11	0.0126
Tapered	High	9	6.030	32.5	25.0	0.12	0.0160
Tapered	High	9	6.040	35.0	27.6	0.15	0.0157
Tapered	High	9	6.020	37.5	29.5	0.14	0.0218
Tapered	High	9	6.010	40.0	32.2	0.17	0.0246
Tapered	High	11	6.020	30.0	22.9	0.14	0.0140
Tapered	High	11	6.030	32.5	25.6	0.13	0.0124
Tapered	High	11	6.010	35.0	28.0	0.14	0.0152
Tapered	High	11	6.030	37.5	30.1	0.18	0.0179
Tapered	High	11	6.020	40.0	32.0	0.16	0.0163

Table-2 Data table for limiting current (A)

Electrode Type	Flow Rate (GPM)	Voltage (V)	Current (A)	Removal Ratio	Stack Resistance (Ω)
Full	7	40.0	14.8	0.75	2.70
Full	7	42.0	15.1	0.79	2.78
Full	7	44.0	15.4	0.86	2.86
Full	7	46.0	15.6	0.91	2.95
Full	7	48.0	15.7	0.92	3.06
Full	7	50.0	15.7	0.92	3.18
Full	7	52.0	15.7	0.91	3.31
Full	7	54.0	15.8	0.90	3.42
Full	7	56.0	15.9	0.90	3.52
Full	7	58.0	16.1	0.90	3.60
Full	7	60.0	16.3	0.90	3.68
Full	9	40.0	16.4	0.59	2.44
Full	9	42.0	17.3	0.59	2.43
Full	9	44.0	18.4	0.58	2.39
Full	9	46.0	19.0	0.59	2.42
Full	9	48.0	19.2	0.60	2.50
Full	9	50.0	19.4	0.61	2.58
Full	9	52.0	19.6	0.62	2.65
Full	9	54.0	20.1	0.63	2.69
Full	9	56.0	20.4	0.64	2.75
Full	11	57.0	25.7	0.80	4.97
Full	11	59.0	25.9	0.81	4.97
Full	11	61.0	26.3	0.83	4.98
Full	11	63.0	26.6	0.86	4.98
Full	11	65.0	26.7	0.88	4.98
Full	11	67.0	26.7	0.88	6.08
Full	11	69.0	26.8	0.88	6.07
Full	11	71.0	26.9	0.89	6.09
Full	11	73.0	27.3	0.89	6.08
Full	11	75.0	27.5	0.88	6.09
Tapered	7	40.0	14.1	0.68	2.84
Tapered	7	42.0	14.3	0.71	2.93
Tapered	7	44.0	14.6	0.77	3.01
Tapered	7	46.0	14.8	0.82	3.10
Tapered	7	48.0	14.9	0.83	3.22
Tapered	7	50.0	14.9	0.83	3.35
Tapered	7	52.0	14.9	0.82	3.49
Tapered	7	54.0	15.0	0.81	3.60
Tapered	7	56.0	15.1	0.81	3.71

Tapered	7	58.0	15.3	0.81	3.79
Tapered	7	60.0	15.5	0.81	3.87
Tapered	9	40.0	15.6	0.69	2.57
Tapered	9	42.0	16.4	0.72	2.56
Tapered	9	44.0	17.5	0.76	2.52
Tapered	9	46.0	18.1	0.79	2.55
Tapered	9	48.0	18.2	0.80	2.63
Tapered	9	50.0	18.4	0.81	2.71
Tapered	9	52.0	18.6	0.83	2.79
Tapered	9	54.0	19.1	0.83	2.83
Tapered	9	56.0	19.4	0.83	2.89
Tapered	11	57.0	23.1	0.64	2.46
Tapered	11	59.0	23.3	0.65	2.53
Tapered	11	61.0	23.7	0.66	2.58
Tapered	11	63.0	23.9	0.69	2.63
Tapered	11	65.0	24.0	0.70	2.70
Tapered	11	67.0	24.0	0.70	2.79
Tapered	11	69.0	24.1	0.70	2.86
Tapered	11	71.0	24.2	0.71	2.93
Tapered	11	73.0	24.6	0.71	2.97
Tapered	11	75.0	24.8	0.70	3.03
Recessed	7	38.0	13.3	0.73	2.86
Recessed	7	40.0	13.8	0.75	2.90
Recessed	7	42.0	14.4	0.79	2.92
Recessed	7	44.0	14.7	0.84	2.99
Recessed	7	46.0	14.8	0.87	3.11
Recessed	7	48.0	15.0	0.88	3.15
Recessed	7	50.0	15.7	0.88	3.18
Recessed	7	52.0	16.2	0.89	3.19
Recessed	9	40.0	17.8	0.75	2.25
Recessed	9	42.0	18.5	0.82	2.27
Recessed	9	44.0	18.9	0.86	2.33
Recessed	9	46.0	19.0	0.87	2.42
Recessed	9	48.0	19.1	0.88	2.51
Recessed	9	50.0	19.6	0.89	2.55
Recessed	9	52.0	19.9	0.89	2.61
Recessed	11	55.0	22.7	0.85	2.42
Recessed	11	57.0	23.2	0.86	2.46
Recessed	11	59.0	23.8	0.87	2.48
Recessed	11	61.0	23.9	0.89	2.55
Recessed	11	63.0	23.9	0.90	2.64
Recessed	11	65.0	24.6	0.91	2.66

Optimization of Algae Production Using Concentrate

RECLAMATION

Managing Water in the West

Desalination & Water Purification Research
and Development Program Report No. XXX *(Reclamation will assign a no.)*

Optimization of Algae Production Using Concentrate

U.S. Department of the Interior



December 2015

REPORT DOCUMENTATION PAGE		Form Approved OMB No. 0704-0188
<p>The public reporting burden for this collection of information is estimated to average 1 hour per response, including the time for reviewing instructions, searching existing data sources, gathering and maintaining the data needed, and completing and reviewing the collection of information. Send comments regarding this burden estimate or any other aspect of this collection of information, including suggestions for reducing the burden, to Department of Defense, Washington Headquarters Services, Directorate for Information Operations and Reports (0704-0188), 1215 Jefferson Davis Highway, Suite 1204, Arlington, VA 22202-4302. Respondents should be aware that notwithstanding any other provision of law, no person shall be subject to any penalty for failing to comply with a collection of information if it does not display a currently valid OMB control number.</p> <p>PLEASE DO NOT RETURN YOUR FORM TO THE ABOVE ADDRESS.</p>		
1. REPORT DATE (DD-MM-YYYY) 15/12/2015	2. REPORT TYPE Final Report	3. DATES COVERED (From - To) September 2014 - September 2015
4. TITLE AND SUBTITLE Optimization of Algae Production Using Concentrate	5a. CONTRACT NUMBER R10AC80283	
	5b. GRANT NUMBER	
	5c. PROGRAM ELEMENT NUMBER	
6. AUTHOR(S) Ali Abdulqafar, Jalal Rastegary, Abbas Ghassemi, Tracey Fernandez, Daniel White	5d. PROJECT NUMBER	
	5e. TASK NUMBER	
	5f. WORK UNIT NUMBER	
7. PERFORMING ORGANIZATION NAME(S) AND ADDRESS(ES) New Mexico State University	8. PERFORMING ORGANIZATION REPORT NUMBER	
9. SPONSORING/MONITORING AGENCY NAME(S) AND ADDRESS(ES) IEE/WERC New Mexico State University P.O. Box 30001 Las Cruces, NM 88003	10. SPONSOR/MONITOR'S ACRONYM(S)	
	11. SPONSOR/MONITOR'S REPORT NUMBER(S)	
12. DISTRIBUTION/AVAILABILITY STATEMENT		
13. SUPPLEMENTARY NOTES		
<p>14. ABSTRACT</p> <p>Desalination can alleviate global water scarcity by removing salt from saline water, but all desalination technologies also produce undesirable concentrate, which contains all of the substances removed from feedwater during desalination. Concentrate is saline to a degree that can threaten the health of many living organisms, and current disposal methods for concentrate are costly, environmentally harmful, and wasteful. Water is precious, and the world's volume of concentrate is a large and mostly unused water source.</p> <p>One of the promising approaches for feasibly and sustainably using desalination concentrate is using it as a growth medium for halotolerant algae. If enough microalgae growth is achieved in the concentrate, the microalgae could be harvested to produce biomass for biofuel, turning a former waste into a valuable product. Furthermore, microalgae consume nutrients from the concentrate, reducing the levels of total dissolved solids, heavy toxic metals in concentrate and facilitating its safe disposal. To improve the feasibility of using concentrate to grow microalgae, this study investigates how modified desalination concentrate – with different levels of phosphorus, nitrogen, and CO₂ – affects the growth of microalgae species <i>Chlorella sorokiniana</i> and <i>Nannochloropsis oculata</i>. Based on biomass production measures, an optimal growth medium composition was determined, and a predictive model for biomass production was developed.</p>		

15. SUBJECT TERMS					
16. SECURITY CLASSIFICATION OF:			17. LIMITATION OF ABSTRACT	18. NUMBER OF PAGES	19a. NAME OF RESPONSIBLE PERSON
a. REPORT	b. ABSTRACT	a. THIS PAGE			19b. TELEPHONE NUMBER <i>(Include area code)</i>

Standard Form 298 (Rev. 8/98)
 Prescribed by ANSI Std. Z39.18

**Desalination & Water Purification Research
and Development Program Report No. XXX**

Optimization of Algae Production Using Concentrate

Prepared for Reclamation Under Agreement No. XXXXXXXXXXXXX

by

**Ali Abdulqafar, Jalal Rastegary, Abbas Ghassemi, Tracey
Fernandez, Daniel White**



**U.S. Department of the Interior
Bureau of Reclamation
Technical Service Center
Water and Environmental Services Division
Water Treatment Engineering Research Team
Denver, Colorado**

December 2015

MISSION STATEMENTS

The mission of the Department of the Interior is to protect and provide access to our Nation's natural and cultural heritage and honor our trust responsibilities to Indian tribes and our commitments to island communities.

The mission of the Bureau of Reclamation is to manage, develop, and protect water and related resources in an environmentally and economically sound manner in the interest of the American public.

Disclaimer

The views, analysis, recommendations, and conclusions in this report are those of the authors and do not represent official or unofficial policies or opinions of the United States Government, and the United States takes no position with regard to any findings, conclusions, or recommendations made. As such, mention of trade names or commercial products does not constitute their endorsement by the United States Government.

Acknowledgements

The authors would like to thank the U.S. Bureau of Reclamation for sponsoring this research project and the Brackish Groundwater National Desalination Research Facility for providing desalination concentrate during the study.

In addition, the authors would like to thank Dr. Leila Karimi, Eahsan Shahriary, and Patrick DeSimio for their help during the project.

Executive Summary

Desalination can alleviate global water scarcity by removing salt from saline water, but all desalination technologies also produce undesirable concentrate, which contains all of the substances removed from feedwater during desalination. Concentrate is saline to a degree that can threaten the health of many living organisms, and current disposal methods for concentrate are costly, environmentally harmful, and wasteful. Water is precious, and the world's volume of concentrate is a large and mostly unused water source.

One of the promising approaches for feasibly and sustainably using desalination concentrate is using it as a growth medium for halotolerant algae. If enough microalgae growth is achieved in the concentrate, the microalgae could be harvested to produce biomass for biofuel, turning a former waste into a valuable product. Furthermore, microalgae consume nutrients from the concentrate, reducing the levels of total dissolved solids, heavy toxic metals in concentrate and facilitating its safe disposal.

To improve the feasibility of using concentrate to grow microalgae, this study investigates how modified desalination concentrate – with different levels of phosphorus, nitrogen, and CO₂ – affects the growth of microalgae species *Chlorella sorokiniana* and *Nannochloropsis oculata*. Based on biomass production measures, an optimal growth medium composition was determined, and a predictive model for biomass production was developed.

The present report consists of two parts:

- I. Lab-scale cultivation of microalgae in desalination concentrate and modification of desalination concentrate to optimize its suitability as a growth medium for microalgae, and
- II. Pilot-scale cultivation of microalgae in desalination concentrate.

Both reports include data on ion removal during microalgae growth.

Contents

PART I

Acknowledgements.....	v
Executive Summary	vi
CHAPTER 1 - INTRODUCTION.....	2
1.1 The Energy Crisis.....	2
1.2 The Water Crisis.....	3
1.3 Desalination.....	5
1.3.1 Membrane Desalination.....	5
1.3.2 Desalination Cost.....	7
CHAPTER 2: LITERATURE REVIEW	10
2.1 Microalgae strains	10
2.2 Effect of CO ₂ on microalgae growth	11
2.3 Effect of nutrients on microalgae growth.....	12
2.3.1 Key elements for microalgae growth.....	14
3.3 Algae metal reduction	15
CHAPTER 3: MATERIAL AND METHODS.....	17
3.1 Experimental Set-Up.....	17
3.2 Algae strains and culture	18
3.3 Design of experiment	18
3.4 Calculations and statistical analysis	21
CHAPTER 4: RESULTS AND DISCUSSION.....	23
4.1 Effect of Media on Growth of Microalgae.....	23
4.2 Predictive model.....	25
4.3 Ion removal	29
CHAPTER 5: CONCLUSION	31
REFERENCES	33

PART II

Abstract.....	39
CHAPTER 1: INTRODUCTION.....	40
CHAPTER 2: MATERIALS AND METHODS	42
CHAPTER 3: RESULTS AND ANALYSIS	46
3.1 Population Analysis.....	46
3.2 pH Analysis.....	50
3.3 Conductivity and Depth Analysis	51
3.4 Element Removal Analysis	53
CHAPTER 4: DISCUSSION.....	70
REFERENCES	71
APPENDIX.....	74

Part I: Lab-Scale Cultivation of Microalgae in Desalination
Concentrate

CHAPTER 1 - INTRODUCTION

The energy and water crises are among the highest-priority challenges to be tackled in the century in which we live. These crises are interrelated: producing energy typically takes large amounts of water (e.g., dammed or running water for hydroelectric plants, steam in nuclear or thermal plants, and water in fracking fluid), and producing clean water takes large amounts of energy (e.g., in thermal and membrane desalination processes). Therefore, solutions that can address both crises simultaneously have a special appeal. In the following sections, the energy and water crises are described, and the use of impaired water to grow algae and produce biofuels is introduced as a potential solution.

1.1 The Energy Crisis

Energy crises mainly result from escalated demands for energy, energy pricing policies, oil import quotas, and depletions of domestic oil and gas reserves (Altin et al., 2001). In 2013, global energy consumption increased by 2.3%, a 0.5% acceleration over 2012. Oil remains the leading fuel, representing 32.9% of global energy consumption (BP, 2014), but the share of oil in global energy consumption is declining. Renewable energy sources are becoming more prominent, and recent conditions where pricing policies brought about overproduction have led to the projected depletion of accessible fossil fuels. The recent growth in U.S. fossil fuel production, as shown in Figure 1, is unlikely to be sustainable.

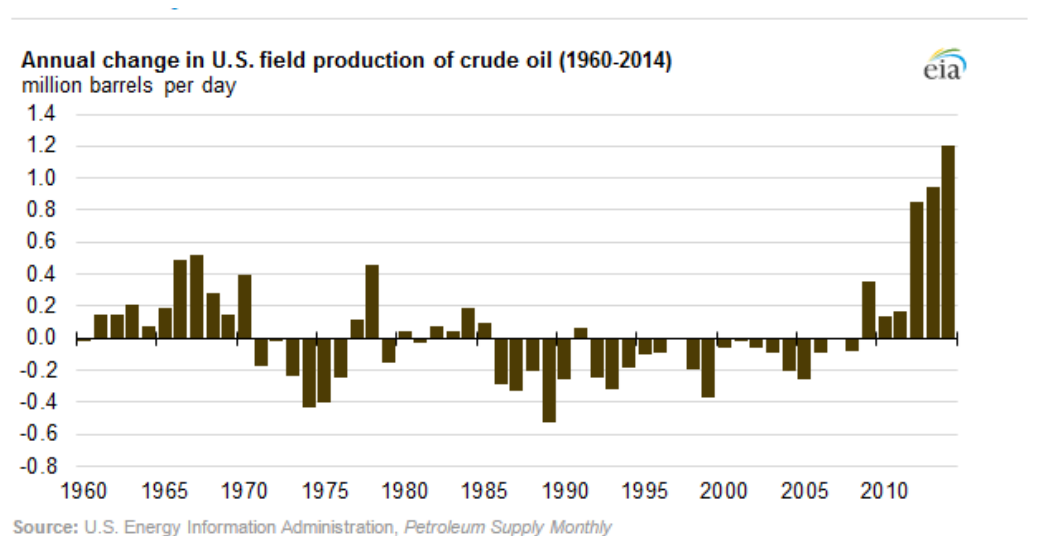


Figure 1. Changes in U.S. fossil fuel production, 1960-2014 (EIA, 2012).

Record growth in fossil fuel consumption also indicates that global CO₂ emissions have grown correspondingly, accelerating climate change. While the use of fossil fuels may continue for years, their finite and non-renewable nature along with their climatic impacts require an immediate effort to reduce growth rates for energy consumption and explore sustainable alternatives for the future.

Biofuels, which are made of living organisms and their byproducts, are seen as a large part of the solution to the energy crisis due to their less-polluting properties and their ability to be produced domestically. The first known biofuels were solid fuels such as wood, sawdust, grass cuttings, domestic refuse, charcoal, agricultural waste, non-food energy crops, and dried manure – i.e., biomass (Ankita, 2013). However, producing this kind of biomass is labor intensive and significant energy inputs are required for harvesting, processing, delivering, and burning the biomass, and then disposing of the residue. Another drawback is that solid biofuels have proven to have limited ability to reduce greenhouse gas emissions (Altin, 2001). Liquid biofuels produced from food crops are also problematic. These fuels can be produced from substances such as converted sugar, starch, vegetable oil, and animal fat, but their use – which has increased at a rate of 7% - competes with food production and can contribute to famine (IEA, 2006). The best biofuels so far are liquid fuels from aquatic organisms such as algae. These organisms are low-input, high-yield feedstocks, which contain a viable source of lipids, from which biodiesel, bioethanol, and bio-hydrogen can be produced through thermochemical or biochemical conversion processes (Ankita, 2013). Algae offer several other benefits including year-round production, no competition with food crops, low land space requirements, and little need for clean water (Chisti, 2008). Contemporary research on microalgae growth is mainly focused on utilizing wastewater as a growth medium, since the availability of water is the only limiting factor for large-scale algae cultivation.

1.2 The Water Crisis

The World Health Organization estimates that more than 750 million people lack access to safe water: that is, 1 in 9 people (Organization, 2012). These numbers are predicted to worsen with industrialization, urbanization, and a growing global population that is expected to reach 9 billion by 2050.

Although the population of the world is increasing, the amount of available freshwater is relatively constant at approximately 200,000 km³, or about 2.5% of the total water available on earth. The relationship between population and water availability is shown in Figure 2.

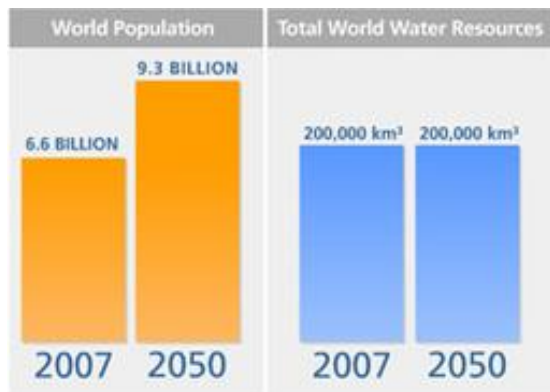
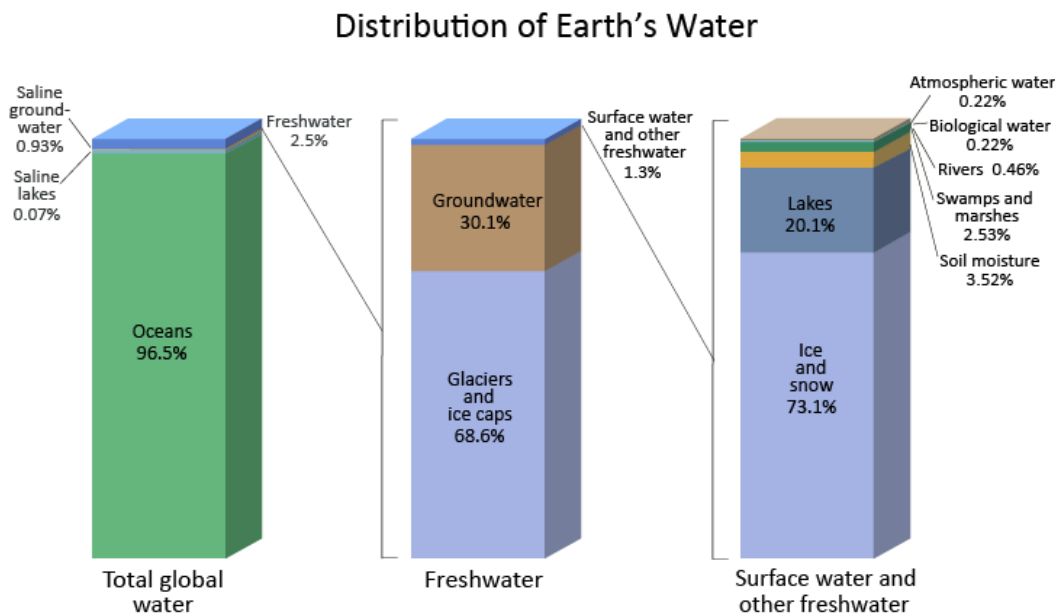


Figure 2. World population in relation to freshwater resources (UNICEF, 2014).

Furthermore, only about 1.3% of freshwater is available on surface of the earth in lakes, rivers, and streams (Figure 3). The remaining freshwater is held in glaciers and groundwater, sources which can be accessible, but which are more difficult to utilize (Altan et al., 2012).



Source: Igor Shiklomanov's chapter "World fresh water resources" in Peter H. Gleick (editor), 1993, *Water in Crisis: A Guide to the World's Fresh Water Resources*.

Figure 3. Distribution of water on earth (Gleick, 1993).

As information on population growth and the availability of freshwater suggests, the current scenario is ominous. Freshwater is finite, and much of its limited quantity is difficult to access. Furthermore, different sectors often compete for the use of freshwater: increases in one sector deprive another, usually household

consumption (Gleick, 1993). Currently, the agricultural sector is a dominant user of freshwater (Chisti, 2008). Under present approaches, the growth of algae would drive agricultural water consumption still higher. Current technologies require a considerable amount of water to grow algae in aqueous suspension: it takes 6000 gallons of water to cultivate 1 gallon of algae oil (Altan et al., 2012). This water not only provides a growth environment, but it also delivers nutrients, removes waste products, and acts as a thermal regulator (Cynthia, 2011). While the water for algae cultivation can be reused in theory, in practice water is lost to evaporation in open ponds at a rate that varies with the climate, temperature, humidity, precipitation, and wind velocity of the location.

1.3 Desalination

Just as energy stress has driven a search for alternative energy sources, water stress has driven a search for alternative water sources. Among alternatives, the reclamation of saline water through desalination processes has been extensively researched and has the potential to provide plentiful drinking water. Desalination can be applied to waters with varying levels of salinity, such as brackish groundwater, estuarine water, or seawater; in some regions, it provides the primary source of drinking water. All desalination technologies produce a product stream of fresh water (called permeate) and a highly concentrated stream of salts and other rejected materials. The latter stream is called desalination concentrate or reject brine, and its safe disposal has been a costly impediment to the installation of desalination plants.

Desalination technology started primarily with thermal process (e.g., flash distillation), but as a result of technological advances, membranes have become a more cost-effective alternative, so membrane technologies comprise an increasing percentage of new desalination systems. Other advances include emerging technologies such as forward osmosis, low temperature distillation, pressure retarded osmosis, and graphene membranes. Hybrid plants and reverse osmosis are gaining wider use in the Middle East, which has traditionally been home to facilities using more energy-intensive thermal technologies (Mike, 2014).

1.3.1 Membrane Desalination

In membrane desalination, reverse osmosis has been the most widely used technology, but other prominent technologies include electrodialysis (ED) and nanofiltration (NF) (Hafez and El-Manharawy, 2002). The differences among the primary desalination technologies are summarized in Table 1 and Figure 4. ED membranes, which typically are used only for brackish water desalination, operate under an electrical current that causes ions to move through parallel membranes (Greenlee et al., 2009). NF, in which pressure is applied to drive water through small pores, has been used to reduce the passage of particles between 1 and 5 nm in size.

Table 1. Differences among filtration processes (Greenlee et al., 2009).

Particular	MF	UF	NF	RO
Membrane	Porous isotropic	Porous asymmetric	Finely porous asymmetric/composite	Nonporous asymmetric/composite
Pore size	50 nm–1 μm	5–20 nm	1–5 nm	–
Transfer mechanism	Sieving and adsorptive mechanisms (the solutes migrate by convection)	Sieving and preferential adsorption	Sieving/electrostatic hydration/diffusive	Diffusive (solutes migrate by diffusion mechanism)
Law governing transfer	Darcy's law	Darcy's law	Fick's law	Fick's law
Typical solution treatment	Solution with solid particles	Solution with colloids and/or macromolecules	Ions, small molecules	Ions, small molecules
Typical pure water flux (L m ⁻² h)	500–10 000	100–2000	20–200	10–100
Pressure requirement (atms)	0.5–5	1–10	7–30	20–100

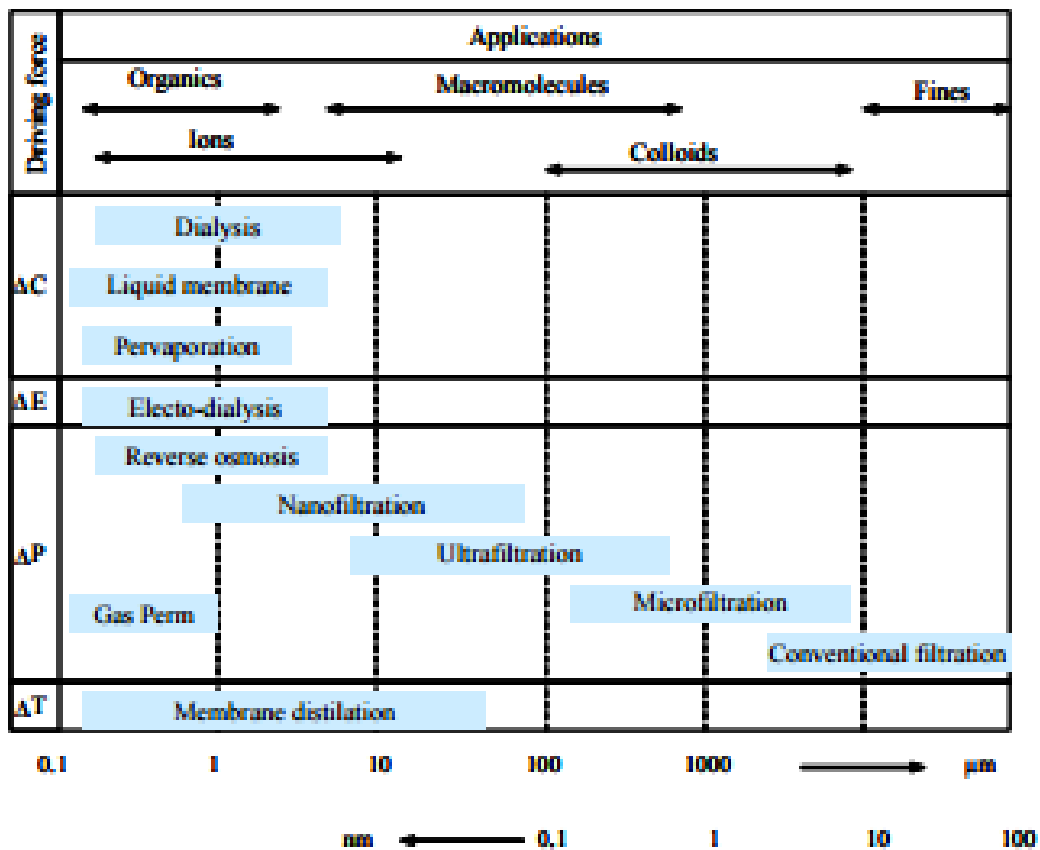


Figure 4. Characteristics of different membrane processes (Shon, 2013).

RO, the most commonly used membrane process, is characterized by an operating pressure that usually is fairly high (20 to 100 bar) and the capacity to remove very fine particles. NF has pore sizes of 1–5 nm and a higher water permeability than RO membranes, so it operates at lower pressure (7 to 30 bar). UF membranes, which have still larger pore sizes of 5 to 20 nm, retain fine colloids, macromolecules, and microorganisms, and operate with a pressure range of 1 to 10 bar. The other membrane technologies used in liquid separation processes are microfiltration (MF), electro dialysis reversal (EDR), and liquid membrane (LM).

1.3.2 Desalination Cost

Over the last decade, the cost for membrane desalination has decreased drastically due to technological advances. All indicators are that the costs associated with the technology will continue to decrease as technologies and efficiencies improve. However, cost comparisons depend on more than the characteristics of the technology. Operating conditions – including feed water characteristics, finished water quality goals, intake type, and disposal method – all play a large role in the overall cost of water (Hafez and El-Manharawy, 2002). Typical cost breakdown for a seawater reverse osmosis (SWRO) desalination plant (Figure 5).

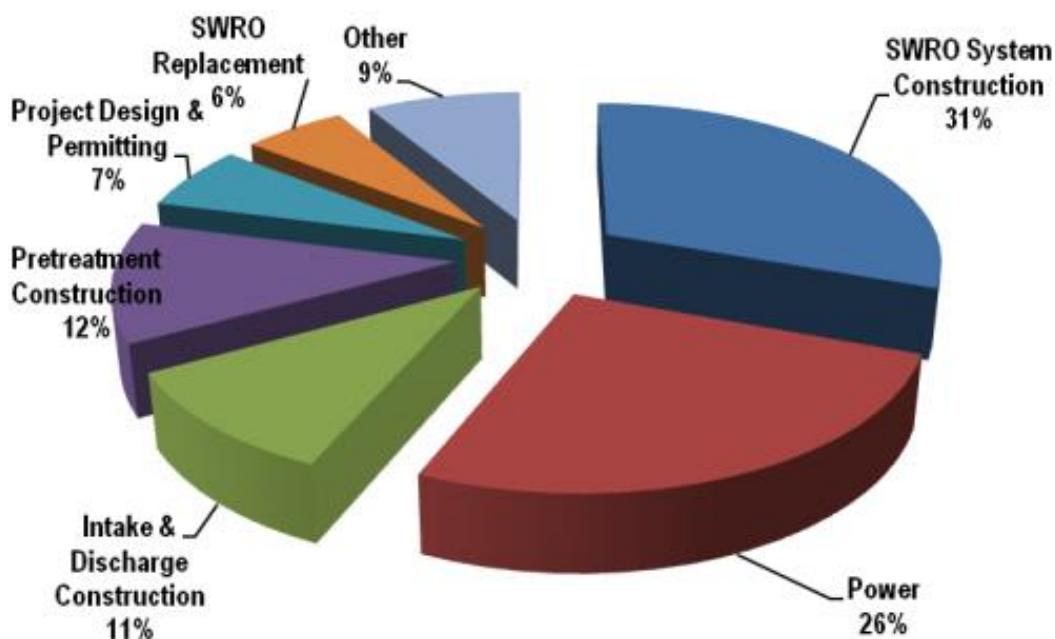


Figure 5. Typical cost breakdown of a sea water reverse osmosis desalination plant (WateRuse, 2009).

The feed water quality affects the pretreatment system required, and typically the pretreatment cost ranges from US\$0.5M/MGD to US\$1.5M/MGD. The lower cost represents a single-stage filtration system, and any additional stages increase this cost. The intake and discharge costs associated with plants are approximately 11 to 12% of the total plant cost (Figure 5). An open intake system typically would cost US\$0.5-1.5M/MGD, but prices up to US\$3M/MGD are possible for complex tunnel and offshore intake systems (Table 2). For discharge, there are several methods to dispose of concentrate, and their cost differs with the varying complexities of the discharge systems.

Table 2. Concentrate disposal methods (WateReuse, 2012)

Disposal Method	Construction Cost	
	(US\$ MM / MGD)	(US\$ MM /acre-foot/day)
New Outfall w/Diffusers	2.0 – 5.5	0.7 - 1.8
Power Plant Outfall	0.2 – 0.6	0.07 - 0.20
Sanitary Sewer	0.1 – 0.4	0.03 - 0.13
WWTP Outfall	0.3 – 2.0	0.1 - 0.7
Deep Well Injection	2.5 – 6.0	0.8 - 2.0
Evaporation Ponds	3.0 – 9.5	1.0 - 3.1
Zero-Liquid Discharge	5.5 – 15.0	1.8 - 4.9

The disposal techniques vary from low- to high-end pricing, and disposal approaches have a considerable impact on the budgeting for a desalination plant. Much of the cost is attributable to environmental regulations put in place by federal agencies, which require permits and formal evaluations of disposal methods in order to protect the environment (Hafez and El-Manharawy, 2002).

In the effort to reduce the cost of concentrate disposal and thereby increase the economic feasibility of desalination plants, microalgae are an auspicious tool. Some researchers have demonstrated that microalgae can be cultivated in desalination concentrate (Hussein et al., 2015; Khaled, 2012), and the microalgae use materials in the concentrate as nutrients, reducing the levels of total dissolved solids (TDS) in the concentrate and facilitating its safe disposal (Shirazi, 2014), all while producing raw materials for biofuels that can alleviate the energy crisis.

Although studies have investigated the use of other impaired waters for algae cultivation (Woertz and Feffer, 2009), few studies have focused on desalination concentrate as a growth medium for microalgae. In the few studies that have been conducted, the main focus has been reducing the salinity of the concentrate solution during algae growth (Hussein et al., 2015; Shirazi, 2014). None of the researchers have investigated the growth of two algae strains, *C. sorokiniana* (fresh water strain) and *N. oculata* (marine strain) using the concentrate stream, and no study has yet investigated the effects of N, P, and CO₂ (three main parameters for algae growth (Grobbelaar, 2004) on the biomass production of the two target microalgae strains.

CHAPTER 2: LITERATURE REVIEW

The first sections of this chapter describe the strains of microalgae used in lipid quantification and characterization studies. The latter section provides information associated with nutrients required for the microalgae and phycoremediation capability of algae species. This section comprehensively provides information on the effect of nutrient and CO₂ capacity used in growth process.

2.1 Microalgae strains

Microalgal products have potential as food supplements, fertilizer, and biofuel feedstocks. Microalgae can also be used for CO₂ sequestration since photoautotrophic algal cultures have the potential to remove CO₂ from the atmosphere, helping alleviate the trend toward global warming.

To reach this goal, it is especially important to achieve two objectives: 1) identifying the microalgae species that performs best in fixing CO₂ (Takagi, 2000), and 2) improving the economic feasibility of microalgae production. For achieving the latter objective, one promising approach is seeking additional value for the system through development of multifunctional, integrated systems, such as combined waste treatment and aquaculture farms (Pedroni et al., 2003). In such systems, algae can sequester CO₂ and produce materials for valuable products while performing other valuable services (e.g., waste water treatment).

In selecting the appropriate microalgae from the more than 72,500 microalgae species (Guiry, 2012), multiple criteria should be considered. As reported by Mata et al. (2010), these criteria include:

- High growth rate
- High performance in competitive mass nature and tolerance to predators
- Appropriate lipid content and energy yield based on type of fuel desired from biomass
- Tolerance to changes in environmental conditions, including resistance to variations in temperature, nutrient inputs (salinity), and light levels
- Availability of nutrients, especially CO₂ when carbon fixation is the goal
- Possibility of obtaining other valuable chemicals
- Degree of easiness of biomass isolation

- Less complex structure and, as a result, easier oil extraction

Some microalgae species, such as *Chlorella*, *Spirulina*, and *Dunaliella*, already have commercial value. *Chlorella* and *Spirulina* are used as food supplements, and *Dunaliella* is a source of beta-carotene (Graham, 2000). *Chlorella* has also been studied for use in CO₂ sequestration and has been shown to grow in conditions of up to 20% CO₂ (Guiry, 2012). For all of these species, commercial profit from biomass production will potentially reduce operational and capital costs for CO₂ sequestration.

The use of marine microalgae for biological CO₂ sequestration has also been considered. Marine algae offer several advantages, including the ability to use plentiful and cheap seawater and brackish water directly as growing media, thereby reducing the costs of microalgae cultivation. CO₂ sources, such as power plants, are also located along coastal areas (Barsanti, 2006), where seawater is available in practically unlimited quantities. Therefore, in addition to algae species that already have demonstrated commercial potential (e.g., *Chlorella*, *Spirulina*, and *Dunaliella*), marine microalgae merit investigation.

One particularly interesting marine microalgae is *Nannochloropsis oculata*, which has a high lipid content of 30% (Malakootian, 2014). Many microalgae can accumulate lipids due to excess photosynthate, and some species can accumulate lipids under heterotrophic or environmental stresses such as nutrient deficiency. The *N. oculata* cultured in 2%, 5%, and 10% CO₂ in a semi-continuous system with a high-cell density of inoculum can be grown optimally in 2% CO₂ (Sheng-Yi, 2009).

From among freshwater algae strains, *Chlorella sorokiniana* has a high growth rate and is tolerant to high irradiance, high temperature, and high CO₂ concentrations (Matsukawa, 2000). Therefore, this strain has clear benefits for use in outdoor cultures and is a good candidate for a CO₂ fixation/conversion system.

2.2 Effect of CO₂ on microalgae growth

Biological CO₂ mitigation is an attractive process since, while achieving CO₂ fixation through photosynthesis, it produces biomass energy as a byproduct (Chang, 2011). Biological mitigation of CO₂ by microalgae mainly focuses on two CO₂ sources: flue gas (with 10–20% CO₂) and air in a closed space (generally around 1.0% CO₂) (Jajesniak, 2014; Matsukawa, 2000). However, to maximize the efficiency of CO₂ removal through bio-regenerative systems, two important factors must be addressed: the need for free CO₂, and the need for superior mechanisms for concentrating carbon.

Presently, nearly all pilot-scale algae cultures depend on purchased CO₂ that contributes substantially (~50%) to the cost of producing biomass (Giordano, 2005). Unless CO₂ is available free, cultivation of algae for fuels is not feasible (Chisti, 2007). Also, even once CO₂ is available, it must be concentrated to levels that are usable by algae. Many algae and cyanobacteria are known to possess mechanisms for concentrating carbon dioxide from the culture mediums into cells (Giordano, 2005), but carbon dioxide absorption from the standard atmosphere into the culture medium is never sufficiently fast to rapidly grow a large concentration of algae. Due to inadequacies in natural carbon concentrating mechanisms, supplementing an algae culture with CO₂ nearly always enhances the biomass growth rate compared to what is possible under a normal atmosphere. Therefore, to enhance algae growth using high concentrations of CO₂, most large-scale cultivation units are situated near coal-fired power stations, which produce plentiful CO₂ as a waste gas.

Algae require 45 pounds of CO₂ to produce a gallon of biodiesel (Pienkos, 2007), and an average power station produces 400 tons of CO₂ in an hour (EIA, 2014). The amount of CO₂-rich flue gas produced from these coal burning power stations can therefore be used productively in algae cultivation. The expected level of CO₂ in a typical flue gas from a power plant is in the range of 10-20% (Mijeong, 2003), which meets or exceeds the amount required for most strains of microalgae.

2.3 Effect of nutrients on microalgae growth

In addition to CO₂, about 30 elements are important to ensure autotrophic growth. According to the amount required by the microalgae, these essential nutrients are grouped into two categories: 1) macronutrients, which are required in the culture medium in relatively large concentrations of g/L; and 2) micronutrients (trace elements), which are required in the culture medium in mg/L or less (Procházková et al., 2013). Most algae nutrient solutions contain both macronutrients (N, P and K) and micronutrients (Raghawan et al., 2008). Key nutrients essential for autotrophic microalgae are shown in Table 3 (Grobbelaar, 2004). If any of these nutrients exist naturally in the water used to grow algae, such waters will provide an economic advantage.

Table 3. Nutrients essential for autotrophic microalgae and elemental

Element	Component added to culture medium	Concentration in culture medium	Cell composition (mg g ⁻¹ dry weight)
C	CO ₂ , HCO ₃ ⁻ , CO ₃ ²⁻	g L ⁻¹	175–650
O	O ₂ , H ₂ O	g L ⁻¹	205–330
H	H ₂ O	g L ⁻¹	29–100
N	NH ₄ ⁺ , NO ₃ ⁻ , NO ₂ ⁻ , urea etc.	g L ⁻¹	10–140
Na	Inorganic salts, i.e. NaCl, Na ₂ SO ₄ , Na ₃ PO ₄	g L ⁻¹	0.4–47
K	Inorganic salts, i.e. KCl, K ₂ SO ₄ , K ₃ PO ₄	g L ⁻¹	1–75
Ca	Inorganic salts, i.e. CaCl ₂ , CaCO ₃	g L ⁻¹	0.0–80
P	Inorganic salts, i.e. Na or K phosphates	g L ⁻¹	0.5–33
S	Inorganic salts, i.e. MgSO ₄ ·7H ₂ O, or amino acids	g L ⁻¹	1.5–16
Mg	Inorganic salts, i.e. Mg sulphates or chlorides	g L ⁻¹	0.5–75
Cl	As Na ⁺ , K ⁺ , Ca ²⁺ or NH ₄ ⁺ salts	g L ⁻¹	*
Fe	In complex with metal ion buffer (e.g. EDTA)	mg L ⁻¹	0.2–34
Zn	Inorganic salts, i.e. ZnSO ₄ , ZnCl ₂	mg L ⁻¹	0.005–1.0
Mn	Inorganic salts, i.e. MnSO ₄ , MnCl ₂	mg L ⁻¹	0.02–0.24
Br	As Na ⁺ , K ⁺ , Ca ²⁺ or NH ₄ ⁺ salts	mg L ⁻¹	*
Si	Na ₃ SiO ₃ ·9H ₂ O	mg L ⁻¹	0–230
B	H ₃ BO ₃	mg L ⁻¹	0.001–0.25
Mo	Na ⁺ or NH ₄ ⁺ molybdate salts	µg L ⁻¹	0.0002–0.001
V	Na ₃ VO ₄ ·16H ₂ O	µg L ⁻¹	*
Sr	As sulphates or chlorides	µg L ⁻¹	*
Al	As sulphates or chlorides	µg L ⁻¹	*
Rb	As sulphates or chlorides	µg L ⁻¹	*
Li	As sulphates or chlorides	µg L ⁻¹	*
Cu	As sulphates or chlorides	µg L ⁻¹	0.006–0.3
Co	Vitamin B ₁₂ , sulphates or chlorides	µg L ⁻¹	0.0001–0.2
I	As Na ⁺ , K ⁺ , Ca ²⁺ or NH ₄ ⁺ salts	µg L ⁻¹	*
Se	SeO ₃ ²⁻ , SeO ₄ ²⁻	ng L ⁻¹	0–0.9 ^a

* Data not available

composition of algal cells (Grobbelaar, 2004)

When considering the composition of growth waters, it is important to distinguish between freshwater, marine, and halotolerant/halophilic algae species. Seawater has a relatively constant pH and composition of major ions (Na^+ , K^+ , Mg_2^+ , Ca_2^+ , Cl^- , SO_4^{2-} , HCO_3^- , CO_3^{2-}), whereas freshwaters have highly variable compositions. Microalgae species that grow in particular waters are appropriately adapted to the chemistries of those waters. For example, when growing in freshwater containing high concentrations of particular metals (e.g., copper) that are toxic to the majority of other phytoplankton species, cells possess particular detoxification or tolerance mechanisms (Sunda, 2005). Another key adaptation possessed by certain species is that, if the concentration of an essential nutrient falls below a required level, the cells interpret the limitation and produce a specific set of genes in order to alter their physiology and adapt to the deficiency (Cade-Menun and Paytan, 2010).

2.3.1 Key elements for microalgae growth

The absolutely essential elements for microalgae growth are nitrogen, phosphorus, and carbon. The roles played by each of these elements are discussed in the following sections.

2.3.1.1 Nitrogen

Nitrogen is an important macronutrient for microalgae: it is the most abundant cellular macromolecule in the form of proteins and nucleic acids. Nitrogen usually is supplied in forms such as NO_3^- , NO_2^- , NH_4^+ , and $(\text{NH}_2)_2\text{CO}$ (urea). The preferred N form for many algae is NH_4^+ since it can be incorporated directly into organic compounds. NH_4^+ concentrations greater than 25 μM are often reported to be toxic for some algal species, so NO_3^- is used more often in synthetic culture media (Barsanti, 2006).

2.3.1.2 Phosphorus

Like nitrogen, phosphorus is an essential macronutrient for the growth of algae. Algal biomass usually contains less than 1% of P, but P levels can exceed 3% by dry weight under certain conditions. The particular importance of phosphorus is in the biosynthesis of nucleic acid and phospholipids, protein function modification, and energy transfer (Powell, 2009). Algae primarily acquire P as inorganic phosphate in the form of either H_2PO_4^- or HPO_4^{2-} .

Larger amounts of P, orthophosphate monoesters (including sugar phosphates, inositol phosphates, and orthophosphate diester degradation products), are found in seawater phytoplankton grown under high light conditions as compared to the same algae grown under low light conditions (Chang, 2011). In freshwater phytoplankton, P is often the main growth-limiting nutrient and it is stored as intracellular polyphosphate. Polyphosphate bodies in eukaryotic algae represent another form of cell protection from metal toxicity, as they can bind incoming metals in a detoxified complex (Cade-Menun and Paytan, 2010).

2.3.1.3 Carbon

Carbon is an essential component of all algae cultures and represents 50% of cell dry weight. Consequently, a limitation in this macronutrient stops biosynthesis (Chisti, 2007). Depending on the source from which carbon is drawn, microalgae species can be divided into autotrophs and heterotrophs. Autotrophic organisms use solar energy to convert and utilize inorganic forms of carbon such as CO₂, carbonate, or bicarbonate. Heterotrophs, in contrast, use the chemical energy of organic forms of carbon (e.g., acetate or glucose) for their metabolic activities (Pires, 2015). Prolonged deprivation of carbon affects photosynthetic energy acquisition and photosynthetic efficiency.

Equation (1) describes the reaction that takes place when gaseous CO₂ is dissolved into water, forming H₂CO₃^{*}, carbonic acid. This reaction occurs between pH 6.5 and 7.5; the other alkaline species, HCO₃⁻ and CO₃²⁻, are not present. However, dissolved carbonic acid, H₂CO₃^{*}, is maximized when the pH is 6.5, and its presence decreases to zero when the pH is 8.5 (Sawyer and McCarty), as H₂CO₃^{*} dissociates to H⁺ and HCO₃⁻ (shown in Eq. (2)) as pH reaches 7.5. The released H⁺ will react with the available calcium carbonate alkalines to form HCO₃⁻, as shown in Eq. (3). More CO₂ dissolved reacts to form HCO₃⁻, Equation (4) (Maung-Thein, 2014).



Autotrophic cultures respond to low levels of CO₂ by increasing the assimilation of the limiting nutrient and at the same time adjusting its capacity, flux rates, and intermediate storage options for the non-limiting nutrients (Giordano, 2005).

2.4 Algae metal reduction

Organic pollutants and heavy metals are considered to be a serious environmental problem during disposal of desalination concentrate. Accumulation of toxic metals e.g. Hg, Cu, Cd, Cr and Zn in humans has several consequences such as growth and developmental abnormalities, carcinogenesis, neuromuscular control defects, mental retardation, renal malfunction and wide range of other illnesses (Dwivedi, 2012).

Microalgae have the ability of reducing heavy metals and its toxicity effects in its habitat; therefore would be effective in reducing the heavy metal toxicity in desalination concentrate. These metals exist in form of free ions, complex ions or in particulate forms (Shaw, 1989). Toxicity of copper, zinc, cadmium, mercury is reduced by calcium and magnesium salts as a result of co-precipitation in some algae, other types of algae synthesize phytochelatins and metallothioneins that can form complexes with heavy metals and translocate them into vacuoles (Sakaguchi et al., 1981).

In order to control heavy metal levels before they are released into the environment, the treatment of the contaminated wastewaters is of great importance since heavy metal ions accumulate in living species with a permanent toxic and carcinogenic effect (Worku and Sahu, 2014).

CHAPTER 3: MATERIAL AND METHODS

3.1 Experimental Set-Up

A lab-scale bioreactor design containing thirty-six 500 mL glass photobioreactors (as shown in Figure 6) was used to conduct the experiments in this study. The photobioreactors were partially filled with 200 mL of growth medium and 50 mL of algae inoculum according to the experimental design, discussed in Section 3.3. The bioreactors were then conditioned with parameters (Table 4) and equipped with an air and CO₂ supply system.



Figure 6. Bioreactor setup.

Table 4. Generalized conditions for culturing microalgae in photobioreactor.

Parameters	Value	Literature
Temp (°C)	24-26	(Crowe et al., 2012; Rocha et al., 2003; Tamburic et al., 2014)
Light intensity ($\mu\text{mol}/\text{m}^2\cdot\text{s}$)	2000	(Aburezq et al., 1999; Sharma et al., 2012)
Photoperiod (light:dark)	16:8	(Sforza and Simionato, 2012; Sharma et al., 2012)
pH	6.7-8.2	(Franco et al., 2012; Rocha et al., 2003)

During the cultivation period, 1 μL of algal broth was sampled at the 3rd, 6th, 10th and 14th days, and then cell count was conducted using an improved

Neubauer haemocytometer to determine the growth rate of the algae species. Deionized water was added during each sampling day to replenish the water lost through evaporation in the bioreactor.

3.2 Algae strains and culture

In this study, two strains of algae were used – *C. sorokiniana* (UTEX 1230) and *N. oculata* (UTEX 2640). These species are fresh water microalgae and marine microalgae, respectively; however, *C. sorokiniana* is halotolerant, and therefore it can grow in desalination concentrate (Ramikrishan, 2014). Growth media suitable for the strains were prepared based of recipe in Table 2: BBM was used for *C. sorokiniana*, and F/2 was used for *N. oculata*. The starting algae used for the experiment were obtained from the University of Texas Algae Collection in Austin, Texas. The algae were obtained in a volume of 500 mL, then cultured and retrieved at exponential growth stage at the concentration 3.7×10^7 cells/mL.

3.3 Design of experiment

The first set of experiments was designed to investigate how ROC and blended ROC affect the growth of the two studied algae strains. Six different growth media were used in the experimental design. For *C. sorokiniana*, these growth media were BBM, ROC, B-ROC, and deionized (DI) water. For *N. oculata*, the growth media were F/2, ROC, F-ROC, and DI water. The DI water was used as a control. The F/2 and BBM media were prepared by adding growth medium components, trace elements, and vitamin solutions to 950 mL of DI water, based on the components shown in Table 5.

ROC was obtained from the RO pilot plant desalination system at the Brackish Groundwater National Desalination Research Facility (BGNDRF) in Alamogordo, New Mexico. BGNDRF has access to four brackish groundwater wells with a wide range of salinities.

Table 5. Components of the F/2 (Guillard, 1978) and BBM (Stein, 1973) growth media.

Component	F/2	BBM
NaNO ₃ (g/L)	75.00	25.00
NaH ₂ PO ₄ ·H ₂ O (g/L)	5.00	17.50
Na ₂ SiO ₃ ·9H ₂ O (g/L)	30.00	30.00
F2 Trace Metal Solution (mL)	1.00	
F2 Vitamin Solution (mL)	0.50	
NaCl (g/L)		2.50
H ₃ BO ₃ (g/L)		5.75
Trace Elements		
FeCl ₃ ·6H ₂ O (g/L)	3.15	
Na ₂ EDTA·2H ₂ O (g/L)	4.36	

CuSO ₄ ·5H ₂ O (g/L)	9.80	
Co(NO ₃) ₂ ·6H ₂ O (g/L)		0.05
Na ₂ EDTA·2H ₂ O (g/L)		4.36

The details of the utilized RO system and the conditions and availabilities of the brackish water in BGNDRF are provided by Karimi et al. (2015). The electrical conductivities (ECs) of the different growth media are given in Table 6. Additionally, the ionic concentration of the ROC, which was obtained from ICP-OES analysis, is provided in Table 7.

Table 6. Electrical conductivities of media.

Medium	BBM	F/2	ROC	B-ROC	F-ROC
EC (mS/cm)	13.2	15.4	9.78-10.44	11.32-11.6	12.4-13.7

Table 7. Ion content in the desalination concentrate.

Ion	K ⁺	Na ⁺	Mg ²⁺	Ca ²⁺	TN*	S	P
Concentration (mg/L)	40.5	880	461.2	905.2	193	1491	17.8

* Total N

A second set of experiments was conducted to determine how different levels of P, N, and CO₂ affect microalgae growth in ROC. The resulting data was used to develop a predictive model that can be used to optimize microalgae growth in concentrate. In this set of experiments, two levels of P (15 and 75 parts per thousand [ppt]) and two levels of N (15 and 75 ppt) were added to ROC at three different CO₂ concentrations based on the volume percentage (0.03% [ambient air], 2%, and 5%).

The fractional factorial design was developed for experiments at different combinations of different factors, as shown in Table 8. For the P and N columns in this table, H indicates 75 ppt and L indicates 25 ppt. In the CO₂ column, L indicates 0.03% CO₂ by volume, M indicates 2% CO₂ by volume, and H indicates 5% CO₂ by volume. Since preliminary experiments identified N as an essential nutrient in growth media for microalgae, most combinations in this set of experiments fixed N at the highest investigated level of 75 ppt. The growths of the two algae strains were measured using the cell counting methods described in

Section 2.3, and the maximum growth of algae was observed during the 10th day, shown in the growth charts for *C. sorokiniana* (Figure 7) and *N. oculata* (Figure 8). Therefore, the response for data analysis was considered the amount of algae growth by day 10.

Table 8. Combinations of different factors.

P (Level)	N (Level)	CO ₂ (Level)
H	L	L
H	L	M
H	L	H
L	H	L
L	H	M
L	H	H
H	H	L
H	H	M
H	H	H

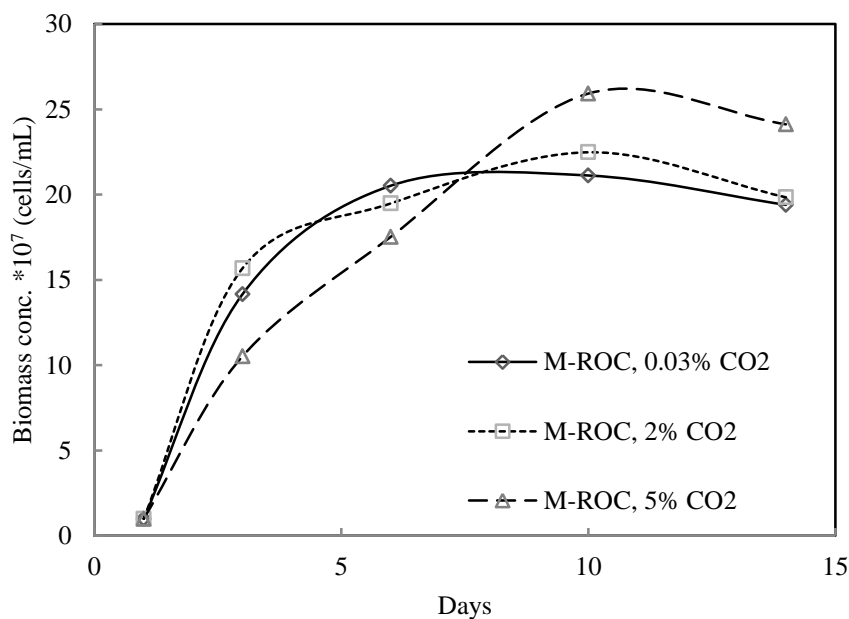


Figure 7. Growth pattern for *C. sorokiniana* species in M-ROC.

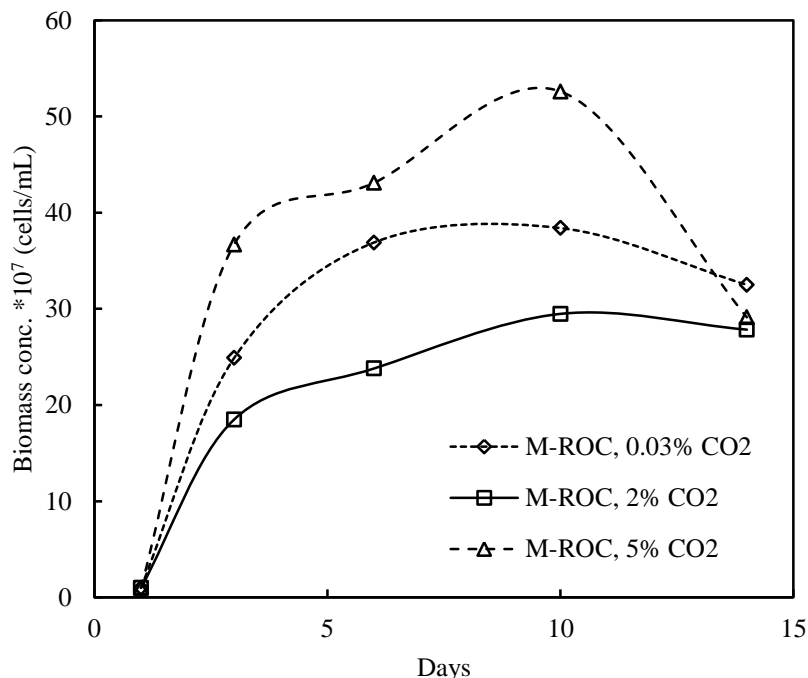


Figure 8. Growth pattern for *N. oculata* species in M-ROC.

At the end of the analysis, the best combination of nutrient were studied for ion content removal. Supernatant from each strain were analyzed on ICP-OES spectroscopy, and the heavy metal concentrations were evaluated.

3.4 Calculations and statistical analysis

Algae growth was reported in concentrations of cells per milliliter of culture, using the equation for Neubauer chamber calculation (Oscar, Technical note- Neubauer chamber cell counting, 2009), shown in Eq. (5):

$$\text{Concentration (cells/mL)} = \frac{(\text{No. of cells} \times 10,000)}{(\text{No. of square} \times \text{dilution})} \quad \text{Eq. (5)}$$

In the first set of experiments, the visual differences between the growths of algae in different growth media were investigated, and statistical analysis was conducted to discern how the studied parameters affect the growth of algae. Equation 1 was also used for the second set of experiments, and from the results, statistical analysis using Minitab 16 was conducted to develop a predictive model for algae growth.

Algae metal reductions were analyzed using difference in metal concentrations before and after culture. The concentrations were from ICP-OES analysis of the

desalination water before the experiment, and supernatant of algae culture after the experiment.

CHAPTER 4: RESULTS AND DISCUSSION

4.1 Effect of Media on Growth of Microalgae

As shown in Figures 7 and 8, the exponential growth of algae cells ended at approximately the tenth day of the experiment for both of the algae strains. Experimental results indicated that the growths for these algal strains varied between the species and among the different media under ambient air CO₂ levels, with the cell concentrations for the strains ranging from 5×10^7 cells/mL to 2.3×10^8 cells/mL for *C. sorokiniana* and 5×10^7 cells/mL to 3.7×10^8 cells/mL for *N. oculata*. The effect of media on the growth of *C. sorokiniana* is shown in Figure 9, which depicts that, although the concentration of main nutrients such as N and P in B-ROC was half the concentration in the BBM media, the maximum growth of *C. sorokiniana* was obtained when B-ROC was used as the media. The main reason for the better growth of *C. sorokiniana* in the medium of B-ROC can be attributed to its lower salinity compared to BBM, because *C. sorokiniana* is a fresh water strain and can survive in fresh water media. However, *C. sorokiniana* could not grow well in the DI water and ROC media because of the lack of nutrients. Additionally, the growth of *C. sorokiniana* was lower in ROC compared to two other conditions, because although ROC had less salinity compared to B-ROC, it had little N, a main nutrient required for algae growth (Raghawan, 2008).

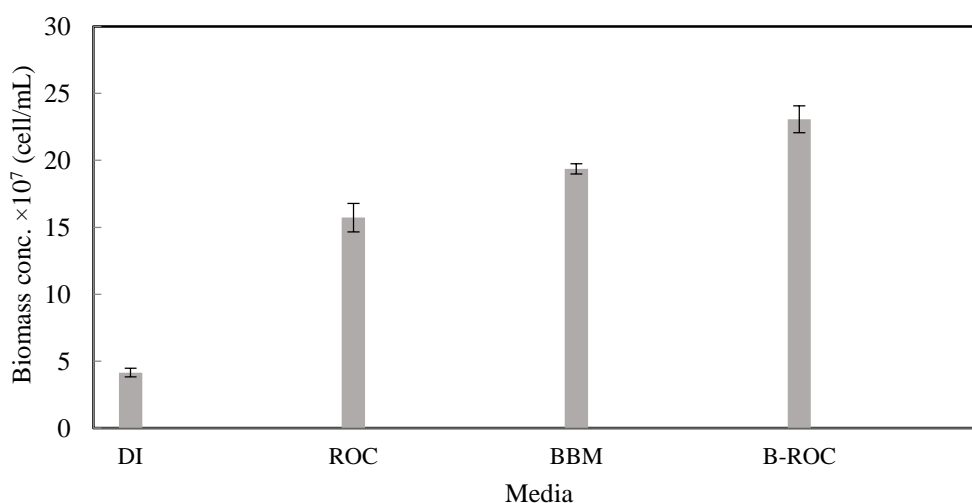


Figure 9. *C. sorokiniana* growth in different media at ambient air CO₂ level.

The influence of media on the growth of *N. oculata* was also investigated, and the results are shown in Figure 10, which shows that the maximum growth of *N. oculata* was obtained when F-ROC was used as the growth media. Although there was no significant difference between *N. oculata* growth in F-ROC and *N. oculata* growth in F/2, the absence of a significant difference means that F-ROC can replace F/2, thereby offering dual benefits for managing brine in inland desalination plants and cultivating *N. oculata* as biomass for biofuel production at lower cost. However, similar to the results observed for the growth of *C. sorokiniana*, ROC resulted in lower growth due to the lack of main nutrients such as N and P. The DI water, used as a control medium for both algae strains, resulted in a small amount of growth for both algae strains.

In a comparison of the growth results for both algae strains, it was found that *N. oculata* grew faster than *C. sorokiniana* in the investigated media, likely because *N. oculata* is a marine algae species and the concentrate media are highly saline. Additionally, *N. oculata* grown in F-ROC media under ambient air conditions produced the highest growth at the 10th day, with a cell concentration of 3.7×10^8 cells/mL.

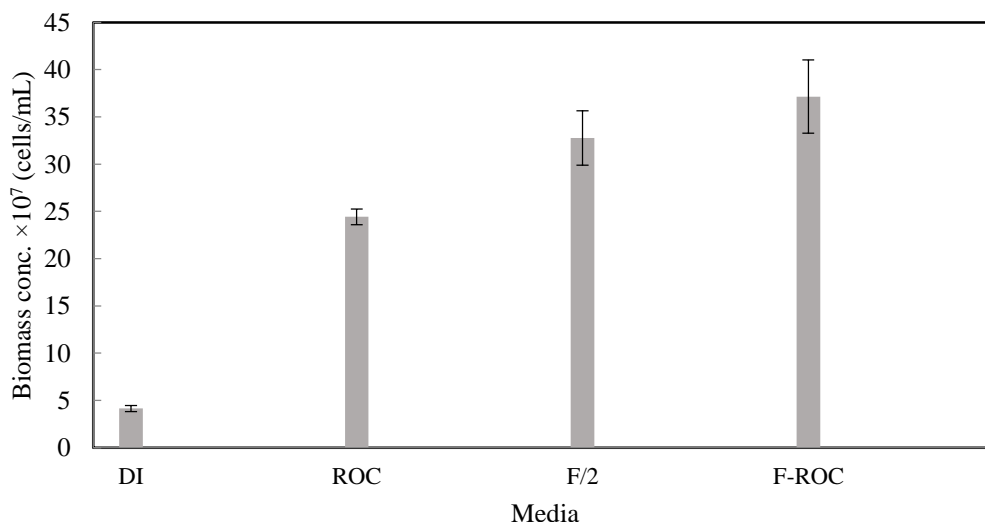


Figure 10. *N. oculata* growth in different media under ambient air CO₂ level.

As compared to ROC and DI water, the conventional media exhibited higher levels of algae growth, which is attributable to the N and P levels in conventional media. This finding led to further study of the concentrate water to produce even better results, which are presented in the following section.

4.2 Predictive Model

In the literature, both wastewater and desalination concentrate have been considered as potential sources of water and media for the production of algal biomass (Hussein, 2013). However, it has been a challenge to select proper conditions under which algae can be grown in concentrate, as there are no established criteria as of yet. According to our experience in algae-based biofuel research and as shown in Section 3.1, a promising medium is expected to satisfy the following requirements: 1) have a high nutrient content, 2) produce a high growth rate, and 3) produce a high cell density at the end of stationary growth stage. According to our recent findings on the effects of media on algae growth, M-ROC was chosen for further investigation on the influence of P, N, and CO₂ levels.

A fractional factorial design of experiments was developed, and the effects of the target parameters were modeled. Linear regression analysis using Minitab software was employed for this purpose. The model was derived using algae concentration as the dependent variable, with N, P, and CO₂ concentrations as the independent variables. In the regression analysis, not only were the three main independent variables taken into account, but all possible interactions among the parameters were incorporated into the model to investigate the possibility that different parameters may have different effects at different levels of other parameters.

In pre-analysis before the regression model was developed, the partial least squares method was used to screen the significant parameters. The selection plot from the procedure determined that the optimal model should have 4 terms for *C. sorokiniana* and 5 terms for *N. oculata*. Loading plots from the partial least squares procedure further clarified the interaction terms that should be eliminated to yield the optimal model: for *C. sorokiniana*, P × N, CO₂, and P × N × CO₂ were eliminated; for *N. oculata*, P × N and P × N × CO₂ were eliminated.

Regression analysis was conducted for the *C. sorokiniana* strain, and the effects of the studied parameters were investigated. As shown in Table 5, the levels of individual parameters, such as P and N, had significant effects on the growth of *C. sorokiniana*, while the effect of CO₂ depended on the level of N and P, as shown by p-values less than 0.05. Based on the effective variables and their interactions, a linear regression model was developed (Equation 6).

Table 5. Factors significance in regression model for *C. sorokiniana*

Source	Coef.	SE Coef.	T-value	p-value
Constant	13.094	0.926	14.15	0

P	-0.0395	0.0117	-3.36	0.004
N	0.0756	0.0102	7.39	0
P*CO ₂	-0.000615	0.000227	-2.71	0.015
N*CO ₂	0.001099	0.000239	4.6	0
R ²	94.88%		R ² (adj)	93.67%
R ² (pred)	91.99%		No. of obs.	21

$$C. \text{ sorokiniana concentration} = 13.094 - 0.0395 \times P + 0.0756 \times N - 0.000615 P \times CO_2 + 0.001099 N \times CO_2 \quad \text{Eq. (6)}$$

As shown in the regression equation, increases in N promote the growth of *C. sorokiniana*. The growth of this algae strain also proved more sensitive than *N. oculata* to variations in the concentration of N. Notably, P had a negative coefficient for microalgae growth in ROC, a result very different from findings in conventional media, where P serves as an essential nutrient. This result merits further research. The effects of P and CO₂ and the effects of N and CO₂ were not independent of each other, as shown by their combined variables. Therefore, an optimum condition should be chosen in consideration of the interactions between these variables. The interaction graphs for the above-mentioned variables are plotted in Figures 11 and 12, which show the interactions between P and CO₂ and N and CO₂, respectively. In the experiments behind Figure 11, N was held constant at 75 ppt, and in the experiments behind Figure 12, P was held constant at 75 ppt. As can be seen in Figure 11, higher levels of CO₂ yielded higher *C. sorokiniana* growth. From Figure 12, it is determined that, although a higher concentration of CO₂ resulted in a higher growth of *C. sorokiniana* at the studied concentration for P when N levels were above 44 ppt, a lower concentration of CO₂ yielded better results at 75 ppt P when the concentration of N was kept at levels lower than 44 ppt.

Ultimately, considering the data reported in Figures 11 and 12, the maximum growth of the *C. sorokiniana* strain (2.68×10^8 cells/mL) in the studied range of parameters can be obtained at higher concentrations of CO₂ and N but at lower concentrations of P.

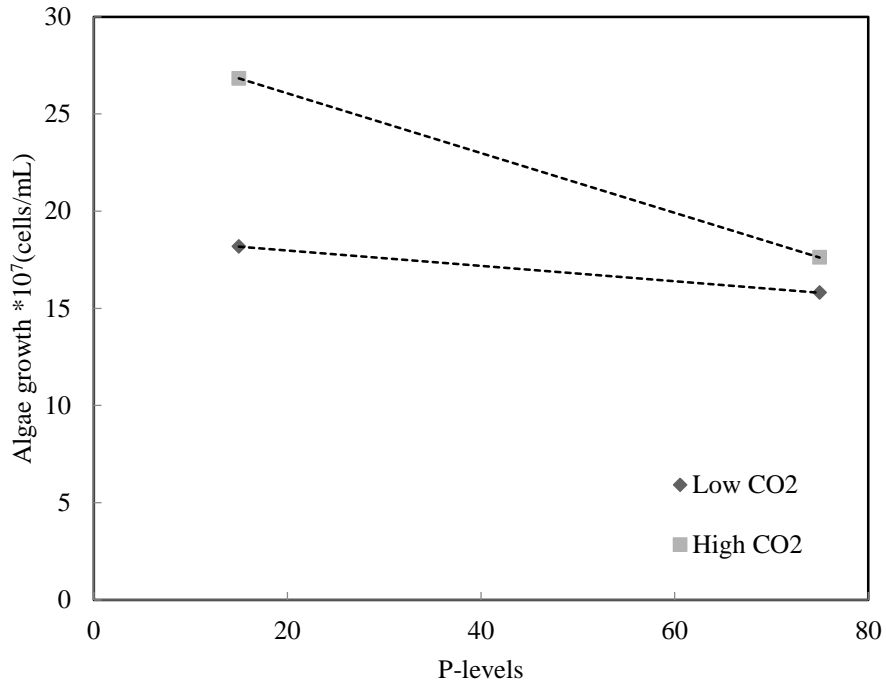


Figure 11. The effect of P-CO₂ interaction on the growth of *C. sorokiniana* at 75 ppt of N.

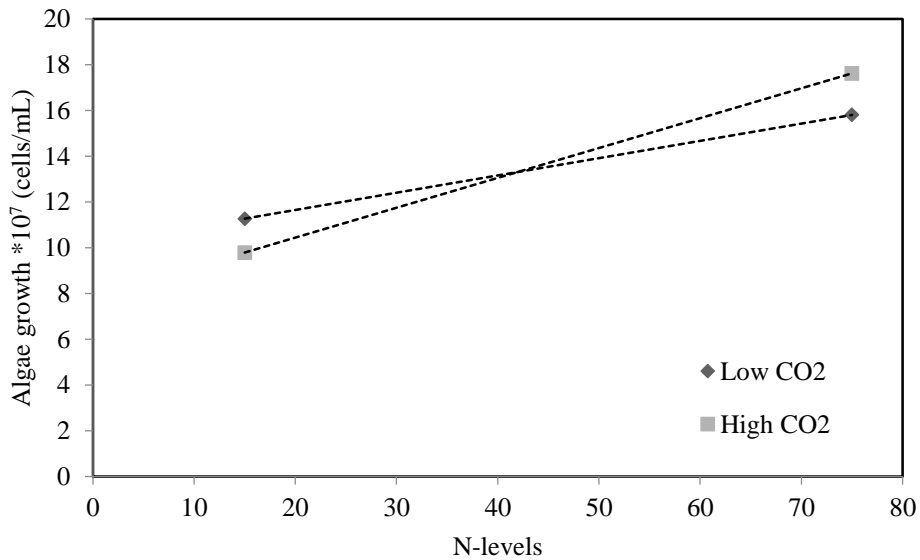


Figure 12. N-CO₂ interaction effect for *C. sorokiniana* at 75 ppt of P.

The partial least squares method was also applied to choose the appropriate variables in the regression analysis. On the basis of this method, the interactions $P \times N$ and $P \times N \times CO_2$ were eliminated for the *N. oculata* strain; the loading plots from the partial least squares procedure showed their insignificance.

Regression analysis was conducted for the *N. oculata* strain, and the effects of the studied parameters were investigated. As shown in Table 6, the levels of individual parameters, such as P, N, and CO_2 , have significant effects on the growth of *N. oculata*. Additionally, the effect of CO_2 varies with the levels of N and P, as shown by *p*-values below 0.05 for these interaction terms. Based on the effective variables and their interactions, a linear regression model is presented, as shown in Equation 7.

Table 6. Factor significance in regression model for *N. oculata* growth.

Source	Coef.	SE Coef.	T-value	P-value
Constant	13.31	4.53	2.94	0
N	0.1119	0.0471	2.37	0.029
P	0.2806	0.0445	6.31	0
CO_2	0.621	0.14	4.45	0
$P \times CO_2$	-0.01159	0.00138	-8.39	0
$N \times CO_2$	0.00464	0.00144	3.21	0.005
R^2	93.80%		R^2 (pred)	89.78%
R^2 (adj)	92.08%		No. of obs.	23

$$N. \textit{oculata} \text{ concentration} = 13.31 + 0.1119 \times N + 0.2806 \times P + 0.621 \times CO_2 - 0.01159 P \times CO_2 + 0.00464 N \times CO_2 \quad Eq. (7)$$

As shown in Equation 7, increasing the concentration of N in the medium has a purely positive effect on the growth of the *N. oculata* strain, a result similar to the findings for *C. sorokiniana*.

Figures 13 and 14 show the effects of combinations of factors on the predicted growth values of *N. oculata*. In Figure 13, N was held constant at 75 ppt; in Figure 14, P was held constant at 75 ppt. As illustrated in these figures, although a higher concentration of CO_2 is typically desired in the studied range of P, a lower concentration of CO_2 is preferred at P levels of 75 ppt and N levels below 55 ppt. From these figures, it is concluded that the maximum growth for *N. oculata* (6.5×10^8 cells/mL) occurs at the highest concentrations of N and CO_2 but at a lower concentration of P.

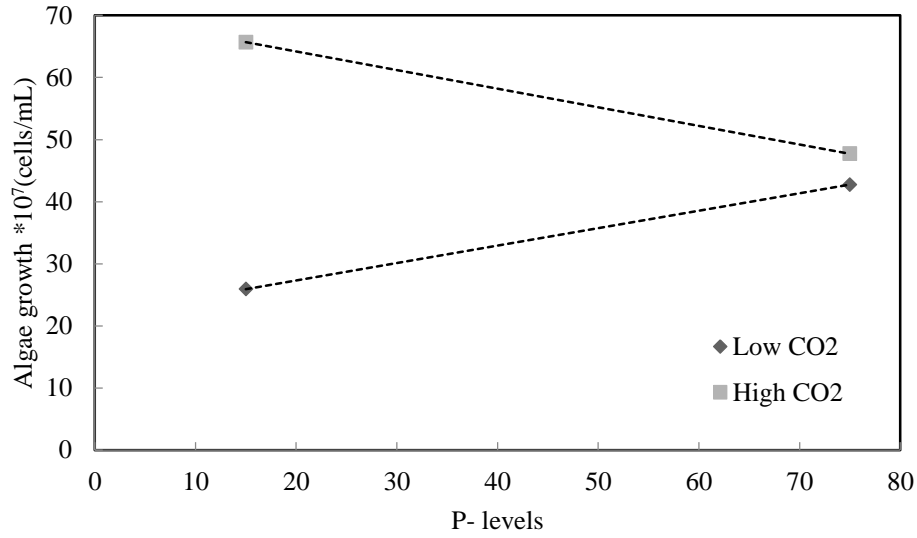


Figure 13. P-CO₂ interaction effect for *N. oculata* 75 ppt of N.

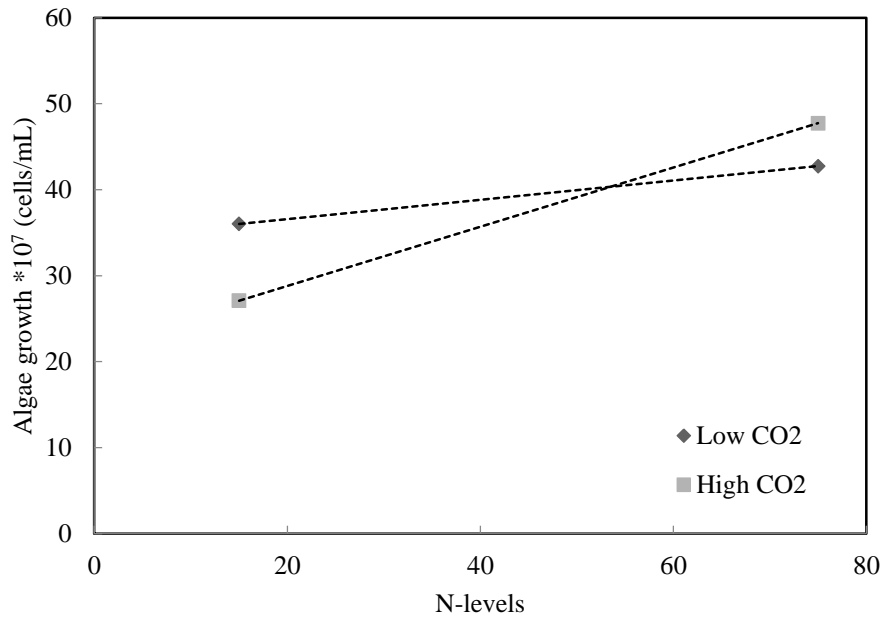


Figure 14. P-CO₂ interaction effect for *N. oculata* 75 ppt of P.

4.3 Ion removal

Figures 15 and 16 offer an analysis of the concentrations of heavy metals before culturing and after the culturing period for both algae species. This result showed

a reduction in metal concentration for *C. sorokiniana* species at all CO₂ levels. Significant reductions in metal concentration were observed at 2% and 5% CO₂ levels. Copper metal was the exception, as it showed an increase in concentration at the end of experiment.

N. oculata species increased the concentrations of the metals at the end of experiment, with the exception of bismuth. These increases in metal concentration may be attributed to bacterial or protozoan breakdown or conversion of other metals present in the desalination water, leading to the accumulation of those heavy metals.

As observed from the results, the differences in species affected the reduction of and tolerance for the heavy metals.

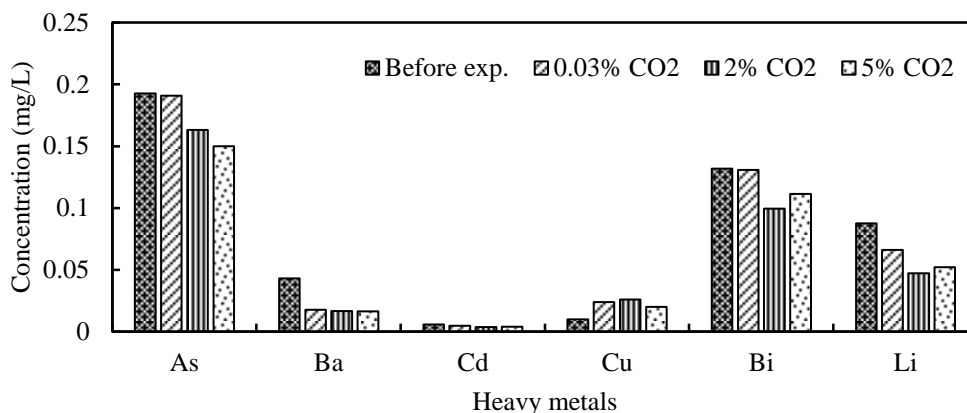


Figure 15. Ion removal in *C. sorokiniana*.

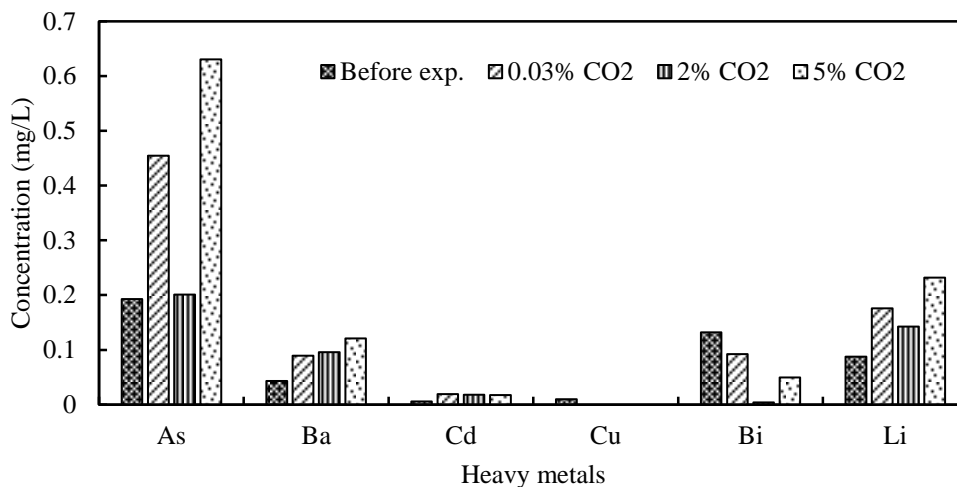


Figure 16. Ion removal in *N. oculata*.

CHAPTER 5: CONCLUSION

The results obtained in this research show that desalination concentrate can be utilized as a microalgae growth medium; however, adding nutrients, such as N, resulted in better microalgae growth. The modified desalination concentrate provided the optimum conditions for cultivating algae. This study suggests that, if N and CO₂ are maintained at a high ratio to P in concentrate water, both freshwater and marine strains of algae could thrive well. In unmodified ROC, *N. oculata* showed better performance than *C. sorokiniana*, achieving roughly 55% higher growth. The use of such species in a growth medium of concentrate or modified concentrate could help alleviate water scarcity in society while providing biomass to curb energy stress.

Differences in heavy metal reduction were observed with the selected microalgae species, as heavy metal concentrations increased in the cultivation media for *N. oculata* but decreased in the cultivation media for *C. sorokiniana*. This suggests that *Chlorella* species is among the species that can tolerate elevated heavy metal concentrations.

Although the algae strains showed good performance in this laboratory experiment, more intensive investigations regarding even lower levels of P and higher levels of N and CO₂ should be implemented in the future, particularly under field stress conditions (like light stress, salt stress, etc.). Lipid content for the strains could also be investigated for nutrient fluctuations. Additionally, future research could pursue an explanation for the negative impacts of high P, usually regarded as a nutrient, when concentrate or blended concentrate is used as a growth medium.

REFERENCES

- Aburezq, T., Musallam, L., Shimmari, J., 1999. Optimum production conditions for different high quality marine microalgae . *Hydrobiologia* 97–107.
- Altan, O., Kerry, K., Lynn, K., Halil, B., 2012. Reduction of water and energy requirement of algae cultivation an algae biofilm photobioreactor. *Bioresour. Technol.* 542–548.
- Altin, R., Cetinkaya, S., Yucesu, H., 2001. Potential of Using Vegetable Oil Fuels as Fuel for Diesel Engines. *Energy Convers. Manag.* 529–538.
- Ankita, J.R.M., 2013. Effects of Environmental Factors and Nutrient and the Biochemical Compostion of Algae for Biomass. *Energies* 6.
- Barsanti, L., 2006. Algal culturing. In *Algae: anatomy, biochemistry and biotechnology*. Boca Ranton, pp. 209–250.
- BP, 2014. Stastical review of world energy consumption.
- Cade-Menun, B.J., Paytan, A., 2010. Nutrient temperature and light stress alter phosphorus and carbon forms in culture-grown algae. *Mar. Chem.* 121, 27–36.
doi:10.1016/j.marchem.2010.03.002
- Chang, J.C., 2011. Cultivation, photobioreactor design and harvesting of microalgae for biodiesel production: a critical review . *Bioresour. Technol.* 71–81.
- Chisti, Y., 2008. Biodiesel from microalgae beats bioethanol.
- Chisti, Y., 2007. Biodiesel from microalgae. *Biotechnol. Adv.* 294–306.
- Crowe, B., Attalah, S., Agrawal, S., 2012. A comparison of *Nannochloropsis salina* growth performance in two outdoor pond design. *Int. J. Chem. Eng.* 2012.

- Cynthia, F., 2011. Energy and water nexus for mass cultivation of algae.
- Dwivedi, S., 2012. Bioremediation of heavy metal by algae: current and future perspective. *J. Adv. Lab. Res. Biol.* III, 195–199.
- EIA, 2012. *World Energy*. IEA.
- Franco, M., Buffing, M., Janssen, M., 2012. Performance of *Chlorella sorokiniana* under extreme winter conditions. *Appl. Phycol.* 693–699.
- Giordano, M.B., 2005. CO₂ concentrating mechanisms in algae: mechanisms, environmental modulation, and evolution. *Annu. Rev. Plant Biol.* 99–131.
- Gleick, P.H., 1993. *Water in crisis a guide to the world's fresh water resources*. *Water Cris. a Guid. to world's fresh water Resour.* 13–24. doi:10.2307/2623756
- Graham, L., 2000. *Algae*. Upper Saddle River, NJ.
- Greenlee, L.F., Lawler, D.F., Freeman, B.D., Marrot, B., Moulin, P., 2009. Reverse osmosis desalination: Water sources, technology, and today's challenges. *Water Res.* 43, 2317–2348. doi:10.1016/j.watres.2009.03.010
- Grobbelaar, J., 2004. *Algal nutrition: mineral nutrition.*, *Handbook of microalgal culture*.
- Guiry, M.D., 2012. How many species of algae are there? *J. Phycol.* doi:10.1111/j.1529-8817.2012.01222.x
- Hafez, A., El-Manharawy, S., 2002. Economics of seawater RO desalination in the red sea region, Egypt. *Desalination* 335–347.
- Hussein, W., Myint, M.T., Ghassemi, A., 2015. Energy usage and carbon dioxide emission saving in desalination by using desalination concentrate and wastes in microalgae production. *Desalin. Water Treat.* 54, 69–83.
doi:10.1080/19443994.2014.884476
- Jajesniak, P.A., 2014. Carbon dioxide capture and utilization using biological systems: opportunities and challenges. *Bioprocess. Biotech.*
- Khaled, A., 2012. Process of growing and harvesting algae in seawater with feather

additives.

Malakootian, M.H., 2014. Evaluation of factors affecting lipid extraction for recovery in *nannochloropsis oculata*. *Environ. Heal. Eng. Manag. J.* 19–24.

Matsukawa, R., 2000. Antioxidants from carbon dioxide fixing *Chlorella sorokiniana*. *J. Appl. Phycol.* 263–267.

Maung-Thein, M., 2014. Using indigenous microalga species to reduce nutrients from high conductivity concentrate. *Desalination* 61–68.

Mijeong, L., 2003. Carbon dioxide mitigation by microalgal photosynthesis. *Bull. Korean Chem. Soc.* 1763.

Mike, R., 2014. Water desalination and energy. *Technol. Bus. Dev.*

Organization, U. and W.H., 2012. Progress on Drinking Water and Sanitation. Update. doi:978-924-1503279

Pedroni, P., Davison, J., Beckert, H., Bergman, P., Benemann, J., 2003. A proposal to establish an international network for biofixation of CO₂ and greenhouse gas abatement with microalgae. *Science* (80-.). II, 1863–1866.

Pienkos, P., 2007. The potential for biofuels from algae., in: National Renewable Energy Laboratory. San Francisco: National Bioenergy Center. p. 2007.

Pires, J., 2015. Mass production of microalgae. In *Handbook of marine microalgae: biotechnology advances*. Elsevier, pp. 55–70.

Powell, N.S., 2009. Toward a luxury uptake process via microalgae-defining the polyphosphate dynamics . *Water Resour.* 4207–4213.

Procházková, G., Brányiková, I., Zachleder, V., Brányik, T., 2013. Effect of nutrient supply status on biomass composition of eukaryotic green microalgae. *J. Appl. Phycol.* 26, 1359–1377. doi:10.1007/s10811-013-0154-9

Raghawan, G., Haridevi, C., Gopinathan, C., 2008. Growth and proximate composition of the *Chaetoceros calcitrans* f. *pumilus* under different temperature, salinity and

- carbon dioxide levels. *Aquac. Res.* 1053–1058.
- Rocha, J.M.S., Garcia, J.E.C., Henriques, M.H.F., 2003. Growth aspects of the marine microalga *Nannochloropsis gaditana*. *Biomol. Eng.* 20, 237–242.
doi:10.1016/S1389-0344(03)00061-3
- Sakaguchi, T., Nakajima, A., Horikoshi, T., 1981. Studies on the accumulation heavy metal elements in biological system XVIII. Accumulation of molybdenum by green microalgae. *Eur. J. App. Microbiol. Biotechnol.* 12, 84–89.
- Sforza, E., Simionato, D., 2012. Adjusted light and dark cycles can optimize photosynthetic efficiency in algae growing in photobioreactor. Open online access.
- Sharma, R., Singh, G., Sharma, V., 2012. Effects of culture conditions on growth and biochemical profile of *Chlorella vulgaris*. *Plant Pathol. Microbiol.* 2012.
- Shaw, J., 1989. *Heavy Metal Tolerance in Plants: evolutionary aspect*. CRC press.
- Sheng-Yi, C., 2009. Lipid accumulation and CO₂ utilization of *Nannochloropsis oculata* in response to CO₂ aeration. *Bioresour. Technol.* 833–838.
- Shirazi, S., 2014. Simultaneous production of biofuel and treatment of concentrate stream of water desalination units using microalgae. New Mexico State University.
- Shon, H.P., 2013. Nanofiltration for water and waste water treatment. , 47-53. *Drink. water Eng. Sci.* 47–53.
- Sunda, W.N., 2005. Trace metal ion buffers and their use in culture., in: *Algal Culturing Techniques*. Elsevier Academic Press, San Diego, pp. 35–64.
- Takagi, M.W., 2000. Limited feeding of potassium nitrate for intracellular lipid and triglyceride accumulation of *Nannochloropsis* sp. *Appl. Microb. Biotechnol.* 112–117.
- Tamburic, B., Guruprasad, S., Radford, D.T., Szabó, M., Lilley, R.M., Larkum, A.W.D., Franklin, J.B., Kramer, D.M., Blackburn, S.I., Raven, J.A., Schliep, M., Ralph, P.J., 2014. The Effect of Diel Temperature and Light Cycles on the Growth of

Nannochloropsis oculata in a Photobioreactor Matrix. PLoS One 9, e86047.

doi:10.1371/journal.pone.0086047

Wateruse, 2009. Seawater Desalination.

Woertz, I., Feffer, A., 2009. Algae grown on dairy and municipal wastewater for simultaneous nutrient removal and lipid production for biofuel feedstock. Environ. Eng. 1115–1122.

Worku, A., Sahu, O., 2014. Reduction of Heavy Metal and Hardness from Ground Water by Algae. J. Appl. Environ. Microbiol. 2, 86–89. doi:10.12691/jaem-2-3-5

Part II: Pilot Scale Cultivation of Microalgae in Desalination
Concentrate

Abstract

Recent research has demonstrated that microalgae grow well in desalination concentrate. The concentrate can serve as a growth medium for the algae, while the algae remove contaminants from the concentrate. However, more investigation is necessary before this method can be implemented on a practical scale. The majority, if not all, of the published research in this field has been completed at the lab scale. Therefore, this research performs a bench-scale cultivation of microalgae in concentrate (brine) to investigate how well *Chlorella sorokiniana* (UTEX 1230) grows in brackish water desalination concentrate. UTEX 1230 was cultivated in two indoor raceway ponds with different concentrations of brine. The experiment was repeated once. Cell population growth, contaminant removal, and the evaporation rates of each pond were examined.

CHAPTER 1: INTRODUCTION

The viability of future generations depends on our commitment to live sustainably today. Five major sustainability concerns are water, food, energy, environmental health, and economic stability. Our current practices in these five areas are unsustainable, and the population growth in most of the world exacerbates the problem. Microalgae cultivated in desalination concentrate can contribute to a viable future in all of these areas.

Treating saline water sources is necessary to meet the growing demand for water resulting from population growth and industrialization. The expansion of saline water treatment is largely inhibited by financial and environmental concerns involved with concentrate disposal. Since algae are enhanced by and remove contaminants from desalination concentrate, their cultivation can alleviate the economic and environmental obstacles hindering the expansion of desalination techniques.

Algae can also contribute to a more sustainable food supply. Microalgae cultivation has the benefits of first-generation biofuels without the disadvantages of requiring arable land or competing with crops. In addition, microalgae may be used for producing nutritional supplements or as an ingredient in animal feed.

Furthermore, microalgae cultivation in concentrate can alleviate the energy crisis by providing feedstock for biodiesel, ethanol, or biogas production. Moreover, algae-based fuels can be used without net carbon dioxide emissions.

Growing microalgae in concentrate can also generate economic value by producing various products and reducing the cost of concentrate disposal. For all of these reasons and more, algae grown in concentrate medium can be a solution to many sustainability concerns.

According to a literature review, the “only two feasible methods available for large-scale production of microalgal biomass” are raceway ponds and tubular photobioreactors [1]. However, the vast majority, if not all, published research on microalgae concentrate management has been conducted at the laboratory scale (Hussein W.Z., 2014; Hussein, Myint, & Ghassemi, 2014; Matos, Morioka, & Sant’Anna, 2011; Matos et al., 2013; Maos et al., 2014; Matos et al., 2015; Matos et al., 2014; Morioka et al., 2014; Myint, 2014; Myint, Ghassemi, and Nirmalakhandan, 2010). This echoes a problem that inhibits algae-based biofuels

in general. As reported by the Food and Agriculture Organization of the United Nation, “Due to a lack of industrial scale experiments, there is insufficient knowledge to adequately judge the economic viability” of algae-based biofuels; “Productivity data is often extrapolated from small experiments and not always presented clearly and consistently” [15].

Chlorella sorokiniana (UTEX 1230) is a freshwater species of microalgae that is adaptive to highly saline environments. In previous lab-scale experiments, UTEX 1230 grew the best in desalination concentrate when compared to six other prospective species. It was therefore chosen to be cultivated in two indoor raceway ponds on a pilot scale. The experiment was run for 31 days under conditions that have been successful in previous research projects. After the first experimental run, the experiment was repeated with a length of 24 days to gain perspective on the variability of the results.

CHAPTER 2: MATERIALS AND METHODS

Desalination concentrate was taken from the Brackish Groundwater Desalination Research Facility (BGNDRF) in Alamogordo, New Mexico. This concentrate was obtained via reverse osmosis desalination of brackish water. The desalination concentrate in the first run of the experiment came from Well 2 at BGNDRF, whose water chemistry has been analyzed in the past and is somewhat consistent. Previous analyses of Well 2 water can be found at the referenced website [16]. An analysis of the ions in concentrate from Well 2 can be found in Paruchuri's referenced work, though this concentrate was produced by electro dialysis reversal (EDR) rather than the RO used in this experiment [13]. Trace element analyses of the concentrate used in both of the experimental runs are located in the appendix of this paper.

Chlorella sorokiniana (UTEX 1230) was obtained from the University of Texas and scaled up in a laboratory. It was subsequently cultivated in 10-L bioreactors at the same facility as the indoor ponds. The bioreactor algae were fed with the same nutrient source as the indoor ponds.

UTEX 1230 was cultivated in two 35-foot indoor raceway ponds at the New Mexico State University WERC A-Mountain greenhouse in Las Cruces, NM. One pond (Pond 7) contained only desalination concentrate and nutrients. The other pond (Pond 8) contained nutrients and concentrate that had been diluted with city water to approximately half of its original electrical conductivity. Both indoor ponds were in a humidified greenhouse. Ambient air was bubbled through both ponds using a 2-horsepower pump during the first run and a 1-horsepower pump during the second run. During the first run of the experiment, a paddle wheel in each pond operated at 24 rpm to ensure raceway circulation. During the second run, an air lift system was constructed to replace the paddle wheels, taking advantage of the air delivery system that was already running. The indoor raceway ponds used in the experiments are shown in Figures 1 and 2, and the bioreactors used to cultivate the inoculating algae are shown in Figure 3.

In Table 1, information is tabulated on the conditions of the ponds at the beginning of each experimental run. The listed information includes the volume of algae taken from the bioreactors for pond inoculation, the amount of nutrients initially fed to each pond, the depths of the ponds, and the ponds' electric conductivities after pond inoculation and feeding.

Table 1. Pond conditions on Day 1.

Volume of Inoculant		Amount of Miracid		Depth (in) Ponds 7/8		Conductivity (mS): Ponds 7/8	
Run 1	Run 2	Run 1	Run 2	Run 1	Run 2	Run 1	Run 2
33 L each	50 L each	1 lb. each	2 lb. each	12/11.5	13/13	8.21/4.40	8.6/4.3

**Figure 1.** Indoor raceway ponds for algae cultivation. Experiment Run 1.

A commercial fertilizer (Miracid) was used as the nutrient for algae cultivation. This fertilizer has a 30:10:10 ratio of N:P:K and also contains trace elements. It has worked well as a nutrient source in previous experiments. The fertilizer was fed to the ponds at an amount in excess of a previously established feeding quantity based on nitrogen (0.1 g N/L/month). In experimental runs 1 and 2, both ponds were fed on day 15 after measurements had been taken (1 lb. in Experiment

1 and 2 lbs. in Experiment 2). In Experiment 1, both ponds were fed about 1/3 lb. of fertilizer on day 27 after measurements had been taken.

The first experimental run ran for 31 days, and the second run ran for 24 days. Depth, pH, and electrical conductivity typically were measured five times per week. Temperature was also measured five times per week during the first run. Photos were taken of the ponds throughout the experiment. Cell count and cell sizing were conducted twice each week. A water analysis was completed once each week.

Conductivity was measured using a Hach sensION5 Conductivity Meter. The pH was measured using an Accumet[®] Basic AB15 pH meter. Temperature was measured using a multimeter. Cell counts were measured using a Hausser Scientific Hemocytometer. Cell counts measured the average UTEX 1230 population in a 4-nL volume. Cell sizing was completed by approximating the average diameter of the UTEX 1230 using an Olympus BX60 microscope. Water analysis was conducted via EPA method 200.7, which uses inductively coupled plasma optical emission spectroscopy (ICP-OES), after algae were filtered out of the mediums with a 0.2 µm filter. Routine measurements began on day -1 of the experimental runs. Raw data are listed in the appendix.

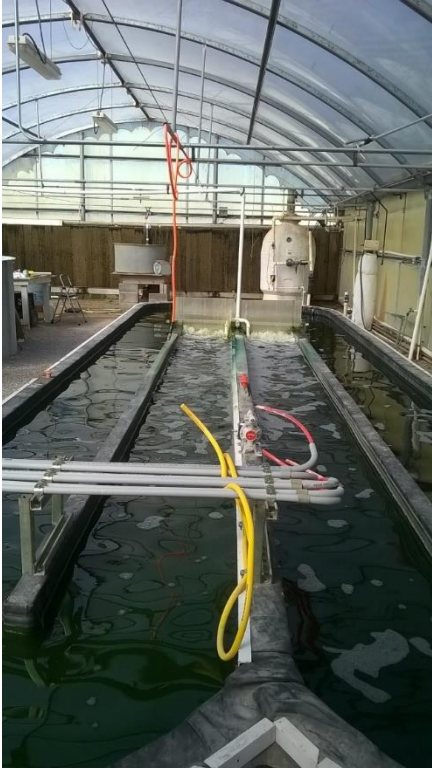


Figure 2. Indoor raceway ponds for algae cultivation. Experiment Run 2.



Figure 3. Bioreactors for Pond Inoculation.

Algae growth in each pond was contrasted to examine the effects of brackish water desalination concentrate on UTEX 1230 growth. Also, evaporation rates and contaminant removal were examined in each pond.

CHAPTER 3: RESULTS AND ANALYSIS

3.1 Population Analysis

During the first run of the experiment, both ponds exhibited healthy cultivation until after population measurements were taken on day 12 (see Figure 4). Pond 7 initially had a stronger growth curve, but it had a lower cell count than Pond 8 on day 15. After a drop in the populations of both ponds between days 15 and 19, the ponds exhibited small recoveries. Finally, the ponds exhibited large declines in cell population after Day 22.

Pond 7 showed higher cell counts than Pond 8 throughout the second run. Both ponds demonstrated population declines after days 6-8. While Pond 8 had a small recovery after its initial population drop, similar to the two ponds during the first run, Pond 7 merely exhibited an increase in population growth rate slope (a less negative slope in Figure 4 between day 12 and day 15).

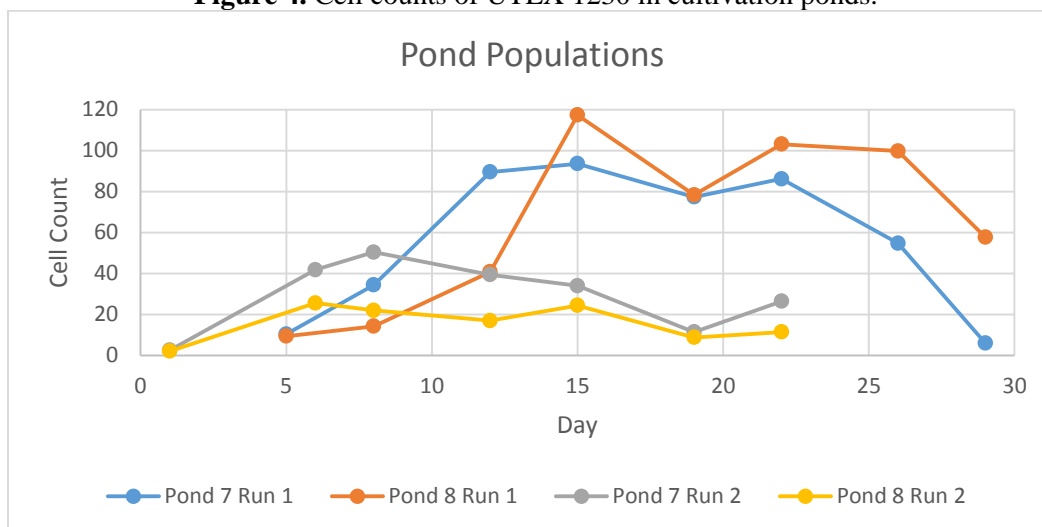
At the beginning of the second run, both ponds demonstrated higher cell counts than their counterparts from the first run (likely due to a higher volume of inoculant). Still, the ponds exhibited unhealthy cell counts by Day 12. In all four pond cultivations, an increase in cell population growth rate was followed by a decrease in growth rate, which was in turn followed by an increase, then a decrease, in population growth rate.

The first-run population drops after day 22 are likely due to foreign species growing in the ponds. Beginning on this day, foreign species were observed to be prevalent in Pond 7 during cell counts. In addition, occasional cells of a contaminating species were found in Pond 8 on both day 19 and day 22.

The contaminating species in Pond 8 had an appearance similar to *Volvox* species, but it was much smaller. The entire cell had a diameter that was only a few times as large as that of a UTEX 1230 cell; it was more prevalent in later cell counts. During the cell count on day 26, foreign species were spread throughout Pond 8. Pond 7 continued as the more highly contaminated pond for the rest of the experiment.

Similarly, the second run's early population drops are likely due to foreign organisms that were observed in the ponds on day 8. On day 12, foreign species appeared to be more dominant in Pond 7 than in Pond 8.

Figure 4. Cell counts of UTEX 1230 in cultivation ponds.



The reasons for the initial population drops in the first run are less clear than the reasons for the other population drops. Still, it is hypothesized that the initial population drops in the first run were also due to contamination, which was demonstrated by algae cells sticking together. The cells may have been stuck together by a biofilm-like substance that is described in later paragraphs. It was noted that many algae cells in Pond 7 were in small groups on day 15. Moreover, the appearance of the algae in both ponds was different on this day than on preceding days, with the algae cells appearing to have an extra coating. On day 19, both ponds had sporadic groups of algae that appeared to be stuck together. The groups of algae were sparser in Pond 8, which could explain why Pond 8 had a better recovery between day 19 and day 22.

The early deceleration of algae growth in Pond 7 during the first run may also be attributable to researchers harvesting algae in Pond 7, but not in Pond 8. This harvesting was conducted again toward the end of the experiment. The days of these harvests are listed in Table 2, along with other events that may have affected experimental measurements.

Uncertainty in interpreting the results of fed-batch experiments is not unheard of. This phenomena is referred to in another research paper: “Despite the application of [batch and fed-batch cultivations] on the evaluation of biomass composition, the microorganisms are submitted to many variables during cultivation, especially nutrient concentration, which makes it difficult to match a biomass composition variation to a certain cause” [8].

Table 2. Events that may have affected experimental measurements.

Run	Day(s)	Event that May Have Affected Measurements
1	4-5	There was a blow-off in the air pump during the weekend. Both ponds were refilled with city water to replace evaporative losses after measurements were taken.
1	8	The ponds were fed 1 lb. of fertilizer each after measurements.
1	15	The ponds were fed 1 lb. of fertilizer each after measurements.
2	15	The ponds were fed 1 lb. of fertilizer each after measurements. Both ponds were refilled with city water to replace evaporative losses after measurements were taken.
1	22	The ponds were fed about 1/3 lb. of fertilizer each after measurements.
1	27	First harvest in Pond 7: after Day 13 measurements and before Day 18 measurements.
1	13 – 18	18 measurements.
1	20 – 24	Second harvest in Pond 7.

During the first run, the foreign species in Pond 7 were often more dominant than those in Pond 8 during cell counts. This was also observed on day 12 of Experiment 2. In addition, the ponds were contaminated earlier during the second run of the experiment than during the first run. It is proposed that these two phenomena can be explained by a factors that was specific to the facility in which the algae were cultivated: how much contaminated air was blowing over each algae cultivation pond.

The wet wall in the greenhouse had algae growing in it. This was typically combatted by bleaching the water that was fed into the wet wall. However, the wet wall was not algae-free during either experimental run. Particularly, during the second run, the wet wall was bleached much less often than during the first experimental run. Upon examining the algae from the wet wall under the microscope during the second run, it was found that the algae were fused together by what appeared to be a biofilm (Figure 5). During the second experimental run, algae bound in a similar biofilm-like substance were also observed in the foam of the ponds after their populations had dropped (Figure 6). This could explain why the ponds were contaminated more quickly during the second run.

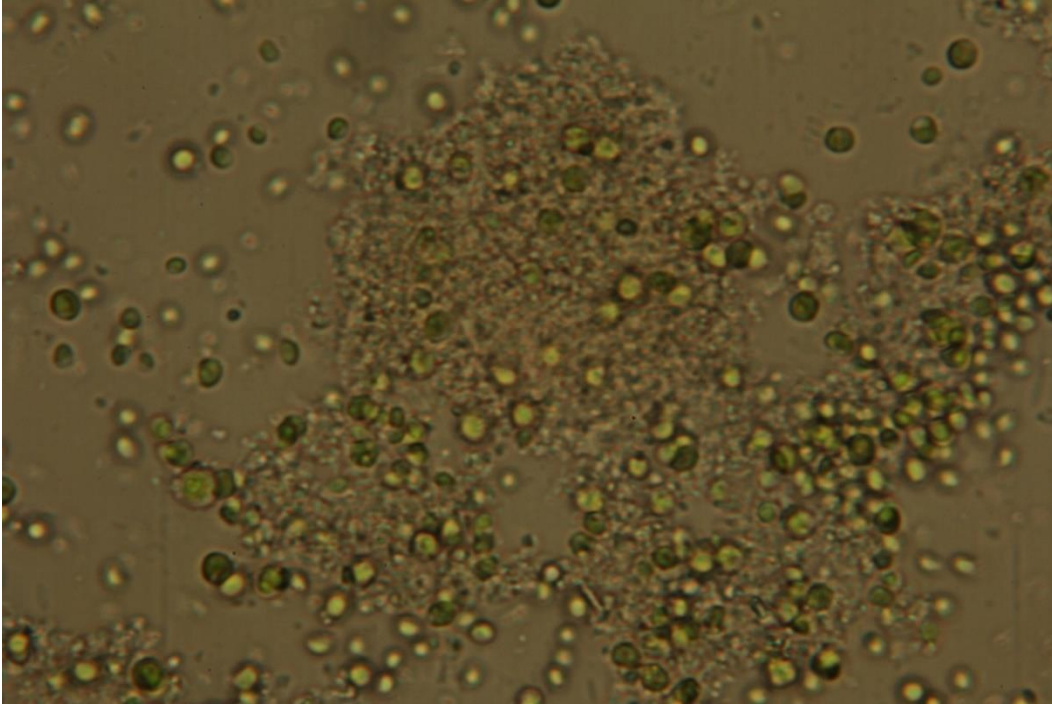


Figure 5. Algae biofilm from wet wall sample on day 20 of the second experimental run.

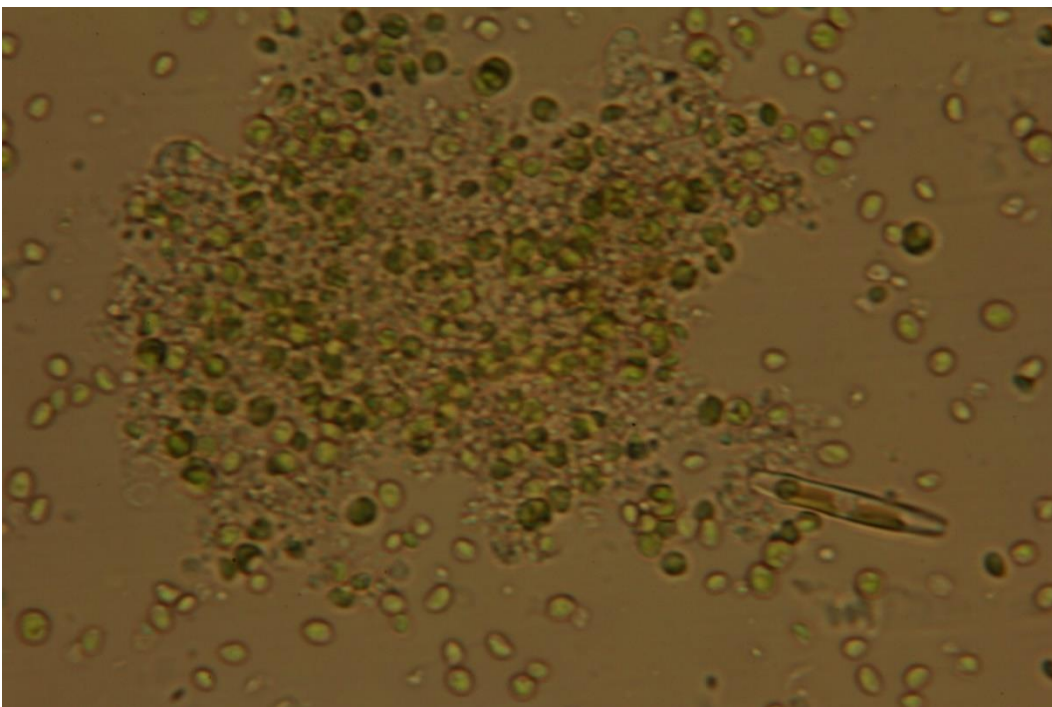


Figure 6. Algae biofilm from Pond 7 foam sample on day 20 of the second experimental run.

The tendency of Pond 7 to be more affected by contamination than Pond 8 may be explained by three factors. First, the wet wall in the greenhouse blew directly over Pond 7, while it did not directly blow over Pond 8; there was an obstruction in front of part of Pond 8. The second factor was Pond 7's proximity to a greenhouse entrance. Oftentimes, the entrance was left open for a short period, allowing outside wind to blow over the ponds. Since Pond 7 was closer to this entrance, it was more exposed to the contamination source. Pond proximity to the greenhouse entrance may have also contributed to the variety of contaminating species in the ponds that were not noted in the wet wall. A third possible reason for Pond 7's tendency to be more contaminated may be related to the water chemistry of the pond. However, it is expected that this is not the case. Further experimentation, in which contamination is better controlled, or in which the two growth media switch locations, may be worthwhile.

If pond composition did not significantly affect how readily ponds were contaminated, the cultivation medium used for Pond 7 (desalination concentrate and nutrients) appears to be a better growth medium than the medium in Pond 8 (nutrients and desalination concentrate diluted with city water to half of the concentrate's normal conductivity). Pond 7 displayed better population counts than Pond 8 during the periods when the ponds were not contaminated.

3.2 pH Analysis

Microalgae population declines were associated with unusual changes in pH. In other research, microalgae health was also linked to pH changes in a medium with high TDS [17]. Further investigation into using pH as an indicator of pond health may be warranted. The pH measurements for cultivation ponds during the first experimental run are plotted in Figure 7. The pH measurements from the second run are omitted because of a discrepancy in the validity of pH measurements.

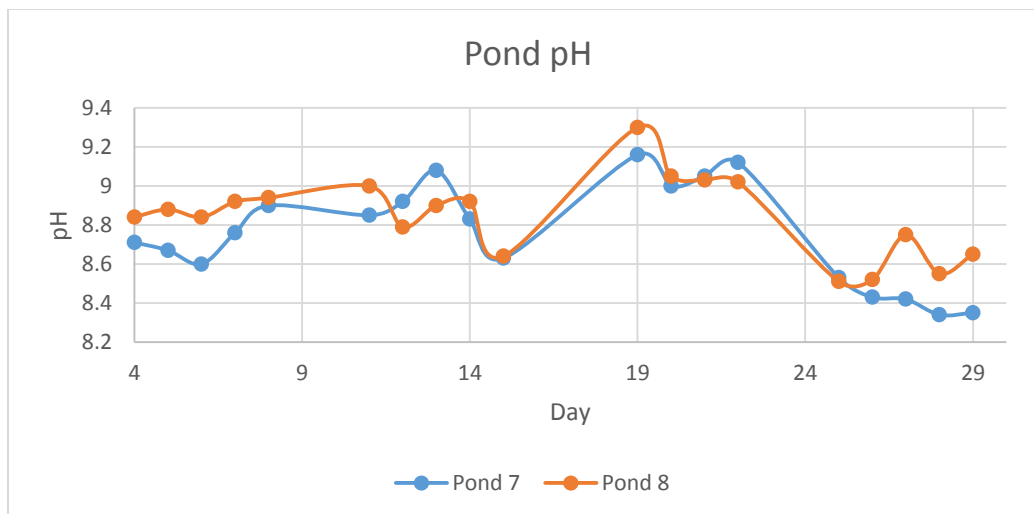


Figure 7. pH of cultivation ponds during the first experimental run.

3.3 Conductivity and Depth Analysis

Overall, the conductivities of the growth mediums were not significantly reduced. This can be seen by the correlation between conductivity and depth measurements during the first run. If conductivities are examined at points where a pond has the same depth on different days, it becomes apparent that only small differences are observed in conductivities over time. This is probably due to the composition of the fertilizer that was used.

This conclusion is supported by previous research. *Spirulina platensis* growth in desalination concentrate with F/2 as nutrients led to an increase in the conductivity of the growth medium (Hussein W. Z., 2014). Conversely, *S. platensis* growth in concentrate with supernatant anaerobic digested sludge (SADS) as nutrients led to a decrease in conductivity. This indicates that nutrient source affects conductivity reduction.

A lack of conductivity reduction, however, does not necessarily discount the current approach in the field of concentrate management. This approach could be incorporated with concentrate disposal via evaporation ponds, providing a revenue stream for owners of evaporation ponds. Still, it is likely that better concentrate management prospects would appear if a different nutrient source were used.

Figure 3. Electrical conductivity of cultivation ponds.

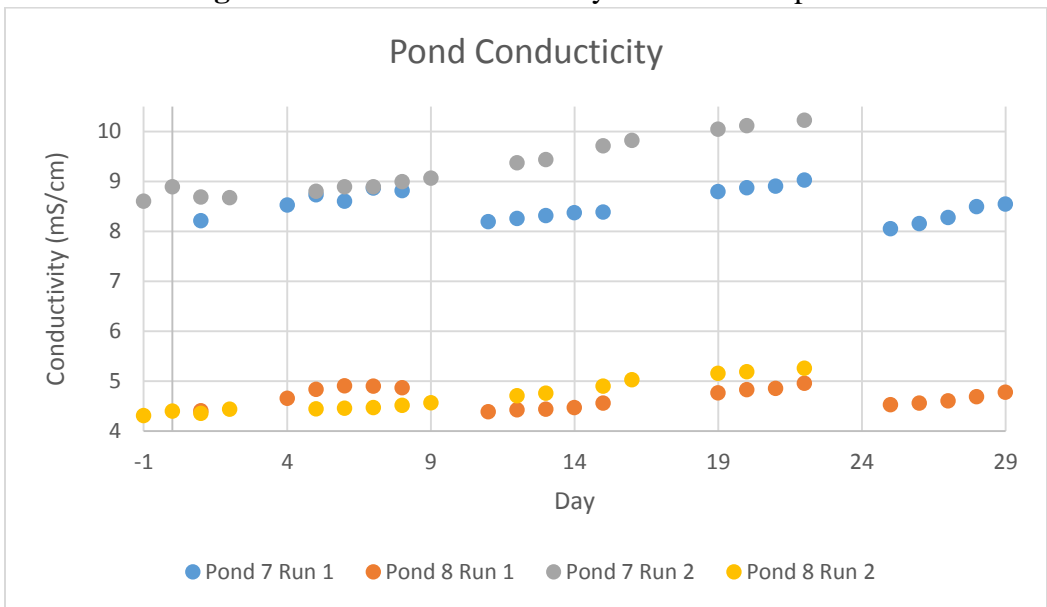
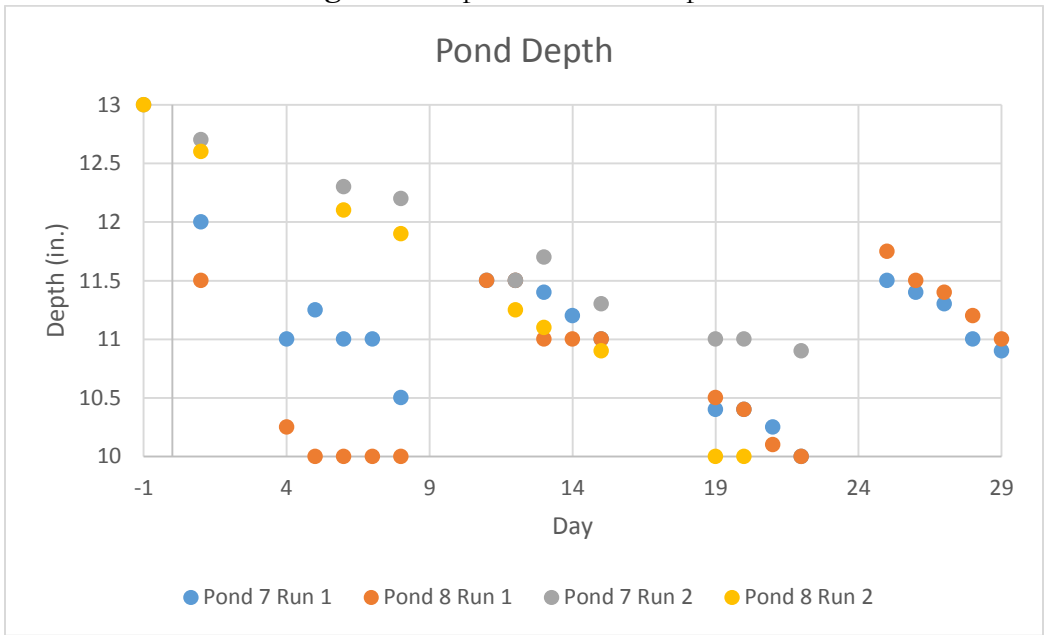


Figure 4. Depth of cultivation ponds.



The average daily evaporative loss was 0.13"/day in both ponds during the first run. Since each pond has a surface area of approximately 172 ft², this equates to a water loss of 14 gal/day/pond. Local weather data are available at the referenced website, and morning temperature measurements of the indoor ponds are listed at

the end of this article [18]. Day 1 of the first run was 5/6/15 and Day 29 was 6/5/15.

During the second run, the average daily water loss was 0.09"/day in Pond 7 and 0.14"/day in Pond 8. It is expected that Pond 8 had a small leak, likely caused by the abrasive cleaning methods that are necessary to clean ponds between cultivations if they become contaminated. The lower water loss in Pond 7 during the second run compared to the first run is expected since the outside weather was cooler during the second experiment. Local weather data are available at the referenced website [18]. Day -1 of the second run was 9/15/15 and day 22 was 10/8/15.

3.4 Element Removal Analysis

Though no significant decreases in the conductivities of the two ponds were observed, water analyses demonstrated that certain elements were removed from the growth medium by the microalgae. The following elements were removed in at least one of the four cultivations: Al, As, B, Ba, Cd, Fe, Mn, Ni, Tl, Zn, Bi, Ca, Li, Mg, P, Sr, K, SiO₂, Na, S and Cu. Tables 3 through 6 contain data from the water analyses. The numbers in the central part of the table represent adjusted concentrations of contaminants in mg/L. Boxes highlighted in blue indicate elements whose presence increased.

Concentrations were adjusted by multiplying each concentration by h'/h . Here, h' is the height of the pond on the given day and h is the initial height of the given pond during a cultivation. For example, $h = 12''$ for Pond 7 during the first run. Also, h was treated as a variable (\hat{h}) in Pond 8 during the second run because of the suspected leak. The variable \hat{h} was calculated using the following formula:

$$\hat{h} = h - (h'_7 - h'_8) \times \frac{h}{0.5(h + h'_8)} = h \left(1 - \frac{h'_7 - h'_8}{0.5(h + h'_8)} \right)$$

Notably, Table 2 states that algae were fed fertilizer before the measurements on Day 22 and Day 29 of the first run. Therefore, the % *Decrease* columns describe the decrease in concentration of a given element between the first and third measurements.

Table 3. Analyses of water samples from Pond 7 Run 1 after microalgae were filtered out of the medium. Concentrations are represented in mg/L.

Element	Day					% Decrease	MDL
	1	8	15	22	29		
Al	0.1101	0.0896	0.088825	0.070166667	0.069033	19.3	0.0026
As	0.2018	0.136763	0.146025	0.124833333	0.118538	27.6	0.0174
B	0.8854	0.8631	0.862492	0.876666667	0.86328	2.6	0.05
Ba	0.0521	0.042263	0.045925	0.039083333	0.047597	11.9	0.001
Be	ND	ND	ND	ND	ND		0.0002
Cd	0.0028	0.002013	ND	ND	0.001726	100	0.001
Co	ND	ND	ND	ND	ND		0.002
Cr	ND	ND	ND	ND	ND		0.003
Fe	0.2235	ND	ND	0.007416667	0.019893	100	0.004
Mn	0.0602	0.017763	0.003575	0.005666667	0.008902	94.1	0.0017
Mo	0.0177	0.0203	0.020717	0.023833333	0.02398	-17.0	0.0017
Ni	0.0051	0.004113	0.003025	ND	ND	40.7	0.002
Pb	ND	ND	ND	ND	ND		0.0027
Se	ND	ND	ND	ND	ND		0.0135
Tl	0.0227	ND	ND	ND	ND	100	0.0068
V	ND	ND	ND	ND	ND		0.0017
Zn	0.195	0.122063	0.113758	0.16675	0.212096	41.7	0.0013
Bi	0.1174	0.09555	0.083783	0.062666667	0.065854	28.6	0.0052
Ca	769.2	583.1875	550.1833	547.1666667	594.2317	28.5	0.0971
Li	0.1251	0.1204	0.124117	0.120833333	0.129801	0.8	0.0014
Mg	400.3	362.5125	347.6917	347.3333333	350.8892	13.1	0.0185
P	6.09	0.607163	0.760833	0.513583333	1.928392	87.5	0.0251
Sr	13.45	12.03125	11.77917	11.825	12.0445	12.4	0.0012
K	23.98	21.04375	19.855	27.05	32.07325	17.2	0.2101
SiO2	56.86	53.2	54.90833	53.75	56.135	3.4	0.0151
Na	1276	1128.75	1085.333	1086.666667	1111.8	14.9	0.0483
S	1502	1420.125	1402.5	1505.833333	1377.033	6.6	0.5
Cu	0.0804	0.015313	0.012925	0.02175	0.034063	83.9	0.0023

* % Decrease between Day 1 and Day 15

^ Method Detection Limit [19].

Table 4. Analyses of water samples from Pond 8 Run 1 after microalgae were filtered out of the medium. Concentrations are represented in mg/L.

Element	Day					% Decrease	MDL
	1	8	15	22	29		
Al	0.0511	0.038435	0.039217	0.027130435	0.029078	23.3	0.0026
As	0.0925	0.065304	0.078339	0.053565217	0.068583	15.3	0.0174
B	0.4436	0.439478	0.452052	0.474086957	0.49567	-1.9	0.05
Ba	0.0539	0.040522	0.047539	0.040608696	0.042948	11.8	0.001
Be	ND	ND	ND	ND	ND		0.0002
Cd	0.0012	0.001043	ND	0.001304348	0.001052	100	0.001
Co	ND	ND	ND	ND	ND		0.002
Cr	ND	ND	ND	ND	ND		0.003
Fe	0.3022	ND	ND	0.003826087	0.010139	100	0.004
Mn	0.1247	ND	ND	ND	0.003061	100	0.0017
Mo	0.0097	0.010609	0.012435	0.014	0.014061	-28.2	0.0017
Ni	0.0024	ND	ND	ND	ND	100	0.002
Pb	ND	ND	ND	ND	ND		0.0027
Se	ND	ND	ND	ND	ND		0.0135
Tl	0.0087	ND	ND	ND	ND	100	0.0068
V	ND	ND	ND	0.002434783	ND		0.0017
Zn	0.1579	0.103217	0.099478	0.162782609	0.201252	37.0	0.0013
Bi	0.0517	0.044609	0.045339	0.03373913	0.034243	12.3	0.0052
Ca	353.3	296.4348	300.5391	316.0869565	337.1739	14.9	0.0971
Li	0.0913	0.086435	0.090774	0.09373913	0.102061	0.6	0.0014
Mg	181.7	169.6522	169.4	175.3913043	177.8174	6.8	0.0185
P	4.939	0.233739	0.312304	0.717304348	1.220522	93.7	0.0251
Sr	6.351	5.929565	5.984957	6	6.160957	5.8	0.0012
K	18.02	15.16522	14.40522	23.47826087	26.88783	20.1	0.2101
SiO ₂	39.29	37.05217	41.03478	40.69565217	44.1913	-4.4	0.0151
Na	582.7	538.2609	541.6783	564.2608696	582.1391	7.0	0.0483
S	722.5	683.1304	685.1565	702.4347826	708.5913	5.2	0.5
Cu	0.0759	0.012957	0.01253	0.031565217	0.038548	83.5	0.0023

*% Decrease between Day -1 and Day 15

^ Method Detection Limit [19].

Table 5. Analyses of water samples from Pond 7 Run 2 after microalgae were filtered out of the medium. Concentrations are represented in mg/L.

Element	Day			% Decrease	MDL ^
	-1	8	15		
Al	0.0756	0.109425	0.23052	-204.9206349	0.0026
As	0.1235	0.448772	0.396369	-220.9467456	0.0174
B	1.1	1.296015	1.362085	-23.82587413	0.05
Ba	0.0194	0.01952	0.016168	16.66137986	0.001
Be	ND	0.003097	ND		0.0002
Cd	ND	ND	0.009301		0.001
Co	ND	ND	ND		0.002
Cr	ND	ND	ND		0.003
Fe	0.6729	ND	ND	100	0.004
Mn	0.0944	ND	0.016863	82.13657106	0.0017
Mo	ND	ND	ND		0.0017
Ni	0.0059	0.013514	ND	100	0.002
Pb	ND	ND	ND		0.0027
Se	ND	ND	ND		0.0135
Tl	0.0061	0.074795	0.039202	-542.6607818	0.0068
V	ND	ND	ND		0.0017
Zn	0.1242	0.057809	0.049807	59.89780751	0.0013
Bi	0.1112	0.237149	0.223827	-101.2832042	0.0052
Ca	704.6	619.0092	641.5792	8.944190921	0.0971
Li	0.0865	0.072543	0.05876	32.06936416	0.0014
Mg	471.4	429.44	442.7862	6.069971607	0.0185
P	8.258	ND	1.904485	76.93770144	0.0251
Sr	10.56	11.32723	11.39562	-7.913024476	0.0012
K	15.45	16.43246	13.98592	9.476226039	0.2101
SiO ₂	31.99	35.20169	35.45592	-10.83439536	0.0151
Na	973.3	924.1031	943.1154	3.101265323	0.0483
S	1606	1434.908	1410.762	12.15681579	0.5
Cu	0.1219	0.018582	0.011822	90.30226541	0.0023

^ Method Detection Limit [19].

Table 6. Analyses of water samples from Pond 8 Run 2 after microalgae were filtered out of the medium. Concentrations are represented in mg/L.

Element	Day			% Decrease	MDL
	-1	8	15		
Al	0.0559	0.048106	0.099367	-77.75856568	0.0026
As	0.2725	0.113092	0.09659	64.55414013	0.0174
B	0.8278	0.546612	0.592644	28.40733169	0.05
Ba	0.0444	0.006095	0.027771	37.45337694	0.001
Be	ND	0.000938	0.000174		0.0002
Cd	0.0065	0.001875	0.003298	49.26506614	0.001
Co	ND	ND	ND		0.002
Cr	ND	ND	ND		0.003
Fe	0.7599	ND	ND	100	0.004
Mn	0.1577	0.003095	0.003558	97.74374063	0.0017
Mo	ND	ND	ND		0.0017
Ni	0.0107	0.002157	ND	100	0.002
Pb	ND	ND	ND		0.0027
Se	ND	ND	ND		0.0135
Tl	0.059	0.010221	ND	100	0.0068
V	ND	0.002063	ND		0.0017
Zn	0.1309	0.071362	0.051983	60.28779201	0.0013
Bi	0.1281	0.060203	0.080188	37.40210922	0.0052
Ca	313.6	274.6659	295.4976	5.772445324	0.0971
Li	0.0851	0.06733	0.067431	20.76294655	0.0014
Mg	192.5	177.5154	183.3734	4.741086939	0.0185
P	8.532	0.628571	2.58875	69.65834505	0.0251
Sr	5.244	4.706548	5.038646	3.915970694	0.0012
K	19.92	17.66714	17.50422	12.12741092	0.2101
SiO2	30.35	27.39157	28.95096	4.609702096	0.0151
Na	420.6	394.5099	405.1051	3.684000109	0.0483
S	619	625.0079	584.0525	5.645791959	0.5
Cu	0.1466	0.042574	0.018919	87.0949592	0.0023

[^] Method Detection Limit [19].

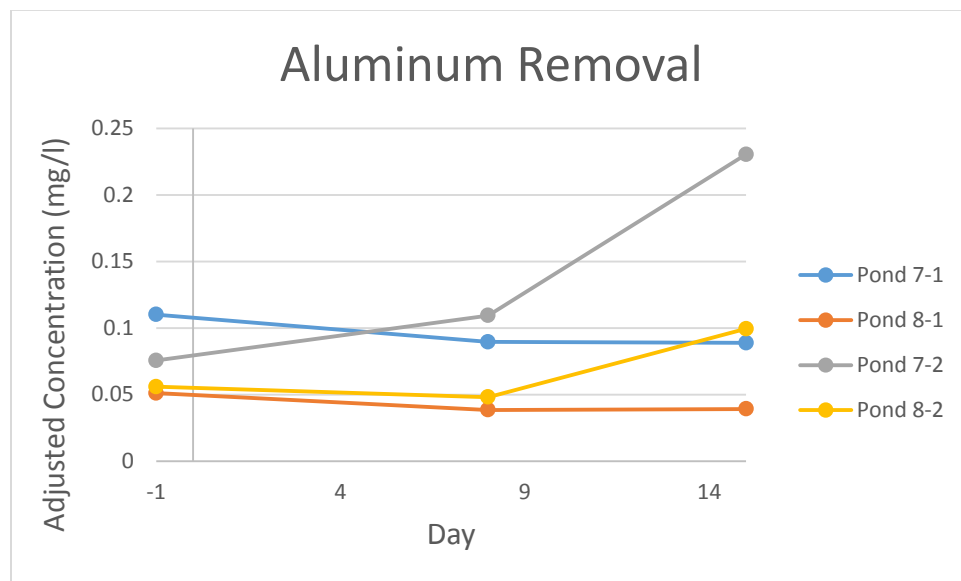
During the cultivations, there were a few elements that increased in concentration. These elements have been contrasted by a highlighted % *Decrease*. Molybdenum is the most prominent of the highlighted elements. Also, some elements in Pond 7 Run 2 increased in concentration during the first interval, then decreased during the second interval. There is no clear explanation for these phenomena. It is also notable that the elements in Table 7 were removed to below their detection limits.

Table 7. Elements that were removed to below their detection limits during cultivations.

Element	Pond 7, Run 1	Pond 8, Run 1	Pond 7, Run 2	Pond 8, Run 2
Cd	✓	✓		
Fe	✓	✓	✓	✓
Mn		✓		
Ni		✓	✓	✓
Tl	✓	✓		✓

In many cases, a contaminant was removed more during the first interval of cultivation than during the second interval. This has implications when using algae to remove specific elements from concentrate with specific water chemistries. More algae or a longer residence time may not be better.

In the following figures, the contaminant removal data is represented in graphical form.

**Figure 5.** Aluminum removal during pond cultivations.

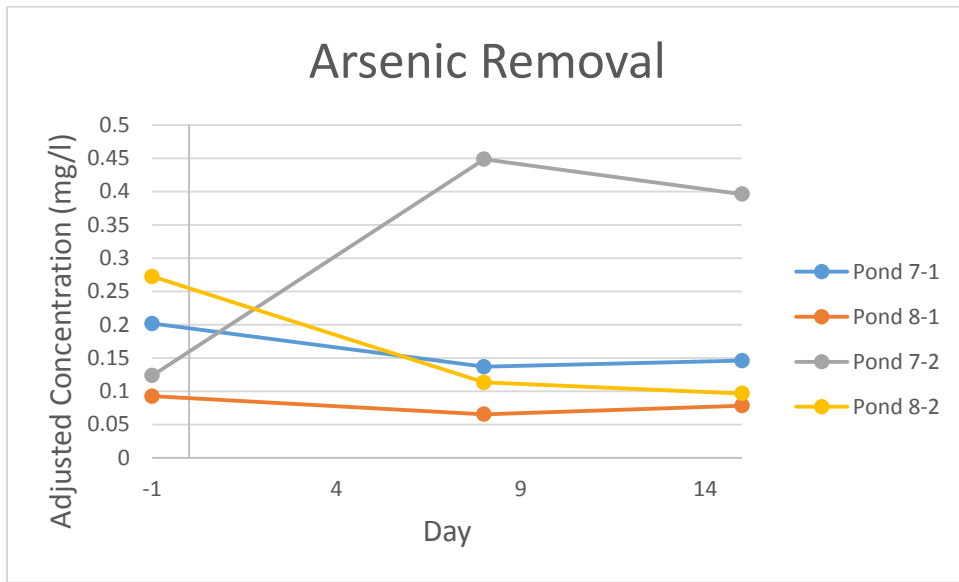


Figure 6. Aluminum removal during pond cultivations.

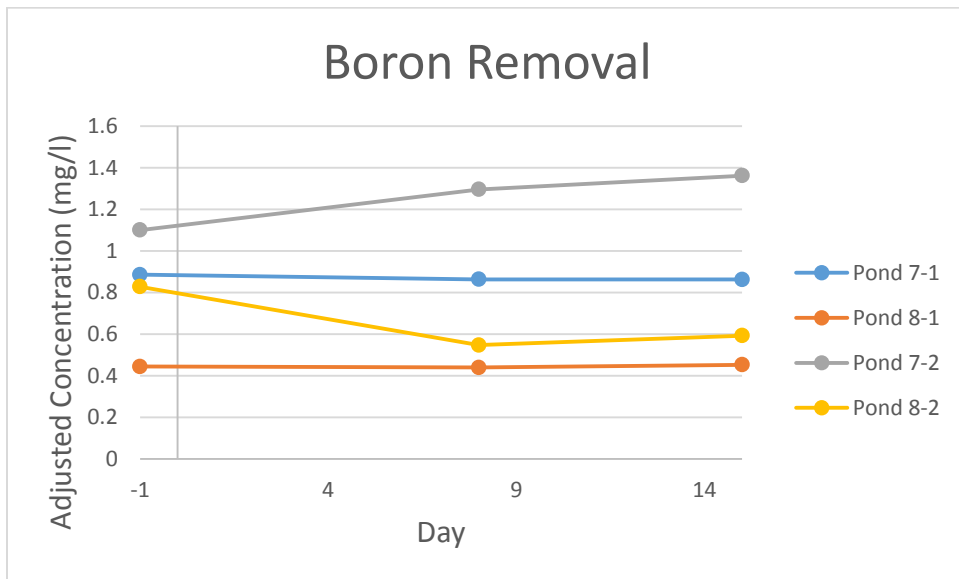


Figure 7. Boron removal during pond cultivations.

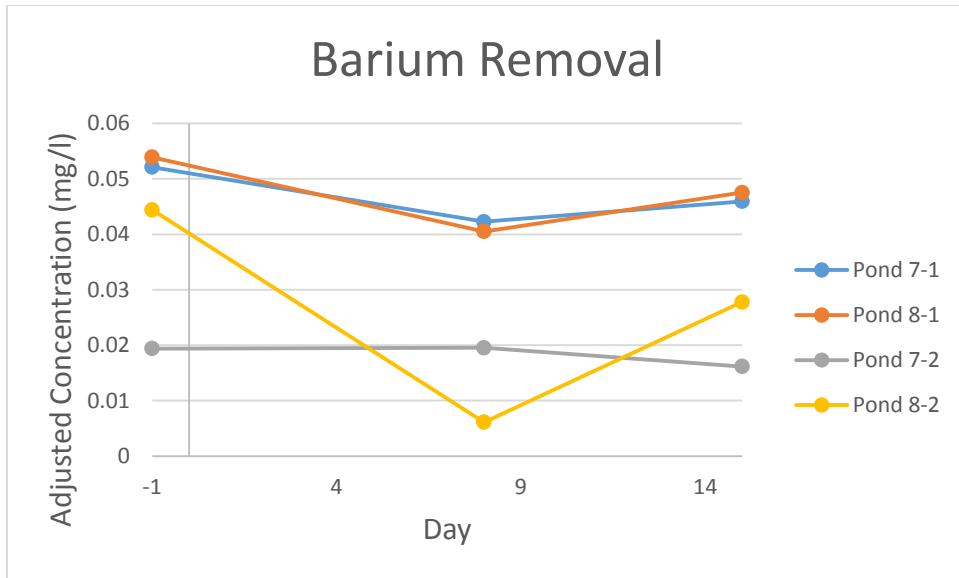


Figure 8. Barium removal during pond cultivations.

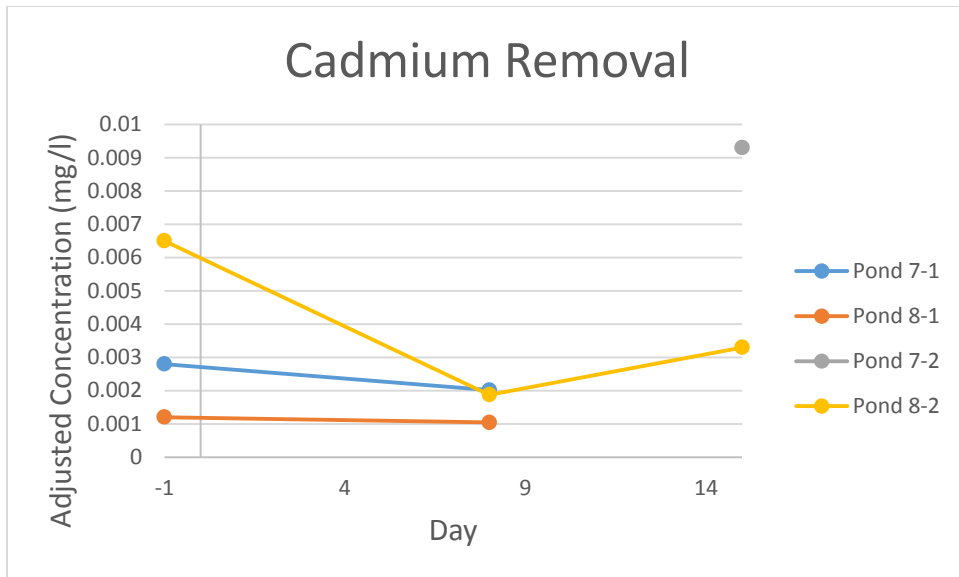


Figure 9. Cadmium removal during pond cultivations.

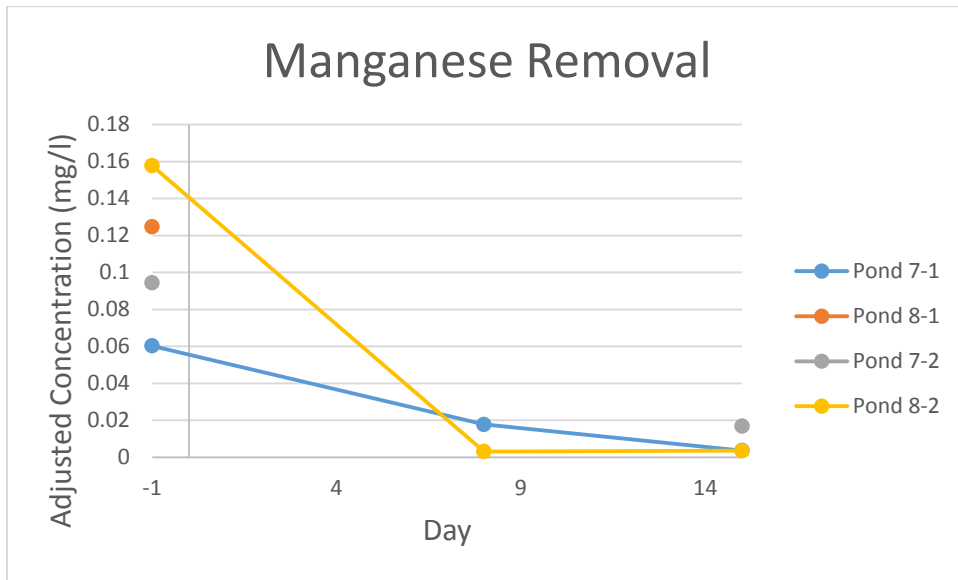


Figure 10. Manganese removal during pond cultivations.

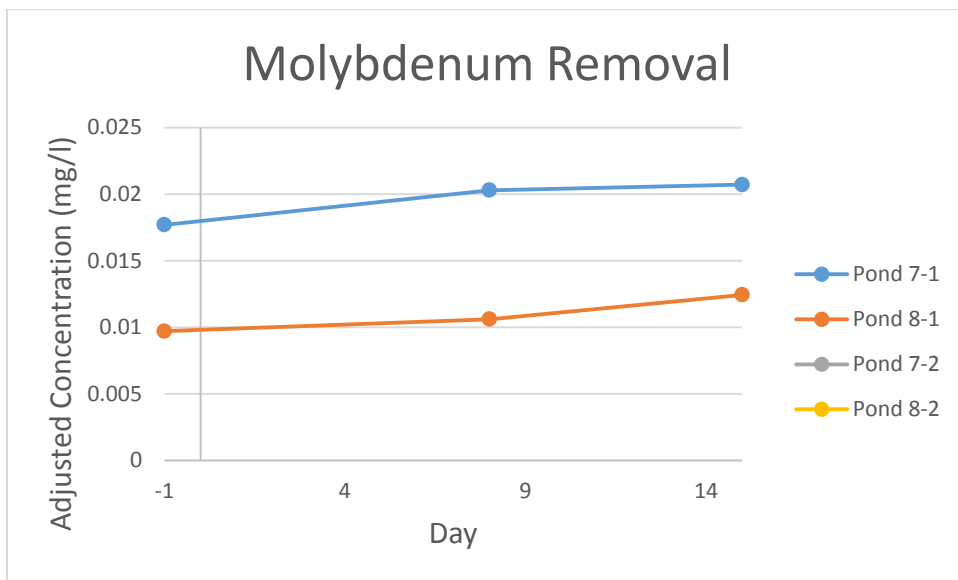


Figure 11. Molybdenum removal during pond cultivations.

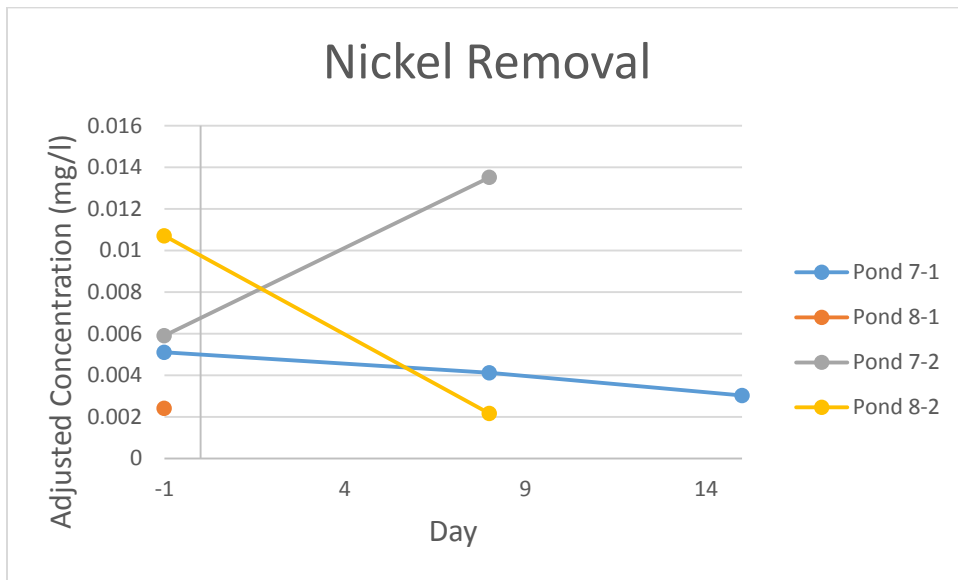


Figure 12. Nickel removal during pond cultivations.

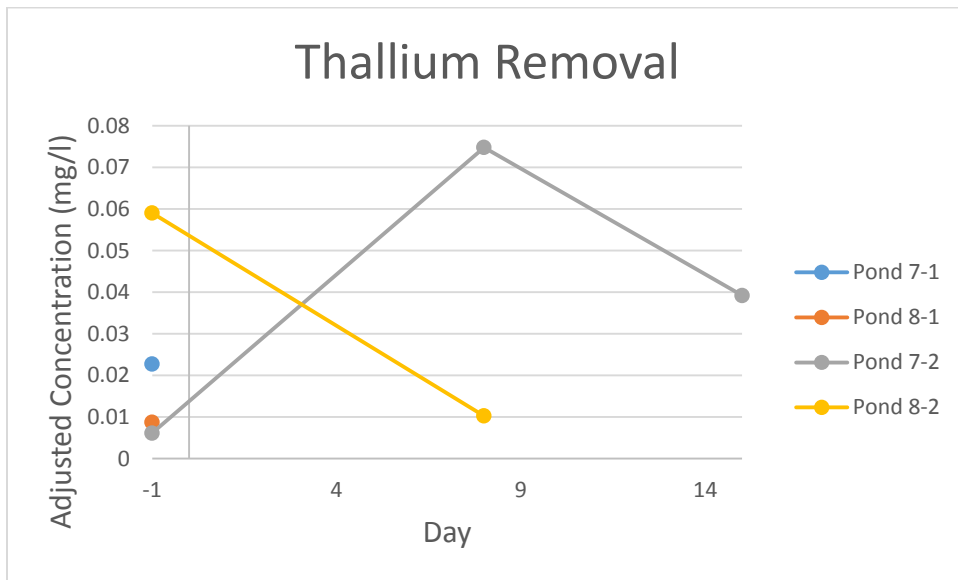


Figure 13. Thallium removal during pond cultivations.

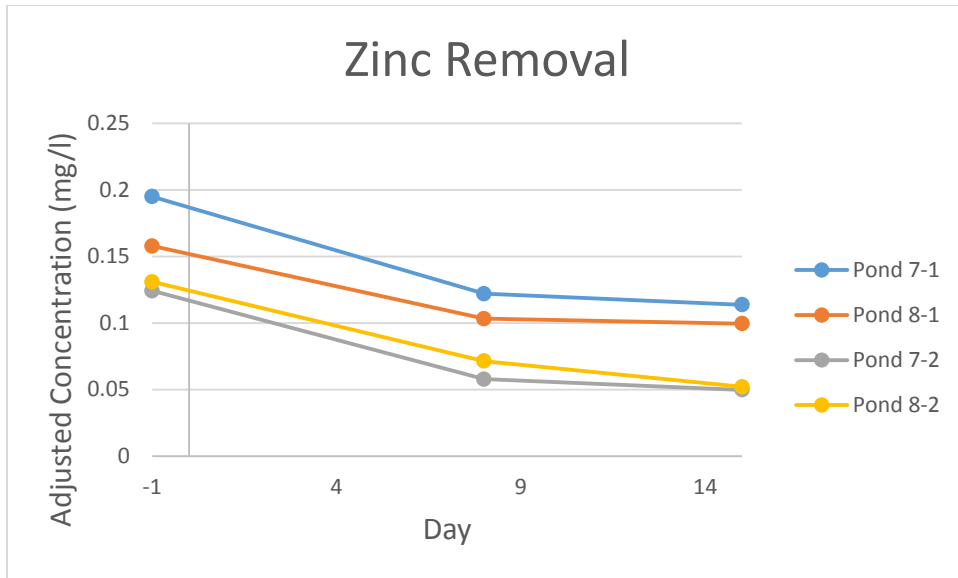


Figure 14. Zinc removal during pond cultivations.

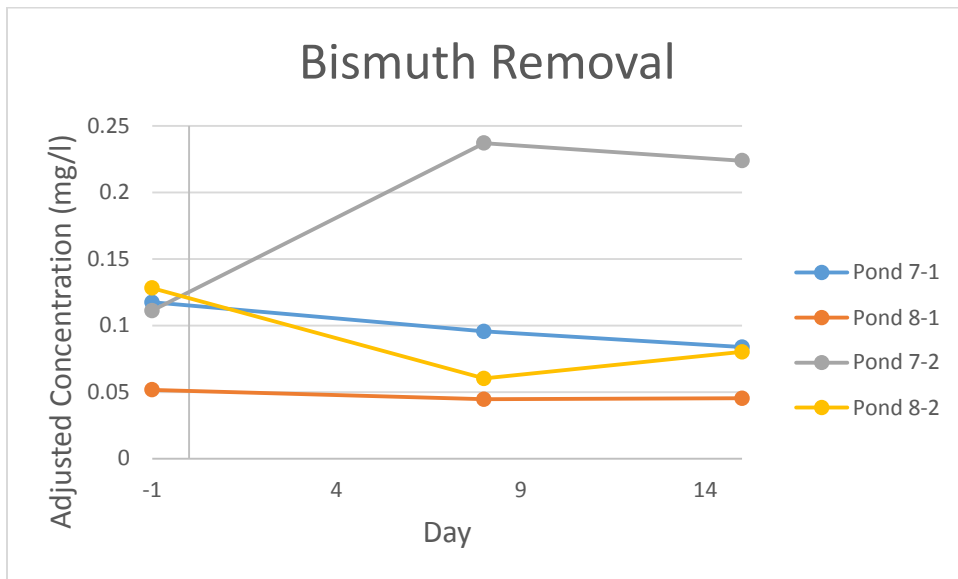


Figure 15. Bismuth removal during pond cultivations.

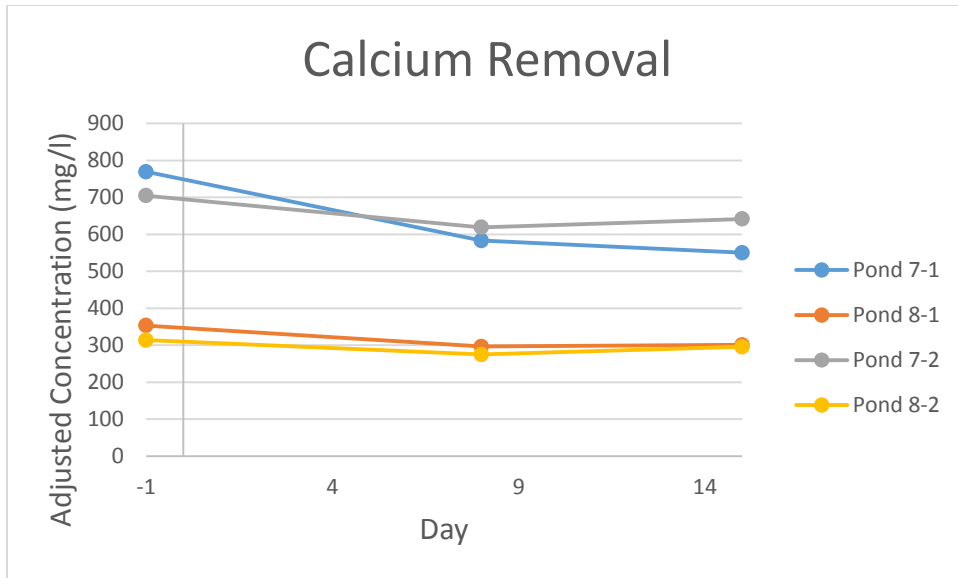


Figure 16. Calcium removal during pond cultivations.

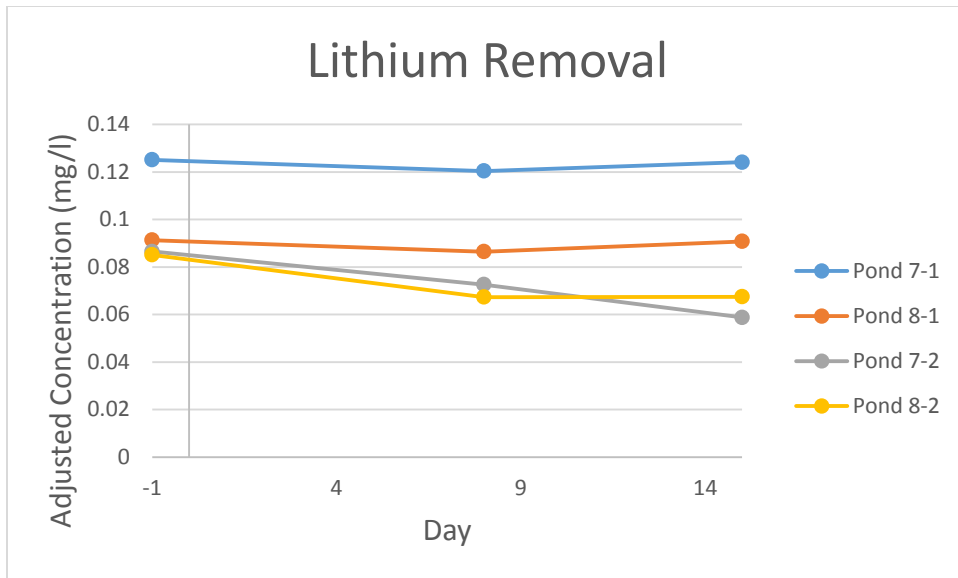


Figure 17. Lithium removal during pond cultivations.

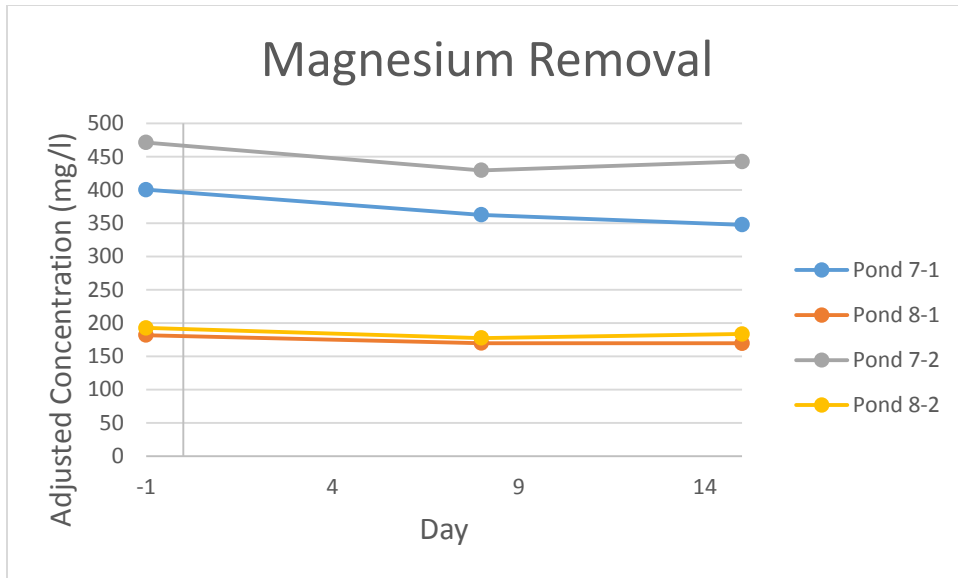


Figure 18. Magnesium removal during pond cultivations.

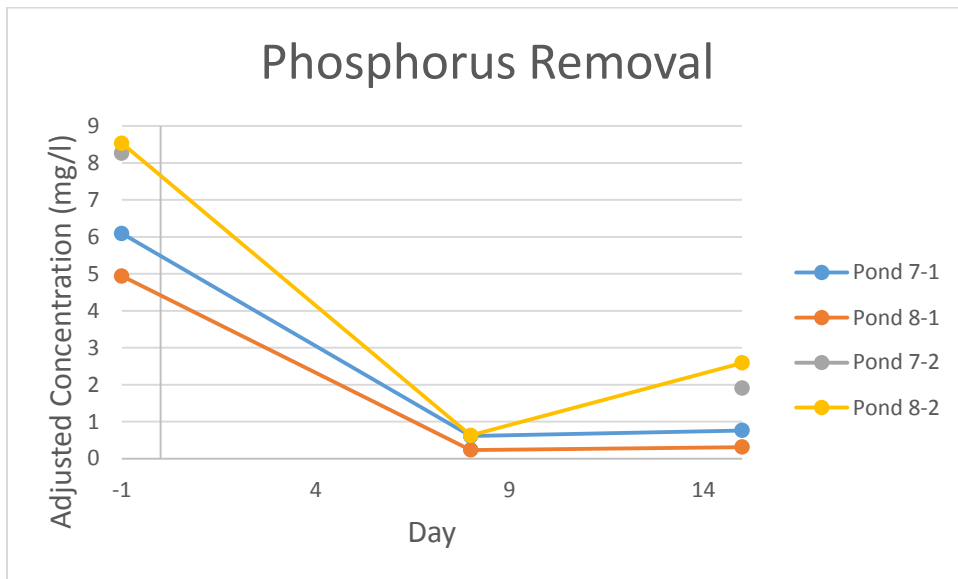


Figure 19. Phosphorus removal during pond cultivations.

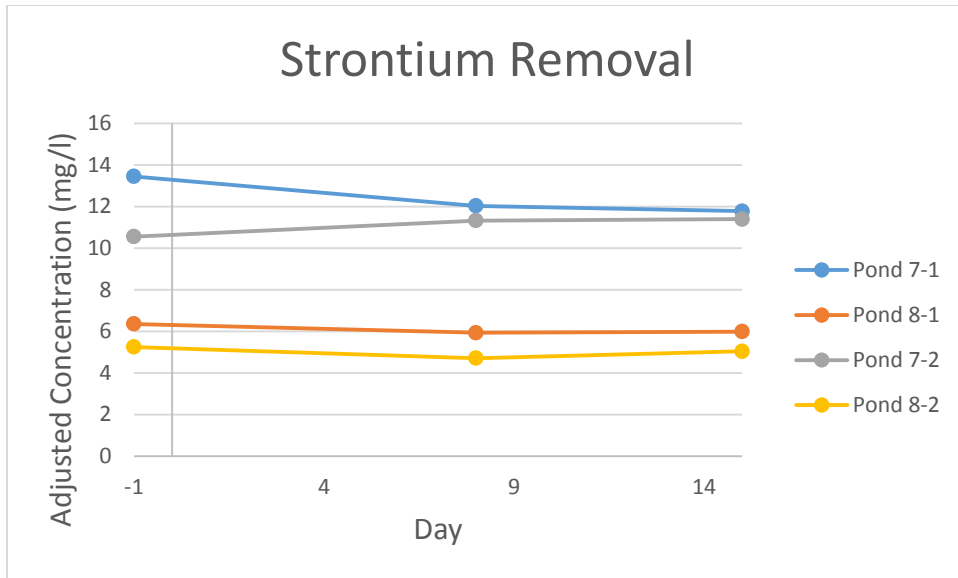


Figure 20. Strontium removal during pond cultivations.

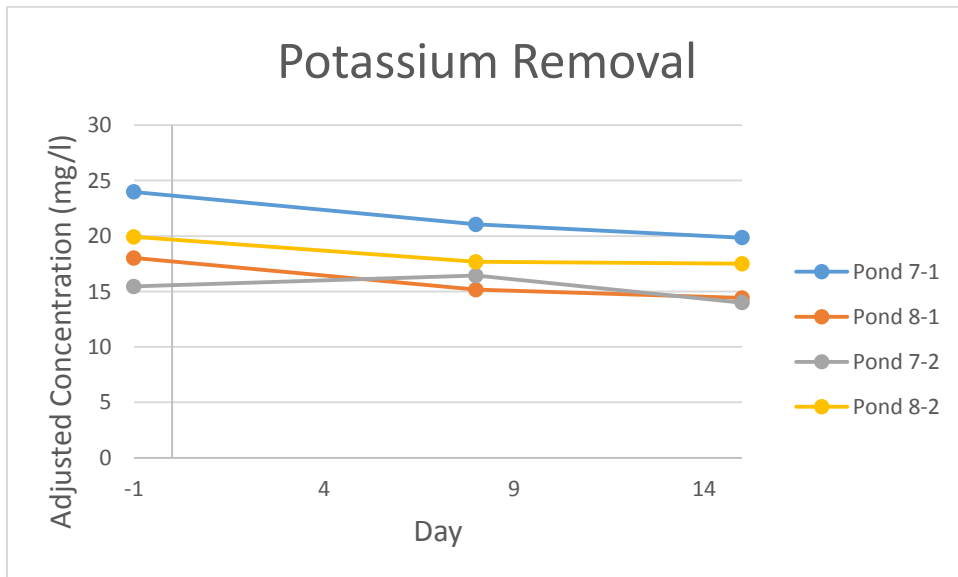


Figure 21. Potassium removal during pond cultivations.

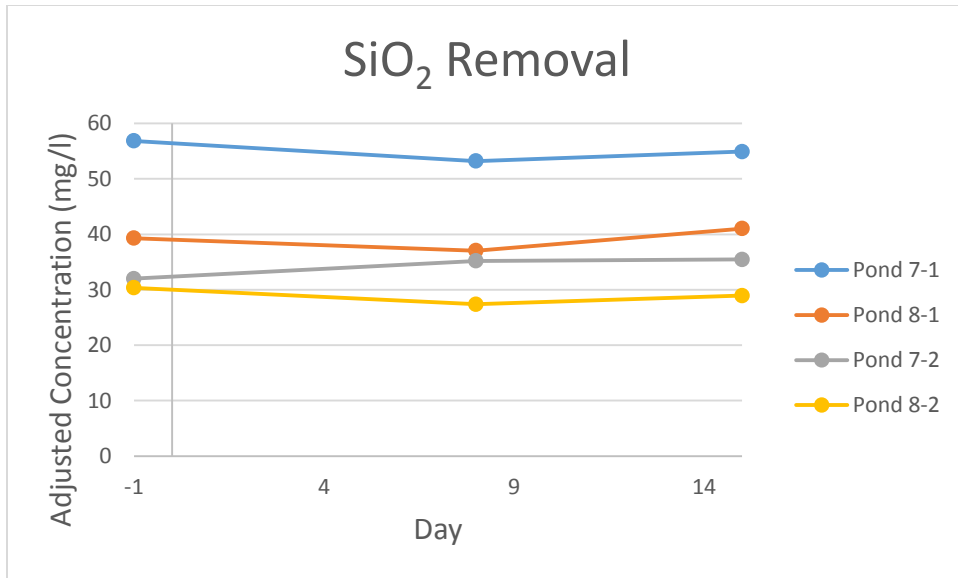


Figure 22. Silicon dioxide removal during pond cultivations.

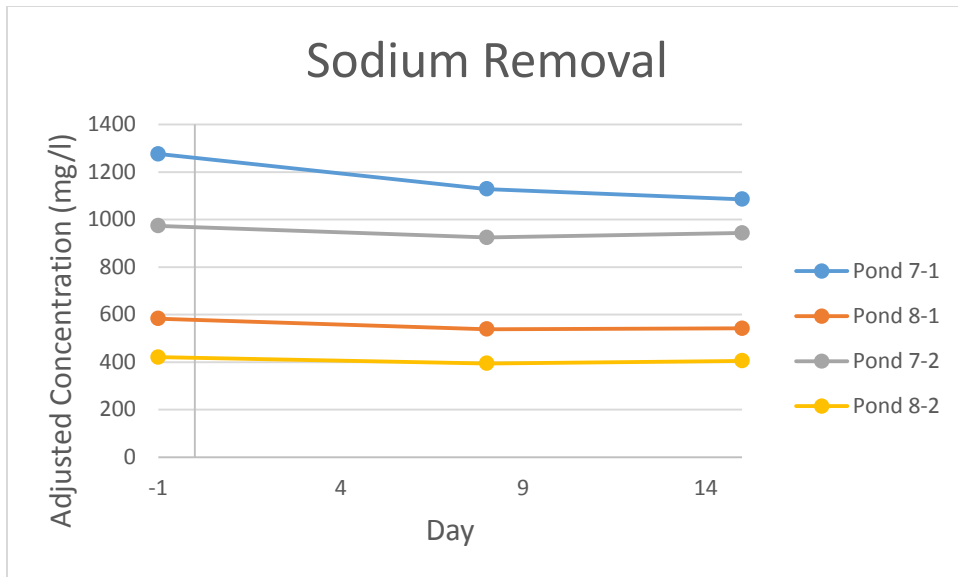


Figure 23. Sodium removal during pond cultivations.

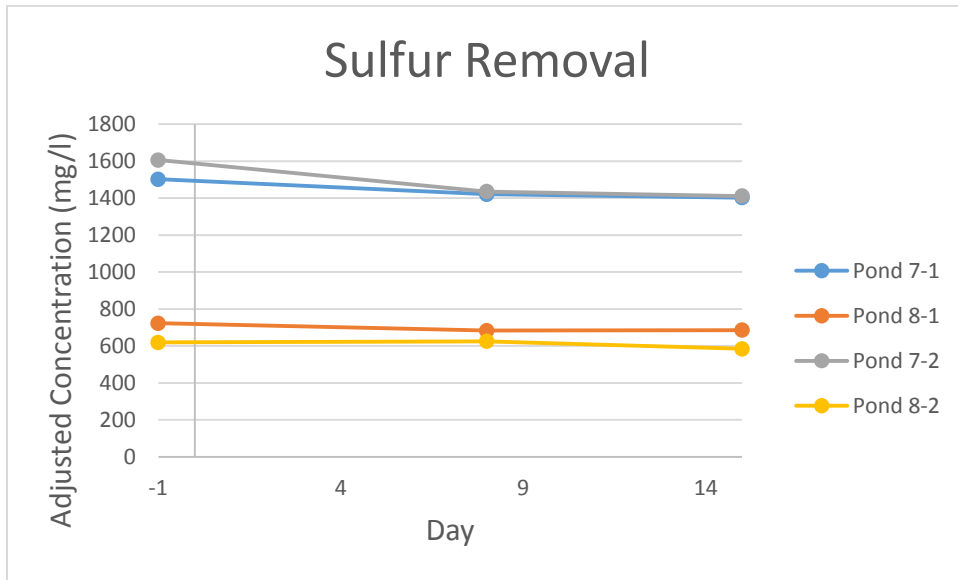


Figure 24. Sulfur removal during pond cultivations.

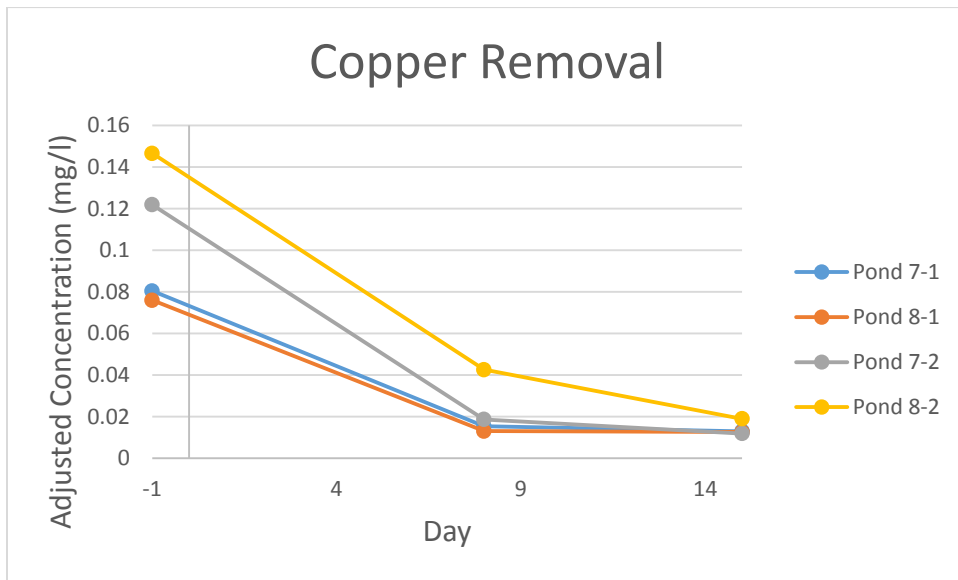


Figure 25. Copper removal during pond cultivations.

If a sum of element removals is taken over the first two intervals of the first run, there was less of an elemental increase in Pond 8 than in Pond 7. Since Pond 8 had a higher biomass-to conductivity ratio during these intervals, this appears to support a conclusion made in previous research: mass conductivity reduction is directly proportional to the mass microalgae-to-conductivity-ratio (Myint, 2014).

However, since there were unexplained increases in some elements during the first interval, and because there was an overall increase in the sum of measured concentrations in Run 1 between Day -1 and Day 15, it appears that there are factors in the experiment that were not accounted for. Therefore, further investigation is necessary to examine the claims made in previous research (Myint, 2014).

CHAPTER 4: DISCUSSION AND CONCLUSION

Chlorella sorokiniana was successfully cultivated in desalination concentrate at a pilot scale. Large amounts of cadmium, iron, manganese, nickel, thallium, zinc, phosphorus, copper and arsenic (Pond 8 Run 2) were removed from the concentrate. Aluminum, boron, barium, bismuth, calcium, lithium, magnesium, strontium, potassium, silicon dioxide, sodium, and sulfur were also removed in at least one of the four cultivations. Some of these elements had higher removals during the first period of cultivation than during the second period. This implies that higher microalgae density and longer residence times may not be better for the removal of specific contaminants.

If further investigation of microalgae growth in desalination concentrate at the pilot scale were conducted, certain changes should be made to the current experimental procedure. First, contamination factors should be controlled more closely. Second, Miracid 30:10:10 is not an appropriate nutrient source when contaminant removal is the goal. Also, cell sizing should be done by a computer. Estimation errors could have large consequences because of the cubic relation between the radius and volume of a sphere. In addition, a more complete water analysis is recommended. This would allow researchers to better understand factors involved with biomass increase and contaminant removal. Particular elemental analyses that may have been helpful in this experiment are analyses of nitrogen and chlorine.

Furthermore, it may have been helpful if a nutrient source with a known composition were used. Continuously fed processes should also be considered. In addition, minimization of variables would be ideal. For example, it would be helpful if harvesting had not taken place in Pond 7 during the first run. Moreover, there were other relevant factors in the experiment that were not analyzed, as is evidenced by the unexplained increase in many elements during the first interval.

Also, this experiment points to other investigations that may be worthwhile. Investigation into the correlation between pH and pond health may be merited. An understanding of this correlation could improve pond maintenance practices. Furthermore, two methodological developments are merited to make comparing biomass between experiments more feasible: a method for correlating algae volume with biomass and a standard method for measuring microalgal biomass.

REFERENCES

- [1] S. A. Shirazi, "Simultaneous Production of Biofuel and Treatment of Concentrate Stream of Water Desalination Units by Using Microalgae," 2014.
- [2] W. Z. Hussein, "Use of Concentrate Stream from Desalination Units and Supernatant Anaerobic Digested Sludge from Water Treatment Plants for Growing Microalgae," 2014.
- [3] W. Hussein, M. T. Myint and A. Ghassemi, "Energy usage and carbon dioxide emission saving in desalination by using desalination concentrate and wastes in microalgae production," *Desalination and Water Treatment*, 2014.
- [4] A. P. Matos, L. I. Morioka and E. S. Sant'Anna, "Potencialidades de *Chlorella vulgaris* cultivada em meio a base de concentrado de dessalinização," *Jornadas de Jovens Investigadores*, 2011.
- [5] A. P. Matos, T. Silva, E. S. Moecke and E. S. Sant'Anna, "Cultivo de *Chlorella vulgaris* em concentrado de dessalinização: Sistema autotrófico, heterotrófico e mixotrófico," *Jornada Unisul de Iniciação Científica*, 2013.
- [6] A. P. Matos, L. R. I. Morioka, E. S. Sant'Anna and K. B. France, "Protein and lipid contents from *Chlorella* sp. Cultivated in residual concentrated desalination," *Rural Science*, 2014.
- [7] Â. P. Matos, W. B. Ferreira, R. C. d. O. Torres, L. R. I. Morioka, M. H. M. Canella, J. Rotta, T. d. Silva, E. H. S. Moecke and E. S. Sant'Anna, "Optimization of biomass production of *Chlorella vulgaris* grown in desalination concentrate," *Journal of Applied Phycology*, 2015.
- [8] Â. P. Matos, R. C. d. O. Torres, L. R. I. Morioka, E. H. S. Moecke, K. B. França and E. S. Sant'Anna, "Growing *Chlorella vulgaris* in Photobioreactor by Continuous Process Using Concentrated Desalination: Effect of Dilution Rate on Biochemical Composition," *International Journal of Chemical Engineering*, 2014.
- [9] L. R. I. Morioka, A. P. Matos, G. Olivo and E. S. Sant'Anna, "Evaluation of flocculation and lipid extraction of *Chlorella* sp. cultivated in concentrated

- desalination," *SciELO*, 2014.
- [10] M. T. Myint, "Using indigenous microalga species to reduce HCO₃⁻, NH₃N, NO₃N, total P, Ca²⁺, SO₄²⁻, and Cl⁻ from a high conductivity concentrate," *Desalination*, 2014.
- [11] M. T. Myint, A. Ghassemi and a. N. Nirmalakhandan, "Review of Nondestructed Anaerobic Digested Sludge," *Environmental Engineering Science*, 2010.
- [12] M. T. Myint, W. Hussein and A. Ghassemi, Microalgal process for treatment of high conductivity concentrates from inland desalination, 2015.
- [13] N. R. K. Paruchuri, "Algal Species Compatibility in EDR Concentrate," 2011.
- [14] H. Volkmann, U. Imianovsky, J. L. Oliveira and E. S. Sant'Anna, "Cultivation of *Arthrospira (spirulina) platensis* in desalinator wastewater and salinated synthetic medium: protein content and amino-acid profile," *Brazilian Journal of Microbiology*, 2008.
- [15] S. v. Iersel, L. Gamba, A. Rossi, S. Alverici, V. Dehue, J. v. d. Staaij and A. Flammini, "Algae-Based Biofuels: A Review of the Challenges and Opportunities for Developing Countries," Food and Agriculture Organization of the United Nations, 2009.
- [16] "Brackish Groundwater National Desalination Research Facility," 2014. [Online]. Available: <http://www.usbr.gov/research/AWT/BGNDRF/>. [Accessed 14 July 2015].
- [17] H. W. Kim, R. Vannela and B. E. Rittmann, "Responses of *Synechocystis* sp. PCC 6803 to total dissolved solids in long-term continuous operation of a photobioreactor," *Bioresourc Technology*, p. 378–384, 2013.
- [18] "LTER Daily Summary Climate Data," 2015. [Online]. Available: <http://jornada-www.nmsu.edu/studies/lter/datasets/climate/wthrstn/day/wyday.php>.
- [19] D. K. Bradshaw and L. Thompson, *The Analysis of Water and Wastes by U.S. EPA Method 200.7 Using the Optima 8300 ICP-OES and prepFAST Auto-Dilution/Calibration System*, PerkinElmer.

APPENDIX**Trace element analyses of concentrate in both experimental runs**

Element	Reported Concentration		Units	MDL
	Run 1	Run 2		
	Al	0.1108		
As	0.1642	0.1282	mg/L	0.0174
B	0.8848	1.152	mg/L	0.05
Ba	0.052	0.019	mg/L	0.001
Be	ND	0.0005	mg/L	0.0002
Cd	0.0032	0.0046	mg/L	0.001
Co	ND	ND	mg/L	0.002
Cr	ND	ND	mg/L	0.003
Fe	0.0558	0.0097	mg/L	0.004
Mn	0.0084	0.0067	mg/L	0.0017
Mo	0.0196	ND	mg/L	0.0017
Ni	0.0041	ND	mg/L	0.002
Pb	ND	ND	mg/L	0.0027
Se	ND	ND	mg/L	0.0135
Tl	ND	ND	mg/L	0.0068
V	ND	ND	mg/L	0.0017
Zn	0.1222	0.0048	mg/L	0.0013
Bi	0.1113	0.1101	mg/L	0.0052
Ca	709.7	686.8	mg/L	0.0971
Li	0.128	0.0878	mg/L	0.0014
Mg	380.8	453.7	mg/L	0.0185
P	2.088	0.028	mg/L	0.0251
Sr	13.65	11.31	mg/L	0.0012
K	15.62	4.982	mg/L	0.2101
SiO ₂	57.95	34.28	mg/L	0.0151
Na	1184	958.5	mg/L	0.0483
S	1519	1504.0	mg/L	0.5
Cu	ND	ND	mg/L	0.0023

**Trace element analyses of Pond 7 during Run 1 after algae were removed
from the medium**

	Day					MDL
	1	8	15	22	29	
Al	0.1101	0.1024	0.0969	0.0842	0.076	0.0026
As	0.2018	0.1563	0.1593	0.1498	0.1305	0.0174
B	0.8854	0.9864	0.9409	1.052	0.9504	0.05
Ba	0.0521	0.0483	0.0501	0.0469	0.0524	0.001
Be	ND	ND	ND	ND	ND	0.0002
Cd	0.0028	0.0023	ND	ND	0.0019	0.001
Co	ND	ND	ND	ND	ND	0.002
Cr	ND	ND	ND	ND	ND	0.003
Fe	0.2235	ND	ND	0.0089	0.0219	0.004
Mn	0.0602	0.0203	0.0039	0.0068	0.0098	0.0017
Mo	0.0177	0.0232	0.0226	0.0286	0.0264	0.0017
Ni	0.0051	0.0047	0.0033	ND	ND	0.002
Pb	ND	ND	ND	ND	ND	0.0027
Se	ND	ND	ND	ND	ND	0.0135
Tl	0.0227	ND	ND	ND	ND	0.0068
V	ND	ND	ND	ND	ND	0.0017
Zn	0.195	0.1395	0.1241	0.2001	0.2335	0.0013
Bi	0.1174	0.1092	0.0914	0.0752	0.0725	0.0052
Ca	769.2	666.5	600.2	656.6	654.2	0.0971
Li	0.1251	0.1376	0.1354	0.145	0.1429	0.0014
Mg	400.3	414.3	379.3	416.8	386.3	0.0185
P	6.09	0.6939	0.83	0.6163	2.123	0.0251
Sr	13.45	13.75	12.85	14.19	13.26	0.0012
K	23.98	24.05	21.66	32.46	35.31	0.2101
SiO ₂	56.86	60.8	59.9	64.5	61.8	0.0151
Na	1276.0	1290.0	1184.0	1304.0	1224.0	0.0483
S	1502.0	1623.0	1530	1807.0	1516.0	0.5
Cu	0.0804	0.0175	0.0141	0.0261	0.0375	0.0023

**Trace element analyses of Pond 8 during Run 1 after algae were removed
from the medium**

	Day					MDL
	1	8	15	22	29	
Al	0.0511	0.0442	0.041	0.0312	0.0304	0.0026
As	0.0925	0.0751	0.0819	0.0616	0.0717	0.0174
B	0.4436	0.5054	0.4726	0.5452	0.5182	0.05
Ba	0.0539	0.0466	0.0497	0.0467	0.0449	0.001
Be	ND	ND	ND	ND	ND	0.0002
Cd	0.0012	0.0012	ND	0.0015	0.0011	0.001
Co	ND	ND	ND	ND	ND	0.002
Cr	ND	ND	ND	ND	ND	0.003
Fe	0.3022	ND	ND	0.0044	0.0106	0.004
Mn	0.1247	ND	ND	ND	0.0032	0.0017
Mo	0.0097	0.0122	0.013	0.0161	0.0147	0.0017
Ni	0.0024	ND	ND	ND	ND	0.002
Pb	ND	ND	ND	ND	ND	0.0027
Se	ND	ND	ND	ND	ND	0.0135
Tl	0.0087	ND	ND	ND	ND	0.0068
V	ND	ND	ND	0.0028	ND	0.0017
Zn	0.1579	0.1187	0.104	0.1872	0.2104	0.0013
Bi	0.0517	0.0513	0.0474	0.0388	0.0358	0.0052
Ca	353.3	340.9	314.2	363.5	352.5	0.0971
Li	0.0913	0.0994	0.0949	0.1078	0.1067	0.0014
Mg	181.7	195.1	177.1	201.7	185.9	0.0185
P	4.939	0.2688	0.3265	0.8249	1.276	0.0251
Sr	6.351	6.819	6.257	6.9	6.441	0.0012
K	18.02	17.44	15.06	27.0	28.11	0.2101
SiO ₂	39.29	42.61	42.9	46.8	46.2	0.0151
Na	582.7	619.0	566.3	648.9	608.6	0.0483
S	722.5	785.6	716.3	807.8	740.8	0.5
Cu	0.0759	0.0149	0.0131	0.0363	0.0403	0.0023

**Trace element analyses of Pond 7 during Run 2 after algae were removed of
the medium**

	Day			Units	MDL
	-1	8	15		
Al	0.0756	0.1166	0.2652	mg/L	0.0026
As	0.1235	0.4782	0.456	mg/L	0.0174
B	1.1	1.381	1.567	mg/L	0.05
Ba	0.0194	0.0208	0.0186	mg/L	0.001
Be	ND	0.0033	ND	mg/L	0.0002
Cd	ND	ND	0.0107	mg/L	0.001
Co	ND	ND	ND	mg/L	0.002
Cr	ND	ND	ND	mg/L	0.003
Fe	0.6729	ND	ND	mg/L	0.004
Mn	0.0944	ND	0.0194	mg/L	0.0017
Mo	ND	ND	ND	mg/L	0.0017
Ni	0.0059	0.0144	ND	mg/L	0.002
Pb	ND	ND	ND	mg/L	0.0027
Se	ND	ND	ND	mg/L	0.0135
Tl	0.0061	0.0797	0.0451	mg/L	0.0068
V	ND	ND	ND	mg/L	0.0017
Zn	0.1242	0.0616	0.0573	mg/L	0.0013
Bi	0.1112	0.2527	0.2575	mg/L	0.0052
Ca	704.6	659.6	738.1	mg/L	0.0971
Li	0.0865	0.0773	0.0676	mg/L	0.0014
Mg	471.4	457.6	509.4	mg/L	0.0185
P	8.258	ND	2.191	mg/L	0.0251
Sr	10.56	12.07	13.11	mg/L	0.0012
K	15.45	17.51	16.09	mg/L	0.2101
SiO ₂	31.99	37.51	40.79	mg/L	0.0151
Na	973.3	984.7	1085	mg/L	0.0483
S	1606	1529	1623	mg/L	0.5
Cu	0.1219	0.0198	0.0136	mg/L	0.0023

**Trace element analyses of Pond 8 during Run 2 after algae were removed
from the medium**

	Day			Units	MDL
	-1	8	15		
Al	0.0559	0.0513	0.1145	mg/L	0.0026
As	0.2725	0.1206	0.1113	mg/L	0.0174
B	0.8278	0.5829	0.6829	mg/L	0.05
Ba	0.0444	0.0065	0.032	mg/L	0.001
Be	ND	0.001	0.0002	mg/L	0.0002
Cd	0.0065	0.002	0.0038	mg/L	0.001
Co	ND	ND	ND	mg/L	0.002
Cr	ND	ND	ND	mg/L	0.003
Fe	0.7599	ND	ND	mg/L	0.004
Mn	0.1577	0.0033	0.0041	mg/L	0.0017
Mo	ND	ND	ND	mg/L	0.0017
Ni	0.0107	0.0023	ND	mg/L	0.002
Pb	ND	ND	ND	mg/L	0.0027
Se	ND	ND	ND	mg/L	0.0135
Tl	0.059	0.0109	ND	mg/L	0.0068
V	ND	0.0022	ND	mg/L	0.0017
Zn	0.1309	0.0761	0.0599	mg/L	0.0013
Bi	0.1281	0.0642	0.0924	mg/L	0.0052
Ca	313.6	292.9	340.5	mg/L	0.0971
Li	0.0851	0.0718	0.0777	mg/L	0.0014
Mg	192.5	189.3	211.3	mg/L	0.0185
P	8.532	0.6703	2.983	mg/L	0.0251
Sr	5.244	5.019	5.806	mg/L	0.0012
K	19.92	18.84	20.17	mg/L	0.2101
SiO2	30.35	29.21	33.36	mg/L	0.0151
Na	420.6	420.7	466.8	mg/L	0.0483
S	619	666.5	673	mg/L	0.5
Cu	0.1466	0.0454	0.0218	mg/L	0.0023

Raw data from electrical conductivity measurements

Day	Conductivity (mS)			
	Pond 7 Run 1	Pond 8 Run 1	Pond 7 Run 2	Pond 8 Run 2
-1			8.6	4.3
0			8.89	4.39
1	8.21	4.4	8.68	4.35
2			8.67	4.43
4	8.52	4.65		
5	8.73	4.83	8.80	4.44
6	8.6	4.9	8.89	4.45
7	8.86	4.89	8.89	4.46
8	8.81	4.86	8.99	4.51
9			9.06	4.56
11	8.19	4.38		
12	8.25	4.42	9.37	4.7
13	8.31	4.43	9.43	4.75
14	8.37	4.46		
15	8.38	4.55	9.71	4.89
16			9.82	5.02
19	8.79	4.76	10.04	5.15
20	8.87	4.82	10.11	5.18
21	8.9	4.85		
22	9.02	4.95	10.22	5.25
25	8.05	4.52		
26	8.15	4.55		
27	8.27	4.6		
28	8.49	4.68		
29	8.54	4.77		

Raw data from pH measurements

Day	pH			
	Pond 7 Run 1	Pond 8 Run 1	Pond 7 Run 2	Pond 8 Run 2
0			8.36	8.47
1			8.66	8.64
2			8.61	8.63
4	8.71	8.84		
5	8.67	8.88	9.56	9.39
6	8.6	8.84	8.82	8.69
7	8.76	8.92	9.33	9.15
8	8.9	8.94	8.75	8.58
9			8.89	8.68
11	8.85	9		
12	8.92	8.79	7.93	8.72
13	9.08	8.9	8.11	8.15
14	8.83	8.92		
15	8.63	8.64	8.15	8.08
16			8.42	8.39
19	9.16	9.3	8.34	8.25
20	9	9.05	8.14	6.62
21	9.05	9.03		
22	9.12	9.02	7.81	6.29
25	8.53	8.51		
26	8.43	8.52		
27	8.42	8.75		
28	8.34	8.55		
29	8.35	8.65		

Raw data from depth measurements

Day	Depth (in)			
	Pond 7 Run 1	Pond 8 Run 1	Pond 7 Run 2	Pond 8 Run 2
-1			13	13
1	12	11.5	12.7	12.6
4	11	10.25		
5	11.25	10		
6	11	10	12.3	12.1
7	11	10		
8	10.5	10	12.2	11.9
11	11.5	11.5		
12	11.5	11.5	11.5	11.25
13	11.4	11	11.7	11.1
14	11.2	11		
15	11	11	11.3	10.9
19	10.4	10.5	11.0	10.0
20	10.4	10.4	11.0	10.0
21	10.25	10.1		
22	10	10	10.9	9.8
25	11.5	11.75		
26	11.4	11.5		
27	11.3	11.4		
28	11	11.2		
29	10.9	11		

Averages of cell counts of UTEX 1230 in a 4 nanoliter volume

Day	Cell Count			
	Pond 7 Run 1	Pond 8 Run 1	Pond 7 Run 2	Pond 8 Run 2
1			2.52	2.08
5	10.4	9.4		
6			41.8	25.6
8	34.4	14.2	50.4	22
12	89.6	40.8	39.4	17
15	93.6	117.4	34	24.4
19	77.4	78.4	11.4	8.8
22	86.2	103.2	26.4	11.4
26	54.8	99.8		
29	6	57.8		

Approximations of average cell diameters.

Day	Average Cell Diameter (Approximate)			
	Run 1		Run 2	
	Pond 7 (μm)	Pond 8 (μm)	Pond 7 (μm)	Pond 8 (μm)
-1	5.0	5.0		
1			3.75	3.125
5	2.5	2.5		
6			2.5	3.0
8	2.0	2.0	2.5	2.5
12	3.0	3.0	2.5	4.0
15	3.0	3.0	2.0	3.0
19	3.0	2.5	2.5	2.5
22	2.5	3.0	2.0	2.0
26	2.5	3.0		
29	1.5-2	2.5		

Raw data from temperature measurements during the first experimental run

Day	Time Measured	Pond Temperature ($^{\circ}\text{F}$)	
		Pond 7	Pond 8
6	10:40 AM	62	62
7	10:35 AM	61	61
8	9:20 AM	59	59
11	8:35 AM	56	57
12	9:50 AM	60	60
13	10:00 AM	61	61
14	9:25 AM	59	59
15	9:20 AM	60	60
19	10:20 AM	62	62
20	9:05 AM	57	58
21	9:20 AM	57	58
22	9:40 AM	58	58
25	9:00 AM	62	62
26	8:35 AM	63	63

27	8:55 AM	60	60
28	8:55 AM	60	60
29	10:10 AM	61	61

The following text summarizes how it was mathematically concluded that Pond 8 had a higher biomass-to-conductivity-ratio during the first run:

Day	Pond 7 Cell Count	Pond 8 Cell Count
-1		
5	10.4	9.4
8	34.4	14.2
12	89.6	40.8
15	93.6	117.4

Day	Pond 7 Avg. Radius	Pond 8 Avg. Radius	Pond 7 Avg. of Avg. Radii	Pond 8 Avg. of Avg. Radii
-1	2.5	2.5		
5	1.25	1.25	Days -1 – 8: 1.583	Days -1 – 8: 1.583
8	1	1		
12	1.5	1.5	Days 8-15: 1.333	Days 8-15: 1.333
15	1.5	1.5		

Day	Pond 7 Biomass nm ³ / 4nl Water	Pond 8 Biomass nm ³ / 4nl Water
-1		
5	172.917526	156.2908408
8	571.9579707	236.0989297
12	889.6369833	405.1025549
15	929.3529201	1165.662744

Assuming biomass is proportional to volume of biomass:

Figure 11. Curve fit for relative biomass in Pond 7 (days -1-12).

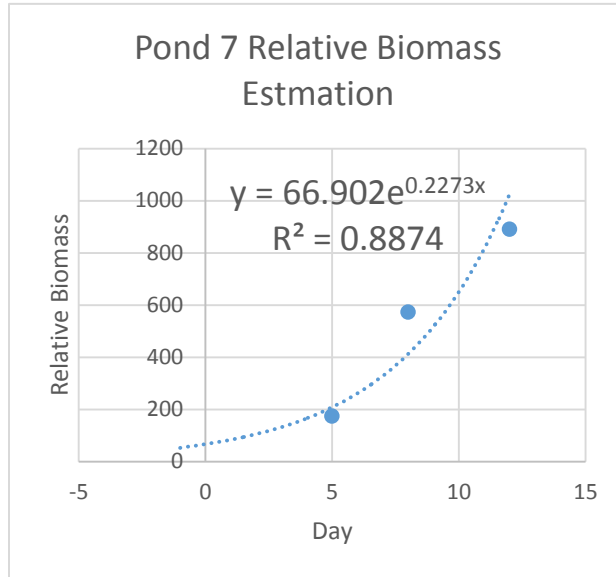


Figure 12. Curve fit for relative biomass in Pond 7 (days 12-15).

Pond 7: Days 1 - 8		
Avg. Rel. Biomass	Average Conductivity	Biomass/Conductivity
175.47	8.56 mS	20.5

Pond 7: Days 8 - 15		
Avg. Rel. Biomass	Average Conductivity	Biomass/Conductivity
779.94*	8.39 mS	93.0

*Used days 8-12 in Figure 11 and days 12-15 in Figure 12.

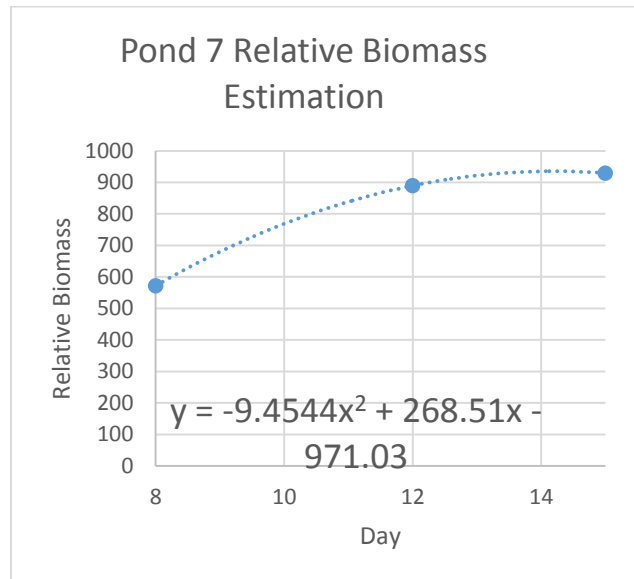
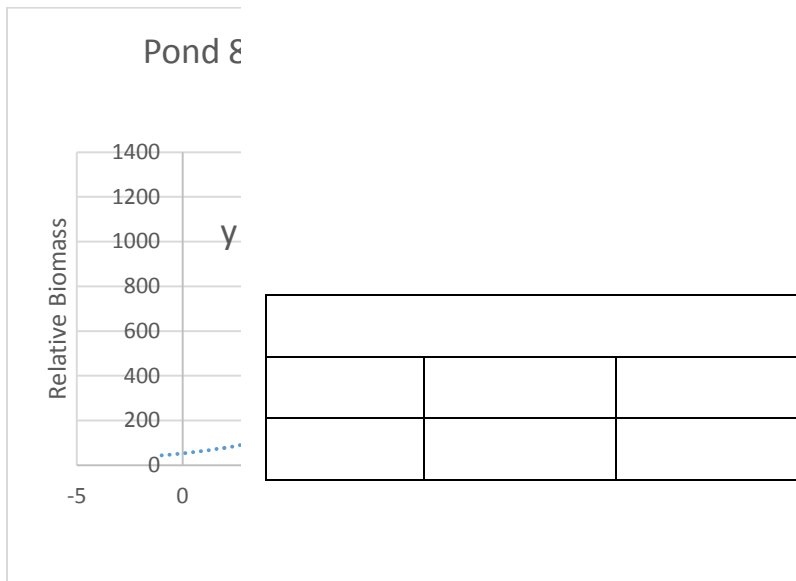


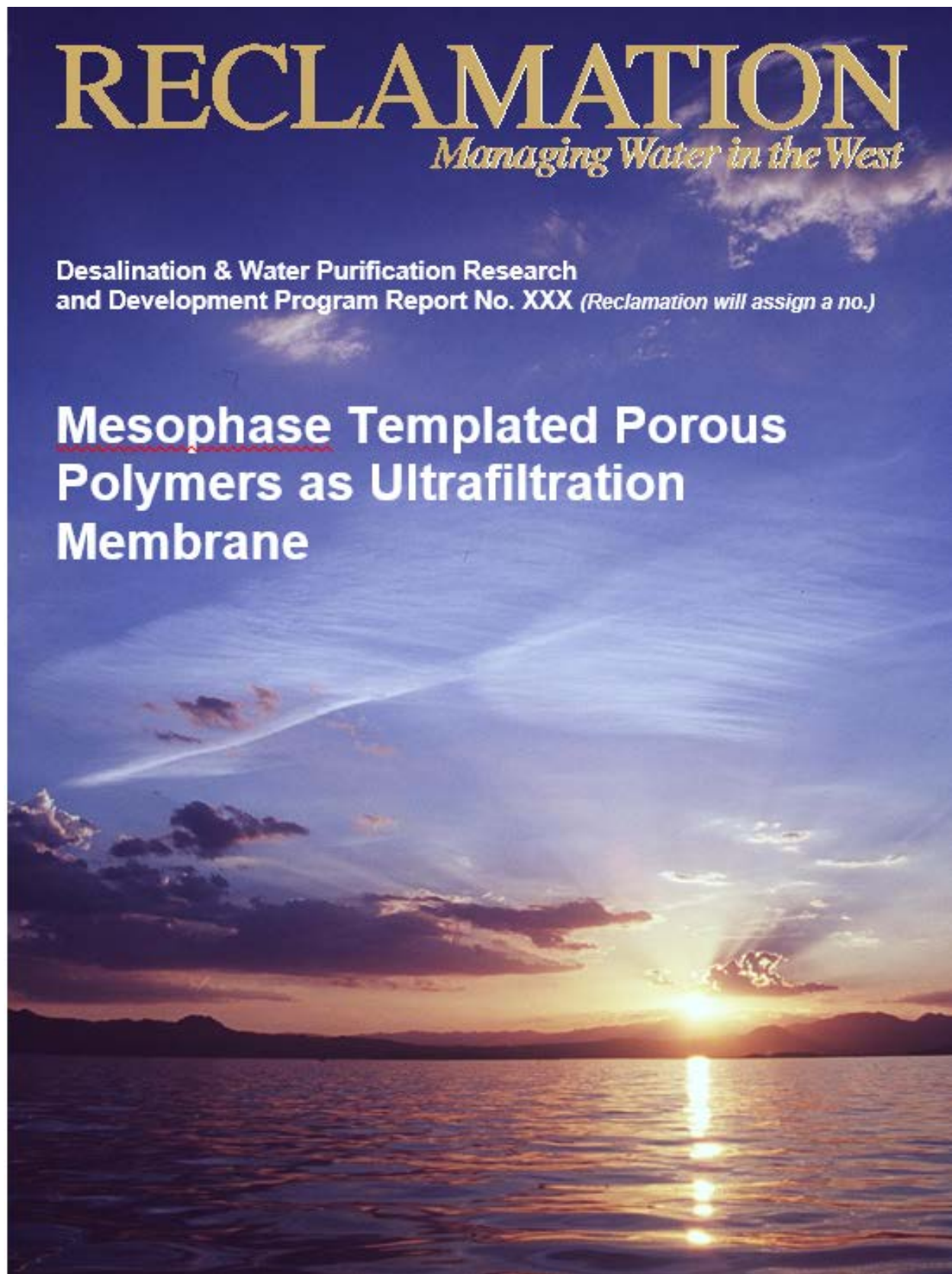
Figure 13. Curve fit for relative biomass in Pond 8.

Pond 8: Days 1 - 8		
Avg. Rel. Biomass	Average Conductivity	Biomass/ Conductivity
117.86	4.70 mS	25.1

Pond 8: Days 8 - 15		
Avg. Rel. Biomass	Average Conductivity	Biomass/ Conductivity
521.47	4.52 mS	115.4



Mesophase Templated Porous Polymers as Ultrafiltration Membrane



REPORT DOCUMENTATION PAGE		<i>Form Approved</i> <i>OMB No. 0704-0188</i>	
<p>The public reporting burden for this collection of information is estimated to average 1 hour per response, including the time for reviewing instructions, searching existing data sources, gathering and maintaining the data needed, and completing and reviewing the collection of information. Send comments regarding this burden estimate or any other aspect of this collection of information, including suggestions for reducing the burden, to Department of Defense, Washington Headquarters Services, Directorate for Information Operations and Reports (0704-0188), 1215 Jefferson Davis Highway, Suite 1204, Arlington, VA 22202-4302. Respondents should be aware that notwithstanding any other provision of law, no person shall be subject to any penalty for failing to comply with a collection of information if it does not display a currently valid OMB control number.</p> <p>PLEASE DO NOT RETURN YOUR FORM TO THE ABOVE ADDRESS.</p>			
1. REPORT DATE (DD-MM-YYYY)	2. REPORT TYPE Proof of Concept Final Report	3. DATES COVERED (From - To)	
4. TITLE AND SUBTITLE Mesophase Templated Porous Polymers as Ultrafiltration Membrane		5a. CONTRACT NUMBER R10AC80283	
		5b. GRANT NUMBER	
		5c. PROGRAM ELEMENT NUMBER	
6. AUTHOR(S) Sahar Qavi, Reza Foudazi		5d. PROJECT NUMBER	
		5e. TASK NUMBER	
		5f. WORK UNIT NUMBER	
7. PERFORMING ORGANIZATION NAME(S) AND ADDRESS(ES) Department of Chemical Engineering, New Mexico State University Regents Row 3055 Williams Avenue		8. PERFORMING ORGANIZATION REPORT NUMBER	
9. SPONSORING/MONITORING AGENCY NAME(S) AND ADDRESS(ES)		10. SPONSOR/MONITOR'S ACRONYM(S)	
		11. SPONSOR/MONITOR'S REPORT NUMBER(S)	

12. DISTRIBUTION/AVAILABILITY STATEMENT			
13. SUPPLEMENTARY NOTES			
14. ABSTRACT			
<p>Clean water scarcity is the number one critical problem in the world. Increasing population gives rises to clean water demand and wastewater production, and thus, further development of water treatment methods. Ultrafiltration is a necessary step for treating the wastewater, in which suspending particles, viruses, and bacteria are removed. Conventional ultrafiltration (UF) membranes are produced by non-solvent induced phase separation (NIPS) technique; but, this method is not ecofriendly and the resultant membranes are anisotropic with low surface area and porosity.</p> <p>Self-assembly of block copolymers in oil/water interface have been widely studies due to its wide range of potential applications in technology and science. The purpose of this research is to utilize self-assembly as a template for producing mesoporous polymeric materials that can be used as UF membranes.</p> <p>In order to study the self-assembly of block copolymers in oil/water interface, different compositions of water/oil/surfactant were studied by changing the monomer and surfactant types and concentrations. Both small molecule surfactants and polymeric surfactants were used in the study. The oil used in this study comprised of butyl acrylate and ethylene glycol dimethacrylate, which can be polymerized by photo and thermal initiators. Ethylene glycol dimethacrylate in the formulations works as cross-linker to provide integrity and appropriate mechanical properties. After forming desired structures of mesophases, oil phase was polymerized to obtain a mesoporous polymer. Polarized light microscopy (PLM), rheology, and small angle X-ray scattering (SAXS) have been used for characterization of the resultant materials. The produced membranes have mesopores in the range of 70 nm and show improved permeability compared to conventional UF membranes. Permeability of membranes was measured in a dead-end flow using a home-made device.</p>			
15. SUBJECT TERMS			
16. SECURITY CLASSIFICATION OF:	17. LIMITATION OF ABSTRACT	18. NUMBER OF PAGES	19a. NAME OF RESPONSIBLE PERSON

a. REPORT	b. ABSTRACT	a. THIS PAGE			19b. TELEPHONE NUMBER <i>(Include area code)</i>

Standard Form 298 (Rev. 8/98)
Prescribed by ANSI Std. Z39.18

**Desalination & Water Purification Research
and Development Program Report No. XXX**

Mesophase Templated Porous Polymers as Ultrafiltration Membrane

**Prepared for Reclamation Under Agreement No.
R10AC80283**

by

Sahar Qavi, Reza Foudazi

MISSION STATEMENTS

The mission of the Department of the Interior is to protect and provide access to our Nation's natural and cultural heritage and honor our trust responsibilities to Indian tribes and our commitments to island communities.

The mission of the Bureau of Reclamation is to manage, develop, and protect water and related resources in an environmentally and

Disclaimer

The views, analysis, recommendations, and conclusions in this report are those of the authors and do not represent official or unofficial policies or opinions of the United States Government, and the United States takes no position with regard to any findings, conclusions, or recommendations made. As such, mention of trade names or commercial products does not constitute their endorsement by the United States Government.

Acknowledgements

The authors would like to thank the U.S. Bureau of Reclamation for providing funding through IEE/NMSU cooperative agreement, Dr. Millicent Firestone at the Center for Integrated Nanotechnologies (CINT) in Los Alamos National Laboratory for helping in Small-angle X-ray Scattering measurements, and New Mexico State University for start-up package.

Contents

Table of Figures.....	4
Glossary.....	6
Executive Summary.....	8
1. Water scarcity.....	9
1.1. Non-solvent induced phase separation method.....	10
1.2. Templating approach for synthesis of porous materials	12
1.3. Self-assembly of amphiphilic block copolymers in oil/water interface	16
2. Experimental.....	21
2.1. Approach	21
2.2. Materials	22
2.3. Set up for making membrane	26
2.4. Characterization techniques	27
2.4.1. Polarized light microscopy (PLM)	27
2.4.2. Small angle X-ray scattering	28
2.4.3. Rheology	31
2.4.4. Permeability.....	32
3. Results and discussion	34
3.1. Polarized light microscopy	37
3.2. SAXS results	40
3.3. Rheology results	45
3.4. Permeability results.....	51
3.5. Rejection Results	53

4. Conclusion.....	54
5. Future wok	55
References	55

Table of Figures

Figure 1. UF membrane can filter particles and impurities in the range of >0.1 μm	9
Figure 2. Chemical structure and schematic representation of a Pluronic block copolymer. X, Y, and Z show the degree of polymerization of different blocks. .	18
Figure 3. Phase diagram of the water/p-xylene/ Pluronic L64 block copolymer ⁴⁰ and water/decanol/CTAB ⁴³	20
Figure 4. Templating approach for making porous materials	21
Figure 5. Chemical structures of monomer (butyl acrylate), cross-linker (ethylene glycol dimethacrylate), initiators (1-hydroxycyclohexyl phenyl ketone, azobisisobutyronitrile, benzoyl peroxide, and 4,N,N-trimethylaniline), block copolymer (Pluronic L64), and small molecule surfactant (CTAB)	24
Figure 6. Eppendorf centrifuge model 5804 used for removing talc from permeate.....	25
Figure 7. Six different compositions used for making mesophases from Pluronic L64.....	25
Figure 8. Processing mesophase to make membrane.....	27
Figure 9. A typical SAXS pattern. q_1 is the principal peak and q_2/q_1 and q_3/q_1 ratios determine the type of crystal symmetry	30
Figure 10. DHR-3 device used for rheometry	32
Figure 11. Home-made filtration set-up.....	33
Figure 12. Cross-polarized light micrographs obtained for mesophases with different compositions containing CTAB before curing	38
Figure 13. Cross-polarized light micrographs obtained for mesophases with different compositions containing Pluronic L64 before curing	39
Figure 14. Cross-polarized light micrographs obtained for mesophase with different compositions containing Pluronic L64 after polymerization.....	40
Figure 15. SAXS spectrum obtained from samples A, B, and C with lamellar pattern. Insets show 2D SAXS images.....	41

Figure 16. SAXS spectrum obtained from samples D and E with hexagonal pattern. Insets show 2D SAXS images.....	42
Figure 17. SAXS spectra of sample A at different temperatures	43
Figure 18. SAXS spectra of samples A, B, and D before and after polymerization	44
Figure 19. Storage modulus, G' , and loss modulus, G'' , versus strain obtained through oscillatory amplitude sweep experiments on samples A and D.....	46
Figure 20. Storage modulus, G' , loss modulus, G'' , and complex viscosity, η^* , versus angular frequency of samples A and D obtained through frequency sweep in small oscillatory amplitude shear regime	49
Figure 21. Schematic illustration of the strain sweep test at a fixed frequency ⁴⁷	50
Figure 22. Oscillatory stress curves versus time (a ,b), and closed-loop plots of normalized stress versus normalized strain (c,d) obtained from amplitude oscillation in large amplitude oscillatory shear regime. a and c plots represent sample A and b and d plots represent sample D	51
Figure 23. membrane surface appearance before and after rejection test with 2 wt.% talc suspension. A cake layer of talc was formed on the membrane surface after the test.	54

Glossary

Term	Description
I_1, L_1	Normal micellar cubic phase
H_1	Normal hexagonal mesophase
L_α	Lamellar mesophase
K, V_2	Gyroid mesophase
H_2	Reverse hexagonal mesophase
I_2, L_2	Reverse micellar cubic phase
Q	Scattering vector ($1/\text{\AA}$)
G'	Storage modulus (Pa)
G''	Loss modulus (Pa)
η^*	Complex viscosity (Pa.s)
UF	Ultra filtration
PEO	Poly(ethylene oxide)
PPO	Poly(propylene oxide)
AIBN	Azobisisobutyronitrile
EGDMA	Ethylene glycol dimethacrylate
CTAB	Cetyltrimethylammonium bromide
BA	Butyl acrylate

K	Darcy's constant (m^2)
L	Membrane thickness (μm)
Q	Flow rate (m^3/s)
M	Feed viscosity (Pa.s)
A	Membrane area (mm^2)
ΔP	Pressure difference along the membrane (Pa)
R	Rejection
C_p	Permeate concentration (g/L)
C_f	Feed concentration (g/L)

Executive Summary

Clean water scarcity is the number one critical problem in the world. Increasing population gives rises to clean water demand and wastewater production, and thus, further development of water treatment methods. Ultrafiltration is a necessary step for treating the wastewater, in which suspending particles, viruses, and bacteria are removed. Conventional ultrafiltration (UF) membranes are produced by non-solvent induced phase separation (NIPS) technique; but, this method is not ecofriendly and the resultant membranes are anisotropic with low surface area and porosity.

Self-assembly of block copolymers in oil/water interface have been widely studied due to its wide range of potential applications in technology and science. The purpose of this research is to utilize self-assembly as a template for producing mesoporous polymeric materials that can be used as UF membranes.

In order to study the self-assembly of block copolymers in oil/water interface, different compositions of water/oil/surfactant were studied by changing the monomer and surfactant types and concentrations. Both small molecule surfactants and polymeric surfactants were used in the study. The oil used in this study comprised of butyl acrylate and ethylene glycol dimethacrylate, which can be polymerized by photo and thermal initiators. Ethylene glycol dimethacrylate in the formulations works as cross-linker to provide integrity and appropriate mechanical properties. After forming desired structures of mesophases, oil phase was polymerized to obtain a mesoporous polymer. Polarized light microscopy (PLM), rheology, and small angle X-ray scattering (SAXS) have been used for characterization of the resultant materials. The produced membranes have mesopores in the range of 70 nm and show improved permeability compared to conventional UF membranes. Permeability of membranes was measured in a dead-end flow using a home-made device.

1. Water scarcity

Water resources become scarcer as the world population continues to grow. Based on United Nation statistics, by 2025, 1.8 billion people will be living in countries or regions with absolute water scarcity, and two-thirds of the world's population could be living under water stressed conditions. Additionally, with the existing climate change scenario, almost half of the world's population will be living in areas of high water stress by 2030, including between 75 million to 250 million people in Africa. Water scarcity in some arid and semi-arid places will displace between 24 million and 700 million people.¹

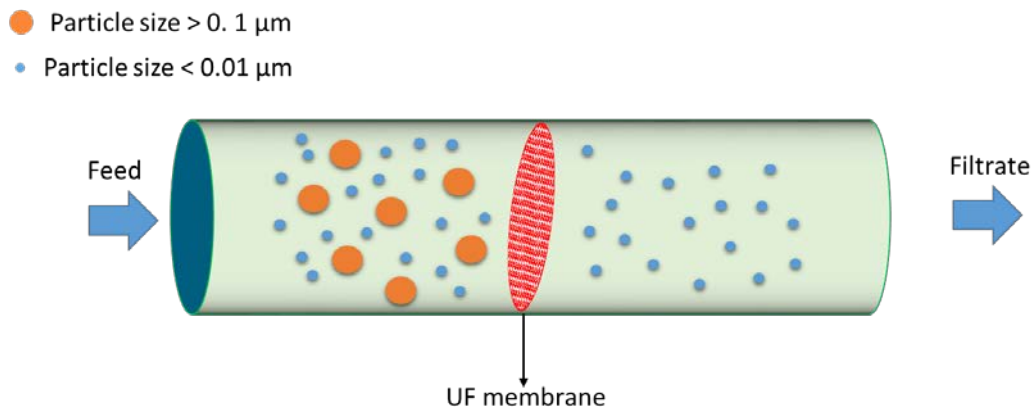


Figure 1. UF membrane can filter particles and impurities in the range of >0.1 μm .

Increase in water usage will raise the amount of wastewater that should be treated sufficiently to meet the environmental regulations. Water treatment processes employ several types of membranes, including microfiltration (MF),

ultrafiltration (UF), nanofiltration (NF), and reverse osmosis (RO).² These processes are usually employed in series in order to purify water efficiently. Figure 1 shows a schematic of a UF membrane. UF uses a finely porous membrane and is a pressure-driven process. Typical UF membranes have the pore size diameter of 0.01-0.1 μm and are used as a pretreatment before NF and RO processes in order to remove proteins, organic acids, oil emulsions, microbes, and viruses from wastewater.

1.1. Non-solvent induced phase separation method

Phase inversion techniques are among the most important and commonly used processes for preparing membranes from a large number of polymeric building blocks. Development of integrally skinned asymmetric membranes by Loeb and Sourirajan in the 1960s is a major breakthrough in membrane technology.³ Over the past half century, a plethora of knowledge has been generated about phase inversion membranes formed by immersion precipitation, also known as non-solvent induced phase inversion (NIPS).

Many different polymers are used in the synthesis of microfiltration, ultrafiltration, nanofiltration, and reverse osmosis membranes using NIPS method. Polysulfone (PSf), polyethersulfone (PES), polyacrylonitrile (PAN), cellulose, poly(vinylidene fluoride) or PVDF, poly(tetrafluoroethylene) or PTFE, polyimides (PI), and polyamides (PA) are among the most common polymeric membrane materials in use today.⁴

Polysulfone (PSf) is one of the most common polymers used to make membranes by phase inversion process. Polysulfone is often selected because of its commercial availability, ease of processing, favorable selectivity-permeability characteristics, and glass transition temperature (T_g) value of 190°C. It possesses good mechanical, thermal, and chemical properties. Moreover, it is generally easy to prepare asymmetric membranes by the phase inversion method, in which a thin layer of PSf solution in an appropriate solvent is immersed into the non-solvent coagulation bath, such as water. The most frequently used solvents for PSf are N-methylpyrrolidone (NMP),⁵ N,N-dimethylacetamide (DMAc),⁶ and N,N-dimethylformamide (DMF).⁷

In NIPS method, the base polymer for membrane production should be dissolved in a significant amount (more than 65 wt.%)⁷ of an organic solvent, which makes the process indeed non-ecofriendly. Moreover, the polymer solution should be usually dilute, and therefore, the process is not efficient in time, energy and raw material consumption. The thickness of membranes produced by NIPS method is limited since a polymer solution film should coagulate through immersion in a non-solvent to form membrane. A development objective that can hardly be achieved by NIPS is to produce 2-3 mm diameter capillary fiber modules which is necessary to lead to lower energy consumption and higher, more stable membrane fluxes.² Therefore, there is a growing need for producing new levels of hierarchical membranes and alternative methods for membrane production with emphasis on ecofriendly processes, higher flux and/or lower operational pressure, and less expensive processes for wastewater treatment and filtration

processes for industrial applications. One alternative method is templating approach for producing mesoporous materials that will be covered in next section.

1.2. Templating approach for synthesis of porous materials

According to the definition of the International Union of Pure and Applied Chemistry (IUPAC), porous materials can be classified into microporous (with pore diameter <2 nm), mesoporous (2–50 nm) and macroporous (>50 nm) materials, respectively.⁸ In the case of mesoporous materials, the structural capabilities at the scale of a few nanometers and high surface area can meet the demands of the growing applications such as adsorption, separation, catalysis, drug delivery, sensors, photonics, energy storage and conversion, and nanodevices. Direct templating by preformed lyotropic liquid crystal (LLC) phases prepared under relatively high surfactant concentrations has been widely used for producing mesoporous oxides, such as silica and niobium oxide.^{9,10}

Inorganic mesoporous materials are limited in terms of processability and mechanical strength.¹¹ Such limitations can be overcome through organic mesoporous materials, which have chemical tunability, mechanical properties, and processability coupled with the high surface area, stability, and reactivity.^{12,13}

When polymerizable surfactants¹⁴ are used templating process is called '**synergistic**' and the material obtained is the cured template. On the other hand,

a **'transcriptive'** synthesis results in a product that is a copy of the template structure, for example when monomer polymerizes around the self-assembled surfactants. In some cases even when the template structure is not retained during polymerization the self-organized reaction medium can still direct polymer growth. In this way, new and typically hierarchically morphologies are formed. Such cases of indirect templating are called **'reconstructive'** synthesis.^{15,16}

Templating within organized solutions is a much more complex process than that Hentze et al.¹⁶ suggested by the simple picture of 'casting' a surfactant assembly. Polymerization reaction progresses within a highly dynamic self-organized medium in a continuously changing physico-chemical environment. As the monomer phase is substituted by a polymer phase, changes of the polarity of the dispersion medium and the partitioning of each compound may occur. Many monomers show some degree of surface activity and consequently segregate at the assembly's interface.¹⁶

Polymerization can cause phase transitions by driving changes in the interface curvature. More severe effects arise due to the loss of entropy or chemical incompatibility of the polymer with the surfactant, and this sometimes drives phase separation and concomitant disruption of the initial structure. In these cases, the surfactant phase still coexists with the demixed polymer phase, so there are usually no significant changes of optical textures or diffractograms recorded before and after polymerization.¹⁶

Given the dilemma that polymerization-induced phase separation is always the enemy of direct synergistic or transcriptive templating, two strategies can be developed for the synthesis of ordered supramolecular materials. One is to suppress phase separation by adjusting thermodynamic and kinetic parameters, either in the original formulation or, perhaps, by changing conditions as the reaction proceeds. To do so, several approaches have been proposed by Hentze and Kaler as follows:¹⁶

- (i) kinetic stabilization by the use of surfactants with slower exchange dynamics (e.g. amphiphilic block copolymers);
- (ii) polymerization within templates with long rearrangement times (e.g. hexagonal and cubic phases);
- (iii) thermodynamic adjustment of the surfactant/monomer/polymer mixture (e.g. by matching the molecular structure to induce some attractive interaction, and thus, compatibility); and
- (iv) cross-linking of the polymer matrix to 'compensate' for the entropy loss caused by producing the polymer matrix in a confined nanogeometry (e.g. monomers with a high number of reactive entities per molecule cross-links upon polymerization, and small multifunctional monomers such as divinylbenzene can be added to mono-functional monomers to form cross-linked networks).

Another strategy for the synthesis of ordered materials, not yet fully developed, is to make use of the high sensitivity of the interaction between polymer network chemistry and surfactant mesophase chemistry. When aiming at the

reconstructive templating of polymers with even more complex morphologies, this sensitivity can be used as a powerful tool for the synthesis of new hierarchical polymer structures. One example is the colloidal ordering of polymer gels by polymerization-induced phase separation within inverse hexagonal phases.¹⁷

Gin and Gu¹² have used cross-linked lyotropic liquid crystal (LLC) phases as catalysts in the development of systems capable of acid catalysis. LLC phases are self-assemblies of amphiphilic molecules that form in a solvent. However, unlike micelles and vesicles which are relatively simple individual structures, LLC phases are highly ordered yet fluid condensed assemblies with specific nanometer-scale geometries. The tails of the amphiphiles in LLC phases form fused hydrophobic regions while the hydrophilic (typically ionic) headgroups define the interfaces of ordered, extended aqueous regions. Depending on the shape of the LLCs and the interfacial curvature, aqueous domains ranging from lamellae to cylindrical channels with dimensions in the 1-10 nm range can be formed.¹⁸

Considerable difficulties arise in templating LLC structures onto organic polymers. It is entropically unfavorable for polymers to exist in the confined dimensions of LLC phases, and thus, phase separation can occur. The sizes of morphologies generated are often in nanometer range, but not the same as the original LLC structure due to uncontrolled phase separation.^{16,19}

Some researches on the polymerization in LLC media have yielded mixed results as lyotropic structures are not typically retained or are significantly altered upon polymerization.²⁰⁻²² On the other hand, a limited number of cases have been

reported showing retained LLC structure upon polymerization. For example, O'Brien et al. polymerized a dienoyl phospholipid in the inverted hexagonal phase with retention of the original lyotropic structure.²³

Lester et al.¹³ have studied the kinetic of photopolymerization in LLC media. They have shown that reactions in the ordered structure of LLC are highly dependent on the type and degree of order, and are significantly different than in an isotropic state. This phenomenon can be attributed to a number of factors including diffusional limitation which reduce termination rates and segregation of the monomeric species increasing both the apparent propagation and termination values.²⁴

1.3. Self-assembly of amphiphilic block copolymers in oil/water interface

Surface-active agents (surfactants) can self-assemble in water/oil mixtures to form mesomorphic phases (mesophases), which are anisotropic structures highly extended in one or two dimensions.^{25,26} Surfactant molecules play a vital role in the formation of mesophases and their stability. Small molecule surfactants have been widely used in several applications for producing mesophase structures.

A polymer is a large molecule, or macromolecule, composed of many repeating units (mer). Copolymers are synthesized by polymerization of more than one type of monomer. If copolymer molecule consists of blocks of different monomers, the resultant copolymer is called a block copolymer. The blocks in

copolymer can be incompatible with one another, e.g. in amphiphilic block copolymers. Literally, amphiphilic means loving both and amphiphilicity can be expressed toward any two solvents which are incompatible with each other, oil and water for instance. Amphiphilic block copolymers have a wide range of applications in pharmaceutical, cosmetics, drug delivery, and catalysis.²⁷ Amphiphilic block copolymers can be used as surfactants at oil/water interfaces as well. Similar to conventional low molar mass surfactants, amphiphilic block copolymers may form micelles, vesicles, or lyotropic mesophases. While polymeric surfactants are less studied than small-molecule surfactants for self-assembly, they offer some opportunities in terms of flexibility, diversity, and functionality.²⁸ Additionally, polymeric amphiphiles self-assemble to structures which are more stable, and have a lower critical micelle concentrations (CMC) compared to their small molecule analogues.²⁹ After all, the block composition is the main determinant of the microstructure observed in solvent-free block copolymers^{30,31} as the chemical composition of typical surfactants (“head group” and “tail”) affects their hydrophilic/lipophilic ratio and self-assembly in solution properties.

Pluronic block copolymers are triblock copolymers of poly (ethylene oxide) (PEO) and poly (propylene oxide) (PPO), often denoted as PEO-PPO-PEO or $(\text{PEO})_x\text{-(PPO)}_y\text{-(PEO)}_z$, are nonionic polymeric surface active agents. Figure 2 shows the chemical structure of typical Pluronic block copolymers. Variation of copolymer composition (PPO/PEO ratio) and molecular weight (PEO and PPO block length) during synthesis leads to the production of molecules with optimum properties

that meet the specific requirements in various areas of technological significance.³²

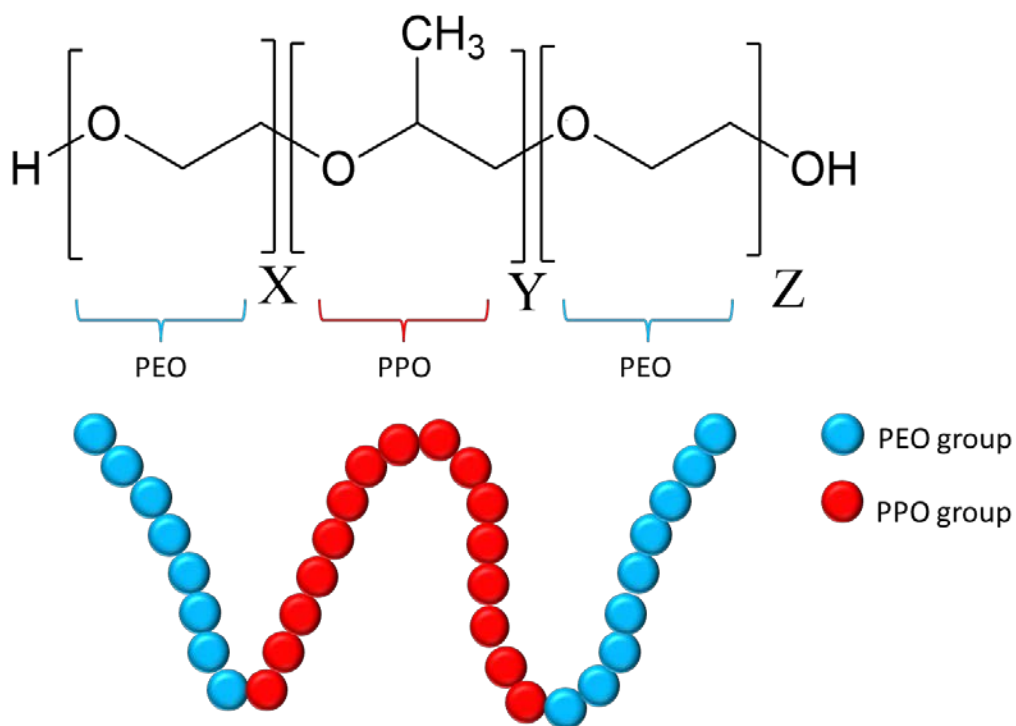


Figure 2. Chemical structure and schematic representation of a Pluronic block copolymer. X, Y, and Z show the degree of polymerization of different blocks.

The Pluronic block copolymers are available in a range of molecular weights and PPO/PEO composition ratios, with relatively low price (compared to small molecule surfactants), low toxicity and stability over a wide pH range.^{33,34} The notation for the Pluronic triblock copolymers starts with the letters L (for liquid), P (for paste), or F (for flakes) followed with a number. The first one or two numbers are indicative of the molecular weight of the PPO block, and the last

number signifies the weight fraction of the PEO block.³² For example, Pluronic F127 and Pluronic L121, have the same molecular weight of PPO, but F127 has 70 wt.% PEO and L121 has 10 wt.% PEO.

Solvent-free block copolymers can self-assemble as spheres, cylinders, and lamellae, similar to small molecule surfactants in solution.³⁵ In the presence of water or in ternary systems with water and oil, PEO/PPO copolymers can self-assemble into lyotropic liquid crystalline structures.^{36,37} Alexandridis et al.^{32,38,39} initiated comprehensive studies on the phase behavior and microstructure of ternary systems consisting of an amphiphilic Pluronic block copolymer and two solvents, one (water) selective for the PEO blocks and another (hydrophobic oil such as p-xylene) selective for PPO block. A rich structural polymorphism has been observed in such ternary copolymer/water/oil systems, with the block copolymer molecules self-assembling to form micro-domains with spherical, cylindrical, or lamellar geometry, discrete or interconnected topology, and liquid-crystalline organization.⁴⁰⁻⁴²

Alexandridis et al.⁴⁰ have examined the ternary phase behavior of Pluronic L64, $(\text{PEO})_{13}\text{-(PPO)}_{30}\text{-(PEO)}_{13}$, in the presence of water and p-xylene as selective solvents of PEO and PPO, respectively. Figure 3 shows the phase diagram of such system. In addition, the ternary phase diagram of water/oil/CTAB is shown for comparison as well. CTAB stands for commonly used small molecule surfactant, cetyl trimethylammonium bromide. Progression of structure in block-copolymer/water/oil phase diagram can be discussed at two levels: i) varying water/oil ratio at constant total copolymer content, and ii) changing total

copolymer content at constant copolymer/oil [copolymer/water] ratio. It can be seen that using different compositions of water/p-xylene in constant surfactant fraction or using different surfactant/water (or surfactant /oil) ratios in constant oil (or water) composition leads to various liquid crystalline structures. L_1 , H_1 , L_α , V_2 , H_2 , and L_2 denote normal (oil-in-water) micellar solution, normal hexagonal, Lamellar, reverse bicontinuous cubic, reverse (water-in-oil) hexagonal, and reverse micellar solution, respectively (all listed in Glossary).

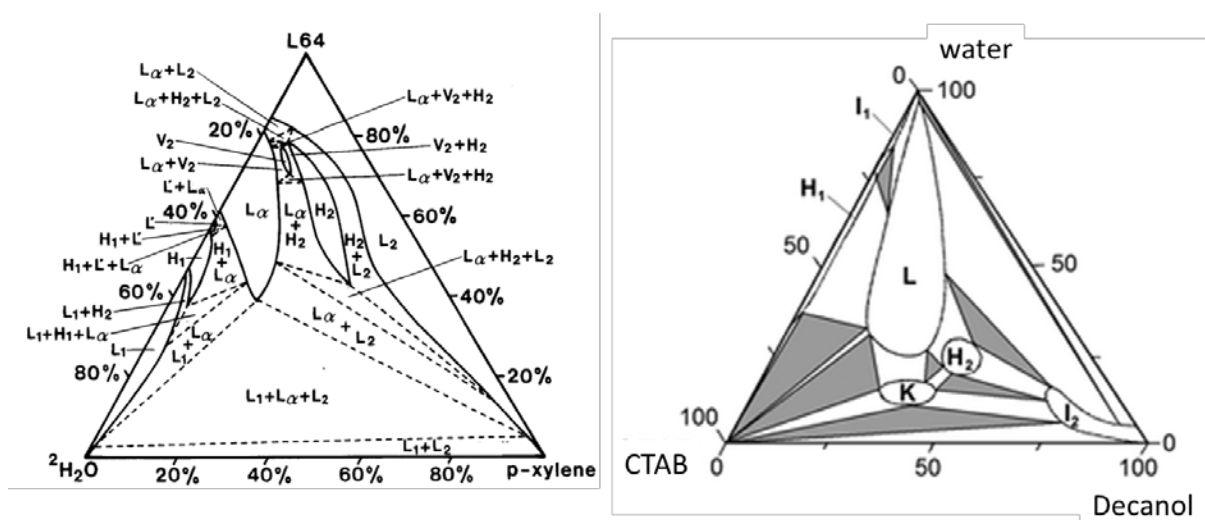


Figure 3. Phase diagram of the water/p-xylene/ Pluronic L64 block copolymer⁴⁰ and water/decanol/CTAB⁴³

The type of structure obtained does not only depend on the ternary copolymer-water-oil composition, but also depends on the PEO/PPO ratio and molecular weight of block copolymer. The ability of the blocks to swell to different extents (based on the amount of solvent available) modulates the interfacial “curvature”, and thus, the resulting structure. An increase in the copolymer

molecular weight for a given block composition increases the block segregation (for the same solvent conditions) and results in an increase of the temperature and composition stability range of the different structures. Higher polymer molecular weight may also lead to the formation of additional structures because of the increase in the range of inter-assembly interactions.⁴¹

2. Experimental

2.1. Approach

In this work, we mainly study the self-assembly of Pluronic L64 block copolymer in oil/water interface and utilize its mesophases as a template for producing UF membranes. To produce mesoporous membranes, polymerizable species (monomer) are used in the oil phase of the system. After self-assembly of oil/water/Pluronic block copolymer in a desired phase state, the monomer is polymerized to obtain the designed porous structure as schematically shown in Figure 4.

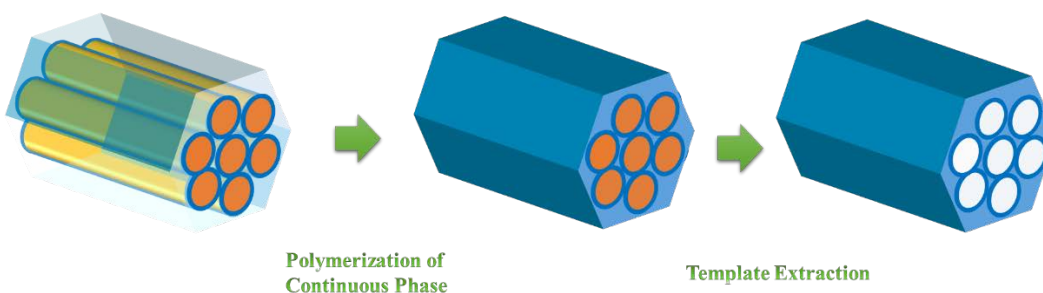


Figure 4. Templating approach for making porous materials

2.2. Materials

Poly(ethylene oxide)-b-poly(propylene oxide)-b-poly(ethylene oxide), Pluronic L64, was kindly provided by BASF corporation. Butyl acrylate ($\geq 99\%$), 4,N,N-trimethylaniline ($\geq 98.5\%$), azobisisobutyronitrile (98%), 1-hydroxycyclohexyl phenyl ketone (99%), and cetyltrimethylammonium bromide (CTAB, $\geq 98\%$) were obtained from Sigma-Aldrich. Ethylene glycol dimethacrylate was purchased from Electron Microscopy Sciences. Benzoyl peroxide was obtained from Fisher Scientific. All chemicals were used as received.

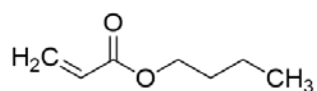
Butyl acrylate (BA) and ethylene glycol dimethacrylate (EGDMA) were used as monomer and cross-linker, respectively. 1-Hydroxycyclohexyl phenyl ketone and azobisisobutyronitrile (AIBN) were used as UV and thermal initiators, respectively. 4,N,N-trimethylaniline and benzoyl peroxide were used as redox initiation system. Chemical structures of small molecule surfactant, block copolymer, monomer, cross-linker, and initiators are shown in Figure 5. The amounts of cross-linker and initiators in the oil phase were kept constant for different compositions.

The experiment comprises of two steps: (i) a simple mixing of all materials in which no chemical reaction takes place, and (ii) a cross-linking polymerization process in which a porous polymeric network (membrane) are formed. For the first step, desired amount of monomer, cross-linker, and initiator were mixed together and centrifuged at alternative directions for several times until a transparent gel (the mesophase) was obtained. Then, mesophases were placed in a UV chamber (Spectrolinker™ XL-1000) in the optimum intensity mode for 4

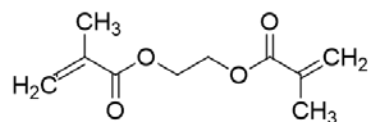
hours. After that, pre-cured samples were placed in drying oven at 60 °C for 3 hours until they were cured completely.

Talc powder and oil-in-water emulsion were used to evaluate the rejection performance of the membranes. 2 g talc powder was dissolved in 1 L water and the suspension was stirred for 30 minutes. 0.5 g NaCl and 5 g Pluronic F 68 were added to stabilize the suspension. Talc suspension was used as feed stream. Talc concentration in the feed and permeate was measured and solute particle rejection was calculated. In order to calculate the permeate concentration, permeate was centrifuged at the speed of 11000 rpm for 15 minutes using an Eppendorf centrifuge model 5804 (Figure 6).

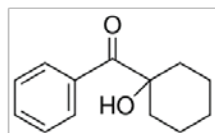
Rejection performance was also tested using an oil-in-water emulsion as feed. Vegetable oil and Pluronic F68 were used as oil phase and surfactant, respectively. First, 1 g Pluronic F68 was added to 1 L DI water and stirred for 15 minutes until it was completely dissolved in water. Then, 25 g vegetable oil was added drop wise (using a syringe pump) to the continuously being stirred solution. Resultant oil-in-water emulsion was used to test the rejection performance of the membranes.



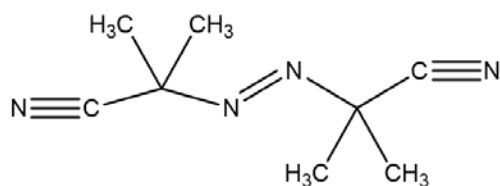
Butyl acrylate



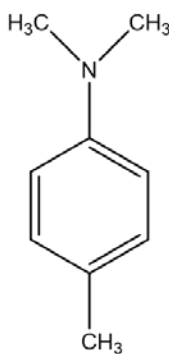
Ethylene glycol dimethacrylate



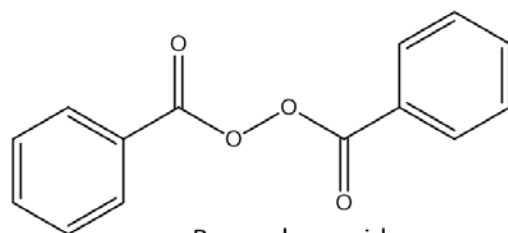
1-Hydroxycyclohexyl phenyl ketone



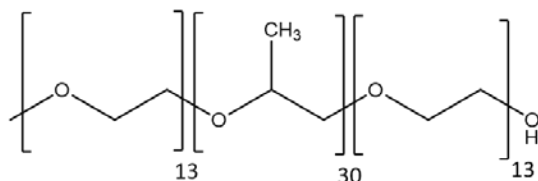
Azobisisobutyronitrile



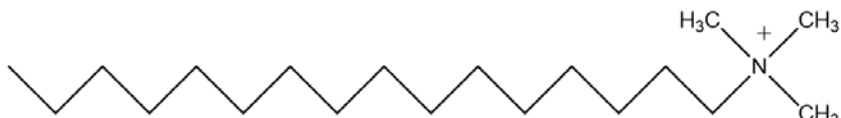
4, N, N-trimethyl aniline



Benzoyl peroxide



Pluronic L64

Br⁻

CTAB

Figure 5. Chemical structures of monomer (butyl acrylate), cross-linker (ethylene glycol dimethacrylate), initiators (1-hydroxycyclohexyl phenyl ketone, azobisisobutyronitrile, benzoyl peroxide, and 4,N,N-trimethylaniline), block copolymer (Pluronic L64), and small molecule surfactant (CTAB)



Figure 6. Eppendorf centrifuge model 5804 used for removing talc from permeate

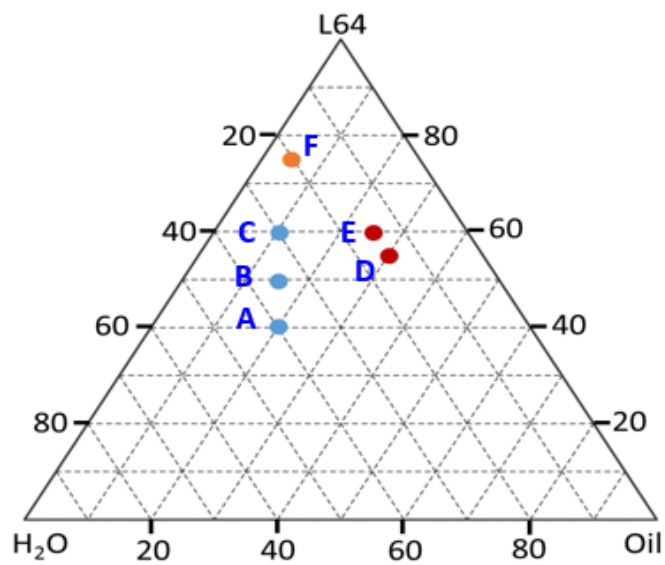


Figure 7. Six different compositions used for making mesophases from Pluronic L64.

Six compositions were chosen in the phase diagram of water/oil/Pluronic L64 to make mesophases (Figure 7). Compositions A, B, and C are expected to be in the lamellar region according to the phase diagram of water/xylene/Pluronic L64 obtained by Alexandridis.⁴⁰ Similarly, compositions D and E are expected to be in the hexagonal region and sample F is expected to be in the continuous cubic (gyroid) region.

2.3. Set up for making membrane

Mesophases show yield stress and do not flow under their weight as will be shown in rheological results. Therefore, processing a mesophase into a membrane needs to be done using a hot press. Such process can be scaled up to industrial scale if needed. For preparation of membranes, a small amount of the monomer gel mixture was first placed on a piece of support layer. In order to avoid biased results and conclusion originated by differences in support layers, we recovered the support from a commercial UF membrane (GE, MW series, MW2540F30) in this work, and fabricated our membranes on it. Then, the gel mixture on the support was sandwiched between Mylar sheets and placed between smooth stainless steel plates. The entire assembly was then pressed using a hot press machine pre-heated to 50 °C, by applying a force of 15 tons for five minutes to infuse the monomer mixture completely through the support layer. For photopolymerization, the resulting infused film (still between Mylar sheets) was placed in the UV chamber for four hours. Afterwards, the film was placed in a drying oven at 70 °C to complete the polymerization (Figure 8).

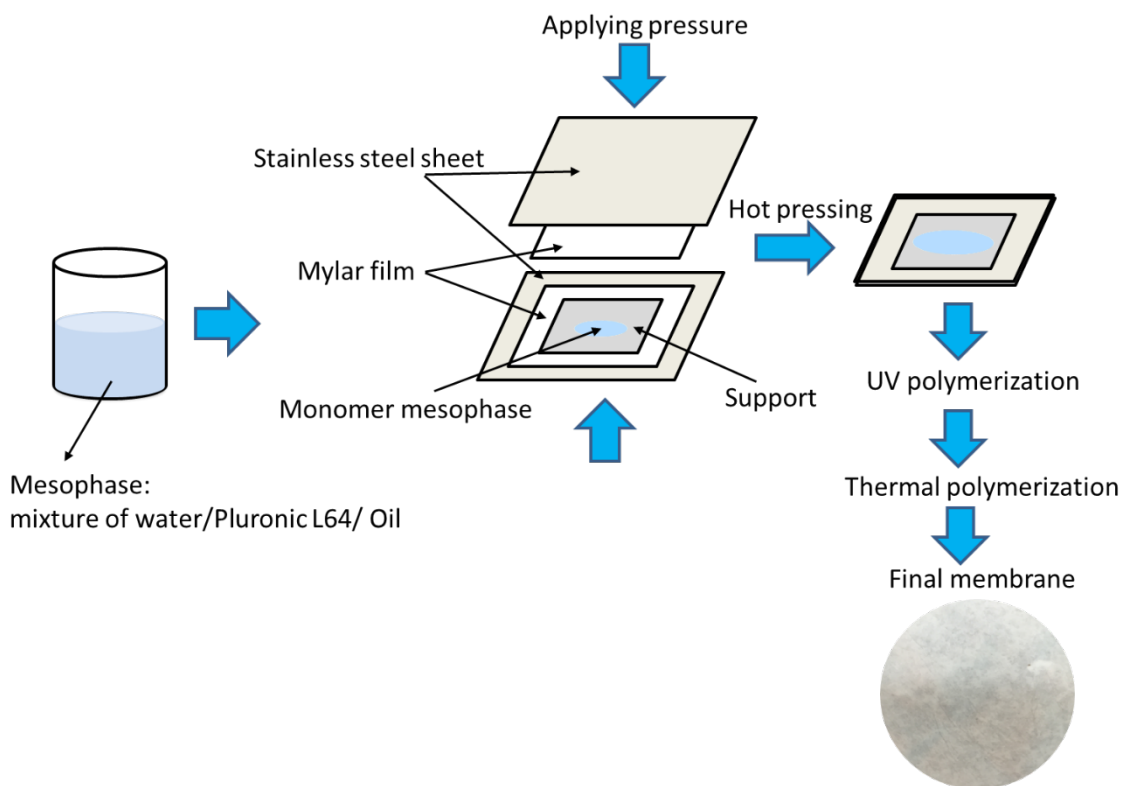


Figure 8. Processing mesophase to make membrane

2.4. Characterization techniques

2.4.1. Polarized light microscopy (PLM)

Olympus microscope (model BX60) with cross-polarized feature was used to characterize the liquid crystalline structure of mesophases before and after the polymerization. A small amount (less than 2 ml) of each mesophase sample (before polymerization) was placed on a glass slide and was covered with cover slip. The cross-polarized images of samples were recorded using a camera

attached to the microscope. In order to characterize samples after polymerization, each mesophase was polymerized on the glass slide using UV initiation system for 3 hours. Obtained samples were covered by a cover slip and studied by cross-polarized light microscopy.

Cross-polarized light microscopy is basically utilized to distinguish between singly refracting (optically isotropic) and doubly refracting (optically anisotropic) media. Anisotropic substances, such as uniaxial or biaxial crystals, oriented polymers, or liquid crystals, generate interference effects in the polarized light microscope, which result in differences of color and intensity in the image as seen through the eyepieces and captured on digital image. This technique is useful for orientation studies of doubly refracting media that are aligned in a crystalline lattice or oriented through long-chain molecular interactions in natural and synthetic polymers.⁴⁴

Lamellar mesophases exhibit distinct optical texture, when confined in thin slabs between crossed polarizers. Typically, the texture is 'streaky' or mosaic-like (to quote the late Krister Fontell⁴⁵), which resembles the marbling in freshly cut steak. Bicontinuous cubic liquid crystals exhibit symmetry and do not display optical texture. Hexagonal mesophases are often identified by a characteristic 'fan' texture in the optical microscope, due to focal conic domains of columns.⁴⁵

2.4.2. Small angle X-ray scattering

Since the pore size of mesoporous materials are in the nanometer range, their structure cannot be seen through current electron microscopes available at New

Mexico State University. In addition, microscopic images are very local and may not reveal the overall structure of prepared mesophase and mesoporous material. Therefore, small angle X-ray scattering (SAXS) measurements, as also frequently used in literature,⁴⁰ were performed in this work. SAXS is an analytical method to determine the structure of mesophase systems in terms of averaged size or shape. In this method, X-rays are sent through the samples and will be scattered as they hit particles that happen to be inside the beam. Thus, the average structure of all illuminated particles in the bulk material is measured. Different structures with long-range order have different SAXS patterns, and thus, can be characterized by this technique.

Figure 9 shows a typical SAXS pattern. q is the scattering vector and its dimension is reciprocal length. Q can be calculated based on the following formula:

$$q = \frac{4\pi}{\lambda} \sin(\theta)$$

where λ and θ are X-ray wavelength and scattering angle, respectively. Distance between the aligned structures can be calculated based on Bragg's law as follows:

$$d_{Bragg} = \frac{2\pi}{q_{peak}}$$

where d_{Bragg} and q_{peak} are distance between the structures and scattering vector at a specific peak, respectively.

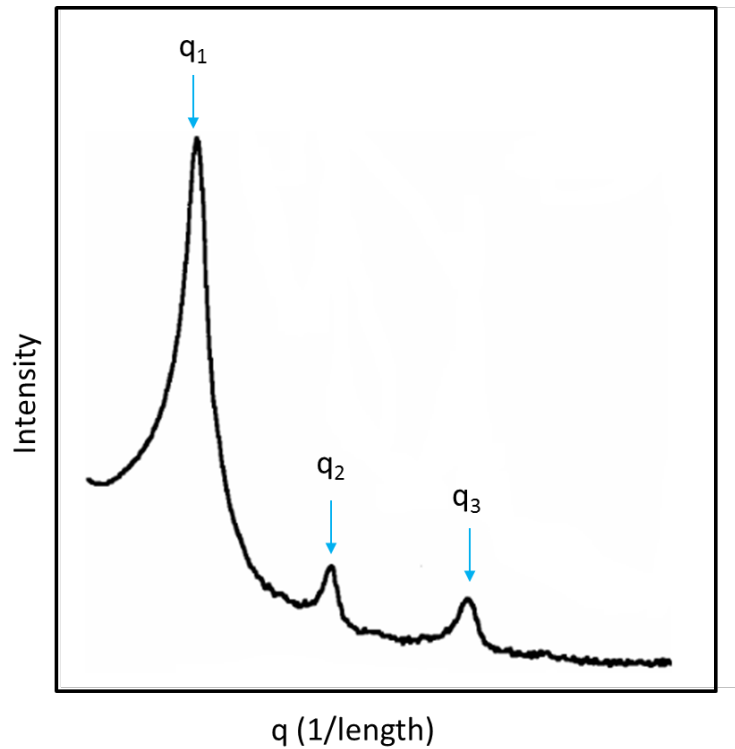


Figure 9. A typical SAXS pattern. q_1 is the principal peak and q_2/q_1 and q_3/q_1 ratios determine the type of crystal symmetry

The structure factor of a crystalline substance is normally called lattice factor. It is a set of peaks at well-defined angles indicative for the crystal symmetry. It can be shown that the ratios of the peak positions on the q -scale have typical values, which reveal the crystal symmetry, for example:

- Lamellar symmetry: 1, 2, 3, 4, 5, ...
- Cubic symmetry: 1, $\sqrt{2}$, $\sqrt{3}$, 2, $\sqrt{5}$, ...
- Hexagonal symmetry: 1, $\sqrt{3}$, 2, $\sqrt{7}$, 3, ...

The samples used for SAXS measurements were filled into a quartz capillary using centrifugation. The cuvette is stoppered using critoseal and epoxy glue. Mesophases were cured in the capillary tubes. SAXS spectra were obtained with a Bruker Nanostar system (located at Los Alamos National Lab) using a monochromated $\text{CuK}\alpha$ radiation source with wavelength of 1.54184 Å. The 2θ angle range of 0.1 to 4.7 was used for measurements.

2.4.3. Rheology

Rheological measurements were done using a discovery hybrid rheometer (DHR-3, TA Instruments). Figure 10 shows the device we used for rheometry. Mesophases are viscoelastic materials and rheometry can be used to measure their viscosity, shear modulus (G'), and loss modulus (G''). In this work, we show that each mesostructure has a rheological fingerprint, so they can be characterized by rheometry. All rheometry measurements were performed at 25 °C. A parallel plate geometry with 40 mm diameter and 1 mm gap was used for all tests. Amplitude sweep measurements were done using an angular frequency of 10 rad/s and over strain range of 0.01 to 1000%. Frequency sweep were performed using a strain amplitude of 1% and over a frequency range of $\omega = 0.01$ to 600 rad/s. Non-linear rheological measurements were performed using amplitude oscillation with sampling time of 10 cycles and conditioning time of 5 cycles.



Figure 10. DHR-3 device used for rheometry

2.4.4. Permeability

Permeability of membranes was measured using a home-made device (Figure 11). The membrane discs were assembled into a stainless steel dead-end filtration cell with an inner diameter of 25 mm and an effective filtration area of 1380 mm².

Darcy's law was used to calculate the permeability as follows:

$$\frac{\kappa}{l} = \frac{Q \mu}{A \Delta P}$$

where, Q , μ , A , ΔP , l , and κ are flow rate, viscosity, membrane area, pressure difference along the membrane, membrane thickness, and Darcy's constant (which features intrinsic permeability), respectively. The ratio of κ/l was considered as an indication of operational permeability in this work. In other words, since different membranes have different thicknesses which is also difficult to be accurately measured, the value of intrinsic permeability itself can be misleading in real application.



Figure 11. Home-made filtration set-up

3. Results and discussion

Different formulations were used for making membranes. In the first set of experiments CTAB, which is a small molecule surfactant, was used. CTAB is highly sensitive to temperature and crystallizes below 30 °C. Samples containing CTAB were polymerized with strict control on the temperature. Samples before polymerization showed liquid crystalline behavior. However, small crystals started to grow inside them upon cooling down to room temperature, which results in the segregation of CTAB molecules through crystallization. Table 1 shows some of the formulations that were prepared using CTAB as surfactant.

Despite the fact that CTAB surfactant can make ordered structures in mesophases, the formulations containing CTAB were excluded from membrane fabrication due to their susceptibility to crystallization at room temperature. Pluronic L64 was used mainly in membrane fabrication as surfactant since it forms stable mesophases as it will be shown later.

First, redox initiation system was used for polymerization. Benzoyl peroxide and 4,N,N-trimethyl aniline are a hydrophobic redox pair and were used to polymerize butyl acrylate. Using this system, polymerization takes place at room temperature after about 10 minutes. For making samples, half of the ingredients were mixed with benzoyl peroxide and 4,N,N-trimethyl aniline was added to the other half. These two halves were mixed together just before applying the mesophase on the support for making membranes. The main drawback of redox system is that we could not control the rate of polymerization efficiently and membrane fabrication was not successful.

Table 1. A summary of formulations that were prepared using CTAB

Oil/water/CTAB composition	Oil phase formulation
30 wt%/40 wt%/30 wt%	UV initiator 7.5 wt.% of monomer Cross-linker 33 wt.% of monomer
10 wt%/70 wt%/20 wt%	Redox initiator 7.5 wt.% of monomer Cross-linker 33 wt.% of monomer
10 wt%/60 wt%/30 wt%	Redox initiator 7.5 wt.% of monomer Cross-linker 33 wt.% of monomer
10 wt%/50 wt%/40 wt%	Redox initiator 7.5 wt.% of monomer Cross-linker 33 wt.% of monomer
10 wt%/40 wt%/50 wt%	Redox initiator 7.5 wt.% of monomer Cross-linker 33 wt.% of monomer
20 wt%/60 wt%/20 wt%	Redox initiator 7.5 wt.% of monomer Cross-linker 33 wt.% of monomer
20 wt%/50 wt%/30 wt%	Redox initiator 7.5 wt.% of monomer Cross-linker 33 wt.% of monomer
20 wt%/40 wt%/40 wt%	Redox initiator 7.5 wt.% of monomer Cross-linker 33 wt.% of monomer
20 wt%/30 wt%/50 wt%	Redox initiator 7.5 wt.% of monomer Cross-linker 33 wt.% of monomer

UV initiator was used instead of redox system in the next set of experiments. The ratios of cross-linker and initiator were kept constant at 33 wt.% of monomer and 5 wt.% of monomer, respectively. UV rays diffusion inside the media is limited, and therefore, UV initiator by itself could not completely polymerize the membranes. Additionally, final membranes did not have enough integrity due to low degree of cross-linking. Therefore, in final series of experiments, the ratio of cross-linker to monomer was increased.

Table 2. A summary of oil phase formulations used to prepare water/oil/Pluronic L64 mesophases

Oil phase formulation	Comment
Redox initiator 5 wt% of monomer Cross-linker 33 wt% of monomer	Controlling the rate of polymerization is challenging. Samples were polymerized before processing into membrane.
UV initiator 5 wt% of monomer Cross-linker 33 wt% of monomer	UV diffusion length is not enough to completely polymerize the samples. Final membrane does not have enough integrity due to low cross-linking.
UV initiator 5 wt% of monomer Thermal initiator 5 wt% of monomer Cross-linker 70 wt% of monomer	Final membranes look homogenous with enough integrity. This is the optimum formulation.

Thermal and UV initiation systems were used in the last set of experiments in conjunction with each other to ensure that mesophases would completely polymerize. The ratios of cross-linker and initiators were kept constant at 70 wt.% of monomer and 5 wt.% of monomer, respectively. Membranes produced by such formulation have good integrity and were used as optimum samples for testing permeability and rejection. Table 2 shows a summary of different oil phase formulations that were used in this project. It should be noted that the produced formulations of mesophases had different fractions of oil phase, water, and Pluronic L64.

3.1. Polarized light microscopy

Figure 12 and Figure 13 show the cross-polarized micrographs obtained for mesophase prepared from CTAB and Pluronic L64 before curing, respectively. All points in Figure 11 show hexagonal textures. However, the sample with 40% CTAB goes rapidly through crystallization of CTAB, and has a different cross-polarized micrograph. As seen in the cross-polarized micrographs of Pluronic L64 mesophases shown in Figure 13, A, B, and C compositions show an oily streak texture that is the characteristic of lamellar mesophases.⁴⁵ Points D and E show focal fan texture that is the characteristic of hexagonally packed mesophases.⁴⁵ Composition F does not have any textures under PLM that could be a characteristic of gyroid type mesophase.⁴⁵

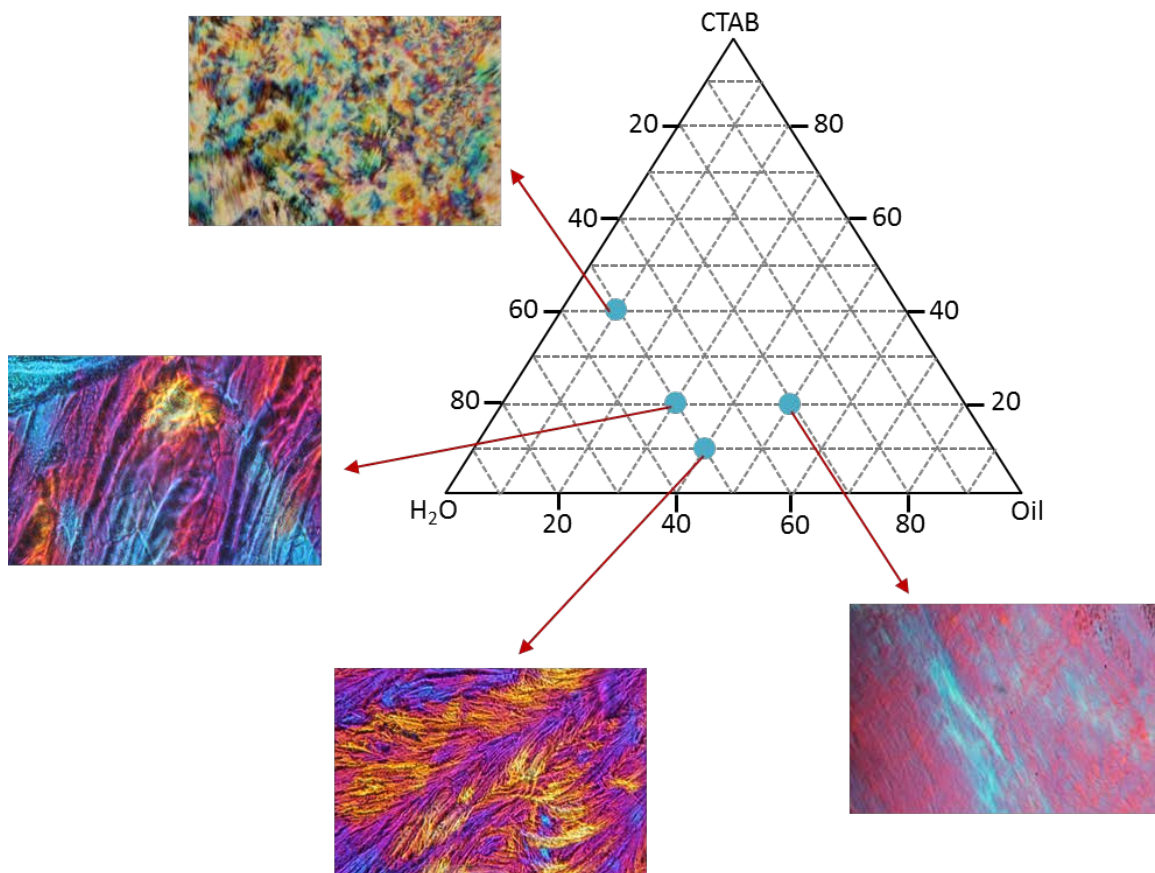


Figure 12. Cross-polarized light micrographs obtained for mesophases with different compositions containing CTAB before curing

Cross-polarized light micrographs of selected mesophases as in Figure 13 after curing are shown in Figure 14. The results show that all mesophases (except gyroid, since it may lose its structure to another non-liquid crystalline mesophase) can preserve their structure under curing. These results are promising for making membranes from mesophases since the structure does not

change during polymerization and we can expect to have a mesoporous material at the end.

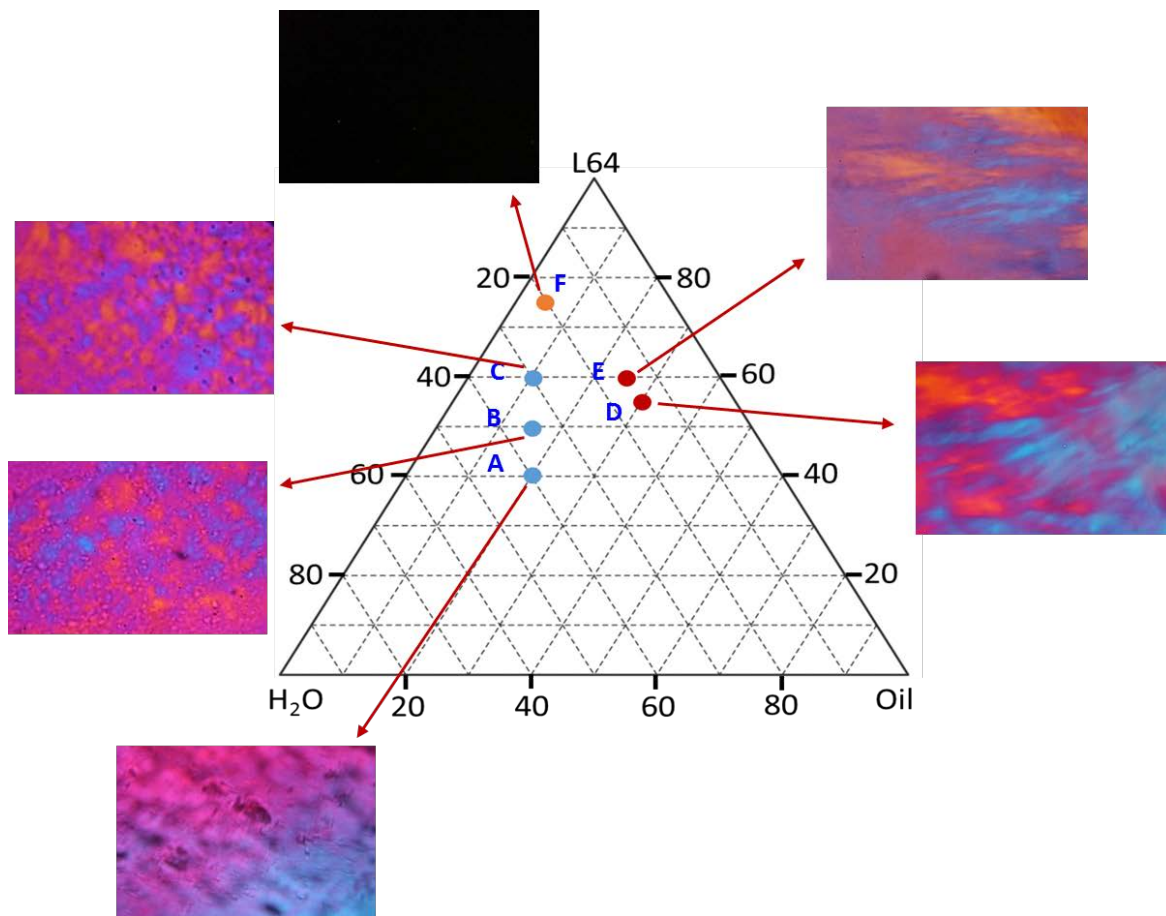


Figure 13. Cross-polarized light micrographs obtained for mesophases with different compositions containing Pluronic L64 before curing

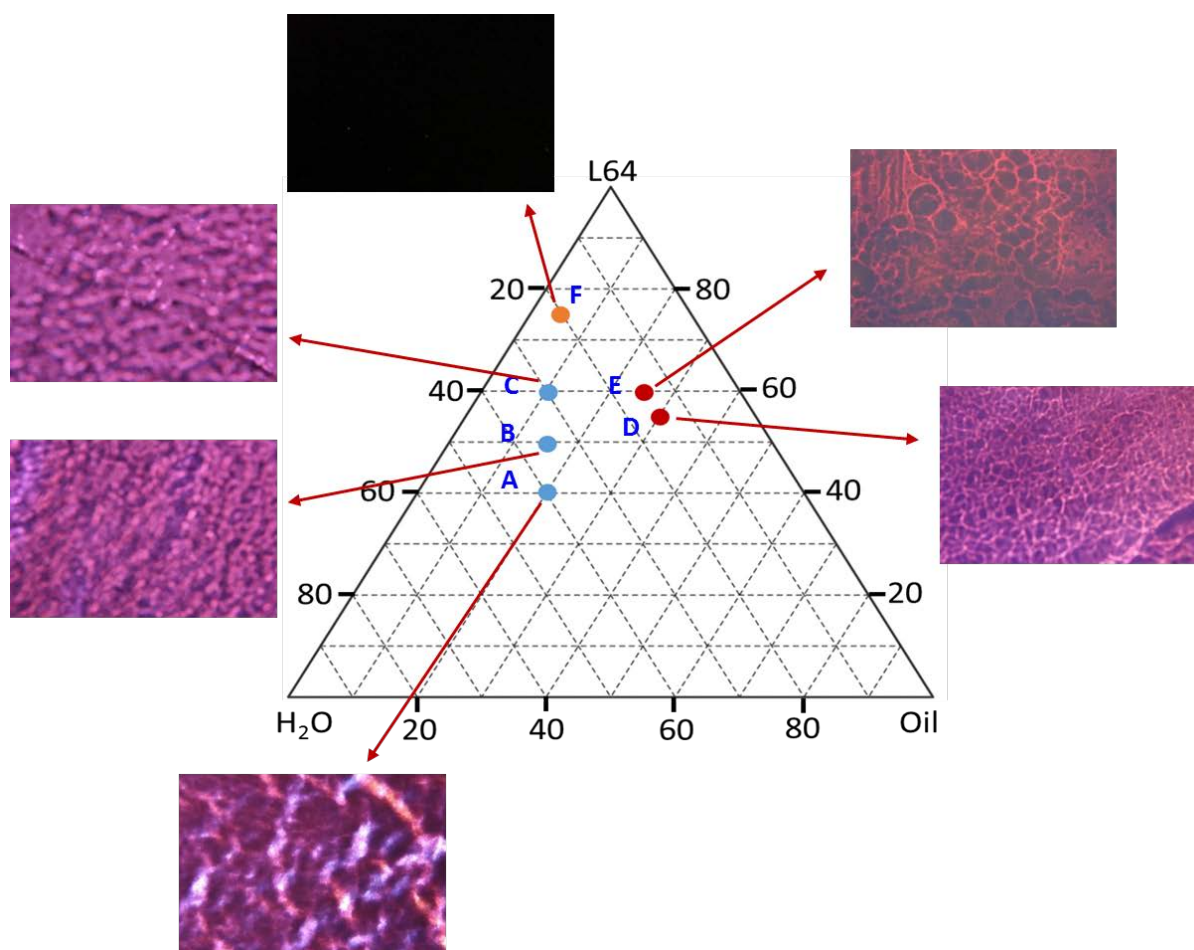


Figure 14. Cross-polarized light micrographs obtained for mesophase with different compositions containing Pluronic L64 after polymerization

3.2. SAXS results

SAXS studies can confirm the data obtained from PLM method. Figure 15 shows the SAXS data obtained for A, B, and C compositions. All patterns resemble the lamellar structure of mesophases. Inset images show the 2D SAXS spectrum with concentric rings which is the characteristics of lamellar mesophases.

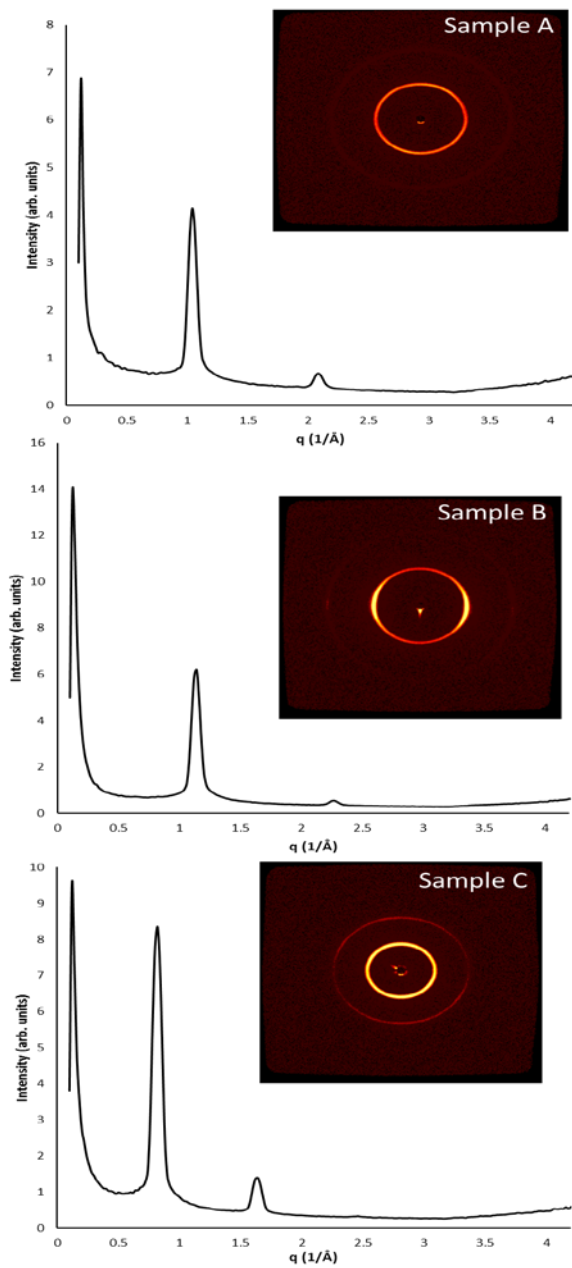


Figure 15. SAXS spectrum obtained from samples A, B, and C with lamellar pattern. Insets show 2D SAXS images

Figure 16 shows the SAXS data obtained for D and E compositions. Both patterns resemble the hexagonal structure of mesophases. Inset images show the 2D SAXS spectrum with one ring, which is the characteristic of hexagonally packed mesophases.

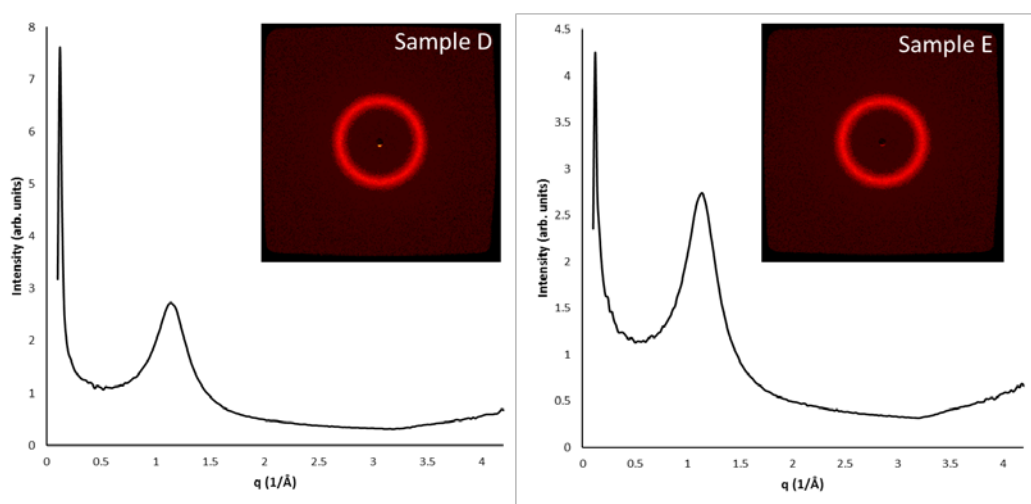


Figure 16. SAXS spectrum obtained from samples D and E with hexagonal pattern. Insets show 2D SAXS images

One important point for making membrane is that mesophases keep their structure during polymerization. Additionally, since thermal initiation is used beside photo initiation, we need to make sure mesophases preserve their structure during heating.

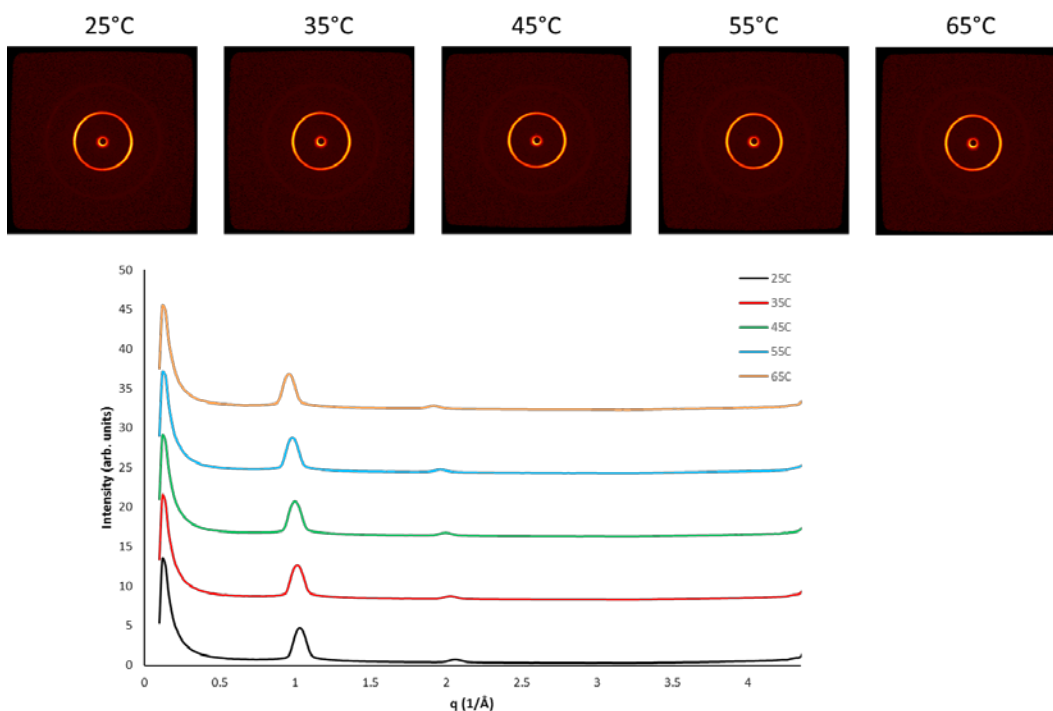


Figure 17. SAXS spectra of sample A at different temperatures

Figure 17 shows the SAXS spectra of sample A at different temperatures. It can be seen that the structure remains intact up to 65°C which proves that using thermal initiation is safe for polymerization of mesophases. Therefore, the scale-up of such membrane fabrication process will be possible.

The produced samples have mesostructure in the range of 70 nm as calculated from Bragg's law.

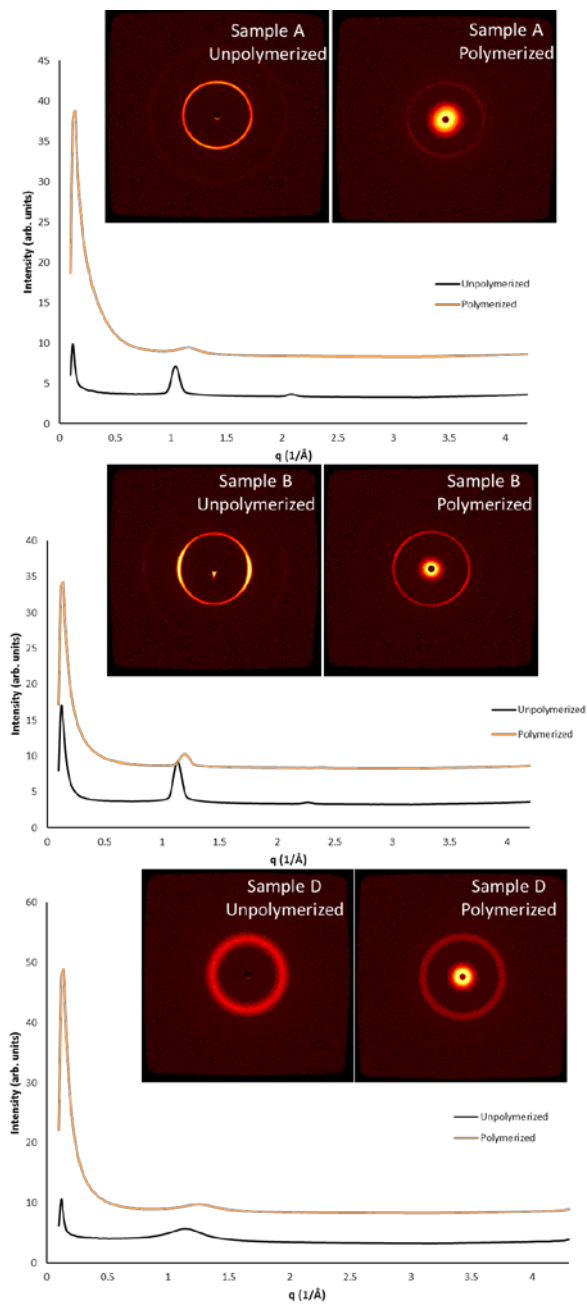


Figure 18. SAXS spectra of samples A, B, and D before and after polymerization

Figure 18 shows the SAXS spectra of samples A, B, and D after polymerization, respectively. As seen, the structure of mesophases remains intact during curing and the polymerized samples have a mesoporous structure at the end. Polymerization usually results in losing one order of crystallinity that is the case here. Additionally, the intensity of the peaks declines upon polymerization due to less ordering, and position of peaks may slightly shift as well.

3.3. Rheology results

All rheological measurements were performed on samples A and D that are located in lamellar and hexagonal regions, respectively. Figure 19 shows the variation of storage modulus, G' , and loss modulus, G'' , versus strain. Storage modulus shows the significance of elastic behavior in materials, while loss modulus is a result of energy dissipation. The viscosity can be calculated from storage and loss moduli as follows:

$$G^* = G' + iG''$$

$$|\eta^*| = \frac{\sqrt{G'^2 + G''^2}}{\omega}$$

where G^* , $|\eta^*|$, and ω are dynamic complex modulus, magnitude of complex viscosity, and angular frequency, respectively.

The results in Figure 19 show Type III non-linear behavior for both systems. Weak strain overshoot and a local maximum in G'' are two important characteristics of such behavior. Polymer solution systems, block copolymer solutions, and highly concentrated emulsion also show such behavior.⁴⁶ It can be

seen that hexagonal structure in sample D shows about one order of magnitude higher moduli compared to lamellar structure in sample A.

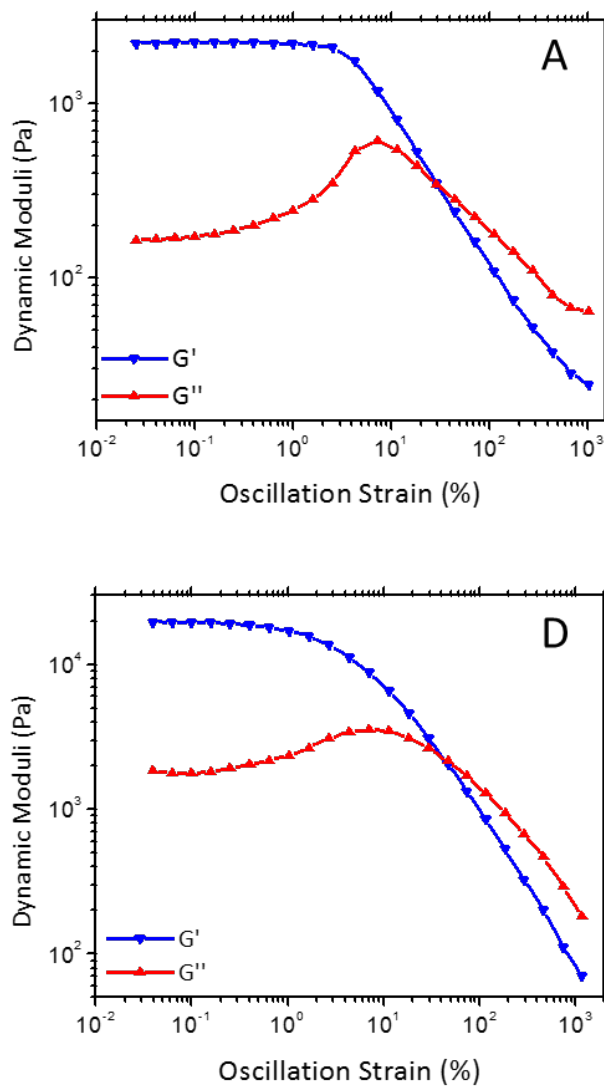


Figure 19. Storage modulus, G' , and loss modulus, G'' , versus strain obtained through oscillatory amplitude sweep experiments on samples A and D

Figure 20 shows the frequency sweep data of sample A and D obtained from small amplitude oscillatory shear experiments. Both samples show solid-like behavior since $G' > G''$. The storage and loss moduli of sample D are one order of magnitude higher than that of sample A. High complex viscosity in both samples shows that they cannot be processed by lab-scale doctor blade film applicator. Instead, we used hot press to make membranes in this work.

Although linear viscoelasticity is useful for understanding the relationship between the microstructure and the rheological properties of complex fluids, it is important to bear in mind that the linear viscoelasticity theory is only valid when the total deformation is quite small. However, in most processing operations the deformation is both large and rapid (therefore in the nonlinear region). Consequently, linear viscoelastic characterization is not sufficient to fully understand practical polymer processing undergoing nonlinear situations. Moreover, since linear viscoelastic experiments use small amplitude oscillatory shear (SAOS test), it has a limited resolution to distinguish complex fluids with similar micro- and nano-structure or molecular structures (e.g. linear or branched polymer topology). Complex fluids with similar linear viscoelastic properties may show different nonlinear viscoelastic properties. This means that even if rheological measurements are only being used for material characterization or quality control, the linear viscoelastic properties may often be insufficient. It can be anticipated that nonlinear viscoelastic characterization will provide much more insight for distinguishing such structural differences.

Thus, it is necessary to study the nonlinear viscoelastic responses of complex fluids in depth.

Figure 21 shows a schematic illustration of the strain sweep test at a fixed frequency. In the linear region, the storage (G') and loss (G'') moduli are independent of the applied strain amplitude at a fixed frequency and the resulting stress is a sinusoidal wave. However, in the nonlinear region, the storage and loss moduli become a function of the strain amplitude, $G'(\gamma_0)$ and $G''(\gamma_0)$, at a fixed frequency and the resulting stress waveforms are distorted from sinusoidal waves. While the SAOS is in the linear region, the application of large amplitude oscillatory shear (LAOS) results in a nonlinear material response.⁴⁷

Large amplitude oscillatory shear (LAOS) data, which represents non-linear viscoelastic behavior, are shown in Figure 22. Figure 22a and c represent oscillatory stress versus time and Figure 22b and d show closed-loop of stress versus strain plots (also known as Lissajous plots). Oscillatory stress plot of sample A shows backward tilted stress, while sample D shows saw tooth stress. Closed-loop plots of two samples are completely different, especially at high shear stresses, which may be considered as fingerprints for lamellar and hexagonal mesostructures. In other words, in addition to SAXS and PLM, rheological measurements can be used to distinguish different mesophases.

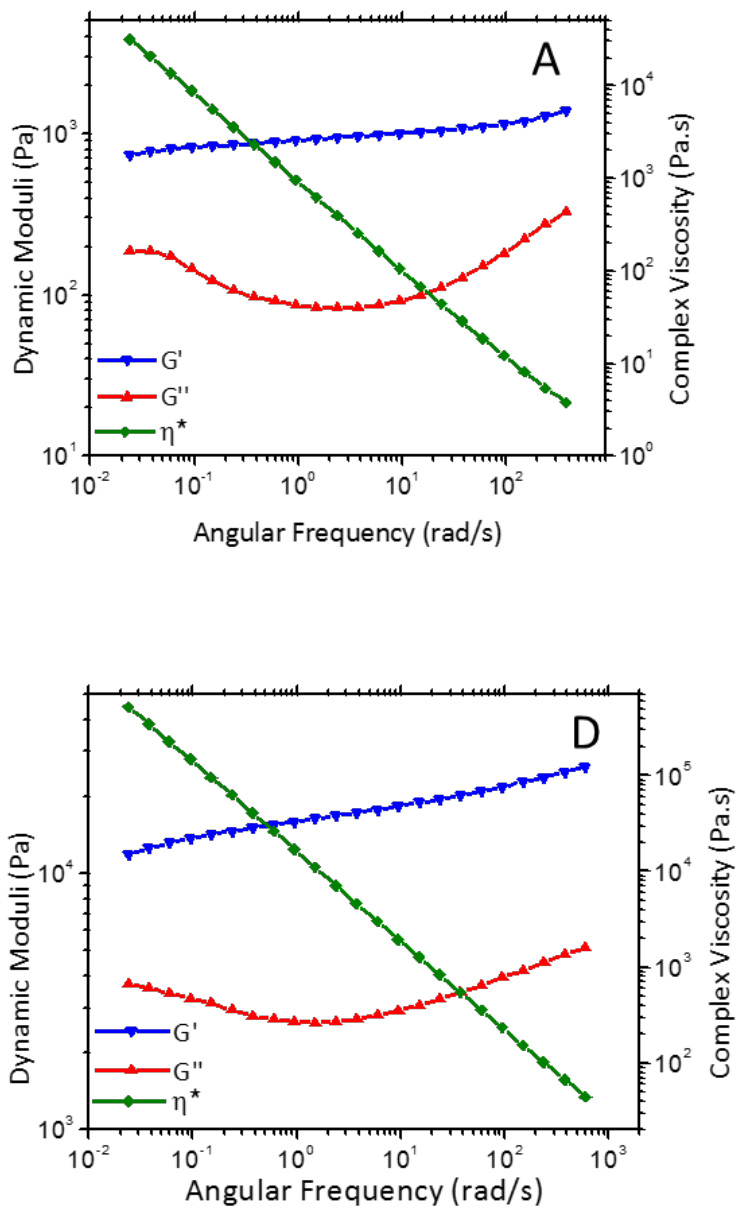


Figure 20. Storage modulus, G' , loss modulus, G'' , and complex viscosity, η^* , versus angular frequency of samples A and D obtained through frequency sweep in small oscillatory amplitude shear regime

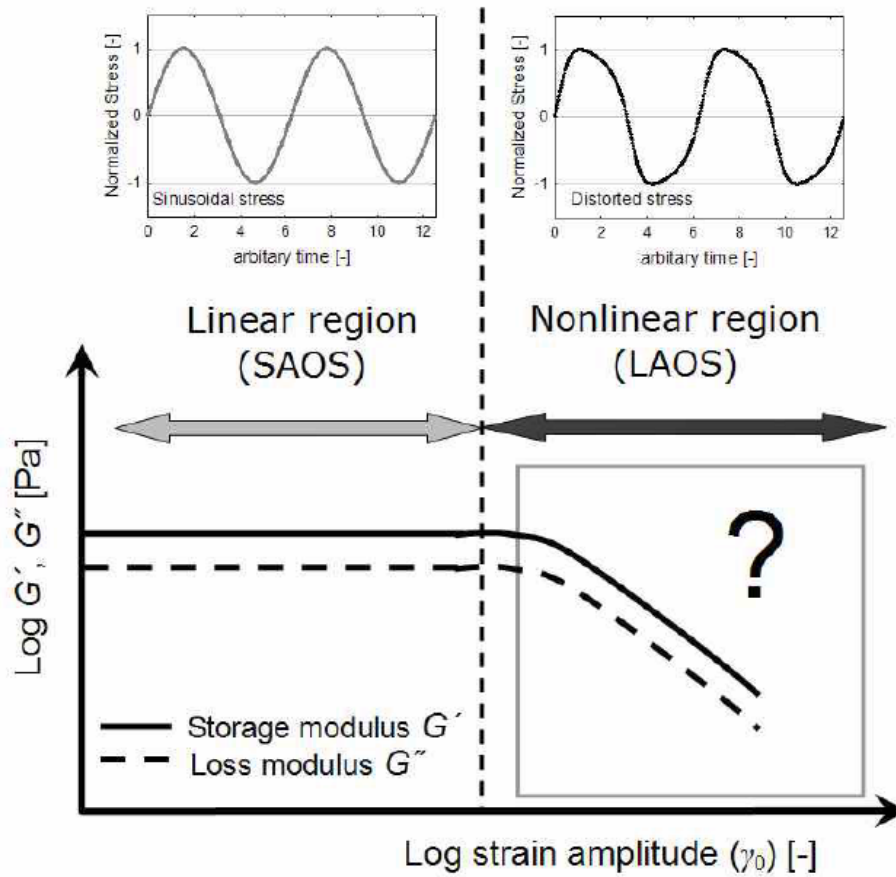


Figure 21. Schematic illustration of the strain sweep test at a fixed frequency⁴⁷

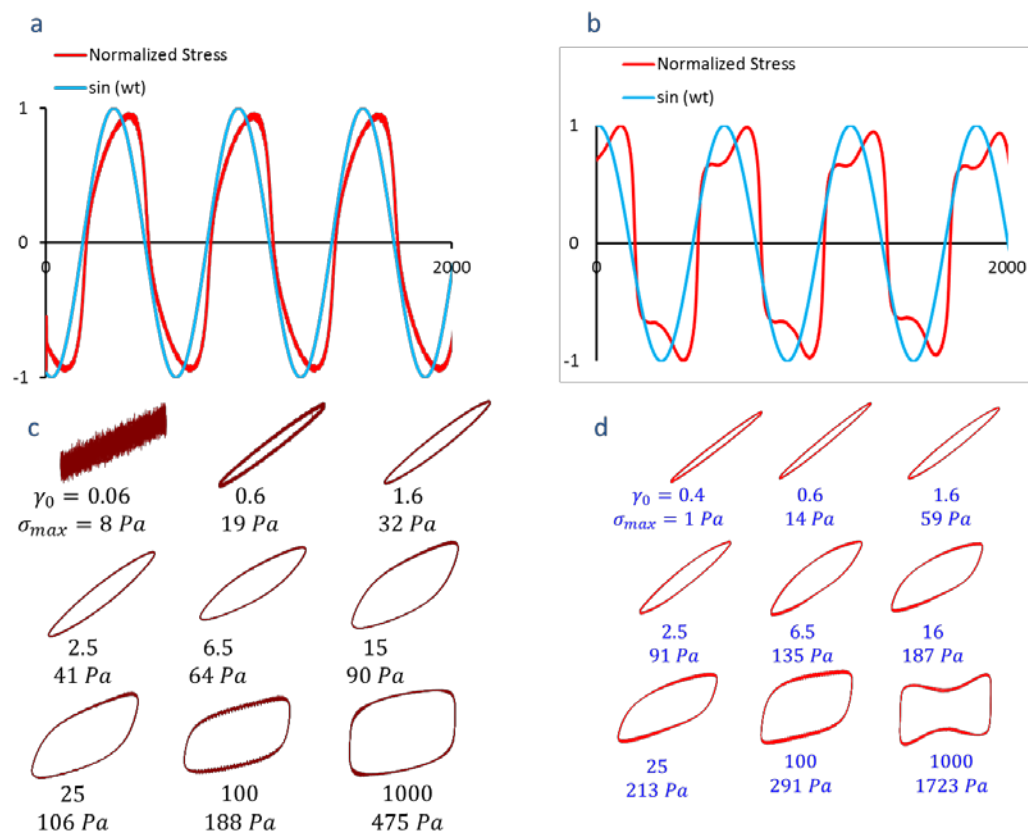


Figure 22. Oscillatory stress curves versus time (a ,b), and closed-loop plots of normalized stress versus normalized strain (c,d) obtained from amplitude oscillation in large amplitude oscillatory shear regime. a and c plots represent sample A and b and d plots represent sample D

3.4. Permeability results

Table 3 shows the obtained permeability results performed by the home-made filtration unit. Membranes A and D have two different mesostructures. As characterized by different techniques, membrane 1 composition (sample A) lies in lamellar region, while membrane 2 composition (sample D) lies in hexagonal region. As Table 3 shows, membrane 1 and 2 have higher permeability compared

to commercial membrane (GE, MW series, MW2540F30) that indicates better performance of fabricated membranes. It should be noted that the mesophase templated membranes were cast on the support layer recovered from GE MW2540F30 membrane in order to cancel the effect of support on the obtained results.

Table 3. Permeability results for membranes

	Commercial membrane (GE, MW2540F30)	Support	Membrane A	Membrane D
Q (ml/s)	1	33.33	47.619	35.088
μ (mPa.s)	1.002	1.002	1.002	1.002
A (mm ²)	1380	1380	1380	1380
ΔP (kPa)	1099	32.05	749	989
l (mm)	0.21	0.11	0.14	0.14
κ/l (ml/mm ²)	6.61×10^{-13}	7.55×10^{-10}	4.62×10^{-11}	2.58×10^{-11}

3.5. Rejection Results

2 g/L talc in water was used as feed solution. Talc concentration in the feed and permeate was measured and solute particle rejection (r) was calculated based on the following equation:

$$r = 1 - \frac{C_p}{C_f} \times 100\%$$

where, C_p and C_f are the concentrations of permeate and feed, respectively. Talc rejection of membranes A and D were measured to be about 99.9% that shows excellent rejection performance of the membranes for suspended particles. Figure 23 shows membrane A before and after rejection test. As seen, a cake layer of talc has formed on the surface of membrane. It should be noted that after 90 min of filtering 2g/L talc suspension, the permeate flow rate reaches zero due to the formation of cake in dead-end configuration of setup.

Rejection performance was also tested for an oil-in-water emulsion (with ~2.4 wt.% oil and prepared as described in the Experimental section) as feed. Oil concentration in permeate and feed streams were measured through centrifugation. The rejection of membrane for the emulsion sample was calculated to be about 65%. The lower rejection here compared to talc suspension can be attributed to the dead-end configuration of set-up, which results in significant increase in filtration pressure and forcing the liquid oil droplets to pass through pores of membrane. It is expected to have a much higher rejection in the cross-flow configuration, where oil droplet will not be pushed through pore of membrane.

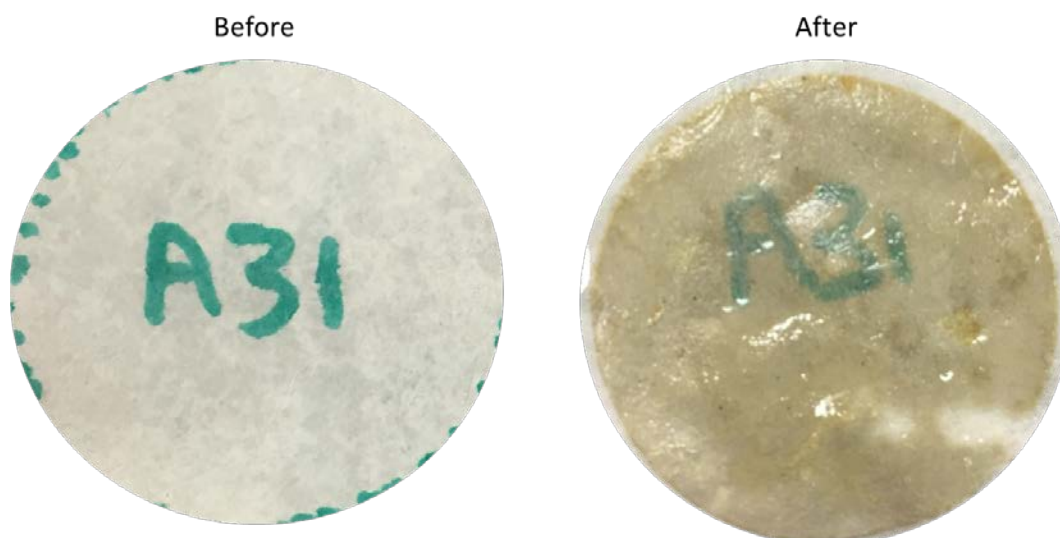


Figure 23. membrane surface appearance before and after rejection test with 2 wt.% talc suspension. A cake layer of talc was formed on the membrane surface after the test.

4. Conclusion

Surfactant self-assembly in the presence of water/oil was used as a template for making UF membranes. Different formulations were tried for oil phase and the optimum cross-linker (ethylene glycol dimethacrylate) and initiator were obtained at 70 wt.% of monomer (butyl acrylate) and 5 wt.% of monomer, respectively. UV (1-hydroxycyclohexyl phenyl ketone) and thermal (AIBN) initiators were used in conjunction for polymerizing mesophases. Cross-polarized light microscopy, SAXS, and rheology were used for characterizing samples. Membranes were cast on a support recovered from a commercially available UF membrane (GE, MW series, MW2540F30). The produced membranes have mesopores in the range of 70 nm according to SAXS measurements. The

permeability and rejection performance of membranes were evaluated by using a home-made dead-end setup. The results indicate that fabricated membranes have higher permeability compared to commercial UF membranes. In addition, 2 g/L talc suspension and 2.4 wt.% oil-in-water emulsion were used to test the rejection performance of the membranes in the dead-end setup. Rejection was calculated to be about 99.9% and 65% for talc suspension and oil-in-water emulsion, respectively. These results confirm that mesophase templated polymers have the potential to be used as ultrafiltration membranes and can be further developed for such applications.

5. Future work

Proposed templating approach is viable for any type of monomer. More hydrophilic monomers could be used in future to improve the permeability of the membranes. Besides, using both hydrophobic and hydrophilic monomers is proposed. Hydrophilic monomers would be added to aqueous phase and guarantee the high permeability, while hydrophobic monomers strengthen the membrane and make it insoluble in water. Rejection performance of the membranes may be done using other feed streams for example proteins and viruses.

References

- (1) <http://www.un.org/waterforlifedecade/scarcity.shtml>
<http://www.un.org/waterforlifedecade/scarcity.shtml>.

- (2) Baker, R. W. *Membrane Technology and Applications*; 2nd editio.; John Wiley & Sons, Ltd.: Chichester, UK, 2004.
- (3) Loeb, G. S.; Sourirajan, S. Sea Water Demineralization by Means of an Osmotic Membrane. *Adv. Chem. Ser* **1968**, *38*, 117.
- (4) Guillen, G. R.; Pan, Y.; Li, M.; Hoek, E. M. V. Preparation and Characterization of Membranes Formed by Nonsolvent Induced Phase Separation: A Review. *Ind. Eng. Chem. Res.* **2011**, *50*, 3798–3817.
- (5) Tsai, H. Effect of Surfactant Addition on the Morphology and Pervaporation Performance of Asymmetric Polysulfone Membranes. *J. Memb. Sci.* **2000**, *176*, 97–103.
- (6) Chakrabarty, B.; Ghoshal, A. K.; Purkait, M. K. Preparation, Characterization and Performance Studies of Polysulfone Membranes Using PVP as an Additive. *J. Memb. Sci.* **2008**, *315*, 36–47.
- (7) Barth, C.; Gonçalves, M. C.; Pires, A. T. N.; Roeder, J.; Wolf, B. A. Asymmetric Polysulfone and Polyethersulfone Membranes: Effects of Thermodynamic Conditions during Formation on Their Performance. *J. Memb. Sci.* **2000**, *169*, 287–299.
- (8) IUPAC Manual of Symbols and Terminology. *Pure Appl. Chem* **1972**, *31*, 578.
- (9) Feng, P.; Bu, X.; Pine, D. J. Control of Pore Sizes in Mesoporous Silica Templated by Liquid Crystals in Block Copolymer–Cosurfactant–Water Systems. *Langmuir* **2000**, *16*, 5304–5310.
- (10) Li, W.; Zhao, D. An Overview of the Synthesis of Ordered Mesoporous Materials. *Chem. Commun. (Camb)*. **2013**, *49*, 943–946.
- (11) Tolbert, S. H. Magnetic Field Alignment of Ordered Silicate-Surfactant Composites and Mesoporous Silica. *Science (80-.)*. **1997**, *278*, 264–268.
- (12) Gin, D. L.; Gu, W. Nanoporous Catalytic Materials with Organic Frameworks. *Adv. Mater.* **2001**, *13*, 1407–1410.

- (13) Lester, C. L.; Colson, C. D.; Guymon, C. A. Photopolymerization Kinetics and Structure Development of Templated Lyotropic Liquid Crystalline Systems. *Macromolecules* **2001**, *34*, 4430–4438.
- (14) Gin, D. L.; Gu, W.; Pindzola, B. A.; Zhou, W.-J. Polymerized Lyotropic Liquid Crystal Assemblies for Materials Applications. *Acc. Chem. Res.* **2001**, *34*, 973–980.
- (15) Mann, S.; Burkett, S. L.; Davis, S. A.; Fowler, C. E.; Mendelson, N. H.; Sims, S. D.; Walsh, D.; Whilton, N. T. Sol–Gel Synthesis of Organized Matter. *Chem. Mater.* **1997**, *9*, 2300–2310.
- (16) Hentze, H.-P.; Kaler, E. W. Polymerization of and within Self-Organized Media. *Curr. Opin. Colloid Interface Sci.* **2003**, *8*, 164–178.
- (17) Hentze, H.-P.; Kaler, E. W. Morphosynthesis of Nanostructured Polymer Gels by Polymerization within Reverse Hexagonal Mesophases. *Chem. Mater.* **2003**, *15*, 708–713.
- (18) Tiddy, G. Surfactant-Water Liquid Crystal Phases. *Phys. Rep.* **1980**, *57*, 1–46.
- (19) Antonietti, M.; Caruso, R. A.; Göltner, C. G.; Weissenberger, M. C. Morphology Variation of Porous Polymer Gels by Polymerization in Lyotropic Surfactant Phases. *Macromolecules* **1999**, *32*, 1383–1389.
- (20) McGrath, K. M.; Drummond, C. J. Polymerisation of Liquid Crystalline Phases in Binary Surfactant/water Systems. *Colloid Polym. Sci.* **1996**, *274*, 316–333.
- (21) McGrath, K. M. Polymerisation of Liquid Crystalline Phases in Binary Surfactant/water Systems. *Colloid Polym. Sci.* **1996**, *274*, 499–512.
- (22) McGrath, K. M.; Drummond, C. J. Polymerisation of Liquid Crystalline Phases in Binary Surfactant/water Systems. *Colloid Polym. Sci.* **1996**, *274*, 612–621.
- (23) Srisiri, W.; Sisson, T. M.; O'Brien, D. F.; McGrath, K. M.; Han, Y.; Gruner, S. M. Polymerization of the Inverted Hexagonal Phase. *J. Am. Chem. Soc.* **1997**, *119*, 4866–4873.

- (24) Guymon, C. A.; Bowman, C. N. Kinetic Analysis of Polymerization Rate Acceleration During the Formation of Polymer/Smectic Liquid Crystal Composites. *Macromolecules* **1997**, *30*, 5271–5278.
- (25) H. T. Davis, J. F. Bodet, L. E. Scriven, W. G. M. *Microemulsions and Their Precursors*; Meunier, J.; Langevin, D.; Boccara, N., Eds.; Springer Proceedings in Physics; Springer Berlin Heidelberg: Berlin, Heidelberg, 1987; Vol. 21.
- (26) Liu, J.; Kim, A. Y.; Wang, L. Q.; Palmer, B. J.; Chen, Y. L.; Bruinsma, P.; Bunker, B. C.; Exarhos, G. J.; Graff, G. L.; Rieke, P. C.; *et al.* Self-Assembly in the Synthesis of Ceramic Materials and Composites. *Adv. Colloid Interface Sci.* **1996**, *69*, 131–180.
- (27) Letchford, K.; Burt, H. A Review of the Formation and Classification of Amphiphilic Block Copolymer Nanoparticulate Structures: Micelles, Nanospheres, Nanocapsules and Polymersomes. *Eur. J. Pharm. Biopharm.* **2007**, *65*, 259–269.
- (28) Liu, S.; Armes, S. P. Recent Advances in the Synthesis of Polymeric Surfactants. *Curr. Opin. Colloid Interface Sci.* **2001**, *6*, 249–256.
- (29) Fenyves, R.; Schmutz, M.; Horner, I. J.; Bright, F. V; Rzayev, J. Aqueous Self-Assembly of Giant Bottlebrush Block Copolymer Surfactants as Shape-Tunable Building Blocks. *J. Am. Chem. Soc.* **2014**, *136*, 7762–7770.
- (30) Khandpur, A. K.; Foerster, S.; Bates, F. S.; Hamley, I. W.; Ryan, A. J.; Bras, W.; Almdal, K.; Mortensen, K. Polyisoprene-Polystyrene Diblock Copolymer Phase Diagram near the Order-Disorder Transition. *Macromolecules* **1995**, *28*, 8796–8806.
- (31) Lohse, D. J.; Hadjichristidis, N. Microphase Separation in Block Copolymers. *Curr. Opin. Colloid Interface Sci.* **1997**, *2*, 171–176.
- (32) Alexandridis, P.; Alan Hatton, T. Poly(ethylene Oxide) poly(propylene Oxide) poly(ethylene Oxide) Block Copolymers and at Interfaces: Thermodynamics, Structure, Dynamics, and Modeling. *Colloids Surfaces A Physicochem. Eng. Asp.* **1995**, *96*, 1–46.
- (33) Hentze, H.-P.; Krämer, E.; Berton, B.; Förster, S.; Antonietti, M.; Dreja, M. Lyotropic Mesophases of Poly(ethylene Oxide)- B -Poly(butadiene) Diblock

Copolymers and Their Cross-Linking To Generate Ordered Gels. *Macromolecules* **1999**, *32*, 5803–5809.

- (34) Alexandridis, P.; Lindman, B. *Amphiphilic Block Copolymers: Self-Assembly and Application*; Elsevier, 2000.
- (35) Bates, F. S. Polymer-Polymer Phase Behavior. *Science* **1991**, *251*, 898–905.
- (36) Alexandridis, P. Amphiphilic Copolymers and Their Applications. *Curr. Opin. Colloid Interface Sci.* **1996**, *1*, 490–501.
- (37) Mortensen, K.; Brown, W.; Nordén, B. Inverse Melting Transition and Evidence of Three-Dimensional Cubatic Structure in a Block-Copolymer Micellar System. *Phys. Rev. Lett.* **1992**, *68*, 2340–2343.
- (38) Svensson, B.; Olsson, U.; Alexandridis, P. Self-Assembly of Block Copolymers in Selective Solvents: Influence of Relative Block Size on Phase Behavior. *Langmuir* **2000**, *16*, 6839–6846.
- (39) Alexandridis, P.; Olsson, U.; Lindman, B. Phase Behavior of Amphiphilic Block Copolymers in Water–Oil Mixtures: The Pluronic 25R4–Water–P-Xylene System. *J. Phys. Chem.* **1996**, *100*, 280–288.
- (40) Alexandridis, P.; Olsson, U.; Lindman, B. Self-Assembly of Amphiphilic Block Copolymers: The (EO)₁₃(PO)₃₀(EO)₁₃-Water-P-Xylene System. *Macromolecules* **1995**, *28*, 7700–7710.
- (41) Holmqvist, P.; Alexandridis, P.; Lindman, B. Phase Behavior and Structure of Ternary Amphiphilic Block Copolymer–Alkanol–Water Systems: Comparison of Poly(ethylene oxide)/Poly(propylene Oxide) to Poly(ethylene oxide)/Poly(tetrahydrofuran) Copolymers. *Langmuir* **1997**, *13*, 2471–2479.
- (42) Alexandridis, P.; Olsson, U.; Lindman, B. Structural Polymorphism of Amphiphilic Copolymers: Six Lyotropic Liquid Crystalline and Two Solution Phases in a Poly(oxybutylene)-B-poly(oxyethylene)–Water–Xylene System. *Langmuir* **1997**, *13*, 23–34.

- (43) Bilalov, A.; Olsson, U.; Lindman, B. Complexation between DNA and Surfactants and Lipids: Phase Behavior and Molecular Organization. *Soft Matter* **2012**, *8*, 11022.
- (44) <http://micro.magnet.fsu.edu/primer/techniques/polarized/configuration.html>
<http://micro.magnet.fsu.edu/primer/techniques/polarized/configuration.html>.
- (45) S., H. *Identification of Lyotropic Liquid Crystal Mesophases, Chap 1. In: Holmberg (ed) Handbook of Applied Surface and Colloid Chemistry*; Wiley, New York, 2001.
- (46) Foudazi, R.; Masalova, I.; Malkin, A. Y. The Rheology of Binary Mixtures of Highly Concentrated Emulsions: Effect of Droplet Size Ratio. *J. Rheol. (N. Y. N. Y.)*. **2012**, *56*, 1299.
- (47) Hyun, K.; Wilhelm, M.; Klein, C. O.; Cho, K. S.; Nam, J. G.; Ahn, K. H.; Lee, S. J.; Ewoldt, R. H.; McKinley, G. H. A Review of Nonlinear Oscillatory Shear Tests: Analysis and Application of Large Amplitude Oscillatory Shear (LAOS). *Prog. Polym. Sci.* **2011**, *36*, 1697–1753.

Primary Evaluation of Algae Biofuel Production from Concentrate Stream

RECLAMATION

Managing Water in the West

Desalination & Water Purification Research
and Development Program Report No. XXX *(Reclamation will assign a no.)*

Primary Evaluation of Algae Biofuel Production from Concentrate Stream



U.S. Department of the Interior
Bureau of Reclamation

December 2014

REPORT DOCUMENTATION PAGEForm Approved
OMB No. 0704-0188

The public reporting burden for this collection of information is estimated to average 1 hour per response, including the time for reviewing instructions, searching existing data sources, gathering and maintaining the data needed, and completing and reviewing the collection of information. Send comments regarding this burden estimate or any other aspect of this collection of information, including suggestions for reducing the burden, to Department of Defense, Washington Headquarters Services, Directorate for Information Operations and Reports (0704-0188), 1215 Jefferson Davis Highway, Suite 1204, Arlington, VA 22202-4302. Respondents should be aware that notwithstanding any other provision of law, no person shall be subject to any penalty for failing to comply with a collection of information if it does not display a currently valid OMB control number.

PLEASE DO NOT RETURN YOUR FORM TO THE ABOVE ADDRESS.

1. REPORT DATE (DD-MM-YYYY) (15-12-2014)	2. REPORT TYPE Proof of Concept Final Report	3. DATES COVERED (From - To) (01-01-2012)-(01-07-2014)
4. TITLE AND SUBTITLE Primary Evaluation of Algae Biofuel Production from Concentrate Stream	5a. CONTRACT NUMBER R10AC80283	
	5b. GRANT NUMBER	
	5c. PROGRAM ELEMENT NUMBER	
6. AUTHOR(S) Saeid Aghahosseini Shirazi, Jalal Rastegary, Abbas Ghassemi	5d. PROJECT NUMBER	
	5e. TASK NUMBER	
	5f. WORK UNIT NUMBER	
7. PERFORMING ORGANIZATION NAME(S) AND ADDRESS(ES)	8. PERFORMING ORGANIZATION REPORT NUMBER	
9. SPONSORING/MONITORING AGENCY NAME(S) AND ADDRESS(ES) IEE/WERC New Mexico State University PO Box 30001 Las Cruces, NM 88003	10. SPONSOR/MONITOR'S ACRONYM(S)	
	11. SPONSOR/MONITOR'S REPORT NUMBER(S)	
12. DISTRIBUTION/AVAILABILITY STATEMENT		
13. SUPPLEMENTARY NOTES		
14. ABSTRACT <p>Drinking water scarcity accentuates the need to find new water sources, such as saline and inland brackish, to provide enough clean water for a growing population. With proper consideration of factors affecting these new sources, such as the lower salinity of inland brackish water compared to seawater, the use of membrane methods to desalinate brackish water can be highly effective. Due to this efficacy, the use of electrodialysis reversal (EDR) and reverse osmosis (RO) technologies has significantly increased over the past two decades. However, environmental effects associated with concentrate disposal have restricted the expansion and practical deployment of desalination technologies for inland brackish water sources.</p> <p>Because water is essential to the production of energy, the looming global energy crisis and the over-reliance on fossil fuels have tied the concept of energy shortage to the production of safe water. Interestingly, microalgae cultivation in desalination concentrate waste may combat the twin water and energy crises by combining increased efficiency for the removal of pollutants from concentrate with the cultivation of algal biomass for biofuel feedstock production. Algae are also a perfect candidate for CO₂ sequestration and greenhouse gas reduction due to algae's ability to use CO₂ as their main carbon source. Other advantages of using microalgae are that they are a sustainable technology capable of growth in most habitats; they do not compete with food crops for resources; they have no NO_x emissions and a short growth cycle; and they are the most rapidly growing option for producing biofuel, fats, oils, sugars, and hydrocarbons, all while fixing carbon dioxide.</p> <p>Furthermore, some algae species naturally live and thrive in brackish water. To investigate the feasibility of using microalgae in pollutant removal and biomass production by growing algae in desalination concentrate, where the algae could use salts and other nutrients to grow, a full factorial experiment was conducted on the growth of two strains of marine algae in concentrate under 16 hours of illumination at 25 °C, and ion removal by algae was observed to characterize the role of algae in removing pollutants.</p>		
15. SUBJECT TERMS		

16. SECURITY CLASSIFICATION OF:			17. LIMITATION OF ABSTRACT	18. NUMBER OF PAGES	19a. NAME OF RESPONSIBLE PERSON
a. REPORT	b. ABSTRACT	a. THIS PAGE			19b. TELEPHONE NUMBER <i>(Include area code)</i>

Standard Form 298 (Rev. 8/98)
 Prescribed by ANSI Std. Z39.18

**Desalination & Water Purification Research
And Development Program Report No. XXX**

Primary Evaluation of Algae Biofuel Production from Concentrate Stream

Prepared for Reclamation Under Agreement No. R10AC80283

By

**Saeid Aghahosseini Shirazi, Jalal Rastegary, Abbas
Ghassemi**



**U.S. Department of the Interior
Bureau of Reclamation
Technical Service Center
Water and Environmental Services Division
Water Treatment Engineering Research Team
Denver, Colorado**

December 2014

MISSION STATEMENTS

The mission of the Department of the Interior is to protect and provide access to our Nation's natural and cultural heritage and honor our trust responsibilities to Indian tribes and our commitments to island communities.

The mission of the Bureau of Reclamation is to manage, develop, and protect water and related resources in an environmentally and economically sound manner in the interest of the American public.

Disclaimer

The views, analysis, recommendations, and conclusions in this report are those of the authors and do not represent official or unofficial policies or opinions of the United States Government, and the United States takes no position with regard to any findings, conclusions, or recommendations made. As such, mention of trade names or commercial products does not constitute their endorsement by the United States Government.

Acknowledgements

I would like to thank the sponsor of this research, Bureau of Reclamation, for their support under the contract R10AC80283.

Contents

	<i>Page</i>
Executive Summary	1
Chapter 1	2
Introduction.....	2
1.1 Background	2
1.2 Research objective.....	3
Conclusions and Recommendations	4
Conclusions	4
Recommendations	5
Chapter 2.....	6
Literature Review.....	6
2.1 Introduction	6
2.2 Renewable energy	6
2.3 Biofuel.....	7
2.4 What are algae?	8
2.5 Algae growth.....	10
2.6 Algal strain selection.....	12
2.7 Carbon dioxide fixation.....	13
2.8 Culture systems in commercial scale	13
2.9 Open ponds.....	14
2.10 Photobioreactors.....	14
2.10.1 Tubular photobioreactor	15
2.10.2 Fence-like solar collector.....	15
2.10.3 Helical tubular photobioreactor	15
2.11 Open raceway ponds vs. photobioreactors	15
2.12 Harvesting	16
2.13 Algal drying.....	17
2.14 Oil extraction.....	17
2.15 Energy conversion from microalgae	18
2.15.1 Biochemical conversion	18
2.15.1.1 Fermentation	18
2.15.1.2 Transesterification.....	18
2.15.2 Thermochemical conversion.....	18
2.15.2.1 Gasification	18
2.15.2.2 Pyrolysis.....	18
2.15.2.3 Liquefaction	18
2.15.2.4 Hydrogenation.....	19
2.16 Biodiesel from algae.....	19
2.17 Ethanol from algae	19
2.18 Methane from algae.....	20
2.19 Economics of biodiesel production	20
2.20 Water scarcity.....	20
2.21 Water desalination.....	21
2.22 Concentrate disposal problem	21

2.23 Objective of this research.....	23
Chapter 3.....	24
Experimental Studies.....	24
3.1 Introduction.....	24
3.2 Strains of algae.....	24
3.3 Culture and medium.....	25
3.3.1 Concentrate medium.....	25
3.3.2 f/2 medium.....	25
3.3.3 50:50 combination of f/2 and concentrate medium.....	25
3.3.4 Deionized medium.....	25
3.4 Photobioreactor set up.....	25
3.5 Design of experiment.....	25
3.5.1 Experimental Apparatus.....	26
3.5.2 Test procedure.....	26
3.6 Analytical method.....	27
3.6.1 Algae growth.....	27
3.6.1.1 Dry biomass weight analysis.....	27
3.6.1.2 Optical density.....	28
3.6.2 Ion removal.....	28
3.6.2.1 Salinity (TDS and EC).....	28
3.6.2.2 Total Nitrogen analysis.....	28
3.6.2.3 Ion content analysis.....	28
Chapter 4.....	29
Results and Discussion.....	29
4.1 Introduction.....	29
4.2 Experiment 1.....	29
4.2.1 Algae growth.....	29
4.2.2 Ion removal.....	31
4.3 Experiment 2.....	32
4.3.1 Algae growth.....	32
4.3.2 Ion removal.....	32
4.4 Growth comparison.....	33
4.5 Ion removal comparison.....	34
Chapter 5.....	36
Conclusion.....	36
5.1 Conclusion.....	36
5.2 Recommendations.....	37
References.....	38
Tables.....	51
Chapter 2.....	51
Chapter 3.....	54
Chapter 4.....	55
Figures.....	60
Chapter 2.....	60
Chapter 3.....	63
Chapter 4.....	64

Chapter 5	72
Appendices.....	73
Appendix A	73
Units of Measure	73
Appendix B	74
Data Record	74

Executive Summary

Drinking water scarcity accentuates the need to find new water sources, such as saline and inland brackish, to provide enough clean water for a growing population. With proper consideration of factors affecting these new sources, such as the lower salinity of inland brackish water compared to seawater, the use of membrane methods to desalinate brackish water can be highly effective. Due to this efficacy, the use of electrodialysis reversal (EDR) and reverse osmosis (RO) technologies has significantly increased over the past two decades. However, environmental effects associated with concentrate disposal have restricted the expansion and practical deployment of desalination technologies for inland brackish water sources.

Because water is essential to the production of energy, the looming global energy crisis and the over-reliance on fossil fuels have tied the concept of energy shortage to the production of safe water. Interestingly, microalgae cultivation in desalination concentrate waste may combat the twin water and energy crises by combining increased efficiency for the removal of pollutants from concentrate with the cultivation of algal biomass for biofuel feedstock production. Algae are also a perfect candidate for CO₂ sequestration and greenhouse gas reduction due to algae's ability to use CO₂ as their main carbon source. Other advantages of using microalgae are that they are a sustainable technology capable of growth in most habitats; they do not compete with food crops for resources; they have no NO_x emissions and a short growth cycle; and they are the most rapidly growing option for producing biofuel, fats, oils, sugars, and hydrocarbons, all while fixing carbon dioxide.

Furthermore, some algae species naturally live and thrive in brackish water. To investigate the feasibility of using microalgae in pollutant removal and biomass production by growing algae in desalination concentrate, where the algae could use salts and other nutrients to grow, a full factorial experiment was conducted on the growth of two strains of marine algae in concentrate under 16 hours of illumination at 25 °C, and ion removal by algae was observed to characterize the role of algae in removing pollutants.

Chapter 1

Introduction

1.1 Background

As population has increased, the demand for energy and water has increased in tandem (Foster et al., 2009). However, finding new and affordable sources of energy and drinking water has become more difficult, and exploiting those sources has become more challenging (Armaroli et al., 2006). The supplies of water and energy are also interrelated: due to water concerns, the operation of some energy facilities has been curtailed, and the construction and operation of new energy facilities must take into account the value of water resources.

Along with availability and cost constraints, one of the paramount concerns related to using fossil fuels is that they release enormous amounts of CO₂ into the atmosphere. This release results in global warming, which affects food and water resources, ecosystems, and other parts of the environment (Foster et al., 2009). Hence, concerted effort is needed to find sustainable, renewable, and CO₂-balanced alternative energy sources that can supplant fossil fuels (Righelato and Spracklen, 2007).

In recent years, biofuel has been considered to have the greatest potential as an alternative to fossil fuels because it is derived from non-toxic, biodegradable, and potentially renewable resources while providing less harmful environmental features (Gouveia and Oliveira, 2009). Furthermore, biofuel can be obtained from various different sources, such as sugar crops, starch crops, oilseed crops, and algae. However, a major concern over biomass-based energy, particularly in large-scale fuel production, is that it will consume vast amounts of farmland and water, compete with food production, and drive up food prices (Patil et al., 2008). While this concern is relevant to biofuel production from sugar crops, starch crops, and oilseed crops, microalgae can produce biofuels by utilizing undeveloped lands and wastewater, without using resources necessary for food production.

Using microalgae as a renewable and sustainable feedstock for the production of biofuels can lessen humanity's dependence on fossil fuels while making worthwhile use of resources that would otherwise be wasted: microalgae can be cultivated in non-arable land in various climates, and they can be grown using brackish water and wastewater, which minimizes or even avoids the use of scarce freshwater as a growth medium (Chisti, 2007; Chisti, 2008). Furthermore, cultivation of algae consumes less total water than other crops to produce the same amount of oil (Dinh et al., 2009), and even while growing with such marginal resources, some strains of algae can yield biomass ranging from 10 to 100 times more than comparable energy crops such as corn, soybean and canola (Oilgae report, 2010).

An additional advantage of algae is their short growth cycle: the majority of microalgae use a photosynthetic process similar to higher plants, and complete

entire growing cycles every few days (da Silva et al., 2009). For this growth, microalgae's main requirements are nutrients, sunlight, CO₂, and water (Demirbas and Demirbas, 2011). Notably, microalgae have a low carbon footprint because they capture CO₂ during photosynthesis (Righelato and Spracklen, 2007).

With no shadow of doubt, water and energy are connected. Water is essential to the production of energy of all forms, and energy is needed to produce safe water. In energy production, a significant amount of water is currently needed, mainly in steam electric power plants. According to a report from the U.S. Department of Energy, about ninety percent of all power plants are thermoelectric, which means that they require billions of gallons of water to cool their machinery and produce the steam used to drive their turbines. Conversely, energy plays an essential role in water treatment and storage. For instance, according to a report from Sandia National Laboratories, about 4 percent of power generation in United States is used for water supply and treatment. Hence, it is crucial to have a combined approach to water and energy.

Water is essential to life as a part of every ecosystem, and it is also essential to industry. Although approximately 70% of the Earth's surface is covered by water, people in developing countries are suffering from water scarcity. Poor water quality is the reason for 80% to 90% of all diseases and 30% of all deaths in developing countries (Leitner, 1998). The continuation of current policies will result in an increase in the number of people affected by water shortages, and the spread of water shortages through both the developed and developing world in the future will worsen for two reasons: 1) population growth, and 2) the increased demands on natural resources from industrialization. In order to ease the crisis, planners must include desalination as a part of the development process. Unfortunately, although desalination has great potential to reduce the impacts of water shortages, the technologies used for desalination are expensive. Accordingly, cost reduction for water desalination is essential to propagating the technology (Miller, 2003). Another barrier to overcome is the problem of desalination concentrate, a highly saline byproduct of desalination that has restricted the use of desalination technologies, especially for inland brackish water sources, because of its environmental impacts and associated costs. Although seawater desalination facilities can simply return the concentrate back to the sea for safe and controllable dilution, this option is not available to inland facilities, which face prohibitive costs for safely disposing of the concentrate. Hence, any attempt to reduce the volume and make beneficial use of concentrate stream could significantly increase the practical deployment of brackish water desalination.

1.2 Research objective

The objective of this research is to increase biofuel production and decrease the cost of desalination by making use of byproducts from the desalination process. The productive use of concentrate, which offers an alternative to disposal, is highly desirable; hence, this study investigates the use of concentrate

from water desalination to cultivate and grow algae. Two strains of algae, *Nannochloropsis oculata* (UTEX-LB 2164) and *Dunaliella tertiolecta* (UTEX-LB 999), were considered and evaluated using concentrate as a growing medium. Additionally, ion removal from concentrate was investigated for both species.

Conclusions and Recommendations

Conclusions

Based on this research, the following conclusions can be reached:

- The concentrate growth medium (80% desalination concentrate and 20% f/2 (the ratio of 4 concentrate and 1 f/2 with algae was used to inoculate)) was an optimal match for the investigated algae species, and it maximized the percentage increase of dry weight biomass better than an f/2 medium. The results of optical density at 750 nm conveyed the same result.
- There was no significant difference in biomass production and ion removal between the two algae species. Both *Nannochloropsis oculata* (UTEX-LB 2164) and *Dunaliella tertiolecta* (UTEX-LB 999) were acceptable, but the combination of *Dunaliella tertiolecta* and concentrate medium yielded the highest biomass production.
- Sufficient evidence indicates that the combination of growth medium and algae species was the determinant factor for biomass production. Temperature, light cycle, light intensity, air flow, and other conditions were controlled.
- The contribution of algal cultures in the removal of ions was not significant, with the exception of specific ions such as nitrate, phosphate and fluoride. Total nitrogen decreased considerably during the experiment, but TDS did not change considerably because the ions responsible for high TDS were not removed noticeably.
- Cultivation of marine algae strains in concentrate disposal of water desalination units is a unique approach that combines the increase of removal efficiency of pollutants in concentrate and the cultivation of the algal biomass for the biofuel feedstock production.
- Results of this research identify a potential to reduce the cost of desalination when biofuel production is included, and can bring about environmentally-friendly benefits, such as CO₂ mitigation and concentrate disposal treatment.

Recommendations

Future research into the growth of microalgae in concentrate streams could benefit from the following approaches:

- Investigating the effect of concentrate on the growth of algae strains that have the capability to survive in saline environments.
- Increasing the amount of inoculum of algae to obtain more reliable results due to the relationship between initial biomass and growth rates.
- Using immobilized algae instead of suspended algae to encourage better ion removal because immobilized algae will increase the effective surface area for reaction.
- Ensuring all ion removal is done by algae by measuring the nutrient uptake by algae and ion removal from the medium, then correlate the two results to determine how much removal is done by algae.
- Examining different combinations of f/2 and concentrate, such as 25:75 and 75:25, may yield additional interesting results.
- Another option for future studies could be analyzing the economic feasibility of the complete process of biofuel generation and desalination concentrate treatment process (figure 5.1).

Chapter 2 Literature Review

2.1 Introduction

This section discusses microalgae and their potential as an alternative fuel source. Additionally, the section presents information on CO₂ fixation, algae cultivation methods and harvesting, oil extraction from microalgae, products of algal biofuel, and problems associated with the disposal of concentrate from water desalination.

2.2 Renewable energy

Renewable energy is defined as the energy that comes from resources which could be repeatedly replaced, and renewable energy is an appropriate choice because it is clean and safe (Demirbas, 2011). Renewable energy sources include hydropower, wind, solar, geothermal, marine, and biofuel energy (Demirbas, 2008). In contrast to fossil and nuclear sources, the distribution of renewable energy resources is almost even around the world.

The global economy is highly dependent on energy, and since the population has increased, the demand for energy has also increased (Patil et al., 2008). If the current growth in energy consumption continues, the world will need about 60% more energy by 2030 (International Energy Agency, 2007). Currently, over 80% of total energy usage is supplied from fossil fuels, including petroleum, coal, and natural gas (Demirbas and Demirbas, 2011). Transportation, manufacturing, electricity, and domestic heating account for the majority of global energy consumption (Gouveia and Oliveira, 2009), and transportation alone uses 27% of this energy (Antoni et al., 2007).

Since fossil fuels resources are finite, they are widely recognized as unsustainable energy (Srivastava and Prasad, 2000). Furthermore, combustion of fossil fuels emit a great deal of greenhouse gases, including CO₂, SO₂, and nitrogen oxide (NO_x) (Patil et al., 2008). Combustion of fossil fuels accounts for almost 98% of carbon emissions (Biofuels Media Ltd, 2007). These greenhouse gas emissions result in global warming (Amin, 2009) and adversely impact the environment and human life. For instance, about one-third of carbon dioxide emitted by fossil fuels is absorbed by oceans, which steadily decreases the water pH, leading to adverse impacts in the marine ecosystems and consequently human life (Ormerod et al., 2002).

The other issue associated with fossil fuels is their availability and cost. Increases in the price of petroleum crude oil over past several decades have had and will continue to have immediate negative impacts on energy accessibility and therefore on human life (Amin, 2009). Fossil fuels are not distributed evenly in the world. As an illustration, almost 63% of petroleum reservoirs are located in

the Middle East (Hacisalihoglu et al., 2009). As a result, fossil fuels are considered to be unsustainable, and production of alternative energy sources seems desirable and ultimately necessary. Replacing petroleum-derived fuels with sustainable, renewable, and carbon-neutral transport fuels will reduce many of the aforementioned adverse effects (Chisti, 2008). Technological requirements to make this evolution happen are becoming available (Demirbas, 2009). Altering the heavy dependence on fossil fuels through the use of renewable energy sources like biofuel can greatly contribute to better control and management of greenhouse gases and their negative effects (Demirbas and Demirbas, 2007; Ragauskas et al., 2006).

2.3 Biofuel

Biomass is a material obtained from living organisms like plants, and is usually derived from energy crop cultivation, forest harvesting, and plant residues (McKendry, 2003). Since plants obtain their energy from the sun during the photosynthesis process, biofuel can be thought of as a natural battery for storing solar energy. Biofuel can be in the form of a solid, liquid, or gas (Patil et al., 2008). Biofuel has the capability to replace a substantial fraction of fossil fuels (Perlack, 2005). Biomass from crops reduces emission of greenhouse gases such as CO₂, nitrogen, and sulfur oxides. As a consequence, biomass prevents climatic changes and global warming. Moreover, biofuels help countries without fossil fuel resources to decrease their degree of dependence on other countries that produce fossil fuels, increasing energy supply security and environmental sustainability (Gouveia and Oliveira, 2009).

There are several different *types of biofuel*, including biodiesel, ethanol, bioalcohols, and biogas. Among these, biodiesel is the most widely used, and is usually produced from soybeans, canola oil, animal fat, palm oil, corn oil, jatropha oil (Barnwal and Sharma, 2005), and waste cooking oil (Felizardo et al., 2006; Kulkarni and Dalai, 2006). Approximately 60–75% of the total cost of biodiesel fuel is based on the feedstock used for biodiesel production (Canakci and Sanli, 2008).

In order to replace the transport fuel consumption in the United States, the country will need at least 0.53 billion cubic meters of biodiesel per year (Chisti, 2007). However, in the U.S., most biodiesel production comes from soybeans - a crop that is also used for food. To better illustrate the difficulty posed by this level of production from biofuel crops, Chisti modeled the land area needed to satisfy 50% of the United States transportation fuel demand (table 2.1).

Obviously, petroleum fuels cannot be significantly replaced by oil crops due to the huge land area needed and the low average oil yield per hectare. In addition, since oil crops are edible plants, using them as a feedstock for biodiesel production will increase food prices without having a significant effect on global warming (Fargione et al., 2008). Furthermore, widespread use of vegetable oils leads to the possibility of malnutrition and even starvation in developing countries

(Demirbas and Demirbas, 2011). Thus, the main concern regarding first generation biofuels (biofuels made from sugar, starch, or vegetable oil) is their inefficiency and unsustainability (Patil et al., 2008). In order for biodiesel to be priced competitively against fossil fuel derived diesel, and avoid competition with food crops, biodiesel must be produced from low cost and non-edible plants.

The solution is a transition to second generation biofuels such as microalgae (Mata et al., 2010). Like other plants, algae are photosynthetic species which are able to convert energy from the sun to chemical energy in the form of proteins, hydrocarbon, and oil (Demirbas and Demirbas, 2011). In contrast to first generation biofuels, microalgae biodiesel has the capability to replace fossil fuels completely, without the negative consequences on food, energy security, and the environment (Patil et al., 2008). Based on calculations done by Chisti, microalgae with an average oil content of 30% dry weight in biomass would require only 3% of the U.S. cropping area. Based on some estimations, although the oil contents are similar between seed plants and microalgae (Mata et al., 2010), algal oil yield per acre is 200 times greater than oilseed crops (Sheehan et al., 2008). As a result, biodiesel production from microalgae would be 10 to 20 times greater than oil crops (Tickell, 2000).

Additionally, microalgae can grow more rapidly than the other crops rich in oil and can double their biomass in less than a day (Demirbas and Demirbas, 2011). Microalgae appear to be the only source of renewable biodiesel that is capable of meeting the global demand for transport fuels due to its advantages, which include higher photosynthetic efficiency, higher biomass production, higher growth rate, higher oil yield, and lower land requirements (Richardson et al., 2009; Minowa et al., 1995).

There are, however, some obstacles to the development of biofuel production, including both technological and non-technological barriers (Patil et al., 2008). Critics of biofuels often believe that biofuel production occupies vast amounts of farmland and increases food prices while not significantly reducing greenhouse gas emissions (Crutzen et al., 2007; Righelato and Spracklen, 2007). However, many studies show that biofuels can supply nearly 30% of global energy demand without affecting food prices or producing greenhouse gas emissions (Koonim, 2006).

2.4 What are algae?

Algae are a large and diverse group of autotrophic organisms that can range from unicellular to multicellular in form. Unicellular algae are called microalgae, and multicellular are called macroalgae. They are mainly aquatic and microscopic (Demirbas, 2011). There are two main populations of algae: phytoplankton and filamentous algae. Phytoplankton are important organisms because they generate oxygen while converting inorganic nutrients and sunlight to biomass. Most phytoplankton are too small to be seen with the naked eye; however, sometimes their aggregated presence in water causes discoloration. Phytoplankton populations can experience rapid growth, which occurs mostly as a

result of excess nutrients. Significant phytoplankton population growth is commonly known as algal bloom, which is one of the most common aquatic plant problems faced by pond owners.

Microalgae typically live in fresh and brackish water and convert sunlight, water, and CO₂ to algal biomass (Shimizu, 1996, 2003; Borowitzka, 1999). Microalgae are present in aquatic ecosystems as well as almost all other ecosystems such as terrestrial systems. An estimated 50,000 species of algae, approximately, are available, but only 30,000 have been studied (Richmond, 2004).

The potential of microalgae as a feedstock for biofuel has been studied for 50 years (Mata et al., 2001), and this research was intensified in the 1970s during the first oil crisis (Spolaore et al., 2006). Today, research on microalgae is taken more seriously due to ever-increasing petroleum prices and global warming concerns associated with the combustion of fossil fuels (Gavrilescu and Chisti, 2005). Microalgae can produce various renewable biofuels such as methane (Spolaore et al., 2006), biodiesel (Roessler et al., 1994; Sawayama et al., 1995; Dunahay et al., 1996) and biohydrogen (Ghirardi et al., 2000; Akkerman et al., 2002; Melis, 2002).

Many algae species have exhibited rapid growth and high productivity. In the exponential phase of microalgae growth, biomass doubling time is usually just about 3.5 hours (Chisti, 2007). A simple microalgae cultivation system is capable of producing 100 g m⁻² d⁻¹ dry biomass (Patil et al., 2005). Approximately 1 kg of biomass can fix almost 1.6-1.8 kg of CO₂. Thus, if algae are cultivated close to power plants or other CO₂ producing facilities, they could consume the CO₂ from the facilities' combustion processes (Klass, 1998; Kong et al., 2007; Sheehan et al., 1998). Additionally, using wastewater as a medium for algae cultures can effectively remove nitrogen, phosphorus, and heavy metals such as As, Cd, and Cr from the wastewater stream (Kong et al., 2007, Sawayama et al., 1995). The use of CO₂ emitted from power plants to grow algae in wastewater, which the algae can treat, can bring about environmental and economic benefits.

Algae consist of chemicals such as proteins, carbohydrates, lipids, and nucleic acids (Demirbas and Demirbas, 2011). Table 2.2 shows the chemical composition of algae on a dry matter basis (%). The percentages vary with the type of algae. Some species have about 40% of their overall mass made up of fatty acids (Becker, 1994). Fatty acids have a vital influence on the quality of biodiesel obtained from these strains of microalgae (Mata et al., 2010).

Common oil levels of microalgae are often between 20 and 50% of dry weight. Table 2.3 shows oil content of some microalgae. Some microalgae, such as *Botryococcus braunii*, contain a high percent of oil content but have low productivity; however, most common microalgae like *Dunaliella* and *Nannochloropsis* have oil content between 20 and 50% and higher productivities (Mata et al., 2010).

Microalgae oil content can even go beyond 80% dry weight biomass (Metting, 1996; Spolaore et al., 2006). Based on reports that have been published regarding lipid content of cells, some species, including *Chlorella* species (Fukuda et al., 2001), *Dunaliella* species (Gerpen, 2005), *Nannochloris* species

(Ghirardi et al., 2000), *Parietochloris incisa* (Haesman et al., 2000), and *Botryococcus braunii* (Harris, 1989) have high quantities of oil content under optimized conditions. The amount of derived oil depends on factors such as algae growth rate and lipid content of dry biomass. Microalgae with high oil content under suitable conditions have the capability to produce 19,000-57,000 l of oil per acre annually (Demirbas and Demirbas, 2011). Lipid accumulation usually happens in the stationary phase, in which most of the nutrients, especially nitrate, have already been consumed for reproducing in the exponential phase (Livansky, 2005). All in all, the effect of nitrate deficiency is that protein content and the chlorophyll level decrease, while carbohydrate and lipid contents increase (Mata et al., 2010).

2.5 Algae growth

The growth of an axenic culture of microalgae in batch reactor is characterized by five phases:

1- Lag phase

In this phase, only a small increase in cell density occurs. This phase is quite long, but it could be made considerably shorter if the added inoculum is in its exponential phase. The lag in growth is attributed to the physiological adaptation of the cell metabolism to growth to promote the growth of additional cells.

2- Exponential phase

In the second phase, the cell density increases as a function of time t according to a logarithmic function:

$$C_t = C_0 \cdot e^{mt} \quad (2-1)$$

Where C_t and C_0 are cell concentrations at time t and 0, respectively, and m is specific growth rate, which is a function of algal species, light intensity, and temperature.

3- Phase of declining growth rate

In this phase, cell division slows down when nutrients, light, pH, carbon dioxide, or other physical and chemical factors begin to limit growth.

4- Stationary phase

In this stage, the limiting factors mentioned in part three and the growth rate are balanced, which results in a quite constant cell density.

5- Death or crash phase

In this phase, due to the deterioration of water quality and depletion of nutrients, cell density decreases very quickly until the culture collapses. The main factors causing this phase are depletion of nutrients, oxygen deficiency, overheating, pH disturbance, or contamination.

Generally, algal cultures in the exponential growth phase contain more protein, while cultures in the stationary phase have more carbohydrates (De Pauw et al., 1984); therefore, the beginning of the stationary phase is the best time to harvest algae. In general, the cost of microalgal biomass production is more than the cost for growing other oil crops (Chisti, 2007). Algae need water, inorganic

nutrients, light, and CO₂ for growth. Since algal biomass consists of 40-50% carbon, it is essential to supply a source of carbon, like CO₂, and light for microalgae to carry out the process of photosynthesis (Moheimani, 2005).

Three main factors that influence algae growth are: abiotic factors, biotic factors, and operational factors. Abiotic factors include light, temperature, nutrient concentration, O₂, CO₂, pH, salinity, and toxic chemicals. Like abiotic factors, biotic factors influence algae growth, but encompass living organisms such as pathogens (e.g., bacteria) and competition between other strains of algae to obtain nutrients. Operational factors also play an important role and include mixing shear, dilution rate, and frequency of harvesting (Mata et al, 2010). As a result, achieving equilibrium among these factors maximizes algae growth (Williams, 2002).

Lighting is a very essential abiotic factor. An increase in light intensity (up to certain limits) will result in an increase in cell concentration (Kaewpintong, 2004). The intensity needed varies greatly based on culture depth and algal culture density. The deeper and denser a culture, the more light intensity is needed to penetrate optimally into the culture. Fluorescents should emit blue or red spectrum because these two are the most effective spectrums for photosynthesis (Oilgae report, 2010).

In addition to light, temperature is another important factor. Generally, in both open and closed systems, most strains of microalgae can stand temperatures 15 °C below their optimum temperature; however, temperatures only 2 °C to 4 °C over their optimum temperature can result in culture loss (Mata et al., 2010). In some closed systems, when the temperature reaches about 55 °C, overheating might be occurring. In such conditions, evaporative cooling systems can be helpful to decrease the temperature to 20-30°C (Moheimani, 2005).

Mixing is essential for the growth of algae. Mixing provides uniformity of heat for the culture, makes the transfer of gases easier, and prevents sedimentation. In order to have rapid circulation, it is desirable to create a moderately turbulent stream, especially in open systems (Barbosa, 2003). However, excessive turbulence can damage the microalgae cells because of the shear stress that excessive turbulence creates (Eriksen, 2008). The ideal degree of turbulence is a function of the strain of algae (Barbosa, 2003).

In all growth systems, salinity is a very important parameter, depending on the temperature. Each algae strain has its individual optimal salinity range. The best method to control the salinity is adding fresh or salt water to the medium, if needed (Mata et al., 2010). Figure 2.2 shows that the nutrition concentration decreases during algal growth, and most of the nutrient depletion occurs in the stationary growth phase. Figure 2.3 shows a schematic diagram for integrated biomass production.

The other factors determining the growth rate of algae are photoperiod (light and dark cycles), pH (between 7 and 9 for optimal growth), CO₂ aeration requirements, and the medium (Oilgae report, 2010).

The growth medium should contain the elements that are essential for the algal cells. These elements are nitrogen, phosphorous, sulphur, potassium,

magnesium, iron, and trace metals like calcium, sodium, cobalt, zinc, copper, and molybdenum (Chisti 2007; Oilgae report, 2010).

Microalgae generally accept nitrate, ammonia, and other sources of organic nitrogen, like urea. Phosphorous is vital for cellular processes, and mostly available in forms of inorganic phosphate or H_2PO_4^- or HPO_4^{2-} . Since sulphur is one of the constituents of essential amino acids, some algae have been known to be capable of utilizing organic sulphur sources. The presence of calcium is also important because it plays a key role in the maintenance of cytoplasm. Calcium is usually deposited on the cell walls of some algae.

Without potassium, an algae culture's photosynthesis will be reduced, creating a deficiency in growth. Sodium is essential for marine algae because it is needed for nitrogen fixation. The presence of sodium is necessary for the transformation of molecular nitrogen to ammonia. For all algal species, magnesium is a requirement because it is a central atom of the chlorophyll molecule. Iron is also important due to its nitrogen assimilation from a growth medium. The availability of trace metals in very small amounts is useful for some strains of algae because these metals have an influence on growth and protein accumulation (Oilgae report, 2010).

Microalgae have four main metabolisms for growth: autotrophic, heterotrophic, mixotrophic, and photoheterotrophic. Autotrophic organisms use light as their only source of energy and convert it to chemical energy through photosynthesis. Heterotrophic organisms cannot fix carbon, and only use organic carbons in order to grow. Mixotrophic organisms can live either autotrophically or heterotrophically, meaning that their growth depends on the concentration of organic compounds and light intensity. Since this metabolism can eliminate or reduce the need for light, it can decrease the cost of the wastewater treatment and biofuel generation processes. Photoheterotrophic organisms need light to use organic carbon (Mata, 2010).

2.6 Algal strain selection

It is estimated that there is a large number of strains of algae available (Richmond, 2004). However, in reality, only some of them could be used for energy production in an economically feasible manner. Thus, selecting the right strain of algae is very important to the production of any kind of bioenergy. Based on previous studies, the following criteria are central to selection of algal species (Mata et al., 2010, Oilgae report, 2010):

- Growth rate;
- High performance in competitive mass nature and tolerance to predators;
- High lipid content and energy yield based on type of fuel from biomass;
- Tolerance to changes in environmental conditions, including resistance to temperature, nutrient input (salinity), and light change;
- Nutrient availability, especially CO_2 , when carbon fixation is the goal;
- Possibility of obtaining other valuable chemicals;
- Degree of easiness of biomass isolation; and

- Less complex structure, and as a result easier oil extraction.

2.7 Carbon dioxide fixation

Excessive carbon dioxide emission has caused global warming; therefore, the mitigation and sequestration of CO₂ is paramount to lowering human impact on the global climate. While there are other approaches to CO₂ sequestration, biological approaches are more economical and are more popular due to the fact that they combine biomass production with CO₂ fixation while reducing or eliminating waste (Pluz and Gross, 2004).

Carbon forms approximately 50% of algal biomass (Sánchez Mirón et al., 2003). This carbon is mostly supplied from CO₂. Microalgae have a voracious appetite for carbon dioxide. Based on estimations, producing 100 tons of biomass will fix nearly 183 tons of CO₂ (Antoni et al., 2007). To grow algal biomass, CO₂ must be injected into the growing medium continuously in daytime. This CO₂ could be supplied from the existing flue gas of coal-fired power plants (Sawayama et al., 1995; Yun et al., 1997) which are responsible for 7% of the total world CO₂ emissions (Kadam, 1997). To completely fix the CO₂ emission of a power plant with the capacity of one MW, roughly 40 acres of algal pond is needed (Awshti and Singh, 2010). This process could be also combined with using wastewater as a medium for algae to grow and recycle CO₂ while treating water (Demirbas and Demirbas, 2011).

2.8 Culture systems in commercial scale

Considering available materials and local conditions, it is possible to design different culture systems with different capacities, materials, and mixing types (Mata et al., 2010). However, in reality, there are only two feasible methods available for large-scale production of microalgal biomass: raceway ponds (Terry and Raymond, 1985; Molina Grima, 1999) and tubular photobioreactors (Molina Grima et al., 1999; Tredici, 1999). Batch, semi-batch, and continuous systems could be used for cultivation (Awasthi and Singh, 2011). In order to select the optimal method, several criteria must be considered (Mata et al., 2010): the selected algae strain, local environmental and climatic conditions, and the availability of nutrients. In large scale commercial production, a continuous method is mainly used, where medium is fed at a constant rate to the algal broth which is harvested continuously (Molina Grima et al., 1999). Photobioreactors can be operated in batch mode as well, but the continuous mode has some advantages over batch, including: higher control, more reliable results due to steady state condition, more control over biomass concentration by changing the dilution rate, and easier system investigation and analysis (Williams, 2002).

2.9 Open ponds

Open ponds have been used for algal production since the 1950s. Species such as *Nannochloropsis*, *Chlorella*, and *Dunaliella salina* have been cultivated in outdoor ponds. A raceway pond consists of closed loop circulation channels that have a 0.3 m depth. Baffles are used at the end of each channel to change the flow direction. Channels are commonly made of concrete and covered with plastic. There is a paddlewheel from where flow begins. Also, feed is injected to the algal broth continuously during the daylight, exactly in front of the paddlewheel. Harvesting is done behind the paddlewheel. The paddlewheel must operate all day long in order to prevent sedimentation (Chisti, 2007). A schematic view of a raceway pond is shown in figure 2.4.

In terms of economics, open ponds are relatively more economical than photobioreactors, but these ponds have drawbacks due to water availability, climatic conditions, contamination by microorganisms like bacteria and fungi, low productivity, and the occupation of a large land area (Mata et al., 2010; Patil et al., 2008; Ugwu, et al., 2008).

2.10 Photobioreactors

Photobioreactors are known as a method for producing a huge amount of algal biomass (Molina Grima et al., 1999; Tredici, 1999; Carvalho et al., 2006). Although artificial illumination is more expensive than natural illumination, artificial illumination has been used successfully in large scale biomass production, and is practically feasible (Pulz, 2001). To prevent sedimentation in the tubes, turbulent flow is provided by either mechanical pump or airlift pump (Molina Grima et al., 1999). Mechanical pumps can be installed and operated more easily; however, they can damage the biomass (García Camacho et al., 2007; Sánchez Mirón et al., 2003; Mazzuca Sobczuk et al., 2006).

In most photobioreactors, dissolved oxygen must be lower than 400% of air saturation; therefore, since the oxygen cannot be removed within the tubes, the length of the tubes must be limited by a continuous mode. For this reason, the culture must be intermittently returned to the degassing zone, where air bubbles strip out the accumulated oxygen. The length of the tube is also a function of other factors such as biomass concentration, light intensity, flow rate, and oxygen concentration at the entrance (Chisti, 2007). Due to these restrictions, the tubes normally should not exceed 80 m (Molina Grima et al., 2001).

An increase in pH will occur when the broth goes forward through the tube due to the consumption of CO₂ (Camacho Rubio et al., 1999); thus, in some cases, carbon injection is needed at certain intervals in order to prevent carbon deficiency and increase the pH (Molina Grima et al., 1999). Photobioreactors must have a cooling device to operate both day and night due to the changes in temperature, which injure the algae and reduce the biomass (Chisti, 2007).

Photobioreactors are more flexible than open ponds because they can be adjusted depending on algal strains, especially the strains that cannot be grown in

open pond; however, the set-up cost of a photobioreactor is much higher than the set-up cost for an open pond (Patil et al., 2008).

2.10.1 Tubular photobioreactor

Tubular photobioreactors have been proven to be the most satisfactory photobioreactor design for large scale algal biomass production (Chisti, 2009). Tubular photobioreactors are made of an array (solar collector) of translucent plastic or glass tubes. The diameter of the tubes must not exceed 0.1 m, because a diameter greater than this does not allow the light to penetrate deep into a culture's denser areas (Chisti, 2007). The tubes are usually oriented north to south for better sunlight capture.

The culture broth is circulated from a degassing zone to a solar collector zone to capture sunlight. The culture is then circulated back to the degassing zone. This circulation is continuously repeated and makes turbulent flow. This flow causes a suspension of the cells, prevents sedimentation, and efficiently mixes gases inside the photobioreactor. Figure 2.5 illustrates the design of a tubular photobioreactor.

2.10.2 Fence-like solar collector

Like figure 2.6, sometimes tubes are located horizontally in parallel to each other, similar to a fence. Thus, this design has been called the fence-like solar collector. This design tries to maximize the number of tubes that can be located in a limited area. The tubes have their ends placed in the north and south direction to optimize sunlight capture. The bottoms of the tubes are either painted with white color or covered with white sheets for better reflection (Chisti, 2007).

2.10.3 Helical tubular photobioreactor

In this design, tubes, instead of being laid either horizontally or vertically, are coiled around a supporting frame. The tubes are made of polyethylene, so they are flexible and capable of being coiled. The diameter of each tube is typically 3 cm. This system is equipped with a gas exchanger tower and a heat exchange system. The device used in this design for circulation is a centrifugal pump. This design is useful for small volumes of microalgal culture (Chisti, 2007).

2.11 Open raceway ponds vs. photobioreactors

The following table (table 2.4) provides the most important criteria for selecting the appropriate microalgal biomass production method for a given situation.

Temperature control is difficult in raceway ponds and evaporation is high due to exposed surface area. This increase in evaporation causes less CO₂ fixation in comparison to photobioreactors. Additionally, low biomass concentrations occur in raceway ponds because of poor mixing (Chisti, 2007). Raceway ponds consume more energy to homogenize nutrients in the growing medium, and the

water depth cannot exceed 15 cm in order to let microalgae receive enough sunlight (Richmond, 2004). The atmosphere contains only 0.03%–0.06% CO₂; therefore, because of this mass transfer limitation in open ponds, microalgae growth will be slow unless CO₂ is injected (Mata et al., 2010). In contrast to photobioreactors, open ponds cannot process single-species culture for a long period of time due to high contamination risks. The harvesting and recovery of biomass for oil extraction typically costs more in open ponds than in photobioreactors because the biomass concentration in the photobioreactor is much denser (almost 30 times) than open pond systems (Chisti, 2007).

Although there are many advantages of photobioreactors over open ponds, these two do not have to be viewed as competing technologies. Photobioreactors have many disadvantages, including high upfront and maintenance costs, cell damage due to higher shear stress, overheating, bio-fouling, hard scaling-up, and oxygen accumulation.

2.12 Harvesting

Harvesting is the process of recovering biomass from the culture medium. This process is very difficult, energy intensive, and expensive (Pimentel et al., 2004). Harvesting accounts for 20%-30% of the total cost of algal cultivation (Grima et al., 2003). In addition to cost, harvesting has other challenges including flocculant toxicity and the difficulty of large scale application (Awshti and Singh, 2011). There are some conventional methods to harvest microalgae from media, including centrifugation (Briens et al., 2008), foam fractionation (Brown et al., 1997), flocculation (Canakci and Van Gerpen, 2001), membrane filtration (Chisti, 2007), and ultrasonic separation (Chynoweth et al., 1993).

Flocculation is easier than centrifugation and filtration because flocculation can treat a large amount of culture. The most effective flocculant agent that has been reported so far is aluminum sulfate, followed by certain cationic polyelectrolytes (Conover, 1975). The role of the flocculant is to aggregate algae cells in order to increase the effective particle size and, as a result, make recovery more convenient (Grima et al., 2003). However, chemical flocculation is too expensive for large scale operations (Amin, 2009).

Another technology to recover biomass is membrane filtration. It can be performed under pressure or in a vacuum to recover biomass, but it is quite slow. This method is appropriate for large size microalgae. For small scale operations, microfiltration and ultra-filtration can be used instead of conventional filtration systems. Filtration is expensive mostly because of membrane replacement and pumping costs (Mata, 2010).

The other method available is froth flotation, which is not broadly used. This method separates algae from the culture by making air bubbles and adjusting optimal pH in order to create a froth of algae that accumulates above the liquid level (Awshti and Singh, 2011). Ultrasound-based methods of algae harvesting are under development.

Based on suggestions (Richmond, 2004), the most important criterion for choosing a harvesting method is the desired final product. For instance, for low-price products, gravity sedimentation coupled with flocculation is appropriate, but for high-quality recovery, centrifugation is of interest because it can process large volumes of biomass.

2.13 Algal drying

Drying or dewatering is a process of reducing the water content of algae from almost 90% to 50% prior to oil extraction. This level of drying is essential for producing a solid material. Several methods have been employed to dry microalgae. The most common drying methods are spray-drying, drum drying, freeze-drying, and solar drying (Richmond, 2004). Solar drying may not require any additional energy sources, but it does require a large land area to be expedient. The most efficient method is to use low-grade waste heat from power plants to dry algae in vessels. Spray-drying is expensive and not economically feasible for low value products, such as biofuel or protein (Mata et al, 2010).

2.14 Oil extraction

There are several methods to extract oil from microalgae for biofuel production. It is possible with either a press or through chemical methods. There are three chemical methods available for oil extraction: solvent method, soxhlet extraction, and supercritical fluid extraction.

Hexane solvent usually is used along with a press method. First, oil is extracted using a press, then the remaining pulp is mixed with cyclo-hexane to extract the remaining oil. The oil dissolves in cyclo-hexane, and the pulp is filtered out. The final stage is the separation of oil and cyclo-hexane by distillation. This method may recover approximately 95% of the total oil in algae.

Soxhlet extraction uses chemical solvents. Oil is extracted through repeated washing with an organic solvent, such as hexane or ether in special glassware.

In supercritical fluid or CO₂ extraction, CO₂ is first liquefied under pressure and heated to the point where it has the properties of both a liquid and a gas (critical point). Next, this liquefied fluid is used as the solvent in oil extraction (Awshti and Singh, 2011). Supercritical fluid extraction is far more efficient than traditional solvent separation methods. Since supercritical fluids are selective, the product would be very pure (Paul and Wise, 1971). The performance of CO₂ extraction is almost 100% (Demirbas and Demirbas, 2011).

2.15 Energy conversion from microalgae

In addition to oil, it is possible to derive non-fuel products from microalgae. Since microalgae contain proteins, carbohydrates and other nutrients, the residual biomass from the transesterification process for biofuel production could be used as animal feed (Schneider, 2006). Additionally, it could be burnt directly to produce heat. These possibilities could reduce the cost of biodiesel. Also, microalgal biomass is available in powder form for the human health food market (Demirbas and Demirbas, 2011).

The energy conversion processes from microalgae can be categorized into biochemical, thermochemical, and direct combustion (Tsukahara and Sawayama, 2005). Biochemical conversion can be subdivided into fermentation and transesterification. Thermochemical conversion can be subdivided into gasification, pyrolysis, liquefaction, and hydrogenation. The chart of energy conversion from microalgae is shown in figure 2.7 and a brief description for each process is detailed in sections 2.16.1 and 2.16.2.

2.15.1 Biochemical conversion

2.15.1.1 Fermentation

The goal of fermentation is to produce ethanol at a large scale. First, the biomass is ground, and then converted to sugar by enzymes. Next, the sugar is converted to ethanol by yeast (McKendry, 2003).

2.15.1.2 Transesterification

Transesterification is the reaction between a fatty acid and alcohol to form esters and glycerol. The result of the reaction is biodiesel (Schuchardt, 1998).

2.15.2 Thermochemical conversion

2.15.2.1 Gasification

Gasification is a chemical process in which hydrocarbons are converted to synthetic gas by partial oxidation with air at high temperature in the range of 800-900 °C (Awshti and Singh, 2010).

2.15.2.2 Pyrolysis

Pyrolysis is a phenomenon related to the decomposition of biomass by heating the biomass at a high temperature (around 500 °C) in the absence of oxygen in order to produce biofuel, charcoal, and gas (McKendry, 2003; Miao et al., 2004).

2.15.2.3 Liquefaction

Microalgal biomass has a high water content (80-90%) after harvesting, and large amounts of energy are required to reduce moisture prior to processing. This drying is a pretreatment to make the biomass ready for heat and power generation. Thus, because more energy is needed, the production cost increases

(Klass, 1998). However, a liquefaction reaction produces biofuel directly without need of drying (Singh and Gu, 2010). The main product of this reaction is bio-crude with a heating value ranging from 30 MJ kg⁻¹ to 35 MJ kg⁻¹ (Goudriaan, 2001).

2.15.2.4 Hydrogenation

Hydrogenation is a reductive reaction in which hydrogen atoms are added to double bonds of a molecule, in the presence of a catalyst and a solvent, under high temperature and pressure conditions. The process forms a three-phase operation in which the contact among the gaseous phase (hydrogen and hydrocarbon phase), the liquid phase (mixture of solvent and liquid product), and the solid particle phase (algal and catalyst) results in algal conversion and the promotion of effective momentum, heat, and mass transfer (Gaffron and Rubin, 1942; Awshti and Singh, 2010).

2.16 Biodiesel from algae

Biodiesel is produced through the process of transesterification. Aquatic unicellular green algae are used in this reaction for biodiesel production. Transesterification is a reaction of parent oil with short chain alcohol (commonly methanol) in the presence of a catalyst. The use of an acid catalyst has been proved possible, but the reaction rates are too slow (Meng et al., 2009); therefore, alkali-catalysts are commonly used commercially because they are 400 times faster (Awshti and Singh, 2010). Products of the reaction are glycerol and fatty acid methyl esters (FAME) or biodiesel (Chisti, 2007; Belarbi et al., 2000).

The energy of biodiesel is similar to petroleum diesel. The heating value of petroleum diesel is 42.7 MJ/kg, and the heating value of biodiesel derived from algae is 41 MJ/kg (Xu et al., 2006). On the other hand, biodiesel from microalgae does have some disadvantages. For instance, it is unstable and contains many polyunsaturated fatty acids (Demirbas and Demirbas, 2011). Biodiesel production from microalgae could be more cost effective and environmentally-friendly if integrated with wastewater treatment and power plant flue gas treatment (CO₂ fixation) (Hodaifa et al., 2008). The schematic process of biodiesel production is shown in figure 2.9.

2.17 Ethanol from algae

Ethanol could be derived from microalgae through either fermentation or gasification due to microalgae's high content of hydrocarbon and polysaccharides (Minowa and Sawayama, 1999). Since bioethanol has only 64% of biodiesel energy and annual U.S. biodiesel needs are 0.53 billion m³, approximately 828 million m³ of bioethanol would be required to fulfill this need. The amount of algae necessary to create enough bioethanol would require 111 M hectares of land

area, almost 61% of the total available cropping area in U.S. Therefore, selecting ethanol over biodiesel would be impractical (Chisti, 2008).

2.18 Methane from algae

Methane can be derived from residual biomass through anaerobic digestion to generate the electrical power needed to run the biomass production facility (Raven and Gregersen, 2007). Studies have indicated that, among different sources of biomass, marine algae offer the greatest potential for biomethanation due to their high growth rate (Chynoweth et al., 1993).

2.19 Economics of biodiesel production

The main obstacle to large-scale production of microalgae is economics. If efficient methods for recovery and oil extraction processes are utilized, microalgal production costs can be minimized (Chisti, 2008). These parameters are very important, but the key for large-scale production of biofuel from microalgae is creating a holistic biorefinery that would integrate several factors (Pushparaj et al., 1993), including biomass production, growth management, wastewater management by using the wastewaters as a growth medium, CO₂ sequestration by using the flue gas of power plants as a carbon source for algae, transport to conversion plants, drying, product separation, recycling, and transport of products to the market place (Patil et al, 2008). The ideal would be to build the biorefinery near power plants, and to design conversion plants within the biorefinery to remove or minimize the cost of transportation (Klass, 1998).

2.20 Water scarcity

Lack of water to meet daily needs is a reality today for one in three people all around the world (Oki and Kanae, 2006). According to a report of the United Nations, about 1.2 billion people are suffering from water scarcity, and another 1.6 billion people are encountering water shortage due to economic factors: i.e., countries lack infrastructure to make use of water from rivers or aquifers. Globally, the problem is getting worse as cities and populations grow, and the demands for water increase in agriculture, industry, and households.

Water scarcity has two causes: natural phenomena and human-made phenomena. An example of a natural phenomenon is that, although there are enough freshwater sources for the current global population, these resources are unevenly distributed geographically. Human-made phenomena include wasting water and global warming.

Because water scarcity forces people to rely on unsafe sources of drinking water, poor water quality can increase the risk of infection from diseases such as

typhoid and paratyphoid fever (Crump and Mintz, 2009). Thus, water scarcity underscores the need for better water management. Since the amount of freshwater on the planet has remained fairly constant over time, there is a crucial need to desalinate and make use of saline and brackish waters. There are many desalination methods that can be applied in combination with available local energy sources for water in dry places. Choosing a specific technique depends on local geographic conditions and the production capacity desired (Belessiotis and Delyannis, 2001).

2.21 Water desalination

Technologies for water purification are based on three main categories: membrane technologies, thermal technologies, and chemical approaches. In some cases, a combination of all three approaches is applicable. The most common desalination approach in the United States is the use of membrane technologies, while thermal methods are rarely used in the United States (Younos and Toulou, 2009).

Generally, membrane technologies use either pressure-driven or electrical-driven technologies. Pressure-driven membrane technologies include reverse osmosis (RO), nanofiltration (NF), ultrafiltration, and microfiltration (Duranceau 2001). Electrical-driven membrane technologies include electrodialysis (ED) and electrodialysis reversal (EDR). The use of EDR and RO systems has significantly increased over the past two decades. There are different typical thermal technologies available, such as solar distillation (SD), multistage-flash, multiple effect evaporation (MEE), thermal vapor compression (TVC), mechanical vapor compression (MVC), and adsorption vapor compression.

Chemical approaches have been considered impractical for treating water with high levels of total dissolved solids (TDS). Such methods are usually used for water softening in a process referred to as ion exchange, which could be described as the interchange of ions between a solid phase and a liquid phase surrounding the solid. There are a limited number of high-quality sources of water in United States; therefore, wastewater, brackish sources, and salt waters, or a combination of the three, are used to meet the demand for water. However, two issues have restricted the expansion and practical deployment of water desalination technologies for inland brackish water: (1) costs associated with treatment technologies, and (2) environmental effects related to concentrate disposal.

2.22 Concentrate disposal problem

Concentrate is a byproduct of desalination that contains between 10 and 50% of the treated water, as shown in figure 2.10. Concentrate has very high salinity, and may have low concentrations of the chemicals used in the pretreatment and post-treatment (cleaning) processes, such as the antiscalants

which are used to prevent scaling in membranes. The types of chemicals left over in the concentrate depend on the type of membrane.

Concentrate features depend on the type of desalination technology used. The amount of the produced concentrate is a function of the desalination process recovery rate. Since membrane technologies have a higher recovery rate, the produced concentrate from membrane technologies is more salty than concentrate produced from thermal or chemical technologies (Younos, 2005).

RO concentrate usually remains at the ambient water temperature. In comparison to freshwater, concentrate has a higher density because of its high salt concentration; therefore, when the concentrate is disposed of into lower salinity water, concentrate has a tendency to sink, which results in problems for the marine environment. These impacts can be mitigated by diluting concentrate before disposing of it (Younos, 2005).

Toxicity in concentrate is connected to three parameters: pH, TDS, and ion imbalance. As a result of adding acidic solution in order to prevent scaling of calcium carbonate in membranes, the pH in concentrate is lower than most surface waters when it leaves the membranes. Low pH waters can add toxicity in marine environments. This pH problem can be solved by adding caustic soda or some similar basic solution. As a result of excessive TDS, the high density of concentrate will have negative benthic impacts if deposited in a body of water. Water mixed with concentrate that has excessive TDS is also toxic to grass, crops, and landscaping. If the feed water is seawater and has an efficient treatment performed on it, the TDS of concentrate can go beyond 36,000 ppm, which is very harmful for the environment. Furthermore, the toxicity created by ions like calcium, fluoride, and potassium is hard to remove. Concentrate has been proved to be toxic to freshwater and marine organisms. The ions that mostly account for this toxicity are calcium, fluoride, and potassium (Mickley 2001). In the case of the treatment of groundwater, which often contains high levels of potentially harmful gases such as carbon dioxide and hydrogen sulfide, the resulting concentrate from groundwater treatment will have a high toxicity (Mickley 2001). Lastly, ion imbalance is also a function of the desalination method used. For instance, in the nanofiltration method, calcium, magnesium, bicarbonate, and fluoride are the ions that deviate from ion balance.

Brine concentrate resulting from seawater desalination contains a level of TDS that exceeds 36,000 mg/L. Therefore, if concentrate is disposed of in an inappropriate fashion, it will create problems for marine and other habitats (Younos, 2005). There are several methods to dispose of concentrate: surface water discharge, sewer discharge, deep well injection, evaporation ponds, infiltration basins, and irrigation. In the United States, the most common methods are surface water discharge (for almost 50% of all plants) and sewer discharge (for about a third of all plants). Surface water discharge includes disposal into freshwater rivers, coastal waters, and freshwater lakes or ponds. Rather than disposing of concentrate in surface waters, sewer disposal puts concentrate underwater. These methods are usually available for coastal areas.

For inland areas like New Mexico, concentrate disposal is a major hindrance for building desalination units because the concentrate cannot be

returned to sea water easily. There are various factors to consider for choosing the disposal method for concentrate from inland brackish water, such as concentrate volume, TDS of concentrate, location of the desalination unit, capital and operating costs, and environmental issues (Younos, 2005).

2.23 Objective of this research

In order to increase the feasibility of the desalination processes, identifying a beneficial use for the concentrate from inland desalination systems is highly desired. The objective of this research is to develop an innovative solution to use concentrate streams from the RO process, which contain high concentrations of dissolved solids, to grow microalgae for the production of biofuel. Specifically, the objective of this research is to:

- Evaluate the growth of two strains of microalgae in desalination concentrate; and
- Evaluate ion removal from concentrate by microalgae.

Chapter 3

Experimental Studies

3.1 Introduction

To examine whether concentrate from inland desalination could be an appropriate medium for growing microalgae while investigating whether microalgae can contribute to concentrate treatment, a full factorial experiment with completely random design (CRD) arrangement was conducted. Two strains of algae, *Nannochloropsis oculata* (UTEX- LB 2164) and *Dunaliella tertiolecta* (UTEX-LB 999), were cultivated in four different media (concentrate, f/2, a 50:50 combination of f/2 and concentrate, and deionized water). The microalgae growth was compared among the different types of growing media. Additionally, ion removal from concentrate by microalgae was studied. This chapter covers experimental apparatus and analytical methods used in this study.

3.2 Strains of algae

In this research, two strains of microalgae, *Nannochloropsis oculata* (UTEX- LB 2164) and *Dunaliella tertiolecta* (UTEX-LB 999), were obtained from the University of Texas Algae Collection in Austin, Texas. The pre-cultures of both strains were cultivated in f/2 medium (Guillard, 1975) for about three weeks in a 10 gallon aquarium aerated with ambient air. The air pumps were connected to air stones for better air distribution. When an optical density of approximately 1.00 was obtained at a wave length of 750 nm for each strain, four liters from each strain was taken for the experiment.

Both *Nannochloropsis oculata* and *Dunaliella tertiolecta* absorb CO₂ efficiently, making these algae species good candidates to test the hypothesis of this paper (Ono et al., 2004).

Nannochloropsis is a green algae that includes approximately six species. *Nannochloropsis* has been considered as a suitable candidate for biofuel production due to its fast reproduction and high oil content, which ranges from 31-68% of dry weight (Chisti, 2007; Apt & Behrens, 1999). *Nannochloropsis oculata* is known as a marine algae; however, this strain also has been observed growing in fresh and brackish water (Karen and Marvin, 2007). This strain was selected for this experiment due to the high salinity of the concentrate.

Dunaliella tertiolecta is a unicellular algae strain with oil content of approximately 40% of dry weight. *Dunaliella tertiolecta* is a very fast growing strain with a high CO₂ fixation rate (Demirbas, 2009). Additionally, *Dunaliella* is a green algae capable of growing in water bodies containing more than 10% salt, such as oceans and brine lakes (Oilgae report, 2010). This strain was selected due to its tolerance of saline environments.

3.3 Culture and medium

In this research, four different media were used: concentrate, f/2, a 50:50 combination of f/2 and concentrate, and deionized water.

3.3.1 Concentrate medium

Concentrate refers to an 80/20 mixture of concentrate and f/2 in this experiment. It was obtained from the reverse osmosis (RO) water desalination process at the Brackish Groundwater National Desalination Research Facility (BGNDRF) in Alamogordo, New Mexico. The concentrate specifications were as follows: TDS was 6240 ppm, electroconductivity (EC) was 10260 $\mu\text{S}/\text{cm}$, and pH was 7.83. The ion content of concentrate is shown in table 3.1. Only ions which are vital for algae to grow were targeted. Since NH_4^+ was not available in the concentrate, that ion is not mentioned in Table 3.1.

3.3.2 f/2 medium

The f/2 medium is a common and widely used general enriched seawater medium designed for growing coastal marine algae. The recipe used in this experiment for making one liter of f/2 is tabulated in table 3.2.

3.3.3 50:50 combination of f/2 and concentrate medium

This combination was incorporated into the experimental design because it is more economical than f/2 while using concentrate.

3.3.4 Deionized medium

This medium served as the control medium in this experiment.

3.4 Photobioreactor set up

In this study, 32 cylindrical, glass UTEX 500-milliliter photobioreactors were used. Each photobioreactor was 14 cm in height and 7 cm in diameter with a working volume of 500 ml and an autoclavable body. Each photobioreactor was equipped with five air delivery modules, a water trap, an air pump, an air stone, and one additional access port for sampling and measurements as shown in figure 3.1.

3.5 Design of experiment

32 runs were conducted in order to provide the data required for testing the various combinations of the 2 types of microalgae and 4 media. Since the experimental design used was a full-factorial design (2X4), eight combinations of microalgae and media were obtained (table 3.3). Furthermore, since four

replications were taken at each level, there were four data points at each combination.

3.5.1 Experimental Apparatus

An experimental apparatus was constructed using the UTEX glass photobioreactors. In order to pass an air tube into the photobioreactor through a check valve on the top of the lid, each photobioreactor had a quarter-inch hole made in the center of the lid. Then, the air tube was connected to the air stone for better air distribution, as well as to create more homogenous bubbles. Each photobioreactor was aerated by a Fusion Air Pump 200 (1.5 W). The lighting device used consisted of four General Electric, F40PL/AQ-ECO, wide-spectrum, 40W florescent tubes with a 3100K color temperature, producing 1900 lumens for each rack. The average distance from the bulbs to the experimental medium was 25 cm. For better light distribution, the floor of each rack was covered with aluminum foil. This addition enabled light from the bottom of the rack to reflect to the underbelly of the photobioreactor.

All weights were measured using an Acculab AL-204 scale with an accuracy of +/- 0.0001g. An Eppendorf 5804 centrifuge was used to isolate biomass from the medium. The wet biomass was dried in a Fisher vacuum oven. An Eppendorf 1-50 ml pipette was used for the inoculation and transfer of algae. Volumes of the medium were measured using volumetric flasks. The pH was measured using an Accumet AB15/15+ pH meter. Before taking each pH sample, the pH meter was calibrated with standard pH 7 solution. A SANYO MLS-3751L was used to autoclave glassware.

3.5.2 Test procedure

In this experiment, concentrate medium with TDS of 6240 mg/l was obtained from concentrate disposed from the RO pilot plant located in BGNDRF in Alamogordo, New Mexico. The f/2 medium was prepared using the standard protocol. To avoid any contamination, all glassware was washed and rinsed with distilled water, and then autoclaved. Eight algae/medium sets with four replications for each treatment were placed separately inside the 32 batch photobioreactors. All the photobioreactors were placed under 16 hours of illumination and 8 hours of darkness at $30\text{ }^{\circ}\text{C} \pm 2.0\text{ }^{\circ}\text{C}$. Then, the inoculums of microalgae were cultivated in four media at the ratio of 1 to 4 in photobioreactors.

The next step was filling the photobioreactors with 320 ml of their respective media. Subsequently, the pH of the media was measured and found to be at 7.8, 6.9, 7.5 and 7.1 for concentrate, f/2, the 50:50 combination of f/2 and concentrate, and deionized water, respectively. Next, 80 ml of stirred homogenous algae was added to each photobioreactor containing 320 ml of medium. The initial biomass of the inoculating algae was defined by taking four 50 ml samples. The samples were centrifuged at 10,000 rpm for three minutes. The supernatant was discarded from each sample, and the remaining algae in each sample were again rinsed with deionized water and then centrifuged a second time. These samples were then dried for 24 hours at $80\text{ }^{\circ}\text{C}$. The initial biomass added to the photobioreactor was 0.052 g and 0.043 g for *Dunaliella tertiolecta* (UTEX-LB

999) and *Nannochloropsis oculata* (UTEX- LB 2164), respectively. The photobioreactors were placed randomly in racks. Air with a volumetric flow rate of 5 ml/s entered each photobioreactor through the air hose inserted through the lid. The experiments ran for 10 days. During this period, pH, optical density at 750 nm, TDS, EC and total nitrogen (TN) were measured every day. Furthermore, dry biomass and the ion content of each concentrate medium were measured in the first and last days of the experiment. The resulting data were analyzed using a general linear model (GLM) procedure. Assumptions were checked using SAS 9.1.3. Means were compared using Tukey's Test ($P < 0.05$).

3.6 Analytical method

3.6.1 Algae growth

One of the main objectives of this experiment is to compare the growth of microalgae between different conventional media. Basically, there are three methods to quantify biomass concentration: measuring dry weight of biomass, counting cell numbers, and using the optical density method. Measuring biomass concentration is difficult and sometimes even unreliable. For instance, dry weight method and cell counting are susceptible to failure if the suspension contains insoluble particulates (Richmond & Hu, 2013). Likewise, if the suspension is not clear, optical density is not very accurate as a measure. Furthermore, optical density does not have the capability to distinguish viable cells from others. The number of cells is counted in order to evaluate the amount of biomass in optical microscopy or flow cytometry (FCM). In this experiment, optical density and dry biomass weight were used in tandem to assess biomass production.

3.6.1.1 Dry biomass weight analysis

Although calculating the dry weight of a sample is challenging, it is the most accurate method to determine biomass production (Richmond & Hu, 2013). To measure dry biomass, a 50 ml sample of culture suspension was taken. Then, the sample was transferred to a pre-weighed 50 ml plastic tube. The plastic tube, with content of algal culture, was centrifuged for 3 minutes at 10,000 RPM, after which the supernatant was extracted. Since the dry weight, especially for marine algae, is heavily affected by the salts and nutrients absorbed on the cell surface, the centrifuged content was rinsed with deionized water in order to reduce the error in determining the amount of dry biomass based on a suggestion by Lee and Shen (Lee & Shen, 2004). Subsequently, the tubes were centrifuged at 10,000 RPM for 3 minutes after rinsing with deionized water. The clear supernatant was discarded, while the tubes containing the biomass were dried in the oven at 80 °C for 24 hours. In order to prevent loss of volatile components in algae cells, the temperature was maintained below 90 °C. The dry biomass was determined by the difference between the initial and final weight of the tube.

3.6.1.2 Optical density

Optical density is determined by the following relationship:

$$A = -\log(I/I_0) \quad (3-1)$$

Where A is absorbance, I_0 is the intensity of light before it enters the sample, and I is the intensity of light that has passed through the sample (transmitted light). Optical density (absorbance) is a fast, indirect, and nondestructive method to measure biomass. The light absorbed by a suspension can be related directly to biomass; the relationship has already been established by calculating chlorophyll A, B, and total chlorophyll for each variety (Griffiths et al., 2011). In order to determine biomass concentration, the optical density value at either 680 or 750 nm must be measured, along with particle size, shape, and refractive index effect optical density. Therefore, there is less congruity between the results of optical density and dry weight biomass.

A HACH DR 5000 Spectrophotometer was used to track the daily algae growth in terms of optical density. Optical density was measured daily at a wavelength of 750 nm, which is the range where chlorophyll is a dominant pigment.

3.6.2 Ion removal

The other central objective of this experiment is to evaluate whether microalgae can contribute significantly to the removal of environmentally hazardous ions from desalination concentrate. There are two methods to measure ion removal: measuring ions accumulated by algae, and measuring the decrease of ions in the medium. The second method was used in this experiment to analyze ion removal.

For this purpose, TDS, EC, and TN were measured daily. The ion content of concentrate was determined from the first and final days.

3.6.2.1 Salinity (TDS and EC)

TDS and EC were measured using a sensION5 Conductivity Meter.

3.6.2.2 Total Nitrogen analysis

Combining the SHIMADZO TNM-1 with a SHIMADZO TOC-VCS/CP analyzer creates a total organic carbon (TOC)/ total nitrogen (TN) simultaneous analysis system which was used for TN analysis in this experiment. The analysis was conducted at the Freeport-McMoRan Water Quality Lab at New Mexico State University.

3.6.2.3 Ion content analysis

Ion content of the concentrate medium was analyzed using a DIONEX ICS-3000 Ion Chromatography System.

Chapter 4

Results and Discussion

4.1 Introduction

A full factorial design experiment with CRD arrangement was conducted for two reasons: (1) to evaluate the growth of the two strains of microalgae (factor A), *Nannochloropsis oculata* (UTEX-LB 2164) and *Dunaliella tertiolecta* (UTEX-LB 999), in a concentrate from water desalination units; and (2) to investigate ion removal from concentrate by these two strains. Four different media (factor B) (concentrate, f/2, a 50:50 combination of f/2 and concentrate, and deionized water) were used to compare microalgae growth. For this purpose, two one-way experiments were run simultaneously to form a full factorial experiment each for ten days. This chapter presents the results obtained from these experiments.

4.2 Experiment 1

In this part of the experiment, *Dunaliella tertiolecta* (UTEX-LB 999) was used in order to investigate the microalgae growth in a concentrate medium with TDS of 6240 ppm. The concentrate solution was obtained from the concentrate disposal of the RO desalination pilot plant in BGNDRF, Alamogordo, New Mexico. Lab scale photobioreactors were used for conducting this experiment. Besides concentrate, three other media were used (f/2, a 50:50 combination of f/2 and concentrate, and deionized water). The deionized water medium was incorporated into this experiment as a control due to the fact that this medium contains no nutrients. Table 4.1 shows the specifications of the media used.

For each combination of microalgae and medium, four replications were considered. Thus, sixteen runs for a period of 10 days were conducted for the required data. Optical density at 750 nm, pH, TDS, electroconductivity and total nitrogen were monitored daily; in addition, the dry biomass and ion content of the concentrate medium were measured on first day and last day. All factors that might affect the biomass growth were kept as constant as possible in order to clarify the effects of algae type and medium on biomass growth.

4.2.1 Algae growth

The initial dry weight biomass was determined by taking three 50 ml samples at three different levels of the glass carboy in which the inoculum algae was located. Each photobioreactor started with 0.052 g of initial biomass. After ten days, the final biomass of all samples was measured. By using the following formula, the percent increase in biomass was calculated for all samples.

$$\frac{(Final\ dry\ weight) - (Initial\ dry\ weight)}{(Initial\ dry\ weight)} \times 100 = (\% \text{ Increase in Biomass})$$

Figure 4.1 depicts the effect of medium on percent increase in biomass. The P-value of 0.004 shows a significant difference in biomass production in different media compared with DI water as control.

Concentrate was the medium that maximized biomass production, and there were no significant differences in percent increase of biomass among other media that did not contain concentrate. This analysis reveals that the high salinity and nutrients available in concentrate provided a better environment for this strain of marine algae to grow than other media. High concentrations of nitrate, phosphate, and NaCl could be possible reasons behind this increased growth.

Compared to f/2 medium, the 50:50 medium demonstrated better performance because it contained the nutrients of both f/2 and the concentrate. This result shows that nutrients available in concentrate can still contribute to algae growth when the nutrients in f/2 are diminishing. Furthermore, there was no significant difference between the growths of the biomass in the f/2 medium when compared with the deionized water medium. This result is because the inoculum algae added to the culture medium were pre-cultivated in f/2 (refer to 3.2); therefore, 20% of deionized water medium was actually f/2. The reason that the percent increase in biomass was used as a measure instead of the actual weight of the biomass increase is that these experimental results were intended to be compared with the results of the second experiment (experiment 2). Since the initial biomasses for these strains of algae were not same, the percent increase is a better criterion for comparison.

Figure 4.2 displays the growth curve for four different media during the ten days of experimentation.

The results obtained from optical density at 750 nm confirm the results obtained from dry weight biomass.

Similar to the results gained from the dry weight test, algae grown in concentrate consistently had the highest optical density from day five to day ten. Aside from concentrate, 50:50 and f/2 media had the next highest optical densities, respectively.

During the first three days, the growth trends in all media were slow and almost the same because the algae cultures are in their lag phases. On the fourth day, the cultures began their exponential phases, which appear to be when the differences in media manifest themselves. The rates of the increase in concentrate and 50:50 media were significantly higher than those in f/2 medium during the exponential phase due to the high concentrations of nitrate and phosphate available in concentrate. *Dunaliella tertiolecta* can accumulate 70% lipid content when salinity is high; however, their high salinity in the initial phase inhibits the cell growth (Takagi, 2006).

On the eighth day, the algae growth in the concentrate medium slowed, mostly because of a depletion of nutrients. The role of light was also important in this stage because the culture becomes very dense and turbid, inhibiting light penetration, especially in the middle of the reactor. However, since the algae cultivated in f/2 and deionized water did not become overly dense, light

penetration was better than in the other media. Hence, they did not exhibit the same inhibitory factor for photosynthesis that the strain in the concentrate medium experienced. It is anticipated that continuation of the experiment for few more days would have resulted in a similar outcome for the cultures cultivated in f/2 and deionized water, which would eventually collapse due to their photosynthetic inhibitions. Based on the results shown in Fig 4.2, the best day for harvesting *Dunaliella tertiolecta* from concentrate is either the ninth or tenth day.

4.2.2 Ion removal

In the preliminary phases of growth, the intracellular substance content—such as lipids and proteins—is relatively low because nutrients are used for biomass production. Once the culture reaches the stable phase, the microalgae begin to accumulate lipids. Furthermore, higher biomass production in a culture results in additional ion reduction. Since removing ions from concentrate for environmental reasons is an important goal of algal concentration processing, TDS, EC, and TN were measured daily; moreover, the ion content of concentrate was determined in the first and final days.

4.3 shows TN removal trending over the period of the experiment, revealing that *Dunaliella tertiolecta* can significantly reduce the nitrogen from concentrate. An exponential regression fit was obtained with an R-squared value of 0.99 (figure 4.3).

The nitrogen removal yield (Y_N) was 0.93, which is considerable, and the volumetric rate of N removal (Q_N) was $1.99 \text{ mg}\cdot\text{dm}^{-3}\cdot\text{day}^{-1}$.

Nitrogen removal is biotic. Since nitrogen is needed for biomass growth, a high nitrogen concentration is important to support the reproduction of microalgae cells. However, the nitrogen concentration is eventually depleted and remains at a level that only supports the synthesis of enzymes and critical cell formation. Under this condition, available carbons are converted into lipids rather than proteins, which slows algal growth because proteins are necessary for continued algal growth (Suali and Sarbatly, 2012). This accentuates the importance of nitrogen removal.

An exponential regression fit was obtained with an R-squared value of 97.8% between total nitrogen and optical density at 750 nm as shown in figure 4.4.

Figure 4.4 shows that a high concentration of nitrogen resulted in a high rate of growth, and shows that when the nitrogen concentration was reduced, the growth rate was also reduced. Under nitrogen deficiency, cells accumulate lipids instead of reproducing.

In addition to TN, the amount of some ions in the concentrate medium was measured in the first and final days. Only ions that are important for algae growth were measured (refer to chapter 2). Table 4.2 and table 4.3 display the concentration of these ions.

The contribution of *Dunaliella tertiolecta* to fluoride, nitrate, and phosphate removal was significant. Phosphorous is removed by two mechanisms: biotic removal, and abiotic removal by chemical perception by forming complex with metal ions. Therefore, phosphorous must be provided in excess because not

all phosphorous is bioavailable. One of the factors that can affect nitrate removal yield is the nitrate level in the medium. Lower nitrate concentration results in higher removal. Overall, TDS of concentrate decreased from 6290 to 5802.5 mg/l and electroconductivity was reduced from 10,180 to 9455 $\mu\text{S}/\text{cm}$.

4.3 Experiment 2

In this portion of the experimental process, *Nannochloropsis oculata* (UTEX- LB 2164) was used. All the conditions were similar to those in Experiment 1. Sixteen runs were performed in order to obtain the data required for assessing the various combinations of media.

4.3.1 Algae growth

The initial biomass was 0.043 g. Figure 4.5 shows the effect of the medium on percent increase in biomass. The P-value of less than 0.0001 shows a significant difference in biomass production in different media.

Again, concentrate was the medium that produced the greatest amount of biomass, and the 50:50 medium produced a larger biomass than the f/2 medium. However, the deionized water and f/2 media showed little difference statistically. Again, high concentrations of some ions – such as nitrate, phosphate and NaCl – were an important parameter causing this difference.

Figure 4.6 depicts the growth curve for the different media in this experiment.

The results obtained from optical density at 750 nm are similar to the results from dry biomass measurement. The vertex point for max biomass happened in the seventh day of the experiment for f/2 and deionized water, indicating that the nutrients in f/2 were diminishing; consequently, growth of algae was decreasing. Lack of nutrients in f/2 and deionized water media caused the stationary phase to be almost one day, which, compared to the other media, was considerably shorter. Thus, the high salinity of concentrate is one of the advantages that can help continuous algae growth. This high salinity of concentrate further explains why the 50:50 medium was still growing after the seventh day.

4.3.2 Ion removal

Figure 4.7 shows TN removal trends over time, which clearly demonstrates that *Nannochloropsis oculata* can meaningfully lessen the amount of nitrogen in concentrate in a similar fashion to the other strain of algae used in this experiment.

An exponential regression fit was obtained with an R-squared value of 0.97. The equation is shown in figure 4.9. The ANOVA table (table 4.5) verifies the accuracy of the model (P-value < 0.00001).

The nitrogen removal yield (Y_N) was 0.91 and volumetric rate of nitrogen removal (Q_N) was $1.81 \text{ mg}\cdot\text{dm}^{-3}\cdot\text{day}^{-1}$.

An exponential regression fit for total nitrogen and optical density at 750 nm has an R-squared value of 99% (P-value < 0.00001) (figure 4.8).

Table 4.6 and table 4.7 show anion and cation concentrations in the samples. Similar to *Dunaliella tertiolecta*, *Nannochloropsis oculata* removed fluoride, nitrate, and phosphate significantly. Since the experiment was designed to avoid cross contamination and because the experiment used pure algae, ion removal was performed by the algae and not any other organisms. TDS of the concentrate decreased from 6270 to 4930 mg/l while EC reduced from 10200 to 8170 $\mu\text{S}/\text{cm}$.

4.4 Growth comparison

The full factorial experiment (factor 1: algae, factor 2: medium), with two levels for factor 1: algae, and four levels for factor 2: medium, considered the interaction of these two factors. Analyzing algae type, medium, and the interaction between the algae and the medium indicated some effects on final biomass production.

Figure 4.9 shows there is no significant difference between levels of factor 1: algae in biomass increase in *Nannochloropsis oculata* (UTEX- LB 2164) and *Dunaliella tertiolecta* (UTEX-LB 999) (P-value = 0.35).

Results show significant variations in dry biomass produced by the four media (P-value < 0.0001). Figure 4.10 illustrates two observations: (1) a significant difference in dry biomass production was observed when concentrate was used, and (2) there was a significant biomass increase in 50:50 medium when compared to f/2. Deionized water and f/2 were essentially the same in terms of percentage increase in biomass because the inoculum of algae used was pre-cultured in f/2; as a result, it contained practically all the main nutrients of f/2.

There were no significant differences among interactions (P-value = 0.2470). Figure 4.11 demonstrates that the interaction of the concentrate medium with *Dunaliella tertiolecta* (UTEX-LB 999) produced the highest dry biomass. The interaction of concentrate medium with *Nannochloropsis oculata* (UTEX- LB 2164) was substantial as well. Interactions of 50:50 medium with both strains of algae yielded considerable amounts of dry biomass, but these amounts were significantly less than the biomass produced in the concentrate medium. Since concentrate alone is less expensive than f/2, concentrate is a better choice than both the 50:50 and f/2 media.

Based on results obtained from dry weight biomass, two kinetic parameters are calculated. Table 4.6 shows volumetric growth rate and specific growth rate, calculated for eight combinations of algae and medium. Specific growth rate could be obtained by using following equation:

$$\mu = \text{Ln} (m_t / m_0) / t \quad (4-1)$$

Volumetric growth rate could be obtained from following equation:

$$Q_x = C_t - C_0 / t \quad (4-2)$$

Based on specific growth rate, the cell concentration of *Dunaliella tertiolecta* in concentrate during the log phase is calculated by the following equation, where C is the cell concentration at any time t (gr/ml):

$$C=1.3*10^{-4}e^{0.19t} \quad (4-3)$$

$1.3*10^{-4}$ is the initial cell concentration (C_0) and 0.19 is the specific growth rate (μ) of *Dunaliella* in concentrate medium.

The equation for *Nannochloropsis oculata* cell concentration is:

$$C=1.075*10^{-4}e^{0.18t} \quad (4-4)$$

For comparison, the growth curve of two cultures of algae in concentrate medium is shown in figure 4.12.

The results indicate that in concentrate medium, *Dunaliella tertiolecta* had a longer lag phase; however, its rate of the growth in the lag phase was higher than that of *Nannochloropsis oculata*.

4.5 Ion removal comparison

For better comparison of the two strains' contributions to concentrate treatment, the results of TN removal and ion removal are shown in table 4.9 and table 4.10, respectively.

Y and Q are removal yield and volumetric removal rate, respectively, which can be obtained from following equations:

$$Y= C_0-C_t/C_0 \quad (4-5)$$

$$Q= C_0-C_t/t \quad (4-6)$$

The elementary composition and C: P: N ratio of microalgal cells usually varies with the strain type; therefore, the absorptive capability of nitrogen and phosphorous may be different for different species of microalgae. Molecular ratios of carbon, nitrogen, and phosphorus in marine algae, usually C: N: P = 106:16:1, allow them to grow quickly and uptake the nutrients available in waste water and salty water. This result from research shows a similar conclusion when the concentrate was used in this experiment. This uptake can occur especially quickly in water bodies with high concentrations of N and P (Lundquist, 2008).

Growth rates of microalgae can also be based on the source of nitrogen present in the body of water. For instance, NH_4^+ can influence growth rate more than urea and nitrate. However, NO_3^- can be removed faster than NH_4^+ and urea. Since the concentrate used in this experiment did not have NH_4^+ available, the growth was not as fast as when it is available. Since the main source of the nitrogen in this experiment was nitrate, the removal yield was high by both strains of algae, as illustrated in table 4.9.

The previous two tables and figure 4.13 reveal that there was no meaningful difference between the two strains of algae for nitrogen and ion removal in terms of statistics.

Figure 4.14 and figure 4.15 show that the TDS and electroconductivity decreased in the concentrate medium during the experiment period as a result of the algae species *Nannochloropsis oculata* and *Dunaliella tertiolecta*.

The presence of ions such as potassium, chloride, sodium, calcium, and sulphate caused high TDS (Bishnoi & Arora, 2007). Table 4.8 shows that these ions were not removed significantly, indicating that TDS was not decreased considerably. The same scenario exists for EC because TDS and EC have the following relationship:

$$\text{TDS} = k_e \text{EC}$$

Where k_e is a correlation factor varying between 0.55 and 0.8 based on the temperature and water type.

Chapter 5 Conclusion

5.1 Conclusion

A full factorial design experiment was developed to investigate algal growth in the desalination concentrate from water desalination units in lab scale photobioreactors. Simultaneously, ion removal from concentrate by algal cultures was examined.

Based on research findings, an optimal match between algae and medium was identified. These findings indicated that, among all the investigated media, a concentrate medium maximized the percentage increase of dry weight biomass better than an f/2 medium, which is a conventional and accepted medium for growing marine algae. The results of optical density at 750 nm conveyed the same result as well.

There was no significant difference in biomass production and ion removal from concentrate between *Nannochloropsis oculata* (UTEX- LB 2164) and *Dunaliella tertiolecta* (UTEX-LB 999). Both strains are acceptable for the purpose of biomass production and ion removal; however, the combination of *Dunaliella tertiolecta* and concentrate medium yielded the highest biomass production.

Since temperature, light cycle, light intensity, air flow, and other conditions were controlled among the four growth media, it can be reasonably concluded that the differences in results were due to the growth media. The variables under study in this experiment, algae and medium, had different effects on the growth rates and biomass production. Based on statistical analysis, there is sufficient evidence to indicate significant increases in biomass occurred due to the selection of specific combinations of medium and algae.

The contribution of algal cultures in the removal of some ions from concentrate was not significant other than for specific ions, such as nitrate, phosphate and fluoride; however, TN decreased considerably during the experiment. TDS did not change considerably because the ions responsible for high TDS were not removed noticeably.

Based on the findings, it can be concluded that the cultivation of marine algae strains in the concentrate disposal of water desalination units is a unique approach that combines an increased efficiency in the removal of pollutants from concentrate with the cultivation of algal biomass for biofuel feedstock production. The results of this research identify a potential to reduce the cost of desalination when biofuel production is included, and can bring about environmentally-friendly benefits, such as CO₂ mitigation and concentrate disposal treatment.

5.2 Recommendations

The next step to continue this study could be to investigate the effect of concentrate on the growth of other strains of algae that have the capability to survive in saline environments. Increasing the amount of inoculum of algae would lead to the acquisition of more reliable results because of the relationship between initial biomass and growth rates. Also, using immobilized algae instead of suspended algae would encourage better ion removal because immobilized algae would increase the effective surface area for reaction. To ensure that all ion removal is done by algae and not by other organisms that may have contaminated the experiment, it would also be a good idea to: 1) measure the nutrient uptake by algae, 2) measure ion removal from the medium, and 3) correlate these two results to find out how much of this removal is done by algae. Also, examining different combinations of f/2 and concentrate, such as 25:75 and 75:25, might yield additional interesting results.

Another option for future studies could be analyzing the economic feasibility of the complete process of biofuel generation and desalination concentrate treatment process (figure 5.1).

References

- Ackman RG, Tocher CS, McLachlan J (1968). Marine phytoplankton fatty acid. *Journal of the Fisheries Research Board of Canada*. 25: 1603-1620.
- Adey WH, Loveland K (2007). *Dynamic aquaria: building living ecosystems*. 3rd Edn, Academic Press, New York, USA.
- Akkerman, I., Janssen, M., Rocha, J., & Wijffels, R. H. (2002). Photobiological hydrogen production: Photochemical efficiency and bioreactor design. In *International Journal of Hydrogen Energy*. 27, 1195–1208.
- Amin, S. (2009). Review on biofuel oil and gas production processes from microalgae. *Energy Conversion and Management*. 50(7). 1834–1840.
- Antoni, D., Zverlov, V. V, & Schwarz, W. H. (2007). Biofuels from microbes. *Applied Microbiology and Biotechnology*, 77, 23–35.
- Antoni, D.; Zverlov, V.V.; Schwarz, H. (2007) Biofuels from Microbes. *Applied Microbiology and Biotechnology*. 77. 23-35.
- Apt K., E., Behrens, P., W. (1999) Commercial development in microalgal biotechnology. *Journal of Phycology*. 35. 215-226.
- Armaroli, N., & Balzani, V. (2006). The future of energy supply: challenges and opportunities. *Angew. Chem., Int. Ed.*, 46, 52–66.
- Awasthi, M., & Singh, R. K. (2011). Development of algae for the production of bioethanol, biomethane, biohydrogen and biodiesel, 14–23.
- Barbosa, M. (2003). *Microalgal photobioreactors : - up and optimisation Scale*. Wageningen Food and Bioprocess Engineering Group.1–166.
- Barnwal, B. K., & Sharma, M. P. (2005). Prospects of biodiesel production from vegetable oils in India. *Renewable and Sustainable Energy Reviews*, 9, 363-378
- Becker EW. (1994) In: Baddiley J et al., editors. *Microalgae: biotechnology and microbiology*. Cambridge (New York): Cambridge Univ. Press.
- Belarbi, E. H., Molina, E., & Chisti, Y. (2000). A process for high yield and scaleable recovery of high purity eicosapentaenoic acid esters from microalgae and fish oil. *Enzyme and Microbial Technology*, 26, 516–529.

Belessiotis, V., & Delyannis, E. (2001). Water shortage and renewable energies (RE) desalination - Possible technological applications. *Desalination*, 139, 133–138.

Benemann, J. R., & Oswald, W. J. (1996). Systems and Economic Analysis of Microalgae Ponds for Conversion of CO₂ to Biomass. *Final Report to the Department of Energy, Pittsburgh Energy Technology Center*. 260.

Bigogno, C., Khozin-Goldberg, I., Boussiba, S., Vonshak, A., & Cohen, Z. (2002). Lipid and fatty acid composition of the green oleaginous alga *Parietochloris incisa*, the richest plant source of arachidonic acid. *Phytochemistry*, 60, 497–503.

Bilanovic D, Shelef G, Sukenik A (1988). Flocculation of microalgae with cationic polymers: effects of medium salinity. *Biomass* 17. 65-76.

Biofuels Media Ltd (2007) Bringing the biofuel markets together. In: Algae: feedstock of the future. <http://www.biofuelsmedia.com/press>. Accessed 8 Sep 2008

Bishnoi, M., & Arora, S. (2007) Potable groundwater quality in some villages of Haryana, India: focus on fluoride. *Journal of Environmental Biology / Academy of Environmental Biology, India*. 28(2), 291–4.

Borowitzka M.A. (1999) Pharmaceuticals and agrochemicals from microalgae. In: Cohen Z, editor. *Chemicals from microalgae*. Taylor & Francis. 313–52.

Briens, C., Piskorz, J., & Berruti, F. (2008). Biomass Valorization for Fuel and Chemicals Production -- A Review. *International Journal of Chemical Reactor Engineering*. 6: 1-49.

Brown, M. R., Jeffrey, S. W., Volkman, J. K., & Dunstan, G. A. (1997). Nutritional properties of microalgae for mariculture. In *Aquaculture*. 151, 315–331.

Camacho Rubio, F., Fernandez, F., Perez, J., Camacho, F., & Grima, E. (1999). Prediction of dissolved oxygen and carbon dioxide concentration profiles in tubular photobioreactors for microalgal culture. *Biotechnology and Bioengineering*, 62, 71–86.

Camacho, F. G., Rodríguez, J. G., Mirón, A. S., García, M. C. C., Belarbi, E. H., Chisti, Y., & Grima, E. M. (2007). Biotechnological significance of toxic marine dinoflagellates. *Biotechnology Advances*. 25.176–94.

Campbell CJ (1997) *the coming oil crisis*. Multi-science Publishing Company and petroconsultants S.A, Essex, England

Campbell, M. N. (2008). Biodiesel : Algae as a Renewable Source for Liquid Fuel. *Guelph Engineering Journal*, 1, 2–7.

Canakci, M., & Gerpen, J. Van. (2001). Biodiesel production from oils and fats with high free fatty acids. *Transactions of the ASAE*, 44, 1429–1436.

Canakci, M., & Sanli, H. (2008). Biodiesel production from various feedstocks and their effects on the fuel properties. *Journal of Industrial Microbiology & Biotechnology*, 35, 431–441.

Carvalho A.P., Meireles L.A., Malcata F.X. (2006) Microalgal reactors: a review of enclosed system designs and performances. *Biotechnol Prog*, 22.1490–506.

Chisti, Y. (2008). Biodiesel from microalgae beats bioethanol. *Trends in Biotechnology*.26 (3), 126-31.

Chynoweth DP, Turick CE, Owens JM, Jerger DE, Peck MW (1993). Biochemical methane potential of biomass and waste feedstocks. *Biomass and Bioenergy* 5: 95-111.

Chynoweth DP, Turick CE, Owens JM, Jerger DE, Peck MW (1993). Biochemical methane potential of biomass and waste feedstocks. *Biomass and Bioenergy* 5: 95-111.

Conover SAM (1975). Partitioning of Nitrogen and Carbon in Cultures of the Marin Diatom *Thalassiosira Fluviatilis* Supplied with Nitrate, Ammonium or Urea. *Mar Biol* 32: 231.

Cravotto G, Boffa L, Mantegna S, Perego P, Avogadro M, Cintas P. (2008) Improved extraction of vegetable oils under high-intensity ultrasound and/or microwaves. *Ultrasonics Sonochemistry*. 15(5).898–902.

Crump, J. A., & Mintz, E. D. (2010). Global trends in typhoid and paratyphoid Fever. *Clinical Infectious Diseases : An Official Publication of the Infectious Diseases Society of America*, 50, 241–246.

Crutzen, P. J., Mosier, A. R., Smith, K. A., & Winiwarter, W. (2007). N₂O release from agro-biofuel production negates global warming reduction by replacing fossil fuels. *Atmospheric Chemistry and Physics Discussions*. 7, 11191-11205.

Da Silva, T. L., Reis, A., Medeiros, R., Oliveira, A. C., & Gouveia, L. (2009). Oil production towards biofuel from autotrophic microalgae semicontinuous

cultivations monitorized by flow cytometry. *Applied Biochemistry and Biotechnology*, 159, 568–578.

Demirbas A. (2008) Biofuels sources, biofuel policy, biofuel economy and global biofuel projections. *Energy Convers Manage* (49:2) 106–16.

Demirbas A. (2009) Future energy sources: part I. *Future Energy Sources*, 1, 1–95.

Demirbas AH. (2009) Inexpensive oil and fats feedstocks for production of biodiesel. *Energy Education Science Technology*, 23, 1–13.

Demirbas, A. H.; Demirbas, I. (2007) Importance of Rural Bioenergy for Developing Countries. *Energy Conversion and Management*, 48(8), 2386-2398.

Demirbas, A., & Fatih Demirbas, M. (2011). Importance of algae oil as a source of biodiesel. *Energy Conversion and Management*. 52(1).163–170.

Dinh, L. T. T., Dinh, L. T. T., Guo, Y. Y., Guo, Y. Y., Mannan, M. S., & Mannan, M. S. (2009). Sustainability Evaluation of Biodiesel Production Using Multicriteria Decision-Making. *Environmental Progress & Sustainable Energy*, 28, 38–46.

Dunahay, T. G., Jarvis, E. E., Dais, S. S., & Roessler, P. G. (1996). Manipulation of microalgal lipid production using genetic engineering. *Applied Biochemistry and Biotechnology*, 57–58, 223–31.

Duranceau, S. J. (2001). Reverse Osmosis and Nanofiltration Technology: Inorganic, Softening and Organic Control. (paper presented at the American Membrane Technology Association's Annual Symposium, Isle of Palms, S.C., August 5-8, 2001).

Eriksen, N. T. (2008). The technology of microalgal culturing. *Biotechnology Letters*, 30, 1525–1536.

Fargione, J., Hill, J., Tilman, D., Polasky, S., & Hawthorne, P. (2008). Land clearing and the biofuel carbon debt. *Science (New York, N.Y.)*, 319, 1235–1238.

Felizardo, P., Neiva Correia, M. J., Raposo, I., Mendes, J. F., Berkemeier, R., & Bordado, J. M. (2006). Production of biodiesel from waste frying oils. *Waste Management*, 26, 487–494.

Foster, R., M. Ghassemi, and A. Cota, (2009). *Solar Energy: Renewable Energy and the Environment*. CRC Press: New York.

- Fukuda, H., Kondo, A., & Noda, H. (2001). Biodiesel fuel production by transesterification of oils. *Journal of Bioscience and Bioengineering*, 92, 405-416.
- Gaffron, H., & Rubin, J. (1942). Fermentative and photochemical production of hydrogen in algae. *The Journal of General Physiology*, 26, 219-240.
- Gavrilescu, M., & Chisti, Y. (2005). Biotechnology - A sustainable alternative for chemical industry. *Biotechnology Advances*, 23, 471-99.
- Ghirardi, M. L., Zhang, L., Lee, J. W., Flynn, T., Seibert, M., Greenbaum, E., & Melis, A. (2000). Microalgae: A green source of renewable H₂. *Trends in Biotechnology*, 18, 506-11.
- Goudriaan, F., Van De Beld, B., Boerefijn, F. R., Bos, G. M., Naber, J. E., Van Der Wal, S., & Zeevalkink, J. A. (2000). Thermal efficiency of the HTU® process for biomass liquefaction. *Progress in Thermochemical Biomass Conversion*, 1325, 1312-1325.
- Gouveia, L., & Oliveira, A. C. (2009). Microalgae as a raw material for biofuels production. *Journal of Industrial Microbiology & Biotechnology*, 36(2), 269-74.
- Gouveia, L., & Oliveira, A. C. (2009). Microalgae as a raw material for biofuels production. *Journal of Industrial Microbiology & Biotechnology*, 36, 269-274.
- Griffiths, M.J., Garcin, C., van Hille, R.P., Harrison, S.T.L. (2011) Interference by pigment in the estimation of microalgal biomass concentration by optical density, *Journal of Microbiological Methods*, 85, 119-123.
- Grobbelaar, J. U. (2004). Algal Nutrition. *Handbook of microalgal culture: biotechnology and applied phycology*, 97-115.
- Grobbelaar, J. U. (2009). Factors governing algal growth in photobioreactors: the “open” versus “closed” debate. *Journal of Applied Phycology*, 21, 489-492.
- Guillard, R. R. L. (1975). Culture of Phytoplankton for Feeding Marine Invertebrates. In *Culture of Marine Invertebrate Animals*. 29-60.
- Hacisalihoglu B, Kirtay E, Demirbas A. (2009) Historical role of Turkey in petroleum between Caspian Sea Basin and the Middle East. *Soc Polit Econ Cultural Res* ,1, 1-25.

Harris EH (1989). The *Chlamydomonas* sourcebook: a comprehensive guide to biology and laboratory use. Academic Press, San Diego, USA.

Heasman, M., Diemar, J., O'connor, W., Sushames, T., & Foulkes, L. (2000). Development of extended shelf-life microalgae concentrate diets harvested by centrifugation for bivalve molluscs ± a summary. *Aquaculture Research*, 31, 637–659.

Hodaifa, G., Martínez, M. E., & Sánchez, S. (2008). Use of industrial wastewater from olive-oil extraction for biomass production of *Scenedesmus obliquus*. *Bioresource Technology*, 99, 1111–1117.

International Energy Agency (2007) World Energy Outlook 2007. China and India Insights.

Kadam, K. L. (1997). Power plant flue gas as a source of CO₂ for microalgae cultivation: Economic impact of different process options. *Energy Conversion and Management*. 38. 505–10.

Kaewpintong, K., Shotipruk, A., Powtongsook, S., & Pavasant, P. (2007). Photoautotrophic high-density cultivation of vegetative cells of *Haematococcus pluvialis* in airlift bioreactor. *Bioresource Technology*, 98, 288–295.

Karen, P. F., and Marven, W. F. (2007) Observation on diversity and ecology of freshwater *Nannochloropsis*(Eustigmatophyceae), with description of new taxa. *Protist*, 158, 325-336.

Kim, W., Park, J., Gim, G., Jeong, S.-H., Kang, C., Kim, D.-J., and Kim, S.(2012) Optimization of culture conditions and comparison of biomass productivity of three green algae. *Bioprocess and Biosystems Engineering*.35(1-2), 19-27.

Klass. D.L. (1998) *Biomass for Renewable Energy, Fuels, and Chemicals*; Academic Press: San Diego, USA, 651.

Klass. D.L. (1998) *Biomass for Renewable Energy, Fuels, and Chemicals*; Academic Press: San Diego, USA, 651.

Klass. D.L. (1998)*Biomass for Renewable Energy, Fuels, and Chemicals*; Academic Press: San Diego,USA, 651.

Kong, Q.; Yu, F.; Chen, P.; Ruan. R. High Oil Content Microalgae Selection for Biodiesel Production. (2007) ASABE Annual International Meeting, Minneapolis, Minnesota, USA, June 17-20; American Society

of Agricultural and Biological Engineers: St. Joseph, Michigan, USA, 2007; 077034.

Koonin, S. E. (2006). Getting serious about biofuels. *Science (New York, N.Y.)*, 311, 435.

Kulkarni, M. G., & Dalai, A. K. (2006). Waste Cooking Oil An Economical Source for Biodiesel: A Review. *Ind. Eng. Chem. Res.*, 45, 2901–2913.

Lee, Y.K. & Shen, H. (2004) Basic culturing techniques. Handbook of Microalgal Culture. Biotechnological and Applied phycology (ed. A. Richmond). 40-56. Black-well Publishing, Oxford

Leitner G. F. (1998) "Is there a water crisis?," *International Desalination and Water Reuse Quarterly*, vol. 7, p. 10, 1998.

Li Y, Horsman M, Wu N, Lan CQ, Dubois-Calero N. Biofuels from microalgae. *Biotechnology Progress* 2008, 24(4), 815–20.

Lívanský, K., Doucha, J., Straka, F. (2005). Utilization of flue gas for cultivation of microalgae *Chlorella* sp.) In an outdoor open thin-layer photobioreactor. *Journal of Applied Phycology*. 17. 403-412.

Lundquist T.J. (2008) Production of algae in conjunction with wastewater treatment. In: NREL—AFOSR workshop on algal oil for jet fuel production.

Mallick, N. (2002). Biotechnological potential of immobilized algae for wastewater N, P and metal removal: a review. *Biometals : An International Journal on the Role of Metal Ions in Biology, Biochemistry, and Medicine*, 15, 377–390.

Mata, T. M., Martins, A. a., & Caetano, N. S. (2010). Microalgae for biodiesel production and other applications: A review. *Renewable and Sustainable Energy Reviews*, 14(1), 217–232.

McKendry P. (2003) Energy production from biomass (part 2): conversion technologies. *Biores Technol.* 83:47–54.

McKendry P. Energy production from biomass (part 2): conversion technologies. *Biores Technol* 2003, 83, 47–54.

McKendry P. (2003) Energy production from biomass (part 2): conversion technologies. *Biores Technol* .83, 47–54.

MELIS, A. (2002). Green alga hydrogen production: progress, challenges and prospects. *International Journal of Hydrogen Energy*. 27.1217–28.

- Meng, X., Yang, J., Xu, X., Zhang, L., Nie, Q., & Xian, M. (2009). Biodiesel production from oleaginous microorganisms. *Renewable Energy*, 34, 1-5
- Metting, F. B. (1996). Biodiversity and application of microalgae. *Journal of Industrial Microbiology & Biotechnology*, 17, 477-89.
- Miao, X., Wu, Q., & Yang, C. (2004). Fast pyrolysis of microalgae to produce renewable fuels. *Journal of Analytical and Applied Pyrolysis*, 71, 855-863.
- Mickley, M.C. 2001. Major Ion Toxicity in Membrane Concentrates. AWWA Research Foundation Project # 290.
- Miller, J. (2003). Review of water resources and desalination technologies. *Sandia National Laboratories Report, SAND2003-0800*, 3-54.
- Minowa, T., Yokoyama, S., Kishimoto, M., & Okakura, T. (1995). Oil production from algal cells of *Dunaliella tertiolecta* by direct thermochemical liquefaction. *Fuel*, 74, 1731-8.
- Moheimani, N. R., & Borowitzka, P. M. (2005). *The culture of Coccolithophorid algae for carbon dioxide bioremediation*. *Algal Biotechnology Laboratory*. Retrieved from <http://www.lib.murdoch.edu.au/adt/browse/view/adt-MU20050901.140745>
- Molina Grima E. (1999) Microalgae, mass culture methods. In: Flickinger MC, Drew SW, editors. *Encyclopedia of bioprocess technology: fermentation, biocatalysis and bioseparation*, vol. 3. Wiley, 1753-69.
- Molina Grima E. Microalgae, mass culture methods. In: Flickinger MC, Drew SW, editors. *Encyclopedia of bioprocess technology: fermentation, biocatalysis and bioseparation*, vol. 3. Wiley; 1999. p. 1753-69.
- Molina Grima, E., Belarbi, E. H., Ación Fernández, F. G., Robles Medina, A., & Chisti, Y. (2003). Recovery of microalgal biomass and metabolites: Process options and economics. *Biotechnology Advances*, 20(7-8), 491-515.
- Molina, E., Fernández, J., Ación, F. G., & Chisti, Y. (2001). Tubular photobioreactor design for algal cultures. In *Journal of Biotechnology*, 92, 113-131.
- Nagle, N., & Lemke, P. (1990). Production of methyl ester fuel from microalgae. *Applied Biochemistry and Biotechnology*, 24-5:355-61.
- Oilgae Report 2010, Academic Edition, Tamilnadu, India.

- Oki, T., & Kanae, S. (2006). Global hydrological cycles and world water resources. *Science (New York, N.Y.)*, 313, 1068–1072.
- Ono, E., Cuello, J.L. (2004) Design parameters of solar concentrating systems for CO₂-mitigating algal photobioreactors. *Energy*. 29. 1651–1657.
- Ormerod WG, Freund P, Smith A, Davison J. (2002) Ocean storage of CO₂. IEA greenhouse gas R&D programme. UK: International Energy Agency
- Patil, V., Reitan, K.I., Knudsen, G.; Mortensen, L., Kallqvist, T., Olsen, E., Vogt, G., Gislerød, H.R. (2005) Microalgae as Source of Polyunsaturated Fatty Acids for Aquaculture. *Current Topics in Plant Biology*. 6, 57-65.
- Patil, V., Tran, K.-Q., & Gislerød, H. R. (2008). Towards sustainable production of biofuels from microalgae. *International Journal of Molecular Sciences*. 9(7). 1188–95.
- Paul PFM, Wise WS. The principle of gas extraction, mills and boon. London; 1971.
- Pauw, N., Morales, J., & Persoone, G. (1984). Mass culture of microalgae in aquaculture systems: Progress and constraints. *Hydrobiologia*. 116/117. 121–34.
- Perlack, R. D., Wright, L. L., Turhollow, A. F., Graham, R. L., Stokes, B. J., & Erbach, D. C. (2005). Biomass as Feedstock for a Bioenergy and Bioproducts Industry: The Technical Feasibility of a Billion-Ton Annual Supply. *Agriculture, DOE/GO-102*, 78.
- Pimentel, D., Berger, B., Filiberto, D., Newton, M., Wolfe, B., Karabinakis, E. Nandagopal, S. (2004). Water Resources: Agricultural and Environmental Issues. 54.909–18.
- Pulz, O. (2001). Photobioreactors: production systems for phototrophic microorganisms. *Applied Microbiology and Biotechnology*, 57, 287–293.
- Pulz, O., & Gross, W. (2004). Valuable products from biotechnology of microalgae. *Applied Microbiology and Biotechnology*, 65, 635–648.
- Pushparaj B, Pelosi E, Torzillo G, Materassi R (1993). Microbial biomass recovery using a synthetic cationic polymer. *Bioresour Technol* 43: 59-62.
- Ragauskas, A.J.; Williams, C.K.; Davison, B.H.; Britovsek, G.; Cairney, J.; Eckert, C.A.;

- Ratledge, C. (1993). Single cell oils--have they a biotechnological future? *Trends in Biotechnology*, *11*, 278–284.
- Ratledge, C., & Wynn, J. P. (2002). The biochemistry and molecular biology of lipid accumulation in oleaginous microorganisms. *Advances in Applied Microbiology*, *51*, 1–51.
- Raven, R. P. J. M., & Gregersen, K. H. (2007). Biogas plants in Denmark: successes and setbacks. *Renewable and Sustainable Energy Reviews*. 11.116–32.
- Richardson J.W., Outlaw J.L., Allison M. (2009) Economics of micro algae oil. In: 13th ICABR conference on the emerging bio-economy Ravello. 17–20.
- Richmond, A. (2004). *Handbook of Microalgal Culture: Biotechnology and Applied Phycology*. *Biotechnology* (Vol. 40, p. 577). doi:10.1111/j.1529-8817.2004.40502.x
- Richmond, A. (2004). *Handbook of Microalgal Culture: Biotechnology and Applied Phycology*.
- Richmond, A., Hu, Q. (2013) *Handbook of Microalgal Culture: Applied Phycology and Biotechnology*, Wiley & Sons Publication
- Righelato, R., & Spracklen, D. V. (2007). Environment. Carbon mitigation by biofuels or by saving and restoring forests? *Science (New York, N.Y.)*, *317*, 902.
- Righelato, R., & Spracklen, D. V. (2007). Environment. Carbon mitigation by biofuels or by saving and restoring forests? *Science (New York, N.Y.)*, *317*, 902.
- Roessler, P. G., Brown, L. M., Dunahay, T. G., Heacox, D. A., Jarvis, E. E., Schneider, J. C., Zeiler, K. G. (1994). Genetic Engineering Approaches for Enhanced Production of Biodiesel Fuel from Microalgae. In *Enzymatic Conversion of Biomass for Fuels Production*. 566. 255–270.
- Rosenberg JN, Oyler GA, Wilkinson L, Betenbaugh MJ. (2008) A green light for engineered algae: redirecting metabolism to fuel a biotechnology revolution. *Current Opinion in Biotechnology* .19(5).430–6.
- Sánchez Mirón, A., Cerón García, M. C., Contreras Gómez, A., García Camacho, F., Molina Grima, E., & Chisti, Y. (2003). Shear stress tolerance and biochemical characterization of *Phaeodactylum tricornutum* in quasi steady-state continuous culture in outdoor photobioreactors. *Biochemical Engineering Journal*, *16*, 287–297.

- Sánchez Mirón, A., Cerón García, M. C., Contreras Gómez, A., García Camacho, F., Molina Grima, E., & Chisti, Y. (2003). Shear stress tolerance and biochemical characterization of *Phaeodactylum tricornutum* in quasi steady-state continuous culture in outdoor photobioreactors. *Biochemical Engineering Journal*, *16*, 287–297.
- Sánchez Mirón, A., Cerón García, M. C., Contreras Gómez, A., García Camacho, F., Molina Grima, E., & Chisti, Y. (2003). Shear stress tolerance and biochemical characterization of *Phaeodactylum tricornutum* in quasi steady-state continuous culture in outdoor photobioreactors. *Biochemical Engineering Journal*, *16*, 287–297.
- Sawayama, S., Inoue, S., Dote, Y., & Yokoyama, S.-Y. (1995). CO₂ fixation and oil production through microalga. *Energy Conversion and Management*. *36*, 729–31.
- Sawayama, S., Inoue, S., Dote, Y., & Yokoyama, S.-Y. (1995). CO₂ fixation and oil production through microalga. *Energy Conversion and Management*. *36*, 729-731.
- Sawayama, S., Inoue, S., Dote, Y., & Yokoyama, S.-Y. (1995). CO₂ fixation and oil production through microalga. *Energy Conversion and Management*. *36*, 729–31.
- Schenk, P. M., Thomas-Hall, S. R., Stephens, E., Marx, U. C., Mussnug, J. H., Posten, C., Hankamer, B. (2008). Second Generation Biofuels: High-Efficiency Microalgae for Biodiesel Production. *BioEnergy Research*. 1.20–43.
- Schneider D. (2006) Grow your own? Would the wide spread adoption of biomass-derived transportation fuels really help the environment. *Am Sci* ,94.408–9.
- Schuchardt, U., Sercheli, R., & Matheus, R. (1998). Transesterification of Vegetable Oils : a Review General Aspects of Transesterification Transesterification of Vegetable Oils Acid-Catalyzed Processes Base-Catalyzed Processes. *J. Braz. Chem. Soc.*, *9*, 199–210.
- Sheehan, J., Dunahay, T., Benemann, J., & Roessler, P. (1998). A Look Back at the U.S. Department of Energy's Aquatic Species Program: Biodiesel from Algae. *Renewable Energy*, *328*, 1–328.
- Sheehan, J., Dunahay, T., Benemann, J., & Roessler, P. (1998). A Look Back at the U.S. Department of Energy's Aquatic Species Program: Biodiesel from Algae. *Renewable Energy*, *328*, 1–328.

- Shimizu, Y. (1996). Microalgal metabolites: a new perspective. *Annual Review of Microbiology*, 50, 431–465.
- Shimizu, Y. (2003). Microalgal metabolites. *Current Opinion in Microbiology*. 6. 236-43.
- Sobczuk, T. M., Camacho, F. G., Grima, E. M., & Chisti, Y. (2006). Effects of agitation on the microalgae *Phaeodactylum tricornutum* and *Porphyridium cruentum*. *Bioprocess and Biosystems Engineering*, 28, 243–250.
- Spolaore, P., Joannis-Cassan, C., Duran, E., & Isambert, A. (2006). Commercial applications of microalgae. *Journal of Bioscience and Bioengineering*, 101, 87–96.
- Srivastava, A.; Prasad, R. (2000) Triglycerides-based Diesel Fuels. *Renewable & Sustainable Energy Reviews*. 4.111-133.
- Suali, E., & Sarbatly, R. (2012). Conversion of microalgae to biofuel. *Renewable and Sustainable Energy Reviews*, 16(6), 4316–4342.
- Sukahara, K. T., & Awayama, S. S. (2005). Liquid Fuel Production Using Microalgae. *Journal of the Japan Petroleum Institute*, 48, 251–259.
- Takagi, M., Watanabe, K., Yamaberi, K., & Yoshida, T. (2000). Limited feeding of potassium nitrate for intracellular lipid and triglyceride accumulation of *Nannochloris* sp. UTEX LB1999. *Applied Microbiology and Biotechnology*, 54, 112–117.
- Terry, K. L., & Raymond, L. P. (1985). System design for the autotrophic production of microalgae. *Enzyme and Microbial Technology*, 7, 474–487.
- Tickell J (2000) From the fryer to the fuel tank. The complete guide to using vegetable oil as an alternative fuel. Tallahassee, USA.
- Tredici M.R., Flickinger, M. C., Drew, S. W., & Wiley, J. (1999). *Encyclopedia of Bioprocess Technology : Fermentation , Biocatalysis , and Builder*.1–5, 2844.
- Tschaplinski, T. (2006) The Path Forward for Biofuels and Biomaterials. *Science*. 311. 484-489.
- Ugwu, C. U., Aoyagi, H., & Uchiyama, H. (2008). Photobioreactors for mass cultivation of algae. *Bioresource Technology*. 99.4021–8.

Van Gerpen, J. (2005). Biodiesel processing and production. *Fuel Processing Technology*, 86, 1097–1107.

Wang, B., Li, Y., Wu, N., & Lan, C. Q. (2008). CO₂ bio-mitigation using microalgae. *Applied Microbiology and Biotechnology*, 79, 707–718.

Weisz, P. B. (2004). Basic Choices and Constraints on Long-Term Energy Supplies. *Physics Today*, 57, 47.

Williams, J. A. (2002). Keys to bioreactor selections. *Chemical Engineering Progress*, 98, 34.

Williams, J. A. (2002). Keys to bioreactor selections. *Chemical Engineering Progress*, 98, 34.

Xu, H., Miao, X., & Wu, Q. (2006). High quality biodiesel production from a microalga *Chlorella protothecoides* by heterotrophic growth in fermenters. *Journal of Biotechnology*, 126, 499–507.

Younos, T. (2005). Environmental Issues of Desalination. *Journal of Contemporary Water Research & Education*, 132, 11–18

Younos, T., Tulou, K. E. (2009). Overview of Desalination Techniques. *Journal of Contemporary Water Research & Education*, 132(1), 3–10.

Yun, Y. S., Lee, S. B., Park, J. M., Lee, C. I., & Yang, J. W. (1997). Carbon Dioxide Fixation by Algal Cultivation Using Wastewater Nutrients. *Journal of Chemical Technology Biotechnology*, 69, 451–455.

Tables

Chapter 2

TABLE 2.1 Comparison between different sources of biodiesel (Chisti, 2007)

Crop	Oil yield (L/ha)	Land area needed (M ha) ^a	Percent of existing US cropping area ^a
Corn	172	1540	846
Soybean	446	594	326
Canola	1190	223	122
Jatropha	1892	140	77
Coconut	2689	99	54
Oil palm	5950	45	24
Microalgae ^b	136,900	2	1.1
Microalgae ^c	58,700	4.5	2.5
a	For meeting 50% of all transport fuel needs of the United States.		
b	70% oil (by wt) in biomass.		
c	30% oil (by wt) in biomass.		

TABLE 2.2 Percentage of chemical composition of algae on a dry basis (Demirbas and Demirbas, 2011)

Species of sample	Proteins	Carbohydrates	Lipids	Nucleic acid
<i>Scenedesmus obliquus</i>	50–56	10–17	12–14	3–6
<i>Scenedesmus quadricauda</i>	47	–	1.9	–
<i>Scenedesmus dimorphus</i>	8–18	21–52	16–40	–
<i>Chlamydomonas reinhardtii</i>	48	17	21	–
<i>Chlorella vulgaris</i>	51–58	12–17	14–22	4–5
<i>Chlorella pyrenoidosa</i>	57	26	2	–
<i>Spirogyra sp.</i>	6–20	33–64	11–21	–
<i>Dunaliella bioculata</i>	49	4	8	–
<i>Dunaliella salina</i>	57	32	6	–
<i>Euglena gracilis</i>	39–61	14–18	14–20	–
<i>Prymnesium parvum</i>	28–45	25–33	22–38	1–2
<i>Tetraselmis maculata</i>	52	15	3	–

<i>Porphyridium cruentum</i>	28–39	40–57	9–14	–
<i>Spirulina platensis</i>	46–63	8–14	4–9	2–5
<i>Spirulina maxima</i>	60–71	13–16	6–7	3–4.5
<i>Synechococcus sp.</i>	63	15	11	5
<i>Anabaena cylindrica</i>	43–56	25–30	4–7	–

TABLE 2.3 Oil content of some microalgae (Chisti, 2007)

Microalga	Oil content (% dry wt)
<i>Botryococcus braunii</i>	25–75
<i>Chlorella sp.</i>	28–32
<i>Cryptocodinium cohnii</i>	20
<i>Cylindrotheca sp.</i>	16–37
<i>Dunaliella primolecta</i>	23
<i>Isochrysis sp.</i>	25–33
<i>Monallanthus salina</i>	20
<i>Nannochloris sp.</i>	20–35
<i>Nannochloropsis sp.</i>	31–68
<i>Neochloris oleoabundans</i>	35–54
<i>Nitzschia sp.</i>	45–47
<i>Phaeodactylum tricornutum</i>	20–30
<i>Schizochytrium sp.</i>	50–77
<i>Tetraselmis sueica</i>	15–23

TABLE 2.4 Comparison of photobioreactor and open pond methods (Chisti, 2007; Mata et al., 2010)

Variable	Photobioreactors	Raceway ponds
Annual biomass production (kg)	100,000	100,000
Volumetric productivity(kg m ⁻³ d ⁻¹)	1.535	0.117
Areal productivity (kg m ⁻² d ⁻¹)	0.048	0.035
Biomass concentration(kg m ⁻³)	4	0.14
Area needed (m ²)	5681	7828
Oil yield (m ³ ha ⁻¹)	136.9	99.4
Annual CO ₂ consumption (kg)	183,333	183,333
Contamination control	Easy	Difficult

Contamination risk	Reduced	High
Process control	Easy	Difficult
Species control	Easy	Difficult
Mixing	Uniform	Very poor
Operation regime	Batch or semi-continuous	Batch or semi-continuous
Space required	A matter of productivity	PBRs \approx Ponds
Area/volume ratio	High (20–200 m ⁻¹)	Low (5–10 m ⁻¹)
Population (algal cell) density	High	Low
Investment	High	Low
Operation costs	High	Low
Capital/operating costs ponds	Ponds 3–10 times lower cost	PBRs >Ponds
Light utilization efficiency	High	Poor
Temperature control	More uniform temperature	Difficult
Productivity	3–5 times more productive	Low
Water losses	Depend upon cooling design	PBRs \approx Ponds
Hydrodynamic stress on algae	Low–high	Very low
Evaporation of growth medium	Low	High
Gas transfer control	High	Low
CO ₂ losses	Depend on pH, alkalinity, etc.	PBRs \approx Ponds
O ₂ inhibition	Greater problem in PBRs	PBRs >Ponds
Biomass concentration	3–5 times in PBRs	PBRs >Ponds
Scale-up	Difficult	Difficult

Chapter 3

TABLE 3.1 Ion content of concentrate medium

Cation (mg/l)	K ⁺	32.93
	Na ⁺	1936.80
	Mg ²⁺	608.60
	Ca ²⁺	495.25
Anion (mg/l)	F ⁻	16.32
	Cl ⁻	2789.20
	NO ₃ ⁻	854.60
	SO ₄ ²⁻	4729.78
	PO ₄ ³⁻	21.90
Total Nitrogen (mg/l)		22.88

TABLE 3.2 Recipe for 1 liter of f/2 medium

Component	Amount	Stock Solution Concentration	Final Concentration
NaNO ₃	1 mL	7.5 g/100 mL dH ₂ O	880 μM
NaH ₂ PO ₄ ·H ₂ O	1 mL	0.5 g/100 mL dH ₂ O	36 μM
Na ₂ SiO ₃ ·9H ₂ O	1 mL	3 g/100 mL dH ₂ O	106 μM
Trace Metals Solution	1 mL/L	See Recipe *	--
Vitamin B12	1 mL/L	See Recipe *	--
Biotin Vitamin Solution	1 mL/L	See Recipe *	--
Thiamine Vitamin Solution	1 mL/L	See Recipe *	--

* Guillard and Ryther 1962, Guillard 1975, f/2 medium

TABLE 3.3 Experimental design

Algae	Medium
<i>Dunaliella tertiolecta</i> (UTEX-LB 999)	Concentrate
<i>Dunaliella tertiolecta</i> (UTEX-LB 999)	f/2
<i>Dunaliella tertiolecta</i> (UTEX-LB 999)	50% f/2 + 50% Concentrate
<i>Dunaliella tertiolecta</i> (UTEX-LB 999)	DI water
<i>Nannochloropsis oculata</i> (UTEX- LB 2164)	Concentrate
<i>Nannochloropsis oculata</i> (UTEX- LB 2164)	f/2
<i>Nannochloropsis oculata</i> (UTEX- LB 2164)	50% f/2 + 50% Concentrate
<i>Nannochloropsis oculata</i> (UTEX- LB 2164)	DI water

Chapter 4

TABLE 4.1 Specifications of media

	pH	EC ($\mu\text{S}/\text{cm}$)	TDS (mg/l)
Concentrate	7.83	10,260	6240
f/2	6.97	113.20	59.80
50:50	7.55	5660	3310
DI	7.15	0.94	0

TABLE 4.2 Analysis of variance for quadratic regression (TN vs. time for *Dunaliella*)

Source	DF	SS	MS	F	P
Regression	2	483.3	241.6	223.3	<0.00001
Error	7	7.5	1.1		
Total	9	490.9			

TABLE 4.3 Anions (Experiment 1)

		Unit=mg/l				
		F ⁻	Cl ⁻	NO ₃ ⁻	SO ₄ ²⁻	PO ₄ ³⁻
Anions	Initial	15.2	2605.8	834.9	3788.4	18.3
	Final	≈0	2383.3	81.3	3608.1	≈0
	Removal	15.2	222.5	753.6	180.3	18.3
	Ion removal yield	≈1	0.1	0.9	0.0	≈1
	Volumetric rate of ion removal	1.52	22.2	75.4	18	1.83

TABLE 4.4 Cations (Experiment 1)

		Unit=mg/l			
		K ⁺	Na ⁺	Mg ²⁺	Ca ²⁺
Cation	Initial	28.7	1889.2	579	464.2
	Final	24.8	1655	537.4	347.3
	Removal	3.9	234.2	41.6	116.9
	Ion removal yield	0.1	0.1	0.1	0.2
	Volumetric rate of ion removal	0.4	23.4	4.1	11.7

TABLE 4.5 Analysis of variance for quadratic regression (TN vs. time for *Nannochloropsis*)

Source	DF	SS	MS	F	P
Regression	2	389.6	194.8	521.7	<0.00001
Error	7	2.614	0.373		
Total	9	392.197			

TABLE 4.6 Anions (Experiment 2)

		Unit=mg/l				
		F⁻	Cl⁻	NO₃⁻	SO₄²⁻	PO₄³⁻
Anion	Initial	15.2	2754.2	834.4	3598.3	20.8
	Final	0	2489.6	72.9	3139.3	0
	Removal	15.2	264.6	761.5	459	20.8
	Ion removal yield	1	0.09	0.9	0.1	1
	Volumetric rate of ion removal	1.52	26.5	76.1	45.9	2.08

TABLE 4.7 Cations (Experiment 2)

		Unit=mg/l			
		K⁺	Na⁺	Mg²⁺	Ca²⁺
Cation	Initial	29.6	1987.6	595.4	445.4
	Final	26.8	1797.9	548.2	351.5
	Removal	2.8	189.7	47.3	93.9
	Ion removal yield	0.1	0.09	0.1	0.2
	Volumetric rate of ion removal	0.3	18.9	4.7	9.4

TABLE 4.8 Kinetic parameters

		Q_x=Volumetric Growth Rate (gr.dm⁻³.day)	μ=Specific Growth Rate (day⁻¹)
<i>Dunaliella</i>	Concentrate	0.08	0.19
<i>tertiolecta</i>	f/2	0.03	0.12
(UTEX-LB 999)	1/2&1/2	0.04	0.14
	DI	0.03	0.11
<i>Nannochloropsis</i>	Concentrate	0.06	0.18
<i>oculata</i> (UTEX-	f/2	0.02	0.09
LB 2164)	1/2&1/2	0.04	0.16
	DI	0.01	0.07

TABLE 4.9 Nitrogen removal (comparison)

	Y_N	$Q_N [=] \text{mg} \cdot \text{dm}^{-3} \cdot \text{day}^{-1}$
Dunaliella tertiolecta	0.93	1.99
Nannochloropsis oculata	0.91	1.81

TABLE 4.10 Ion removal (comparison)

		<i>Dunaliella tertiolecta</i>		<i>Nannochloropsis oculata</i>	
		Y	$Q [=] \text{mg} \cdot \text{dm}^{-3} \cdot \text{day}^{-1}$	Y	$Q [=] \text{mg} \cdot \text{dm}^{-3} \cdot \text{day}^{-1}$
Anion	F⁻	≈1	1.52	≈1	1.52
	Cl⁻	0.1	22.2	0.09	26.5
	NO₃⁻	0.9	75.4	0.9	76.1
	SO₄²⁻	0.04	18	0.1	45.9
	PO₄³⁻	≈1	1.83	≈1	2.08
Cation	K⁺	0.1	0.4	0.1	0.3
	Na⁺	0.1	23.4	0.09	18.9
	Mg²⁺	0.1	4.1	0.1	4.7
	Ca²⁺	0.2	11.7	0.2	9.4

Figures

Chapter 2

FIGURE 2.1 Five growth phases of microalgae cultures.

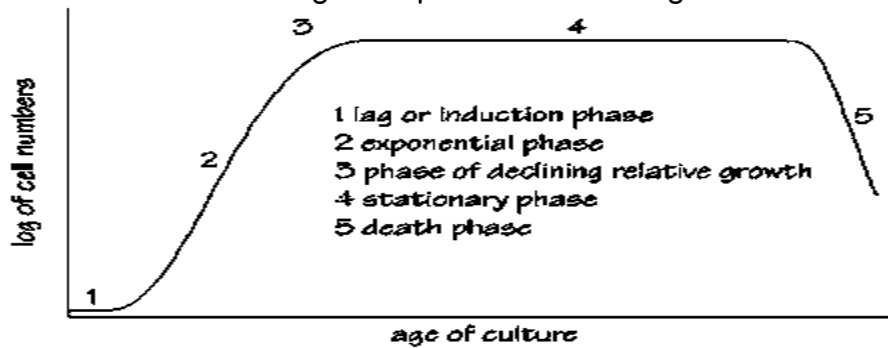


FIGURE 2.2 Algae growth rate in batch culture (solid line) and nutrient concentration (dashed line) in batch system (Mata et al., 2010)

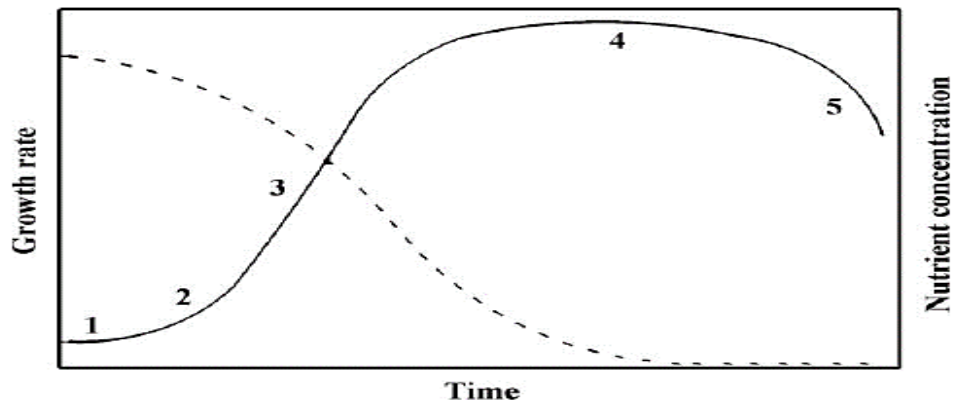


FIGURE 2.3 Schematic diagram for integrated biomass production

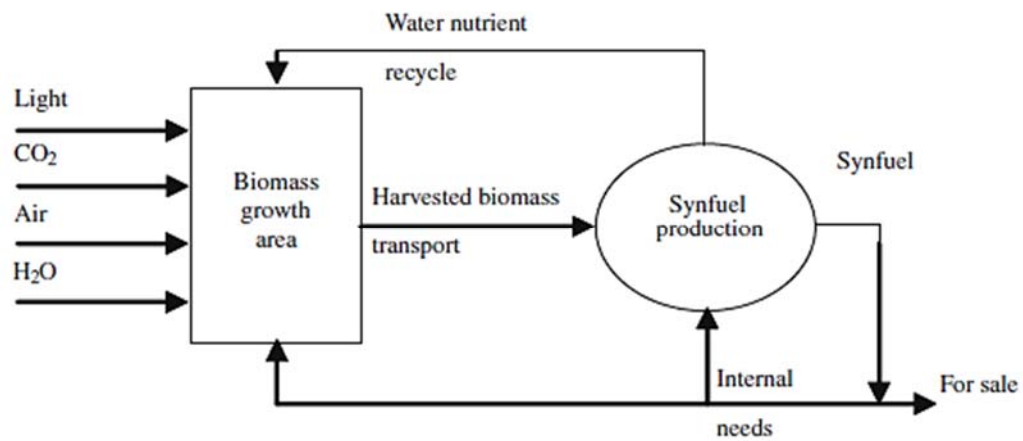


FIGURE 2.4 Schematic view of a raceway pond

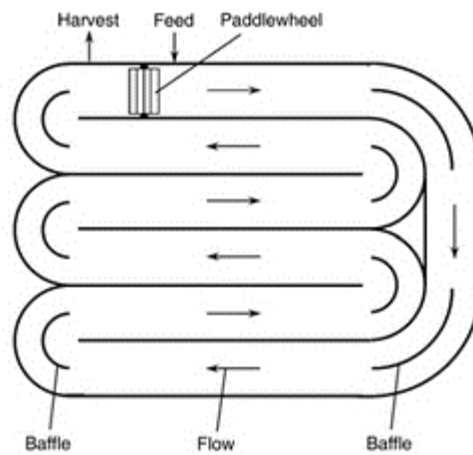


FIGURE 2.5 Tubular photobioreactor with parallel run horizontal tubes

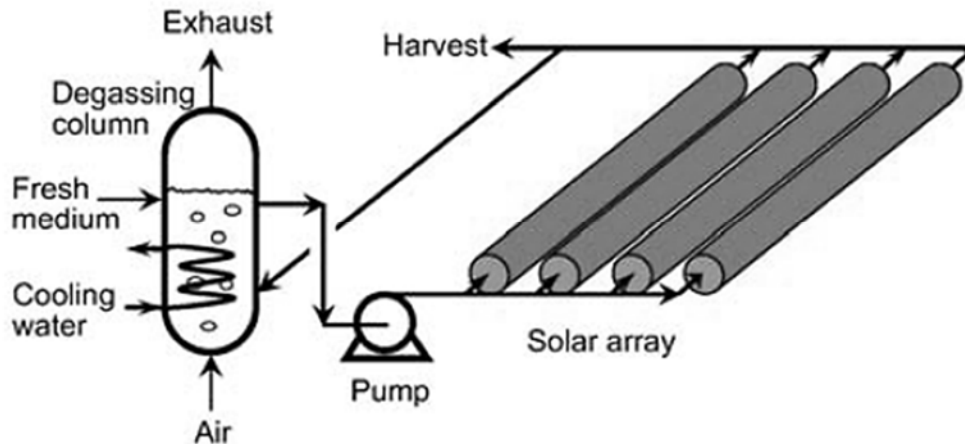


FIGURE 2.6 A fence-like solar collector

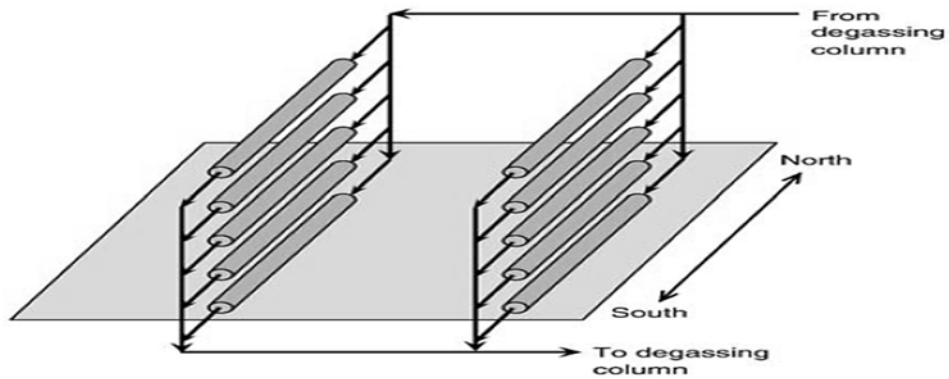


FIGURE 2.7 Energy conversion processes from microalgae

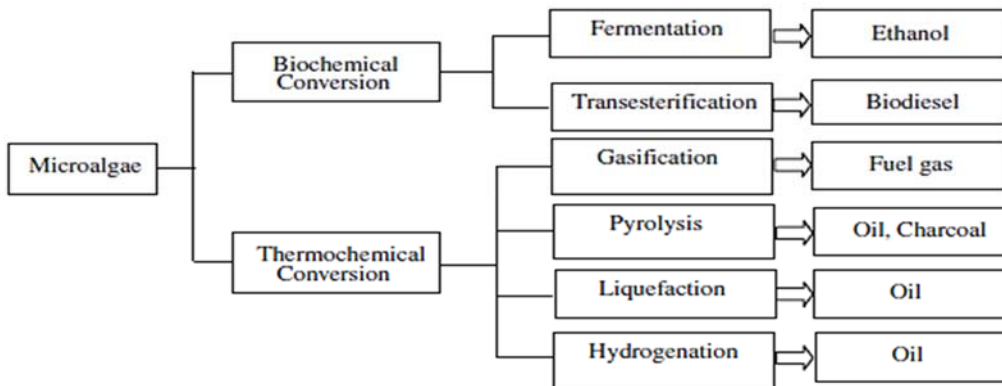


FIGURE 2.8 Transesterification of oil to biodiesel

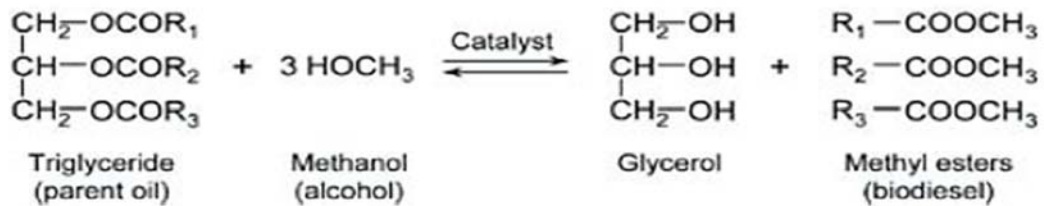


FIGURE 2.9 Schematic process of biodiesel production

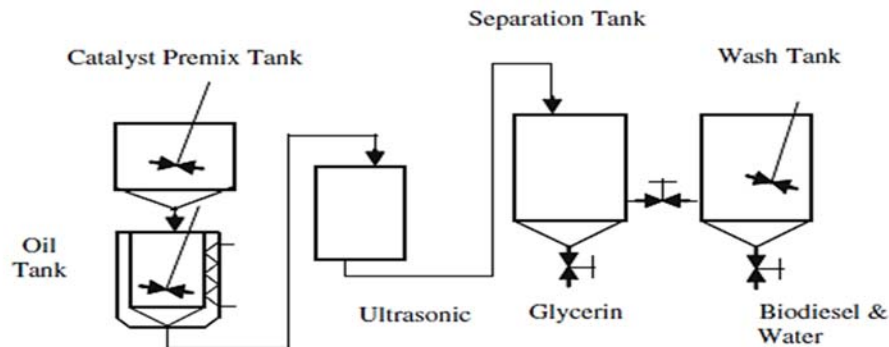
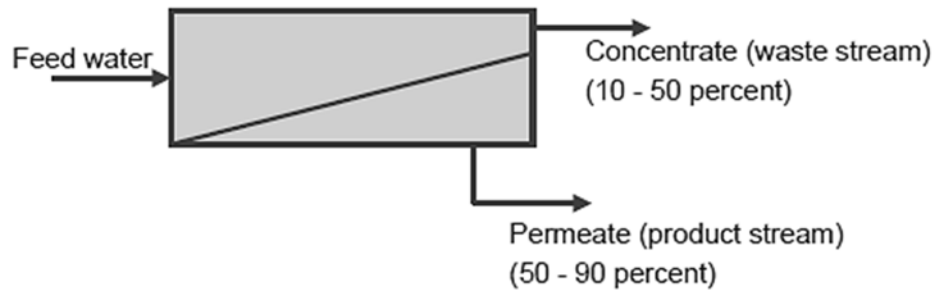


FIGURE 2.10 Schematic view of reverse osmosis (RO)

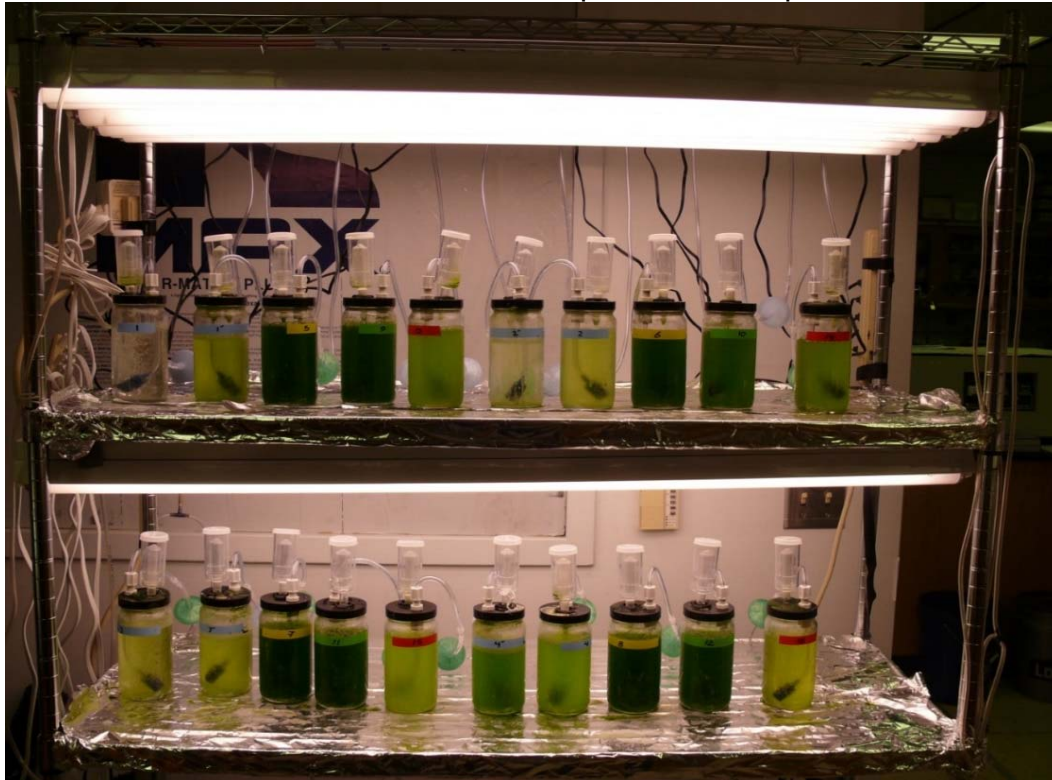


Chapter 3

FIGURE 3.1 UTEX photobioreactor



FIGURE 3.2 Experiment set-up



Chapter 4

FIGURE 4.1 Effect of medium on biomass production for *Dunaliella tertiolecta*

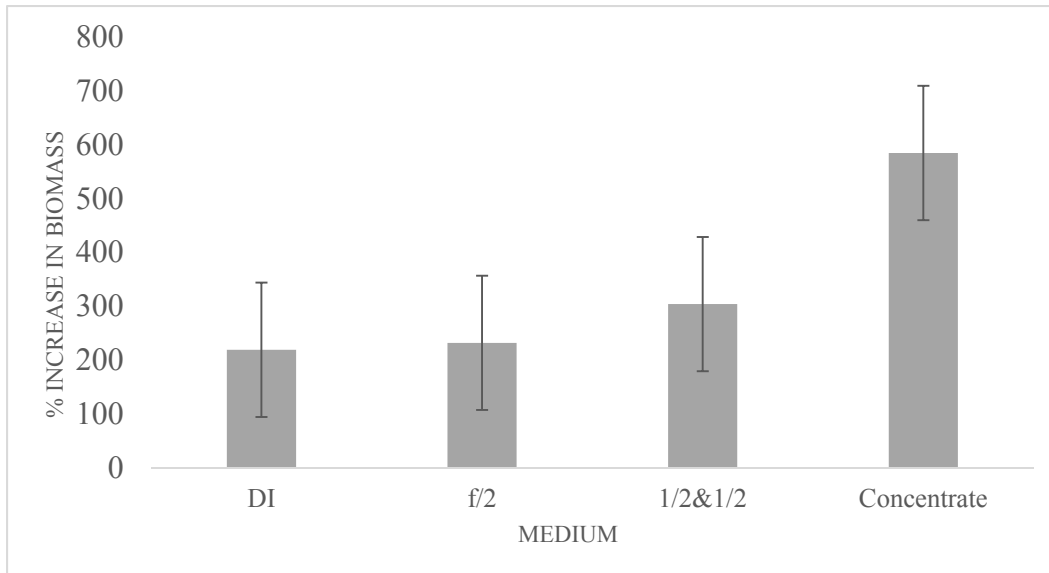


FIGURE 4.2 Growth curve for *Dunaliella tertiolecta*

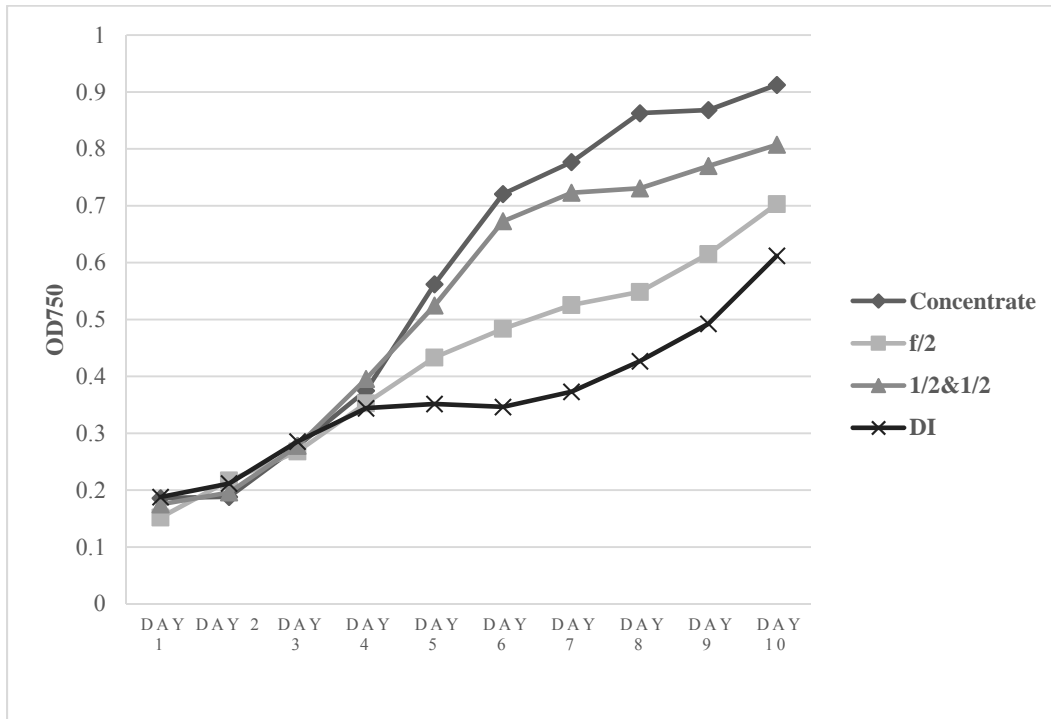


FIGURE 4.3 Total nitrogen removal from concentrate by *Dunaliella tertiolecta*

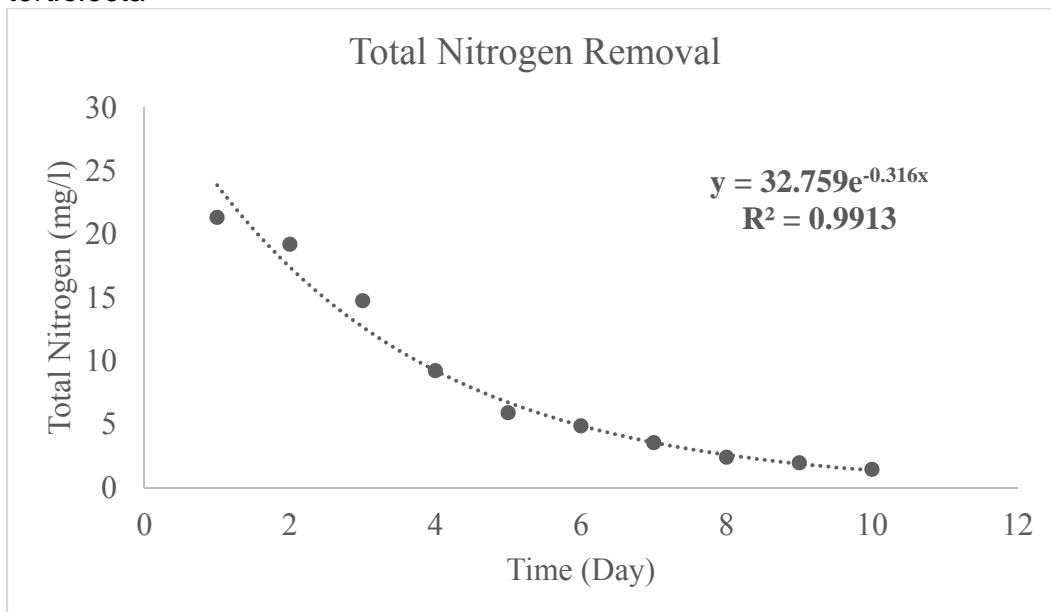


FIGURE 4.4 Correlation between TN and OD 750 for *Dunaliella tertiolecta* cultivated in concentrate

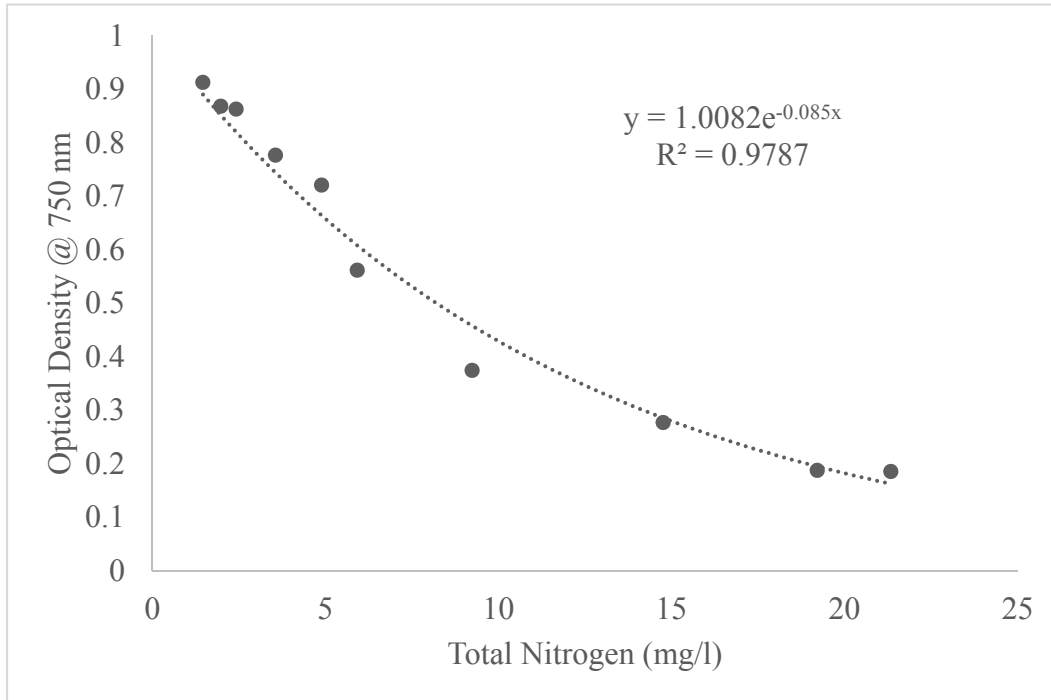


FIGURE 4.5 Effect of medium on biomass production for *Nannochloropsis oculata*

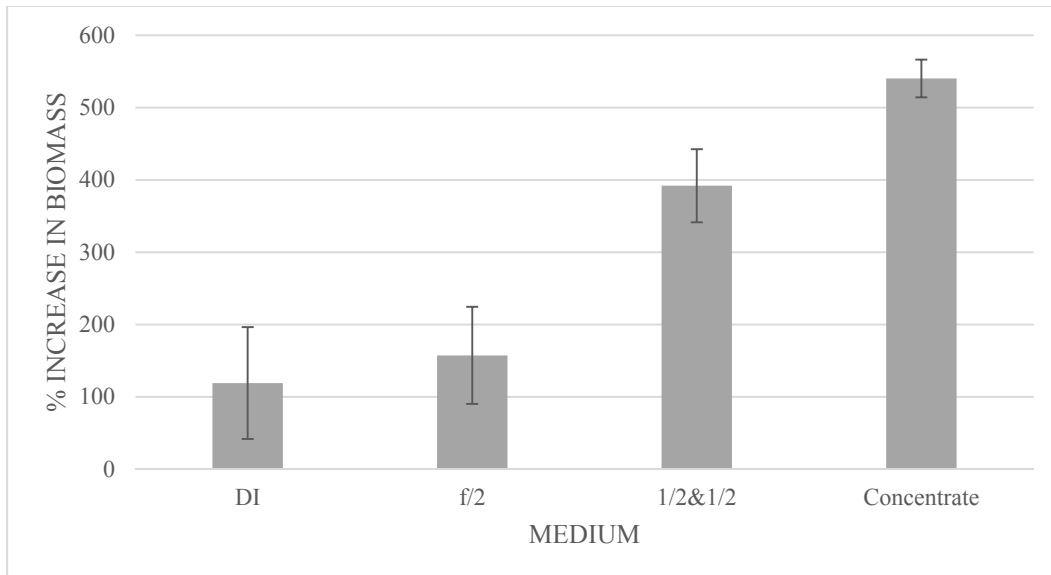


FIGURE 4.6 Growth curve for *Nannochloropsis oculata*

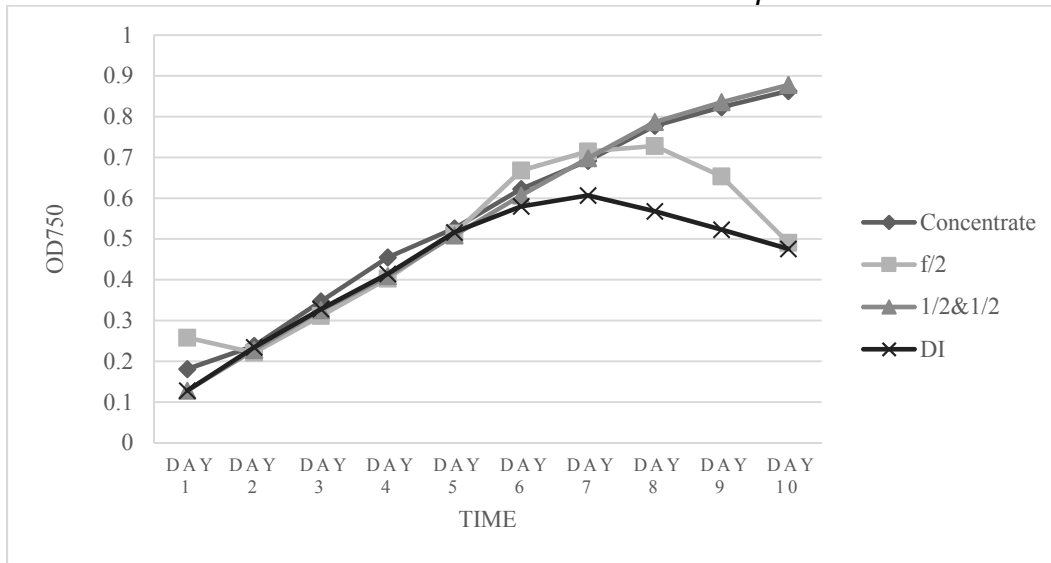


FIGURE 4.7 Total Nitrogen Removal from concentrate by *Nannochloropsis oculata*

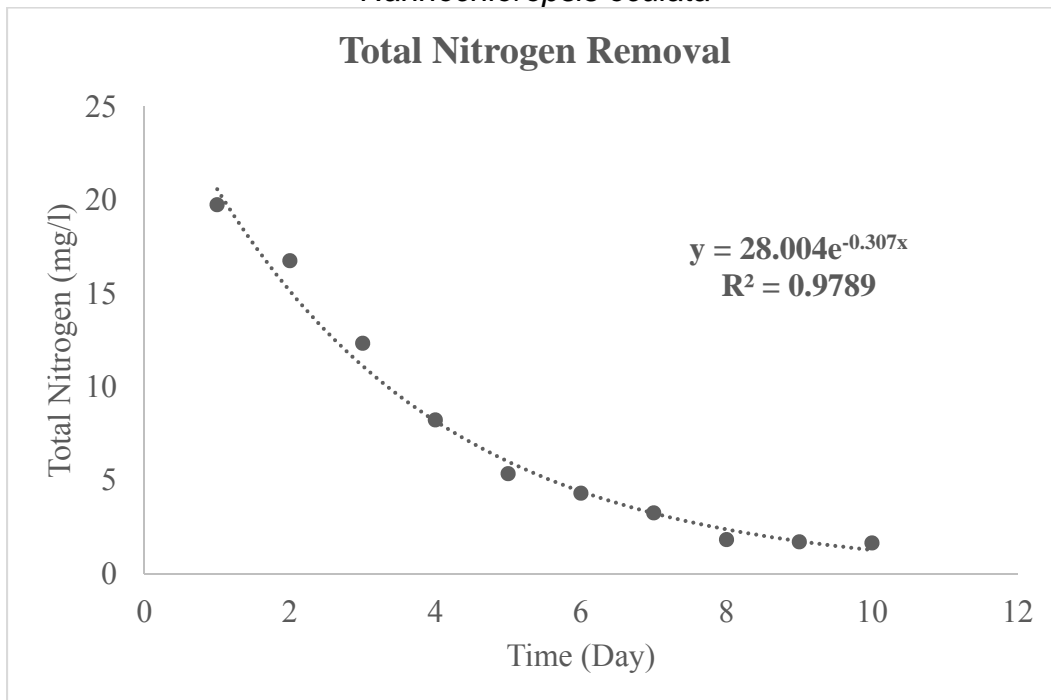


FIGURE 4.8 Correlation between TN and OD 750 for *Nannochloropsis oculata* cultivated in concentrate

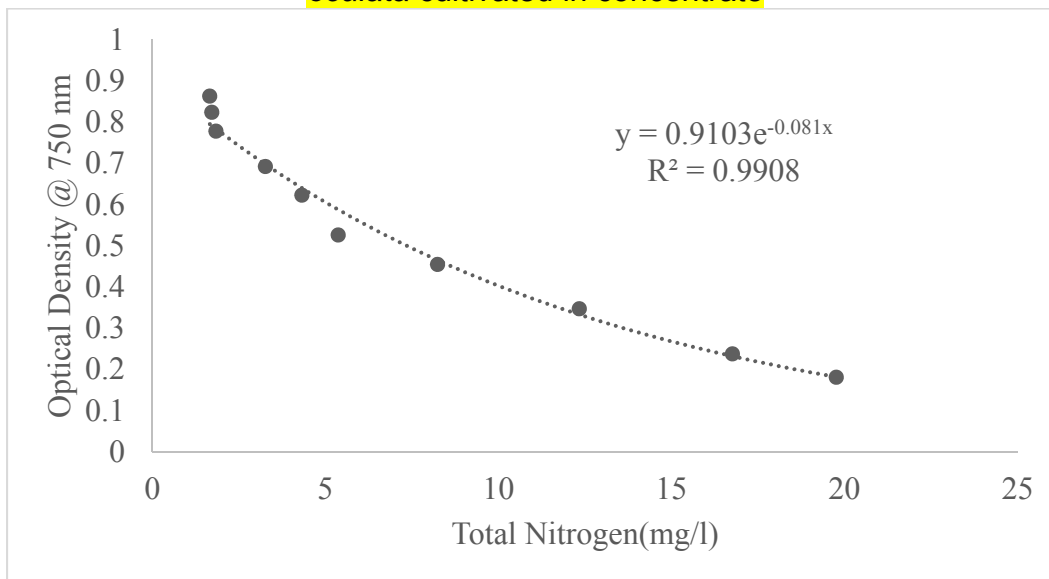


FIGURE 4.9 Algae effect on dry biomass production

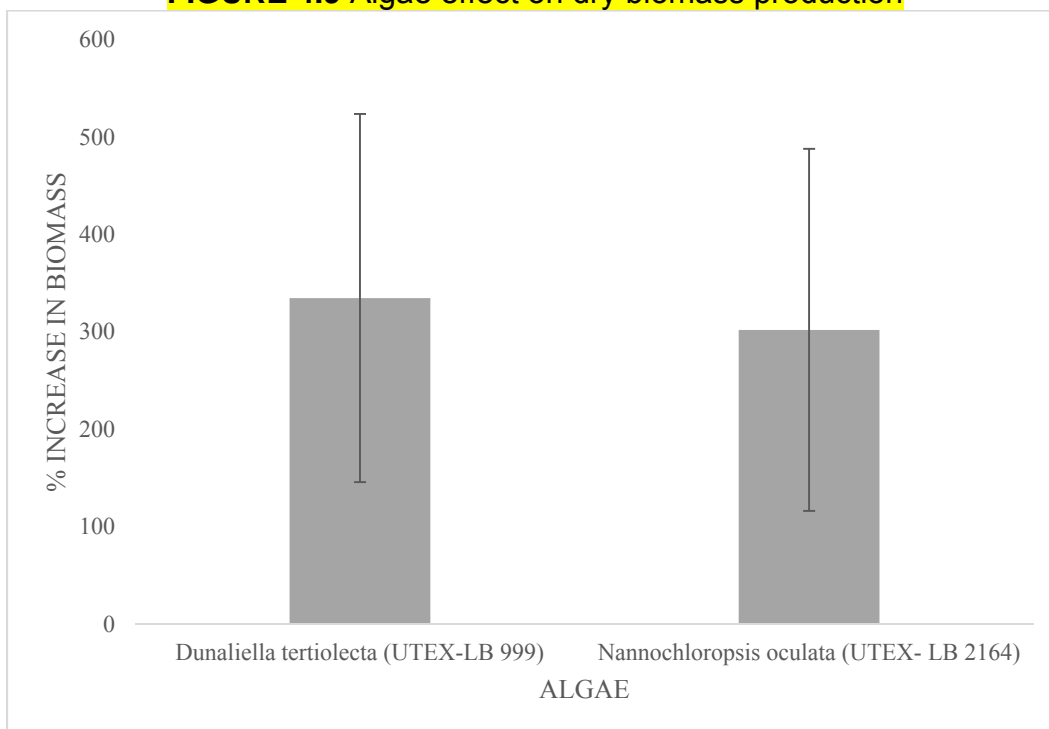


FIGURE 4.10 Medium effect on dry biomass production

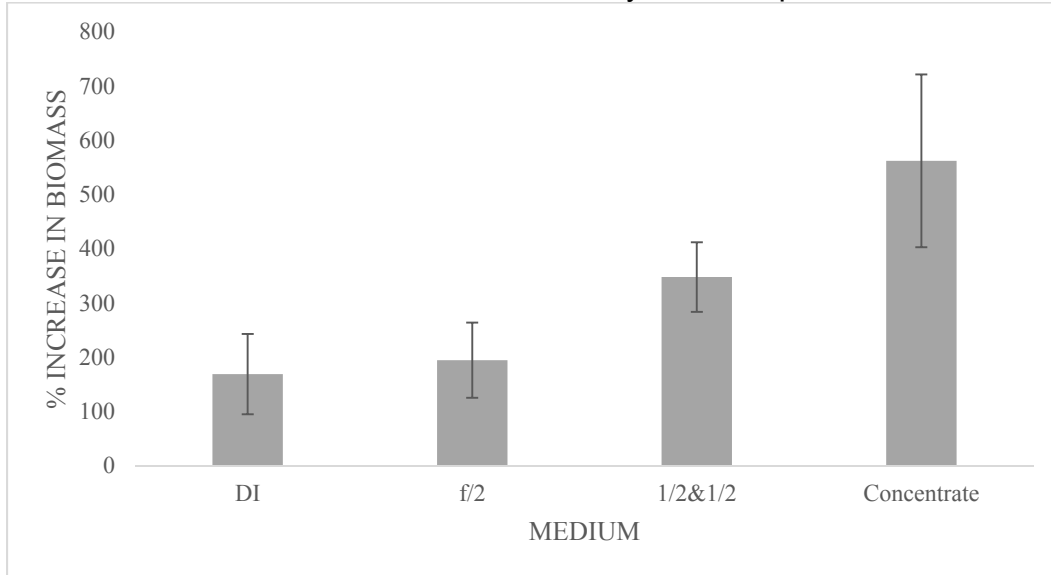


FIGURE 4.11 Algae-Medium interaction effect on dry biomass

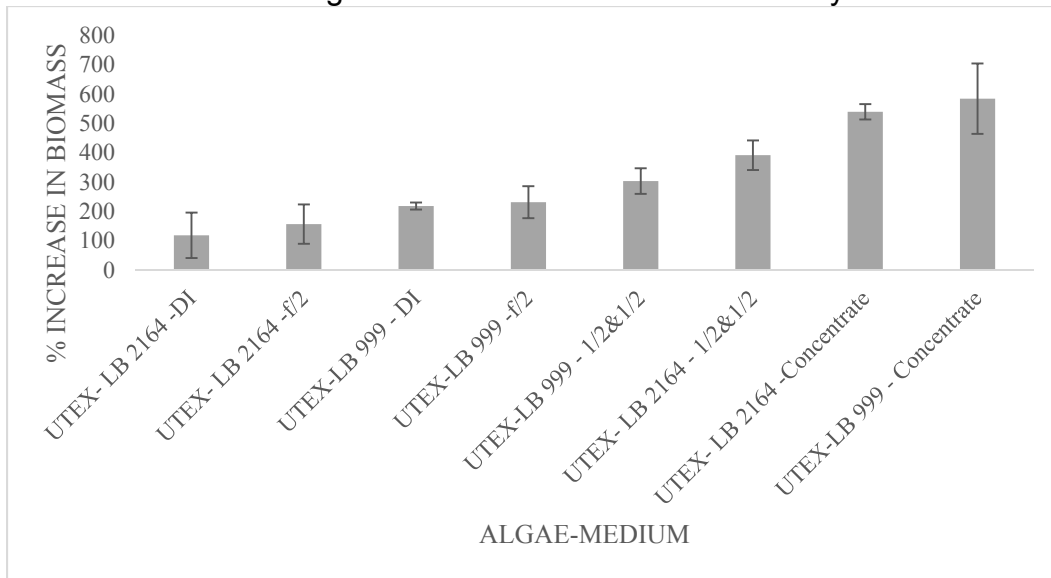


FIGURE 4.12 Effect of algae on biomass concentration in concentrate

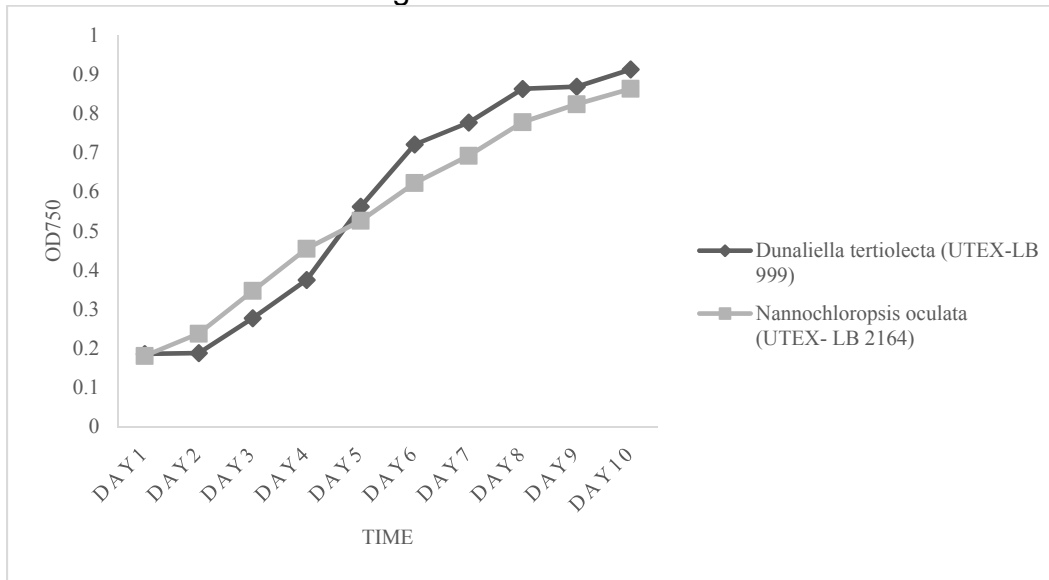


FIGURE 4.13 Ion removal from concentrate by two cultures of algae

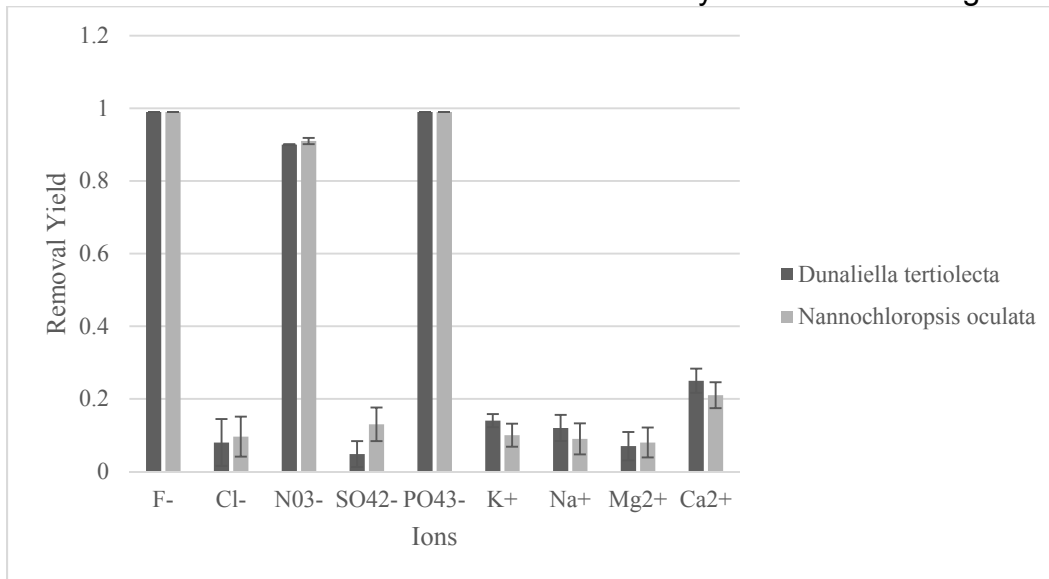


FIGURE 4.14 TDS reduction in concentrate medium by two strains of algae

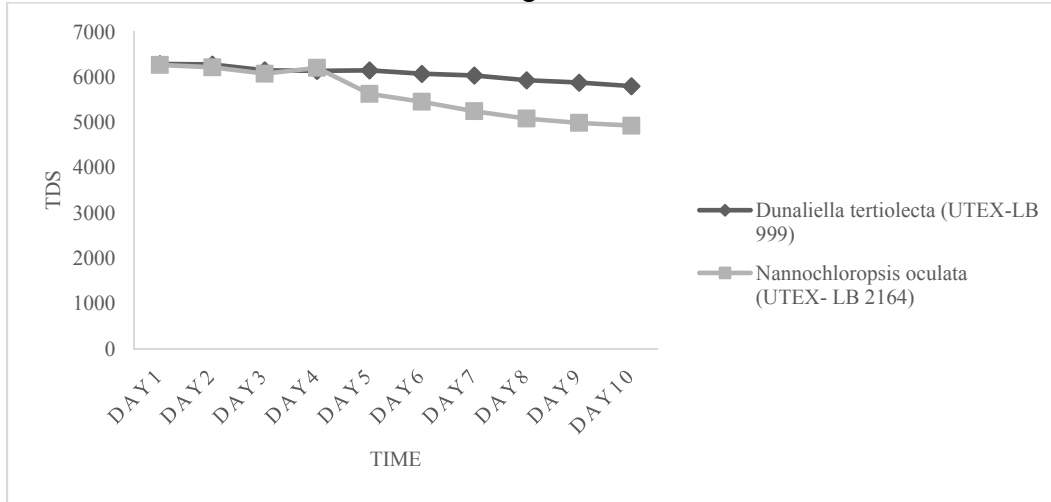
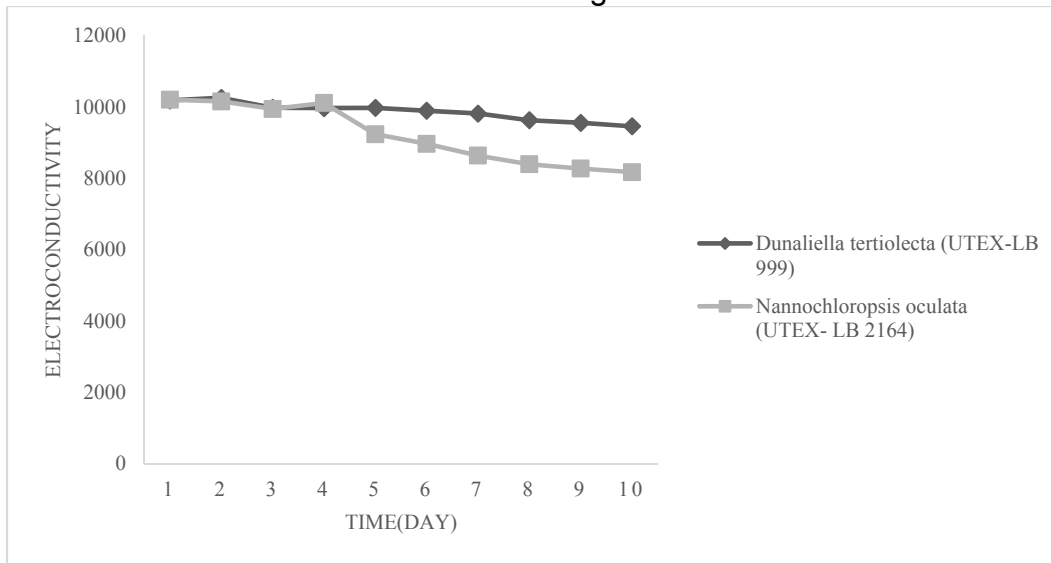
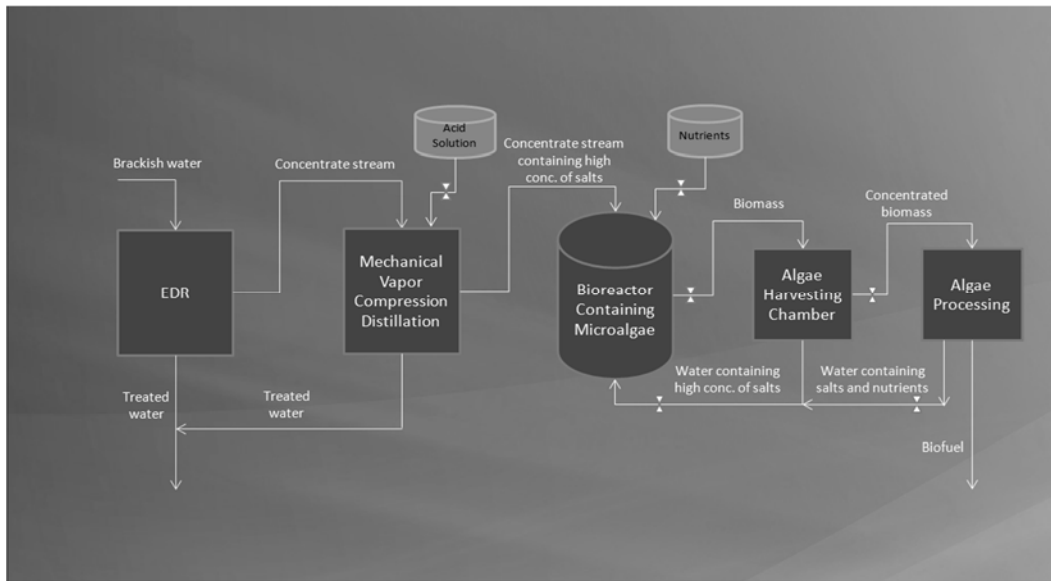


FIGURE 4.15 Electroconductivity reduction in concentrate medium by two strains of algae



Chapter 5

FIGURE 5.1 Process overview



Appendices

Appendix A

Units of Measure

°C	Degree(s) Celsius
°F	Degree(s) Fahrenheit
ft	Feet
g	Gram(s)
g/L	Gram(s) per liter
g/L/d	Gram(s) per liter per day
g. MJ ⁻¹	Gram(s) per mega joule(s)
GPD	Gallon(s) per day
Kg	kilogram
KWh	kilowatt hour
L	Liter(s)
m ³	Cubic meter(s)
mg/L	Milligram(s) per liter
MJ	Mega Joule
MGD	Million gallon(s) per day
ppm	Part per million
Rpm	Revolutions per minute
µm	Micrometer(s)
µS/cm	Micro-Siemens per centimeter
%	Percentage

Appendix B

Data Record

1. Initial Media Characteristics

	pH	EC ($\mu\text{S/cm}$)	TDS (mg/l)	Initial Biomass (g)
Concentrate	7.83	10,260	6240	0
f/2	6.97	113.2	59.8	0
50% f/2 + 50% Concentrate	7.55	5660	3310	0
DI water	7.15	0.94	0	0
<i>Dunaliella tertiolecta</i> inoculum	9.32	20,600	13,200	0.052
<i>Nannochloropsis oculata</i> inoculum	8.73	21,300	13,690	0.043

2. Initial Cation, Anion, and TN Characteristics of Concentrate

	Cations (mg/l)				Anions (mg/l)					TN
	K	Na	Mg	Ca	F ⁻	Cl ⁻	NO ₃ ⁻	SO ₄ ²⁻	PO ₄ ³⁻	
Concentrate	32.93	1936.8	608.6	495.25	16.32	2789.2	854.6	4729.78	21.9	22.88

3. Anion Removal by *D. tertiolecta*

	Initial Concentration (mg/l)	Final Concentration (mg/l)	Removal (mg/l)	Removal Yield	Volumetric Rate of Removal
F ⁻	15.20	≈0	15.2	≈1	1.52
Cl ⁻	2605.81	2383.33	222.48	0.08	22.248
NO ₃ ⁻	834.90	81.31	753.59	0.90	75.36
SO ₄ ²⁻	3788.44	3608.1	180.34	0.048	18.03
PO ₄ ³⁻	18.3	≈0	18.3	≈1	1.83

4. Anion Removal by *N. oculata*

	Initial Concentration (mg/l)	Final Concentration (mg/l)	Removal (mg/l)	Removal Yield	Volumetric Rate of Removal
F ⁻	15.2	0	15.2	1	1.52
Cl ⁻	2754.23	2489.64	264.59	0.096	26.46
NO ₃ ⁻	834.4	72.86	761.54	0.91	76.15
SO ₄ ²⁻	3598.3	3139.3	459	0.13	45.9
PO ₄ ³⁻	20.8	0	20.8	1	2.08

5. Cation Removal *D. tertiolecta*

	Initial Concentration (mg/l)	Final Concentration (mg/l)	Removal (mg/l)	Removal Yield	Volumetric Rate of Removal
K	28.67	24.76	3.91	0.14	0.39
Na	1889.19	1655.01	234.19	0.12	23.42
Mg	578.96	537.37	41.59	0.07	4.16
Ca	464.22	347.33	116.89	0.25	11.69

6. Cation Removal by *N. oculata*

	Initial Concentration (mg/l)	Final Concentration (mg/l)	Removal (mg/l)	Removal Yield	Volumetric Rate of Removal
K	29.63	26.78	2.855	0.1	0.28
Na	1987.6	1797.86	189.73	0.09	18.97
Mg ²⁺	595.44	548.17	47.27	0.08	4.73
Ca ²⁺	445.44	351.55	93.89	0.21	9.39

7. TDS Reduction

		TDS (mg/l)				
		Day				
Algae	Medium	1	2	3	4	5
<i>Dunaliella tertiolecta</i> (UTEX-LB 999)	Concentrate	6290.0	6280.0	6152.5	6140.0	6150.0
<i>Nannochloropsis oculata</i> (UTEX- LB 2164)	Concentrate	6270.0	6217.5	6077.5	6207.5	5632.5

		TDS (mg/l)				
		Day				
Algae	Medium	6	7	8	9	10
<i>Dunaliella tertiolecta</i> (UTEX-LB 999)	Concentrate	6075.0	6037.5	5932.5	5880.0	5802.5
<i>Nanno-chloropsis oculata</i> (UTEX- LB 2164)	Concentrate	5457.5	5250.0	5087.5	4992.5	4930.0

8. EC Reduction

		Electroconductivity ($\mu\text{S}/\text{cm}$)				
		Day				
Algae	Medium	1	2	3	4	5
<i>Dunaliella tertiolecta</i> (UTEX-LB 999)	Concentrate	10,180.0	10,250.0	9972.5	9965.0	9970.0
<i>Nannochloropsis oculata</i> (UTEX- LB 2164)	Concentrate	10,200.0	10,152.5	9942.5	10,110.0	9232.5

		Electroconductivity ($\mu\text{S}/\text{cm}$)				
		Day				
Algae	Medium	6	7	8	9	10
<i>Dunaliella tertiolecta</i> (UTEX-LB 999)	Concentrate	9890.0	9812.5	9625.0	9552.5	9455.0
<i>Nannochloropsis oculata</i> (UTEX- LB 2164)	Concentrate	8965.0	8635.0	8392.5	8272.5	8170.0

9. pH Levels during Growth

		pH									
		Day									
Algae	Medium	1	2	3	4	5	6	7	8	9	10
<i>Dunaliella tertiolecta</i> (UTEX-LB 999)	Concentrate	8.14	8.62	8.36	8.44	8.45	8.44	8.38	8.39	8.27	8.27
<i>Dunaliella tertiolecta</i> (UTEX-LB 999)	f/2	9.25	7.62	7.60	8.16	8.56	8.52	8.33	8.29	8.06	7.73
<i>Dunaliella tertiolecta</i> (UTEX-LB 999)	50% f/2 + 50% Concentrate	8.37	8.41	8.43	8.56	8.54	8.54	8.51	8.43	8.38	8.35
<i>Dunaliella tertiolecta</i> (UTEX-LB 999)	DI water	9.35	7.58	7.57	8.42	8.33	7.96	7.79	7.76	7.70	7.37
<i>Nannochloropsis oculata</i> (UTEX- LB 2164)	Concentrate	7.93	8.56	8.51	8.49	8.43	8.36	8.29	8.36	8.42	8.39
<i>Nannochloropsis oculata</i> (UTEX- LB 2164)	f/2	8.42	7.76	8.12	8.28	8.42	8.37	8.21	8.12	8.04	7.84
<i>Nannochloropsis oculata</i> (UTEX- LB 2164)	50% f/2 + 50% Concentrate	8.17	8.49	8.59	8.64	8.58	8.535	8.435	8.605	8.66	8.645
<i>Nannochloropsis oculata</i> (UTEX- LB 2164)	DI water	8.75	7.79	8.16	8.54	8.27	8.16	7.84	7.61	7.71	7.66

10. Optical Density

		Optical Density at 750 nm									
		Day									
Algae	Medium	1	2	3	4	5	6	7	8	9	10
<i>Dunaliella tertiolecta</i> (UTEX-LB 999)	Concentrate	0.186	0.162	0.251	0.338	0.456	0.652	0.767	0.811	0.861	0.795
<i>Dunaliella tertiolecta</i> (UTEX-LB 999)	Concentrate	0.186	0.185	0.264	0.347	0.572	0.700	0.778	0.881	0.837	0.894
<i>Dunaliella</i>	Concen-	0.186	0.185	0.295	0.396	0.624	0.767	0.728	0.893	0.911	0.981

<i>tertiolecta</i> (UTEX-LB 999)	trate										
<i>Dunaliella tertiolecta</i> (UTEX-LB 999)	Concen- trate	0.186	0.221	0.300	0.419	0.596	0.764	0.834	0.866	0.864	0.980
<i>Dunaliella tertiolecta</i> (UTEX-LB 999)	f/2	0.152	0.293	0.249	0.343	0.394	0.405	0.439	0.439	0.525	0.608
<i>Dunaliella tertiolecta</i> (UTEX-LB 999)	f/2	0.152	0.196	0.306	0.362	0.430	0.457	0.532	0.597	0.670	0.785
<i>Dunaliella tertiolecta</i> (UTEX-LB 999)	f/2	0.152	0.182	0.242	0.350	0.484	0.568	0.600	0.656	0.716	0.798
<i>Dunaliella tertiolecta</i> (UTEX-LB 999)	f/2	0.152	0.197	0.275	0.356	0.425	0.505	0.531	0.502	0.550	0.621
<i>Dunaliella tertiolecta</i> (UTEX-LB 999)	50% f/2 + 50% Concen- trate	0.175	0.175	0.248	0.368	0.505	0.679	0.676	0.657	0.692	0.744
<i>Dunaliella tertiolecta</i> (UTEX-LB 999)	50% f/2 + 50% Concen- trate	0.175	0.194	0.313	0.409	0.529	0.606	0.685	0.658	0.686	0.715
<i>Dunaliella tertiolecta</i> (UTEX-LB 999)	50% f/2 + 50% Concen- trate	0.175	0.228	0.282	0.507	0.603	0.773	0.817	0.850	0.865	0.857
<i>Dunaliella tertiolecta</i> (UTEX-LB 999)	50% f/2 + 50% Concen- trate	0.175	0.187	0.268	0.298	0.461	0.633	0.713	0.757	0.836	0.913
<i>Dunaliella tertiolecta</i> (UTEX-LB 999)	DI water	0.188	0.207	0.264	0.319	0.309	0.306	0.320	0.354	0.447	0.611
<i>Dunaliella tertiolecta</i> (UTEX-LB 999)	DI water	0.188	0.206	0.269	0.351	0.418	0.387	0.420	0.476	0.550	0.619
<i>Dunaliella tertiolecta</i> (UTEX-LB 999)	DI water	0.188	0.218	0.294	0.345	0.346	0.353	0.383	0.425	0.471	0.576
<i>Dunaliella tertiolecta</i> (UTEX-LB 999)	DI water	0.188	0.216	0.315	0.361	0.333	0.339	0.369	0.452	0.502	0.642
<i>Nanno- chloropsis oculata</i> (UTEX- LB 2164)	Concen- trate	0.181	0.236	0.321	0.472	0.497	0.603	0.674	0.772	0.815	0.858
<i>Nanno- chloropsis</i>	Concen- trate	0.181	0.239	0.347	0.439	0.542	0.634	0.704	0.786	0.842	0.881

<i>oculata</i> (UTEX- LB 2164)											
<i>Nanno- chloropsis oculata</i> (UTEX- LB 2164)	Concen- trate	0.181	0.229	0.352	0.449	0.529	0.618	0.691	0.770	0.808	0.853
<i>Nanno- chloropsis oculata</i> (UTEX- LB 2164)	Concen- trate	0.181	0.247	0.368	0.459	0.536	0.635	0.699	0.783	0.829	0.860
<i>Nanno- chloropsis oculata</i> (UTEX- LB 2164)	f/2	0.258	0.214	0.293	0.361	0.448	0.556	0.641	0.627	0.566	0.438
<i>Nanno- chloropsis oculata</i> (UTEX- LB 2164)	f/2	0.258	0.220	0.312	0.405	0.513	0.643	0.723	0.716	0.590	0.399
<i>Nanno- chloropsis oculata</i> (UTEX- LB 2164)	f/2	0.258	0.230	0.335	0.450	0.584	0.852	0.793	0.827	0.781	0.646
<i>Nanno- chloropsis oculata</i> (UTEX- LB 2164)	f/2	0.258	0.221	0.305	0.395	0.509	0.621	0.702	0.742	0.677	0.480
<i>Nanno- chloropsis oculata</i> (UTEX- LB 2164)	50% f/2 + 50% Concen- trate	0.128	0.228	0.328	0.396	0.507	0.612	0.707	0.817	0.857	0.907
<i>Nanno- chloropsis oculata</i> (UTEX- LB 2164)	50% f/2 + 50% Concen- trate	0.128	0.225	0.318	0.393	0.482	0.577	0.670	0.737	0.794	0.825
<i>Nanno- chloropsis oculata</i> (UTEX- LB 2164)	50% f/2 + 50% Concen- trate	0.128	0.233	0.336	0.425	0.535	0.633	0.710	0.811	0.848	0.890
<i>Nanno- chloropsis oculata</i> (UTEX- LB 2164)	50% f/2 + 50% Concen- trate	0.128	0.224	0.319	0.421	0.511	0.605	0.705	0.782	0.843	0.889
<i>Nanno- chloropsis oculata</i> (UTEX- LB 2164)	DI water	0.128	0.216	0.300	0.394	0.497	0.560	0.566	0.472	0.379	0.329
<i>Nanno- chloropsis oculata</i> (UTEX- LB 2164)	DI water	0.128	0.282	0.306	0.388	0.478	0.538	0.579	0.471	0.390	0.366
<i>Nanno- chloropsis oculata</i>	DI water	0.128	0.221	0.340	0.466	0.579	0.635	0.671	0.677	0.657	0.551

(UTEX- LB 2164)											
<i>Nannochloropsis oculata</i> (UTEX- LB 2164)	DI water	0.128	0.218	0.366	0.409	0.511	0.587	0.611	0.652	0.665	0.657

11. Total Nitrogen vs. Optical Density

	Day				
	1	2	3	4	5
Optical Density at 750 nm	0.18600	0.18825	0.2775	0.37500	0.56200
Total Nitrogen (mg/l)	21.34	19.21	14.76	9.24	5.92

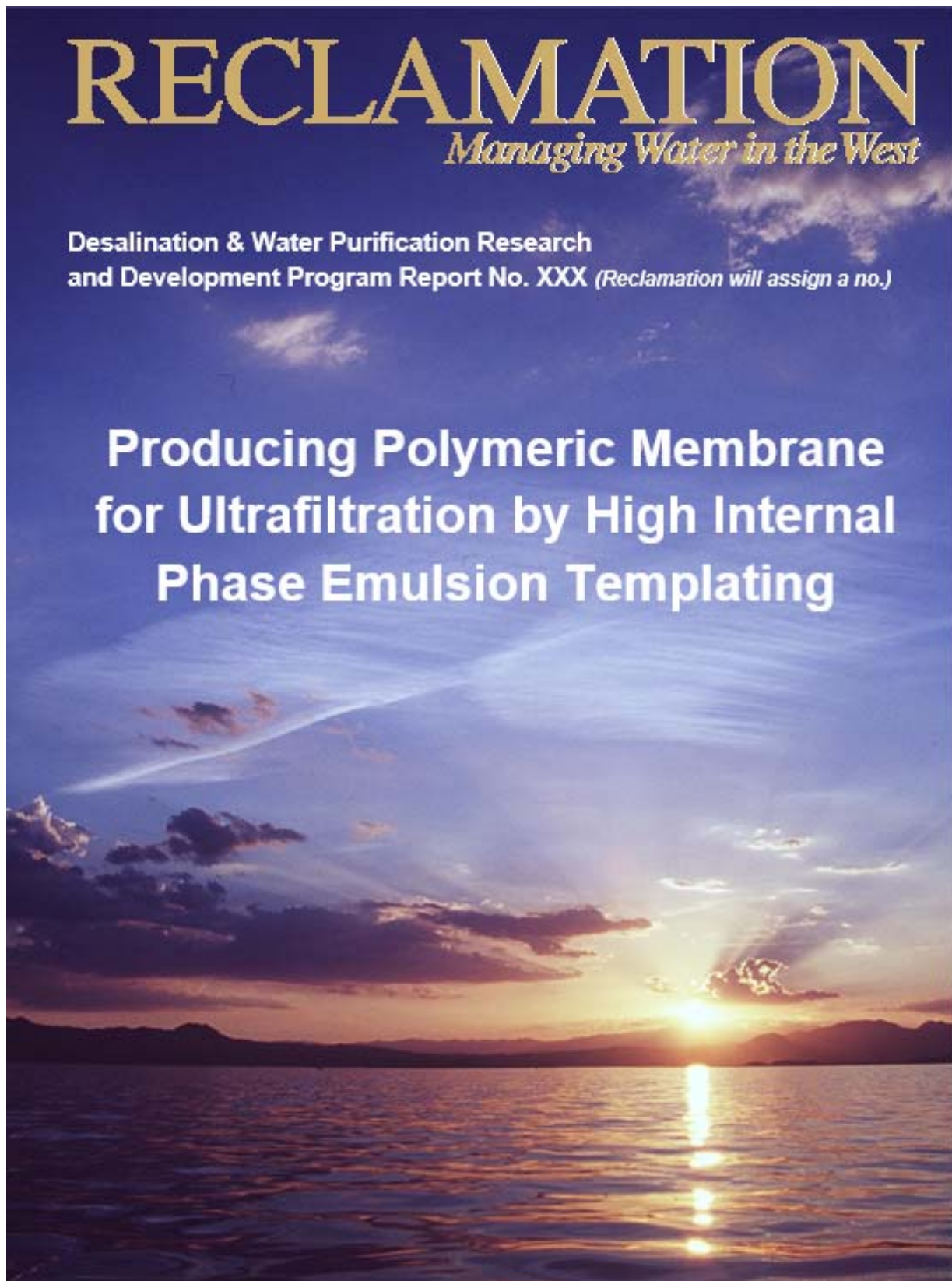
	Day				
	6	7	8	9	10
Optical Density at 750 nm	0.72075	0.77675	0.86275	0.86825	0.9125
Total Nitrogen (mg/l)	4.89	3.56	2.42	1.98	1.46

12. Algae-Medium Interaction Effect on Biomass

Algae	Medium	Treatment 1	Treatment 2	Initial Biomass (g)	Final Biomass (g)
<i>Dunaliella tertiolecta</i> (UTEX-LB 999)	Concentrate	1	1	0.05224	0.2952
<i>Dunaliella tertiolecta</i> (UTEX-LB 999)	Concentrate	1	1	0.05224	0.3224
<i>Dunaliella tertiolecta</i> (UTEX-LB 999)	Concentrate	1	1	0.05224	0.5424
<i>Dunaliella tertiolecta</i> (UTEX-LB 999)	Concentrate	1	1	0.05224	0.2704
<i>Dunaliella tertiolecta</i> (UTEX-LB 999)	f/2	1	2	0.05224	0.1496
<i>Dunaliella tertiolecta</i> (UTEX-LB 999)	f/2	1	2	0.05224	0.148
<i>Dunaliella tertiolecta</i> (UTEX-LB 999)	f/2	1	2	0.05224	0.2008
<i>Dunaliella tertiolecta</i> (UTEX-LB 999)	f/2	1	2	0.05224	0.1952
<i>Dunaliella tertiolecta</i> (UTEX-LB 999)	50% f/2 + 50% Concentrate	1	3	0.05224	0.208
<i>Dunaliella tertiolecta</i> (UTEX-LB 999)	50% f/2 + 50% Concentrate	1	3	0.05224	0.2056
<i>Dunaliella tertiolecta</i> (UTEX-LB 999)	50% f/2 + 50% Concentrate	1	3	0.05224	0.2424
<i>Dunaliella tertiolecta</i> (UTEX-LB 999)	50% f/2 + 50% Concentrate	1	3	0.05224	0.188
<i>Dunaliella tertiolecta</i> (UTEX-LB 999)	DI water	1	4	0.05224	0.1576
<i>Dunaliella tertiolecta</i> (UTEX-LB 999)	DI water	1	4	0.05224	0.1688

(UTEX-LB 999)					
<i>Dunaliella tertiolecta</i> (UTEX-LB 999)	DI water	1	4	0.05224	0.168
<i>Dunaliella tertiolecta</i> (UTEX-LB 999)	DI water	1	4	0.05224	0.172
<i>Nannochloropsis oculata</i> (UTEX- LB 2164)	Concentrate	2	1	0.043456	0.2808
<i>Nannochloropsis oculata</i> (UTEX- LB 2164)	Concentrate	2	1	0.043456	0.2928
<i>Nannochloropsis oculata</i> (UTEX- LB 2164)	Concentrate	2	1	0.043456	0.2664
<i>Nannochloropsis oculata</i> (UTEX- LB 2164)	Concentrate	2	1	0.043456	0.2728
<i>Nannochloropsis oculata</i> (UTEX- LB 2164)	f/2	2	2	0.043456	0.0976
<i>Nannochloropsis oculata</i> (UTEX- LB 2164)	f/2	2	2	0.043456	0.0808
<i>Nannochloropsis oculata</i> (UTEX- LB 2164)	f/2	2	2	0.043456	0.148
<i>Nannochloropsis oculata</i> (UTEX- LB 2164)	f/2	2	2	0.043456	0.1208
<i>Nannochloropsis oculata</i> (UTEX- LB 2164)	50% f/2 + 50% Concentrate	2	3	0.043456	0.2336
<i>Nannochloropsis oculata</i> (UTEX- LB 2164)	50% f/2 + 50% Concentrate	2	3	0.043456	0.1824
<i>Nannochloropsis oculata</i> (UTEX- LB 2164)	50% f/2 + 50% Concentrate	2	3	0.043456	0.2184
<i>Nannochloropsis oculata</i> (UTEX- LB 2164)	50% f/2 + 50% Concentrate	2	3	0.043456	0.2208
<i>Nannochloropsis oculata</i> (UTEX- LB 2164)	DI water	2	4	0.043456	0.0584
<i>Nannochloropsis oculata</i> (UTEX- LB 2164)	DI water	2	4	0.043456	0.0776
<i>Nannochloropsis oculata</i> (UTEX- LB 2164)	DI water	2	4	0.043456	0.1112
<i>Nannochloropsis oculata</i> (UTEX- LB 2164)	DI water	2	4	0.043456	0.1336

Producing Polymeric Membrane for Ultrafiltration by High Internal Phase Emulsion Templating



REPORT DOCUMENTATION PAGE

Form Approved
OMB No. 0704-0188

The public reporting burden for this collection of information is estimated to average 1 hour per response, including the time for reviewing instructions, searching existing data sources, gathering and maintaining the data needed, and completing and reviewing the collection of information. Send comments regarding this burden estimate or any other aspect of this collection of information, including suggestions for reducing the burden, to Department of Defense, Washington Headquarters Services, Directorate for Information Operations and Reports (0704-0188), 1215 Jefferson Davis Highway, Suite 1204, Arlington, VA 22202-4302. Respondents should be aware that notwithstanding any other provision of law, no person shall be subject to any penalty for failing to comply with a collection of information if it does not display a currently valid OMB control number.

PLEASE DO NOT RETURN YOUR FORM TO THE ABOVE ADDRESS.

1. REPORT DATE (DD-MM-YYYY) 30/11/2015	2. REPORT TYPE Proof of Concept Final Report	3. DATES COVERED (From - To)
4. TITLE AND SUBTITLE Producing Polymeric Membrane for Ultrafiltration by High Internal Phase Emulsion Templating		5a. CONTRACT NUMBER
		5b. GRANT NUMBER
		5c. PROGRAM ELEMENT NUMBER
6. AUTHOR(S) Anna Malakian Reza Foudazi		5d. PROJECT NUMBER
		5e. TASK NUMBER
		5f. WORK UNIT NUMBER
7. PERFORMING ORGANIZATION NAME(S) AND ADDRESS(ES)		8. PERFORMING ORGANIZATION REPORT NUMBER
9. SPONSORING/MONITORING AGENCY NAME(S) AND ADDRESS(ES)		10. SPONSOR/MONITOR'S ACRONYM(S)
		11. SPONSOR/MONITOR'S REPORT NUMBER(S)
12. DISTRIBUTION/AVAILABILITY STATEMENT		
13. SUPPLEMENTARY NOTES		
14. ABSTRACT Clean water scarcity is a critical concern in the world. In order to make water drinkable, different filtration steps need to be done. Ultrafiltration is one of the main steps by which bacteria, viruses, oils, and organic minerals are removed from water. In this project, application of polymerized high internal phase emulsions, polyHIPEs, as ultrafiltration and microfiltration membranes was studied. Oil phase as continuous phase of emulsions containing butyl acrylate monomer was polymerized. For improving the mechanical properties, ethylene glycol dimethacrylate as a cross-linker was added to the oil phase. Polyglycerol polyricinoleate was mainly used as surfactant to stabilize emulsions. Aqueous dispersed phase comprised of salt and in some formulations initiator. Different initiation systems such as redox, thermal, and photo initiator were investigated for optimum polymerization. We found that mixtures of thermal and photo initiator provide satisfactory stability and polymerization. Then, the volume fraction,		

speed and time of mixing, and surfactant concentration were varied to produce different polyHIPE membranes. The membranes performance was evaluated in terms of pore size, porosity, and window formation. The optimum formulation was considered as the one with mechanical properties high enough to withstand the filtration pressure, the highest window formation (compared to other synthesized polyHIPEs in this work), and the smallest possible pore size. Since hydrophobic matrix and hydrophilic surface can result in improved rejection and permeability of porous membranes, in-situ functionalization of polyHIPEs was investigated through incorporation of a hydrophilic monomer (sodium acrylate) in the aqueous phase prior to polymerization. After successful functionalization, the membrane performance was studied. The results show that polyHIPEs can successfully be used as ultrafiltration (UF) membranes in upper bond (~0.1 μm) as well as microfiltration (MF) membranes, especially for removal of suspended particles. The results show that the permeability of polyHIPE membranes is significantly higher than commercial ones. Therefore, UF/MF membranes can successfully be produced from high internal phase emulsion templating with potential to utilize different monomers for tuning membrane performance. In addition, the fabrication of polyHIPE membranes is ecofriendly since it uses water to generate pores instead of organic solvent.

15. SUBJECT TERMS

16. SECURITY CLASSIFICATION OF:			17. LIMITATION OF ABSTRACT	18. NUMBER OF PAGES	19a. NAME OF RESPONSIBLE PERSON
a. REPORT	b. ABSTRACT	a. THIS PAGE			19b. TELEPHONE NUMBER <i>(Include area code)</i>

**Desalination & Water Purification Research
and Development Program Report No. XXX**

Producing Polymeric Membrane for Ultrafiltration by High Internal Phase Emulsion Templating

Prepared for Reclamation Under Agreement No. XXXXXXXXXXXXX

by

Anna Malakian and Reza Foudazi



U.S. Department of the Interior
Bureau of Reclamation
Technical Service Center
Water and Environmental Services Division
Water Treatment Engineering Research Team
Denver, Colorado

November 2015

MISSION STATEMENTS

The mission of the Department of the Interior is to protect and provide access to our Nation's natural and cultural heritage and honor our trust responsibilities to Indian tribes and our commitments to island communities.

The mission of the Bureau of Reclamation is to manage, develop, and protect water and related resources in an environmentally and economically sound manner in the interest of the American public.

Disclaimer

The views, analysis, recommendations, and conclusions in this report are those of the authors and do not represent official or unofficial policies or opinions of the United States Government, and the United States takes no position with regard to any findings, conclusions, or recommendations made. As such, mention of trade names or commercial products does not constitute their endorsement by the United States Government.

Acknowledgements

The authors would like to thank the U.S. Bureau of Reclamation and New Mexico State University for their support.

Contents

Executive Summary	1
1. Introduction	2
1.1. Water scarcity	2
1.2. Emulsions.....	3
1.3. High Internal Phase Emulsions	6
1.4. Polymerization of High Internal Phase Emulsions	8
2. Experimental.....	11
2.1. Materials	11
2.2. Emulsion preparation	11
2.3. Sample preparation	16
2.4. Characterization	19
2.4.1. Morphology.....	19
2.4.2. Surface Chemistry.....	19
2.4.3. Mechanical Properties.....	20
2.4.4. Filtration test	21
3. Results and Discussion	22
3.1. Morphology.....	22
3.2. In-situ functionalization	28
3.3. Mechanical properties	31
3.4. Permeability	32
4. Conclusion	35
5. References	36

Table of Figures

Figure 1. Schematic of different types of emulsions	4
Figure 2. Schematic of the emulsion instability processes	6
Figure 3. Schematic representation of high internal phase emulsions.....	7
Figure 4. Typical micrographs of (a) HIPE and (b) polyHIPE [20]	9
Figure 5. Structure of majorly used chemicals	11
Figure 6. Oven used to polymerize samples containing thermal initiator	16
Figure 7. UV cross-linker used to polymerize samples containing photo initiator	17
Figure 8. Schematic process of polyHIPE synthesis.	17
Figure 9. HIPE preparation setup.....	18
Figure 10. Casting thin layer of HIPE on support for membrane applications.....	18
Figure 11. Soxhlet setup for washing polyHIPES.....	19
Figure 12. conductometric titration setup	20
Figure 13. Mechanical tester equipment used to determine the resistance of membranes against pressure	21
Figure 14. Homemade filtration setup	22
Figure 15. Optical micrographs of sample #17 after A) 0 min, B) 5 min, C) 10 min, D) 30 min, and E) 60 min of mixing. The scale bar is equal to 10 μm	23
<i>Figure 16. Optical microscopy of sample #27: A) 0 min, and B) 5 min after casting on glass slide. The scale bar is equal to 10 μm.....</i>	24
<i>Figure 17. Comparison of (A) droplet size of HIPE before polymerization obtained by optical microscopy (scale bar: 10 μm), and (B) void size of polyHIPE after polymerization obtained by SEM (scale bar: 50μm) for sample #14.</i>	25
Figure 18. Droplet/void size distribution before and after polymerization (Sample #100)	25
Figure 19. Different window formation: A) SEM of sample #26: no window formation, B) SEM of sample #35: some window formation, C) SEM of sample #46: some window formation, D) SEM of sample #100: intermediate window formation in term of size and volume, E) SEM of sample #62: large window formation. The scale bar is equal to 5 μm	26

Figure 20. Pore size distribution of sample #100	27
Figure 21. Window size distribution of sample #100	27
<i>Figure 22. Schematic of in-situ functionalization process of polyHIPE developed in this work.....</i>	<i>28</i>
Figure 23. Comparing FTIR results of polyHIPE before and after washing with solvent to study the reactivity of surfactant (sample #21)	29
Figure 24. FTIR results show change in surface chemistry for polyHIPEs with (sample #47) and without sodium acrylate (sample #21)	29
Figure 25. Titration curve for: (A) DI water, (B) polyHIPE without sodium acrylate, and (C) polyHIPE with 1 wt.% sodium acrylate	30
Figure 26. Stress versus strain curve of polyHIPE with different pore volume fraction (samples #89, 90, and 91).....	32
Figure 27. Drying kinetics of polyHIPE without (sample #10), with 0.5% (sample #40), with 1% (sample #45), and with 2% (sample #50) sodium acrylate	34

Glossary

HIPE	High Internal Phase Emulsions
polyHIPE	Polymerized high Internal Phase Emulsions
EPA	Environmental Protection Agency
UF membrane	Ultrafiltration membrane
MF membrane	Microfiltration membrane
W/O	Water-in-oil emulsions
O/W	Oil-in-water emulsions
O/O	Oil-in-oil emulsions
W/W	Water-in-water emulsions
O/W/O	Oil-in-water-in-oil emulsions
W/O/W	Water-in-oil-in-water emulsions
HLB	Hydrophilic-lipophilic balance
BA	Butyl Acrylate
SA	Sodium Acrylate
Span 80	Sorbitane monooleate
PGPR	Polyglycerol polyricinoleate
DVB	Divinylbenzene
KPS	Potassium persulfate
1-HPK	1-Hydroxycyclohexyl phenyl ketone
BPO	Benzoyl Peroxide
DMT	N,N-dimethyl-p-toluidine
EGDMA	Ethylene Glycol Dimethacrylate
SEM	Scanning electron microscopy
FTIR	Fourier transform infrared spectroscopy
κ	Darcy's constant (m^2)
l	Membrane thickness (μm)
Q	Flow rate (m^3/s)
μ	Feed viscosity (Pa.s)
A	Membrane area (mm^2)
ΔP	Pressure difference along the membrane (Pa)
R	Rejection
C_p	Permeate concentration (g/L)
C_f	Feed concentration (g/L)

Executive Summary

Presently, over one-third of the world's population lives in water-stressed countries, and this figure is predicted to rise to nearly two-thirds by 2025 [1]. Demand for membrane systems and disinfection equipment will increase as the Environmental Protection Agency (EPA) implements new regulations that stipulate maximum allowable limits for disinfection byproducts, volatile organic compounds, perchlorates, and other potentially hazardous contaminants [2]. Therefore, adequate access to low-cost, energy-efficient methods for advanced water treatment, without further stressing the environment, requires designing and evaluating new membrane technologies.

In this project, high Internal Phase Emulsions (HIPEs) are used as template for producing porous polymers with high porosity and permeability [3]. Porous polymers from HIPE templating are synthesized with a highly interconnected pore network, and thus, have the potential to be utilized for producing microfiltration and ultrafiltration membranes. In this work, oil phase as continuous phase containing butyl acrylate monomer was polymerized through radical polymerization. For improving the mechanical properties, ethylene glycol dimethacrylate as a cross-linker was added to the oil phase. Polyglycerol polyricinoleate was mainly used as surfactant to stabilize HIPEs. Aqueous dispersed phase containing salt and in some formulations initiator was added drop-wise to the oil phase while mixing was performed with an overhead mixer. Different initiation systems such as redox, thermal, and photo initiator were investigated for optimum polymerization of HIPE. We found that mixtures of thermal and photo initiator provide satisfactory stability and polymerization. Then, the volume fraction, speed and time of mixing, and surfactant concentration were varied to produce different polyHIPE membranes. The membranes performance was evaluated in terms of pore size, porosity, and window formation. The optimum formulation was considered as the one with mechanical properties high enough to withstand the filtration pressure, the highest window formation (compared to other synthesized polyHIPEs in this work), and the smallest possible

pore size. Hydrophobic matrix and hydrophilic surface can result in improved rejection and permeability of porous membranes. Therefore, in-situ functionalization of polyHIPEs was investigated through incorporation of a hydrophilic monomer (sodium acrylate) in the water phase of HIPE prior to polymerization. After successful functionalization, the membrane performance was studied. The results show that polyHIPEs can successfully be used as ultrafiltration (UF) membranes in upper bond ($\sim 0.1 \mu\text{m}$) as well as microfiltration (MF) membranes, especially for removal of suspended particles. The produced polyHIPE membranes have higher permeability than typical commercial UF membranes. Therefore, they require less energy for filtration compared to current membranes in the market.

1. Introduction

1.1. Water scarcity

As the world population continues to grow, water resources become scarcer, particularly in arid and semi-arid regions. Consequently, there will be an increase in the production of wastewater containing enough harmful material to damage ground water and/or surface water quality, which should be treated to meet the environmental regulations. Small communities face unique challenges in finding wastewater management solutions since they simply lack the capacity to pay for capital improvements and costs associated with the operation and maintenance of a wastewater system. Additionally, over one-third of the world's population lives in water-stressed countries, and this figure is predicted to rise to nearly two-thirds by 2025 [1].

Demand for membrane systems and disinfection equipment will increase as the Environmental Protection Agency (EPA) implements new regulations that stipulate maximum allowable limits for disinfection byproducts, volatile organic compounds, perchlorates, and other potentially hazardous contaminants [2]. Therefore, adequate access to low-cost, energy-efficient methods for advanced water treatment, without further stressing the environment, requires designing and

evaluating new membrane technologies. In this project, the high internal phase emulsions templating is used to produce new generation of ultrafiltration and microfiltration membranes. The aim is to develop membranes through ecofriendly process, while increasing their permeability in order to reduce the cost of water treatment.

1.2. Emulsions

An emulsion is a dispersion of one liquid (the dispersed or internal phase) in a second immiscible liquid (the continuous or external phase). Emulsions are part of a more general class of two-phase systems of matter called colloids. Examples of emulsions include butter, margarine, mayonnaise, and cream. As schematically shown in Figure 1, emulsions are classified based on the dispersion of droplets in continues phase. The system which consists of water droplets dispersed in an oil phase is known as a water-in-oil (w/o) emulsion, while the dispersed oil droplets in an aqueous phase is an oil-in-water (o/w) emulsion. Additionally, there are more complicated cases such as oil-in-water-in-oil (o/w/o) and water-in-oil-in-water (w/o/w) emulsions, known as multiple emulsions.

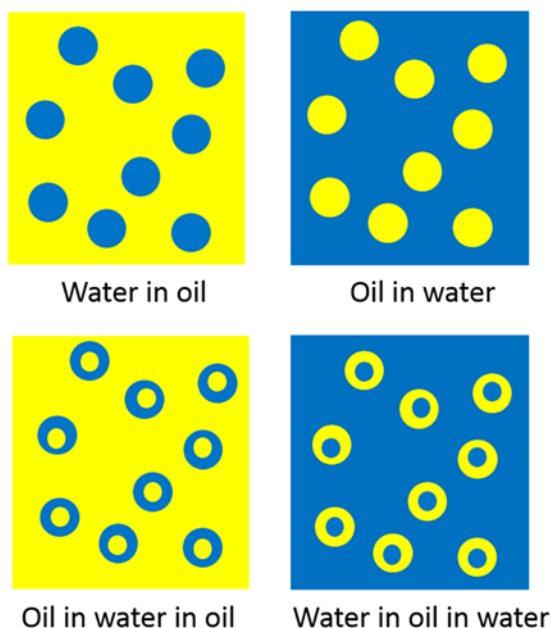


Figure 1. Schematic of different types of emulsions

Beside the oil and water phases, emulsions contain surfactant that stabilizes the dispersed droplets. In other word, while emulsions are not thermodynamically stable systems, they can kinetically be stabilized over a period of time by using proper surfactants. The molecular structure of surfactants contains two moieties: one has attraction for water, known as a lyophobic (hydrophilic) part or “head”, while the other part has strong attraction for oil, called the lyophilic (hydrophobic) segment or simply “tail”. Such molecular structure is known as amphipathic or amphiphilic. In the case of a surfactant dissolved in aqueous medium, the lyophobic (hydrophobic) group distorts the structure of the water by breaking hydrogen bonds between the water molecules and by structuring the water in the vicinity of the hydrophobic group [4]. Therefore, the free energy increases, and the system responds in some fashion to minimize the contact between the lyophobic group and the water phase. Formation of micelles by surfactant molecules is a result of such tendency.

Based on the first emulsification rule developed by Bancroft in 1913 [5], surfactants improve the dispersion of the phase in which they do not dissolve very well. Surfactant can be classified by their hydrophilic-lipophilic balance (HLB) which for first time was introduced by Griffin [6] in 1946. One of the popular formula for calculation of HLB is the Davies expression [7]:

$$HLB = 7 + (\text{Hydrophilic group number}) - 0.45 n_c$$

where hydrophilic group number is obtained form group contribution theory and n_c is the number of $-\text{CH}_2-$ groups in the lipophilic part of the molecule. Surfactants with an HLB number in the range of 3 to 6 form water-in-oil (w/o) emulsions, whereas those with HLB numbers of 8 to 18 are expected to form oil-in-water (o/w) emulsions. Surfactants should be insoluble in the droplet phase to prevent emulsion inversion at high internal phase volume fractions. Depending on the nature of the hydrophilic head group, surfactants are classified as ionic (anionic, cationic, zwitterionic) which have a charged head group connected to a neutral tail, or nonionic which have an uncharged, polar head group connected to

a hydrocarbon tail. As mentioned above, surfactants play a major role in the preparation and stabilization of emulsions. They can be adsorbed strongly at the interface between the continuous and dispersed phases and reduce the energetic driving force to coalescence by lowering the interfacial tension and/or forming a mechanical barrier between droplets.

The interfacial chemistry and rheology, the dynamic of adsorption, and the physicochemical kinetics of surfactants are important parameters in emulsion stability [2]. There are two principal types of stability for colloidal emulsions, droplet stability and dispersion stability. Droplet stability is dependent on the bulk properties of the fluids and the nature of the surfactant. Several breakdown processes may occur that depend on the particle size distribution and the density difference between droplets and the medium. However, the physical phenomena involved in each instability process are not simply described, requiring analysis of the various forces involved [8]. Generally, the solubility of the dispersed droplets and the particle size distribution determine Ostwald ripening and the stability of the liquid film between the droplets determines coalescence and phase inversion. Ostwald ripening is a process where large drops grow at the expense of smaller ones, as the larger droplets are energetically more favorable. Dispersion stability is the stability against aggregation, flocculation (coagulation), and macroscopic phase separation [9]. Emulsion droplets come into contact with each other due to Brownian motion. Consequently, coagulation (flocculation) can occur, which may lead to the formation of larger droplets and coalescence. By forming a thin film around the dispersed phase, as mentioned previously, the surfactant provides a barrier against coalescence and lowers the interfacial tension of the system. A continuous phase with high viscosity can reduce creaming and flocculation by impeding Brownian motion. However, an increase in the viscosity of the continuous phase can lead to inefficient mixing of the two phases [10]. Figure 2 (adapted from ref. [8]) schematically shows different instability in emulsion systems.

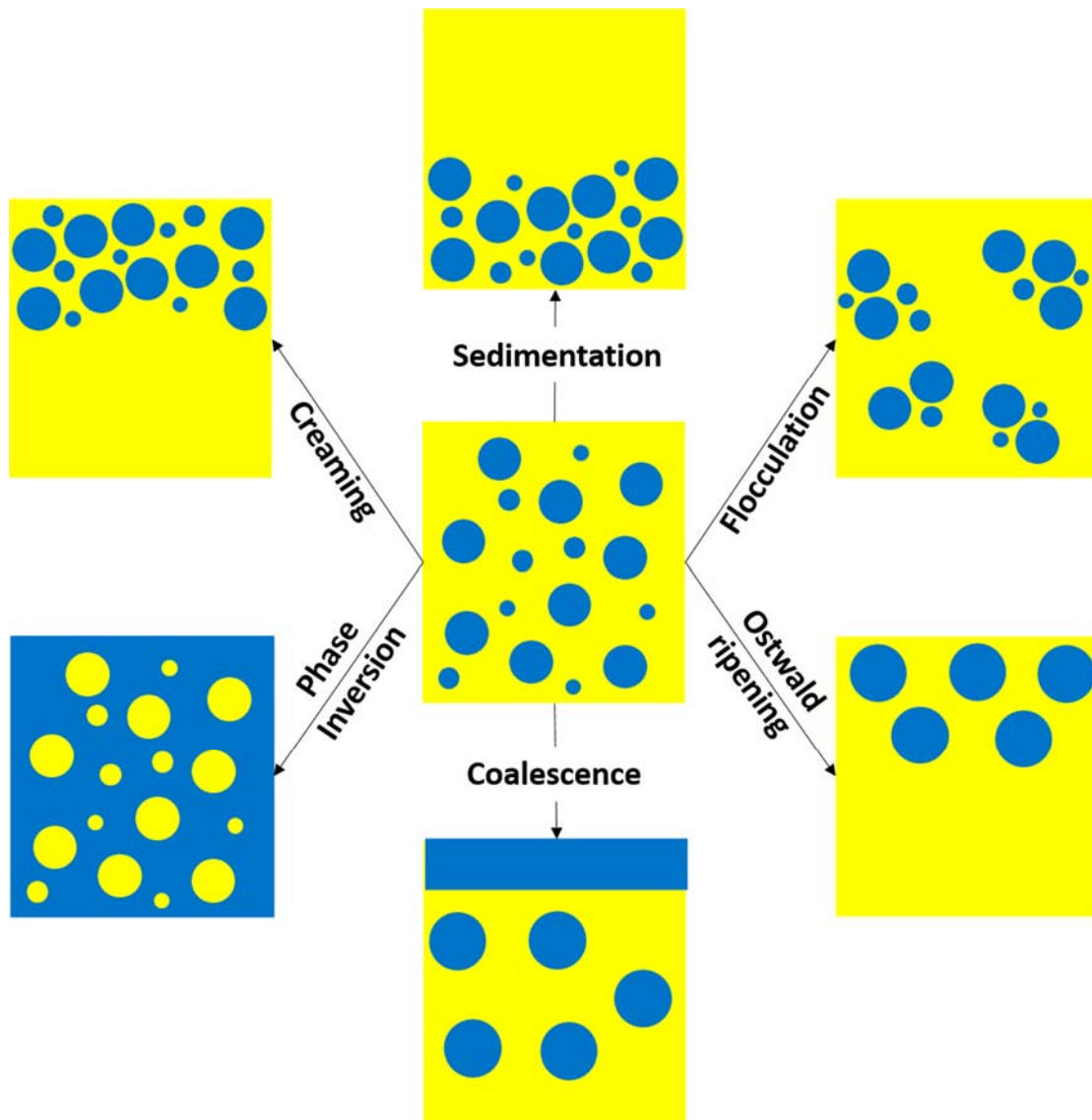
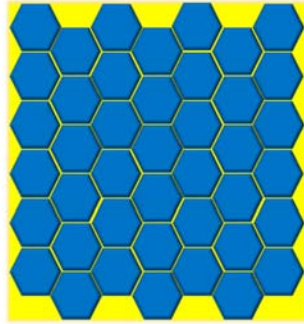


Figure 2. Schematic of the emulsion instability processes

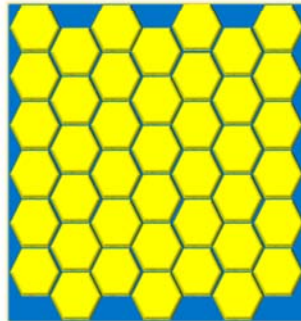
1.3. High Internal Phase Emulsions

The shape of droplets in dispersed phase is spherical (minimum surface area in constant volume) as schematically shown in Figure 1. The volume fraction of maximum closest packing of monodispersed spheres is 74.01% [11]. If the concentration of dispersed phase exceeds this fraction, droplets will be deformed into polyhedrons. This deformation will create large areas of contact between droplets and a packed configuration which induces mechanical interference between droplets, thus prohibiting their free movement (Figure 3). Such emulsions are known as “high internal phase emulsions” (HIPES) or “highly

concentrated emulsions” (HCEs), as introduced by Lissant [12] for the first time in 1964.



High internal phase emulsion (water-in-oil)



High internal phase emulsion (oil-in-water)

Figure 3. Schematic representation of high internal phase emulsions

HIPES similar to other emulsions are thermodynamically unstable and may go through instability. Coalescence in HIPE can occur through the rupture of thin films between the adjacent droplets, eventually leading to complete phase separation of the HIPE. Creaming/sedimentation is the formation of a concentrated layer above/below the bulk emulsion, due to density differences between the two phases.

One of the methods to improve the stability of HIPES is the addition of electrolytes to the aqueous phase. Aronson and Petko [13] studied the effect of electrolytes on properties and stability of HIPES. They found that the emulsion stability is improved by decreased solubility of aqueous phase in oil phase.

However, they concluded that even though Ostwald ripening contributed to HIPE destabilization and was prevented in the presence of the electrolyte, the coalescence is still dominant in HIPE instability. Kizling and Kronberg [14] suggested that lowering van der Waals interaction through polarizability or increasing the refractive index of the aqueous phase towards that of the oil phase could reduce the rate of coalescence.

HIPES have been investigated extensively for decades [15]–[19] and are used in a range of common practical applications in food, cosmetic formulations, drug delivery, and formation of porous materials [5], [7], [9]–[14], [20]. The most common application of HIPES is the synthesis of porous polymer as will be reviewed in next section.

1.4. Polymerization of High Internal Phase Emulsions

HIPES can be polymerized if one or both phases of the emulsion contain monomeric species [21]. This process yields a range of products with widely different properties. Emulsions can be used in three ways as a template for polymer synthesis: (i) polymerization of both phases (continuous and dispersed phases) to produce composites, (ii) polymerization of dispersed phase in order to produce colloidal particles, and (iii) polymerization of continuous phase and removing the dispersed phase to produce porous materials [22]. Polymerized High Internal Phase Emulsions also known as PolyHIPES, are usually produced by curing the continuous phase of HIPES. The continuous phase of emulsions should contain a cross-linker in addition to monomer and surfactant to provide the integrity to polyHIPE upon polymerization. The cross-linker forms the polymer network structure. Once cured, the dispersed phase is removed and the polyHIPE is washed by Soxhlet extractor and dried. If HIPE is stabilized by particles instead of surfactants, the product is known as poly-Pickering-HIPES [23]. Following polymerization of the continuous phase, the emulsion droplets are embedded in the resulting material. Under the correct conditions (*vide infra*), small interconnecting windows are formed between adjacent emulsion droplets upon

polymerization allowing the droplet phase to be removed by drying and form voids (where droplet were before) in the polyHIPE. Consequently, a highly porous and permeable material is produced with complex pore morphology [4]. Typical micrographs of HIPEs and polyHIPEs are shown in Figure 4.

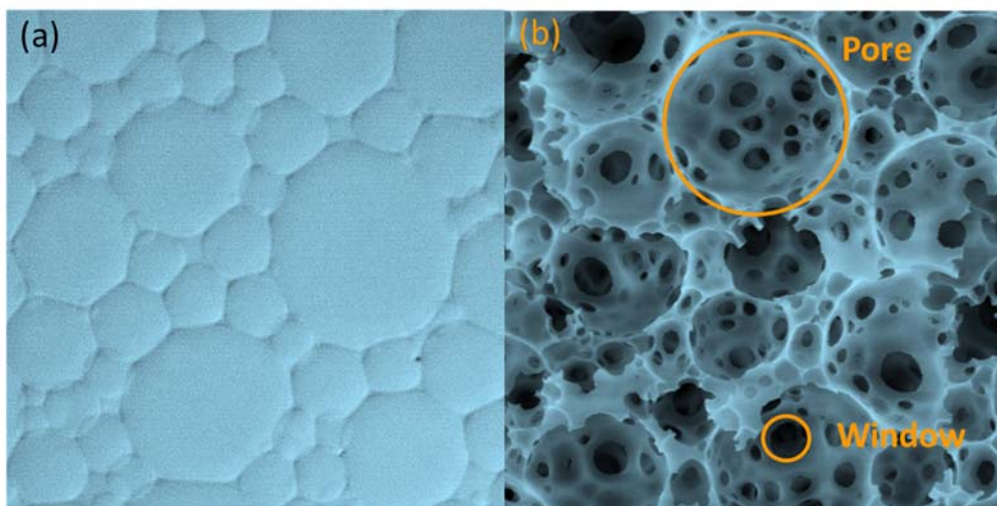


Figure 4. Typical micrographs of (a) HIPE and (b) polyHIPE [20]

The porous materials obtained from polymerization of HIPE are useful for a wide range of advanced applications, such as catalyst supports, ion-exchange modules, separation media, electrochemical sensing [5], supports for cell cultures, bone grafts, setting cement for oil well applications, porous electrodes [7], and separators in lithium ion batteries [8]. The open cellular morphology also makes the polyHIPE a potential candidate for thermal and acoustic insulation [5] within engine compartments and other enclosures. The highly interconnected macroporous structures can be advantageous for achieving high transport rates to microporous walls for molecular storage applications. They can also be formed into macroporous beads [10].

Because of flexibility of polyHIPEs to be produced in any shape and structure, controllable pore size, and high porosity (at least 74.05%), they have the potential to be utilized in liquid separation devices as membranes. Zhao et al. [24]

produced thin layers of polyHIPEs by reactive molding them between two flat plates, separated by poly(ethylene terephthalate) films. The other methods are the slicing the polyHIPE monoliths [25], and polymerization of blade-cast HIPEs on the support.

PolyHIPEs are mostly used as filter for protein purification or gas separation [24], [26]–[29]. Bhumgara [30] used HIPE to produce filter device with 48 cross-flow channels, by pumping a prepared HIPE into a mold before polymerization. The device could successfully filter calcium carbonate particles with 11 μm diameter. In addition, Krajnc et al. [28] produced monoliths for protein separation. The polyHIPE monoliths were modified to bear weak-anion exchange groups for separation of standard protein mixture containing myoglobin, conalbumine, and trypsin inhibitor. Good separation was achieved in a very short time similar to the separation obtained by commercial methacrylate monoliths. However, higher dispersion of protein was observed with polyHIPEs. The other separation application of polyHIPEs is as a permeable barrier with high mechanical properties in oil wells, replacing traditional gravel packs, which has been successfully produced by Ikem et al. [31].

Interaction between the mold and HIPE which results in a low permeability surface on final polyHIPE, as well as droplet coalescence during polymerization of HIPE are disadvantages of polymerizing thin layers of HIPE [27]. However, Krajnc et al. [32] could successfully produce a polyHIPE membrane with thickness between 30-500 μm . The oil phase of HIPEs contained styrene, divinylbenzene, vinylbenzyl chloride, and ethylhexyl acrylate. The pinhole-free membranes were prepared by casting HIPEs onto glass by using an appropriate blade. The mechanical flexibility of polyHIPEs was controlled by the degree of cross-linking and the addition of ethylhexyl acrylate.

2. Experimental

2.1. Materials

Butyl acrylate (BA, 99% , Sigma-Aldrich) and sodium acrylate (SA, 97%, Sigma- Aldrich) as monomers; sorbitane monooleate (Span 80, Sigma-Aldrich), Polyglycerol polyricinoleate (PGPR 4125, Palsgaard), and Pluronic L121 (BASF) as surfactants; divinylbenzene (DVB, 80%, Sigma-Aldrich) and ethylene glycol dimethacrylate (EGDMA, 98%, Sigma-Aldrich) as cross-linker; potassium persulfate (KPS, 99%, Acros) as thermal initiator; 1-hydroxycyclohexyl phenyl ketone (1-HPK, 99%, Sigma-Aldrich) as photo initiator; and benzoyl peroxide (BPO, 75%, Sigma-Aldrich) and N,N-dimethyl-p-toluidine (DMT, 99%, Sigma-Aldrich) as redox initiator were used as received. Structures of majorly used chemicals are shown in Figure 5.

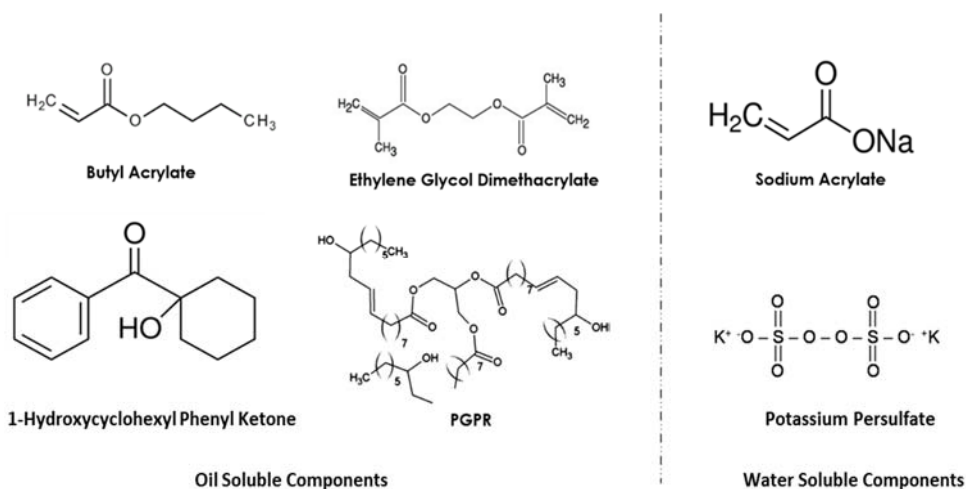


Figure 5. Structure of majorly used chemicals

2.2. Emulsion preparation

The oil phase of emulsion was a mixture of monomer (butyl acrylate), surfactant (PGPR 4125, Span80, or Pluronic L121) and cross-linker (EGDMA or DVB). For some samples photo-initiator (1-hydroxycyclohexyl phenyl ketones) or redox initiator (N,N-dimethyl-4-toluidine and benzoyl peroxide) were also added. Table 1 shows all samples in details. In this table volume fraction and composition of all samples are included.

Table 1. Composition of prepared samples and corresponding morphological observation

Sample Number	Oil Phase									Aqueous Phase				HIPE Formation	Open pore Formation	Window Formation
	Water Phase (wt. %)			Surfactant (wt.%)			Initiator (wt.%)			Monomer	Initiator (wt.%)		Salt			
	BA (ratio)	EDGMA (ratio)	DVB (ratio)	PGPR	Span 80	Pluronic L121	I-HPK	DMT (wt %)	SA (wt.%)	KPS	BPO	NaCl (wt.%)				
1	75	3	1	-	10	-	-	-	-	-	0.5	-	2	Yes	Yes	Some
2	75	3	1	-	15	-	-	-	-	-	0.5	-	2	Yes	Yes	Some
3	75	3	1	-	20	-	-	-	-	-	0.5	-	2	Yes	Yes	Some
4	75	3	1	-	25	-	-	-	-	-	0.5	-	2	Yes	Yes	Some
5	75	3	1	-	30	-	-	-	-	-	0.5	-	2	Yes	Yes	Some
6	80	3	1	-	10	-	-	-	-	-	0.5	-	2	Yes	Yes	Some
7	80	3	1	-	15	-	-	-	-	-	0.5	-	2	Yes	Yes	Some
8	80	3	1	-	20	-	-	-	-	-	0.5	-	2	Yes	Yes	Some
9	80	3	1	-	25	-	-	-	-	-	0.5	-	2	Yes	Yes	Some
10	80	3	1	-	30	-	-	-	-	-	0.5	-	2	Yes	Yes	Some
11	85	3	1	-	10	-	-	-	-	-	0.5	-	2	Yes	Yes	Some
12	85	3	1	-	15	-	-	-	-	-	0.5	-	2	Yes	Yes	Some
13	85	3	1	-	20	-	-	-	-	-	0.5	-	2	Yes	Yes	Some
14	85	3	1	-	25	-	-	-	-	-	0.5	-	2	Yes	Yes	Some
15	85	3	1	-	30	-	-	-	-	-	0.5	-	2	Yes	Yes	Some
16	85	3	1	-	10	-	-	-	-	-	0.5	-	2	Yes	Yes	Some
17	90	3	1	-	10	-	-	-	-	-	0.5	-	2	Yes	Yes	Some
18	90	3	1	-	15	-	-	-	-	-	0.5	-	2	Yes	Yes	Some
19	90	3	1	-	20	-	-	-	-	-	0.5	-	2	Yes	Yes	Some
20	90	3	1	-	25	-	-	-	-	-	0.5	-	2	Yes	Yes	Some
21	90	3	1	-	30	-	-	-	-	-	0.5	-	2	Yes	Yes	Some
22	90	3	1	-	10	-	-	-	-	-	0.5	-	2	No	-	-
23	95	3	1	-	10	-	-	-	-	-	0.5	-	2	No	-	-
24	95	3	1	-	15	-	-	-	-	-	0.5	-	2	No	-	-
25	95	3	1	-	20	-	-	-	-	-	0.5	-	2	No	-	-
26	95	3	1	-	25	-	-	-	-	-	0.5	-	2	No	-	-
27	95	3	1	-	30	-	-	-	-	-	0.5	-	2	No	-	-
28	90	3	1	-	10	-	-	-	-	-	0.5	-	5	No	-	-
29	90	3	1	-	15	-	-	-	-	-	0.5	-	5	No	-	-
30	90	3	1	-	20	-	-	-	-	-	0.5	-	5	No	-	-

Sample Number	Water Phase (wt. %)	Oil Phase								Aqueous Phase				HIPE Formation	Open pore Formation	Window Formation	
		Monomer		Cross-linker		Surfactant (wt.%)			Initiator (wt.%)		Monomer	Initiator (wt.%)					Salt
		BA (ratio)	EDGMA (ratio)	DVB (ratio)	PGPR	Span 80	Pluronic L121	1-HPK	DMT (wt %)	SA (wt.%)	KPS	BPO	NaCl (wt.%)				
31	90	3	1	-	25	-	-	-	-	-	0.5	-	5	No	-	-	
32	90	3	1	-	30	-	-	-	-	-	0.5	-	5	No	-	-	
33	90	3	1	-	10	-	-	-	-	-	0.5	-	5	No	-	-	
34	95	3	1	-	10	-	-	-	-	-	0.5	-	5	No	-	-	
35	95	3	1	-	15	-	-	-	-	-	0.5	-	5	No	-	-	
36	95	3	1	-	20	-	-	-	-	-	0.5	-	5	No	-	-	
37	95	3	1	-	25	-	-	-	-	-	0.5	-	5	No	-	-	
38	95	3	1	-	30	-	-	-	-	-	0.5	-	5	No	-	-	
39	75	3	1	-	30	-	-	-	-	0.5	0.5	-	2	Yes	Yes	Some	
40	80	3	1	-	30	-	-	-	-	0.5	0.5	-	2	Yes	Yes	Some	
41	85	3	1	-	30	-	-	-	-	0.5	0.5	-	2	Yes	Yes	Some	
42	90	3	1	-	30	-	-	-	-	0.5	0.5	-	2	Yes	Yes	Some	
43	95	3	1	-	30	-	-	-	-	0.5	0.5	-	2	Yes	Yes	Some	
44	75	3	1	-	30	-	-	-	-	1	0.5	-	2	Yes	Yes	Some	
45	80	3	1	-	30	-	-	-	-	1	0.5	-	2	Yes	Yes	Some	
46	85	3	1	-	30	-	-	-	-	1	0.5	-	2	Yes	Yes	Some	
47	90	3	1	-	30	-	-	-	-	1	0.5	-	2	Yes	Yes	Some	
48	95	3	1	-	30	-	-	-	-	1	0.5	-	2	Yes	Yes	Some	
49	75	3	1	-	30	-	-	-	-	2	0.5	-	2	Yes	Yes	Some	
50	80	3	1	-	30	-	-	-	-	2	0.5	-	2	Yes	Yes	Some	
51	85	3	1	-	30	-	-	-	-	2	0.5	-	2	Yes	Yes	Some	
52	90	3	1	-	30	-	-	-	-	2	0.5	-	2	Yes	Yes	Some	
53	95	3	1	-	30	-	-	-	-	2	0.5	-	2	Yes	Yes	Some	
54	75	3	-	1	-	10	-	-	-	-	0.5	-	5	No	-	-	
55	75	3	-	1	-	15	-	-	-	-	0.5	-	5	No	-	-	
56	75	3	-	1	-	20	-	-	-	-	0.5	-	5	No	-	-	
57	75	3	-	1	-	25	-	-	-	-	0.5	-	5	No	-	-	
58	75	3	-	1	-	30	-	-	-	-	0.5	-	5	some	-	-	
59	75	3	-	1	-	35	-	-	-	-	0.5	-	5	Yes	Yes	Yes	
60	80	3	-	1	-	35	-	-	-	-	0.5	-	5	Yes	Yes	Yes	
61	85	3	-	1	-	35	-	-	-	-	0.5	-	5	Yes	Yes	Yes	

Sample Number	Water Phase (wt. %)	Oil Phase								Aqueous Phase				HIPE Formation	Open pore Formation	Window Formation	
		Monomer		Cross-linker		Surfactant (wt.%)			Initiator (wt.%)		Monomer	Initiator (wt.%)					Salt
		BA (ratio)	EDGMA (ratio)	DVB (ratio)	PGPR	Span 80	Pluronic L121	1-HPK	DMT (wt %)	SA (wt.%)	KPS	BPO	NaCl (wt.%)				
62	90	3	-	1	-	35	-	-	-	-	0.5	-	5	Yes	Yes	Yes	
63	95	3	-	1	-	35	-	-	-	-	0.5	-	5	No	-	-	
64	75	3	1	-	-	-	10	-	-	-	0.5	-	5	No	-	-	
65	75	3	1	-	-	-	15	-	-	-	0.5	-	5	No	-	-	
66	75	3	1	-	-	-	20	-	-	-	0.5	-	5	No	-	-	
67	75	3	1	-	-	-	25	-	-	-	0.5	-	5	No	-	-	
68	75	3	1	-	-	-	30	-	-	-	0.5	-	5	some	-	-	
69	75	3	1	-	-	-	35	-	-	-	0.5	-	5	Yes	Yes	Some	
70	80	3	1	-	-	-	35	-	-	-	0.5	-	5	Yes	Yes	Some	
71	85	3	1	-	-	-	35	-	-	-	0.5	-	5	Yes	Yes	Some	
72	90	3	1	-	-	-	35	-	-	-	0.5	-	5	No	-	-	
73	95	3	1	-	-	-	35	-	-	-	0.5	-	5	No	-	-	
74	75	3	1	-	20	-	-	0.5	-	-	-	-	5	No	-	-	
75	80	3	1	-	20	-	-	0.5	-	-	-	-	5	No	-	-	
76	85	3	1	-	20	-	-	0.5	-	-	-	-	5	No	-	-	
77	90	3	1	-	20	-	-	0.5	-	-	-	-	5	No	-	-	
78	95	3	1	-	20	-	-	0.5	-	-	-	-	5	No	-	-	
79	75	3	1	-	20	-	-	-	0.25	-	-	0.25	5	No	-	-	
80	80	3	1	-	20	-	-	-	0.25	-	-	0.25	5	No	-	-	
81	85	3	1	-	20	-	-	-	0.25	-	-	0.25	5	No	-	-	
82	90	3	1	-	20	-	-	-	0.25	-	-	0.25	5	No	-	-	
83	95	3	1	-	20	-	-	-	0.25	-	-	0.25	5	No	-	-	
84	75	3	1	-	30	-	-	0.25	-	-	0.25	-	5	Yes	Yes	Yes	
85	80	3	1	-	30	-	-	0.25	-	-	0.25	-	5	Yes	Yes	Yes	
86	85	3	1	-	30	-	-	0.25	-	-	0.25	-	5	Yes	Yes	Yes	
87	90	3	1	-	30	-	-	0.25	-	-	0.25	-	5	No	-	-	
88	95	3	1	-	30	-	-	0.25	-	-	0.25	-	5	No	-	-	
89	75	3	1	-	30	-	-	0.25	-	0.5	0.25	-	5	Yes	Yes	Yes	
90	80	3	1	-	30	-	-	0.25	-	0.5	0.25	-	5	Yes	Yes	Yes	
91	85	3	1	-	30	-	-	0.25	-	0.5	0.25	-	5	Yes	Yes	Yes	
92	75	3	1	-	30	-	-	0.25	-	1	0.25	-	5	Yes	Yes	Yes	

Sample Number	Water Phase (wt. %)	Oil Phase								Aqueous Phase				HIPE Formation	Open pore Formation	Window Formation	
		Monomer		Cross-linker		Surfactant (wt.%)			Initiator (wt.%)		Monomer	Initiator (wt.%)					Salt
		BA (ratio)	EDGMA (ratio)	DVB (ratio)	PGPR	Span 80	Pluronic L121	1-HPK	DMT (wt %)	SA (wt.%)	KPS	BPO	NaCl (wt.%)				
93	80	3	1	-	30	-	-	0.25	-	1	0.25	-	5	Yes	Yes	Yes	
94	85	3	1	-	30	-	-	0.25	-	1	0.25	-	5	Yes	Yes	Yes	
95	75	3	1	-	30	-	-	0.25	-	2	0.25	-	5	Yes	Yes	Yes	
96	80	3	1	-	30	-	-	0.25	-	2	0.25	-	5	Yes	Yes	Yes	
97	85	3	1	-	30	-	-	0.25	-	2	0.25	-	5	Yes	Yes	Yes	
98	75	3	1	-	35	-	-	0.25	-	-	0.25	-	5	Yes	Yes	Yes	
99	80	3	1	-	35	-	-	0.25	-	-	0.25	-	5	Yes	Yes	Yes	
100	85	3	1	-	35	-	-	0.25	-	-	0.25	-	5	Yes	Yes	Yes	
101	75	3	1	-	35	-	-	0.25	-	0.5	0.25	-	5	Yes	Yes	Yes	
102	80	3	1	-	35	-	-	0.25	-	0.5	0.25	-	5	Yes	Yes	Yes	
103	85	3	1	-	35	-	-	0.25	-	0.5	0.25	-	5	Yes	Yes	Yes	
104	75	3	1	-	35	-	-	0.25	-	1	0.25	-	5	Yes	Yes	Yes	
105	80	3	1	-	35	-	-	0.25	-	1	0.25	-	5	Yes	Yes	Yes	
106	85	3	1	-	35	-	-	0.25	-	1	0.25	-	5	Yes	Yes	Yes	
107	75	3	1	-	35	-	-	0.25	-	2	0.25	-	5	Yes	Yes	Yes	
108	80	3	1	-	35	-	-	0.25	-	2	0.25	-	5	Yes	Yes	Yes	
109	85	3	1	-	35	-	-	0.25	-	2	0.25	-	5	Yes	Yes	Yes	

The oil phase with different weight fractions was mixed with overhead mixer with 500 rpm for 10 minutes. Then, aqueous phase containing water, salt (NaCl) as stabilizer, and thermal initiators (KPS) if present was added dropwise to the oil phase. In some samples, second monomer (sodium acrylate) was also included in the aqueous phase. The weight fraction of aqueous phase was varied from 75 to 95%. Three last columns of Table 1 summarize the result of experiments, which will be elaborated in the Results and Discussion section. Some compositions could not form high internal phase emulsion and after a while one of instability processes (as schematically shown in Figure 2), mostly phase inversion, took place. In other words, HIPE formation is a critical step before one can synthesize

polyHIPE. Since window formation and open-pore structure have direct effect on permeability of membrane, they are also addressed in Table 1.

2.3. Sample preparation

After preparation of HIPEs, they should be polymerized to produce porous materials. In the case of thermal initiators, the samples were placed in an oven (Thermo Scientific, Heratherm oven, as shown in Figure 6) at temperature of 65-70 °C for 2 h. For photo-initiation, the samples were placed in a UV chamber (Spectroline, Select Series, as shown in Figure 7) at wavelength of 240 nm for 2 h.



Figure 6. Oven used to polymerize samples containing thermal initiator

For redox initiation, two different emulsions were prepared, each of them containing one component of redox initiator (either BPO or DMT). Then, these two emulsions were mixed together and placed under foam hood for 24 h for polymerization to be completed. The process of polyHIPE synthesis is schematically shown in Figure 8 and the setup used for HIPE preparation is shown in Figure 9.



Figure 7. UV cross-linker used to polymerize samples containing photo initiator

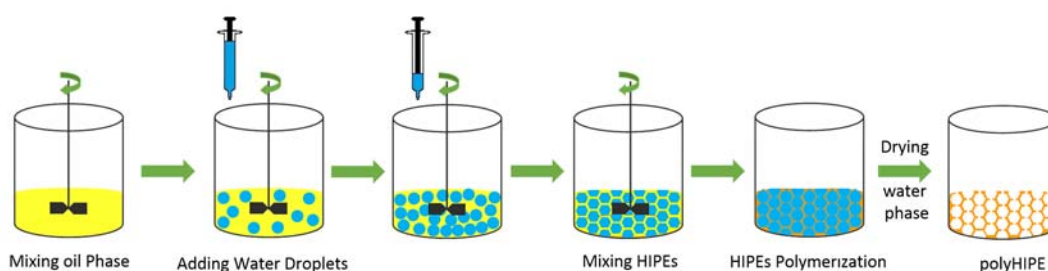


Figure 8. Schematic process of polyHIPE synthesis.

For thin-layer polyHIPE which is needed for membrane performance test, HIPE samples were cast on the support which was recovered from a commercial membrane (GE, MW series, MW2540F30) through washing with chloroform in Soxhlet for 24 h. The HIPE samples were cast on the support by sandwiching the support, HIPE, and a frame with 0.2 mm thickness between two stainless steel plates covered with Mylar sheets. Then, a constant pressure of 0.4 MPa was applied by a mechanical press to prepare a uniform thickness of HIPE and improve its diffusion in the support. Figure 10 shows the casting process schematically. Afterwards, samples were cured by UV and/or heating as will be discussed in the Results and Discussion.

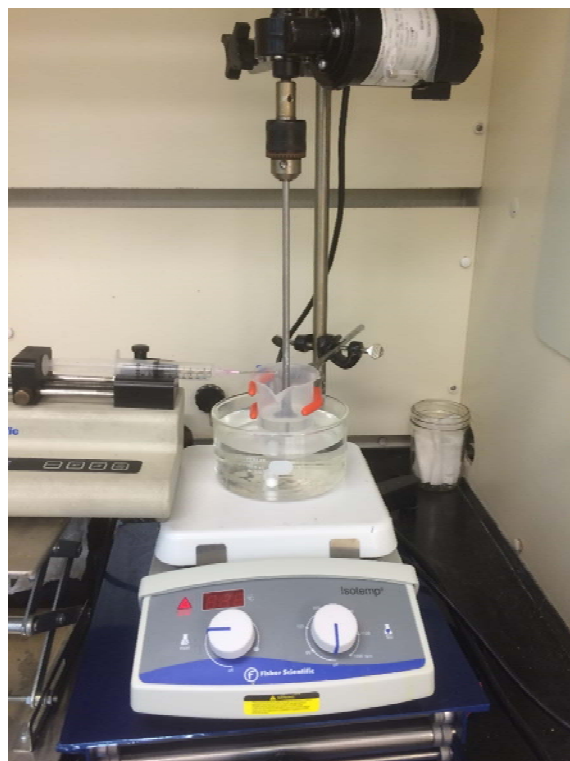


Figure 9. HIPE preparation setup

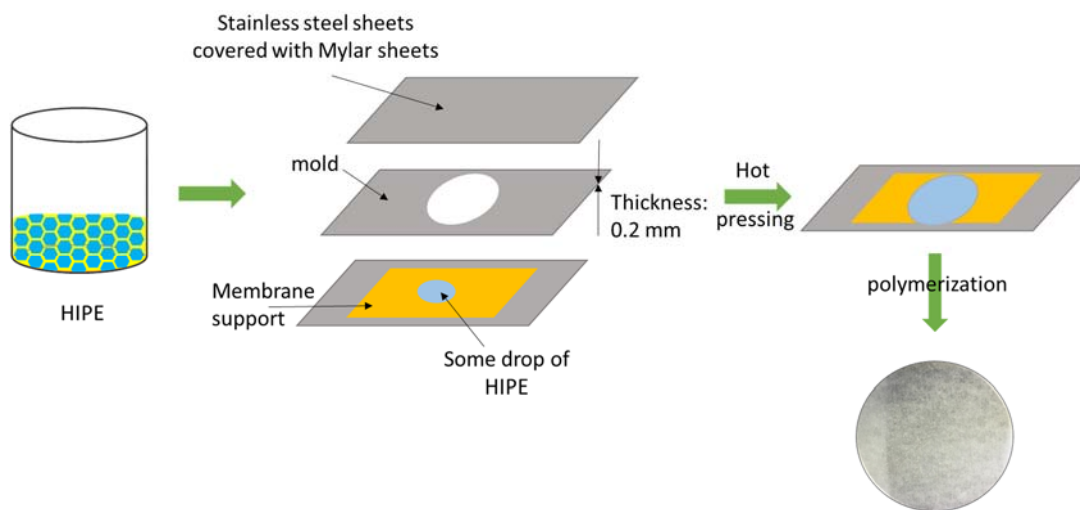


Figure 10. Casting thin layer of HIPE on support for membrane applications

All samples after polymerization were washed first with DI water for 24 h, and then with 2-propanol for another 24 h by a Soxhlet apparatus (shown in Figure 11).

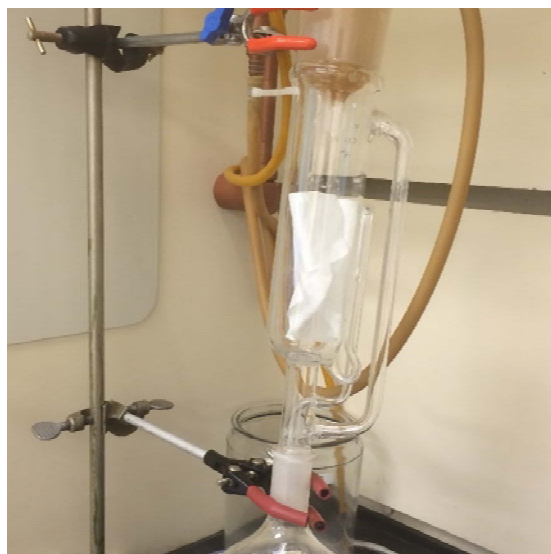


Figure 11. Soxhlet setup for washing polyHIPEs

2.4. Characterization

2.4.1. Morphology

As a primary characterization, morphology of prepared samples was studied to define a proper formulation of polyHIPE with desired structure (based on pore sizes and window formation). Scanning electron microscopy (SEM, S-3400N Type II, Hitachi High-Technologies Corp.) and optical microscopy (Nikon, Eclipse E400) were used to observe the morphology of polyHIPE and HIPE samples, respectively. The samples for optical microscopy were prepared by putting a drop of HIPE between a glass slide and a cover glass.

Sample preparation for SEM was performed by fracturing the dried polyHIPE in liquid nitrogen. Then, a piece of fractured sample was adhered on the sample holder with carbon conductive tape, and coated through gold sputtering.

2.4.2. Surface Chemistry

Fourier transform infrared spectroscopy (FTIR, Perkin-Elmer Spectrum One FTIR Spectrometer), and surface charge were investigated for characterizing the surface properties of polyHIPEs.

Surface charge density of membranes was studied by conductometric titration. PolyHIPE samples were grinded and dispersed in water (10 wt.%) 30 min before starting the experiment. The pH and conductivity of dispersion was recorded simultaneously by ultra pH/conductivity meter (hq40d, Hach Co.). A magnetic stirrer was used to continuously mix the dispersion. The HCL 0.1 N and NaOH 0.1 N were used for titration. The setup is shown in Figure 12.



Figure 12. conductometric titration setup

2.4.3. Mechanical Properties

Mechanical properties of selected samples were studied by compression test with mechanical tester machine (AGS-X, Shimadzu Co., shown in Figure 13) to determine the tolerance of samples to filtration pressures. PolyHIPE monoliths were cut into cylinders with 2.5 cm height and 1.5 cm diameter. Then, they placed between two plates of mechanical tester machine and compressing test was started with speed of 1 mm/min.



Figure 13. Mechanical tester equipment used to determine the resistance of membranes against pressure

2.4.4. Filtration test

A home-made setup was used for filtration measurement (Figure 14). Two sets of experiments were performed. First, the water flux was measured to calculate the permeability of prepared membranes. In the second experiment, the capabilities of polyHIPE membrane to remove suspended oil droplets was studied by filtering a mixture of vegetable oil (25g), NaCl (500 mg), Pluronic F68 (5 g) and DI water (1L). This mixture was prepared through stirring prior to filtration by a magnetic stirrer bar (3/8 in. diameter, 2 in. length) in a 1 L flat-bottom Erlenmeyer flask at a constant speed of 600 rpm at 60°C for 24 h [12]. Additionally, for particle filtration, another feed mixture containing 10 wt.% talc, $\text{H}_2\text{Mg}_3(\text{SiO}_3)_4$, was prepared. Since talc is insoluble in water, 2 wt.% Pluronic F 68 was also added to stabilize the suspension.

The permeability of polyHIPEs can also be measured through drying kinetics test after saturation with water. PolyHIPEs after washing with 2-propanol and water were dried in the oven at 45°C for 48 h and then immersed in DI water for 6h. Each sample was weighted after saturation with water, and then placed in the

oven. The drying kinetics of samples was obtained by measuring their weight in 30 min intervals.



Figure 14. Homemade filtration setup

3. Results and Discussion

3.1. Morphology

PolyHIPEs as membrane have potential application for filtration of suspending particles and bacteria. To produce optimum morphology, several formulations were synthesized as summarized in Table 1. Since the pore size and pore formation are controlled by droplet size of emulsion in HIPE templating, the time of mixing, speed of mixing, and surfactant concentration (10-35 wt%) were varied from 0-90 min, 400-650 rpm, and 10-35 wt.% in different formulations, respectively. For example, as shown in Figure 15, by increasing the mixing time, the droplet size is decreased.

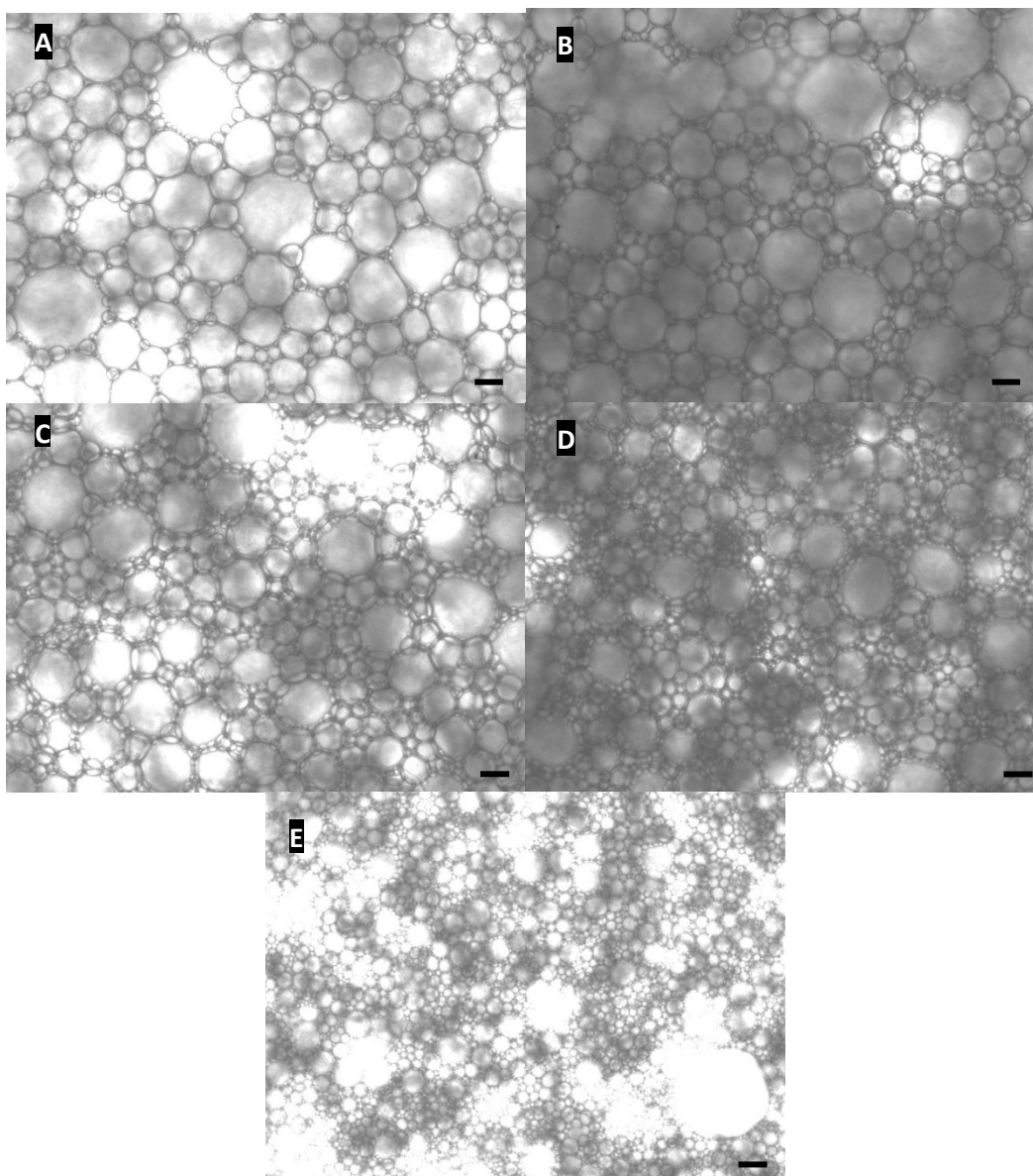


Figure 15. Optical micrographs of sample #17 after A) 0 min, B) 5 min, C) 10 min, D) 30 min, and E) 60 min of mixing. The scale bar is equal to 10 μm .

The concentration and type of surfactant affect the stability of emulsion. For example as shown in Table 1, the water does not emulsify in oil containing Span 80 as a surfactant with concentration lower than 30%. The stability of emulsions were investigated through monitoring their morphology with time. The variation of surfactant concentration shows two satisfactory observations: (i) higher

stability of emulsions (as shown in Figure 16), and (ii) smaller droplet sizes (discussed below) by increasing the surfactant concentration.

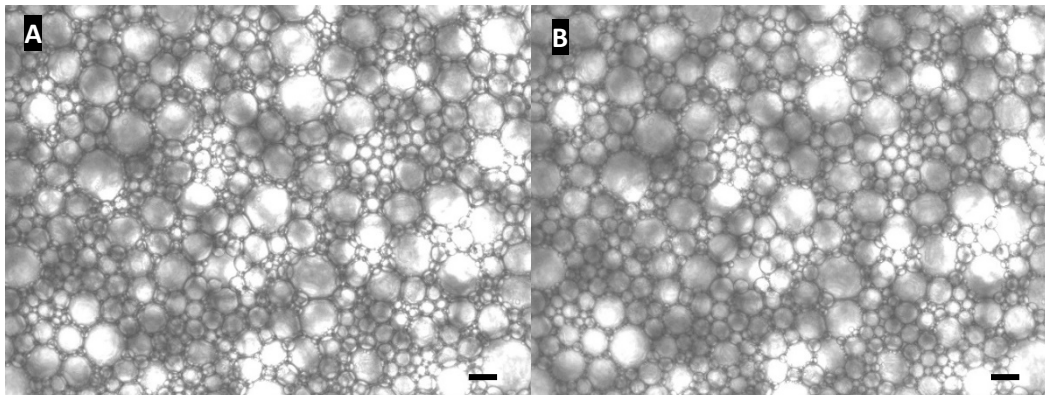


Figure 16. Optical microscopy of sample #27: A) 0 min, and B) 5 min after casting on glass slide. The scale bar is equal to 10 μm .

The second method to study the stability of HIPE is to compare the droplet sizes of HIPE (by optical microscopy before polymerization) and the void size of polyHIPE (by SEM after polymerization) since polymerization with thermal initiation may affect the stability of emulsions and final microstructure in polyHIPE. As seen in Figure 16, the domain size of sample 14 increases upon polymerization (note that the scale bar in SEM micrograph is equal to 50 μm , while it is equal to 10 μm in optical micrograph), which can be attributed to the increase in coalescence rate at high temperatures. To overcome this shortcoming, a photo-initiator was incorporated in formulations (sample 74-78). The role of photo-polymerization is to set the HIPE structure in the absence of intensive thermal initiation. We observed that HIPE samples cannot be prepared only via photo-polymerization (see for instant #74 to 78 in Table 1) since the white color of emulsions limits the penetration length of UV light. Therefore, a combination of thermal and photo-polymerization was investigated (sample 79-97 in Table 1). In other words, photo-polymerization as pre-polymerization stage was firstly performed and then thermal polymerization was used to complete the curing of samples. Additionally, we observed that increasing the salt concentration from 2

wt.% to 5 wt.% in the water phase improves the stability of HIPE during polymerization (by comparing sample #1 and #54).

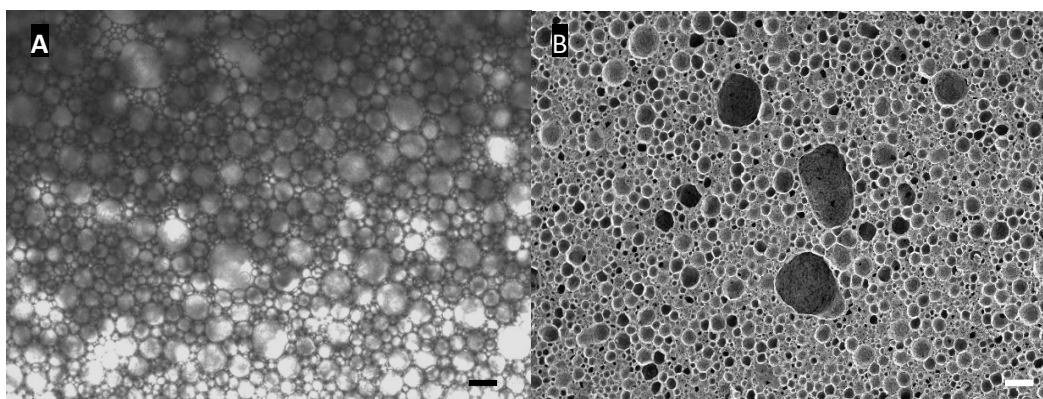


Figure 17. Comparison of (A) droplet size of HIPE before polymerization obtained by optical microscopy (scale bar: 10 μm), and (B) void size of polyHIPE after polymerization obtained by SEM (scale bar: 50 μm) for sample #14.

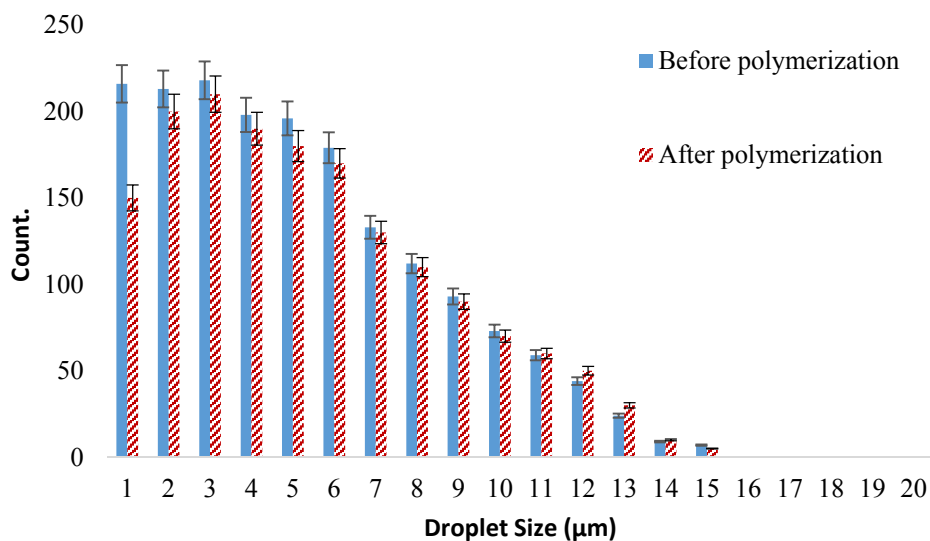


Figure 18. Droplet/void size distribution before and after polymerization (Sample #100)

To quantify the stability of emulsions, droplet size distributions before and after polymerization were investigated through image analysis of optical micrographs and scanning electron micrographs, respectively. As seen in Figure 17, the size distribution does not change in the sample that goes through first

photo- and then thermal polymerization. Therefore, the developed method of combined initiation in this work can successfully be employed in the scale-up of process.

Since window size directly affects the permeability of polyHIPE membranes, different formulations were made to produce different windows as shown in Figure 18.

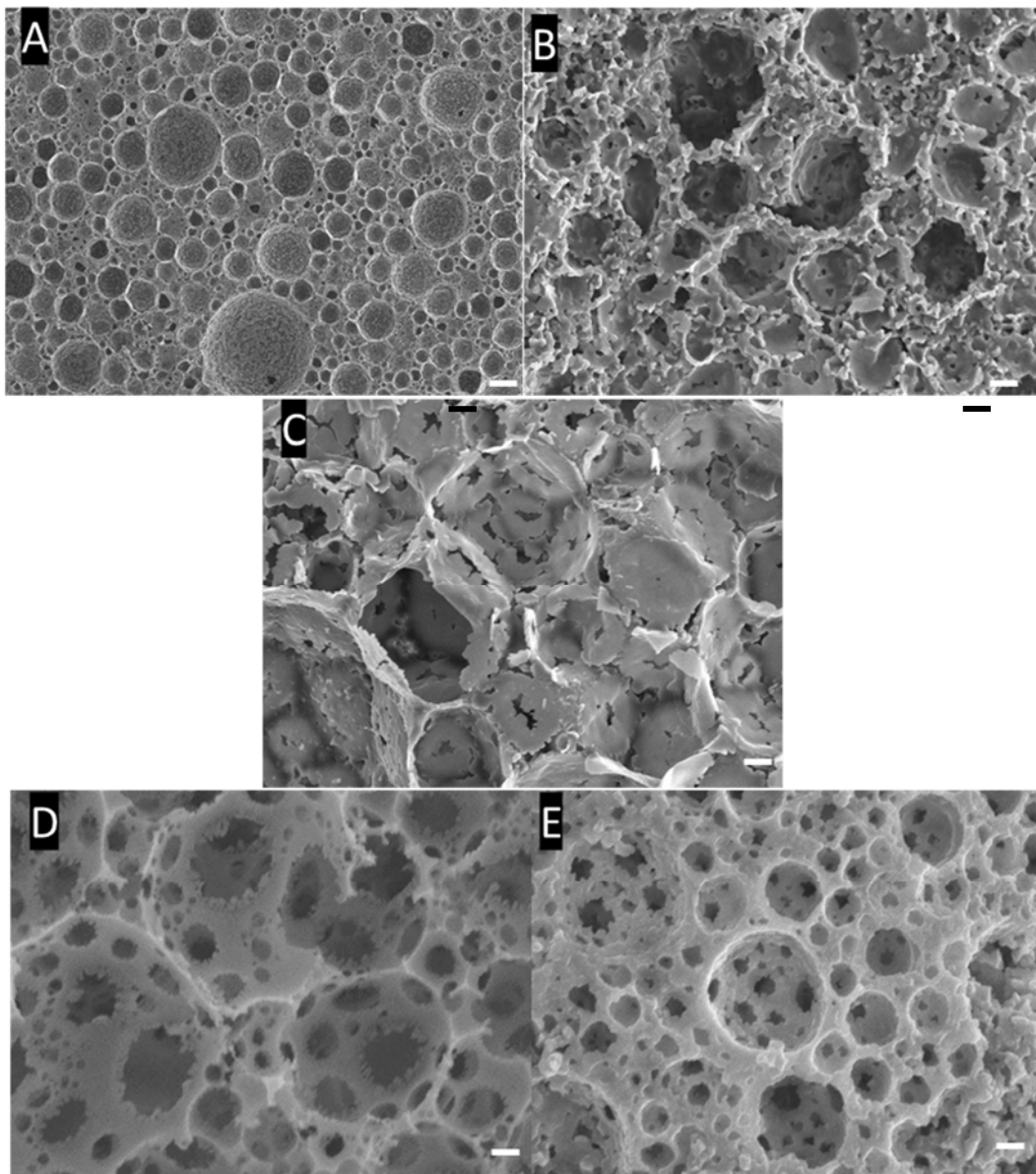


Figure 19. Different window formation: A) SEM of sample #26: no window formation, B) SEM of sample #35: some window formation, C) SEM of sample #46: some window formation, D) SEM of sample #62: large window formation, E) SEM of sample #100: intermediate window formation in term of size and volume. The scale bar is equal to 5 μ m.

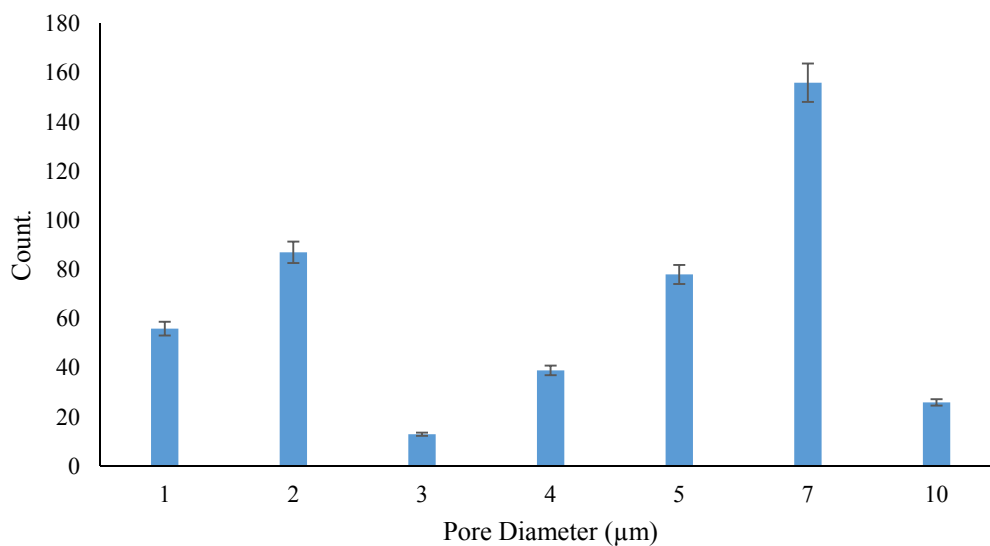


Figure 20. Pore size distribution of sample #100

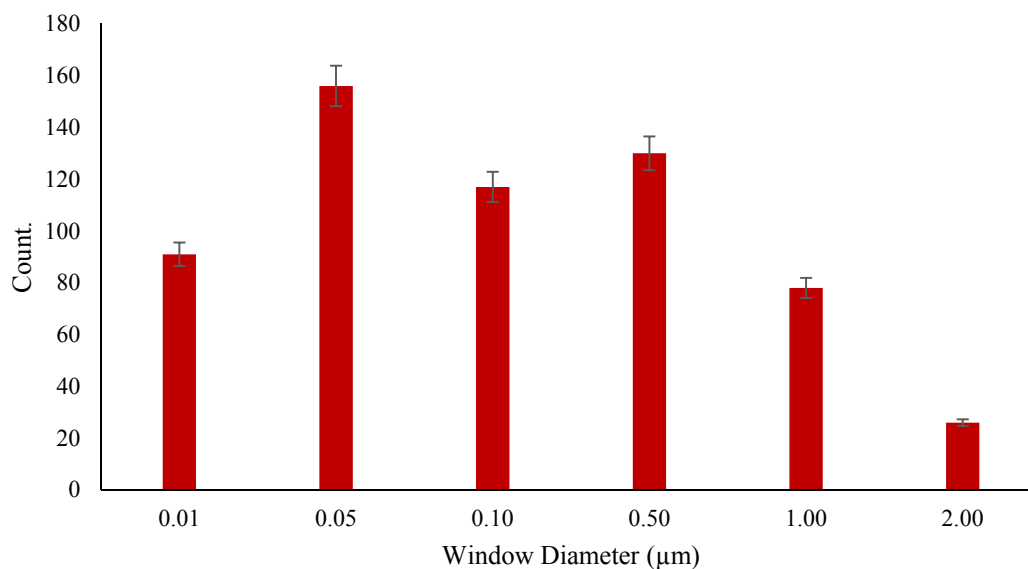


Figure 21. Window size distribution of sample #100

The size distribution of pores and windows was investigated for sample #100 – which was found to be the optimum formulation in terms of stability, polymerization, and window formation – as shown in Figure 20 and 21. This sample has window size between 0.01 to 1 μm . Therefore, membranes made from

this polyHIPE are on the upper bond of ultrafiltration and can be also utilized as microfiltration membranes.

3.2. In-situ functionalization

For water purification, the ideal ultrafiltration and microfiltration membranes should have hydrophilic surface and hydrophobic structure, because: (i) the hydrophilic surface will interact with water and reject the hydrophobic particles which in turn decrease the fouling, and (ii) a hydrophilic body of membrane will result in swelling of membrane during filtration which will decrease its performance. Therefore, surface of commercialized membranes is usually treated. In this study, for the first time the surface modification is performed in-situ, which means during the polymerization of membrane.

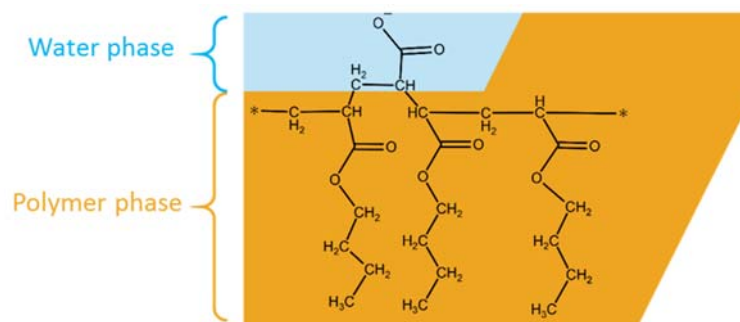


Figure 22. Schematic of in-situ functionalization process of polyHIPE developed in this work

The nature of synthesized polyHIPE membrane is hydrophobic (the employed monomers form hydrophobic polymer); therefore, a water-soluble monomer (sodium acrylate) was added in the aqueous phase to produce a hydrophilic surface during polymerization as schematically shown in Figure 22. In addition, the employed surfactant has unsaturated carbon-carbon bonds, and thus, can be copolymerized with continuous phase.

The FTIR of two samples (#21 and #47) are shown in Figure 23 and 24. Sodium acrylate has O^- functional group while butyl acrylate does not; therefore,

the observed broad peak in $3200\text{-}3600\text{ cm}^{-1}$ in FTIR of samples can be due to the -O- group belongs to sodium acrylate at the surface and/or the -OH functional group of PGPR surfactant.

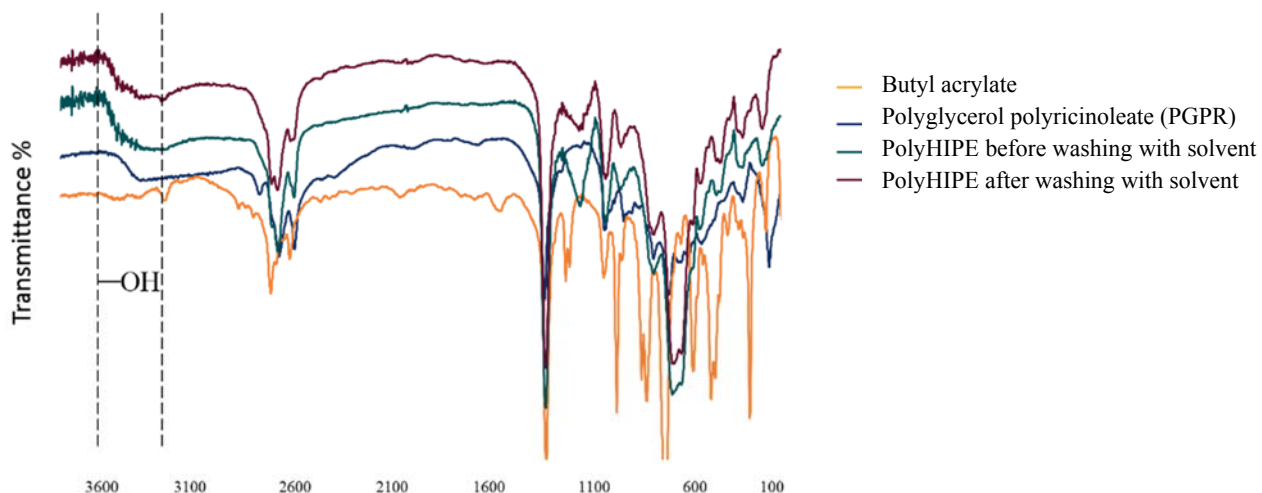


Figure 23. Comparing FTIR results of polyHIPE before and after washing with solvent to study the reactivity of surfactant (sample #21)

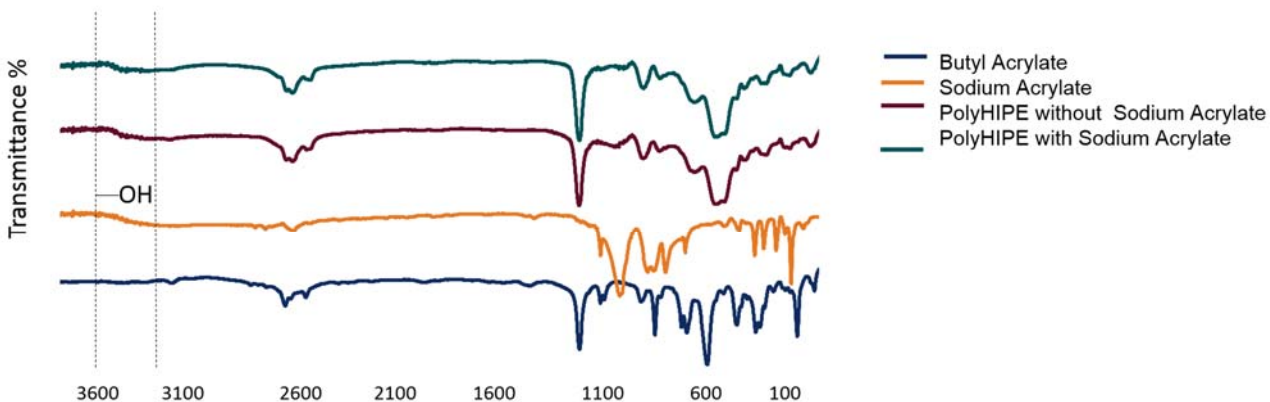


Figure 24. FTIR results show change in surface chemistry for polyHIPEs with (sample #47) and without sodium acrylate (sample #21)

FTIR results in Figure 23 shows that even after washing samples with 2-propanol which dissolves PGPR, the peaks in the $3200\text{ to }3600\text{ cm}^{-1}$ range are still present in polyHIPE sample. PGPR also shows similar peaks in the same range.

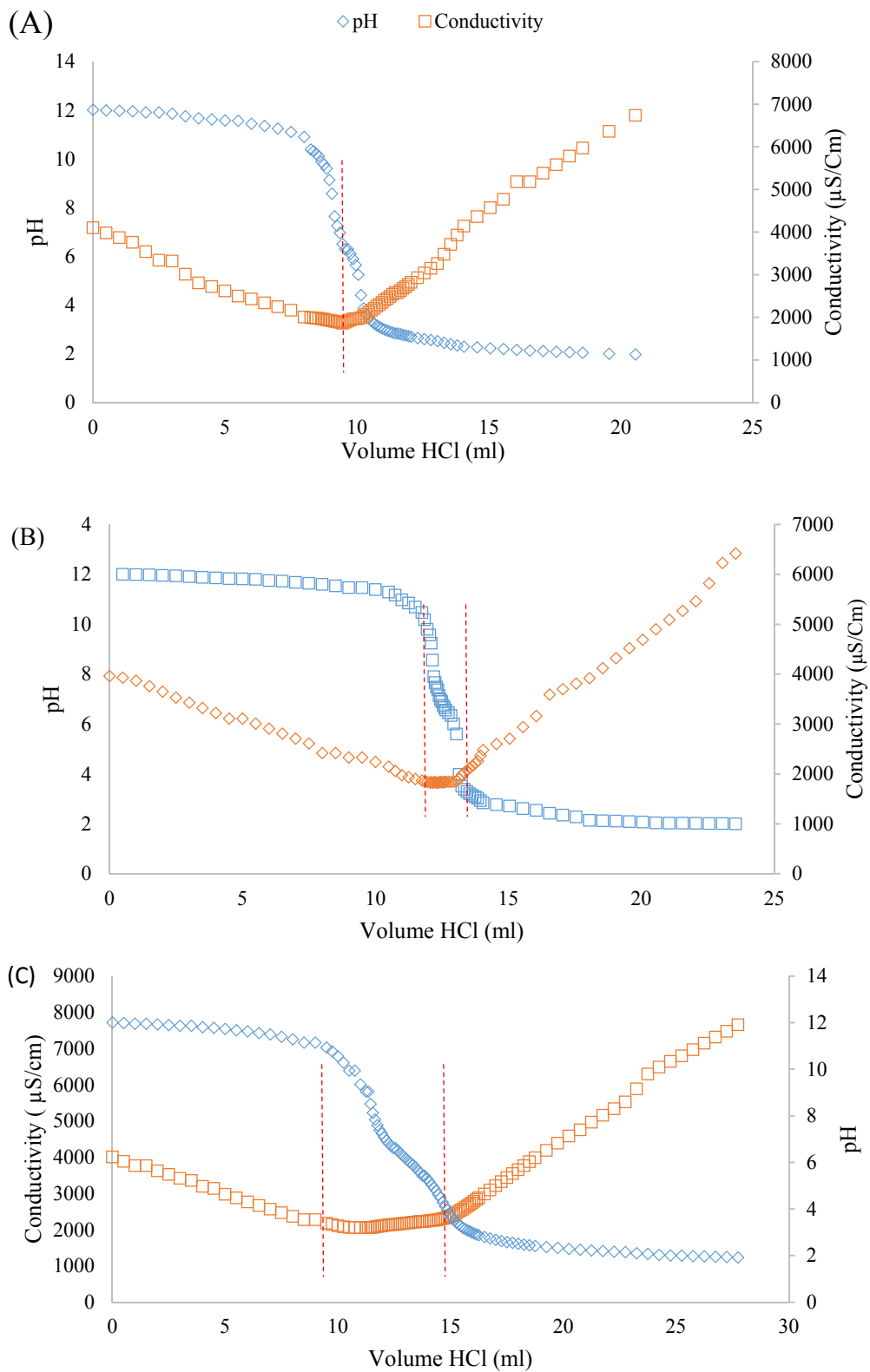


Figure 25. Titration curve for: (A) DI water, (B) polyHIPE without sodium acrylate, and (C) polyHIPE with 1 wt.% sodium acrylate

The results in Figure 23 confirm that the surfactant is copolymerized with BA and EGDMA through the existing double bonds in its chemical structure. In Figure 24, the FTIR results of polyHIPE with/without SA are presented. The peak in the 3200 to 3600 cm^{-1} range as seen in Figure 23 appears in both samples, which shows that SA may also reacted with BA. To confirm the copolymerization of SA with continuous phase at the surface of polyHIPE, the charge density of polyHIPE is also studied by conductometric titration (Figure 25).

Comparing the charge density of membranes without and with sodium acrylate in the formulation, as shown in Table 2, shows that the charge density increases by increasing the percentage of sodium acrylate in the continuous phase. The results confirm that by adding sodium acrylate to the aqueous phase, in-situ functionalization takes place. The titration results also show that the polyHIPE without sodium acrylate (sample #100) has some surface charge which can be related to the copolymerization of PGPR with continuous phase. It should be noted that DI water was tested as control sample to make sure that the obtained results are not artifact.

Table 2. Charge density for samples No. 103, 106, 109

Sample	Charge Density (C.m^{-2})
Control (DI water)	0
PolyHIPE without SA (sample #100)	0.45
PolyHIPE with 1% SA (sample #106)	1.92
PolyHIPE with 2% SA (sample #109)	3.16

3.3. Mechanical properties

One of the important properties of ultrafiltration and microfiltration membranes is mechanical properties since the filtration process is normally done

at high pressures (around 5 to 10 bar, equal to 0.5 to 1 MPa). As shown in Figure 25, by increasing the volume fraction, mechanical properties is decreased. However, even the sample with the lowest mechanical properties in this study is strong enough to withstand the pressure of filtration process.

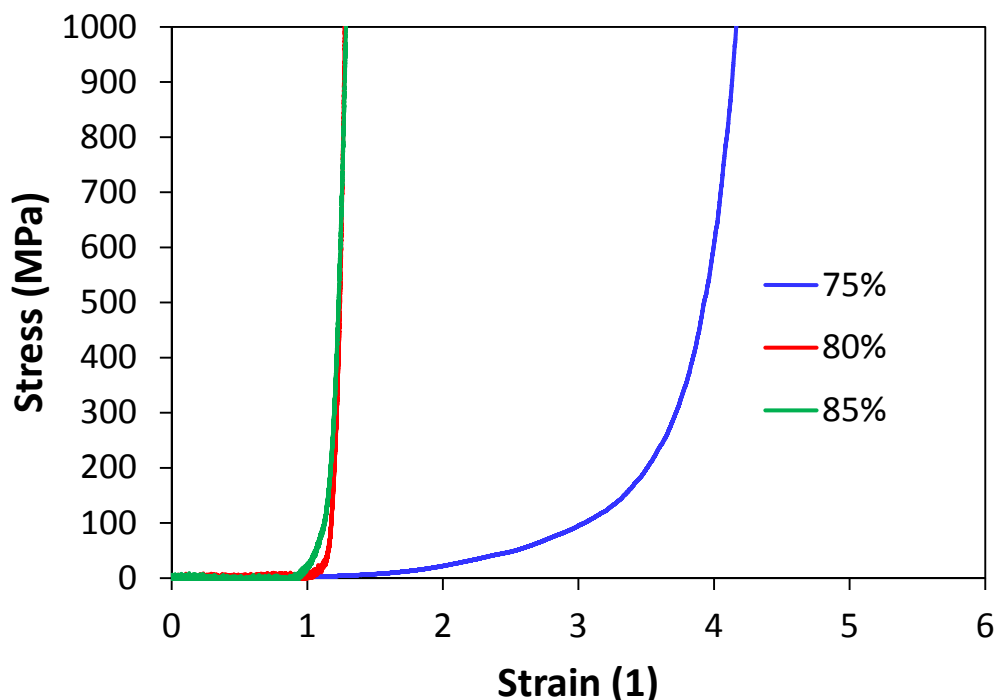


Figure 26. Stress versus strain curve of polyHIPE with different pore volume fraction (samples #89, 90, and 91)

3.4. Permeability

Performance of synthesized membranes was evaluated by carrying out pure water permeation, flux and rejection, and drying kinetics. Pure water permeation and drying kinetics are directly related to the membrane pore size and porosity, and thus its permeability. However, the permeate flux is influenced by several other factors such as feed solute molecular weight, feed concentration, and solute physical structure. Pure water permeation was studied based on Darcy's coefficient by dead-end filtration setup. Darcy's law was used to calculate the permeability as follows:

$$\frac{\kappa}{l} = \frac{Q \mu}{A \Delta P}$$

where, Q , μ , A , ΔP , l , and κ are flow rate, viscosity, membrane area, pressure difference along the membrane, membrane thickness, and Darcy's constant (which features intrinsic permeability), respectively. The ratio of κ/l was considered as an indication of operational permeability in this work. In other words, since different membranes may have different thicknesses which is also difficult to be accurately measured, the value of intrinsic permeability itself can be misleading in real application.

The results are shown in Table 3, in which the synthesized membranes show higher permeability than commercial UF membranes due to high porosity of polyHIPEs. Therefore, UF/MF membranes can successfully be produced from HIPE templating not only with potential to utilize different monomers but also with higher permeability. In addition, the fabrication of polyHIPE membranes is ecofriendly since it uses water to generate pores instead of organic solvent.

The kinetics of drying was also studied, which shows that by adding SA, because of hydrophilic surface, the drying process is faster (higher slope at short times) as shown in Figure 27.

Table 3. Pure water permeation result based on Darcy's law

	Sample #100	Sample #103	Sample #106	Sample #109	Commercial UF (GE)
P atm (KPa)	101	101	101	101	101
P pump (KPa)	482	965	517	482	1200
Area (mm ²)	1380	1380	1380	1380	1380
Q (ml/sec)	26.316	31.250	29.412	30.303	1.0
Thickness (mm)	0.2	0.2	0.2	0.2	0.2
κ/l (m)	5.02×10^{-11}	2.63×10^{-11}	5.13×10^{-11}	5.77×10^{-11}	6.61×10^{-13}

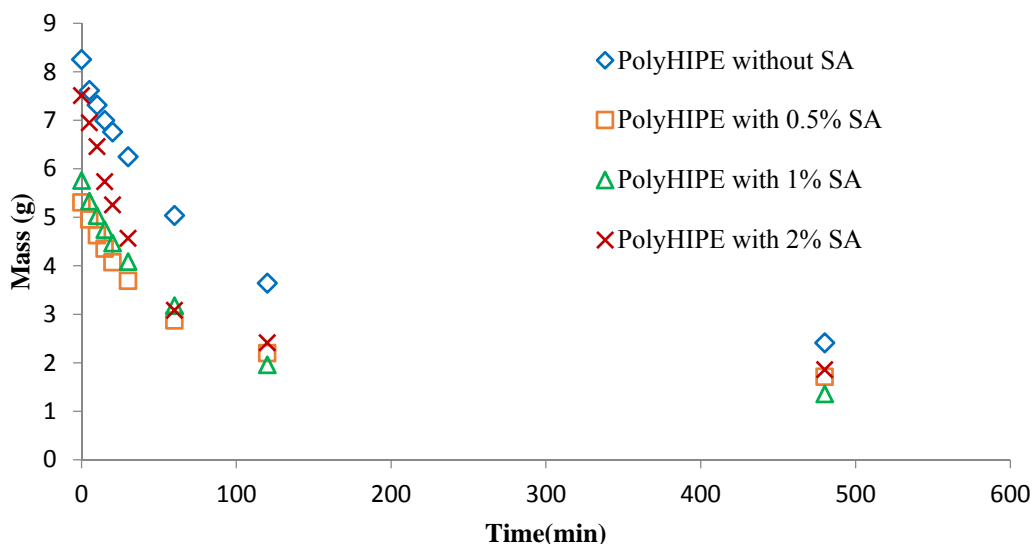


Figure 27. Drying kinetics of polyHIPE without (sample #10), with 0.5% (sample #40), with 1% (sample #45), and with 2% (sample #50) sodium acrylate

After studying the water flux permeation, permeability for filtering of oil-in-water emulsion (occurs in applications such as fracking) was studied. The sample feed composed of vegetable oil, NaCl, water, and Pluronic F 68 as surfactant. Sample #100 was used as membranes in this experiment. During the test, pressure increased to values higher than 1000 KPa which suggests that the polyHIPE membrane act as a barrier for oil droplets. However, since the experiments were performed in dead-end configuration and resulted in such a high pressure, droplets are pushed through membrane and went through refining process to pass the small pores of polyHIPE membrane. Another experiment was performed in which sample feed containing talc, prepared as explained in Experimental section, was filtered through sample #100 as membrane. Synthesized membranes showed 99.9% rejection of particles and the permeability after 60 second was decreased to zero, which demonstrates the formation of cake and pore blockage due to the dead-end configuration. Therefore, the polyHIPE has the capability for removing suspending particles from water. The permeability for such experiment is shown in Table 4. It is expected that polyHIPE membranes have a much a better performance in the cross-flow configuration, where oil droplet will not be pushed

through pore of membrane and particles will be washed away from membrane surface (much lower pore blockage compared to dead-end configuration).

Table 4. Particle filtration permeability of synthesized membrane

	Sample No. 103
P atm (KPa)	101
P pump (KPa)	1430
Volume (ml)	20
Q (ml/sec)	0.33
Thickness(mm)	0.2
κ/l (m)	1.80×10^{-13}

4. Conclusion

The aim of this project was to study the possibility of using polyHIPEs as ultrafiltration (UF) and microfiltration (MF) membrane. In this regard, morphology, surface chemistry, mechanical properties, and filtration ability of polyHIPE porous materials were studied. The results show that polyHIPEs can be used as membranes because of high porosity (at least 74.05%), high pore connectivity, and acceptable mechanical properties. Also, in-situ functionalization was performed to improve permeability and rejection of membrane through incorporation of a hydrophilic monomer (sodium acrylate) in the water phase of HIPE prior to polymerization.

Comprehensive investigation of several formulations was performed and a polyHIPE with 85 wt% water phase which contains 5 wt% salt, and 0.5 wt% SA and 15 wt% oil phase contain 35 wt% PGPR as a surfactant, 0.25 wt% KPS as thermal initiator and 0.25 wt% HPK as photo initiator and monomer to cross-linker ratio of 4:1 was found as an optimum formulation for membrane fabrication in this work. Optical Microscopy, SEM, FT-IR, and conductometric titration were used for membrane characterization. Based on rejection test which shows 99.9% rejection of talc particle, the polyHIPE can be used as a particle filtration membrane. Significant increase in the pumping pressure upon filtration of oil

droplets also demonstrates that the polyHIPE membranes have the potential for oil droplet removal in industrial configuration which are cross-flow rather than dead-end. The results show that the permeability of polyHIPE membranes is significantly higher than commercial ones. Therefore, UF/MF membranes can successfully be produced from HIPE templating with potential to utilize different monomers for tuning membrane performance. In addition, the fabrication of polyHIPE membrane is ecofriendly since it uses water to generate pores instead of organic solvent.

As recommendation for future work, polyHIPE can be made with nanoemulsion to produce nanofiltration membranes.

5. References

- [1] R. F. Service, "Desalination freshens up," *Science* (80-.), vol. 313, no. 5790, pp. 1088–1090, Aug. 2006.
- [2] ed Sjoblom, Johan, *Emulsions and Emulsion Stability: Surfactant Science Series/61*, vol. 21. CRC Press, 2005.
- [3] K. J. Lissant and K. G. Mayhan, "A study of medium and high internal phase ratio water/polymer emulsions," *J. Colloid Interface Sci.*, vol. 42, no. 1, pp. 201–208, Jan. 1973.
- [4] E. D. Goddard, *Surfactants and interfacial phenomena*, vol. 40. 1989.
- [5] B. Y. W. D. Bancroft, "Bancroft, W. D. The Theory of Emulsification V.," *Changes*, vol. 3, no. 1904, pp. 501–519, 1913.
- [6] W. C. Griffin, "Classification of surface-active agents by 'HLB,'" *J Soc Cosmet. Chem.*, vol. 1, pp. 311–326, 1946.
- [7] I. Congress and S. Activity, "Emulsion Type . I . Physical Chemistry of," pp. 426–438, 1957.
- [8] T. F. Tadros, *Applied Surfactants: Principles and Applications*. Wiley-VCH Verlag GmbH & Co., 2005.
- [9] E. Ruckenstein and N. Churaev, "A possible hydrodynamic origin of the forces of hydrophobic attraction," *J. Colloid Interface Sci.*, vol. 147, no. 2, pp. 535–538, Dec. 1991.
- [10] J. R. Carnachan, "Emulsion-derived (PolyHIPE) foams for structural

- materials applications,” 2004.
- [11] N. R. Cameron, “High internal phase emulsion templating as a route to well-defined porous polymers,” *Polymer (Guildf.)*, vol. 46, no. 5, pp. 1439–1449, Feb. 2005.
- [12] K. . Lissant, “The geometry of high-internal-phase-ratio emulsions,” *J. Colloid Interface Sci.*, vol. 22, no. 5, pp. 462–468, Nov. 1966.
- [13] M. P. Aronson and M. F. Petko, “Highly Concentrated Water-in-Oil Emulsions: Influence of Electrolyte on Their Properties and Stability,” *J. Colloid Interface Sci.*, vol. 159, no. 1, pp. 134–149, Aug. 1993.
- [14] J. Kizling and B. Kronberg, “On the formation and stability of concentrated water-in-oil emulsions, aphrons,” *Colloids and Surfaces*, vol. 50, pp. 131–140, Jan. 1990.
- [15] H. M. Princen, “Highly concentrated emulsions. I. Cylindrical systems,” *J. Colloid Interface Sci.*, vol. 71, no. 1, pp. 55–66, 1979.
- [16] T. D. Dimitrova and F. Leal-Calderon, “Rheological properties of highly concentrated protein-stabilized emulsions,” *Adv. Colloid Interface Sci.*, vol. 108, pp. 49–61, 2004.
- [17] V. G. Babak and M.-J. Stébé, “Highly Concentrated Emulsions: Physicochemical Principles of Formulation,” *J. Dispers. Sci. Technol.*, vol. 23, no. 1–3, pp. 1–22, Jan. 2002.
- [18] I. Masalova, R. Foudazi, and A. Y. Malkin, “The rheology of highly concentrated emulsions stabilized with different surfactants,” *Colloids Surfaces A Physicochem. Eng. Asp.*, vol. 375, no. 1–3, pp. 76–86, Feb. 2011.
- [19] R. Foudazi, S. Qavi, I. Masalova, and A. Y. Malkin, “Physical chemistry of highly concentrated emulsions,” *Adv. Colloid Interface Sci.*, vol. 220, pp. 78–91, 2015.
- [20] R. Foudazi, P. Gokun, D. L. Feke, S. J. Rowan, and I. Manas-Zloczower, “Chemorheology of Poly(high internal phase emulsions),” *Macromolecules*, vol. 46, no. 13, pp. 5393–5396, Jun. 2013.
- [21] N. R. Cameron and D. C. Sherrington, *High internal phase emulsions (HIPES) — Structure, properties and use in polymer preparation*. Berlin, Heidelberg: Springer Berlin Heidelberg, 1996.
- [22] H. Zhang and A. I. Cooper, “Synthesis and applications of emulsion-templated porous materials,” *Soft Matter*, vol. 1, no. 2, pp. 107–113, 2005.
- [23] P. J. Colver and S. a F. Bon, “Cellular polymer monoliths made via

- pickering high internal phase emulsions,” *Chem. Mater.*, vol. 19, no. 13, pp. 1537–1539, 2007.
- [24] C. Zhao, E. Danish, N. R. Cameron, and R. Katakya, “Emulsion-templated porous materials (PolyHIPEs) for selective ion and molecular recognition and transport: applications in electrochemical sensing,” *J. Mater. Chem.*, vol. 17, no. 23, pp. 2446–2453, Jun. 2007.
- [25] A. M. Shakorfow, “Process intensification in the demulsification of water-in-crude oil emulsions via crossflow microfiltration through a hydrophilic polyHIPE polymer (PHP),” 2012.
- [26] I. Pulko, V. Smrekar, A. Podgornik, and P. Krajnc, “Emulsion templated open porous membranes for protein purification,” *J. Chromatogr. A*, vol. 1218, no. 17, pp. 2396–401, 2011.
- [27] M. Tebboth, A. Menner, A. Kogelbauer, and A. Bismarck, “Polymerised high internal phase emulsions for fluid separation applications,” *Curr. Opin. Chem. Eng.*, vol. 4, pp. 114–120, 2014.
- [28] P. Krajnc, N. Leber, D. Štefanec, S. Kontrec, and A. Podgornik, “Preparation and characterisation of poly(high internal phase emulsion) methacrylate monoliths and their application as separation media,” *J. Chromatogr. A*, vol. 1065, no. 1, pp. 69–73, Feb. 2005.
- [29] J. Su, J. Flanagan, Y. Hemar, and H. Singh, “Synergistic effects of polyglycerol ester of polyricinoleic acid and sodium caseinate on the stabilisation of water–oil–water emulsions,” *Food Hydrocoll.*, vol. 20, no. 2–3, pp. 261–268, 2006.
- [30] Z. Bhumgara, “Polyhipe foam materials as filtration media,” *Filtr. Sep.*, vol. 32, no. 3, pp. 245–251, Mar. 1995.
- [31] V. O. Ikem, A. Menner, T. S. Horozov, and A. Bismarck, “Highly permeable macroporous polymers synthesized from pickering medium and high internal phase emulsion templates,” *Adv. Mater.*, vol. 22, no. 32, pp. 3588–92, Aug. 2010.
- [32] I. Pulko and P. Krajnc, “Open cellular reactive porous membranes from high internal phase emulsions,” *Chem. Commun. (Camb)*, no. 37, pp. 4481–3, 2008.